WATER RESOURCES OF WADI SYSTEMS OF SOUTHERN SAUDI ARABIA

Saleh A. S. Bajabaa

A Thesis Submitted for the Degree of PhD
at the
University of St Andrews

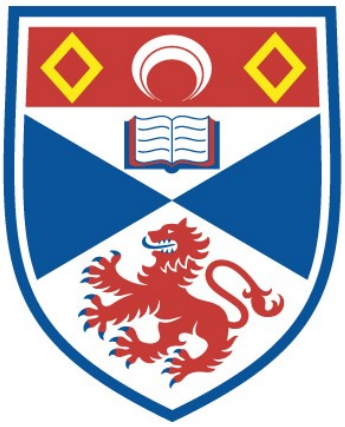

1996

WATER RESOURCES OF WADI SYSTEMS OF SOUTHERN SAUDI ARABIA

Thesis submitted for the award of
Doctor of Philosophy

University of St. Andrews

by

Saleh A. S. Bajabaa B.Sc. University of King Abdulaziz,
M.Sc. South Dakota School of Mines and Technology,
School of Geography and Geology,
The University of St Andrews

July 1995

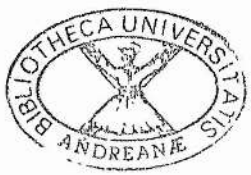

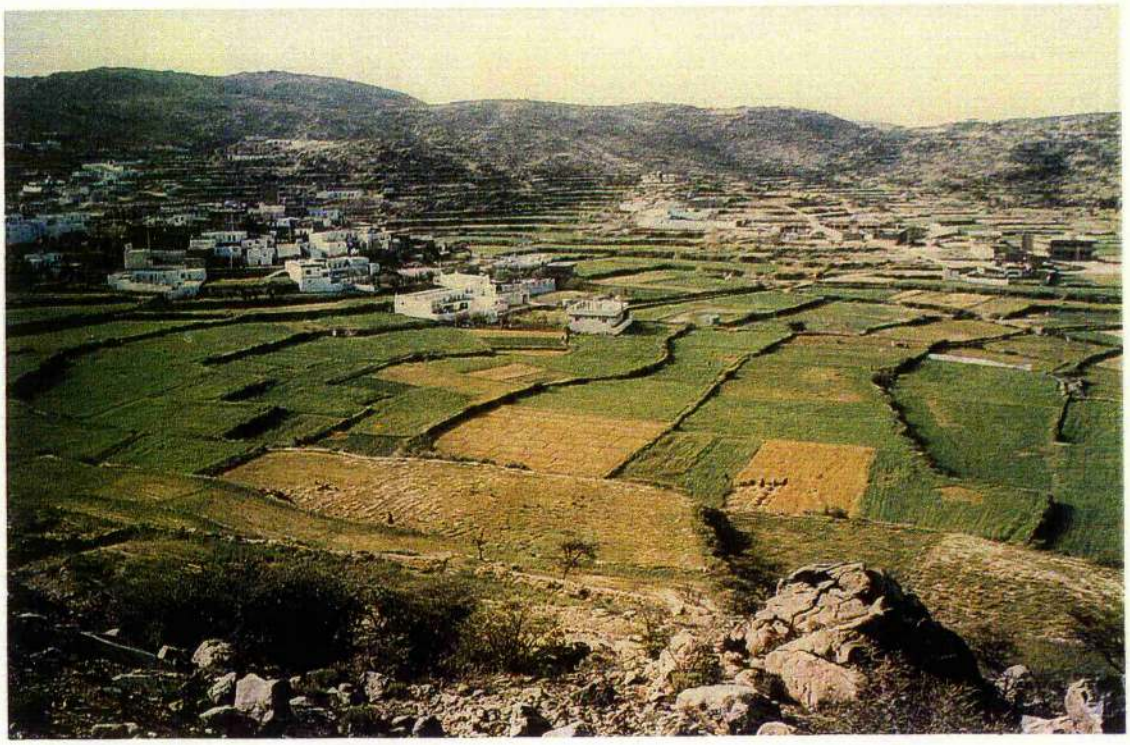

Declarations

I, **Saleh Amer S. Bajabaa**, hereby certify that this thesis, which is approximately **88000** words in length, has been written by me, that it is the record of work carried out by me and that it has not been submitted in any previous application for a higher degree.

date 26/6/1995 signature of candidate.

I was admitted as a research student in October 1988 and as a candidate for the degree of PhD. in September 1989; the higher study for which this is a record was carried out in the University of St. Andrews between October 1988 and June 1995.

date 26/6/1995 signature of candidate.

I hereby certify that the candidate has fulfilled the conditions of the Resolution and Regulations appropriate for the degree of PhD. in the University of St. Andrews and that the candidate is qualified to submit this thesis in application for that degree.

date..... signature of supervisor.....

I hereby certify that the candidate has fulfilled the conditions of the Resolution and Regulations appropriate for the degree of .PhD. in the University of St. Andrews and that the candidate is qualified to submit this thesis in application for that degree.

date..26.6.95 signature of supervisor.....

Copyright

In submitting this thesis to the University of St. Andrews I wish access to it to be subject to the following conditions: for a period of five years from the date of submission, the thesis shall be withheld from use;

I understand , however, that the title and abstract of the thesis will be published during this period of restricted access; and that after the expire of this period the thesis will be made available for use in accordance with the regulations of the University Library for the time being in force, subject to any copyright in the work not being affected thereby, and a copy of the work may be made and supplied to any bona fide library or research worker.

date 26/6/1995 signature of candidate.

DEDICATION

FOR..MY MOTHER S. BAJABAA AND IN MEMORY OF ..MY FATHER A. BAJABAA

ABSTRACT

WATER RESOURCES OF WADI SYSTEMS OF SOUTHERN SAUDI ARABIA

Saleh A. S. Bajabaa
University of St Andrews

This study is a water resources assessment of two wadi systems in the southern Arabian Shield using seismic refraction, electrical resistivity (VES) and borehole geophysical techniques, pumping tests and ground water quality data and an examination of artificial recharge. Wadi Baysh (flowing southwest to the Red Sea) and Wadi Habawnah (flowing east to the Rub Al Khali) have similar catchment areas (approximately 10000 km^2) and are underlain by igneous and metamorphic rocks but contrast in their hydrological cycles.

The mean annual rainfall of Wadi Baysh is 350 mm while Wadi Habawnah receives 150 mm. The mean annual water discharges of Wadi Baysh and Wadi Habawnah are 75 and 10 mcm respectively.

Hydrochemical classification, evolution of groundwater and its suitability for agricultural and domestic usage were studied in both wadis. In the upper and middle parts of both wadis the solute concentrations reach 1200 mg/l whereas in the lower parts solute concentrations range between 2000 and 3500 mg/l.

Both wadis show high average values of transmissivity and storativity determined from pumping tests and grain size analysis.

The geophysical surveys confirmed that the unconfined aquifer thickness is less than 42 m in both wadis. The seismic velocities of the aquifers range between 536 and 1817 m s^{-1} while the resistivities range between 23 and 125 ohm-m in both wadis. The igneous and metamorphic bedrock resistivity range between 3400 and 10260 ohm-m.

The sediment has a high potential for water supply in the middle and lower parts of both wadis.

The transverse resistance of the saturated part of the aquifers is used for correlation with the hydraulic transmissivity in which a computed empirical function may be applicable to similar aquifers in other Arabian Shield wadis.

This study introduces a plan for the surface and subsurface storage that should help to manage the perennial yield and minimise the mining yield. The analysis reveals that building small reservoirs in both wadis is economically justifiable.

ACKNOWLEDGEMENTS

The completion of this thesis would not have been possible without the help and guidance of many people.

The author is indebted to his thesis advisors, Professor John McManus, who visited the study area with the writer, and Dr Rob Duck who gave helpful advice, continuous effort and great encouragement during the study. They also critically reviewed the thesis and offered many suggestions.

Dr. J. Jarvis, Dr Andrew Black, Dr J Henderson, Mr R Batchelor contributed greatly by introducing the author to the Tektronix 4596 digitising tablet and 4051 computer, Uniras Program, Principal Component Package and Macintosh system respectively, and thanks are extended to them for their assistance.

I owe great thanks to my mother, brother and sister for their support and encouragement and during being abroad for their financial support during the year in which my scholarship was stopped.

My thanks and appreciation goes to my wife and children for their patience, love and support.

I want to express my appreciation to the Department of Hydrogeology representative, Dr A.S. Bazuhair and Dr M A Sharaf, and the Earth Science Faculty members represented by Mohammed Nasseef in King Abdulaziz University, who gave me more than one chance to complete my education.

Thanks go to Dr. Assad Mofti who gave permission for access to geochemistry lab for analysing water samples. Also thanks extended to Dr Talal Mokhtar for access to the resistivity and seismic equipment.

Thanks go to Dr Abdulaziz Radien and Dr Fawaz Zaker and Professor Zaki Shen for their suggestions and help during preparation for the field work and to the geophysics team, the drivers and the labourers for their help in the field.

Thanks and appreciation are extended to personnel of the Ministry of Agriculture and Water Resources in Riyadh, Saudi Arabia, especially Mohammed Al Fa'ar and Eyad Al-Khatib, Saleh Alshalan for providing the writer with valuable information

The writer is also pleased to express his sincere thanks to Mr Bin Mutlagah, the director of Najran branch of Ministry of agriculture and water resources and the Amir of Wadi Habawnah, Mr M Al-Kahatani for their help in providing the accommodation and their generous invitations during the field camps.

Thanks and appreciation are extended to personnel of the Educational Mission Of Saudi Arabia in London representative in Mr Abdullah Al Naser and Dr Kamal M Ali for their help and support during my education in St Andrews University.

My thanks goes to the University library staff particularly Miss S.G. Rowe, Mrs M Grundy and F.D. Story in the main library office and Mrs M.Sandeson of the Purdie Building library for their time and consideration.

My thanks go to Professor G. Whittington, Professor R. Hay, Dr WEStephens, Dr Bowden, Dr CH Donaldson, Dr GJH Oliver, Dr J. Kinnaird, Dr J. Baldwin, Mr A. Bahabri, Mr H. Alwashmi, Mrs F. McAndie, Mrs L. Young, Mr S Harvey, Mr A. Mackie, Mr A. Calder, Mr C. Cameron, Mr S. Allison, Mr A. Danby, Mr T. Clifford, Mr J Bews, Mr P. Pogorzetek and my friend and colleagues at the school of Geography and Geology and school of Chemistry with many of whom I had very constructive discussions.

I am grateful to my internal and external examiners who will spend their valuable time reading and examining this work.

I am also thankful to all persons who helped put this work in its present form especially Mrs R. McCormack, Mrs L. Stewart. and Ms. E. Martinez

I am sincerely thankful for my government represented by the King Abdulaziz University for granting me a scholarship for the PhD study and for generously financing this research.

CONTENTS

LIST OF FIGURES

LIST OF TABLES

LIST OF APPENDICES

CHAPTER ONE: INTRODUCTION

1.1 General Introduction

The southern part of the Asire region (Najran region and Tehamat Asir) of Saudi Arabia includes some of the best agricultural land in the country which produces quite a significant quantity of crops thereby playing a vital role in alleviating, in part, a serious food shortage in the Asir region. Although the rainfall is variable, it causes floods mostly in winter, spring, summer and autumn in Wadi Baysh and during the spring in Wadi Habawnah. The latter is an area that experiences monsoonal climatic conditions and suffers serious shortages of flood recharge during the summer period, due to prolonged dry conditions.

The study area (Figure 1.1) consists of Wadi Baysh and Wadi Habawnah. Both wadis contain ephemeral streams that originate in the Asir Mountains in the south west of Saudi Arabia.

Wadi Baysh is located within the area of lat. 17° 00' and 18° 00' N and long. 42° 00' and 43° 00'E and is partly bounded on the west by the Red Sea and on the east by Yemen Arab Republic. The major drainage pattern dominates the north and the north east part of the area and drains an area of 4987 km^2 towards the south west to the Red Sea . Altitude in the catchment area ranges from 5m close to the sea coast to 700m at the foothills and above 3000m in the Asir provinces.

Wadi Habawnah is in the extreme south eastern part of the Asir province, east of long. 43° 30' E and extends southwards from lat. 18° 15' to 17° 30' N. Wadi Habawnah flows in the eastern side towards the Rub Al Khali desert. Altitudes of the area range from about 1200m above sea level in the main channel of the wadi to more than 3000m in the Asir provinces. The catchment area is 4640 km^2.

The upper hard-rock area, which includes about 85% of the watershed of both wadis, is rugged mountainous terrain composed chiefly of igneous and metamorphic rocks and minor amounts of alluvial sediments. The lower alluvial area has little relief and is composed primarily of alluvium.

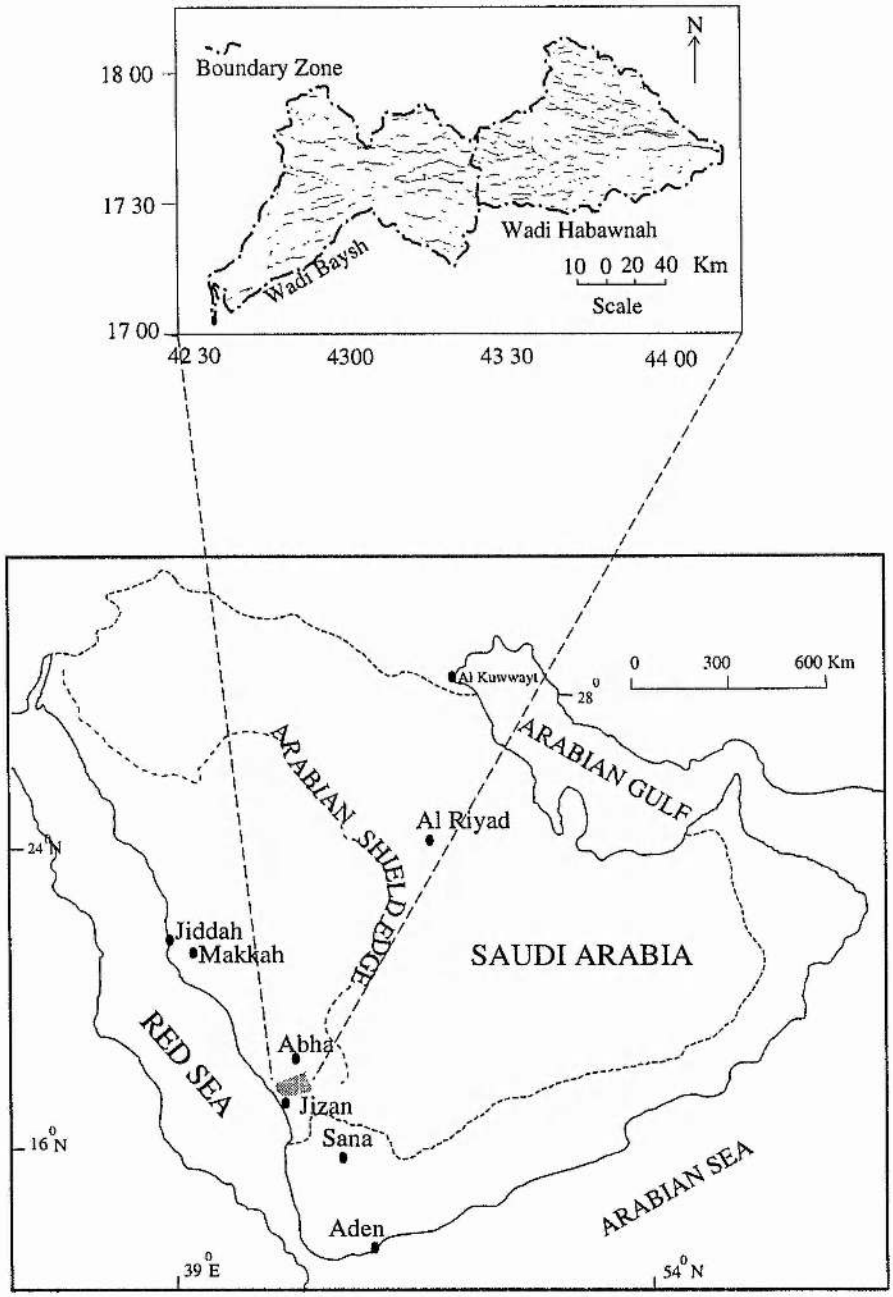

Figure 1.1 Map of Saudi Arabia showing the location of the study area (shaded).

The rainy season of the area is influenced by Mediterranean-type distribution and monsoonal type of rain. Both wadis show different rates of precipitation. Wadi Baysh has an annual rainfall which varies from 500 mm in the upper part of the catchment area to 100-150 mm in the coastal plain; while Wadi Habawnah has an average rainfall of about 150 mm per year.

Wadi Baysh and Wadi Habawnah were selected for the evaluation of the groundwater resources of the region. Both the quality and the effects of groundwater development have been taken into consideration. The aquifers of the study area differ from the upper part to the lower part of each wadi. In each case, major unconfined aquifers hold the principal groundwater resources of the area. The ground water resource is the only source of irrigation water to ensure normal crop production in Wadi Habawnah. However, in Wadi Baysh the farming community depends on floods for irrigation. Considerable volumes of ground water are currently withdrawn from underground storage. An important cause for concern in the area is the occurrence of poor quality ground water in the lower part of both wadis. All these background problems have encouraged the author to carry out a detailed hydrogeological study using the latest available conventional and selected numerical techniques to extract as much information as possible on groundwater availability. The purpose of the study is to evaluate the present state of ground water potential of these finite resources, to devise a possible solution as to how they can best be utilised for domestic use and irrigation, and to maximise their potability.

1.2 Previous Studies

Previous investigations in Wadi Baysh and Wadi Habawnah include 1: 500,000-scale reconnaissance mapping in the Asir province by the U. S. Geological Survey (Brown and Jackson, 1959). Wadi Baysh quadrangle was mapped at a scale of 1:100,000 by Anderson (1979) and Fairer (1982) and explanatory notes to the geological map of Wadi Baysh at 1:250,000 were prepared by Fairer (1985). Prospecting and stream sediment sampling in the western part of Wadi Habawnah were carried out by the Riofinex Geological Mission (1978), and Parker (1982). In 1985, Sable described the geological features of the area with reference to a 1:250,000 scale map.

A number of hydrological research activities have taken place in the Arabian Shield as regional studies since the early 1970s. The Ministry of Agriculture and Water Resources of Saudi Arabia (MAWR) has contracted projects of agricultural development in the Saudi Arabian shield to Italconsult, Sogriah, and McClaren companies (in 1967, 1968 and 1978 respectively) (El-Khatib 1980). El-Khatib (1980) published a book (Seven Green Spikes) providing a general view of the progress of agricultural development and the supply of domestic water in Saudi Arabia since 1973. Al-Jerash (1982), who studied rainfall-runoff relationships in south Saudi Arabia, found that the ratio of run-off to rainfall stands at an annual average of 0.44 for Wadi Baysh (and consequently on the western side of the main watershed of the Asir highland) and at 0.33 for the east-sloping Wadi Bishah. Alehaideb (1985) studied the precipitation distribution in the south west of Saudi Arabia.

Sorman and Abdurazzak (1987) undertook the regional analysis of flood characteristics for 18 wadis of the south-western region of Saudi Arabia which drain towards the Red Sea. The amount of surface runoff generated in this area is estimated to comprise 40% of the water resources for the entire country. The previous studies, did not fully encompass the scope of the present investigation. However Some investigators have worked on some of the indivisual concepts that can all be part of the data record. The literature relting to any particular topic is reviewed in its respecting chapters.

1.3 The Available Data

The available data can be summarised as follows:

1- Air photo at a scale of 1 : 1000000.

2- Topographic map at scales of 1: 50,000, 1 : 250,000 and 1: 500,000.

3- Landsat image (Path 179 and Row 048), date acquired Oct. 30,1975.

4- Preliminary landsat image map of the Asir Quadrangle at a scale of 1 : 500,000.

5- Geological map of Wadi Baysh quadrangle and Wadi Najran quadrangle with scales 1: 250,000 and 1: 500,000.

6- Rainfall-runoff and meteorological data were provided for different periods of records from the area.

7- Lithological descriptions for 11 core wells (drilled 1978) in the lower part of Wadi Baysh and 6 core wells in Wadi Habawnah. Well log records of seven geophysical logs and the grain size analysis data of seventy five core samples were provided by MAWR for the Wadi Baysh drilling wells.

1.4 Justification

From the above mentioned previous works one can see that some of the studies are now about 10 years old, and some of these were based on limited data concerning the climate, rainfall and evaporation.

Most of the ground water data, qualitative or quantitative measurements, were carried out during short periods of time providing very limited records. Today the conditions are different (i.e. new data and data processing methods have come into existence) and the data recording systems have long records of more than 15 years.

The south west region of Saudi Arabia is one of the fast developing areas and the need for water for different uses is increasing every day.

One of the challenging methods that has not yet been studied is the artificial recharge characteristics of the area. Recharge is an essential element in any ground water development and management plans, especially in an area where flash floods are the main resource for the ground water recovery.

Sedimentological parameters such as grain size and sorting have direct relationships with porosity and permeability of water bearing formations and consequently of well yield.

The internal relationship between the geological formation and groundwater quality is an important aspect that has been little considered in the area.

These investigations deal only with the principal wadi alluvium of the lower reaches of Wadi Baysh and Wadi Habawnah, with main channels of length 42 and 55 km respectively.

1.5 Scope and Objectives

The primary purpose of this study was to provide a comprehensive approach to evaluate the water resources in both wadis. The analyses comprise geology, hydrology,

hydrochemistry, ground water parameters, geophysics and the conjunctive use strategy. Consequently, this work involves the estimation of flood volumes produced from the watershed after effective rainfall. Since the resource of groundwater recharge in the wadis depends on direct recharge from rainfall as well as from floods during their flow over unsaturated zones, the purpose of the study is mainly to propose empirical approaches to estimate flood volumes and eventually ground water recharge. Furthermore, controlling the flood flow for a course of the artificial recharge of the aquifer would be a significant advance in developing the water resources of the area.

The analysis is limited to the shallow unconfined aquifers systems with the water table at shallow depths. The analytical approach assumes that the aquifer can be characterised as uniform, homogenous, already extensive and horizontal. Using the methods documented in this study, it should be possible for a designer to characterise the aquifer system, select appropriate hydraulic parameters and to implement the conjunctive use system in both wadis.

In this, the scope included :

1- Review present published literature

2- Review data collected by MAWR

3- Determine the aquifer parameters

4- Evaluate the ground water quality

5- Evaluate Rainfall-runoff distribution

6- Study thickness variations and characteristics of wadi floor sediments

7- Development of guidelines for planning a field investigation programme and presentation of a series of field methods

8- Presentation of case studies from other countries in the world for the evaluation and design of artificial recharge in the area

9- Preparation of this study to be used as a guide by evaluators and designers as a source of reference for water resources and artificial recharge feasibility for controlling water use in other wadis of Arabian Shield during periodic droughts.

1.6 Field Design

The entire research work was based firstly on the collection of pre-existing hydrogeological data and, secondly on subsequent field exploration and sampling carried out during two seasonal visits to the study area. The total time proposed for the field work A and B was 3 months each, divided into two periods. Field work periods A (13 May-28 July 1989), consisted of collecting data related to water quality, pumping test analyses, well inventories, aquifer volume evaluation, water balances, water level monitoring, and infiltration rates. The geophysical study (resistivity and seismic refraction) was carried out in the period of field work B, (14 December 1989 - 15 February 1990).

1.7 Utilisation

The results of this study will have its direct effects on development projects in the area. The author believes that using desalinated water as an alternative to increased water supply is costly; where the artificial recharge by controlling flood water would provide a greater recovery for the aquifer in the long term. The present study has also built a data base which will facilitate the subsequent monitoring of both surface and ground water activities in the area.

1.8 Thesis Structure

Chapter **one** presents a brief description of the background to this investigation, and Chapter **two** describes the geology and topography of the catchment areas of both wadis within the framework of groundwater exploration.

Chapter **three** describes the rainfall characteristics of both wadis and discusses the influence of elevation and the air mass systems affecting rainfall distribution. The magnitude of floods of varying recurrence intervals are also estimated.

In Chapter **four**, the water chemistry of both wadi is described. The groundwater quality for use as drinking water and for irrigation is evaluated.

In Chapter **five**, the characteristics of ground water flow, aquifer properties, their definitions and pumping test methods are outlined before accounts of the Papadopulos-Cooper method, the modified volumetric method, the Ferris method and the step draw

down method are given.

In Chapter **six**, the results of electrical resistivity and seismic refraction methods to determine aquifer thicknesses are evaluated. Aquifer geometry and water levels are determined.

In Chapter **seven**, the geoelectric studies for predicting aquifer properties are described. The relationships between the resistivity measurements and the permeability and transmissivity of the wadi floor sediments are developed.

Chapter **eight** discusses the geophysical logs of the wadi aquifers. The lithologies of the rocks penetrated by the wells permits identification of the aquifer types on the basis of their lithological characteristics. The second section deals with grain size analyses of 75 samples collected from different subsurface units in which the permeability and the transmissivity of the aquifers were determined using the Hazen method, the Masch and Denny method and pumping tests. Computations of ground water flows have been made. The geophysical logs of Self Potential, Normal Resistivity (long and short) and Natural Gamma Ray emission were used to determine the characteristics of the subsurface lithology in relation to the hydrogeological units of the aquifers. The Archie formula and electric conductivity data have been used to calculate the formation factors. The graphical relationships between the effective grain size, permeability and formation factors were determined for wadi floor sediments.

In Chapter **nine**, the artificial recharge feasibility is discussed based on the previous chapters, taking into consideration the conjunctive use for the groundwater development in the area.

Chapter **ten** is a general conclusion with further suggestions for water quality monitoring and the planning and development of water resources.

CHAPTER TWO: GEOLOGY

2.1 Introduction

The Arabian Peninsula has two main geological provinces, the Arabian Shield in the west and the Arabian Shelf in the east (Figure 2.1). The catchment areas of both wadis are located in the southwestern and southeastern part of the Arabian Shield.

Tertiary and Quaternary sediments and volcanics stretch from the margin of the Red Sea to the foothills of the Tehamt Asir. The Precambrian rocks of the Arabian Shield are locally covered by Palaeozoic and Mesozoic sedimentary rocks in addition to Tertiary and Quaternary of the volcanics and sediments.

Johnson *et al.*, (1987) believed that Arabian Shield, during late Precambrian times, was subjected to a complex process of microplate accretion. This process was dominated by Precambrian metavolcanic, metasedimentary and plutonic rocks. Each of the microplates was subjected to several cycles of metamorphism, tectonism and plutonism.

Stoeser and Camp (1985) defined five paleomicroplates characterised by ophiolitic associations along their accretionary boundaries (sutures). Figure 2.2 shows the paleomicroplate terranes as :

(1) The western part of the Arabian Shield divided into three intraoceanic island-arc terranes namely Midyan, Hijaz and Asir.

(2) The eastern part divided into two terranes namely Afif, having continental affinity, and Ar Rayn showing possible continental affinity terranes. Their accretionacy boundaries or sutures (the line of splitting) separating these terranes are divided into two types according to their genetic, island arc-island arc collisional sutures (Bir Umq and Yanbu) or island arc-continental collisional sutures (Nabitah and Al Amer).

Both wadi catchment areas are located in the Asir terrane and the Nabitah orogenic belt which extend to the Shield in Yemen (Republic of Yemen).

During the Oligocene, the Red Sea rift valley (Figure 2.1) began to open by rifting of the lithosphere and a drifting apart of the lithospheric plates (Arabian and

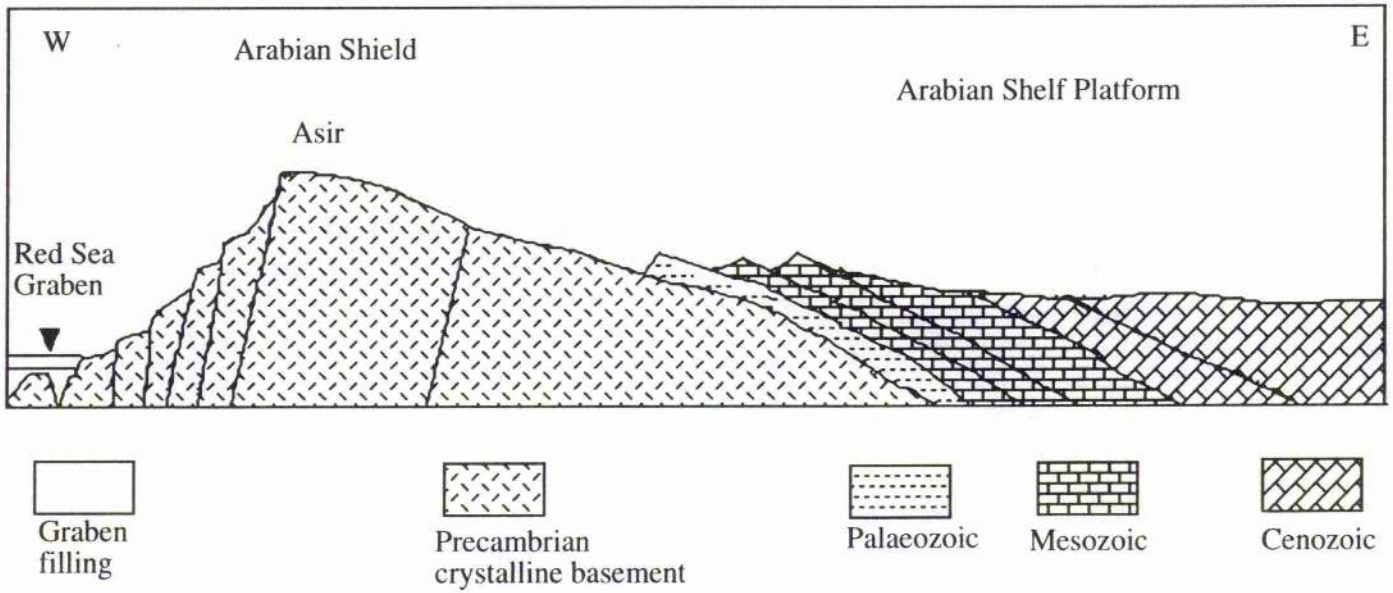

Figure 2.1 Geological cross section along the crystalline basement of the Arabian Peninsula showing the tilted position of the uplifted western part, where the Precambrian basement outcrops.

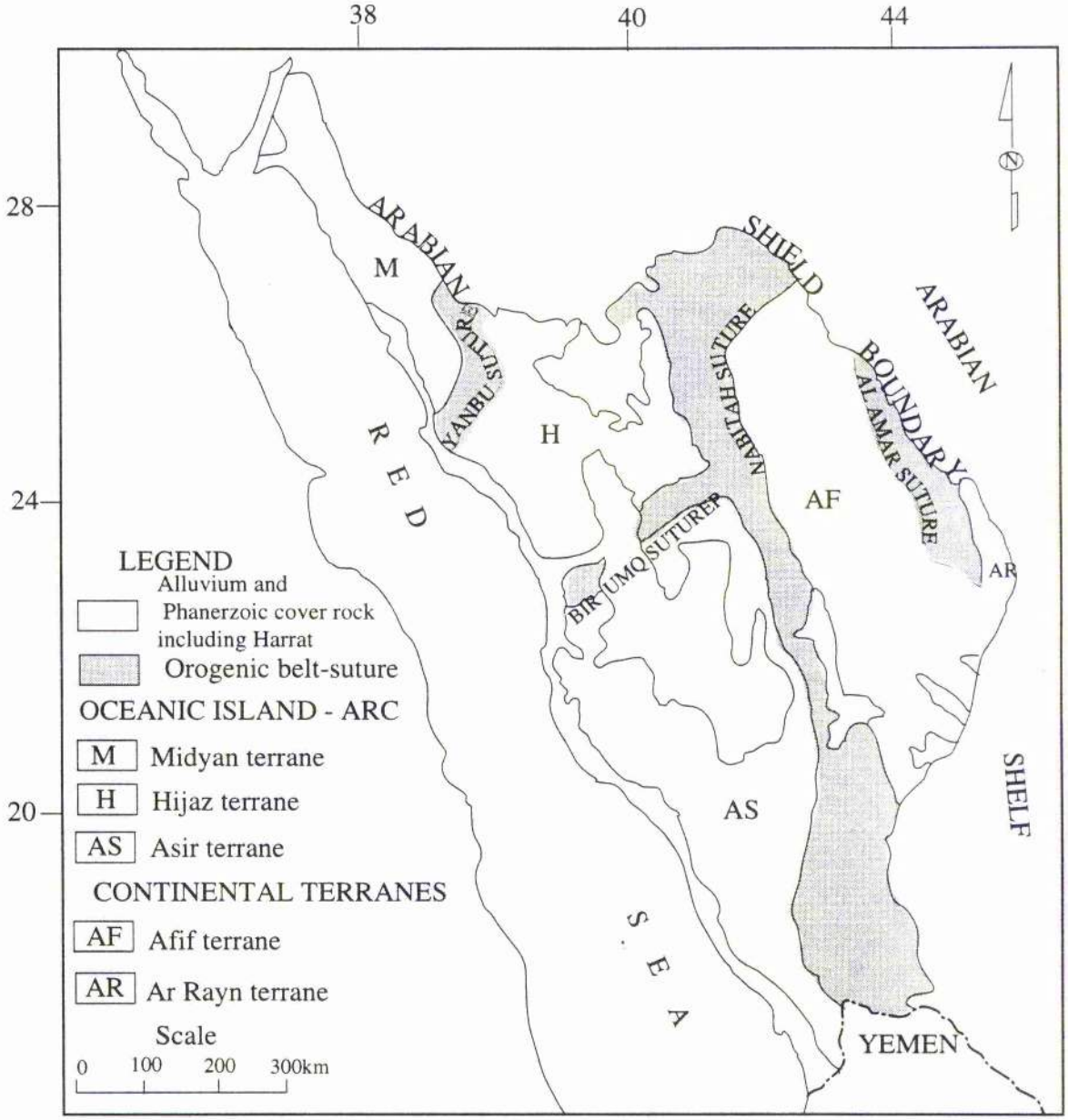

Figure 2.2 Map of the Arabian Shield illustrating the terranes and suture zones (modified from Stoeser and Camp, 1985).

Nubian shields) caused by the movement of rising oceanic crust which is still extending.

The physiography of the Arabian Shield is complex, resulting from an interplay between its tectonic and climatic histories. The Arabian Shield separation from the Nubian shield during the structural evolution of the Red Sea rift valley and the uplift along its western margin were the principal structural events forming the main physiographic features of the area. Brown (1960) indicated that the escarpment mountains and the development of the major wadi systems were related to uplift along the Red Sea margin and to a presumably more humid climate than at present.

The physiographic features of the study area comprise (from the west to the east) the Red Sea coastal lowlands (Tihamah Asir plain), through the entire Asir mountain belt and into the eastern margin of the Arabian Shield: (1) In the east is a major plateau forming a gently inclined eastward dipping peneplain. It is penetrated by west-east trending wadis such as the drainage system of Wadi Habawnah, which flows eastwards into the Al Rub Al-Khali desert. (2) The dissected Highlands, which form a narrow belt of strongly eroded terrane. In the north west, this zone reaches a peak of 3200m (MAWR, 1984). (3) The western scarp mountains form the western front of the dissected Highlands. They are underlain by the same facies as the Assarah Mountains. The scarp descends westward in a steep slope towards the Red Sea coastal plain. (4) The intermediate foothills zone is a gently sloping plain of low elevation which forms a transition between the coastal plain and the Assarah Mountains. These features are presented in general form in Figure 2.3. Further description of the topographic characteristics and description of the physiographic features will be given in the geological and geomorphological analysis below.

The geological map of the Wadi Baysh and Wadi Habawnah catchment areas (Figure 2.4) has been compiled from geological maps of scale 1: 250,000 of Wadi Baysh quadrangle (Fairer, 1985) and Wadi Najran quadrangle (Sable, 1985). The compilation was also aided significantly by using the available Landsat image data (scale 1: 250,000) and topographic maps (1: 250,000 and 1: 500,000) to determine the catchment area

Figure 2.3 Topographic model of Wadi Baysh (flowing toward the southwest) and Wadi Habawnah (flowing toward the east)

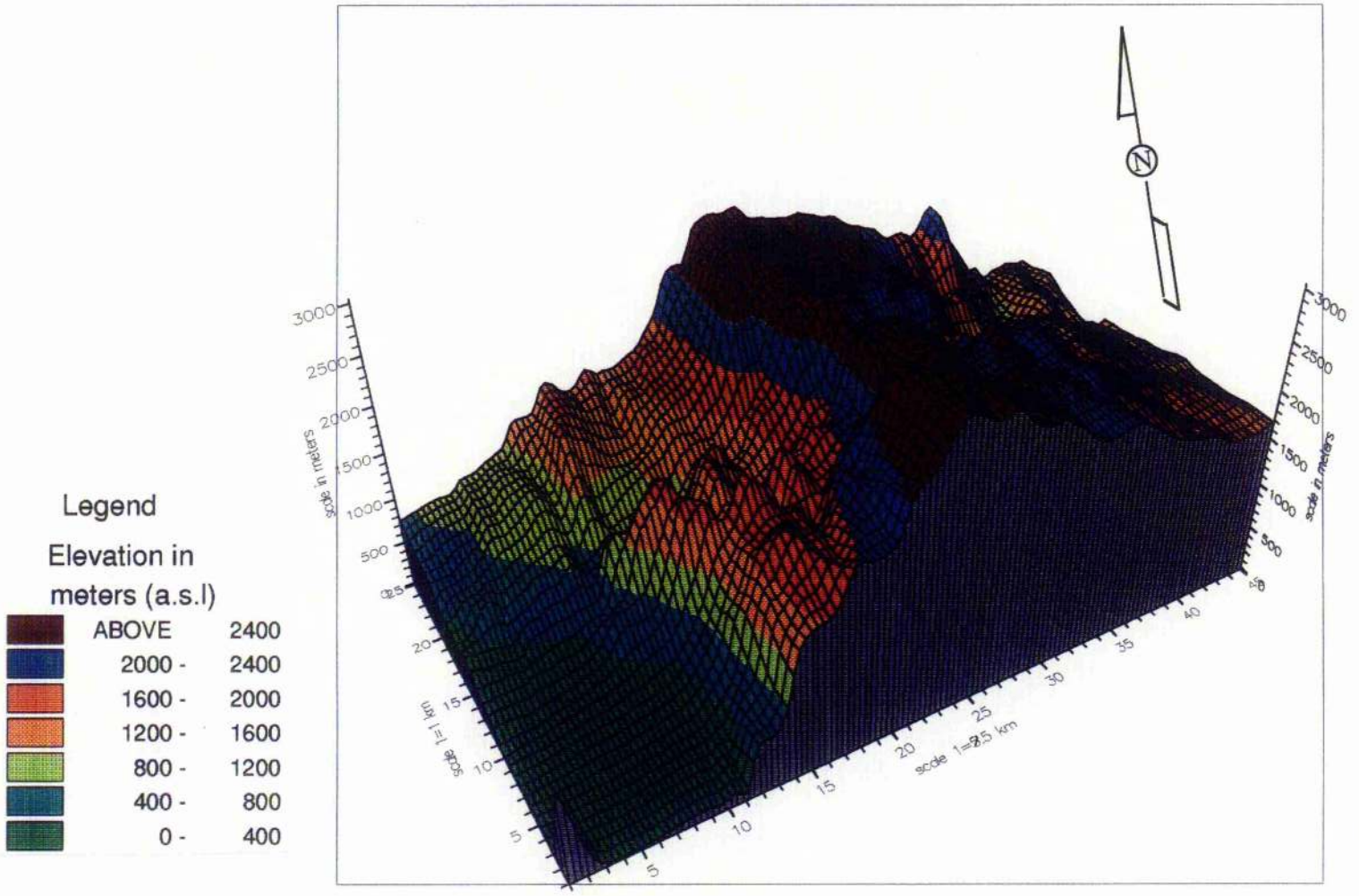

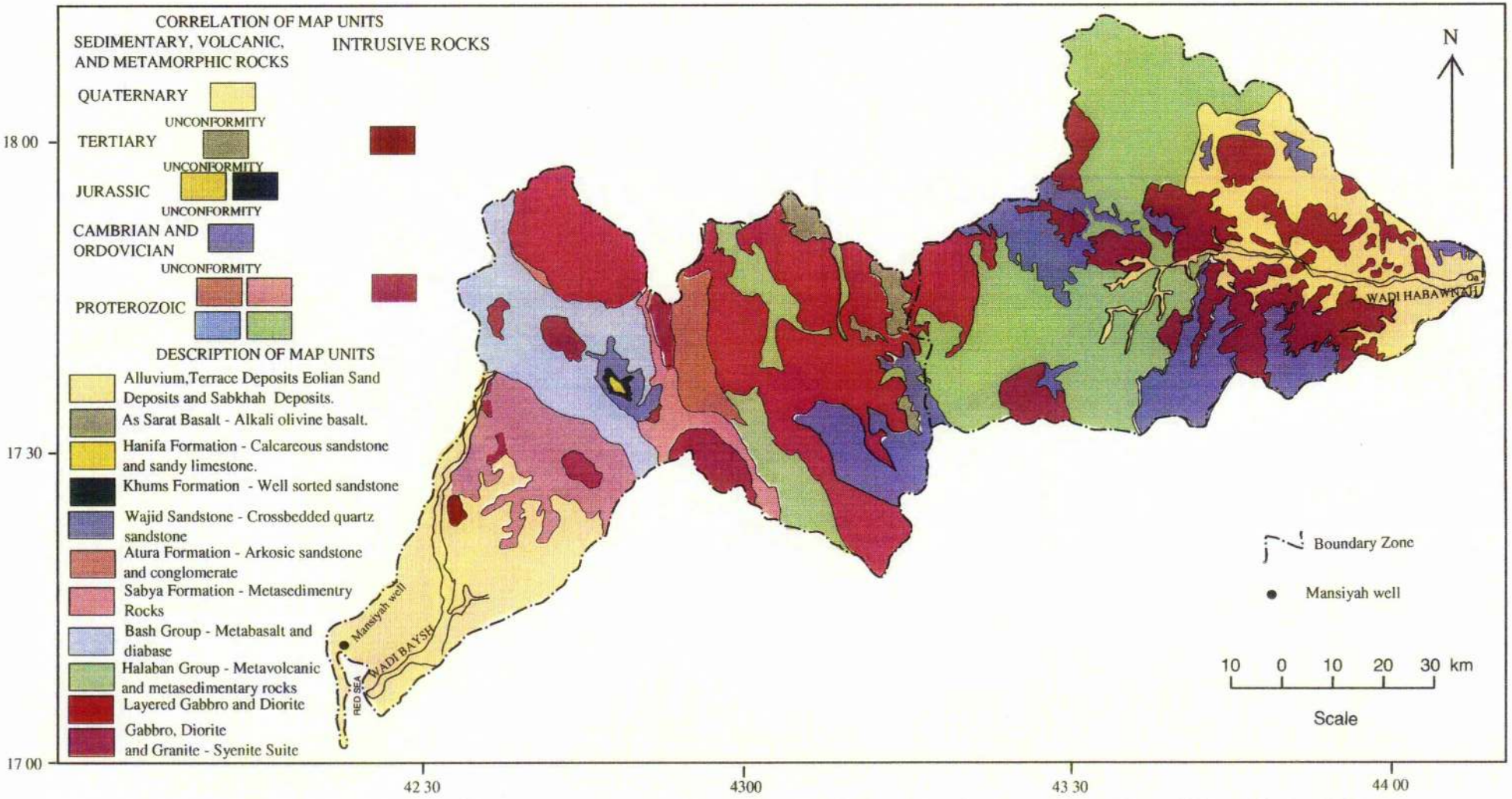

Figure 2.4 Geologic map of Wadi Baysh and Wadi Habawnah in the south of the Arabian Shield, Saudi Arabia (Adapted from Fairer, 1985 and Sable, 1985).

boundaries. Also a geological summary has been compiled to show the lithostratigraphic units (Figure 2.4) and the structural provinces (Figure 2.5) of the area. The stratigraphies given by Sable (1985) and Fairer (1985) are allocated different colour units on the map. The upper catchment area of Wadi Baysh and Wadi Habawnah are of Proterozoic volcanic and sedimentary rocks, intruded by plutonic rocks. These are overlain by Palaeozoic and Mesozoic sedimentary rocks as well as Tertiary and Holocene sedimentary and volcanic rocks. All geological investigations represented in this study have been carried out within the framework of ground water exploration.

2.2 Geology

The geology of the area will be discussed as a two main sections, the upper hard-rock area and the lower alluvial area.

2.2.1 The Consolidated Rocks of the Uplands

The upper hard-rock area forms a rugged mountainous terrain that has great relief and steep slopes. The average gradient of Wadi Baysh through this area is 20 m/km while in Wadi Habawnah it is 12 m/km.

Precambrian rocks outcrop in most part of the study catchment areas and form the hill pediment of the Asir mountains. The two catchments have essentially similar geological components, although detail varies from site to site. The basal Proterozoic layered gneisses of sedimentary and volcanic origin are intruded by sequences of later Proterozoic igneous masses varying from early tonalite-diorites to later granites and granodiorites. The Precambrian basement is overlain unconformably by the sub-horizontal Wajid Sandstone of Cambro-Ordovician age. This is a thin unit which is covered paraconformably by Jurassic sediments. Lateritisation of all pre-existing units preceded Tertiary volcanic activity which gave rise to basaltic flows and ash horizons principally in the Wadi Baysh catchment area. Small discontinuous deposits of unconsolidated Quaternary alluvium are found along the main wadi channel of the upper catchment area. Brief descriptions of the main lithological units are given below in chronological order.

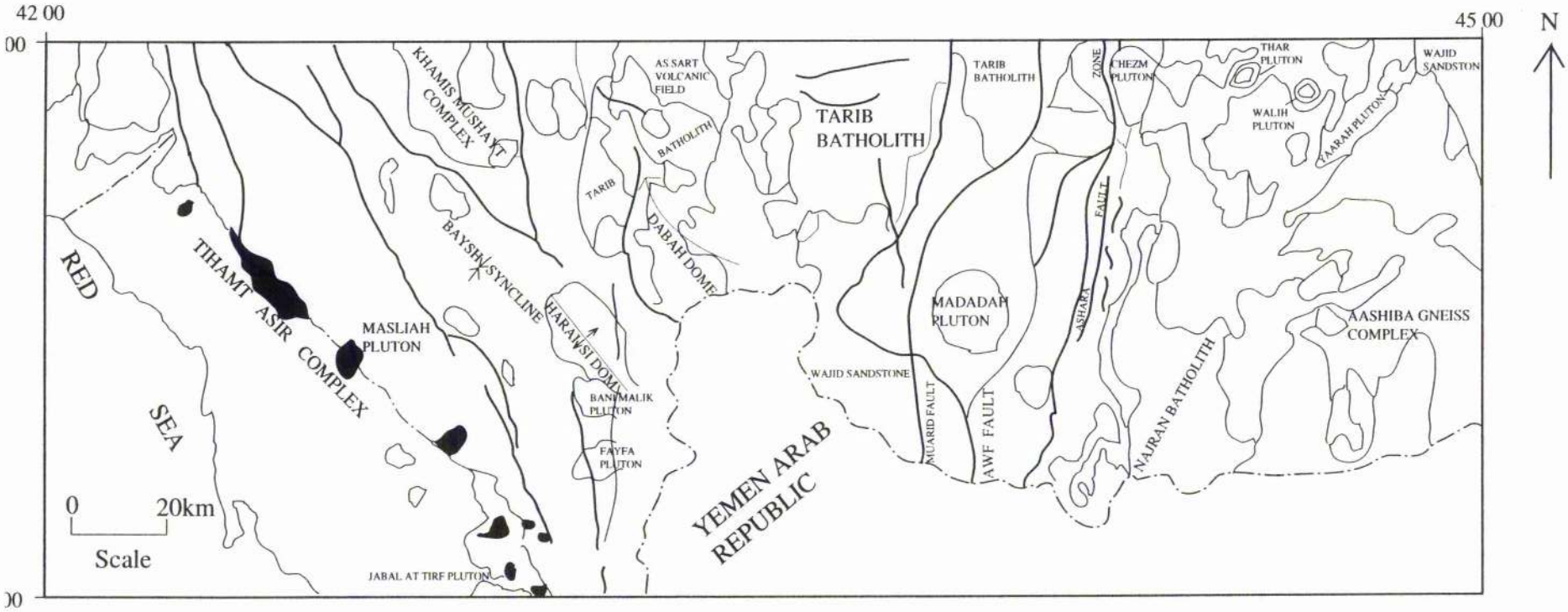

Figure 2.5 Structure sketchal map of Wadi Baysh and Wadi Habawnah to show the location of major intrusive rocks and the fault zones of the area (simplified and compiled from Wadi Baysh quadrangle by Fairer, 1985 and Wadi Habawnah quadrangle by Sable, 1985).

2.2.1.1 Proterozoic Sedimentary, Volcanic and Metamorphic Rocks

2.2.1.1.1 Sabya Formation

Generally, the Sabya Formation can be considered as sequence of sedimentary rocks that were deposited in a basin bounded by the African craton to the southwest and the early Arabian arc to the northeast (Fairer, 1985).

The Sabya Formation is of meta sedimentary rocks that include quartzite quartz-pebble conglomerate, argillite, limestone, and greywacke, widely converted to micaceous schist. The entire Formation has been effected by regional metamorphism to amphibolite and granulite facies. The most common rock of the Sabya Formation is quartz-sericite schist see (Figure 2.6). The base of the Sabya Formation is not exposed. The upper contact of the Sabya Formation with the overlying Baysh Group is sheared almost everywhere. According to Fairer (1985), where the contact is undeformed, it is marked by basaltic lapilli tuff resting conformably on quartz-sericitic schist. The tuff is overlain by basalt flows and pillow basalts of the Baysh Group. As shown in Figure 2.4, the Sabya Formation is located in the south west of the area but is absent in the east

2.2.1.1.2 Baysh Group

The Baysh Group was originally named the Baysh greenstone by Brown and Jackson (1959) to describe metabsalt and diabase that are well exposed along the course of Wadi Baysh. The Baysh Group occurs interbeded with the Sabya Formation.

Fairer (1982) reported that The Baysh Group consists mainly of a thick sequence of basaltic flows and spilitic pillow basalts intercalated with minor discontinuous beds of metagreywacke, metachert, schist, and marble. The Baysh Group occupies the centre of the northwestern area as a plunging syncline (Baysh syncline, Figure 2.5). In the study area, the Baysh Group is exposed as greenschist-facie rocks. Fairer (1985) pointed out that, on the eastern limb of the Baysh syncline, the contact with the underlying Sabya Formation is conformable but commonly shows bedding plane shearing.

Figure 2.6 Sabya Formation (mainly sericite schist) rocks with vertical slope located about 9km northeast of Misliyah. Along the right bank of Wadi Baysh, the terraces are mainly of sand supporting luxuriant growth of Hyphaen (Doom).

2.2.1.1.3 Halaban Group

The Halaban Group consists of a metavolcanic unit and metasedimentary unit. The metavolcanic unit consists of basalt flows, pillow lavas, andesitic and dacitic pyroclastic rocks. It outcrops in the northeast of Wadi Baysh, where the rocks are generally massive and are metamorphosed to an assemblage of greenschist, amphibolite or hornblende-hornfels facies. The metasedimentary unit is composed of greywackes and siltstones derived largely from volcanic rocks. They have a moderate to strong cleavage and schistosity and are metamorphosed to greenschist and amphibolite facies (Greenwood, 1985). They are preserved in two major blocks that extend south into the east centre of the upper part of the Wadi Baysh catchment area. However in the western side of the upper part of Wadi Habawnah, the Halaban Group refers to the belt of rocks along the Ashara fault zone (Figure 2.5). Most of Halaban Group is dominated by meta andesite and meta basalt.

Meta sedimentary rocks form several north-trending belts east of the Hadadah pluton (Figure 2.5). The unit consists of fine grained schist or slate to meta greywacke.

Sable (1985) suggested that the great thickness of Halaban Group (as much as several kilometres) indicates deposition and emplacement in a sinking trough, possibly on the flank of an island arc.

2.2.1.1.4 Atura Formation

The Atura Formation is a thick, north-trending sequence of predominantly sedimentary strata metamorphosed to greenschist and amphibolite facies (Figure 2.4). It consists mainly of metamorphosed arkosic sandstone, polymictic conglomerate and diamictite (poorly sorted and containing a wide range of particle sizes in a mud matrix). The unit is several kilometres thick, but the true thickness is unknown due to internal deformation and erosion of its uppermost part (Anderson 1979). The base of the Atura Formation is well exposed as the unconformable contact between it and the underlying plutonic rocks of the Tarib batholith. In Wadi Habawnah this Formation is not present (see Figure 2.4).

2.2.1.2 Proterozoic Intrusive Rocks

Proterozoic intrusive rocks (Figures 2.4 and 2.5) dominate the upper parts of Wadi Baysh and most of the Wadi Habawnah area. They consist of plutonic and hypabyssal igneous rocks which range from gabbro to alaskite in composition.

2.2.1.2.1 Proterozoic Intrusive Rocks of the Wadi Baysh Area

Fairer (1985) interpreted the Proterozoic intrusive rocks of Wadi Baysh area as forming major igneous suites as follows:

2.2.1.2.1.1 Gabbro - Diorite Suite

The oldest rocks believed to be contemporaneous with Baysh Group layered rocks, this suite consists of numerous thin sheets of gabbro and minor bodies of granodiorite in the upper part of the Sabya Formation as hypabyssal sills that are coeval with the Baysh basalt. Also it occurs as pyritiferous diorite (fine to medium-grained diorite) along the eastern border of the Wadi Baysh catchment area.

2.2.1.2.1.2 Tonalite - Diorite Suite

The Tonalite - Diorite Suite postdates the Halaban Group layered rocks which are represented in the study area by rocks of the Tarib batholith (Figure 2.5). Also it occurs on the west and northwest side of the Wadi Baysh catchment area, adjacent to the Daba'ah dome (Figures 2.4 and 2.5). In Wadi Habawnah, the tonalite-diorite suite dominates the western sectors of the catchment.

2.2.1.2.1.3 Granodiorite - Granite Suite

The suite consists of intermediate to felsic rocks, characterised by strong internal foliation. It has two major units:

a - Foliated granite rocks are exposed in the Hairis dome and in the Shada pluton to the southeast (Figure 2.5).

b - The Khamis Mushayt complex consists mainly of granodiorite gneiss. Structural features show that the dome deformed the overlying rocks of the Sabya Formation and Baysh Group along its western margin. The Sabya Formation is extensively

sheared and tectonically thinned between the Khamis Mushayt complex and the Baysh Group (see Figures 2.4 and 2.5).

2.2.1.2.1.4 Granite - Syenite Suite

Fairer (1985) indicated that rocks in the granite syenite suite forms subcircular pluton that cut most Proterozoic structures. The suite of rocks consists of diorite in the Raha pluton (Figure 2.5) and syenite in Jabal Fayfa and Jabal Bani Malik. Monzogranite occurs in two bodies that intrude the Khamis Mushat complex and the Autra Formation. The monzogranite forms discordant circular to subcircular plutons as large as 150 km^2 (Fairer, 1985), sheeted to lenticular bodies, and ring dykes. The pluton intrudes the Baysh Formation and the Sabya Formation as the Shadan pluton (Figures 2.4 and 2.5).

2.2.1.2.2 Proterozoic Intrusive Rocks of the Wadi Habawnah Area

Proterozoic intrusive rocks in the Wadi Habawnah catchment area are summarised on the basis of the Sable (1985) description as three major suites of plutonic and hypabyassal intrusive rocks, all of which are interpreted as postdating the Halaban Group.

2.2.1.2.2.1 Tonalite - Diorite Suite

Tonalite - Diorite Suite, containing metadiorite and metagabbro, biotite-hornblende tonalite, biotite tonalite and metadiabase, forms the southernmost part of the Tarib batholith (Figures 2.4 and 2.5) in the western part of Wadi Habawnah.

2.2.1.2.2.2 Tonalite - Granite Suite

The Tonalite - Granite Suite consists of a wide variety of plutonic rocks of the Aashiba gneiss complex in the southwest (Figure 2.5). In the Hadadah pluton this suite is exposed as granodiorite tonalite gabbro and diorite. Altered and unaltered rocks underlie a large area in the eastern part of Wadi Habawnah and diorite forms the Tary plutons in the western part of Wadi Habawnah (Figure 2.5).

2.2.1.2.2.3 Granite - Syenite Suite

The Granite - Syenite Suite is widespread and is particularly abundant east of the Ashara fault zone. In the Najran Batholith in the southern area it occurs in irregular, sheet form, and subcircular to ovoid bodies (Figure 2.5).

2.2.1.3 Palaeozoic and Mesozoic Rocks

2.2.1.3.1 Wajid Sandstone

The Wajid Sandstone is Ordovician and Cambrian in age (Powers *et al.*, 1966). It is about 395m thick at Jabal Abu Hassan in Wadi Baysh (Figures 2.4 and 2.5), (Fairer, 1982). McKee (1963) indicated the Wajid Sandstone is an erosional remnant of a Nubian Sandstone blanket. It rests unconformably on Proterozoic metamorphic and plutonic rocks. In the Wadi Habawnah area, it is exposed in the northwestern, central, and northeastern parts of the catchment. The northeastern exposures are part of an extensive blanket of strata that dip gently east under Quaternary deposits in the Al Rub Al Khali basin. The Wajid Sandstone overlies a nearly planar unconformity on Proterozoic rocks. It is computed of mostly grey to red quartz arenite, which is coarse grained and moderately well sorted. Cross bedding is common. The ferruginous cement which typifies the upper part of the Wajid Sandstone is characteristic in the lower part of Wadi Habawnah. Tabular and trough cross beds are characteristic; foreset beds dip northwards over a large area (Sable, 1982). The thickest erosional remnants of the Wajid Sandstone range from about 135 to 270 m in Wadi Habawnah (see Figure 2.7a), (Sable, 1982). However, the Wajid sandstone is exposed in Habawnah town as small remnants with thicknesses of about 7m while at the Hausaniah village (about 53km to the east of Habawnah town) the Wajid Sandstone is 35m in thickness (Figure 2.7b).

2.2.1.3.2 Khums Formation

The Khums Formation is Jurassic in age (Brown and Jackson, 1959) and rests upon the Wajid Sandstone paraconformably at Jabal Abu Hassan (Fairer, 1982). It is composed of white to buff coloured, medium-grained, well sorted quartz sandstone which contains rounded quartz pebbles and commonly has a ferruginous cement. However, in the

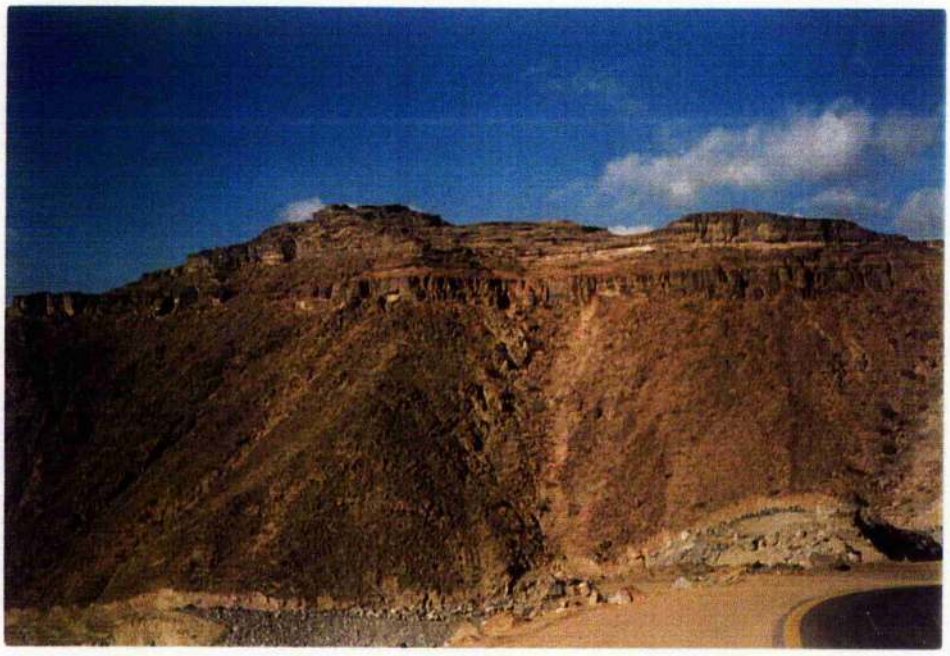

Figure 2.7a View of the Wajid Sandstone with ferruginous cement capping plutonic rocks (mainly granite) and displaying slope and feeder-channel characteristics, 20km northwest of Al-Magma village, Wadi Habawnah.

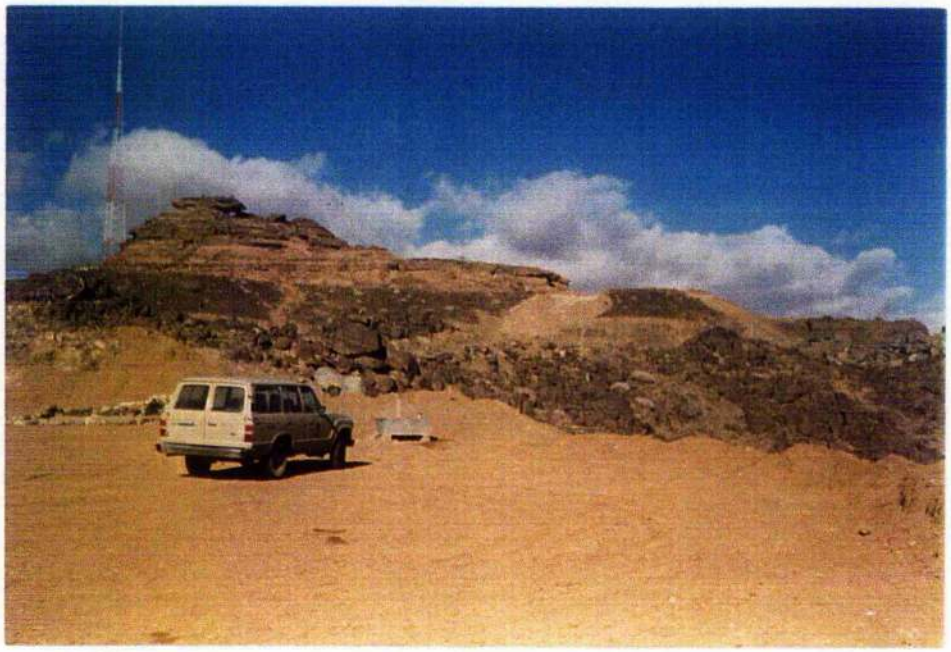

Figure 2.7b Outcrop of approximately 35m of Upper Wajid Sandstone east of Hausaniah village (about 55 km to the east of Habawnah town on the left bank of Wadi Habawnah).

Wadi Habawnah area this formation is absent (Figure 2.4).

2.2.1.3.3 Hanifa Formation

The principal components of the Hanifa Formation are fossiliferous limey sandstones and sandy limestones mapped as 'calcareous rocks' by Anderson (1979). It rests upon the Khums Formation paraconformably at Jabal Abu Hassan (Fairer, 1982) in the centre of the Wadi Baysh area, while it is not present in Wadi Habawnah (see Figure 2.4).

2.2.1.4 Tertiary Rocks

2.2.1.4.1 As Sarat Basalt

The As Sarat Basalt is flat lying and grey to black in colour. More than 20 basalt flows, with an aggregate thickness of about 600 m, are exposed on a deeply dissected ridge to the north and northeastern side of Wadi Baysh (Figure 2.4) (Fairer, 1985). They range from mainly alkali picrite through alkali olivine basalt to hawaiite. Most of the basalts are fairly dense and non-vesicular (Colman *et al.*, 1977).

2.2.1.4.2 Tihamah Asir Complex

The Tihamah Asir Complex is exposed in the Tihamah Province (coastal plain) (Figure 2.4 and 2.5). The Tihamah Asir Complex is of granophyric rocks which form isolated hills surrounded or capped by Quaternary basalt. They are of a medium to fine grained quartz monzogabbro which has an age of 21 Ma at Misliyah (Gettings and Stoeser, 1981). Layered gabbro, and diorite crop out in the Misliyah and Jabal at Tirf plutons (Figure 2.5). Colman *et al.* (1979) indicated that the rocks of the Jabal at Tirf were emplaced during the Middle Miocene near the end of the initial phase of spreading along the Red Sea rift.

2.2.1.4.3 Tihamah Asir Deposits

Due to structure development as a result of the opening of the Red Sea graben, the facial character of the Tihamah Asir Tertiary deposits varies greatly. Brown *et al.* (1959) indicated that, during late Miocene, the deposition of the Baid Formation occurred. It contains a large volume of tuffaceous material originating from volcanic activity associated with Tertiary tectonic movements. However, in the Wadi Baysh area there is no surface outcrop of this formation. In the coastal area, Mansiyah Well No. 1 penetrated a thick continental series, underlain by massive salt sequences and finally marine clastic deposits. Gillmann (1968) indicated that this well (Figure 2.4) penetrated about 4000m of the Baid Formation (see Figure 2.8). He summarised the lithological features of the sequence as: 0 to 171m sandy limestone with minor sandstone or clay layers; 171 to 999m "Upper Continental Member" red shale with metamorphic and volcanic rock pebbles; 999 to 1250m " Middle continental member" red shale with thin dolomite and anhydrite beds; 1250 to 2230m "Lower continental member" red shale with sandstone and conglomerate; 2230 to 3472m Evaporite series (halite) with rare anhydrite layers; 3472 to 3992m infra evaporitic series, grey shale with conglomerate, silt and grey, fine-grained sandstone.

Intensive tectonic movements between the end of Miocene and the Pleistocene have produced large quantities of clastic material in the rift zone which covered the Tihamah plain from the foothills to the coast (Brown *et al.*, 1959).

2.2.2 Unconsolidated Alluvia of the Wadi Floors

In sharp contrast to the upper hard-rock area, the lower alluvial area has little relief and gentle slopes. The channels of both wadis have average gradients of about 4m/km.

The lower alluvial area is underlain chiefly by poorly consolidated alluvial deposits, which are Quaternary in age. These deposits unconformably overlie metamorphic or granite and related crystalline rocks. Wadi alluvium occupies the beds of all major wadis. It consists of silt, sand, gravel and boulders, and is unconsolidated, poorly sorted and more or less stratified. Figures 2.9a and b show the wadi channels and flood plains of both wadis. Based on the borehole data, the wadi alluvium shows variations in thickness

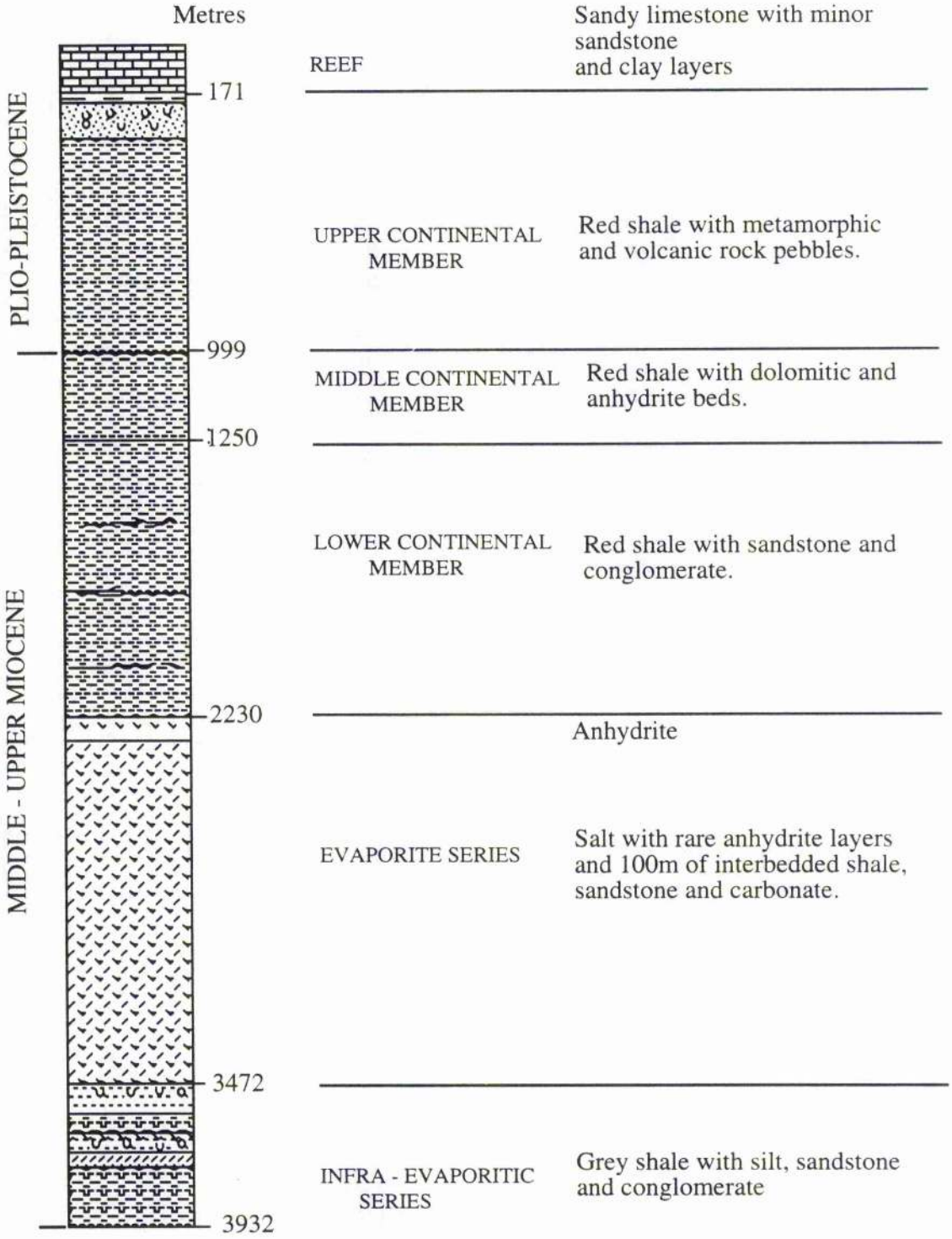

Figure 2.8 Stratigraphic section of eastern Red Sea coast (Mansiyah Well No. 1 after Gillmann, 1968).

A

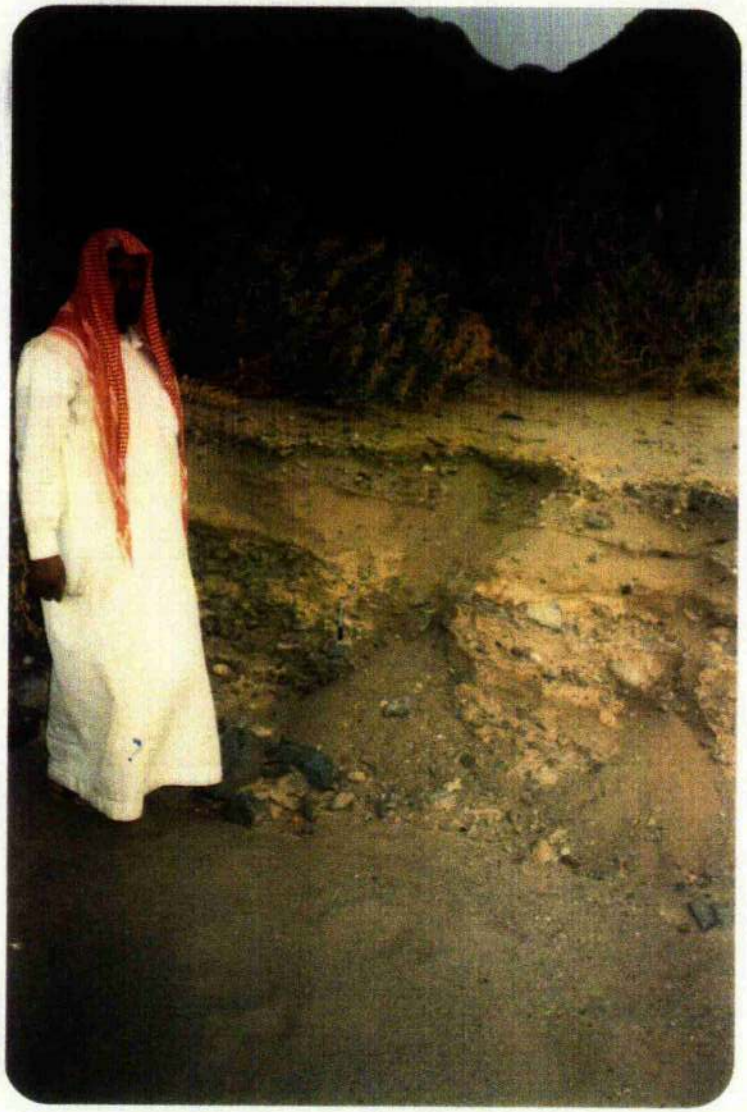

B

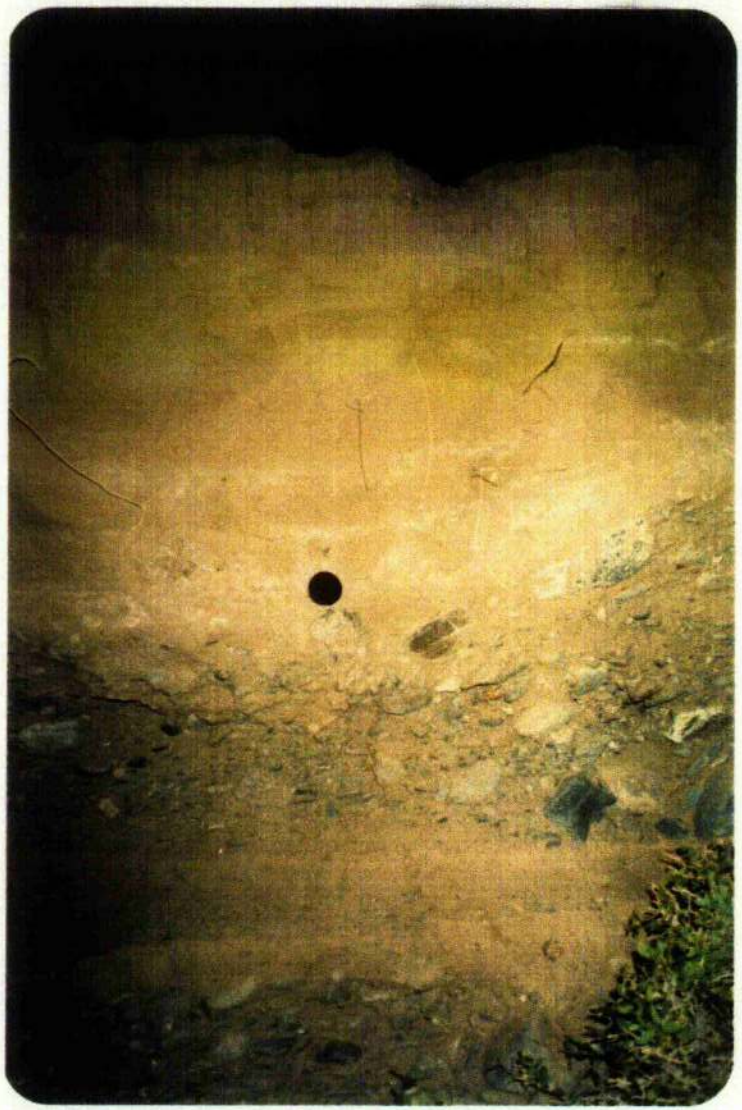

Figures 2.9 Typical sequences of flood plain stratigraphy in Wadi Habawnah (a) and Wadi Baysh (b). The lower part of each section is composed of coarse grained deposits overlain by silt .

from 13m to 20m near Misliyah village in Wadi Baysh and at Habawnah town in Wadi Habawnah (a more detailed description will be given in Chapters 6 and 8).

The alluvial terrace deposits which cross the west side of the area consist mainly of sand, cobbles and gravel and have been not disturbed by farming. These older terraces are flat and support only sparse vegetation (see Figure 2.10). They are thought to be Pleistocene in age (Muller, 1977). Thin terrace gravel of Quaternary age unconformably overlie the unconsolidated alluvium in both wadis.

The broad flat channels and plains of Wadi Habawnah and Wadi Baysh (Figure 2.11 a and b) are underlain by as much as 150 and 50m respectively of unconsolidated Quaternary alluvium which consists of gravel, sand and clay. The unconsolidated alluvium of Wadi Baysh was deposited in the Tihamah plain (the Tihamah plain belongs to the eastern margin of the Red Sea rift valley), while in Wadi Habawnah it was deposited in a channel cut into the crystalline rocks on the eastern part of the lower alluvial area. The subsurface lithology of the Quaternary deposits of both wadis will be examined further in Chapters 6 and 8.

Sabkhah deposits covered by a thin layer of saline, sandy mud are present on the coast in the southwest corner of the Wadi Baysh area and in Wadi Habawnah near the Empty Quarter desert (see Figure 2.12a). Where separated from the Red Sea by beach dunes, white crusts of salt cover the saturated mud.

Eolian and alluvial sand areas are present along the coast and inland in the lower part of the Baysh plain. The eolian deposit is large enough to be easily recognised (Figure 2.12a). It acts as a barrier for water flow in the wadi channel. Reworked alluvium extends over large areas on the western side of the plain. It contains cobbles, sand and derived from alluvial terrace deposits and from overbank deposits of the present drainage.

In Wadi Habawnah, the eolian sand deposits overlie gravel plain deposits and show dunes that trend generally northwest. The linear sand dune deposits include active

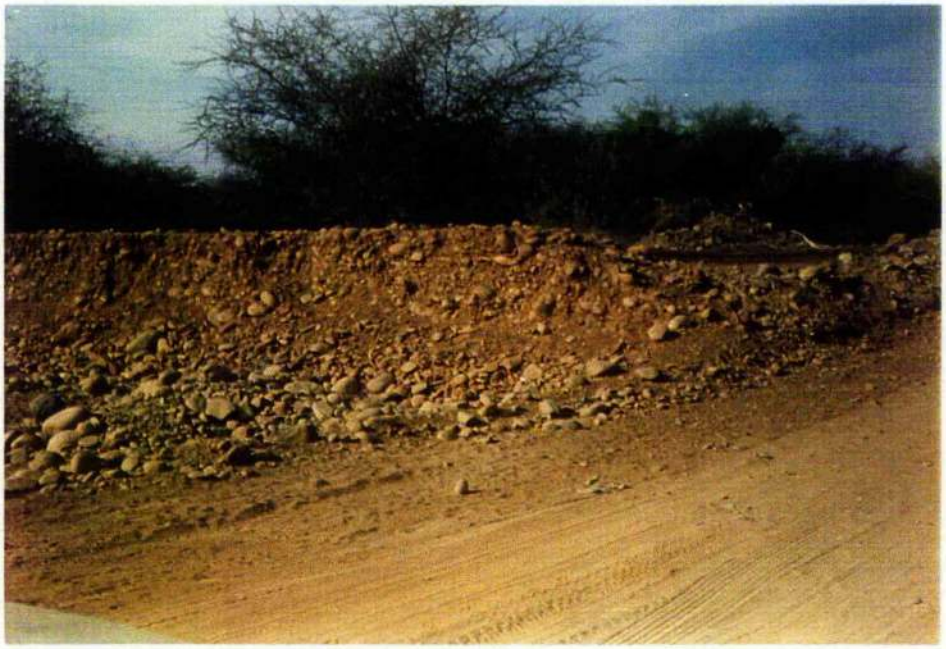

Figure 2.10 Photograph of an alluvial terrace (2km north of Mysliah) along the right bank of Wadi Baysh. The thin light coloured layer at the top represents a thin layer of recent material (gravel and sand) while the reddish colour represents the weathered gravels and boulders. The area has many species of Acacia trees (Salam).

A

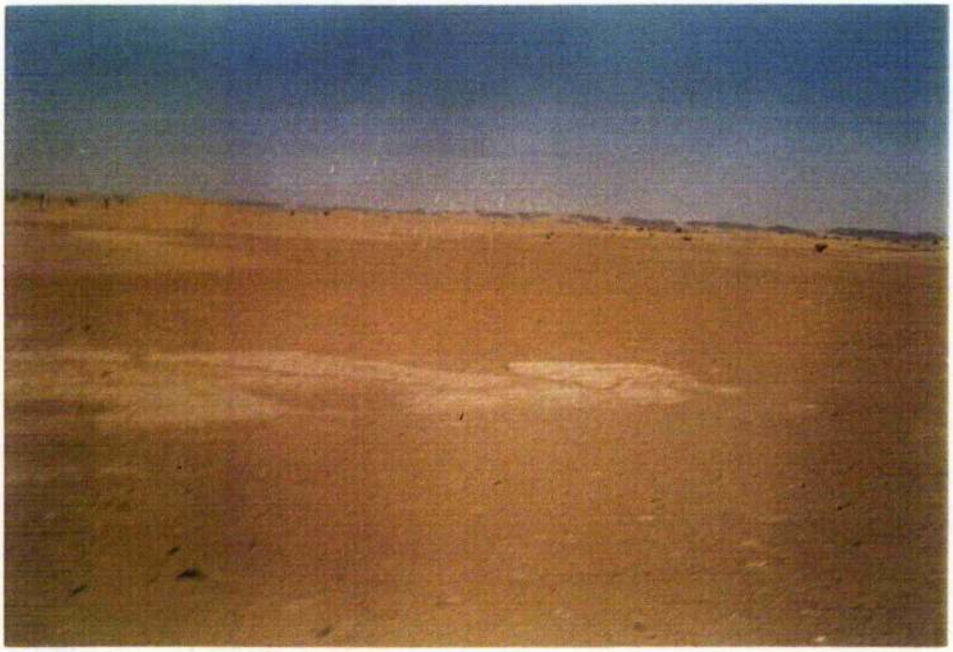

B

Figures 2.11 Sandy ephemeral wadis showing great width and planar channels, (a) Wadi Habawnah and (b)Wadi Baysh.
(a) a sheet of calcite deflated from occasionally surrounding Sabkhah. As sand is removed by wind, the Sabkhah becomes exposed to the surface. (b) residual runoff southwest of Misliyah one day after flood in December, 1989. This part of the wadi and the area above supports a luxuriant growth of Hyphaen (Doom) along the wadi bank.

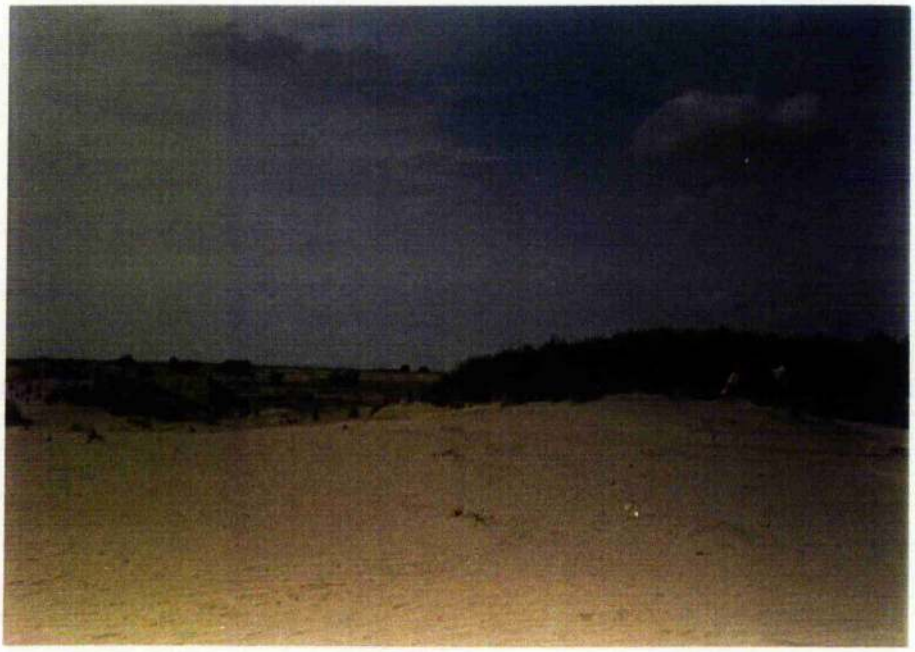

Figure 2.12a Eolian deposits on the high river terraces of Wadi Baysh (17km southwest Misliyah village) with some natural tree vegetation, mainly of Salvadora (Arak).

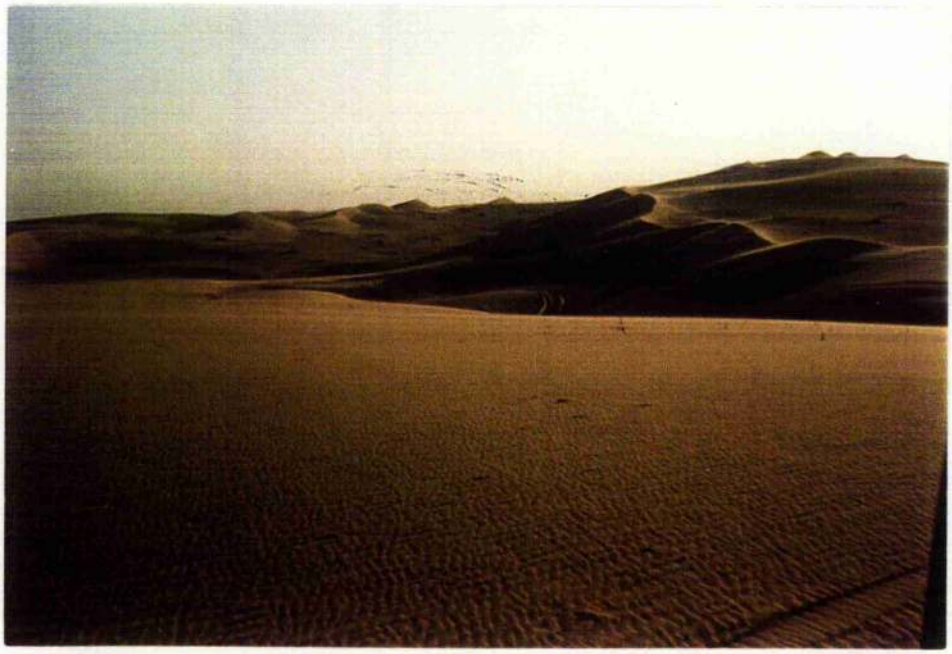

Figure 2.12b Active seif dunes in the eastern part of Wadi Habawnah (about 15 km east of Al Husaniah).

seifs and linear dune complexes in the eastern part of the area, along the junction of the Wadi Habawnah with the Al Rub Al Khali desert (Figure 2.12b). Sand features interpreted as remnants of older stabilised seif termini, have been mapped east of Wadi Habawnah (Sable 1982). They and the currently active seifs may reflect two separate episodes of linear dune encroachment, which represent periods of aridity interrupted by a pluvial period (Sable 1982). The periods of aridity, have given rise to the huge sand deposit basin which is known as the Al Rub Al Khali desert (Figure 2.13).

2.3 Wadi Baysh and Wadi Habawnah Drainage Systems

The drainage systems of both wadis show well developed dendritic patterns (Figure 2.14) which are locally modified by differential erodibility of the bedrocks and by geological structures such as faults. Most of the tributaries enter the main wadis nearly at right angles which may indicate a control by fault planes guiding both the tributary and the main channel. This influence of faulting on surface drainage may also have a control on ground water circulation and deep weathering which leads to erosion of the rocks along faults.

The wadi catchments have a combined area of about 10000km^2. The lower reaches of the main wadis have lengths of 240km for Wadi Baysh and 160km for Wadi Habawnah.

Both wadis are rather narrow, particularly in their upper parts. However, their widths vary from less than 100m to more than 1km farther downstream where alluvium becomes widespread and thicker at sites such as Baysh Bridge and Habawnah Bridge (Figures 2.15 and 2.16a).

The upper course of Wadi Baysh is directed toward the southwest, its middle course runs north to south, between Misliyah and a few kilometres below Wadi Baysh bridge while its lower course trends southwest, perpendicular to the edge of the graben (Red Sea coast) (Figure 2.15). However, the main course of Wadi Habawnah trends west to east runs WE (Figure 2.16a). Both wadis are influenced in their direction by the fault systems in the area.

Figure 2.13 Shows part of the SW area of the Rub al Khali Desert (the world's largest contiguous sand desert with an area about 640,000 km^2, MAWR,1984). It is covered by gigantic linear dunes of draa type, spaced from 2 to 6 km apart and with an average direction of N60E. This type of dune is up to 260 km long but is commonly 150 km long and up to 230m high (Edgell, 1990). Formation of these huge longitudinal dunes is due to vortex-type wind flow alternating from the northeast and southwest. In the early Holocene, there were many lakes and considerable areas of grassy vegetation with wild life (Clark, 1989). However, the last 6,000 years have been mostly hyperarid and many different types of dunes have formed in the Rub Al Khali (Wilson 1973). One of the main sources of siliceous sandy sediments for the Rub. Al Khali is the Arabian shield, Wajid Sandstone and sand-filled wadi systems that formed in more pluvial intervals of the early Quaternary, such as the Wadi Habawnah. (Edgell, 1990).

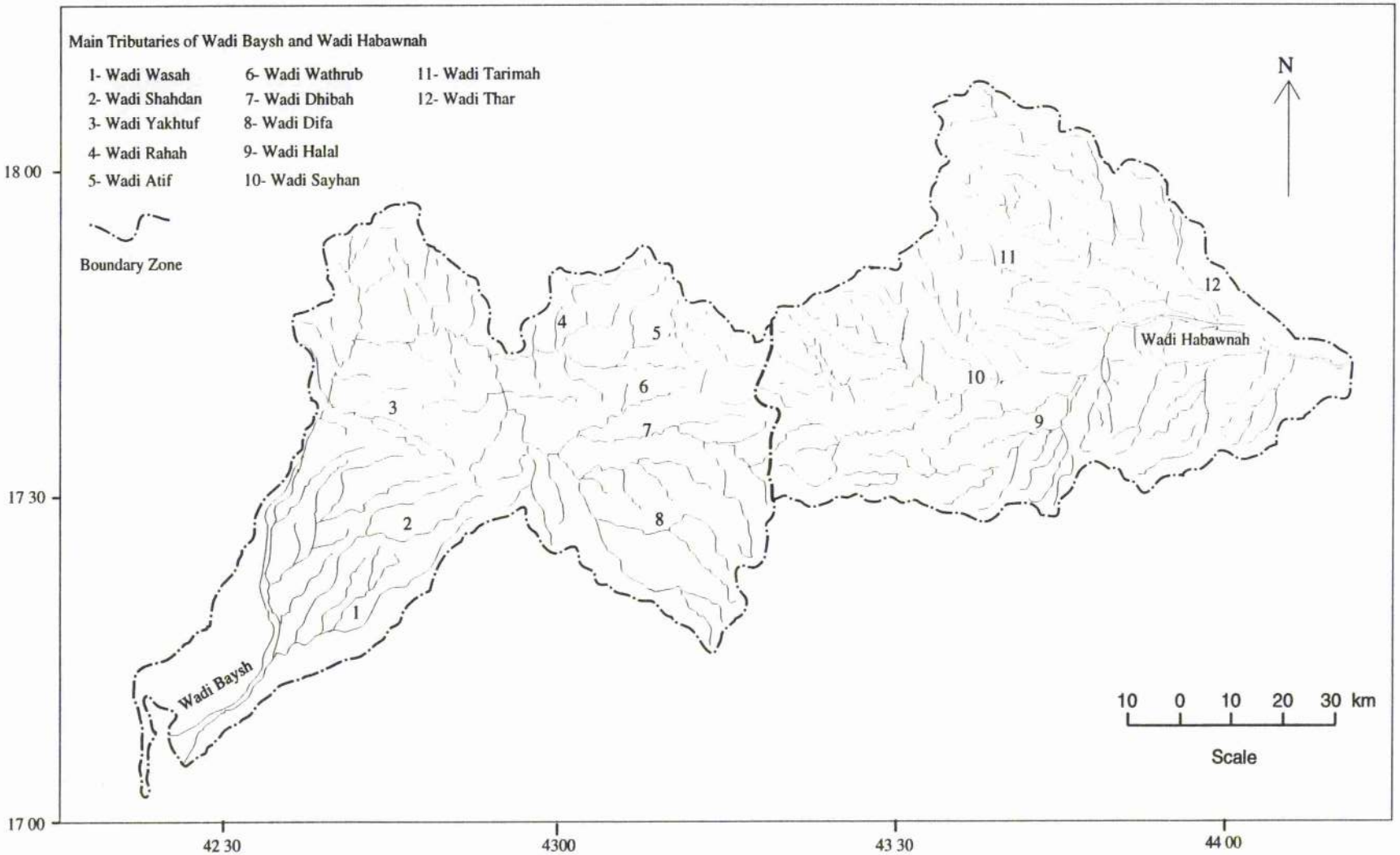

Figure 2.14 Drainage map of Wadi Baysh and Wadi Habawnah in the south of the Arabian Shield, Saudi Arabia.

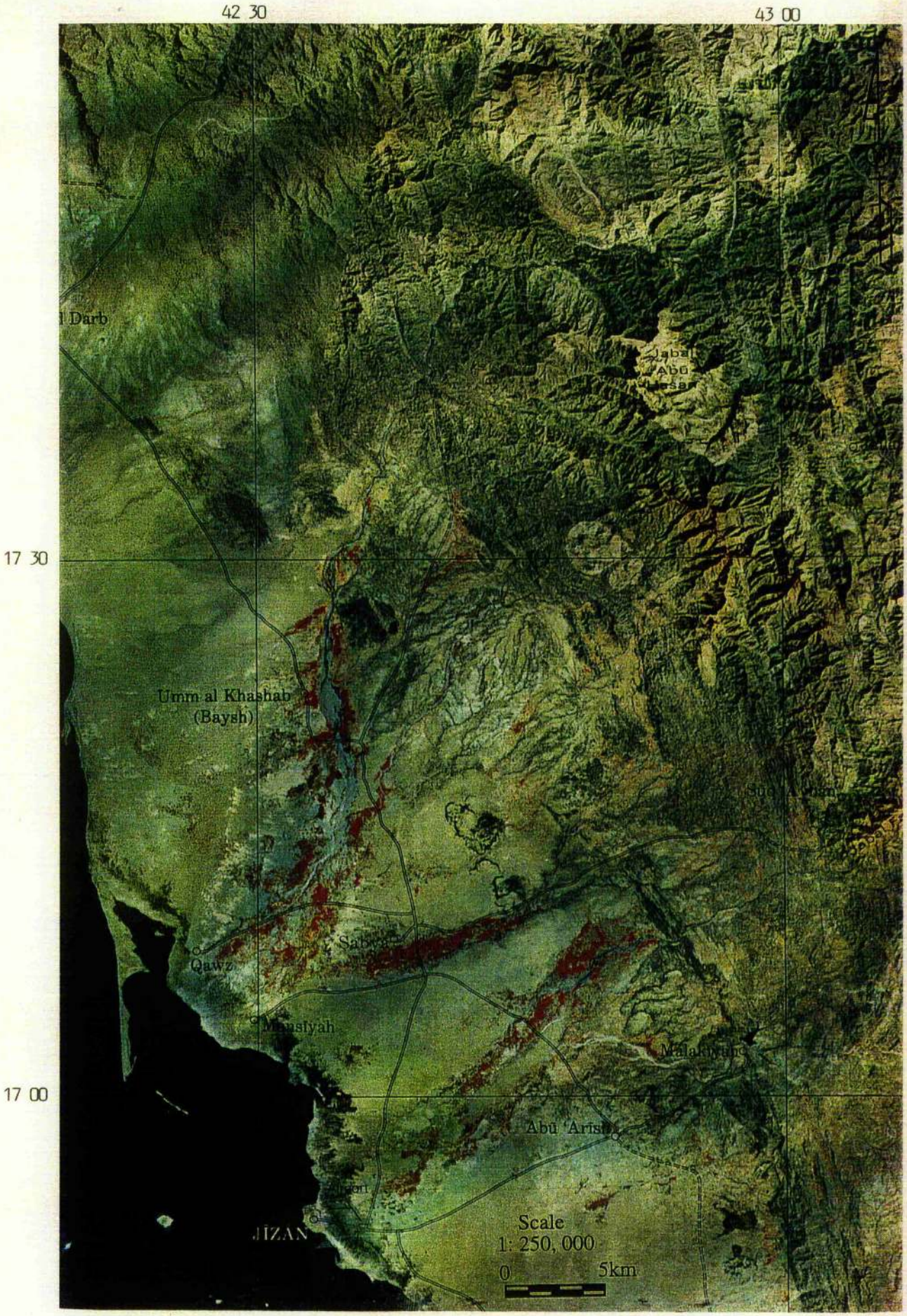

Figure 2.15: Landsat image of the erosional scarp of Asir lat.17 N. Red Sea lower on left, bordered by the Tihamah 'Asir (coastal plain) and then foot-hills in the left side. It shows Wadi Baysh and Wadi Sabya penetrating the coastal plain and flowing to the Red Sea. The red patches along the wadis indicate the agriculture areas.

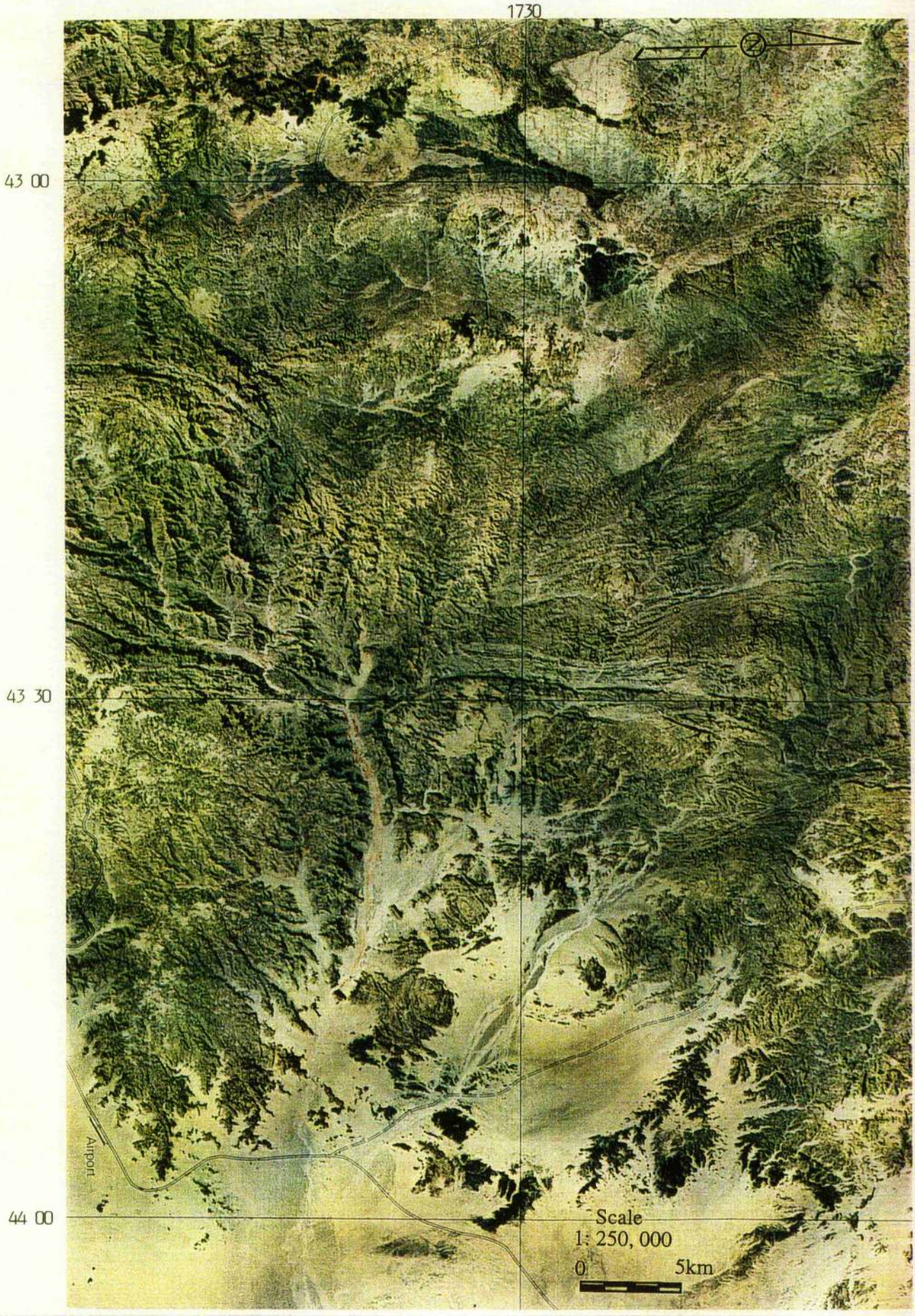

Figure 2.16a: Landsat image of Wadi Habawnah lat.17 N. In the west side of this image at the point where it has cut through the escarpment of the Highlands (cutting the Ashara Fault Zone), cultivated fields extend along Wadi Habawnah as patches of red in colour. Farther west in the highland zone, small scattered red coloured areas occur around lava flows indicating the development of cultivation where runoff is entrapped by adjacent impervious rock.

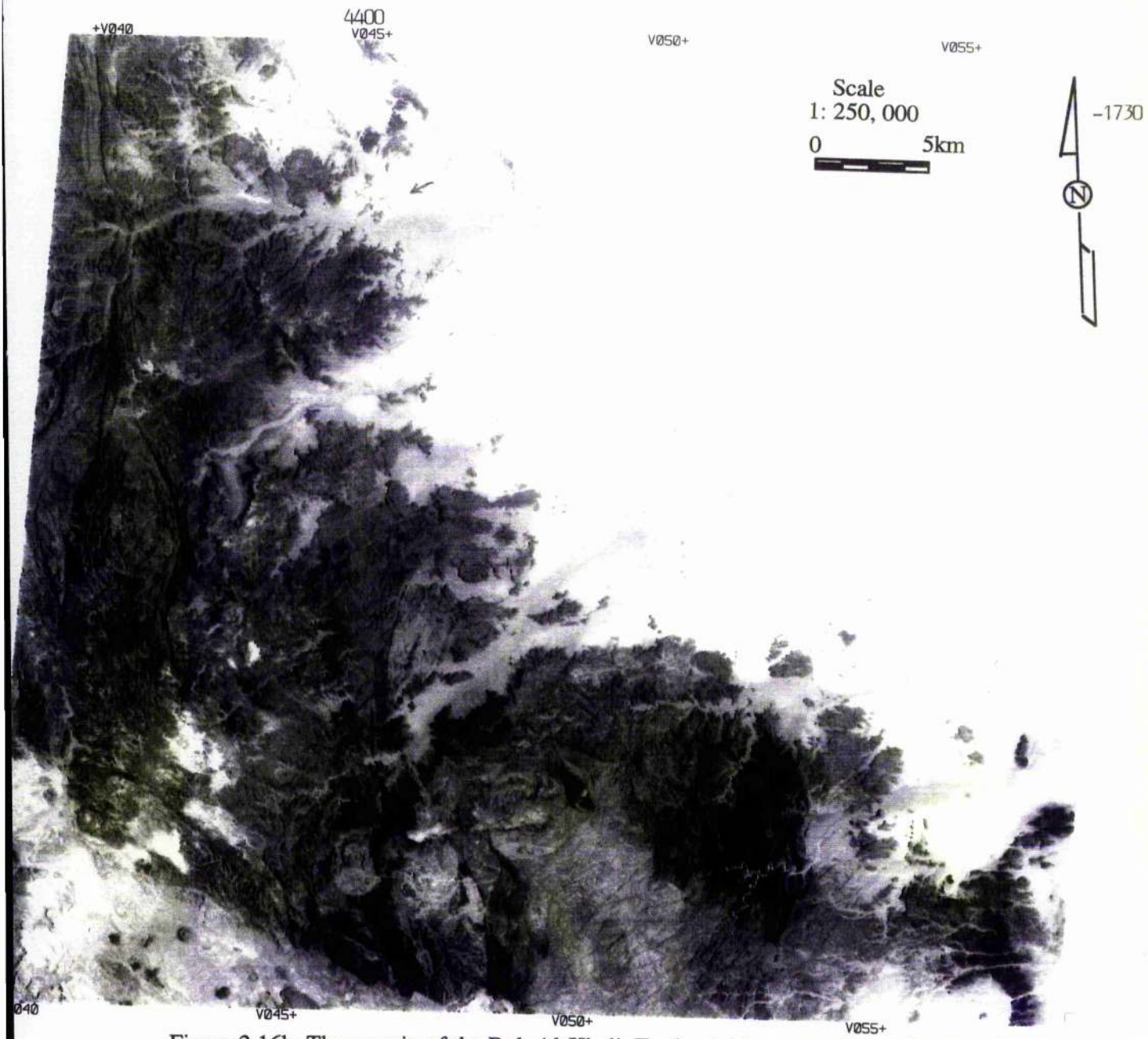

Figure 2.16b: The margin of the Rub Al-Khali. To the right are seen linear dunes and aeolian sand fields. These dunes serve as a natural barrier for the ephemeral runoff that originates further west in the Wadi Habawnah to the left of the image.

2.4 Geomorphology

2.4.1 Introduction

The geomorpholgical development of the Arabian Shield was influenced by two main factors, climate and tectonism, which were particularly important during the Cainozoic (Bower,1960). Most of the major faults and fractures visible in the present landscape of the area formed as result of deformation during the Precambrian. However, the development of major scarps associated with the Red Sea rifting was all important in the Miocene. The relatively horizontal disposition of the extensive peneplains and terraces is indicative that little tectonic activity has occurred east of the Highlands in late Cainozoic times, (Italconsult, 1965).

From the Oligocene to the Pliocene the climate changed from tropical to subtropical and/or semi-arid (Al-Otaiby, 1981). The study of the geomorphology of Wadi Bishah (Northeast of Wadi Habawnah) shows the existence of boulders at high levels indicating that humidity increased during the Tertiary (Al-Otaiby, 1981). The upper basins developed during the Tertiary were further eroded in a drier intermediate period (i.e. Middle to Upper Pleistocene). Such erosion may have resulted in a change from the major silt accumulations found in the lower basin to overlying, younger sands and gravels. Subsequent to the soil removal the streams commenced transporting granular material to the gravel layers overlying the terraces throughout the lower basins.

A further more humid period permitted the wadi to erode a new valley in the terraces Subsequently the entrenched valleys were filled with more recent alluvium. Al-Otaiby (1981) indicated that the presence of terraces at various elevations along the wadi confirms the ongoing evolution of the wadi floor sequence.

The forms of the land and other physical features of the study area are not in harmony with the current climatic regime. The most striking phenomenon is the presence of a fluvial drainage network, or a wadi system, in areas presently under fully arid to semi-arid climatic conditions.

The drainage system has high channel density in most of the interior basin, especially on the broad slopes that are drained by the wadis. This dense drainage network

can only be explained by a much larger runoff rate, compared to that of today. Moreover, the drainage system has an integrated arrangement: small valleys terminate in larger ones, which in turn end in a few master wadis, where Wadi Baysh reaches the Red Sea and Wadi Habawnah reaches the Empty Quarter Desert.

Increasing valley size indicates that at some previous time discharge also increased downstream. Today's flow may only occasionally reach the wadi's end.

Both Wadis are deeply entrenched into bedrock and have thick alluvial fills. Such features load and cutting power with large discharge reflect coarse bed. In Wadi Habawnah and Wadi Baysh, the alluvium reaches at least 50m and 150m in thickness respectively.

The streams of considerable transporting capacity is characterise the various wadis in the region by the presence of well-rounded gravels that transport along the wadis channels. Figure 2.10 shows the pebbles gravels have been in the transported long distances from upstream of their current position, from igneous and metamorphic rock complexes of the Asir highlands, over distance approximately of 130km. Today the ends of the lower parts of both wadis are completely covered by sands.

The cross-profiles of wadis in arid areas exhibit form elements that are similar to valleys in humid regions. Cross sections in the upper reaches are V-shaped, but in the middle courses these are box-shaped. The amount of alluvium increases downstream. The headwater and middle sections of the wadis display evidence of "active erosion", while extensive alluvial plains characterise their lower reaches. This description is appropriate for the two wadis under examination.

Hotzl and Zotl (1984) indicate that during the Pliocene/Early Pleistocene, there was an intensive, long, humid (pluvial) phase in Arabian Peninsula. The entrenchment of the wadi systems of Arabia occurred during this time. The southeast wadis drainage system of Asir Highlands ware responsible for the deposition of the alluvial plain of Al Rub Al Khali that covers vast areas of southeast Arabia.

According to Hotzl and Zotl (1984), Arabian Peninsula is believed to have experienced arid conditions with minor humid phases of little geomorphic and stratigraphic significance during the entire middle Pleistocene.

Carbon-14 measurements made from calcite crusts collected from gravels below the surface of terraces in Wadi Ar Rummah revealed ages of 28,900±1,300 and 30,200±1,300 B.P (Hotzl and Zotl,1984).

In the Mugabil loam pit of Wadi Ranyah, samples collected from crusts at depths of 0.7 and 1.0m below the land surface have carbon-14 ages of 26,400 and 29,840 years B.P for the origin of the calcite horizons (Hotzl and Zotl, 1984). Endlessly there was enough precipitation to produce soil caliche during this period.

A series of lake beds in the lee of seif dunes in southwestern Al Rub Al Khali yielded with C^{14} dates ranging from about 36,000 years B.P. to about 17,000 years B.P. (McClure, 1978). The period 17,000 - 9,000 years B.P. was hyperarid, characterised by arid conditions, with strong deflation in Al Rub Al khali. (McClure, 1978).

A sub pluvial lake with radio carbon dates ranging from 9,000 to 6000 years B.P. is found separating red, eolian sand deposits in southwest Al Rub Al Khali (McClure, 1978). Hotzl and Zotl (1984) believe that the rest of the Holocene have had similar arid conditions to those that prevail today over Arabia, with some intervals of minor increase in precipitation.

2.4.2 Wadi System Geomorphology

Both wadis show geomorphological features typical of the south Arabian Shield which can be divided into three majors units as follows:

2.4.2.1 The First Major Unit

The First Major Unit of Wadi Baysh is the mountain zone. It is part of the Assarah mountains uplifted by Tertiary orogeny which lowered the Red Sea coastal plain some 3 km below the shield (Chapman, 1978). According to Brown (1960), the wadis which flow through the mountains towards the Red Sea were originally related to structure. However, subsequent erosion has deepened and enlarged the wadis so that deep canyons cut into Precambrian rocks and now extend from the foot hills to the head waters. The highest elevation at a frontier mark between Saudi Arabia and Yemen is 2,784m (Philby, 1952).

The southwest mountains are formed by a succession of faults which developed a chain of ridges and increase in elevation eastwards in a series of steps. By comparison, the Wadi Habawnah mountain zone shows a gently sloping landscape draining to the east and northeast by way of shallow, poorly defined valleys. The head-water areas of many of the valleys have elevations of about 3,000m.

The headwaters of both wadis are mainly of crystalline basement of Precambrian age. Remnants of Cambrian to Ordovician Wajid Sandstone occur in the southern limits of the Highlands. The amount of overburden varies with the slope and degree of agricultural terracing on the upper valley sides.

2.4.2.2 The Second Major Unit

The Second Major Unit of Wadi Baysh can be considered as the foothills zone while in Wadi Habawnah it is the transition wadis.

In Wadi Baysh, the foothills zone is located between the Highlands and the coastal plain and has an average width of 25 km (Muller 1977). In the west this zone begins as a line of low hills which rise to 100-200m, on average. This band of hills is followed to the east by a second band which reaches elevations of 200-700m (Muller 1977).

The terrain in the foothills zone is highly eroded due to erosion by run-off originating in the Highlands. Gullying is widespread in this zone and steep hillsides are common. Gullying is probably related to the higher average annual rainfall in this area (500mm pa). Soil erosion caused by run-off and steep terrane restricts agricultural activities to the lower areas.

In Wadi Habawnah, the transitional wadis characterise the zone connecting the dissected Highlands with the pediplains to the east and north east. In the upper part of this unit, broader wadis exist separated by small segments of the dissected Highlands. Some have steep narrow valleys which are aligned with local and regional structural lineaments. The alluvial deposits are coarse gravels although fine sediments are found locally. Within the wadis are recognised pediments, terraces and wadi channels.

The wadi channels are generally narrow. This width is no more than 40m above

Habawnah town but increases to 1,300m near the Hausaniah bridge. Local accumulations of fine sands and silts are developed as a result of erosion from the terrace deposits. Coarse sands and gravels are brought in to this area by flow resulting from occasional torrential storms.

2.4.2.3 The Third Major Unit

The Third Major Unit of Wadi Baysh is the lowland zone while in Wadi Habawnah it is the pediplains.

The lowlands of Wadi Baysh can be divided into two main zones: the wadi area and the Khabt area. The wadi area consists of a network of wadis and their flood plains which are dominated by agricultural activity. The Khabt (Arabian word) area (Plural Khuboot) constitutes the flat plains between the wadis. Most Khuboot areas consist of continental terraces with wind eroded surfaces (Figure 2.17). The Wadi area can be considered as an area between Misliyah and about 10 km from the Red Sea coast (Figure 2.15), where the wadi enters a vast delta. Abdul-kar (1988) indicated that such a boundary could be located only a few kilometres east of the coast, on the basis of topography, vegetation, ground water resources and the distribution of Sabkhah. The high plain reaches only 5m above sea level and is characterised by small sand dunes, that vary according to tides and seasons. The area bordering the shore line is dominated by sabkhah which exceeds 10km in width (Abdul-kar, 1988).

In Wadi Habawnah, the pediplains consist of broad plains of silts, sands and gravels. Due to the overall subdued relief within this unit the pediments and associated terraces are wider than in the transitional valleys. Eolian reworking of the finer materials creates broad deflation surfaces which provide material for accumulation features such as sand dunes formed on the leeward side of small obstacles near the wadis. However, these eolian accumulations, although significant, in no way compare with the dune fields associated with the zones bordering the Al Rub Al Khali Desert (see Figure 2.13). Due to the infrequent flow of water in the lower zones of these wadis, the degree of channel entrenchment is generally limited or minimal. Within the lower sections of Wadi Habawnah there is evidence that major river flows do occur and that they flow occasionally

Figure 2.17 A flat plain located about 5km north of Misliyah consisting of high level terraces in an area between the wadis. The terrace surface is wind eroded (Khabat area).

into the Al Rub Al Khali (Empty Quarter) Desert (Figure 2.16b).

2.5 Structural Geology

An east-west profile through the Arabian-Nubian Precambrian shield shows a very broad anticlinal structure with the Red Sea forming a graben at its crest.

The two physiographic units of the study area, the Highlands, sloping gently to the east (Wadi Habawnah), and the upper part of Wadi Baysh and the Assarah Mountains, facing the rift valley of the Red Sea with a very steep scarp, correspond to two different structural environments.

According to Sable (1985) there are three Proterozoic structural provinces in the Najran quadrangle: (1) Southernmost exposures of the Tarib batholith in the north western part of the quadrangle (Figure 2.5), (2) North trending belts of layered rocks east of the Tarib batholith and west of the Ashara fault zone (Figures 2.5 and 2.16), (3) A complex of layered rock remnants within younger Proterozoic intrusive suites east of the Ashara fault zone that are characterised by northeasterly to northerly structural trends (Figures 2.5 and 2.16a).

The Wadi Baysh quadrangle lies in a series of broad northwest trending structural belts (Greenwood *et al.*, 1982). The Tertiary structural features also show that, of the overlying deformed rocks of the Sabya Formation and the Baysh Group along the western margin, the Sabya is extensively sheared and tectonically thinned between the Khamis Mushayt complex (granodioritic gneiss dome) and the Baysh Group (see Figures 2.4 and 2.15a).

In the Tihamah Asir plain (Asir coastal plain), two large flexure-like zones of westward dipping faults have developed during the deposition of the Baid Formation (Gillmann, 1968). In the east of the plain, the flexure belt stretches parallel to the foothills and corresponds with the eastern edge of the Red Sea graben. This fault zone cuts the basement and the Khums and Baid Formations, creating a deepening of the sediment basin (see Figure 2.18a)

In the east of Wadi Baysh (in Wadi Shahdan) some of the faults trend in a

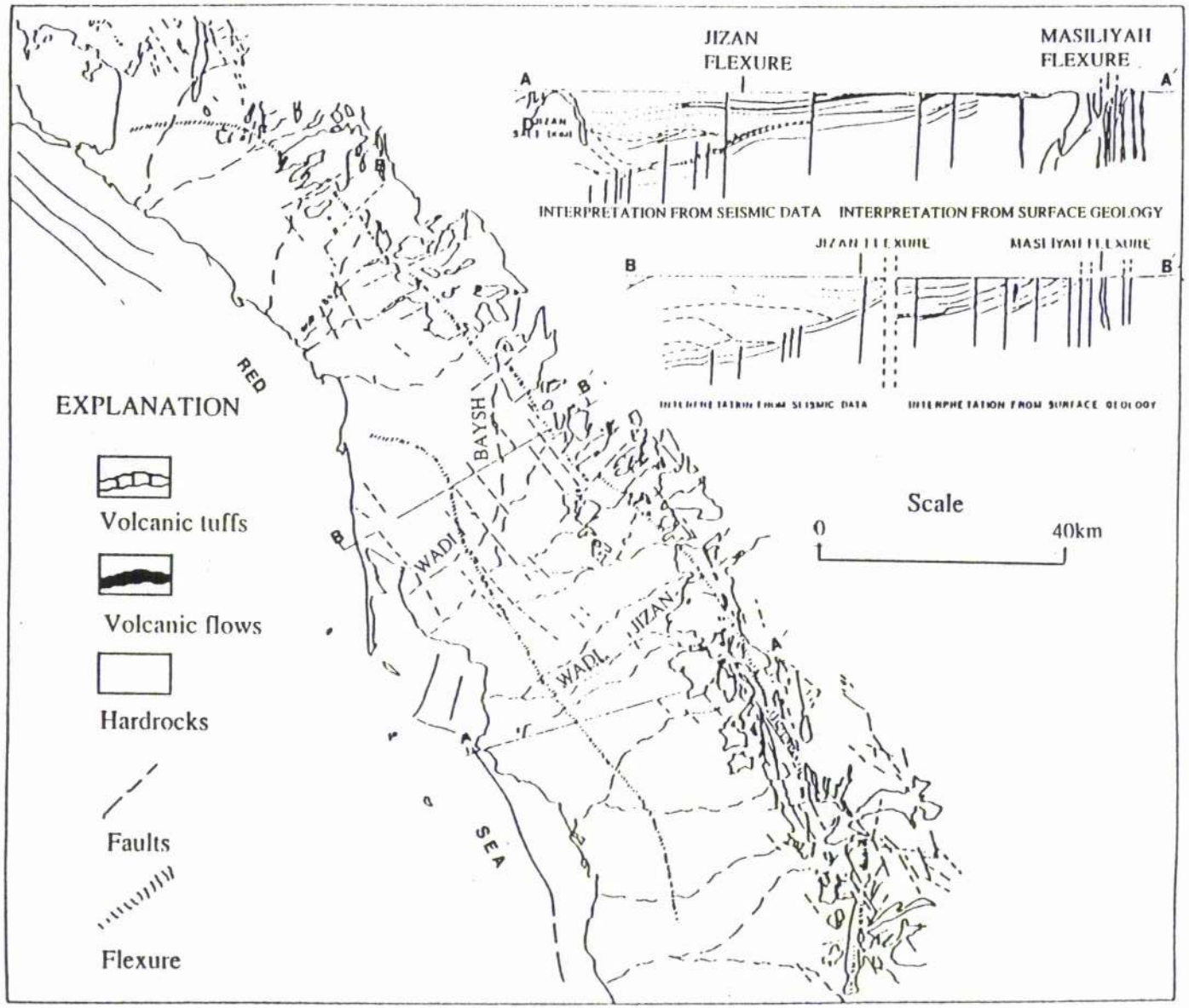

Figure 2.18a Structural map of the Tihamat Asir plain (modified from Gillman, 1978)

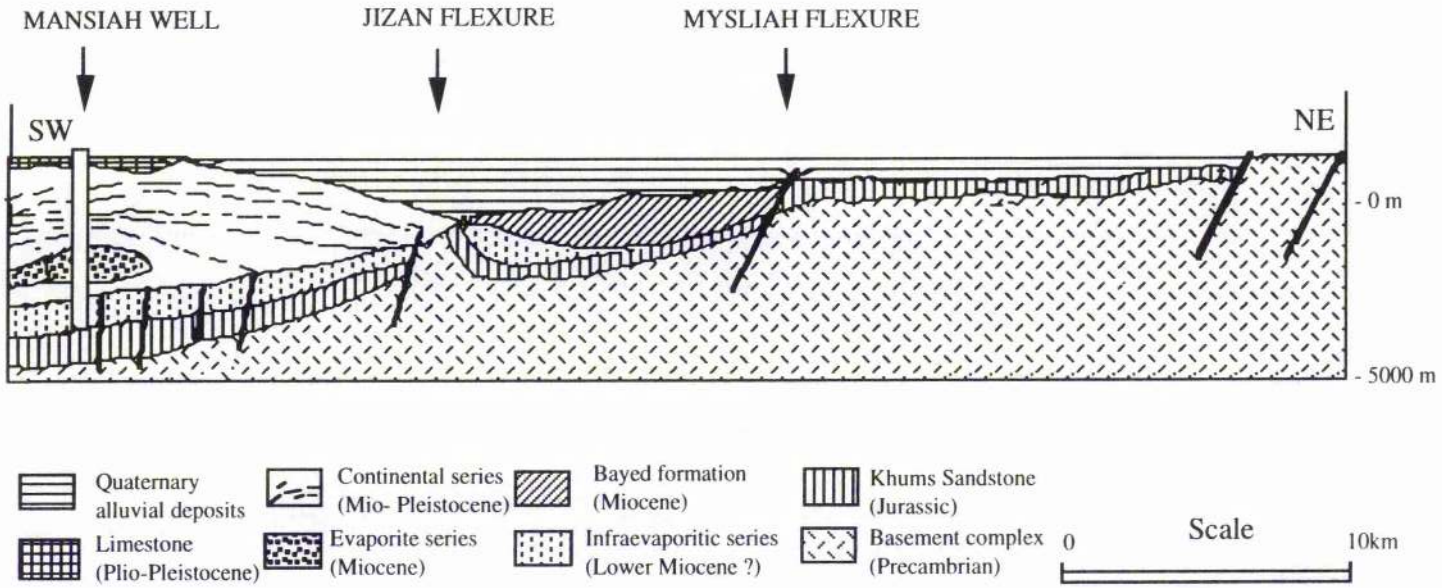

Figure 2.18b Generalized geological cross section of the Tihamat Asir showing the approximate location of the Misliyah flexure, the Jizan flexure and the Mansiyah well (modified from Gillmann, 1968 and Jado et al., 1984).

northwest-southeast direction. However, this system of faults provokes lateral displacements of the flexure. Jado *et al.*(1984) indicated that Wadi As Sirr displacement (one of the set of faults) is perhaps responsible for the change in direction of Wadi Baysh northeast of Misliyah, after this wadi has left the foothills (see Figure 2.15). On the basis of aeromagnetic and seismic surveys Gillmann (1968) determined that there is a homocline west of this flexured area. The homocline is about 25-35 km wide with northwest-southeast strike and low westward dip. A result of the northwest trending faulting of this homocline, is believed to be the deposition area of the Baid Formation (see Figures 2.8 and 2.18a). A second flexure zone (Jizan Flexure) is located parallel to the first one (see Figure 2.18a). This second flexure zone is limited the second homocline in the west and provokes westward thickening of the continental series (clastic deposits).

Figure 2.18b shows cross section of Tihamah Asir Plain (varying thickness of the Quaternary layers) based on seismic reflection and resistivity profiles and aeromagnetic surveys by Gillmann (1968).

Near to the coastal plain, the Mansiyah anticline consists of continental deposits overlain by marine, calcareous sediment, which is followed eastward by a wide, slightly asymmetrical syncline. The synclinal axis is approximately in the middle of Tihamah (Jizan Flexure). The alluvial deposits have a thickness of several hundred metres within the Jizan Flexure. On the western limb of the syncline, the alluvial deposits are superimposed upon the continental series and interfinger with the marine calcareous sediments. Eastward, in the Mansiyah flexure area, the alluvial deposits overlie the Jurassic Khums Sandstone. This zone is nearly 10km wide. The crystalline basement is exposed at the surface after further step faults eastward of this flexure.

The alluvial filling of the wadi syncline shows a differentiated sequence, which is described further in Chapters 6 and 8.

Moore (1983) defined several groups of lineations from his aeromagnetic data. These are: (1) North-northwest to northwest trend in the Red Sea coastal strip. (2) Northwest trend which are faults of the Najd fault system. (3) North to northeast trend which are boundary faults of Proterozoic volcano-sedimentary and serpentine belts.

Qari (1990) indicates that the southern Arabian Shield has been affected by the following events (1) East-West structural trend (2) North-South trend which resulted from East-West compression (3) Northwest-Southeast trend which resulted from the Najd faulting system (4) Northeast-Southwest trend, presumably the signature of a conjugate set of fractures developed at the same time as the Najd system.

Based on the above information the author believes that Wadi Baysh and Wadi Habawnah show typical influences of the East-West structural trend (Wadi Habawnah), and also of the NE-SW trend (Wadi Baysh), (Figures 2.15 and 2.16).

2.6 Summary and Conclusion

Wadi Baysh and Wadi Habawnah are representative systems of Arabian Shield wadis. They have nearly the same size of catchment area but different flow directions under the influence of the Shield physiography which slopes to the west and to the east.

An east-west profile through the Arabian-Nubian Precambrian shield shows an anticlinal structure with the Red Sea forming a graben at its crest.

The two physiographic units of the area, the Highlands sloping gently to the east (Wadi Habawnah) and the upper part of Wadi Baysh which faces the rift valley of the Red Sea, correspond to two different structural environments as follows:

The Proterozoic structure has left a clear mark on the physiographic features of Wadi Habawnah. In the west part of the catchments, The Halaban Group was affected by the Ashara fault zone in which the Group trends the N-S perpendicular to the wadi course (W-E). In Wadi Baysh the Sabya Formation is extensively sheared and tectonically thinned between the Khamis Mushayt complex and the Baysh Group.

The Tertiary evolution of the Red Sea formed the Wadi Baysh physiographic features. The graben shoulder rifting along the western margin of the Arabian Shield is the main event which formed the physiography of the west scarp of the mountain chains to the east, the foothills of the interior and the Tihamah Asir plain (coastal plain in the west).

The upland area slopes of Wadi Baysh and Wadi Habawnah have average

gradients of 20 m/km and 12m/km, respectively, while in the lower parts of both wadis the gradients are approximately 4m/km.

The stratigraphic rock units of Wadi Habawnah and the upper areas of Wadi Baysh consist of Proterozoic metavolcanic and metasedimentary rocks intruded by Proterozoic intrusive rocks, mainly gabbro, diorite and a granite-syenite suite. The lower land area is intruded by Tertiary rocks (layered gabbro and diorite). In both wadis Proterozoic rock units are overlain partially by Palaeozoic sedimentary rocks as well as Tertiary to Holocene sediments and volcanic rocks. The Mesozoic sedimentary rocks are present only in the Wadi Baysh area. The hard rocks of the Wadi Habawnah catchment outcrop over about 90% of the area while in Wadi Baysh they outcrop over about 80 % of the catchment area.

The lowland deposits of Wadi Habawnah are mainly alluvium overlying bedrock, while the Wadi Baysh coastal plain shows a thick alluvial deposit that covers the Tertiary rocks (mainly the Baid Formation with a total thickness of nearly 4km).

CHAPTER THREE: RAINFALL, RUNOFF AND FLOODS

3.1 Introduction

The Wadi Baysh and Wadi Habawnah catchment areas have been drawn on the basis of the topographic maps of Sabya and Najran regions (Figure 3.1). The total catchment area of both wadis is approximately 10,000 km^2. The catchment area above the outlet (SA-124) of the upper part of Wadi Baysh is about 3511 km^2, while that of Wadi Habawnah is about 4425 km^2 at the outlet (N-406). Wadi Baysh and Wadi Habawnah have eight and four major tributaries respectively (see Figure 3.1). The boundary of the Wadi Baysh basin reaches to within 10 km of the Red Sea, and the boundary of Wadi Habawnah is 15 km from the Empty Quarter Desert.

The wadis are separated by the escarpment crest of the Asir Mountains which trends northwest-southeast through the region. The Wadi Habawnah catchment is developed on the moderate dip slope while the Wadi Baysh catchment is formed on the steeper scarp slope which becomes flatter only towards the coast of the Red Sea (Figure 3.1). The area is of mountainous terrain and is bounded to the west by the Red Sea and to the east by the Empty Quarter Desert. This location provides a good example of the unique hydrological cycle of a semi arid and arid zone.

The data on climate and rainfall-runoff within and near the study area were obtained from the Department of Water Resources (Minister of Agriculture and Water Resources, see bibilography), Kingdom of Saudi Arabia, during the field work in the summer 1990 and from the study of the climatic water balance in Saudi Arabia 1970-1986 by Al-Jarach (1989). The locations of meteorological and the rainfall run-off stations are shown on Figure 3.2.

There are nine meteorological stations: Habawnah (N-002NP) and Sarat Abidah stations are located within the Wadi Habawnah catchment area, while the rest of the stations (Najran airport, Najran, Khamis Mushait, Sira Lisa-A006, Abha-A001, Sabya (SA-002), Jizan airport and Malaki (SA-001)) are near the study area. The available data records of the meteorological stations are for different periods (between 1 and 16 years) and consist of data for sunshine hours, solar radiation, air humidity, wind speed, temperature,

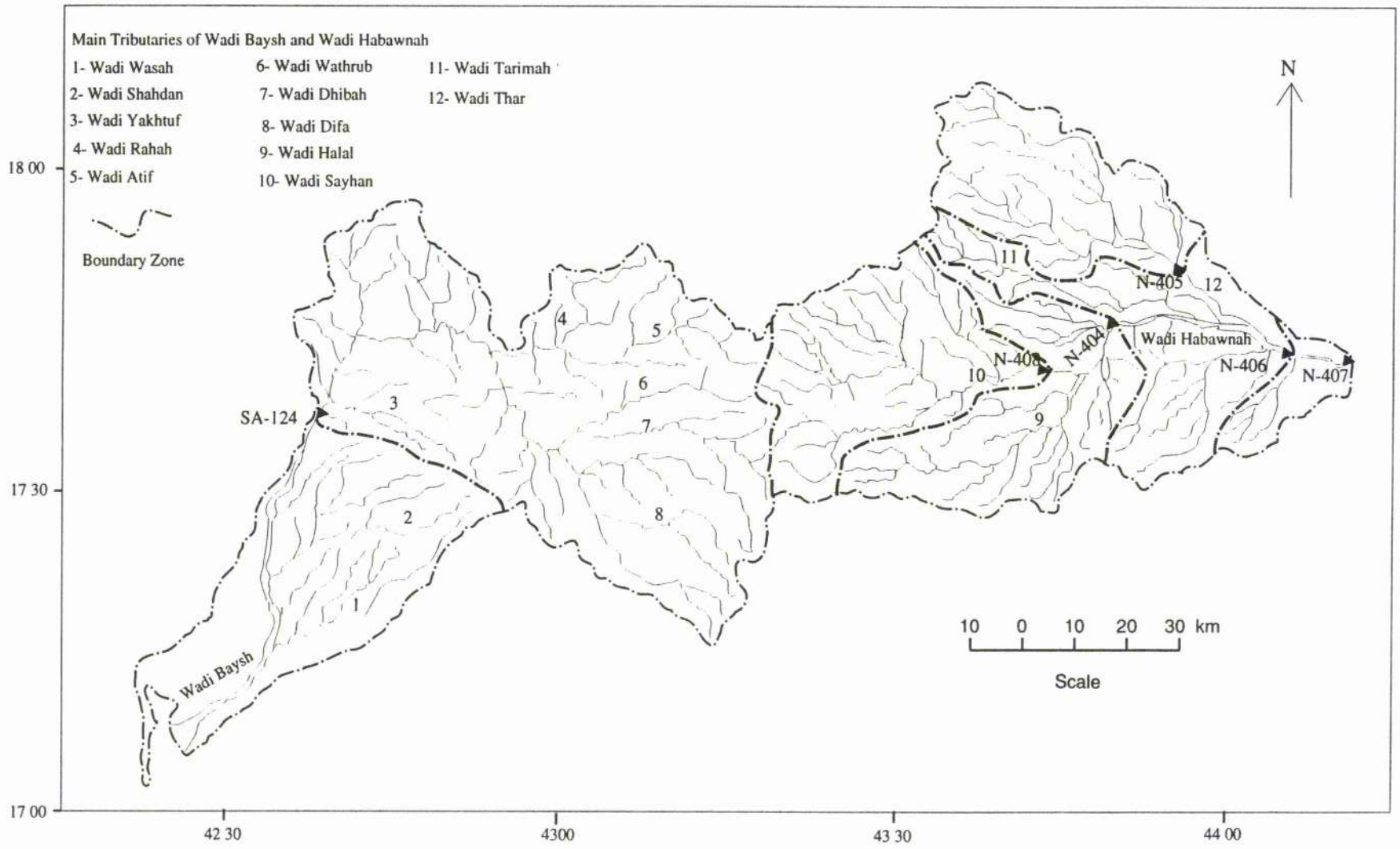

Figure 3.1 Drainage map with outlet stations of Wadi Baysh and Wadi Habawnah in the south of the Arabian Shield, Saudi Arabia.

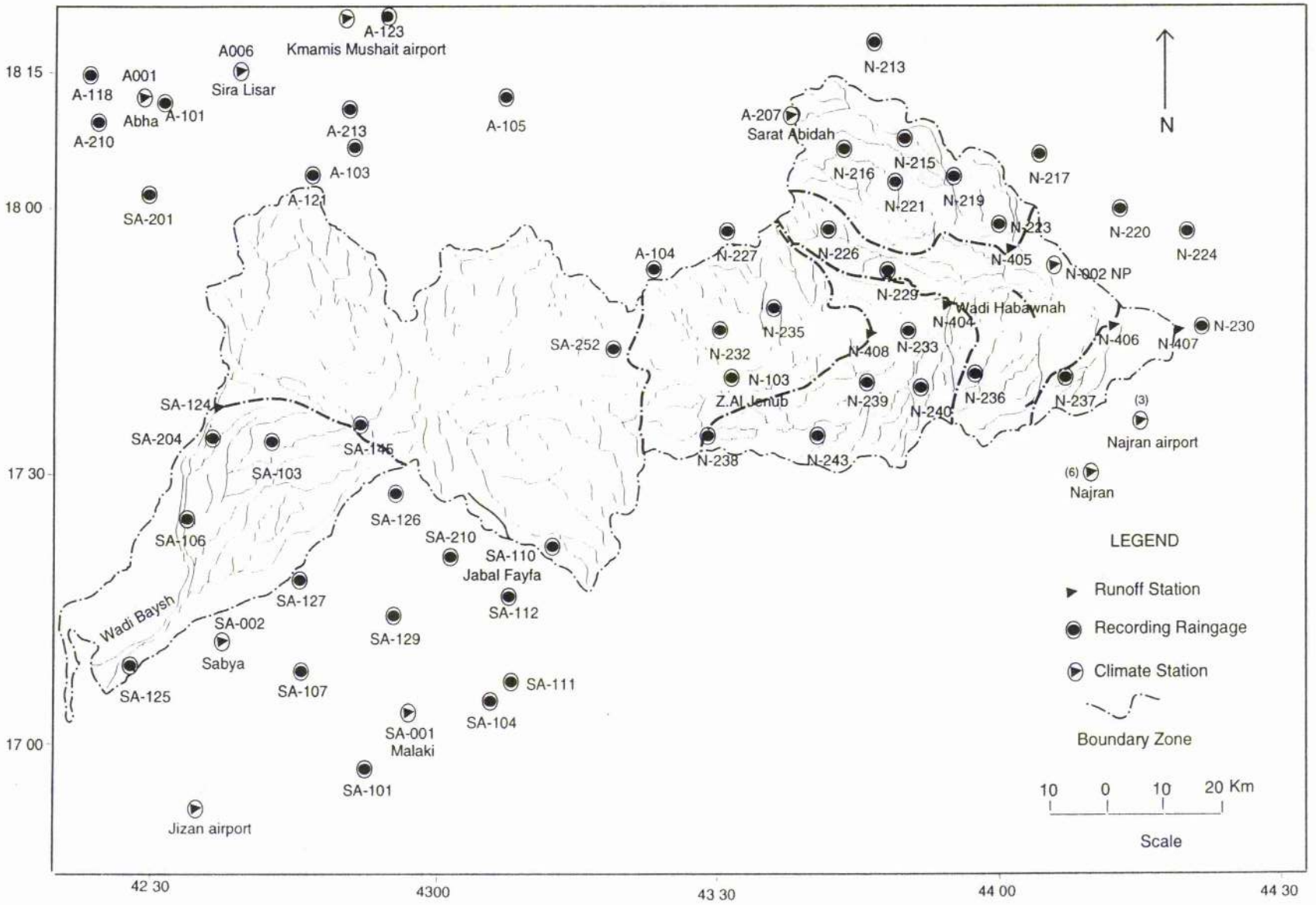

Figure 3.2 Meteorological, rainfall and runoff stations within and near the catchment areas of Wadi Baysh and Wadi Habawnah in the southern Arabian Shield.

evaporation and evapotranspiration (Tables 3.1, 3.2, and 3.3). The rainfall station records consist of four years of monthly rainfall data for 27 stations within and near Wadi Habawnah, and monthly averages of rainfall data for 4 to 24 years of records of 31 stations within Wadi Baysh and the nearby area (Table 3.4). The intergauge spacing varies between 8 km and 108 km in Wadi Habawnah, and 4 to 152 km in Wadi Baysh (see Figure 3.2). There is a 15 year monthly record of runoff for station SA-124. This is the only existing outlet station for the upper part of the catchment area of Wadi Baysh. In Wadi Habawnah, there are five subcatchment stations each having three years' records of monthly runoff (see Table 3.5).

In both wadis the meteorology and topography differ greatly in the upper and lower parts. The historical flood records show that the centres of storms occur in the upper part of the catchments. Most of the catchment area of both wadis is characterised by impervious hard rocks, which converts rainfall to run-off in a short time. As shown in Figure 3.3 and Table 3.4, the catchment of Wadi Baysh drains into the Red Sea and the elevation generally increases from south-west to north-east with the rainfall stations varying between 200 and 2200m in altitude. The Wadi Habawnah basin is situated further inland where the elevation increases from east to west, with the height of the rain stations varying between 1160 and 2290m above sea level. It can be seen that the topography of the catchment is quite varied and it is likely to exert a significant influence on spatial patterns of climatic parameters.

The south-west of Saudi Arabia experiences cyclonic and monsoon climatic conditions. The cyclonic systems move across the region from the north during the winter. The monsoon moves across the region from the southwest in the summer. These two types of weather systems vary in duration both seasonally and annually and this makes it difficult to explain the regional climate.

The daily temperature ranges between 22°C and 32°C throughout the region. The seasonal daily rates of evaporation on the western and eastern slopes are approximately 9 and 11 mm/day, while the evapotranspiration rate is 5 and 6 mm/day respectively.

Table 3.1 Climatological data for the Malaki, Sabya, Habawnah and Abha stations

SUN SHINE HOURS

STATION			JAN	FEB	MAR	APR	MAY	JUN	JUL	AUG	SEP	OCT	NOV	DEC
Abha	1982-85	MAX	*	*	*	*	*	*	*	*	*	*	*	*
		MEAN	7.2	7	7	9	8	8.5	7.4	7.4	9	8.7	8	7
		MIN	*	*	*	*	*	*	*	*	*	*	*	*
Habawnah	1984-87	MAX	*	*	*	*	*	*	*	*	*	*	*	*
		MEAN	9.5	9.2	8.3	9	9.4	9.4	9.1	8.6	10	10.3	10.3	9.1
		MIN	*	*	*	*	*	*	*	*	*	*	*	*

SOLARRADIATION (Cal/cm^2/d)

STATION			JAN	FEB	MAR	APR	MAY	JUN	JUL	AUG	SEP	OCT	NOV	DEC
Abha	1966-75	MAX	*	*	*	*	*	*	*	*	*	*	*	*
		MEAN	420	430	560	450	580	510	490	440	510	510	480	430
		MIN	*	*	*	*	*	*	*	*	*	*	*	*
Habawnah	1984-87	MAX	*	*	*	*	*	*	*	*	*	*	*	*
		MEAN	440	465	499	548	573	584	580	551	559	535	463	424
		MIN	*	*	*	*	*	*	*	*	*	*	*	*
Malaki	1966-75	MAX.	403	437	537	642	641	623	579	601	577	570	494	473
		MEAN	369	396	501	543	564	427	484	502	509	514	431	397
		MIN.	316	294	453	499	497	450	413	419	419	407	344	362
Sabya	1966-75	MAX.	410	450	520	560	577	566	482	468	520	482	471	477
		MEAN	363	403	480	526	539	503	435	451	475	466	395	371
		MIN.	311	356	427	446	491	473	357	378	409	411	340	316

AIR-HUMIDITY (%)

STATION			JAN	FEB	MAR	APR	MAY	JUN	JUL	AUG	SEP	OCT	NOV	DEC
Abha	1984-87	MAX. (%)	89	90	99	96	96	33	30	40	27	55	64	95
		MEAN (%)	34	30	34	36	23	13	12	15	15	16	25	36
		MIN. (%)	25	24	24	22	17	11	10	12	12	14	19	25
Habawnah	1966-75	MAX. (%)	83	77	75	77	68	55	63	68	64	66	77	72
		MEAN (%)	59	59	57	59	49	42	47	51	45	46	53	50
		MIN. (%)	46	43	40	44	41	30	34	37	34	37	42	41
Malaki	1966-75	MAX. (%)	70	68	68	64	58	61	60	69	67	64	65	62
		MEAN (%)	60	65	60	54	51	52	52	60	59	61	59	55
		MIN. (%)	52	59	43	46	45	36	41	55	44	49	53	50
Sabya	1966-75	MAX. (%)	75	75	72	70	66	60	66	70	75	73	78	77
		MEAN (%)	70	69	67	62	60	59	56	62	65	63	63	69
		MIN. (%)	65	63	64	55	53	50	53	50	54	60	61	63

WIND SPEED (km/h)

STATION			JAN	FEB	MAR	APR	MAY	JUN	JUL	AUG	SEP	OCT	NOV	DEC
Abha	1966-75	MAX.	11.6	11	11.8	10.2	8.3	9.9	11	10.3	9	9.7	8	10
		MEAN	9.5	9.5	9.7	8.9	8	8.8	9.1	8.7	8.2	8	7.7	8.2
		MIN.	6.9	8	7.7	7.7	7.4	6.8	7.9	6.7	7	7.3	7	6.1
Habawnah	1984-87	MAX.	19.6	22	20.6	21.3	21.6	21	23	22.7	21.8	19.1	19.4	19.4
		MEAN	8.3	9.7	10.5	10.4	10.4	10	12	11	10.8	9.3	8.6	8.9
		MIN.	*	*	*	*	*	*	*	*	*	*	*	*
Malaki	1966-75	MAX.	7.2	8.3	8.4	9	8.4	9.2	10	9.6	7.9	8.9	7	7.1
		MEAN	6.5	7.4	7.7	7.9	8.1	8.3	8.8	8.2	7	6.9	6.3	6.9
		MIN.	5.9	6.3	7.1	7.2	7.7	7.7	7.6	7.2	6	6.7	6.1	5.6
Sabya	1966-75	MAX.	7.6	8.4	7.9	9.3	9.4	10	11	10.5	8.7	8.7	8.1	7.1
		MEAN	6.8	7.3	7.5	8	8.3	8.7	10	9.3	8.1	7.6	6.6	6.7
		MIN.	5.9	6	6.2	6.2	7.6	7.4	9.3	8	6.5	6.7	6	5

(*) not available

Table 3.2 Temperature data (in Celsius) for meteorological stations near the catchment area.

STATION KHAMIS MUSHAIT AIRPORT

Year		JAN	FEB	MAR	APR	MAY	JUN	JUL	AUG	SEP	OCT	NOV	DEC
1970-86	MAX	14.4	17.1	18.8	20.2	23.5	25.9	24.6	25.7	25.6	24.3	17.4	15.1
	MEAN	13.4	14.8	17.0	18.4	21.1	23.0	23.1	23.1	21.7	18.7	15.5	13.5
	MIN	12.1	12.3	14.8	17.1	18.8	21.1	21.5	21.5	19.7	17.2	14.4	12.3

STATION SIR LASAN (A-006)

Year		JAN	FEB	MAR	APR	MAY	JUN	JUL	AUG	SEP	OCT	NOV	DEC
1974-76	MAX	14.2	14.7	16.72	18.72	21.5	22.89	25.1	22.78	23.5	20.5	16.11	13.72
	MEAN	12.7	14.5	15.57	16.75	18.71	20.91	16.8	21.34	19.64	15.38	13.76	12.59
	MIN	10.9	10.3	13.39	14.22	13.22	18.5	21.4	19	16	11.89	12.39	9.89

STATION ABHA (A-101)

Year		JAN	FEB	MAR	APR	MAY	JUN	JUL	AUG	SEP	OCT	NOV	DEC
1970-86	MAX	14.3	15.6	16.39	19.61	20.28	22.39	24.2	23.89	21.89	18.39	15.78	14.22
	MEAN	10.8	11.9	15.5	17.1	19.6	22.1	22.1	21.5	20.7	17.2	14.7	12.9
	MIN	9.5	9.61	14.61	14.5	17.11	16	19.6	18.22	18.61	14.39	14	11.61

STATION SERAT ABIDAH

Year		JAN	FEB	MAR	APR	MAY	JUN	JUL	AUG	SEP	OCT	NOV	DEC
1982-86	MAX	15.3	15.3	17.8	18.9	21.0	22.2	24.6	23.7	22.5	18.7	15.3	14.6
	MEAN	12.8	13.5	16.4	17.5	20.3	21.7	22.7	23.0	21.5	17.7	14.7	13.1
	MIN	11.7	12.0	15.2	17	18.5	20.7	21.4	21.9	20.4	17.0	13.2	12.1

STATION NAJRAN AIRPORT

Year		JAN	FEB	MAR	APR	MAY	JUN	JUL	AUG	SEP	OCT	NOV	DEC
1977-86	MAX	19.1	21.4	24.2	27.3	29.3	34.5	35.8	37.2	33.6	29.9	22.5	19.4
	MEAN	17.2	18.9	23.1	25.9	28.6	30.8	32.0	31.8	28.5	23.5	19.9	16.9
	MIN	16.0	16.4	22.1	24.7	27.4	30	29.4	30.9	26.8	21.6	18.0	14.9

STATION NAJRAN

Year		JAN	FEB	MAR	APR	MAY	JUN	JUL	AUG	SEP	OCT	NOV	DEC
1974-76	MAX	18.3	20.0	23.3	25.7	28.0	28.3	31.2	31.4	27.5	22.3	18.9	17.0
	MEAN	16.1	17.8	21.3	24.2	26.4		30.7	29.6	26.2	21.0	17.0	15.4
	MIN	12.2	14.4	18.7	22.2	16.1	27.7	29.4	28.9	24.7	19.0	15.5	13.3

STATION SABYA (SA-002)

Year		JAN	FEB	MAR	APR	MAY	JUN	JUL	AUG	SEP	OCT	NOV	DEC
1970-86	MAX	27.4	29.3	30.5	33.2	34.7	34.7	36.0	35.4	37.5	33.7	39.8	28.0
	MEAN	26.3	27.1	28.5	31.1	33.5	34.0	34.9	34.3	33.7	31.3	28.9	25.5
	MIN	24.9	25.4	27.0	29.8	32.3	33.0	33.3	32.9	33.2	29.5	27.0	24.6

STATION MALAKI (SA-001)

Year		JAN	FEB	MAR	APR	MAY	JUN	JUL	AUG	SEP	OCT	NOV	DEC
1970-86	MAX	27.8	28.4	30.3	33.0	34.5	36.6	35.6	35.6	34.6	32.5	30.4	28.1
	MEAN	26.2	27.2	29.2	31.5	33.9	35.0	34.5	33.8	33.0	31.2	29.1	27.2
	MIN	24.7	25.0	27.0	30.1	32.4	32.5	32.0	31.5	31.8	29.6	27.2	26.2

STATION JIZAN AIRPORT (SA-001)

Year		JAN	FEB	MAR	APR	MAY	JUN	JUL	AUG	SEP	OCT	NOV	DEC
1970-86	MAX	27.0	27.6	28.8	30.9	33.0	34.3	34.5	33.9	33.7	33.8	29.6	27.5
	MEAN	25.4	26.0	27.6	29.9	32.0	33.0	33.1	33.0	32.4	30.9	28.6	26.1
	MIN	23.7	22.9	24.2	26.4	27.7	29.5	30.1	32.6	29.0	27.9	27.8	21.6

Table 3.3 The average values of potential evaporation and evapotranspiration of different stations and different altitudes

POTENTIAL EVAPORATION (PE)

Month	Sabya*	Malaki*	Abha*	Sarat Abidah*	Habawnah**
	mm	mm	mm	mm	mm
JAN	172	201	136	54	289
FEB	183	227	156	55	321
MAR	251	280	212	79	322
APR	300	359	215	88	371
MAY	354	386	256	116	359
JUN	359	367	304	124	344
JULY	375	377	297	138	363
AUG	346	320	255	133	363
SEP	310	288	288	114	363
OCT	302	296	246	82	360
NOV	216	220	175	63	329
DEC	186	215	137	54	285
Mean	279	295	223	92	339
Sum	3352	3536	2678	1100	4070
mm/day	9	10	7	3	11

POTENTIAL EVAPOTRANSPIRATION (PT)

Month	Sabya*	Malaki*	Abha*	Sarat Abidah*	Habawnah**
	mm	mm	mm	mm	mm
JAN	127	124	34	10	90
FEB	126	128	37	11	104
MAR	154	160	54	30	135
APR	177	181	66	34	186
MAY	199	203	89	36	171
JUN	199	199	109	15	210
JULY	206	206	110	11	222
AUG	198	196	104	14	207
SEP	182	181	90	5	207
OCT	170	170	65	6	162
NOV	144	145	46	2	147
DEC	131	134	37	3	108
Mean	168	169	70	15	162
Sum	2012	2025	839	177	1949
mm/day	6	6	2.3	0.5	5

(*) mean values of monthly record of 16 years)

(**) mean values of monthly record of 1 year)

Table 3.4 Rainfall data in and near the catchment areas of Wadi Baysh and Wadi Habawnah.

Wadi Baysh rainfall mean data (in mm)

Station No.	Latitude N	Longtitude E	Elevation (m)	Year record	JAN mean	FEB mean	MAR mean	APR mean	MAY mean	JUN mean	JUL mean	AUG mean	SEP mean	OCT mean	NOV mean	DEC mean	Annual mean
SA-145	17° 37' 00"	42° 48' 00"	600	1972-76*	73.3	46.3	47.2	66	57.3	18.4	16.9	16.4	15.6	18.6	62.9	95.4	582.8
SA-126	17° 27' 00"	42° 53' 00"	540	1967-84	24.3	35.3	18.8	28.8	68.4	43.9	67.5	108.2	97.9	96.3	50	29.5	668.7
SA-129	17° 10' 00"	42° 54' 00"	150	1967-84	11.4	3.4	17	5.2	15.6	9.5	74.6	69.8	49.6	35.4	14.4	6.5	312.5
SA-107	17° 07' 00"	42° 47' 00"	70	1966-84	11.6	4.1	13.4	8	3.2	4	38.6	26.2	21.8	29.6	8.9	12	181.4
SA-101	16° 58' 00"	42° 50' 00"	69	1960-84	13.9	5.8	13.2	6.7	13	1.5	35.9	40.3	24.7	22	12.8	16.1	206.1
SA-002	17° 10' 00"	42° 37' 00"	40	1966-84	7	3.3	6.1	3.4	5.9	0	27.8	7.1	13	17.3	6.8	7.2	105
SA-127	17° 16' 00"	42° 45' 00"	110	1967-84	18.8	16	9.5	3.3	8.4	5.3	42.5	27.5	36.4	22.5	15	11.6	217
SA-103	17° 31' 00"	42° 42' 00"	190	1966-84	19.3	13.3	2.4	5.8	3.6	10.1	44.1	24.1	26.2	27	27.6	20.4	223.8
SA-204	17° 34' 00"	42° 36' 00"	200	1970-84	20.5	7.4	9.4	7.9	11.3	6.4	20.5	31.3	29.1	30.7	9.7	22.3	194.2
SA-124	17° 34' 00"	42° 37' 00"	200	1967-84	19.2	7.4	8.5	7.2	11	12.3	24.9	27.9	24.5	26.8	11.5	19.8	201
SA-125	17° 08' 00"	42° 27' 00"	5	1967-84	10.1	6.2	7.7	1.5	3.4	0.3	9.3	6.1	3.6	13.9	7.8	7.6	77.5
A-118	18° 15' 00"	42° 22' 00"	2820	1965-84	25.8	46.8	50	69.4	87.1	22.3	42.1	75.4	21	18.5	32.5	15.6	506.5
A-210	18° 11' 00"	42° 25' 00"	2670	1967-84	34.3	29.2	45.8	65.5	60.7	24.4	45.8	54.5	5.5	12.3	45.6	18.2	441.9
A-001	18° 12' 00"	42° 29' 00"	2200	1966-84	25.5	40.9	57.8	59.4	48.9	14	42.9	40.6	5.2	10.3	17.5	7.9	370.8
A-101	18° 13' 00"	42° 29' 00"	2190	1960-84	27.3	29.6	52.9	80.5	37.3	16	36.2	38.6	2.7	3	38.2	16.9	379.2
A-006	18° 15' 00"	42° 36' 00"	2100	1982-84	6.5	120.1	31.3	36.3	31.9	3.8	7.7	24.3	0.3	3.3	5.8	10.4	218.6
A-123	18° 19' 00"	42° 54' 00"	1900	1965-84	6.1	10.1	25.9	38.1	35	4.9	17.1	18.3	2.7	1.2	9.3	3.5	172.4
A-105	18° 14' 00"	43° 11' 00"	2060	1967-84	3	6.8	21.3	26.5	20.3	1.4	5.8	1.4	0	1.4	3.6	2.5	93.8
SA-001	17° 03' 00"	42° 57' 00"	190	1962-84	14.2	4.8	11.9	10	17	8.6	62.8	114.7	51.9	39.6	24.2	3.8	363.5
A-103	18° 06' 00"	42° 47' 00"	2100	1965-84	17.4	40.7	43	55.4	59.7	12.9	22.4	54.1	7.6	4.3	12	6.4	335.8
A-121	18° 02' 00"	42° 45' 00"	2300	1965-84	37.7	46.7	64.3	70.4	72.8	15	29.2	47	10.7	16.3	26.9	15.9	452.9
SA-110	17° 16' 00"	43° 08' 00"	860	1960-84	33.6	33	34.2	73.5	66.6	47.7	84.7	93.6	48.8	28.4	37	40.9	622
SA-112	17° 12' 00"	43° 03' 00"	800	1960-84	34.4	33.6	34.3	69.6	61.7	46.7	76	84.2	46.4	29.5	36.3	39.9	592.5
SA-111	17° 03' 00"	43° 07' 00"	900	1960-84	34.6	24.3	14.2	39.9	44.8	53.4	105.2	99.6	52	32.5	56.5	63.5	615.7
SA-104	17° 03' 00"	43° 05' 00"	223	1964-84	18.1	12.3	7.5	25	33.1	37.9	70.8	82.5	63.6	43.1	41.2	25.3	460.4
A-213	18° 10' 00"	42° 50' 00"	2030	1966-84	10	30.5	35.8	33.6	23.6	12.3	15.9	23	3.4	4.1	11.1	6.8	210.1
SA-201	18° 02' 00"	42° 29' 00"	820	1968-73	23.4	15.1	29.1	33.3	30.1	11.5	8.2	19.5	13.5	11.9	11.7	5.1	212.4
SA-210	17° 19' 00"	43° 02' 00"	305	1968-71	26.8	14.9	31.4	65.5	51.4	34.2	68.9	58.8	44.4	20.1	27.6	19.6	463.5
SA-252	17° 43' 00"	43° 20' 00"	2200	1984-87	11.2	2.2	29.7	60.3	37.3	9.8	0.4	13.0	0.0	0.2	4.7	6.5	175.0
JAIZAN	16° 52' 00"	42° 35' 00"	3	1970-84	13.5	0.8	11.4	4.8	4.3	0.5	2.5	6.6	5.8	14.2	3.3	16.8	84.6

Continued on next page

Table 3.4 continued

Wadi Habawnah rainfall mean data (in mm)

Station No.	Latitude N	Longtitude E	Elevation (m)	Year record	JAN mean	FEB mean	MAR mean	APR mean	MAY mean	JUN mean	JUL mean	AUG mean	SEP mean	OCT mean	NOV mean	DEC mean	Annual mean
N-217	18° 05' 00"	44° 03' 00"	1340	1984-87	0.6	1.0	10.1	34.3	6.6	0.6	0.0	0.2	0.1	0.0	0.2	1.1	54.6
N-219	18° 03' 00"	44° 53' 00"	1460	1984-87	2.5	0.0	16.7	53.7	6.0	0.1	0.5	0.5	0.2	0.0	0.0	0.3	80.3
N-220	18° 00' 00"	44° 15' 00"	1306	1984-87	1.7	0.0	7.6	25.0	7.5	0.1	0.0	0.1	0.0	0.0	0.0	0.3	42.2
N-223	17° 58' 00"	44° 00' 00"	1300	1984-87	3.6	0.0	11.1	36.4	8.1	0.0	0.7	0.9	0.4	0.0	0.0	0.6	61.7
N-224	17° 52' 00"	44° 23' 00"	1250	1984-87	2.5	0.0	9.2	26.7	5.2	0.0	0.7	0.0	0.0	0.0	0.0	0.7	44.8
N-229	17° 49' 00"	43° 46' 00"	1300	1984-87	4.6	0.0	12.3	41.9	9.1	0.0	0.1	0.3	0.1	0.0	0.0	0.2	68.4
N-230	17° 45' 00"	44° 25' 00"	1160	1984-87	0.4	0.0	12.9	27.1	4.7	0.0	0.0	0.2	0.0	0.0	0.0	1.4	46.5
N-233	17° 44' 00"	43° 48' 00"	1360	1984-87	4.3	1.7	9.3	47.9	7.2	4.5	0.8	1.2	1.4	0.0	0.0	0.8	78.9
N-236	17° 38' 00"	44° 32' 54"	1400	1984-87	7.8	1.0	10.6	46.7	9.0	0.0	0.0	0.1	0.1	0.0	0.0	0.4	75.5
N-237	17° 40' 00"	44° 05' 00"	1400	1984-87	4.2	0.2	12.8	30.2	7.4	0.0	0.0	0.6	0.0	0.0	0.0	0.6	55.9
N-239	17° 40' 00"	43° 45' 00"	1500	1984-87	5.9	0.5	8.7	69.7	7.9	4.7	1.0	1.2	1.5	0.3	0.0	2.1	103.1
N-215	18° 07' 00"	43° 48' 00"	1600	1984-87	4.8	0.8	19.5	27.3	2.5	0.1	0.0	0.2	0.1	0.0	0.0	0.3	55.5
N-216	18° 05' 00"	43° 42' 00"	2120	1984-87	6.0	0.2	14.9	59.3	12.9	0.9	0.6	2.1	0.0	0.0	0.0	0.4	97.0
N-221	18° 22' 00"	43° 50' 00"	1630	1984-87	3.2	0.1	17.4	47.2	5.5	1.0	0.7	0.1	0.0	0.0	0.0	0.3	75.3
N-226	17° 57' 00"	43° 40' 00"	1980	1984-87	3.8	0.1	10.2	80.1	12.8	0.2	1.6	1.6	1.1	0.0	0.0	0.7	112.0
N-227	17° 56' 00"	44° 33' 00"	2320	1984-87	13.3	0.1	21.4	40.3	21.5	2.4	0.3	1.8	0.2	0.0	4.5	1.4	107.0
N-232	17° 46' 00"	43° 32' 00"	2200	1984-87	10.7	2.0	20.5	9.6	39.0	5.0	1.8	9.9	2.1	0.8	2.0	3.9	107.1
N-235	17° 45' 00"	43° 38' 00"	1620	1984-87	2.8	0.0	8.8	49.0	12.6	0.1	1.5	0.5	0.1	0.0	0.0	1.2	76.4
N-238	17° 33' 00"	43° 30' 00"	2140	1984-87	5.8	2.0	34.6	59.9	30.8	1.0	1.1	5.5	0.3	0.0	0.3	7.3	148.4
N-240	17° 35' 00"	43° 52' 00"	1770	1984-87	6.1	0.8	20.4	42.4	11.6	0.3	0.2	0.4	0.0	0.0	0.0	1.2	83.1
N-243	17° 34' 00"	43° 42' 00"	2080	1984-87	6.1	0.7	17.1	34.3	19.5	0.8	7.0	2.9	0.0	0.0	0.0	2.5	90.7
N-213	18° 02' 00"	42° 29' 00"	1880	1984-87	3.6	1.8	20.5	26.6	12.5	0.0	0.1	1.7	0.1	0.0	0.0	0.2	67.0
NAJAIR"	17° 33' 00"	44° 14' 00"	1250	1970-84	2.8	8.1	22.6	17.5	4.6	0	1.5	1.8	0	8.1	0.5	3.8	71.3
NAJRAN	17° 29' 00"	44° 26' 00"	1210	1970-84	2.5	3	21.6	21.6	4.6	0	0.3	9.1	0	10.7	6.6	0.3	111.4
A-207	18° 10' 00"	43° 06' 00"	2400	1966-84	16	35.8	48.2	43.9	38.2	4.3	19.6	17.6	1.6	3.5	9.9	5.9	244.2
A-104	17° 56' 00"	43° 22' 00"	2250	1966-84	16	26	45.2	44.3	33.2	0	16.5	15	0	4.6	8.7	3.6	213.3
N-103	17° 40' 00"	43° 38' 00"	2020	1964-84	11.9	17.5	34.9	54.7	31	1.3	16	19.1	0.4	5.6	4.4	8.9	205.7

(*) 1972-76/1980-1984

(") Najran airport

Table 3.5 Monthly runoff data within the catchment areas of Wadi Baysh and Wadi Habawnah

Wadi Baysh

Runoff data of Station SA-124 (elevation 200 m a.ms.l,catchment area 3511 km^2)

Year record	JAN mcm	FEB mcm	MAR mcm	APR mcm	MAY mcm	JUN mcm	JUL mcm	AUG mcm	SEP mcm	OCT mcm	NOV mcm	DEC mcm	Annual mcm
1970	0.61	1.16	6.45	0.581	0.189	0.091	4.05	3.43	5.29	0.199	0.052	0.044	22.1
1971	0.123	0.029	0.13	29.6	20.7	4	14.9	5.7	3.28	0.53	5.04	1.5	85.5
1972	0.492	5.49	20.1	48.5	13.9	9.76	11.1	9.2	4.95	5.3	2.92	2.37	134.1
1973	10	1.6	0.994	2.57	2.79	0.337	9.69	8.48	5.27	0.429	0.527	3.11	45.8
1974	0.586	0	16.1	6.12	13.6	7.87	15.5	12.3	6.76	4.3	1.54	2.47	87.1
1975	2	2.97	3.16	26.5	2.73	3.76	2.84	25.2	2.83	2.43	1.22	1.24	76.9
1976	1.34	0.903	6.48	4.32	4.78	3.07	5.13	5.24	5.32	3.83	4.04	0.333	45.4
1977	4.98	0.643	0.656	2.79	5.04	3.04	3.76	3.77	2.77	3.91	5	0.295	36.7
1978	7.94	2.72	1.93	1.7	2.42	1.05	3.13	7.08	3.03	2.12	1.04	0.939	35.1
1979	4.09	2.86	2.86	3.59	7.23	3.85	3.12	4.94	3.25	1.45	0.556	2.3	40.1
1980	0.748	1.3	1.13	3.88	7.78	4.85	9.7	4.93	1.6	1.13	0.294	0.645	38.0
1981	0.408	0.24	21.2	5.94	27.1	8.05	9.77	6.92	8.46	4.88	1.42	1.36	95.7
1982	6.05	26.5	13.4	18.7	7.43	6.44	7.29	12.4	7.22	5.95	4.73	5.06	121.2
1983	1.94	24.7	12.1	32.2	17.5	17.6	15.6	12.5	7.05	3.29	3.08	3.38	150.9
1984	3.29	2.88	2.85	3.13	16	8.62	9.96	7.19	3.57	2.28	2.2	3.88	65.9
1985	6.45	3.7	3.9	18.54	13.43	9.95	15.03	13.09	6.1	6.87	7.48	6.54	111.1
Average	3.19	4.856	7.09	13.04	10.16	5.771	8.786	8.898	4.797	3.056	2.571	2.25	74.5

Wadi Habawnah

Runoff data of Station N-408 (elevation 1452 m a.ms.l,catchment area 1307 km^2)

Year record	JAN mcm	FEB mcm	MAR mcm	APR mcm	MAY mcm	JUN mcm	JUL mcm	AUG mcm	SEP mcm	OCT mcm	NOV mcm	DEC mcm	Annual mcm
1984	0	0	0	0	0.188	0	0	0	0	0	0	0	0.2
1985	1.122	0	0.35	6.259	3.549	0.235	0.062	0	0	0	0	0	11.6
1986	0	0.041	1.667	12.382	1.356	0.039	0.005	0.095	0	0	0	0	15.6
Average	0.374	0.014	0.672	6.214	1.698	0.091	0.022	0.032	0	0	0	0	9.1

Runoff data of Station N-404 (elevation 1339 m a.ms.l,catchment area 2391 km^2)

Year record	JAN mcm	FEB mcm	MAR mcm	APR mcm	MAY mcm	JUN mcm	JUL mcm	AUG mcm	SEP mcm	OCT mcm	NOV mcm	DEC mcm	Annual mcm
1984	0	0	0	0.225	0.292	0.074	0	0	0	0	0	0	0.6
1985	0.682	0	0.286	9.16	2.708	0.061	0	0	0	0	0	0	12.9
1986	0	0	0.972	14.119	1.448	0.007	0.069	0	0	0	0	0	16.6
Average	0.227	0	0.419	7.835	1.483	0.047	0.023	0	0	0	0	0	10.0

Runoff data of Station N-405 (elevation 1303m a.ms.l,catchment area 940 km^2)

Year record	JAN mcm	FEB mcm	MAR mcm	APR mcm	MAY mcm	JUN mcm	JUL mcm	AUG mcm	SEP mcm	OCT mcm	NOV mcm	DEC mcm	Annual mcm
1984	0	0	0	0.417	0	0	0	0	0	0	0	0	0.4
1985	0	0	0.041	5.067	0.621	0	0	0	0	0	0	0	5.7
1986	0	0	0.003	6.244	0	0	0	0	0	0	0	0	6.2
Average	0	0	0.015	3.909	0.207	0	0	0	0	0	0	0	4.1

Runoff data of Station N-406 (elevation 1212m a.ms.l,catchment area 4425 km^2)

Year record	JAN mcm	FEB mcm	MAR mcm	APR mcm	MAY mcm	JUN mcm	JUL mcm	AUG mcm	SEP mcm	OCT mcm	NOV mcm	DEC mcm	Annual mcm
1984	0	0	0.091	0	0	0	0	0	0	0	0	0	0.1
1985	0.105	0	0	15.813	1.103	0	0	0	0	0	0	0	17.0
1986	0	0.016	0.295	11.068	0	0	0	0	0	0	0	0	11.4
Average	0.035	0.005	0.129	8.96	0.368	0	0	0	0	0	0	0	9.5

Runoff data of Station N-407 (elevation 1166m a.ms.l,catchment area 4682 km^2)

Year record	JAN mcm	FEB mcm	MAR mcm	APR mcm	MAY mcm	JUN mcm	JUL mcm	AUG mcm	SEP mcm	OCT mcm	NOV mcm	DEC mcm	Annual mcm
1984	0	0	0	0	0	0	0	0	0	0	0	0	0.0
1985	0.454	0	0	5.313	0.173	0	0	0	0	0	0	0	5.9
1986	0	0	0.232	5.122	0	0	0	0	0	0	0	0	5.4
Average	0.151	0	0.077	3.478	0.058	0	0	0	0	0	0	0	3.8

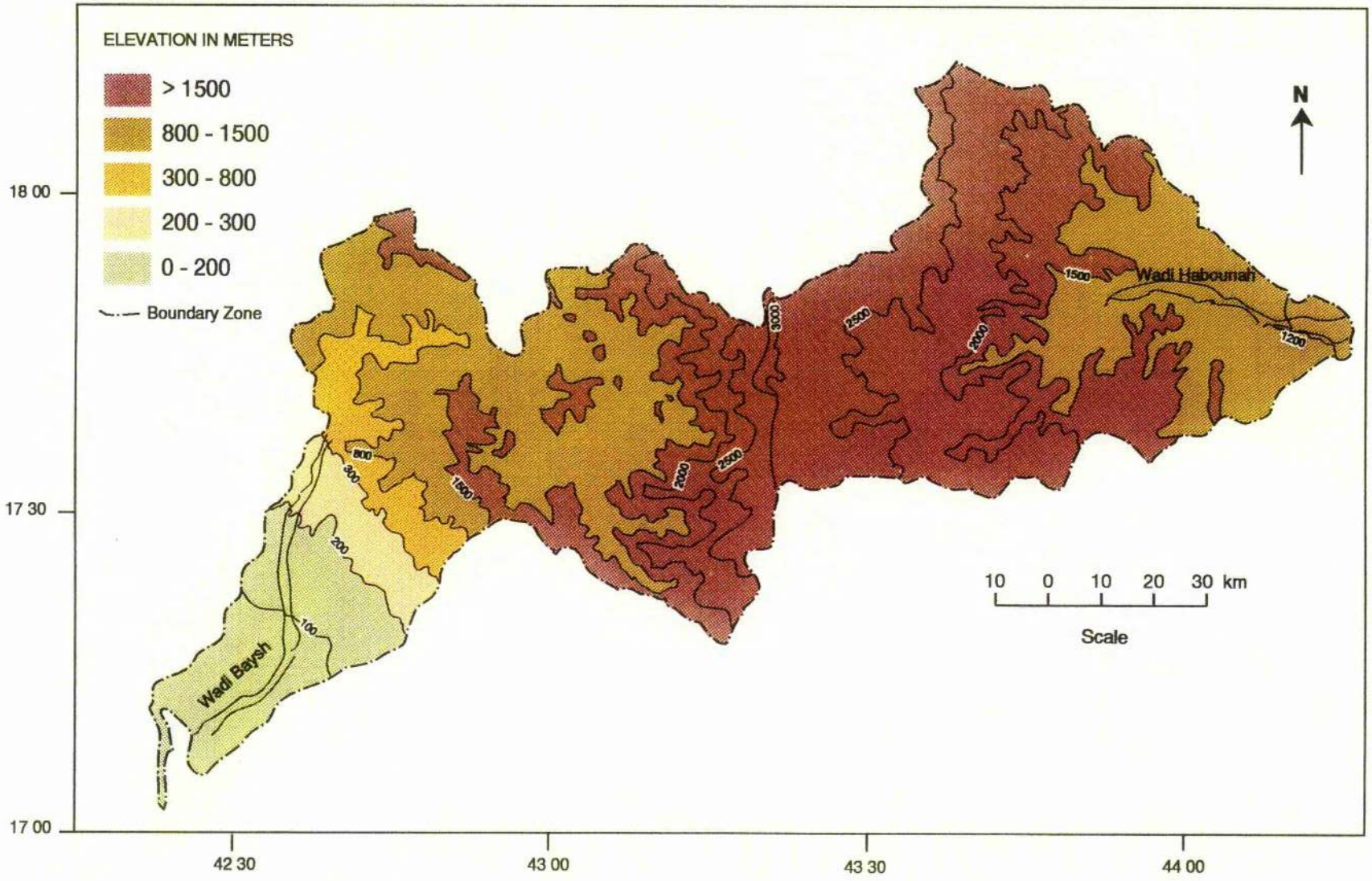

Figure 3.3 Topographic map of Wadi Baysh (flowing towards the southwest) and Wadi Habawnah (flowing towards the east) south of Arabian Shield Saudi Arabia.

The precipitation shows a large annual and geographic variation. The large variation from year to year results from the effect of the cyclonic and monsoon wet systems. The large geographical variations are due to orographic effects.

The mean annual precipitation is 400 mm on the scarp slope of the Asir Mountains and 175 mm on the dip slope. Mean rainfall decreases with distance from the crest of the escarpment as altitude decreases. However, the mid-south of the Wadi Baysh catchment area has a high mean rainfall of 622 mm. An isohyet map (see Figure 3.20) was drawn using mean monthly rainfall values (Table 3.4).

The main aim of this chapter is to investigate how much water flows to the lower part of the wadis where the agricultural area is located. The first section describes the climatic parameters in both wadis. The second section discusses the rainfall characteristics of both wadis and studies rainfall seasonality and rainfall-runoff relationships. The high quality of the data resulting from the relatively high rain gauge density and long record makes it easy to determine the rainfall - runoff characteristics in the region. The available data were analysed both graphically and statistically. The third section studies the probability of floods using the historical records of floods in both wadis.

3.2 Section One: Climate

3.2.1 Climatic Conditions

The climatic conditions of the catchment areas of both wadis are influenced by the topography of the region and its proximity to the Red Sea on the west side and its nearness to the Empty Quarter Desert on the east side. The meteorological data consist of temperature, solar radiation, sunshine, air humidity, wind speed and evaporation information and have been adapted from the data manual known as the Climatic Water Balance in Saudi Arabia (Al-Jerash 1989) (see Table 3.1, 3.2 and 3.3).

Taha *et al.* (1981) indicated that the south-west of Arabia can be divided into three main climatic types:

1- The warm, rainy climatic type with a dry winter which prevails in the Asir Mountains.

2- The hot steppe climatic type which prevails on the plateau.

3- The hot desert climatic type which prevails in the Red Sea coast area.

As a result of the catchments being situated in the south-west of Saudi Arabia, the climate is influenced by the interaction of local circulation and the general circulation of the surrounding regions.

There are two different mean annual precipitations of 400 mm for the western scarp slope and 175 mm for eastern dip slope. However, the rainfall decreases sharply to the west and east of the crest, sharing a close correlation with altitude. The study area is characterised by high air temperatures during the summer with mean annual temperatures exceeding 24°C throughout the lowland areas. The average temperature is less than 20°C in the Asir Mountains. The average wind speed at the Asir escarpment is 6-12 km/hr while in the lower part of Wadis Baysh and Habawnah it is 6 to 10 and 19 to 23 km/hr, respectively. The major winds blow from the south-west and south-east. The relative humidity ranges between 56% and 70% in the coastal areas. In the interior of the study area the relative humidity is between 46% and 59%. (Table 3.1)

The greatest sunlight intensity in the summer ranges between 493 and 584 cal/cm^2/day in Wadi Habawnah and between 363 to 539 cal/cm^2/day in Wadi Baysh

(Table 3.1). Both solar radiation and temperature can be related to elevation in the region. The average number of sunshine hours is distributed fairly evenly throughout the year. The daily average for Wadi Baysh is 9 hours which is slightly less than that for Wadi Habawnah which varies between 8.3 and 10.3 hours (Table 3.2).

The monthly average for evaporation is 279 mm at Sabya, 295 mm at Malaki, 223 mm at Abha and 484 mm at the Habawnah meteorological station (Table 3.3).

In addition to the influence of topography, the climate is influenced by different air mass systems (Figure. 3.4).

3.2.1.1 Air Masses

Al-Qurashi (1981) indicates that the south-west of Arabia is influenced mainly by four air masses during the year as follows:

1- Polar continental air mass (cp)

2- Modified polar continental air masses (mcp) are found over central Asia and Europe, respectively, during the winter season. The (mcp) is cold and dry air, modified as it travels across the Mediterranean it picks up moisture and forms small amounts of cloud.

3- Tropical continental air (ct) originates in the Sahara in the summer, late spring, and early autumn (Taha *et al.*, 1981). It is characterised by hot and dry air and moves from west to east over the northern Red Sea.

4- The maritime tropical air mass (MT) is associated with depressions of maritime tropical air from the Indian Ocean and the Red Sea. The major air mass influencing the southern region, it is characterised by warm moist air. It brings the majority of the rainfall to the region.

3.2.1.2 Climatic Seasons of the Area

ITALCONSULT (1973) reported that the south-west of Saudi Arabia, situated between a sub-tropical belt of high pressure and the tropics, in front of the mountains of Africa, is under the influence of the intertropical front and the humid atmosphere from the Indian Ocean. During the northern winter the intratropical front is in the southern

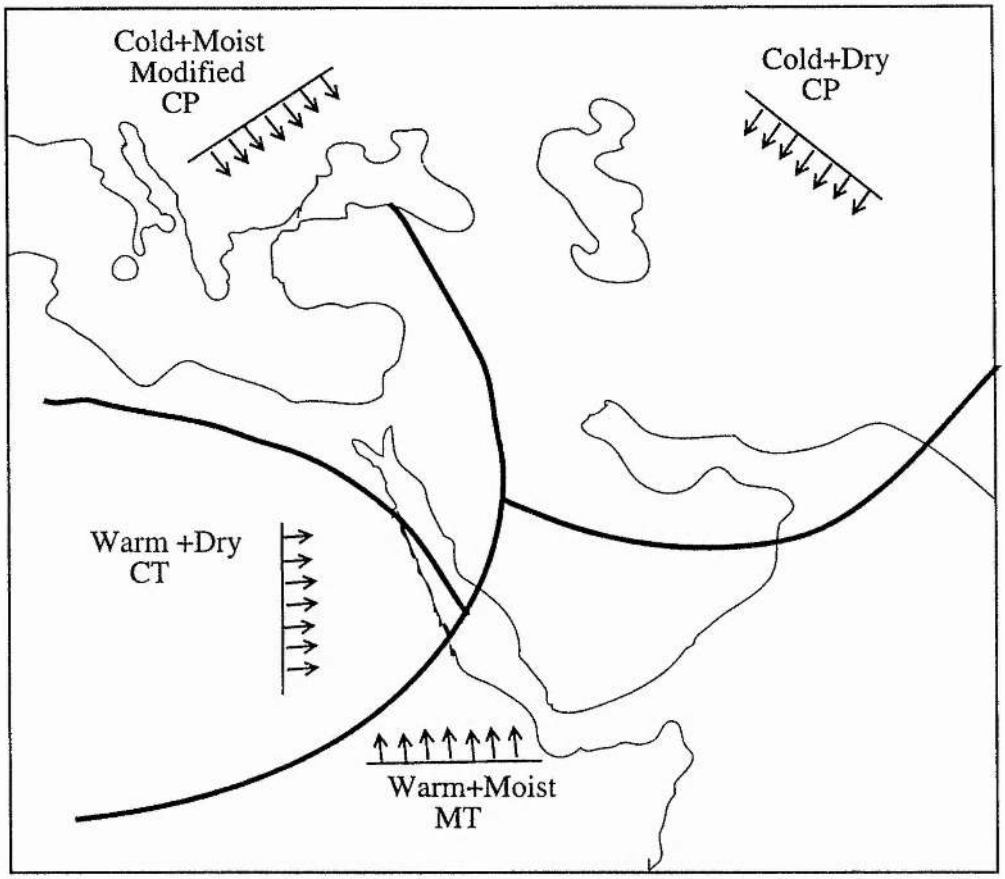

Figure 3.4 Different air mass systems influence the Arabian Peninsula climate (modified from Al-Qurashi, 1981).

hemisphere and there is a balance between the continental air masses and the humid air masses from the Indian Ocean. The continental air masses, cold and only slightly humid, do not bring much rain. During the summer the northern intratropical front moves towards the north and humid air masses from the Indian Ocean, pushed by south-east winds, influenced by the Ethiopian mountains, arrive from the west in the southern part of Saudi Arabia and bring rain. The climate varies from season to season as a result of the different air masses achiving dominance.

Alehaideh (1985) explained the seasonal climate of the south-west of Saudi Arabia based on the interpretation of Hastenrath *et al.* (1979) as follows:

In winter (December-February) the northerly flows (Figure 3.5) influence the region in which the westerly Mediterranean air is associated with depressions that move across northern Arabia. The Red Sea convergence is found over the southern Red Sea. The westerly flow moves into the Red Sea trough and causes orographic rainfall on the mountains. In spring (March-May), the flow patterns are less marked compared to the winter season (Figure 3.5). The north-east monsoon over the region is less uniform, while the south-easterly monsoon flow becomes the main influence. The Red Sea convergence zone is still in existence and, associated with the south-easterly monsoon flow, will produce widespread rainfall over the area.

During summer (June-August), the flow pattern is well-defined. Hastenrath *et al.* (1979), indicate that two major air mass flows dominate the region, the south-west monsoon flow from the equator and the north-easterly flow from the north over Arabia. These two air masses merge together along an extended confluence zone over the Gulf of Aden and the South of Arabia. In the summer, the south-west of Saudi Arabia comes under the influence of a moist south-westerly air flow which brings rainfall to the area.

In autumn (October-November), the flow pattern is less distinctive. The north-westerly flow continues while the south-westerly monsoon flow retreats.

3.2.1.3 Relationship between Altitude and Rainfall

Rainfall in the highlands is greater than in the lowlands (Pacl 1973). Critchfield (1974) explained that the maximum annual rainfall occurs where mountain barriers lie

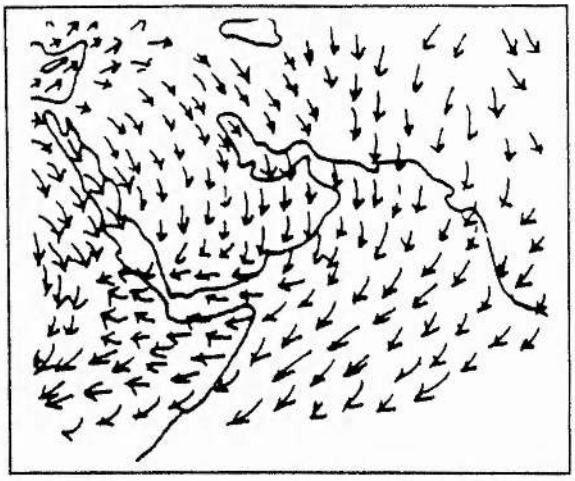

JANUARY

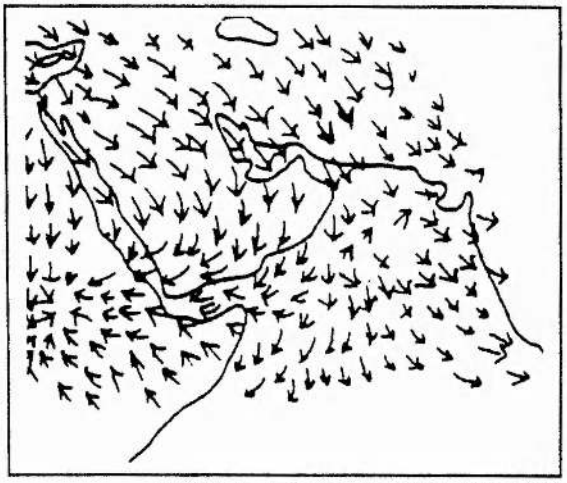

APRIL

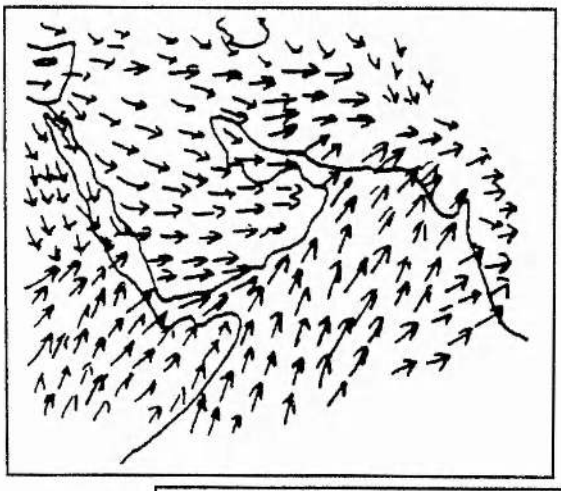

JULY

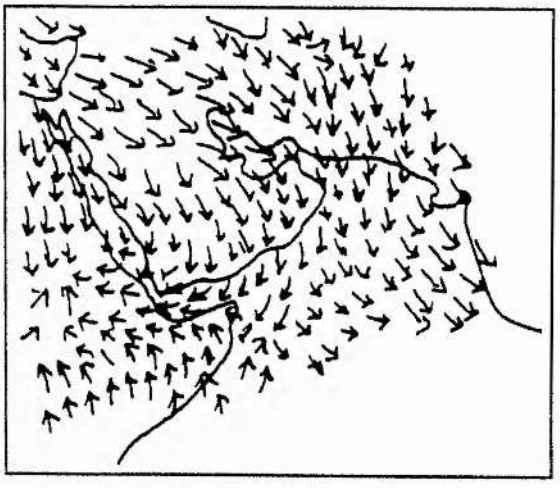

OCTOBER

Figure 3.5 Air flow variation across the Arabian Peninsula (after Hastenrath, et al., 1979)

across the path of moisture-bearing winds.

Sawyer (1956) indicated that there are three factors which influence the orographic precipitation:

1- airmass characteristics and pressure patterns

2- local vertical motion due to terrain

3- microphysical processes in the cloud and evaporation of falling drops.

In Tanzania, Barry (1992) shows that the annual rainfall total exhibits an increase with elevation. However, at very high elevation, the rainfall decreases. Nieuwold (1974) indicates that such phenomena may occur where the depletion of the atmospheric water becomes a limiting factor.

There are two maximum zones of rainfall in Wadi Baysh which show a positive correlation of rainfall with elevation (Figure 3.6a and Table 3.6). The first maximum zone of rainfall is located near sea-level up to an elevation of 0.9 km while the second zone is between the elevation 1.9 and 2.82 km. In the first zone, the maximum rainfall occurs between an elevation of 0.5 km and 0.9 km and is characterised by high intensity with low variation (Figure 3.7a) where annual rainfall ranges between 550 and 650mm.

The Wadi Habawnah catchment shows similar characteristics and also shows a positive correlation between rainfall and elevation (1.3-2.5 km) but the rainfall intensity is low compared to Wadi Baysh (Figure 3.6b, c and Table 3.6). The lower part of the catchment area shows low rainfall intensity (>50 mm/yr) and low variation with elevation (Figure 3.7b). Mean annual rainfall generally increases with an increase in altitude. However, at low altitude in both wadis the rainfall shows less variation with an increase in elevation (Figure 3.7a, b). Further disction followes later in the chapter that shows that Arabian Shiled has a great influence on the rainfall distribution of the areafor .

When rainfall is correlated with altitude a correlation coefficient of +0.78 is obtained for Wadi Baysh and +0.76 for Wadi Habawnah (see Figure 3.6a, b), which indicates a similar relation between the rainfall and the elevation in both wadis.

There are 14 and 12 stations within and nearby Wadis Baysh and Habawnah

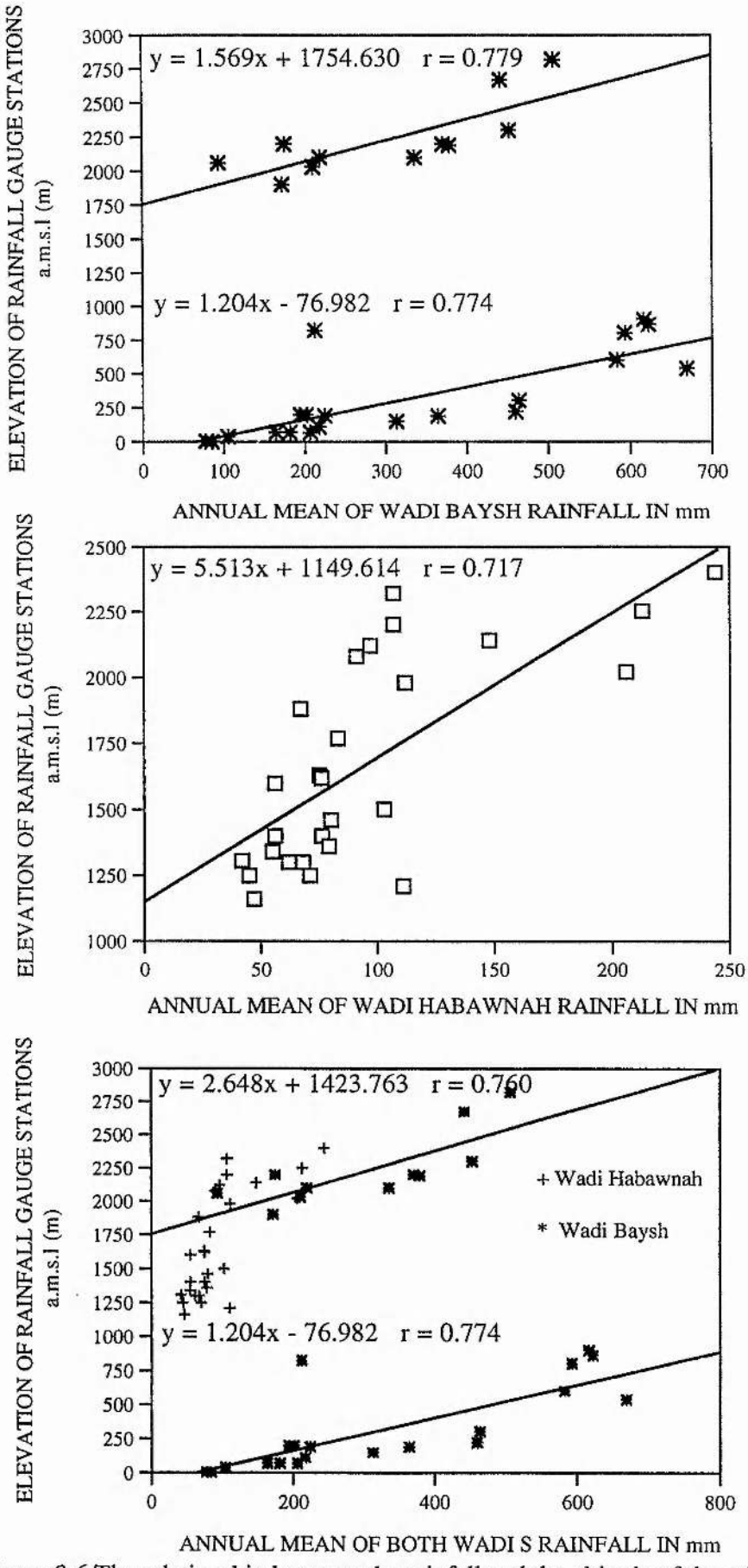

Figure 3.6 The relationship between the rainfall and the altitude of the rain gauge station in both wadis.

Table 3.6 The relationship between the mean annual rainfall (mm) and the altitude of the catchment areas of Wadi Baysh, Wadi Habawnah and the nearby area.

Wadi Baysh rainfall mean data (in mm) of upper part of the catchment area

Station No.	Elevat. (m)	Annual mean
A-118	2820	507
A-210	2670	442
A-121	2300	453
A-001	2200	371
SA-252	2200	175
A-101	2190	379
A-006	2100	219
A-103	2100	336
A-105	2060	94
A-213	2030	210
A-123	1900	172

Wadi Baysh rainfall mean data (in mm) of lower part of the catchment area

Station No.	Elevat. (m)	Annual mean
SA-111	900	616
SA-110	860	622
SA-201	820	212
SA-112	800	593
SA-145	600	583
SA-126	540	669
SA-210	305	464
SA-104	223	460
SA-204	200	194
SA-124	200	201
SA-103	190	224
SA-001	190	364
SA-129	150	313
SA-127	110	217
SA-107	70	181
SA-106	70	164
SA-101	69	206
SA-002	40	105
SA-125	5	78
JAIZAN	3	85

Wadi Habawnah rainfall mean data (in mm)

Station No.	Elevat. (m)	Annual mean
A-207	2400	244
N-227	2320	107
A-104	2250	213
N-232	2200	107
N-238	2140	148
N-216	2120	97
N-243	2080	91
N-103	2020	206
N-226	1980	112
N-213	1880	67
N-240	1770	83
N-221	1630	75
N-235	1620	76
N-215	1600	56
N-239	1500	103
N-219	1460	80
N-236	1400	76
N-237	1400	56
N-233	1360	79
N-217	1340	55
N-220	1306	42
N-223	1300	62
N-229	1300	68
N-224	1250	45
NAJAIR	1250	71
NAJRAN	1210	111
N-230	1160	47

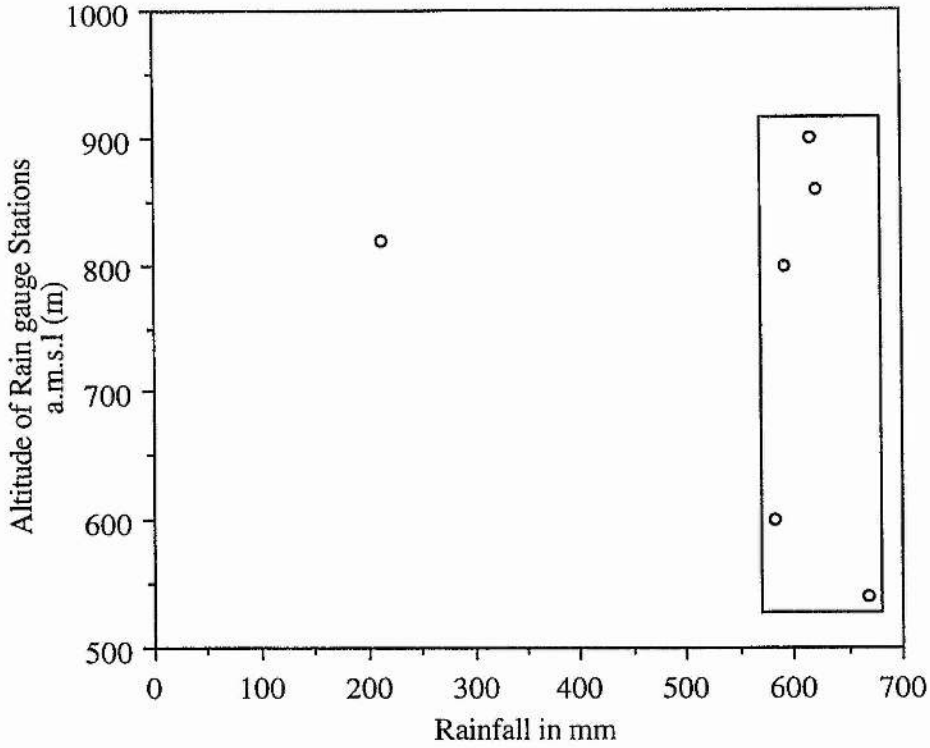

Figure 3.7a Rainfall (mm) versus the altitude of the rain gauge stations of Wadi Baysh (middle part of the catchment area).

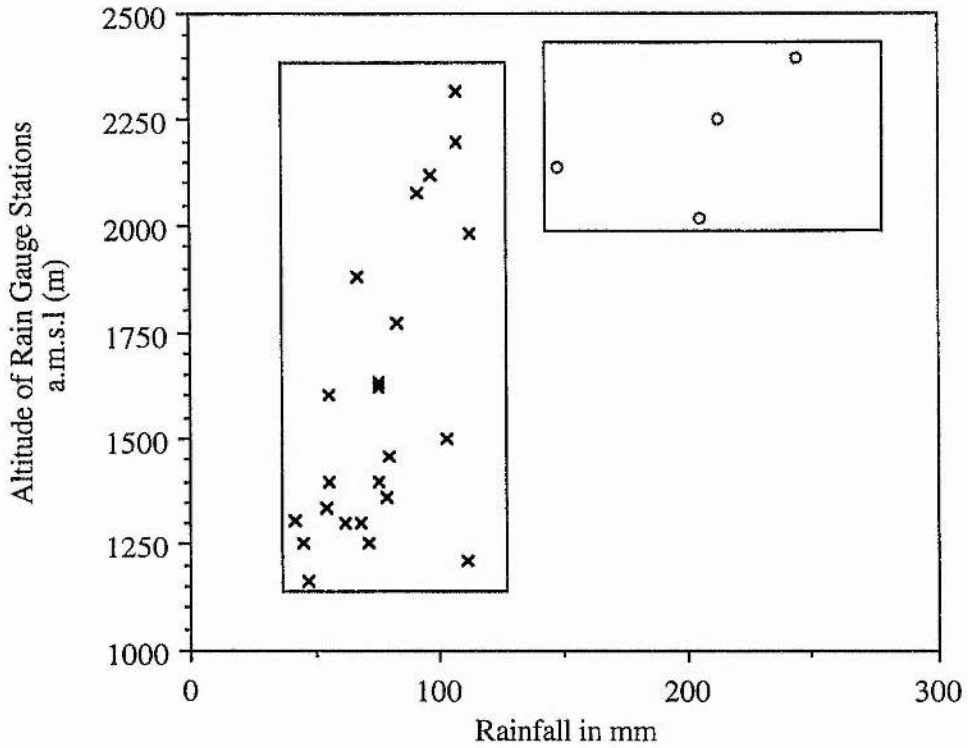

Figure 3.7b Rainfall (mm) versus the altitude of the rain gauge stations of Wadi Habawnah (lower, middle and upper part of the catchment area).

respectively. Table 3.7 and Figures 3.8a, b, 3.9 and 3.10 have been constructed to show the relationship between the annual rainfall and the elevation for those stations which are located either on the same longitude or latitude. Generally there is an increase in rainfall with elevation. However, Stations SA-204, and A-006 are at longitude 42° 36' and they have approximately similar annual rainfall (194 and 201 mm) but different elevations (200m and 2100m respectively). The station A-006 is located in the northern part of the study area, 75.6 km from station SA-204 in the south. Outside the catchment of Wadi Baysh, station A-213 in the north and station SA 101 to the south on the same line of longitude (42° 50) (Figure 3.7a and Table 3.7) have similar annual rainfalls (210 and 206 mm respectively) but different elevations (69 and 2030m respectively). These examples show that elevation is not the only factor affecting rainfall in the Wadi Baysh catchment area.

In Wadi Habawnah, the stations at high elevations receive high rainfall. However, there are two main zones of rainfall, approximately above and below the elevation 2050 m in the upper part of the catchment. At Stations N-227 and N-103 (at longitude 43° 31' and elevations of 2320 and 2020 m respectively) the latter site has an annual rainfall nearly double (206 mm) that of the former (107 mm). Stations N-216 and N-243 (at longitude 43° 42') have low annual rainfalls of 97 and 91 mm respectively despite their elevation above 2070 m. Stations located on longitudes 43°45, 43°48', 43°53' and 44°25' are characterised by relatively low annual rainfall, where located at elevations of above 1600 m when compared to sites below 1600 m. The rainfall distribution results from the airflow systems influencing the area. In winter this is a northern flow from the Mediterranean while in the summer it is a south-western flow.

In both wadis, stations located at the same latitude show high annual rainfall on higher ground. However, the stations of Wadi Baysh consist of two zones: the first zone consists of the stations at latitudes 17°03',17°10',17°16' and 18°02' which have relatively high rainfall (105 - 622 mm) but low elevations (between 40 and 900 m) while the second zone consists of the stations at latitudes 18°02' and 18°15' with high elevations

Table 3.7 Rainfall data within the catchment areas of Wadi Baysh and Habawnah

Wadi Baysh rainfall mean data (in mm)

Station No.	Latitude N	Longtitude E	Elevat. (m)	Year record	JAN mean	FEB mean	MAR mean	APR mean	MAY mean	JUN mean	JUL mean	AUG mean	SEP mean	OCT mean	NOV mean	DEC mean	Annual mean
SA-125	17° 08' 00"	42° 27' 00"	5	1967-84	10.1	6.2	7.7	1.5	3.4	0.3	9.3	6.1	3.6	13.9	7.8	7.6	77.5
SA-106	17° 22' 00"	42° 32' 00"	70	1967-84	14.9	13.7	8.7	6.2	5.2	4.2	26.5	26.1	10.5	19.6	8.6	20	164.2
SA-103	17° 31' 00"	42° 42' 00"	190	1966-84	19.3	13.3	2.4	5.8	3.6	10.1	44.1	24.1	26.2	27	27.6	20.4	223.8
SA-204	17° 34' 00"	42° 36' 00"	200	1970-84	20.5	7.4	9.4	7.9	11.3	6.4	20.5	31.3	29.1	30.7	9.7	22.3	194.2
SA-124	17° 34' 00"	42° 37' 00"	200	1967-84	19.2	7.4	8.5	7.2	11	12.3	24.9	27.9	24.5	26.8	11.5	19.8	201
SA-145	17° 37' 00"	42° 48' 00"	600	1972-76	73.3	46.3	47.2	66	57.3	18.4	16.9	16.4	15.6	18.6	62.9	95.4	582.8
SA-110	17° 16' 00"	43° 08' 00"	860	1960-84	33.6	33	34.2	73.5	66.6	47.7	84.7	93.6	48.8	28.4	37	40.9	622
SA-252	17° 43' 00"	43° 20' 00"	2200	1984-87	11.2	2.2	29.7	60.3	37.3	9.8	0.4	13.0	0.0	0.2	4.7	6.5	175.0
				Mean	25.3	16.2	18.5	28.5	24.5	13.6	28.4	29.8	19.8	20.6	21.2	29.1	280.1
				Maximum	73.3	46.3	47.2	73.5	66.6	47.7	84.7	93.6	48.8	30.7	62.9	95.4	622.0
				Minimum	10.1	2.2	2.4	1.5	3.4	0.3	0.4	6.1	0.0	0.2	4.7	6.5	77.5

Wadi Habawnah rainfall mean data (in mm)

Station No.	Latitude N	Longtitude E	Elevat. (m)	Year record	JAN mean	FEB mean	MAR mean	APR mean	MAY mean	JUN mean	JUL mean	AUG mean	SEP mean	OCT mean	NOV mean	DEC mean	Annual mean
N-219	18° 03' 00"	43° 53' 00"	1460	1984-87	2.5	0.0	16.7	53.7	6.0	0.1	0.5	0.5	0.2	0.0	0.0	0.3	80
N-223	17° 58' 00"	44° 00' 00"	1300	1984-87	3.6	0.0	11.1	36.4	8.1	0.0	0.7	0.9	0.4	0.0	0.0	0.6	62
N-229	17° 49' 00"	43° 46' 00"	1300	1984-87	4.6	0.0	12.3	41.9	9.1	0.0	0.1	0.3	0.1	0.0	0.0	0.2	68
N-230	17° 45' 00"	44° 25' 00"	1160	1984-87	0.4	0.0	12.9	27.1	4.7	0.0	0.0	0.2	0.0	0.0	0.0	1.4	47
N-233	17° 44' 00"	43° 48' 00"	1360	1984-87	4.3	1.7	9.3	47.9	7.2	4.5	0.8	1.2	1.4	0.0	0.0	0.8	79
N-236	17° 38' 00"	43° 58' 54"	1400	1984-87	7.8	1.0	10.6	46.7	9.0	0.0	0.0	0.1	0.1	0.0	0.0	0.4	76
N-237	17° 40' 00"	44° 05' 00"	1400	1984-87	4.2	0.2	12.8	30.2	7.4	0.0	0.0	0.6	0.0	0.0	0.0	0.6	56
N-239	17° 40' 00"	43° 45' 00"	1500	1984-87	5.9	0.5	8.7	69.7	7.9	4.7	1.0	1.2	1.5	0.3	0.0	2.1	103
N-215	18° 07' 00"	43° 50' 00"	1600	1984-87	4.8	0.8	19.5	27.3	2.5	0.1	0.0	0.2	0.1	0.0	0.0	0.3	55
N-216	18° 05' 00"	43° 42' 00"	2120	1984-87	6.0	0.2	14.9	59.3	12.9	0.9	0.6	2.1	0.0	0.0	0.0	0.4	97
N-221	18° 22' 00"	43° 48' 00"	1630	1984-87	3.2	0.1	17.4	47.2	5.5	1.0	0.7	0.1	0.0	0.0	0.0	0.3	75
N-226	17° 57' 00"	43° 40' 00"	1980	1984-87	3.8	0.1	10.2	80.1	12.8	0.2	1.6	1.6	1.1	0.0	0.0	0.7	112
N-232	17° 46' 00"	43° 29' 00"	2200	1984-87	10.7	2.0	20.5	9.6	39.0	5.0	1.8	9.9	2.1	0.8	2.0	3.9	107
N-235	17° 45' 00"	43° 38' 00"	1620	1984-87	2.8	0.0	8.8	49.0	12.6	0.1	1.5	0.5	0.1	0.0	0.0	1.2	76
N-238	17° 33' 00"	43° 28' 00"	2140	1984-87	5.8	2.0	34.6	59.9	30.8	1.0	1.1	5.5	0.3	0.0	0.3	7.3	148
N-240	17° 35' 00"	43° 52' 00"	1770	1984-87	6.1	0.8	20.4	42.4	11.6	0.3	0.2	0.4	0.0	0.0	0.0	1.2	83
N-243	17° 34' 00"	43° 42' 00"	2080	1984-87	6.1	0.7	17.1	34.3	19.5	0.8	7.0	2.9	0.0	0.0	0.0	2.5	91
A-207	18° 10' 00"	43° 06' 00"	2400	1966-84	16	35.8	48.2	43.9	38.2	4.3	19.6	17.6	1.6	3.5	9.9	5.9	244
N-103	17° 40' 00"	43° 31' 00"	2020	1964-84	11.9	17.5	34.9	54.7	31	1.3	16	19.1	0.4	5.6	4.4	8.9	206
				Mean	5.8	3.3	17.9	45.3	14.5	1.3	2.8	3.4	0.5	0.5	0.9	2.0	98
				Maximum	16.0	35.8	48.2	80.1	39.0	5.0	19.6	19.1	2.1	5.6	9.9	8.9	244
				Minimum	0.4	0.0	8.7	9.6	2.5	0.0	0.0	0.1	0.0	0.0	0.0	0.2	47

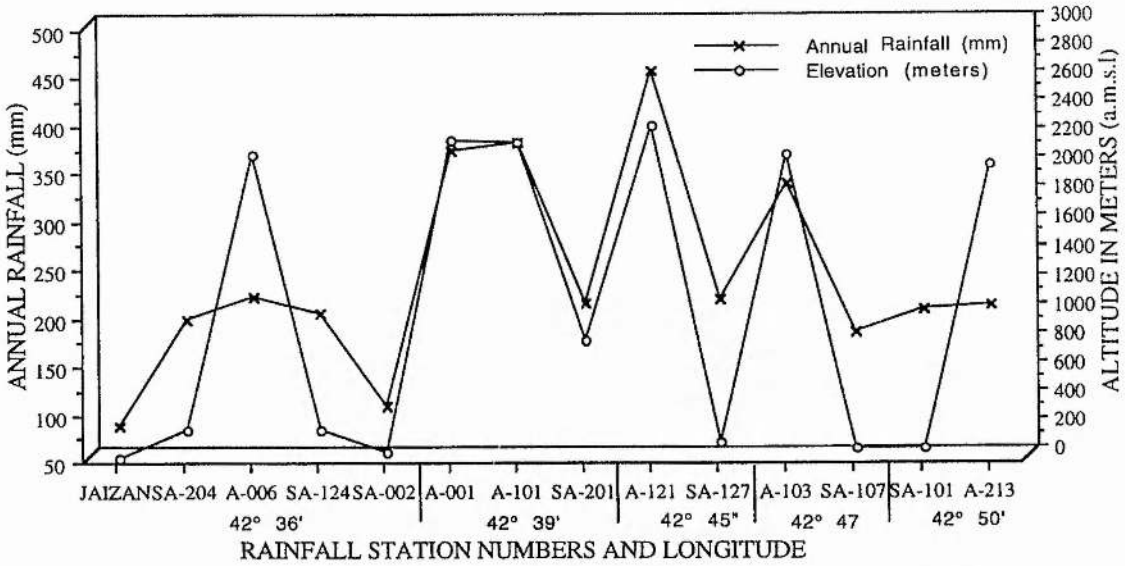

Figure 3.8a Relationships between the annual rainfall stations and the altitude on the same longitude within and near by Wadi Baysh.

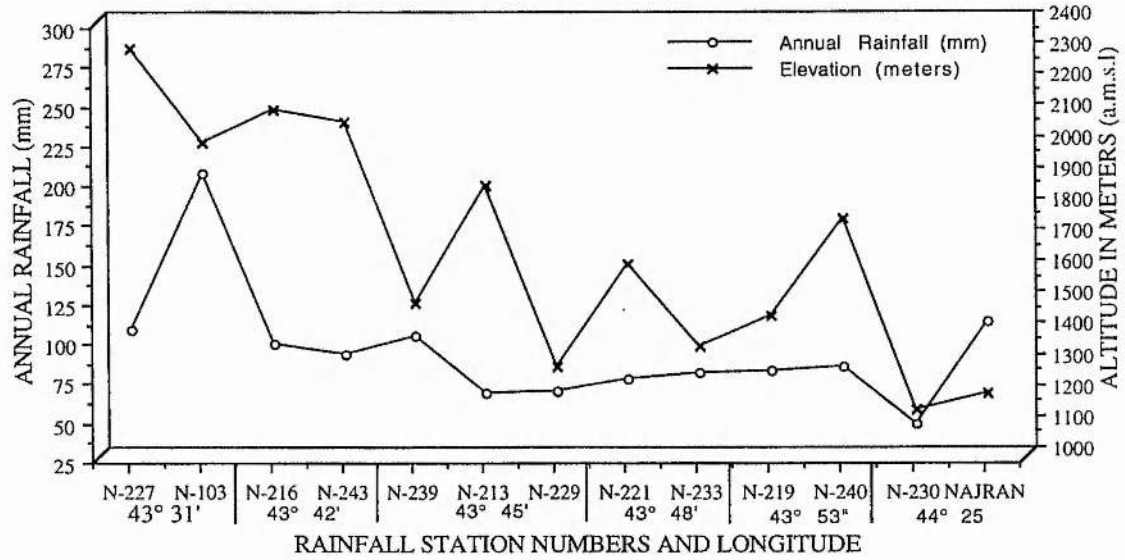

Figure 3.8b Relationships between the annual rainfall stations and the altitude on the same longitude within and near by Wadi Habawnah.

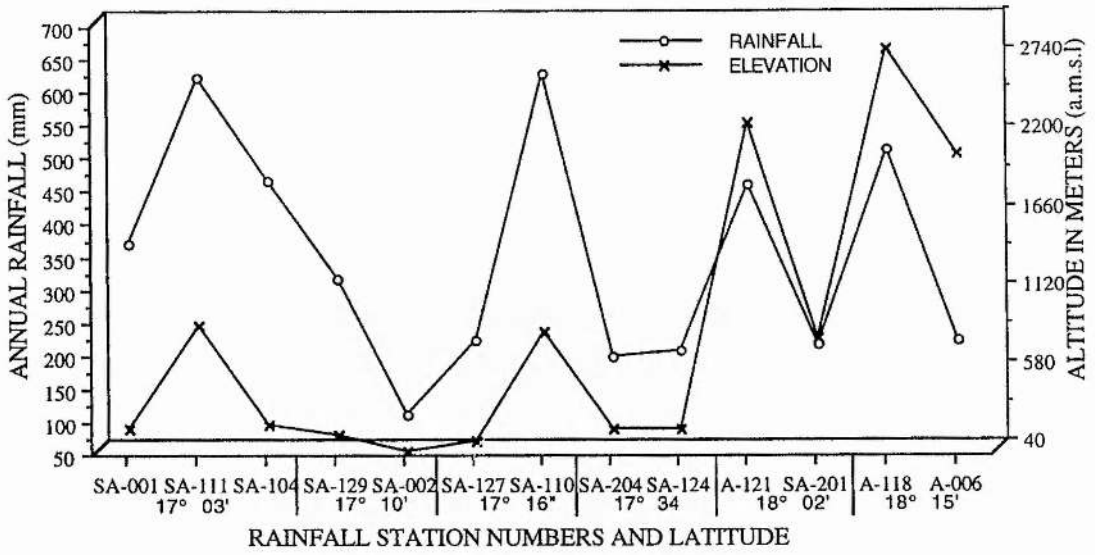

Figure 3.9 Relationships between the annual rainfall stations and the altitude on the same latitude within and near by Wadi Baysh.

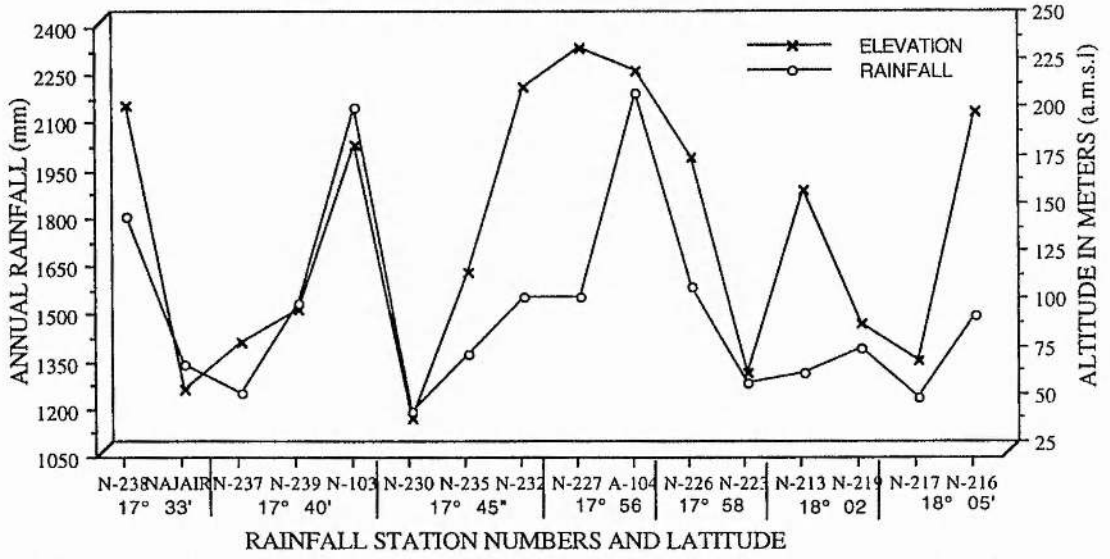

Figure 3.10 Relationships between the annual rainfall stations and the altitude on the same latitude within and near by Wadi Habanah.

ranging between 820 and 2300 m (Figure 3.9 and Table 3.7). The rainfall decreases toward the north and increases towards the south under the influence of southwesterly flow systems.

The Wadi Habawnah stations which are located on the same latitude show a good correlation of the rainfall and elevation. In the area between latitude 17°45' and 17°56' the stations have a higher elevation and rainfall than the rest of the catchment area (see Figure 3.10 and Table 3.7).

3.2.1.4 Air Temperature

The climate is distinguished by high air temperatures during summer with the annual average exceeding 20°C throughout the lowlands. The warm period is from April through August with maximum temperatures of 35°C in July (see Table 3.2 and Figures 3.11, 3.12 and 3.13). However, in the mountains of Asir the annual average temperature is only 12-15°C.

The area is greatly influenced by the weather from the southwest. However, during January the average air temperatures in the coastal area are the highest in the area. The high temperatures are due to the Asir Mountains preventing the penetration of cold northerly winds into the Wadi Baysh Basin. The mean monthly temperatures of Habawnah station (N002NP) and the nearby station (Najran Airport) range from 31 to 33°C in July and from 16 to 18°C in January, as shown in Figure 3.11 and Table 3.2.

In Wadi Baysh, the mean monthly temperatures of Baysh station (Malaki) and the nearby stations (Sabya and Jizan Airport) range from 33 to 35°C in July and from 26 to 27°C in January, as shown in Figure 3.12 and Table 3.2. According to data recorded at the Serat Abidah meteorological station in the upper part of the catchment area and nearby stations (Khamis Mushait airport, Sir Lasan and Abha (Table 3.2; Figure 3.13), the temperature normally ranges from 21 to 23°C in June, and from 11 to 12°C in January.

3.2.1.5 Potential Evaporation

Potential evaporation is a very important factor affecting the water budget in the

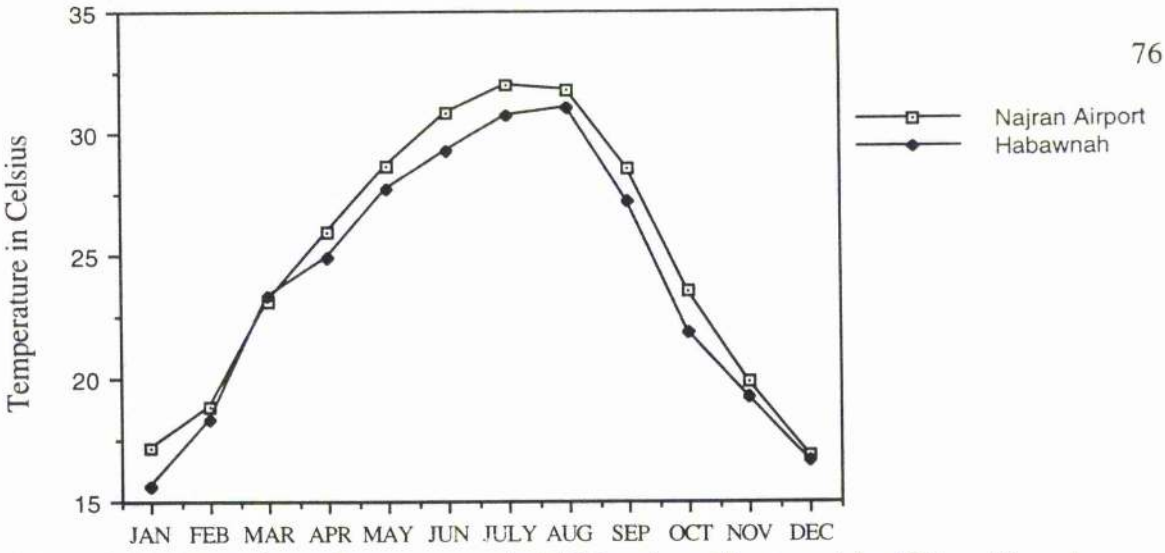

Figure 3.11 Comparison of temperature in Celsius (monthly mean) for Najran Airport and Najran Stations (altitude is 1250 and 1210 m, respectively).

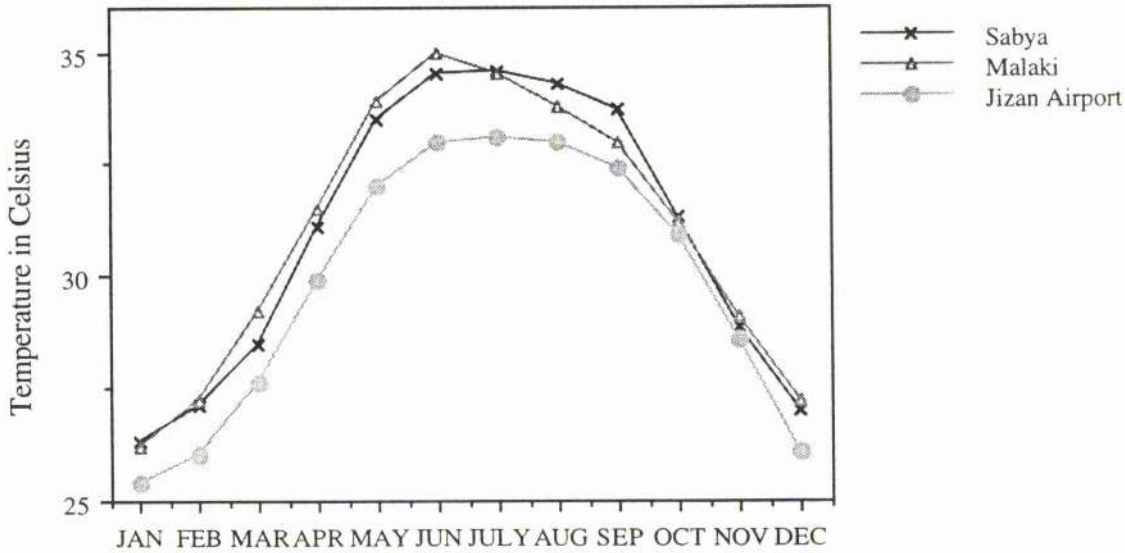

Figure 3.12 Comparison of temperature in Celsius (monthly mean) for Sabya, Malaki and Jizan Airport Stations (altitude is 40, 190 and 3 m, respectively).

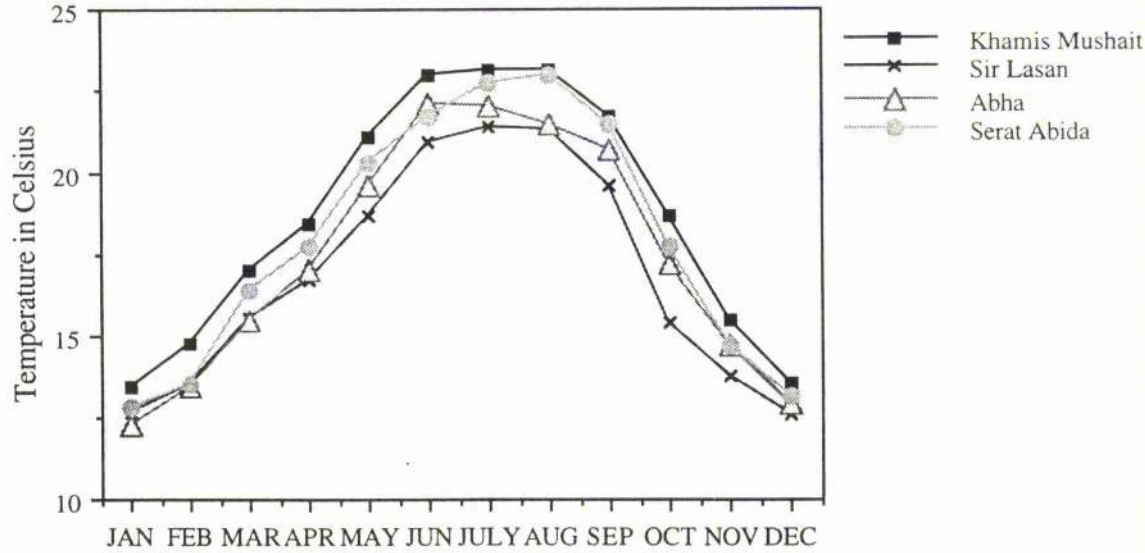

Figure 3.13 Comparison of temperature in Celsius (monthly mean) for Khamis Mushait, Sir Lasan, Abha and Serat Abida Stations (altitude is 2057, 2100, 2200 and 2190 m, respectively).

area. Table 3.3 and Figures 3.14, 3.15 and 3.16 show the variation in values for pan evaporation at the five climatological stations. The mean values of monthly records were taken over 16 years for the Sabya, Malaki and Abha stations, while the Wadi Habawnah climatic station (N-OO2NP) data are from only one year. These stations represent different elevations near and within the catchment area. The maximum evaporation ranges between 289 and 363mm in Wadi Habawnah while in Wadi Baysh it ranges between 201 and 386mm. The annual pan evaporation shows high evaporation over all the area with the maximum of 4070mm in the lower part of Wadi Habawnah. The upper parts of the catchments of both wadis reveal a minimum of 2678mm while the lower part of Wadi Baysh shows 3536mm near the foothills and 3352mm in the Tihamah Plain (Sabya).

3.2.1.6 Potential Evapotranspiration

Potential evapotranspiration (PT): this term can be defined as the transpiration of water from vegetation and soil. Table 3.16 shows evapotranspiration values in both areas. The maximum PT in the Wadi Habawnah area occurs in July (222mm), which may be due to the high air temperature in this month, and in Wadi Baysh in July (206mm) and August (196mm). Table 3.3 and Figures 3.14, 3.15 and 3.16 show the mean monthly potential evapotranspiration within and nearby the study areas.

The seasonal variation of potential transpiration can be recognised from data records. The winter season (December, January and February) is characterised by the lowest value of monthly mean PT. PT in Wadi Baysh ranges from 124mm to 134mm, while in Wadi Habawnah it ranges between 90 and 108mm. In the summer season (June, July and August), PT ranges between 196 and 206mm in Wadi Baysh and from 207 to 222mm in Wadi Habawnah.

Higher winter PT in Wadi Baysh than in Wadi Habawnah can be interpreted as a result of the higher air temperatures in Wadi Baysh.

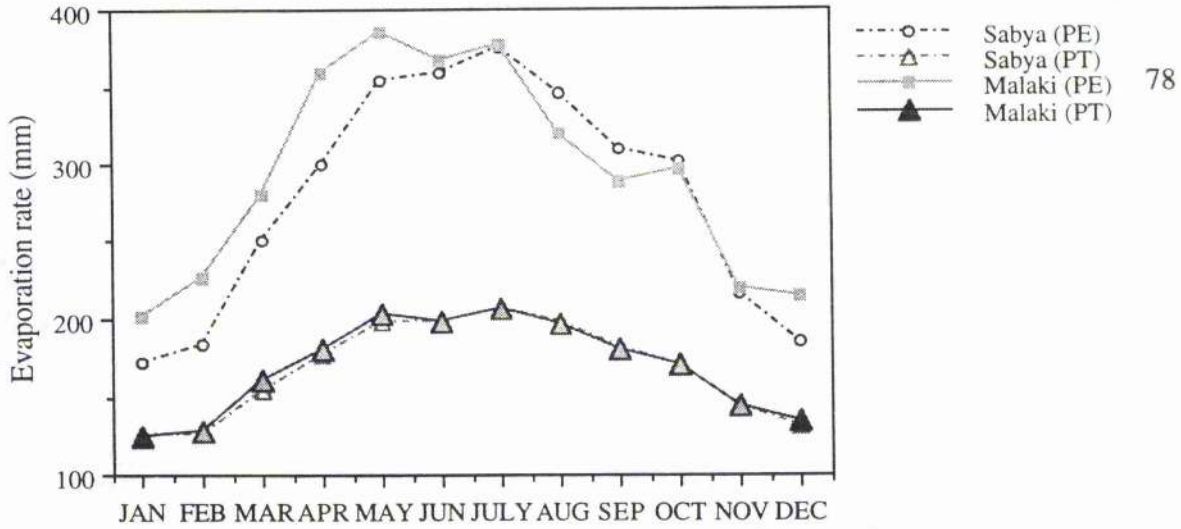

Figure 3.14 Potential evaporation and evapotranspiration (monthly mean) for Sabya and Malaki stations (altitude is 65 and 190 m, respectively).

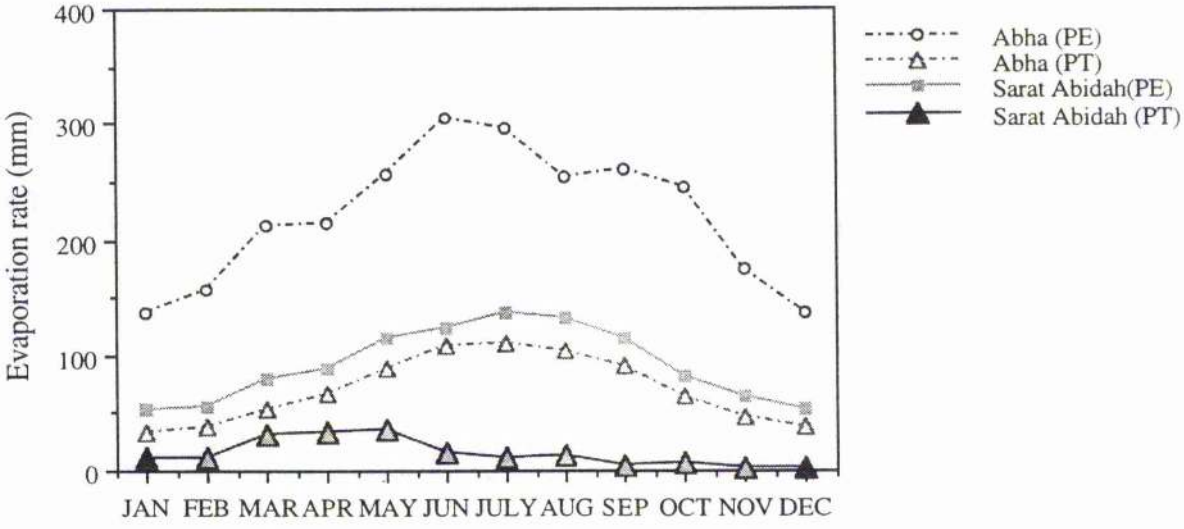

Figure 3.15 Potential evaporation and evapotranspiration (monthly mean) for Abha and Serat Abida Stations (altitude is 2200 and 2400 m, respectively).

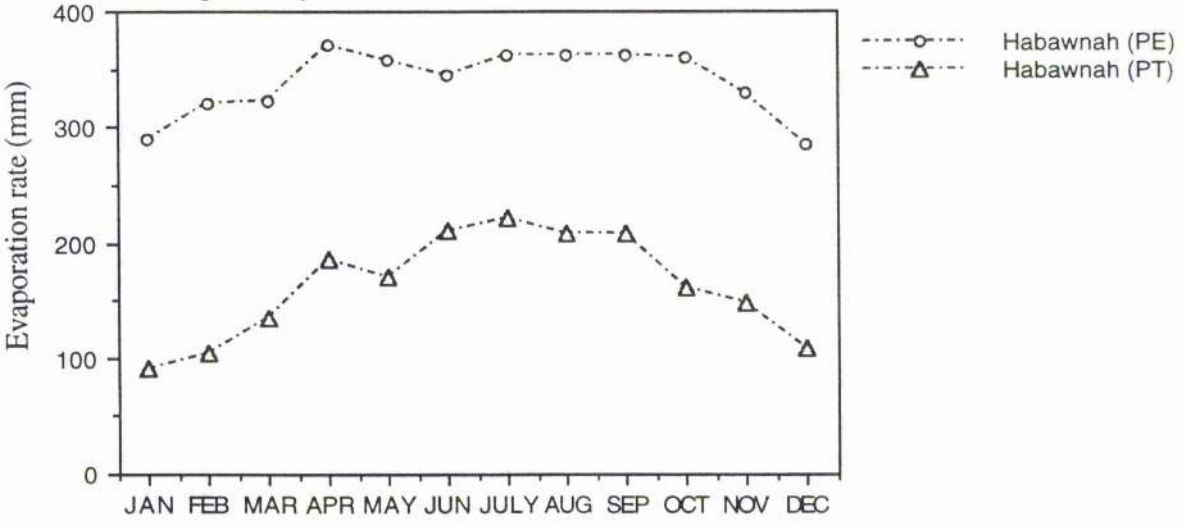

Figure 3.16 Potential evaporation and evapotranspiration (monthly mean) for Habawnah Station (altitude is 1210 m).

3.2.2 Hydrological Cycle

3.2.2.1 Introduction

The major hydrogeological components of the study area are presented schematically in Figure 3.17. In the west, the basement complex and volcanic rocks are essentially impermeable. Precipitation ranges from 78 to 669 mm/yr in Wadi Baysh and 51 to 244 mm/yr in Wadi Habawnah (see Table 3.4). Groundwater is found only in alluvial infilling and in the coastal-plain deposits of the Red Sea area Tehamah Plain. To the east, the sedimentary formations contain many aquifers and have a structure which produces a major unconfined and artesian groundwater basin.

The largest amounts of precipitation in Wadi Baysh occur during the months from July until November and from February until May, while in Wadi Habawnah it falls between February and May. The monsoon regime affects the southern part of the Arabian Peninsula during the winter and spring, when cloudbursts occur in association with thunderstorms.

Rainfall varies in the study area because of two main factors: altitude, and distance from the escarpment. In the escarpment area, relatively large amounts of precipitation occur and the mean annual rainfall in Wadi Baysh is 400mm while in Wadi Habawnah it is 117mm. Mean annual rainfall values decrease to the west (i.e. towards the Red Sea) in the Baysh Basin and to the east (towards Empty Quarter) in the Habawnah basin, with mean values of 194mm and 65mm (Table 3.8), respectively.

3.2.2.2 The Annual Variations of Rainfall

The annual variation of rainfall is the dominant factor in evaluating the availability of water. Precipitation data within Wadi Baysh and Wadi Habawnah are available from 7 and 19 stations respectively (Table 3.7). The annual rainfall varies from one station to another within each catchment area. The greatest annual value was recorded at station SA-110 (622 mm) in Wadi Baysh and the least (77 mm) at station SA-125. According to the records, station SA-124 had the greatest amounts of precipitation in six years out of 19 years, with the mean annual rainfall ranging between 298 and 386mm, while the years

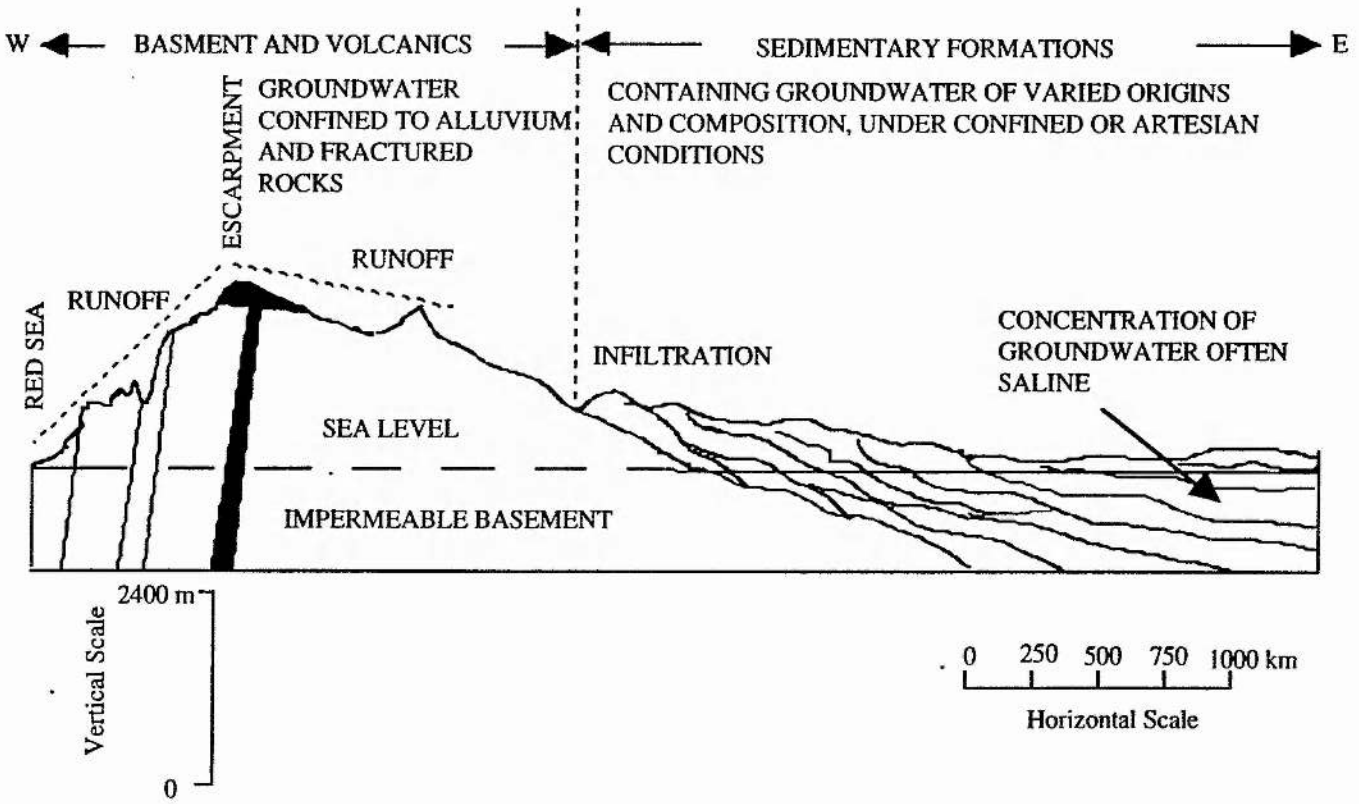

Figure 3.17 Geohydrological cross-section of the Arabian Peninsula (redrawn from Burdon and Ockum, 1968).

Table 3.8a Rainfall data with the same longitude or latitude within and nearby the catchment areas of Wadi Baysh and Habawnah

Wadi Baysh rainfall mean data (in mm) with the longitude

Station No.	Year record	Longtitude E	Elevat. (m)	Annual mean	Intergauge Distance (km)
JAIZAN	1970-84	42° 35' 00"	3	85	77.9
SA-204	1970-84	42° 36' 00"	200	194	
A-006	1982-84	42° 36' 00"	2100	219	75.6
SA-124	1967-84	42° 37' 00"	200	201	
SA-002	1966-84	42° 37' 00"	40	105	44.5
A-001	1966-84	42° 39' 00"	2200	371	
A-101	1960-84	42° 39' 00"	2190	379	2.2
SA-201	1968-73	42° 39' 00"	820	212	18.9
A-121	1965-84	42° 45' 00"	2300	453	
SA-127	1967-84	42° 45' 00"	110	217	84.5
A-103	1965-84	42° 47' 00"	2100	336	
SA-107	1966-84	42° 47' 00"	70	181	109
SA-101	1960-84	42° 50' 00"	69	206	
A-213	1966-84	42° 50' 00"	2030	210	22.2

Wadi Habawnah rainfall mean data (in mm) with the longitude

Station No.	Year record	Longtitude E	Elevat. (m)	Annual mean	Intergauge Distance (km)
N-227	1984-87	43° 31' 00"	2320	107	
N-103	1964-84	43° 31' 00"	2020	206	29.6
N-216	1984-87	43° 42' 00"	2120	97	
N-243	1984-87	43° 42' 00"	2080	91	57.4
N-239	1984-87	43° 45' 00"	1500	103	
N-213	1984-87	43° 45' 00"	1880	67	66.7
N-229	1984-87	43° 46' 00"	1300	68	50.1
N-221	1984-87	43° 48' 00"	1630	75	
N-233	1984-87	43° 48' 00"	1360	79	70.5
N-219	1984-87	43° 53' 00"	1460	80	
N-240	1984-87	43° 53' 00"	1770	83	51.9
N-230	1984-87	44° 25' 00"	1160	47	
NAJRAN	1970-84	44° 26' 00"	1210	111	29.7

Wadi Baysh rainfall mean data (in mm) with the latitude

Station No.	Year record	Latitude N	Elevat. (m)	Annual mean	Intergauge Distance (km)
SA-001	1960-84	17°03"00	190	364	
SA-111	1960-84	17°03"00	900	616	18.1
SA-104	1964-84	17°03"00	223	460	13.8
SA-129	1967-84	17°10"00	150	313	
SA-002	1966-84	17°10"00	40	105	29.7
SA-127	1967-84	17°16"00	110	217	
SA-110	1960-84	17°16"00	860	622	40.3
SA-204	1970-84	17°34"00	200	194	
SA-124	1967-84	17°34"00	200	201	2.1
A-121	1965-84	18°02"00	2300	453	
SA-201	1968-84	18°02"00	820	212	28.5
A-118	1965-84	18°15"00	2820	507	
A-006	1982-84	18°15"00	2100	219	24.3

Wadi Habawnah rainfall mean data (in mm) with the latitude

Station No.	Year record	Latitude N	Elevat. (m)	Annual mean	Intergauge Distance (km)
N-238	1984-87	17°33"00	2140	148	
NAJAIR"	1964-84	17°33"00	1250	71	25.4
N-237	1984-87	17°40"00	1400	56	
N-239	1964-84	17°40"00	1500	103	71
N-103	1984-87	17°40"00	2020	206	46.6
N-230	1984-87	17°45"00	1160	47	
N-235	1984-87	17°45"00	1620	76	22.2
N-232	1984-87	17°46"00	2200	107	6.7
N-227	1984-87	17°56"00	2320	107	
A-104	1984-87	17°56"00	2250	213	5.3
N-226	1984-87	17°57"00	1980	112	
N-223	1984-87	17°58"00	1300	62	71.3
N-213	1984-87	18°02"00	1880	67	
N-219	1984-87	18°03"00	1460	80	27.8
N-217	1970-84	18°05"00	1340	55	
N-216	1970-84	18°05"00	2120	97	68.7

Table 3.8b The annual rainfall (mm) of the consolidated area and the basin area of both wadis

Wadi Baysh rainfall mean data (in mm) of the consolidated area

Station No.	Elevat. (m)	Annual mean
A-118	2820	507
A-210	2670	442
A-121	2300	453
A-001	2200	371
SA-252	2200	175
A-101	2190	379
A-006	2100	219
A-103	2100	336
A-105	2060	94
A-213	2030	210
A-123	1900	172
SA-111	900	616
SA-110	860	622
SA-201	820	212
SA-112	800	593
SA-145	600	583
SA-126	540	669
SA-210	305	464
SA-104	223	460
	Mean	399
	Maximum	669
	Minimum	94

Wadi Baysh rainfall mean data (in mm) of the basin area

Station No.	Elevat. (m)	Annual mean
SA-204	200	194
SA-124	200	201
SA-103	190	224
SA-001	190	364
SA-129	150	313
SA-127	110	217
SA-107	70	181
SA-106	70	164
SA-101	69	206
SA-002	40	105
SA-125	5	78
JAIZAN	3	85
	Mean	194
	Maximum	364
	Minimum	78

Wadi Habawnah rainfall mean data (in mm) of the consolidated area

Station No.	Elevat. (m)	Annual mean
A-207	2400	244
N-227	2320	107
A-104	2250	213
N-232	2200	107
N-238	2140	148
N-216	2120	97
N-243	2080	91
N-103	2020	206
N-226	1980	112
N-213	1880	67
N-240	1770	83
N-221	1630	75
N-235	1620	76
N-215	1600	56
N-239	1500	103
N-219	1460	80
	Mean	117
	Maximum	244
	Minimum	56

Wadi Habawnah rainfall mean data (in mm) of the basin area

Station No.	Elevat. (m)	Annual mean
N-236	1400	76
N-237	1400	56
N-233	1360	79
N-217	1340	55
N-220	1306	42
N-223	1300	62
N-229	1300	68
N-224	1250	45
NAJAIR	1250	71
NAJRAN	1210	111
N-230	1160	47
	Mean	65
	Maximum	111
	Minimum	42

1971, 1980, 1981, 1984 and 1988 had little rainfall (<100mm) (Figure 3.18 and Table 3.9). Although the record for Wadi Habawnah is too short to reveal patterns of change in the annual rainfall, comparison of the data from station A-232 (Figure 3.19 and Table 3.9) shows that the four years of rain followed a pattern very similar to that during the same years in Wadi Baysh.

3.2.2.3 Mean Annual Rainfall

Annual rainfall totals in Wadi Baysh and the surrounding area, for different lengths of records between 1960 and 1988, and in Wadi Habawnah, for the period of 1984-1987 are shown in Table 3.4. In this table, the annual means were computed for each station. The mean values were used to plot isohyets (lines connecting points of equal precipitation), on the map of the study area (Figure 3.20). The accuracy of the isohyets is greater in Wadi Baysh because of a long record despite Wadi Habawnah having a denser network of rainfall stations. The isohyet map has been prepared using mean annual rainfall in both wadis to show the rainfall distribution pattern over the area. It may be seen that in Wadi Baysh, the highest amounts of rainfall (>650mm) occur in the central southern part of catchment. The Wadi Habawnah isohyet map (Figure 3.20) shows that the highest rainfall (>100<250mm) occurs in the western and northwest parts of the catchment area, while the lowest precipitation (<100mm) occurs in the centre and southern parts of the catchment area.

The mean annual rainfall varies within the study area, from the 100mm isohyet near the Red Sea to 600 mm near the highland station S-110 in the south east of Wadi Baysh. However, in Wadi Habawnah the lowest rainfall value of 50mm is found near the Empty Quarter Desert, while in the highland (west of Wadi Habawnah) the 150mm isohyet is located. Rainfall decreases rapidly towards the east of Wadi Habawnah and towards the south-west of Wadi Baysh, as a result of a decrease in the altitude.

The average precipitation in the upper and middle Wadi Baysh watershed area was calculated from an isohyet map (Figure 3.20).

Rainfall values recorded at various stations throughout the study area (Figure 3.2 and Table 3.4) were used by the author to draw isohyets (see Figure 3.20). These

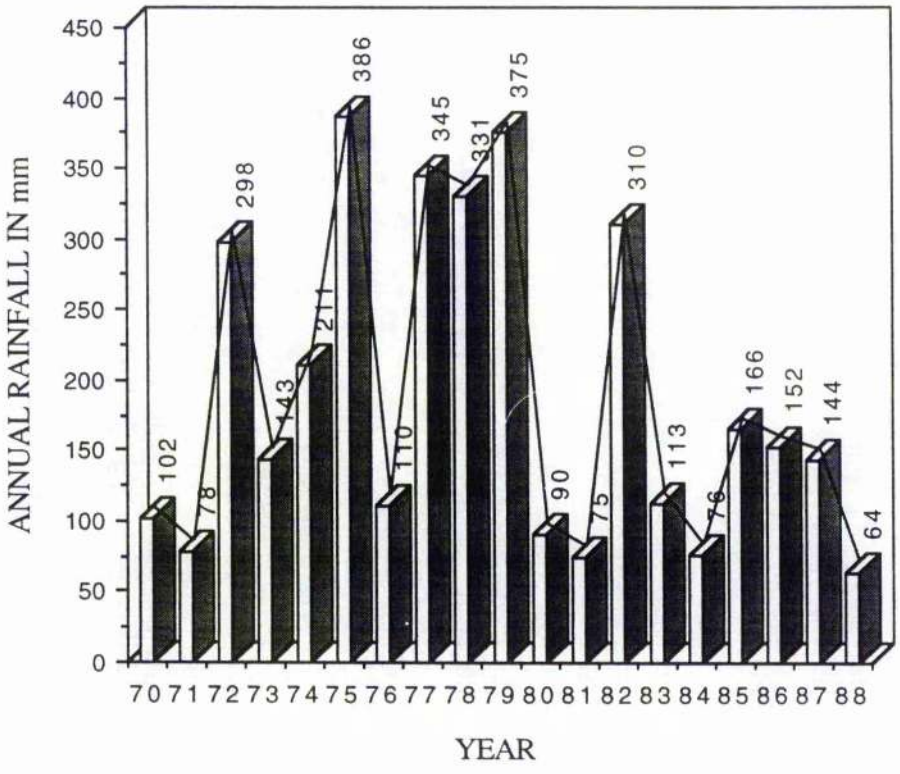

Figure 3.18 Annual variation record of 18 years rainfall in Wadi Baysh (Rainfall gauge SA-124).

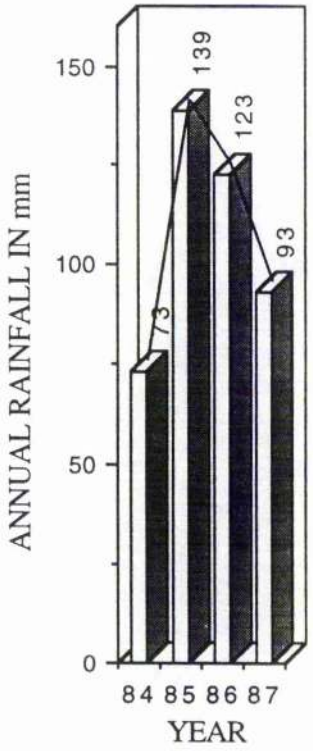

Figure 3.19 Annual variation record of 4 years rainfall in Wadi Habawnah (Rainfall gauge A-232).

Table 3.9 Rainfall variation of rain gauge station (SA-124) and (N-232) in Wadi Baysh and Wadi Habawnah, respectively

Raingauge Station (SA-124) Wadi Baysh

Station No	Elevation m (a.m.s.l.)	Year	JAN mm	FEB mm	MAR mm	APR mm	MAY mm	JUN mm	JUL mm	AUG mm	SEP mm	OCT mm	NOV mm	DEC mm	TOTAL mm
SA-124	200	1970	150	0	0	0	0	0.6	35.6	13.4	16.2	18.8	0	2	102
		1971	1.7	0	0	7	3.5	0	5.2	9.5	12	14.2	12.4	12.7	78
		1972	0	5.6	9	37.3	50	65.8	35	10.1	23.4	66.5	51.3	28.8	298
		1973	19.8	0	0	0	0	0	4.5	9.8	34.5	6.8	14.7	53.2	143
		1974	7.3	0	63	0	7.5	12	5.4	50	14.9	32.7	0	18.6	211
		1975	0	29.5	17.6	48.7	0	2.6	25.6	127.1	12.7	0	0	21.7	386
		1976	0	1.5	4.6	0.6	0.2	0.7	41.5	0	1	16.4	43	0	110
		1977	89.1	0	0	0	13.1	0	0	107	7.7	115.1	12.9	0	345
		1978	37.5	14.2	0	0	3.1	0	158.6	16	39.7	52.2	0	0	331
		1979	103.3	0	2.6	0	9.8	10.8	0.2	52.8	77.6	4.4	0	76.6	375
		1980	4.2	7.6	0	0.6	5	0	3.4	22.2	37.2	0	6.2	3.4	90
		1981	0	1	16.7	1.6	0	0	18.9	5.6	2.6	28.3	0	0	75
		1982	19.2	22.8	1.6	0	26	0	13.1	1.7	49.2	55.8	56.8	63.8	310
		1983	0	0	0	23.1	5.6	4.5	0	21.3	5.2	1.4	0	52.2	113
		1984	9	0	0	0	40.7	0	25.3	0	0.6	0.2	0	0	76
		1985	17.1	0	0	29.1	22.4	0	0	11.6	62.6	12.2	0	10.7	166
		1986	1	0	18.9	53.6	0	0.2	13.8	14.7	10.6	4.2	0	26.4	152
		1987	7.5	0	8.8	41	8.8	0	16	13	15.2	26.2	7.4	0	144
		1988	7.8	5.8	0	9.6	0	0	16.9	8.6	14.4	0	0	2.4	64
		Mean	36.5	12.57143	17.85	25.22	16.30833	13.88571	139.6667	29.08235	24.29444	30.36	29.24286	31.04167	198.25

Raingage Station (N232) Wadi Habawnah

Station No	Elevation m (a.m.s.l.)	Year	JAN mm	FEB mm	MAR mm	APR mm	MAY mm	JUN mm	JUL mm	AUG mm	SEP mm	OCT mm	NOV mm	DEC mm	TOTAL mm
N-232	2200.0	1984.0	0.0	0.0	15.4	8.6	44.4	3.0	0.4	0.0	0.0	0.0	0.0	1.0	73
		1985.0	20.8	0.0	8.2	3.6	59.8	0.0	6.8	25.8	0.0	3.2	7.8	3.4	139
		1986.0	0.0	4.0	32.6	4.0	39.0	17.0	0.0	7.4	8.2	0.0	0.0	11.0	123
		1987.0	22.0	4.0	25.6	22.2	12.8	0.0	0.0	6.2	0.0	0.0	0.0	0.0	93
		MEAN	21.4	4.0	20.5	9.6	39.0	10.0	2.7	20.0	4.1	1.7	3.7	7.5	107

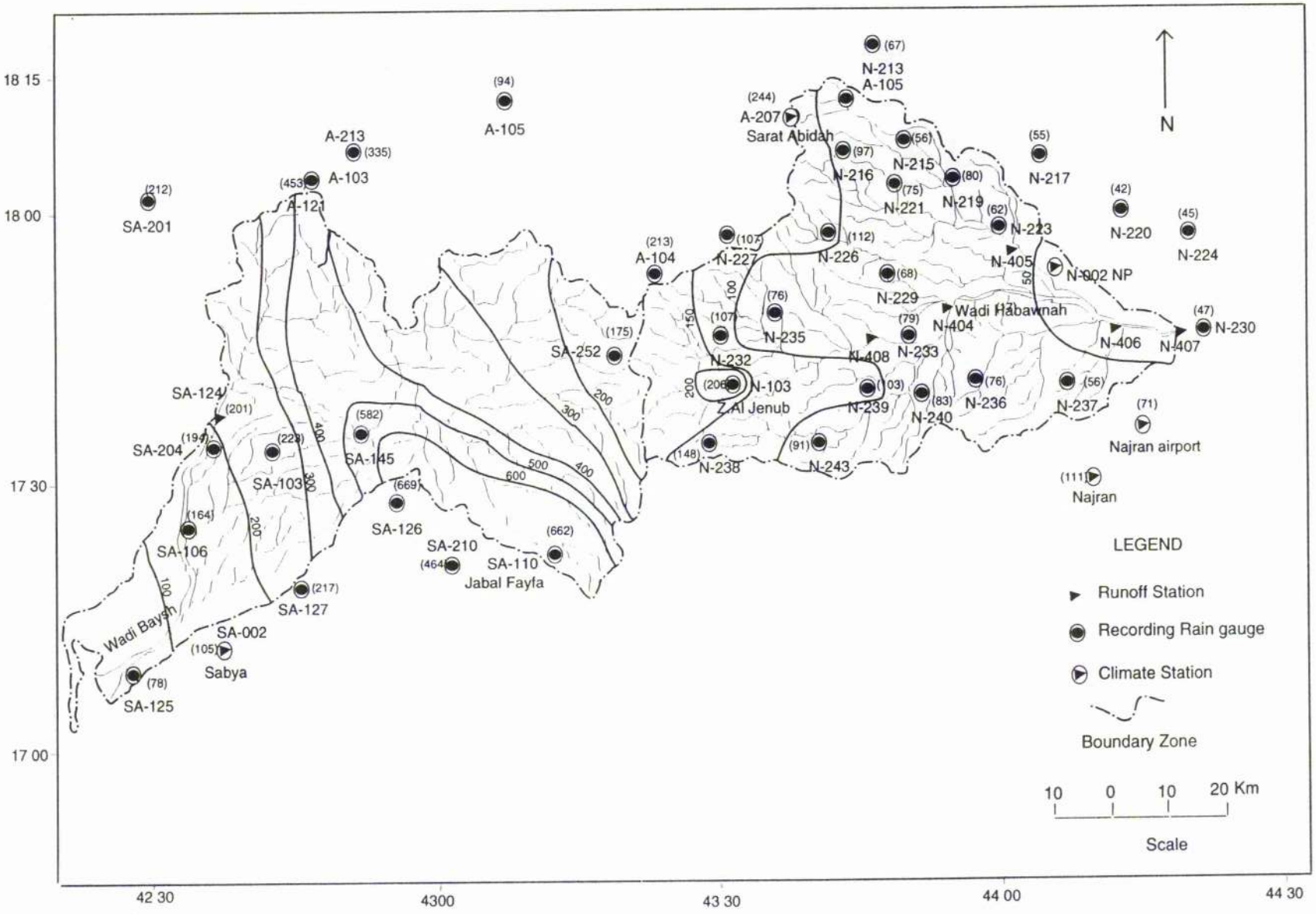

Figure 3.20 Isohyets showing to annual rainfall in mm in Wadi Baysh (flowing towards the southwest) and Wadi Habawnah (flowing towards the east) south of Arabian Shield.

lines were located by visual interpolation between stations, and sketched as smooth curves. The interval between lines depends on variations in precipitation and rain gauge density. An interval of 50mm was selected.

Assuming that the arithmetic mean of isohyets represents the average precipitation P_{av} for a particular area (a) enclosed between isohyets the total precipitation falling in the catchments was calculated (Table 3.10).

The following simple equation was used to derive the average rate of precipitation for the upper Wadi Baysh and Habawnah catchment areas:

$$P_{av} = \frac{\sum P \times a}{A} \qquad (3.1)$$

where average precipitation equals the sum of precipitation (P) multiplied by area (a) for all sectors, divided by the total area (A) of the upper Wadi Baysh and/or Wadi Habawnah catchment area.

The average annual precipitation over the catchment area of Wadi Baysh is 331 mm/yr and Wadi Habawnah is 98 mm/yr. Therefore, the average volumes of annual precipitation for Wadi Baysh and Habawnah are 1536 mcm (million cubic metres) and 455 mcm m^3/year respectively.

3.2.2.4 Mean Monthly Rainfall

The mean, maximum and minimum monthly rainfall of both wadis are shown in Table 3.11 and Figures 3.21, 22, 23, 24 and 25. There are variations between the monthly rainfall means within each wadi. For example, the highest monthly means for Wadi Baysh are in April (32 mm), August (30 mm) and December (30 mm) each of which represent 10% to 11% of the annual rainfall. The lowest monthly mean rainfalls occur in February (3.2 mm) and June (0.3 mm). However, the maximum rainfall values were recorded in August (95 mm) and December (93 mm) in SA-110 and SA- 145 stations. The greatest mean monthly rainfall at Wadi Habawnah is in April during which rain stations N-226 and N-239 receive 71% (80 mm) and 68% (69 mm) of their mean annual rainfall respectively. During this month, most of the rainfall stations show high rainfall means between 36 mm (67%) and 80 mm (68%). According to the four year period, the driest months in the

Table 3.10 Calculation of average precipitation over the catchment areas of Wadi Baysh and Wadi Habawnah

Wadi Baysh for the years 1963-1984

Isohyet (mm)	Sector No.	Enclosed Area km^2	Incremental Area km^2	Average Precipitation mm	Product (mm*km^2)
250	a	319	319	200	63831
300	b	799	480	250	120117
400	c	1536	737	350	257936
500	d	2177	641	450	288382
600	e	2469	292	550	160716
700	f	2931	462	650	300098
400	g	3218	287	350	100478
300	h	3825	607	250	151639
200	i	4352	527	150	79051
100	k	4640	288	50	14406
		4640			1536653

Average Precipitation (P) = 1536653 / 4640 = 331 mm / year
Volume of average precipitation in wadi Baysh catchment area =
Average Precipitation (P) * Total Area = (331/1000) * 4640*10^6 = 1536 *10^6 m^3 / year

Wadi Habawnah for the years 1984-1987

Isohyet (mm)	Sector No.	Enclosed Area km^2	Incremental Area km^2	Average Precipitation mm	Product (mm*km^2)
150	A	456	456	175	79739
200	B	526	70	200	13985
100	C	1412	886	150	132891
50	D	4298	2887	75	216516
25	E	4647	349	37	12906
		4647			456036

Average Precipitation (P) = 456036 / 4647 = 98 mm / year
Volume of average precipitation in wadi Habawnah catchment area =
Average Precipitation (P) * Total Area = (98/1000) * 4647*10^6 = 455 * 10^6 m^3 / year

Table 3.11Rainfall data within the catchment areas of Wadi Baysh and Habawnah

Wadi Baysh rainfall (mean values in mm)

Station No.	Elevat. (m)	Year record	JAN mean	D	%	FEB mean	D	%	MAR mean	D	%	APR mean	D	%	MAY mean	D	%	JUN mean	D	%	JUL mean	D	%	AUG mean	D	%	SEP mean	D	%	OCT mean	D	%	NOV mean	D	%	DEC mean	D	%	Annual mean
SA-125	5	1967-84	10	-11	13	6.2	-17	8.0	7.7	-18	10	1.5	-32	2	3.4	-30	4.4	0.3	-16	0.4	9.3	-30	12	6.1	-39	7.9	3.6	-21	4.6	13.9	-8	18	7.8	-15	10	7.6	-12	9.8	77.5
SA-103	190	1966-84	19	-2	9	13.3	-10	5.9	2.4	-23	1	5.8	-28	3	3.6	-29	1.6	10	-6	4.5	44	5	20	24.1	-21	11	26.2	1.6	12	27	5.2	12	27.6	5.1	12	20.4	0.8	9.1	223.8
SA-204	200	1970-84	21	-1	11	7.4	-16	3.8	9.4	-16	5	7.9	-26	4	11	-22	5.8	6.4	-10	3.3	21	-19	11	31.3	-14	16	29.1	4.5	15	30.7	8.9	16	9.7	-13	5	22.3	2.7	11	194.2
SA-124	200	1967-84	19	-2	10	7.4	-16	3.7	8.5	-17	4	7.2	-26	4	11	-22	5.5	12	-4	6.1	25	-14	12	27.9	-17	14	24.5	0	12	26.8	5	13	11.5	-11	5.7	19.8	0.2	9.9	201
SA-145	600	1972-76*	73	52	13	46.3	23	7.9	47.2	22	8	66	32	11	57	24	9.8	18	2.3	3.2	17	-22	2.9	16.4	-29	2.8	15.6	-9	2.7	18.6	-3	3.2	62.9	40	11	95.4	76	16	582.8
SA-110	860	1960-84	34	12	5	33	9.6	5.3	34.2	9	5	73.5	40	12	67	34	11	48	32	7.7	85	46	14	93.6	49	15	48.8	24	7.8	28.4	6.6	4.6	37	14	5.9	40.9	21	6.6	622
SA-252	2200	1984-87	11	5	6	2.2	-1.8	1.3	29.7	10	17	60.3	17	34	37	22	21	9.8	8.8	5.6	0.4	-2.6	0.2	13	9	7.4	0	0	0	0.15	-1	0.1	4.7	2.7	2.7	6.45	4.5	3.7	175
		Maximum	73			46			47			74			67			48			85			94			49			31			63			95			622
		mean	27		9	17		6	20		7	32		11	27		9	15		5	29		10	30		10	21		7	21		7	23		8	30		10	297
		Minimum	10.1			2.2			2.4			1.5			3.4			0.3			0.4			6.1			0.0			0.2			4.7			6.5			77.5
		SUM	187		9	116		6	139		7	222		11	191		9	105		5	201		10	212		10	148		7	146		7	161		8	213		10	2076

Wadi Habawnah rainfall (mean values in mm)

Station No.	Elevat. (m)	Year record	JAN mean	D	%	FEB mean	D	%	MAR mean	D	%	APR mean	D	%	MAY mean	D	%	JUN mean	D	%	JUL mean	D	%	AUG mean	D	%	SEP mean	D	%	OCT mean	D	%	NOV mean	D	%	DEC mean	D	%	Annual mean
N-219	1460	1984-87	2.5	-3.6	3.1	0.0	-3.0	0.0	16.7	-1	21	53.7	9	67	6.0	-8.1	7.4	0.1	-0.9	0.1	0.5	-2.5	0.6	0.5	-2.6	0.6	0.2	0.2	0.2	0.0	-1.0	0.0	0.0	-1.0	0.0	0.3	-1.8	0.3	80.3
N-223	1300	1984-87	3.6	-2.5	5.8	0.0	-3.0	0.0	11.1	-7	18	36.4	-9	59	8.1	-5.9	13.1	0.0	-1.0	0.0	0.7	-2.4	1.1	0.9	-2.1	1.5	0.4	0.4	0.6	0.0	-1.0	0.0	0.0	-1.0	0.0	0.6	-1.5	0.9	61.7
N-229	1300	1984-87	4.6	-1.4	6.7	0.0	-3.0	0.0	12.3	-6	18	41.9	-3	61	9.1	-4.9	13.3	0.0	-1.0	0.0	0.1	-3.0	0.1	0.3	-2.7	0.4	0.1	0.1	0.1	0.0	-1.0	0.0	0.0	-1.0	0.0	0.2	-1.9	0.2	68.4
N-230	1160	1984-87	0.4	-5.6	0.9	0.0	-3.0	0.0	12.9	-5	28	27.1	-18	58	4.7	-9.4	10.0	0.0	-1.0	0.0	0.0	-3.0	0.0	0.2	-2.9	0.3	0.0	0.0	0.0	0.0	-1.0	0.0	0.0	-1.0	0.0	1.4	-0.6	3.0	46.5
N-233	1360	1984-87	4.3	-1.8	5.4	1.7	-1.3	2.2	9.3	-9	12	47.9	3	61	7.2	-6.9	9.1	4.5	3.5	5.7	0.8	-2.2	1.0	1.2	-1.9	1.5	1.4	1.4	1.8	0.0	-1.0	0.0	0.0	-1.0	0.0	0.8	-1.2	1.0	78.9
N-236	1400	1984-87	7.8	1.8	10	1.0	-2.0	1.3	10.6	-7	14	46.7	2	62	9.0	-5.1	11.9	0.0	-1.0	0.0	0.0	-3.0	0.0	0.1	-3.0	0.1	0.1	0.1	0.1	0.0	-1.0	0.0	0.0	-1.0	0.0	0.4	-1.6	0.5	75.5
N-237	1400	1984-87	4.2	-1.9	7.4	0.2	-2.8	0.4	12.8	-5	23	30.2	-15	54	7.4	-6.6	13.2	0.0	-1.0	0.0	0.0	-3.0	0.0	0.6	-2.5	1.0	0.0	0.0	0.0	0.0	-1.0	0.0	0.0	-1.0	0.0	0.6	-1.4	1.1	55.9
N-239	1500	1984-87	5.9	-0.1	5.7	0.5	-2.6	0.4	8.7	-9	8	69.7	25	68	7.9	-6.2	7.6	4.7	3.7	4.5	1.0	-2.1	0.9	1.2	-1.9	1.1	1.5	1.5	1.5	0.3	-0.8	0.2	0.0	-1.0	0.0	2.1	0.0	2.0	103.1
N-215	1600	1984-87	4.8	-1.3	8.6	0.8	-2.2	1.4	19.5	2	35	27.3	-18	49	2.5	-12	4.5	0.1	-0.9	0.2	0.0	-3.0	0.0	0.2	-2.8	0.4	0.1	0.1	0.2	0.0	-1.0	0.0	0.0	-1.0	0.0	0.3	-1.8	0.5	55.5
N-216	2120	1984-87	6.0	0.0	6.1	0.2	-2.9	0.2	14.9	-3	15	59.3	14	61	12.9	-1.2	13.3	0.9	-0.1	0.9	0.6	-2.5	0.6	2.1	-1.0	2.1	0.0	0.0	0.0	0.0	-1.0	0.0	0.0	-1.0	0.0	0.4	-1.6	0.4	97.0
N-221	1630	1984-87	3.2	-2.8	4.3	0.1	-3.0	0.1	17.4	-1	23	47.2	2	63	5.5	-8.5	7.3	1.0	-0.1	1.3	0.7	-2.4	0.9	0.1	-2.9	0.1	0.0	0.0	0.0	0.0	-1.0	0.0	0.0	-1.0	0.0	0.3	-1.8	0.3	75.3
N-226	1980	1984-87	3.8	-2.2	3.4	0.1	-3.0	0.0	10.2	-8	9	80.1	35	71	12.8	-1.2	11.4	0.2	-0.8	0.2	1.6	-1.4	1.4	1.6	-1.4	1.4	1.1	1.1	1.0	0.0	-1.0	0.0	0.0	-1.0	0.0	0.7	-1.4	0.6	112.0
N-232	2200	1984-87	10.7	4.7	10	2.0	-1.0	1.9	20.5	2	19	9.6	-35	9	39.0	25.0	36.4	5.0	4.0	4.7	1.8	-1.2	1.7	9.9	6.9	9.2	2.1	2.1	1.9	0.8	-0.2	0.7	2.0	1.0	1.8	3.9	1.9	3.6	107.1
N-235	1620	1984-87	2.8	-3.2	3.7	0.0	-3.0	0.0	8.8	-9	12	49.0	4	64	12.6	-1.4	16.5	0.1	-1.0	0.1	1.5	-1.6	1.9	0.5	-2.5	0.7	0.1	0.1	0.1	0.0	-1.0	0.0	0.0	-1.0	0.0	1.2	-0.8	1.6	76.4
N-238	2140	1984-87	5.8	-0.2	3.9	2.0	-1.0	1.3	34.6	17	23	59.9	15	40	30.8	16.8	20.8	1.0	-0.1	0.6	1.1	-2.0	0.7	5.5	2.5	3.7	0.3	0.3	0.2	0.0	-1.0	0.0	0.3	-0.8	0.2	7.3	5.3	4.9	148.4
N-240	1770	1984-87	6.1	0.0	7.3	0.8	-2.3	0.9	20.4	2	25	42.4	-3	51	11.6	-2.5	13.9	0.3	-0.7	0.4	0.2	-2.9	0.2	0.4	-2.7	0.4	0.0	0.0	0.0	0.0	-1.0	0.0	0.0	-1.0	0.0	1.2	-0.8	1.4	83.1
N-243	2080	1984-87	6.1	0.0	6.7	0.7	-2.3	0.8	17.1	-1	19	34.3	-11	38	19.5	5.5	21.5	0.8	-0.2	0.9	7.0	4.0	7.7	2.9	-0.2	3.1	0.0	0.0	0.0	0.0	-1.0	0.0	0.0	-1.0	0.0	2.5	0.5	2.8	90.7
A-207	2400	1966-84	16.0	10	6.6	35.8	33	15	48.2	30	20	43.9	-1	18	38.2	24.2	15.6	4.3	3.3	1.8	19.6	16.6	8.0	17.6	14.6	7.2	1.6	1.6	0.7	3.5	2.5	1.4	9.9	8.9	4.1	5.9	3.9	2.4	244.2
N-103	2020	1964-84	11.9	5.9	5.8	17.5	15	8.5	34.9	17	17	54.7	10	27	31.0	17.0	15.1	1.3	0.3	0.6	16.0	13.0	7.8	19.1	16.1	9.3	0.4	0.4	0.2	5.6	4.6	2.7	4.4	3.4	2.1	8.9	6.9	4.3	205.7
		Maximum	16			36			48			80			39			5			20			19			2			6			10			9			244
		mean	6		6	3		3	18		18	45		46	14		15	1		1	3		3	3		3	0.5		0.5	0.5		1	0.9		1	2.0		2	98.2
		Minimum	0.4			0.0			8.7			9.6			2.5			0.0			0.0			0.1			0.0			0.0			0.0			0.2			46.5
		SUM	110		6	63		3	341		18	861		46	275		15	24		1	53		3	64		3	9		0.5	10		1	17		1	39		2	1865

(D) deviation from the mean

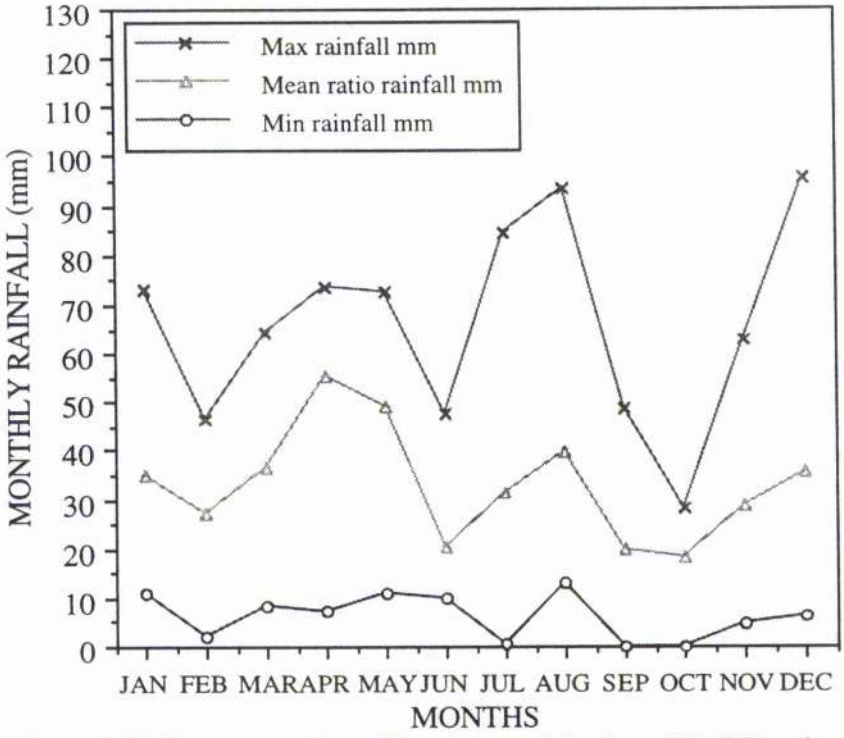

Figure 3.21 Sequence of monthly area precipitation : Wadi Baysh .

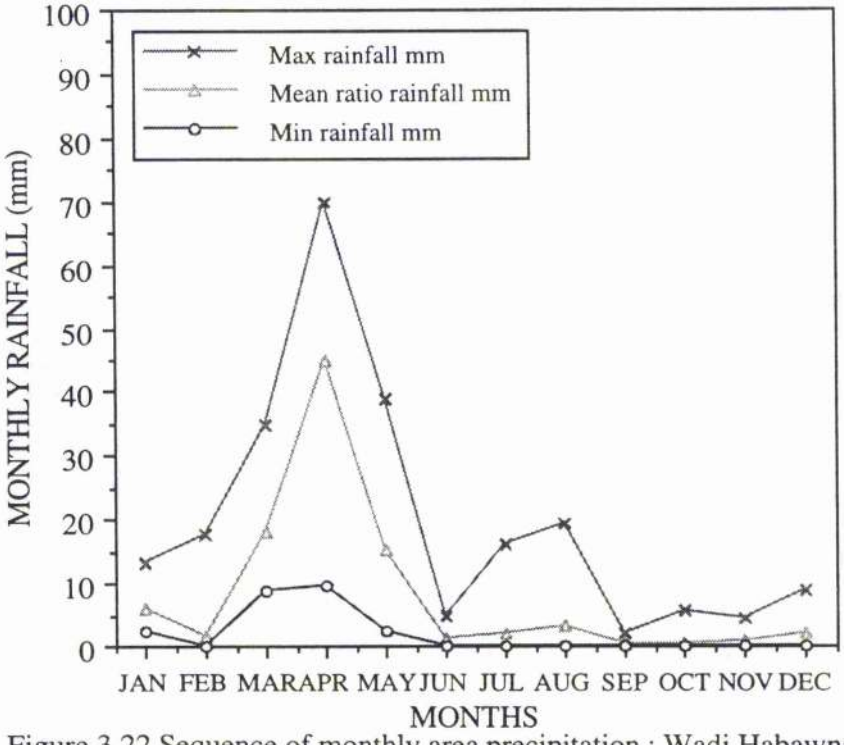

Figure 3.22 Sequence of monthly area precipitation : Wadi Habawnah .

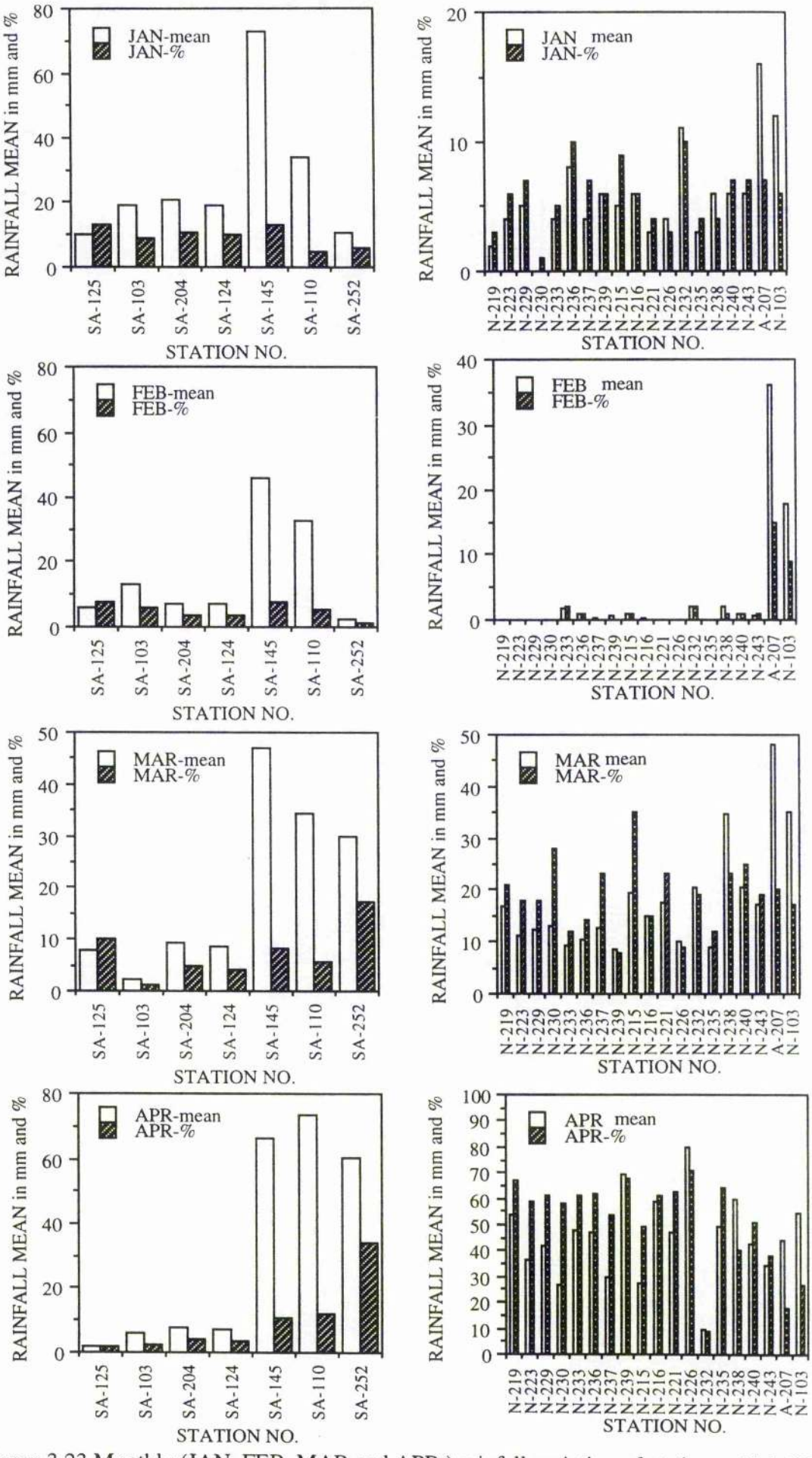

Figure 3.23 Monthly (JAN, FEB, MAR and APR) rainfall variation of stations within Wadi Baysh (left side) and Wadi Habawnah (right side).

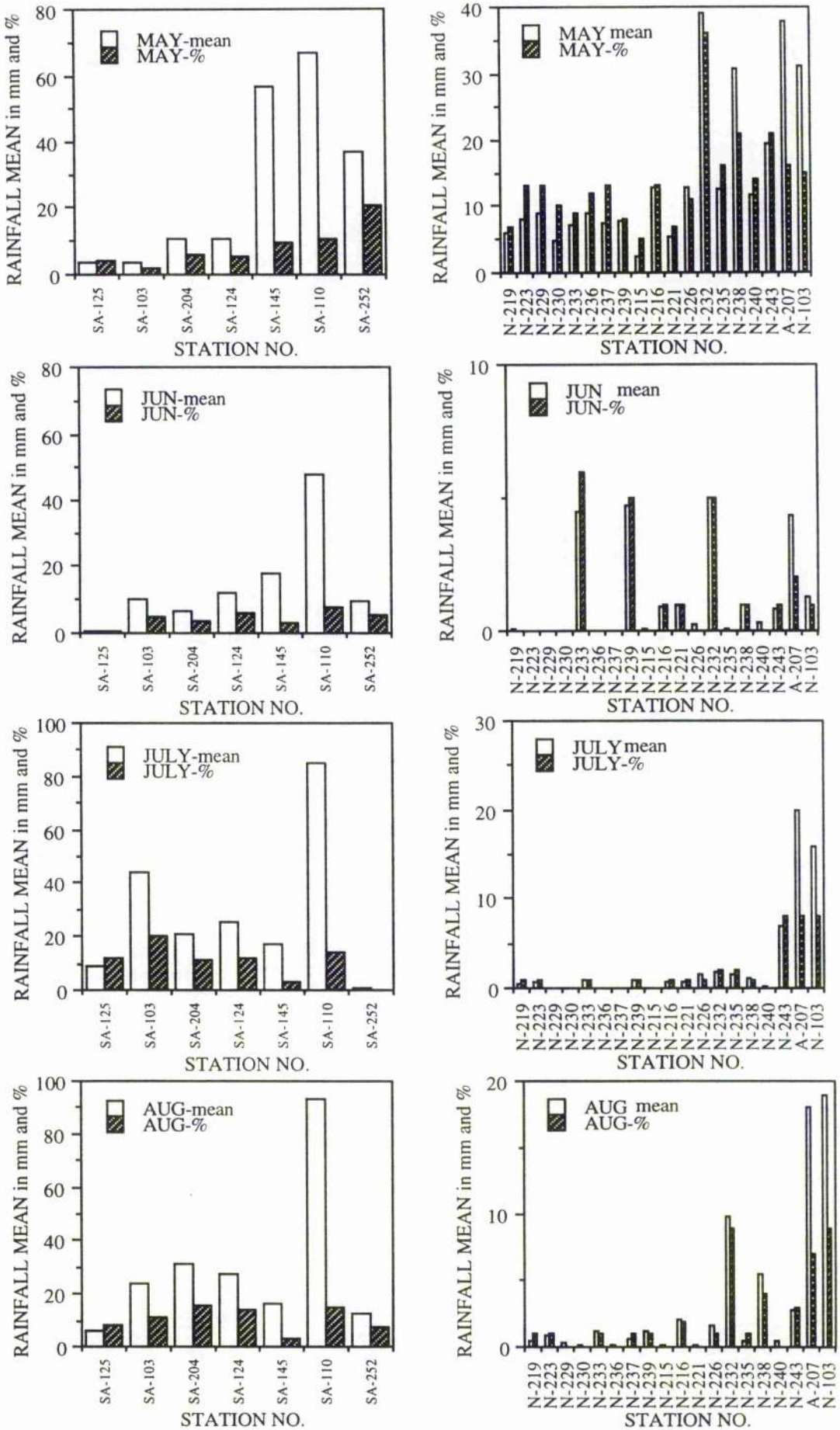

Figure 3.24 Monthly (MAY, JUN, JUL and AU) rainfall variation of stations within Wadi Baysh (left side) and Wadi Habawnah (right side).

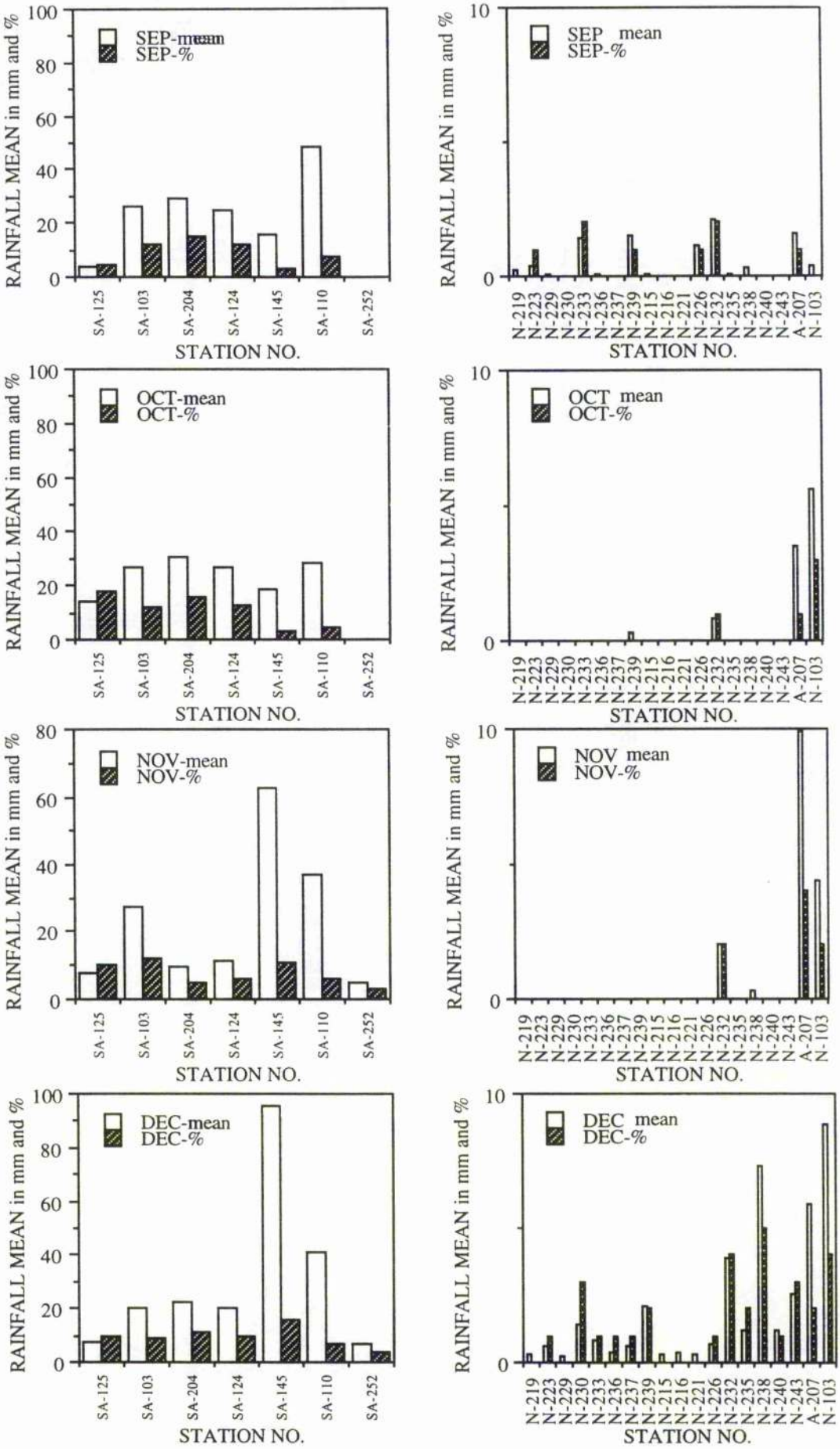

Figure 3.25 Monthly (SEP,OCT,NOV and DEC) rainfall variation of stations within Wadi Baysh (left side) and Wadi Habawnah (right side).

year period, in the catchment area are June to December.

3.2.2.5 Seasonal Distribution of Rainfall

In order to demonstrate the rainfall distribution seasonally in both wadis, data from the rainfall stations within the catchment area, have been summarised in Table 3.12 and Figure 3.26. The year has been divided into four seasons: Winter (December-February), Spring (March-May), Summer (June-August) and Autumn (September-November). Wadi Baysh has four rainy seasons, with the spring season contributing the most rainfall during the year. However, in Wadi Habawnah spring is the only rainy season, during which the rainfall exceeds 30 mm. Isohyet maps for the four seasons have been drawn (see Figures 3.27, 3.28, 3.29 and 3.30) based on the mean ratio of the monthly rainfall within and nearby the catchment area (see Table 3.13). The rainfall volumes for each season were determined (see Table 3.14) as the product of the average precipitation P_{av} for a particular area (a) enclosed between isohyets multiplied by area (a) of the sector, the rainfall volume summation of each of the sectors will represent the total rainfall volume for each season in both wadis.

2.2.2.5.1 Winter Rainfall

The winter season is a relatively dry season in Wadi Baysh. The average rainfall is 56mm when only 18% of the mean annual rainfall falls. Figure 3.27 shows rainfall variations of the winter season. Rain station SA-145 shows the highest percentage (37%, 46mm) of winter rainfall. The lowest percentage of winter rainfall is found at SA-252 with 11% (20mm). The total volume of the winter rainfall is 92 mcm (see Table 3.14). The winter season is also one of the driest seasons in Wadi Habawnah. The average winter rainfall is 11mm with 11% of the total annual rainfall in the area. Rain stations A-207 and N-103 show a mean rainfall range between 58 and 30mm and a percentage of 24% and 19% respectively. On the other hand, the rest of the rain stations show rainfall less than 30 mm p.a. for, Figure 3.27 has been drawn to show the distribution of winter isohyet rainfall for both wadis. The Wadi Baysh isohyets show that most of the rainfall occurs in the mid south and decreases in the rest of the area, while the Wadi Habawnah isohyet map shows

Table 3.12 Rainfall data within the catchment areas of Wadi Baysh and Wadi Habawnah.

Wadi Baysh rainfall (mm)

Station No.	Elevat-ation (m)	Year record	Winter DEC mean	Winter JAN mean	Winter FEB mean	Winter Total mm	Winter Total/Annual %	Spring MAR mean	Spring APR mean	Spring MAY mean	Spring Total mm	Spring Total/Annual %	Summer JUN mean	Summer JUL mean	Summer AUG mean	Summer Total mm	Summer Total/Annual %	Autumn SEP mean	Autumn OCT mean	Autumn NOV mean	Autumn Total mm	Autumn Total/Annual %	Annual mean
SA-125	5	1967-84	10.1	6.2	7.7	24	31	1.5	3.4	0.3	5	7	9.3	6.1	3.6	19	25	13.9	7.8	7.6	29	38	77.5
SA-204	200	1970-84	22.3	20.5	7.4	50	17	9.4	7.9	11.3	29	10	6.4	20.5	31.3	58	19	29.1	30.7	9.7	70	23	194.2
SA-124	200	1967-84	19.8	19.2	7.4	46	15	8.5	7.2	11	27	9	12.3	24.9	27.9	65	22	24.5	26.8	11.5	63	21	201
SA-103	190	1966-84	20.4	19.3	13.3	53	18	2.4	5.8	3.6	12	4	10.1	44.1	24.1	78	26	26.2	27	27.6	81	27	223.8
SA-145	600	1972-76*	95.4	73.3	46.3	215	72	47.2	66	57.3	171	57	18.4	16.9	16.4	52	17	15.6	18.6	62.9	97	32	582.8
SA-110	860	1960-84	40.9	33.6	33	108	36	34.2	73.5	66.6	174	58	47.7	84.7	93.6	226	75	48.8	28.4	37	114	38	622
SA-252	2200	1984-87	6.45	11.2	2.2	20	7	29.7	60.3	37.3	127	42	9.75	0.4	13	23	8	0	0.15	4.7	5	2	175
		SUM	215	183	117	516	25	133	224	187	544	26	114	198	210	521	25	158	139	161	459	22	2076
		Average	30.8	26.2	16.8	73.7	Average	19.0	32.0	26.8	77.8	Average	16.3	28.2	30.0	74.5	Average	22.6	19.9	23.0	65.5	Average	296.6
		STD	30.5	22.5	16.4	68.6	STD	17.9	32.6	26.9	76.4	STD	14.3	28.6	29.6	70.2	STD	15.2	11.7	21.2	37.9	STD	214.3

Wadi Habawnah rainfall (mm)

Station No.	Elevat. (m)	Year record	Winter DEC mean	Winter JAN mean	Winter FEB mean	Winter Total mm	Winter Total/Annual %	Spring MAR mean	Spring APR mean	Spring MAY mean	Spring Total mm	Spring Total/Annual %	Summer JUN mean	Summer JUL mean	Summer AUG mean	Summer Total mm	Summer Total/Annual %	Autumn SEP mean	Autumn OCT mean	Autumn NOV mean	Autumn Total mm	Autumn Total/Annual %	Annual mean
N-219	1460	1984-87	0.3	2.5	0.0	3	3	16.7	53.7	6.0	76	95	0.1	0.5	0.5	1	1	0.2	0.0	0.0	0	0	80.3
N-223	1300	1984-87	0.6	3.6	0.0	4	7	11.1	36.4	8.1	56	90	0.0	0.7	0.9	2	3	0.4	0.0	0.0	0	1	61.7
N-229	1300	1984-87	0.2	4.6	0.0	5	7	12.3	41.9	9.1	63	92	0.0	0.1	0.3	0	1	0.1	0.0	0.0	0	0	68.4
N-230	1160	1984-87	1.4	0.4	0.0	2	4	12.9	27.1	4.7	45	96	0.0	0.0	0.2	0	0	0.0	0.0	0.0	0	0	46.5
N-233	1360	1984-87	0.8	4.3	1.7	7	9	9.3	47.9	7.2	64	81	4.5	0.8	1.2	6	8	1.4	0.0	0.0	1	2	78.9
N-236	1400	1984-87	0.4	7.8	1.0	9	12	10.6	46.7	9.0	66	88	0.0	0.0	0.1	0	0	0.1	0.0	0.0	0	0	75.5
N-237	1400	1984-87	0.6	4.2	0.2	5	9	12.8	30.2	7.4	50	90	0.0	0.0	0.6	1	1	0.0	0.0	0.0	0	0	55.9
N-239	1500	1984-87	2.1	5.9	0.5	8	8	8.7	69.7	7.9	86	84	4.7	1.0	1.2	7	7	1.5	0.3	0.0	2	2	103.1
N-215	1600	1984-87	0.3	4.8	0.8	6	10	19.5	27.3	2.5	49	89	0.1	0.0	0.2	0	1	0.1	0.0	0.0	0	0	55.5
N-216	2120	1984-87	0.4	6.0	0.2	7	7	14.9	59.3	12.9	87	90	0.9	0.6	2.1	4	4	0.0	0.0	0.0	0	0	97.0
N-221	1630	1984-87	0.3	3.2	0.1	4	5	17.4	47.2	5.5	70	93	1.0	0.7	0.1	2	2	0.0	0.0	0.0	0	0	75.3
N-226	1980	1984-87	0.7	3.8	0.1	5	4	10.2	80.1	12.8	103	92	0.2	1.6	1.6	3	3	1.1	0.0	0.0	1	1	112.0
N-232	2200	1984-87	3.9	10.7	2.0	17	15	20.5	9.6	39.0	69	65	5.0	1.8	9.9	17	16	2.1	0.8	2.0	5	4	107.1
N-235	1620	1984-87	1.2	2.8	0.0	4	5	8.8	49.0	12.6	70	92	0.1	1.5	0.5	2	3	0.1	0.0	0.0	0	0	76.4
N-238	2140	1984-87	7.3	5.8	2.0	15	10	34.6	59.9	30.8	125	84	1.0	1.1	5.5	7	5	0.3	0.0	0.3	1	0	148.4
N-240	1770	1984-87	1.2	6.1	0.8	8	10	20.4	42.4	11.6	74	89	0.3	0.2	0.4	1	1	0.0	0.0	0.0	0	0	83.1
N-243	2080	1984-87	2.5	6.1	0.7	9	10	17.1	34.3	19.5	71	78	0.8	7.0	2.9	11	12	0.0	0.0	0.0	0	0	90.7
A-207	2400	1966-84	5.9	16	35.8	58	24	48.2	43.9	38.2	130	53	4.3	19.6	17.6	42	17	1.6	3.5	9.9	15	6	244.2
N-103	2020	1964-84	8.9	11.9	17.5	38	19	34.9	54.7	31	121	59	1.3	16	19.1	36	18	0.4	5.6	4.4	10	5	205.7
		SUM	39	110	63	212	11	341	861	275	1477	79	24	53	64	141	8	9	10	17	36	2	1865
		Average	2.0	5.8	3.3	11.2	Average	17.9	45.3	14.5	77.7	Average	1.3	2.8	3.4	7.4	Average	0.5	0.5	0.9	1.9	Average	98.2
		STD	2.6	3.7	8.8	13.9	STD	10.5	16.3	11.5	25.4	STD	1.8	5.5	5.8	11.9	STD	0.7	1.5	2.4	4.1	STD	70.5

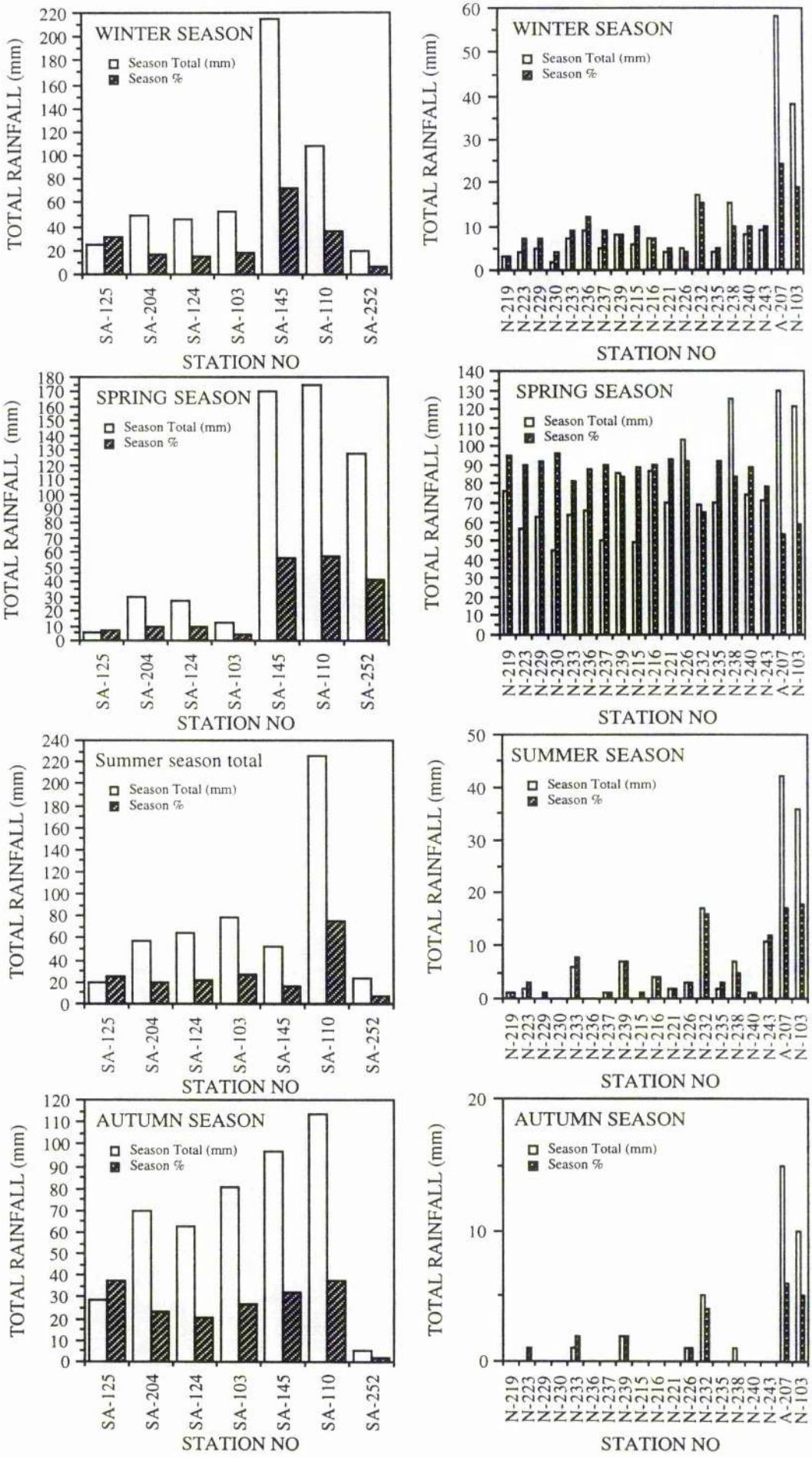

Figure 3.26 Variation of total rainfall (mm) in a season at Wadi Baysh (left side) and Wadi Habawnah (right side).

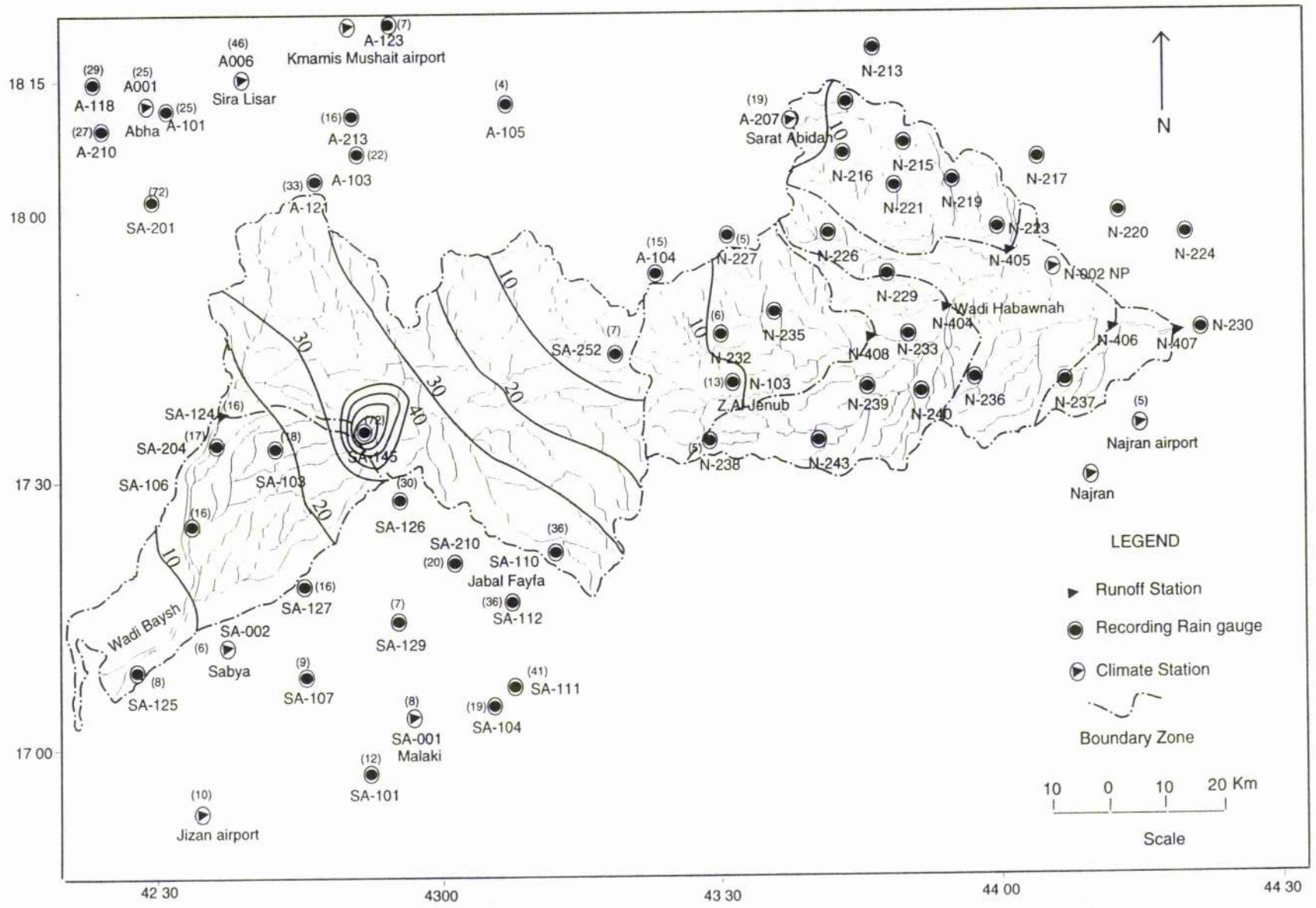

Figure 3.27 Isohyets of Winter Rainfall (mm) for Wadi Baysh (flowing towards the southwest) and Wadi Habawnah (flowing towards the east) south of Arabian Shield.

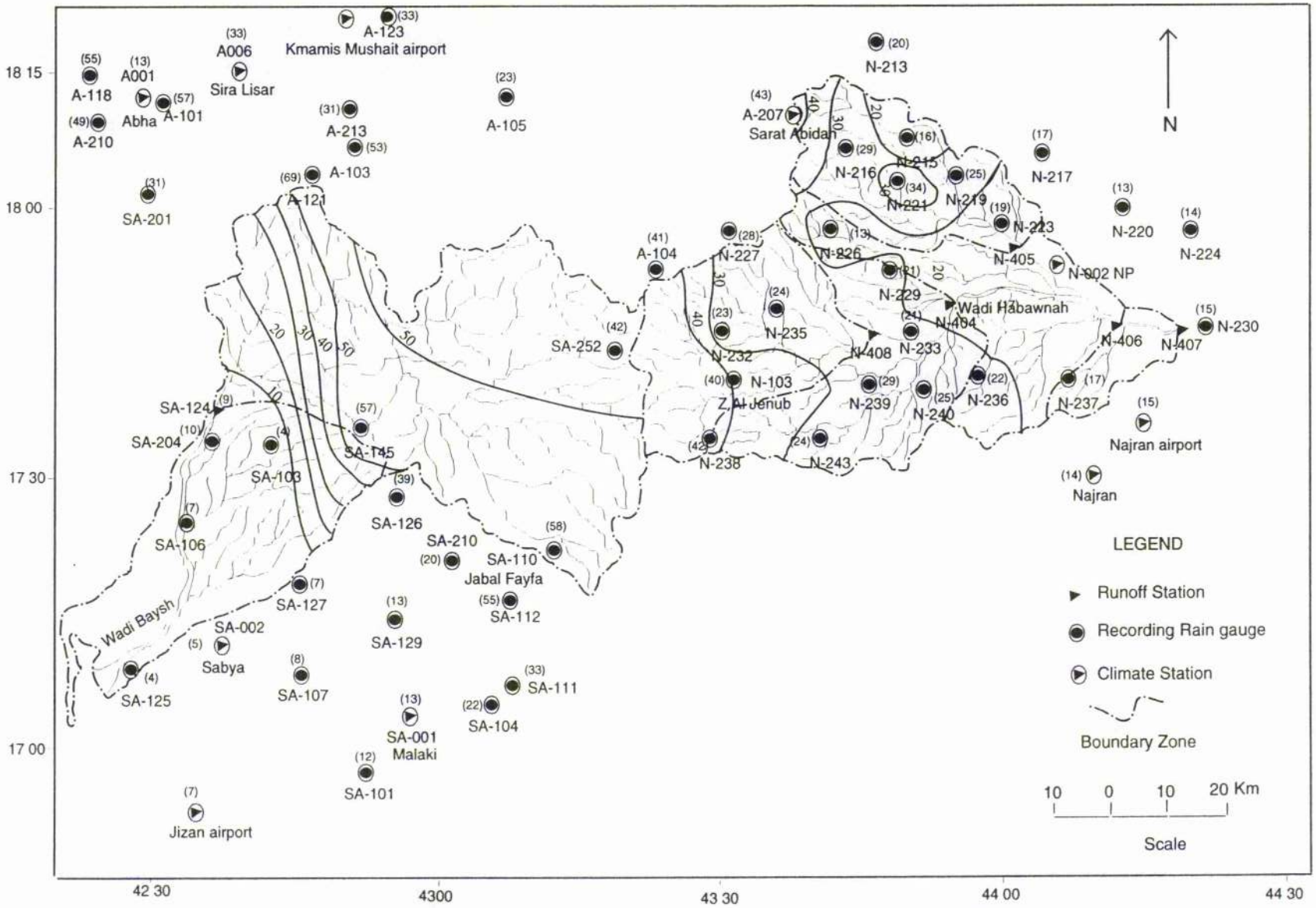

Figure 3.28 Isohyets of Spring Rainfall (mm) for Wadi Baysh (flowing towards the southwest) and Wadi Habawnah (flowing towards the east) south of Arabian Shield.

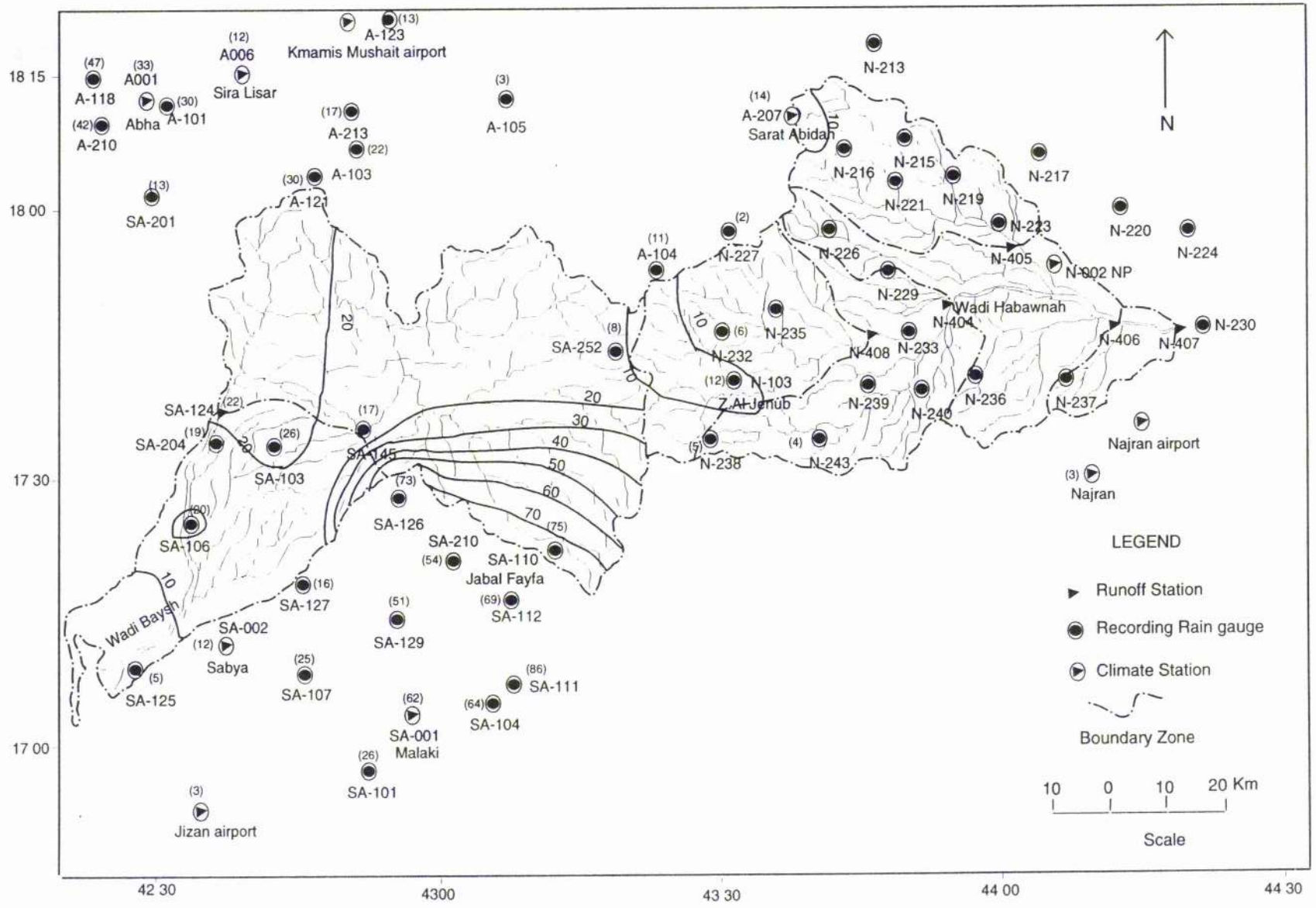

Figure 3.29 Isohyets of Summer Rainfall (mm) for Wadi Baysh (flowing towards the southwest) and Wadi Habawnah (flowing towards the east) south of Arabian Shield.

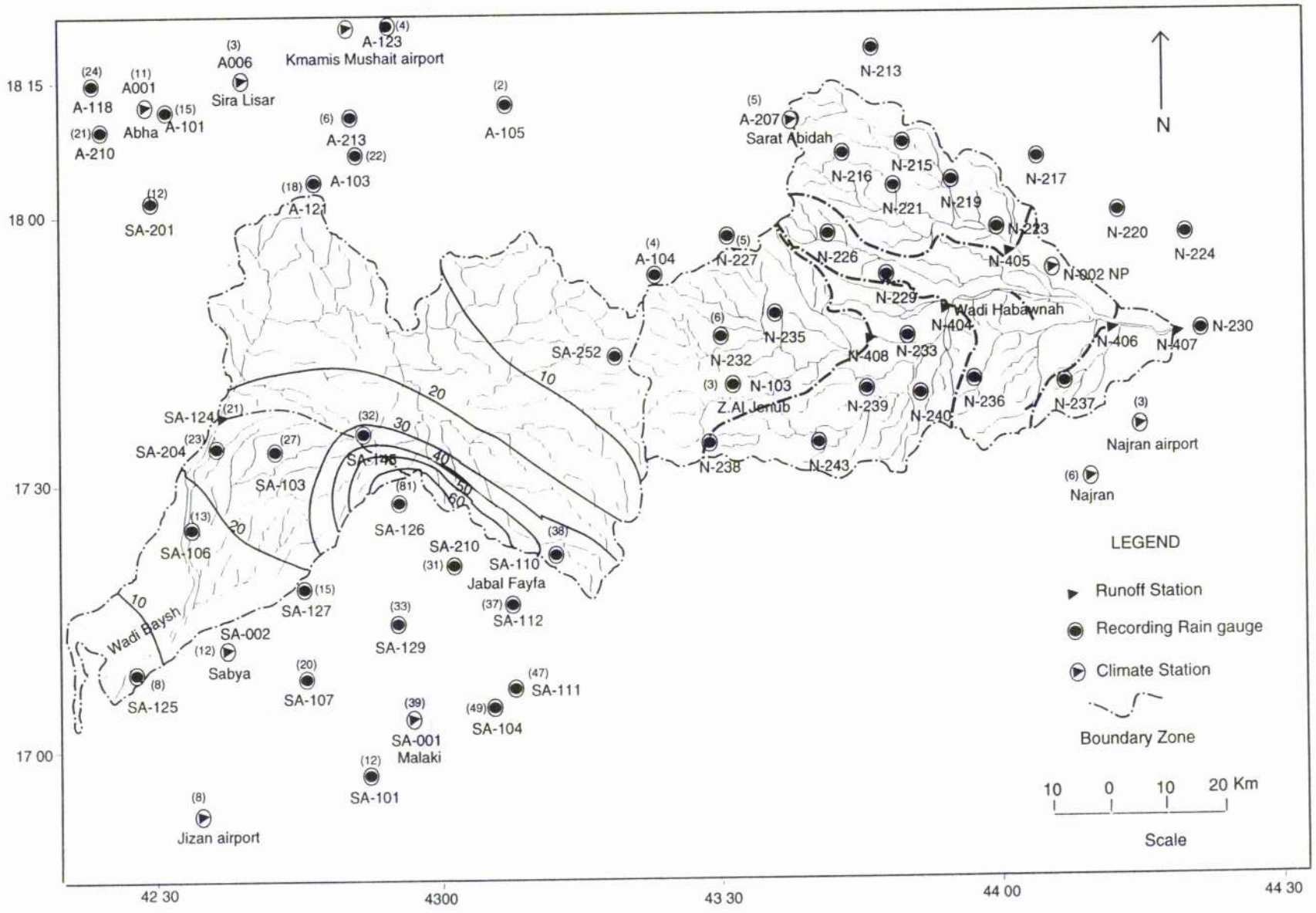

Figure 3.30 Isohyets of Autumn Rainfall (mm) for Wadi Baysh (flowing towards the southwest) and Wadi Habawnah (flowing towards the east) south of Arabian Shield.

Table 3.13 Rainfall data in and nearby catchment areas of Wadi Baysh and Habawnah

Wadi Baysh rainfall (mm)			Winter					Spring					Summer					Autumn					
Station No.	Elevation (m)	Year record	DEC mean	JAN mean	FEB mean	Total mm	Season mean (mm)	MAR mean	APR mean	MAY mean	Total mm	Season mean (mm)	JUN mean	JUL mean	AUG mean	Total mm	Season mean (mm)	SEP mean	OCT mean	NOV mean	Total mm	Season mean (mm)	Annual mean
SA-145	600	1972-76*	95.4	73.3	46.3	215	72	47.2	66	57.3	171	57	18.4	16.9	16.4	52	17	15.6	18.6	62.9	97	32	582.8
SA-126	540	1967-84	29.5	24.3	35.3	89	30	18.8	28.8	68.4	116	39	43.9	67.5	108	220	73	97.9	96.3	50	244	81	668.7
SA-103	190	1966-84	20.4	19.3	13.3	53	18	2.4	5.8	3.6	12	4	10.1	44.1	24.1	78	26	26.2	27	27.6	81	27	223.8
SA-204	200	1970-84	22.3	20.5	7.4	50	17	9.4	7.9	11.3	29	10	6.4	20.5	31.3	58	19	29.1	30.7	9.7	70	23	194.2
SA-124	200	1967-84	19.8	19.2	7.4	46	15	8.5	7.2	11	27	9	12.3	24.9	27.9	65	22	24.5	26.8	11.5	63	21	201
SA-125	5	1967-84	10	6.2	7.7	24	8	1.5	3.4	0.3	5	2	9.3	6.1	3.6	19	6	13.9	7.8	7.6	29	10	77.5
A-118	2820	1965-84	15.6	25.8	46.8	88	29	50	69.4	87.1	207	69	22.3	42.1	75.4	140	47	21	18.5	32.5	72	24	506.5
A-210	2670	1967-84	18.2	34.3	29.2	82	27	45.8	65.5	60.7	172	57	24.4	45.8	54.5	125	42	5.5	12.3	45.6	63	21	441.9
A-001	2200	1966-84	7.9	25.5	40.9	74	25	57.8	59.4	48.9	166	55	14	42.9	40.6	98	33	5.2	10.3	17.5	33	11	370.8
A-101	2190	1960-84	16.9	27.3	29.6	74	25	52.9	80.5	37.3	171	57	16	36.2	38.6	91	30	2.7	3	38.2	44	15	379.2
A-006	2100	1982-84	10.4	6.5	120	137	46	31.3	36.3	31.9	100	33	3.8	7.7	24.3	36	12	0.3	3.3	5.8	9	3	218.6
A-123	1900	1965-84	3.5	6.1	10.1	20	7	25.9	38.1	35	99	33	4.9	17.1	18.3	40	13	2.7	1.2	9.3	13	4	172.4
A-105	2060	1967-84	2.5	3	6.8	12	4	21.3	26.5	20.3	68	23	1.4	5.8	1.4	9	3	0	1.4	3.6	5	2	93.8
SA-001	190	1962-84	3.8	14.2	4.8	23	8	11.9	10	17	39	13	8.6	62.8	115	186	62	51.9	39.6	24.2	116	39	363.5
A-103	2100	1965-84	6.4	17.4	40.7	65	22	43	55.4	59.7	158	53	12.9	22.4	54.1	89	30	7.6	4.3	12	24	8	335.8
A-121	2300	1965-84	15.9	37.7	46.7	100	33	64.3	70.4	72.8	208	69	15	29.2	47	91	30	10.7	16.3	26.9	54	18	452.9
SA-110	860	1960-84	40.9	33.6	33	108	36	34.2	73.5	66.6	174	58	47.7	84.7	93.6	226	75	48.8	28.4	37	114	38	622
SA-112	800	1960-84	39.9	34.4	33.6	108	36	34.3	69.6	61.7	166	55	46.7	76	84.2	207	69	46.4	29.5	36.3	112	37	592.5
SA-111	900	1960-84	63.5	34.6	24.3	122	41	14.2	39.9	44.8	99	33	53.4	105	99.6	258	86	52	32.5	56.5	141	47	615.7
SA-104	223	1964-84	25.3	18.1	12.3	56	19	7.5	25	33.1	66	22	37.9	70.8	82.5	191	64	63.6	43.1	41.2	148	49	460.4
A-213	2030	1966-84	6.8	10	30.5	47	16	35.8	33.6	23.6	93	31	12.3	15.9	23	51	17	3.4	4.1	11.1	19	6	210.1
SA-201	820	1968-73	5.1	23.4	15.1	44	15	29.1	33.3	30.1	93	31	11.5	8.2	19.5	39	13	13.5	11.9	11.7	37	12	212.4
SA-210	305	1968-71	19.6	26.8	14.9	61	20	31.4	65.5	51.4	148	49	34.2	68.9	58.8	162	54	44.4	20.1	27.6	92	31	463.5
SA-252	2200	1984-87	6.5	11.2	2.2	20	7	29.7	60.3	37.3	127	42	9.8	0.4	13.0	23	8	0.0	0.2	4.7	5	2	175.0

Continued on next page

Table 3.13 continued

Wadi Habawnah rainfall (mm)

Station No.	Elevat-ation (m)	Year record	Winter DEC mean	JAN mean	FEB mean	Total mm	Season mean (mm)	Spring MAR mean	APR mean	MAY mean	Total mm	Season mean (mm)	Summer JUN mean	JUL mean	AUG mean	Total mm	Season mean (mm)	Autumn SEP mean	OCT mean	NOV mean	Total mm	Season mean (mm)	Annual mean
N-217	1340	1984-87	1.1	0.6	1.0	3	1	10.1	34.3	6.6	51	17	0.6	0.0	0.2	1	0	0.1	0.0	0.2	0	0	54.6
N-219	1460	1984-87	0.3	2.5	0.0	3	1	16.7	53.7	6.0	76	25	0.1	0.5	0.5	1	0	0.2	0.0	0.0	0	0	80.3
N-220	1306	1984-87	0.3	1.7	0.0	2	1	7.6	25.0	7.5	40	13	0.1	0.0	0.1	0	0	0.0	0.0	0.0	0	0	42.2
N-223	1300	1984-87	0.6	3.6	0.0	4	1	11.1	36.4	8.1	56	19	0.0	0.7	0.9	2	1	0.4	0.0	0.0	0	0	61.7
N-224	1250	1984-87	0.7	2.5	0.0	3	1	9.2	26.7	5.2	41	14	0.0	0.7	0.0	1	0	0.0	0.0	0.0	0	0	44.8
N-229	1300	1984-87	0.2	4.6	0.0	5	2	12.3	41.9	9.1	63	21	0.0	0.1	0.3	0	0	0.1	0.0	0.0	0	0	68.4
N-230	1160	1984-87	1.4	0.4	0.0	2	1	12.9	27.1	4.7	45	15	0.0	0.0	0.2	0	0	0.0	0.0	0.0	0	0	46.5
N-233	1360	1984-87	0.8	4.3	1.7	7	2	9.3	47.9	7.2	64	21	4.5	0.8	1.2	6	2	1.4	0.0	0.0	1	0	78.9
N-236	1400	1984-87	0.4	7.8	1.0	9	3	10.6	46.7	9.0	66	22	0.0	0.0	0.1	0	0	0.1	0.0	0.0	0	0	75.5
N-237	1400	1984-87	0.6	4.2	0.2	5	2	12.8	30.2	7.4	50	17	0.0	0.0	0.6	1	0	0.0	0.0	0.0	0	0	55.9
N-239	1500	1984-87	2.1	5.9	0.5	8	3	8.7	69.7	7.9	86	29	4.7	1.0	1.2	7	2	1.5	0.3	0.0	2	1	103.1
N-215	1600	1984-87	0.3	4.8	0.8	6	2	19.5	27.3	2.5	49	16	0.1	0.0	0.2	0	0	0.1	0.0	0.0	0	0	55.5
N-216	2120	1984-87	0.4	6.0	0.2	7	2	14.9	59.3	12.9	87	29	0.9	0.6	2.1	4	1	0.0	0.0	0.0	0	0	97.0
N-221	1630	1984-87	0.3	3.2	0.1	4	1	17.4	47.2	5.5	70	23	1.0	0.7	0.1	2	1	0.0	0.0	0.0	0	0	75.3
N-226	1980	1984-87	0.7	3.8	0.1	5	2	10.2	80.1	12.8	103	34	0.2	1.6	1.6	3	1	1.1	0.0	0.0	1	0	112.0
N-227	2320	1984-87	1.4	13.3	0.1	15	5	21.4	40.3	21.5	83	28	2.4	0.3	1.8	4	1	0.2	0.0	4.5	5	2	107.0
N-232	2200	1984-87	3.9	10.7	2.0	17	6	20.5	9.6	39.0	69	23	5.0	1.8	9.9	17	6	2.1	0.8	2.0	5	2	107.1
N-235	1620	1984-87	1.2	2.8	0.0	4	1	8.8	49.0	12.6	70	23	0.1	1.5	0.5	2	1	0.1	0.0	0.0	0	0	76.4
N-238	2140	1984-87	7.3	5.8	2.0	15	5	34.6	59.9	30.8	125	42	1.0	1.1	5.5	7	2	0.3	0.0	0.3	1	0	148.4
N-240	1770	1984-87	1.2	6.1	0.8	8	3	20.4	42.4	11.6	74	25	0.3	0.2	0.4	1	0	0.0	0.0	0.0	0	0	83.1
N-243	2080	1984-87	2.5	6.1	0.7	9	3	17.1	34.3	19.5	71	24	0.8	7.0	2.9	11	4	0.0	0.0	0.0	0	0	90.7
N-213	1880	1984-87	0.2	3.6	1.8	6	2	20.5	26.6	12.5	60	20	0.0	0.1	1.7	2	1	0.1	0.0	0.0	0	0	67.0
NAJAIR**	1250	1970-84	3.8	2.8	8.1	15	5	22.6	17.5	4.6	45	15	0	1.5	1.8	3	1	0	8.1	0.5	9	3	71.3
NAJRAN	1210	1970-84	0.3	2.5	3	6	2	21.6	21.6	4.6	48	16	0	0.3	9.1	9	3	0	10.7	6.6	17	6	111.4
A-207	2400	1966-84	5.9	16	35.8	58	19	48.2	43.9	38.2	130	43	4.3	19.6	17.6	42	14	1.6	3.5	9.9	15	5	244.2
A-104	2250	1966-84	3.6	16	26	46	15	45.2	44.3	33.2	123	41	0	16.5	15	32	11	0	4.6	8.7	13	4	213.3
N-103	2020	1964-84	8.9	11.9	17.5	38	13	34.9	54.7	31	121	40	1.3	16	19.1	36	12	0.4	5.6	4.4	10	3	205.7

(*) 1972-76/1980-1984

(**) Najran airport

Table 3.14 Seasonality calculation of rainfall within the catchment area of both wadis based on the isoheyt map of each season

Wadi Baysh

SUMMER RAINFALL (mm)

Outlet Gauge No.	Rainfall	Area	Area	Rainfall
SA-124	(mm)	(cm^2)	km^2	mcm**
(3511)*	10	2.1	245	2
	15	10.8	1260	19
	25	9.2	1073	27
	35	1.7	198	7
	45	1.9	222	10
	55	1.5	175	10
	65	1.7	198	13
	75	1.20	140	88
		3511	3511	173

AUTUMN RAINFALL (mm)

Outlet Gauge No.	Rainfall	Area	Area	Rainfall
SA-124	(mm)	(cm^2)	km^2	mcm**
(3511)*	10	7.18	837	8
	15	14.1	1645	25
	25	5.3	618	15
	35	2.12	247	9
	45	0.7	82	4
	55	0.5	58	3
	65	0.203	24	2
		3511	3511	66

WINTER RAINFALL (mm)

Outlet Gauge No.	Rainfall	Area	Area	Rainfall
SA-124	(mm)	(cm^2)	km^2	mcm**
(3511)*	10	4.1	478	5
	15	5.73	668	10
	25	8.1	945	24
	35	11	1283	45
	60	1.17	136	8
		3511	3511	92

Wadi Habawnah

SUMMER RAINFALL (mm)

Outlet Gauge No.	Rainfall	Area	Area	Rainfall
N-405	(mm)	(cm^2)	km^2	mcm**
(940)*	10.00	0.50	58	1
	5	7.56	882	4
		sum	940	5
N-408	10.00	2.50	292	3
(1307)*	7.50	8.70	1015	8
		sum	1307	11
N-404	10.00	2.50	292	3
(2391)*	7.50	8.70	1015	8
	5	11.8	1376	7
	sum	23	2391	18
N-406	10.00	0.50	58	1
(4425)*	5	7.56	882	4
	10.00	2.50	292	3
	7.50	8.70	1015	8
	5	11.8	1376	7
	0	6.87	801	0
	sum	37.9	4425	23
N-407	10.00	0.50	58	1
(4647)*	5	7.56	882	4
	10.00	2.50	292	3
	7.50	8.70	1015	8
	5	11.8	1376	7
	0	14.93	1741	0
	0	1.91	223	0
	sum	39.8	4647	23

AUTUMN RAINFALL (mm)

Outlet Gauge No.	Rainfall	Area	Area	Rainfall
N-407	(mm)	(cm^2)	km^2	mcm**
(4647)*	0.00	39.8	4647	0

WINTER RAINFALL (mm)

Outlet Gauge No.	Rainfall	Area	Area	Rainfall
N-408	(mm)	(cm^2)	km^2	mcm**
(1307)*	10.00	4.10	478	5
	7.50	7.10	828	6
			1307	11
N-405	15.00	0.90	105	2
(940)*	5	7.16	835	4
			940	6
N-404	10.00	4.10	478	5
(2391)*	7.50	7.10	828	6
	5.00	9.30	1085	5
			2391	19
N-406	10.00	4.10	478	5
(4425)*	7.50	7.10	828	6
	5.00	9.30	1085	5
	15.00	0.90	105	2
	5	7.16	835	4
	5	9.38	1094	5
			4425	28
N-407	10.00	4.10	478	5
(4647)*	7.50	7.10	828	6
	5.00	9.30	1085	5
	15.00	0.90	105	2
	5	7.16	835	4
	5	9.38	1094	5
	5	1.9	222	1
			4647	29

Continued on next page

Table 3.14 continued

SPRING RAINFALL (mm)					SPRING RAINFALL (mm)				
Outlet Gauge N0.	Rainfall (mm)	Area (cm^2)	Area km^2	Rainfall mcm**	Outlet Gauge N0.	Rainfall (mm)	Area (cm^2)	Area km^2	Rainfall mcm**
SA-124	45	9.2	1073	48	N-408	40.00	4.40	513	21
(3511)*	50	14.3	1668	83	(1307)*	35.00	1.90	222	8
	45	1.15	134	6		25.00	4.90	572	14
	35	1.1	128	4				1306	43
	25	1.4	163	4	N-404	40.00	4.40	513	21
	15	1.5	175	3	(2391)*	35.00	1.90	222	8
	10	1.45	169	2		25.00	4.90	572	14
		3511	3511	151		40.00	0.40	47	2
						35.00	1.60	187	7
						25.00	7.30	851	21
								2391	63
					N-405	40.00	0.17	20	1
					(940)*	35.00	0.79	92	3
						25.00	3.61	421	11
						30.00	0.49	57	2
						20.00	0.92	107	2
						17.00	2.08	243	4
								940	23
					N-406	40.00	4.4	513	21
					(4425)*	35.00	1.9	222	8
						25.00	4.9	572	14
						40.00	0.4	47	2
						35.00	1.6	187	7
						25.00	7.3	851	21
						40.00	0.17	20	1
						35.00	0.79	92	3
						25.00	3.61	421	11
						40.00	0.49	57	2
						35.00	0.92	107	4
						25.00	2.08	243	6
						25.00	0.40	47	1
						25.00	1.38	161	4
						17.00	7.60	886	15
								4425	142
					N-407	40.00	4.4	513	21
					(4647)*	35.00	1.9	222	8
						25.00	4.9	572	14
						40.00	0.4	47	2
						35.00	1.6	187	7
						25.00	7.3	851	21
						40.00	0.17	20	1
						35.00	0.79	92	3
						25.00	3.61	421	11
						40.00	0.49	57	2
						35.00	0.92	107	4
						25.00	2.08	243	6
						25.00	0.40	47	1
						25.00	1.38	161	4
						17.00	7.60	886	15
						17.00	1.90	222	4
								4647	146

(*) The total area (km^2) of the outlet drainage area of subcatchment

** million cubic meters

limited areas of rainfall in the west and north west with 10 mm. The rainfall volumes falling in Wadi Baysh and Habawnah are 92 and 29 mcm respectively (see Table 3.14). Both of the study areas are mainly influenced by the Mediterranean depressions that penetrate the Arabian peninsula during the winter season. These depressions have less effect southwards.

3.2.2.5.2 Spring Rainfall

Spring is the main rainfall season in both wadis with more than half of the annual precipitation (see Figure 3.28 and Tables 3.13 and 3.14). In Wadi Baysh the greatest amount of spring rain falls in the mid-south while in Wadi Habawnah the highest rainfall falls at the western end of the catchment.

The spring rainfall, in Wadi Baysh ranges between 5mm and 58mm (see Table 3.12). The greatest rainfall is found at SA-110, whereas the lowest rainfall is found at SA-125 (Fig. 2.30). Station SA-110 is much higher than station SA-125 (see Table 3.4).

Wadi Habawnah rain-station A-207 shows the highest rainfall of 130mm which is 53% of the annual total (see Table 3.12). However, rain-stations N-238, A-107 and N-103 are characterised by high rainfall with annual average of 125, 123 and 121mm respectively. Rain-station N-230 shows a lower spring rainfall of 45mm (see Table 3.12).

Spring is the wettest season in both wadis. Since the Mediterranean depressions are weaker during the spring (Al-Blehed 1984) the author believes that, at that time, the study area comes under the influence of the southeast monsoon which prevails over the southern half of the Arabian Peninsula. On the basis of the rainfall data it appears that the storms penetrate most of the upper parts of both wadis. The spring rain volume in Wadi Baysh is 151 mcm and in Wadi Habawnah it is 146 mcm.

3.2.2.5.3 Summer Rainfall

In the summer about 25% of the total annual precipitation falls in Wadi Baysh while Wadi Habawnah has a dry summer, during which most rain-stations have recorded negligible amounts of rainfall. The highest rainfall in Wadi Habawnah during the

summer is shown by rain station N-230 (15 mm) with 6% of the annual total. The rest of the rain-stations within the Wadi Habawnah catchment show ranges between zero and 10mm.

The summer rainfall in Wadi Baysh shows a high total of 521mm over the catchment area. The highest summer rainfall occurs at station SA-110 in which the rainfall for the 3 months is 226mm. However, the other rain-stations show a variation of rainfall between 19mm and 78mm. (See Figure 3.29 and Table 3.12).

Summer precipitation over Wadi Baysh is brought mainly by the south-west monsoon flow, which is characterised by moist cool air. The author believes that the Arabian escarpment becomes a barrier, and the south-western monsoon winds that bring great amounts of moisture from the Indian Ocean and Arabian Sea through the Red Sea cannot cross the mountains to enter Wadi Habawnah. During this season, generally, the precipitation increases with increasing elevation.

The monsoon winds precipitate most of their moisture on the crest of the escarpment and along windward western slopes so that the foothills and the western slopes of the study area receive more precipitation than the eastern slopes (in Wadi Habawnah).

The southern part of Wadi Baysh shows high precipitation compared to the northern part. The foothills receive more precipitation during summer than the ridge crest and adjacent areas (see Table 3.12 and Figure 3.29).

Table 3.12 shows that rainfall station SA-110 with an elevation of 860m has a mean summer rainfall of 226mm while rain station SA-252 received only 23mm of rainfall at an elevation of 2200m. The former station is located in the southern foothills. These lie across the south-western monsoon which does not continue sufficiently far inland to reach the latter station near the crest of the escarpment. According to Table 3.14 and Figure 3.29, Wadi Baysh receives a rainfall volume of 173 mcm while in Wadi Habawnah it is 23 mcm during the summer months.

3.2.2.5.4 Autumn Rainfall

The autumn rainfall is spread through Wadi Baysh (see Figure 3.30 and Table 3.14). However, in Wadi Habawnah it is very dry. In general, the Wadi Baysh area receives less rainfall in autumn than any other season. Figure 3.30 shows that foothill stations receive more rainfall than the higher stations. The highest rainfall mean is recorded at station SA-110 (114mm).

Also the foothill rainfall stations receive more rainfall than the stations located at the crest of the escarpment because the foothill rainfall stations are again influenced mainly by the south-western monsoon.

However, the autumn is a transition period from the summer to the winter. The influence of the monsoon is effective during the early autumn (September) while the Mediterranean depressions begin to become important later (Algrashi 1981). The rainfall volume of this season is 66 mcm for Wadi Baysh while in Wadi Habawnah there is no rain (Table 3.14).

3.2.2.6 The Aridity of the Study Area

The comparison between precipitation and evaporation can be used to define whether a region is arid or semi-arid. UNESCO (1979) considered that the degree of aridity is based on the ratio of mean annual precipitation to mean annual potential evaporation estimated by the Penman approach. The ratio is used to define arid and semi-arid zones as follows:

1- Arid zone: 0.03 - 0.2

2- Semi-arid zone: 0.2 - 50

According to this classification the south-western and north-eastern parts of Wadi Baysh (Table 3.15) can be considered as being arid since the ratios of the mean annual precipitation of the SA-106 (165mm), SA-103 (224mm) and SA-252 (175mm) stations to the mean annual evaporation of Sabya (3352mm), Malaki (3536mm) and Abha (2678mm) stations respectively are 0.06. However, the south-eastern part of Wadi Baysh is semi-arid because the ratio of the annual rainfall of SA-110 (622) to the annual evaporation of the Abha station is 0.23 (see Table 3.15). On the other hand, Wadi Habawnah is located

Table 3.15 Aridity of the study area based on rainfall (R)/potential evaporation (PE) ratio of UNESCO Classification,1979

Wadi Baysh Rainfall Station No.	Annual rainfall mean (mm)	PE Station No.	Annual PE mean (mm)	Ratio R/PE	Aridity type
SA-106*	165	Sabya*	3352	0.05	Arid zone
SA-103*	224	Malaki*	3536	0.06	Arid zone
SA-252*	175	Abha*	2678	0.07	Arid zone
SA-110**	622	Abha**	2678	0.23	Semiarid zone
		Malaki**	3536	0.20	Semiarid zone

Wadi Baysh Rainfall Station No.	Annual rainfall mean (mm)	PE Station No	Annual PE mean (mm)	Ratio R/PE	Aridity type
Sarat Abidah*	155	Sarat Abidah*	1100	0.14	Arid zone
N-223*	61	N-002NP*	4070	0.01	Arid zone

* Approximately , it has same elevation

** SA-110 (860 m amsl) located between Malaki (200 m amsl) and Abha (2200 m amsl)

in an arid zone in which the ratios of the annual mean of the precipitation of the Sarat Abidah (155mm) and N-223 (61mm) stations to the annual mean of evaporation of Sarat Abidah (1100mm) (5814mm) are 0.14 and 0.01, respectively (see Table 3.15).

3.2.2.6.1 Rainfall and Potential Evapotransportation

It is known that an agricultural area should have a rainfall rate that exceeds the potential evapotranspiration (PT) level. Brown and Cocheme (1972) indicate that the conditions for agricultural land can be classified on the basis of the rainfall and potential evapotranspiration as follows:

1- Humid: rainfall rate > PT

2- Moist: rainfall rate $>^1/_2$ PT

3- Intermediate: rainfall rate is between PT and half of it.

4- Moderately dry: rainfall rate equals half PT

5- Dry: rainfall is equal to $^1/_{10}$ of PT

Five meteorological stations within and nearby the study area were examined according to the above classification. The monthly rainfall means were selected for the rainfall stations within the catchment areas of both wadis, and plotted against the PT, $^1/_2$ PT and $^1/_{10}$ PT for the climate station that has the same elevation as the rain station. Figures 2.31 and 2.32 and Table 3.16 show the relationship between the rainfall and PT in the study area (SA-103 -SA-106 forWadi Baysh and N-233 for Wadi Habawnah).

The lower parts of both wadis show that the rainfall intersects only the $^1/_{10}$ PT value, which indicates that the water availability may be classified as dry. However, the upper parts of both catchment areas (SA-252 station of Wadi Baysh and Sarat Abidah of Wadi Habawnah) are characterised by humid to intermediate conditions in which the rainfall intersects the PT and $^1/_2$ PT levels.

Generally speaking, the upper parts of both catchments receive more water than the lower parts. The only possibility of replenishment in the lower parts of both wadis is where groundwater aquifers are present.

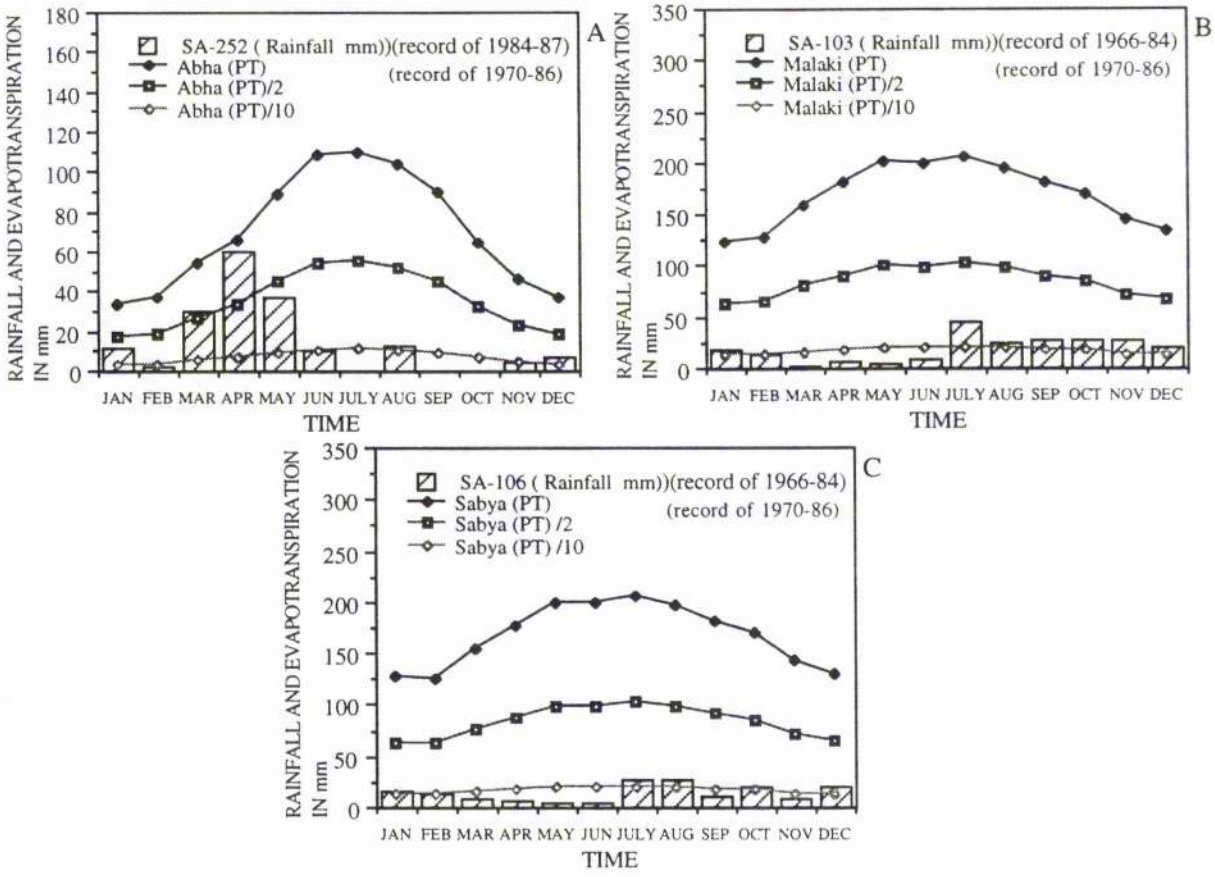

Figure 3.31 Average values of rainfall and potential evapotranspiration (mm) of Abha (A), Malaki (B) and Sabya (C) Stations.

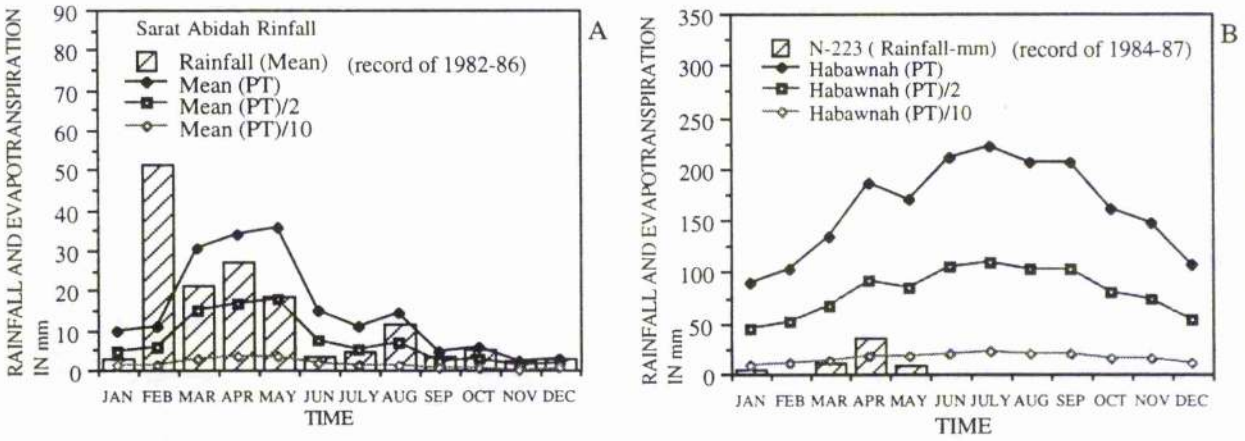

Figure 3.32 Average values of rainfall and potential evapotranspiration (mm) of Sarat Abidah (A) and Habawnah (B) Stations.

Table 3.16 Average value of temperature (°C), evaporation (mm) Class A pan (PE), potential evapotransparation (mm) (PT) and rainfall for meteorological different altitudes (Sabya 65 m); (Malaki 190 m); (Abha 2200m); (Sarat Abidah 2400 m) and (Habawnah 1160 m)

Wadi Baysh

Month	Sabya* Temp. (°C)	Sabya* PE mm	Sabya* PT mm	Station No. SA-106 Rainfall mm	Malaki* Temp. (°C)	Malaki* PE mm	Malaki* PT mm	Station No. SA-103 Rainfall mm	Abha* Temp. (°C)	Abha* PE mm	Abha* PT mm	Station No. SA-252 Rainfall mm	Station No. SA-110 Rainfall mm
JAN	26.3	172	127	15	26	201	124	19	12	136	34	11	34
FEB	27.1	183	126	14	27	227	128	13	13	156	37	2	33
MAR	28.5	251	154	9	29	280	160	2	16	212	54	30	34
APR	31.1	300	177	6	32	359	181	6	17	215	66	60	74
MAY	33.5	354	199	5	34	386	203	4	20	256	89	37	67
JUN	34.5	359	199	4	35	367	199	10	22	304	109	10	48
JULY	34.6	375	206	27	35	377	206	44	22	297	110	0.4	85
AUG	34.3	346	198	26	34	320	196	24	22	255	104	13	94
SEP	33.7	310	182	11	33	288	181	26	21	288	90	0.0	49
OCT	31.3	302	170	20	31	296	170	27	17	246	65	0.2	28
NOV	28.9	216	144	9	29	220	145	28	15	175	46	5	37
DEC	27	186	131	20	27	215	134	20	13	137	37	7	41
Mean		279	168	14		295	169	19		223	70	15	622
Sum		3352	2012	165		3536	2025	224		2678	839	175	
mm/day		9	6			10	6			7	2		

Continued on next page

Table 3.16 continued

Wadi Habawnah

Month	Sarat Abidah^ Temp. (°C)	Sarat Abidah^ PE mm	Sarat Abidah^ PT mm	Sarat Abidah^ Rainfall mm	Habawnah** Temp. (°C)	Habawnah** PE mm	Habawnah** PT mm	Station No. N-223 Rainfall mm
JAN	13	54	10	3	16	289	90	3.6
FEB	14	55	11	51	18	321	104	0.0
MAR	16	79	30	22	23	322	135	11.1
APR	18	88	34	27	25	371	186	36.4
MAY	20	116	36	19	28	359	171	8.1
JUN	22	124	15	3	29	344	210	0.0
JULY	23	138	11	5	31	363	222	0.7
AUG	23	133	14	12	31	363	207	0.9
SEP	22	114	5	3	27	363	207	0.4
OCT	18	82	6	5	22	360	162	0.0
NOV	15	63	2	2	19	329	147	0.0
DEC	13	54	3	3	17	285	108	0.6
Mean		92	15	13		339	162	5.2
Sum		1100	177	155		4070	1949	61.8
mm/day		3.0	0.5			11	5	

(^) mean values of monthly record for 5 years)

(*) mean values of monthly record for 16 years)

(**) mean values of monthly record for 1 years)

3.3 Section Two: Runoff

3.3.1 Runoff

3.3.1.1 Introduction

Wadi flows are generally ephemeral due to the erratic rainfall in both catchment areas. The surface runoff which occurs in the wadi systems is mainly generated by rain storms on the higher areas of the catchment. Wadi Baysh has a much larger mean annual rainfall 1355 mcm and runoff 75 mcm than Wadi Habawnah which has a lower mean annual rainfall of 426 mcm and runoff 14.3 mcm. The runoff occurs in the form of spates or flash flood flows (Figure 3.33a).

A dominant feature of the surface runoff is the infiltration at the wadi bed. This represents a transmission loss for surface runoff, but is the primary mode of groundwater recharge throughout the basin. As a result, the flood flow decreases significantly in magnitude downstream, unless augmented by subsequent tributary inflows. Transmission losses are discussed later in this section.

The channel network is shown in Figure 3.1. The length of the longest watercourse of Wadi Habawnah is 148km with maximum slope and mean slope of 23m/km and 4/km, respectively. Wadi Baysh has a watercourse length of 120km with maximum slope and mean slope of 12m/km and 3m/km, respectively. Both wadis contain integrated trunk channels from several subcatchments, each characterised by steep drainage basins (Figure 3.33b). Each subcatchment is defined by a local wadi name (see Figure 3.1). Table 3.17 summarises the characteristics of both wadis. There is one gauging station (SA-124) at the outlet of the upper part of Wadi Baysh below a drainage area of 3511km^2. For the present study the basin outlet of this wadi is defined as the point of emergence near the Red Sea where the total catchment area (Figure 3.1) is 4625km^2. The elevation ranges from over 3000 m to sea level. There are five gauging stations in the Habawnah catchment area, N-408, N-404, N-405, N-406 and N-407 with drainage areas of 1307, 2391, 940, 4425 and 4682km^2 respectively (Figure 3.2). The basin outlet of Wadi Habawnah is the point of emergence by the town of Husaniah at gauge N-407, above which the catchment area

a

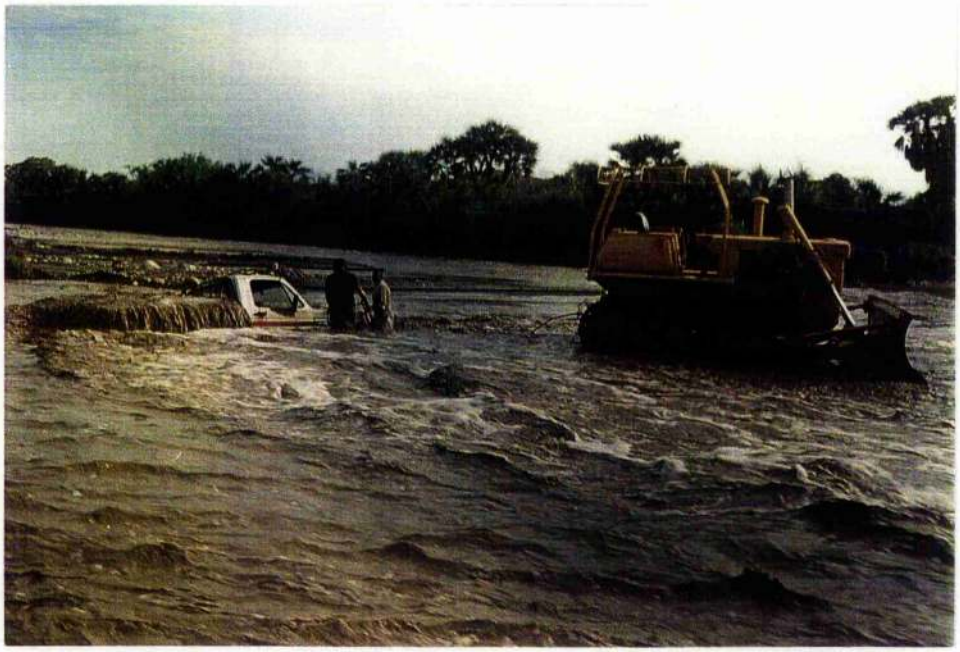

b

Figure 3.33 (a) First day of flood in Wadi Baysh (photo taken on December 22 1990).
(b) Wadi Habawnah, showing the steep drainage of the Wadi.

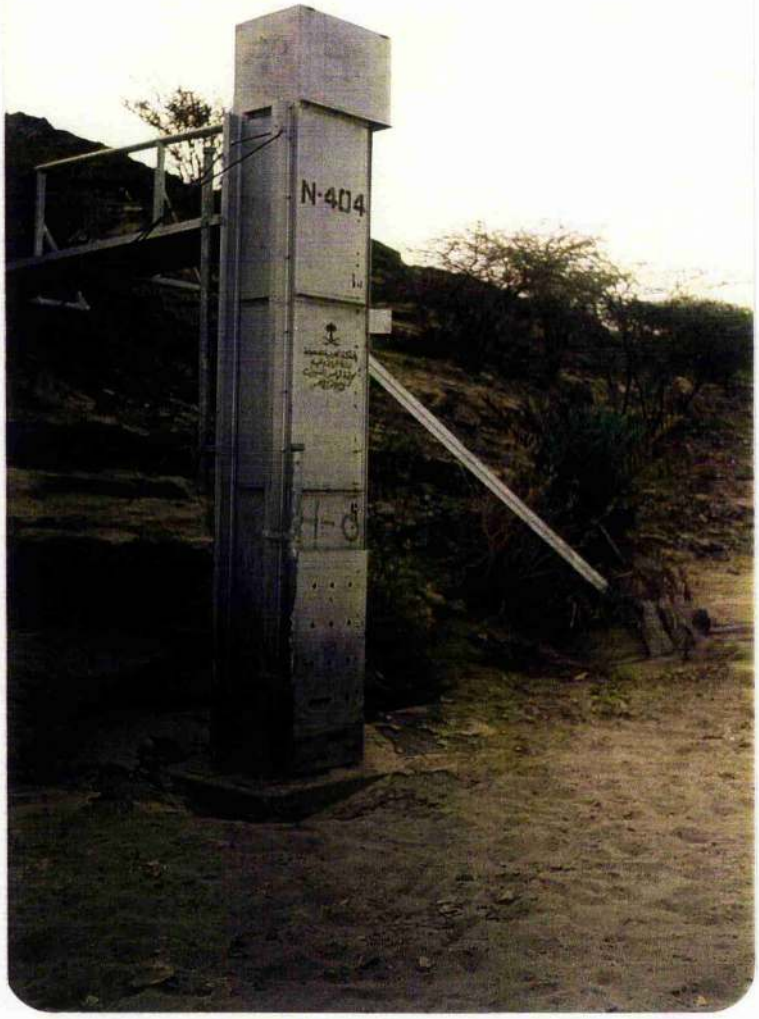

Figure 3.34 Runoff station N-404, Wadi Habawnah-float-type water stage recorders which are generally installed in a shelter house and stilling well.

(Figure 3.1) is 4647km^2. Elevation range is over 1500m, from 3000 to less than 1200m. The above gauge stations are float-type water stage recorders which are generally installed in a shelter house and stilling well (Figure 3.34). Both wadi basins show good average hydraulic conductivity (of 1.6 m/h, Chapter 4). In Wadi Baysh, the infiltration area (the area of the main wadi channel) is approximately 45 km^2 while in Wadi Habawnah it is smaller (27 km^2) (see Chapter 8).

Table 3.17 Wadi Baysh and Wadi Habawnah characteristics.

Wadi Baysh (Upper part of the catchment area).				
Mean annual rainfall 10^6 m^3	Drainage area A (km^2)	Main stream length L (km)	Relief ΔH (m)	Slope S = ΔH/L
1356	3511	118	2100	18m/km
Wadi Baysh (Lower part of the catchment area).				
Main stream length L (km)	Relief ΔH (m)	Hydraulic conductivity K (m/hr)	*Infiltration area A_i (km^2)	Slope S = ΔH/L
60	200	1.5	45	3m/km
Wadi Habawnah (Upper part of the catchment area).				
Mean annual rainfall 10^6 m^3	Drainage area A (km^2)	Main stream length L (km)	Relief ΔH (m)	Slope S = ΔH/L
426	3331	95	1140	12m/km
Wadi Habawnah (Lower part of the catchment area).				
Main stream length L (km)	Relief ΔH (m)	Hydraulic conductivity K (m/hr)	*Infiltration area A_i (km^2)	Slope S = ΔH/L
50	173	1.7	27	3m/km

3.3.1.2 Rainfall-Runoff Relationship

The rainfall-runoff relationships have been investigated for monthly and annual totals to permit the assessment of surface water resources in the wadis. The rainfall of both wadis represents the main source of water for runoff. The rainfall-runoff of the study area is seasonal in which the intensity of rainfall and the river flow vary from one season to another. When the capacity of surface storage is exceeded the water begins to runoff in a short time and this gives rise to a flash flood since the catchment areas of both wadis are mostly impervious and steep. A flood is defined as the result of the runoff in quantities too great to be confined in the low water stream channels. The flood, in its role as a major source of recharge to the aquifer and main water supply for irrigation, is the most important factor in the hydrological balance of the study area.

3.3.1.2.1 Rainfall-Runoff Seasonal Variation

The rainfall runoff relationships in both wadis according to seasons are shown in Figures 3.35, 3.36, 3.37 and 3.38. Wadi Baysh is characterised by rainfall runoff throughout the four seasons while in Wadi Habawnah, although there are flows in the winter and the spring, there is no runoff during the rest of the year. However, the rainfall runoff volumes differ greatly in the two wadis. Wadis Baysh and Habawnah both have high rainfall runoffs in the spring season. In April the Wadi Baysh record shows 195 mcm of rainfall and 13 mcm of runoff while in Wadi Habawnah there is 149 mcm of rainfall and 11.7 mcm of runoff. During the summer and the autumn, there is no rain in Wadi Habawnah, while in Wadi Baysh, August has the highest rainfall and runoff volume of the summer season, which amounted to 139 mcm and 8.9 mcm, respectively. The autumn season is characterised by low rainfall and runoff volume of 70 mcm and 4.8 mcm, respectively.

The winter seasons in both wadis show low rainfall and runoff volumes. Generally, the monthly record of rainfall runoff indicates that no runoff occurs when the rainfall volume is less than 17 mcm.

The runoff coefficient was determined using the average monthly and annual values of rainfall and runoff for both wadis (Table 3.18 and Figure 3.39). The monthly runoff coefficient of Wadi Baysh varied between 0.02 and 0.07 while in the Wadi Habawnah subcatchments area it varied between 0 and 0.076. However, the annual runoff coefficient of Wadi Baysh has a high value of 0.1 compared with Wadi Habawnah which varied between less than 0.05 and over 0.022 (see Figure 3.39). In general, the monthly and annual runoff coefficients of both wadis are low, which reflects the irregularity of the rainfall of both wadi catchments.

3.3.1.2.2 Rainfall-Runoff Annual Variation

The rainfall-runoff relationship is not direct since there is a general cause and effect on this relationship, such as evaporation, infiltration, depression storage etc. The intensity of storms and the season of precipitation, as shown previously, play major roles in runoff variation. For instance, Figure 3.40 shows that the 16 years of the Wadi Baysh flood

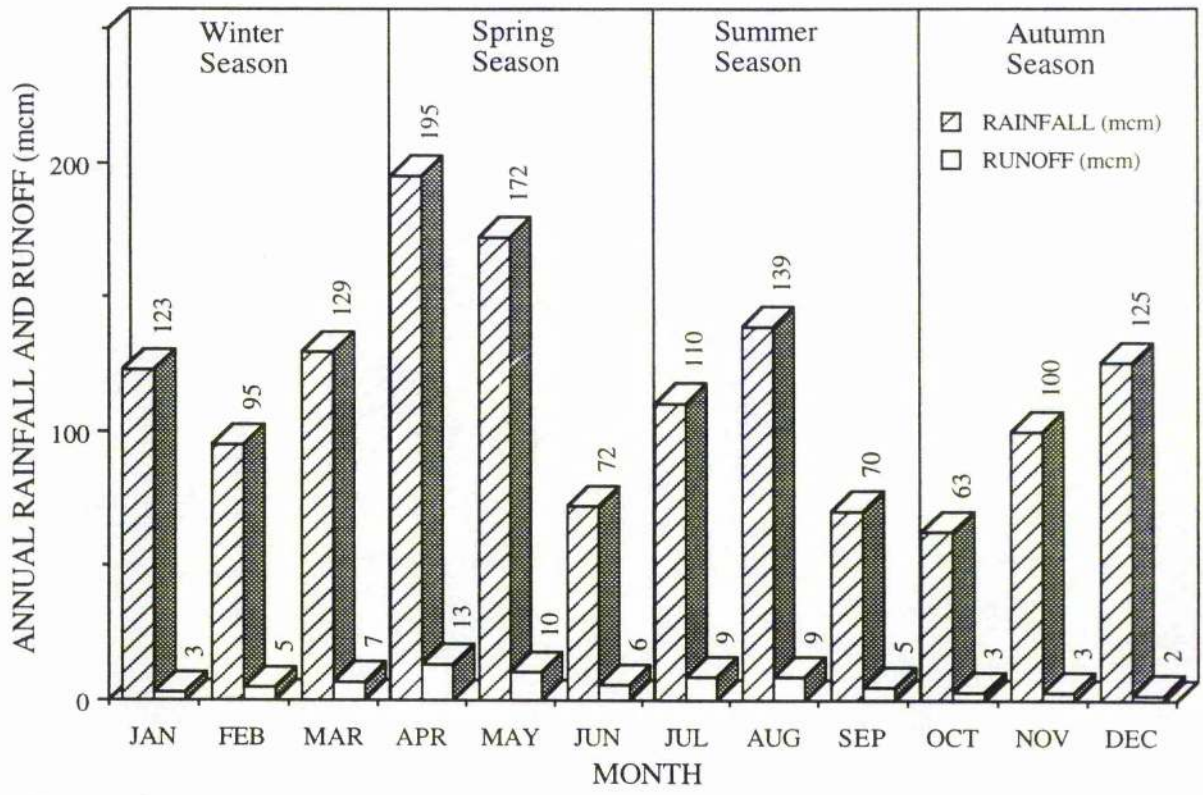

Figure 3.35 Variation of Rainfall - Runoff volume by season within the catchment area of Wadi Baysh.

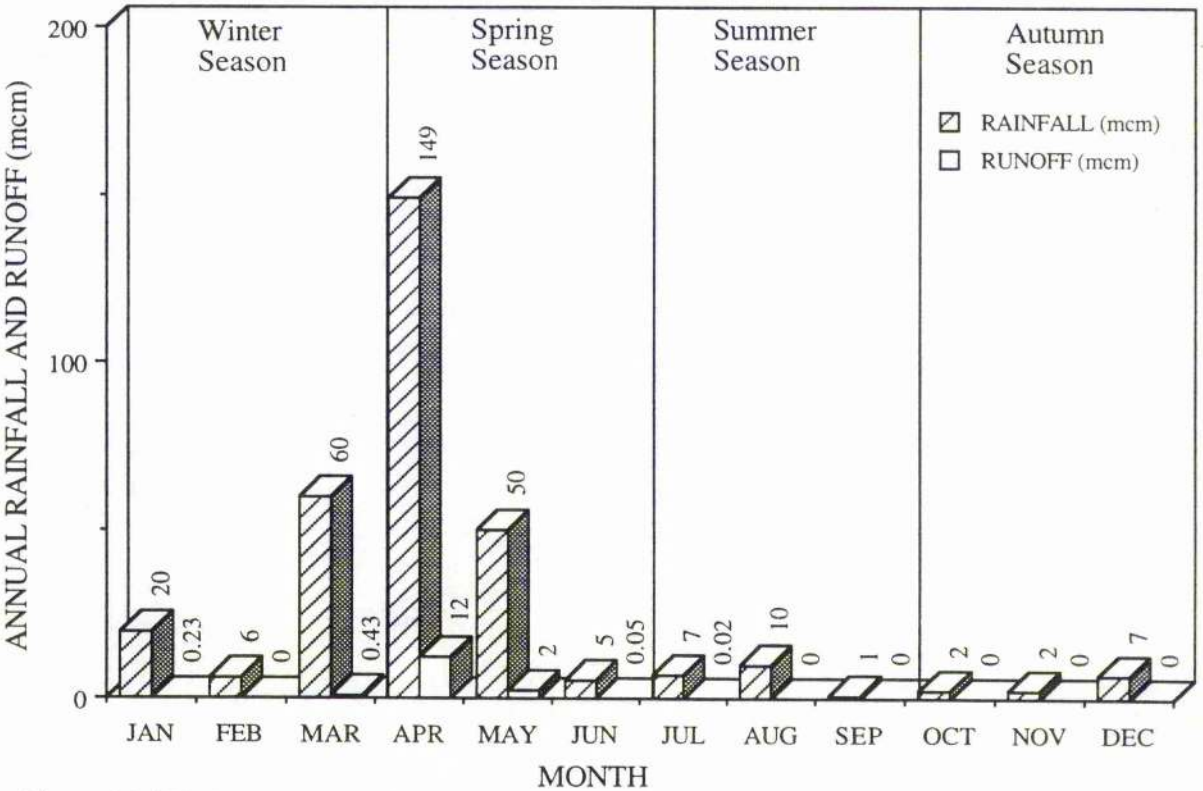

Figure 3.36 Variation of Rainfall - Runoff volume by season within the catchment area of Wadi Habawnah.

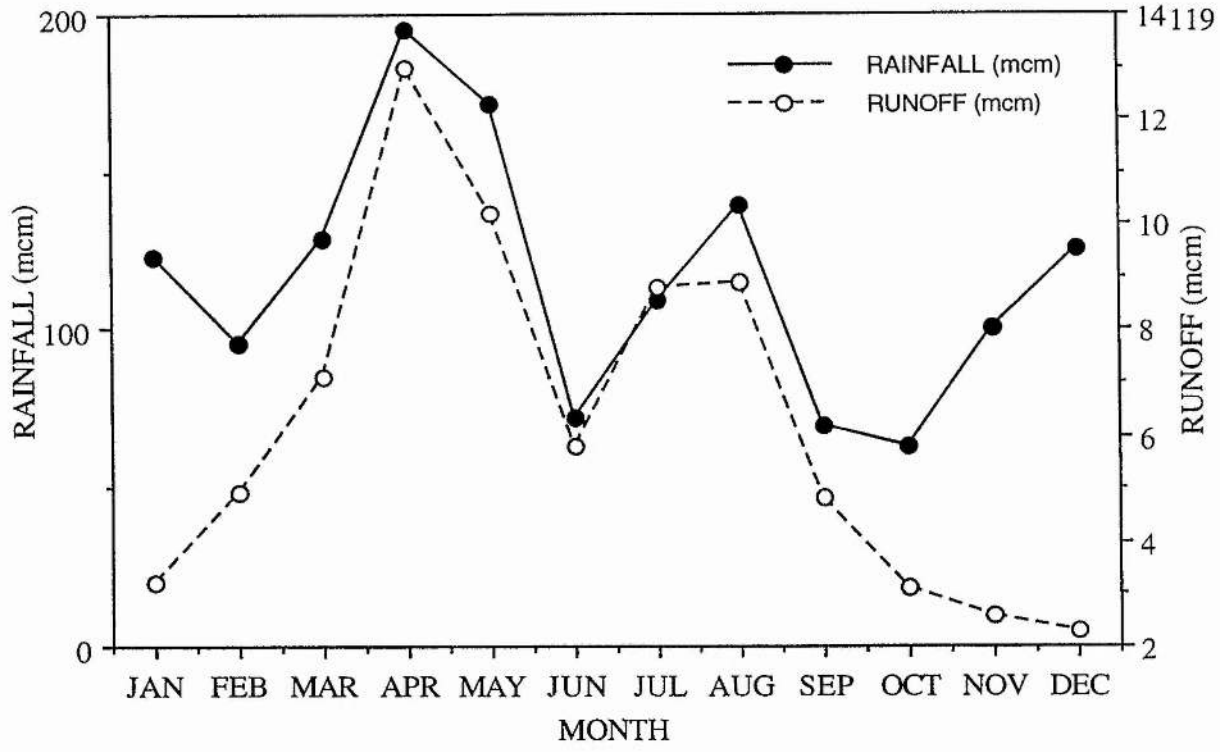

Figure 3.37 Rainfall - Runoff variation within the catchment area of Wadi Baysh .

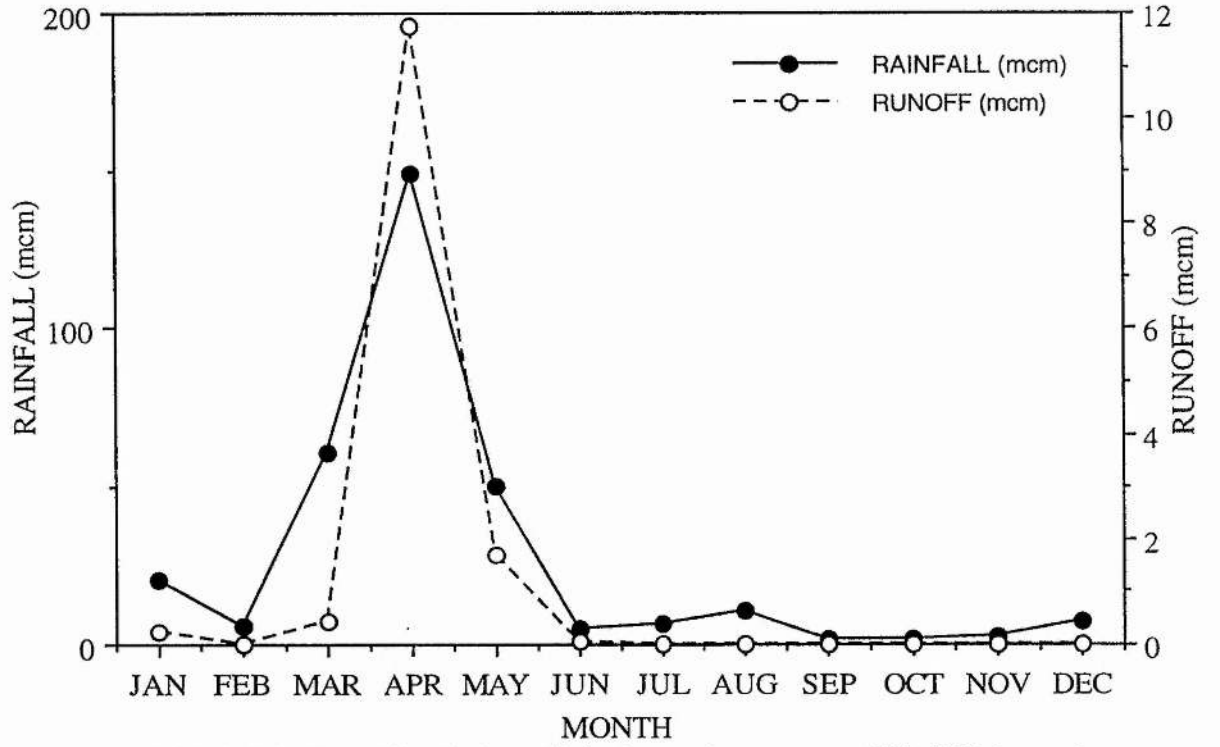

Figure 3.38 Rainfall - Runoff variation within the catchment area of Wadi Habawnah .

Table 3.18 The mean ratio of monthly and annual Rainfall-Runoff data of Wadi Baysh and Wadi Habawnah and the determination of the runoff coefficient

Wadi Baysh rainfall mean ratio (in mm and mcm)

Station	Year	JAN	FEB	MAR	APR	MAY	JUN	JUL	AUG	SEP	OCT	NOV	DEC	Annual
		mean	mean	mean	mean	mean	mean	mean	mean	mean	mean	mean	mean	mean
No.	record	mm	mm	mm	mm	mm	mm	mm	mm	mm	mm	mm	mm	mm
SA-124	1967-84	19.2	7.4	8.5	7.2	11	12.3	24.9	27.9	24.5	26.8	11.5	19.8	201
SA-145	1972-76	73.3	46.3	47.2	66	57.3	18.4	16.9	16.4	15.6	18.6	62.9	95.4	583
SA-110	1960-84	33.6	33	34.2	73.5	66.6	47.7	84.7	93.6	48.8	28.4	37	40.9	622
SA-252	1984-87	11.2	2.2	29.7	60.3	37.3	9.8	0.4	13.0	0.0	0.2	4.7	6.5	175
A-121	1965-84	37.7	46.7	64.3	70.4	72.4	15.0	29.2	47.0	10.7	16.3	26.9	15.9	453
	Mean ratio	35	27	37	55	49	21	31	40	20	18	29	36	407
Rainfall in mcm		123	95	129	195	172	72	110	139	70	63	100	125	1428

Wadi Baysh

Runoff data of Station SA-124 (elevation 200 m a.ms.l,catchment area 3511 km^2)

	Year	JAN	FEB	MAR	APR	MAY	JUN	JUL	AUG	SEP	OCT	NOV	DEC	Annual
	record	mcm	mcm	mcm	mcm	mcm	mcm	mcm	mcm	mcm	mcm	mcm	mcm	mcm
	1970	0.61	1.16	6.45	0.581	0.189	0.091	4.05	3.43	5.29	0.199	0.052	0.044	22
	1971	0.123	0.029	0.13	29.6	20.7	4	14.9	5.7	3.28	0.53	5.04	1.5	86
	1972	0.492	5.49	20.1	48.5	13.9	9.76	11.1	9.2	4.95	5.3	2.92	2.37	134
	1973	10	1.6	0.994	2.57	2.79	0.337	9.69	8.48	5.27	0.429	0.527	3.11	46
	1974	0.586	0	16.1	6.12	13.6	7.87	15.5	12.3	6.76	4.3	1.54	2.47	87
	1975	2	2.97	3.16	26.5	2.73	3.76	2.84	25.2	2.83	2.43	1.22	1.24	77
	1976	1.34	0.903	6.48	4.32	4.78	3.07	5.13	5.24	5.32	3.83	4.04	0.933	45
	1977	4.98	0.643	0.656	2.79	5.04	3.04	3.76	3.77	2.77	3.91	5	0.295	37
	1978	7.94	2.72	1.93	1.7	2.42	1.05	3.13	7.08	3.03	2.12	1.04	0.939	35
	1979	4.09	2.86	2.86	3.59	7.23	3.85	3.12	4.94	3.25	1.45	0.556	2.3	40
	1980	0.748	1.3	1.13	3.88	7.78	4.85	9.7	4.93	1.6	1.13	0.294	0.645	38
	1981	0.408	0.24	21.2	5.94	27.1	8.05	9.77	6.92	8.46	4.88	1.42	1.36	96
	1982	6.05	26.5	13.4	18.7	7.43	6.44	7.29	12.4	7.22	5.95	4.73	5.06	121
	1983	1.94	24.7	12.1	32.2	17.5	17.6	15.6	12.5	7.05	3.29	3.08	3.38	151
	1984	3.29	2.88	2.85	3.13	16	8.62	9.96	7.19	3.57	2.28	2.2	3.88	66
	1985	6.45	3.7	3.9	18.54	13.43	9.95	15.03	13.09	6.1	6.87	7.48	6.54	111
	Mean ratio	3.19	4.86	7.09	13.04	10.16	5.77	8.79	8.90	4.80	3.06	2.57	2.25	74
Runoff coefficients		0.03	0.05	0.05	0.07	0.06	0.08	0.08	0.06	0.07	0.05	0.03	0.02	0.1

Continued on next page

Table 3.18 continued

Wadi Habawnah

Rainfall mean ratio (in mm and mcm) of sub catchment N-408

Station	Year	JAN	FEB	MAR	APR	MAY	JUN	JUL	AUG	SEP	OCT	NOV	DEC	Annual
		mean	mean	mean	mean	mean	mean	mean	mean	mean	mean	mean	mean	mean
No.	record	mm	mm	mm	mm	mm	mm	mm	mm	mm	mm	mm	mm	mm
A-104	1966-84	16	26	45.2	44.3	33.2	0	16.5	15	0	4.6	8.7	3.6	213
N-238	1984-87	5.8	2.0	34.6	59.9	30.8	1.0	1.1	5.5	0.3	0.0	0.3	7.3	148
N-103	1964-84	11.9	17.5	34.9	54.7	31	1.3	16	19.1	0.4	5.6	4.4	8.9	206
N-235	1984-87	2.8	0.0	8.8	49.0	12.6	0.1	1.5	0.5	0.1	0.0	0.0	1.2	76
N-227	1984-87	13.3	0.1	21.4	40.3	21.5	2.4	0.3	1.8	0.2	0.0	4.5	1.4	107
N-235	1984-87	2.8	0.0	8.8	49.0	12.6	0.1	1.5	0.5	0.1	0.0	0.0	1.2	76
	Mean ratio	8.77	7.59	25.61	49.51	23.62	0.78	6.13	7.06	0.17	1.70	2.98	3.93	138
Rainfall in mcm		12.98	11.24	37.93	73.32	34.98	1.16	9.07	10.45	0.25	2.52	4.41	5.81	204

Runoff data of Station N-408 (elevation 1452 m a.ms.l,catchment area 1481 km^2)

	Year	JAN	FEB	MAR	APR	MAY	JUN	JUL	AUG	SEP	OCT	NOV	DEC	Annual
	record	mcm	mcm	mcm	mcm	mcm	mcm	mcm	mcm	mcm	mcm	mcm	mcm	mcm
	1984	0	0	0	0	0.188	0	0	0	0	0	0	0	0.2
	1985	1.122	0	0.35	6.259	3.549	0.235	0.062	0	0	0	0	0	12
	1986	0	0.041	1.667	12.382	1.356	0.039	0.005	0.095	0	0	0	0	16
	Mean ratio	0.37	0.01	0.67	6.21	1.70	0.09	0.02	0.03	0.00	0.00	0.00	0.00	9
Runoff coefficients		0.03	0.00	0.02	0.08	0.05	0.08	0.00	0.00	0.00	0.00	0.00	0.00	0.04

Rainfall mean ratio (in mm and mcm) of sub catchment N-404

Station	Year	JAN	FEB	MAR	APR	MAY	JUN	JUL	AUG	SEP	OCT	NOV	DEC	Annual
		mean	mean	mean	mean	mean	mean	mean	mean	mean	mean	mean	mean	mean
No.	record	mm	mm	mm	mm	mm	mm	mm	mm	mm	mm	mm	mm	mm
N-238	1984-87	5.8	2.0	34.6	59.9	30.8	1.0	1.1	5.5	0.3	0.0	0.3	7.3	148
N-243	1984-87	6.1	0.7	17.1	34.3	19.5	0.8	7.0	2.9	0.0	0.0	0.0	2.5	91
N-239	1984-87	5.9	0.5	8.7	69.7	7.9	4.7	1.0	1.2	1.5	0.3	0.0	2.1	103
N-240	1984-87	6.1	0.8	20.4	42.4	11.6	0.3	0.2	0.4	0.0	0.0	0.0	1.2	83
N-233	1984-87	4.3	1.7	9.3	47.9	7.2	4.5	0.8	1.2	1.4	0.0	0.0	0.8	79
N-229	1984-87	4.6	0.0	12.3	41.9	9.1	0.0	0.1	0.3	0.1	0.0	0.0	0.2	68
	Mean ratio	5.44	0.93	17.04	49.32	14.33	1.87	1.67	1.88	0.54	0.04	0.04	2.33	95
Rainfall in mcm		5.90	1.01	18.49	53.51	15.54	2.03	1.81	2.03	0.59	0.05	0.05	2.53	104

Continued on next page

Table 3.18 continued

Runoff data of Station N-404 (elevation 1339 m a.ms.l,catchment area 1085 km^2)

Year	JAN	FEB	MAR	APR	MAY	JUN	JUL	AUG	SEP	OCT	NOV	DEC	Annual
record	mcm	mcm	mcm	mcm	mcm	mcm	mcm	mcm	mcm	mcm	mcm	mcm	mcm
1984	0	0	0	0.225	0.292	0.074	0	0	0	0	0	0	0.6
1985	0.682	0	0.286	9.16	2.708	0.061	0	0	0	0	0	0	13
1986	0	0	0.972	14.119	1.448	0.007	0.069	0	0	0	0	0	17
Mean ratio	0.23	0.00	0.42	7.83	1.48	0.05	0.02	0.00	0.00	0.00	0.00	0.00	10
Runoff coefficients	0.01	0.00	0.01	0.06	0.03	0.01	0.00	0.00	0.00	0.00	0.00	0.00	0.03

Rainfall mean ratio (in mm and mcm) of sub catchment N-405

Station	Year	JAN	FEB	MAR	APR	MAY	JUN	JUL	AUG	SEP	OCT	NOV	DEC	Annual
		mean	mean	mean	mean	mean	mean	mean	mean	mean	mean	mean	mean	mean
No.	record	mm	mm	mm	mm	mm	mm	mm	mm	mm	mm	mm	mm	mm
A-207	1966-84	16	35.8	48.2	43.9	38.2	4.3	19.6	17.6	1.6	3.5	9.9	5.9	244
N-213	1984-87	3.6	1.8	20.5	26.6	12.5	0.0	0.1	1.7	0.1	0.0	0.0	0.2	67
N-216	1984-87	6.0	0.2	14.9	59.3	12.9	0.9	0.6	2.1	0.0	0.0	0.0	0.4	97
N-215	1984-87	4.8	0.8	19.5	27.3	2.5	0.1	0.0	0.2	0.1	0.0	0.0	0.3	55
N-221	1984-87	3.2	0.1	17.4	47.2	5.5	1.0	0.7	0.1	0.0	0.0	0.0	0.3	75
N-219	1984-87	2.5	0.0	16.7	53.7	6.0	0.1	0.5	0.5	0.2	0.0	0.0	0.3	80
N-223	1984-87	3.6	0.0	11.1	36.4	8.1	0.0	0.7	0.9	0.4	0.0	0.0	0.6	62
	Mean ratio	5.64	5.51	21.17	42.04	12.23	0.91	3.14	3.29	0.34	0.50	1.41	1.11	97
Rainfall in mcm		5.12	5.01	19.24	38.22	11.12	0.82	2.86	2.99	0.31	0.45	1.29	1.01	88

Runoff data of Station N-405 (elevation 1303m a.ms.l,catchment area 909 km^2)

Year	JAN	FEB	MAR	APR	MAY	JUN	JUL	AUG	SEP	OCT	NOV	DEC	Annual
record	mcm	mcm	mcm	mcm	mcm	mcm	mcm	mcm	mcm	mcm	mcm	mcm	mcm
1984	0	0	0	0.417	0	0	0	0	0	0	0	0	0.4
1985	0	0	0.041	5.067	0.621	0	0	0	0	0	0	0	6
1986	0	0	0.003	6.244	0	0	0	0	0	0	0	0	6
Mean ratio	0.00	0.00	0.01	3.91	0.21	0.00	0.00	0.00	0.00	0.00	0.00	0.00	4
Runoff coefficients	0.0000	0.0000	0.0008	0.0600	0.0186	0.0000	0.0000	0.0000	0.0000	0.0000	0.0000	0.0000	0.0467

Continued on next page

Table 3.18 continued

Rainfall mean ratio (in mm and mcm) of sub catchment N-406

Station	Year	JAN	FEB	MAR	APR	MAY	JUN	JUL	AUG	SEP	OCT	NOV	DEC	Annual
		mean	mean	mean	mean	mean	mean	mean	mean	mean	mean	mean	mean	mean
No.	record	mm	mm	mm	mm	mm	mm	mm	mm	mm	mm	mm	mm	mm
N-226	1984-87	3.8	0.1	10.2	80.1	12.8	0.2	1.6	1.6	1.1	0.0	0.0	0.7	112
N-229	1984-87	4.6	0.0	12.3	41.9	9.1	0.0	0.1	0.3	0.1	0.0	0.0	0.2	68
N-236	1984-87	7.8	1.0	10.6	46.7	9.0	0.0	0.0	0.1	0.1	0.0	0.0	0.4	76
	Mean ratio	5.40	0.35	11.00	56.20	10.28	0.07	0.55	0.65	0.40	0.00	0.00	0.40	85
Rainfall in mcm		5.79	0.38	11.80	60.30	11.03	0.07	0.59	0.70	0.43	0.00	0.00	0.43	92

Runoff data of Station N-406 (elevation 1212m a.ms.l,catchment area 1073 km^2)

	Year	JAN	FEB	MAR	APR	MAY	JUN	JUL	AUG	SEP	OCT	NOV	DEC	Annual
	record	mcm	mcm	mcm	mcm	mcm	mcm	mcm	mcm	mcm	mcm	mcm	mcm	mcm
	1984	0	0	0.091	0	0	0	0	0	0	0	0	0	0.1
	1985	0.105	0	0	15.813	1.103	0	0	0	0	0	0	0	17
	1986	0	0.016	0.295	11.068	0	0	0	0	0	0	0	0	11
	Mean ratio	0.04	0.01	0.13	8.96	0.37	0.00	0.00	0.00	0.00	0.00	0.00	0.00	9
Runoff coefficients		0.0012	0.0003	0.0015	0.0398	0.0051	0.0000	0.0000	0.0000	0.0000	0.0000	0.0000	0.0000	0.0195

Rainfall mean ratio (in mm and mcm) of sub catchment N-407

Station	Year	JAN	FEB	MAR	APR	MAY	JUN	JUL	AUG	SEP	OCT	NOV	DEC	Annual
		mean	mean	mean	mean	mean	mean	mean	mean	mean	mean	mean	mean	mean
No.	record	mm	mm	mm	mm	mm	mm	mm	mm	mm	mm	mm	mm	mm
N-237	1984-87	4.2	0.2	12.8	30.2	7.4	0.0	0.0	0.6	0.0	0.0	0.0	0.6	56
N-230	1984-87	0.4	0.0	12.9	27.1	4.7	0.0	0.0	0.2	0.0	0.0	0.0	1.4	47
	Mean ratio	2.28	0.04	4.35	15.52	2.25	0.00	0.00	0.12	0.00	0.00	0.00	0.33	23
Rainfall in mcm		0.72	0.01	1.37	4.89	0.71	0.00	0.00	0.04	0.00	0.00	0.00	0.11	7

Runoff data of Station N-407 (elevation 1166m a.ms.l,catchment area 315 km^2)

	Year	JAN	FEB	MAR	APR	MAY	JUN	JUL	AUG	SEP	OCT	NOV	DEC	Annual
	record	mcm	mcm	mcm	mcm	mcm	mcm	mcm	mcm	mcm	mcm	mcm	mcm	mcm
	1984	0	0	0	0	0	0	0	0	0	0	0	0	0.0
	1985	0.454	0	0	5.313	0.173	0	0	0	0	0	0	0	6
	1986	0	0	0.232	5.122	0	0	0	0	0	0	0	0	5
	Mean ratio	0.15	0.00	0.08	3.48	0.06	0.00	0.00	0.00	0.00	0.00	0.00	0.00	4
Runoff coefficients		0.0050	0.0000	0.0009	0.0151	0.0008	0.0000	0.0000	0.0000	0.0000	0.0000	0.0000	0.0000	0.0076

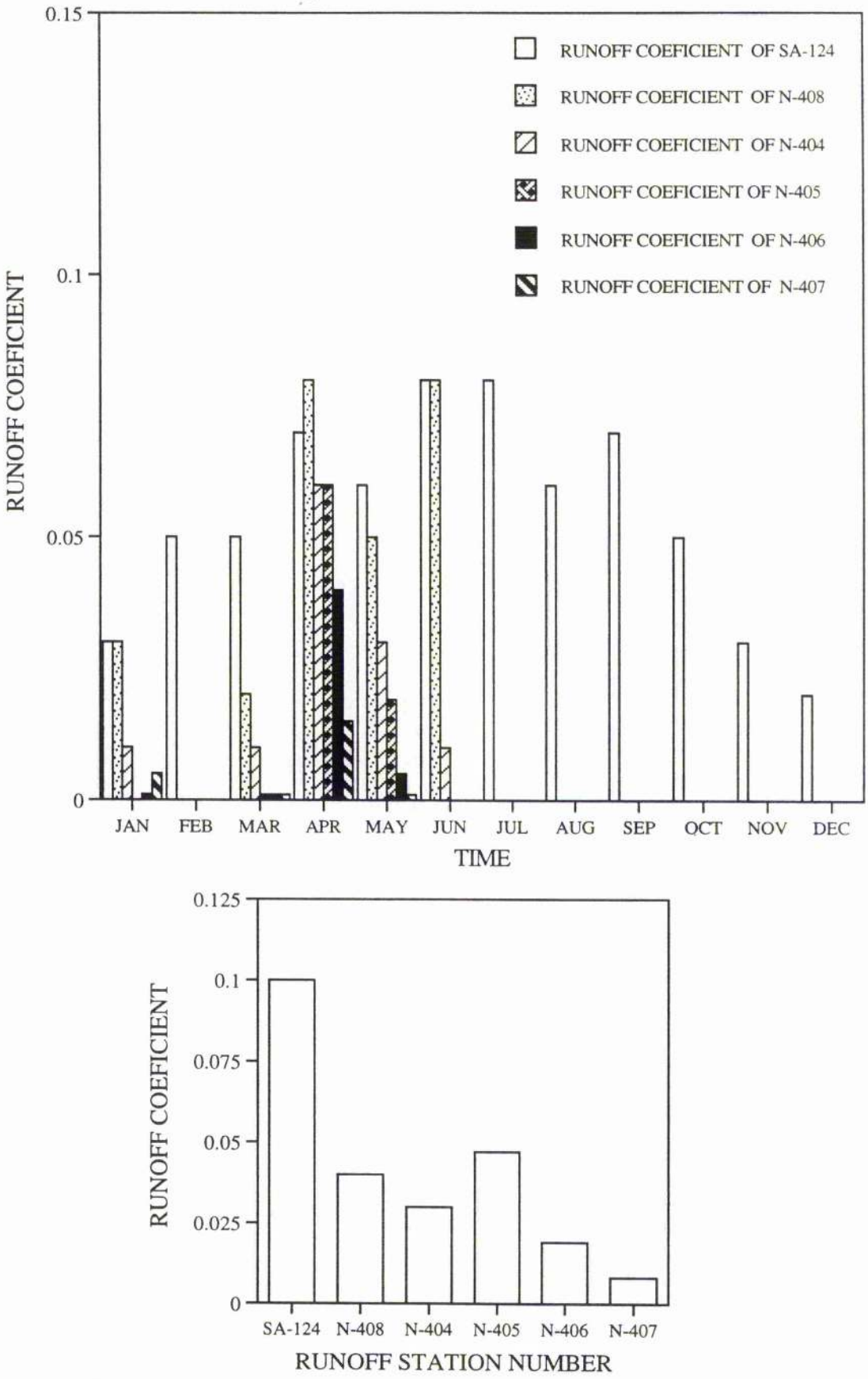

Figure 3.39 Monthly (above) and annual (below) runoff coeficient within Wadi Baysh (SA-124) and Wadi Habawnah (N-408, N-404, N-405, N-406 and N-407).

record has two main periods that were characterised with high volumes of annual flood; the period between 1971 and 1975 and the period between 1981 and 1985, where the annual flood volume ranged from 45.8 to 137.1 mcm and 65.9 to 150.9 mcm, respectively. The five years (1976-1980) between these two high flood periods were characterised with low annual flood volumes ranging from 35.1 to 45.4 mcm.

Wadi Habawnah has five major sub-catchments, but they have short (3 year) records of annual floods (1984-1986). However, 1984 shows a low volume of annual flood throughout the catchment area and the flood volume ranged between zero at station N-407 and 0.56 mcm in station N-404 (Figure 3.41). The years 1985 and 1986 were characterised by variations of annual flood volumes. The stations of the upper part of the catchment area (N-408 and N-404) contributed lower annual flood volumes in 1985 (12.9 mcm) than compared to 1986 (16.62 mcm), while the station in the lower catchment (N-406) showed a higher annual volume of 17.0 mcm in 1985 than in 1986.

The author suggests that the reduction in the flood volume in the lower parts of the catchment area is partly due to the diversion of water for the agricultural lands and partly due to infiltration into groundwater aquifers.

3.3.1.2.3 Rainfall-Runoff Correlation

The rainfall-runoff relationships indicate the proportion of rainfall that gives rise to surface runoff. Rainfall-runoff relationships are essential for predicting future discharges (i.e. flood forecasting) (Linsley, *et.al* ., 1982), and it may be possible to establish an empirical relationship for a particular catchment based on the precipitation and the runoff data (Wilson, 1990). In order to show the interrelationship, the author considered the mean rainfall and runoff volumes for the monthly records of both wadis (Table 3.19) as plotted in Figures 3.42 and 43.

The best fit lines have the equations as follows:

for Wadi Baysh

$$\text{Runoff} = (0.062 \times \text{Rainfall} - 0.965) \qquad (3.2)$$

and for Wadi Habawnah

$$\text{Runoff} = (0.060 \times \text{Rainfall} - 1.005) \qquad (3.3)$$

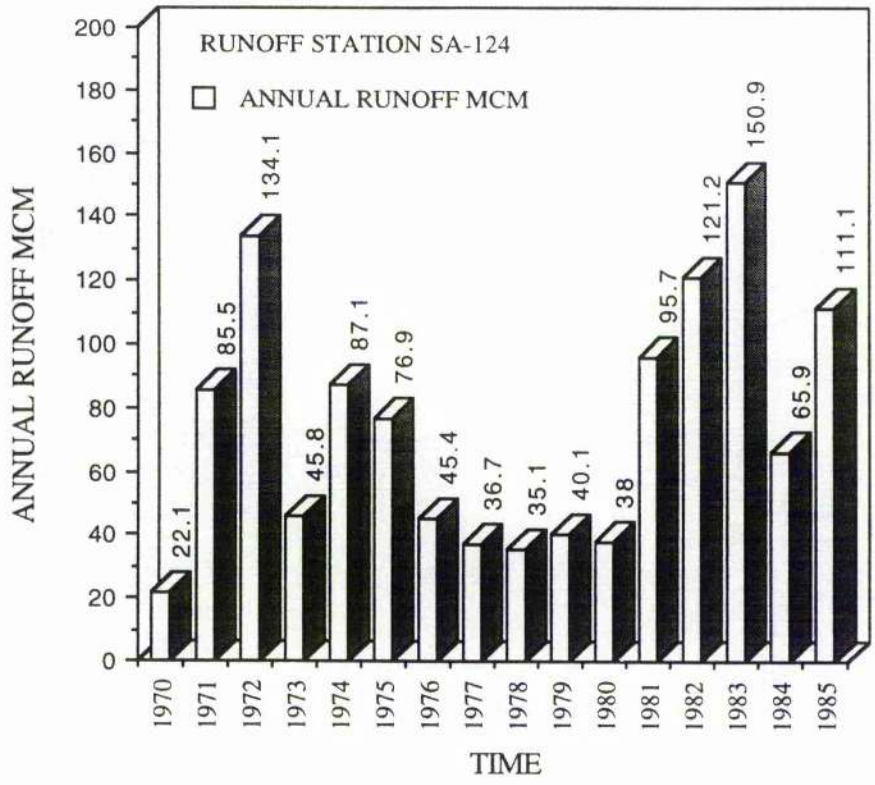

Figure 3.40 Annual runoff variation of Wadi Baysh.

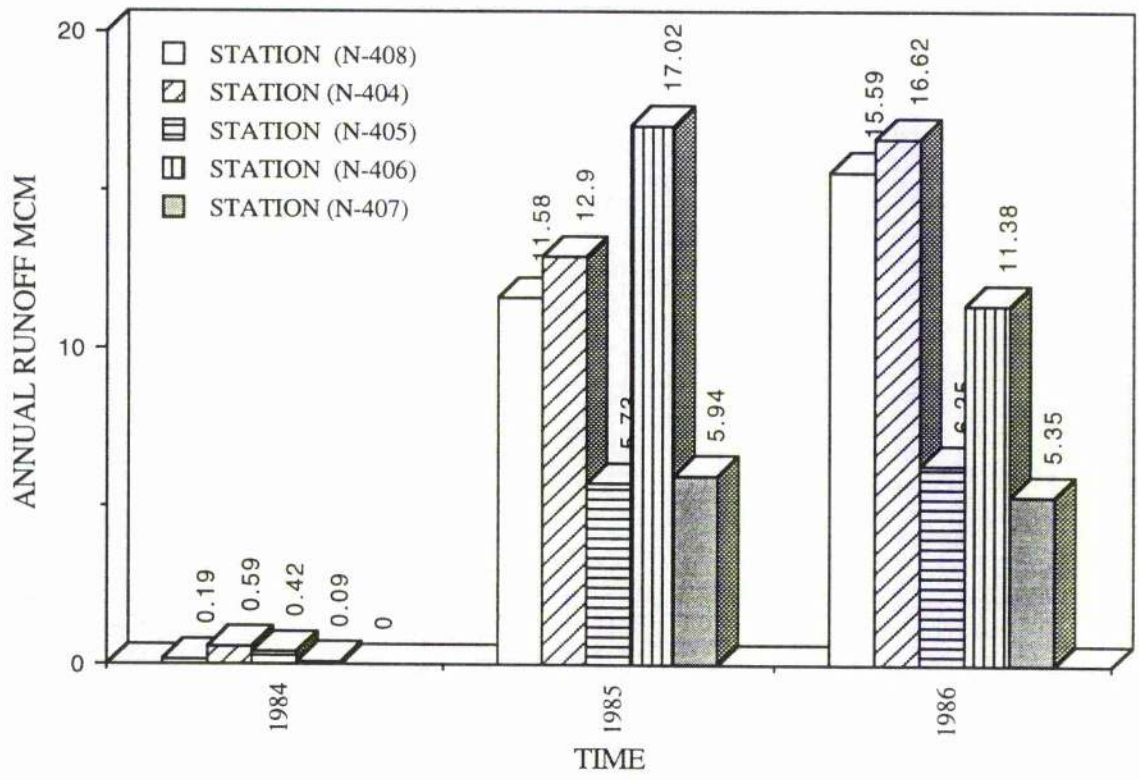

Figure 3.41 Annual runoff variation of Wadi Habawnah.

Table 3.19 The average monthly and annual Rainfall - Runoff (mcm) within the catchment areas of Wadi Baysh and Wadi Habawnah

Wadi Baysh rainfall and runoff

		JAN	FEB	MAR	APR	MAY	JUN	JUL	AUG	SEP	OCT	NOV	DEC	Annual
		mcm	mcm	mcm	mcm	mcm	mcm	mcm	mcm	mcm	mcm	mcm	mcm	mcm
Total rainfall in (mcm)		123	95	129	195	172	72	110	139	70	63	100	125	1428
Runoff in (mcm)	Mean ratio	3.19	4.86	7.09	13.04	10.16	5.77	8.79	8.90	4.80	3.06	2.57	2.25	74.47

Wadi Habawnah rainfall and runoff

		JAN	FEB	MAR	APR	MAY	JUN	JUL	AUG	SEP	OCT	NOV	DEC	Annual
		mcm	mcm	mcm	mcm	mcm	mcm	mcm	mcm	mcm	mcm	mcm	mcm	mcm
Total rainfall in (mcm)	Mean ratio	27	17	85	205	66	4	13	15	1	3	5	9	450
Runoff in (mcm)	Mean ratio	0.11	0.02	0.19	13.44	1.10	0.00	0.00	0.00	0.00	0.00	0.00	0.00	14.25

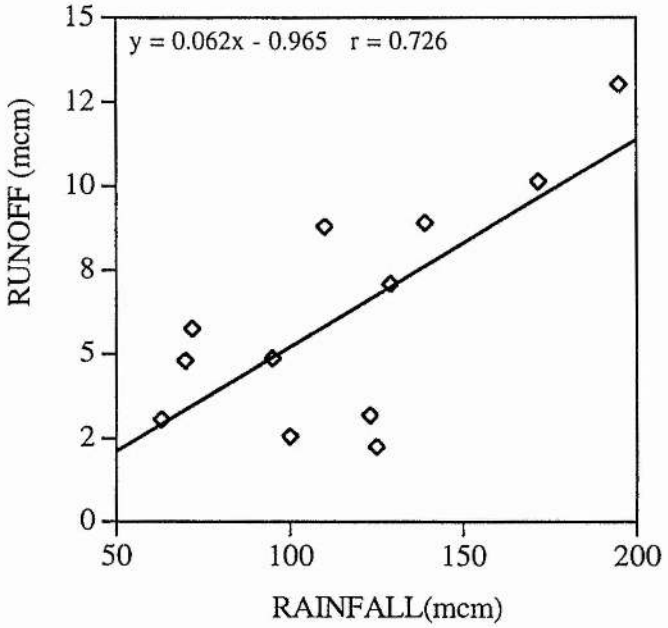

Figure 3.42 Rainfall-Runoff mean volume of flow of Wadi Baysh (1970-1985).

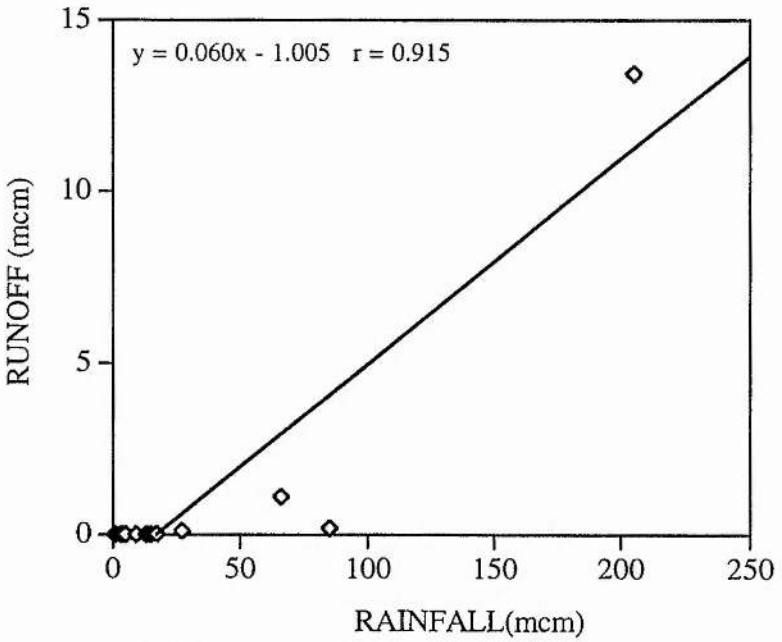

Figure 3.43 Rainfall-Runoff mean volume of flow of Wadi Habawnah (1984-1987).

with both parameters measured in mcm.

The rainfall runoff correlation coefficient of both wadis is high (Wadi Baysh, 0.726 and Wadi Habawnah, 0.9), due to the runoff that in Wadi Habawnah the interrelationship, which is mainly for the influence of spring rainfall, shows a higher coefficient value than in Wadi Baysh influenced by all four seasons as indicated previously. However the winter season (November - January) caracterise with high rainfall and low run off in at Wadi Bays . This abnormality can be explained by the fact that the parched soil absorbed much of the rainfall and lessened the runoff total since the summer season characterise with high evaporation in addition to the rainfall variability as arid and semi arid zone.

3.3.1.3 Factors Affecting Runoff

Factors that appear to affect runoff are evaporation, infiltration, and miscellaneous abstractions such as the route and timing that depend on the character of the drainage basin and precipitation intensity in which each path affects the rate and amount of runoff in a different way. In the study area, the evaporation and infiltration characteristics are probably the most important. These two main factors are discussed below.

3.3.1.3.1 Evaporation

The study area is in an arid to semi arid zone, characterised by hot weather and irregular rainfall. In Wadi Baysh the average annual rainfall is 500 mm for the upper part of the catchment, falling to 165mm on the lower part of the catchment area (station SA-106) in which the potential evaporation is 3352mm/y (see Table 3.16). In Wadi Habawnah, the potential evaporation in the lower part of the catchment is 4070mm/y, where the annual mean of the rainfall is 62mm at station N-223. The upper part of the catchment shows a lower value of evaporation and evapotranspiration but receives higher rainfall. At Sarat Abidah and Abha, the annual values of PE range between 1100 and 2678mm/yr while the PE range between 177 and 839mm/yr, respectively. The annual rainfall at Sarat Abidah and Abha is 155mm and 175mm, respectively.

The foothills of Wadi Baysh (Malaki station) are characterised by higher values of PE and PT than the station in the lower part of the wadi SA-106 (see Table 3.16), close to

the Red Sea. The PE and PT daily rate of the lower part of Wadi Baysh were determined as 9 and 6mm, while Wadi Habawnah has PE and PT daily rates of 11 and 5mm, respectively. However, because of the short duration of most runoff events in both Wadi basins, the author has assumed that the effect of the evaporation on the channel transmission losses is small and insignificant.

3.3.1.3.2 Infiltration

Runoff infiltration is the main factor controlling groundwater recharge of both wadi basins. However, ephemeral flow is one of the main features of wadi channels where the runoff occurs only following infrequent storms. Channel transmission loss is seen as flow reduction which takes place when the flood flows occur in the normally dry stream beds. Lane (1983) indicated that the transmission loss reduces the volume of runoff progressively at downstream points along the channel.

The infiltration capacity will yield information on subsurface recharge. The bedrock in the area of investigation consists mostly of metamorphic and igneous rocks which are largely impervious and favourable to runoff. However, the wadi floors are filled with porous alluvial deposits into which water infiltrates readily. It is usual to see the wadi floor during each runoff event as unsteady flow with rapid rise and fall of water levels. Both wadis have large drainage areas which provide large quantities of water, in the rainy season. Chow (1964) assumes 10% of the rainfall can be considered as groundwater recharge in arid regions. This assumption will lead to total amounts of 135.6 mcm and 42.6 mcm that will recharge the groundwater of Wadi Baysh and Wadi Habawnah, respectively. However, the annual ratio of runoff and rainfall shows a value of 6% for Wadi Habawnah and 3% for Wadi Baysh, which are lower than Chow's estimate. Such a low ratio of runoff to rainfall is a result of evaporation and mostly due to loss on the upper catchment terraces in which some of the runoff is diverted for agricultural purposes. Generally, both wadis show that runoff occurs when the rainfall exceeds 25 mm/month. However, Cordery *et al* . (1983) found that runoff occured in arid western New South Wales, Australia on all occasions when there was more than 16mm of rain in a storm event.

According to the basin conductivity, both wadis are characterised by permeable

material with an average of 1.6 m/hr of hydraulic conductivity based on pumping test analysis (see Chapter 5) which suggests that conditions for surface recharge are favourable.

Sorman, *et al.* (1993) studied the infiltration recharge through the Wadi Tabalah Basin about 300 km northwest of Wadi Habawnah and derived a regression equation to evaluate the groundwater recharge depth as follows:

$$GR = 0.01 + 0.302\ (V_{up}) \qquad (3.4)$$

GR is groundwater recharge as depth in m, (V_{up}) is inflow volume (upstream runoff).

The annual volume of groundwater recharge per kilometre in the main wadi channel may be expressed as channel transmission loss (m^3/km) based on the water balance equation below:

$$T_L\ (m^3/km) = [V_{up}\ (mcm/year) - V_{ud}\ (mcm/year)]/X\ (km) \qquad (3.5)$$

where T_L is transmission loss, V_{ud} is downstream runoff and X is the distance between the two measuring stations in kilometres.

Accordingly, the equations 3.4 and 3.5 were used to estimate the groundwater recharge depth and volume for Wadi Habawnah using the annual and monthly runoff data of the five stations. The distance between these runoff stations, starting from upstream, are listed in Table 3.20 (see Figure 3.2).

Table 3.20 Distance between runoff stations within Wadi Habawnah main channel

Runoff Station No.(upstream)	Runoff Station No	Distance in km
Start point of main channel for Wadi Habawnah	N-407	130
N-408	N-404	19.5
N-404	N-406	34
Start point of main channel for Wadi Thar	N-407	93
N-405	N-406	25
N-406	N-407	13

The groundwater recharge depth and channel transmission losses from the monthly records have been determined (see Table 3.21 for Wadi Habawnah). There is an increase in channel loss that is associated with an increase in the ground recharge depth. The maximum channel loss was 81,000 m^3/km/month of water and the groundwater recharge depth was 3.2 m (see Tables 3.21 and 3.22). There is a strong positive correlation between the transmission loss and the groundwater recharge depth (see Figure 3.44). The correlation coefficient is 0.907. The groundwater recharge depth can be determined using the

Table 3.21 The monthly runoff data (mcm) within the catchment area of Wadi Habawnah, the ground water recharge depth (m) and the transmission loss (m^3/km/month) determination of the main channel of the wadi basin

Runoff data (mcm) of Station N-408 (elevation 1452 m a.ms.l,catchment area 1307 km^2).

Year	JAN	JAN	JAN	FEB	FEB	FEB	MAR	MAR	MAR	APR	APR	APR	MAY	MAY	MAY	JUN	JUN	JUN	JUL	JUL	JUL	AUG	AUG	AUG	SEP	SEP	SEP	OCT	OCT	OCT	NOV	NOV	NOV	DEC	DEC	DEC
	Runoff	GR*	TL^	Runoff	GR*	TL^	Runoff	GR*	TL^	Runoff	GR*	TL^	Runoff	GR*	TL^	Runoff	GR*	TL^	Runoff	GR*	TL^	Runoff	GR*	TL^	Runoff	GR*	TL^	Runoff	GR*	TL^	Runoff	GR*	TL^	Runoff	GR*	TL^
record	mcm	m	m^3/km	mcm	m	m^3/km	mcm	m	m^3/km	mcm	m	m^3/km	mcm	m	m^3/km	mcm	m	m^3/km	mcm	m	m^3/km	mcm	m	m^3/km	mcm	m	m^3/km	mcm	m	m^3/km	mcm	m	m^3/km	mcm	m	m^3/km
1984	0			0			0			0			0.188			0			0			0			0			0			0			0		
1985	1.122			0			0.35			6.259			3.549			0.235			0.062			0			0			0			0			0		
1986	0			0.041			1.667			12.382			1.356			0.039			0.005			0.095			0			0			0			0		

Runoff data (mcm) of Station N-404 (elevation 1339 m a.ms.l,catchment area 2391 km^2), ground water recharge depth (m) and transmission loss (m^3/km/month).

Year	JAN	JAN	JAN	FEB	FEB	FEB	MAR	MAR	MAR	APR	APR	APR	MAY	MAY	MAY	JUN	JUN	JUN	JUL	JUL	JUL	AUG	AUG	AUG	SEP	SEP	SEP	OCT	OCT	OCT	NOV	NOV	NOV	DEC	DEC	DEC
	Runoff	GR*	TL^	Runoff	GR*	TL^	Runoff	GR*	TL^	Runoff	GR*	TL^	Runoff	GR*	TL^	Runoff	GR*	TL^	Runoff	GR*	TL^	Runoff	GR*	TL^	Runoff	GR*	TL^	Runoff	GR*	TL^	Runoff	GR*	TL^	Runoff	GR*	TL^
record	mcm	m	m^3/km	mcm	m	m^3/km	mcm	m	m^3/km	mcm	m	m^3/km	mcm	m	m^3/km	mcm	m	m^3/km	mcm	m	m^3/km	mcm	m	m^3/km	mcm	m	m^3/km	mcm	m	m^3/km	mcm	m	m^3/km	mcm	m	m^3/km
1984	0	0.01	0	0	0.01	0	0	0.01	0	0.225	-0.06	-11532	0.292	-0.02	-5330	0.074	-0.01	-3793	0	0.01	0	0	0.01	0	0	0.01	0	0	0.01	0	0	0.01	0	0	0.01	0	0
1985	0.682	0.14	22551	0	0.01	0	0.286	0.03	3280	9.16	-0.87	-148685	2.708	0.26	43104	0.061	0.06	8918	0	0.03	3178	0	0.01	0	0	0.01	0	0	0.01	0	0	0.01	0	0	0.01	0	0
1986	0	0.01	0	0	0.02	2101	0.972	0.22	35621	14.119	-0.51	-89026	1.448	-0.02	-4715	0.007	0.02	1640	0.069	-0.01	-3280	0	0.04	4869	0	0.01	0	0	0.01	0	0	0.01	0	0	0.01	0	0

Runoff data (mcm) of Station N-405 (elevation 1303m a.ms.l,catchment area 940 km^2).

Year	JAN	FEB	MAR	APR	MAY	JUN	JUL	AUG	SEP	OCT	NOV	DEC
	Runoff	Runoff	Runoff	Runoff	Runoff	Runoff	Runoff	Runoff	Runoff	Runoff	Runoff	Runoff
record	mcm	mcm	mcm	mcm	mcm	mcm	mcm	mcm	mcm	mcm	mcm	mcm
1984	0	0	0	0.417	0	0	0	0	0	0	0	0
1985	0	0	0.041	5.067	0.621	0	0	0	0	0	0	0
1986	0	0	0.003	6.244	0	0	0	0	0	0	0	0

Runoff data (mcm) of Station N-406 (elevation 1212m a.ms.l,catchment area 4425 km^2), ground water recharge depth (m) and transmission loss (m^3/km/month).

Year	JAN	JAN	JAN	FEB	FEB	FEB	MAR	MAR	MAR	APR	APR	APR	MAY	MAY	MAY	JUN	JUN	JUN	JUL	JUL	JUL	AUG	AUG	AUG	SEP	SEP	SEP	OCT	OCT	OCT	NOV	NOV	NOV	DEC	DEC	DEC
	Runoff	GR*	TL^	Runoff	GR*	TL^	Runoff	GR*	TL^	Runoff	GR*	TL^	Runoff	GR*	TL^	Runoff	GR*	TL^	Runoff	GR*	TL^	Runoff	GR*	TL^	Runoff	GR*	TL^	Runoff	GR*	TL^	Runoff	GR*	TL^	Runoff	GR*	TL^
record	mcm	m	m^3/km	mcm	m	m^3/km	mcm	m	m^3/km	mcm	m	m^3/km	mcm	m	m^3/km	mcm	m	m^3/km	mcm	m	m^3/km	mcm	m	m^3/km	mcm	m	m^3/km	mcm	m	m^3/km	mcm	m	m^3/km	mcm	m	m^3/km
1984	0	0.01	0	0	0.01	0	0.091	-0.02	-3619	0	0.20	25532	0	0.10	11613	0	0.03	2943	0	0.01	0	0	0.01	0	0	0.01	0	0	0.01	0	0	0.01	0	0	0.01	0	0
1985	0.454	0.08	9068	.0	0.01	0	0	0.11	13005	15.813	-0.47	-63076	1.103	0.68	88529	0	0.03	2426	0	0.01	0	0	0.01	0	0	0.01	0	0	0.01	0	0	0.01	0	0	0.01	0	0
1986	0	0.01	0	0.016	0.01	-636	0.295	0.22	27044	11.068	2.82	369664	0	0.45	57587	0	0.01	278	0	0.03	2744	0	0.01	0	0	0.01	0	0	0.01	0	0	0.01	0	0	0.01	0	0

Runoff data (mcm) of Station N-407 (elevation 1166m a.ms.l,catchment area 4682 km^2), ground water recharge depth (m) and transmission loss (m^3/km/month).

Year	JAN	JAN	JAN	FEB	FEB	FEB	MAR	MAR	MAR	APR	APR	APR	MAY	MAY	MAY	JUN	JUN	JUN	JUL	JUL	JUL	AUG	AUG	AUG	SEP	SEP	SEP	OCT	OCT	OCT	NOV	NOV	NOV	DEC	DEC	DEC
	Runoff	GR*	TL^	Runoff	GR*	TL^	Runoff	GR*	TL^	Runoff	GR*	TL^	Runoff	GR*	TL^	Runoff	GR*	TL^	Runoff	GR*	TL^	Runoff	GR*	TL^	Runoff	GR*	TL^	Runoff	GR*	TL^	Runoff	GR*	TL^	Runoff	GR*	TL^
record	mcm	m	m^3/km	mcm	m	m^3/km	mcm	m	m^3/km	mcm	m	m^3/km	mcm	m	m^3/km	mcm	m	m^3/km	mcm	m	m^3/km	mcm	m	m^3/km	mcm	m	m^3/km	mcm	m	m^3/km	mcm	m	m^3/km	mcm	m	m^3/km
1984	0	0.01	0	0	0.01	0	0	0.04	7024	0	0.01	0	0	0.01	0	0	0.01	0	0	0.01	0	0	0.01	0	0	0.01	0	0	0.01	0	0	0.01	0	0	0.01	0	0
1985	0.105	0.12	26938	0	0.01	0	0	0.01	0	5.313	3.18	810463	0.173	0.29	71784	0	0.01	0	0	0.01	0	0	0.01	0	0	0.01	0	0	0.01	0	0	0.01	0	0	0.01	0	0
1986	0	0.01	0	0	0.01	1235	0.232	0.03	4863	5.122	1.81	458954	0	0.01	0	0	0.01	0	0	0.01	0	0	0.01	0	0	0.01	0	0	0.01	0	0	0.01	0	0	0.01	0	0

(*) Ground water recharge depth m based on the equation GR=0.01+0.302(Inflow volume = (Vup = Upstream runoff - Downstream runoff).
(^) Transmission loss (m^3/km/month) = (Upstream runoff - Downstream runoff) / Distance between the Upstream runoff station and the Downstream runoff station) (km).
(-) It indicates that there is a local storm which limited to the downstream in which the surface runoff occurs while upstream there was no flow.

Table 3.22 Ground water recharge (m) and channel transmission loss m^3/km/month determined on the basis of monthly runoff records (1984-1986) for five subcatchment areas of Wadi Habawnah

GROUND WATER RECHARGE DEPTH GR (m)	TRANSSIMISION LOSS TL m^3/km/month
0.14	22551
0.08	9068
0.12	26938
0.02	2101
0.01	1235
0.03	3280
0.22	35621
0.11	13005
0.22	27044
0.04	7024
0.03	4863
0.2	25532
2.82	369664
3.18	810463
1.81	458954
0.26	43104
0.1	11613
0.68	88529
0.45	57587
0.29	71784
0.06	8918
0.02	1640
0.03	2943
0.03	2426
0.01	278
0.03	3178
0.03	2744
0.04	4869

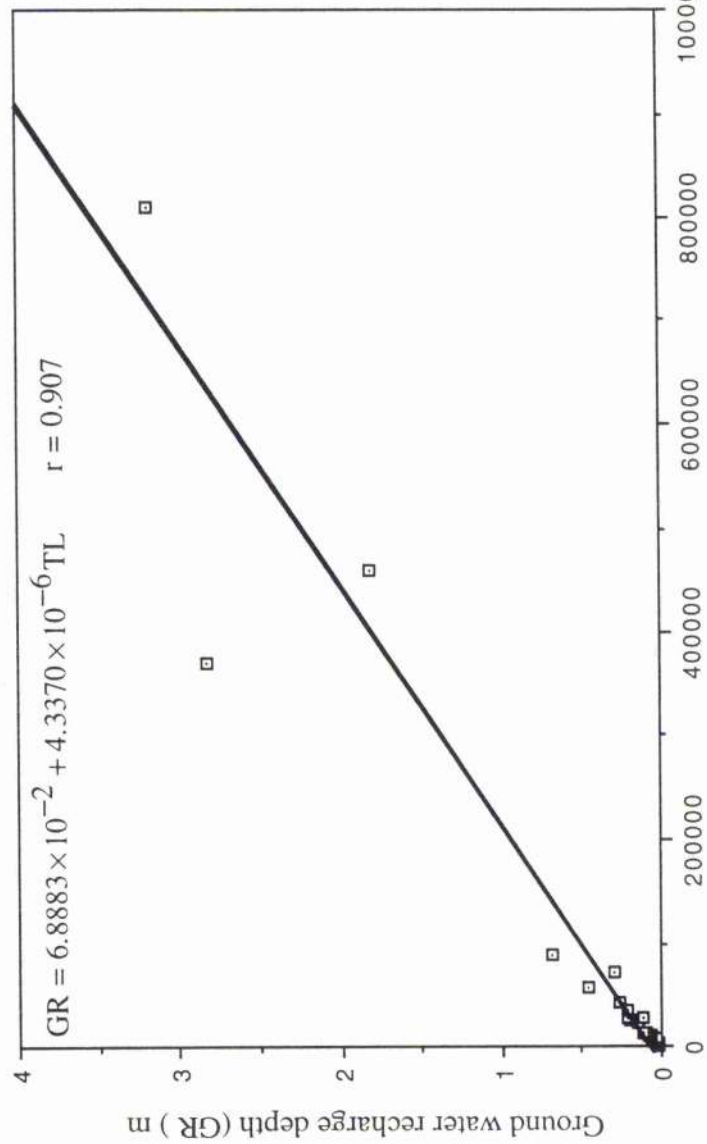

Figure 3.44 Relation of transmission loss (TL) to ground water recharge depth (GR) in the main channel of the Wadi Habawnah basin.

following regression :

$$GR(m) = 6.8883 \times 10^{-2} + 4.3370 \times 10^{-6} TL \quad (3.6)$$

Equation 3.6 shows a strong correlation coefficient (r = 0.907) in which the two parameters can be determined with low error.

There is only one runoff station for Wadi Baysh, which makes it difficult to use the above equations to determine the channel loss and the groundwater recharge depth since there require measurements from more than one runoff station. However, the runoff record of station SA-124 is the only outlet for the upper catchment flow to the Wadi Baysh basin, which is the main resource for groundwater recharge of downstream aquifers. The mean annual runoff is 75 mcm (see Table 3.5). The well inventory (see chapter 5 and 6) reveals that the water table depth ranges between 2 and 20 m below the surface within the irrigated area and it is thought normally to be too deep to receive recharge from the intermittently flooded surface.

With respect to the 80 mcm annual runoff of Wadi Jizan (70 km to south of Wadi Baysh), Sir William Halcrow (1972) estimated the groundwater recharge on the wadi bed as 31% of the annual runoff. Using 31% of the annual runoff of Wadi Baysh (2.16 mcm), the annual amount of groundwater recharge from the main wadi channel, over a distance of 54 km, results in a minimum loss rate of 40,000 m^3/km/y.

3.4 Section Three: Floods

3.4.1 Regression-Flood Frequency Methods

Flood data have an inherent randomness which may be analysed and explained in a probabilistic sense. For instance, it is not possible to predict the wadi floods on a purely deterministic basis since it is impossible to know all the causal mechanisms quantitatively. Fortunately statistical methods such as regression flood frequency analysis are able to reduce the observed data to a form that facilitates their interpretation and evaluation.

The observed flood record is a sample of the total population of floods that have occurred and may occur again. Probabilities can show how frequently a wadi flood will equal or exceed a specific value.

The past records of flood events of both wadis are very important in estimating the probability of future occurrences of flooding. Estimation of the flood volume requires some measures of its rarity, in which the water supply management in both wadis would require to know whether discharges of, for example, 100 mcm, are likely to occur once, or a number of times, during the project life, or if they are not likely to occur at all.

In flood frequency analysis, peak flows, Q (q_1, q_2, q_3), are used as variables. All possible flows form a population while the sample represents the subset of the population. The probability distribution used for the number of occurrences of a certain flood flow is plotted as a proportion of the total. The cumulative distribution function (cdf) of the population refers to the probability that any randomly selected flow will be less than a given value. In other words it is a probability of nonexceedance as a function of a continuous random variable.

Flood estimation and prediction will assist in the efficient management of the surface water storage design so that the agricultural areas will avoid drought seasons. The study presents flood discharge analyses for both wadis.

This section deals with more than one technique for flood frequency analysis to show the best average value for the N-year event of a given flood in both wadis. There are two outlet stations to be considered, SA-124 in Wadi Baysh, and N-406 in Wadi Habawnah (see Figure 3.1). The flood discharge parameters are determined. The flood

magnitudes with different recurrence intervals are evaluated using Gumbel's distribution, Log Pearson Type III and normal distribution methods. The ratios of estimated maximum flood volumes for different recurrences are calculated to show the frequency values for Wadis Baysh and Habawnah. However, the fitting of the distributions are restricted to point data, that is observations at a single station of measurement.

The measured data (Wadi Baysh) and synthesised data (Wadi Habawnah) were adopted for the normal distribution, the Log Pearson Type III and Gumbel's distribution analysis to compute flood magnitude (volumes) corresponding to return periods of from 2 to 100 years.

The various methodologies will be compared for several return periods, with emphasis on 2 year volumes because of the short period of records. The author extrapolated the Wadi Habawnah flood record by the rational method and regression analysis which will be explained later in this section. Flood volumes (monthly and annual) of observed and synthesised data have been calculated for both wadis. In other words the Wadi Baysh flood volumes have been analysed for a record of 16 years (1970-1985) and the record for Wadi Habawnah was extended backwards for the period 1985 to 1970.

3.4.1.1 Data Selection

The mean annual runoff is determined for gauged Wadis Baysh and Habawnah (see Table 3.5) as the sum of the mean values of the months. The monthly natural flow values of runoff station SA-124 at Al Fatiyah in Wadi Baysh and Wadi Habawnah runoff stations N-408, N-404, N-405, N-406 and N-407 are given in Table 3.5. The annual mean flow at Wadi Baysh is 74.5 mcm based on the mean ratio of monthly flow of station SA-124 available for the period 1970-1985. The annual mean flow at Wadi Habawnah is 14.17 mcm for the period 1984-1986 (see Figure 3.2), equal to the summation of the flows of Wadi Thar (runoff station N-405) and Wadi Sayhan (runoff station N-404) which flow into Wadi Habawnah (runoff station N-406).

The runoff record of station SA-124, (at Wadi Baysh) could not be extended to a longer duration. However, there is a longer record of rainfall data and this can be used to predict the runoff records of Wadi Baysh using the equation developed by Sorman and

Abdulrazzag (1987) for the south-west region of Arabia:

$$\overline{Q} = 0.0108 \times (AP)^{1.204} \times (K)^{-0.459} \quad (3.7)$$

$$\overline{Q} = 0.020 \times (AP)^{1.086} \times (K)^{-0.60} \times (S)^{0.39} \quad (3.8)$$

Equations 3.7 and 3.8 can be used to predict the runoff ($\overline{Q}$) based on the number of available parameters of annual precipitation (AP), hydraulic conductivity (K) and the drainage slope (S). However, the long record of rainfall for Wadi Baysh is available as an average value, for e.g. 1963-1985 (see Table 3.4). Since the Wadi Habawnah record is insufficient for a frequency analysis of measured volumes, because the runoff record is very short (3 years), the probabilities derived cannot be expected to be reliable. It is necessary therefore to establish a record of equal length for both wadis which have similar catchment areas but with different slopes. The ratio factor and regression methods were used to create a long runoff record based on the Wadi Baysh runoff record which can then be used as an input to compute a synthesised record of flood volumes for Wadi Habawnah. In Wadi Habawnah there are five runoff stations but all have the same short time of record which cannot be used to extend their record for longer periods.

The Wadi Habawnah runoff record was extended using two methods :

1- As a rational method the ratio factor of the runoff of both wadis was used to extend the Wadi Habawnah runoff record. The runoff records (Table 3.23) show that, on average, Wadi Habawnah experiences as much as 31% of the runoff encountered in Wadi Baysh. For simplicity, the author considers the 31% of the spring record of the Wadi Baysh runoff as a suitable previous record to be considered for Wadi Habawnah spring flow since Wadi Habawnah floods mainly occur in the spring (see Figures 3.35 and 3-36). In predicting the maximum monthly runoff of the annual flow of Wadi Baysh the author used the same ratio factor (31%) to determine the maximum monthly runoff for likely Wadi Habawnah records (see Table 3.23).

2- The period 1984 until 1985, as two years' runoff records for both wadis, was used for regression analysis. In order to show the relation between runoff of both wadis, the mean ratio of monthly runoff volumes during the spring season and during the rest of the year (see Tables 3.24 and 3.25) are plotted in Figure 3.45 and 3.46. The spring season of both

Table 3.23 Observed Spring monthly runoff data of station SA-124 within the catchment areas of Wadi Baysh (catchment area 3511 km^2) and the synthesised runoff data of station N-406 within Wadi Habawnah (catchment area 4425 km^2)

Wadi Baysh

Observed runoff data of Station SA-124

Year record	Spring season MAR mcm	APR mcm	MAY mcm	Total runoff mcm
1970	6.45	0.581	0.189	7.2
1971	0.13	29.6	20.7	50.4
1972	20.1	48.5	13.9	82.5
1973	0.994	2.57	2.79	6.4
1974	16.1	6.12	13.6	35.8
1975	3.16	26.5	2.73	32.4
1976	6.48	4.32	4.78	15.6
1977	0.656	2.79	5.04	8.5
1978	1.93	1.7	2.42	6.1
1979	2.86	3.59	7.23	13.7
1980	1.13	3.88	7.78	12.8
1981	21.2	5.94	27.1	54.2
1982	13.4	18.7	7.43	39.5
1983	12.1	32.2	17.5	61.8
1984	2.85	3.13	16	22.0
1985	3.9	18.54	13.43	35.9
			Average	30.3

Wadi Habawnah

Observed Runoff data of Station N-406

Year record	Spring season MAR mcm	APR mcm	MAY mcm	Total runoff mcm
1984	0.091	0	0	0.1
1985	0	15.813	1.103	16.9
1986	0.295	11.068	0	11.4
			Average	9.5

Wadi Habawnah

Synthesised Runoff data of Station N-406

Year	Spring season Synthesised data** mcm	Maximum monthly value Synthesised data** Time	mcm
1970	2.3	March,1970	2.0
1971	15.8	April,1971	9.3
1972	25.9	April,1972	15.2
1973	2.0	May,1973	0.9
1974	11.2	March,1974	5.0
1975	10.2	April,1975	8.3
1976	4.9	March,1976	2.0
1977	2.7	May,1977	1.6
1978	1.9	May,1978	0.8
1979	4.3	May,1979	2.3
1980	4.0	May,1980	2.4
1981	17.0	May,1981	8.5
1982	12.4	April,1982	5.9
1983	19.4	April,1983	10.1
1984	6.9	May,1984	5.0
1985	11.3	April,1985	5.8

(**) predicted data based on the spring average Wadi Habawnah runoff (9.5mcm) to the spring average of Wadi Bayash runoff (30.0mcm) defined as ratio factor = 0.31 or 31%

Table 3.24 Monthly runoff data of the Spring Season within the catchment areas of Wadi Baysh and Wadi Habawnah

Wadi Baysh

Runoff data of Station SA-124 (elevation 200 m a.ms.l,catchment area 3511 km^2)

Year	MAR	APR	MAY	Season
record	mcm	mcm	mcm	mcm
1984	2.85	3.13	16	22.0
1985	3.9	18.54	13.43	35.9

Wadi Habawnah

Runoff data of Station N-408 (elevation 1452 m a.ms.l,catchment area 1307 km^2)

Year	MAR	APR	MAY	Season
record	mcm	mcm	mcm	mcm
1984	0	0	0.188	0.2
1985	0.35	6.259	3.549	10.2

Runoff data of Station N-404 (elevation 1339 m a.ms.l,catchment area 2391 km^2)

Year	MAR	APR	MAY	Season
record	mcm	mcm	mcm	mcm
1984	0	0.225	0.292	0.5
1985	0.286	9.16	2.708	12.2

Runoff data of Station N-405 (elevation 1303m a.ms.l,catchment area 940 km^2)

Year	MAR	APR	MAY	Season
record	mcm	mcm	mcm	mcm
1984	0	0.417	0	0.4
1985	0.041	5.067	0.621	5.7

Runoff data of Station N-406 (elevation 1212m a.ms.l,catchment area 4425 km^2)

Year	MAR	APR	MAY	Season
record	mcm	mcm	mcm	mcm
1984	0.091	0	0	0.1
1985	0	15.813	1.103	16.9

Runoff data of Station N-407 (elevation 1166m a.ms.l,catchment area 4682 km^2)

Year	MAR	APR	MAY	Season
record	mcm	mcm	mcm	mcm
1984	0	0	0	0.0
1985	0	5.313	0.173	5.5

Table 3.25 Monthly runoff data of the rest of the year (Summer, Autumn and Winter) within the catchment areas of Wadi Baysh and Wadi Habawnah

Wadi Baysh

Runoff data of Station SA-124 (elevation 200 m a.ms.l,catchment area 3511 km^2)

Year record	DEC mcm	JAN mcm	FEB mcm	JUN mcm	JUL mcm	AUG mcm	SEP mcm	OCT mcm	NOV mcm	Total mcm
1984	3.88	3.29	2.88	8.62	9.96	7.19	3.57	2.28	2.2	40.0
1985	6.54	6.45	3.7	9.95	15.03	13.09	6.1	6.87	7.48	68.7

Wadi Habawnah

Runoff data of Station N-408 (elevation 1452 m a.ms.l,catchment area 1307 km^2)

Year record	DEC mcm	JAN mcm	FEB mcm	JUN mcm	JUL mcm	AUG mcm	SEP mcm	OCT mcm	NOV mcm	Total mcm
1984	0	0	0	0	0	0	0	0	0	0.19
1985	0	1.122	0	0.235	0.062	0	0	0	0	1.42

Runoff data of Station N-404 (elevation 1339 m a.ms.l,catchment area 2391 km^2)

Year record	DEC mcm	JAN mcm	FEB mcm	JUN mcm	JUL mcm	AUG mcm	SEP mcm	OCT mcm	NOV mcm	Total mcm
1984	0	0	0	0.074	0	0	0	0	0	0.07
1985	0	0.682	0	0.061	0	0	0	0	0	0.74

Runoff data of Station N-405 (elevation 1303m a.ms.l,catchment area 940 km^2)

Year record	DEC mcm	JAN mcm	FEB mcm	JUN mcm	JUL mcm	AUG mcm	SEP mcm	OCT mcm	NOV mcm	Total mcm
1984	0	0	0	0	0	0	0	0	0	0.00
1985	0	0	0	0	0	0	0	0	0	0.00

Runoff data of Station N-406 (elevation 1212m a.ms.l,catchment area 4425 km^2)

Year record	DEC mcm	JAN mcm	FEB mcm	JUN mcm	JUL mcm	AUG mcm	SEP mcm	OCT mcm	NOV mcm	Total mcm
1984	0	0	0	0	0	0	0	0	0	0.00
1985	0	0.105	0	0	0	0	0	0	0	0.11

Runoff data of Station N-407 (elevation 1166m a.ms.l,catchment area 4682 km^2)

Year record	DEC mcm	JAN mcm	FEB mcm	JUN mcm	JUL mcm	AUG mcm	SEP mcm	OCT mcm	NOV mcm	Total mcm
1984	0	0	0	0	0	0	0	0	0	0.00
1985	0	0.454	0	0	0	0	0	0	0	0.45

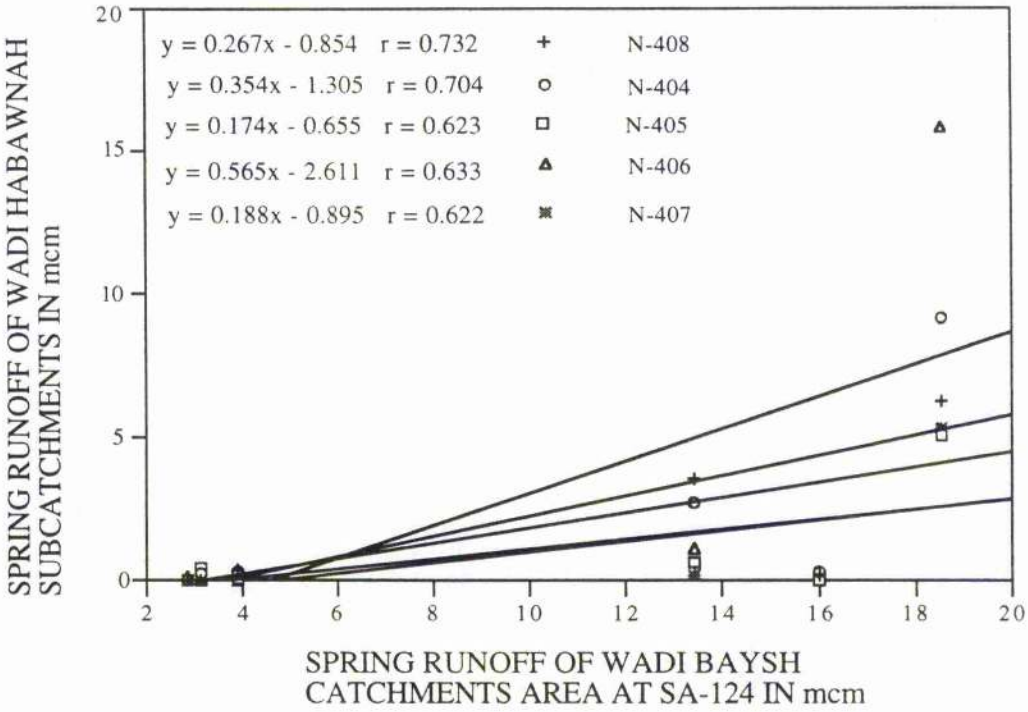

Figure 3.45 Spring runoff correlation between Wadi Baysh (Station SA-124) and Wadi Habawnah subcatchments (stations N-408, N-404, N-405, N-406 and N-407).

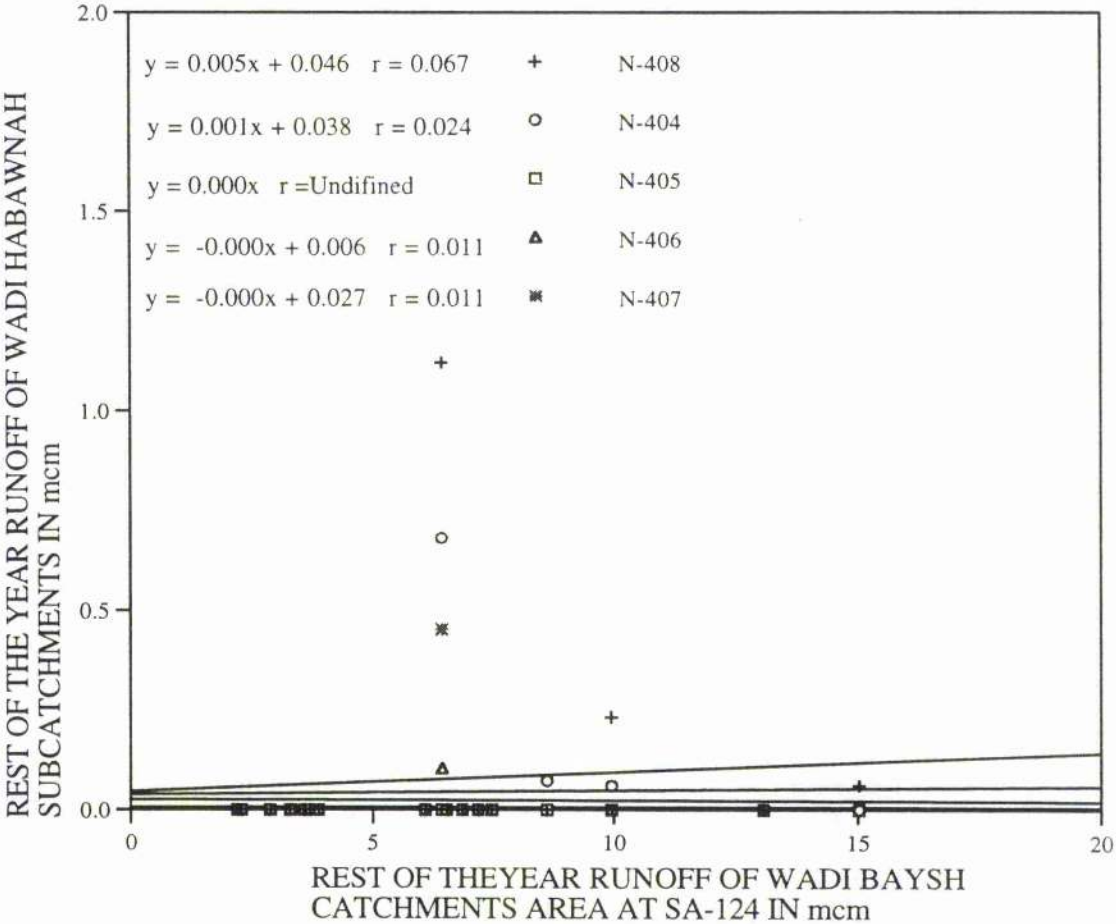

Figure 3.46 Rest of the year runoff correlation between Wadi Baysh (Station SA-124) and Wadi Habawnah subcatchments (stations N-408, N-404, N-405, N-406 and N-407).

wadis was chosen because both wadis have the major quantity of runoff during this season (see Figure 3.35 and 3.36). The correlation between the spring seasons of the runoff for both wadis were considered. The fit of the linear regression is shown in Figure 3.45 and 3.46. The fitted line for the spring runoff (Figure 3.45) has r = 0.732 for station SA-124 versus N-408, while runoff stations N-404, N-405, N-406 and N-407 have r = 0.704, 0.623, 0.633 and 0.622, respectively. Generally r values are low. However, the author considers that the fitted line of the spring runoff for station SA-124 versus N-406 which has a regression equation:

Runoff of Wadi Habawnah = - 2.6107 + 0.56476 × (Runoff of Wadi Baysh) (3.9)

is most suitable for prediction of the runoff for Wadi Habawnah (see Table 3.26) for two reasons:

(a) Runoff station N-406 records the whole of the Wadi Habawnah catchment flow since the two major subcatchments (N-404 and N-405) flow into it.

(b) The catchment area of N-406 is large, similar in area to the Wadi Baysh catchment. The runoff records for the rest of the year of 1984 and 1985 do not show significant correlation; r varied between zero and 0.011 (Figure 3.46). Such lack of correlation is to be expected, since in Wadi Habawnah, runoff occurs mostly in the spring while during the rest of the year almost no flow occurs (see Table 3.5). However, Wadi Baysh experienced runoff during all seasons.

3.4.1.2 Plotting Positions

Two main parameters were determined by plotting the wadi flows: the probability and the return period. Probability (P) is defined by analysis of the likelihood of the flood flow being equalled or exceeded in any year, while the return period (T_r) is often used in lieu of probability to describe a design structure for flood storage. Probability and return period are inversely related, i.e.

$$P = \frac{1}{T_r} \tag{3.10}$$

The wadi flood flows were plotted as a cumulative frequency curve using a probability and return period associated with each flood. There are various formulae for defining this

Table 3.26 Observed Spring monthly runoff data of station SA-124 within the catchment of Wadi Baysh and the synthesised runoff data of station N-406 within Wadi Habawnah

Wadi Baysh Spring Season Runoff Observed Runoff Data of Station SA-124				Wadi Habawnah Spring Season runoff Synthesised Runoff Data of Station N-406 Synthesised Data Using Ratio Factor**				Synthesised Data Using Regression Equation***			
		Maximum Monthly Value			Spring Season	Maximum Monthly Value			Spring Season	Maximum Monthly Value	
Year record	Total mcm		Runoff mcm	Year record	Runoff mcm		Runoff mcm	Year record	Runoff mcm		Runoff mcm
1970	7.2	March,1970	6.45	1970	2.26	March,1970	2.02	1970	1.46	March,1970	1.03
1971	50.4	April,1971	29.6	1971	15.80	April,1971	9.28	1971	25.85	April,1971	14.11
1972	82.5	April,1972	48.5	1972	25.87	April,1972	15.21	1972	43.98	April,1972	24.78
1973	6.4	May,1973	2.79	1973	2.01	May,1973	0.87	1973	1.00	May,1973	0.00
1974	35.8	March,1974	16.1	1974	11.22	March,1974	5.05	1974	17.61	March,1974	6.5
1975	32.4	April,1975	26.5	1975	10.16	April,1975	8.31	1975	15.69	April,1975	12.36
1976	15.6	March,1976	6.48	1976	4.89	March,1976	2.03	1976	6.20	March,1976	1.05
1977	8.5	May,1977	5.04	1977	2.67	May,1977	1.58	1977	2.19	May,1977	0.24
1978	6.1	May,1978	2.42	1978	1.91	May,1978	0.76	1978	0.83	May,1978	0.00
1979	13.7	May,1979	7.23	1979	4.30	May,1979	2.27	1979	5.13	May,1979	1.47
1980	12.8	May,1980	7.78	1980	4.01	May,1980	2.44	1980	4.62	May,1980	1.78
1981	54.2	May,1981	27.1	1981	16.99	May,1981	8.50	1981	28.00	May,1981	12.69
1982	39.5	April,1982	18.7	1982	12.38	April,1982	5.86	1982	19.70	April,1982	7.95
1983	61.8	April,1983	32.2	1983	19.38	April,1983	10.10	1983	32.29	April,1983	15.57
1984	22.0	May,1984	16	1984	6.90	May,1984	5.02	1984	9.81	May,1984	6.43
1985	35.9	April,1985	18.54	1985	11.26	April,1985	5.81	1985	17.66	April,1985	7.86

(**) predicted data based on the spring average Wadi Habawnah runoff (9.5mcm) to the spring average of Wadi Bayash runoff (30.0mcm) defined as ratio factor = 0.31 & 31%

(***) predicted data based on the regression equation (see Figure 2.45) that Wadi Habawnah runoff = 0.56476*Wadi Baysh runoff data of the spring season - 2.6107 }

value, known as the plotting position (Benson, 1962), such as Weibull's formula:

$$P = \frac{m}{n+1} \tag{3.11}$$

or

$$T_r = \frac{n+1}{m} \tag{3.12}$$

and Gringorten's formula:

$$T_r = \frac{(n+0.12)}{(m-0.44)} \tag{3.13}$$

where n is the length of record in number of years and m is the rank of the event, with the largest event having rank equal to n.

In this study, the Gringorten plotting technique is applied because it gives longer return periods for the bigger floods in the series. This recognises that the true return period of the higher floods is probably longer than the value calculated with Weibull's formula.

Tables 3.27, 28, 29, 30, 31and 32 were plotted in semi- log form for Q_{T_r} (mcm) against return period (year) T_r (logarithmic) (see Figure 4.47, 4.48 and 4.49)

The probability P of an N-year event of return period (T_r) is

$$P = \frac{100}{T_r} \text{ percent.} \tag{3.14}$$

Table 3.26 is a listing of the annual values of flood volumes and maximum monthly values for Wadi Baysh and Wadi Habawnah for the years 1970-1985. The annual and monthly series of flood volumes with return periods and probabilities were calculated for Wadi Baysh (see Table 3.27 and 3.28) and Wadi Habawnah (see Table 3.29, 30, 31 and 32) from the equations (3.13) and (3.14).

3.4.1.3 Normal Distribution

Figures 3.47, 48, and 49 were used to predict Q_{T_r} at different T_r (2-, 10-, 20-, 50-, 100 year) (see Table 3.33).

Table 3.27 Maximum monthly flood volume (Q) observed in mcm for water-years1970-1985, at Fatiyah station SA-124 of Wadi Baysh

Water year	(Q) mcm	number of event	Rank m	Return period Tr (year)*	Percentage probability P	Log Q (mcm)	Log Q^2 (mcm)	(logQ - averge log Q)^3 (mcm)
March, 1970	6.45	1	15	1.1	90	0.810	0.655	-0.046
April, 1971	29.60	1	3	6.3	16	1.471	2.165	0.028
April, 1972	48.50	1	1	28.8	3	1.686	2.842	0.139
January, 1973	10.00	1	10	1.7	59	1.000	1.000	-0.005
March, 1974	16.10	1	8	2.1	47	1.207	1.456	0.000
April, 1975	26.50	1	5	3.5	28	1.423	2.026	0.017
March, 1976	6.48	1	14	1.2	84	0.812	0.659	-0.045
May, 1977	5.04	1	16	1.0	97	0.702	0.493	-0.101
January, 1978	7.94	1	12	1.4	72	0.900	0.810	-0.019
May, 1979	7.23	1	13	1.3	78	0.859	0.738	-0.029
July, 1980	9.70	1	11	1.5	66	0.987	0.974	-0.006
May, 1981	27.10	1	4	4.5	22	1.433	2.053	0.019
February, 1982	26.50	1	6	2.9	34	1.423	2.026	0.017
April, 1983	32.20	1	2	10.3	10	1.508	2.274	0.039
May, 1984	16.00	1	9	1.9	53	1.204	1.450	0.000
April, 1985	18.54	1	7	2.5	41	1.268	1.608	0.001
Q(av)	18							
Q (stdev)	12							
log Q (sum)	18.693							
log Q^2 (sum)	23.228							
log Q^3 (sum)	0.007							
log Q (av)	1.168							
log Q (stdev)	0.304							
G	0.019							

(*) Tr equal to (n + 0.12) / (m - 0.44)

Table 3.28 Annual mean of floods volumes (Q) observed in mcm for water-years1970-1985, at Fatiyah station SA-124 of Wadi Baysh

Water year	(Q) mcm	number of event	Rank m	Return period Tr (year)*	Percentage probability P	Log Q (mcm)	Log Q^2 (mcm)	(logQ - averge log Q)^3 (mcm)
1970	22	1	16	1.0	97	1.342	1.802	-0.102
1971	86	1	7	2.5	41	1.934	3.742	0.002
1972	134	1	2	10.3	10	2.127	4.525	0.032
1973	46	1	10	1.7	59	1.663	2.765	-0.003
1974	87	1	6	2.9	34	1.940	3.762	0.002
1975	77	1	8	2.1	47	1.886	3.559	0.000
1976	45	1	11	1.5	66	1.653	2.733	-0.004
1977	37	1	14	1.2	84	1.568	2.459	-0.014
1978	35	1	15	1.1	90	1.544	2.384	-0.019
1979	40	1	12	1.4	72	1.602	2.567	-0.009
1980	38	1	13	1.3	78	1.580	2.496	-0.012
1981	96	1	5	3.5	28	1.982	3.929	0.005
1982	121	1	3	6.3	16	2.083	4.338	0.021
1983	151	1	1	28.8	3	2.179	4.748	0.051
1984	66	1	9	1.9	53	1.820	3.311	0.000
1985	111	1	4	4.5	22	2.045	4.183	0.013
Q(av)	75							
Q (stdev)	40							
log Q (sum)	28.949							
log Q^2 (sum)	53.303							
log Q^3 (sum)	-0.036							
log Q (av)	1.809							
log Q (stdev)	0.248							
G	-0.177							

(*) Tr equal to (n + 0.12) / (m - 0.44)

Table 3.29 Maximum volume of monthly flood (Q) in mcm using ratio factor analysis for water-years 1970-1985, at station N-406 of Wadi Habawnah.

Water year	Q mcm	number of event	Rank m	Return period Tr (year)*	Percentage probability P	Log Q (mcm)	Log Q^2 (mcm)	(logQ - averge log Q)^3 (mcm)
March,1970	2.00	1	12	1.4	72	0.301	0.091	-0.023
April,1971	9.30	1	3	6.2	16	0.968	0.938	0.057
April,1972	15.20	1	1	27.0	4	1.182	1.397	0.214
May,1973	0.9	1	15	1.1	90	-0.046	0.002	-0.250
March,1974	5.00	1	8	2.1	47	0.699	0.489	0.002
April,1975	8.30	1	5	3.5	28	0.919	0.845	0.038
March,1976	2.00	1	13	1.3	78	0.301	0.091	-0.023
May,1977	1.60	1	14	1.2	84	0.204	0.042	-0.055
May,1978	0.8	1	16	1.0	96	-0.097	0.009	-0.316
May,1979	2.30	1	11	1.5	65	0.362	0.131	-0.011
May,1980	2.40	1	10	1.7	59	0.380	0.145	-0.008
May,1981	8.50	1	4	4.5	22	0.929	0.864	0.041
April,1982	5.90	1	6	2.9	35	0.771	0.594	0.007
April,1983	10.10	1	2	10.1	10	1.004	1.009	0.074
May,1984	5.00	1	9	1.9	53	0.699	0.489	0.002
April,1985	5.80	1	7	2.5	41	0.763	0.583	0.006
Q(av)	5							
Q (stdev)	4							
log Q (sum)	9.341							
log Q^2 (sum)	7.716							
log Q^3 (sum)	-0.246							
log Q (av)	0.584							
log Q (stdev)	0.388							
G	-0.32							

(*) Tr equal to (n + 0.12) / (m - 0.44)

Table 3.30 Annual mean of floods volumes (Q) in mcm using ratio factor analysis for water-years 1970-1985, at station N-406 of Wadi Habawnah

Water year	Q mcm	number of event	Rank m	Return period Tr (year)*	Percentage probability P	Log Q (mcm)	Log Q^2 (mcm)	(logQ - averge log Q)^3 (mcm)
1970	2.3	1	14	1.2	84	0.362	0.131	-0.111
1971	15.8	1	4	4.5	22	1.199	1.437	0.045
1972	25.9	1	1	28.8	3	1.413	1.997	0.186
1973	2.0	1	15	1.1	90	0.301	0.091	-0.158
1974	11.2	1	7	2.5	41	1.049	1.101	0.009
1975	10.2	1	8	2.1	47	1.009	1.017	0.005
1976	4.9	1	10	1.7	59	0.690	0.476	-0.003
1977	2.7	1	13	1.3	78	0.431	0.186	-0.069
1978	1.9	1	16	1.0	97	0.279	0.078	-0.179
1979	4.3	1	11	1.5	66	0.633	0.401	-0.009
1980	4.0	1	12	1.4	72	0.602	0.362	-0.014
1981	17.0	1	3	6.3	16	1.230	1.514	0.059
1982	12.4	1	5	3.5	28	1.093	1.196	0.016
1983	19.4	1	2	10.3	10	1.288	1.658	0.089
1984	6.9	1	9	1.9	53	0.839	0.704	0.000
1985	11.3	1	6	2.9	34	1.053	1.109	0.009
Q(av)	10							
Q (stdev)	7							
log Q (sum)	13.472							
log Q^2 (sum)	13.458							
log Q^3 (sum)	-0.126							
log Q (av)	0.842							
log Q (stdev)	0.375							
G	-0.18							

(*) Tr equal to (n + 0.12) / (m - 0.44)

Table 3.31 Maximum volume of monthly flood (Q) in mcm using regression analysis for water-years 1970-1985, at station N-406 of Wadi Habawnah

Water year	Q mcm	number of event	Rank m	Return period Tr (year)*	Percentage probability P	Log Q (mcm)	Log Q^2 (mcm)	(logQ - averge log Q)^3 (mcm)
March,1970	1.03	1	13	1.3	78	0.013	0.000	0.007
April,1971	14.11	1	3	6.2	16	1.150	1.321	2.329
April,1972	24.78	1	1	27.0	4	1.394	1.944	3.871
May,1973	0.000001	1	15	1.1	90	-6.000	36.000	-197.544
March,1974	6.50	1	8	2.1	47	0.813	0.661	0.967
April,1975	12.36	1	5	3.5	28	1.092	1.193	2.039
March,1976	1.05	1	12	1.4	72	0.021	0.000	0.008
May,1977	0.24	1	14	1.2	84	-0.620	0.384	-0.087
May,1978	0.000001	1	16	1.0	96	-6.000	36.000	-197.544
May,1979	1.47	1	11	1.5	65	0.167	0.028	0.040
May,1980	1.78	1	10	1.7	59	0.250	0.063	0.078
May,1981	12.69	1	4	4.5	22	1.103	1.218	2.095
April,1982	7.95	1	6	2.9	35	0.900	0.811	1.247
April,1983	15.57	1	2	10.1	10	1.192	1.422	2.562
May,1984	6.43	1	9	1.9	53	0.808	0.653	0.953
April,1985	7.86	1	7	2.5	41	0.895	0.802	1.230
Q(av)	7							
Q (stdev)	7							
log Q (sum)	-2.820							
log Q^2 (sum)	82.499							
log Q^3 (sum)	-377.751							
log Q (av)	-0.176							
log Q (stdev)	2.338							
G	-2.25							

(*) Tr equal to (n + 0.12) / (m - 0.44)

Table 3.32 Annual mean of flood volumes (Q) in mcm using regression analysis for water-years 1970-1985, at station N-406 of Wadi Habawnah

Water year	Q mcm	number of event	Rank m	Return period Tr (year)*	Percentage probability P	Log Q (mcm)	Log Q^2 (mcm)	(logQ - averge log Q)^3 (mcm)
1970	1.5	1	14	1.2	84	0.176	0.031	-0.397
1971	25.9	1	4	4.5	22	1.413	1.997	0.127
1972	44.0	1	1	28.8	3	1.643	2.701	0.393
1973	1.0	1	15	1.1	90	0.000	0.000	-0.756
1974	17.6	1	7	2.5	41	1.246	1.551	0.037
1975	15.7	1	8	2.1	47	1.196	1.430	0.023
1976	6.2	1	10	1.7	59	0.792	0.628	-0.002
1977	2.2	1	13	1.3	78	0.342	0.117	-0.184
1978	0.8	1	16	1.0	97	-0.097	0.009	-1.024
1979	5.1	1	11	1.5	66	0.708	0.501	-0.008
1980	4.6	1	12	1.4	72	0.663	0.439	-0.015
1981	28.0	1	3	6.3	16	1.447	2.094	0.154
1982	19.7	1	5	3.5	28	1.294	1.676	0.056
1983	32.3	1	2	10.3	10	1.509	2.278	0.214
1984	9.8	1	9	1.9	53	0.991	0.983	0.001
1985	17.7	1	6	2.9	34	1.248	1.557	0.038
Q(av)	15							
Q (stdev)	13							
log Q (sum)	14.573							
log Q^2 (sum)	17.993							
log Q^3 (sum)	-1.342							
log Q (av)	0.911							
log Q (stdev)	0.561							
G	-0.58							

(*) Tr equal to (n + 0.12) / (m - 0.44)

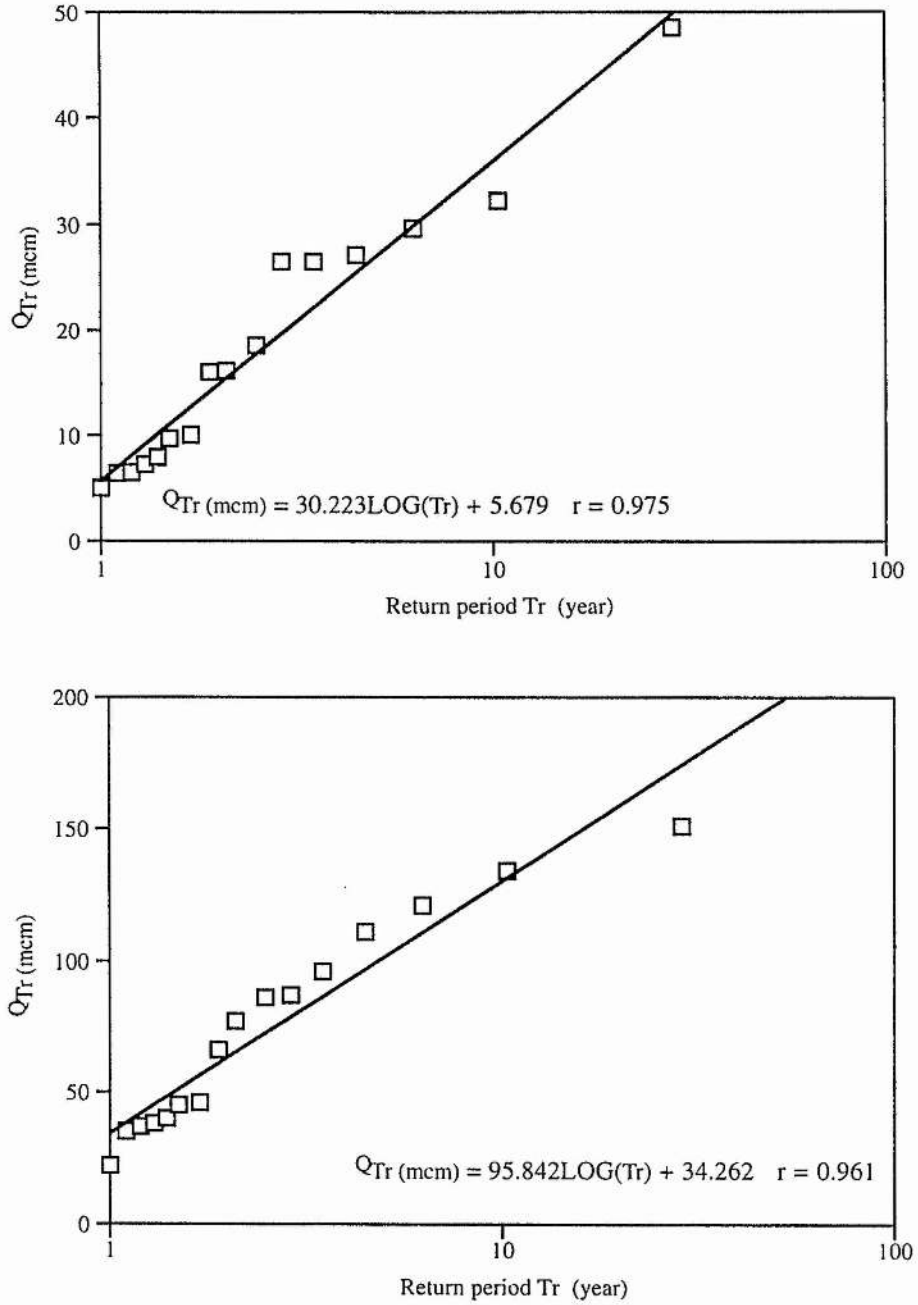

Figure 3.47 Maximum monthly (above) and annual mean (below) of flood volumes in Wadi Baysh, 1970-1985.

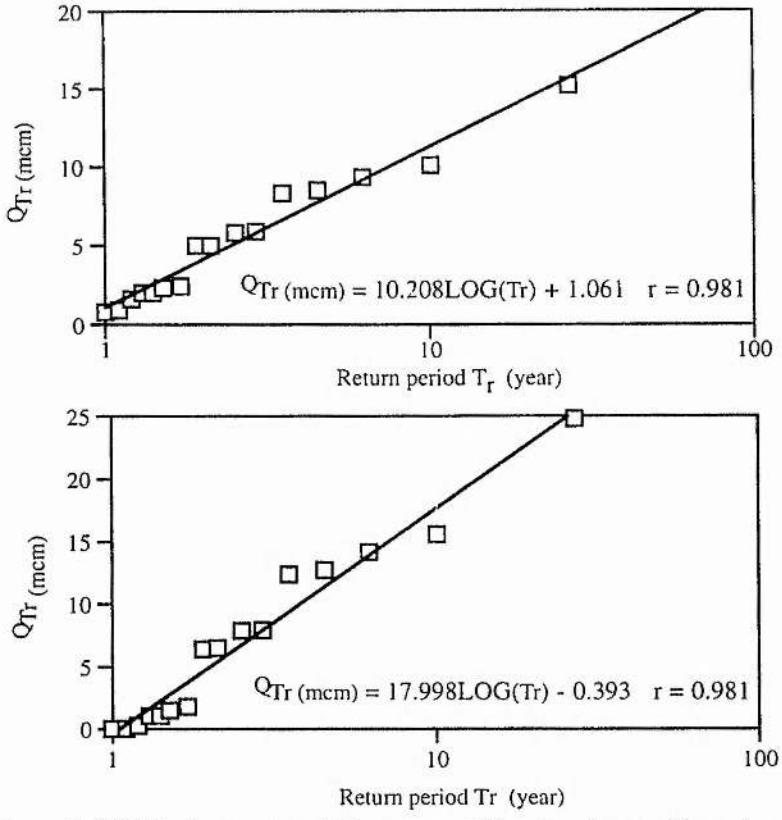

Figure 3.48 Maximum monthly mean of flood volumes (based on ratio factor ; above) and regression equation (below) in Wadi Habawnah,1970-1985.

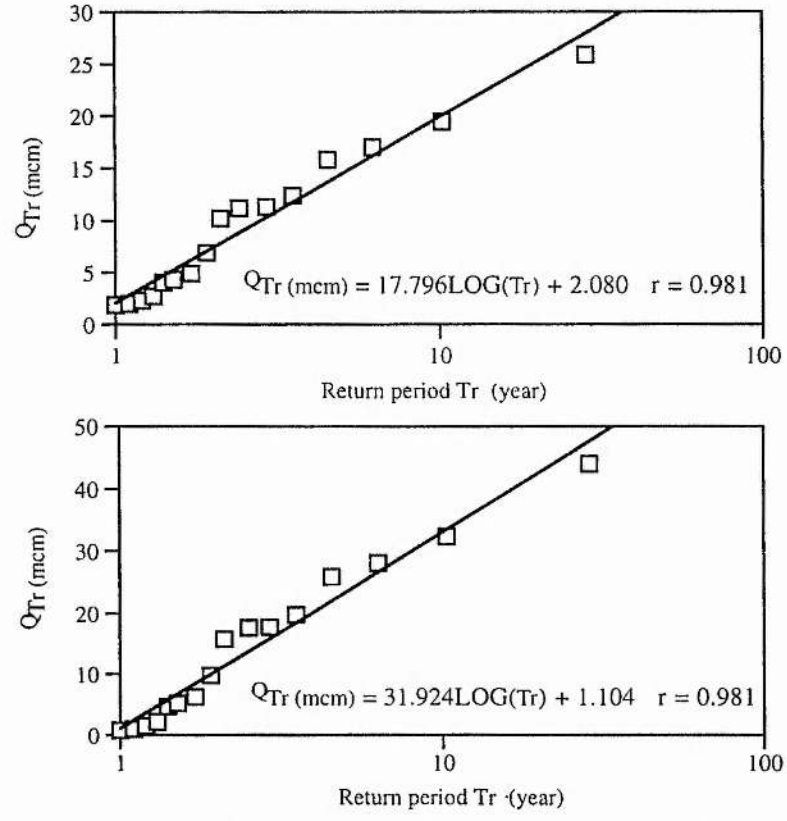

Figure 3.49 Annual mean of flood volumes (based on ratio factor ; above) and regression equation (below) in Wadi Habawnah, 1970-1985.

Table 3.33 Determining the flood volume magnitude (mcm) of the N-year event for both wadis .

Wadi Baysh flood volume magnitude of the N-year event using maximum monthly flood (based on observed data) within the year.				
[Qr=30.223*LOG(Tr)+5.679] Based on observed data				
Tr (year)	2	10	50	100
P%	50	10	5	1
Qr (mcm)	14.8	35.9	57.0	66.1
Wadi Baysh flood volume magnitude of the N-year event using the annual flood (based on observed data) within the wadi flood record.				
[Qr=95.842*LOG(Tr)+34.262] Based on observed data				
Tr (year)	2	10	50	100
P%	50	10	5	1
Qr (mcm)	63.1	130.1	197.1	225.9
Wadi Habawnah flood volume magnitude of the N-year event using maximum monthly flood (based on ratio factor) within the year.				
[Qr=10.208*LOG(Tr)+1.061]				
Tr (year)	2	10	50	100
P%	50	10	5	1
Qr (mcm)	4.1	11.3	18.4	21.5
Wadi Habawnah flood volume magnitude of the N-year event using maximum monthly flood (based on regression equation) within the year.				
[Qr=17.998*LOG(Tr)+0.393]				
Tr (year)	2	10	50	100
P%	50	10	5	1
Qr (mcm)	5.8	18.4	31.0	36.4
Wadi Habawnah flood volume magnitude of the N-year event using the annual flood (based on the ratio factor) within the annual flood record.				
[Qr=17.796*LOG(Tr)+2.080]				
Tr (year)	2	10	50	100
P%	50	10	5	1
Qr (mcm)	7.4	19.9	32.3	37.7
Wadi Habawnah flood volume magnitude of the N-year event using the annual flood (based on the regression equation) within the annual flood record.				
[Qr=31.924*LOG(Tr)+1.104]				
Tr (year)	2	10	50	100
P%	50	10	5	1
Qr (mcm)	10.7	33.0	55.3	65.0

3.4.1.4 Log Pearson Type III Distribution

One of the most popular methods to determine the flood magnitude of the N-year event is by the Log Pearson Type III distribution (PT3D) where the logarithm of the variant Q shows that the annual flood series will plot as straight lines. It has been widely adapted as the standard method for flood frequency analysis in which the transform y = log x is used to reduce skewness (Viessman *et al.*, 1977).

From Tables 3.26, 3.27, 3.28, 3.29, 3.30 and 3.31, N-year events were calculated using logarithms of the variant and a skewness coefficient (G) given by

$$\text{Skewness coefficient : } G = \left[\frac{n\sum\left(\log x - \overline{\log x}\right)^3}{(n-1)(n-2)\left(\sigma_{\log x}\right)^3} \right] \qquad (3.16)$$

where log x = log Q
and $\sigma_{\log x}$ = standard deviation on n values of x. The calculation of 10, 50 and 100 year return periods for flood Q from the maximum monthly and the annual flood record requires the following steps:

1- All n values of Q in the flood record were transformed to their logarithms

base (10) $\log x = \log Q$

2- The mean of all values of x were determined as below:

3- The standard deviation of n values of log x were computed using the equation below:

$$\text{Standard deviation : } \sigma_{\log x} = \sqrt{\frac{\sum\left(\log x - \overline{\log x}\right)^2}{n-1}} \qquad (3.17)$$

4- The Skewness of the x values, G, is calculated using equation 3.16.

5- The Q_{T_r} (return flood discharge) was calculated using the equation below

$$\text{Log}Q_{T_r} = \text{Log}Q_{av} + K\sigma_{\log x} \qquad (3.18)$$

where K is selected from Table 3.34a for particular probability (P) and Skewness (G) and Q_{T_r} based on equation (3.18) for different K. The flood magnitude at 2, 10, 50, and 100

Table 3.34a Values for the Pearson Type III distribution

	Recurrence interval, years							
	1.0101	1.25000	2	5	10	25	50	100
Skew coefficient	Percent chance							
G	99	80	50	20	10	4	2	1
3.0	-0.667	-0.636	-0.396	0.420	1.180	2.278	3.152	4.051
2.8	-0.714	-0.666	-0.384	0.460	1.210	2.275	3.114	3.973
2.6	-0.769	-0.696	-0.368	0.499	1.238	2.267	3.071	3.889
2.4	-0.832	-0.725	-0.351	0.537	1.262	2.256	3.023	3.800
2.2	-0.905	-0.752	-0.330	0.574	1.284	2.249	2.970	3.705
2.0	-0.990	-0.777	-0.307	0.609	1.320	2.219	2.912	3.605
1.8	-1.087	-0.799	-0.282	0.643	1.318	2.193	2.848	3.499
1.6	-1.197	-0.817	-0.254	0.675	1.329	2.163	2.780	3.388
1.4	-1.318	-0.832	-0.225	0.705	1.337	2.128	2.706	3.271
1.2	-1.449	-0.844	-0.915	0.732	1.340	2.087	2.626	3.149
1.0	-1.588	-0.852	-0.164	0.758	1.340	2.043	2.542	3.022
0.8	-1.733	0.856	-0.132	0.780	1.336	1.993	2.453	2.891
0.6	-1.880	-0.857	-0.099	0.800	1.328	1.939	2.359	2.755
0.4	-2.029	-0.855	-0.066	0.816	1.317	1.880	2.261	2.615
0.2	-2.178	-0.850	-0.033	0.830	1.301	1.818	2.159	2.472
0	-2.326	-0.842	0.	0.842	1.282	1.751	2.054	2.326
-0.2	-2.472	-0.830	0.033	0.850	1.258	1.680	1.945	2.178
-0.4	-2.165	-0.816	0.066	0.855	1.231	1.606	1.834	2.029
-0.6	-2.755	-0.800	0.099	0.857	1.200	1.528	1.720	1.880
-0.8	-2.891	-0.780	0.132	0.856	1.166	1.448	1.606	1.733
-1.0	-3.022	-0.758	0.164	0.852	1.128	1.366	1.492	1.588
-1.2	-3.149	-0.732	0.195	0.844	1.086	1,282	1.379	1.449
-1.4	-3.271	-0.705	0.225	0.832	1.041	1.198	1.270	1.318
-1.6	-3.388	-0.675	0.254	0.817	0.994	1.116	1.166	1.197
-1.8	-3.499	-0.643	0.282	0.799	0.945	1.035	1.069	1.087
-2.0	-3.605	-0.609	0.307	0.777	0.895	0.959	0.980	0.990
-2.2	-3.705	-0.574	0.330	0.752	0.844	0.888	0.900	0.905
-2.4	-3.800	-0.537	0.351	0.725	0.795	0.823	0.830	0.832
-2.6	-3.889	-0.499	0.368	0.696	0.747	0.764	0.768	0.769
-2.8	-3.973	-0.460	0.384	0.666	0.702	0.712	0.714	0.714
-3.0	-4.051	-0.420	0.396	0.636	0.660	0.666	0.666	0.667

(after Linsley, *et al.* 1986)

Table 3.34b Values of K for 6 the extreme-value (Type I) distribution

Return period, years	Probability	Reduced variate y	K
1.58	0.63	0.000	-0.450
2.00	0.50	0.367	-0.164
2.33	0.43	0.579	0.001
5	0.20	1.500	0.719
10	0.10	2.250	1.30
20	0.05	2.970	1.87
50	0.02	3.902	2.59
100	0.01	4.600	3.14
200	0.005	5.296	3.68
400	0.0025	6.000	4.23

(after Linsley, *et al.* 1986)

year recurrence intervals was estimated (see Table 3.35). The distribution data of both wadis exhibit small skewness values (Wadi Baysh, G = -0.18 to 0.019, Wadi Habawnah, G = -2.25 to -0.18) and are approximately log normal.

3.4.1.5 Gumbel's Distribution

Gumbel (1958; in Viessman, Jr. *et al* ., 1977) was the first to suggest the use of the extreme value distribution for floods which is commonly referred to as the Gumbel distribution. The flood data of both wadis were used to find the magnitude of the 2, 10, 50 and 100 year floods with Gumbel's distribution methods.

The event, X, of return period, T_r years, is defined as Q_{T_r}, and is given by

$$Q_{T_r} = Q_{av} + \sigma \times K = Q_{av} + \sigma \times K \qquad (3.19)$$

where Q_{av}= average of all values of 'annual flood' Q_{max}, σ= standard deviation of the series where n = number of years of record = number of Q_{max} values, $\sum Q_{max}$ = sum of the squares of n values of Q_{max}. Table 3.34b gives values of K as a function of T_r. The results are shown in Table 3.36.

3.4.1.6 Illustrative Example

Using the data of Tables 3.26 and 3.29, the magnitude of the 50 and 100 year floods with Gumbel and Log-Pearson Type III distribution were determined for both wadis as follows: Wadi Baysh

For Gumbel,

Q_{av} =18 mcm σ = (stdev) =12 (see Table 3.27)

From Table 3.34-b, $K_{50} = 2.59$ and $K_{100} = 3.14$

Using equation 3.19:

$$Q_{50} = 18 + (2.3 \times 12) = 497 \text{ mcm}$$

$$Q_{100} = 18 + (3.14 \times 12) = 678 \text{ mcm}$$

For Log-Pearson Type III, Table 3.29 (Wadi Habawnah) was used to determine the following:

$\overline{\log x}$ = (log Q_{av}) = 0.842, σ_{logQ} = log Q (stdev) = 0.375 and G = -0.18

Table 3.35 Determining the flood volume magnitude (mcm) of the N-year event for both wadis using the Log-Pearson Type III method

Log-Pearson Type III distrubution

Wadi Baysh

Data Type	Maximum monthly logQ(average)	LogQ(std)	G	K(2)	K(10)	K(25)	K(50)	K(100)	Q(2) mcm	Q(10) mcm	Q(50) mcm	Q(100) mcm
Observed data	1.2	0.3	0.019	-0.033	0.830	1.818	2.159	2.472	15.492	28.119	55.6416	70.4206

Wadi Habawnah

Data Type	Maximum monthly logQ(average)	LogQ(std)	G	K(2)	K(10)	K(25)	K(50)	K(100)	Q(2) mcm	Q(10) mcm	Q(50) mcm	Q(100) mcm
Ratio data	0.6	0.4	-0.3	0.033	1.258	1.680	1.945	2.170	4.1039	12.682	18.7068	23.8781
Regression data	-0.2	2.3	-2.3	0.330	0.844	0.888	0.900	0.905	3.9404	62.701	79.4592	84.7618

Wadi Baysh

Data Type	Annualy logQ(average)	LogQ(std)	G	K(2)	K(10)	K(25)	K(50)	K(100)	Q(2) mcm	Q(10) mcm	Q(50) mcm	Q(100) mcm
Observed data	1.8	0.2	-0.2	0.033	1.258	1.680	1.945	2.178	64.296	129.41	164.68	191.584

Wadi Habawnah

Data Type	Annualy logQ(average)	LogQ(std)	G	K(2)	K(10)	K(25)	K(50)	K(100)	Q(2) mcm	Q(10) mcm	Q(50) mcm	Q(100) mcm
Ratio data	0.8	0.4	-0.2	0.033	1.258	1.680	1.945	2.178	7.1511	20.594	29.6483	37.2713
Regression data	0.9	0.6	-0.6	0.099	1.200	1.528	1.720	1.880	9.1075	41.687	65.5843	85.5067

Table 3.36 Determining the flood volume magnitude (mcm) of the N-year event for both wadis using Pearson Type III and Gumbel methods .

Gumbel's distrubution

Wadi Baysh

Data Type	Maximum monthly Q(average) mcm	Q(std) mcm	K(2)	K(10)	K(20)	K(50)	K(100)	Q(2) mcm	Q(10) mcm	Q(50) mcm	Q(100) mcm
Observed data	18.0	12.0	-0.164	1.300	1.870	2.590	3.140	16.032	33.6	40.44	49.08

Wadi Habawnah

Data Type	Maximum monthly Q(average) mcm	Q(std) mcm	K(2)	K(10)	K(20)	K(50)	K(100)	Q(2) mcm	Q(10) mcm	Q(50) mcm	Q(100) mcm
Ratio data	5.0	4.0	-0.164	1.300	1.870	2.590	3.140	4.344	10.2	12.48	15.36
Regression data	7.0	7.0	-0.164	1.300	1.870	2.590	3.140	5.852	16.1	20.09	25.13

Wadi Baysh

Data Type	Annualy Q(average) mcm	Q(std) mcm	K(2)	K(10)	K(20)	K(50)	K(100)	Q(2) mcm	Q(10) mcm	Q(50) mcm	Q(100) mcm
Observed data	75.0	40.0	-0.164	1.300	1.870	2.590	3.140	68.44	127	149.8	178.6

Wadi Habawnah

Data Type	Annualy Q(average) mcm	Q(std) mcm	K(2)	K(10)	K(20)	K(50)	K(100)	Q(2) mcm	Q(10) mcm	Q(50) mcm	Q(100) mcm
Ratio data	10.0	7.0	-0.164	1.300	1.870	2.590	3.140	8.852	19.1	23.09	28.13
Regression data	15.0	13.0	-0.164	1.300	1.870	2.590	3.140	12.868	31.9	39.31	48.67

From Table 3.34a, $K_{50} = 1.945$ and $K_{100} = 2.178$

using equation 3.18

$$\log Q_{50} = 0.842 + (1.945 \times 0.375) = 1.571$$

$$Q_{50} = \text{antilog}1.571 = 37.24 \text{ mcm}$$

$$\log Q_{100} = 0.842 + (2.178 \times 0.375) = 1.658$$

$$Q_{100} = \text{antilog}1.658 = 45.5 \text{ mcm}$$

The flood volumes of both wadis were estimated for different return periods (see Table 3.35).

The average flood discharge of different return periods are calculated for the previous three methods (see Table 3.37). Table 3.38 illustrates the flood volumes estimation for Wadi Baysh and Wadi Habawnah for different return periods as two different ratios, $Q100_{/Q2}$ and $Q10_{/Q2}$, as sampled data for three theoretical probability distribution functions.

It can be seen that the presented frequency ratios show: that the characteristics of runoff rate show that Wadi Baysh is likely to produce more water than Wadi Habawnah.

3.5 Summary and Conclusion

The relationship between rainfall and elevation in the study area was determined. The isohyet method and regression-correlation were used to analyse the rainfall distribution and to study the effect of elevation and topography. The results can be summarised as follows:

The study area does not have uniform rainfall due to several combined topographic and climatic factors. In Wadi Baysh, the rainfall varies from one season to another while in Wadi Habawnah it is limited to winter and spring.

In the winter season, most rain falls along the northern part of the mountainous area because this part of the area is affected by the north-westerly air flow. In the spring, the rainfall falls mainly in the high land while the low land in the eastern part of Wadi Habawnah and along the Red Sea receives little rain as it is influenced by south-easterly monsoon air flow.

From Table 3.34a, $K_{50} = 1.945$ and $K_{100} = 2.178$

using equation 3.18

$$\log Q_{50} = 0.842 + (1.945 \times 0.375) = 1.571$$

$$Q_{50} = \text{antilog}1.571 = 37.24 \text{ mcm}$$

$$\log Q_{100} = 0.842 + (2.178 \times 0.375) = 1.658$$

$$Q_{100} = \text{antilog}1.658 = 45.5 \text{ mcm}$$

The flood volumes of both wadis were estimated for different return periods (see Table 3.35).

The average flood discharge of different return periods are calculated for the previous three methods (see Table 3.37). Table 3.38 illustrates the flood volumes estimation for Wadi Baysh and Wadi Habawnah for different return periods as two different ratios, $Q100_{/Q2}$ and $Q10_{/Q2}$, as sampled data for three theoretical probability distribution functions.

It can be seen that the presented frequency ratios show:

1 - The probability distributions of floods in both wadis are similar.

2 - The characteristics of runoff rate show that Wadi Baysh is likely to produce more water than Wadi Habawnah.

3.5 Summary and Conclusion

The relationship between rainfall and elevation in the study area was determined. The isohyet method and regression-correlation were used to analyse the rainfall distribution and to study the effect of elevation and topography. The results can be summarised as follows:

The study area does not have uniform rainfall due to several combined topographic and climatic factors. In Wadi Baysh, the rainfall varies from one season to another while in Wadi Habawnah it is limited to winter and spring.

In the winter season, most rain falls along the northern part of the mountainous area because this part of the area is affected by the north-westerly air flow. In the spring, the rainfall falls mainly in the high land while the low land in the eastern part of Wadi Habawnah and along the Red Sea receives little rain as it is influenced by south-easterly

Table 3.37 Determining the average of the flood volume magnitude (mcm) of the N-year event for both wadis using the regression, Log-Pearson Type III and Gumbel's distribution methods

Wadi Baysh				
Monthly flood ,Qr(average)				
Return interval Year (Tr)	2	10	50	100
Pecent Chance (P%)	50	10	5	1
Qr (mcm)	15	36	57	66
Qr (mcm)*	16	34	40	49
Qr (mcm)**	15	28	56	70
AVERAGE	15	33	51	62
Annualy flood ,Qr(average)				
Return interval Year (Tr)	2	10	50	100
Pecent Chance (P%)	50	10	5	1
Qr (mcm)	63	130	197	226
Qr (mcm)*	68	127	150	179
Qr (mcm)**	64	129	165	192
AVERAGE	50	81	113	139
Wadi Habawnah				
maximum monthly , Qr(avcrage)				
Return interval Year (Tr)	2	10	50	100
Pecent Chance (P%)	50	10	5	1
Qr (mcm) (ratio facter data)	4	11	18	21
Qr (mcm)(regression data)	6	18	31	36
Qr (mcm)* (ratio facter data)	4	10	12	15
Qr (mcm)*(regression data)	6	16	20	25
Qr (mcm)** (ratio facter data)	4	13	19	24
Qr (mcm)**(regression data)	4	63	79	85
AVERAGE	5	22	30	34
Annualy monthly , Qr(average)				
Return interval Year (Tr)	2	10	50	100
Pecent Chance (P%)	50	10	5	1
Qr (mcm) (ratio facter data)	7	20	32	38
Qr (mcm)(regression data)	11	33	55	65
Qr (mcm)* (ratio facter data)	9	19	23	28
Qr (mcm)*(regression data)	13	32	39	49
Qr (mcm)** (ratio facter data)	7	21	30	37
Qr (mcm)**(regression data)	9	42	66	86
AVERAGE	9	28	41	50

* CALCULATED USING REGRESSION METHODS

** CALCULATED USING PEARSON TYPE III DISTRIBUTION METHODS

***CALCULATED USING GUMBEL'S DISTRIBUTION METHOD

Table 3.38 Illustration of different frequency analysis ratio of flood return period for both wadis

Wadi Baysh							
Monthly flood ,Q (average)			Q10/Q2		Q50/Q2		Q100/Q2
Return interval Year (T)	2	10		50		100	
Percent Chance (P%)	50	10		5		1	
Q (mcm)*	15	36	2	57	4	66	4
Q (mcm)**	16	34	2	40	3	49	3
Q (mcm)***	15	28	2	56	4	70	5
AVERAGE	15	33	2	51	3	62	4
Annualy flood ,Qr(average)			Q10/Q2		Q50/Q2		Q100/Q2
Return interval Year (T)	2	10		50		100	
Percent Chance (P%)	50	10		5		1	
Q (mcm)*	63	130	2	197	3	226	4
Q (mcm)**	68	127	2	150	2	179	3
Q (mcm)***	64	129	2	165	3	192	3
AVERAGE	50	81	2	113	2	139	3
Wadi Habawnah							
maximum monthly , Qr(average)			Q10/Q2		Q50/Q2		Q100/Q2
Return interval Year (T)	2	10		50		100	
Pecent Chance (P%)	50	10		5		1	
Q (mcm)* (ratio facter data)	4	11	3	18	4	21	5
Q (mcm)*(regression data)	6	18	3	31	5	36	6
Q (mcm)** (ratio facter data)	4	10	2	12	3	15	4
Q (mcm)**(regression data)	6	16	3	20	3	25	4
Q (mcm)*** (ratio facter data)	4	13	3	19	5	24	6
Q (mcm)***(regression data)	4	63	16	79	20	85	22
AVERAGE	5	22	5	30	6	34	7
Annualy monthly , Qr(average)			Q10/Q2		Q50/Q2		Q100/Q2
Return interval Year (T)	2	10		50		100	
Pecent Chance (P%)	50	10		5		1	
Q (mcm)* (ratio facter data)	7	20	3	32	4	38	5
Q (mcm)*(regression data)	11	33	3	55	5	65	6
Q (mcm)** (ratio facter data)	9	19	2	23	3	28	3
Q (mcm)**(regression data)	13	32	2	39	3	49	4
Q (mcm)*** (ratio facter data)	7	21	3	30	4	37	5
Q (mcm)***(regression data)	9	42	5	66	7	86	9
AVERAGE	9	28	3	41	4	50	5

* data interpreted using curve fitting

** data interpreted using Gumbel's distribution

*** data interpreted using Type III distrebution

During the summer the Wadi Baysh foothills receive more precipitation while the eastern slopes receive no rain at all because the southwest monsoon rain falls along the western slopes of the mountains. The N-S orientation of the Asir Mountains creates a barrier, with the eastern slopes being in a rain shadow.

During autumn, and especially in the early autumn, the foothills of Wadi Baysh receive more rain than the higher elevations because the foothills are exposed to the south-westerly monsoon. In Wadi Habawnah (eastern slope) no significant rain occurs.

The mid-south elevation of 860m (a.m.s.l) of Wadi Baysh receives more rainfall than at higher elevations where the annual rainfall is 662mm with a mean of 400mm, because the mountain orientation is nearly perpendicular to the southwest flow which produces orographic rainfall. The resulting rainfall regime is characterised by high intensity and short duration events, and by variability.

The mean annual rainfall correlates with elevation in both wadis. There are zones of varying rainfall intensity. In Wadi Baysh, the correlation coefficient (r) of rainfall to elevation on the mountain side is 0.78 and along the Red Sea up to the foothills, the correlation coefficient has similar value of 0.77. In Wadi Habawnah, the correlation between mean annual rainfall and elevation shows a similar value ($r = 0.7$) to that of Wadi Baysh, which indicates that, in both wadis, elevation exhibits the same influence on rainfall distribution.

The latitude and longitude of the rainfall station clearly shows the influence of the elevation and the air mass/weather system (south-west monsoon and north-westerly flow) on the rainfall distribution of the area. However, in the mid-south, such a relationship is not clear.

The hydrological potential evaluations of the Wadi Baysh and Wadi Habawnah runoff records performed are based on 16 years and 3 years of observation. The major shortcomings are where no discharge measurements exist for the small tributary wadis in Wadi Baysh and Wadi Habawnah and where both records of rainfall and runoff have only a short record. The worst limitation is the shortness of the observation periods. However, the author has used the ratio factor and regression analysis to extend the runoff record of

Wadi Habawnah based on the Wadi Baysh runoff record since the problem could not be overcome by extending the record length of rainfall through the regression method for following reasons:

1- A long record of rainfall for Wadi Baysh is available as an average value for the whole period, for e.g. 1963-1985. However, there is not a yearly record available.

2- The runoff record of Wadi Baysh is from 1970 -1985 as monthly and annual data while the Wadi Habawnah record of runoff is from 1984 - 1987 as monthly and annual data.

The flood volume of Wadi Baysh shows a mean of 75 mcm while Wadi Habawnah it is 14 mcm per year.

The flood frequency of gauged sites was determined for both wadis. The mean coefficient of variation and coefficient of skewness were estimated from the flood data and calculated for SA-124 and N-407 stations.

The fitted distribution was used to estimate the magnitude of floods of 5, 10, 20, 50 and 100 year return periods. The results are necessarily estimates for both wadis since the historical data from both wadis are short.

There are two common probability distributions which provide the least error of estimate, namely the Pearson Type III and Gumbel distributions. The flood discharges of the return period are determined for each theoretical fitting function. Also, the ratios to the 2 year return period flood volumes are computed in order to illustrate their variation, in dimensionless form, of the regional frequency values for the study zones.

The estimated flood volumes for different return periods of both wadis show similarity using both the Pearson Type III and Gumbel distributions, while linear regression shows high values. The frequency analyses were shown in terms of three different ratios, $Q10/Q2$, $Q50/Q2$ and $Q100/Q2$. The dimensionless values of frequency ratios do not differ much for both probability distributions in Wadi Baysh and Wadi Habawnah. The Pearson Type III distribution shows the largest recurrence flood magnitudes and high dimensionless frequency ratios compared with the Gumbel method, when the synthesised data of the regression interpolation of Wadi Habawnah runoff was used (see Table 3.38). It can be concluded that the Gumbel distribution method will be useful to estimate the flood

discharge for different return periods in both wadis, since the flood magnitudes at different return periods and the dimensionless frequency ratios for this method are similar to the average values of the above methods (see Tables 3.37 and 3.38).

CHAPTER FOUR: WATER CHEMISTRY

4.1 Introduction

The purpose of this study has been to collect pertinent data from both wadis for the interpretation of the hydrochemistry and the definition of the water quality. Of great importance for the hydrochemical part of the study was the acquisition of new data. Lists of existing chemical data were collected and additional water samples were analysed from both wadis.

A comprehensive sampling program was undertaken in order to take account of the diversity in physiography, geology, hydrology and water chemistry in the different parts of the wadis. Both wadis were subdivided into upper, middle and lower parts on the basis of the hydrochemical analyses. The definition of aquifers with hydrochemical similarity and contrast was essential, in the context of aquifer characterisation, for the Arabian Shield.

Water samples were collected from 62 hand dug wells in Wadi Habawnah and from 20 in Wadi Baysh (Figures 4.1 and 4.2). The samples were analysed at the King Abdulaziz Earth Science Laboratory in Jeddah, Saudi Arabia. However, the temperature, pH and EC were determined in the field immediately after collection.

The computer programme WATEQF (Ball *et al.*, 1980) was used to calculate the equilibrium relations of the aqueous and mineral phases. Major ion data were analysed by linear regression and cluster multivariance analysis (Cluster and PCA) to determine the statistical significance of any correlation between variables.

The purposes of the hydrochemistry chapter is to:

1- Examine the concentration of chemicals in the groundwaters.

2- Determine the probable sources of dissolved substances

3- Quantify geochemical processes that control groundwater chemistry such as water reaction with aquifer strata, evaporation, ion exchange and redox reaction

4- Provide information that can be transferred from these wadis to the other wadis, as yet underdeveloped, in the Arabian Shield.

5- Evaluate the groundwater quality of Wadi Habawnah and Wadi Baysh for use as drinking water and for irrigation.

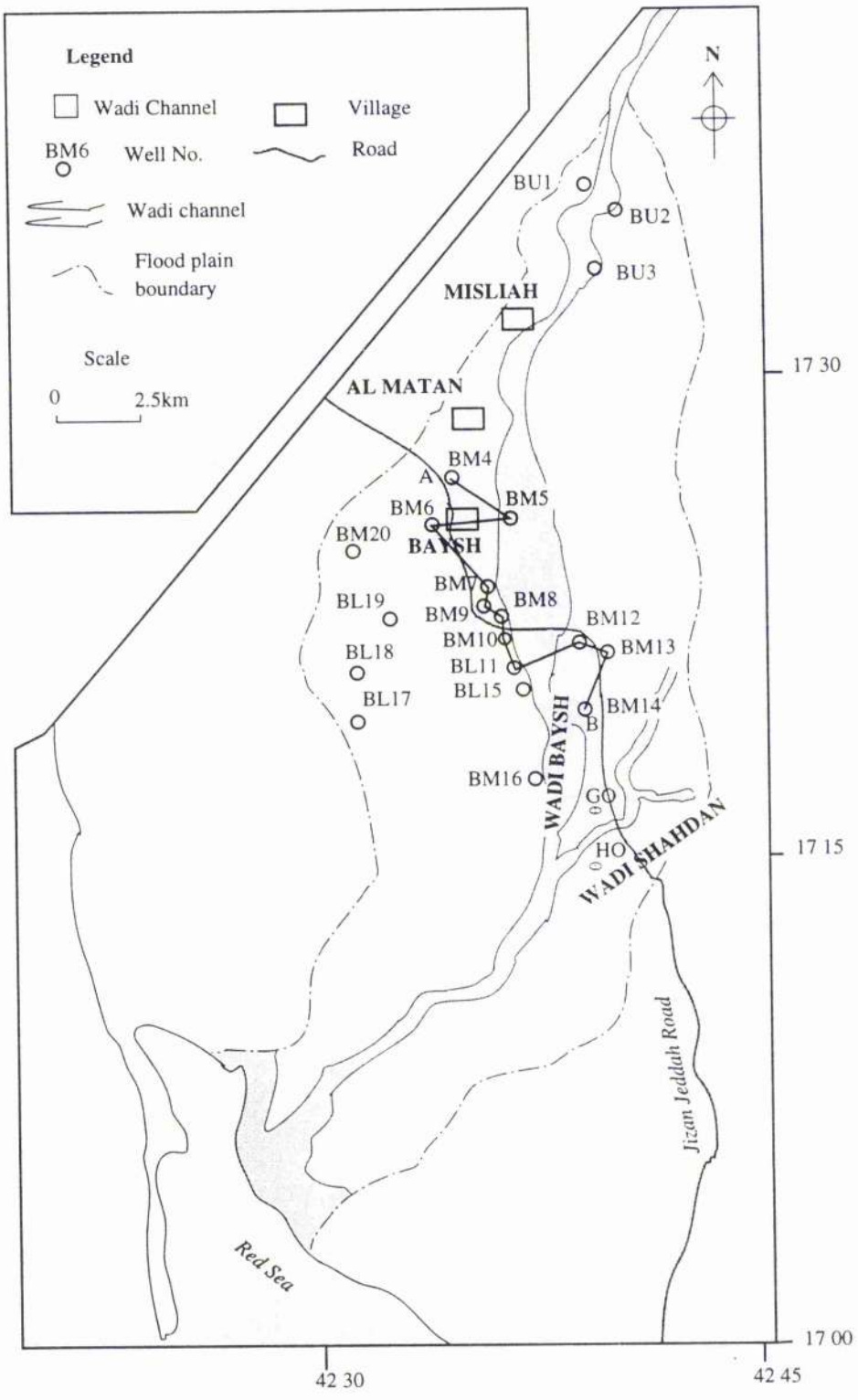

Figure 4.1 Wadi Baysh well locations.

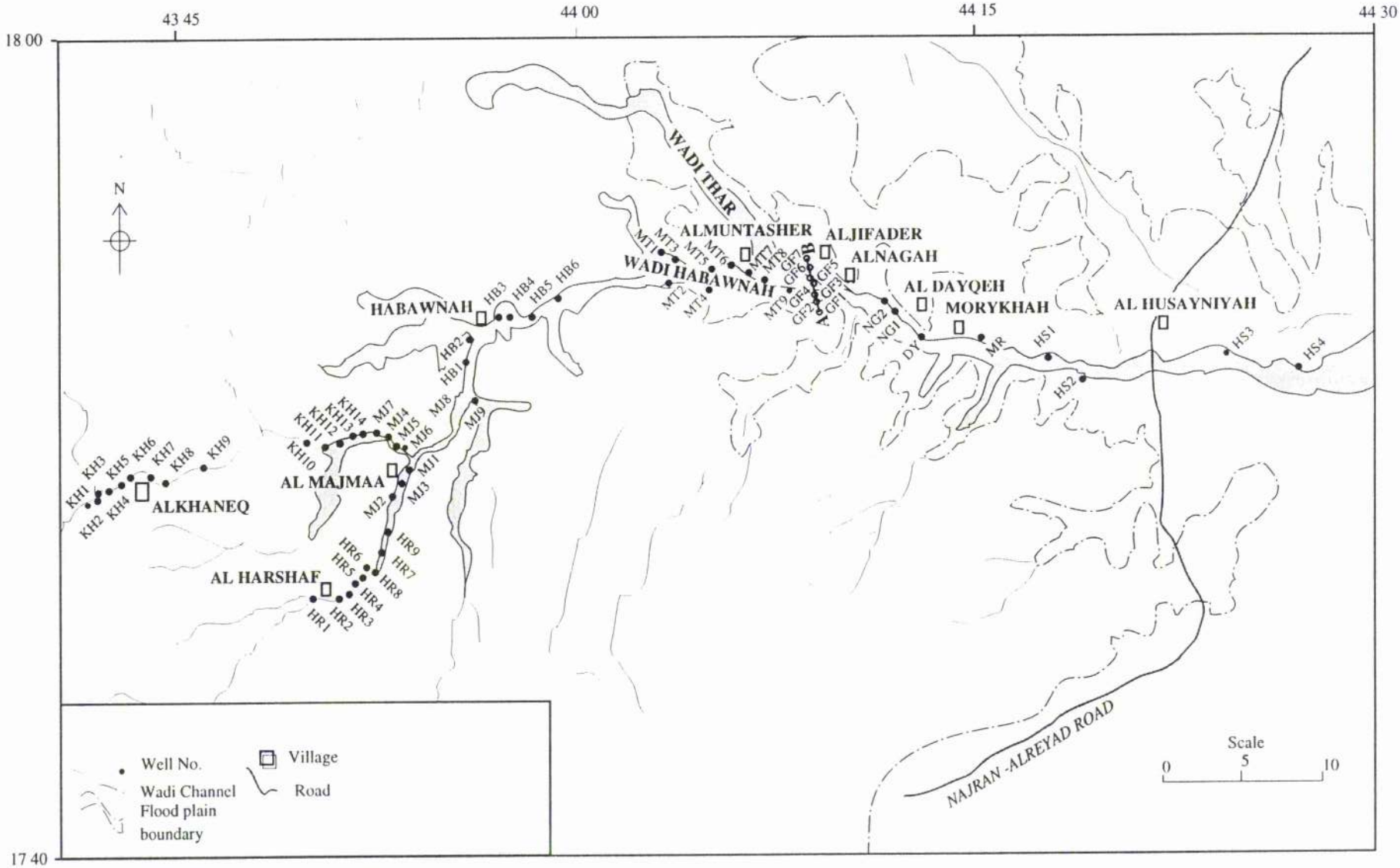

Figure 4.2 Wadi Habawnah well locations.

4.2 Previous Study

Water quality studies, dealing primarily with dissolved solids at different locations within a regional context, have been carried out at several sites in the Arabian Shield. MAWR, through contractors such as Italconsult and Maclaren, evaluated the quality of water along the main course of the south-west Arabian Shield during regional studies in 1963 and 1978. The author will refer to their data as providing a 'previous record', which may help to illustrate changes in the water quality.

4.3 Field Collection of Groundwater Samples

After careful evaluation of the distribution of the MAWR sampling data it became evident that both Wadi Habawnah and Wadi Baysh had a serious shortage of groundwater quality information. In Wadi Habawnah there were chemical analyses for only 17 hand dug wells, for which no sampling location map is available. There are records of the analysis of four samples of surface (flood) waters. However, in Wadi Baysh six water samples had been analysed, although the recorded data were an average value of all six samples. Such data are quite inadequate for the interpretation and evaluation of the hydrochemical behaviour of groundwater in either wadi.

To overcome this inadequacy, field visits were made during December 1989 and January 1990 to collect groundwater samples from pre-existing wells which have pumps. A total of 20 samples were collected from 20 hand dug wells located in the upper, middle and lower part of the Wadi Baysh (see Figures 4.1 and 4.2), while 62 samples were collected from 62 hand dug wells of the Wadi Habawnah and its major tributaries. Usually the only means of evaluating the quality of water tapped by a well is by an analysis of a pumped sample, therefore all samples are pumped well samples collected from the rising main of the pump after it had been running for some time. This was in order to minimise disturbance and contamination. Most of the wells located in Habawnah and Baysh were near or in the wadi channels or on the margin of the surrounding rocks. They were all shallow (less than 70m in depth). In the upper part of the wadis, where the water table is low, the permissible pumping periods are less than one hour whereas in the lower section of the wadis the water table is more stable and the pumping period is six hours on average.

None of the samples were filtered. All water samples were preserved in airtight polypropylene plastic containers and stored at a low temperature before being transferred to the University laboratory for analysis.

The measurements in the field at the well head were:

1- Electrical conductivity (EC).

2- pH - using a glass electrode meter which was calibrated at the beginning of each sampling day.

3- The total depth of the well, the diameter of the casing, the water level and the water temperature.

4.4 Chemical Analysis of Groundwater Samples

The groundwater samples were analysed to determine the concentrations of the major ions (Ca^{2+}, Mg^{2+}, Na^{+}, K^{+}, CO_3^{2-}, HCO_3^{-}, SO_4^{2-} and Cl^{-}) and some trace elements (Fe^{2+}, Mn^{2+}, Ni^{2+}, Pb^{2+} and Al^{3+}).

The methods used in the water analyses are well standardised (Suess, 1982). The following is a list of the constituents with the method used to analyse them and the lower limit of detection (LLD) for each method:

1 - Atomic Absorption for Ca^{2+} and Mg^{2+} with (LLD 0.1mg/l)

2 - Flame photometric method for Na^{+} and K^{+} (LLD 0.1mg/l).

3 - EDTA titrimetric method for $CaCO_3$ (Hardness) (LLD 0.1mg/l)

4 - Titrimetry for CO_3^{2-} and HCO_3^{-} (LLD 1mg/l)

5 - Specific electrode for Cl^{-} (LLD 0.5mg/l)

6 - Nephelometric method for SO_4^{2-} (LLD 0.5mg/l)

7 - Direct current plasma for trace elements (LLD 0.1 ppb)

8 - Gravimetric method (105 C°) for TDS (LLD 1mg/l)

The chemical analyses of 82 groundwater samples have been considered in the present study (Tables 4.1 and 4.2).

4.5 Quality of Analytical Data

The criteria of ionic-balance and the comparison of total dissolved solids (TDS)

Table 4.1 Chemical composition of groundwater in Wadi Baysh

Chemical composition of groundwater in the middle part of Wadi Baysh

Sample	Na^+	Na^+	K^+	K^+	Ca^{2+}	Ca^{2+}	Mg^{2+}	Mg^{2+}	SO_4^{2-}	SO_4^{2-}	Cl^-	Cl^-	HCO_3^-	HCO_3^-	CO_3^{2-}	CO_3^{2-}	TDS	TDS	Error**
NO	ppm	meq/l	ppm	meq/l	ppm	meq/l	ppm	meq/l	ppm	meq/l	ppm	meq/l	ppm	meq/l	ppm	meq/l	meq/l	ppm	%
BU1	32.0	1.4	5.9	0.2	52.1	2.6	25.3	2.1	102.3	2.1	69.8	2.0	112.3	1.8	0.0	0.0	12.2	342.4	2.4
BU2	33.1	1.4	7.0	0.2	54.9	2.7	27.5	2.3	115.3	2.4	69.8	2.0	151.9	2.5	0.0	0.0	13.5	382.1	-1.9
BU3	39.1	1.7	10.2	0.3	87.0	4.3	36.0	3.0	155.6	3.2	69.8	2.0	106.2	1.7	18.0	0.6	16.8	467.7	10.1

Chemical composition of groundwater in the middle part of Wadi Baysh

Sample	Na^+	Na^+	K^+	K^+	Ca^{2+}	Ca^{2+}	Mg^{2+}	Mg^{2+}	SO_4^{2-}	SO_4^{2-}	Cl^-	Cl^-	HCO_3^-	HCO_3^-	CO_3^{2-}	CO_3^{2-}	TDS	TDS	Error**
NO	ppm	meq/l	ppm	meq/l	ppm	meq/l	ppm	meq/l	ppm	meq/l	ppm	meq/l	ppm	meq/l	ppm	meq/l	meq/l	ppm	%
BM4	33.1	1.4	10.2	0.3	156.3	7.8	28.7	2.4	147.5	3.1	176.9	5.0	151.9	2.5	0.0	0.0	22.4	627.1	5.8
BM5	43.9	1.9	3.1	0.1	60.1	3.0	40.6	3.3	162.3	3.4	69.8	2.0	106.2	1.7	30.0	1.0	16.4	462.0	1.5
BM6	360.1	15.7	14.1	0.4	300.6	15.0	132.5	10.9	1487.5	31.0	282.9	8.0	122.0	2.0	30.0	1.0	83.9	2667.5	0.i
BM7	120.0	5.2	1.6	0.0	91.0	4.5	41.3	3.4	296.3	6.2	106.0	3.0	137.3	2.3	0.0	0.0	24.6	723.5	7.3
BM8	66.2	2.9	2.3	0.1	125.5	6.3	30.1	2.5	299.7	6.2	106.0	3.0	90.9	1.5	0.0	0.0	22.4	674.4	4.3
BM9	60.0	2.6	2.3	0.1	207.6	10.4	57.6	4.7	206.5	4.3	319.0	9.0	122.0	2.0	0.0	0.0	33.1	913.0	7.5
BM10	68.1	3.0	5.1	0.1	53.3	2.7	32.8	2.7	158.0	3.3	69.8	2.0	122.0	2.0	0.0	0.0	15.7	446.9	7.6
BM11	43.0	1.9	5.5	0.1	97.4	4.9	28.6	2.4	122.0	2.5	66.6	1.9	253.8	4.2	0.0	0.0	17.8	487.4	3.6
BM12	43.9	1.9	8.2	0.2	123.0	6.1	29.2	2.4	162.3	3.4	88.6	2.5	269.1	4.4	0.0	0.0	21.0	587.2	1.8
BM13	45.1	2.0	8.6	0.2	79.0	3.9	34.0	2.8	121.0	2.5	66.6	1.9	305.7	5.0	0.0	0.0	18.3	504.1	-2.7
BM14	52.0	2.3	12.9	0.3	192.0	9.6	39.6	3.3	213.3	4.4	124.1	3.5	410.6	6.7	0.0	0.0	30.1	835.0	2.5

Chemical composition of groundwater in the lower part of Wadi Baysh

Sample	Na^+	Na^+	K^+	K^+	Ca^{2+}	Ca^{2+}	Mg^{2+}	Mg^{2+}	SO_4^{2-}	SO_4^{2-}	Cl^-	Cl^-	HCO_3^-	HCO_3^-	CO_3^{2-}	CO_3^{2-}	TDS	TDS	Error**
NO	ppm	meq/l	ppm	meq/l	ppm	meq/l	ppm	meq/l	ppm	meq/l	ppm	meq/l	ppm	meq/l	ppm	meq/l	meq/l	ppm	%
BL15	200.0	8.7	7.0	0.2	247.3	12.3	90.7	7.5	772.8	16.1	319.0	9.0	244.1	4.0	0.0	0.0	57.8	1756.5	-0.7
BL16	165.1	7.2	5.1	0.1	264.5	13.2	96.6	8.0	755.0	15.7	343.1	9.7	233.1	3.8	0.0	0.0	57.7	1743.7	-1.3
BL17	530.0	23.1	5.5	0.1	413.4	20.6	161.0	13.2	0.0	0.0	2197.1	62.0	76.3	1.3	0.0	0.0	120.3	3344.3	-5.1
BL18	719.9	31.3	7.4	0.2	408.8	20.4	159.9	13.2	0.0	0.0	2355.5	66.5	32.3	0.5	0.0	0.0	132.0	3667.4	-1.5
BL19	310.0	13.5	10.2	0.3	344.7	17.2	97.3	8.0	0.0	0.0	1382.8	39.0	24.4	0.4	0.0	0.0	78.4	2156.9	-0.6
BL20	200.0	8.7	1.2	0.0	352.7	17.6	97.3	8.0	2.4	0.1	1235.4	34.9	61.0	1.0	0.0	0.0	70.2	1918.9	-2.2

**Ionic balance error

Table 4.2 Chemical composition of groundwater in Wadi Habawnah

Chemical composition of groundwater in Al KHANEQ

Sample No.	Na^+ meq/l	Na^+ ppm/l	K^+ meq/l	K^+ ppm/l	Ca^{2+} meq/l	Ca^{2+} ppm/l	Mg^{2+} meq/l	Mg^{2+} ppm/l	SO_4^{2-} meq/l	SO_4^{2-} ppm/l	Cl^- meq/l	Cl^- ppm/l	HCO_3^- meq/l	HCO_3^- ppm/l	TDS meq/l	TDS ppm	Error* %
KH1	2.5	57.9	0.2	6.6	3.2	64.1	3.1	37.2	4.8	231.5	3.0	106.0	2.5	151.9	18.0	579.4	-7.0
KH2	4.5	103.0	0.2	9.0	10.1	203.2	6.5	78.5	11.1	532.7	8.0	282.9	2.5	151.9	41.6	1285.2	-0.6
KH3	10.9	249.9	0.4	14.9	17.3	347.5	13.6	165.3	25.5	1222.4	14.0	495.9	2.5	151.9	82.9	2571.9	0.3
KH4	4.7	108.1	0.2	7.8	10.5	209.6	7.5	90.9	13.0	626.3	10.0	354.1	2.5	151.9	47.1	1472.9	-5.5
KH5	5.6	128.1	0.2	5.9	11.4	228.5	7.9	95.6	12.6	605.2	10.0	354.1	2.0	122.0	48.6	1478.3	0.8
KH6	13.1	300.1	0.3	10.2	24.7	494.2	10.9	133.0	20.3	975.5	24.9	881.6	2.5	151.9	95.3	2870.5	1.3
KH7	16.5	380.1	0.3	11.0	26.0	521.0	18.0	218.9	28.9	1386.2	33.0	1169.1	1.8	112.3	123.6	3742.4	-2.3
KH8	7.8	180.0	0.2	7.8	9.3	187.2	7.4	90.2	12.0	577.8	10.0	354.1	2.5	151.9	48.1	1473.1	0.6
KH9	9.6	220.1	0.3	11.0	16.1	323.4	10.1	122.3	15.8	758.4	18.0	638.1	2.0	122.0	70.8	2134.2	0.4
KH10	4.8	109.9	0.2	9.0	8.8	175.6	5.3	64.9	10.3	496.2	8.0	282.9	1.5	90.9	38.2	1183.9	-1.8
KH11	2.8	65.1	0.2	7.8	2.9	58.1	2.2	27.2	3.4	164.7	3.0	106.0	2.5	151.9	15.8	504.9	-4.3
KH12	3.5	80.0	0.2	7.8	3.7	73.3	2.6	31.6	4.6	220.0	4.0	141.1	1.5	90.9	19.2	599.3	-0.6
KH13	3.9	89.9	0.2	7.8	5.1	103.0	3.6	43.8	7.4	357.3	4.0	141.1	2.0	122.0	25.3	803.9	-2.1
KH14	9.6	220.1	0.2	7.0	17.6	352.7	10.7	129.6	23.6	1132.6	11.0	388.9	1.5	90.9	73.3	2276.3	2.6

Chemical composition of groundwater in Al-JIFA

Sample No.	Na^+ meq/l	Na^+ ppm/l	K^+ meq/l	K^+ ppm/l	Ca^{2+} meq/l	Ca^{2+} ppm/l	Mg^{2+} meq/l	Mg^{2+} ppm/l	SO_4^{2-} meq/l	SO_4^{2-} ppm/l	Cl^- meq/l	Cl^- ppm/l	HCO_3^- meq/l	HCO_3^- ppm/l	TDS meq/l	TDS ppm	Error* %
GF-1	4.7	108.1	0.1	5.1	6.3	125.5	3.4	41.3	6.4	306.9	6.1	214.5	2.5	151.9	28.2	877.3	-1.5
GF2	4.0	92.9	0.1	5.1	6.3	125.5	3.0	36.5	7.0	335.7	5.0	176.9	2.0	122.0	26.4	833.5	-2.0
GF3	7.4	169.9	0.1	3.1	8.9	177.6	4.1	50.3	11.2	536.5	7.0	248.1	2.0	122.0	39.6	1246.6	0.7
GF4	7.4	169.9	0.1	2.0	6.3	127.1	3.3	39.6	8.2	391.9	6.0	212.0	2.0	122.0	32.2	1003.5	2.7
GF5	4.5	103.0	0.1	3.9	5.6	112.2	4.4	53.5	6.6	315.1	6.0	212.0	2.0	122.0	28.1	860.7	0.1
GF6	7.8	180.0	0.1	4.7	25.0	501.0	12.0	145.9	21.0	1009.1	20.0	709.0	2.5	151.9	87.2	2625.7	1.6
GF7	4.9	112.0	0.1	3.5	4.7	94.2	3.0	36.0	4.3	205.1	5.0	176.9	3.5	212.9	23.6	734.1	-0.5

Continued on next page

Table 4.2 continued

Chemical composition of groundwater in AL-HARSHAF

Sample No.	Na^+ meq/l	Na^+ ppm/l	K^+ meq/l	K^+ ppm/l	Ca^{2+} meq/l	Ca^{2+} ppm/l	Mg^{2+} meq/l	Mg^{2+} ppm/l	SO_4^{2-} meq/l	SO_4^{2-} ppm/l	Cl^- meq/l	Cl^- ppm/l	HCO_3^- meq/l	HCO_3^- ppm/l	TDS meq/l	TDS ppm	Error* %
HR1	10.0	229.9	0.4	14.1	10.0	200.4	6.8	82.7	15.8	759.8	10.0	354.1	2.5	151.9	54.2	1717.0	-2.1
HR2	10.4	240.1	0.3	12.9	10.5	211.2	7.3	88.3	16.2	778.1	10.0	354.1	3.0	183.0	56.3	1776.2	-1.1
HR3	9.1	209.9	0.3	12.9	11.7	235.3	7.3	88.3	15.3	736.8	11.0	388.9	2.0	122.0	55.8	1733.0	0.3
HR4	7.4	169.9	0.2	9.0	10.0	200.4	4.3	51.8	11.9	571.1	8.0	282.9	1.5	90.9	42.5	1330.5	1.2
HR5	23.5	539.9	0.2	6.3	20.3	406.0	11.9	144.4	35.6	1708.0	21.0	744.1	2.0	122.0	113.3	3609.6	-2.4
HR6	5.7	129.9	0.3	11.0	8.9	179.2	4.6	55.7	11.6	554.8	6.9	245.7	1.5	90.9	38.7	1221.6	-1.3
HR7	7.8	180.0	0.3	11.0	8.7	175.2	5.1	61.5	10.5	504.8	8.0	282.9	2.0	122.0	41.4	1276.3	3.3
HR8	9.6	220.1	0.3	11.0	15.4	308.6	7.0	85.6	17.8	856.9	11.0	388.9	2.0	122.0	62.1	1932.0	2.3
HR9	9.6	220.1	0.3	12.9	12.2	244.5	7.5	90.7	17.1	822.3	11.0	388.9	2.5	151.9	58.9	1855.2	-1.7

Chemical composition of groundwater in AL-MAJMAA

Sample No.	Na^+ meq/l	Na^+ ppm/l	K^+ meq/l	K^+ ppm/l	Ca^{2+} meq/l	Ca^{2+} ppm/l	Mg^{2+} meq/l	Mg^{2+} ppm/l	SO_4^{2-} meq/l	SO_4^{2-} ppm/l	Cl^- meq/l	Cl^- ppm/l	HCO_3^- meq/l	HCO_3^- ppm/l	TDS meq/l	TDS ppm	Error* %
MJ1	3.6	82.5	0.1	5.1	6.1	123.0	3.3	39.6	6.7	322.8	5.0	176.9	1.5	90.9	25.6	795.4	-0.3
MJ2	5.0	115.0	0.1	2.3	9.4	188.4	5.1	62.5	9.6	462.1	8.0	282.9	2.0	122.0	38.2	1174.1	0.0
MJ3	4.4	100.0	0.1	3.5	5.7	113.4	3.6	43.8	6.6	317.0	6.0	212.0	2.0	122.0	27.3	850.7	-3.1
MJ4	3.9	89.9	0.1	5.5	6.3	125.5	3.9	47.9	6.4	306.9	7.0	248.1	2.0	122.0	28.6	884.8	-3.8
MJ5	5.7	129.9	0.2	8.6	8.3	165.5	5.3	64.9	9.9	476.0	8.7	307.0	2.5	151.9	39.3	1227.9	-3.9
MJ6	6.1	140.0	0.2	6.3	11.3	227.3	7.5	90.7	12.3	590.3	10.0	354.1	2.0	122.0	48.3	1469.7	1.6
MJ7	4.1	95.0	0.2	9.0	5.3	107.0	3.2	39.1	6.2	297.3	5.0	176.9	2.0	122.0	25.1	785.3	-1.0
MJ8	7.8	180.0	0.3	10.2	14.0	280.6	3.5	43.0	13.1	627.3	9.0	319.0	2.0	122.0	48.7	1521.1	3.2
MJ9	3.4	77.9	0.2	5.9	4.1	81.4	2.8	34.0	5.0	239.7	4.0	141.1	2.5	151.9	20.6	655.9	-4.8

Continued on next page

Table 4.2 continued

Chemical composition of groundwater in HABAWNAH

Sample	Na^+	Na^+	K^+	K^+	Ca^{2+}	Ca^{2+}	Mg^{2+}	Mg^{2+}	SO_4^{2-}	SO_4^{2-}	Cl^-	Cl^-	HCO_3^-	HCO_3^-	TDS	TDS	Error*
No.	meq/l	ppm/l	meq/l	ppm/l	meq/l	ppm/l	meq/l	ppm/l	meq/l	ppm/l	meq/l	ppm/l	meq/l	ppm/l	meq/l	ppm	%
HB1	6.3	143.9	0.2	7.0	6.5	131.1	3.9	46.9	8.2	392.9	6.4	227.9	2.5	151.9	32.7	1025.8	-0.7
HB2	4.5	103.0	0.2	7.8	7.2	144.3	3.4	40.8	7.2	347.3	5.0	176.9	2.0	122.0	28.5	881.1	3.5
HB3	7.0	160.0	0.2	8.6	9.3	187.2	4.9	59.1	11.3	542.3	6.0	212.0	2.0	122.0	39.7	1230.2	5.2
HB4	3.5	80.0	0.2	7.8	7.3	145.5	2.8	34.0	5.7	275.7	4.0	141.1	2.0	122.0	24.5	745.2	8.0
HB5	5.6	128.1	0.2	6.6	8.6	172.3	4.7	56.9	8.9	425.6	7.0	248.1	2.0	122.0	35.9	1098.7	3.2
HB6	4.5	103.9	0.1	5.1	6.3	127.1	3.0	36.5	6.3	302.1	7.0	248.1	2.0	122.0	28.3	883.8	-4.4

Chemical composition of groundwater in AL-MUNTASHER

Sample	Na^+	Na^+	K^+	K^+	Ca^{2+}	Ca^{2+}	Mg^{2+}	Mg^{2+}	SO_4^{2-}	SO_4^{2-}	Cl^-	Cl^-	HCO_3^-	HCO_3^-	TDS	TDS	Error*
No.	meq/l	ppm/l	meq/l	ppm/l	meq/l	ppm/l	meq/l	ppm/l	meq/l	ppm/l	meq/l	ppm/l	meq/l	ppm/l	meq/l	ppm	%
MT1	7.0	160.0	0.1	3.9	14.1	281.8	7.7	94.1	10.6	510.6	16.0	567.2	1.5	90.9	56.2	1663.0	1.3
MT2	4.6	105.1	0.1	2.7	5.3	107.0	2.8	34.0	7.0	335.7	5.0	176.9	1.5	90.9	25.5	806.9	-2.7
MT3	4.4	100.0	0.2	5.9	4.6	92.2	2.8	34.0	4.8	232.0	5.6	197.1	1.5	90.9	23.0	706.6	0.1
MT4	5.7	129.9	0.2	7.0	6.7	135.1	4.1	50.1	7.6	365.5	6.0	212.0	2.3	142.8	31.5	971.0	0.5
MT5	3.9	89.9	0.2	5.9	4.6	92.2	2.7	33.3	7.9	378.0	4.0	141.1	4.0	244.1	25.3	862.4	-16.3
MT6	3.5	80.0	0.1	3.1	13.9	277.8	3.6	43.8	5.6	266.6	11.0	388.9	3.0	183.0	39.0	1151.6	3.7
MT7	1.1	24.6	0.1	2.3	7.7	155.1	2.2	26.7	3.6	174.4	5.0	176.9	2.5	151.9	20.9	636.0	-0.3
MT8	4.4	100.0	0.2	7.0	8.3	167.1	3.8	46.2	6.1	292.0	7.0	248.1	3.0	183.0	31.3	952.1	1.8
MT9	3.2	72.9	0.1	5.1	10.6	212.4	3.3	40.6	5.5	264.2	6.3	221.6	4.5	273.9	31.2	953.7	3.0

Chemical composition of groundwater in MORYKHAH

Sample	Na^+	Na^+	K^+	K^+	Ca^{2+}	Ca^{2+}	Mg^{2+}	Mg^{2+}	SO_4^{2-}	SO_4^{2-}	Cl^-	Cl^-	HCO_3^-	HCO_3^-	TDS	TDS	Error*
No.	meq/l	ppm/l	meq/l	ppm/l	meq/l	ppm/l	meq/l	ppm/l	meq/l	ppm/l	meq/l	ppm/l	meq/l	ppm/l	meq/l	ppm	%
MR	4.8	109.9	0.2	7.8	4.6	92.2	3.3	40.6	5.3	253.6	6.0	212.0	2.5	151.9	25.4	792.1	-3.1

Continued on next page

Table 4.2 continued

Chemical composition of groundwater in AL-NGAH

Sample No.	Na^+ meq/l	Na^+ ppm/l	K^+ meq/l	K^+ ppm/l	Ca^{2+} meq/l	Ca^{2+} ppm/l	Mg^{2+} meq/l	Mg^{2+} ppm/l	SO_4^{2-} meq/l	SO_4^{2-} ppm/l	Cl^- meq/l	Cl^- ppm/l	HCO_3^- meq/l	HCO_3^- ppm/l	TDS meq/l	TDS ppm	Error* %
NG-1	4.0	92.9	0.1	5.1	5.1	103.0	3.0	36.2	6.1	293.0	5.0	176.9	2.5	151.9	24.6	783.0	-5.0
NG-2	5.2	120.0	0.1	3.1	7.5	149.5	4.7	56.9	10.3	493.3	6.0	212.0	2.3	142.8	34.9	1106.2	-4.8

Chemical composition of groundwater in AL-DAYQAH

Sample No.	Na^+ meq/l	Na^+ ppm/l	K^+ meq/l	K^+ ppm/l	Ca^{2+} meq/l	Ca^{2+} ppm/l	Mg^{2+} meq/l	Mg^{2+} ppm/l	SO_4^{2-} meq/l	SO_4^{2-} ppm/l	Cl^- meq/l	Cl^- ppm/l	HCO_3^- meq/l	HCO_3^- ppm/l	TDS meq/l	TDS ppm	Error* %
DY	11.7	269.9	0.1	3.9	15.5	309.8	7.5	91.2	17.2	828.0	13.5	477.5	2.0	122.0	66.5	2041.4	3.1

Chemical composition of groundwater in AL-HUSAYNIAH

Sample No.	Na^+ meq/l	Na^+ ppm/l	K^+ meq/l	K^+ ppm/l	Ca^{2+} meq/l	Ca^{2+} ppm/l	Mg^{2+} meq/l	Mg^{2+} ppm/l	SO_4^{2-} meq/l	SO_4^{2-} ppm/l	Cl^- meq/l	Cl^- ppm/l	HCO_3^- meq/l	HCO_3^- ppm/l	TDS meq/l	TDS ppm	Error* %
HS-1	16.1	370.0	0.3	10.2	23.7	475.8	14.8	179.9	26.3	1265.1	24.3	861.4	2.5	153.1	106.8	3238.9	1.6
HS-2	15.7	360.1	0.2	7.8	15.3	307.4	11.7	141.7	21.2	1018.3	13.0	460.1	3.0	183.0	78.5	2387.0	7.1
HS-3	18.7	430.0	0.2	9.0	23.7	474.9	17.2	209.1	30.7	1473.6	23.3	827.0	2.5	151.9	115.1	3499.6	2.9
HS-4	6.8	155.9	0.1	3.1	16.0	320.0	7.9	95.6	10.1	484.1	15.0	531.0	2.0	122.0	56.8	1650.8	6.3

*Ionic errors

were adopted to check the validity of the analytical data. The data which show seriously erroneous values (> 10%) can be excluded from further geochemical interpretations. The following empirical formula was used to calculate the ionic-balance (Tables 4.3 and 4.4) as percentage differences:

$$[(\Sigma \text{ cation} - \Sigma \text{ anion}) / (\Sigma \text{ cation} + \Sigma \text{ anion})] \times 100$$

A total of 89 % of the Wadi Habawnah and 15% of the Wadi Baysh groundwater samples respectively show ionic-balance errors of less than 5 %. The rest of the samples showed errors of less than 10 %. The percentage error of total dissolved solids (TDS) was calculated using the same formula with Σ cations and Σ anions replaced by the TDS obtained by the residue on evaporation and the calculated TDS respectively. The empirical formula has the following form:

(TDS residual - TDS calculated) / (TDS residual + TDS calculated)] x 100

The groundwater samples from both wadis may be classified on the basis of two factors; such as the percentage of ionic and TDS balance errors:

- Good balance (error < 5 %) was obtained for 15% and 27% of the Wadi Baysh and Wadi Habawnah groundwater samples, respectively.

2- An acceptable balance (error < 10 %) was obtained for a further 85 % and 66 % of the Wadi Baysh and Wadi Habawnah groundwater samples, respectively.

3- Although 7 % of the Wadi Habawnah water samples showed high TDS balance errors, both the ionic balance and total dissolved solids balance jointly were in good agreement for most of the analysed groundwater samples.

4.6 Scientific Background

Rainwater is the main resource that can be used to describe a typical evolutionary sequences of the groundwater chemistry. Rainfall is a very dilute solution, predominantly containing NaCl of marine origin and dissolved CO_2. In the soil zone, this water gains more CO_2 as a result of the soil porosity connected with the atmosphere air. Also such waters leach NO_3^-, PO_4^{2-}, and Cl^- together with Na^+ and K^+ originally applied to the soil as a fertilisers.

The chemical reactions in groundwater can be considered mainly as acid-base

Table 4.3 Chemical composition of Wadi Baysh groundwater with error percantage

Chemical composition of groundwater in the upper part of Wadi Baysh

Sample NO	Na^+ meq/l	K^+ meq/l	Ca^{2+} meq/l	Mg^{2+} meq/l	SO_4^{2-} meq/l	Cl^- meq/l	HCO_3^- meq/l	CO_3^{2-} meq/l	Error* %	TDS(calc) mg/l	TDS AT 105 C Over night mg/l	Error** %	EC µmhos/cm	T.Hard. CaCO3 mg/l
BU1	1.4	0.2	2.6	2.1	2.1	2.0	1.8	0.0	2.4	342.4	406.0	8.5	800.0	219.4
BU2	1.4	0.2	2.7	2.3	2.4	2.0	2.5	0.0	-1.9	382.1	470.0	10.3	700.0	230.6
BU3	1.7	0.3	4.3	3.0	3.2	2.0	1.7	0.6	10.1	467.7	570.0	9.9	1000.0	358.9

Chemical composition of groundwater in the middle part of Wadi Baysh

Sample NO	Na^+ meq/l	K^+ meq/l	Ca^{2+} meq/l	Mg^{2+} meq/l	SO_4^{2-} meq/l	Cl^- meq/l	HCO_3^- meq/l	CO_3^{2-} meq/l	Error* %	TDS(calc) mg/l	TDS AT 105 C Over night mg/l	Error** %	EC µmhos/cm	T.Hard. CaCO3 mg/l
BM4	1.4	0.3	7.8	2.4	3.1	5.0	2.5	0.0	5.8	627.1	732.0	7.7	1400.0	636.3
BM5	1.9	0.1	3.0	3.3	3.4	2.0	1.7	1.0	1.5	462.0	536.0	7.4	1000.0	251.5
BM6	3.0	0.1	2.7	2.7	3.3	2.0	2.0	0.0	7.6	446.9	530.0	8.5	3000.0	224.2
BM7	5.2	0.0	4.5	3.4	6.2	3.0	2.3	0.0	7.3	723.5	829.0	6.8	1200.0	374.9
BM8	2.9	0.1	6.3	2.5	6.2	3.0	1.5	0.0	4.3	674.4	817.0	9.6	1300.0	512.8
BM9	2.6	0.1	10.4	4.7	4.3	9.0	2.0	0.0	7.5	913.0	1057.0	7.3	1400.0	841.5
BM10	16.0	0.4	15.6	11.0	31.0	8.0	2.0	1.0	1.2	2667.5	3140.0	8.1	3378.0	1213.0
BM11	1.9	0.1	4.9	2.4	2.5	1.9	4.2	0.0	3.6	487.4	595.0	9.9	922.0	400.6
BM12	1.9	0.2	6.1	2.4	3.4	2.5	4.4	0.0	1.8	587.2	679.0	7.3	1066.0	503.2
BM13	2.0	0.2	3.9	2.8	2.5	1.9	5.0	0.0	-2.7	504.1	589.0	7.8	892.0	326.8
BM14	2.3	0.3	9.6	3.3	4.4	3.5	6.7	0.0	2.5	835.0	987.0	8.3	1543.0	778.9

Chemical composition of groundwater in the lower part of Wadi Baysh

Sample NO	Na^+ meq/l	K^+ meq/l	Ca^{2+} meq/l	Mg^{2+} meq/l	SO_4^{2-} meq/l	Cl^- meq/l	HCO_3^- meq/l	CO_3^{2-} meq/l	Error* %	TDS(calc) mg/l	TDS AT 105 C Over night mg/l	Error** %	EC µmhos/cm	T.Hard. CaCO3 mg/l
BL15	8.7	0.2	12.3	7.5	16.1	9.0	4.0	0.0	-0.7	1756.5	1983.0	6.1	3000.0	1000.0
BL16	8.7	0.0	17.6	8.0	0.1	34.9	1.0	0.0	-2.2	1918.9	2128.0	5.2	2845.0	1422.0
BL17	23.1	0.1	20.6	13.2	0.4	62.0	1.3	0.0	-5.1	3344.3	3893.0	7.6	4340.0	1665.0
BL18	31.3	0.2	20.4	13.2	2.0	66.5	0.5	0.0	-1.5	3667.4	3857.0	2.5	4198.0	1646.0
BL19	13.5	0.3	17.2	8.0	0.1	39.0	0.4	0.0	-0.6	2156.9	2350.0	4.3	3894.0	1390.0
BL20	7.2	0.1	13.2	8.0	15.7	9.7	3.8	0.0	-1.3	1743.7	1965.0	6.0	3100.0	1069.0

*Ionic balance errors

**TDS errors

Table 4.4 Chemical composition of groundwater in Wadi Habawnah with the error percantage

Chemical composition of groundwater in Al-KHANEQ

Sample No.	Na^+ meq/l	K^+ meq/l	Ca++ meq/l	Mg++ meq/l	SO^{--} meq/l	Cl^- meq/l	HCO_3^- meq/l	Error* %	TDS (calc.) mg/l	T.D.S at 105 C Over Night mg/l	Error*** %	EC µmhos/cm	T.HARD. CaCO3 mg/l
KH1	2.5	0.2	3.2	3.1	4.8	3.0	2.5	-7.0	579.4	693.0	8.9	1100.0	269.4
KH2	4.5	0.2	10.1	6.5	11.1	8.0	2.5	-0.6	1285.2	1390.0	3.9	2200.0	825.8
KH3	10.9	0.4	17.3	13.6	25.5	14.0	2.5	0.3	2571.9	2643.0	1.4	3300.0	1390.0
KH4	4.7	0.2	10.5	7.5	13.0	10.0	2.5	-5.5	1472.9	1630.0	5.1	2200.0	838.4
KH5	5.6	0.2	11.4	7.9	12.6	10.0	2.0	0.8	1478.3	1710.0	7.3	2300.0	914.0
KH6	13.1	0.3	24.7	10.9	20.3	24.9	2.5	1.3	2870.5	2947.0	1.3	3100.0	1991.8
KH7	16.5	0.3	26.0	18.0	28.9	33.0	1.8	-2.3	3742.4	3851.0	1.4	4500.0	2099.0
KH8	7.8	0.2	9.3	7.4	12.0	10.0	2.5	0.6	1473.1	1705.0	7.3	2200.0	763.8
KH9	9.6	0.3	16.1	10.1	15.8	18.0	2.0	0.4	2134.2	2217.0	1.9	3000.0	1308.6
KH10	4.8	0.2	8.8	5.3	10.3	8.0	1.5	-1.8	1183.9	1335.0	6.0	2000.0	717.4
KH11	2.8	0.2	2.9	2.2	3.4	3.0	2.5	-4.3	504.9	689.0	15.4	930.0	249.4
KH12	3.5	0.2	3.7	2.6	4.6	4.0	1.5	-0.6	599.3	813.0	15.1	1000.0	310.2
KH13	3.9	0.2	5.1	3.6	7.4	4.0	2.0	-2.1	803.9	894.0	5.3	1400.0	429.0
KH14	9.6	0.2	17.6	10.7	23.6	11.0	1.5	2.6	2276.3	2460.0	3.9	2800.0	1427.8

Chemical composition of groundwater in AL-HARSHAF

Sample No.	Na^+ meq/l	K^+ meq/l	Ca++ meq/l	Mg++ meq/l	SO^{--} meq/l	Cl^- meq/l	HCO_3^- meq/l	Error* %	TDS (calc.) mg/l	T.D.S at 105 C Over Night mg/l	Error*** %	EC µmhos/cm	T.HARD. CaCO3 mg/l
HR1	10.0	0.4	10.0	6.8	15.8	10.0	2.5	-2.1	1717.0	1937.0	6.0	2400.0	812.6
HR2	10.4	0.3	10.5	7.3	16.2	10.0	3.0	-1.1	1776.2	2008.0	6.1	2500.0	855.8
HR3	9.1	0.3	11.7	7.3	15.3	11.0	2.0	0.3	1733.0	1939.0	5.6	2500.0	952.2
HR4	7.4	0.2	10.0	4.3	11.9	8.0	1.5	1.2	1330.5	1516.0	6.5	1900.0	812.6
HR5	23.5	0.2	20.3	11.9	35.6	21.0	2.0	-2.4	3609.6	3850.0	3.2	4400.0	1635.0
HR6	5.7	0.3	8.9	4.6	11.6	6.9	1.5	-1.3	1972.0	2064.0	2.0	430.0	1200.0

Continued on next page

Table 4.4 continued

Chemical composition of groundwater in AL-HARSHAF

Sample No.	Na^+ meq/l	K^+ meq/l	Ca++ meq/l	Mg++ meq/l	SO^{--} meq/l	Cl^- meq/l	HCO_3^- meq/l	Error* %	TDS (calc.) mg/l	T.D.S at 105 C Over Night mg/l	Error*** %	EC µmhos/cm	T.HARD. CaCO3 mg/l
HR7	7.8	0.3	8.7	5.1	10.5	8.0	2.0	3.3	2120.0	2490.0	8.0	510.0	194.0
HR8	9.6	0.3	15.4	7.0	17.8	11.0	2.0	2.3	3155.0	3247.0	1.0	471.0	213.0
HR9	9.6	0.3	12.2	7.5	17.1	11.0	2.5	-1.7	3008.0	3320.0	5.0	520.0	239.0

Chemical composition of groundwater in AL-MAJMAA

Sample No.	Na^+ meq/l	K^+ meq/l	Ca++ meq/l	Mg++ meq/l	SO^{--} meq/l	Cl^- meq/l	HCO_3^- meq/l	Error* %	TDS (calc.) mg/l	T.D.S at 105 C Over Night mg/l	Error*** %	EC µmhos/cm	T.HARD. CaCO3 mg/l
MJ1	3.6	0.1	6.1	3.3	6.7	5.0	1.5	-0.3	940.0	509.0	8.3	1500.0	-0.3
MJ2	5.0	0.1	9.4	5.1	9.6	8.0	2.0	1.0	1174.1	1376.0	7.9	1700.0	770.6
MJ3	4.4	0.1	5.7	3.6	6.6	6.0	2.0	-3.1	850.7	983.0	7.2	1400.0	470.6
MJ4	3.9	0.1	6.3	3.9	6.4	7.0	2.0	-3.8	884.8	1094.0	10.6	1500.0	519.0
MJ5	5.7	0.2	8.3	5.3	9.9	8.7	2.5	-3.9	1227.9	1418.0	7.2	1400.0	679.0
MJ6	6.1	0.2	11.3	7.5	12.3	10.0	2.0	1.6	1469.7	1700.0	7.3	2400.0	926.2
MJ7	4.1	0.2	5.3	3.2	6.2	5.0	2.0	-1.0	785.3	831.0	2.8	1300.0	445.0
MJ8	7.8	0.3	14.0	3.5	13.1	9.0	2.0	3.2	1521.1	1825.0	9.1	2100.0	1139.4
MJ9	3.4	0.2	4.1	2.8	5.0	4.0	2.5	-4.8	655.9	817.0	10.9	1500.0	342.6

Chemical composition of groundwater in HABAWNA

Sample No.	Na^+ meq/l	K^+ meq/l	Ca++ meq/l	Mg++ meq/l	SO^{--} meq/l	Cl^- meq/l	HCO_3^- meq/l	Error* %	TDS (calc.) mg/l	T.D.S at 105 C Over Night mg/l	Error*** %	EC µmhos/cm	T.HARD. CaCO3 mg/l
HB1	6.3	0.2	6.5	3.9	8.2	6.4	2.5	-0.7	1025.8	1243.0	9.6	1600.0	538.4
HB2	4.5	0.2	7.2	3.4	7.2	5.0	2.0	3.5	881.1	1132.0	12.5	2000.0	577.2
HB3	7.0	0.2	9.3	4.9	11.3	6.0	2.0	5.2	1230.2	1429.0	7.5	1300.0	748.8
HB4	3.5	0.2	7.3	2.8	5.7	4.0	2.0	8.0	745.2	865.0	7.4	1400.0	582.0
HB5	5.6	0.2	8.6	4.7	8.9	7.0	2.0	3.2	1098.7	1318.0	9.1	1300.0	689.2
HB6	4.5	0.1	6.3	3.0	6.3	7.0	2.0	-4.4	883.8	1017.0	7.0		508.4

Continued on next page

Table 4.4 continued

Chemical composition of groundwater in AL-MUNTASHER

Sample No.	Na^+ meq/l	K^+ meq/l	Ca^{++} meq/l	Mg^{++} meq/l	SO^{--} meq/l	Cl^- meq/l	HCO_3^- meq/l	Error* %	TDS (calc.) mg/l	T.D.S at 105 C Over Night mg/l	Error*** %	EC µmhos/cm	T.HARD. CaCO3 mg/l
MT1	7.0	0.1	14.1	7.7	10.6	16.0	1.5	1.3	1663.0	1840.0	5.1	1400.0	1145.2
MT2	4.6	0.1	5.3	2.8	7.0	5.0	1.5	-2.7	806.9	946.0	7.9	1600.0	446.0
MT3	4.4	0.2	4.6	2.8	4.8	5.6	1.5	0.1	706.6	811.0	6.9	1300.0	386.8
MT4	5.7	0.2	6.7	4.1	7.6	6.0	2.3	0.5	971.0	1162.0	9.0	1800.0	558.4
MT5	3.9	0.2	4.6	2.7	7.9	4.0	4.0	-16.3	862.4	994.0	7.1	1600.0	386.8
MT6	3.5	0.1	13.9	3.6	5.6	11.0	3.0	3.7	1151.6	1309.0	6.4	1900.0	1129.2
MT7	1.1	0.1	7.7	2.2	3.6	5.0	2.5	-0.3	636.0	732.0	7.0	1100.0	638.4
MT8	4.4	0.2	8.3	3.8	6.1	7.0	3.0	1.8	952.1	1130.0	8.5	1000.0	686.4
MT9	3.2	0.1	10.6	3.3	5.5	6.3	4.5	3.0	953.7	1029.0	3.8	1400.0	867.6

Chemical composition of groundwater in Al-JIFA

Sample No.	Na^+ meq/l	K^+ meq/l	Ca^{++} meq/l	Mg^{++} meq/l	SO^{--} meq/l	Cl^- meq/l	HCO_3^- meq/l	Error* %	TDS (calc.) mg/l	T.D.S at 105 C Over Night mg/l	Error*** %	EC µmhos/cm	T.HARD. CaCO3 mg/l
GF1	4.7	0.1	6.3	3.4	6.4	6.1	2.5	-1.5	877.3	1127.0	12.5	1471.0	523.0
GF2	4.0	0.1	6.3	3.0	7.0	5.0	2.0	-2.0	833.5	970.0	7.6	1371.0	523.0
GF3	7.4	0.1	8.9	4.1	11.2	7.0	2.0	0.7	1246.6	1382.0	5.2	2032.0	731.4
GF4	7.4	0.1	6.3	3.3	8.2	6.0	2.0	2.7	1003.5	1100.0	4.6	1660.0	529.4
GF5	4.5	0.1	5.6	4.4	6.6	6.0	2.0	0.1	860.7	1034.0	9.2	1456.0	469.8
GF6	7.8	0.1	25.0	12.0	21.0	20.0	2.5	1.6	2625.7	2851.0	4.1	4423.0	2025.0
GF7	4.9	0.1	4.7	3.0	4.3	5.0	3.5	-0.5	734.1	928.0	11.7	1269.0	397.8

Chemical composition of groundwater in MORYKHAH

Sample No.	Na^+ meq/l	K^+ meq/l	Ca^{++} meq/l	Mg^{++} meq/l	SO^{--} meq/l	Cl^- meq/l	HCO_3^- meq/l	Error* %	TDS (calc.) mg/l	T.D.S at 105 C Over Night mg/l	Error*** %	EC µmhos/cm	T.HARD. CaCO3 mg/l
MR	4.8	0.2	4.6	3.3	5.3	6.0	2.5	-3.1	792.1	893.0	6.0	1300.0	392.8

Continued on next page

Table 4.4 continued

Chemical composition of groundwater in ALHARSHAF

Sample No.	Na^+ meq/l	K^+ meq/l	Ca^{2+} meq/l	Mg^{2+} meq/l	SO^{2-} meq/l	Cl^- meq/l	HCO_3^- meq/l	Error* %	TDS (calc.) mg/l	T.D.S at 105 C Over Night mg/l	Error*** %	EC µmhos/cm	T.HARD. CaCO3 mg/l
No.	meq/l	meq/l	meq/l	meq/l	meq/l	meq/l	meq/l	%	mg/l	Over Night mg/l	%	µmhos/cm	CaCO3 mg/l
NG-1	4.0	0.1	5.1	3.0	6.1	5.0	2.5	-5.0	783.0	917.0	7.9	1400.0	431.0
NG-2	5.2	0.1	7.5	4.7	10.3	6.0	2.3	-4.8	1106.2	1300.0	8.1	1800.0	617.0

Chemical composition of groundwater in AL-DAYQAH

Sample No.	Na^+ meq/l	K^+ meq/l	Ca^{2+} meq/l	Mg^{2+} meq/l	SO^{2-} meq/l	Cl^- meq/l	HCO_3^- meq/l	Error* %	TDS (calc.) mg/l	T.D.S at 105 C Over Night mg/l	Error*** %	EC µmhos/cm	T.HARD. CaCO3 mg/l
Dy	11.7	0.1	15.5	7.5	17.2	13.5	2.0	3.1	2041.4	2145.0	2.5	4400.0	1262.2

Chemical composition of groundwater in AL-HUSAYNIAH

Sample No.	Na^+ meq/l	K^+ meq/l	Ca^{2+} meq/l	Mg^{2+} meq/l	SO^{2-} meq/l	Cl^- meq/l	HCO_3^- meq/l	Error* %	TDS (calc.) mg/l	T.D.S at 105 C Over Night mg/l	Error*** %	EC µmhos/cm	T.HARD. CaCO3 mg/l
HS-1	16.1	0.3	23.7	14.8	26.3	24.3	2.5	1.6	3238.9	3681.0	6.4	4400.0	1926.2
HS-2	15.7	0.2	15.3	11.7	21.2	13.0	3.0	7.1	2387.0	2867.0	9.1	3600.0	1252.6
HS-3	18.7	0.2	23.7	17.2	30.7	23.3	2.5	2.9	3499.6	3610.0	1.6	3100.0	1922.6
HS-4	6.8	0.1	16.0	7.9	10.1	15.0	2.0	6.3	1650.8	1823.0	5.0	2900.0	1303.0

*Ionic balance errors
**TDS. errors

reactions, redox reactions and solid phase interactions (solution-precipitation and adsorption including ion exchange). These types of chemical reactions in water are reversible and can be described in terms of equilibrium:

$$A+B \leftrightarrow C+D.$$

In the groundwater, CO_2 charged water dissolves $CaCO_3$ and $MgCO_3$, in which they become $Ca(HCO_3)_2$ and $Mg(HCO_3)_2$ solutions via a sequence of acid-base reactions. However the silica occurrence may be contributed by silicate minerals and sulphate by the oxidation of sulphides such as pyrite.

As the water becomes more reducing it may leach iron oxides, or conversely may precipitate transition metal sulphides (FeS_2). In aquifers that contained dominantly sodium chloride water, ion exchange occurs, changing the calcium bicarbonate water to a sodium bicarbonate water. At the end of the flow path some saline water may remain, producing a sodium chloride water by mixing. Lloyd (1985) indicated that nearly static water at the end of the flow path actively participates in the diagenesis of the aquifer. Edmunds (1977) studied the elements involved in hydrological processes, and their controls. Below there is a summary of the common processes, which Edmunds recognised as controlling the occurrences of the major cations and anions in the groundwater. The implications of these controls are discussed later in the chapter.

Processes controlling the occurrences of the major cations and anions of groundwater (Edmunds, 1977).

		Geochemical					
Ion	Dispersion	Complex formation	Ionic strength	Acid-base	Oxidation reduction	Solution precipitation	Adsorption
Ca^{2+}	X	(X)	X			(X)	X
Mg^{2+}	X	(X)	X			(X)	X
Na^{+}	X						X
K^{+}	X						X
HCO_3^-	X	(X)		X			
SO_4^{2-}	X	(X)	(X)	(X)	X	(X)	(X)
Cl^-	X	(X)					

The parentheses indicate minor controls.

4.6.1 Dispersion

The dispersion can be considered as the spreading of any moving solute front. Slow transport in the groundwater is dominated by bulk movement of water induced by hydraulic gradients. Besides the transport as a main factor, time has an influence in the chemical processes of an aquifer. Lloyd (1984) indicated that the persistence of undersaturation far into the aquifer is important in the development of secondary permeability.

4.6.2 Complex Formation

Complex formation is simply any combination of two or more atoms that can exist as a complex. It is another factor that might enhance the solubility of the molecules by the possible association of its ions to form complexes. For example $CaCO_3$ is more soluble because Ca^{2+} and CO_3^{2-} have no tendency to associate in solution, except from a solid precipitate when the product of their concentration exceeds the solubility product (see Lloyd, 1984 for further detail).

4.6.3 Ionic Strength

The ionic strength of a solution (I) is defined as equal to one half of the sum of the products of the concentration of each ion multiplied by square of its valency, or

$$I = \frac{1}{2}\sum_i C_i Z_i^2,$$

where C_i is the ionic concentration in moles per litre of solution and Z_i is the valency of the ion concerned, e.g. for a solution containing 0.1M $CaCO_3$ and 0.04 M $NaNO_3$, the ionic strength would be:

$$I = \frac{1}{2}(0.1\times 4 + 0.1\times 4 + 0.04\times 1 + 0.04\times 1) = 0.88.$$

Empirically it is found that the ionic strength gives a good measure of the effect of electrolytes on solubility. However the solubility of a salt, when it is measured at different ionic strengths, will reflect the quantity which called activity. As the ionic strength of a solution increases so the activity coefficient decreases.

4.6.4 Acid-Base Reactions

Acids and bases are known in terms of proton transfer, where acids are proton donors and bases are proton acceptors. In groundwater, acid-base pairs are mostly present with carbonic acid and water itself. Many aquifers of sedimentary origin contain significant amounts of solid carbonate such as calcite ($CaCO_3$) or dolomite $CaMg(CO_3)2$ which participate in the carbonic acid equilibrium via the reactions

$$CO_2 + H_2O \Leftrightarrow H_2CO_3$$
$$H_2CO_3 \Leftrightarrow H^+ + HCO_3^-$$
$$HCO_3^- \Leftrightarrow H^+ + CO_3^{2-}$$
$$CaCO_3 \Leftrightarrow Ca^{2+} + CO_3^{2-}$$

The carbonate chemistry of many aquifers is described largely on the basis of the above equations (Lloyd, 1985). The above example shows the affects of the reactions limited to acids and bases. This is clear when the calcite dissolution contributes carbonate ions to the solution which is considered as a strong base. So the solution reduces the hydrogen ion concentration, thus making the solution more alkaline.

4.6.5 Oxidation-Reduction Potential

Oxidation-reduction potential is one of the devices that describe the tendency of substances to react with one another. It is used for reactions involving oxidation and reduction processes. The redox reactions can be treated as electron transfer reactions in much the same way as acid-base reactions are proton transfer reactions.

4.6.6 Solution-Precipitation

Water has powerful solvent properties. The solution precipitation reactions with the aquifer matrix are important in controlling groundwater chemistry.

Usually, the mineral dissolution in groundwater is described by equilibrium relationships: the concentrations in waters in contact with minerals increases to a level which may reach saturation. The concentration of a saturated solution is the solubility of the mineral and in general it depends on temperature and pressure and sometimes on external

chemical factors (Lloyd, 1985). As Table 4.5 shows, the solubility of some sedimentary minerals under surface conditions vary considerably.

Table 4.5 Solubilities of minerals that dissolve in water at 25°C and 1 bar total pressure (After Seidell, 1958).

Mineral	Formula	Solubility at pH 7 (mg/l)
Gibbsite	$Al_2O_3.2H_2O$	0.001
Quartz	SiO_2	12
Hydroxyapatite	$Ca_3(OH)(PO_4)_3$	30
Amorphous silica	SiO_2	120
Fluorite	CaF_2	160
Dolomite	$CaMg(CO_3)_2$	90[a]
Calcite	$CaCO_3$	100[a]
Gypsum	$CaSO_4 \cdot 2H_2O$	2100
Sylvite	KCl	264000
Epsomite	$MgSO_4 \cdot 7H_2O$	267000
Mirabillite	$NaSO_4 \cdot 10H_2O$	280000
Halite	NaCl	360000

[a] CO_2 of partial pressure 10^{-3}

As an example of the solution process in aquifers of sedimentary origin is calcite which described by the reaction as follows, $CaCO_3 \Leftrightarrow Ca^{2+} + CO_3^{2-}$

At 25°C and 10^{-3} bar partial pressure of carbon dioxide, the calcite solubility is 90 mg/l and rises to 480 mg/l at 10^{-1} bar partial pressure of carbon dioxide.

However, rock forming silicates dissolve producing a solid phase during dissolution reactions, e.g. orthoclase, derived from granites, and a common mineral in sandstones may dissolve in water acording to the reaction below:

$$11H_2O + 2KAlSi_3O_8(s) \Leftrightarrow 2K^+ + 2OH^- + 4Si(OH)_4 + Al_2SiO_2(OH)$$

Orthoclase Kaolinite

4.6.7 Adsorption

The adsorption describes surface phenomena where some dissolved constituents in water are concentrated at interfaces between solids and solutions. However, for ions with the same charge, the ion with smallest hydrated radius is most strongly adsorbed and therefore Ca^{2+} is favoured over Mg^{2+}. Recharge water entering a sodium-saturated aquifer would make the ions of the aquifer (Ca^+ and Mg^{2+}) to become replaced by sodium until

the exchange capacity of the aquifer is exhausted. Some of the adsorption may occur in the reverse direction with the replacement of sodium by calcium, when saline water percolates through terrigenous clay deposits in river estuaries (Lloyd, 1985). Some cations are adsorbed irreversibly on clay minerals and are therefore fixed, e.g. large unhydrated ions (K^+ and NH_4^+), small highly hydrated ions (Li^+) and, to some extent, Mg^{2+} which becomes part of the clay mineral lattice (Lloyd, 1985).

4.7 Sources of Dissolved Species

4.7.1 Major Cations

The major cations of the groundwater are Calcium, Magnesium, Sodium and Potassium while the major anions of the groundwater are Sulphate, Chloride and Bicarbonate/Carbonate (Gorham, 1961).

4.7.1.1 Calcium

Calcium is the major component of solute in most fresh groundwater, since it is distributed in rock minerals and soil. Calcium, as well as other alkaline earths, ionises and forms moderately soluble compounds such as carbonate, fluoride, hydroxides and phosphates. The weathering of plagioclase would release an amount of calcium and sodium based on the anorthite-albite ratio in the bedrock (Hems, 1989).

The ferromagnesian minerals of the pyroxene and amphibole groups are minor sources. Limestones, although absent from the area, are major sources of calcium. Gypsum and anhydrite, though not widespread, may be considered as main sources where they occur in playas or evaporites.

4.7.1.2 Magnesium

Magnesium, also an alkaline earth, behaves geochemically differently from calcium, because of its smaller ionic radius, 0.66Å, compared with the calcium ionic radius of 0.99Å. Magnesium is incorporated in ferromagnesian minerals during early crystallisation of magma. Thus, in primary rock genesis, mangesium is more important than calcium (Rankam and Sahama, 1950). Silicate sources of magnesium are the ferromagnesian

minerals augite, hornblende and biotite. Dolomite, if present, may be a major source of magnesium.

4.7.1.3 Sodium

Sodium is one of the more abundant elements and is a common constituent of natural waters. It is part of the alkali metal group. Sodium compounds are highly water soluble, and the most widespread source of sodium is the weathering of feldspars. Halite (Na Cl) where present in the aquifer fill, can cause large concentrations of solute sodium.

4.7.1.4 Potassium

The potassium concentration in most natural waters remains relatively low. It rarely approaches 20 mg/l (Allen and Minea, 1982). This is due in part to resistance to chemical weathering of the potassium minerals. Potassium feldspar, orthoclase and microcline ($KAlSi_3O_8$) are the major source of potassium. Micas and the feldspathoid leucite ($KAlSi_2O_6$) also contain potassium and may be additional sources. Hems (1985) indicates that potassium is an essential element for both plants and animals. The element is present in plant material and is lost from agricultural soil by crop harvesting and removal as well as by leaching and runoff acting on organic residues.

4.7.2 Major Anions

4.7.2.1 Sulphate

Sulphate is a common ion in the earth's crust and high concentrations may be present in groundwater due to leaching of gypsum, sodium sulphate and some shale and as a result of redox weathering of pyrite. In natural water, sulphate concentrations may range from a few mg/l to several thousand mg/l.

4.7.2.2 Chloride

Chloride, the ionised form, occurs in the alkali rocks, pegmatite, volcanic emanates and hydrothermal solutions characterised by large concentrations of chloride (Rankama and Sahama, 1950 in Hem, 1989). Owing to the high solubility of most chloride compounds, particularly halite, the compounds are concentrated in evaporites or playa deposits.

However, Hem (1989) reviewed the behaviour of chloride ions in natural water as follows:

1- They do not significantly enter into oxidation or reduction reactions.

2- Form no important solute complexes with other ions unless the chloride concentration is extremely high.

3- Do not form of salts of low solubility

4- Are not significantly adsorbed on mineral surfaces

4.7.2.3 Bicarbonate/Carbonate

Bicarbonate (HCO_3^-) and Carbonate (CO_3^{2-}) can arise when carbon dioxide gas (CO_2) is dissolved in water to form carbonic acid (H_2CO_3) and also from the oxidation of organic matter by bacteria. The other major source of carbonate and bicarbonate in natural water is dissolved carbonate minerals such as calcite. Carbonic acid is the main agent for chemical weathering of silicate minerals as well as carbonate minerals.

4.7.3 Minor Ions

The minor ions analysed in this study were the elements of aluminium, manganese, iron, nickel, barium and lead.

4.7.3.1 Aluminium

Although aluminium is among the most abundant elements in the earth's crust, it is present only in trace concentrations in natural waters. Aluminium is present in water at near neutral pH and rarely exceeds a few tenths of a milligramme per litre.

4.7.3.2 Manganese

A relatively common element in rocks and soils, manganese exists as oxides and hydroxides in the (II), (III) or (IV) oxidation state. These compounds strongly absorb other metallic cations and, along with iron oxides, are of great importance in controlling the concentrations of various trace metals present in natural waters.

4.7.3.3 Iron

Surface waters within normal pH range of 6 to 9 rarely carry more than 1mg of dissolved iron per litre. However, subsurface water removed from atmospheric oxidative

conditions is low in iron concentration unless it has contact with iron bearing minerals with high concentrations of ferrous iron.

The form and solubility of iron in natural waters is strongly dependent upon the pH and the oxidation-reduction potential of the water. Iron is ferrous in +2 and ferric in +3 oxidation states.

Since ferric iron is found in solution only at a pH of less than 3, it is logical that the Fe of samples collected from the study area is in the ferrous (2+) iron state.

4.7.3.4 Nickel

The concentration of nickel in natural waters is probably controlled by its absorption on solid phases, such as iron and manganese oxides, rather than by the precipitation of $Ni(OH)_2$ or other nickel containing compounds. However, the median river water concentration of nickel is, 10 mg/l.

4.7.3.5 Barium

Barium is found in minor concentrations in natural waters. The U.S.A. has a reported range of 0.49-90 ppb, while an EPA study cited a range of 2-300 ppb for water examined in the U.S.A.

A likely control over the concentration of barium in natural waters is the solubility of barite ($BaSO_4$), which is a fairly common mineral. The solubility product for this material is near 10^{-10} (Sillen and Martell, 1964) and at sulphate molar activities near 10^{-4} (~10 mg/l) or 10^{-3} (~100 mg/l). Also the absorption by metal oxides or hydroxides would influence the concentration of barium in natural water. It is found in freshwater manganese oxide deposits (Ljunggren, 1955).

4.7.3.6 Lead

Lead is a relatively minor element in the earth's crust but is widely distributed in low concentrations in uncontaminated sedimentary rocks and soil. Its natural mobility is low, however, due to the low solubility of lead hydroxy carbonates and phosphate. Also the adsorption of lead onto organic and inorganic sediment surfaces and the coprecipitation of lead with manganese oxide tend to maintain low concentration levels in surface and

groundwaters (Hem, 1989).

4.8 Major Chemical Composition of Groundwater of Both Wadis

4.8.1 Major Cations

Major Cations were determined in Tables 4.1 and 4.2 and are described as follows:

4.8.1.1 Calcium

In Wadi Baysh the Ca^{2+} concentration varied from 52 to 414 mg/l as shown in the distribution map (Figure 4.3a). In the upper part of the wadi, calcium concentration was low (52 - 87 mg/l). The south west section concentrations were high (270 - 415 mg/l).

In Wadi Habawnah calcium is the principal cation of the groundwater. Its concentration varied from 58 to 521 mg/l but most values fell between 190 and 285 mg/l. Generally concentrations increased down wadi. The highest values were detected in the west (Al-Khaneg and Al Harshf area) but there is a substantial area with high calcium content in the east of the wadi near Al Husaniah (Figure 4.3b).

4.8.1.2 Magnesium

In Wadi Baysh the magnesium concentration varied between 25 mg/l and 161 mg/l, although mostly the concentrations were at the lower end of this range (25-70 mg/l, Table 4.1). The concentrations increased down wadi and reached their highest values in the southwest (Figure 4.4a). In Wadi Habawnah the magnesium concentrations varied between 21 and 219 mg/l with most sites showing 27-135 mg/l (Table 4.6). In general the concentrations increased down wadi although they decreased again in the extreme east (Figure 4.4b).

4.8.1.3 Sodium

The sodium concentration varied greatly in the study area: in both Wadi Baysh and Wadi Habawnah the waters showed a considerable variation, 32 to 720 mg/l and 24 to 540 mg/l, respectively (Table 4.6).

The distribution map (Figure 4.5a) shows that over most of Wadi Baysh the waters contained 140-300mg/l of sodium, but the sodium content increased systematically towards

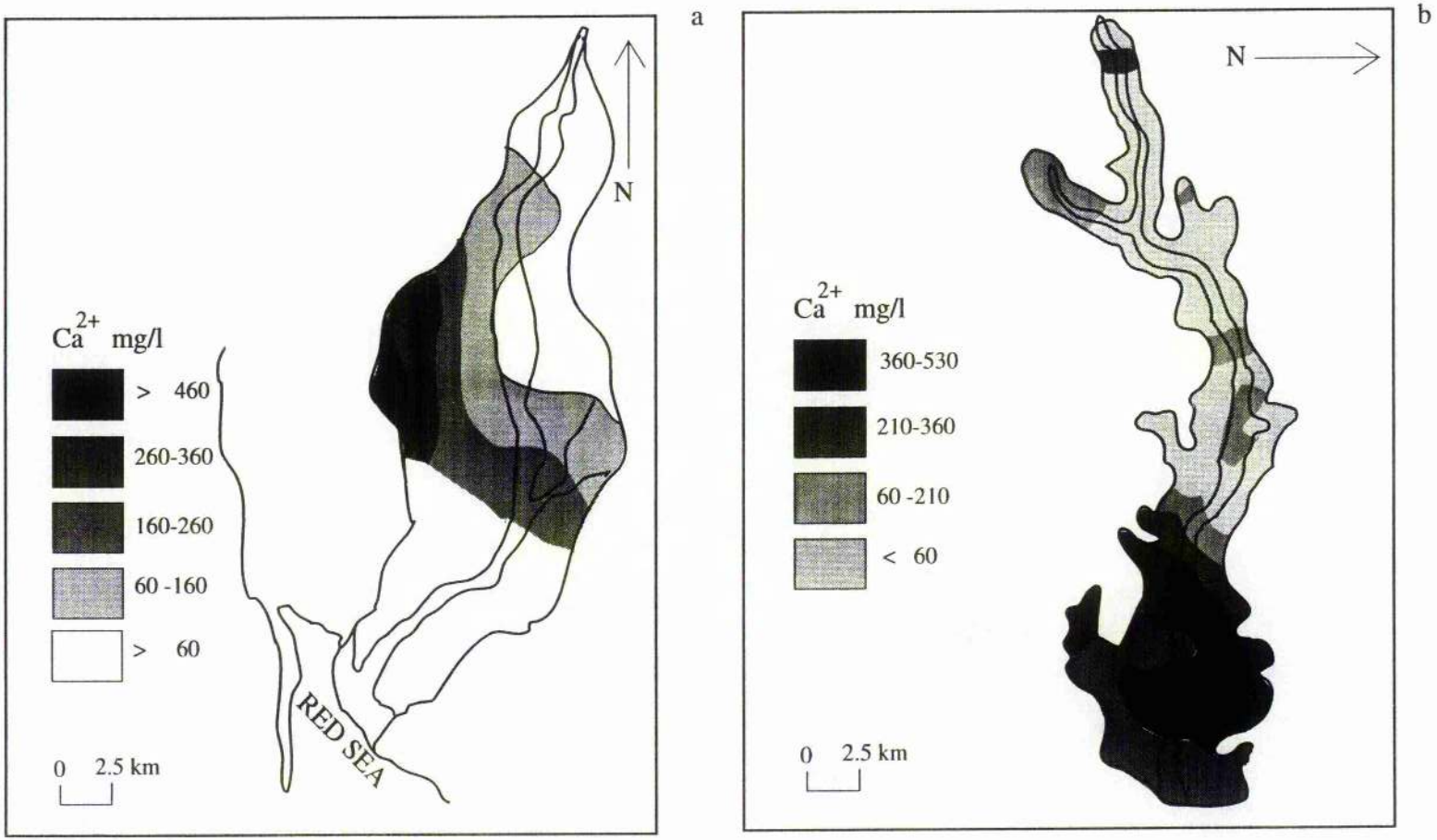

Figure 4.3 Areal distribution map of calcium in Wadi Baysh (a) and Wadi Habawnah (b) groundwater.

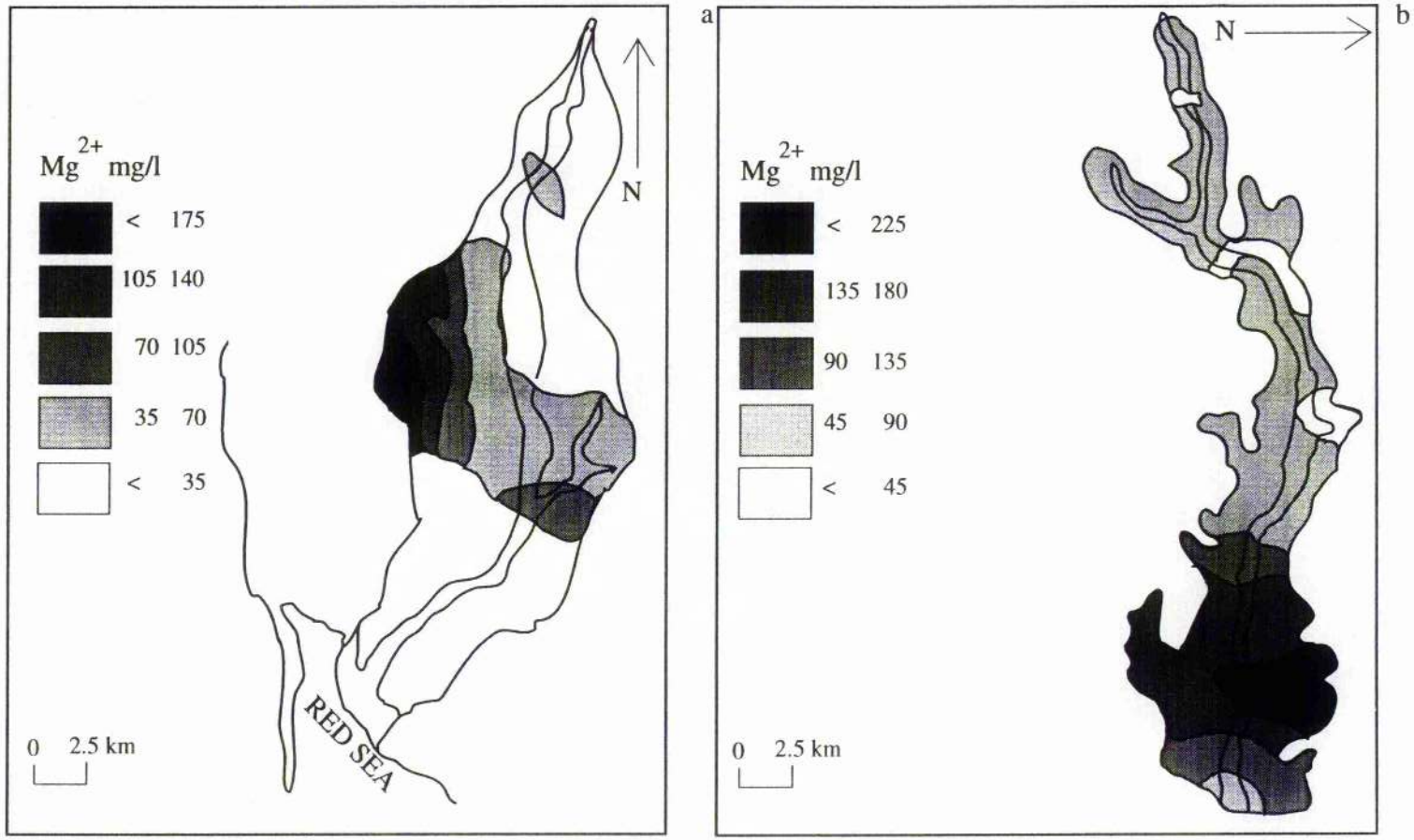

Figure 4.4 Areal distribution map of magnesium in Wadi Baysh (a) and Wadi Habawnah (b) groundwater.

Table 4.6 Variation of ionic composition in the groundwater of Wadi Baysh and Wadi Habaunah.

Wadi Baysh ionic concentrations (mg/l)

Location	UPPER PART			MIDDLE PART			LOWER PART		
Number of Samples	3			11			6		
Ions Conc. in mg/l	MAX	MEAN	MIN	MAX	MEAN	MIN	MAX	MEAN	MIN
Sodium (Na)	39	35	32	360	85	33	720	354	165
Potassium (K)	10	8	5	14	7	2	10	6	1
Calcium (Ca)	87	65	52	301	135	53	413	339	247
Magnesium (Mg)	36	30	25	133	45	29	161	117	91
Sulphate (SO4)	156	124	102	1488	307	121	773	255	0
Chloride (Cl)	70	70	69	319	134	67	2355	1305	319
Bicarbonate (HCO3)	152	124	106	410	190	91	244	112	24
Carbonate (CO3)	18	6	0	30	5	0	0	0	0
Total dissolved solids (TDS)	468	397	342	2667	812	447	3667	2431	1744

Wadi Habawnah ionic concentrations (mg/l)

Location	AL-KHANEQ			AL-JIFA			AL-HARSHAF			AL-MAJMAA			HABAWNAH			AL-MUNTASHER			MOR.&AL-NG.&DY*			AL-HUSAYNIAH		
Number of Samples	14			7			9			9			6			9			4			4		
Ions Conc. in mg/l	MAX	MEAN	MIN	MAX	MEAN	MIN	MAX	MEAN	MIN	MAX	MEAN	MIN	MAX	MEAN	MIN	MAX	MEAN	MIN	MAX	MEAN	MIN	MAX	MEAN	MIN
Sodium (Na)	380	164	58	180	134	93	540	238	130	180	112	78	160	120	80	160	96	24	270	148	93	430	329	156
Potassium (K)	15	9	6	5	4	2	14	11	6	10	6	2	9	7	5	7	5	2	8	5	3	10	8	3
Calcium (Ca)	521	239	58	501	180	94	406	240	175	280	157	81	187	151	127	282	169	92	310	164	92	476	395	307
Magnesium (Mg)	219	95	27	146	58	36	144	83	52	91	52	34	59	46	34	94	45	27	91	56	36	209	157	96
Sulphate (SO4)	1386	663	165	1009	443	205	1708	810	505	627	404	240	542	381	276	511	313	174	828	467	254	1474	1060	484
Chloride (Cl)	1169	407	106	709	279	177	744	381	246	354	246	141	248	209	141	567	259	141	478	270	177	861	670	460
Bicarbonate (HCO3)	152	130	91	213	144	122	183	129	91	152	125	91	152	127	122	274	161	91	152	142	122	183	153	122
Total dissolved solids (TDS)	3742	1641	505	2626	1169	734	3610	1828	1222	1521	1041	656	1230	978	745	1663	967	636	2041	1181	783	3500	2694	1651

*MORYKHAH,AL-NGAH and AL-DAYQAH

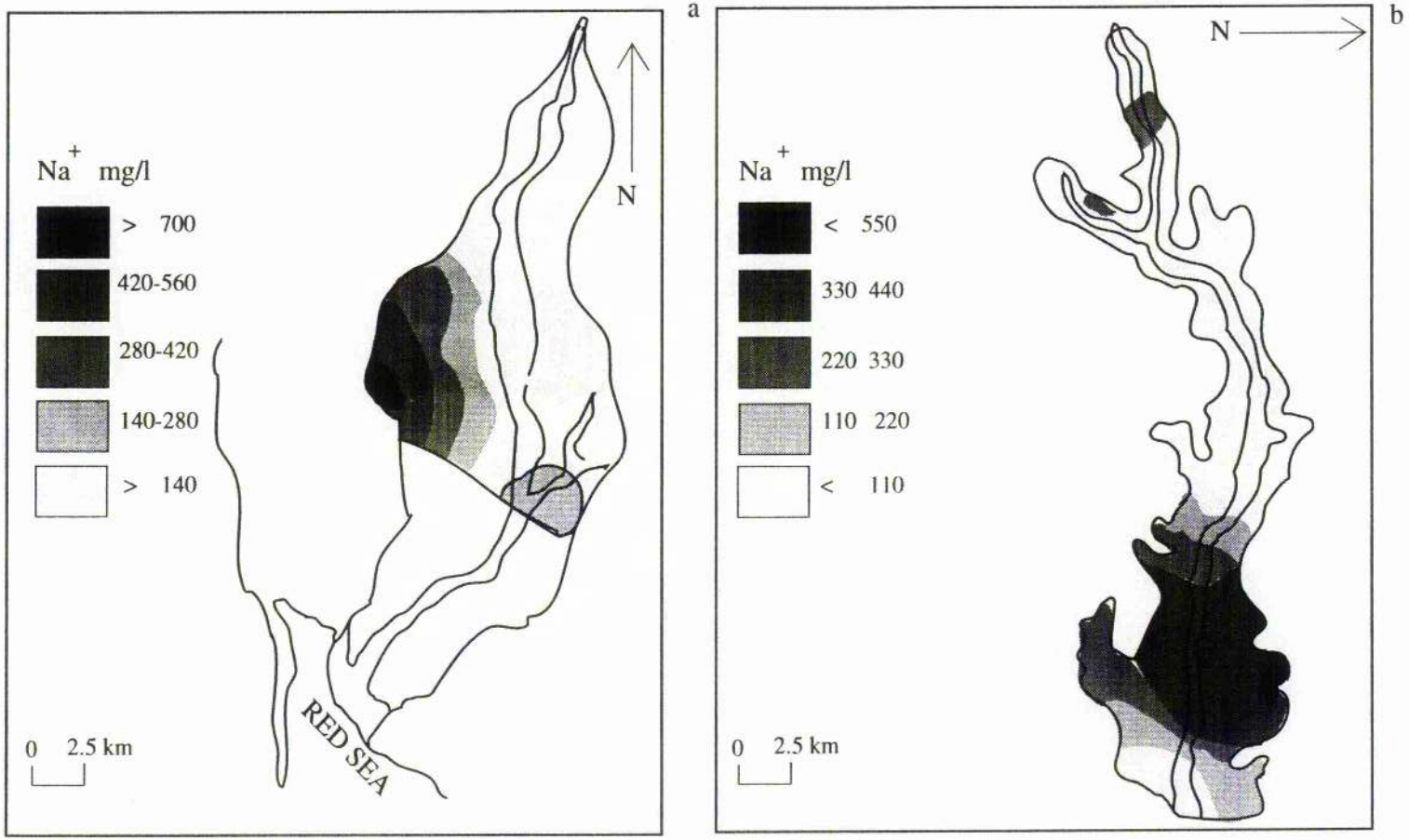

Figure 4.5 Areal distribution map of sodium in Wadi Baysh (a) and Wadi Habawnah (b) groundwater.

the southwest with peak values in well BL18. In the western part of Wadi Habawnah the sodium contents were generally below 168 mg/l but the concentrations rose to over 400 mg/l towards the mouth of the wadi before decreasing still further eastwards beyond the Najran - Al Riyadh Road (Figure 4.5b).

4.8.1.4 Potassium

The potassium content in the waters varied between 1.2 and 14.1 mg/l in Wadi Baysh and between 2 and 11.2 mg/l, in Wadi Habawnah (Figure 4.6).

There was little evidence of systematic change of concentration, but in Wadi Baysh concentrations were highest in the west and least in the central areas. In Wadi Habawnah concentrations were greatest in the headwaters and towards the Riyadh road. Concentrations were least in the extreme east.

4.8.2 Major Anions

Major anion concentrations are listed in Table 4.6.

4.8.2.1 Sulphate

In Wadi Baysh, 70% of the samples had less than 250 mg/l of sulphate in solution. Of the remainder, only those of the extreme southeast and extreme west yielded notable patterns, with peak a concentration of 1488 mg/l (Figure 4.7a). In Wadi Habawnah most of the samples contained less than 600 mg/l of sulphate. Least in the headwater and central reaches of the wadi sulphate increases to the north of the Riyadh road with a peak of 1708 mg/l (Figure 4.7b).

4.8.2.2 Chloride

The chloride concentrations in Wadi Baysh ranged between 69 mg/l and 2355 mg/l^{-1} (Figure 4.8a).

In both wadis most of the water samples contained less than 250 mg/l of chloride. In Wadi Baysh the chloride content varied down wadi with exceptionally high peaks in the extreme southwest. In Wadi Habawnah the chloride content is marginally higher in the

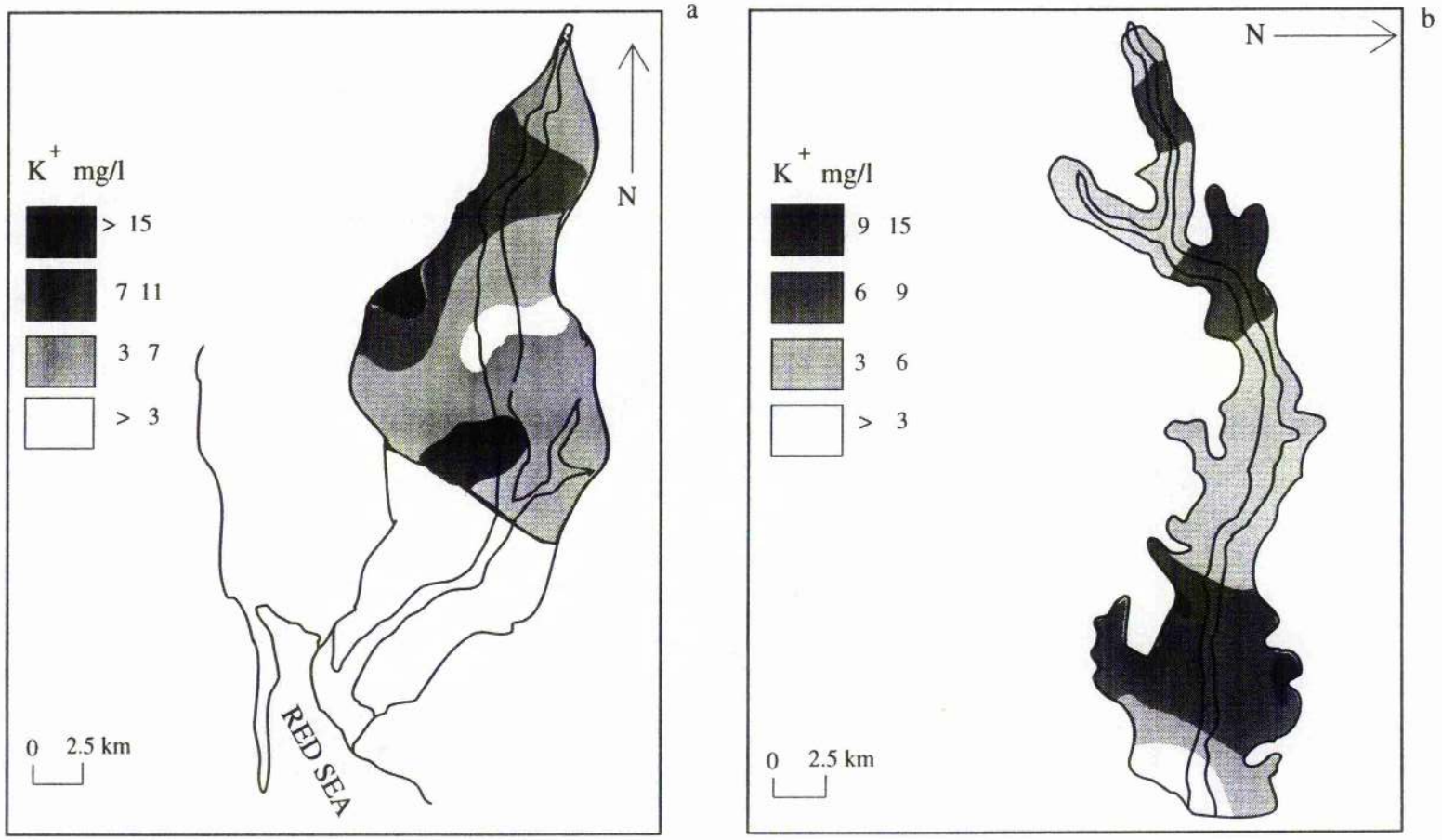

Figure 4.6 Areal distribution map of potassium in Wadi Baysh (a) and Wadi Habawnah (b) groundwater.

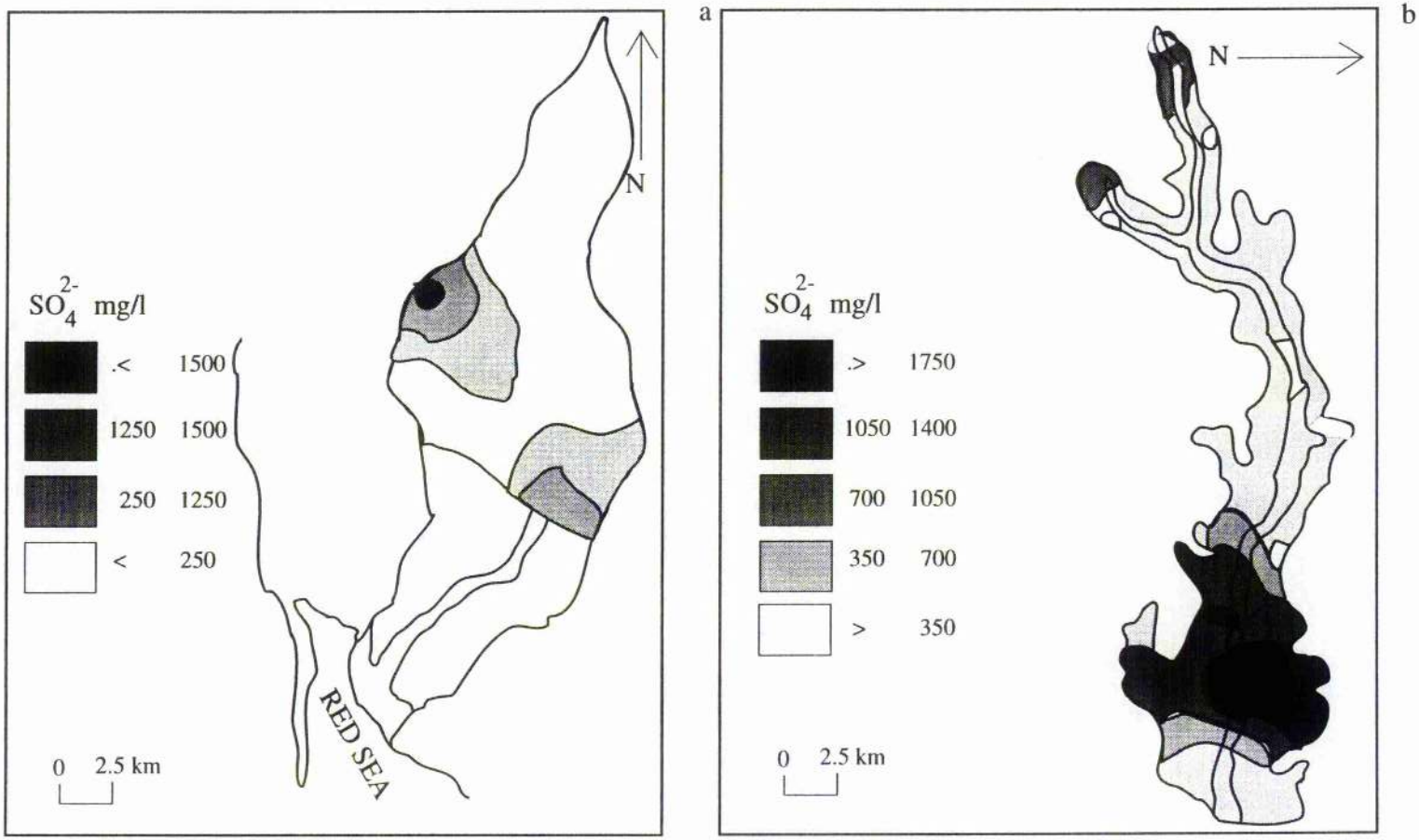

Figure 4.7 Areal distribution map of sulphate in Wadi Baysh (a) and Wadi Habawnah (b) groundwater.

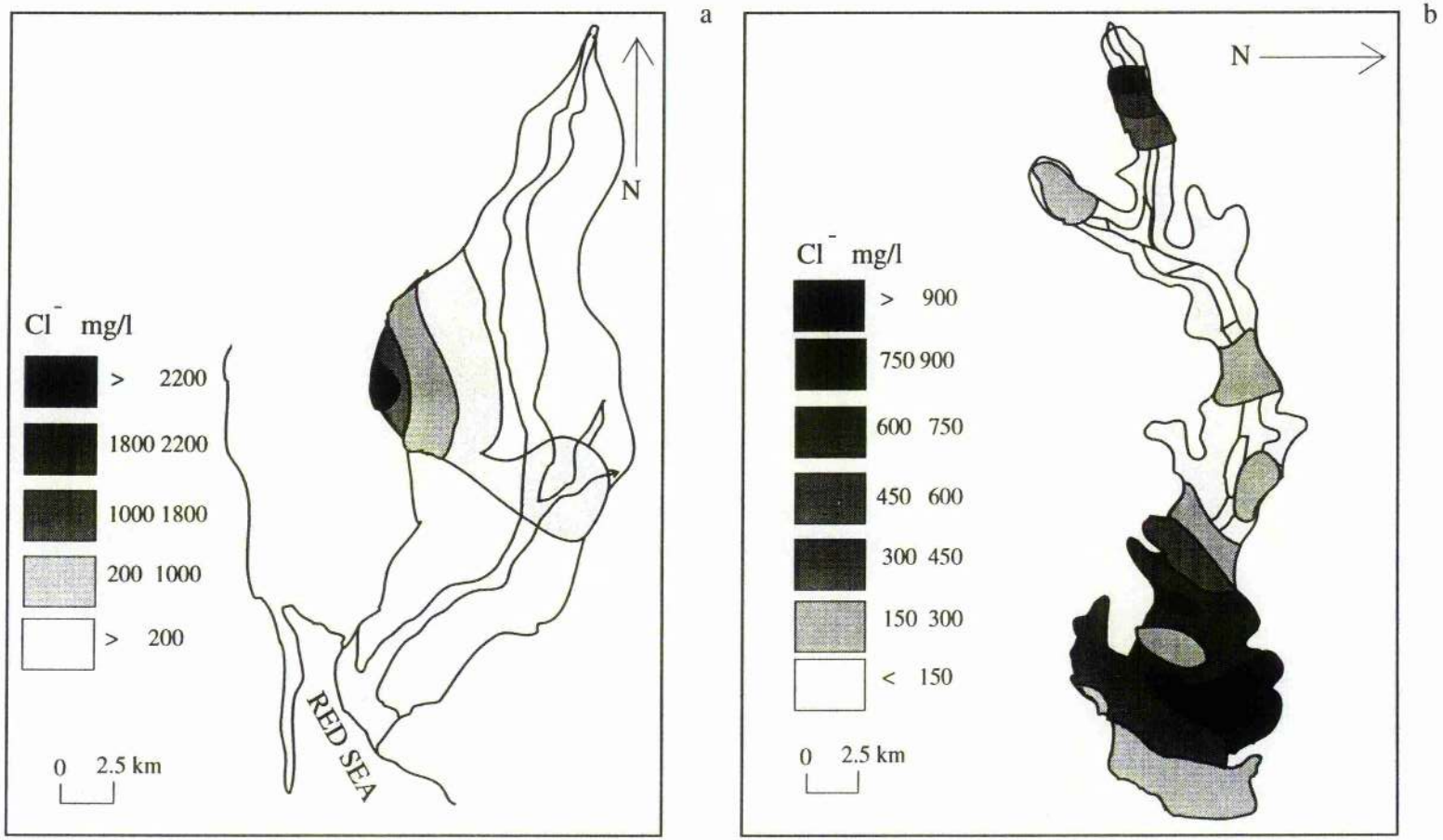

Figure 4.8 a and b Areal distribution map of chloride in Wadi Baysh (a) and Wadi Habawnah (b) groundwater

headwaters but 20km west of Al Husaniyah concentrations increased substantially before decreasing still further eastwards (Figure 4.8b).

In the lower part of Wadi Baysh, the lithological sequences include the presence of a buried salt dome structure some 1000m below the surface (Chapter 2). The author believes that it is unlikely that halite from the salt dome would influence the aquifer layer which is entirely within the upper section and extends to no more than 150m below the surface.

4.8.2.3 Bicarbonate/Carbonate

Wadi Baysh groundwater samples contain bicarbonate (HCO_3^-) in concentrations of 24.4 to 410 mg/l, while bicarbonate in Wadi Habawnah ranges from 91 to 271 mg/l. The bicarbonate distribution maps (see Figure 4.9) show that in Wadi Baysh and Wadi Habawnah the waters normally contain less than 350 mg/l but that there is one limited area in the lower wadi with greater concentrations. In Wadi Habawnah concentrations are mostly below 200 mg/l with two localised zones carrying greater concentrations. The carbonate (CO_3^{2-}) anion is absent in most of the water samples.

4.8.3 Minor Ions

Minor ions in the waters of both wadis are listed in Tables 4.7 and 4.8.

4.8.3.1 Aluminium

In Wadi Baysh no sample yielded more than 1 mg/l of aluminium (range 0.043 to 0.982). No systematic variation with site was detected. In Wadi Habawnah the aluminium concentrations were substantially lower, rising to 0.551 in the lower part of the wadi.

4.8.3.2 Manganese

In Wadi Baysh concentrations were generally low, in the region of 0.15-0.19 mg/l, two exceptions with more Mn^{2+} occurring in the lower part of the wadi. In Wadi Habawnah concentrations lay in the range of 0.15 to 0.22 mg/l, with higher values in the lower part of the wadi.

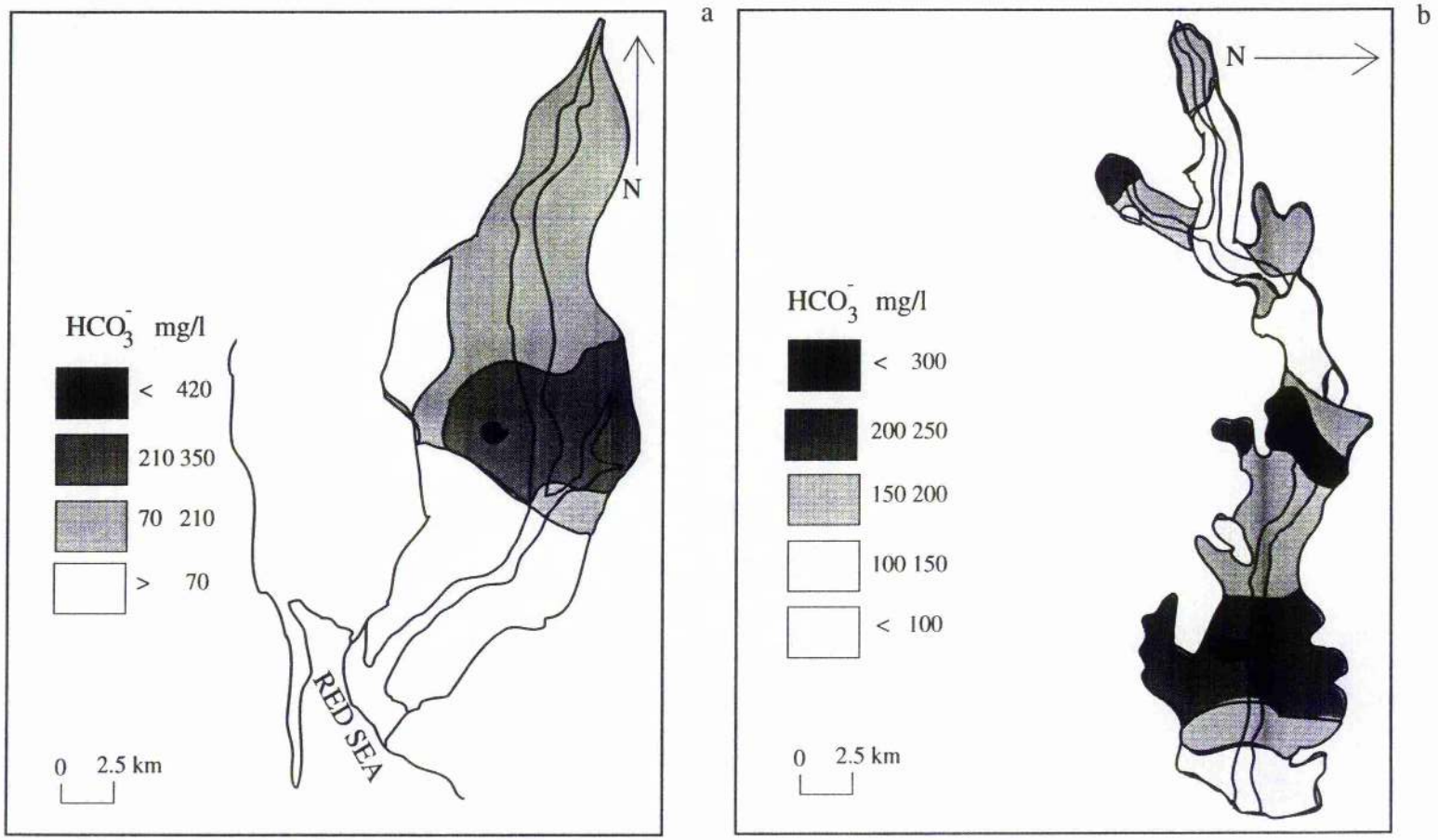

Figure 4.9 Areal distribution map of bicarbonate in Wadi Baysh (a) and Wadi Habawnah (b) groundwater.

Table 4.7 Chemical analyses of groundwater minor ions of Wadi Baysh

Chemical Analyses of Groundwater Minor Ions of the upper part of Wadi Baysh

Sample NO	Al^{3+} ppm	Ba^{2+} ppm	Fe^{2+} ppm	Mn^{2+} ppm	Ni^{2+} ppm	Pb^{2+} ppm
BU1	0.552	0.014	0.821	0.154	0.063	0.004
BU2	0.419	0.020	0.964	0.186	0.078	0.008
BU3	0.453	0.017	0.725	0.155	0.066	0.005

Chemical Analyses of Groundwater Minor Ions of the middle part of Wadi Baysh .

Sample NO	Al^{3+} ppm	Ba^{2+} ppm	Fe^{2+} ppm	Mn^{2+} ppm	Ni^{2+} ppm	Pb^{2+} ppm
BM4	0.117	0.019	0.519	0.155	0.071	0.008
BM5	0.043	0.026	0.922	0.185	0.075	0.009
BM6	0.862	0.023	0.998	0.177	0.074	0.011
BM7	0.218	0.015	0.264	0.180	0.114	0.007
BM8	0.431	0.015	0.178	0.900	0.068	0.014
BM9	0.053	0.027	0.103	0.180	0.095	0.013
BM10	0.134	0.021	0.546	0.161	0.070	0.008
BM11	**	**	**	**	**	**
BM12	**	**	**	**	**	**
BM13	**	**	**	**	**	**
BM14	**	**	**	**	**	**

Chemical Analyses of Groundwater Minor Ions of the lower part of Wadi Baysh .

Sample NO	Al^{3+} ppm	Ba^{2+} ppm	Fe^{2+} ppm	Mn^{2+} ppm	Ni^{2+} ppm	Pb^{2+} ppm
BL15	0.790	0.015	0.869	0.163	0.054	0.005
BL16	**	**	**	**	**	**
BL17	0.403	0.050	0.284	0.694	0.086	0.010
BL18	**	**	**	**	**	**
BL19	**	**	**	**	**	**
BL20	0.982	0.017	0.161	0.337	0.045	0.003

**No data available

Table 4.8 Chemical analyses of groundwater minor ions of Wadi Habawnah

Chemical Analyses of Groundwater Minor Ions of Al-KHANEQ.

Sample No.	Al^{3+} ppm	Ba^{2+} ppm	Fe^{2+} ppm	Mn^{2+} ppm	Ni^{2+} ppm	Pb^{2+} ppm
KH1	0.169	0.045	0.614	0.223	0.13	0.017
KH2	**	**	**	**	**	**
KH3	**	**	**	**	**	**
KH4	**	**	**	**	**	**
KH5	**	**	**	**	**	**
KH6	**	**	**	**	**	**
KH7	**	**	**	**	**	**
KH8	**	**	**	**	**	**
KH9	**	**	**	**	**	**
KH10	**	**	**	**	**	**
KH11	**	**	**	**	**	**
KH12	**	**	**	**	**	**
KH13	**	**	**	**	**	**
KH14	**	**	**	**	**	**

Chemical Analyses of Groundwater Minor Ions of Al-HARSHAF

Sample No.	Al^{3+} ppm	Ba^{2+} ppm	Fe^{2+} ppm	Mn^{2+} ppm	Ni^{2+} ppm	Pb^{2+} ppm
HR1	0.1	0.027	0.848	0.216	0.095	0.01
HR2	0.243	0.032	0.821	0.191	0.086	0.011
HR3	0.116	0.103	0.567	0.195	0.131	0.035
HR4	0.114	0.025	0.557	0.171	0.076	0.009
HR5	0.32	0.021	0.693	0.154	0.066	0.012
HR6	0.289	0.032	0.682	0.18	0.087	0.011
HR7	0.094	0.022	0.4	0.159	0.067	0.009
HR8	0.216	0.025	0.496	0.156	0.068	0.01
HR9	0.168	0.019	0.37	0.174	0.069	0.008

Chemical Analyses of Groundwater Minor Ions of AL-MAJMAA

Sample No.	Al^{3+} ppm	Ba^{2+} ppm	Fe^{2+} ppm	Mn^{2+} ppm	Ni^{2+} ppm	Pb^{2+} ppm
MJ1	0.13	0.023	0.455	0.158	0.064	0.007
MJ2	0.083	0.021	0.37	0.165	0.069	0.008
MJ3	0.257	0.033	0.679	0.176	0.098	0.013
MJ4	0.25	0.021	0.516	0.155	0.075	0.007
MJ5	0.26	0.026	0.638	0.158	0.072	0.008
MJ6	0.297	0.02	0.483	0.174	0.069	0.0017
MJ7	0.179	0.02	0.535	0.162	0.073	0.009
MJ8	0.259	0.022	0.503	0.158	0.073	0.01
MJ9	0.335	0.046	0.782	0.226	0.12	0.011

Chemical Analyses of Groundwater Minor Ions of HABAWNA

Sample No.	Al^{3+} ppm	Ba^{2+} ppm	Fe^{2+} ppm	Mn^{2+} ppm	Ni^{2+} ppm	Pb^{2+} ppm
HB1	0.385	0.031	0.611	0.171	0.095	0.01
HB2	0.617	0.031	0.545	0.203	0.097	0.009
HB3	0.024	0.034	0.483	0.194	0.107	0.01
HB4	0.06	0.032	0.648	0.174	0.098	0.01
HB5	0.093	0.035	0.537	0.198	0.097	0.011
HB6	0.247	0.046	0.387	0.179	0.125	0.011

Continued on next page

Table 4.8 continued

Chemical Analyses of Groundwater Minor Ions of Al-MUNTASHER

Sample No.	Al^{3+} ppm	Ba^{2+} ppm	Fe^{2+} ppm	Mn^{2+} ppm	Ni^{2+} ppm	Pb^{2+} ppm
MT1	0.119	0.032	0.497	0.173	0.085	0.009
MT2	0.033	0.029	0.481	0.166	0.078	0.012
MT3	0.317	0.016	0.781	0.161	0.064	0.005
MT4	0.211	0.023	0.565	0.159	0.071	0.008
MT5	0.076	0.029	0.605	0.179	0.072	0.008
MT6	0.082	0.034	0.491	0.15	0.078	0.009
MT7	0.032	0.029	0.426	0.161	0.08	0.009
MT8	0.064	0.028	0.455	0.169	0.079	0.008
MT9	0.032	0.029	0.447	0.161	0.077	0.01

Chemical Analyses of Groundwater Minor Ions of Al-JIFA.

Sample No.	Al^{3+} ppm	Ba^{2+} ppm	Fe^{2+} ppm	Mn^{2+} ppm	Ni^{2+} ppm	Pb^{2+} ppm
GF-1	**	**	**	**	**	**
GF2	**	**	**	**	**	**
GF3	**	**	**	**	**	**
GF4	**	**	**	**	**	**
GF5	**	**	**	**	**	**
GF6	0.259	0.047	0.595	0.245	0.115	0.018
GF7	**	**	**	**	**	**

Chemical Analyses of Groundwater Minor Ions of MORYKHAH

Sample No.	Al^{3+} ppm	Ba^{2+} ppm	Fe^{2+} ppm	Mn^{2+} ppm	Ni^{2+} ppm	Pb^{2+} ppm
MR	0.551	0.025	0.3455	0.172	0.068	0.009

Chemical Analyses of Groundwater Minor Ions of Al-NGAH

Sample No.	Al^{3+} ppm	Ba^{2+} ppm	Fe^{2+} ppm	Mn^{2+} ppm	Ni^{2+} ppm	Pb^{2+} ppm
NG-1	**	**	**	**	**	**
NG-2	0.055	0.041	0.404	0.165	0.129	0.008

Chemical Analyses of Groundwater Minor Ions of Al-DAYQEH

Sample No.	Al^{3+} ppm	Ba^{2+} ppm	Fe^{2+} ppm	Mn^{2+} ppm	Ni^{2+} ppm	Pb^{2+} ppm
DY	0.254	0.026	0.591	0.147	0.067	0.01

Chemical Analyses of Groundwater Minor Ions of Al-HUSAYNIYAH

Sample No.	Al^{3+} ppm	Ba^{2+} ppm	Fe^{2+} ppm	Mn^{2+} ppm	Ni^{2+} ppm	Pb^{2+} ppm
HS-1	0.206	0.045	0.625	0.219	0.156	0.019
HS-2	0.451	0.045	0.574	0.212	0.15	0.016
HS-3	**	**	**	**	**	**
HS-4	**	**	**	**	**	**

**No available data

4.8.3.3 Iron

In Wadi Baysh concentrations were always below 1 mg/l, with two groups of analyses, one in the range 0.1-0.3 mg/l in the central part of the wadi and the other samples 0.5-1 mg/l from all other areas. In Wadi Habawnah the Fe^{2+} ranges between 0.37 and 0.85 mg/l. In any individual reach there appears to be a down wadi decrease of concentrations but this is not the case along the whole wadi.

4.8.3.4 Nickel

In Wadi Baysh the nickel content ranges from 0.045-0.114mg/l, being normally between 0.06 and 0.08mg/l. In Wadi Habawnah the nickel content ranged between 0.066 and 0.156mg/l with many samples higher than 0.09mg/l. The highest values occurred in the lower part of the wadi but west of Riyadh-Najran road.

4.8.3.5 Barium

In Wadi Baysh barium varies in concentration between 0.014 and 0.050 mg/l but most samples were in the range 0.015 to 0.027 mg/l. In Wadi Habawnah concentrations showed a much greater range 0.016 to 0.103mg/l with nearly half containing more than 0.03mg/l. Most samples contained between 0.02 and 0.45mg/l. Values tended to be lower in the upper parts of the wadi.

4.8.3.6 Lead

In Wadi Baysh the lead concentrations were least in the upper and lower reaches with a very small range of low values (0.003-0.014mg/l). The Wadi Habawnah the waters carry more lead (0.005 to 0.100mg/l). However, most water samples contained less than 0.02mg/l.

4.9 Hydrogen Ion Concentration (pH)

The dominant value of pH in the distribution map (Figure 4.10) is close to the neutral value of 7. The groundwaters of Wadi Habawnah are dominated by a natural pH value.

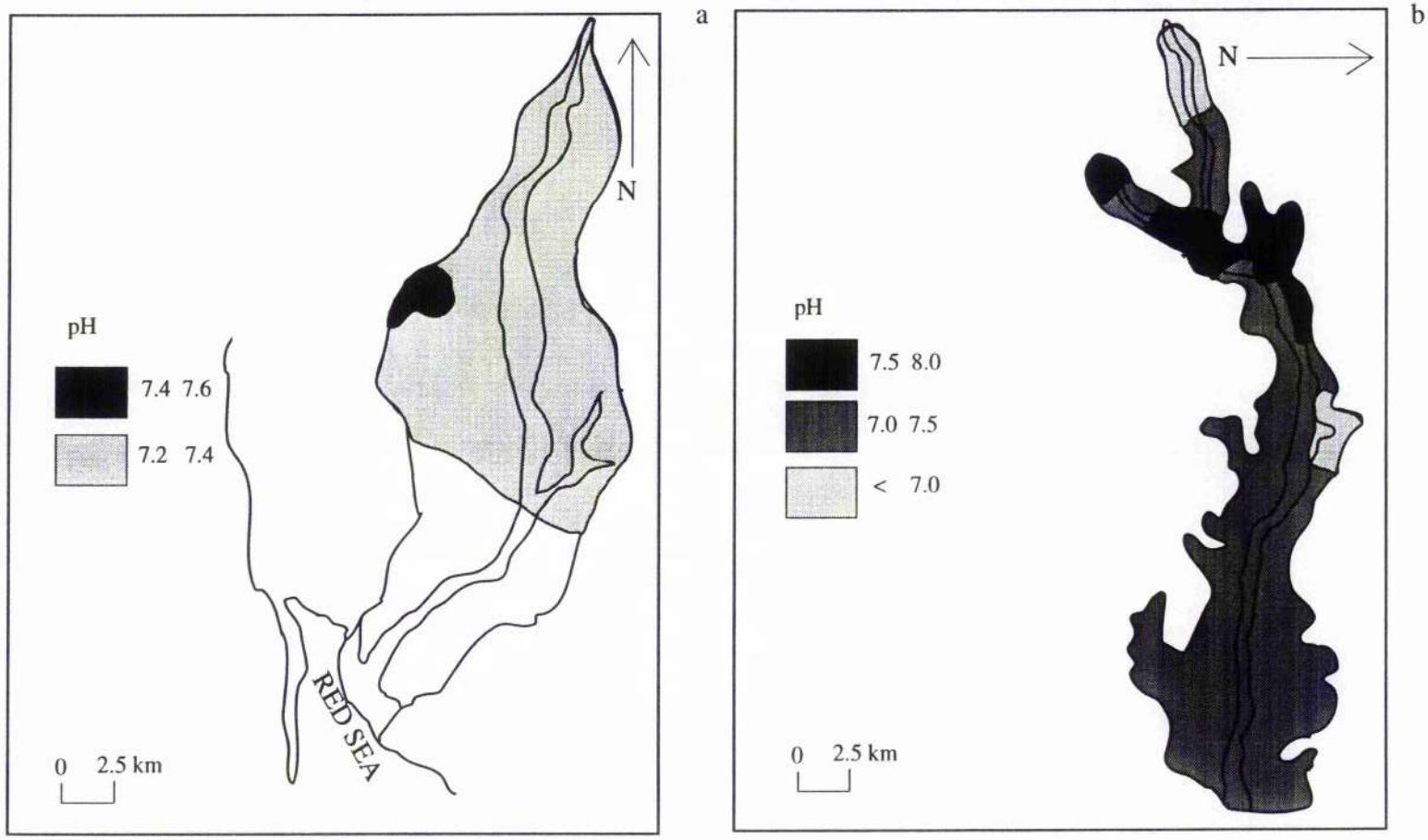

Figure 4.10 Areal distribution map of hydrogen-ion activity (pH) in Wadi Baysh (a) and Wadi Habawnah (b) groundwater.

4.10 Electrical Conductivity (EC)

Based on the fact that, for most groundwater, conductivity is a good measure of the relative mineralisation, total dissolved solids (TDS) in mg/l may be estimated by multiplying conductivity (μohm/cm at 25°C) by an empirical factor. The factor may range from 0.55 to 0.9, depending on the nature of the dissolved constituents. The Wadi Habawnah and Wadi Baysh samples both show linear relationships by plotting the EC against TDS (Figure 4.11). Thus EC measurements can be used to interpret the salinity in both sites. The field measurements of EC indicate a high concentration of dissolved solids in most of Wadi Habawnah with dominant values between 1279 and 2779 μohm/cm in the western part (Figure 4.12a) while in the lower sections the range is higher (2779 to 4279 μohm/cm). The main channel of Wadi Baysh shows a low range of EC distribution of 1000 to 1500 μohm/cm (Figures 4.12b). This value increases in the south west of the wadi to reach a range of 3000 to 6504 μmho/cm at sites relatively remote from the main channel.

4.11 Graphical Methods and Hydrochemical Facies

The author used several graphical methods for interpretation of the chemical data from the well fields in both wadis. Because of large number of analyses, the X-Y plots, Piper diagram and Durov diagram were adapted. These diagrams are useful for describing the similarity and the differences in major chemistry in groundwater systems. Also the water composition was reflected by identifiable groups or categories using the concept of hydrochemical facies. Feeze and Cherry (1979) defined the hydrochemical facies as distinct zones that have cation and anion concentrations describable within defined composition categories. The definition of a composition category is commonly based on subdivision of the trilinear diagram in the manner suggested by Back and Hanshaw (1965). These subdivisions are shown in Figure 4.13. The figure shows a classification diagram for anion-cation facies in terms of major-ion percentages. Water types are designated according to the domain in which they occur on the diagram segments (Back, 1966). Potassium and sodium are normally plotted as a single parameter. Definition of separate facies for the 0-10% and 90-100% domains on the diamond-shaped cation-anion graph is used in this study as it best displays the chemical characteristics of the waters in the study area.

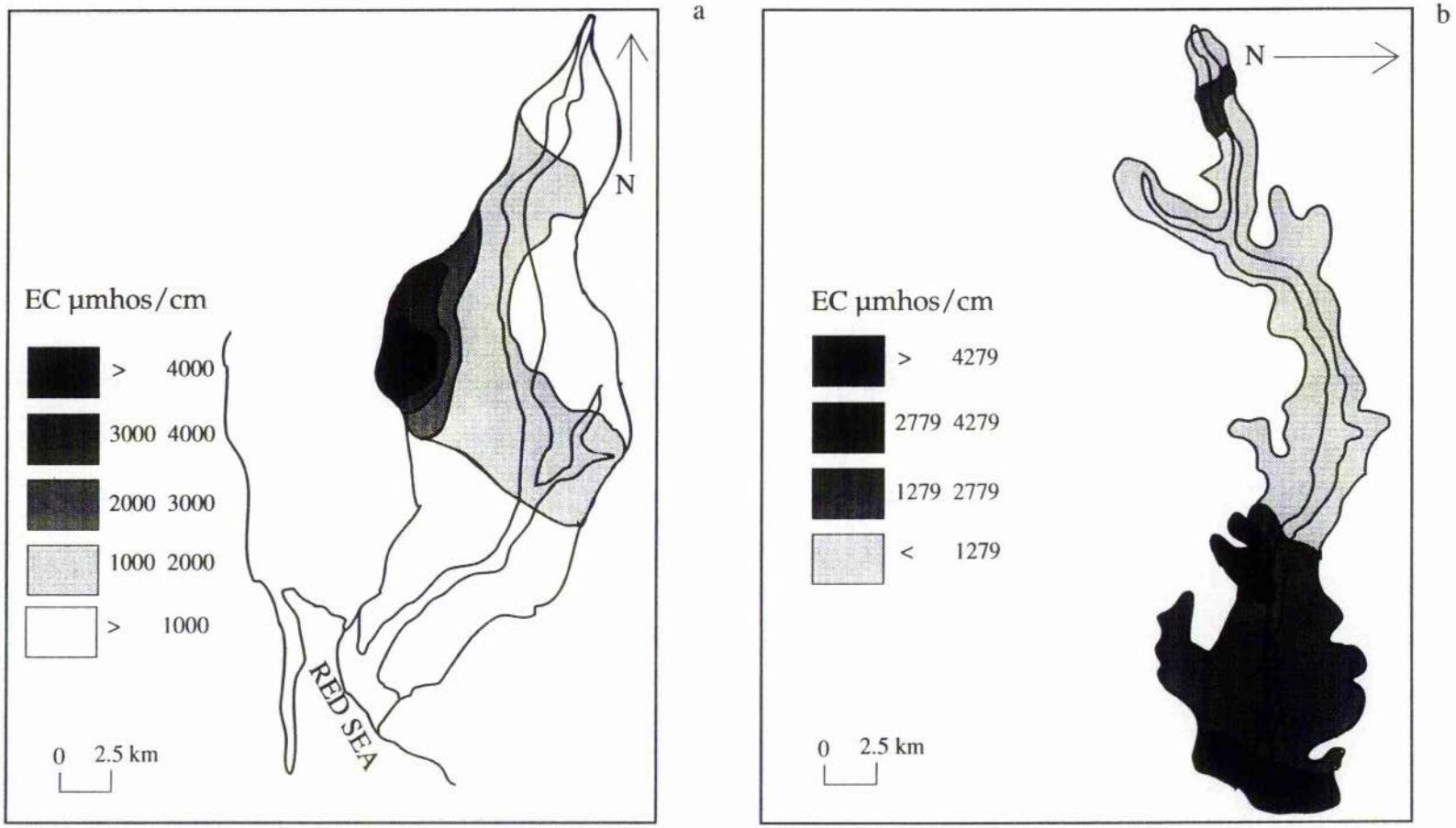

Figure 4.11 Areal distribution map of electrical conductivity (EC) in Wadi Baysh (a) and Wadi Habawnah (b) groundwater

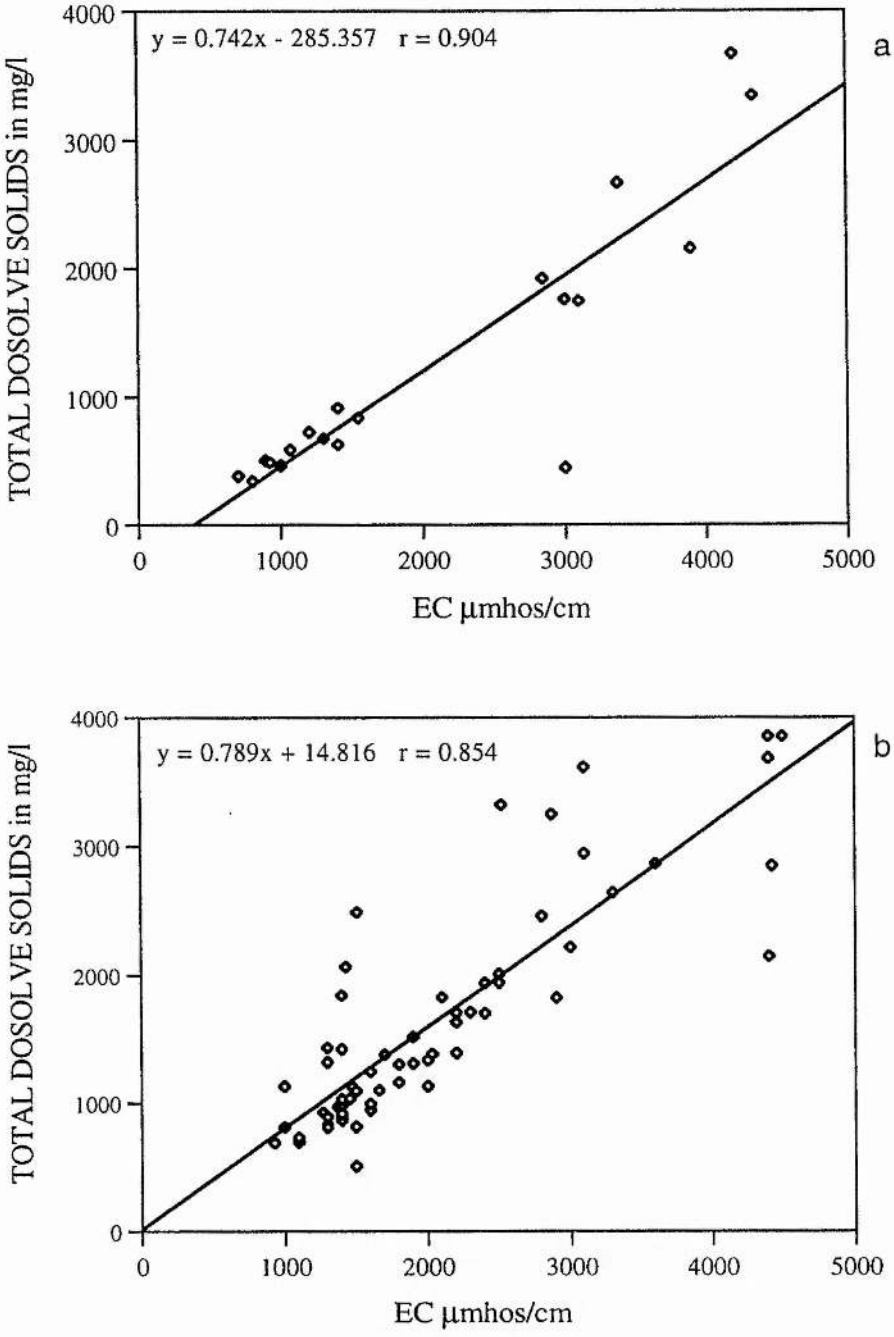

Figure 4.12 Relationship between electrical conductivety and total dissolved solids in Wadi Baysh (a) and Wadi Habawnah (b).

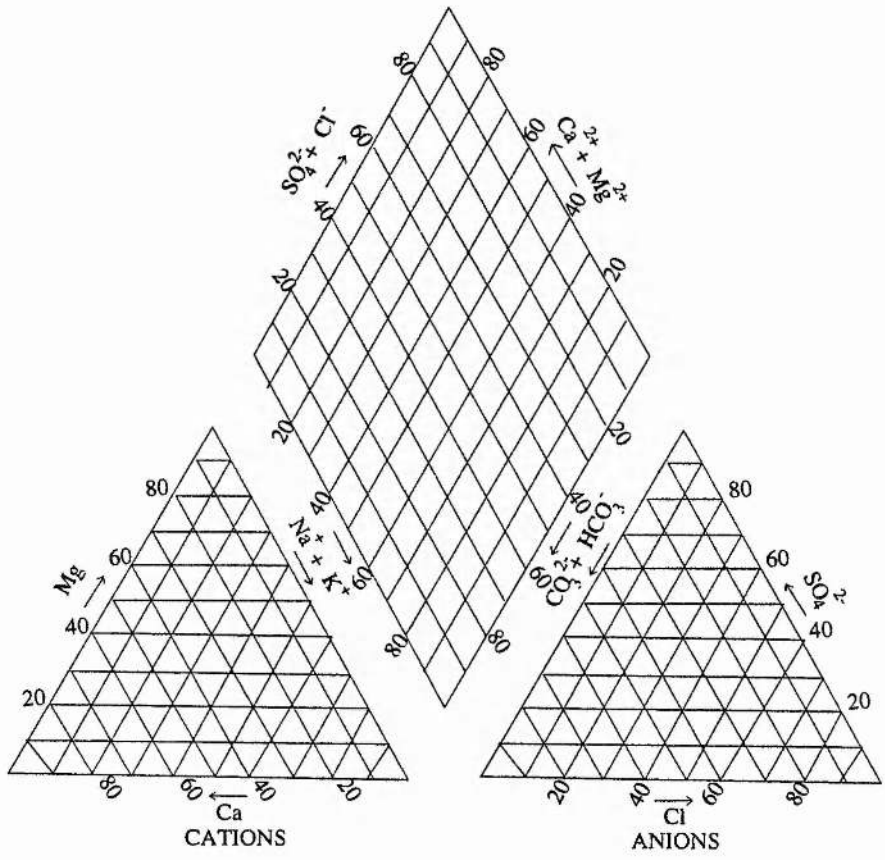

Figure 4.13 Trilinear diagram (after Piper 1944).

4.11.1 Linear Plots of Major Ions

Linear plots (X-Y plots) provide the initial approach to the interpretation of the hydrochemical data. They demonstrate the stoichiometric balance between ions and indicate the possible processes affecting the solutions. The major ions in the groundwater samples from both wadis were subjected to this technique in order to examine possible process effects.

The correlation diagrams of chloride and total dissolved solid (TDS) versus the major ions are plotted to show the behaviour of anions and cations against each other in both wadis. In this study Cl^- was chosen as a reference ion to demonstrate the effects of evaporation, due to the fact that it is not removed or supplied significantly by interaction with rocks, and it is not precipitated as a salt until very high salinity is reached. Drever (1982) explained that the chloride concentration in groundwater indicates the amount of evaporation that has taken place since the water started out as rainfall.

The author adopted the Mazor concepts (1991) for the X-Y plot interpretation as follows.

The composition diagram of Figures 4.14 and 4.15 are for the data given in Tables 4.1 and 4.2. The composition diagrams of Figures 4.16 and 4.17 portray the composition of Wadi Baysh and Wadi Habawnah in a visual form. The following features can be observed: (1) The well samples vary considerably in their concentrations; (2) The data plot on straight lines, revealing a positive correlation of Na^+, Ca^{2+}, Mg^{2+}, Cl^-, SO_4^{2-} with TDS. (3) The data plots of K^+ and HCO_3^- and CO_3^{2-} reveal a poor correlation with TDS. These mixing lines characterised by positive correlation indicate that the aquifer waters mix in various proportions with recharge water.

However, these mixing lines in the above figures, show three variations as follows: (a) the line extrapolates to the zero points, indicating mixing of aquifer water with recharge water that has negligible concentration (dilution) of the ion that plots on the Y-axis (Na^+ and Ca^{2+} of Wadi Habawnah water samples); (b) the line extrapolates to a point on the TDS axis, indicating the recharge water contains significant concentration of ions other than the one represented by the Y-axis (Na^+ and Cl^- in Wadi Baysh and Mg^{2+}, SO_4^{2-}, Cl^- in

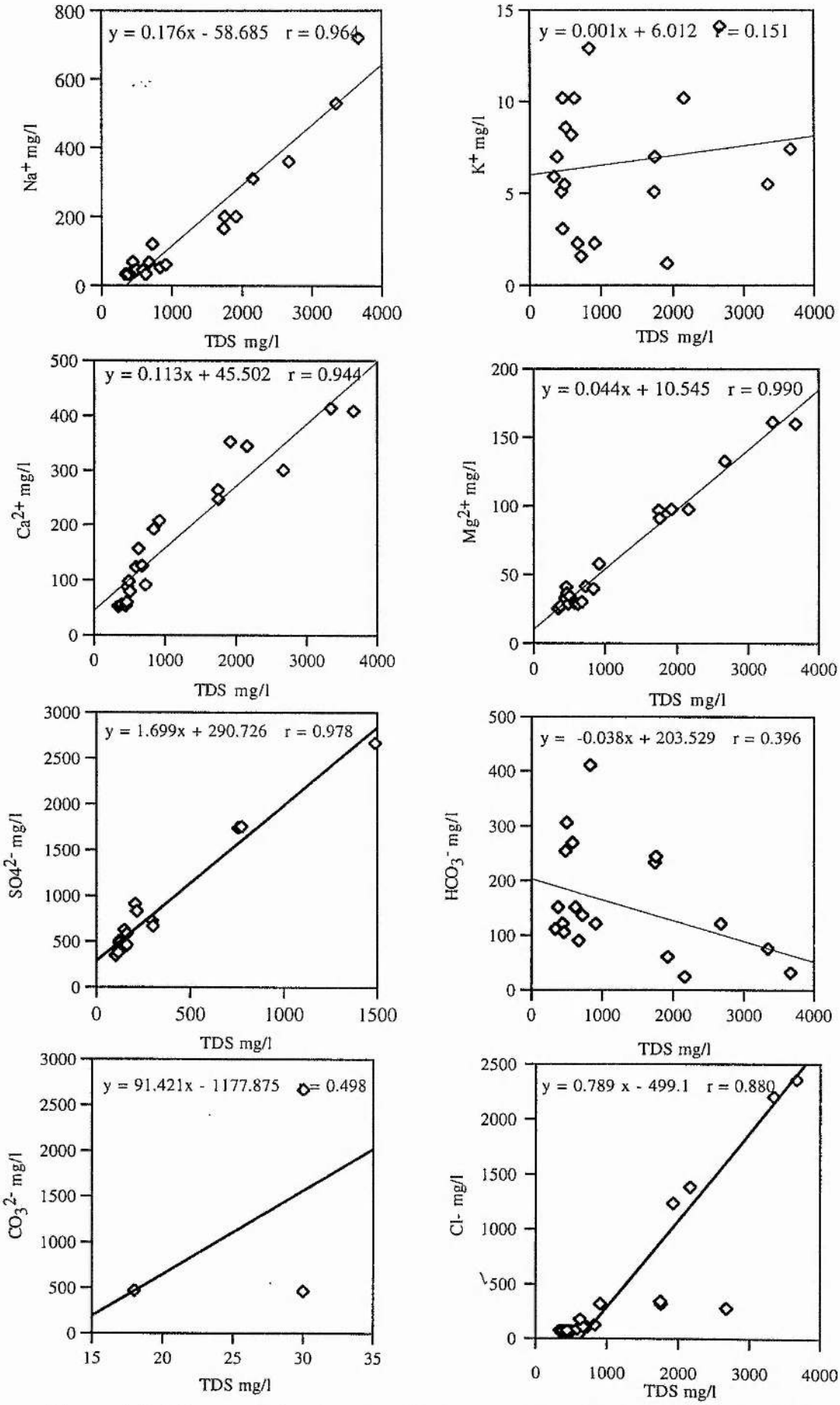

Figure 4.14 The correlation between TDS and the ions of Wadi Baysh groundwater.

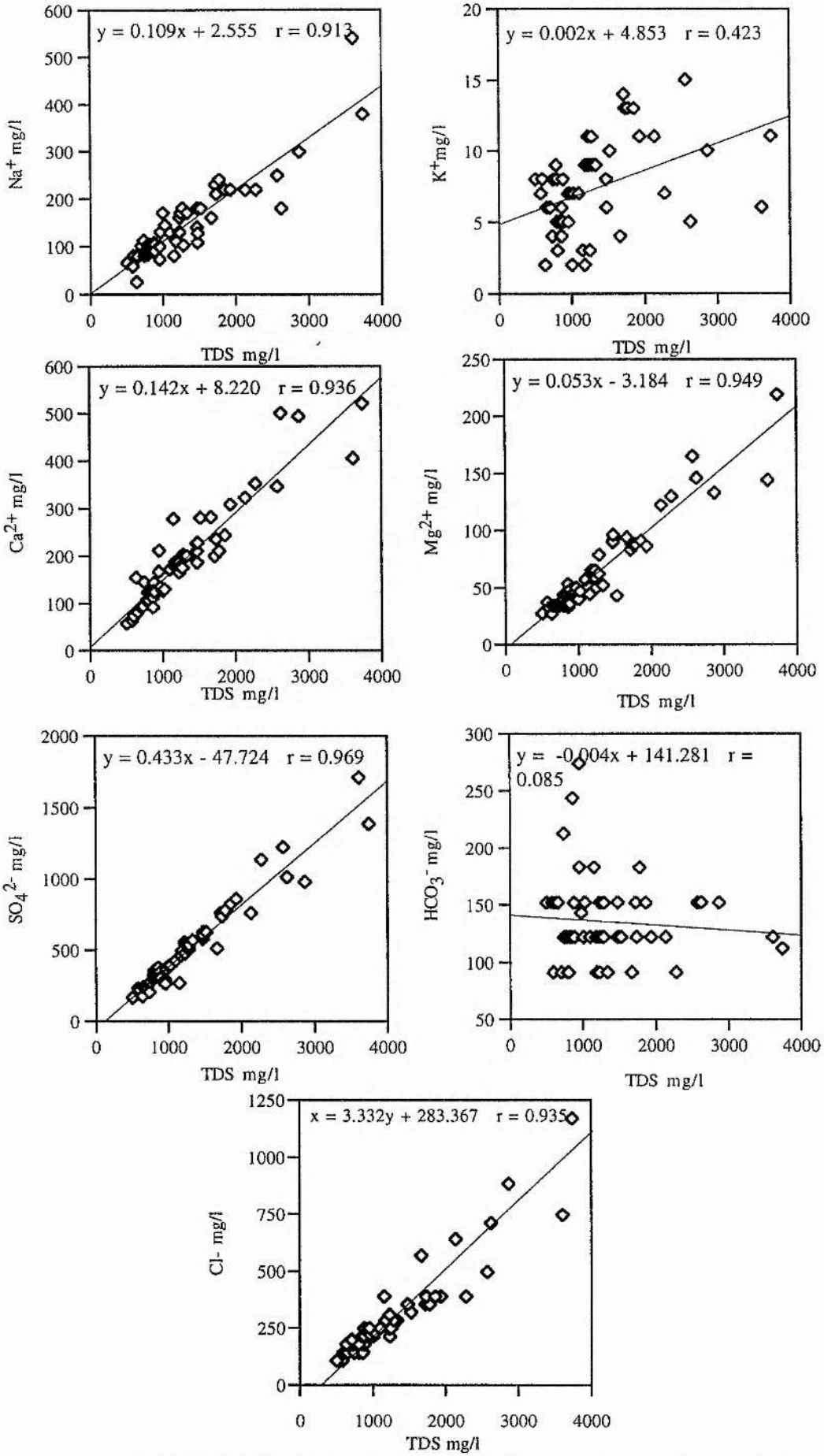

Figure 4.15 The correlation between TDS and the major ions of Wadi Habawnah groundwater.

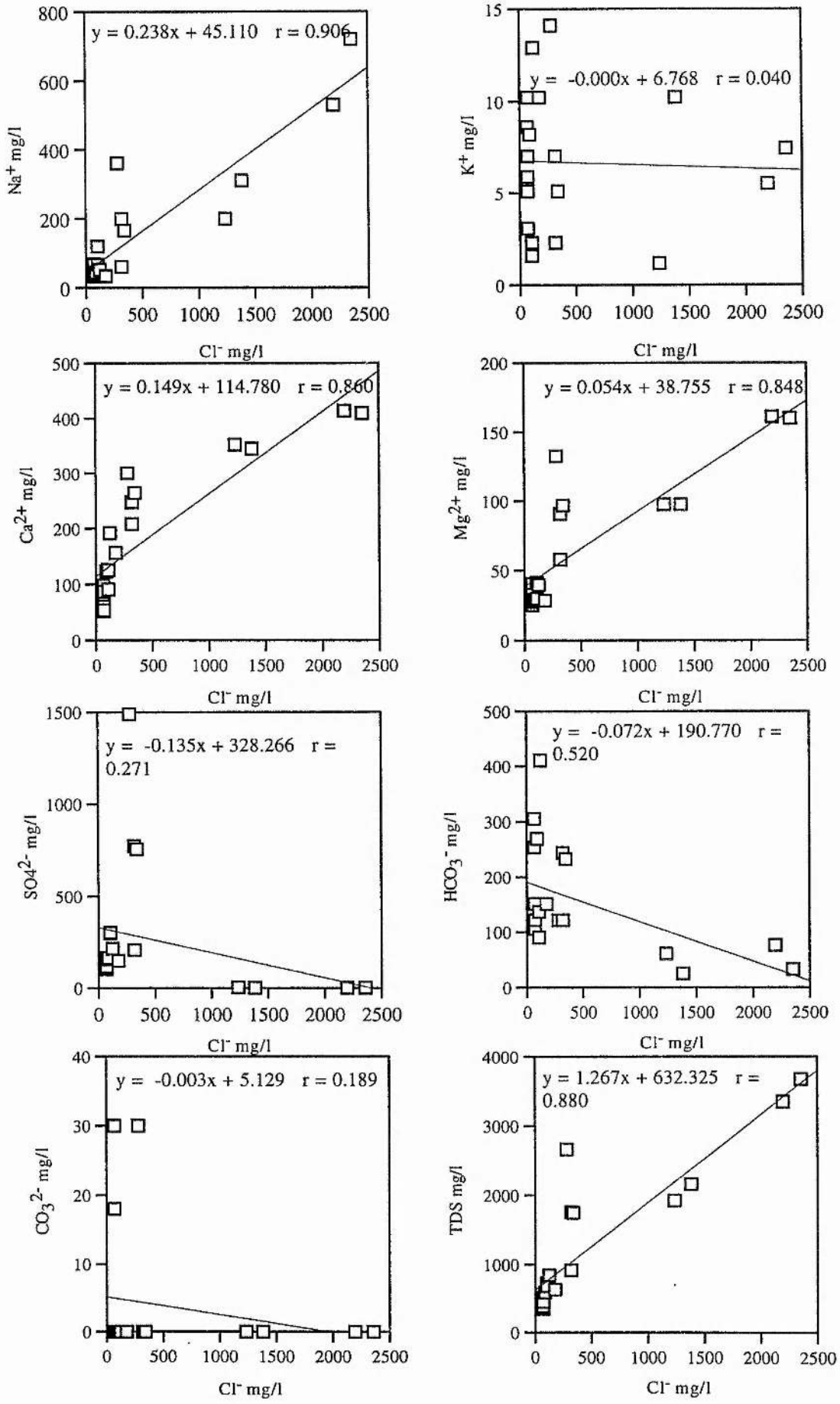

Figure 4.16 The correlation between Cl^- and the ions of Wadi Baysh groundwater.

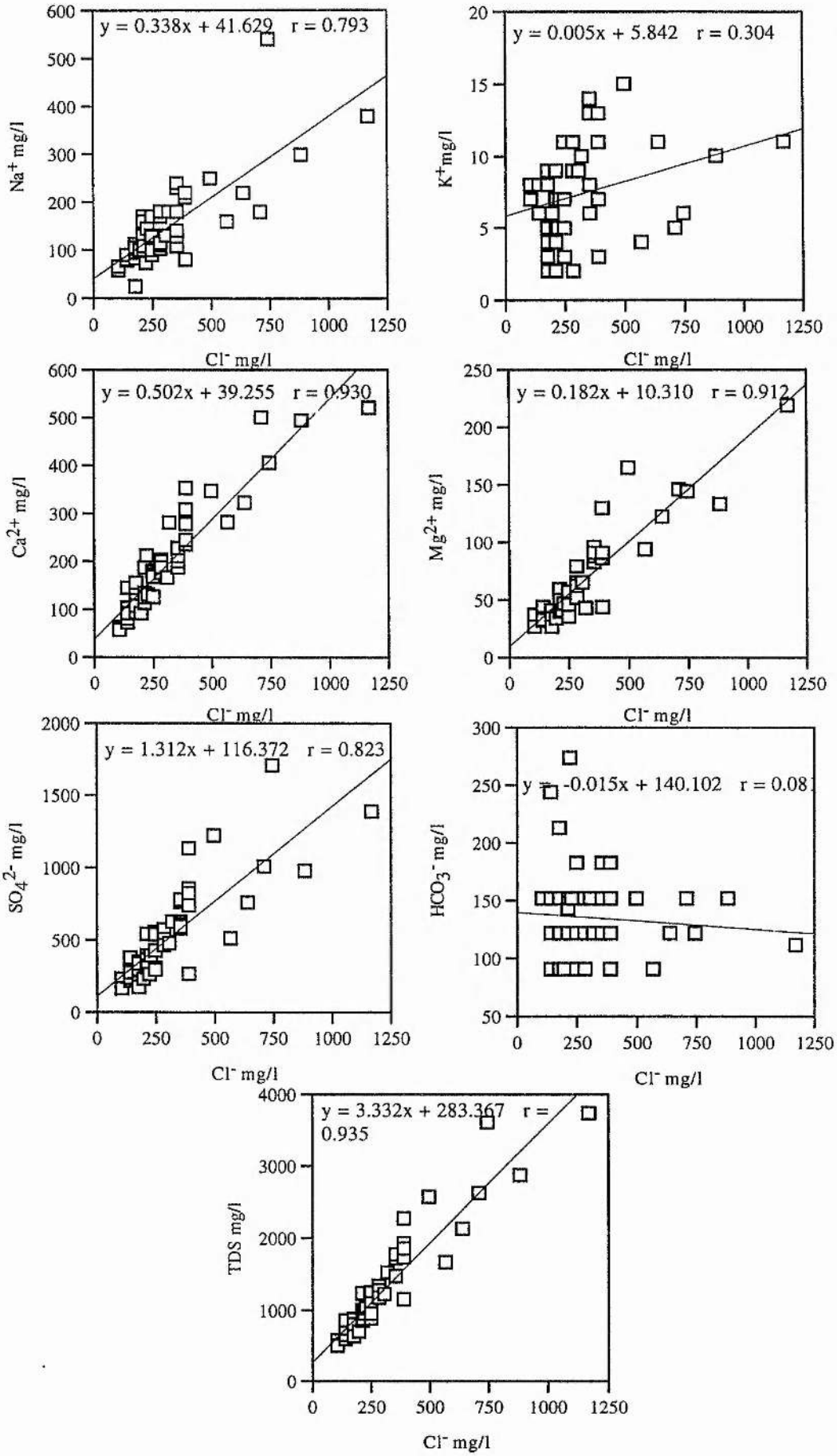

Figure 4.17 The correlation between Cl^- and the major ions of Wadi Habawnah groundwater.

Wadi Habawnah); and (c) The line extrapolates to the Y-axis, indicating both intermixing waters contain significant concentrations of the ion represented by the Y-axis (Ca^{2+}, Mg^{2+} in Wadi Baysh).

Figures 4.14 and 4.15 also show a case where data from a study area in Wadi Baysh and Wadi Habawnah reveal a random distribution on a composition diagram of K^+, HCO_3^- and CO_3^{2-} versus TDS in Baysh and K^+, HCO_3^- versus TDS in Wadi Habawnah. These random distributions may indicate that high variation of these ion concentrations were affected by wetting and drying cycles in the area.

Figures 4.16 and 4.17 show the correlation between Cl^- and Na^+ and other ions in different locations in the area. The correlation coefficient of Na^+ with Cl^- in Wadi Baysh has a higher value (0.9) than Wadi Habawnah (0.79). In Wadi Baysh the relation between Cl^- and Na^+ indicates that a simple dissolution or mixing between waters is the main process in the aquifer. However, in Wadi Habawnah the Cl^- concentration exceed the Na^+ concentration, which may be due to reverse ion exchange, where $CaCl_2$ water type is abundant in the wadi.

Figures 4.16 and 4.17 also show that the SO_4^{2-} concentration exceeds the Cl^- concentration in all water samples along Wadi Habawnah and in some areas in the lower part of Wadi Baysh. However, the correlation coefficient of Cl^- versus SO_4^{2-} is high (0.823) in Wadi Habawnah while in Wadi Baysh it is very low value. Such a case can be interpreted as being due to the influence of the bedrock types on the drainage systems

In Wadi Habawnah, the Cl^- versus Ca^{2+} and Mg^{2+} shows a high correlation coefficient which indicates that the water has a simple mixing influence with water type $CaCl_2$ and $MgCl_2$. However, the K^+ concentration versus Cl^- has a low correlation coefficient of 0.15 and 0.3 in Wadi Baysh and Wadi Habawnah respectively. This can be interpreted as the K^+ solubility is low compared to the rest of the cations of the fresh water while the solubility of Cl^- is greater than the other components.

Figures 4.18 and 4.19 show that there is a strong correlation ($r = 0.9$) between (Ca^{2+}+Mg^{2+}) and ($HCO_3^- + SO_4^{2-}$) in both wadis. Such a feature indicates that simple dissolution and mixing are the main processes dominant in the aquifers.

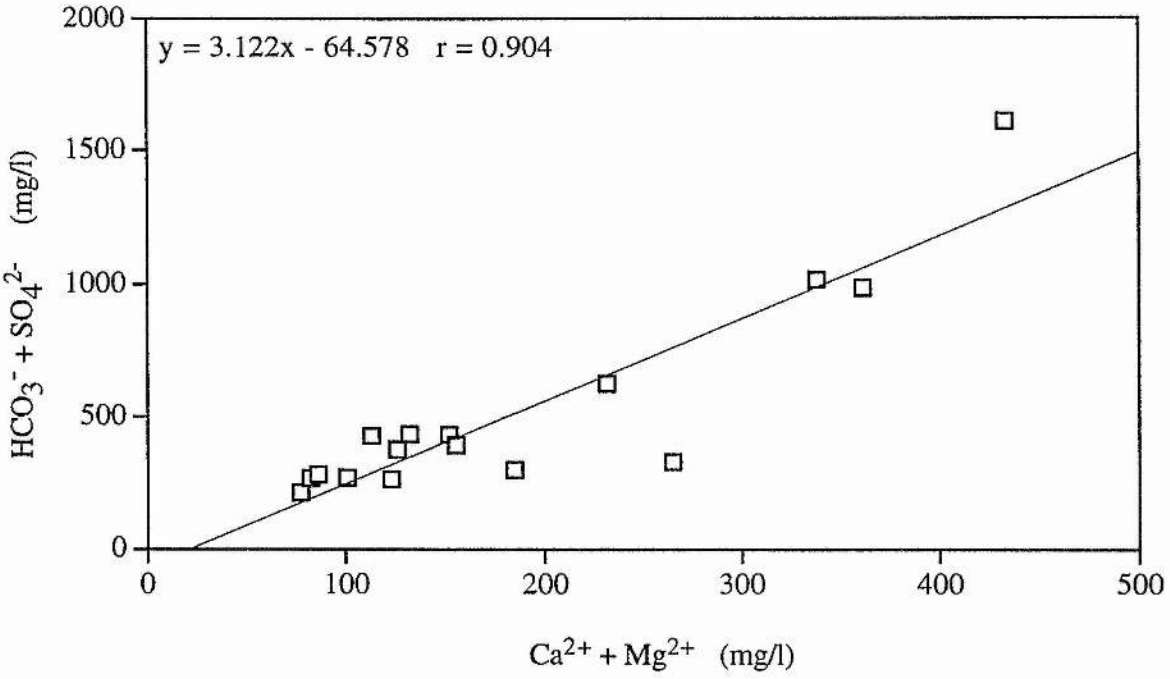

Figure 4.18 The correlation between (Ca^{2+} + Mg^{2+}) and (HCO_3^- + SO_4^{2-}) of Wadi Baysh groundwater.

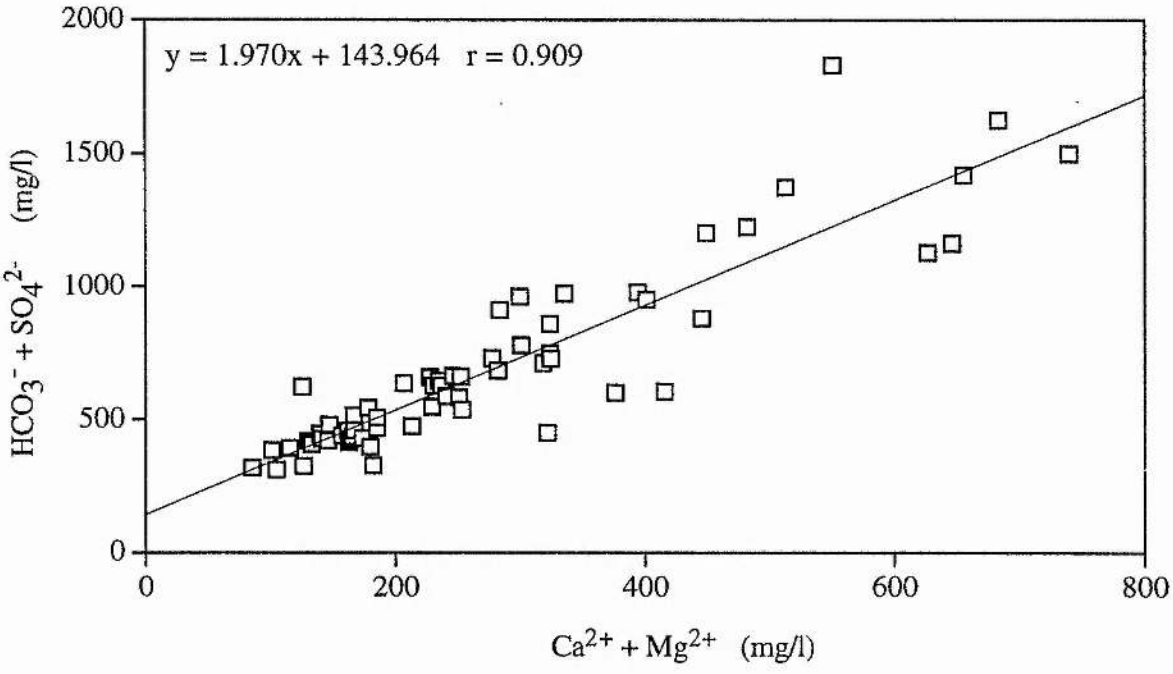

Figure 4.19 The correlation between (Ca^{2+}+ Mg^{2+}) and (HCO_3^- + SO_4^{2-}) of Wadi Habawnah groundwater.

4.11.2 Piper Trilinear Diagram

The concentrations of the major cations (Ca^{2+}, Mg^{2+}, $Na^{+} + K^{+}$) and major anions (Cl^{-}, SO_4^{2-}, CO_3^{2-}, HCO_3^{-}) of the study area are plotted on two base triangular diagrams based on the percentage of each. Each apex of a triangle represents a 100% concentration of one of the three constituents.

The diamond-shaped field between these two triangles is used to represent the composition of water with respect to both cations and anions (Hem, 1989; Fetter, 1988).

The data for each groundwater sample from Wadi Habawnah (62 wells) and Wadi Baysh (20 wells) were plotted as percentage milliequivalents (Figures 4.20 and 21). These figures show that there are distinct differences between the water types in the two wadis.

The diagram for Wadi Habawnah (Figure 4.20) shows that the cation composition is dominated by calcium (40-60%) with subsidiary magnesium (20-30%), while sulphate (40-60%) is the dominant anion with subsidiary chloride (30-50%). In terms of hydrochemical facies, the groundwater of Wadi Habawnah (Figure 4.21) is principally a calcium-sulphate type. Sodium-chloride and magnesium-sulphate water types are also present but less common.

For Wadi Baysh, the trilinear diagram differs from that of Wadi Habawnah. Chloride, the stable fraction, normally represents 20-30% of the groundwater anion (Figures 4.22 and 4.23). The water type is characteristically of the calcium-sulphate and sodium-chloride facies with some examples of magnesium-sulphate or calcium bicarbonate water types.

However, the Maclaren chemistry data of Wadi Habawnah groundwater from 1978 was plotted in Figures 4.24 and 4.25. They show that the cation composition is dominated by sodium, while sulphate is the dominant anion with subsidiary chloride. This change in the water types of Wadi Habawnah may be considered to be result of an ion exchange reaction in which the calcium replaces the sodium (see section 4.15 for further discussion).

4.11.3 Durov's Diagram

Durov (1948) developed a diagram based upon the percentage of major ion milli-equivalent values, in which the cations and anions together total 100%. It differs from the

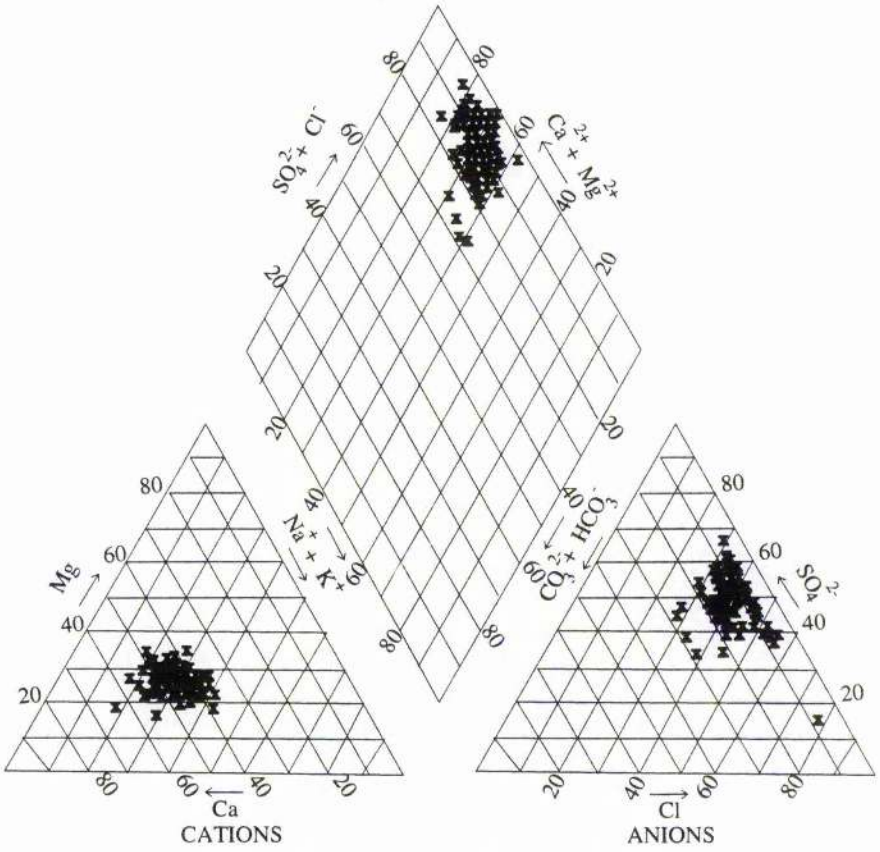

Figure 4.20 A trilinear diagram showing the chemical composition of water samples of Wadi Habawnah (Field data 1990).

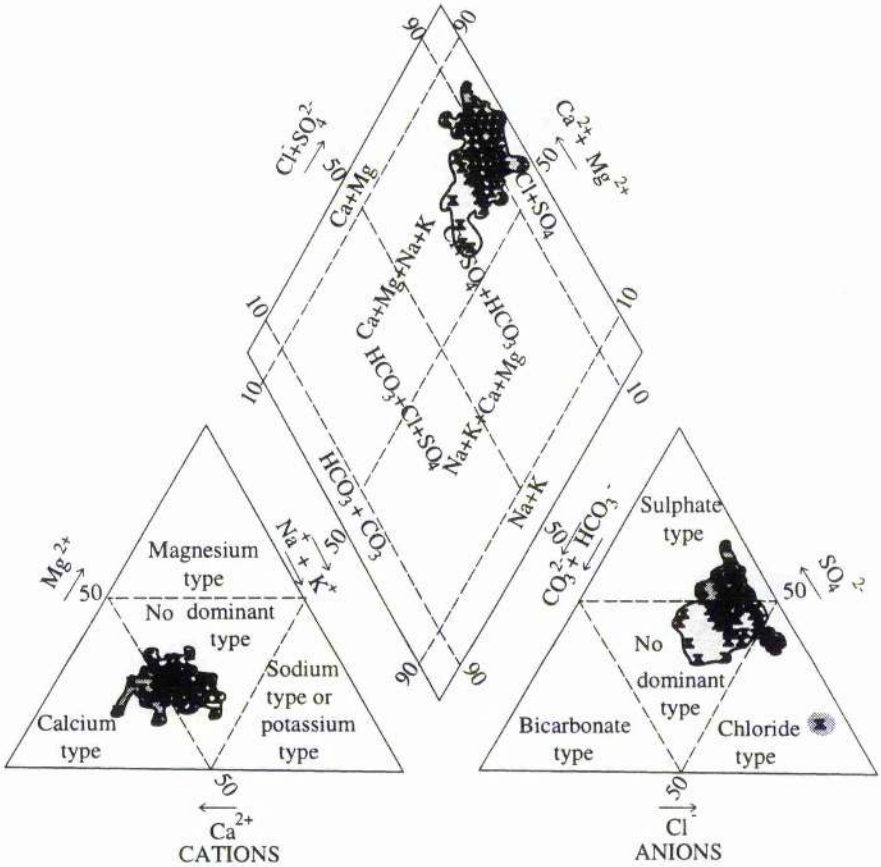

Figure 4.21 A trilinear diagram showing the chemical composition of water samples and the dominant chemical facies in Wadi Habawnah (Field data 1990).

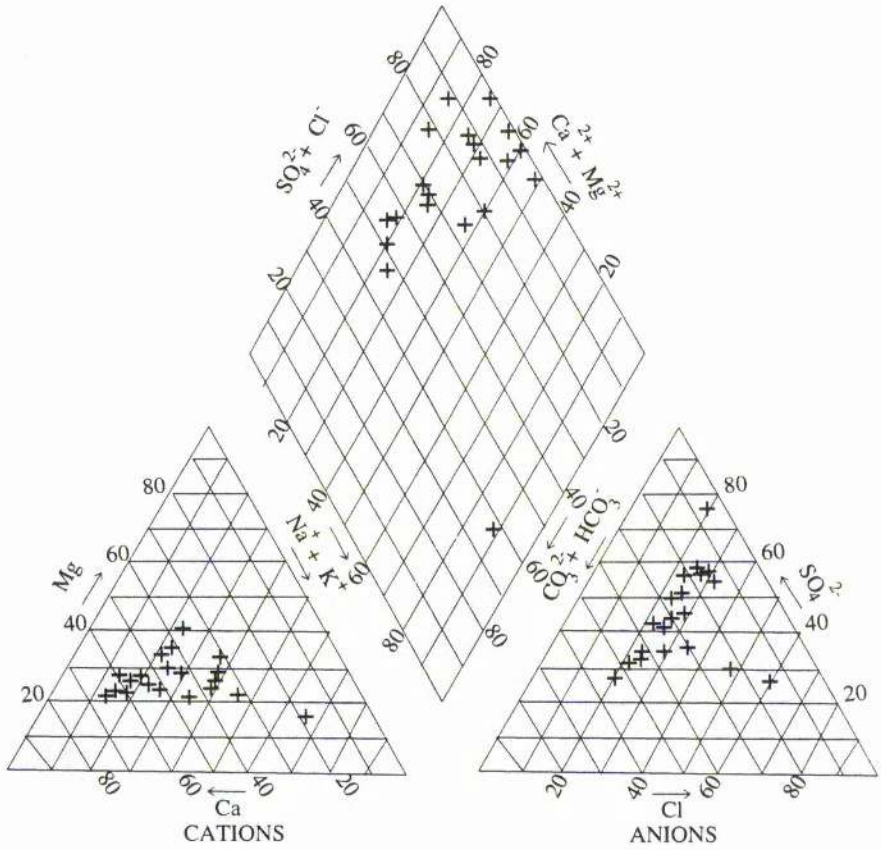

Figure 4.22 A trilinear diagram showing the chemical composition of water samples of Wadi Baysh (Field data 1990).

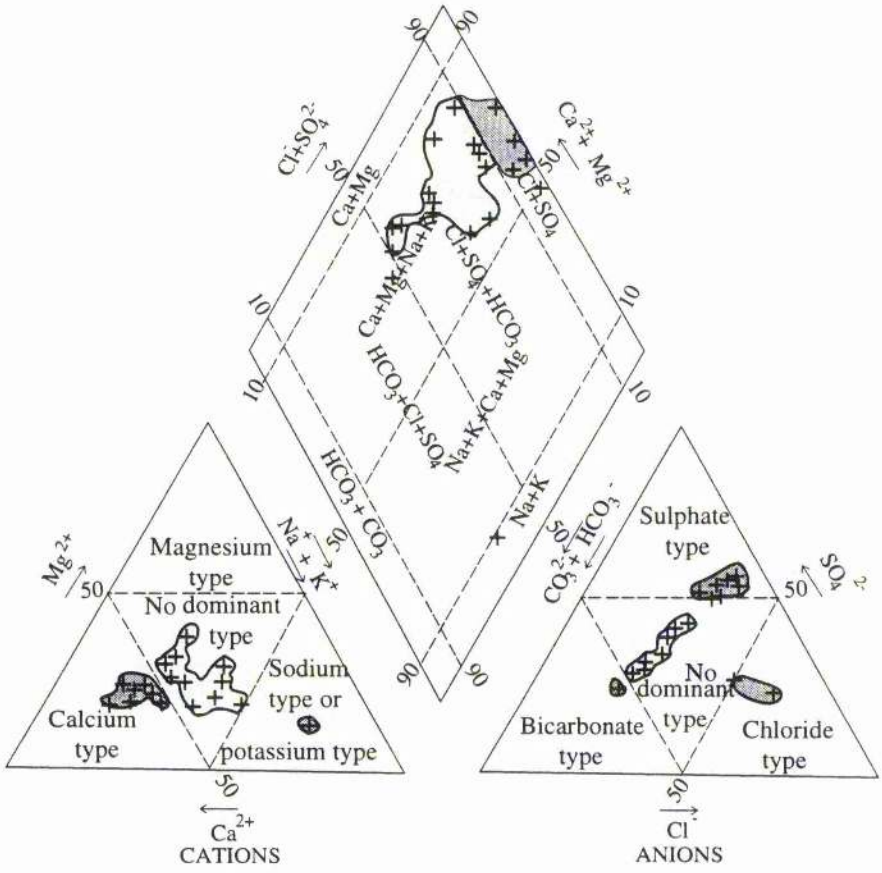

Figure 4.23 A trilinear diagram showing the chemical composition of water samples and the dominant chemical facies in Wadi Baysh (Field data 1990).

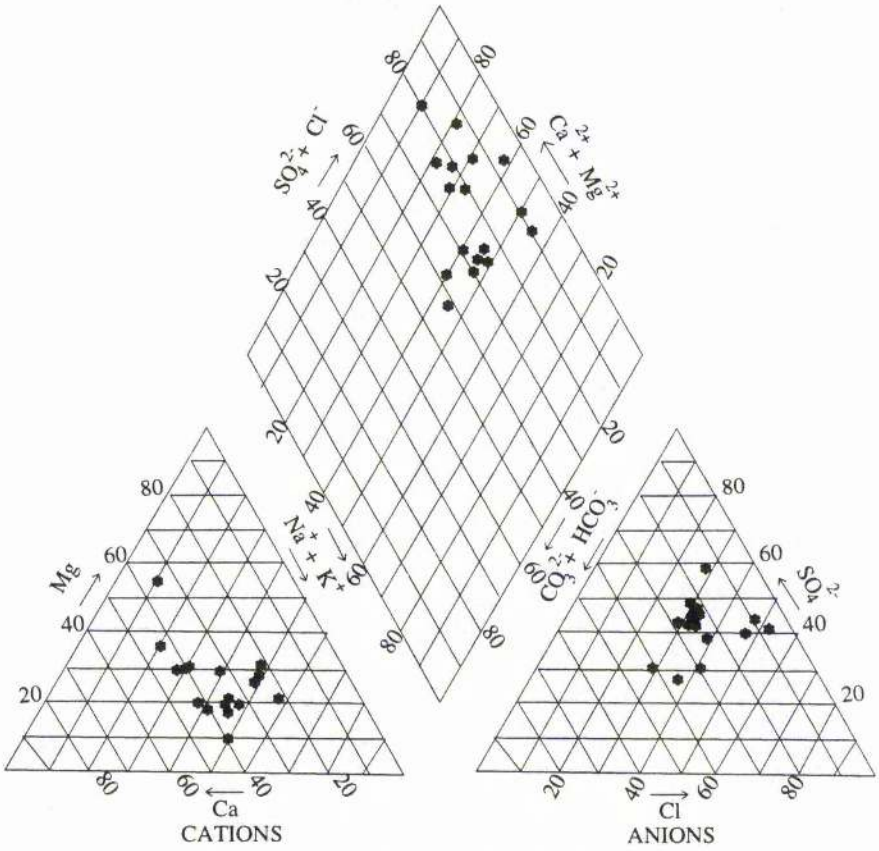

Figure 4.24 A trilinear diagram showing the chemical composition of water samples of Wadi Habawnah (Using Maclaren data 1978).

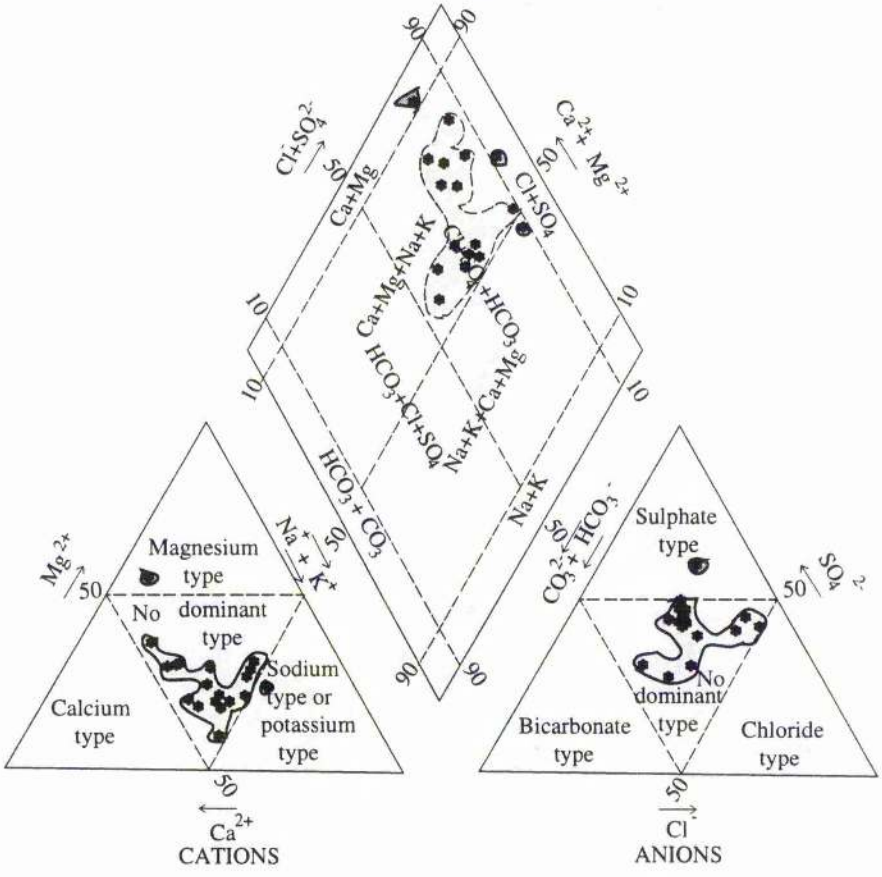

Figure 4.25 A trilinear diagram showing the chemical composition of water samples and the dominant chemical facies in Wadi Habawnah (Using Maclaren data 1978).

Trilinear diagram in which both the cations and the anions each separately total 100%. The percentages of the cation and anion concentrations are plotted on triangular diagrams and projected into a square main field as shown in Figures 4.26.

Lloyd and Heathcote (1985) expanded the Durov diagram into nine convenient fields (Figure 4.26) to provide a better classification which leads to an understanding of the hydrochemical groupings of groundwater composition.

Field 1- HCO_3^- and Ca^{2+} dominant, frequently indicates recharging of waters in limestone or sandstone.

Field 2- Indicates waters often associated with dolomites; where Ca^{2+} and Na^+ are important and partial ion exchange may be indicated.

Field 3- HCO_3^- and Ca^{2+} dominant, normally indicates ion-exchanged waters.

Field 4- Sulphate and calcium dominance frequently indicates a recharge water in lava and gypsiferous deposits; otherwise a mixed water or a water exhibiting simple dissolution (see Figure 4.26).

Field 5- No dominant anion or cation, indicates water exhibiting simple dissolution or mixing.

Field 6- SO_4^{2-} dominant or anions indiscriminate and Na^+ dominant, is a water type not frequently encountered and indicates probable mixing influences.

Field 7- Cl^- and Ca^{2+} dominant, is infrequently encountered; the waters may result from reverse ion exchange of sodium and chloride waters.

Field 8- Cl^- dominant and no dominant cation indicates that the groundwaters may be related to reverse ion exchange of sodium and chloride waters.

Field 9- Cl^- and Na^+ dominant frequently indicates end-point waters.

The Baysh and Habawnah data (Tables 4.1 & 4.2) were plotted using the expanded Durov diagram (Figures 4.27 and 4.28).

In Wadi Baysh (Figure 4.27) a simple dissolution is dominant for 30% of the samples plot in Field 1 and 10% each in Fields 5 and 9. The water type could therefore be Ca $(HCO_3)_2$ and NaCl. 30% of the samples fall in Field 4 where Ca^{2+} and SO_4^{2-} are dominant suggesting a mixed water or a water exhibiting simple dissolution within basin

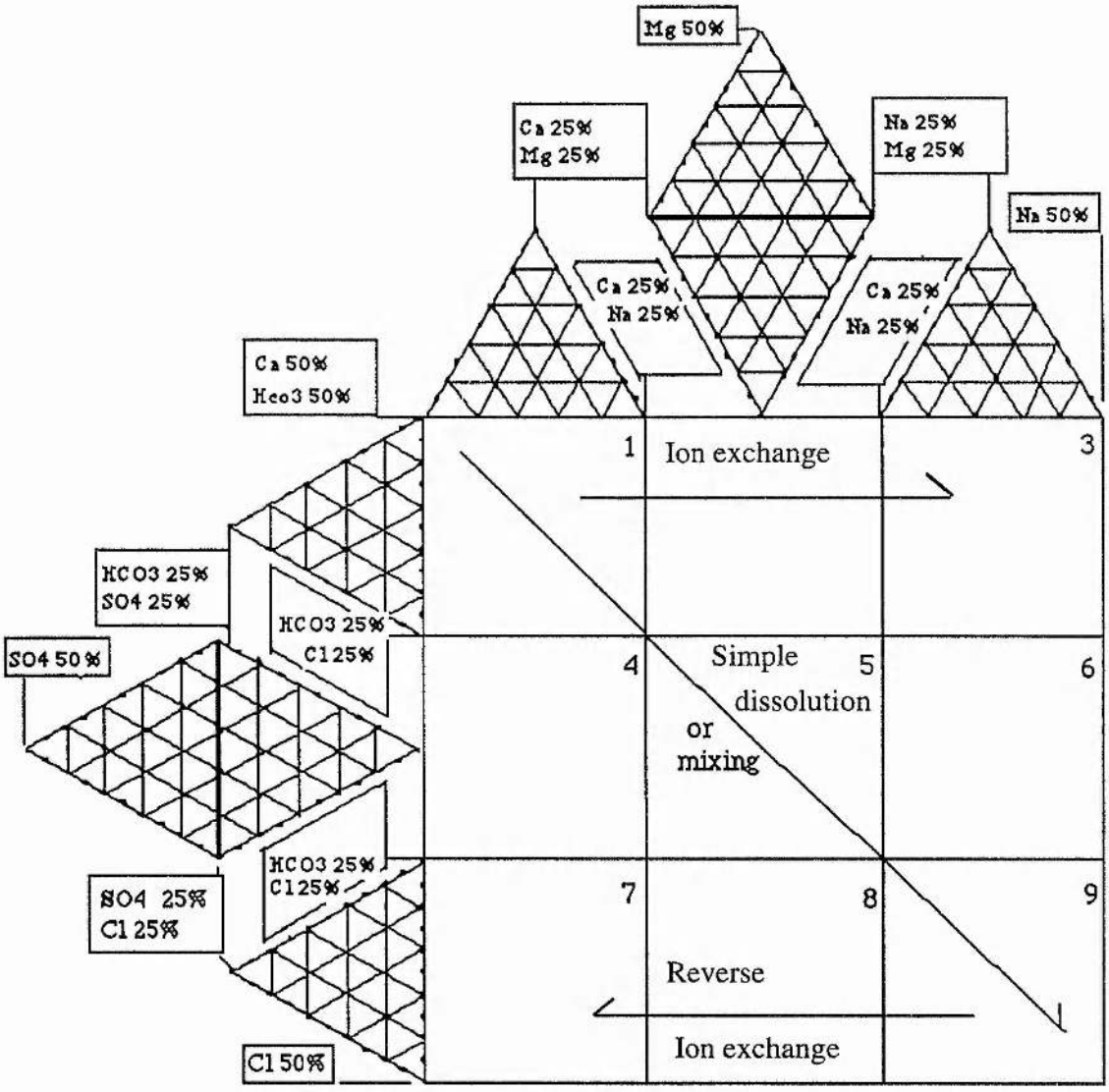

Figure 4.26 An expanded Durov diagram with subdivision and processes after Lloyd and Heathcote (1985).

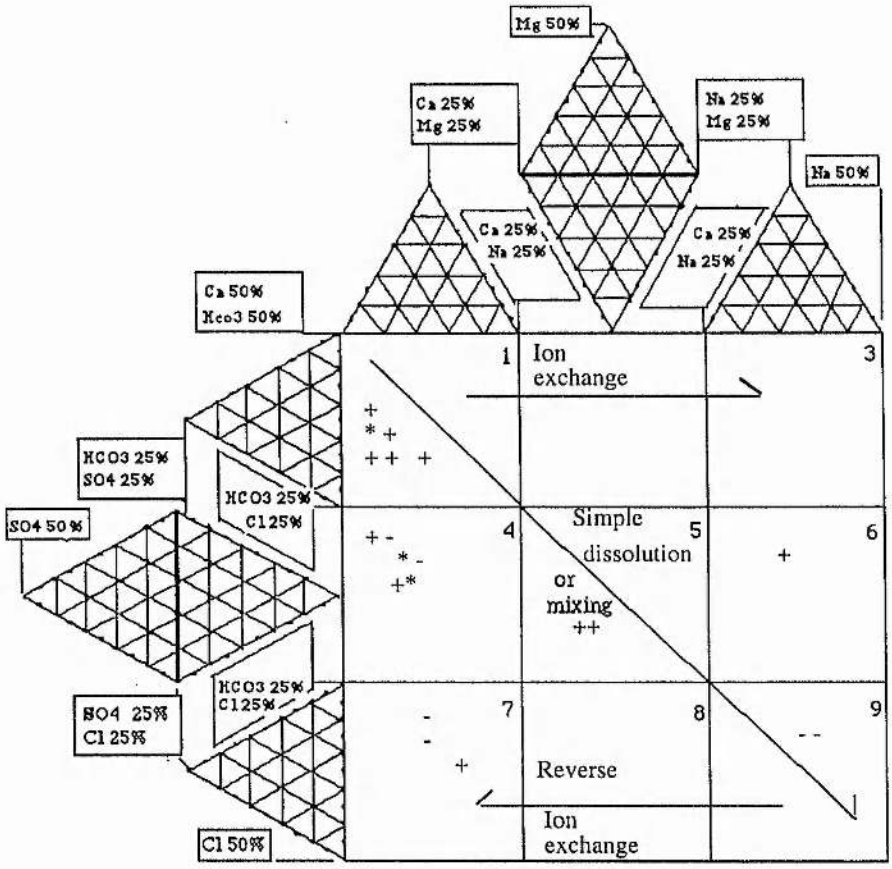

* Upper part Field Percentage (1) 05% (4)10 %
\+ Middle part Field Percentage (1) 25% (4)10% (5) 10% (6)05% (7) 05%
\- Lower Part Field Percentage (1) ---- (4)10% (5) ------(6) ---- (7)10% (9) 10%

Total Field Percentage (1) 30% (4)30% (5)10% (6) 05% (7) 15% (9) 10%

Figure 4.27 Classification of the percentage of groundwater types of Wadi Baysh using an expanded Durov diagram after Lloyd and Heathcote (1985).

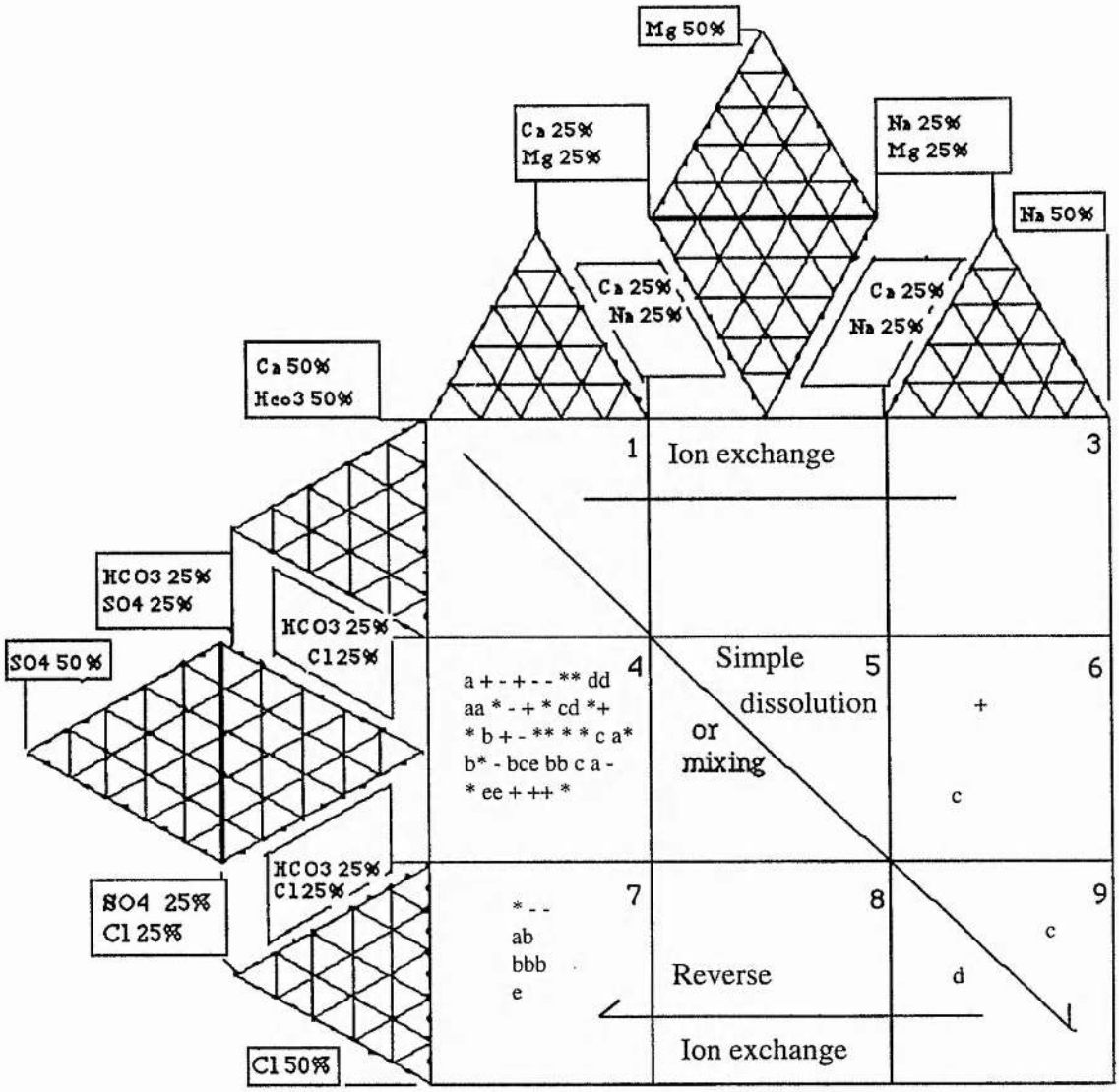

* Al Khaneq	Field Percentage (4) 21% (6) ----- (7) 0.169 (9) -----
+ Al Harshaf	Field Percentage (4) 13% (6) 1.6%(7) 3.4% (9) -----
- Al Majama	Field Percentage (4) 11% (6) ----- (7)1.6% (9) -----
a Habawnah	Field Percentage (4) 08% (6) ----- (7) 6.4% (9) -----
b Al Muntasher	Field Percentage (4) 08% (6) ----- (7) ------ (9) -----
c Al Jifader	Field Percentage (4) 08% (6)1.6% (7) ------- (9) -----
d Group **	Field Percentage (4) 05% (6)1.6% (7) 0.169(9)1.6%
e Al Husayniyh	Field Percentage (4) 05% (6) ----- (7) 0.169 (9) -----
Total	Field Percentage (4) 79% (6)4.6%(7)14.6%(9)1.6%

**Morykhah , Al Nagah and Al Dayqeh

Figure 4.28 Classification of the percentage of groundwater types of Wadi Habawnah using the expanded Durov diagram after Lloyd and Heathcote (1985).

fill. However, 15% and 5% of the data plot in Fields 7, and 6 respectively which clearly reflect a reverse ion exchange in which the water chemistry may result from reverse ion exchange of Na - Cl water. The 5% occurrence in of Field 6 shows SO_4^{2-} and Na^+ as the dominant ions. These waters therefore exhibit mixing influences.

In Wadi Habawnah (Figure 4.28) 79% of the samples plot in Field 4, which indicates a $CaSO_4$ water type reflecting a simple dissolution or mixing. This may be due to the fact that recharge of the aquifer in the upper part of the wadi occurs by runoff over basement rocks.

Of the remaining samples, 14.6%, 4.8% and 1.6 % plot within Fields 7, 6 and 9, respectively.

In Field 7 the samples reflect Ca^{2+} as the dominant ion. This may result from reverse ion exchange. The rest of the samples indicate probable mixing influences.

The expanded Durov diagram for the Wadi Baysh groundwater samples (Figure 4.27) shows that 6% reflect $CaSO_4$ and NaCl water types. This compares with 79% of the Wadi Habawnah samples being of Ca SO_4 type, a similar interpretation to that derived from the Piper diagram. About 45% of the Wadi Habawnah samples, out of the 79% which plot in Field 4, are from the upper part of the wadi (Al Khaneg, Al Harshaf and Al Majma). In Wadi Baysh the middle parts influence the water type of Field 1, while in Field 2 the water shows equal influence from all parts of the wadi. This may be as a result of mixing processes and evaporation effects.

4.12 Aqueous Speciation and Saturation Data

Robertson (1991) indicated that the selection of phases is based partly on the groundwater saturation state with respect to the possible minerals, during the derived mass transfer that must be consistent with thermodynamic or solubility constraints placed on the reactants and products. The derived minerals, dissolved or precipitated, should agree with those observed and those determined by the aqueous speciation.

The speciation of the solution supplies the activities and concentrations of the dissolved species, including some of those not analysed, calculates the partial pressure of several gases, and determines the mineral saturation indices. To accomplish such analysis

the author applied the WATEQF hydrochemical model.

4.12.1 Application of WATEQF Hydrochemical Model

The WATEQF Hydrochemical Model determines the detailed composition of a solution, the concentrations and activities of all species.

Since the major ions (Ca^{2+}, Mg^{2+}, $Na^{+}+K^{+}$, SO_4^{2-}, $Cl^{-}$and HCO_3^{-}) dominate the water content, the states of the water (under saturated or super saturated) were evaluated. Based on the chemical analysis and site measurement of temperature, and pH for the groundwater samples, the WATEQF Model was applied. Truesdell and Jones (1977) indicate that the examination of reaction states may suggest the origin of the dissolved constituents and assist in the prediction of the chemical effects of groundwater production, recharge and irrigation.

The evaluation of the groundwater equilibrium state with respect to soluble solids, as a result of the continued action of chemical processes, is made in terms of saturation indices (SI). A saturation indices is defined as a measure of the thermodynamic state of a solution relative to equilibrium with a specified solid-phase mineral. In other words the saturation indices describe the saturation state of dissolved species with respect to selected mineral phases. In terms of the saturation indices(SI), the saturation state is defined as follows:

$$SI = \text{Log}\frac{IAP}{K},$$

where IAP is the ion activity product and K is the equilibrium constant. The term $\frac{IAP}{K}$ defines the ratio of the aqueous ion activity product to the solubility products in equilibrium with a given mineral phase

A water is in equilibrium with a given mineral phase when the saturation indice is zero. If the SI is less than zero, the groundwater is undersaturated with respect to a mineral and the mineral will dissolve. If the SI is greater than zero, the water is saturated or supersaturated with respect to a mineral and the mineral may precipitate.

Input data required for the speciation are a chemical analysis, field pH, temperature, alkalinity.

4.12.1.1 Description of Model Results

The model output shows a list of results from 20 and 62 water samples of Wadi Baysh and Wadi Habawnah, for which species calculations have been completed. Model calculated results of water sample HS1 were chosen to demonstrate the output Tables 4.9.

Tables 4.10 and 4.11 show that most of the groundwater samples are sub-saturated except for a few samples which are supersaturated. The groundwater of both wadis are sub-saturated with respect to anhydrite and gypsum. However, there are six, eleven and ten sites in the middle and the lower parts of Wadi Baysh where the water are supersaturated with respect to aragonite, calcite and dolomite. In Wadi Habawnah, the super saturated sites in respect to aragonite, calcite and dolomite were found along the wadi in ten, fifteen and twenty sites respectively.

4.13 Application of Cluster and Principal Component Analysis to Groundwater Data

4.13.1 Application of Cluster Analysis

Cluster analysis was used in this study to classify the groundwater samples into related groups based on the similarities and differences using the major constituents and other parameters such as pH, EC and TDS as well as calculated variables such as saturation indices for aragonite, calcite and dolomite. The wide range in the units and values among the variables were converted to a standard form to remove the effects of using different units in describing the variables (see Table 4.12 and 4.13).

The cluster results are displayed in dendrograms of two subsets of 62 and 20 samples. The sequential numbers listed on the left are the field numbers (see Figure 4.29 and Table 14). In Figure 4.29 the X- axis of the diagram indicates the value of the distance function, the values being higher for lower similarity (Davis, 1986). The cluster can be selected at similar distances and each cluster then represents a facies.

4.13.1.1 Results

Based on the Figure 4.29, the satiable coefficients for Wadi Habawnah and Baysh are 7.352 and 2.503, respectively. Four clusters were determined in each wadi which may

Table 4.9 A modified form of the WATEQF model calculated results output for well HS1.

Speciation and Calculation for Well HS1, Wadi Habawnah.

Total Concenteration of Input Species in Molalities.

Element	Molality	Log Molality
Ca^{++}	$7.40*10^{-03}$	-2.13
Mg^{++}	$1.20*10^{-02}$	-1.92
Na^{+}	$1.60*10^{-02}$	-1.97
K^{+}	$2.60*10^{-04}$	-3.58
Cl^{-}	$2.40*10^{-02}$	-1.61
SO_4^{--}	$1.30*10^{-02}$	-1.8
HCO_3^{-}	$2.50*10^{-03}$	-2.6
Fe^{++}	$1.00*10^{-05}$	-4.9

Description of solution

pH	7.10
PE	0.00
Activity H2O	1.00
Ionic Strength	0.07
Temperature	27.00
Tot. Alkalinity	2.27MEQ

Result

Phase	log IAP	Log KT	Log IAP/KT(S.I)
Anhydrite	-5.063	-4.405	-0.658
Aragonite	-8.608	-8.349	-0.259
Calcite	-8.608	-8.491	-0.117
Dolmite	-16.9	-17.136	0.14
Gypsum	-5.064	3.46	-0.461
Halite	-3.606	6.42	-5.19

Table 4.10 Summary of saturation indices of certain mineral matrix of Wadi Baysh groundwater .

Summary of saturation indices of certain mineral matrix of Wadi Baysh Groundwater (Upper Part).

Sample No.	Ionic Strength	Anhydrite SI	Aragonite SI	Calcite SI	Dolomite SI	Gypsum SI
BU1	$8.40*10^{-2}$	-1.86	-0.509	-0.37	-0.628	-1.7
BU2	$9.40*10^{-3}$	-1.8	-0.354	-0.216	-0.298	-1.656
BU3	$1.20*10^{-2}$	-1.545	-0.227	-0.088	-0.132	-1.4

Summary of Saturation Indices of certain mineral matrix of Wadi Baysh Groundwater (Middle Part).

Sample No.	Ionic Strength	Anhydrite SI	Aragonite SI	Calcite SI	Dolomite SI	Gypsum SI
BM4	$1.58*10^{-2}$	-1.378	- 0.077	+ 0.061	- 0.186	-1.23
BM5	$1.10*10^{-2}$	-1.67	- 0.617	- 0.478	- 0.701	-1.515
BM6	$1.08*10^{-2}$	-1.707	- 0.593	- 0.455	- 0.686	-1.566
BM7	$1.66*10^{-2}$	-1.33	- 0.408	- 0.268	- 0.46	-1.171
BM8	$1.57*10^{-2}$	-1.168	+ 0.413	- 0.275	- 0.735	-1.027
BM9	$2.33*10^{-2}$	-1.218	+ 0.101	+ 0.24	+ 0.343	-1.059
BM10	$5.16*10^{-2}$	-0.485	- 0.068	+ 0.071	+ 0.22	-0.336
BM11	$1.22*10^{-2}$	-1.6	- 0.034	+ 0.105	+ 0.103	-1.45
BM12	$1.43*10^{-2}$	-1.418	+ 0.067	+ 0.206	+ 0.215	-1.268
BM13	$1.22*10^{-2}$	-1.69	- 0.047	+ 0.092	+ 0.246	-1.541
BM14	$2.04*10^{-2}$	-1.213	+ 0.487	+ 0.626	+ 0.989	-1.06

Summary of Saturation Indices of certain mineral matrix of Wadi Baysh Groundwater(lower Part).

Sample No.	Ionic Strength	Anhydrite SI	Aragonite SI	Calcite SI	Dolomite SI	Gypsum SI
BL15	$3.71*10^{-2}$	- 0.731	+ 0.236	+ 0.375	+ 0.74	- 0.573
BL16	$4.78*10^{-2}$	- 3.1	- 0.138	+ 0.001	- 0.135	- 2.919
BL17	$7.70*10^{-2}$	*	- 0.141	- 0.002	+ 0.021	*
BL18	$8.30*10^{-2}$	*	- 0.111	+ 0.028	+ 0.083	*
BL19	$5.18*10^{-2}$	*	- 0.332	- 0.193	- 0.505	*
BL20	$3.72*10^{-2}$	- 0.0709	+ 0.367	+ 0.506	+ 1.007	- 0.56

*NO PHAS

Table 4.11 Summary of saturation indices of certain mineral matrix of Wadi Habawnah groundwater and its major tributaries.

Saturation Indices (SI) of certain mineral matrix of Al-KHANEQ.

Sample No.	Ionic Strength	Anhydrite SI	Aragonite SI	Calcite SI	Dolomite SI	Gypsum SI
KH1	0.01	-1.582	- 0.672	- 0.529	- 0.875	- 1.385
KH2	0.03	-1.13	- 0.372	- 0.229	- 0.102	- 0.922
KH3	0.05	-0.649	- 0.059	+0.084	+ 0.449	+0.452
KH4	0.03	-1.024	- 1.607	- 1.464	- 2.622	- 0.817
KH5	0.03	-1.02	- 1.231	- 1.089	- 1.846	- 0.823
KH6	0.06	-0.865	- 1.237	- 1.094	- 1.67	- 0.658
KH7	0.08	-0.582	+0.335	- 0.191	- 0.056	- 0.375
KH8	0.03	-1.058	- 0.439	- 0.296	- 0.331	- 5.839
KH9	0.05	-0.917	- 1.93	- 1.786	- 3.206	- 0.71
KH10	0.03	-1.21	- 0.341	- 0.198	- 0.022	- 1.003
KH11	0.01	-1.83	- 0.572	- 0.429	- 0.594	- 1.622
KH12	0.01	-1.683	- 0.865	- 0.722	- 1.143	- 1.475
KH13	0.02	-1.417	- 0.435	- 0.292	- 0.272	- .21
KH14	0.05	-0.761	- 1.76	- 1.617	- 2.851	- 0.553

Saturation Indices (SI) of certain mineral matrix of Al-HARSHAF

Sample No.	Ionic Strength	Anhydrite SI	Aragonite SI	Calcite SI	Dolomite SI	Gypsum SI
HR1	0.04	-0.843	+0.198	+0.341	+0.682	-0.641
HR2	0.04	-0.827	+0.288	+0.431	+0.863	-0.62
HR3	0.04	-1.001	- 0.236	- 0.094	+0.194	-0.804
HR4	0.03	-0.891	- 0.85	- 0.708	-1.615	-0.696
HR5	0.07	-0.4	- 0.593	- 0.451	-0.946	-0.213
HR6	0.03	-0.924	- 0.874	- 0.732	-1.573	-0.739
HR7	0.03	-0.993	- 0.098	+0.044	+0.024	-5.934
HR8	0.04	-0.651	- 0.727	- 0.59	-1.335	-0.454
HR9	0.04	-0.748	+0.07	+0.212	+0.384	-0.551

Saturation Indices (SI) of certain mineral matrix of AL-MAJMAA

Sample No.	Ionic Strength	Anhydrite SI	Aragonite SI	Calcite SI	Dolomite SI	Gypsum SI
MJ1	0.02	-1.222	-0.414	-0.272	-0.648	-1.025
MJ2	0.03	-0.99	-0.161	-0.019	+0.13	-0.793
MJ3	0.02	-1.27	-0.114	+0.028	+0.028	-1.073
MJ4	0.02	-1.252	-0.072	+0.07	+0.106	-1.055
MJ5	0.03	-1.032	+0.085	+0.227	+0.435	-0.835
MJ6	0.03	-0.873	+0.696	+0.838	+1.668	-0.676
MJ7	0.02	-1.289	-0.536	-0.395	- 0.827	-1.108
MJ8	0.03	-0.756	-0.147	-0.004	- 0.44	-0.553
MJ9	0.01	-1.629	-0.288	-0.146	+0.035	-1.431

Saturation Indices (SI) of certain mineral matrix of HABAWNA

Sample No.	Ionic Strength	Anhydrite SI	Aragonite SI	Calcite SI	Dolomite SI	Gypsum SI
HB1	0.02	-1.386	- 0.537	-0.394	- 0.392	-1.189
HB2	0.02	-1.48	+0.157	+0.299	+1.097	-1.282
HB3	0.03	-1.218	- 0.463	-0.321	- 0.188	-1.02
HB4	0.02	-1.624	- 0.51	-0.368	- 0.157	-1.427
HB5	0.03	-1.334	+0.273	+0.416	+1.266	-1.137
HB6	0.02	-1.566	- 0.495	-0.352	+0.213	-1.369

Continued on next page

Table 4.11 continued

Saturation Indices (SI) of certain mineral matrix of Al-MUNTASHER

Sample No.	Ionic Strength	Anhydrite SI	Aragonite SI	Calcite SI	Dolomite SI	Gypsum SI
MT1	0.04	-0.86	- 0.14	+0.002	-0.076	- 0.673
MT2	0.02	-1.246	- 0.571	-0.429	-0.963	- 1.059
MT3	0.02	-1.429	- 1.319	-1.178	-2.397	- 1.241
MT4	0.02	-1.161	- 1.01	-0.869	-1.775	- 0.974
MT5	0.02	-1.265	- 0.686	-0.544	-1.139	+0.982
MT6	0.03	-1.056	- 0.6	-0.458	-1.331	- 0.865
MT7	0.02	-1.337	- 0.246	-0.105	-0.578	- 1.154
MT8	0.02	-1.176	- 0.1	+0.043	-0.091	- 0.979
MT9	0.02	-1.126	+0.191	+0.332	+0.339	- 0.938

Saturation Indices (SI) of certain mineral matrix of Al-JIFA.

Sample No.	Ionic Strength	Anhydrite SI	Aragonite SI	Calcite SI	Dolomite SI	Gypsum SI
GF1	0.02	-1.510	-0.564	-0.421	-0.411	-1.313
GF2	0.02	-1.510	-0.081	-0.668	-0.841	-1.323
GF3	0.03	-1.275	-0.411	-0.269	-0.028	-1.087
GF4	0.02	-1.443	-0.687	-0.546	-0.625	-1.256
GF5	0.02	-1.390	-0.658	-0.516	-0.761	-1.193
GF6	0.06	-0.791	-0.646	-0.504	-0.506	-0.604
GF7	0.02	-1.678	-1.012	-0.871	-1.367	-1.49

Saturation Indices (SI) of certain mineral matrix of MORYKHAH

Sample No.	Ionic Strength	Anhydrite SI	Aragonite SI	Calcite SI	Dolomite SI	Gypsum SI
MR	0.02	-1.425	-0.302	-0.16	-0.293	-1.228
NG-1	0.04	-0.649	-0.214	-0.074	-0.261	-0.481
NG-2	0.02	-1.556	-0.499	-0.357	-0.31	-4.008
DY	0.02	-1.235	-0.284	-0.142	+0.097	-1.047

Saturation Indices (SI) of certain mineral matrix of Al-HUSAYNIYAH

Sample No.	Ionic Strength	Anhydrite SI	Aragonite SI	Calcite SI	Dolomite SI	Gypsum SI
HS-1	0.07	-0.658	-0.259	-0.117	+0.148	-0.461
HS-2	0.05	-0.761	-0.467	-0.324	- 0.355	-0.564
HS-3	0.07	-0.547	-0.096	+0.045	+0.417	-0.361
HS-4	0.04	-1.145	+0.265	-0.123	+0.24	-0.958

Table 4.12 Standardized Wadi Baysh cluster analyses.

Cluster 1

Sample	Na^+ meq/l	K^+ meq/l	Ca^{++} meq/l	Mg^{++} meq/l	SO_4^{--} meq/l	Cl^- meq/l	HCO_3^- meq/l	TEMP C	pH	EC µmhos/cm	TDS ppm	Aragonite SI**	Calcite SI**	Dolomite SI**
BL-16	-1.037	-1.291	-0.751	-0.867	1.500	-0.986	0.515	-0.867	-0.548	-0.627	-0.988	0.417	0.417	-0.004
BL-17	0.388	-0.155	0.925	0.880	-0.500	0.715	1.143	-0.867	-1.095	-0.688	0.663	0.388	0.388	0.587
BL-18	1.209	0.362	0.798	0.850	-0.500	0.996	-0.666	0.867	1.095	1.454	1.037	0.682	0.682	0.822
BL-19	-0.562	1.085	-0.972	-0.867	-0.500	-0.725	-0.992	0.867	0.548	-0.141	-0.713	-1.487	-1.487	-1.405

Cluster 1

Sample	Na^+ meq/l	K^+ meq/l	Ca^{++} meq/l	Mg^{++} meq/l	SO_4^{--} meq/l	Cl^- meq/l	HCO_3^- meq/l	TEMP C	pH	EC µmhos/cm	TDS ppm	Aragonite SI**	Calcite SI**	Dolomite SI**
BL-20	-0.018	-0.635	0.506	0.367	0.130	0.740	0.057	-0.730	1.790	0.599	0.215	0.653	0.653	0.953
BL-15	0.260	-0.248	0.112	0.202	0.163	0.468	0.149	-0.730	-0.447	0.790	0.233	0.052	0.052	0.220
BM-14	-0.919	0.914	-1.153	-1.212	-0.900	-1.732	1.556	1.095	-0.447	-1.002	-1.000	1.204	1.204	0.904
BM-10	1.535	1.146	1.330	1.360	1.521	0.060	-0.881	1.095	-0.447	0.790	1.449	-1.342	-1.342	-1.209

Cluster 3

Sample	Na^+ meq/l	K^+ meq/l	Ca^{++} meq/l	Mg^{++} meq/l	SO_4^{--} meq/l	Cl^- meq/l	HCO_3^- meq/l	TEMP C	pH	EC µmhos/cm	TDS ppm	Aragonite SI**	Calcite SI**	Dolomite SI**
BM-9	-0.855	-1.177	-0.795	-0.714	-0.912	0.468	-0.881	-0.730	-0.447	-1.178	-0.896	-0.567	-0.567	-0.871
BM-7	2.657	-1.531	0.058	1.725	1.900	0.562	-0.359	-1.968	-0.944	0.837	1.708	-0.603	-0.467	-0.434
BM-13	-0.254	0.819	-0.291	0.349	-0.685	-0.619	1.878	1.124	-0.944	-0.640	-0.121	0.539	1.013	1.444
BM-12	-0.298	0.688	0.991	-0.569	-0.076	0.040	1.391	-0.422	0.540	0.194	0.569	0.899	1.482	1.362
BM-11	-0.334	-0.226	0.245	-0.683	-0.671	-0.619	1.189	-0.422	0.540	-0.496	-0.262	0.580	1.067	1.064
BM-4	-0.718	1.341	1.958	-0.661	-0.295	2.689	-0.165	-0.422	-0.944	1.795	0.902	0.444	0.886	0.295
BU-3	-0.486	1.341	-0.058	0.716	-0.175	-0.523	-0.772	-0.422	0.540	-0.122	-0.420	-0.031	0.273	0.439
BU-2	-0.718	0.296	-0.991	-0.890	-0.770	-0.523	-0.165	-0.422	0.540	-1.560	-1.135	-0.432	-0.253	-0.003

Cluster 4

Sample	Na^+ meq/l	K^+ meq/l	Ca^{++} meq/l	Mg^{++} meq/l	SO_4^{--} meq/l	Cl^- meq/l	HCO_3^- meq/l	TEMP C	pH	EC µmhos/cm	TDS ppm	Aragonite SI**	Calcite SI**	Dolomite SI**
BU-1	-0.763	-0.095	-1.072	-1.303	-0.961	-0.523	-0.691	1.124	0.540	-1.081	-1.467	-0.923	-0.886	-0.880
BM-6	0.639	-0.356	-1.037	0.119	-0.140	-0.523	-0.562	1.124	-0.944	-0.122	-0.594	-1.188	-1.235	-1.035
BM-5	-0.298	-1.009	-0.839	1.587	-0.076	-0.523	-0.772	-0.422	-0.944	-0.122	-0.470	-1.264	-1.330	-1.074
BM-8	0.568	-1.270	1.061	-0.385	1.950	0.562	-0.975	1.124	2.024	1.316	1.293	1.993	-0.495	-1.165

** Saturated indixes

Table 4.13 Standardized Wadi Habawnah cluster analyses.

Cluster 1

Sample	Na^+ meq/l	K^+ meq/l	Ca^{++} meq/l	Mg^{++} meq/l	SO_4^{--} meq/l	Cl^- meq/l	HCO_3^- meq/l	TEMP °C	pH	EC µmhos/cm	TDS ppm	Aragonite SI**	Calcite SI**
HS4	-1.2	-1.17	-0.84	-1.06	-1.4	-0.76	-0.44	0.76	1.11	-0.74	-1.28	1.37	0.84
MT1	-1.17	-0.93	-1.24	-1.09	-1.34	-0.61	-1.55	-0.63	1.11	-2.16	-1.27	0.2	0.1
HS2	0.33	0.27	-0.97	-0.11	-0.14	-1.07	1.75	0.76	-0.37	-0.07	-0.4	-0.74	-0.56
DY1	-0.35	-0.93	-0.95	-1.15	-0.59	-1	-0.44	0.76	0.37	0.69	-0.81	-0.22	0.5
GF6	-1.02	-0.69	1.06	-0.02	-0.16	0.02	0.63	-0.63	-0.74	0.69	-0.11	-1.26	-0.92
HS1	0.4	0.99	0.79	0.68	0.45	0.68	0.68	0.76	0.37	0.69	0.63	-0.14	0.62
HS3	0.85	0.63	0.79	1.29	0.94	0.53	0.63	0.76	0.74	-0.55	0.94	0.33	1.26
KH7	0.48	1.23	1.27	1.49	0.73	2.03	-0.79	-2.02	-1.86	0.78	1.23	1.57	0.14
HR5	1.67	-0.21	0.06	-0.05	1.49	0.17	-0.44	-0.49	-0.74	0.69	1.07	-1.11	-1.95

Cluster 2

Sample	Na^+ meq/l	K^+ meq/l	Ca^{++} meq/l	Mg^{++} meq/l	SO_4^{--} meq/l	Cl^- meq/l	HCO_3^- meq/l	TEMP °C	pH	EC µmhos/cm	TDS ppm	Aragonite SI**	Calcite SI**
KH4	-1	-0.78	-0.36	0.17	-0.15	-0.19	1.35	-1.32	-1.01	-0.06	-0.25	-0.86	-0.84
KH5	-0.7	-1.74	-0.2	0.29	-0.23	-0.19	0.17	-0.57	0.3	0.09	-0.24	0.06	0.39
KH9	0.72	0.78	0.6	1.04	0.33	1.14	0.17	-0.57	-1.68	1.11	0.75	-1.66	-1.76
KH14	0.72	-1.16	0.84	1.24	1.71	-0.03	-1.06	-0.57	-1.01	0.82	0.97	-1.24	-1.2
KH6	1.95	0.39	2.04	1.34	1.13	2.29	1.35	-0.57	-0.34	1.26	1.87	0.04	0.67
HR8	0.72	0.78	0.47	0.02	0.7	-0.03	0.17	-0.57	1.34	0.82	0.45	1.3	1.2
HR4	-0.05	-0.19	-0.44	-0.92	-0.36	-0.53	-1.06	0.34	1.01	-0.5	-0.47	1	0.75
HR6	-0.67	0.78	-0.62	-0.82	-0.42	-0.7	-1.06	0.95	1.01	-1.52	-0.63	0.94	0.82
MT3	-1.13	-1.74	-1.35	-1.42	-1.6	-0.93	-1.06	1.93	0.34	-1.37	-1.42	-0.16	-0.48
MT4	-0.67	-1.16	-0.99	-0.97	-1.11	-0.86	0.99	0.95	0.34	-0.64	-1.02	0.6	0.5

Cluster 3

Sample	Na^+ meq/l	K^+ meq/l	Ca^{++} meq/l	Mg^{++} meq/l	SO_4^{--} meq/l	Cl^- meq/l	HCO_3^- meq/l	TEMP °C	pH	EC µmhos/cm	TDS ppm	Aragonite SI**	Calcite SI**
HR9	1.08	1.02	0.77	0.54	1.02	0.98	0.8	-0.29	-2.03	-0.31	1.02	0.35	0.03
HR3	0.89	1.02	0.6	0.45	0.63	0.98	-0.58	-0.48	-0.08	0.91	0.72	-0.66	-0.29
HR1	1.27	1.37	-0.07	0.26	0.73	0.52	0.8	-0.78	0.57	0.7	0.68	0.77	0.54
HR2	1.46	1.02	0.14	0.45	0.82	0.52	2.23	-0.48	0.57	0.91	0.83	1.06	0.85
KH3	1.65	1.6	2.74	3.11	2.86	2.39	0.8	0.51	-0.4	2.53	2.74	-0.08	0.14
HB5	-0.66	-0.82	-0.6	-0.63	-0.8	-0.87	-0.58	1.5	-0.08	-1.32	-0.81	1.01	1.54
HB2	-1.14	-0.47	-1.14	-1.18	-1.16	-1.8	-0.58	1.5	1.88	-1.12	-1.33	0.63	1.25
MJ6	-0.44	-0.93	0.45	0.54	-0.05	0.52	-0.58	-2.37	2.2	0.7	0.09	2.4	2.22
MJ4	-1.39	-1.16	-1.5	-0.94	-1.35	-0.87	-0.58	-0.48	0.25	-1.12	-1.32	-0.12	-0.44
MJ2	-0.91	-2.08	-0.3	-0.44	-0.64	-0.41	-0.58	-0.48	-0.4	-0.72	-0.62	-0.41	-0.4
MJ5	-0.63	-0.24	-0.73	-0.35	-0.57	-0.1	0.8	-0.48	0.25	-1.32	-0.49	0.4	0.12
MJ8	0.32	0.22	1.46	-1.11	0.12	0.06	-0.58	1	-0.73	0.1	0.21	-0.36	-1.38
HB3	-0.06	-0.24	-0.32	-0.55	-0.27	-1.34	-0.58	1.5	-0.4	-0.11	-0.49	-1.4	-0.95
KH10	-1.01	-0.13	-0.54	-0.35	-0.48	-0.41	-2.01	0.51	0.25	-0.11	-0.6	-1	-0.66
HR7	0.32	0.45	-0.55	-0.47	-0.44	-0.41	-0.58	-0.19	-0.08	-0.31	-0.38	-0.2	-0.58
KH8	0.32	-0.47	-0.32	0.52	-0.1	0.52	0.8	-0.48	-1.05	0.3	0.1	-1.32	-1.19
KH2	-1.14	-0.13	-0.01	0.12	-0.31	-0.41	0.8	0.01	-0.73	0.3	-0.36	-1.1	-0.8

Continued on next page

Table 4.13 continued

Cluster 4 Sample	Na^+ meq/l	K^+ meq/l	Ca^{++} meq/l	Mg^{++} meq/l	SO_4^{--} meq/l	Cl^- meq/l	HCO_3^- meq/l	TEMP °C	pH	EC µmhos/cm	TDS ppm	Aragonite SI**	Calcite SI**
KH1	-1.27	0.55	-1.29	-0.33	-0.87	-1.52	0.1	-1.17	-0.44	-1.15	-1.48	-0.82	-0.78
KH11	-1.04	1.15	-1.42	-1.69	-1.64	-1.52	0.1	-2.06	0.47	-1.78	-1.91	-0.44	-0.18
KH12	-0.56	1.15	-1.09	-1.09	-1	-0.91	-1.29	-1.17	0.02	-1.52	-1.37	-1.55	-1.35
KH13	-0.24	1.15	-0.46	0.57	0.59	-0.91	-0.58	-1.17	0.93	-0.04	-0.2	0.09	0.51
GF1	0.34	-0.24	0.01	0.24	0	0.37	0.1	-0.27	0.02	0.22	0.21	-0.41	0.21
GF2	-0.14	-0.24	0.01	-0.43	0.34	-0.29	-0.58	0.62	-0.44	-0.15	-0.03	1.44	-0.71
GF3	2.34	-1.24	1.12	1.46	2.65	0.95	-0.58	0.62	0.93	2.29	2.32	0.18	1.03
GF4	2.34	-1.83	0.05	0	0.98	0.32	-0.58	0.62	0.02	1.07	0.93	-0.88	-0.24
GF5	0.18	-0.84	-0.27	1.89	0.1	0.32	-0.58	-0.27	-0.44	0.14	0.12	-0.77	-0.53
GF7	0.47	-1.04	-0.65	-0.49	-1.17	-0.29	1.5	0.62	-2.26	-0.6	-0.6	-2.12	-1.83
MJ1	-0.48	-0.24	-0.04	0	0.19	-0.29	-1.29	-2.06	0.47	0.33	-0.25	0.17	-0.29
MJ3	0.09	-1.04	-0.24	0.57	0.12	0.32	-0.58	0.8	1.38	-0.04	0.06	1.31	1.15
MJ7	-0.08	1.74	-0.38	-0.06	-0.11	-0.29	-0.58	1.24	-0.44	-0.41	-0.31	-0.3	-0.68
MJ9	-0.63	0.15	-0.92	-0.76	-0.77	-0.91	0.1	2.4	1.38	0.33	-1.05	0.65	1.17
HB1	1.5	0.75	0.13	1	1	0.6	0.1	-0.27	0.02	0.7	1.06	-0.3	0.26
HB4	-0.56	1.15	0.44	-0.76	-0.36	-0.91	-0.58	-0.27	0.93	-0.41	-0.54	-0.2	0.76
HB6	0.21	-0.24	0.05	-0.43	-0.05	0.95	-0.58	-0.27	0.93	-0.41	0.25	-0.14	1.55
MT2	0.25	-1.44	-0.38	-0.76	0.34	-0.29	-1.29	0.62	0.02	0.7	-0.19	-0.43	-0.97
MT5	-0.24	0.15	-0.69	-0.86	0.82	-0.91	2.21	0.62	-1.8	0.7	0.13	-0.87	-1.34
MT6	-0.56	-1.24	3.25	0.57	-0.46	3.41	0.82	0.26	-2.71	1.81	1.78	-0.54	-1.75
MT7	-2.34	-1.63	0.64	-1.75	-1.53	-0.29	0.1	1.06	-0.44	-1.15	-1.16	0.81	-0.14
MT8	0.09	0.75	0.9	0.9	-0.17	0.95	0.82	-0.27	0.02	-1.52	0.64	1.36	0.9
MT9	-0.79	-0.24	1.86	0.14	-0.49	0.49	2.89	0.62	0.02	-0.04	0.65	2.47	1.82
MR1	0.4	1.15	-0.69	0.14	-0.61	0.32	0.1	-0.27	0.47	-0.41	-0.27	0.59	0.47
NG1	-0.14	-0.24	-0.46	-0.46	-0.16	-0.29	0.1	-0.27	0.47	-0.04	-0.32	0.93	0.54
NG2	0.73	-1.24	0.52	2.36	2.15	0.32	-0.1.	-0.27	0.47	1.44	1.52	-0.16	0.43

** Saturated indixes

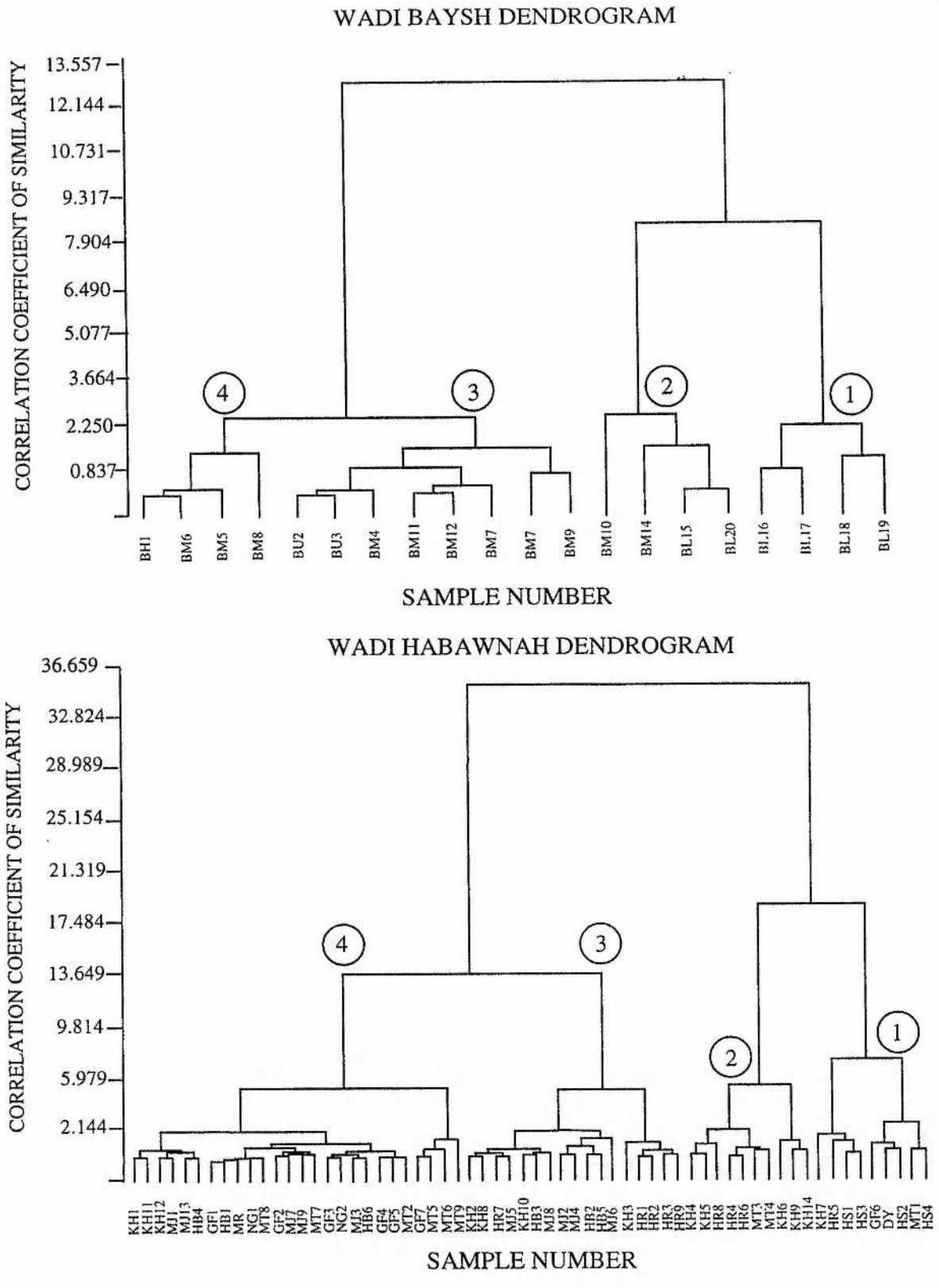

Figure 4.29 Dendrogram showing hierarchical clustering of the groundwater samples collected in 1989 from Wadi Baysh (above) and in 1990 from Wadi Habawnah (below).

Table 4.14 Cluster analyses of Wadi Baysh and Wadi Habawnah

Cluster analyses of Wadi Baysh

Cluster 1					Cluster 2					Cluster 3					Cluster 4				
Variable	MIN	MAX	MEAN	STDEV	Variable	MIN	MAX	MEAN	STDEV	Variable	MIN	MAX	MEAN	STDEV	Variable	MIN	MAX	MEAN	STDEV
Na^+	200.0	720.0	440.0	232.0	Na^+	52.0	360.1	194.3	127.3	Na^+	33.1	120.0	52.2	28.7	Na^+	32.0	68.1	52.6	17.6
K^+	1.2	10.2	6.1	3.8	K^+	5.1	14.1	9.8	4.4	K^+	1.6	10.2	6.7	3.3	K^+	2.3	5.9	4.1	1.7
Ca^{--}	345.0	413.0	380.0	36.0	Ca^{--}	192.0	30.6	251.1	45.2	Ca^{--}	54.9	207.6	112.0	49.1	Ca^{--}	52.1	125.5	72.7	35.3
Mg^{++}	97.0	161.0	128.8	36.7	Mg^{++}	39.6	132.5	89.8	38.3	Mg^{++}	27.5	57.6	35.4	10.2	Mg^{++}	25.3	40.6	32.2	6.4
SO_4^{--}	60.0	755.0	249.0	338.0	SO_4^{--}	213.0	1488.0	807.0	523.0	SO_4^{--}	115.3	296.3	165.8	60.5	SO_4^{--}	102.3	299.7	180.6	84.0
Cl^-	24.4	76.3	48.5	24.3	Cl^-	122.0	410.6	252.5	119.0	Cl^-	106.2	305.7	187.2	76.5	Cl^-	90.9	122.0	107.9	13.0
HCO_3^-	0.4	1.3	0.8	0.4	HCO_3^-	2.0	6.7	4.1	2.0	HCO_3^-	1.7	5.0	3.1	1.3	HCO_3^-	1.5	2.0	1.8	0.2
TEMP	32.0	33.0	32.5	0.6	TEMP	31.0	32.0	31.5	0.6	TEMP	31.0	33.0	31.9	0.6	TEMP	32.0	33.0	32.8	0.5
pH	7.2	7.6	7.4	0.2	pH	7.3	7.4	7.3	0.1	pH	7.2	7.3	7.3	0.1	pH	7.2	7.4	7.3	0.1
EC	3000.0	6504.0	4125.0	1636.0	EC	1543.0	3000.0	2597.0	706.0	EC	700.0	1400.0	1072.5	247.9	EC	80.0	1300.0	1025.0	206.0
TDS	1919.0	3667.0	2772.0	863.0	TDS	835.0	2667.0	1751.0	748.0	TDS	382.0	913.0	586.5	168.9	TDS	342.0	674.0	481.2	139.1
ARAG*	-0.3	-0.1	-0.2	0.1	ARAG*	-0.7	0.5	0.3	0.2	ARAG*	-0.4	0.1	-0.1	0.2	ARAG*	-0.6	0.4	-0.3	0.5
CALC**	-0.2	0.0	0.0	0.1	CALC**	0.1	0.6	0.4	0.2	CALC**	-0.3	0.2	0.0	0.2	CALC**	-0.5	-0.3	-0.4	0.1
DOL***	-0.5	0.1	-0.1	0.3	DOL***	0.2	1.0	0.7	0.4	DOL***	-0.5	0.3	0.0	0.3	DOL***	-0.7	-0.6	-0.7	0.0

Cluster analyses of WadiHabawnah

Cluster 1					Cluster 2					Cluster 3					Cluster 4				
Variable	MIN	MAX	MEAN	STDEV	Variable	MIN	MAX	MEAN	STDEV	Variable	MIN	MAX	MEAN	STDEV	Variable	MIN	MAX	MEAN	STDEV
Na^+	155.9	539.9	316.2	133.6	Na^+	100.0	300.0	172.6	65.1	Na^+	90.0	249.9	162.9	52.9	Na^+	24.6	169.9	95.8	32.5
K^+	3.1	11.0	6.7	3.0	K^+	5.9	11.0	8.6	2.1	K^+	2.3	14.9	9.4	3.4	K^+	2.0	9.0	5.3	2.0
Ca^{--}	281.1	521.0	399.7	96.0	Ca^{--}	92.2	494.2	252.4	118.6	Ca^{--}	125.5	347.5	204.2	52.6	Ca^{--}	58.1	277.8	126.1	49.1
Mg^{++}	91.2	218.9	146.8	48.3	Mg^{++}	34.0	133.0	84.9	35.9	Mg^{++}	40.8	165.3	75.1	28.9	Mg^{++}	26.7	53.5	38.9	6.8
SO_4^{--}	484.0	1708.0	1076.0	423.0	SO_4^{--}	232.0	1132.0	667.8	271.6	SO_4^{--}	306.9	1222.4	600.5	217.4	SO_4^{--}	164.7	536.5	301.0	81.7
Cl^-	460.1	1169.1	705.2	288.4	Cl^-	197.1	881.6	394.3	212.6	Cl^-	176.9	495.9	313.7	76.1	Cl^-	106.0	388.9	191.8	60.8
HCO_3^-	90.9	183.0	134.3	27.8	HCO_3^-	90.9	151.9	117.6	25.6	HCO_3^-	90.9	183.0	134.3	21.6	HCO_3^-	90.9	273.9	146.9	46.6
TEMP	26.0	30.0	29.0	1.4	TEMP	25.0	29.3	26.8	1.3	TEMP	23.1	27.0	25.5	1.0	TEMP	25.0	30.0	27.3	1.2
pH	6.5	7.3	7.0	0.3	pH	6.0	6.9	6.5	0.3	pH	6.8	8.1	7.4	0.3	pH	6.6	7.5	7.2	0.2
EC	1400.0	4500.0	3678.0	1054.0	EC	1200.0	3100.0	2240.0	685.0	EC	1400.0	3300.0	2053.0	493.0	EC	930.0	2030.0	1400.0	274.6
TDS	1651.0	3742.0	2718.0	833.0	TDS	707.0	2871.0	1639.0	658.0	TDS	881.0	2572.0	1433.0	415.0	TDS	504.0	1246.0	832.5	177.5
ARAG*	-0.7	0.3	-0.2	0.3	ARAG*	-1.9	-0.7	-1.3	0.4	ARAG*	-0.5	0.7	0.0	0.3	ARAG*	-1.0	0.2	-0.5	0.3
CALC**	-1.0	0.4	-0.1	0.4	CALC**	-3.2	-1.3	-2.1	0.6	CALC**	-0.4	1.7	0.4	0.6	CALC**	-1.4	0.3	-0.5	0.5

ARAG* (Aragonite) CALC** (Calcite) DOL***(Dolomite)

give a meaningful interpretation of groundwater facies.

To assist the interpretation of the differences among the four clusters in each wadi, some statistical parameters were calculated (see Table 4.14). From the average values of the TDS in Wadi Habawnah and Wadi Baysh, the data can be ranked as: Cluster one > Cluster two > Cluster three > Cluster four.

Clusters one and two both show high ranges in the mineral concentration. Clusters three and four show low mineral concentration (Table 4.14).

Wadi Baysh groundwater analysis:

Cluster one: has high Na^+ and Ca^{2+} and high mean of TDS with positive calcite saturation indices (water type Ca^{2+}, Na^+).

Cluster two: has high SO_4^{2-}, Ca^{2+}, Cl^- and Na^+ with positive calcite and dolomite saturation indices. (water type Ca^{2+}, SO_4^2, Cl^-).

Cluster three: has high SO_4^{2-} and Cl^-

Cluster four: has higher SO_4^{2-} and Cl^- than the rest of the variables.

Wadi Habawnah groundwater analysis:

Cluster one: has high Ca^{2+}, Na^+, SO_4^{2-}, Cl^-.

Cluster two: has high Mg^{2+}, Na^+, HCO_3^-, SO_4^{2-}, Cl^-.

Cluster three: has high Ca^{2+}, SO_4^{2-}

Cluster Four: has high Ca^{2+}, Na^+, Mg^{2+}, HCO_3^- and SO_4^{2-}.

The Cluster zone maps (Figures 4.30 and Table 4.14) shows that cluster one is dominant in the lower part of Wadi Baysh in which the hydrochemical facies may be calcite and halite. The upper part is a mix of clusters two and three in which the hydrochemical facies may be $CaCO_3$ and $CaSO_4$. The middle part of the wadi is dominated by clusters two, three, and four, in which the hydrochemical facies are thought to be $CaCO_3$ and NaCl.

In Wadi Habawnah most of the upper part is dominated by cluster three in which the hydrochemical facies may be $CaSO_4$. The middle part of the wadi is dominated by cluster four in which the hydrochemical facies may be $CaCO_3$, NaCl and $CaMgSO_4$. Cluster one dominates the lower part of the wadi in which the hydrochemical facies are

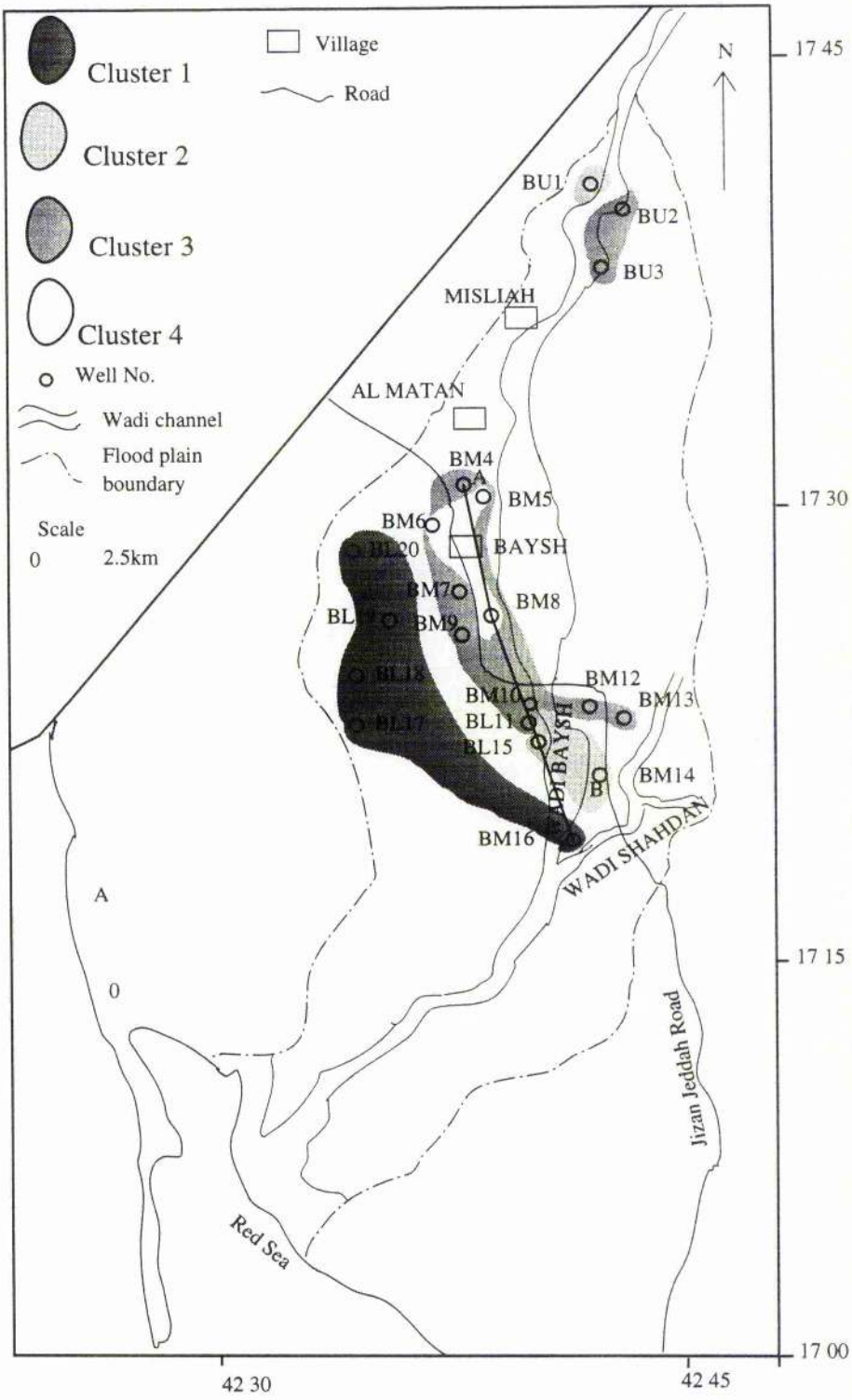

Figure 4.30a Cluster zones of Wadi Baysh groundwater.

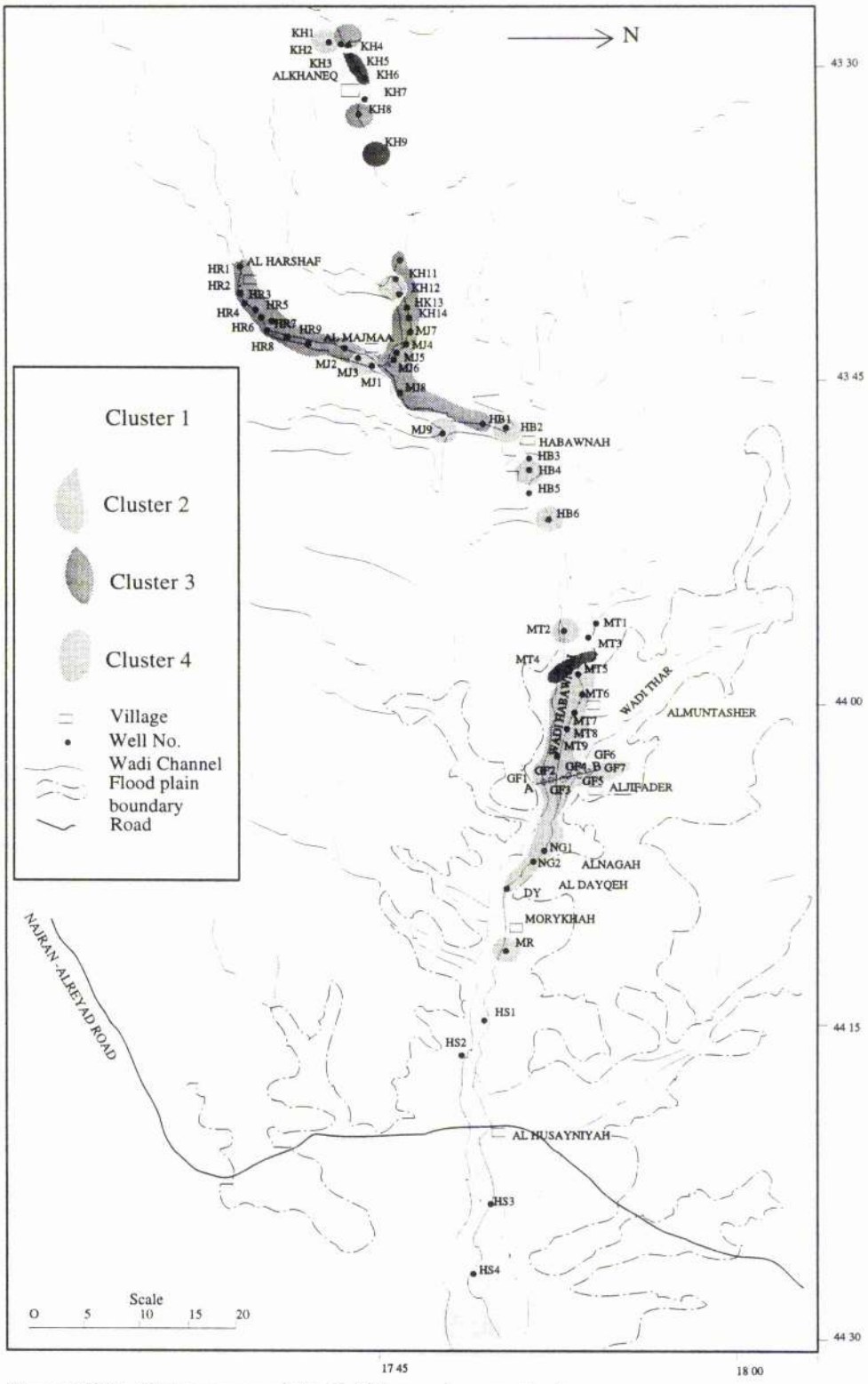

Figure 4.30b Cluster zones of Wadi Habawnah groundwater.

thought to be $CaCO_3$ and NaCl. The Cluster two data are scattered along the wadi.

The cluster analysis has been useful and has produced a classification of waters. The ground water mineralisation of both wadis tends to increase in a down slope direction, which shows the influence of the aquifer lithology and the evaporation effects.

4.13.2 Principal Component Analysis

Principal Components Analysis: multivariate data analysis techniques such as principal component analysis (PCA) have often been used in an attempt to confirm geochemical characteristic of groundwater. PCA has the capability to group different geochemical variables on the basis of the degree of co-variation among samples.

The same variables used in cluster analyses were used in PCA. In cluster analysis they are used to classify groundwater samples on the basis of their similarity while in PCA they will show the degree of co-variation among samples and help identify the loads which contribute most to the variation in Wadi Baysh and Wadi Habawnah.

Both data sets of groundwater chemistry were subjected to PCA analysis using a statistical program (Minitab) for standardised data (see Table 4.12 and 4.13) in order to give the variables the same weighting.

The co-ordination between the variables and a component is known as the component loading and squares of their values indicate the proportion of the variance in the individual variable that can be encountered in the component (Johnston, 1980). The eigenvalue of the component would be the same as the squared variable loading which indicates the total variance accounted for by the component. The components that are interpreted would have eigenvalues exceeding 1.0 (Johnston, 1980).

4.13.2.1 Results

The result of the PCA analyses of both groundwater chemistry in Wadi Baysh (20 samples) and Wadi Habawnah (62 samples) are given in Tables 4.15 and 4.16.

Four components had eigenvalues >1, while for the other ten components the eigenvalues were less than unity. Those components in which the eigenvalue was less than one represent 19% of the total variance. However, this percentage will be reduced to

Table 4.15 Eigenanalysis of the covariance matrix of hydrochemical analysis of the Wadi Baysh water samples variables

Eigenvalue	4.0569	3.2692	1.5453	1.2600	0.9351	0.5347
Proportion	0.324	0.261	0.124	0.101	0.075	0.043
Cumulative	0.324	0.586	0.709	0.810	0.885	0.927
Eigenvalue	0.3507	0.2081	0.1717	0.0897	0.0509	0.0284
Proportion	0.028	0.017	0.014	0.007	0.004	0.002
Cumulative	0.955	0.972	0.986	0.993	0.997	0.999
Eigenvalue	0.0097	0.0011				
Proportion	0.001	0.000				
Cumulative	1.000	1.000				
Variable	PC1	PC2	PC3	PC4	PC5	PC6
Na^+	0.372	-0.124	0.143	-0.088	0.358	0.219
K^+	-0.077	0.167	-0.344	-0.622	0.040	0.030
Ca^{2+}	0.369	0.237	-0.158	-0.177	-0.142	-0.143
Mg^{2+}	0.310	-0.124	0.304	-0.253	0.213	0.451
$SO4^{--}$	0.319	-0.129	0.091	0.329	0.310	-0.398
Cl^-	0.377	0.104	-0.103	-0.073	-0.584	-0.075
$HCO3^-$	-0.138	0.402	0.303	-0.088	0.270	-0.210
TEMP	-0.122	-0.060	-0.522	-0.218	0.489	-0.212
PH	0.034	0.085	-0.501	0.460	0.080	0.584
EC	0.409	0.059	-0.230	-0.041	-0.052	-0.097
TDS	0.448	0.093	-0.002	-0.082	0.129	-0.052
ARO	0.068	0.426	-0.109	0.362	0.159	-0.154
CALC	-0.025	0.509	0.091	0.037	0.001	0.033
DOL	-0.041	0.483	0.158	-0.084	0.073	0.310
Variable	PC7	PC8	PC9	PC10	PC11	PC12
Na^+	-0.238	-0.418	-0.438	0.241	-0.104	0.103
K^+	0.519	-0.055	-0.076	0.312	0.089	-0.236
Ca^{2+}	0.121	-0.267	0.475	-0.211	-0.105	0.508
Mg^{2+}	-0.031	0.422	0.472	-0.006	-0.010	-0.126
$SO4^{--}$	0.514	0.068	0.001	-0.011	-0.419	-0.256
Cl^-	-0.333	-0.082	0.002	0.046	-0.315	-0.517
$HCO3^-$	-0.077	-0.261	0.051	-0.483	0.271	-0.366
TEMP	-0.455	0.112	0.119	-0.126	-0.315	-0.011
PH	0.168	-0.207	0.056	-0.219	0.048	-0.173
EC	0.014	0.520	-0.476	-0.373	0.315	0.084
TDS	-0.036	-0.263	0.050	0.100	0.351	-0.037
ARO	-0.197	0.228	0.202	0.558	0.273	-0.110
CALC	0.040	0.130	-0.200	0.135	-0.273	0.366
DOL	0.015	0.109	-0.157	-0.135	-0.385	-0.089
Variable	PC13	PC14				
Na^+	0.344	0.144				
K^+	0.103	0.093				
Ca^{2+}	0.312	-0.037				
Mg^{2+}	-0.014	0.218				
$SO4^{--}$	-0.024	0.015				
Cl^-	-0.015	0.164				
$HCO3^-$	0.111	0.270				
TEMP	-0.136	-0.006				
PH	-0.048	0.160				
EC	0.142	0.013				
TDS	-0.674	-0.321				
ARO	0.299	-0.061				
CALC	-0.413	0.524				
DOL	0.075	-0.644				

Table 4.16 Eigenanalysis of the covariance matrix of hydrochemical analysis of the Wadi Habawnah water samples variables

Eigenvalue	5.2779	2.2542	1.1449	1.1264	0.8873	0.5865
Proportion	0.427	0.182	0.093	0.091	0.072	0.047
Cumulative	0.427	0.609	0.702	0.793	0.864	0.912
Eigenvalue	0.3013	0.2832	0.222	0.1489	0.0792	0.0465
Proportion	0.024	0.023	0.018	0.012	0.006	0.004
Cumulative	0.936	0.959	0.977	0.989	0.996	0.999
Eigenvalue	0.0075					
Proportion	0.001					
Cumulative	1					

Variable	PC1	PC2	PC3	PC4	PC5	PC6
Na^+	0.336	-0.041	-0.138	-0.252	-0.347	-0.106
K^+	0.111	-0.095	-0.592	0.367	-0.483	0.439
Ca^{2+}	0.349	-0.036	0.231	0.180	0.234	0.367
Mg^{2+}	0.366	-0.068	-0.102	-0.051	0.090	-0.140
$SO4^{--}$	0.371	-0.059	-0.109	-0.278	-0.156	-0.134
Cl^-	0.362	-0.027	0.108	0.160	0.293	0.281
$HCO3^-$	0.138	0.036	0.248	0.660	-0.313	-0.571
TEM	-0.082	-0.021	0.648	-0.184	-0.585	0.367
PH	-0.150	-0.522	-0.126	-0.298	-0.070	-0.138
EC	0.357	0.031	0.122	-0.218	-0.016	-0.189
TDS	0.417	-0.052	0.072	-0.055	0.004	0.035
ARO	-0.019	-0.561	0.143	0.229	0.167	0.120
CALC	-0.014	-0.622	0.073	0.056	-0.017	-0.115

Variable	PC7	PC8	PC9	PC10	PC11	PC12
Na^+	0.543	-0.365	0.208	0.020	0.037	0.431
K^+	-0.222	0.024	-0.003	-0.117	0.026	-0.036
Ca^{2+}	-0.303	-0.042	0.109	0.553	-0.001	0.411
Mg^{2+}	0.072	0.778	-0.139	-0.250	-0.128	0.333
$SO4^{--}$	-0.062	0.001	-0.460	0.346	-0.017	-0.472
Cl^-	0.256	-0.025	0.432	-0.327	-0.154	-0.451
$HCO3^-$	-0.038	-0.015	0.099	0.087	-0.183	-0.047
TEM	0.009	0.207	-0.028	-0.110	-0.062	-0.039
PH	-0.262	0.031	0.402	0.136	-0.571	-0.031
EC	-0.619	-0.308	0.027	-0.505	0.172	0.096
TDS	0.102	-0.026	-0.037	0.172	-0.065	-0.243
ARO	0.157	-0.303	-0.560	-0.250	-0.233	0.151
CALC	0.038	0.165	0.199	0.074	0.711	-0.106

Variable	PC13
Na^+	0.113
K^+	-0.041
Ca^{2+}	0.153
Mg^{2+}	0.028
$SO4^{--}$	0.411
Cl^-	0.281
$HCO3^-$	0.057
TEM	0.031
PH	-0.009
EC	-0.019
TDS	-0.842
ARO	0.005
CALC	0.011

11.6% if component five is excluded.

In Wadi Baysh, the variables are ranked from the higher to the lower weightings as follows:

Component 1 accounts for 32.4 % : TDS > Na^+ > Ca^{2+} > Cl^- > SO_4^{2-}

Component 2 accounts for 26 %: Calcite > Dolomite > Aragonite > HCO_3^- > Ca^{2+}

Component 3 accounts for 12%: Mg^{2+} > Dolomite > HCO_3^-

Component 4 accounts for 10 %: Aragonite > SO_4^{2-}

According to the above results of Wadi Baysh, component 1 accounts for 32.4% of the total variance. It has high a loading of TDS, Na^+, Ca^{2+}, Mg^{2+}, Cl^- and SO_4^{2-}. All are positively correlated with component 1 weightings. Thus component 1 represents the degree of overall mineralisation of the groundwater. Low weightings on component 1 may represent mixing of older concentrated water with dilute recharge. The 26% of the groundwater dominated with supersaturated water of $CaCO_3$, $CaMg(CO_3)_2$. The 12% and 10% of the wadi water shows that Mg^{2+} and $CaCO_3$, dominate the water type while the $CaMg(CO_3)_2$, SO_4^{2-} and HCO_3 show small influnces.

Wadi Habawnah : PCA results are determined as follows:

Component 1 accounts for 42.7%: TDS > SO_4^{2-} > Mg^{2+} > Ca^{2+}

Component 2 accounts for 18 % : HCO_3^-

Component 3 accounts for 9.3%: HCO_3^- > Ca^{2+} > Aragonite

Component 4 accounts for 9.1% : HCO_3^- > K^+ > Aragonite

In Wadi Habawnah, 43% of the water samples show high total dissolved solids that are dominated by SO_4^{2-} Mg^{2+} and Ca^{2+} while HCO_3^- dominated 18%. However 9% of the water samples are characterised by HCO_3^- and Ca^{2+}.

Accordingly, Wadi Habawnah groundwater has a high loading of total dissolved solids, sodium, calcium, chloride and sulphate. Bicarbonate has significantly loaded components 2, 3 and 4. It probably reflects the initial dissolution of minerals by groundwater. The low variance associated with this component probably reflects buffering of the HCO^-_3 content by CO_2 exchange between groundwater and the atmosphere. Also there is loading of saturation indices of aragonite. It may indicate that the water type is

dominated by $CaCO_3$ that possibly occurs within the basin fill. Component 4 shows a high loading of K^+ that may be released into the groundwater, possibly by weathering of K-feldspar.

Accordingly, Wadi Habawnah and Wadi Baysh groundwater has a high loading of total dissolved solids with 42% and 32% respectively. However, in Wadi Baysh the dominant ion sequence is $Na^+ > Ca^{2+} > Mg^{2+} > Cl^- > SO_4^{2-}$, while in Wadi Habawnah the dominant ion sequence is $SO_4^{2-} > Mg^{2+} > Ca^{2+}$. These ions dominate in both wadis and give clear evidence that the catchment area, with the influence of evaporation mechanism plays the main role in controlling the water type, as discussed further in section 4.15.

4.14 Water Type Classification

The groundwaters of both wadis have been described and the areal distribution of both the major and minor chemical concentrations were described in previous sections. In order to understand the hydrological process taking place, the groundwater samples were classified into distinct types on the basis of:

1- highest average concentration of cation/anion in each aquifer zone

2- the geographical/geohydrological location of the water samples.

The lower parts of both wadis are groundwater discharge areas. However, the middle parts of both wadis are transition zones. The author considers the upper part of Wadi Baysh (Mislyah region) as a recharge area since there is no data available for the catchment area. The middle area of Wadi Baysh consists of the Baysh area. In Wadi Habawnah the middle area consists of Al Muntasher, Al Dyagah, Al Nagah and Morayakhah areas. The lower parts of Wadi Baysh and Wadi Habawnah (basins area) are located 2km south west of Baysh Bridge and within the Al Hausaniah area respectively.

The main ions that dominate the groundwater in each selected zone, are indicated in Tables 4.17 and 4.18. In Wadi Baysh and Wadi Habawnah there are three main compositional categories into which most natural groundwater in the wadi floor deposits can be placed and in which the total hardness was classified according to Durfor and Becker (1964) classifications (see section 4.17.1.1.2).

Wadi Baysh: Water Type (I) is calcium sulphate dominated. The waters in the upper

Table 4.17 Analytical data for selected wells in the recharge and down-gradient areas of Wadi Baysh

	RECHARGE AREA UPPER PART					DOWNGRADIENT AREA MIDDLE PART					LOWER PART				
	Number of wells	Mean		SD		Number of wells	Mean		SD		Number of wells	Mean		SD	
pH(units)	3	7.3		0		11	7.3		0.1		6	7.4		0.1	
Temp. °C	3	32.3		0.6		11	32		0.7		6	32		0.9	
Na^+	3	1.5	(35)	0.2	(4)	11	3.7	(85)	4.1	(94)	6	15.4	(354)	9.7	(224)
K^+	3	0.23	(8)	0.1	(2.2)	11	0.2	(6.7)	0.1	(4.4)	6	0.2	(6.1)	0.1	(3)
Ca^{2+}	3	3.2	(65)	1	(19)	11	6.7	(135)	3.7	(74)	6	17	(339)	3.5	(70)
Mg^{2+}	3	2.4	(30)	0.5	(5.7)	11	3.7	(45)	2.5	(30)	6	9.6	(117)	2.8	(37)
SO_4^{2-}	3	2.6	(124)	0.6	(28)	11	6.4	(307)	8.3	(396)	6	5.3	(255)	8.2	(394)
Cl^-	3	2	(70)	0	(0)	11	3.8	(134)	2.5	(89)	6	37	(1306)	2.5	(873)
HCO_3^-	3	2	(123)	0.4	(25)	11	3	(190)	1.7	(104)	6	1.8	(112)	1.6	(100)
CO_3^{2-}	3	0.19	(6)	0.38	(10)	11	0.2	(5.5)	0.4	(12)	6	0	(0)	0	(0)
Al^{3+}	3		(0.475)		(0.07)	7		(0.265)		(0.294)	3		(0.725)		(0.295)
Ba^{2+}	3		(0.02)		(0.003)	7		(0.021)		(0.005)	3		(0.027)		(0.02)
Fe^{2+}	3		(0.837)		(0.12)	7		(0.504)		(0.352)	3		(0.438)		(0.378)
Mn^{2+}	3		(0.165)		(0.018)	7		(0.277)		(0.275)	3		(0.398)		(0.271)
Ni^{2+}	3		(0.069)		(0.01)	7		(0.081)		(0.017)	3		(0.062)		(0.022)
Pb^{2+}	3		(0.006)		(0.002)	7		(0.01)		(0.003)	3		(0.006)		(0.004)
TDS	3		(397)		(64)	11		(812)		(634)	6		(2431)		(852)
T-HARD	3		(283)		(71)	11		(522)		(294)	6		(1327)		(300)

[In milliequivalents per liter unless otherwise indicated; values in parentheses are in milligrams per liter; SD is standard deviation.]

Table 4.18 Analytical data for selected wells in the recharge and down-gradient areas of Wadi Habawnah

	RECHARGE AREA CATCHMENT AREA					DOWNGRADIENT AREA UPPER PART					MIDDLE PART					LOWER PART				
	Number of wells	Mean		SD		Number of wells	Mean		SD		Number of wells	Mean		SD		Number of wells	Mean		SD	
pH(units)	39	7.1		0.4		6	7		1.2		13	6.5		2		4	7.1		0.2	
Temp. °C	39	26		1.4		6	27		0		13	26		6.4		4	30		0	
Na^+	39	7.1	(164)	4.1	(94)	6	5.2	(120)	1.3	(30)	13	4.9	(112)	2.5	(57)	4	14.3	(329)	5.2	(120)
K^+	39	0.2	(8)	0.1	(3)	6	0.2	(7.2)	0.03	(1.2)	13	0.1	(4.8)	0.05	(1.8)	4	0.2	(7.5)	0.1	(3.1)
Ca^{2+}	39	10.5	(210)	6	(120)	6	7.5	(151)	1.2	(24)	13	8.3	(167)	3.9	(78)	4	20	(395)	4.7	(94)
Mg^{2+}	39	6.2	(76)	3.5	(43)	6	3.8	(46)	0.9	(10.5)	13	4	(48)	1.7	(21)	4	13	(157)	4	(49)
SO_4^{2-}	39	12.4	(598)	7.2	(346)	6	7.9	(388)	2	(96.5)	13	7.5	(361)	3.6	(171)	4	22	(1060)	8.9	(427)
Cl^-	39	9.6	(341)	6.2	(220)	6	5.9	(209)	1.2	(43)	13	7.4	(262)	6.7	(131)	4	19	(670)	5.8	(204)
HCO_3^-	39	2.1	(131)	0.4	(26)	6	2.1	(127)	0.2	(12)	13	2.5	(155)	0.9	(56)	4	2.5	(153)	0.4	(25)
Al^{3+}	19		(0.204)		(0.082)	6		(0.238)		(0.23)	13		(0.16)		(0.153)	2		(0.329)		(0.173)
Ba^{2+}	19		(0.031)		(0.019)	6		(0.035)		(0.006)	13		(0.03)		(0.008)	2		(0.045)		(0)
Fe^{2+}	19		(0.579)		(0.144)	6		(0.535)		(0.093)	13		(0.514)		(0.113)	2		(0.6)		(0.036)
Mn^{2+}	19		(0.176)		(0.023)	6		(0.187)		(0.014)	13		(0.17)		(0.024)	2		(0.216)		(0.005)
Ni^{2+}	19		(0.084)		(0.022)	6		(0.103)		(0.011)	13		(0.082)		(0.019)	2		(0.153)		(0.004)
Pb^{2+}	19		(0.020)		(0.025)	6		(0.01)		(0.001)	13		(0.009)		(0.003)	2		(0.018)		(0.002)
TDS	39		(1461)		(786)	6		(977)		(175)	13		(1032)		(616)	4		(2694)		(842)
T-HARD	39		(834)		(467)	6		(565)		(98)	13		(400)		(267)	4		(1628)		(421)

[In milliequivalents per liter unless otherwise indicated; values in parentheses are in milligrams per liter; SD is standard deviation.]
*No available data

part of Wadi Baysh (Misliah area), are slightly alkaline, fresh waters (<400 mg/l TDS). The water is hard (293 mg/l).

Water Type II is calcium sulphate and sodium chloride waters. This type characterises the groundwater of the middle zone (Baysh area). It is slightly alkaline fresh water (< 812 mg/l TDS). The water is hard (522 mg/l).

Water Type III is calcium sulphate and sodium chloride waters. It occurs in the lower zone, in semi-confined to confined aquifers (basin area). This water type is slightly alkaline; brackish water (< 2450 mg/l TDS) and it is hard (<1350 mg/l).

Wadi Habawnah: Water Type I is dominated by calcium sulphate. This water type dominates in the groundwater of the west side of the catchment (Al Khanig, Alharashf, Al Majma and the upper zone, Habawnah village area. It is slightly alkaline, freshwater (> 999 <1500 mg/l TDS > 900 mg/l), and is very hard (< 840 mg/l TH > 500 mg/l).

Water Type II is calcium sulphate water with chloride becoming increasingly dominant. This type characterises the groundwater in the middle part of the wadi (Al Mumtasher, Alnagah, Al Daugah and Morayekhah areas). In this area, the aquifer outcrops are crossed by two main tributaries: Wadi Tarimah and Wadi Thar which flow from the northern part of the catchment area. The water is slightly acidic, and fresh (< 1100 mg/l TDS).

Type III is calcium sulphate and sodium chloride water. It occurs only in the eastern part of the area, in the semi confined aquifer of the Wadi Habawnah outlet. It is slightly alkaline, brackish water (< 2700 mg/l TDS) and very hard (<1650 mg/l).

4.15 Major Factors Influencing the Groundwater Chemistry

The chemical composition of groundwater in both wadis is under the influence of constant rock weathering that appears to control ionic concentrations in the groundwater and the extremes of simple evaporative concentration. The factors controlling these variations will be discussed below and interpretations of data from these systems reached.

The alluvial aquifers in both wadis consist of mixtures of minerals derived from various sedimentary, igneous, or metamorphic source rocks in the catchment area. These minerals can vary from bed to bed in layered sequences. Such variations can cause large

differences in the chemistry of groundwater from bed to bed and from region to region. There are large variations in the major cations of the groundwater flow in both wadis. However, in the upper parts of both wadis, the waters show lower values of TDS than in the lower parts. In such a system groundwater moves along the saturated zone from the upper parts of the wadi to the lower part of the wadi, increases of total dissolved solids and of most of the major ions occur.

Chebotarev (1955) observed that groundwater evolution is normally accompanied by the following regional changes in dominant anion species:

Travel along flow path - - - - →

$$HCO_3^- \rightarrow HCO_3^- + SO_4^{2-} \rightarrow SO_4^{2-} + HCO_3^- \rightarrow$$

$$SO_4^{2-} + Cl^- \rightarrow Cl^- + SO_4^{2-} + Cl^-$$

Increasing age - - - - - - →

The above changes occur as the water flows from the recharging zones through the intermediate zone into the zone where the flow is very sluggish and the water is old. Domenico (1972) correlated the Chebotarev sequences with depth in large sedimentary basins as:

1- Upper zone groundwater has HCO_3^- as dominant anion and is low in total dissolved solids

2- Intermediate zone (less active groundwater circulation) has higher TDS, sulphate is normally the dominant anion

3- The lower zone (very sluggish groundwater flow) has a high TDS content and high Cl^- concentration.

Freeze and Cherry (1979) indicated that chemical analysis of waters from crystalline rock terrain (granites, diorites, basalts, and amphibolites) in various parts of the world generally have very low major ion concentrations (see Table 4.19). However, HCO_3^- is the dominant anion and SiO_2 is present in high concentrations. They assumed that Cl^- and SO_4^{2-} can be attributed to atmospheric sources, decomposition of organic matter in the soil and trace impurities in the rocks. The least abundant of the cations in all samples was K^+.

Table 4.19 Water samples analyses (in mg/l) of Groundwater and Groundwater-Derived Surface in Primarily Igneous Rock Areas (after Freeze and Cherry, 1979).

Location*	Number	pH	HCO_3^-	Cl^-	SO_4^{2-}	SiO_2	Na^+	K^+	Ca^{2+}	Mg^{2+}
(1) Vosges, France	51	6.1	15.9	3.4	10.9	11.5	3.3	1.2	5.8	2.4
(2) Brittany, France	7	6.5	13.4	16.2	3.9	15.0	13.3	1.3	4.4	2.6
(3) Central Massif, France	10	7.7	12.2	2.6	3.7	15.1	4.2	1.2	4.6	1.3
(4) Alrance Spring F, France	77	5.9	6.9	<3	1.15	5.9	2.3	0.6	1.0	0.4
(5) Alrance Spring A, France	47	6.0	8.1	<3	1.1	11.5	2.6	0.6	0.7	0.3
(6) Corsica	25	6.7	40.3	22.0	8.6	13.2	16.5	1.4	8.1	4.0
(7) Senegal	7	7.1	43.9	4.2	0.8	46.2	8.4	2.2	8.3	3.7
(8) Chad	2	7.9	54.4	<3	1.4	85	15.7	3.4	8.0	2.5
(9) Ivory Coast (Korhogo, dry season)	54	5.5	6.1	<3	0.4	10.8	0.8	1.0	1.0	0.10
(10) Ivory Coast (Korhogo, wet season)	59	5.5	6.1	<3	0.5	8.0	0.2	0.6	<1	<0.1
(11) Malagasy (high plateaus)	2	5.7	6.1	1	0.7	10.6	0.95	0.62	0.40	0.12
(12) Sierra Nevada, Calif. (ephemeral springs)		6.2	2.0	0.5	1.0	16.4	3.03	1.09	3.11	0.70
(13) Sierra Nevada, Calif. (perennial springs)		6.8	54.6	1.06	2.38	24.6	5.95	1.57	10.4	1.70
(14) Kenora, NW Ontario (unconfined aquifer)	12	6.3	24.0	0.6	1.1	18.7	2.07	0.59	4.8	1.54
(15) Kenora, NW Ontario (confined aquifer)	6	6.9	59.2	0.7	0.8	22.1	3.04	1.05	11.9	4.94

*(1), A spring after thawing, 1967; and (3), streams after several dry months, summer 1967;(4) and (5), two springs throughout 1966; (6), streams throughout the Island after 6 dry months, 1967; (7), streams in eastern regions, dry season 1967; (8), stream in Guera, dry season 1967; (9) and (10), streams in Korhogo area, 1965; (11), on the high plateaus and on the eastern coast, dry season 1967; (12) and (13), spring during 1961; (14) and (15), piezometers in glacial sands derived from granitic Precambrian rocks.

In crystalline terrain (silicate minerals), there is no tendency toward development of SO_4^{2-} and Cl^- facies as groundwater moves over the rocks. Thus the Chebotarev hydrochemical evolution sequence is not relevant in crystalline rock terrain.

The chemical evolution of this water is controlled by interactions with aluminosilicate minerals. According to Robertson (1991) such interactions may be described by a few simple chemical equations. Carbonic acid (H_2CO_3) is the major material to attack silicate minerals. This acid forms as a product of carbon dioxide CO_2 combining with water. The reaction of carbon dioxide and water supplies hydrogen ions i.e.:

$$CO_2\,(g) + H_2O \Leftrightarrow H_2CO_3\,(aq) \Leftrightarrow H^+(aq) + HCO_3^-(aq)$$

Hydrogen ions aid in the attack on feldspars, which become changed to clay minerals, here represented by kaolinite and cations are released.

$$2NaAlSi_3O_8 + 2H^+ \Leftrightarrow Al_2Si_2O_5(OH)_4 + 2Na^+ + 4H_4Si_3O_8^+$$

$$CaAl_2Si_3O_8 + H_2O + 2H^+ \Leftrightarrow Al_2Si_2O_5(OH)_4 + Ca^{2+}$$

The influence of the weathering process can be detected from the groundwater analysis data, where the major cation is dominant. As Na^+ and Ca^{2+} are both released, the dominant concentration of Ca^{2+} may be a result of the ion exchange process and K^+ may also be released from the potash feldspars which occur in low abundance in the local rocks. The clay mineral kaolinite is an aluminosilicate residue.

Sulphide bearing rocks including massive sulphide deposits, mostly associated with andesitic to basaltic volcanic flow rocks and earthy gossans (weathered massive sulphides) are present in both wadis. In Wadi Habawnah such deposits occur in three areas, recognised by Sable (1984). From west to east they are : 1) near the central western border of the Wadi Najran quadrangle; 2) west of Wadi Arjan; 3) along Wadi Gurra. Carbonate rocks with massive sulphide gossans in metavolcanic flow rocks are exposed in a tributary of Wadi Arjan at about latitude 17°42'09" N and longitude 44°09'29" E.

Todd (1980) indicated that groundwater has a higher concentration of dissolved constituents than the surface water because of the greater exposure to soluble material in geological strata. Also the soluble salts in groundwater are originally from solution of rock materials.

Freeze and Cherry (1979) explained that the longer the journey of groundwater in the saturated zone, the greater the concentrations of total dissolved solids and most of the major ions present. In Wadi Baysh the shallow groundwaters of the upper part of the wadi are lower in dissolved solids than the groundwaters of the lower parts of the wadi. However, in Wadi Habawnah, the salinity of waters in the upper part of the wadi was high but decreased when brought into contact with a second aquifer of low salinity at Tarimah and Thar (see Figure 4.2) where the salinity is lowered by dilution and increased in the wadi outlet.

Evaporation takes place in all climates whereby pure water is removed from solution so that the concentration of all dissolved components tends to increase. Szikszay *et al.* (1990) indicated in their study that the chemical composition of water (Ca^{2+}, Mg^{2+}, Na^{+}, K^{+} and SO_4^{2-}, Cl^{-}, NO_3^{2-}, HCO_3^{-}) in the upper part of the unsaturated zone was influenced by climate, whereas the lower part of the unsaturated zone showed that important variations in the chemistry of the water at depth could be linked to the local lithology. In arid climates the build up of dissolved components through evaporation is a major control on water composition and cyclic wetting and drying is an important process in the arid zone (Drever 1982). Complete evaporation of water and deposition of all the solutes in it may occur during a dry period, followed by partial re-solution of those solutes during a wet period. The end result of an evaporation-solution cycle is a water that contained all the ions which had precipitated only as highly soluble salts, but has lost some of the ions which precipitated as less soluble compounds. Hotal and Zoxl (1984) indicated that in an arid zone, where evaporation exceeds precipitation, soluble salts accumulate in the soils and the water table fluctuations have an impact on water quality and in many places form Wadi-Sabkhah layers.

Bower (1978) indicates that the most important sulphate deposits are found in evaporitic sedimentary rocks. Leaching of sulphate from the upper soil layers may be significant, causing sulphate to be the principal anion in the underlying groundwater.

Both wadi outlets are within the arid zone where the evaporation causes concentration of the water ions near the surface. The agricultural water system of Wadi

Habawnah depends totally on pumping machines, which enable evaporation rates to increase locally, while in Wadi Baysh farmers depend mostly on floods for irrigation water. The field investigations show that the lower parts of both wadis are covered with a silty layer that is probably responsible for keeping the relatively saline water from being flushed out by the occasional wadi flow.

The high-salinity waters occur away from the main channel, where the agricultural area is located. These may show the influence of the irrigation waters passing into infiltration.

Lloyd *et al.* (1985) indicated in their conceptual hydrochemical model of Wadi Bishah, northeast of Wadi Baysh, that there are two types of return which occur, one in which the sulphate water is concentrated and the other in which chloride dominant water develops, probably as a result of return, through the irrigation use of the main wadi recharge water.

On the basis of isotope data they showed that:

1- The water type characteristic of a thin alluvial spread was $Ca(HCO_3)_2$ where the precipitation produced minor recharge.

2- Following the water through the thin alluvial channel, the water may have dissolved gypsum that is known to occur, and was subjected to partial evaporation. They considered the water type was Na_2SO_4 rich, whereas the water type of the main channel was NaCl and $CaSO_4$ rich. They believed that Na_2SO_4 water recharge occurred at the wadi edge. The edge effect was maintained by the flow of the flood which was characterised by $Ca(HCO_3)_2$ and entered the aquifer as indirect recharge.

3- Salinity anomalies away from the alluvial edge were attributed to irrigation return effects; Na_2SO_4 waters could be concentrated by this means, and NaCl waters produced from the main wadi recharge.

4- Evaporation would increase the salt content in the soil, but in the rainy season, the salt may be dissolved and flushed out to percolate down to the zone of saturation. Such a process may led to seasonal variations in the groundwater quality.

The flood flow has a short time of contact with the soil or vegetation compared to

that of the groundwater aquifers. However, reaction in the soil zone shows that runoff has much higher dissolved solids concentration than the original rain (Figures 4.31 and 4.32). Hem (1984) indicated that, in addition to mixing of groundwater and runoff, the natural factors influencing stream water composition include reactions of water with mineral solids in the streambed and in suspension, as well as losses of water by evapotranspiration. These natural factors result in fluctuations of composition that bear little relation to flood rate.

Kennedy and Brown (1966) found that sodium saturated natural sediments from Brandywine Creek, Delaware, U.S.A, exchange 90 percent of their adsorbed sodium for calcium in 3-7 minutes in laboratory experiments. Also oxidation of ferrous to ferric iron may reach equilibrium quickly in the runoff (Hem, 1989). However, both wadi basins are located in arid to semi arid zones in which the build-up of dissolved components through evaporation is a major control on water composition. In addition to the excess of evaporation over precipitation, water from shallow unconfined aquifers (as in the Al Khaneq and Al Harshaf major tributaries of Wadi Habawnah) may also become evaporated.

The graphical plots of the ionic composition of the waters of both wadis, are given in Figures 4.31 and 4.32. The chemical concentrations in rainfall are about an order of magnitude lower than those in flood waters and the floodwaters have up to an order of magnitude less chemicals than the groundwaters. The very close parallelism of patterns of composition of rain and floodwaters in the upper and middle parts of both wadis (Figures 4.31 and 4.32) demonstrates their close chemical interrelationship, perhaps through evaporation concentration processes. Similar evaporation may lead to increasing concentrations within the groundwaters. In the lower part of Wadi Habawnah the flood waters and rainwater diverge, with floodwaters showing greatly enhanced concentrations of Ca^{2+} and HCO_3^- and substantial reduction of Cl^- and SO_4^{2-}.

In the upper part of Wadi Baysh the groundwater concentrations are similar to those encountered in floodwater but the groundwater concentrations increase into the middle reaches and become still more highly concentrated in the lower reaches where the Mg^{2+}, SO_4^{2-}, Cl^- and HCO_3^- patterns ape those of sea water although an order of magnitude

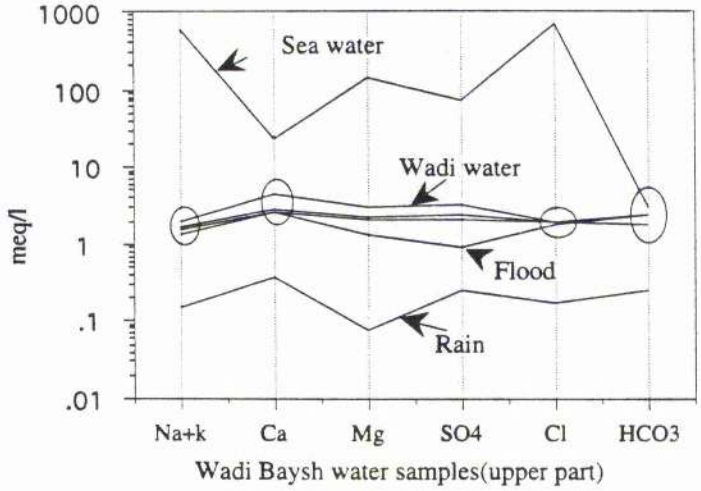

Wadi Baysh water samples(upper part)

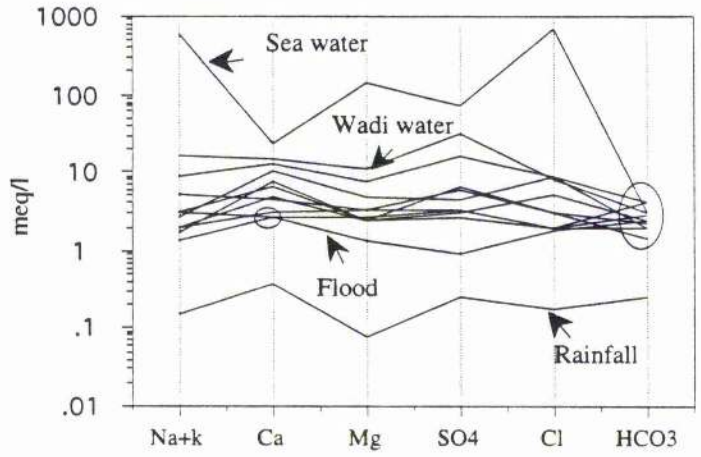

Wadi Baysh water samples (middle part)

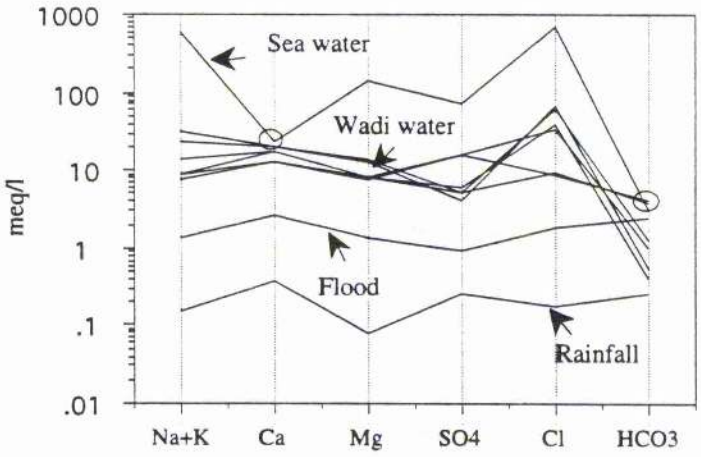

Wadi Baysh water samples (lower part)

Figure 4.31 Diagrams to show chemical analyses of Wadi Baysh water samples (upper, middle and lower part of the wadi)

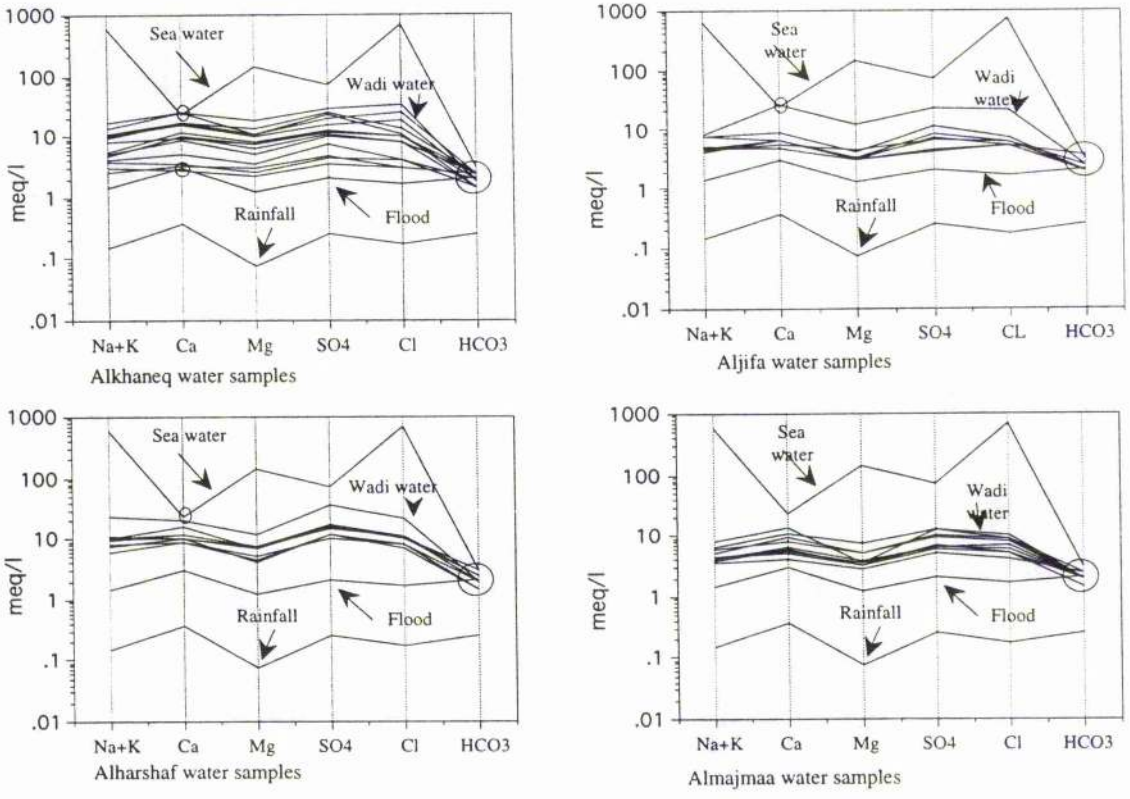

(Four major tributaries of the western part of the catchment area)

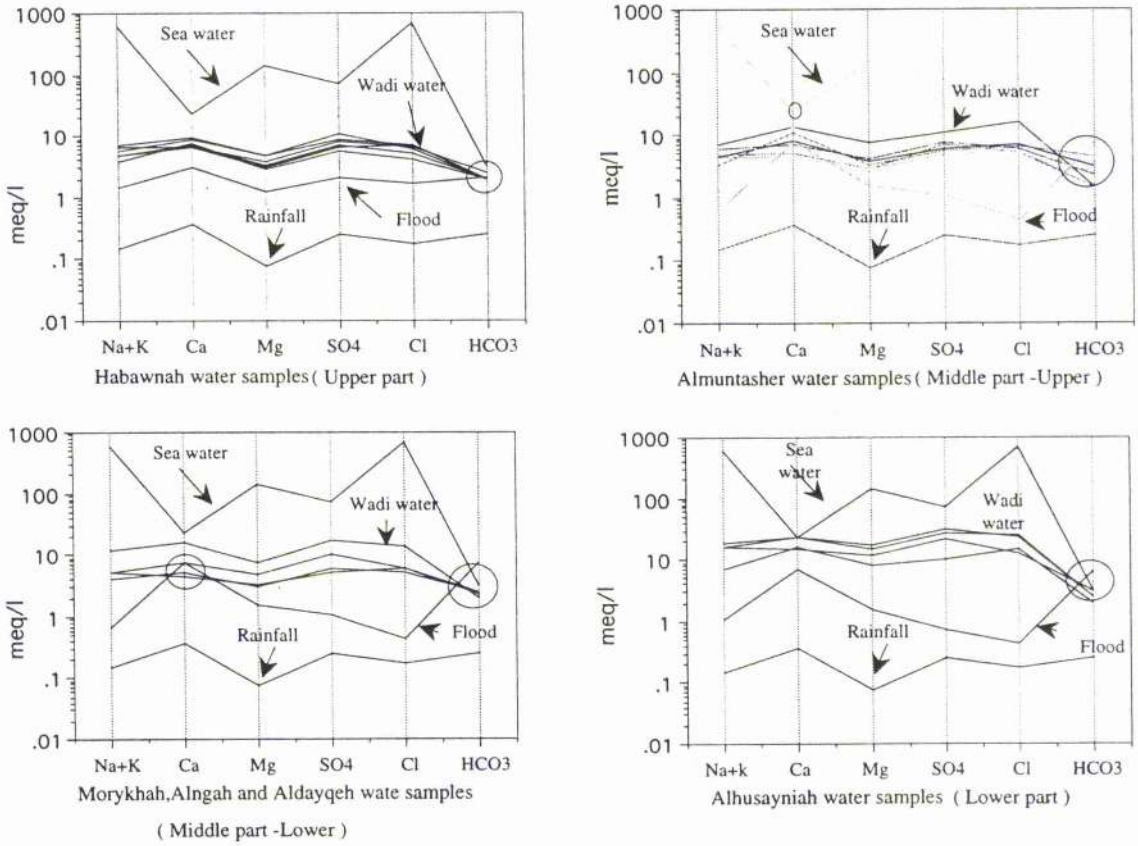

Figure 4.32 Diagrams to show chemical analyses of Wadi Habawnah groundwater and its major tributaries with flood,rainfall and sea water.

lower in value.

Most of the saturation indices (SI) data for the major cations and anions show that in both wadis the most waters are under saturated with respect to gypsum dolomite, halite, aragonite and calcite (Table 4.10 and 4.11). This may indicate that the aquifer lithology has a greater influence on the water quality than evaporation.

In the case of a rainstorm of sufficient intensity for the water to percolate through the soil zone and recharge the groundwater system, the soluble salts (such as gypsum) will dissolve. The water reaching the groundwater system will thus appear to have lost sulphate. However the solution will be under saturated with respect to gypsum because there was not sufficient contact time between gypsum and water for equilibrium to be established.

In the case of water table fluctuation, Hellwig (1974) explained that, when the water table is near the ground surface, water drawn up above the water table by capillary action will evaporate and deposit salts. If rainfall occurs, these salts may be leached by percolating water; chlorides will dissolve rapidly whereas gypsum will not.

Sowagan and Allayla (1989) explained, in their model for the groundwaters of Wadi Ar-Rumah in north central Saudi Arabia, that at the end of the pluvial period, the aquifer was fully recharged with water, in nature probably similar in quality to that of the alluvial water. Later the wadi floor held an ephemeral stream. Because of the low gradient of the wadi channel and the reduction in the flow volume, fine-grained sediments began to be deposited along the wadi channel and the flood plain. This sediment has low permeability, and it was difficult for groundwater and surface water to mix during flow. However, evaporation of groundwater has since taken place (as a result of capillary draw and vapour transport). Some of the groundwater infiltrated downward taking with it the most soluble salts such as gypsum, which were then left in the interstices of the sediments. Such a model is similar to Drever and Smith's (1978) cycle of wetting and drying.

In the study area, conditions are mostly influenced by aquifer lithology and the evaporation mecanism since both discharges area are characterised by high total dissolved solids compare to the recharge areas.

4.16 Evolution of Groundwater Chemistry in the Recharge and Discharge Areas of Both Wadis

In order to determine the chemical evolution of the groundwater in both wadi basins, two hydrochemical processes were identified as follows:

1- the reaction of flood water as it infiltrates the soil zone and percolates through the unsaturated zone to the water table in the recharge area and

2- the reaction of groundwater as it moves from the recharge area down-gradient to discharge areas.

Figures 4.31 and 4.32 show the average values of the major ions of the groundwater samples in each zone of both wadis plotted against the rainfall, flood and sea water data for the same major ions. The chemical concentrations in rainfall are about an order of magnitude lower than those of flood waters and the flood waters have up to an order of magnitude less chemicals than the groundwaters which shows the influence of the unsaturated zone on the groundwater quality. The very close parallelism of patterns of composition of rain and flood waters in the upper and middle parts of both wadis (Figures 4.31 and 4.32) demonstrates their close chemical interrelationship perhaps through evaporation concentration processes. Similar evaporation may lead to increasing concentrations within the groundwaters. In the lower part of Wadi Habawnah the flood waters and rainwater diverge with floodwaters showing greatly enhanced concentrations of Ca^{2+} and HCO_3^- and substantial reduction of Cl^- and SO_4^{2-} .

In the upper part of Wadi Baysh the groundwater concentrations are similar to those encountered in floodwater but the groundwater concentrations increase into the middle reaches and became still more highly concentrated in the lower reaches where the Mg^{2+}, SO_4^{2-}, Cl^- and HCO_3^- patterns ape those of sea water although an order of magnitude lower in value.

In the recharge and downgradient areas, interactions between flood water, gases, and minerals may occur to a large degree in the soil and unsaturated zones. However downgradient reactions occur mostly within the saturated zone since the floods occasionally reach the basin area.

The wadi floor deposits have had a substantial effect on aquifer water chemistry as shown in the water type classification described previously. Therefore, the hydrochemical data for both wadis have been used to construct two hydrochemical cross sections (Figure 4.33) along the flow lines (see Figures 4.1 and 4.2) and across different water types downgradient and another two cross perpendicular to the flow system (Figures 4.34 and 4.35). These cross sections along the flow line of both wadi systems represent the composition of the groundwater, which are defined by an average of chemical analyses of water from wells along each wadi. In Wadi Habawnah, a greater number of wells are located in recharge areas than is desirable because of the differences in evolution of these waters and the waters downgradient. However, in Wadi Baysh there are no data available for the wells in the catchment area, and instead the limited number of wells in the upper areas was used.

The water chemistry of the recharge, middle and downgradient areas of both wadis is summarised in Tables 4.17 and 4.18 and Figure 4.33 as follows:

In Wadi Baysh, the groundwater chemistry of the **Recharge Areas** is typically a calcium magnesium sulphate type. The calcium, magnesium and sulphate concentration are 3.2meq/l (65 mg/l), 2.4 meq/l (30 mg/l) and 2.6 meq/l (126 mg/l) respectively. Sodium, potassium, chloride and bicarbonate have low concentrations. However the large variability of the CO_3^{2-} is reflected in the large standard deviation and the extreme values all influence the mean values. The pH of the groundwater is slightly alkaline (7.3).

In the **Middle Areas** the composition of the groundwater evolves into either calcium magnesium mixed-anion type or as calcium magnesium bicarbonate type. Also calcium magnesium chloride types may occur.

In the downgradient areas (**Lower Zone**), the composition evolves into either calcium sodium chloride or calcium magnesium bicarbonate and sodium chloride. However, the sulphate concentration is variable with large standard deviation. The total dissolved solids of 397 mg/l and 812 mg/l in the recharge and middle areas respectively may increased to more than 2400 mg/l owing to dissolution reaction.

The concentration of trace elements reveals increasing manganese in the middle

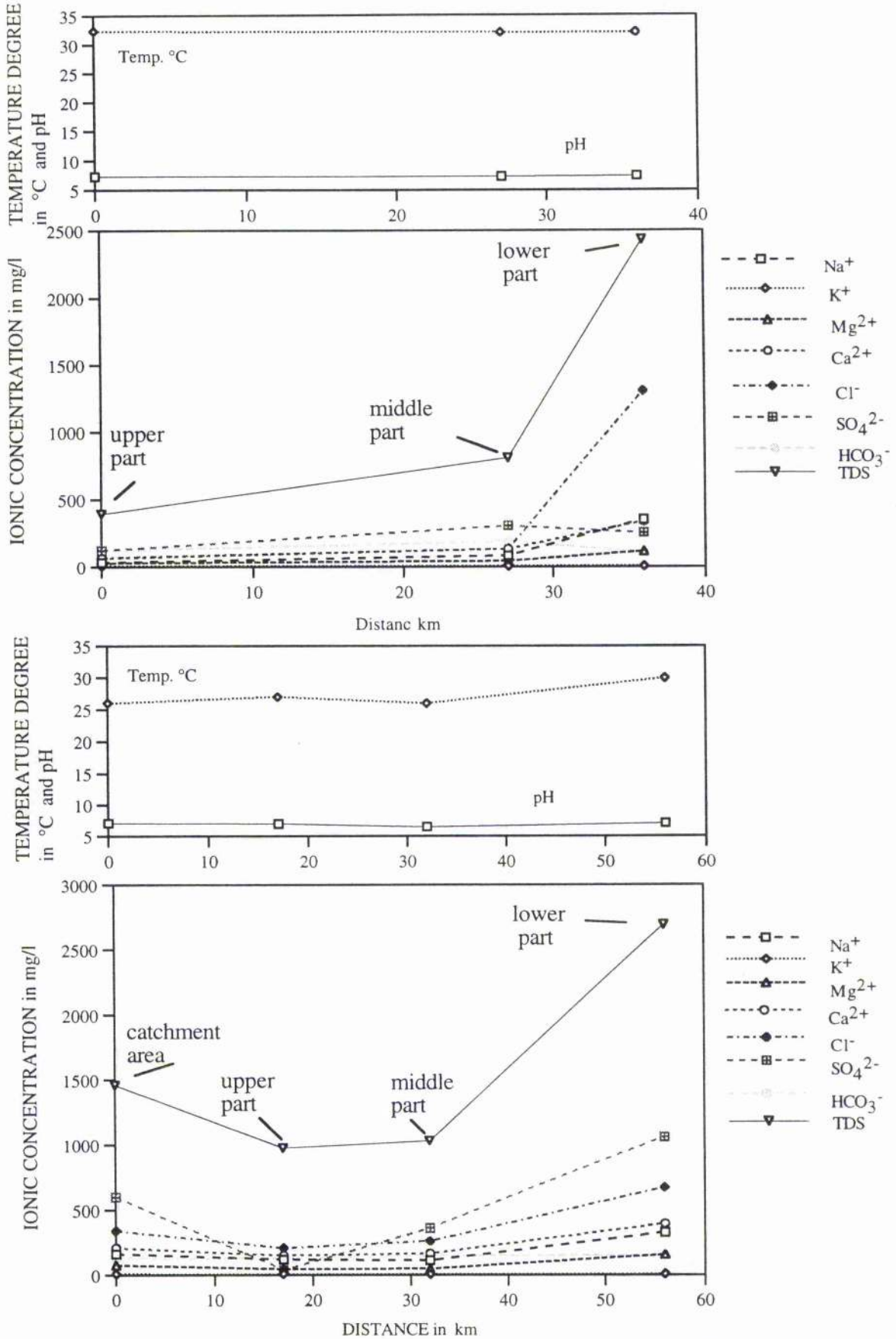

Figure 4.33 The mean concentrations of major ions, total disolved solids, temperature and pH of the groundwater along the upper, middle and lower parts of Wadi Baysh (above) and the catchment, upper, middle and lower parts of Wadi Habawnah (below).

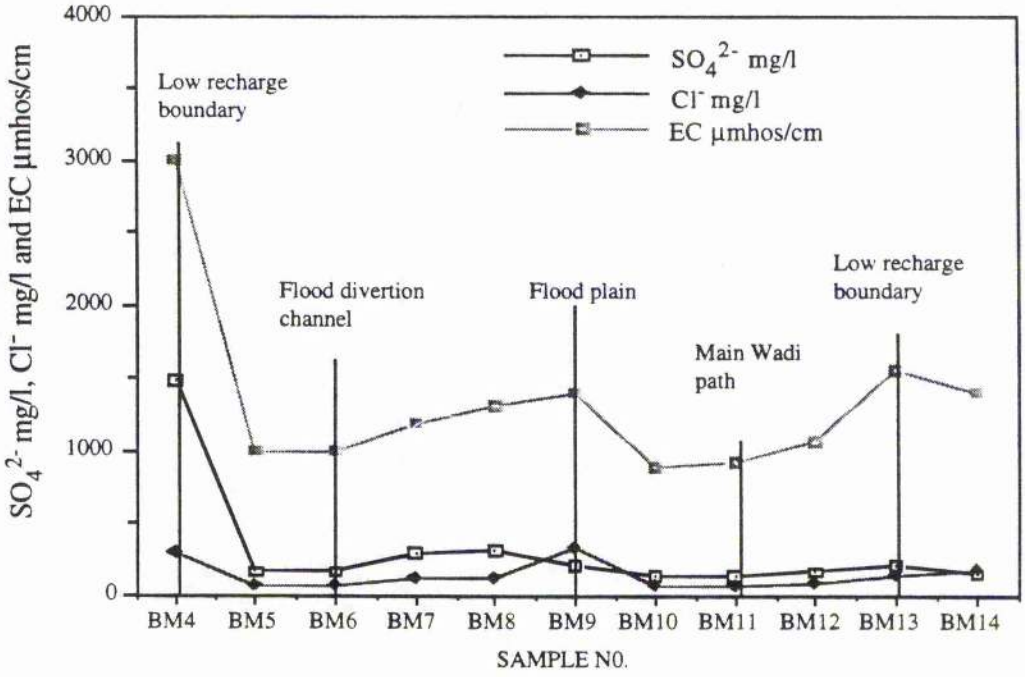

Figure 4.34 Schematic section across Wadi Baysh showing some major ions and conductivity data at A- B on Figure 4.1

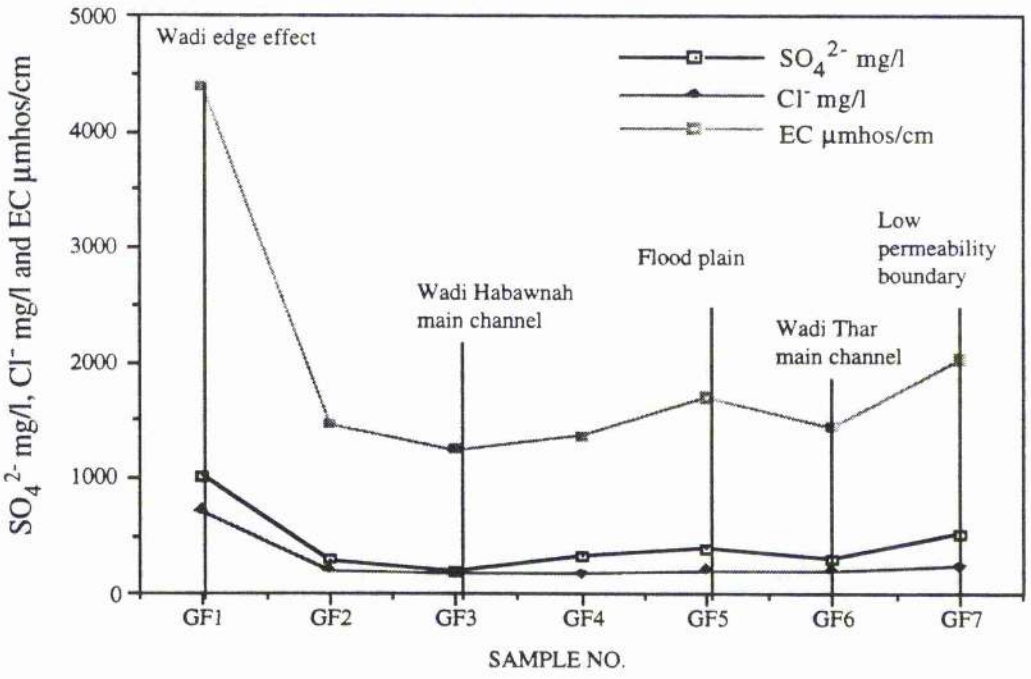

Figure 4.35 Schematic section across Wadi Habawnah showing some major ions and conductivity data at A - B on Figure 4.2

(0.277 mg/l) and down gradient areas (0.398 mg/l). It is suggested that such an increase in manganese is due to the fact that the Mn^{2+} ion, under conditions to be expected in a natural water system, will be as dissolved manganese in the 2+ oxidation state. In general, however, the Mn^{2+} ion is considerably more stable in aerated water, and it can be transported at higher concentrations without the protection of complexation (Hem, 1989).

In the recharge areas of Wadi Habawnah and the upper area (Habawnah village area), the groundwater is typically a calcium sulphate type and sodium chloride type. The recharge areas generally contain large concentrations of sulphate (12.4 meq/l (598 mg/l)) and calcium (10.5 meq/l (210 mg/l)), chloride (9.6 meq/l (341 mg/l)) and sodium (7.1 meq/l(210 mg/l)).

In the upper area, the concentration of the above ions is lower. The bicarbonate and potassium concentrations are relatively small in both areas. However, bicarbonate in the catchment area is variable with a high standard deviation. The pH of the groundwater is generally neutral. The TDS in the catchment area are 1461 mg/l while in the upper area they decrease to less than 1000 mg/l. The decrease of the TDS may be due to precipitation occuring in this part of the wadi.

The groundwater chemistry of the middle part is typically a calcium sulphate and a calcium bicarbonate type. The middle areas generally contain large concentrations of calcium (8.3 meq/l (167 mg/l)), sulphate (7.5 meq/l (361 mg/l)) and bicarbonate (2.5 meq/l (155 mg/l)). The calcium and bicarbonate show higher concentrations while the trace element concentrations are lower in this area than in the upper part of the wadi. This may be as a result of the chemical influence of the groundwater of Wadi Thar that flows from the northern part of the catchment into the middle area near Al Muntasher. The groundwater is slightly acid with a pH of 6.5 and a temperature of generally 26°C.

In the lower downgradient areas of Wadi Habawnah, the composition evolves into either a calcium sulphate and sodium chloride type or, as dissolved solids increase, into a calcium sodium sulphate type or calcium magnesium sulphate type. The TDS and trace elements also increase basinwards.

The cross sections drawn perpendicular to the groundwater flow systems are

shown in Figures 4.34 and 4.35 for the section across the wadis marked A-B on Figure 4.1 and Figure 4.2. The two sections with plots of the total salinity, sulphate and chloride data of the well water samples represent the middle zones of both wadis (see Tables 4.1 and 4.2). Both sections show indirect recharge by low salinity wadi water occurring at the main channel of the wadi, while sulphate dominance over chloride is shown towards the edges of the wadi.

Since clay minerals are often rich in Na^+ while the groundwater in the study area is dominated by Ca^{2+}, ion-exchange may take place either to replace the Ca^{2+} in the water by Na^+ or the reverse may occur (known as reverse ion-exchange).

The hydrochemical analyses show that Ca^{2+} is the dominant cation in most of the Wadi Habawnah and Wadi Baysh samples. This suggests that there may be other sources supplying Ca^{2+} besides the evaporation phenomenon, such as rock-weathering, reverse ion-exchange and adsorption.

The Ca^{2+} and Cl^- plot (Figure 4.16) shows that Ca^{2+} concentrations are higher than would be expected if the groundwater were simply evaporated precipitation. It is suggested that reverse ion-exchange may have taken place where the Ca^{2+} has been replaced by Na^+, as shown by the Durov diagram (Figures 4.26 and 4.28).

Redox reaction may take place in both wadis. Both show high concentration of SO_4^{2-}. Since SO_4^{2-} concentration values are very high compared to those in the rainfall it may be assumed that weathering processes play a role. It is known that pyrite is a widespread accessory mineral in the igneous and metamorphic rocks which dominate both catchment areas of Wadi Baysh and Habawnah.

It is shown in Figures 4.17 and 4.18 that relationships of $Ca^{2+}$with HCO_3^-, SO_4^{2-} and $HCO_3^- + SO_4^{2-}$ that $HCO_3^- + SO_4^{2-}$ do balance the concentration trend of Ca^{2+}. Such a case may indicate that oxidation of pyrite for example would supply H_2SO_4 to the runoff, which in turn would make the rock-water interaction (mainly silicate minerals) a major source of such ions in the groundwater.

The redox weathering of pyrite may be expressed by the following reaction.

$$4FeS_2 + 15O_2 + 14H_2O \Rightarrow 4Fe(OH)_3 + 16H^+ + 8SO_4$$

However, the reaction releases a large number of hydrogen ions; for every mole of pyrite 4 moles of H^+ ions are produced, so the weathering solution becomes very acid : pH values of 2 or lower may be reached (Henderson 1986). Since the groundwater pH is in the range of 6.8 to 8.1, the redox weathering of pyrite may develop in the upper part of the catchment area where sulphate and pyrite are exposed.

4.17 Groundwater Quality Criteria

The groundwater is the main water resource in the study area. It is used mainly for domestic and agricultural water supply. Therefore the following discussion will be limited to drinking and irrigation aspects of water quality.

4.17.1 Drinking Water Quality

Groundwater potability is based on the soluble solids concentrations. Some of these soluble solids have low concentrations while other more harmful materials are present in high concentrations. To maintain groundwater quality there are three major, international agencies which recommend standard limits for most of the dissolved materials. These agencies are :

1- WHO (World Health Organisation)

2- USEPA (US Environmental Protection Agency)

3- EEC (European Economic Community)

The groundwater ion measurements in both wadis are compared with the three major international standards in Tables 4.20 and 4.21. The maximum and minimum concentrations of ions measured are compared to show the range of the differences in the international standards. The MAC term is the maximum admissible concentration and MRC is the minimum required concentration, while GL is the guide level.

4.17.1.1 Wadi Baysh

TDS (total dissolved solids): The maximum admissible concentration (MAC) for drinking water is 1500 mg/l. The measured TDS values are below the recommended limit in the upper and middle sections except for well BM6 (Figure 4.1) where, at a depth of 17 m, the water has TDS of 2667 mg/l. This high TDS value at shallow depth results from

Table 4.20 Comparative tabulation of potable water quality with selected international standards (Wadi Baysh)

ITEM	WHO 1984		USEPA 1988		EEC 1975			UPPER PART STUDY RESULTS IN 1989 NO. OF WELLS (3)	
	MAC mg/l	MRC mg/l	MAC mg/l	MRC mg/l	MAC mg/l	MRC mg/l	GIL mg/l	MIN mg/l	MAX mg/l
TDS	1000	-	500	-	1500	-	-	342.4	467.7
PH	6.5-8.5	-	6.5-8.5	-	-	6	6.5-8.5	7.3	7.3
Na^+	200	-	-	-	100	-	20	32	39.1
K^+	-	-	-	-	12	-	10	5	10.2
Ca^{++}	100-300	-	-	-	-	10	100	52	87
Mg^{++}	-	-	-	-	50	5	30	25	36
Fe^{++}	0.3	-	0.3	-	0.3	-	0.1	0.725	0.964
Mn^{++}	0.1	-	0.05	-	0.05	-	0.02	0.154	0.186
SO_4^{--}	400	-	250	-	250	-	5	102.3	155.6
Cl^-	250	-	250	-	200	-	25	69	69.8
HCO_3^-	-	-	-	-	-	-	30	106.2	151.9
CO_3^{--}	-	-	-	-	-	10	35	0	18
EC*^	-	-	-	-	1250	-	400	700	1000

ITEM	WHO 1984		USEPA 1988		EEC 1975			MIDDLE PART STUDY RESULTS IN 1989 NO. OF WELLS (11)	
	MAC mg/l	MRC mg/l	MAC mg/l	MRC mg/l	MAC mg/l	MRC mg/l	GIL mg/l	MIN mg/l	MAX mg/l
TDS	1000	-	500	-	1500	-	-	447	2668
PH	6.5-8.5	-	6.5-8.5	-	-	6	6.5-8.5	7.2	7.3
Na^+	200	-	-	-	100	-	20	33.1	360.1
K^+	-	-	-	-	12	-	10	1.6	14.1
Ca^{++}	100-300	-	-	-	-	10	100	53.3	300.5
Mg^{++}	-	-	-	-	50	5	30	28.6	132.5
Fe^{++}	0.3	-	0.3	-	0.3	-	0.1	0.103	0.998*
Mn^{++}	0.1	-	0.05	-	0.05	-	0.02	0.155	0.9*
SO_4^{--}	400	-	250	-	250	-	5	121	1488
Cl^-	250	-	250	-	200	-	25	66.6	319
HCO_3^-	-	-	-	-	-	-	30	90.9	410
CO_3^{--}	-	-	-	-	-	10	35	0	30
EC*^	-	-	-	-	1250	-	400	892	3000

ITEM	WHO 1984		USEPA 1988		EEC 1975			LOWER PART STUDY RESULTS IN 1989 NO. OF WELLS (6)	
	MAC mg/l	MRC mg/l	MAC mg/l	MRC mg/l	MAC mg/l	MRC mg/l	GIL mg/l	MIN mg/l	MAX mg/l
TDS	1000	-	500	-	1500	-	-	1744	3667
PH	6.5-8.5	-	6.5-8.5	-	-	6	6.5-8.5	7.3	7.6
Na^+	200	-	-	-	100	-	20	165	719.9
K^+	-	-	-	-	12	-	10	1.2	10.2
Ca^{++}	100-300	-	-	-	-	10	100	247.3	413.4
Mg^{++}	-	-	-	-	50	5	30	90.7	161
Fe^{++}	0.3	-	0.3	-	0.3	-	0.1	0.161	0.869**
Mn^{++}	0.1	-	0.05	-	0.05	-	0.02	0.163	0.694**
SO_4^{--}	400	-	250	-	250	-	5	0	773
Cl^-	250	-	250	-	200	-	25	319	2355
HCO_3^-	-	-	-	-	-	-	30	24.4	244.1
CO_3^{--}	-	-	-	-	-	10	35	0	0
EC*^	-	-	-	-	1250	-	400	2845	6504

*Based on 7 samples **Based on 3 samples EC*^ µmhos/cm

Table 4.21 Comparative tabulation of potable water quality with selected international standards (Wadi Habawnah)

ITEM	WHO 1984		USEPA 1988		EEC 1975			AL-KHANG STUDY RESULTS IN 1990 NO. OF WELLS (14)	
	MAC mg/l	MRC mg/l	MAC mg/l	MRC mg/l	MAC mg/l	MRC mg/l	GIL mg/l	MIN mg/l	MAX mg/l
TDS	1000	-	500	-	1500	-	-	854	6225
pH	6.5-8.5	-	6.5-8.5	-	-	6	6.5-8.5	6.2	7.4
Na^+	200	-	-	-	100	-	20	57.9	380.1
K^+	-	-	-	-	12	-	10	5.9	14.9
Ca^{++}	100-300	-	-	-	-	10	100	58.1	521
Mg^{++}	-	-	-	-	50	5	30	27.2	218.9
Fe^{++}	0.3	-	0.3	-	0.3	-	0.1	0.614	0.614**
Mn^{++}	0.1	-	0.05	-	0.05	-	0.02	0.223	0.223**
SO4	400	-	250	-	250	-	5	165	1386
Cl^-	250	-	250	-	200	-	25	106	1169
HCO_3	-	-	-	-	-	-	30	90.9	151.9
CO_3^{--}	-	-	-	-	-	10	35	0	0
EC*^	-	-	-	-	1250	-	400	930	4500

ITEM	WHO 1984		USEPA 1988		EEC 1975			AL-JIFA STUDY RESULTS IN 1990 NO. OF WELLS (7)	
	MAC mg/l	MRC mg/l	MAC mg/l	MRC mg/l	MAC mg/l	MRC mg/l	GIL mg/l	MIN mg/l	MAX mg/l
TDS	1000	-	500	-	1500	-	-	1269	4423
pH	6.5-8.5	-	6.5-8.5	-	-	6	6.5-8.5	6.7	7.4
Na^+	200	-	-	-	100	-	20	92.9	180
K^+	-	-	-	-	12	-	10	2	5.1
Ca^{++}	100-300	-	-	-	-	10	100	94.2	501
Mg^{++}	-	-	-	-	50	5	30	36	145.9
Fe^{++}	0.3	-	0.3	-	0.3	-	0.1	0.595	0.595**
Mn^{++}	0.1	-	0.05	-	0.05	-	0.02	0.245	0.245**
SO4	400	-	250	-	250	-	5	205	1009
Cl^-	250	-	250	-	200	-	25	176.9	709
HCO_3	-	-	-	-	-	-	30	122	212.9
CO_3^{--}	-	-	-	-	-	10	35	0	0
EC*^	-	-	-	-	1250	-	400	1982	6900***

ITEM	WHO 1984		USEPA 1988		EEC 1975			AL-HARSHAF STUDY RESULTS IN 1990NO. OF WELLS (9)	
	MAC mg/l	MRC mg/l	MAC mg/l	MRC mg/l	MAC mg/l	MRC mg/l	GIL mg/l	MIN mg/l	MAX mg/l
TDS	1000	-	500	-	1500	-	-	1200	4400
pH	6.5-8.5	-	6.5-8.5	-	-	6	6.5-8.5	6.8	7.6
Na^+	200	-	-	-	100	-	20	129.9	539.9
K^+	-	-	-	-	12	-	10	6.3	14.1
Ca^{++}	100-300	-	-	-	-	10	100	175.2	406
Mg^{++}	-	-	-	-	50	5	30	51.8	144.4
Fe^{++}	0.3	-	0.3	-	0.3	-	0.1	0.37	0.848
Mn^{++}	0.1	-	0.05	-	0.05	-	0.02	0.154	0.216
SO4	400	-	250	-	250	-	5	505	1708
Cl^-	250	-	250	-	200	-	25	245.7	744.1
HCO_3	-	-	-	-	-	-	30	90.9	183
CO_3^{--}	-	-	-	-	-	10	35	0	0
EC*^	-	-	-	-	1250	-	400	1875	6875***

continued on next page

Table 4.21 continued

ITEM	WHO 1984		USEPA 1988		EEC 1975			AL-MAJMA STUDY RESULTS IN 1990 NO. OF WELLS (9)	
	MAC mg/l	MRC mg/l	MAC mg/l	MRC mg/l	MAC mg/l	MRC mg/l	GIL mg/l	MIN mg/l	MAX mg/l
TDS	1000	-	500	-	1500	-	-	1095	2466
pH	6.5-8.5	-	6.5-8.5	-	-	6	6.5-8.5	7.1	8.1
Na^+	200	-	-	-	100	-	20	77.9	180
K^+	-	-	-	-	12	-	10	2.3	10.2
Ca^{++}	100-300	-	-	-	-	10	100	81.4	280
Mg^{++}	-	-	-	-	50	5	30	34	90.7
Fe^{++}	0.3	-	0.3	-	0.3	-	0.1	0.37	0.78
Mn^{++}	0.1	-	0.05	-	0.05	-	0.02	0.155	0.226
SO4	400	-	250	-	250	-	5	239.7	627.3
Cl^-	250	-	250	-	200	-	25	141.1	354.1
HCO_3	-	-	-	-	-	-	30	90.9	151.9
CO_3^{--}	-	-	-	-	-	10	35	0	0
EC*^	-	-	-	-	1250	-	400	1300	2400

ITEM	WHO 1984		USEPA 1988		EEC 1975			AL-HABWNAH STUDY RESULTS IN 1990 NO. OF WELLS (6)	
	MAC mg/l	MRC mg/l	MAC mg/l	MRC mg/l	MAC mg/l	MRC mg/l	GIL mg/l	MIN mg/l	MAX mg/l
TDS	1000	-	500	-	1500	-	-	1273	2033
pH	6.5-8.5	-	6.5-8.5	-	-	6	6.5-8.5	7.2	8
Na^+	200	-	-	-	100	-	20	80	160
K^+	-	-	-	-	12	-	10	5.1	8.6
Ca^{++}	100-300	-	-	-	-	10	100	127.1	187.2
Mg^{++}	-	-	-	-	50	5	30	34	59.1
Fe^{++}	0.3	-	0.3	-	0.3	-	0.1	0.387	0.648
Mn^{++}	0.1	-	0.05	-	0.05	-	0.02	0.171	0.203
SO4	400	-	250	-	250	-	5	275.7	542.3
Cl^-	250	-	250	-	200	-	25	141.1	248.1
HCO_3	-	-	-	-	-	-	30	122	151.9
CO_3^{--}	-	-	-	-	-	10	35	0	0
EC*^	-	-	-	-	1250	-	400	1300	2000

ITEM	WHO 1984		USEPA 1988		EEC 1975			AL-MUNTASHER STUDY RESULTS IN 1990 NO. OF WELLS (9)	
	MAC mg/l	MRC mg/l	MAC mg/l	MRC mg/l	MAC mg/l	MRC mg/l	GIL mg/l	MIN mg/l	MAX mg/l
TDS	1000	-	500	-	1500	-	-	1109	2849
pH	6.5-8.5	-	6.5-8.5	-	-	6	6.5-8.5	6.6	7.3
Na^+	200	-	-	-	100	-	20	24	160
K^+	-	-	-	-	12	-	10	2.3	7
Ca^{++}	100-300	-	-	-	-	10	100	92.2	281.8
Mg^{++}	-	-	-	-	50	5	30	26.7	94.1
Fe^{++}	0.3	-	0.3	-	0.3	-	0.1	0.426	0.781
Mn^{++}	0.1	-	0.05	-	0.05	-	0.02	0.15	0.173
SO4	400	-	250	-	250	-	5	174.4	510.6
Cl^-	250	-	250	-	200	-	25	141.1	567.2
HCO_3	-	-	-	-	-	-	30	90.9	273.9
CO_3^{--}	-	-	-	-	-	10	35	0	0
EC*^	-	-	-	-	1250	-	400	1100	1900

Continued on next page

Table 4.21 continued

ITEM	WHO 1984		USEPA 1988		EEC 1975			MOR.&AL-NG.&DY* RESULTS IN 1990NO. OF WELLS (4)	
	MAC mg/l	MRC mg/l	MAC mg/l	MRC mg/l	MAC mg/l	MRC mg/l	GIL mg/l	MIN mg/l	MAX mg/l
TDS	1000	-	500	-	1500	-	-	1294	3376
pH	6.5-8.5	-	6.5-8.5	-	-	6	6.5-8.5	7.1	7.3
Na^+	200	-	-	-	100	-	20	92.9	269.9
K^+	-	-	-	-	12	-	10	3.1	7.8
Ca^{++}	100-300	-	-	-	-	10	100	92.2	309.8
Mg^{++}	-	-	-	-	50	5	30	36.2	91.2
Fe^{++}	0.3	-	0.3	-	0.3	-	0.1	0.404	0.591
Mn^{++}	0.1	-	0.05	-	0.05	-	0.02	0.147	0.172
SO4	400	-	250	-	250	-	5	254	828
Cl^-	250	-	250	-	200	-	25	176.9	477.5
HCO_3	-	-	-	-	-	-	30	122	151.9
CO_3^{--}	-	-	-	-	-	10	35	0	0
EC*^	-	-	-	-	1250	-	400	1300	4400

ITEM	WHO 1984		USEPA 1988		EEC 1975			AL-HUSAYNIAH STUDY RESULTS IN 1990 NO.OF WELLS (4)	
	MAC mg/l	MRC mg/l	MAC mg/l	MRC mg/l	MAC mg/l	MRC mg/l	GIL mg/l	MIN mg/l	MAX mg/l
TDS	1000	-	500	-	1500	-	-	2888	5817
pH	6.5-8.5	-	6.5-8.5	-	-	6	6.5-8.5	6.9	7.3
Na^+	200	-	-	-	100	-	20	155.9	430
K^+	-	-	-	-	12	-	10	3.1	10.2
Ca^{++}	100-300	-	-	-	-	10	100	307.4	475.8
Mg^{++}	-	-	-	-	50	5	30	95.6	209.1
Fe^{++}	0.3	-	0.3	-	0.3	-	0.1	0.574	0.625
Mn^{++}	0.1	-	0.05	-	0.05	-	0.02	0.212	0.219
SO4	400	-	250	-	250	-	5	484	1474
Cl^-	250	-	250	-	200	-	25	460	861
HCO_3	-	-	-	-	-	-	30	122	183
CO_3^{--}	-	-	-	-	-	10	35	0	0
EC*^	-	-	-	-	1250	-	400	2900	4400

*MORYKHAH, AL-NGAH and AL-DAYQAH **LIMTED DATA ***CALCULATED *^mmhos/cm

high concentrations of Na^+ and Ca^{2+}, SO_4^{2-} and Cl^-. This high salinity of groundwater may be as a result of the location of the well far from the main wadi channel (2 km) where the flood recharge is very rare, the rainfall rate is small and the evaporation rate is high.

In the lower part of Wadi Baysh, all of the analyses of TDS were above the EEC limit. Such high salinity may be a result of irrigation which diverts the flood waters to many farmers lands, exposing a large area of surface water to evaporation. This would affect the groundwater chemistry because the percolated water would have enhanced the soluble mineral content.

pH: The MAC and MRC levels for hydrogen ion concentration are 8.5 and 6.5, respectively. All of the well data were lay within the recommended limits (Figure 4.9b)

4.17.1.1.1 Major Ions

The analytical lists (Tables 4.16 and 4.17) show that the concentration of all major ions in the upper section of Wadi Baysh were within the EEC recommended safety limits. However, trace elements Fe^{2+} and Mn^{2+} exceeded the EEC limits with concentrations of 0.725-0.964 and 0.154-0.186 mg/l, respectively.

4.17.1.1.2 Hardness

The groundwater hardness may be defined as the ion concentration in the water that will react with a sodium soap to precipitate an insoluble residue. It is caused primarily by calcium and magnesium cations, although some heavy metals such as iron and manganese also consume soap (Table 4.22).

Hardness of water may be divided into two types, carbonate and non-carbonate. Carbonate hardness includes that portion of calcium and magnesium that combines with bicarbonate and the small amount of carbonate present. This is known as temporary hardness because it can be removed by boiling, which precipitates calcium and magnesium carbonate and sulphate minerals. Non-carbonate hardness is the difference between total hardness and carbonate hardness. It is caused by those amounts of calcium and magnesium that combine normally with sulphate, chloride and nitrate ions, plus the slight hardness contributed by minor constituents such as iron. Non-carbonate hardness cannot be removed

Table 4.22 Groundwater characteristics of Wadi Baysh to show the suitability of water use for irrigation.

Groundwater characteristics of the upper part of Wadi Baysh.

Sample No.	Temp. °C	PH	TDS ppm	TH mg/l	SAR meq/l	RC meq/l
BU1	33	7.3	406	234	-2.8	-0.76
BU2	32	7.3	470	250	-2.5	-0.3
BU3	32	7.3	570	365	-5	-2.0

Groundwater characteristics of the middle part of Wadi Baysh.

Sample No.	Temp. °C	PH	TDS ppm	TH mg/l	SAR meq/l	RC meq/l
BM4	32	7.2	732	508	-7.7	-5.31
BM5	32	7.2	536	317	-3.6	-0.26
BM6	32	7.3	530	1295	-3.0	-12
BM7	31	7.2	829	397	-5.7	-2.29
BM8	33	7.4	817	437	-7.3	-4.77
BM9	31	7.3	1057	755	-1.31	-8.36
BM10	33	7.2	3140	268	-3.4	-0.66
BM11	32	7.3	595	361	-3.1	-0.7
BM12	32	7.3	679	427	-4.1	-1.73
BM13	33	7.2	589	337	-1.7	1.07
BM14	32	7.3	987	642	-6.1	-2.85

Groundwater characteristics of the lower part of Wadi Baysh.

Sample No.	Temp. °C	PH	TDS ppm	TH mg/l	SAR meq/l	RC meq/l
BL15	31	7.3	1983	990	-1.58	-8.34
BL16	31	7.4	2128	1058	-1.73	-9.38
BL17	32	7.2	3893	1693	-3.26	-19.38
BL18	33	7.6	3857	1677	-3.3	-19.87
BL19	33	7.5	2350	1260	-2.48	-16.8
BL20	32	7.3	1965	1280	-2.46	-16.6

Temperature in centigrade degrees (Temp.°C)
Hydrogen ion concenteration (pH)
Total dissolved solids (TDS mg/l)
Total hardness(TH mg/l)
Sodium adsorprtion ratio (SAR)
Residual carbonate (RC)

by boiling.

Since the calcium and magnesium ions are known in mg/l, total hardness can be determined using the expression:

Total hardness as $CaCO_3 = 2.5\ (Ca^{+}) + 4.1\ (Mg^{2+})$ (see Todd, 1980)

The terms "hard water" and "soft water" are relative expressions of hardness. Numerical values for hardness have meaning only in the relative sense because consumer acceptance of hardness varies widely. Durfor and Becker (1964) used the following classifications:

Hardness range mg/l of $CaCO_3$	Description
0 - 60	soft
61 - 120	moderately hard
121 - 180	hard
More than 180	very hard

The World Health Organisation (1971) suggested an upper limit of 500 mg/l for potable waters. The Wadi Baysh groundwater is very hard water with a range of 234 to 1694 mg/l.

4.17.1.2 Wadi Habawnah

TDS (total dissolved solids): About 70% of the wells in Wadi Habawnah yield water below the EEC MAC (Table 4.21). The wells above the recommended level are mostly located in the lower part of Wadi Habawnah (Al Gifah and Al Husaniah).

pH: With the exception of the well at Al Khaneq, the waters were all within the EEC recommended level (6.5-8.5). At Al Khang the pH values (6.5, 6.3) were below those recommended.

4.17.1.2.1 Major Ions

The water sample analysis data (Table 4.21) indicate that calcium, magnesium, sodium, sulphate, and chloride vary from below to above the EEC recommended safety limit. The Fe^{2-} and Mn^{2+} concenteration are above the EEC limit. In the Al Husaniah area (lower part) all water ions showed concentrations above those required by the EEC limits. In most samples, concentrations were lower than the recommended EEC limits.

4.17.1.2.2 Hardness

The groundwater hardness value in Wadi Habawnah was between 313 and 2045

mg/l. According to the Durfor and Becker classifications of hardness, the Wadi Habawnah groundwater is very hard.

4.17.2 Irrigation Water

Groundwater is most extensively used for irrigation purposes throughout the year. In Wadi Habawnah the irrigation system depends on pumping from wells while in Wadi Baysh most of the farmers depend on floods to irrigate their farms. This study, will be focused on hydrochemical factors determining the suitability of irrigation water. Several empirical indices may be used:

1- Total dissolved solids (TDS)

2- Sodium absorption ratio (SAR)

3- Bicarbonate hazard (RSC)

4- Salinity expressed either as TDS or EC.

4.17.2.1 Total Dissolved Solids (TDS)

Dissolved-solids values are widely used in evaluating water quality and are a convenient means of comparing water quality from site to site.

Robinove *et al.* (1958) assigned terms for water of high dissolved solids contents as follows:

	Dissolved solids (mg/l)
Slightly saline	1,000 - 3,000
Moderately saline	3,000 - 10,000
Very saline	10,000 - 35,000
Briny	more than 35,000

According to Robinove's salinity classification, the Wadi Baysh and Wadi Habawnah groundwaters are slightly to moderately saline. Figure 4.36 indicates that fresh water is dominant in most of the upper and middle parts of the wadi while saline waters dominate the lower parts of the area. Some of the area in the upper part of Wadi Habawnah (Al Harshaf) shows high salinity waters, either because of the location of the well, far from the wadi channel, or because the alluvium is thin and evaporation increases the salinity of the aquifer.

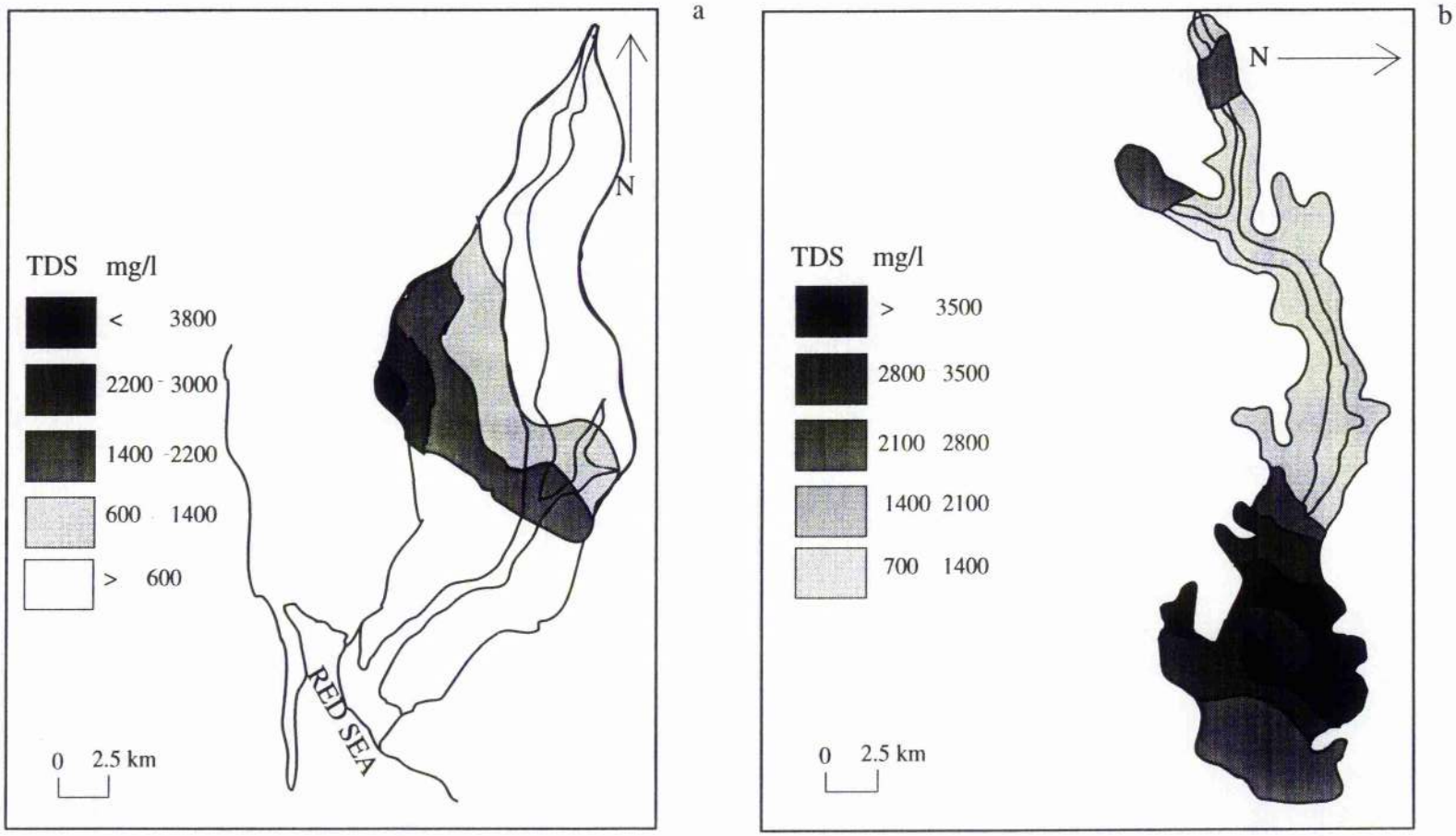

Figure 4.36 Areal distribution map of total dissolved solids (analysed data) in Wadi Baysh (a) and Wadi Habawnah (b) groundwater.

4.17.2.2 Sodium Absorption Ratio (SAR)

Measuring the effect of sodium ions is a very important factor for agricultural use. It is the ratio of sodium to calcium and magnesium which determines the characteristics of the soil. When sodium-rich water is applied to soil, some of the sodium is taken up by clay and the clay gives up calcium and magnesium in exchange. Driscoll (1986) indicates that clay which takes up sodium becomes sticky and slick when wet and has low permeability. When it dries the clay shrinks into hard clods that are difficult to cultivate. On the other hand, when the same clay carries excess calcium or magnesium ions, it tills easily and has good permeability.

The method of measuring the effect of sodium ions is by means of the Sodium Absorption Ratio (SAR). The SAR is calculated from the following equation:

$$SAR = [Na/\{(Ca+Mg)/2\}1/2]$$

where sodium, calcium and magnesium are in meq/l from the water analysis. The sodium hazard is low to medium in both wadis except for one sample in the lower part of Wadi Baysh which shows a high sodium hazard (Figure 4.37 and Table 4.22). Low sodium water as described by Wilcox (1955) can be used for irrigation on almost all soils with little danger of the development of harmful levels of exchangeable sodium. Quoting from the U.S. salinity report (1954) "low salinity water can be used for irrigation with most crops on most soils with little likelihood that a salinity problem will develop". Some leaching is required but this occurs under normal irrigation practices except in soils of extremely low permeability. Medium salinity water can be used if a moderate amount of leaching occurs. Plants with moderate salt tolerance can be grown in most instances without special practices for salinity control.

Based on US salinity laboratory (1954), SAR values below 10 indicate little danger of a sodium problem. In Figure 4.37 and Tables 4.22 and 4.23, the SAR ratio is within the safe limit. In Wadi Habawnah the SAR ranges between 2 and 6 while in Wadi Baysh it shows a range between less than 1 to 7.

The US Department of Agriculture has devised a classification for irrigation water based on a combination of parameters. In their classification they have considered the SAR

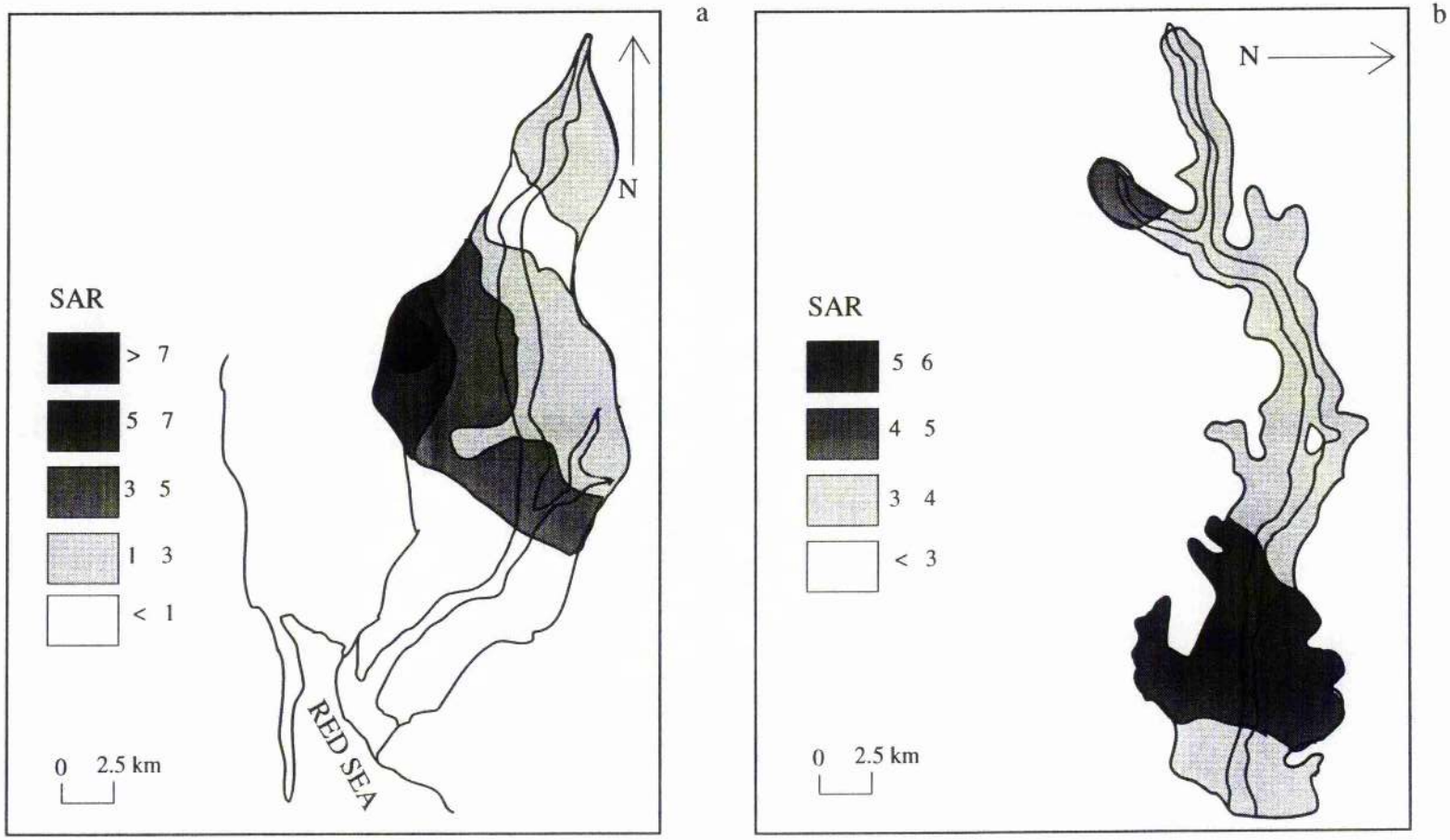

Figure 4.37 Areal distribution map of sodium adsorption ratio in Wadi Baysh (a) and Wadi Habawnah (b) groundwater

Table 4.23 Groundwater characteristics of Wadi Habawnah to show the suitability of water use for irrigation.

Groundwater characteristics of Al-KHANEQ

Sample No.	Temp. °C	PH	TDS mg/l	TH mg/l	SAR meq/l	Na %	RC meq/l
KH1	26	7.1	579	313	1.42	30	-3.8
KH2	25.5	7.2	1285	830	1.56	22	-14.1
KH3	26	7.3	2572	1547	2.76	27	-28.5
KH4	25	6.2	1473	897	1.57	21	-15.5
KH5	26	6.5	1478	963	1.79	23	-17.3
KH6	26	6.4	2871	1780	3.09	27	-33.1
KH7	26	6.5	3742	2201	3.52	28	-42.2
KH8	25	7.1	1473	838	2.7	32	-14.3
KH9	26	6	2134	1310	2.64	27	-24.2
KH10	26	7.5	1184	705	1.8	26	-12.6
KH11	25	7.3	505	257	1.77	37	-2.7
KH12	26	7.2	599	313	1.97	37	-4.8
KH13	26	7.4	804	437	1.87	32	-6.7
KH14	26	6.2	2276	1413	2.55	26	-26.8

Groundwater characteristics of Al-JIFA

Sample No.	Temp. °C	PH	TDS mg/l	TH mg/l	SAR meq/l	Na %	RC meq/l
GF-1	27	7.2	877	483	2.14	33	-7.2
GF2	28	7.1	834	463	1.88	31	-7.3
GF3	28	7.4	1247	650	2.9	36	-11
GF4	28	7.2	1004	480	3.37	44	-7.6
GF5	27	7.1	861	500	2	31	-8
GF6	28	6.8	2626	1850	1.82	18	-34.5
GF7	28	6.7	734	383	2.49	39	-4.2

Groundwater characteristics of AL-HARSHAF

Sample No.	Temp. °C	PH	TDS mg/l	TH mg/l	SAR meq/l	Na %	RC meq/l
HR1	24.7	7.6	1717	840	3.45	38	-14.3
HR2	25	7.6	1776	890	3.5	38	-14.8
HR3	25	7.4	1733	950	2.96	33	-17
HR4	27.2	6.8	1331	713	2.77	35	-12.8
HR5	28.2	6.8	3610	1607	5.86	42	-30.1
HR6	28	6.8	1222	676	2.17	30	-12
HR7	25.3	7.4	1276	690	2.98	37	-11.8
HR8	26	6.9	1932	1122	2.86	31	-20.4
HR9	25.2	6.8	1855	983	3.05	33	-17.2

Groundwater characteristics of AL-MAJMAA

Sample No.	Temp. °C	PH	TDS mg/l	TH mg/l	SAR meq/l	Na %	RC meq/l
MJ1	25	7.3	795	470	1.66	28	-7.9
MJ2	25	7.3	1174	727	1.85	26	-12.5
MJ3	28.2	7.5	851	463	2.02	32	-7.3
MJ4	25	7.5	885	510	1.73	28	-8.2
MJ5	25	7.5	1228	680	2.17	30	-11.1
MJ6	23.1	8.1	1470	940	1.99	25	-16.8
MJ7	28.7	7.1	785	428	2	34	-6.6
MJ8	26.5	7.2	1521	877	2.64	32	-15.5
MJ9	30	7.5	656	343	1.83	34	-4.4

Groundwater characteristics of HABAWNA

Sample No.	Temp. °C	PH	TDS mg/l	TH mg/l	SAR meq/l	Na %	RC meq/l
HB1	27	7.2	1026	520	2.75	38	-7.9
HB2	27	8	881	528	1.95	31	-8.6
HB3	27	7.3	1230	710	2.61	34	-12.2
HB4	27	7.4	745	503	1.55	27	-8.1
HB5	27	7.4	1099	664	2.16	30	-11.3
HB6	27	7.4	884	467	2.09	33	-7.3

Continued on next page

Table 4.23 continued

Groundwater characteristics of AL-MUNTASHER

Sample No.	Temp. °C	PH	TDS mg/l	TH mg/l	SAR meq/l	Na %	RC meq/l
MT1	28	7.3	1663	1090	2.11	24	-20.3
MT2	28	7.2	807	407	2.27	36	-6.7
MT3	29.3	6.6	707	370	2.26	38	-5.9
MT4	28	6.6	971	543	2.42	35	-7.9
MT5	28	6.8	862	367	2.04	36	-3.3
MT6	27.6	6.6	1152	873	1.18	17	-14.5
MT7	28.5	7.1	636	497	0.48	10	-7.5
MT8	27	7.2	952	607	1.77	27	-9.1
MT9	28	7.2	954	697	1.2	19	-9.5

Groundwater characteristics of MORYKHAH

Sample No.	Temp. °C	PH	TDS mg/l	TH mg/l	SAR meq/l	Na %	RC meq/l
MR	27	7.3	792	397	2.4	39	-5.5

Groundwater characteristics of AL-NGAH

Sample No.	Temp. °C	PH	TDS mg/l	TH mg/l	SAR meq/l	Na %	RC meq/l
NG-1	27	7.3	783	406	2.01	34	-5.6
NG-2	27	7.3	1106	607	2.12	30	-9.2

Groundwater characteristics of AL-DAYQAH

Sample No.	Temp. °C	PH	TDS mg/l	TH mg/l	SAR meq/l	Na %	RC meq/l
DY	30	7.1	2041	1148	3.46	34	-21

Groundwater characteristics of AL-HUSAYNIAH

Sample No.	Temp. °C	PH	TDS mg/l	TH mg/l	SAR meq/l	Na %	RC meq/l
HS-1	30	7.1	3239	1927	3.67	30	-36
HS-2	30	6.9	2387	1350	4.26	37	-24
HS-3	30	7.2	3500	2045	4.14	32	-38.4
HS-4	30	7.3	1651	1192	1.96	22	-21.8

Temperature in centigrade degrees (Temp. °C)
Hydrogen ion concenteration (pH)
Total dissolved solids (TDS mg/l)
Total hardness(TH mg/l)
Sodium adsorprtion ratio (SAR)
Residual carbonate (RC)

in combination with electrical conductivity which has proved very convenient and is widely used in assessing irrigation water quality. The actual plot (Figure 4.38) of calculated SAR value and the measured EC values suggest that, although the sodium risk is higher, nevertheless most of the water falls within the category of medium to high salinity hazard in both wadis.

On the basis of the latter criterion for different categories of hazards, it may be concluded that most of the waters are not suitable for most crops. Nevertheless, selective cropping patterns (such as parley, sorgum, palm tree) would be more appropriate in areas having high salinity hazard such as the lower parts of both wadis.

4.17.2.3 Residual Carbonate (RC)

The bicarbonate hazard (RC) arises when the sum of carbonate and bicarbonate is in excess of calcium and magnesium, and there is almost complete precipitation of the latter

$$RC = (CO_3^{2-} + HCO_3^-) - (Ca^{2+} + Mg^{2+})$$

where all the concentrations are expressed in meq/l.

Since the safe margin of RC is 204 meq/l, the present sets of data, indicates that the water of both wadis is suitable for agricultural use (Tables 4.22 and 4.23). In the lower part of both areas most of the wells show high salinities but with ionic compositions maintaining a suitable balance for agricultural purposes.

For the present sets of data from the lower parts of both wadis, the evaluation of the groundwater conditions may need to be based on the salinity conditions rather than the SAR and RC.

This is because the lower parts of both wadis are characterised by high evaporation and low rainfall (120-80mm). Using groundwater with high salinity for irrigation would damage the agricultural water supply. A subsurface drainage system to reduce the evaporation effect and the planting of suitable crops for such high salinity in this part of the study area is recommended.

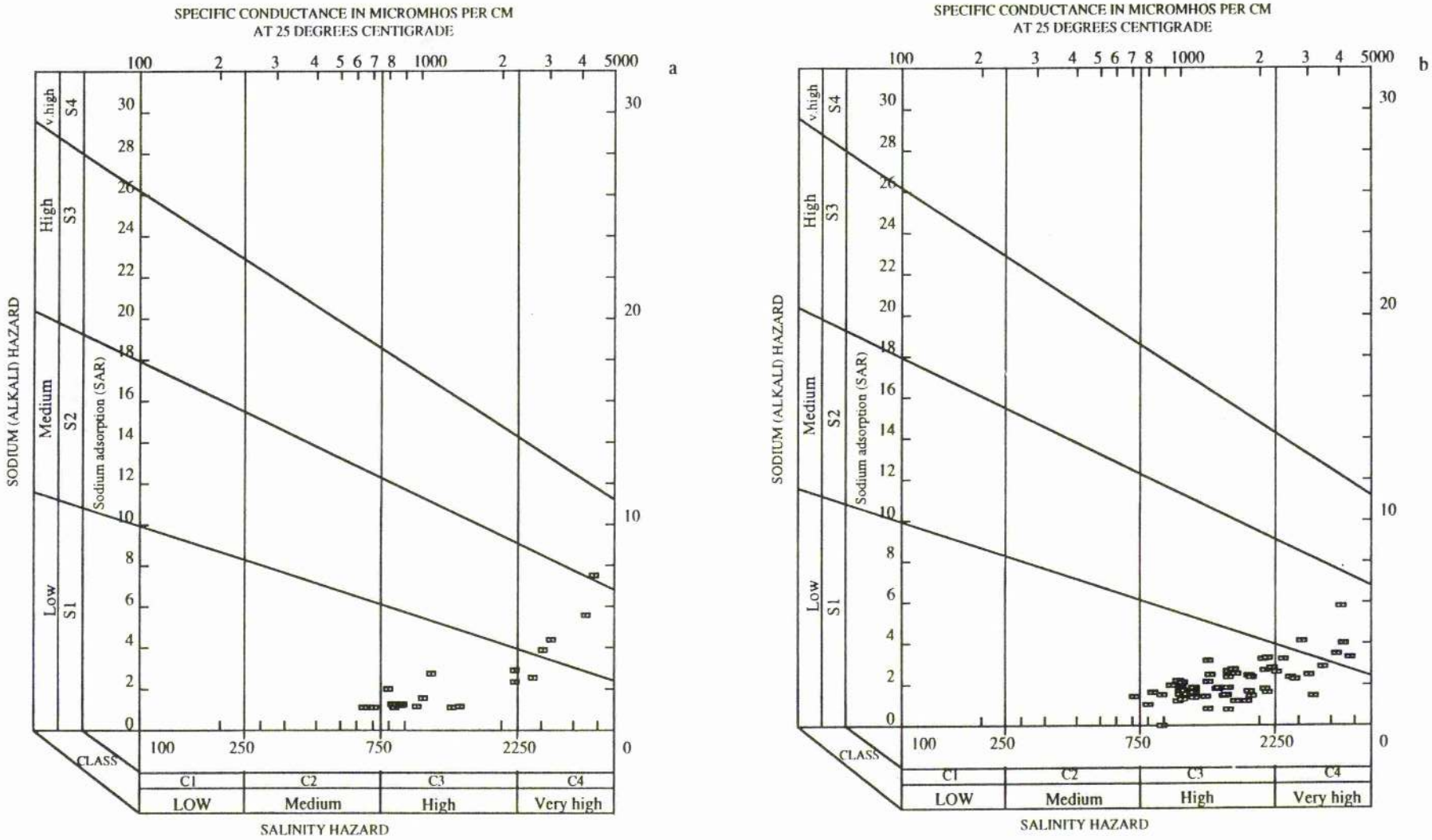

Figure 4.38 U.S. Salinity diagram for use in interpreting the analysis of irrigation water of Wadi Baysh (b) and Wadi Habawnah with it's major tributaries (b) in January 1990.

4.18 Summary and Conclusion

Groundwater in the alluvial systems of Wadi Baysh and Wadi Habawnah has been the subject of geochemical and water quality investigations as part of this study.

Water samples were collected from 62 and 20 hand dug wells in Wadi Habawnah and Wadi Baysh respectively. The groundwater sample concentrations of the major ions (Ca^{2+}, Mg^{2+}, Na^{+}, K^{+}, CO_3^{2-}, HCO_3^{-}, SO_4^{2-} and Cl^{-}) and some trace elements (Fe^{2+}, Mn^{2+}, Ni^{2+}, Pb^{2+} and Al^{3+}) were determined.

The description of major ions in the groundwater analyses has been augmented by areal distribution maps of each ion to show the variation of the groundwater quality in both wadis. The ionic distribution maps of calcium, sodium, magnesium, sulphate and chloride show high concentrations in the water in the lower part of both wadis. This indicates a high natural abundance of these ions and may point to their high solubility .

Several graphical methods for interpreting the chemical data from the well fields in both wadis were adopted because of the large number of analyses, such as X-Y plots, the Piper diagram and the Durov diagram. It can be observed from the linear plots of major ions that: (1) The well samples vary considerably in their solute concentrations; (2) The data plot on straight lines, revealing a positive correlation of Na^{+},Ca^{2+},Mg^{2+},Cl^{-}, SO_4^{2-} with TDS. (3) The data plots of K^{+} and HCO_3^{-} and CO_3^{2-}, show a poor correlation with TDS. These mixing lines are characterised by positive correlations and indicate that the aquifer waters mix in various proportions with recharge water.

The correlation coefficient of Cl^{-} against Na^{+} in the aquifer in Wadi Baysh has a higher value (0.9) than that in Wadi Habawnah (0.79). In Wadi Baysh the relationship between Cl^{-} and Na^{+} indicates that a simple dissolution or mixing between waters is the main process in the aquifer. However, the Wadi Habawnah analyses show that the Cl^{-} concentration exceeds the Na^{+} concentration, which may be due to reverse ion exchange, where $CaCl_2$ water type is abundant.

The relationship between (Ca^{2+}+Mg^{2+}) and ($HCO_3^{-} + SO_4^{2-}$) displays a strong correlation coefficient (0.9) in both wadis. Such a feature indicates that simple dissolution and mixing are the main processes in the aquifers.

The Piper trilinear diagram for Wadi Habawnah (Figures 4.7 and 4.8) shows that the cation composition is dominated by calcium (40-60%) with subsidiary magnesium (20-30%), while sulphate (40-60%) is the dominant anion with subsidiary chloride (30-50%). In terms of hydrochemical facies, the groundwater of Wadi Habawnah is principally a calcium-sulphate type. Sodium-chloride and magnesium-sulphate water types are also present but less common.

The trilinear diagram for Wadi Baysh, differs from that of Wadi Habawnah. Chloride, the stable fraction, normally represents 20-30% of the groundwater anions. The water type is characteristically of the calcium-sodium-chloride facies with some examples of magnesium-sulphate or calcium bicarbonate water types.

Durov's Diagram shows that in Wadi Baysh simple dissolution is dominant for 30% of the samples, which plot in Field 1, and 10% each in Fields 5 and 9. The water type could therefore be Ca (HCO_3) and NaCl. Some 30% of the samples fall in Field 4 where Ca^{2+} and SO_4^{2-} are dominant, suggesting a mixed water or a water exhibiting simple dissolution within the basin fill.

The expanded Durov diagram for the Wadi Baysh groundwater samples (Figure 4.24) shows that only 6% reflect $CaSO_4$ and Na Cl water types. This compares with 79% of the Wadi Habawnah samples being of Ca SO_4 type, a similar interpretation to that derived from the Piper diagram. About 45% of the Wadi Habawnah samples, out of the 79% which plot in Field 4, are from the upper part of the wadi (Al Khaneg, Al Harshaf and Al Majma). In Wadi Baysh the middle parts influence the water type of Field 1 while in Field 2 the water shows equal influence from all parts of the wadi. This may be as a result of mixing processes and evaporation.

The computer programme WATEQF results show that aqueous speciation and saturation data of most of the groundwater samples are sub-saturated, except for a few samples from the middle and lower part of Wadi Baysh and from scatterd sites along Wadi Habawnah which are super-saturated in respect of $CaCO_3$ and $CaMg(CO_3)_2$. application of cluster analysis shows that the recharge area of Wadi Baysh is characterised by the hydrochemical facies of $CaCO_3$ while the Wadi Habawnah recharge area is characterised by

the hydrochemical facies of $CaCO_3$ and $CaSO_4$. The discharge area of Wadi Baysh is dominated by the hydrochemical facies of $CaCO_3$ and NaCl while the Wadi Habawnah discharge area is largely dominated by the hydrochemical facies of $CaSO_4$ and NaCl. The middle part of Wadi Baysh is dominated by the same hydrochemical facies as in the discharge area while the middle part of Wadi Habawnah is dominated by the hydrochemical facies of $CaCO_3$ and $CaMg(SO_4)_2$.

Principal component analysis shows that the Wadi Habawnah groundwater has a high loading of total dissolved solids, sodium, calcium, chloride and sulphate. These high values of groundwater constituents are most likely the result of evaporation.

Bicarbonate has significantly loaded components 2, 3 and 4. It probably reflects the initial dissolution of minerals by groundwater. The low variance associated with this component probably reflects buffering of the HCO_3^- content by CO_2 exchange between groundwater and the atmosphere. Also there is loading of saturation indices of aragonite. It may indicate precipitation of aragonite and possible calcite within the basin fill. Component 4 shows a high loading that may be released into the groundwater by weathering of K-feldspar. It is removed, perhaps, by ion exchange or uptake as a plant nutrient.

In Wadi Baysh the groundwater has a high loading for total dissolved solids, sodium, calcium, chloride and sulphate. Also there is loading of saturation indices of aragonite. This may indicate precipitation of aragonite and possible dolomite.

Water type classification, based on the average ionic content with low standard deviation that dominates the groundwater in each zone of each wadi (upper, middle, lower zone), has been applied. Accordingly, in Wadi Baysh and Wadi Habawnah three main water types can be identified:

The upper part of Wadi Baysh (Misleyah area) is characterised by Water Type (I) as calcium sulphate rich.Water Type (II) is of calcium sulphate and sodium chloride waters which represents the groundwater in the middle zone (Baysh area). Water Type (III) is calcium sulphate and sodium chloride waters. It occurs in the lower part, in semi confined to confined aquifers (basin area).

Wadi Habawnah: Water Type (I) dominates the recharge area (Al Khanig,

Alharashf, Al majma and Habawnah village area). Water Type (II) is calcium sulphate water with chloride becoming increasingly dominant in the middle part (Almuntasher, Alnagah, Al Daugah and Morayekhah areas). The unconfined to semi confined aquifer in the Wadi Habawnah outlet is characterised by Type (III), calcium sulphate and sodium chloride waters.

Assuming that the water points are representative of the whole hydrological column in both wadis, analysing the results using different graphical interpretations as well as chemical simulation, shows that:

1- The dominant chemical processes occurring in the groundwater of both wadis continue throughout the aquifer with the flow directions.

2- Simple mixing between waters with different degrees of salinity, from recharge area to discharge area, is likely to be the main chemical process dominating the study areas.

3- The recharge area and the evaporation processes play principal roles in determining the ground water type of both wadis.

The groundwater is used mainly as a domestic and agricultural water supply. The drinking and irrigation aspects of groundwater quality criteria are more suitable in the upper and middle parts of both wadis compared to the lower parts of the wadis. The drinking water quality of Wadi Baysh and Wadi Habawnah are mostly within the recommended limit in the upper and middle sections. However, all of the TDS analyses were above the EEC limit in the lower parts of both wadis. The trace elements Fe^{2+} and Mn^{2+} exceeded the EEC limits slightly with concentrations of 0.725-0.964 and 0.154-0.186 mg/l, respectively. The groundwater hardness of both wadis is very hard water with a range of 234 to 1694 mg/l in Wadi Habawnah and 313 to 2045 mg/l in Wadi Habawnah.

The irrigation waters of Wadi Baysh and Wadi Habawnah groundwaters are slightly to moderately saline in the lower parts of the area. However, some of the area in the upper part of Wadi Habawnah (Al Harshaf) shows moderate salinity in the groundwater.

The sodium hazard is low to medium in both wadis. Medium salinity water can be used if a moderate amount of leaching occurs. Plants with moderate salt tolerance can be

grown in most instances without special practices for salinity control. In Wadi Habawnah, the SAR ranges between 2 and 6 while in Wadi Baysh it shows a range between less than 1 to 7.

The calculated SAR value and the measured EC values suggest that, although the sodium risk is higher, nevertheless most of the water falls within the category of medium to high salinity hazard in both wadis.

On the basis of the latter criterion for different categories of hazards, it may be concluded that most of the waters are not suitable for most crops. Nevertheless, selective cropping patterns (such as barley, sorghum, wheat and palm tree) would be more appropriate in areas having high salinity hazard, such as the lower parts of both wadis.

Since the safe margin of Residual Carbonate (RC) is 204 meq/l, the present sets of data indicate that the water of both wadis is suitable for agricultural use. In the lower part of both areas, most of the wells show high salinities but with ionic compositions maintaining a suitable balance for agricultural purposes.

For the present sets of data from the lower parts of both wadis, the evaluation of the groundwater conditions may need to be based on the salinity conditions rather than the SAR and RC. This is because the lower parts of both wadis are characterised by high evaporation and low rainfall (120 mm-80 mm). Using groundwater with high salinity for irrigation would damage the agricultural water supply. A subsurface drainage system to reduce the evaporation effect and the planting of suitable crops (wheat, sorghum and corn) for such high salinity groundwater in this part of the study area is recommended.

CHAPTER FIVE: AQUIFER PARAMETERS

5.1 Hydraulic Properties of Aquifers

5.1.1 Introduction

Transmissivity (T), permeability (K) and storativity (S) are hydraulic properties of aquifers that determine how fast water moves through a porous and permeable medium, and how ground water levels are affected (Bouwer, 1978).

Of all the hydraulic testing procedures that are most commonly used in alluvial aquifers, pumping tests are used exclusively for evaluating groundwater parameters and for determining the transmissivity and storage properties of the aquifer.

In this section the author will restrict the discussions to large diameter test wells, since all of the available wells are of this kind. The tests require single pumping wells in which it is possible to measure the response to pumping. These procedures originated with the work of Papadopulos and Cooper (1967). The characteristics of groundwater flow, aquifer properties, their definitions and pumping test methods will be outlined before accounts of the Papadopulos-Cooper method, the modified volumetric method, the Ferris (1962) method and the step draw down method are given.

5.1.2 Groundwater Flow, Aquifer Properties and Definition

Darcy's Law is the foundation of groundwater hydraulics (Todd, 1960). It states that the flow rate through a porous medium is proportional to the head loss and inversely proportional to the length of the flow path (see Figure 5.1). The Law is applicable when the flow is laminar. The Law formulae can be expressed in several forms most of which are derivations of $Q = AV$.

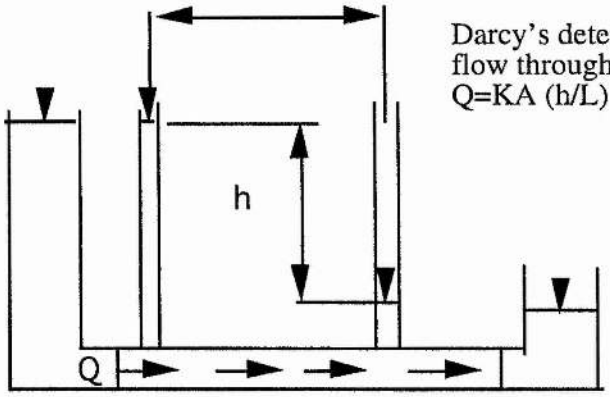

Darcy's determination of rate of flow through a porous medium: Q=KA (h/L)

Figure 5.1 Illustration of Darcy's law

$$V = Ki \tag{5.1}$$

$$Q = KiA \tag{5.2}$$

$$Q = KA\frac{h_1 - h_2}{L} \tag{5.3}$$

$$K = \frac{Q}{iA} = \frac{\frac{L^3}{t}}{L^2} = \frac{L}{t} \tag{5.4}$$

where V = velocity (L / t), K = permeability or hydraulic conductivity of the porous medium (L / t), i = hydraulic gradient = $\frac{h_1 - h_2}{L}$ (non-dimensional) (5.5)

h_1 and h_2 = the water level or potential at two points on a line parallel to the direction of flow, L = length of flow path between h_1 and h_2, A = area normal to the direction of flow (L^2), Q = Rate of flow (L^3 / t) andt = time

As a result of rearrangement, Darcy's equation leads to

$$K = \frac{V}{i} = \frac{Q}{iA} \tag{5.6}$$

Since the hydraulic conductivity shows variation in all directions and from place to place in an aquifer, Theis (1935) introduced the term transmissivity, T = KM, which is equal to the average permeability multiplied by the saturated thickness of the aquifer, to clarify this deficiency. The transmissivity has the dimensions of L^2 / t. K is the hydraulic conductivity of a unit cross-sectional area of the aquifer, while T is the hydraulic conductivity of a unit width of the full thickness of the aquifer.

Storativity: this is a term used to express the storage capacity of an aquifer. It is

defined as the volume of water released from, or taken into storage, per unit surface area of aquifer per unit change in the component of hydraulic head normal to that surface (Figure 5.2).

Storativity is expressed as the ratio : $S = \frac{V'}{V}$ (5.7)

where V' equals the volume of water released and V is the volume of material drained in a free aquifer or the volume defined by the change in piezometric head for an artesian aquifer. Since $V' / V = L^3 / L^3$, S is non dimensional.

In an unconfined aquifer, S is a function of the size and number of inter-connected voids and represents the actual volume of water drained from the aquifer by the lowering of the water table. The S value ranges from as low as 0.001 to 0.1 (Kruseman and De Ridder, 1970). The less uniform, finer grained and more dense the material, the smaller the S value.

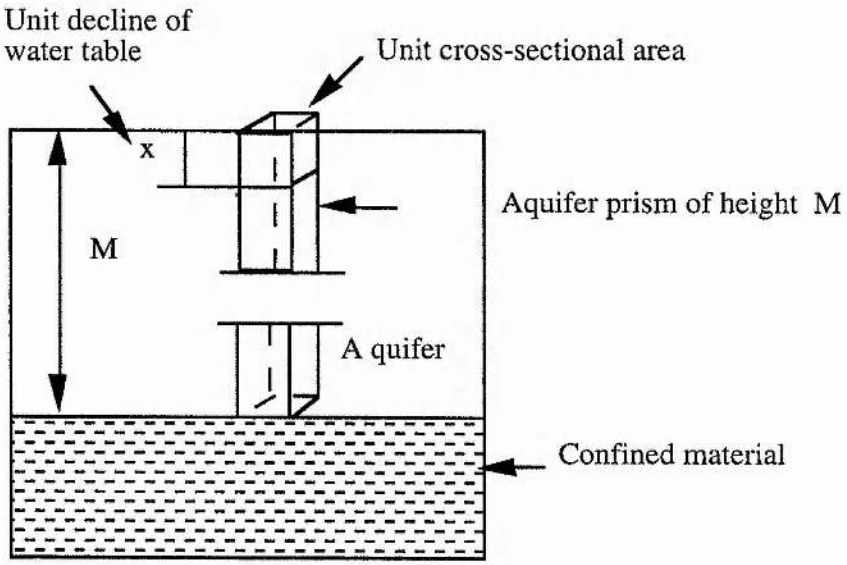

Figure 5.2 Sketch diagram to illustrate the storativity.

L- unit length, V- The volume involved in a unit drop or increase in water table elevation within a prism of 1-unit^2 cross section (L^3). V' - the volume of water released (drained or recharged) by a change in water table elevation within (L^3).

5.2 Well Structure and Field Measurements

5.2.1 Dug Wells (Large Diameter Wells)

The farmers in both Wadi Habawnah and Wadi Baysh use dug wells to take water from an aquifer. A hole is dug into the saturated material and is then lined to prevent collapse of its sides. Such a hole is called an intake. Water from the aquifer will flow through the intake until the level of the water surface within the well coincides with the surrounding water table, when the natural flow will stop.

The water in both wadis is extracted from the wells using a centrifuge pump with pipes between three and four inches in diameter. As soon as the water is extracted the level inside falls causing a decrease in the internal water pressure which is compensated by an upward flow through the intake.

The hand dug wells in Wadi Habawnah have been constructed with circular cross sections lined with concrete and stone, while in Wadi Baysh they were constructed from stone. However, the quantity of water entering the wells in both wadis is sufficient to equal the amount withdrawn in most of the wells. A balance is reached with the water level within the well being some distance below the natural water level. This distance is known as the 'draw down'.

Most wells that were surveyed by the author showed that increasing the depth gives an improvement to the yield which is greater than that obtained by enlarging the diameter of the well. Also it has been observed in Wadi Habawnah that, when a number of wells are sited close together, pumping large quantities from one affects the output of others near by. This results when the total volume of water extracted from the wells is in excess of the capacity of the aquifer, so the underground storage will be depleted and the water table throughout the area drops. This is not likely to happen for the selected pumping well tests. Further explanation will follow later.

5.2.2 Field Measurements

The farm wells constructed in both wadis are the large diameter dug wells. There are over two hundred such dug wells in Wadi Habawnah while in Wadi Baysh there are

about 100 wells.

A total of thirty dug wells in Wadi Habawnah and twenty dug wells in Wadi Baysh have been investigated in detail regarding well depth and the saturated thickness of the aquifer (see Table 5.1).

The dug wells varied in depth according to their location. In the upper parts of both wadis, the wells ranged between 6 and 20m in depth while in the lower parts the well depths range between 32 and 43m in Wadi Habawnah and between 24 and 84m in Wadi Baysh. These wells are generally round in plan with an average diameter of 3m with the exception of well HB2 (Wadi Habawnah) which has a diameter of 5.25m.

The wells of Wadi Baysh are lined with stone while the majority of wells in Wadi Habawnah are lined with concrete (Figure 5.3) or stone to prevent the wells from caving in. All of the wells are equipped with pumps of the centrifugal type driven by petrol engines. Pumping normally lasts 0.5-1 hour in the upper part of Wadi Habawnah while in the middle and the lower parts it ranges over 8-24 hours. In the upper part of Wadi Baysh, the pumping lasts 2-3 hours while in the lower part it ranges between 6 and 24 hours. The discharge rate of the dug wells ranges between 288 and 720 m^3/day in Wadi Baysh while in Wadi Habawnah it ranges from 331 to 720 m^3/day (see Table 5.1).

Twenty aquifer tests were performed within the boundaries of the study area in Wadi Baysh and Wadi Habawnah during the summer of 1989.

The distances separating the tested wells in both wadis were large so that there were no draw down effects from the other wells during testing. The selected wells were planned to cover most of the study area, to provide a good estimation of the aquifer parameters in both wadis. Unfortunately, most of the pumping wells were pumped for short periods of time because the owners of such wells do not use pumps for periods longer than their needs for irrigation or stock watering.

5.2.3 Small Diameter Wells

Eleven small diameter wells were drilled in the lower part of Wadi Baysh while six small diameter wells (see Figures 5.4 and 5.5) were drilled along Wadi Habawnah (MAWR, 1978).

Table 5.1 Well discharge estimation from horizontal pipe flowing full in m^3/day in Wadi Baysh and Wadi Habawnah

Wadi Baysh

Well Identification	Distance X, in inches. at 12 inches drop	Pipe diameter inches	Discharge rate (Q) gpm	Discharge rate (Q) m^3/min	Discharge rate (Q) m^3/day
BU1	7	3	53	0.20	288
BU2	6	4	79	0.30	432
BU3	8	4	106	0.40	576
BM5	8	4	106	0.40	576
BM7	10	4	132	0.50	720
BM12	8	4	106	0.40	576
BL16	9	4	119	0.45	648

Wadi Habawnah

Well Identification	Distance X, in inches. at 12 inches drop	Pipe diameter inches	Discharge rate (Q) gpm	Discharge rate (Q) m^3/min	Discharge rate (Q) m^3/day
HB2	6	4	87	0.33	475
HB3	8	3	61	0.23	331
HB6	7	4	92	0.35	504
MT1	9	4	119	0.45	648
MT9	7	4	90	0.34	489
GF2	8	4	111	0.42	604
GF5	8	4	111	0.42	604
NG1	8	4	106	0.40	576
MR	10	4	132	0.50	720
HS2	8	4	111	0.42	604
HS4	10	4	132	0.50	720

Figure 5.3 Well number MT1 in Wadi Habawnah with concrete lining.

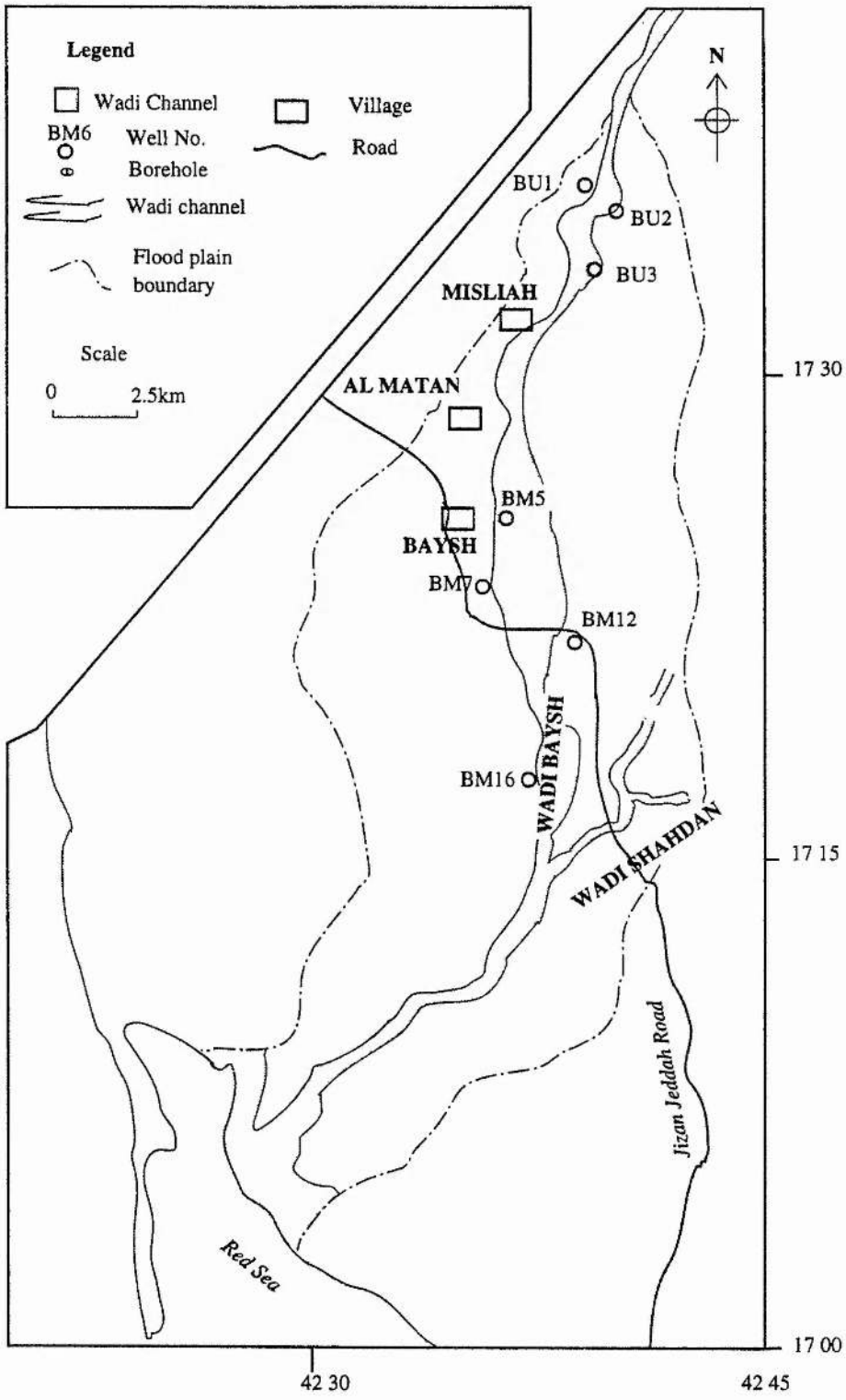

Figure 5.4 Wadi Baysh well locations of pumping tests.

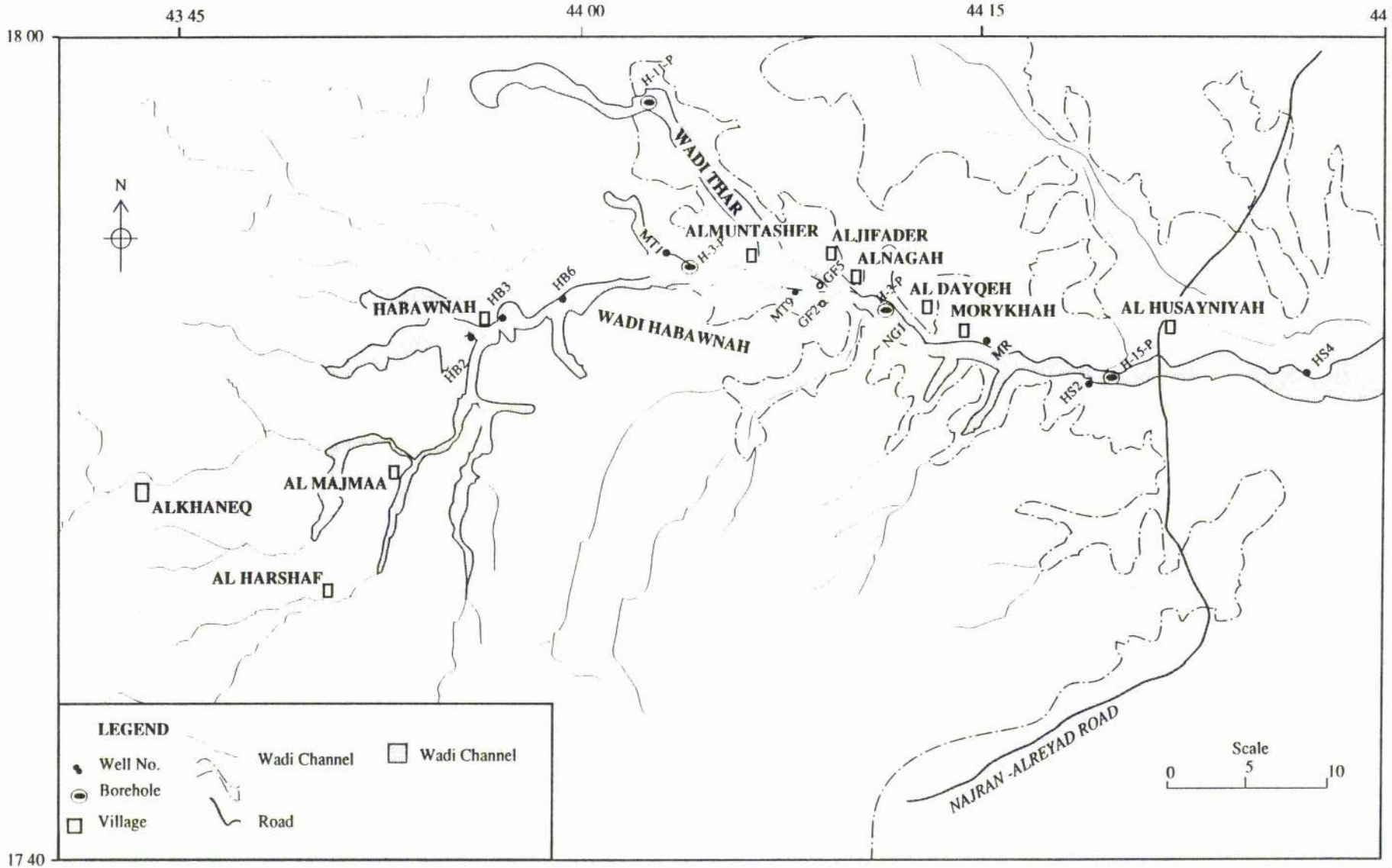

Figure 5.5 Wadi Habawnah well locations of pumping tests.

All of the above wells were drilled in completely unconsolidated sediments (alluvial sand and gravel) using direct rotary drilling, in which the borehole is drilled by rotating a bit. Cuttings are removed by the continuous use of drilling fluid as the bit penetrates the formation.

The small well diameter is 12.25 inches. The depth of these wells in Wadi Baysh is 40 to 150m, while in Wadi Habawnah it is 30 to 36m. None of this group of wells was used for water supply in the area (see Chapters 6 and 7 for more detail).

5.3 Aquifer Test

5.3.1 Introduction

The wadi floor sediments of the study area form three main subdivisions in each wadi. These three sections can be characterised as the upper and middle parts of the wadi in which the aquifer is of shallow to medium depth, and is of boulder and gravel sized material, while in the lower section it is fine grained. This characteristic of the aquifer material is reflected in the changes of the aquifer conditions from unconfined in the upper and middle wadi to semi confined and confined in the lower parts of the wadi (see chapters 6, 7 and 8).

Twenty pump tests (see Figures 5.4 and 5.5) were carried out by the author, eight in Wadi Baysh and twelve in Wadi Habawnah. Each well was pumped for a considerable time under constant discharge. In two cases step draw down tests were undertaken in which the well was pumped at a low constant discharge for a fixed time and then the discharge rate was increased. This process was repeated throughout the test, with at least three steps of differing duration. During the pumping the changes in water level (draw down) were measured in the well itself in the absence of observation wells available. When a well is pumped during aquifer testing the water level declines with time giving the draw down response which is measured at specified time intervals.

The draw down measurements from the pumped well facilitate the application of matching curves of draw down with time using the Papadopulos-Cooper (1967) method in the analysis of the aquifer parameters, such as hydraulic conductivity (K), transmissivity

(T) and storativity (S) for both wadis.

5.3.2 Boundary Condition in Wadi Baysh and Wadi Habawnah

The aquifer boundaries are based on the results of geophysical analysis, well inventories and geological studies of the area and can be summarised as follows:

1- The aquifer is unconfined in Wadi Habawnah but in Wadi Baysh it consists of an unconfined aquifer that dominates the upper and middle parts while in the lower parts it is mostly a confined aquifer.

2- The aquifers in Wadi Habawnah and the upper and middle parts of Wadi Baysh are underlain by crystalline bed rock. However, the aquifer of the lower part of Wadi Baysh is underlain by a thick layer of clay or silty clay and is commonly beneath similar materials which serve as aquicludes.

3- The aquifers of Wadi Habawnah and the upper parts of Wadi Baysh are bounded laterally by impervious crystalline rocks. The lateral boundaries of aquifers in the lower parts of Wadi Baysh are mainly of fine grained sediments.

4- The lower boundaries of the aquifers in both wadis slope irregularly downwards to the east in Wadi Habawnah and to the southwest in Wadi Baysh. This basal surface is steep in the upper parts of both wadis but is more gentle in the lower reaches. Most of the tests were conducted in the middle and lower parts of both wadis in which the flow system was assumed to be horizontal to simplify the pumping test analysis.

5.3.3 Methods of Analysis of Pumping Tests

An aquifer test is a technique to determine the hydraulic properties of an aquifer. The technique involves pumping a well at a known rate and observing the draw down of the water table in observation wells or at the pumped well itself. Water level changes in the wells are measured with respect to time, which allows hydraulic properties, such as transmissivity and coefficient of storage, to be calculated.

It is preferable that a pumping test should be continued until a steady state condition is reached, in which the pumping rate is equal to the rate of aquifer recharge. In practice this cannot be reached for all types of aquifer conditions. An advantage of longer pumping

of a well is that it may reveal the presence of some previously unknown boundary condition.

The draw down observed in each pumping well was then plotted against the corresponding time on double logarithmic graph paper to produce time draw down curves. The aquifer properties and well performance were obtained mathematically.

Four methods of analysis were selected which satisfied both the aquifer conditions and the well types under examination:

1- Papadopulos-Cooper (1967) in which the aquifer transmissivity was determined

2- Volumetric method (1982) to determine the aquifer storativity

3- Modified Ferris method (1963) to determine the aquifer storativity

4- Step draw down test using the Jacob method (1947) to determine the well performance.

Each of the above methods is outlined below.

5.3.3.1 Papadopulos-Cooper (1967) Method

The large diameter well test is a pump test in which the effect of water stored within the well casing is taken into account.

In small diameter wells this storage can be ignored without significantly affecting the analysis of the aquifer's hydrological properties. In the study area, where the pumping tests were run on large diameter hand dug wells, storage within the well bore cannot be ignored and must be taken into account.

5.3.3.1.1 Introduction

The assumptions made in the work of Papadopulos and Cooper (1962) are:

1- The aquifer is confined at both the top and the bottom by impermeable beds.

2- The aquifer is level and infinite in horizontal extent.

3- The aquifer is homogeneous and isotropic.

4- The pumping well fully penetrates the aquifer.

5- Discharge from the well is at a constant rate.

A diagram of a typical large diameter well is shown in Figure 5.6.

The Papadopulos and Cooper solution for the draw down in a well of large

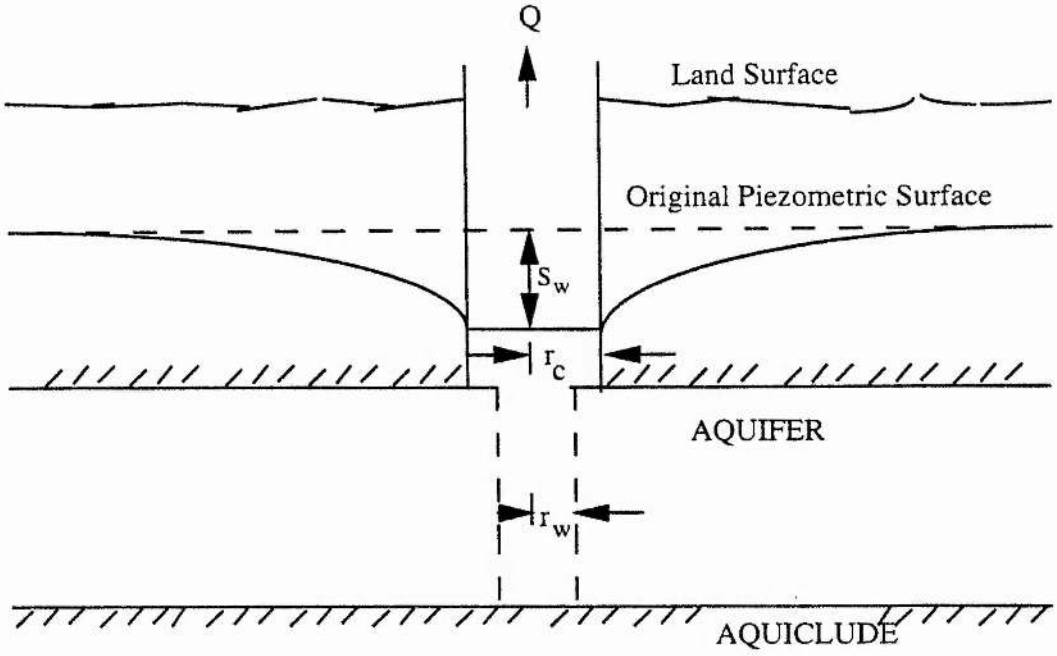

Figure 5.6 Diagram of a typical large diameter well setup (modified after Papadopulos and Cooper, 1967).

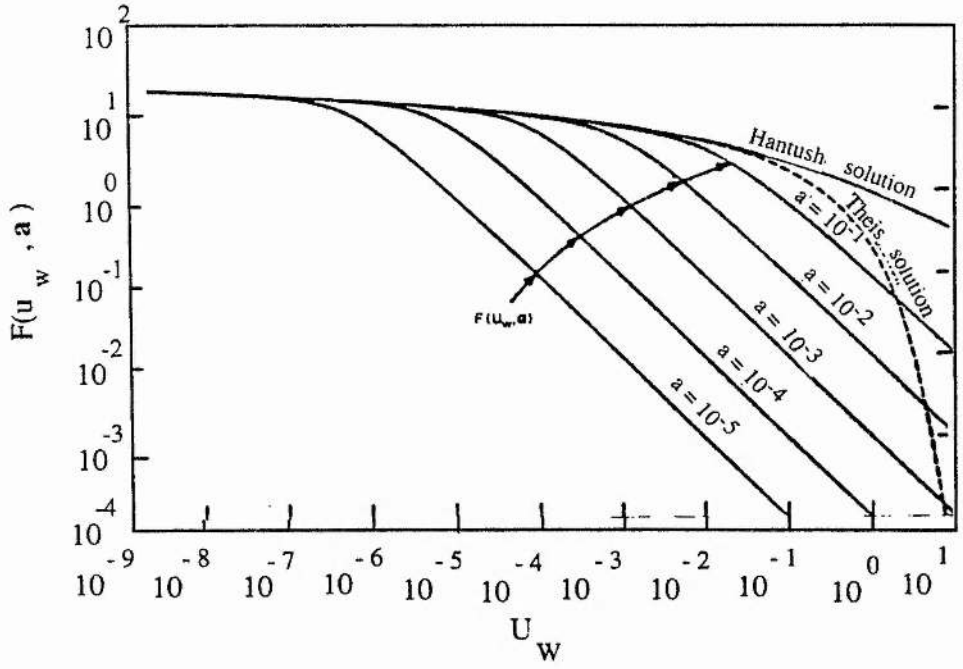

Figure 5.7 Type curves for the drawdown in a large diameter well (after Papadopulos and Cooper, 1967).

diameter is similar in form to that of Theis (1935); however, their well function, $F(U_w, a)$, is more complicated. The draw down in a well of large diameter is given by equation 5.8.

$$S = \frac{Q}{4\pi T} F(U_w, \alpha) \tag{5.8}$$

where

$$F(U_w, \alpha) = \frac{32\alpha^2}{\pi^2} \int_0^{\infty} \frac{\left(1 - e^{-2B^2/4u_w}\right)}{B^3 \Delta(B)} dB, \tag{5.9}$$

$$U_w = \frac{r_w^2 S}{4 T t} \tag{5.10}$$

and

$$\alpha = \frac{r_w^2 S}{r_c^2} \tag{5.11}$$

Values of U_W vs. $F(U_w, \alpha)$ in equation 5.9 and 5.10 for varying values of alpha (equation 5.11) can be plotted to produce type curves (Figure 5.7) to be used to match with data obtained from a large diameter well pump test.

5.3.3.1.2 General Solution Algorithm

The general solution is the same for log-log curve matching using confined or unconfined pumping tests.

An example of how to perform the log-log curve matching technique for a pump test conducted within an unconfined aquifer using the large diameter well-test curves:-

1- The values of time vs. draw down are plotted on log-log paper. The author used SI units.

2- A type curve of Papadopulos and Cooper will be a set of 'α' values ranging between 10^{-1} and 10^{-5}. The aquifer curves are superimposed on the plotted field data. The type curves are plotted at the same scale as the field data. The author tried different type curves (different 'α' values) to obtain the best match with the field data. The author's experience in such aquifer parameters helped in the selection of appropriate values for the aquifers under examination.

3- The type curve selected in step 2 is matched with the data plotted in step 1 by superimposing the curve over the data and keeping the coordinate axes parallel. When the first type curve does not match the data very well, then step 2 is repeated until a good match is achieved.

4- Once the type curve is superimposed over the field data an arbitrary match point will be selected together with the paired values of time, draw down $F(U_w, \propto)$ and U_w.

5- The values obtained in step 3 along with the pumping rate (Q) and the well radius (r_c) are used in the following equations to calculate the transmissivity and storativity of the aquifer:-

$$T = \frac{Q F(U_{w,} \propto)}{4 \pi S_w} \tag{5.12}$$

$$S = \alpha \frac{r_c^2}{r_w^2} \tag{5.13}$$

Hydraulic conductivity, K, is:-

$$K = \frac{T}{b} \tag{5.14}$$

Definition of variables:-

T	= Transmissivity (L^2K)
K	= Hydraulic conductivity (L/T)
b	= aquifer thickness (L)
S	= storativity or storage coefficient
Q	= pumping well discharge rate (L^3/t)
t	= time
r_c	= radius of casing over length of water level decline (L)
r_w	= radius of well in aquifer
S_w	= draw down (L)
$F(U_w, \propto)$	= well function
U_w	= well function
$\propto$	= type curve values

5.3.3.1.3 GWAP Program

The Graphical Well Analysis Package (GWAP) written by Dansby and Price, (1992) is designed to simplify the tedious graphical solutions approach currently applied in aquifer test analysis.

Table 5.2 Pumping tests result using the Papadopulos and Cooper (1967) method for the field data of large diameter wells in Wadi Baysh and Wadi Habawnah (1989)

Wadi Baysh

Well Identification	Date of aquifer test	Aquifer thickness (m)	Discharge rate (Q) m^3/day	Effective radius (m)	Match Point alpha	Match Point t (min)	Match Point s (m)	Match Point 1/Uw	Match Point F(Uw , a)	Solution T (m^2/day)	Solution K m/day	Solution Storativity (S)
BU1	1/7/89	2	288	1.2	-1	1	0.31	30.2	2.5	190	95	$1.00x10^{-1}$
BU2	2/7/89	6	432	1.7	-4	1	0.31	0.0074	1.4	156	26	$1.00x10^{-4}$
BU3	3/7/89	12	576	2.5	-1	1	0.31	2.3	0.6	87	7	$1.00x10^{-1}$
BM5	4/7/89	11	576	1.5	-1	1	0.31	2.5	0.5	75	7	$1.00x10^{-1}$
BM7	5/7/89	13	720	1.6	-1	1	0.31	5.6	0.77	147	11	$1.00x10^{-1}$
BM12	6/7/89	21	576	1.2	-1	1	0.31	11.7	1	150	7	$1.00x10^{-1}$
BL16	7/7/89	37	648	1.5	-1	1	0.31	8.13	0.76	130	3	$1.00x10^{-1}$

Wadi Habawnah

Well Identification	Date of aquifer test	Aquifer thickness (m)	Discharge rate (Q) m^3/day	Effective radius (m)	Match Point alpha	Match Point t (min)	Match Point s (m)	Match Point 1/Uw	Match Point F(Uw , a)	Solution T (m^2/day)	Solution K m/day	Solution Storativity (S)
HB2	9/6/89	7	475	2.6	-1	1	0.31	40	1.3	207	29	$1.00x10^{-1}$
HB3	10/6/89	5	331	1.4	-5	1	0.31	96000	4.3	371	74	$1.00x10^{-5}$
HB6	11/6/89	4	504	1.5	-3	1	0.31	19000	1.44	190	48	$1.00x10^{-3}$
MT1	12/6/89	17	648	1.5	-5	1	0.31	110000	1.7	285	17	$1.00x10^{-5}$
MT9	13/6/89	19	489	1.5	-5	1	0.31	520000	4	520	27	$1.00x10^{-5}$
GF2	14/6/89	19	604	1.5	-5	1	0.31	575500	4.7	738	39	$1.00x10^{-5}$
GF5	15/6/89	16	604	1.5	-5	1	0.31	645700	1.8	281	18	$1.00x10^{-5}$
NG1	17/6/89	12	576	1.5	-5	1	0.31	363100	2.24	337	28	$1.00x10^{-5}$
MR	16/6/89	12	720	1.5	-5	1	0.31	676100	3.5	652	54	$1.00x10^{-5}$
HS2	18/6/89	19	604	1.5	-5	1	0.31	1148000	4.6	734	37	$1.00x10^{-5}$
HS4	19/6/89	21	720	1.5	-2	1	0.31	79.43	1.4	254	12	$1.00x10^{-2}$

ranges of values. In the upper parts of the wadis, the transmissivities range from 75 to 190 m^2/day and from 190 to 371 m^2/day in Wadi Baysh and Wadi Habawnah respectively. The middle and lower parts of Wadi Baysh and Wadi Habawnah show higher values of transmissivity, in which the transmissivity ranges between 130 and 150 m^2/day to between 281 and 738 m^2/day respectively.

According to the criteria given by Ghearghe (1979), a high potential aquifer should have a transmissivity equal to or greater than 500 m^2/day while for moderate potential aquifers it ranges from 50 to 500 m^2/day.

Under the Ghearghe (1979) criteria, the aquifer of Wadi Baysh can be considered as of moderate potential since all the transmissivity values are below 500 m^2 / day while Wadi Habawnah shows two orders of transmissivity: moderate potential which dominates the upper part of the wadi whereas the lower part of the wadi contains the aquifer with high potential.

At most sites in Wadi Baysh the value of storativity was 0.1 except well no BU2 where it is very low (0.0001). In Wadi Habawnah, storativity values are very low (0.00001) with the exceptions of wells no HB2 and HS4 which have relatively high storativity values of 0.1 and 0.01, respectively.

It seems that storativity values derived from the Papadopulos-Cooper method are not reliable because the field data curves could be matched with more than one type curve. This results in slight changes in the transmissivity values but large variations in the storativity values.

The storativity values obtained by the Papadopulos-Cooper method seem to be low for the unconfined aquifer of Wadi Habawnah, and two alternative methods have been used: The Volumetric method of Sen (1983) and the modified Ferris (1963 in All- Hageri, 1977) method.

5.3.3.2 Volumetric Method

The Volumetric method was developed by Sen (1983) for the hydraulic solution of large diameter wells using the same assumptions as in the Papadopulos-Cooper method. The volumetric method is based on the storativity concept in which:

$$S\ (\text{Storativity}) = \frac{\text{Volume of water obtained from aquifer}, V_{a(t)}}{\text{Volume of aquifer dewatered}, V_{(t)}} \qquad (5.16)$$

or

$$S = \frac{V_{a(t)} = Q\,t - \pi r_w^2 S_{w(t)}}{V_{(t)} = r_w^2 Q\left\{\exp\left(4\pi T S_{w(t)} / Q\right)\right\} / 4T - \pi r_w^2 S_{w(t)}} \qquad (5.17)$$

This formula yields an approximate estimation of the storativity provided that the well discharge (Q) and the well draw down (S_W) in the main well are measured while the transmissivity (T) is determined from the pumping test formula of Papadopulos and Cooper.

5.3.3.2.1 Results

The storativity is calculated by substituting the values of transmissivity imported from the Papadopulos - Cooper method together with the corresponding values of r_W, Q, $S_{W(t)}$ and t for each test into the above equation. The $S_{W(t)}$ values should be taken as the last draw down record in the pumping well.

The storativity shows low values (7.3×10^{-4} to 8.69×10^{-3}) in Wadi Baysh and very low values (1.25×10^{-6} to 1.87×10^{-3}) in Wadi Habawnah (see Table 5.3). With low values of storativity (storage coefficient), ambiguity arises because the values should be higher for unconfined aquifers. It seems that the assessment method needs a long time of draw down before the steady state is reached. Such a condition was not achieved in the pumping tests.

5.3.3.3 Modified Ferris Method

The analogous drain solution was developed from the Ferris method (1963) by Al Hageri (1977) due to the fact that the seepage area of a well is equivalent to the seepage area of a drain or gallery. The Ferris solution can be modified to determine the aquifer parameters such as the transmissivity and the storativity.

Ferris (1963) described the draw down distribution around a line sink or line of sources under constant discharge, as follows:

$$S' = \frac{qy}{T} F(U) \qquad (5.18)$$

Table 5.3 Determination of aquifer storativity of Wadi Baysh and Wadi Habawnah using the volumetric method

Wadi Baysh Well Identification	Discharge rate (Q) m^3/day	Effective radius (m)	Drawdown s (m)	Time t (day)	T (m^2/day)	Va (t) * m^3	V (t)** m^3	Storativity S***
BU1	288	1.2	0.2	0.01	190.08	4	$4.59x10^2$	$8.69x10^{-3}$
BU2	432	1.7	1	0.08	156.00	32	$2.02x10^4$	$1.60x10^{-3}$
BU3	576	2.5	0.3	0.13	86.60	71	$5.72x10^3$	$1.25x10^{-2}$
BM5	576	1.5	2	0.10	75.00	59	$9.86x10^3$	$5.93x10^{-3}$
BM7	720	1.6	0.9	0.10	146.88	74	$1.84x10^4$	$4.04x10^{-3}$
BM12	576	1.2	3	0.17	150.00	94	$1.29x10^5$	$7.29x10^{-4}$
BL16	648	1.5	2	0.19	129.60	119	$7.39x10^4$	$1.61x10^{-3}$
Wadi Habawnah Well Identification	Discharge rate (Q) m^3/day	Effective radius (m)	Drawdown s (m)	Time t (day)	T (m^2/day)	Va (t) * m^3	V (t)** m^3	Storativity S***
HB2	475.00	2.6	0.27	0.03	207.00	13	$6.96x10^3$	$1.87x10^{-3}$
HB3	331.00	1.4	0.86	0.13	371.00	42	$2.25x10^5$	$1.86x10^{-4}$
HB6	504.00	1.5	0.5	0.09	190.00	47	$1.34x10^4$	$3.51x10^{-3}$
MT1	648.00	1.5	1.8	0.10	285.12	64	$1.79x10^5$	$3.57x10^{-4}$
MT9	489.00	1.5	1.6	0.13	520.00	60	$1.92x10^6$	$3.10x10^{-5}$
GF2	604.00	1.5	5	0.54	737.60	308	$4.21x10^6$	$7.32x10^{-5}$
GF5	604.00	1.5	1	0.17	280.50	99	$1.57x10^5$	$6.35x10^{-4}$
NG1	576.00	1.5	3.3	0.29	336.96	161	$1.29x10^8$	$1.25x10^{-6}$
MR	720.00	1.5	1.3	0.21	651.80	148	$5.48x10^6$	$2.70x10^{-5}$
HS2	604.00	1.5	1.4	0.17	734.40	99	$8.55x10^6$	$1.16x10^{-5}$
HS4	720.00	1.5	0.9	0.13	254.00	89	$6.65x10^4$	$1.34x10^{-3}$

* [Va (t)] is a volume of water obtained from aquifer

** [V (t) is a volume of aquifer dewatered]

*** S [Va/V(t)]

in which

$$U = y^2 \frac{S}{4Tt} \tag{5.19}$$

where

S' = the draw down during time t, q = the rate of discharge per unit length of line sink, y = the distance from the centre of the drain to the observation point, T = the transmissivity of the aquifer and S = the storativity of the aquifer

F(U) and U are well functions which can be determined from a table given by Ferris *et al.* (1962) or by using the following equation:

$$D(U) = \frac{e^{-U}}{\sqrt{\pi U}} - \text{erfc}\sqrt{U} \tag{5.20}$$

or

$$D(U) = \frac{e^{-U}}{\sqrt{\pi U}} - \left(1 + \frac{2}{\sqrt{\pi}} \int_0^{\frac{x}{2}\sqrt{\frac{\pi}{s}}} e^{-U^2}\, dU\right) \tag{5.21}$$

Since

$$\text{erfc}\sqrt{U} \equiv 1 + \frac{2}{\sqrt{\pi}} \int_0^{\frac{x}{2}\sqrt{\frac{\pi}{s}}} e^{-U^2}\, dU \tag{5.22}$$

The seepage drain length (L_e) used by Ferris is related to the large diameter well circumference as follows:

$$L_e = 2\pi r_w \tag{5.23}$$

where r_w is the radius of the large diameter well

Since the rate of discharge of the drain per unit length (q) is equal to the drain discharge (Q) divided by the drain length (L_e), the q value of the large diameter well can be determined as

$$q = \frac{Q}{2\pi r_w} \tag{5.24}$$

where Q and $2\pi r_w$ are the discharge rate and the circumference of a large diameter well, respectively.

The draw down measurements in the large diameter well are taken along the circumference of the well. Similarly, in the analogous drain, the draw down is the same at

all points along the circumference, which can be expressed as:

$$y = \sqrt{(\pi r)^2 + \left(\frac{r}{4}\right)^2} \tag{5.25}$$

assuming that $r = r_w$, the above equation can be rewritten as follows:

$$y = \sqrt{(\pi r_w)^2 + \left(\frac{r_w}{4}\right)^2} \Rightarrow \quad y = r_w\sqrt{\pi^2 + \frac{1}{16}} \tag{5.26}$$

As a simplification of the equation above, it can be written as $y = \pi\ r_w$ where the term $\sqrt{\frac{1}{16}}$ is omitted because it is small in value.

5.3.3.3.1 Results

The author has used the transmissivity values calculated using the Papadopulos - Cooper method together with the corresponding values of r_w, Q, $S_{w(t)}$ and t for each test substituted into the above equation to calculate the storativity for both wadis.

Table 5.4 shows results believed to be representative of the storage coefficients in both wadis. The storativity coefficient of Wadi Baysh has a range of values between $7.9x10^{-3}$ and $4.1x10^{-1}$ while for Wadi Habawnah, its values range between $9.7x10^{-3}$ and $2.0x10^{-1}$

The values of storativity in both wadis fall within the acceptable range (0.1 to 0.001) for unconfined aquifers (Kruseman and De Ridder, 1970).

5.3.3.4 Step Drawdown Test

Well performance testing is a procedure to determine aquifer losses and well losses. Aquifer losses can be defined as the head losses that occur in an aquifer where the flow is laminar. Well losses are usually divided into linear losses (i.e. caused by damage of the aquifer during the well construction) and non-linear losses (which occur inside the well screen, in the suction pipe and adjacent to the well where the flow is turbulent). These losses make the draw down inside the well high.

Well performance tests consist of two main types: the recovery test and the step

Table 5.4 Analogous drain solution of large diameter wells in Wadi Baysh and Wadi Habawnah

Wadi Baysh

Well Identification	Discharge rate (Q) m^3/day	Effective radius (m)	Drawdown s (m)	Time t (min)	Le* m	q** Q"/Le	x*** m	T (m^2/min)	K m/day m/day	D (U)!	U!!	Storativity S!!!
BU1	0.2	1.2	1.2	70	7.5	0.03	3.8	0.13	95	1.584	0.053	$1.38x10^{-1}$
BU2	0.3	1.7	4.6	200	10.7	0.03	5.3	0.11	26	3.322	0.018	$5.47x10^{-2}$
BU3	0.4	2.5	3.7	280	15.7	0.03	7.9	0.06	7	1.113	0.084	$9.18x10^{-2}$
BM5	0.4	1.5	4.5	330	9.4	0.04	4.7	0.05	7	1.172	0.078	$2.42x10^{-1}$
BM7	0.5	1.6	3.1	420	10.0	0.05	5.0	0.10	11	1.265	0.071	$4.82x10^{-1}$
BM12	0.4	1.2	5.8	540	7.5	0.05	3.8	0.10	7	3.021	0.02	$3.17x10^{-1}$
BL16	0.45	1.5	4.5	360	9.4	0.05	4.7	0.09	3	1.800	0.044	$2.57x10^{-1}$

Wadi Habawnah

Well Identification	Discharge rate (Q) m^3/day	Effective radius (m)	Drawdown s (m)	Time t (min)	Le*	q** Q"/Le	x*** m	T (m^2/min)	K m/day m/day	D (U)!	U!!	Storativity S!!!
HB2	0.33	2.6	0.94	80	16.3	0.02	8.2	0.14	29	0.819	0.12	$8.28x10^{-2}$
HB3	0.23	1.4	1.83	230	8.8	0.03	4.4	0.26	74	4.102	0.0125	$1.53x10^{-1}$
HB6	0.35	1.5	3.8	180	9.4	0.04	4.7	0.13	48	2.865	0.0222	$9.51x10^{-2}$
MT1	0.45	1.5	6.1	360	9.4	0.05	4.7	0.20	17	5.368	0.00797	$1.02x10^{-1}$
MT9	0.34	1.5	5.4	720	9.4	0.04	4.7	0.36	27	11.485	0.00205	$9.61x10^{-2}$
GF2	0.42	1.5	11.8	1440	9.4	0.04	4.7	0.51	39	28.820	0.000358	$4.76x10^{-2}$
GF5	0.42	1.5	7.2	660	9.4	0.04	4.7	0.19	18	6.687	0.00544	$1.26x10^{-1}$
NG1	0.40	1.5	8.4	720	9.4	0.04	4.7	0.23	28	9.828	0.00272	$8.26x10^{-2}$
MR	0.50	1.5	4.3	600	9.4	0.05	4.7	0.45	54	7.785	0.00415	$2.03x10^{-1}$
HS2	0.42	1.5	5.1	660	9.4	0.04	4.7	0.51	37	12.402	0.00177	$1.07x10^{-1}$
HS4	0.50	1.5	6.3	780	9.4	0.05	4.7	0.18	12	4.445	0.0109	$2.70x10^{-1}$

* [Le is the equivalent length of the drain which is equivalent to the large diameter well circumference Le = 2*3.14*r)]

** [q is the rate of discharge per unit length of the drain can be expressed as follows (q= Q/Le)]

*** [x is the most remote point along the circumference from the centre and it is expressed as $x = (3.14*r)^2 + (r/4)^2$

! [D(U) is a well function = s* T/q*x*100]

!! [U is a well function = x^2*S/4*T*t]

!!! [S = 4*U*T*t/x^2]

draw down test. The recovery test can be defined as the measurement of the water level rise in a well after the pump has been shut down. In this the skin factor (i.e. the difference between the total draw down observed in a well and the aquifer loss component; De Marsily, 1986) and the transmissivity can be determined. Unfortunately, in the two wadis there were no observation wells near by to permit such measurements to be made. The step draw down test is a single well test in which the draw down of the water level is measured under different rates of pumping through at least three steps. Each step is characterised by having nearly equal duration while the pumping rate is increased progressively at each step of the tests. The following discussion will be limited to the step draw down test in which the aquifer and the well losses can be determined.

5.3.3.4.1 Theoretical

Jacob (1947) provided an equation in which the aquifer and the well loss were combined into a single term (B (r_{ew}, t) as follows:

$$S_w = B(r_{ew}, t)\,Q + C\,Q^2 \qquad (5.27)$$

where

$$B(r_{ew}, t) = B_{1(r_w, t)} + B_2 \qquad (5.28)$$

$B_{1(r_w, t)}$ = linear well - loss cofficient

B_2 = linear aquifer loss cofficient

C = non – linear well loss cofficient

r_{ew} = effective radius of the well

r_w = actual radius of the well

t = pumping time

Rorabaugh (1953) and Lennox (1966) modified the Jacob equation to:

$$S_w = BQ + C\,Q^p \qquad (5.29)$$

in which the value of P has a range of 1.5 to 3.5 depending on the discharge rate (Q). In this study the author has assumed P = 2 as Jacob suggested, a value which is still widely used (see Skinner, 1988).

The step draw down test makes it possible to determine the aquifer losses, B, and

the well losses in which the draw down inside the well can be predicted for any discharge, Q, after a given time, t.

5.3.3.4.2 Analysis Methods of the Step Drawdown Test

Several methods are available for analysis of the step draw down test based on the Jacob (1947) equation. The most important of these are; Hantush (1964), and Bierschenk (1963) method, Eden-Hazel method (1973) and Rorabaugh (1953) method.

The Hantush-Bierschenk method has been applied in this study because the following conditions and the assumptions are satisfied in the field areas:

1- The aquifer is unconfined, leaky or confined;

2- The aquifer is pumped step-wise at increased discharge rates;

3- The flow of the well is in an unsteady state.

The Hantush-Bierschenk method expresses the draw down ($S_{w(n)}$) in the pumping well during the n-th step of a step-draw down test as:

$$S_{w(n)} = \sum_{i=1}^{n} \Delta Q_i B(r_{ew}, t - t_i) + CQ_n^2 \qquad (5.30)$$

where $S_{w(n)}$ = total draw down in the well during the n-th step at time t, Q_n = constant discharge during the n-th step, Q_i = constant discharge during the i-th step of that preceding the n-th step, $\Delta Q_i = Q_i - Q_{i-1}$ = discharge increment beginning at time t_i.

t_i = time at which the $i-th$ step begins $(t_i = 0)$

r_{ew} = effective radius of the well

The draw down values at fixed intervals of time from the beginning of each step $(t - t_i = \Delta t)$ can be added together using the following equation:

$$\sum_{i=1}^{n} \Delta s_{w(i)} = S_{w(n)} = B(r_{ew}, \Delta t_i) Q_n + CQ_n^2 \qquad (5.31)$$

where $\Delta S_{w(n)}$ = the draw down increment taken between the i-th step and that preceding it, taken at time $t_i + \Delta t$ from the beginning of the i-th step.

The equation above was rearranged to the form below for use in the graphic solution

$$\frac{S_{w(n)}}{Q_n} = B\left(r_{ew}, \Delta t_i\right) + CQ_n \qquad (5.32)$$

From this expression, plotting $S_{w(n)} / Q_n$ versus Q_n yields a straight line with slope equal to C. The value of B can be determined either from the straight line intercept with the line of $S_{w(n)} / Q_n$ or from the equation above.

5.3.3.4.3 Procedures

The author used the Cricket Graph program to plot the observed drawdown (see Appendix 5A&B) in the well, S_w, against the corresponding time t, using the arithmetic scale and the curve was extrapolated from the end of each step to the start of the next step (Figure 5.8).

The draw down increments $\Delta S_{w(i)}$ for each step are determined as equal to the difference between the draw down at a fixed time interval Δt of each step (from the beginning to the end of each step) with the corresponding draw down on the extrapolated curve of the preceding step;

After determining the value of DS_w (n) which corresponds to Q_n from

$$\Delta S_{w(n)} = \Delta S_{w(1)} + \Delta S_{w(2)} + ...+ \Delta S_{w(n)}, \qquad (5.33)$$

the ratio $S_{w(n)} / Q_n$ for each step can be calculated and plotted on arithmetic paper versus the corresponding values of Q_n (Figure 5.9).

The slope of the straight line $S_{w(n)} / Q_n$ is the value of C and the intercept of this line in the Q = 0 axis gives the value of B on the $S_{w(n)} / Q_n$ axis

The well efficiency is a parameter of the ratio of laminar head loss to the total head loss, expressed as a percentage :

$$L_p = \frac{BQ}{BQ + CQ^2} \times 100 \qquad (5.34)$$

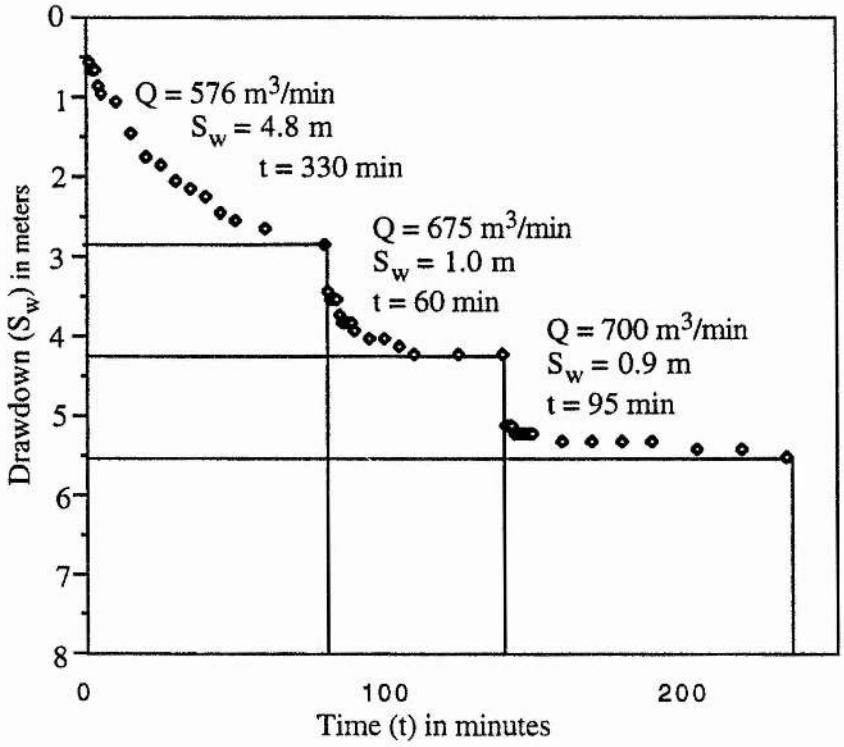

Figure 5.8 Determination of the drawdown for each step using a step drawdown test for well no (BM5) in Wadi Baysh.

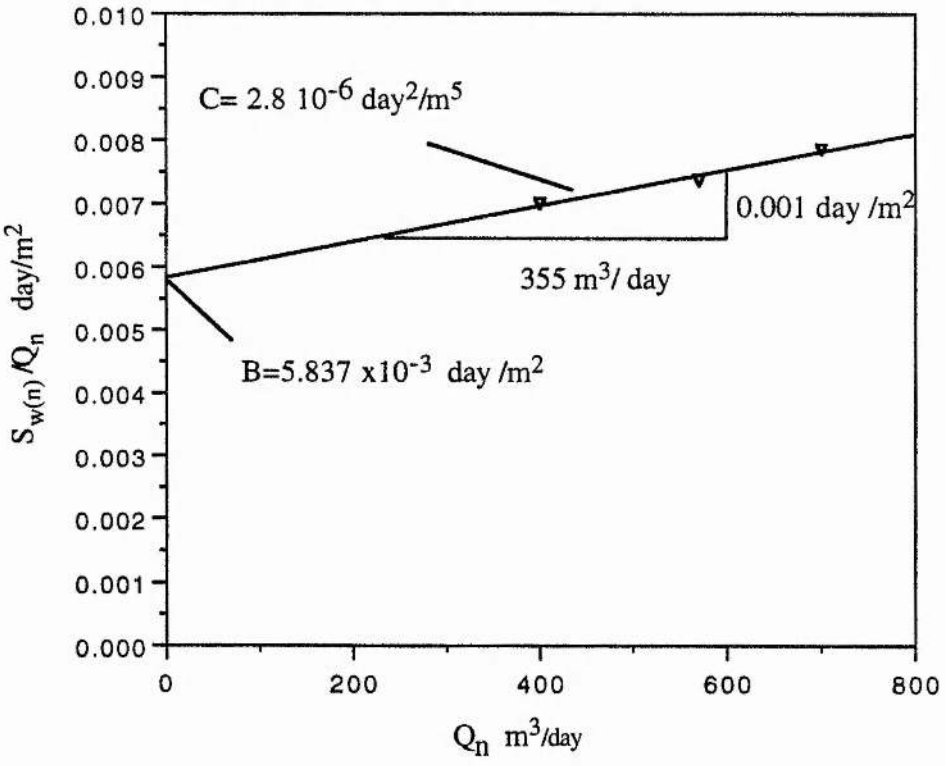

Figure 5.9 Determination of the parameters B and C of well no (BM5) using a step drawdown test in Wadi Baysh.

5.3.3.4.4 Results

The calculation of the linear (B) and non-linear (C) aquifer-loss coefficients shows that the B values (0.0058 d/m^2) and C ($3x10^{-6}$) of well BM5 in Wadi Baysh were higher than the corresponding values for B and C in Wadi Habawnah (B = 0.0008 d/m^2 and C = 10^{-6}; see Figures 5.9, 5.10 and 5.11, Table 5.5 and Appendix 5A&B). The percentage of the total head loss attributable to laminar flow is an average of 80 % in Wadi Baysh while in Wadi Habawnah it is 65%.

On the basis of the Jacob (1974) assumptions, Table 5.5 indicates that the well losses in BM5 were higher than those of well HB2. Also the aquifer loss of Wadi Baysh averaged 3m which is much higher than the average value of the aquifer loss in Wadi Habawnah (0.36m). Lp, which is used as a measure of well efficiency, shows that well BM5 has a high efficiency value of 80% where the discharge value is low (i.e. 400 m^3/day). The efficiency decreased to 75% when the discharge rate became higher (700 m^3/day).

Well HB2 reached the high efficiency value of 78 % when the rate of discharge was 215m^3/day but at a higher discharge rate of 670 m^3/ day the well efficiency decrease to 53%.

5.4 Summary and Conclusion

The main problems in the determination of aquifer parameters are to find the most suitable analytical methods. In spite of a range of different methods being available, each is valid only under a set of limited assumptions. Assumptions concerning aquifer homogeneity, isotropy, and uniformity in thickness, are seldom, if ever, satisfied.

The Papadopulos-Cooper method was used in this investigation as the most suitable method to evaluate the properties of the unconfined aquifer using the pumping test for large diameter wells.

The GAWP computer program helped to minimise the human error in selection of the proper match point. Close agreement was achieved between the field data curves and the type curve for this method (Appendix 5A&B).

The transmissivity values of the unconfined aquifer in both wadis are believed to be

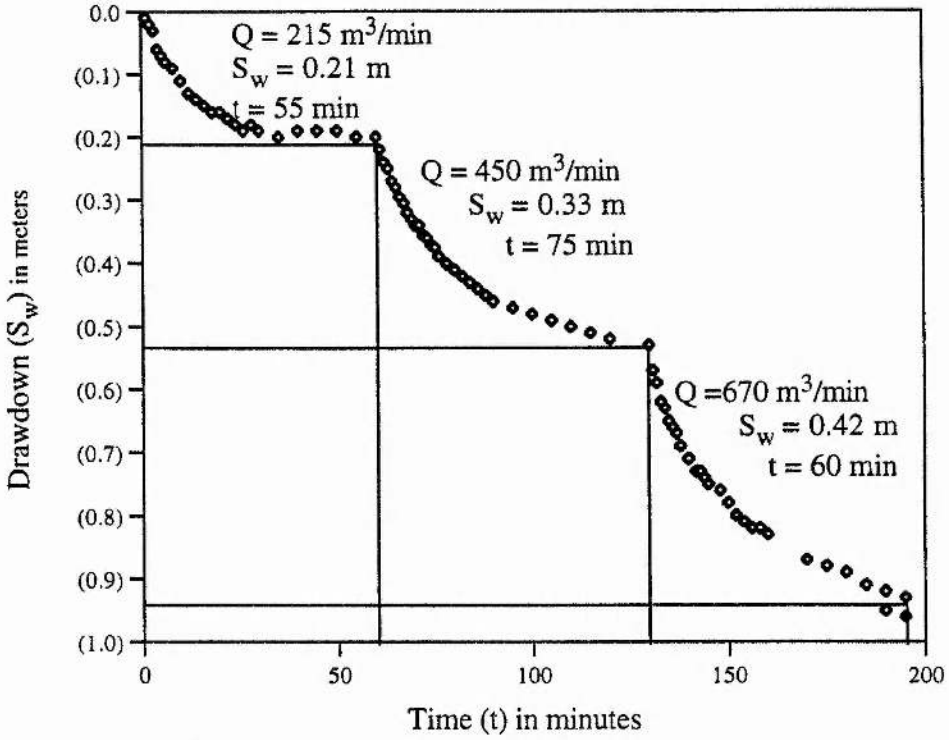

Figure 5.10 Determination of the drawdown for each step using a step drawdown test for well no (HB2) in Wadi Habawnah.

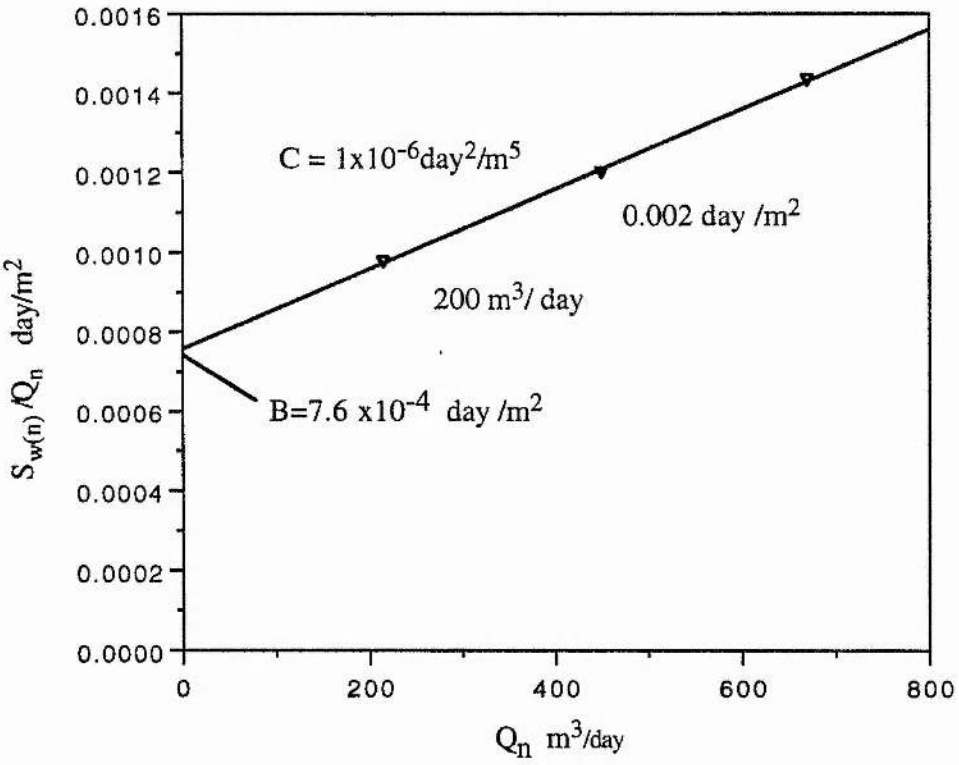

Figure 5.11 Determination of the parameters B and C using a step drawdown test for well no (HB2) in Wadi Habawnah.

Table 5.5 Specific drawdown calculated using the Hantush-Bierschenk method: step draw down test well.

Wadi Baysh (Well no. BM5)

Step No	Pumping rate Q (m^3/day)	Resulting drawdown S_w (m)	Specific drawdown S_w/Q (day/m^2)
1	400	2.80	0.0070
2	570	4.20	0.0074
3	700	5.50	0.0079

Wadi Baysh (Aquifer loss) Well loss

Step No	ΔQ	ΔS_w m	B day/m^2	C $(day)^2/m^5$	BxQ m	CxQ^2 m	Lp %
Step 1	170	2.80	$5.8x10^{-3}$	$2.8x10^{-6}$	2.34	0.45	84
Step 2	130	1.40			3.33	0.91	79
Step 3		1.30			4.10	1.37	75

Wadi Habawnah (Well No HB2)

Step No	Pumping rate Q (m^3/day)	Resulting drawdown S_w (m)	Specific drawdown S_w/Q (day/m^2)
1	215	0.21	0.0010
2	450	0.54	0.0012
3	670	0.96	0.0014

Wadi Habawnah (Aquifer loss) Well loss

Step No	ΔQ	ΔS_w m	B day/m^2	C $(day)^2/m^5$	BxQ m	CxQ^2 m	Lp %
Step 1	195	0.21	$0.8x10^{-3}$	$1x10^{-6}$	0.17	0.05	78
Step 2	220	0.33			0.36	0.20	63
Step 3		0.42			0.54	0.45	53

ΔS_w = total draw down in the well during the n-th step at time t.
ΔQ = constant discharge during the n-th step.
B = linear aquifer - loss coefficient
C = non linear aquifer - loss coefficient
Lp is the percentage of the total head loss that is attributable to laminar flow

reliable figures. The average value of the transmissivity in Wadi Baysh is 134 m^3/day while the average of the transmissivity of Wadi Habawnah is 515 m^3/day on the basis of the Ghearghe (1979) criteria.

Wadi Habawnah can be considered as having moderate to high potential while Wadi Baysh has only moderate potential. This different characteristic of the wadis is most probably due to the nature of the wadi floor sediments (see Chapters 6 and 8).

Both wadis show high values of transmissivity in the main course of the wadi system, where highly permeable wadi floor sediments are present, but lower values outside the main channel where sediments of low permeability are present.

The storativity (S) values obtained using the Papadopulos and Cooper method, although theoretically exact, are questionable from the practical viewpoint for the following reasons:

1- The field data curves of the pumping tests can easily be matched to more than one curve relating to the theoretical solution of different values of alpha.

2- The type curve family shows slight differences where the alpha value differs by an order of magnitude, so that, as a result, the reliability of the storativity determination is questionable (Kruseman and De Ridder, 1970). The transmissivity values change slightly compared to the storativity when the data match more than one single type curve.

The volumetric method was not helpful in determining a realistic value for the storativity. All the values calculated were very low. This method needs a long record of draw down to avoid the effects of well storage on the draw down compared to the aquifer drain. Such long period testing was not possible at the sites investigated.

The modification to the Ferris method yields more reliable values of storativity (Table 5.6). The modified Ferris method, using approximation techniques, gives what are believed to be still more reliable results for determining the storativity of the unconfined aquifers (storage coefficient) using the large diameter well test. The step draw down test shows that the efficiency of wells tested in both wadis is high. The values obtained confirm that large diameter wells are suitable for water supply in the wadis of the Arabian shield. According to the location of the two wells, the author believes that the pumping rate in the

Table 5.6 Average values of storativites using the Papadopulose and Cooper (1967) method, volumetric method and analogous drain solution method of large diameter wells in Wadi Baysh and Wadi Habawnah

Wadi Baysh Well Identification	Discharge rate (Q) (m^3/day)	T (m^2/day)	K m/day	S*	S**	S***	S(average)
BU1	288	190.08	95	$1.00x10^{-1}$	$8.69x10^{-3}$	$1.38x10^{-1}$	$8.22x10^{-2}$
BU2	432	156.00	26	$1.00x10^{-4}$	$1.60x10^{-3}$	$5.47x10^{-2}$	$1.88x10^{-2}$
BU3	576	86.60	7	$1.00x10^{-1}$	$1.25x10^{-2}$	$9.18x10^{-2}$	$6.81x10^{-2}$
BM5	576	75.00	7	$1.00x10^{-1}$	$5.93x10^{-3}$	$2.42x10^{-1}$	$1.16x10^{-1}$
BM7	720	146.88	11	$1.00x10^{-1}$	$4.04x10^{-3}$	$4.82x10^{-1}$	$1.95x10^{-1}$
BM12	576	150.00	7	$1.00x10^{-1}$	$7.29x10^{-4}$	$3.17x10^{-1}$	$1.39x10^{-1}$
BL16	648	129.60	3	$1.00x10^{-1}$	$1.61x10^{-3}$	$2.57x10^{-1}$	$1.20x10^{-1}$
Wadi Habawnah							
Well Identification	Discharge rate (Q) (m^3/day)	T (m^2/day)	K m/day	S*	S**	S***	S(average)
HB2	475	207.00	29	$1.00x10^{-1}$	$1.87x10^{-3}$	$8.28x10^{-2}$	$6.16x10^{-2}$
HB3	331	371.00	74	$1.00x10^{-5}$	$1.86x10^{-4}$	$1.53x10^{-1}$	$5.12x10^{-2}$
HB6	504	190.00	48	$1.00x10^{-3}$	$3.51x10^{-3}$	$9.51x10^{-2}$	$3.32x10^{-2}$
MT1	648	285.12	17	$1.00x10^{-5}$	$3.57x10^{-4}$	$1.02x10^{-1}$	$3.43x10^{-2}$
MT9	489	520.00	27	$1.00x10^{-5}$	$3.10x10^{-5}$	$9.61x10^{-2}$	$3.20x10^{-2}$
GF2	604	737.60	39	$1.00x10^{-5}$	$7.32x10^{-5}$	$4.76x10^{-2}$	$1.59x10^{-2}$
GF5	604	280.50	18	$1.00x10^{-5}$	$6.35x10^{-4}$	$1.26x10^{-1}$	$4.22x10^{-2}$
NG1	576	336.96	28	$1.00x10^{-5}$	$1.25x10^{-6}$	$8.26x10^{-2}$	$2.75x10^{-2}$
MR	720	651.80	54	$1.00x10^{-5}$	$2.70x10^{-5}$	$2.03x10^{-1}$	$6.78x10^{-2}$
HS2	604	734.40	37	$1.00x10^{-5}$	$1.16x10^{-5}$	$1.07x10^{-1}$	$3.58x10^{-2}$
HS4	720	254.00	12	$1.00x10^{-2}$	$1.34x10^{-3}$	$2.70x10^{-1}$	$9.39x10^{-2}$

S* is Storativity values using Papadoplus's method
S** is Storativity values using volumetric method
S*** is Storativity values using Analogous drain solution method

upper and middle part of Wadi Baysh and in the lower part of Wadi Habawnah should be within the range of 400 and 215 m^3/day to satisfy the high percentage of well efficiency (see Table 5.5).

CHAPTER SIX: SURFACE GEOPHYSICS EXPLORATION FOR GROUND WATER

6.1 Introduction

Geophysical methods have been used successfully for ground water exploration world-wide. They can provide specific information on the stratigraphy and structure of local geological formations as well as on aquifer properties.

Aquifers exist within the alluvial deposits in the basins of Wadi Baysh and Wadi Habawnah where they form significant water bearing formations. The use of geophysical methods has aided in the determination of the aquifer distributions and their regional boundaries. In addition geophysical methods have been used to study the hydrological parameters of the aquifers.

This chapter will focus on descriptions of the surface methods while the aquifer parameters and borehole methods will be described in the following chapters. A complete description is not possible within the scope of this work, but an attempt is made to provide an overview of each method. Zohdy, Eaton and Mabey (1980) describe the application of surface geophysics to ground water investigations. Keys and MacLary (1971) provided a complete discussion of borehole geophysical methods.

During the field work in the study area, seismic refraction and electrical resistivity surveys were conducted on the bed of both Wadi Baysh and Wadi Habawnah (Figures 6.1 , 6.2, 6.15 and 6.16). Previously borehole geophysical exploration had been carried out by MAWR, (1978), using electric logging and radioactive logging in the downstream reaches of Wadi Baysh. The location of these boreholes is shown in Figure 6.1.

The main aquifer investigated in Wadi Habawnah extends over an area of about 50 km^2 from Habawnah village in the west to Al Husaniah village in the east (Figure 6.2). The principal aquifer of Wadi Baysh occupies an area of about 47 km^2 (7 km north east of Masliyah village to 10 km west of Baysh Bridge).

The lower parts of Wadi Baysh and Wadi Habawnah have flood plains varying in width from 2 to 5 km and 0.7 to 2 km, respectively. In the upper part of Wadi Baysh, the flood plain is about 90 m above mean sea level and is bordered by low hills rising to

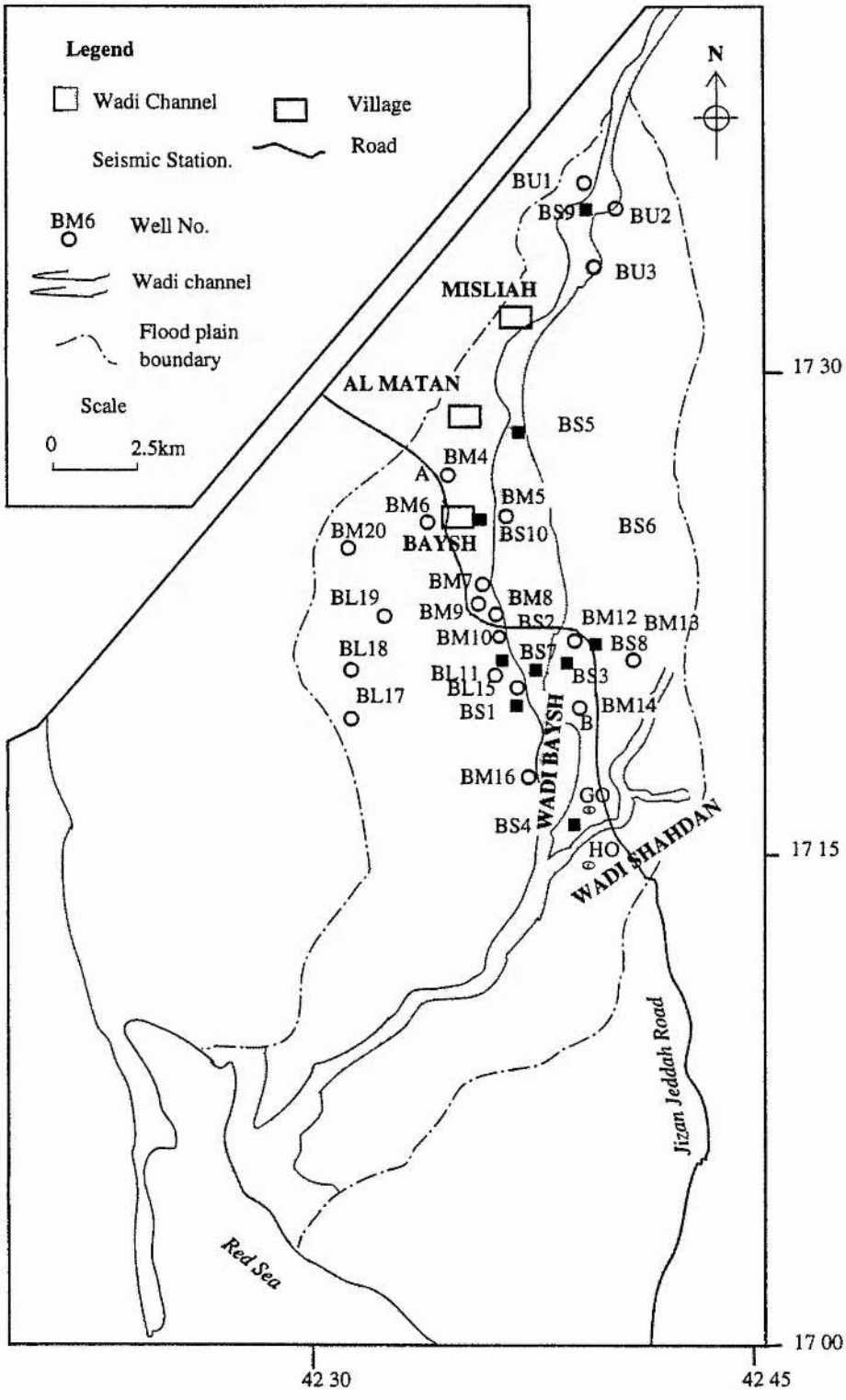

Figure 6.1 Location map of Wadi Baysh wells and seismic stations.

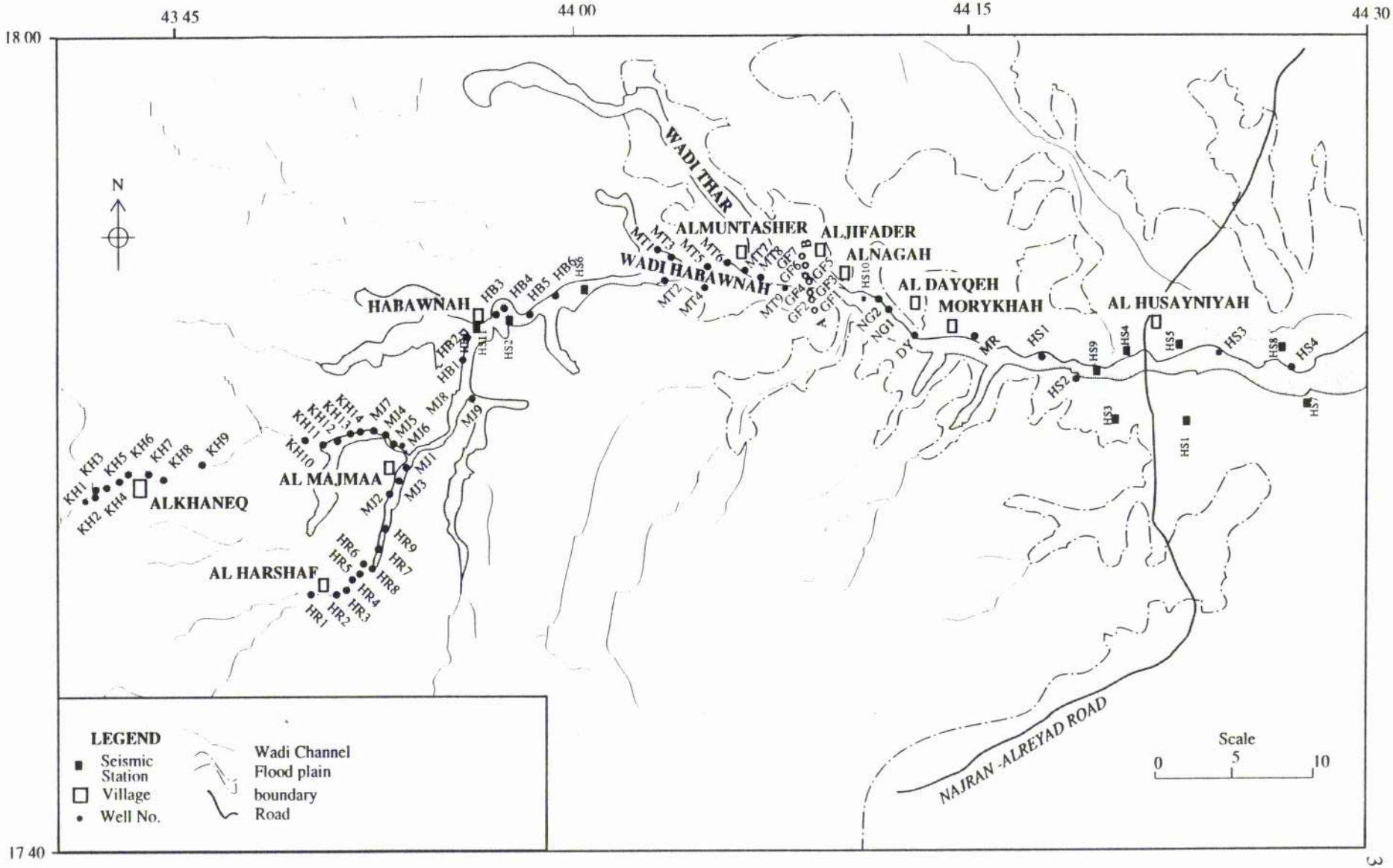

Figure 6.2 Location map of Wadi Habawnah wells and seismic stations.

elevations of approximately 140 m in the north east. In the south west the flood plain becomes wider with an elevation of 3 to 10 m above sea level. The flood plain of Wadi Habawnah is about 1150 m above mean sea level.

This chapter is divided into two sections which are briefly described below:

Section one, deals with shallow seismic refraction surveys to determine the depth of the water table and the bedrock in both wadis.

Section two deals with electrical resistivity surveys to determine the depth of the water table and the bedrock in both wadis.

6.2 Section One: Seismic Refraction Method

6.2.1 Study Area

The surface geophysical studies were carried out in Wadis Baysh and Habawnah, to delineate the gravel beds. Such permeable strata would serve as conduits for the flow of water. The sediments of wadis on the Arabian Shield are Quaternary in age (Brown, 1956). The floors of the two wadis are lined with thick gravels forming a flood plain with two levels of terraces. The younger and older terraces are 1-2 m and 3-4 m higher, respectively, than the floor of the wadi. Both terraces generally consist of assorted boulders in addition to sandy and silty alluvium. The entire channel surfaces of the upper and middle parts of both wadis are covered by thick riverine alluvium. In the lower parts of both wadis, these alluvial deposits are overlain by blown sand and silt that become thicker near the Red Sea coast and the Empty Quarter Basin respectively. The seaward portion of the coastal plain in which Wadi Baysh occurs (Tihamat Plain) has been studied by seismic reflection methods (Gillmann, 1968 Figure 2.18a). This work indicated that the surface of the basement dips toward the Red Sea at an average angle of about 10°, its depth increasing from about 2 km some 20 km inland to nearly 5 km in the vicinity of the Mansiyah Well 1 and the Jizan Dome on the coastline. Basinwards the Mansiyah Well 1 penetrated a thick continental series, then a massive salt sequence and finally marine clastic deposits of Miocene and Pliocene age (see Chapter 1).

Ten seismic refraction stations were occupied in Wadi Baysh and eleven stations in Wadi Habawnah, (Figures 6.1, 6.2 and Appendix 6A). Both wadis were dry throughout the time of the survey, but a stream intermittently carried small amounts of water in Wadi Baysh. The numbers of survey stations was restricted due to limitations of manpower availability. In general the floors of both wadis exhibit gentle slopes, Wadi Baysh towards the south west and Wadi Habawnah towards the east. The main channel is generally of low gradient except for small irregularities such as the stream margin banks. In the several surveys such surface irregularities were avoided to minimise their effects on the readings.

6.2.2 Theory of Seismic Refraction Interpretation

Although seismic refraction surveys are used routinely for several kinds of investigations, the methods used to collect and interpret seismic data have not changed significantly in the last two decades. The following sections summarise the major points of theory of seismic refraction interpretation.

Refraction surveys are based on the detection of seismic waves which have been refracted at interfaces of different seismic velocity (representing boundaries between differing sediment types) and have arrived at the ground surface. The wave path, schematic record, and travel-time are demonstrated in Figure 6.3.

Snell's Law describes the physical principle of wave refraction where the wave phenomena will travel from one point to another along a path that requires the minimum amount of time. Snell's Law states that the ratio of the sine of the angle incidence (I) to the sine of the angle of refraction (R) is a constant for any pair of media as follows

$$\frac{\sin I}{\sin R} = \frac{V_I}{V_R} \qquad (6.1)$$

where I is the angle of incidence with respect to the normal to a velocity interface, R is the angle of refraction, V_I is the seismic velocity in the incident layer (layer 1) and V_R is the velocity in the refracting layer (layer 2) as shown in Figure 6.4.

It is known that at a critical angle of incidence for the underlying high speed layer, a seismic wave is refracted along the interface between two layers (i.e. angle R = 90°). Refraction will be towards the interface if V_2 is greater than V_1. If $\sin I = \frac{V_1}{V_2}$, the refracted ray will be parallel to the interface and some of the energy will return to the surface at the original angle of incidence. However, at greater incident angles there can be no reflected ray and all the energy is refracted.

The associated wave fronts in layer 1 lag behind those in layer 2 creating a "bow wave" effect (Heiland, 1968). A portion of the refracted energy, therefore, returns to the ground surface where geophones detect it (Figure 6.5).

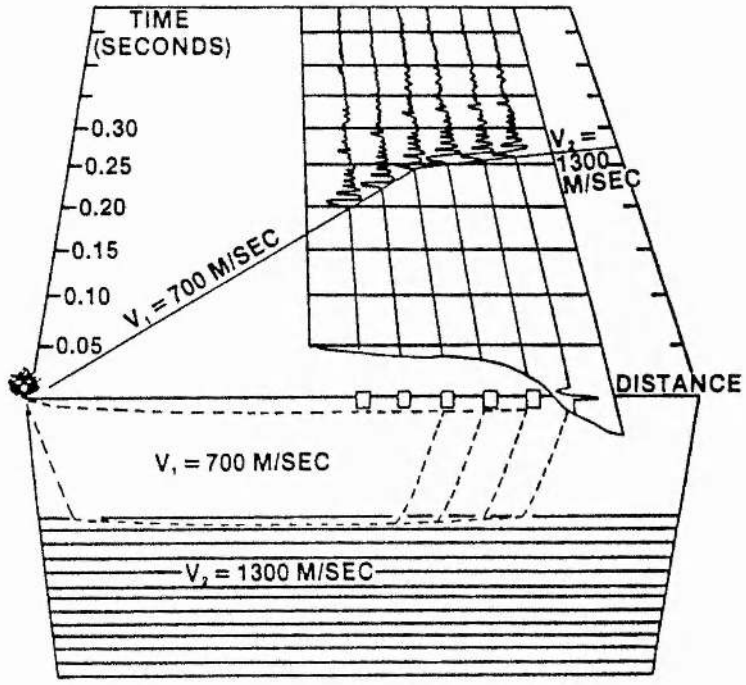

Figure 6.3 Wave path, schematic record and travel-time curve in a single-layer refraction problem (After Heiland, 1951).

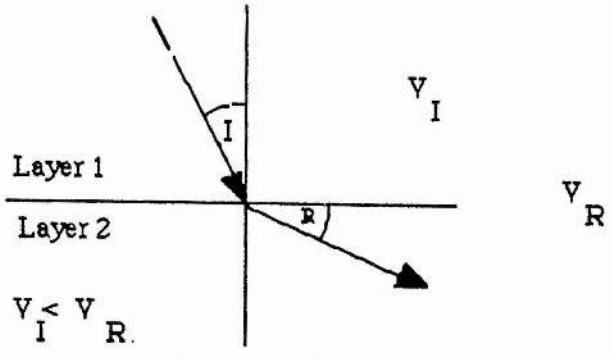

Wave refraction

I = angle of incidence, R = angle of refraction
V_1 = seismic velocity in layer 1, V_2 = seismic velocity in layer 2

Figure 6.4 Illustration the path of seismic wave during refraction.

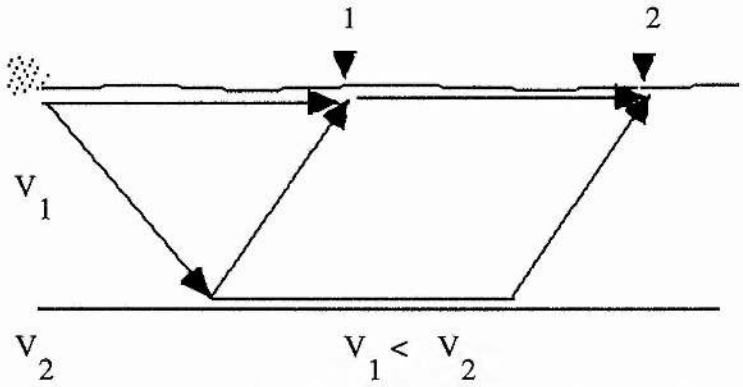

Figure 6.5 Direct and refracted waved arrivals. At geophone 1, the direct arrival will be faster , while the refracted wave at geophone 2 arrives sooner than the direct wave.

6.2.3 Interpretation Methods

Four types of waves can be transmitted by an elastic body according to the theory of elasticity. Two of these, the compressional waves and shear waves (P-waves and S-waves) are body waves. P-waves are compressional waves in which the particle motion in the medium is parallel to the direction of propagation. S-waves are shear waves in which the particle motion is perpendicular to the direction of propagation. The other two waves known as surface waves (Rayleigh waves and Love waves) are confined to a region near to the free surface of the medium.

No use is made of shear waves and surface waves in hydrological exploration because of the following reasons:

1- Shear wave velocities are less affected by moisture content than compressional waves.

2- The surface wave amplitudes decrease with depth in the medium.

3- The elastic wave propagation in this study is concerned with compressional waves (P-waves). These waves have the highest velocity of the above types discussed and, therefore, the shortest travel time for a given propagation path.

4- The refraction schemes usually use arrival times (amount of time taken by seismic waves to travel from source to each receiver) and offsets (service-to-receiver distances) as input.

There are many different methods of interpreting seismic refraction data. The differences result from the assumptions made about the subsurface wave travel path.

Sjogren, (1984) indicates that the required assumptions for all standard refraction interpretations are that the layer velocities increase with depth, and that the contrast between layer velocities is large. The various interpretation methods are distinguished according to whether they depend on the assumption of the refractors being planar or undulating and whether individual layer velocities are constant or varying (Palmer, 1981).

Commonly, the interpretation methods are derived from the reciprocal method or method of differences (Hawkins et al, 1961; Palmer, 1981). These methods use arrival times from waves that have refracted along the target layer. The required data are arrival times from shot points on opposite sides of the geophone spread. The interpretation methods can be classified on the basis of the structure of the layers as parallel interfaces (assuming the layer is horizontal or dipping:

6.2.3.1 Parallel Interfaces

6.2.3.1.1 Intercept Method

The intercept method uses the so-called intercept time for each refractor, with the time derived by extrapolating the apparent refractor velocity segment back to the shot location. Overburden velocities are calculated as apparent velocities of travel time curve segments using both forward and reverse shots, the arithmetic mean velocities are assumed to provide representative average layer velocities.

The interpretation proceeds as follows: assign arrivals to layers, forming straight line segments on the travel time curves. Extrapolate line segments representing layers back to the shot point location. Define the intercept time t_i for the i^{th} layer (see Figure 6.6)

Several equations have been developed to calculate the depth or the thickness (D) of different layers from plots like Figure 6.6. Dobrin (1988) used the following expression for thickness of a particular layer in a multilayered profile:

$$D_n = \frac{V_n V_{n+1}}{2\sqrt{V_{n+1}^2 V_n^2}} \left[t_{i(n+1)} - 2D_1 \frac{\sqrt{V_{n+1}^2 V_1^2}}{V_1 V_{n+1}} - 2D_2 \frac{\sqrt{V_{n+1}^2 - V_2^2}}{V_2 V_{n+1}} \right.$$

$$\left. \ldots -2D_{n-1} \frac{\sqrt{V_{n+1}^2 V_{n-1}^2}}{V_{n-1} V_{n+1}} \right] \qquad (6.2)$$

Sjogren, (1984) indicates that the required assumptions for all standard refraction interpretations are that the layer velocities increase with depth, and that the contrast between layer velocities is large. The various interpretation methods are distinguished according to whether they depend on the assumption of the refractors being planar or undulating and whether individual layer velocities are constant or varying (Palmer, 1981).

Commonly, the interpretation methods are derived from the reciprocal method or method of differences (Hawkins et al, 1961; Palmer, 1981). These methods use arrival times from waves that have refracted along the target layer. The required data are arrival times from shot points on opposite sides of the geophone spread. The interpretation methods can be classified on the basis of the structure of the layers as parallel interfaces (assuming the layer is horizontal or dipping:

6.2.3.1 Parallel Interfaces

6.2.3.1.1 Intercept Method

The intercept method uses the so-called intercept time for each refractor, with the time derived by extrapolating the apparent refractor velocity segment back to the shot location. Overburden velocities are calculated as apparent velocities of travel time curve segments using both forward and reverse shots, the arithmetic mean velocities are assumed to provide representative average layer velocities.

The interpretation proceeds as follows: assign arrivals to layers, forming straight line segments on the travel time curves. Extrapolate line segments representing layers back to the shot point location. Define the intercept time t_i for the i^{th} layer (see Figure 6.6)

Several equations have been developed to calculate the depth or the thickness (D) of different layers from plots like Figure 6.6. Dobrin (1988) used the following expression for thickness of a particular layer in a multilayered profile:

$$D_n = \frac{V_n V_{n+1}}{2\sqrt{V_{n+1}^2 V_n^2}} \left[t_{i(n+1)} - 2D_1 \frac{\sqrt{V_{n+1}^2 V_1^2}}{V_1 V_{n+1}} - 2D_2 \frac{\sqrt{V_{n+1}^2 - V_2^2}}{V_2 V_{n+1}} \right.$$
$$\left. \ldots -2D_{n-1} \frac{\sqrt{V_{n+1}^2 V_{n-1}^2}}{V_{n-1} V_{n+1}} \right] \qquad (6.2)$$

where D_n = thickness of nth layer (for the top layer, n = 1), V_n = sound velocity in the nth layer (reciprocal of slope for the nth straight section of a data curve) and $t_{i(n)}$ = intercept of extended straight line for nth layer with t axis (Figure 6.6).

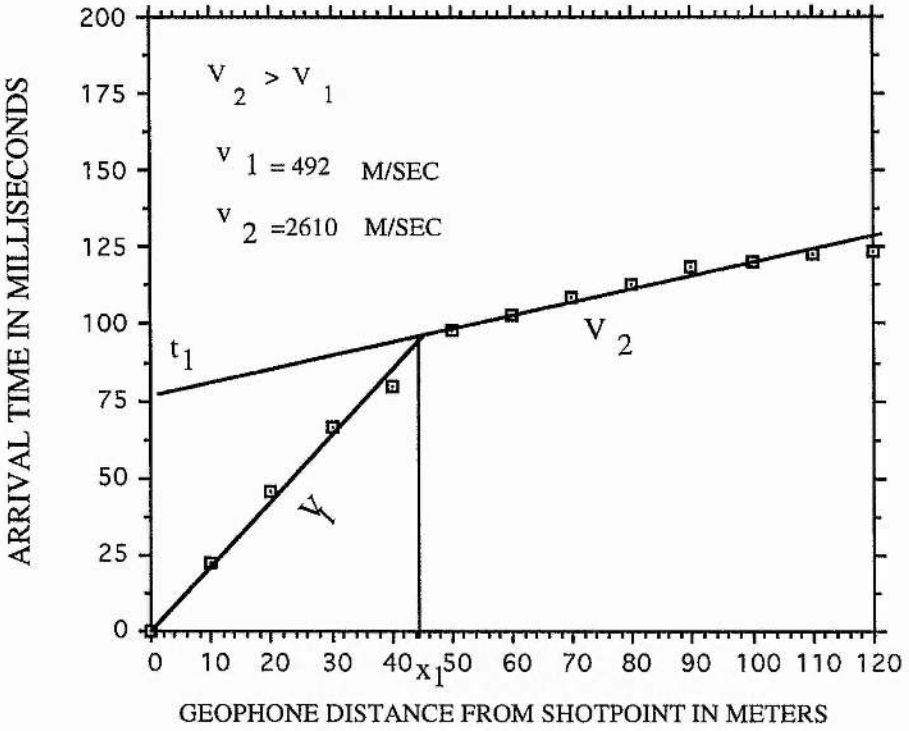

Figure 6.6 Hypothetical relation between arrival time and geophone distance for a two-layer case.

This expression is commonly reduced to calculate the top layer and second layer thicknesses as D_1 and D_2, respectively (see Tables 6.1, 6.2 and 6.3 and Appendix 6A).

$$D_1 = \frac{V_1 V_2}{\sqrt{V_2^2 - V_1^2}} t_{i2}; \tag{6.3}$$

$$D_2 = \frac{V_2 V_3}{\sqrt{V_3^2 - V_2^2}} \left[t_{i3} - 2D_1 \frac{\sqrt{V_3^2 - V_1^2}}{V_3 V_1} \right] \tag{6.4}$$

6.2.3.1.2 Critical Distance Method

The critical distance method (Heiland, 1968) is similar to the intercept method in that it is applicable to horizontally layered targets which are characterised by constant velocities. Such a method is interpreted on the basis of the observation that, at some offset from the shot, the refracted arrival from a given layer will arrive before the direct or

Table 6.1 Seismic refraction analysis of Wadi Baysh and Wadi Habawnah (Forward profile)

Wadi Baysh

Station No.	V_1 ms^{-1}	V_2 ms^{-1}	V_3 ms^{-1}	$(T_1)^*$ ms^{-1}	$(T_2)^*$ ms^{-1}	$(X_1)^*$ meter	$(X_2)^*$ meter	D_1(useT_1) Calc.	D_2(useT_2) Calc.	X_1** meter	X_2** meter	X_1 pct	X_2 pct	D_1(useX_1*) Calc.	D_2(use X_2*) Calc.
BS1	180	416		165		51		16		52		3		16	
BS2	185	500		148		40		15		43		8		14	
BS3	235	370		70		48		11		45		6		11	
BS4	170	260		150		80		17		74		9		18	
BS5	439	1069		43		29		10		32		9		9	
BS6	389	999		46		29		10		29		1		10	
BS7	494	733		25		34		8		38		10		8	
BS8	365	178.6***													
BS9	245	1806		42		13		5		12		9		6	
BS10	415	736		50		43		13		48		10		11	

Wadi Habawnah

Station No.	V_1 ms^{-1}	V_2 ms^{-1}	V_3 ms^{-1}	$(T_1)^*$ ms^{-1}	$(T_2)^*$ ms^{-1}	$(X_1)^*$ meter	$(X_2)^*$ meter	D_1(useT_1) Calc.	D_2(useT_2) Calc.	X_1** meter	X_2** meter	X_1 pct	X_2 pct	D_1(useX_1*) Calc.	D_2(use X_2*) Calc.
HS1	313	1786	6073	30	43	12	34	5	12	11	33	-6	4	5	11
HS2	324	1797	5000	30	57	13	78	5	26	12	76	10	3	5	25
HS3	347	950		25		15		5		14		10		5	
HS4	360	743		18		11		4		12		10		3	
HS5	385	927		35		23		7		23		0		7	
HS6	493	2610		76		45		19		46		2		19	
HS7	333	909		85		47		15		45		5		16	
HS8	345	777		40		26		8		25		5		8	
HS9	337	710	2851	21	80	13	52	4	21	13	54	3	1	4	20
HS10	333	1238	3086	21	55	11	73	4	22	10	70	7	5	4	22
HS11	325	2381	4930	43	53	15	49	7	12	16	44	7	10	7	12

Critical Distance (X_1&X_2)& Time Intercept (T_1&T_2)

The total depth of the first and the second layer{ (D_1)&(D_2) respectively

*from the graph & ** calculated

Percent of error (pct)

Table 6.2 Seismic refraction data analysis of Wadi Baysh (B) and Wadi Habawnah (H) (Reverse profile)

Wadi Baysh

Station No.	V_1 ms^{-1}	V_2 ms^{-1}	V_3 ms^{-1}	(T_1)* ms^{-1}	(T_2)* ms^{-1}	(X_1)* meter	(X_2)* meter	D_1(useT_1) Calc.	D_2(useT_2) Calc.	X_1** meter	X_2** meter	X_1 pct	X_2 pct	D_1(useX_1*) Calc.	D_2(use X_2*) Calc.
BS1	181	390		160		50		16		54		7		15	
BS2	185	606		150		43		15		40		8		16	
BS3	167*													#VALUE!	
BS4	196	425		200		80		22		73		10		24	
BS5	437	1170		40		25		9		28		10		8	
BS6	389	963		45		29		10		29		1		9	
BS7	485	741		25		34		8		35		3		8	
BS8	364	232***												#VALUE!	
BS9	252	1806		42		13		5		12		6		6	
BS10	598	736		50		41		26		43		-4		7	

Wadi Habawnah

Station No.	V_1 ms^{-1}	V_2 ms^{-1}	V_3 ms^{-1}	(T_1)* ms^{-1}	(T_2)* ms^{-1}	(X_1)* meter	(X_2)* meter	D_1(useT_1) Calc.	D_2(useT_2) Calc.	X_1** meter	X_2** meter	X_1 pct	X_2 pct	D_1(useX_1*) Calc.	D_2(use X_2*) Calc.
HS1	345	1625	4777	30	42	13	36	5	11	13	33	1	9	5	11
HS2	329	1670	2907	30	54	13	64	5	24	12	93	6	10	5	23
HS3	360	1603		39		19		7		18		5		8	
HS4	367	856		16		11		3		10		7		3	
HS5	410	912		26		19		6		19		2		6	
HS6	413	709		72		34		18		71		9		9	
HS7	330	1086		90		43		16		43		2		16	
HS8	357	792		41		27		8		27		1		8	
HS9	348	833	3420	35	71	19	42	7	14	21	37	9	9	6	13
HS10	333	1095	2907	23	55	10	74	4	18	11	55	9	3	4	18
HS11	320	5617	4912	45		16		7		15		7		8	

Critical Distance (X_1&X_2)& Time Intercept (T_1&T_2)

The total depth of the first and the second layer{ (D_1)&(D_2) respectively

*from the graph & ** calculated

Percent of error (pct)

***Affected velocity as a result of changing in the dip of the layer

Table 6.3 The average depth of seismic refraction layers based on the intercept time method and the critical distance method in Wadi Baysh and Wadi Habawnah (H)

Wadi Baysh

Station No.	D_1(use t_1) Calc.(F)	D_2(use t_2) Calc.(F)	D_1(use T_1) Calc.(R)	D_2(use T_2) Calc.(R)	D_1(useX_1) Calc.(F)	D_2(use X_2) Calc.(F)	D_1(useX_1) Calc.(R)	D_2(use X_2) Calc.(R)	D_1 (m) Average	D_2 (m) Average
BS1	16		16		16		15		16	
BS2	15		15		14		16		15	
BS3	11				11				5	
BS4	17		22		18		24		20	
BS5	10		9		9		8		9	
BS6	10		10		10		9		10	
BS7	8		8		8		8		8	
BS8	*									
BS9	5		5		6		6		5	
BS10	13		26		11		7		14	

Wadi Habawnah

Station No.	D_1(use t_1) Calc.(F)	D_2(use t_2) Calc.(F)	D_1(use T_1) Calc.(R)	D_2(use T_2) Calc.(R)	D_1(useX_1) Calc.(F)	D_2(use X_2) Calc.(F)	D_1(useX_1) Calc.(R)	D_2(use X_2) Calc.(R)	D_1 (m) Average	D_2 (m) Average
HS1	5	12	5	11	5	11	5	11	5	11
HS2	5	26	5	24	5	25	5	23	5	24
HS3	5		7		5		8		6	
HS4	4		3		3		3		3	
HS5	7		6		7		6		7	
HS6	19		18		19		9		16	
HS7	15		16		16		16		16	
HS8	8		8		8		8		8	
HS9	4	21	7	14	4	20	6	13	5	17
HS10	4	22	4	18	4	22	4	18	4	20
HS11	7	12	7		7	12	8		7	6

The total depth of the first and second layer using intercept time method [D_1(use T_1)&D_2(use T_2)

The total depth of the first and second layer using critical distance method [D_1(use X_1)&D2(use X_2)

*unable to calculate the depth since the velocity decreases with depth

refracted arrival from the overlying layer (Figure 6.5). By measuring this offset (cross-over distance) and calculating the layer velocities from forward and reverse shots the thickness of materials overlying the refractor may be determined. The interpretation process consists of assigning arrivals to straight travel time curve segments similar to the intercept method.

However, instead of defining the intercept time of a segment, the "critical" distance, x, of the point where the slope of the curve changes at which the wave is refracted (see Figure 6.6), the layer depth under the shot is calculated by the equation given below by Dobrin and Savit (1988) (See Tables 6.1, 6.2, 6.3 and Appendix 6A)

$$D_1 = \frac{x_1}{2}\sqrt{\frac{V_2 - V_1}{V_2 + V_1}} \qquad (6.5)$$

and for the second layer, an approximate equation used to calculate D_2 is presented in modified form by Bower (1978)

$$D_2 = \frac{x_2}{2}\sqrt{\frac{V_3 - V_2}{V_3 + V_2}} - \frac{D_1}{6} \qquad (6.6)$$

6.2.3.2 Dipping Layer

6.2.3.2.1 Mooney Computer Program

The Mooney Computer program (Mooney, 1977) was adopted to solve the dipping layer problem of refraction seismology for any number of layers (see Appendix 6B).

A reversed profile which represents all of the refraction data in both wadis, is required for a complete interpretation (Appendix 6A).

To summarise the computation procedure, using an observed travel time graph for a reversed seismic profile, a straight line segment is inserted onto the graph so as to best fit the observation points and to satisfy the condition of reciprocity. The number of line segments from position A is equal to the number of line segments from position B. The number of layers in the subsurface structure is also equal to the number of time segments. The computer program will take the apparent velocities from position A and B and the intercept times at position A and B as inputs, (Tables 6.1 and 6.2) and provide depths, dips and velocities of the structure as outputs (Tables 6.4 and 6.5). The input data include a

Table 6.4 Analysis for the dipping-layers structure of Wadi Baysh using Mooney's computer program

Station No	Depth A m	Layer No	Depth B m	Velocity m/sec	Thickness A m	Thickness B m	DIP	Error %
BS1		1		181	17	17	*	<10
	17		17					
		2		403				
BS2		1		185	15	15	*	<10
	15		15					
		2		588				
BS4		1		183	17	23	-10	>10
	17		23					
		2		318				
BS5		1		438	10	10	*	<10
	10		10					
		2		1117				
BS6		1		389	10	10	0	<10
	10		10					
		2		980				
BS7		1		490	8	8	0	<10
	8		8					
		2		737				
BS9		1		249	5	5	0	<10
	5		5					
		2		1806	9	12		
BS10		1		507	17	17	0	<10
	17		17					
		2		736				

- Indicates the dip direction upstream E-W

*Dip < 5°

0 Horizontal

Table 6.5 Analysis for the dipping-layers structure of Wadi Habawnah using Mooney's computer program

Station No	Depth A m	Layer No	Depth B m	Velocity m/sec	Thickness A m	Thickness B m	DIP	Error %
HS1		1		329	5	5	*	<10
	5		5				*	
		2		1702	11	10		
		3		5348				
HS2		1		327	5	5	*	<10
	5		5					
		2		1730	26	23	6	
		3		3658				
HS3		1		354	5	7	*	>10
	5		7					
		2		1189				
HS4		1		364	4	3	*	
	4		3					>10
		2		795				
HS5		1		397	8	6	*	<10
	8		6					
		2		920				
HS6		1		453	19	19	15	>10
	19		19					
		2		1078				
HS7		1		331	15	16	*	<10
	15		16					
		2		989				
HS8		1		350	8	8	*	<10
	8		8					
		2		785				
HS9		1		343	4	7	*	<10
	4		7				*	
		2		766	22	13		
		3		3103				
HS10		1		333	4	4	*	<10
	4		4				*	
		2		1162	21	20		
		3		2989				
HS11		1		323	7	7	*	<10
	7		7					
		2		3342				

* Dip < 5

quantity, M, which is set equal to zero since the intercept times are read in seconds as requested by the program. The symbol X designates the seismic profile length from A to B in metres and the apparent velocities are also in m s^{-1}. The dips of less than 5° are ignored for simplicity.

6.2.4 Field Procedures Using Bison Portable Seismograph Model 1980

With Bison seismograph instruments, the seismic wave is generated with a sledge hammer striking a steel plate on the ground. This was the form of apparatus used in the stations in the upper part of the wadis, but a 70kg heavy weight was used to generate the seismic waves in the lower part of the wadis where the sediments were believed to be of greater thickness (Figure 6.7).

With a geophone at each end of the survey line, it is possible to obtain a time-distance curve both backward and forward along the line (a reversed profile). Sometimes it was found that to get good geophone contact, the ground around the geophone needed to be wetted because most of the station sites were dry. The time it takes for a P-wave to travel from the impact source to the geophone is read on the refraction-seismic instrument. The amplified wave forms from the geophone outputs are displayed on the viewing screen. When the seismic signal is desired for refraction surveys, the marker pip which appears on the wave form is moved back and forth until it coincides with the first positive P-Wave arrival.

The maximum depth of penetration in such investigations varies with the types of material involved (i.e is dependent upon material density) or the horizontal distance that can be obtained between geophone and the shock wave source (approx 1:3). Two people operate the portable refraction seismic instrument, one person is stationed at the instrument to record time readings while the second swings the hammer. When the hammer strikes the plate, a mercury switch on the hammer handle closes, sending a signal through a cable which starts the seismograph. This measures time intervals in milliseconds. When a first arrival of a P-wave is received by a geophone, it stops the instrument. The hammer blows are repeated until a repeatable reading has been established. The lowest of these readings is plotted on the graph. The repeatable readings, generally, vary by only 1 or 2 milliseconds.

Figure 6.7 Surveying team using a heavy weight dumper (70 kg) to generate energy at a seismic station in the middle part of Wadi Baysh.

Non-repeated readings are disregarded. An S facility, using enhancement seismograph, which permits the storage of a signal, is built into the instrument. This helps to build a strong signal from a number of weaker signals from a distant hammer station (e.g. 70 m).

After selecting the survey line which runs parallel to the main wadi channel, the geophone is placed into the ground at one end of the line at a site thereafter considered to be station zero. A second geophone is moved progressively forward from the zero point and F_1, F_2, F_3 etc. readings obtained. This is accomplished by the Marker Position control. The travel time corresponding to the location of the marker pip appears as a four digit number (in milliseconds) directly above the wave form on the display screen. After the time reading has been obtained, the Clear Memory command button is pressed and the next hammer station is established.

6.2.5 Results and Interpretation

Two and three layer interpretations of the travel time curve yielded depths of 5 m to 20 m for the base of the top layer with seismic velocities of 200 to 600 ms^{-1} in Wadi Baysh (Tables 6.4 and 6.6). In Wadi Habawnah depths of 3 m to 29 m were measured to the base of the top material with seismic velocities of 300 to 400 m s^{-1} (Tables 6.5 and 6.7). The farmers' wells in Wadi Habawnah show that the dry gravel and boulder layer of Wadi Habawnah is an average of 8 m in thickness above the bed rock surface, while in the lower part of the wadi it reaches an average of 16 m in depth (Table 6.8). However, in Wadi Baysh the dry surface layer has a thickness of 5 to 20 m below the surface.

The seismic station BS9 was placed mid-way between water wells BU1 and BU2 while the seismic station B1 was placed near the water well BL14 in Wadi Baysh (Figure 6.1). However, in Wadi Habawnah the seismic stations HS2 and HS7 were placed near water wells H-7-P and HB3 (Figure 6.2). This was done to facilitate comparison of results of the seismic method with the known well lithology (Tables 6.8 and 6.9).

There is 0 to 13% difference between the seismic data and the well data in Wadi Baysh, and 9 to 12% in Wadi Habawnah (Table 6.9). On the whole, the seismic methods give relatively good agreement in predicting locally the total thickness of the shallow aquifer.

Table 6.6 The average depth and thickness of the dipping-layers structure of Wadi Baysh using Mooney's computer program (1977).

Station No	Layer No	Depth A m	Depth B m	Thickness A m	Thickness B m	Average depth (m)	Average Thicknnes (m)
BS1	1			17	17		17
		17	17			17	
	2						
BS2	1			15	15		15
		15	15			15	
	2						
BS4	1			17	23		20
		17	23			20	
	2						
BS5	1			10	10		10
		10	10			10	
	2						
BS6	1			10	10		10
		10	10			10	
	2						
BS7	1			8	8		8
		8	8			8	
	2						
BS9	1			5	5		5
		5	5			5	
	2						
				9	12		11
BS10	1			17	17		17
		17	17				
	2						

Table 6.7 The average depth and thickness of the dipping-layers structure of Wadi Habawnah using Mooney's computer program

Station No	Layer No	Depth A m	Depth B m	Thickness A m	Thickness B m	Average Depth (m)	Average Thickness (m)
HS1	1	5	5	5	5	5	5
	2			11	10		11
	3						
HS2	1	5	5	5	5	5	5
	2	31	28	26	23		25
	3						
HS3	1	5	7	5	7	6	6
	2						
HS4	1	4	3	4	3	3	3
	2						
HS5	1	8	6	8	6	7	7
	2						
HS6	1	19	19	19	19	19	19
	2						
HS7	1	15	16	15	16	15	15
	2						
HS8	1	8	8	8	8	8	8
	2						
HS9	1	4	7	4	7	5	5
	2	26	19	22	13		18
	3						
HS10	1	4	4	4	4	4	4
	2	25	24	21	20		21
	3						
HS11	1	7	7	7	7	7	7
	2						

Table 6.8 The inventory data (1989&1990) of the Farmer's Wells and MAWR observation wells

Wadi Habawnah Wells					Wadi Baysh Wells				
Well Location No.	Aquifer Thickness (m)	Water table depth (m)	Saturated Thickness (m)	Unsaturated Thickness (m)	Well Location No.	Aquifer Thickness (m)	Water table depth (m)	Saturated Thickness (m)	Unsaturated Thickness (m
HB1	12	10	2	10	BU1	7	5	2	6
HB2	16	9	7	9	BU2	12	6	6	6
HB3	17	12	5	12	BU3	20	7	13	7
HB4	16	12	4	12	BM4	30	11	19	11
HB5	16	12	4	12	BM5	24	13	11	13
HB6	17	13	4	13	BM6	27	13	14	13
H-11-P*	20	8	12	8	BM7	30	17	13	17
H-7-B*	33	14	19	14	BM8	70	16	54	16
MT1	32	15	17	15	BM9	75	16	59	16
MT2	34	10	24	10	BM10	68	17	51	17
MT3	30	10	20	10	BM11	54	18	36	18
MT4	30	11	19	11	BM12	40	19	21	19
MT5	31	11	20	11	BM13	62	19	43	19
MT6	37	11	26	11	BM14	43	18	25	18
MT7	36	12	24	12	BL15	70	22	48	22
MT8	38	12	26	12	BL16	60	23	37	23
MT9	33	14	19	13	BL17	90	24	66	24
H-3-P*	34	11	19	11	BL18	90	24	66	24
GF1	35	15	20	15	BL19	87	25	62	25
GF2	30	11	19	12	BL20	84	28	56	28
GF3	40	13	27	13	GO*	75	24	51	24
GF4	40	14	26	16	EO*	150	23	127	23
GF5	29	13	11	13					
GF6	30	14	16	14					
GF7	35	15	20	15					
NG1	24	12	12	12					
NG-2	40	13	27	13					
MR	26	14	12	14					
DY	42	19	23	19					
HS1	43	15	28	15					
HS2	37	18	19	18					
HS-3	43	17	26	17					
HS-4	38	17	21	17					
H-15-P*	35	16	19	16					

* Observation well of MAWR

Table 6.9 Comparison of seismic refraction data and direct measurements indicating the water table depth and the lithology at selected wells in Wadi Baysh and Wadi Habawnah

Wadi Baysh Geophysical Station No.	Seismic Refraction V_1 ms^{-1}	V_2 ms^{-1}	V_3 ms^{-1}	D_1 (m)	D_2 (m)	Well No	Well Inventory Data Description	Depth (m)	Total depth Error %	Remark
BS9	250	1800		5		BU1	Gravel , Sand	5	0	Field measurement
						BU2	Gravel , Sand	6	16	
BS1	200	400		17		BL14	Gravel , Sand	15	13	Farmer interview
							Sand , Silt and Clay	23		

Wadi Habawnah Geophysical Station No.	Seismic Refraction V_1 ms^{-1}	V_2 ms^{-1}	V_3 ms^{-1}	D_1 (m)	D_2 (m)	Well No	Well Inventory Data Description	Depth (m)	Total depth Error %	Remark
HS2	350	1000		15		HB3	Gravel , sand and silt	17	12	Field measurement
HS7	350	1750	4000	5	25	H-7-P	Coarse Sand	7		MAWR data
							Gravel Cobbles	18	9	
							clay	8		
							Bed rock			

As noted above, seismic refraction methods determine the level of the water table in both wadis. However, the saturated weathered bed rocks showed high seismic refraction with seismic velocities of 1700 to 1800 ms^{-1} as shown in station BS9 and HS2 (Tables 6.1 and 6.2). Below the water table the alluvial aquifer shows a seismic velocity range of 800 to 1400 ms^{-1} (Tables 6.6 and 6.7). The igneous and metamorphic bed rock depth were determined at eight seismic stations in Wadi Habawnah (see Table 6.7). The bed rock depth is 3 to 30 metres. The seismic velocities of the bed rocks range from 3400 to 6100 ms^{-1}. The depth to bed rock of Wadi Baysh could not be determined, and the maximum seismic velocity (V_2) recorded was 1200 ms^{-1} (Table 6.2) at seismic station (BS5).

According to Atlas Copco ABEM/AB (1986) (Figure 6.8), the typical P-wave velocities of igneous and metamorphic rocks range from 4000 m s^{-1} to 6500 m s^{-1} (see Table 6.2).

The seismic methods exhibit general agreement with water table depth measurement, the well lithology and bed rock in Wadi Habawnah. However, the seismic method becomes increasingly insensitive with depth, as shown in the lower part of Wadi Baysh, where the depths of the boreholes and farmers' wells ranged from 43 m to 150 m (Borehole EO) see (Tables 6.6 and 6.8). Seismic refraction wave energy decreases with depth because of the limited amount of energy which can be generated with a hammer or 70kg dumper.

The maximum horizontal distance of wave detection for a geophone varies from 70 to 100m from the shock point, so that the maximum depth that can be measured is 25 to 45 m, respectively.

6.2.6 Unimap Program Interpolation

Unimap, a program available on the Sun System at St. Andrews University, was used to interpolate the seismic data from both wadis. Seismic velocity maps of the dry layer and the saturated zone were constructed (Figures 6.9 and 6.10).

The bed rock seismic velocity of Wadi Habawnah was mapped and the water table contour lines and the thickness of the sediment for both wadis are established (Figures 6.9 and 6.10).

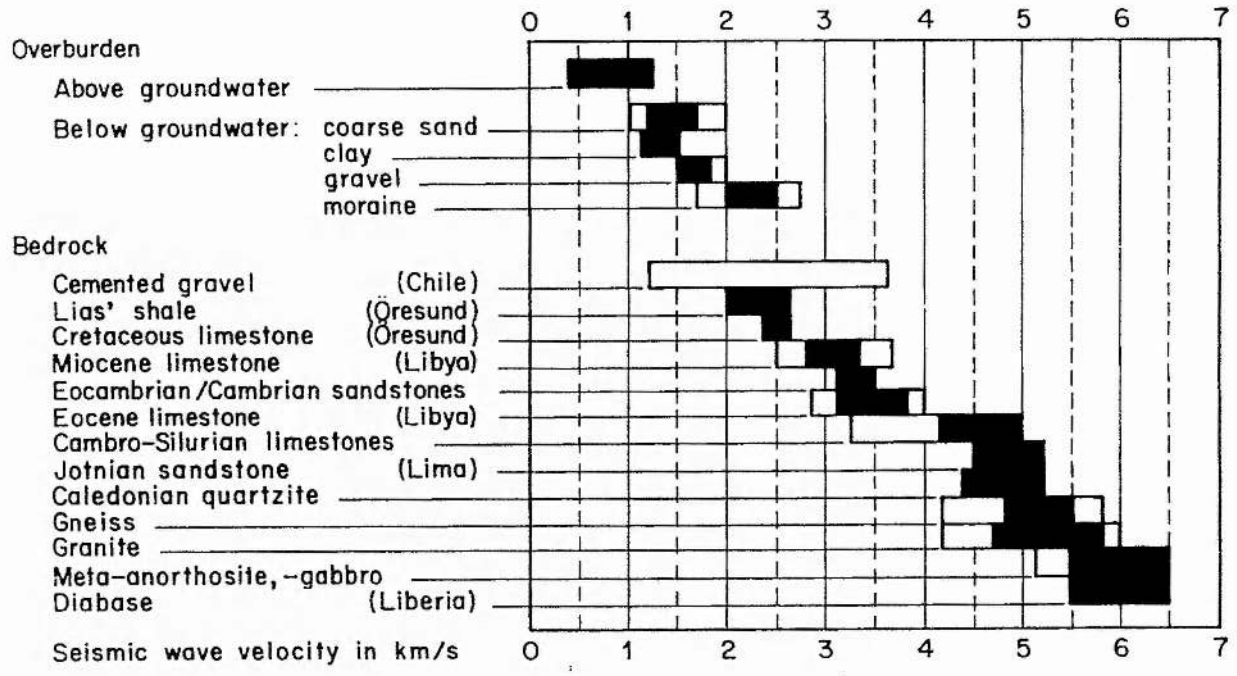

Figure 6.8 Typical values of P - wave seismic velocities (Atlas Copco ABEM.AB after Sjoren 1984).

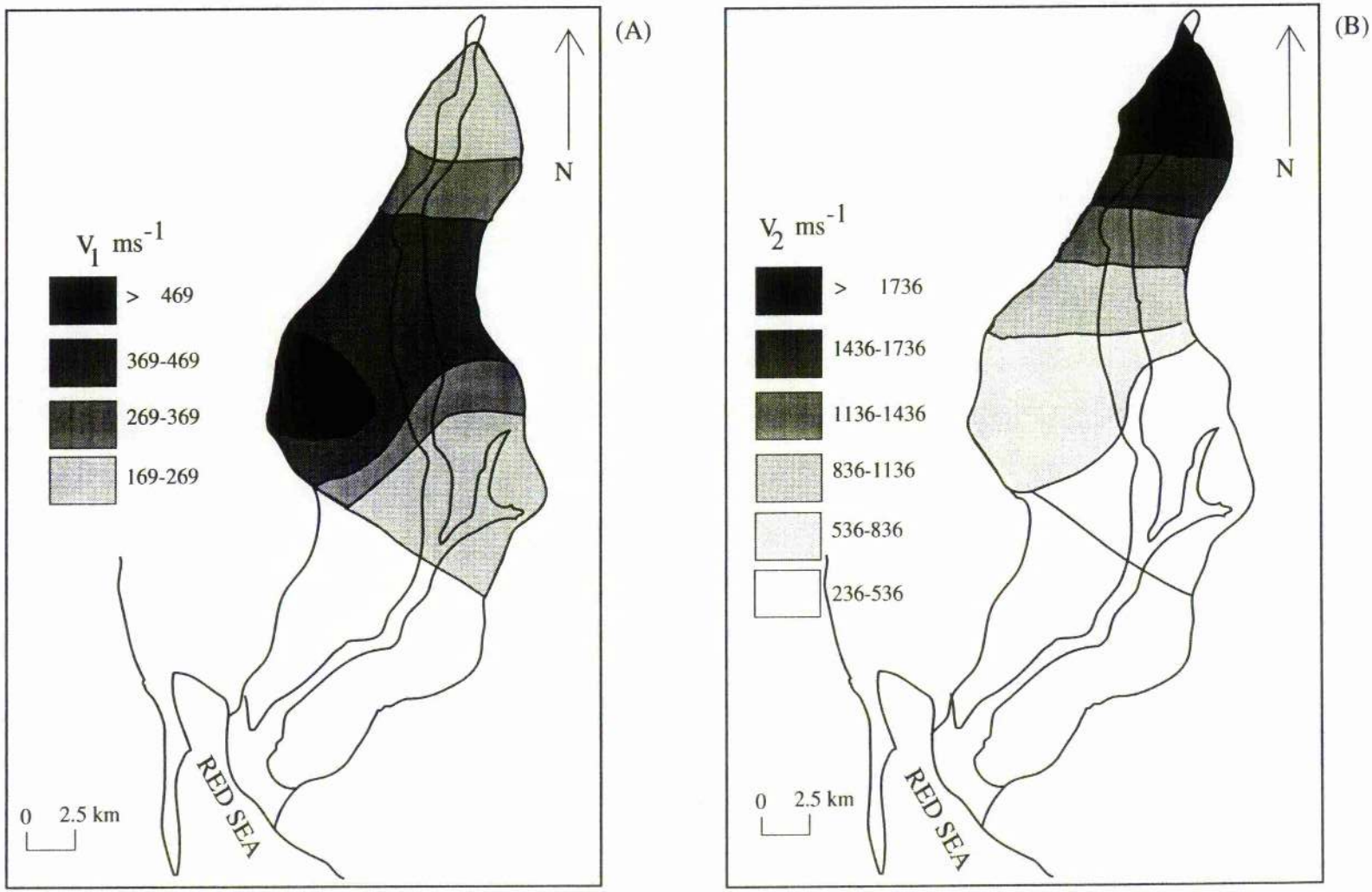

Figure 6.9 Shallow seismic refraction map showing velocities of surface layer (A) and saturated zone (B) in Wadi Baysh.

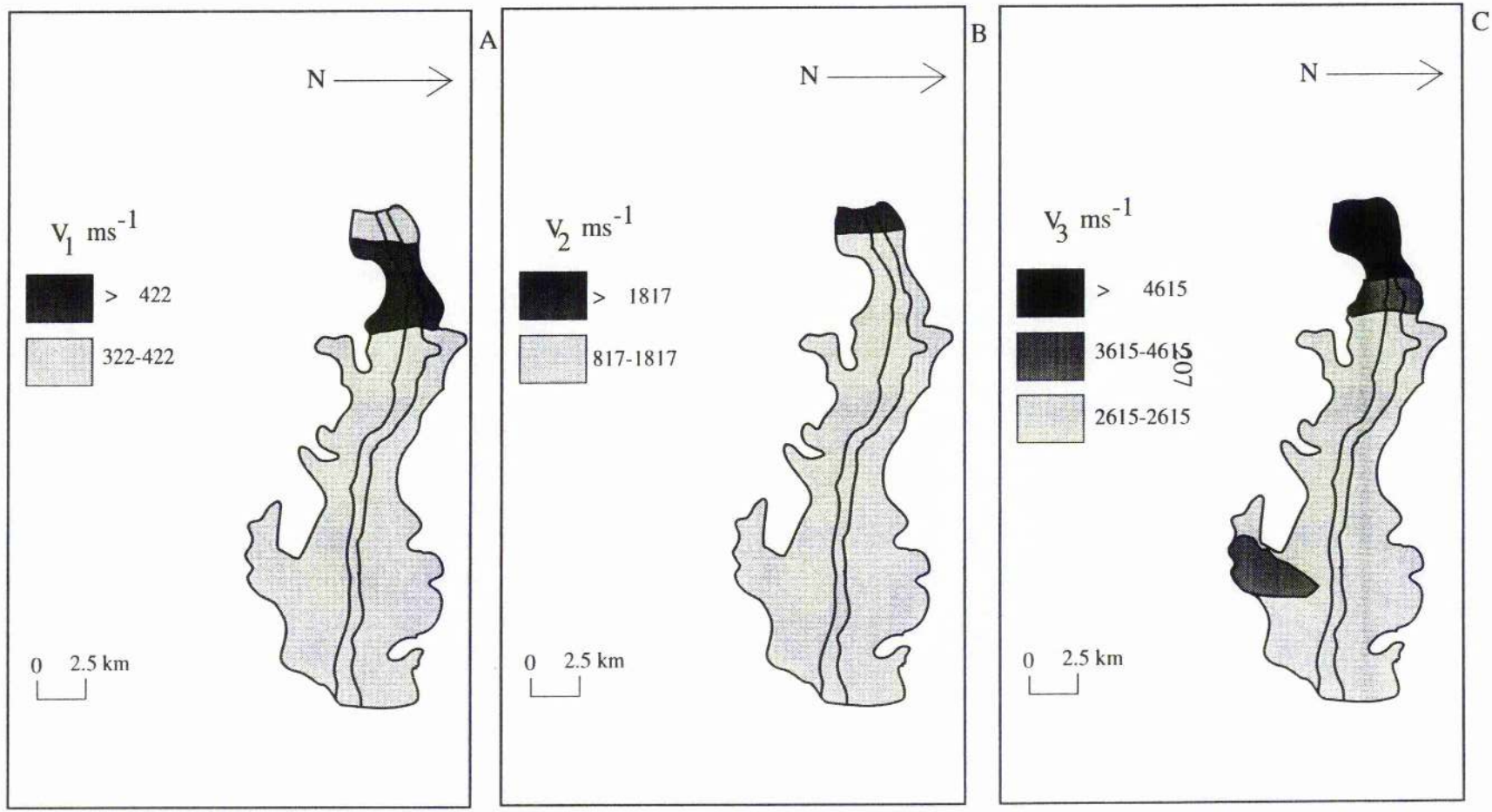

Figure 6.10 Shallow seismic refraction map showing velocities of surface layer (A), and saturated zone (B) and bedrock in Wadi Habawnah.

Figures 6.9a and 6.10a show that the seismic velocity in the near surface layers ranges from 200 to 500 m s^{-1} in Wadi Baysh, while in Habawnah the range was from 300 to 400 m s^{-1}. The water table depth (Figure 6.10b) was detected in most of Wadi Habawnah with seismic refraction method. These seismic refraction velocities range from 200 to 800 = (V_1) m s^{-1}. The saturated zone is detected in the middle part of Wadi Baysh with refraction velocities ranging from 800 to 1700 ms^{-1} (Figure 6.9b). The bedrock in Habawnah shows a seismic velocity (V_3) range from 4000 to 5000 m s^{-1} (see Figure 6.10c). This is characteristic of the granitic and metamorphic bed rocks (Sjogren, 1984) into which the wadi has been cut. However, the bedrock of Wadi Baysh was detected only in the upper part of the wadi with the low velocity of 1800 m s^{-1} which may reflect the weathering bed rocks (see Figure 6.9b).

The depth to the water saturated zone, as determined by seismic refraction measurements (Figures 6.9b and 6.10b), ranges from 5 to 10m in Wadi Habawnah and from 5 to 16m at Wadi Baysh (Tables 6.4 and 6.5). The lower part of wadi floor sediments show variations in thickness between 50 m and 150 m in Wadi Baysh while in Wadi Habawnah the thickness ranges between 28 m and 39m according to the borehole data (see Figures 6.13 and 6.14). The water table elevation of Wadi Baysh shows a variation in elevation between 96m (amsl) in the upper area (10 km north Misliyah) to 36m near Baysh Bridge. In Wadi Habawnah, the water table elevation is about 1250m in the upper area (Habawnah village) to less than 1110m at the wadi outlet.

6.2.7 Structure

The reciprocal slopes of the time-distance lines define apparent seismic velocities. The seismic travel-time graphs show reversed profiles from Wadi Baysh and Wadi Habawnah (Figures 6.11 and 6.12), respectively. They exhibit subsurface structures that influence the seismic velocity and the thickness of the layer (Table 6.10). The reversed profile technique helps to eliminate several possible interpretations.

On the basis of Mooney's catalogue (1977) of expected travel-time graphs for seismic interpretations and also on a geological field study of the area, the author evaluated these measurements in terms of possible subsurface structures as follows:

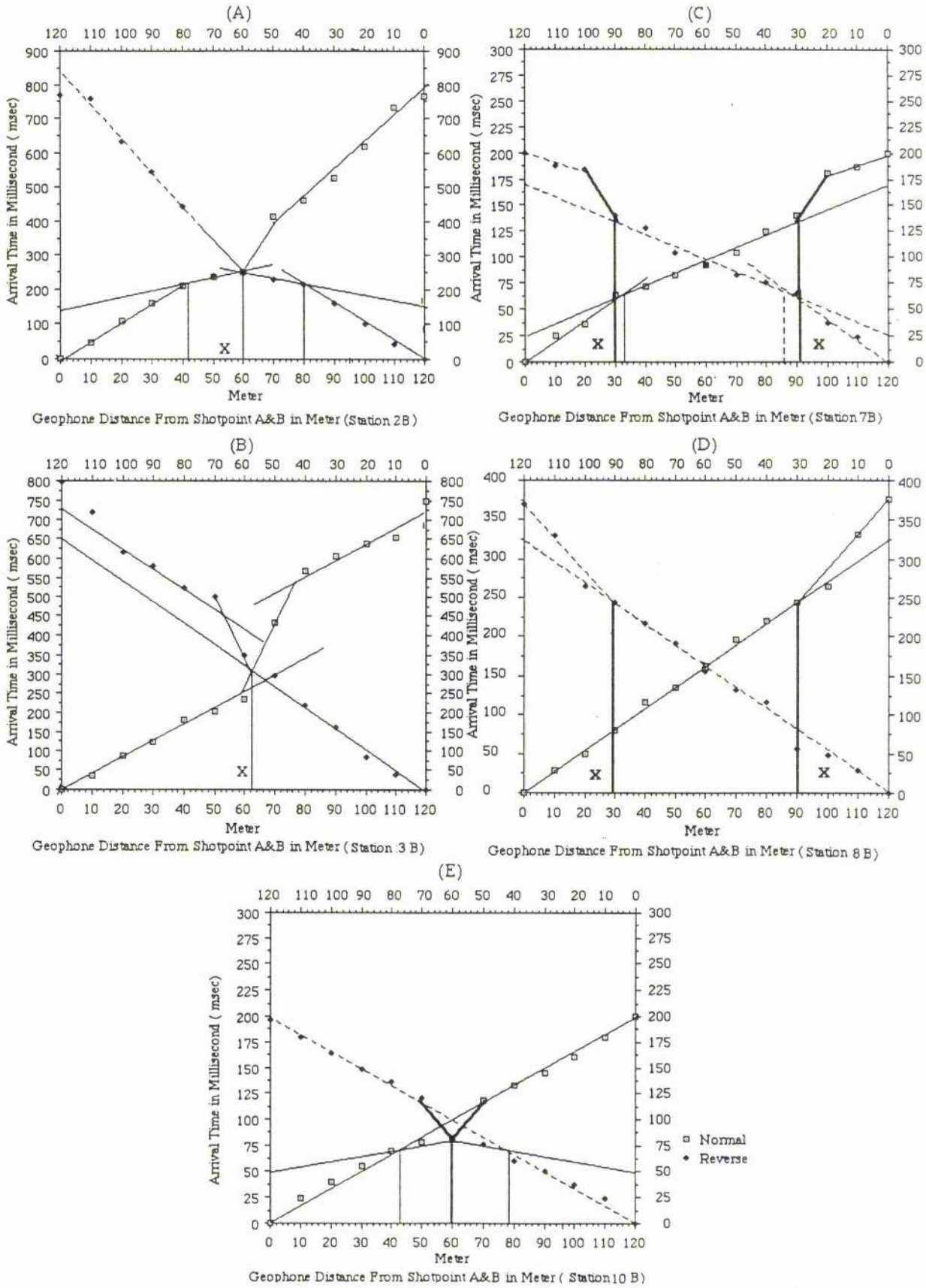

Figure 6.11 Reversed travel-time graph (A, B, C, D, and E) for the dipping layers of Wadi Baysh affected by the subsurface structure.

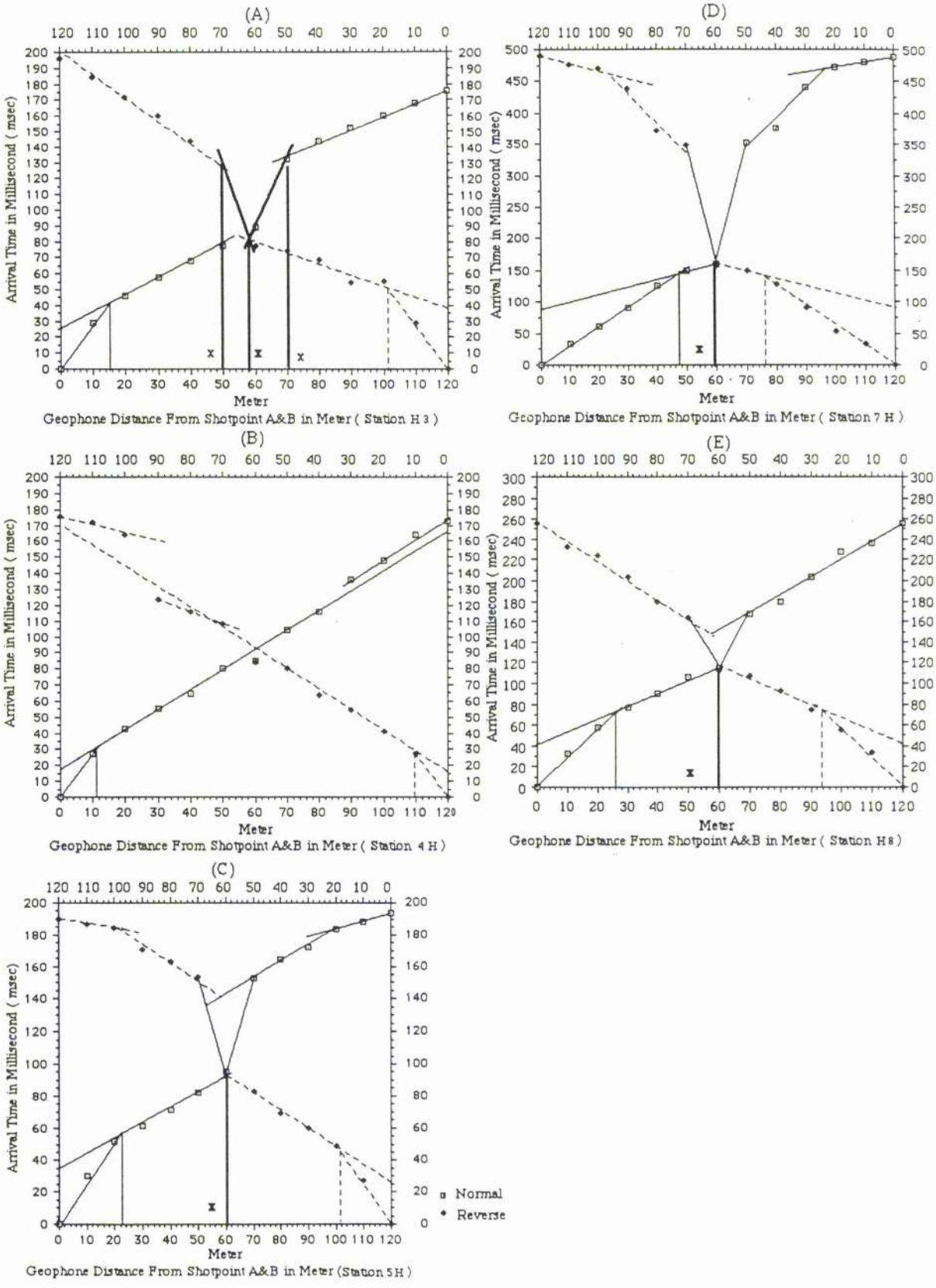

Figure 6.12 Reversed travel-time graph (A, B, C, D, and E) for the dipping layers of Wadi Habawnah affected by the subsurface structure.

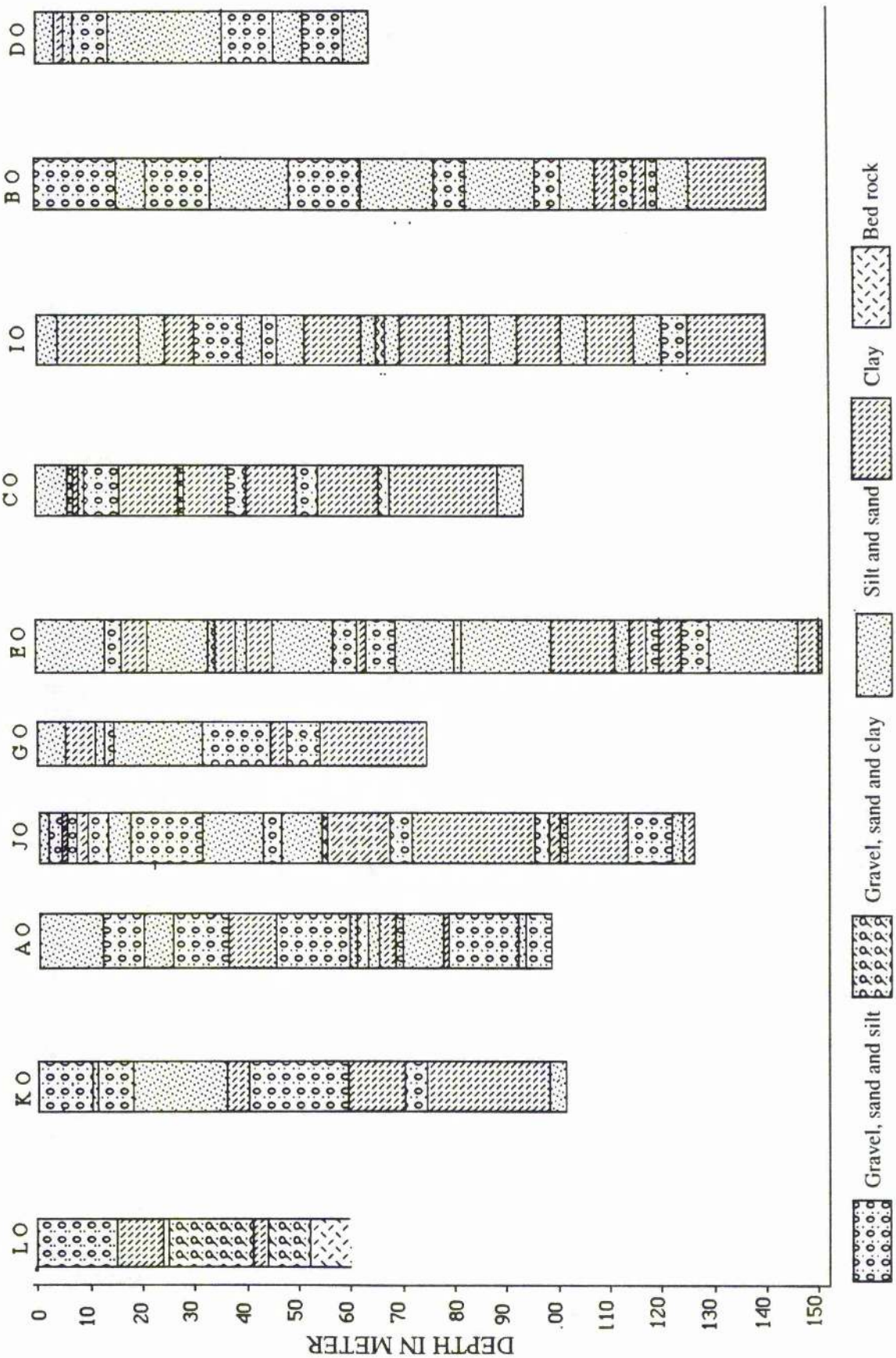

Figure 6.13 The borehole lithology of the lower part of Wadi Baysh.

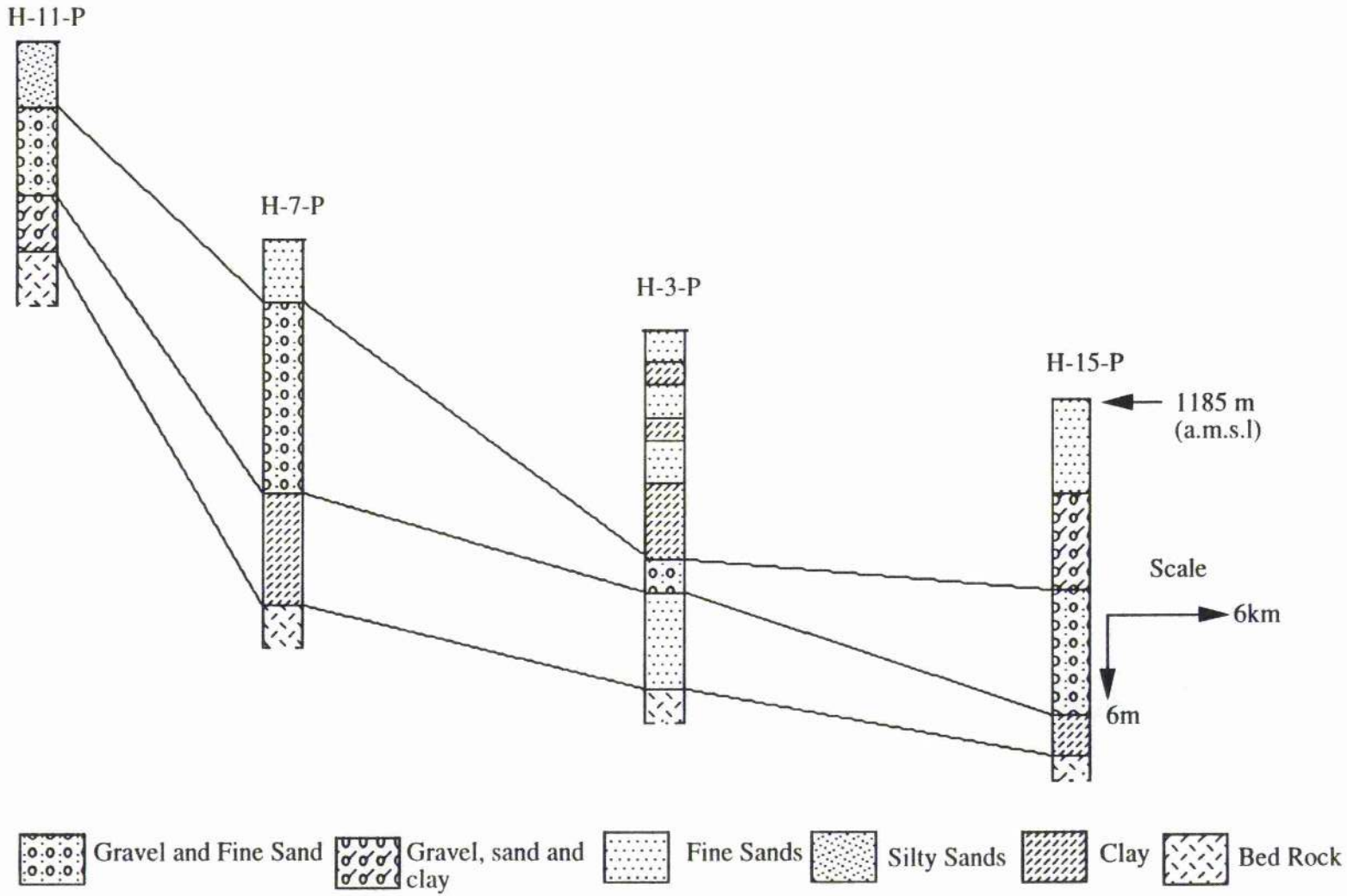

Figure 6.14 The borehole lithology of Wadi Habawnah in which the high (gravel and sand) and the low permeable layer (clay) were determined

Table 6.10 The effect of the subsurface structure on the seismic refraction velocities of some of the seismic stations in Wadi Baysh and Wadi Habawnah

Wadi Baysh

Station No.	$V_{1(n)}$ m s^{-1}	$V_{2(n)}$ m s^{-1}	$V_{2(n)'}$ m s^{-1}	$V_{2(n)''}$ m s^{-1}	$T_{1(n)}$ msec	$X_{1(n)}$ meter	$D_{1(n)}$ CALC	Station No.	$V_{1(r)}$ m s^{-1}	$V_{2(r)}$ m s^{-1}	$V_{2(r)'}$ m s^{-1}	$V_{2(r)''}$ m s^{-1}	$T_{1(r)}$ msec	$X_{1(r)}$ meter	$D_{1(r)}$ CALC
BS2	200	500	150*		148	40	15	B2	200	600	100*		150	43	16
BS3	250	400	350*		70	48	11	B3	200	200*					
BS7	500	750	1050*		25	34	8.5	B7	500	750	1250*		25	34	8
BS8	400	200*						B8	400	250*					
BS10	450	750	400*		50	43	13	B10	600	750	600*		50	41	26

Wadi Habawnah

Station No.	$V_{1(n)}$ m s^{-1}	$V_{2(n)}$ m s^{-1}	$V_{2(n)'}$ m s^{-1}	$V_{2(n)''}$ m s^{-1}	$T_{1(n)}$ msec	$X_{1(n)}$ meter	$D_{1(n)}$ CALC	Station No.	$V_{1(r)}$ m s^{-1}	$V_{2(r)}$ m s^{-1}	$V_{2(r)'}$ m s^{-1}	$V_{2(r)''}$ m s^{-1}	$T_{1(r)}$ msec	$X_{1(r)}$ meter	$D_{1(r)}$ CALC
HS3	350	1000	1200*		25	15	5	H3	400	1600	750*		39	19	7
HS4	400	750			18	11	4	H4	400	900	1250*	1700*	16	11	3
HS5	400	950	950*	2000*	35	23	7	H5	400	1000	3600*		26	19	6
HS7	350	900	250*	1000*	85	47	15	H7	400	1100	250*	1250*	90	43	17
HS8	350	800	600*		40	26	7.5	H8	400	800	600*		41	27	8

$V_{2(f)}$ and $V_{2(r)}$ velocities are affected by subsurface structures
Critical Distance (X_1&X_2)
Intercept Time (T_1&T_2)
The total depth of the first layer (D_1)
* Affected velocities

Graphs A, C and E of Figure 6.11 of Wadi Baysh show similar patterns. Since V2 differs substantially from V2" (see Table 6.10) the most probable interpretation is that profile passes over the down dropped edge of a buried vertical step or fault near position X. It is suggested that the throw of the fault may be large. There is no direct evidence of the trend of this fault, however, there is a suite of faults trending NW-SE locally and this fault might be assumed, parallel to the Red Sea structural trend.

Graph B (Figure 6.13) shows that V1 is equal to V1" in reversed direction and approximately equal to V1" in broken line in the forward direction. The most probable interpretation is that the profile may cross a zone of lower-velocity near -surface material near position X.

Graph D (Figure 6.13) shows V1 > V2 (Table 6.10). This may be explained by suggesting that the seismic profile crosses a vertical contact such as a channel margin near location X.

Graph A, E and D (Figure 6.12) of Wadi Habawnah, shows V2 > V2" in reverse profile while A and D show V2 < V2" in the forward profile (see Table 6.10). This may show the effect of buried vertical dyke on the seismic velocity.

Graph B (Figure 6.12) show a scatter of data points in the graph. This graph may reflect the effect of the boulder rich alluvial overburden on the seismic measurements.

6.2.8 Summary and Discussion

The deposits of Wadi Habawnah and the uppermost layer of Wadi Baysh are believed to be of Quaternary age (Brown, 1966). They can be traced continuously from local wells, boreholes and also by seismic refraction survey. The seismic velocity is characteristic of an unconsolidated dry overburden above the water table and bedrock. Well lithology near the profile indicates that this material is predominantly interbeded gravel, silt and medium to coarse sand. Thin lenses of calcareous sand were noticed in Wadi Habawnah (Al Montasher) see Chapter 8. The computed thickness of the Quaternary deposits examined ranged from 3.5 to 150 m in Wadi Baysh and from 4 to 50 m in Wadi Habawnah (see Figures 6.13 and 6.14) according to the borehole data.

The refraction surveys in both wadis show that the unconsolidated surface sediment (alluvium) is characterised by low seismic velocities (200 to 600 m s^{-1}). This is due to the

fact that low density material has a low P-wave velocity, this may be a direct indication of high total porosity and potential water storage capacity and could be a useful guide to unconsolidated aquifers. The uppermost layer, 80% of the total area of both wadis, shows a low seismic velocity. It is difficult to show a strong correlation between seismic velocity and aquifer parameters such as permeability. The velocity and permeability depend on different properties of the pore spaces. Rubin *et al.* (1992) indicates that seismic velocity in a fluid-saturated rock depends on the compliance (ratio of the pore strain to the applied stress) of the pore space and on the compressibility of the pore fluid. However, the permeability depends on pore size, conductivity and tortuousity. In spite of the influence of different parameters on the seismic velocity and permeability variables, seismic refraction surveys may give useful primary information about the aquifer. The local shallow structure may be predicted using seismic refraction techniques. The data point distribution reflects the influence of the subsurface structure. The change in the seismic velocity while the sediment thickness of the layer is the same (reverse profile) may reflect the dips of the interface. The change in the seismic refraction velocity and the thickness may indicate that the bedrock topography is highly irregular.

6.2.9 Conclusion

The seismic refraction study shows that in both wadis the aquifers consist of three main zones; unsaturated zone, saturated zone, and bedrock. The unsaturated zone thickness varied between 3 to 29 m with P-Wave velocities ranging between 200 and 600 m s^{-1}. The saturated thicknesses varied between 3 and 30 meters in Wadi Habawnah and in the upper -middle parts of Wadi Baysh while in the lower part it was not determined. The lower aquifer boundaries of Wadi Habawnah and the upper and middle part of Wadi Baysh were defined as a contact with igneous and metamorphic rocks with seismic velocity ranges between 3400 and 9000 m s^{-1}.

6.3 Section Two: Groundwater Investigation of Wadi Foor Sediments Using Schlumberger Resistivity Sounding

6.3.1 Introduction

Aquifer electrical resistivities were determined for 16 and 14 vertical electrical soundings (VES) in Wadi Baysh and Wadi Habawnah respectively (Figures 6.1 and 6.2). Resistivities for the different aquifer materials, water depth and bedrock were determined with boreholes and dug wells providing lithological control. Data used in this study were collected principally during two geophysical studies in December 1989 and February 1990. Agricultural development of Wadis Baysh and Habawnah has resulted in the drilling of many water wells, from which some data were available. Depth to ground water increases eastwards in Wadi Habawnah and southwestwards in Wadi Baysh. The study used combined information from these sources to refine understanding of the ground water flow system.

6.3.2 Data Sources

Sources for data used in this study consist of Schlumberger's vertical electrical resistivity sounding, detailed lithology of the boreholes, hand dug wells, and water quality formation. The sites of eighteen pumping test dug wells and two observation wells of MAWR are shown in Figures 6.15 and 6.16. The wadi deposits of the upper, middle and lower parts of Wadi Baysh and Wadi Habawnah were selected for lithological comparison and resistivty interpretation as follows:

Wadi Baysh: the upper part (3 wells); the middle part (3 wells) the lower part (2 wells)

Wadi Habawnah: the upper part (3 wells); the middle part (6 wells); the lower part (3 wells).

The VES station numbering system used in this chapter indicates the location of the station with the region and the name of the wadi with a number. The first two letters designate the region as TR for the Tehamah Region or AR the Asir Region then the second two letters which indicate the wadi names as (WB) Wadi Baysh and (WH) Wadi Habawnah. The letter N with a number indicates the sequences in a number of wells.

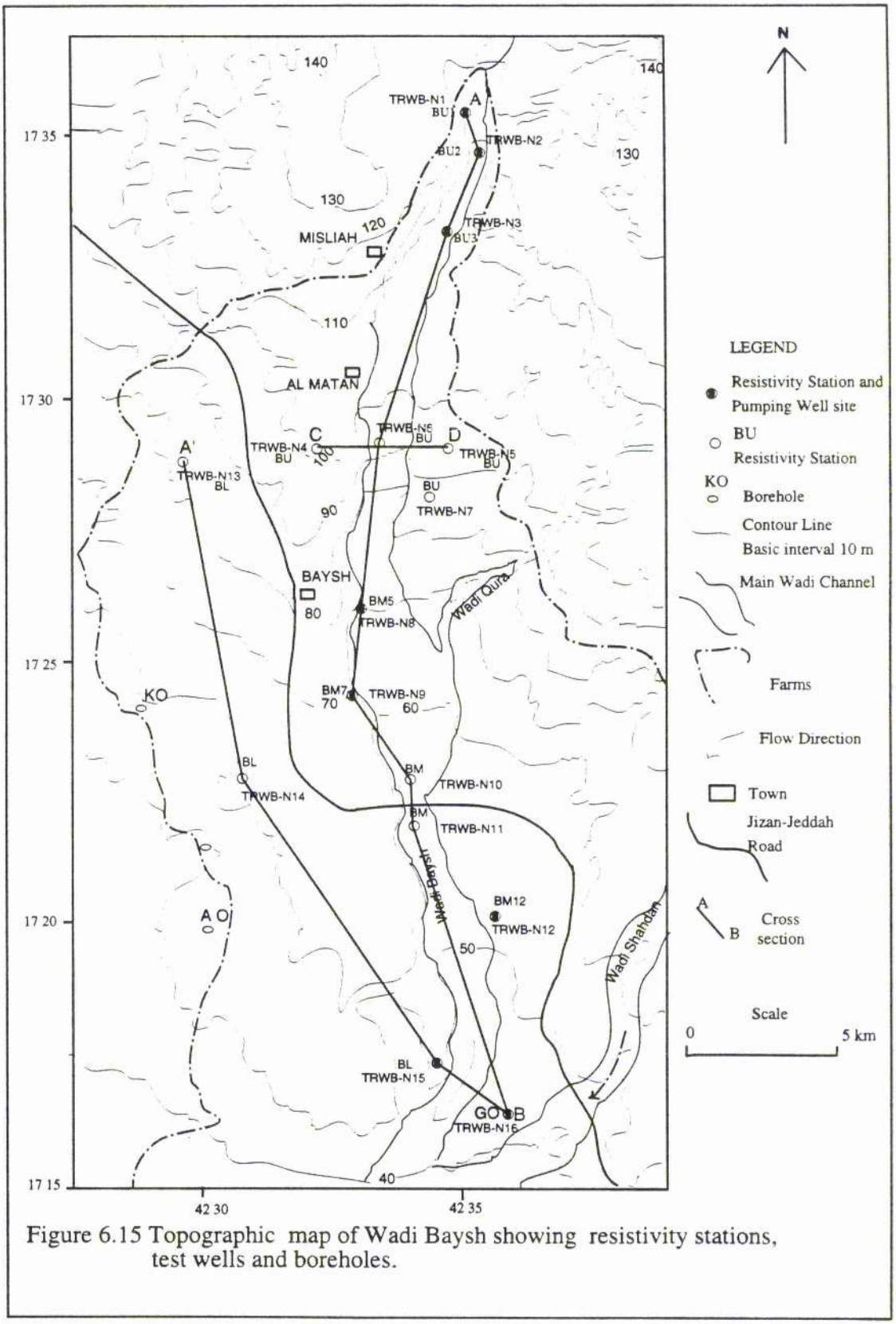

Figure 6.15 Topographic map of Wadi Baysh showing resistivity stations, test wells and boreholes.

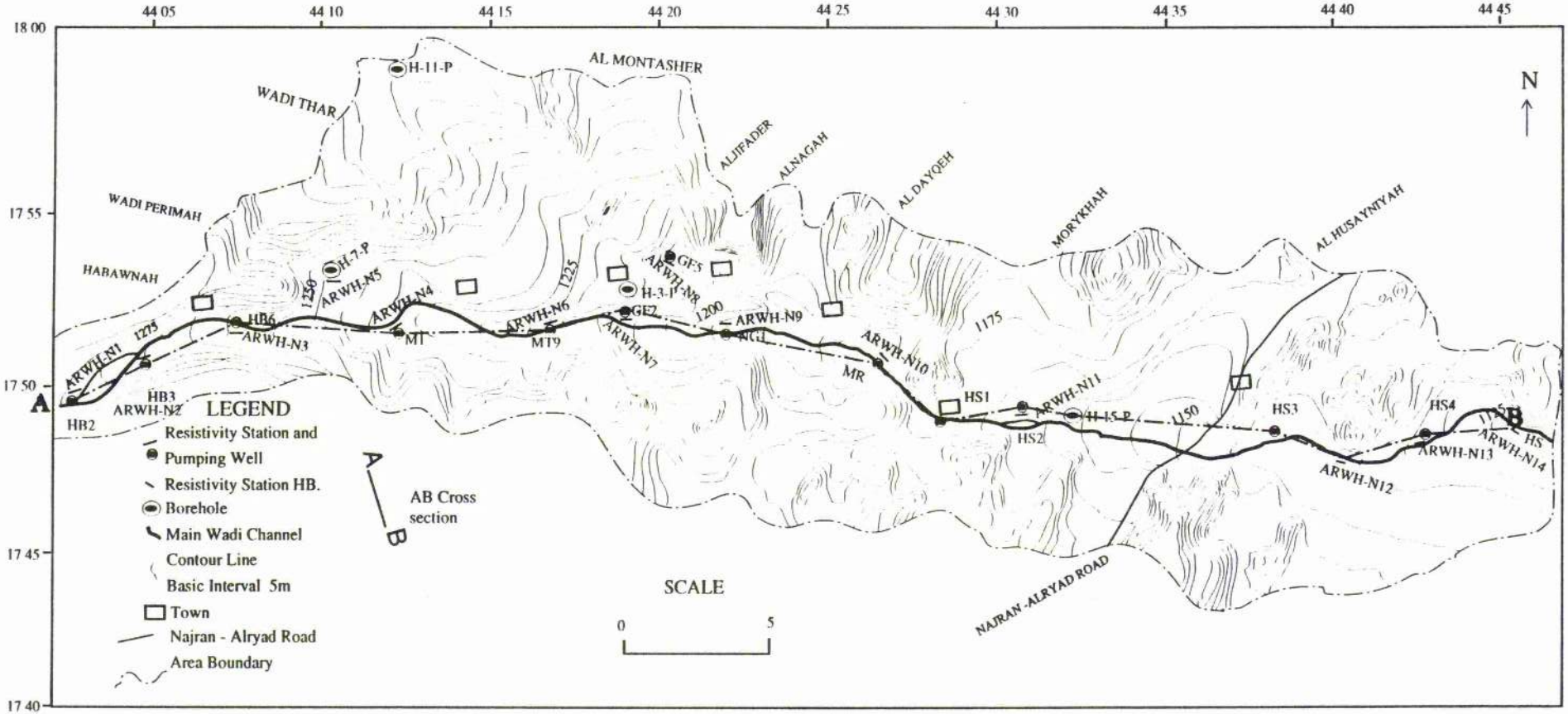

Figure 6.16 Topographic map of Wadi Habawnah showing resistivity stations, test wells and boreholes.

6.3.3 Definition and Method

The electrical resistance, R, of a material is well known and is directly proportional to the length L, and inversely proportional to its cross-sectional area, A. That is:

$$R \alpha \frac{L}{A} \quad \text{or} \quad R = \rho \frac{L}{A} \tag{6.7}$$

The constant of proportionality (ρ) is known as the electrical resistivity of that material. It can be seen that electrical resistivity is a characteristic of the material and is independent of its shape or size. According to Ohm's Law, the resistance of a material can be given by

$$R = \frac{\Delta V}{I} \tag{6.8}$$

where ΔV is the potential difference across the material and I is the electric current through the material. Substituting equation 6.7 in equation 6.8 and rearranging, gives

$$\rho = (\frac{A}{L}) \times (\frac{\Delta V}{I}) \tag{6.9}$$

Equation 6.9 may be used to determine the resistivity (ρ) of homogeneous and isotropic materials having unit cross-sectional areas and lengths.

The units of resistivity are ohm-m.

6.3.4 DC Electrical Resistivity

The DC electrical resistivity is one of the most widely used surface methods for measuring earth resistivity. In this method, a direct current from a dry battery is introduced into the ground through two current electrodes (A and B). Two other electrodes (M and N) are used to measure the potential differences caused by the introduced direct current into the earth. Therefore, four electrodes are used to perform a resistivity measurement.

There are many electrode configurations which can be used to perform vertical electrical sounding and constant separation traversing (Keller, 1966). The Schlumberger, Wenner, and Dipole are the three most commonly used electrode configurations (Figure 6.17).

The vertical sounding survey is carried out by increasing the electrode spacing gradually after each measurement in order to study resistivity variations with depth. The

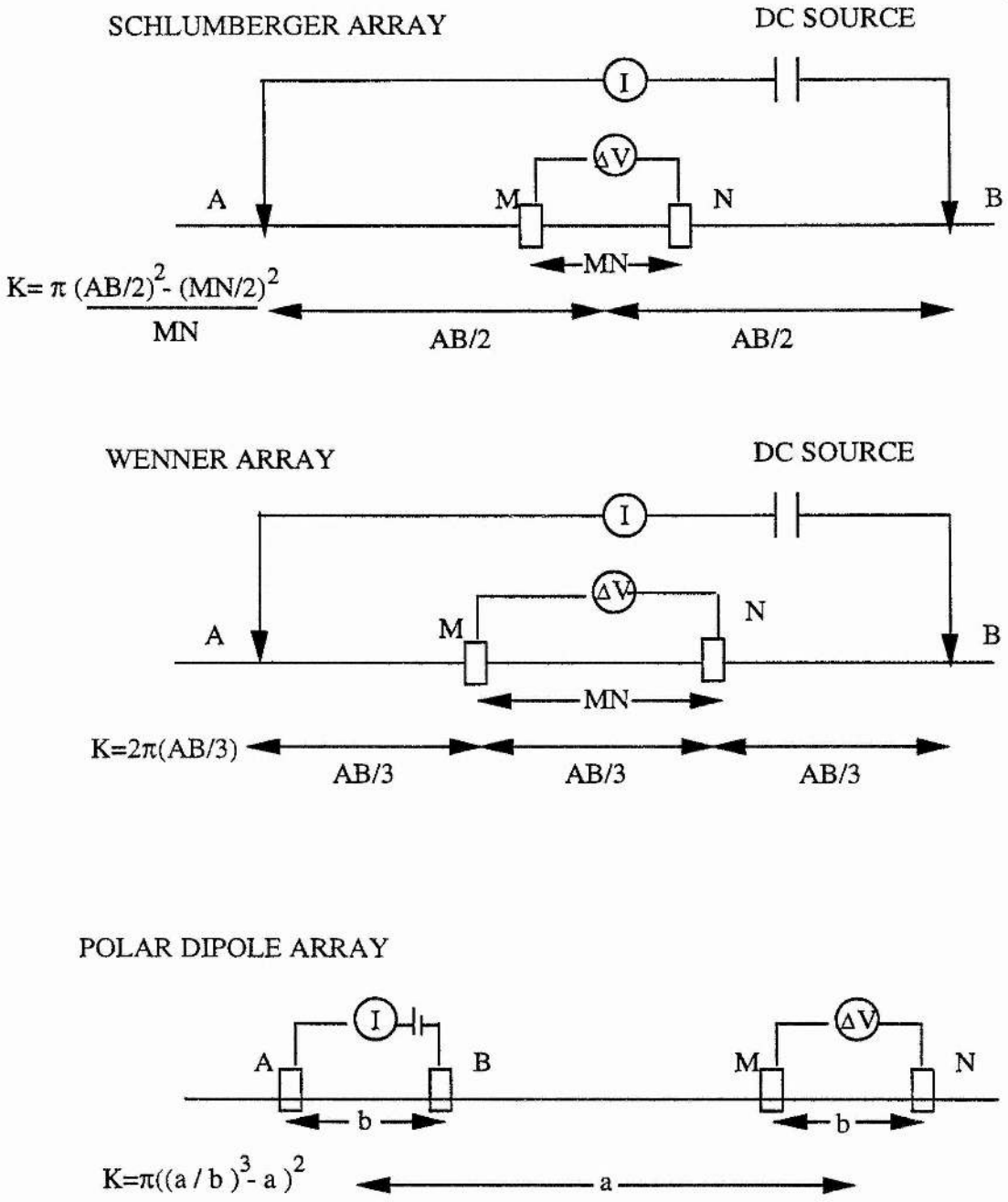

Figure 6.17 Types of electrode arrays most commonly used in DC resistivity survey.

Schlumberger configuration of electrode layout was used for the vertical electrical sounding (VES) in the study area. The configuration has the following advantages:

1- It is less sensitive to unknown lateral inhomogeneities because the potential electrodes (M and N) are changed after a number of changes the positions of A and B (the current electrodes) (Figure 6.17) and it is a relatively rapid method.

2- The analytical-graphical method of construction of empirical curves is applicable in the case of the Schlumberger method.

3- The technique of partial curve matching is possible with sufficient accuracy.

4- The introduction of personal error in this method is small since only two electrodes are changed at a time.

6.3.5 The DC Resistivity Equipment

The DC resistivity equipment is made light and simple, so that two people can handle a resistivity survey. The equipment mainly consists mainly of a dry battery as a direct current source, a potentiometer to measure voltage across the potential electrodes, four reels of insulated wire, and measuring tape.

6.3.6 Principles of the Resistivity Method

A resistivity survey is based on the study of subsurface resistivity. The method assumes that a direct current of strength, I, (low frequency current, i.e. <1Hz) flows into a homogeneous and isotropic earth by means of two electrodes, denoted A and B. The potential difference is measured between the two other electrodes, denoted M and N, (see Figure 6.17).

The potential difference between the two points M and N on the surface is commonly given using the equation below:

$$\Delta V = \frac{I\rho}{2\pi}\left\{\left(\frac{1}{AM}-\frac{1}{BM}\right)-\left(\frac{1}{AN}-\frac{1}{BN}\right)\right\} \qquad (6.10)$$

where ρ is the resistivity of the ground. Thus, the resistivity of the homogenous earth can be determined from the measurements on the surface. So the resistivity can be calculated

from the current, potential differences, and electrode configuration measurements by the following equation:

$$\rho = \frac{2\pi}{\left(\frac{1}{AM}\right)-\left(\frac{1}{BM}\right)-\left(\frac{1}{AN}\right)+\left(\frac{1}{BN}\right)} x \frac{\Delta V}{I} \qquad (6.11)$$

$$\text{The factor} = \frac{2\pi}{\left(\frac{1}{AM}\right)-\left(\frac{1}{BM}\right)-\left(\frac{1}{AN}\right)+\left(\frac{1}{BN}\right)} = \pi\left(\frac{AB}{2}\right)^2 - \left(\frac{MN}{2}\right)^2 \qquad (6.12)$$

is usually called the geometric factor of the electrode arrangement and is commonly given the variable name K. It is shown to be dependent only upon the spacing (or configuration) of the current and potential electrodes (AM, AN, BM, and BN). So the above equation can be reduced to

$$\rho = K\left(\frac{\Delta V}{I}\right) \qquad (6.13)$$

Using the above equation, the resistivity value ρ, is the true resistivity assuming that the measurements are made for a homogeneous and isotropic material. Mooney *et al.* (1966) explained that for the non-homogeneous case, the apparent resistivity ρ_a may be defined as the resistivity of an equivalent homogeneous medium in which the same current I, would produce the same potential drop, ΔV. Since the geological formations of both wadis are characterised by having several layers of non-homogeneous and/or anisotropic material, the resistivity measured is an apparent resistivity (ρ_a). Zohdy *et al.* (1969b) indicated that the apparent resistivity is a function of : (1) the electrode spacing, (2) the geometry of the electrode array, (3) the true resisivity of the subsurface material, and (4) the factors such as layer thickness, angles of dip etc. The apparent resistivity may be larger than, smaller than or equal to the true value.

In carrying out resistivity sounding measurements, equation 6.13 is used to calculate the apparent resistivity values, ρ_a.

6.3.7 Field Procedures (VES)

An ABEM SAS 300 Terrameter instrument was used to perform a total of 30 sets of VES measurements in both wadis (Figure 6.18). There is a compensating device designed in the instrument to eliminate the background noise from power lines and industrial plant.

The electrodes are set in a straight line in the surface of the ground. This arrangement is shown schematically in Figure 6.19. Current flows in an arc-like pattern between the current electrodes creating a hemispherical equipotential surface assuming the subsurface material is uniform. As the current electrodes are moved apart, the current penetrates deeper into the ground (deviation from uniform ground conditions will distort the pattern of current flow).

Voltage and current are measured directly and resistance of the material is computed. The sounding locations were chosen along the main wadi axis, to minimise the effect of the lateral variation of the sediments on the VES measurements. From results of the seismic surveys above it may be assumed that the geological structure can be approximated by layers which are horizontal or nearly so along the main axis of the wadi channels. All the electric soundings were carried out from 1.5 m up to 130 m AB/2 electrode spacing. All of these soundings were parallel and along or close to the wadi channel. This permits tracing of the thicker part of the sediments but it is also the easy way to spread out the electrodes.

The following electrode spacings were arranged for the electric sounding according to complete measurement test at ARWH-N10.

MN = 0.5 m for $AB/2$ = 1.5, 3, 5, 9, 15 m

MN = 5.0 m for $AB/2$ = 15, 20, 25, 30, 37.5, 45 m

MN = 10 m for $AB/2$ = 45, 60, 75, 90, 105, 120, 130 m

There is a common $AB/2$ spacing at each single change of the potential electrode spacing, MN (Appendix 6C). The Schlumberger array is designed to measure approximately the potential gradient or electric field using closely spaced electrodes. However, the potential gradient or electric field is an infinitesimal amount which is beyond the potential accuracy of the instrument. In consequence, the potential gradient is defined as

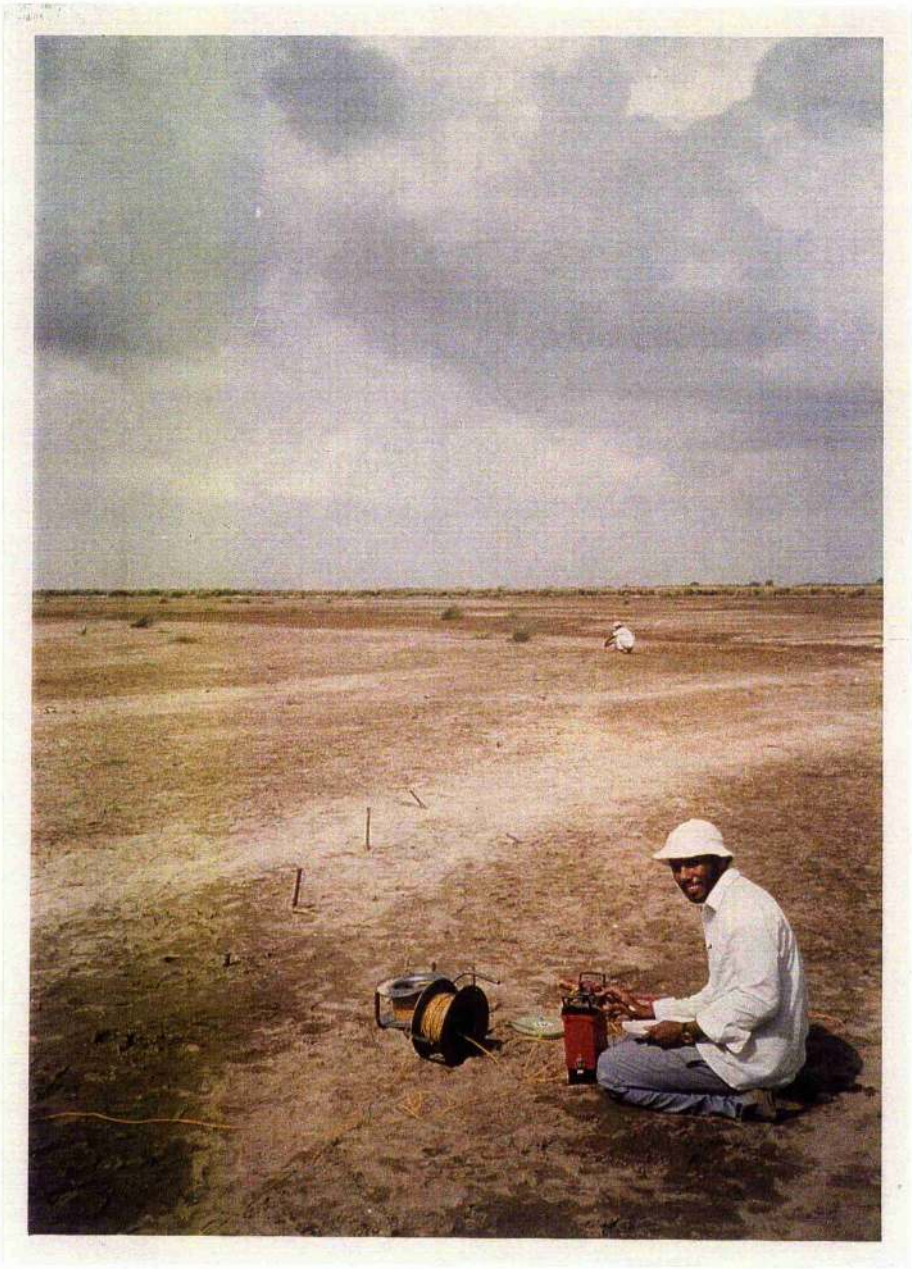

Figure 6.18 Field use of resistivity equipment showing the control unit and electrodes set up the along a traverse in the lower part of Wadi Baysh.

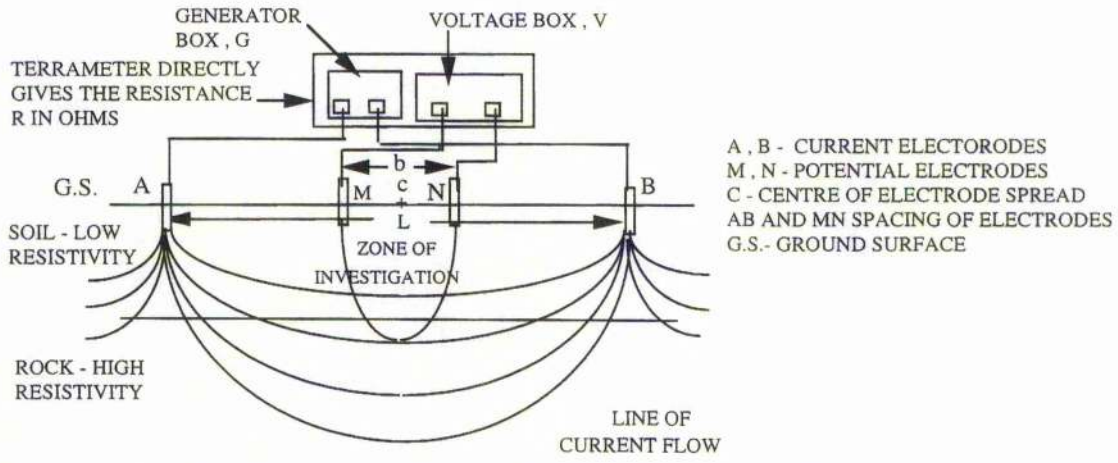

Figure 6.19 Current and potential electrodes for the Schlumberger configuration during resistivity measurement.

the voltage measured with two electrodes at an infinitesimal spacing. This is the reason for increasing the spacing of the MN measuring electrodes occasionally to maintain sufficient voltage.

6.3.8 Resix Program Interpretations

Resix is a forward and inverse modelling program for DC resistivity data interpretation. It was written by Interpex Limited, USA, in 1990. This program is used in this study for interpreting resistivity sounding data in terms of a layered earth model. The sounding curves are entered as a function of $AB/_2$ for Schlumberger soundings.

Resistivity estimates can be derived directly from the apparent resistivities, with some extrapolation necessary at the shortest and longest spacing. Since the author desired to construct the model manually, the observed data were entered, and then checked for correctness. The interactive graphics mode was then entered using the 'interpret' command, and a two layer model chosen which nearly fits the sounding data at small values of spacing. Resistivity estimates can be determined directly from the apparent resistivities, with some extrapolation necessary at the shortest and longest spacings.

Depths can be derived from the spacing at the midpoint between wings in the curves by multiplying by a constant factor (0.5 for Schlumberger soundings) (Interpex Limited, 1990). The substratum (lower layer) was divided into two layers and resistivities entered that best define the intermediate part of the sounding. Finally, the depth and physical properties of the substrata were adjusted to better define the sounding curve at maximum spacing. The process is interactive. The layer depths and physical properties were moved slightly over several iterations to get an acceptable fit, in which the field data match with the theoretical curve.

6.3.8.1 Example of Interpretation

The general features of many sounding curves in both wadis are explained with a 3 and 4 layer model. For example, Table 6.11 and Figure 6.20 show observed resistivity data from site ARWH-N1. The field data are displayed on the screen, after using the INTERPRET command to enter the interactive graphics mode.

Table 6.11 Resistivity interpretation of station ARWH-N1 using the Resix program

DATA SET: ARWH-N1

CLIENT: KING ABDULAZIZ UNIVERSITY DATE: JAN. 1990
LOCATION: WADI HABAWNAH SOUNDING: V.E.S
COUNTY: ASIR REGION AZIMUTH: E-W
PROJECT: Ph.D THISES S.BAJABAA EQUIPMENT: TERRAM SAS30
ELEVATION: 1280.00
SOUNDING COORDINATES: X: 1.0000 Y: 1.0000

Schlumberger Configuration

FITTING ERROR: 2.873 PERCENT

L #	RESISTIVITY (ohm-m)	THICKNESS (meters)	ELEVATION (meters)	LONG. COND. (Siemens)	TRANS. RES. (Ohm-m^2)
			1280.0		
1	1267.9	4.03	1275.9	0.00318	5119.2
2	1129.3	4.11	1271.8	0.00364	4642.9
3	54.36	7.07	1264.7	0.130	384.5
4	8925.8				

ALL PARAMETERS ARE FREE

No.	SPACING (m)	RHO-A (ohm-m) DATA	SYNTHETIC	DIFFERENCE (percent)
1	1.50	1260.0	1271.2	-0.892
2	3.00	1263.0	1256.1	0.543
3	5.00	1227.0	1204.7	1.81
4	9.00	986.0	1008.3	-2.26
5	15.00	650.0	656.5	-1.00
6	15.00	647.0	653.4	-1.00
7	20.00	468.0	445.4	4.82
8	25.00	327.0	332.9	-1.82
9	30.00	287.0	288.2	-0.431
10	37.50	289.0	288.5	0.158
11	45.00	310.0	322.9	-4.16
12	45.00	310.0	322.9	-4.16
13	60.00	420.0	416.7	0.768
14	75.00	530.0	514.6	2.90
15	90.00	650.0	610.9	6.00

PARAMETER RESOLUTION MATRIX:
"F" INDICATES FIXED PARAMETER

* Dept. of Geography and Geology *

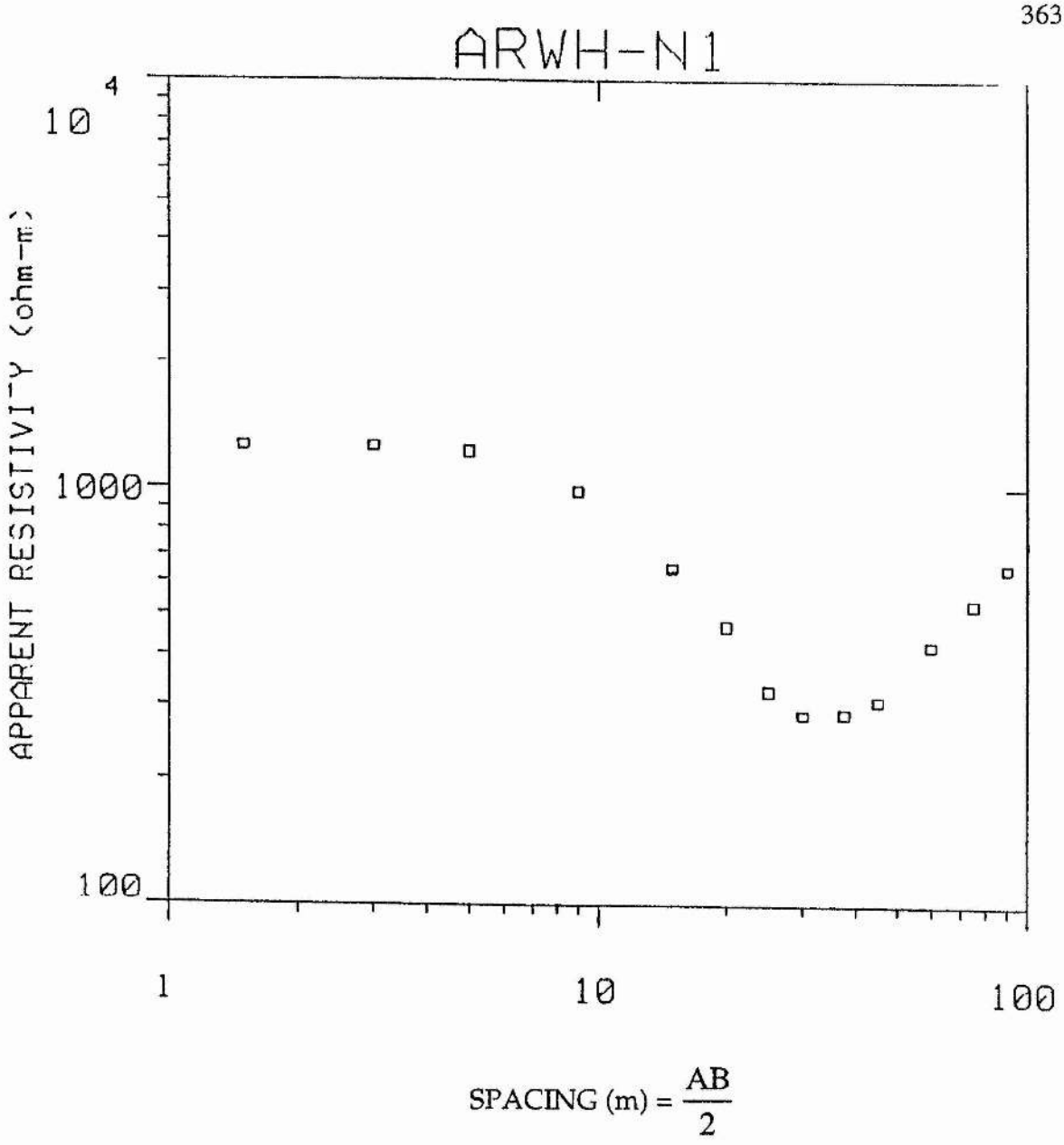

Figure 6.20 VES resistivity curve plots of station ARWH-N1 using the Resix Program.

The sounding curve shows a four layer sequence. The author begins by estimating that the first layer resistivity is about 1300 ohm-m, the second layer is 1100, and the thickness is about 4 m (one half of $AB/_2 = 9$). Then forward calculations are performed and the result is shown in Figure 6.21.

The next layer is added and the third layer resistivity is estimated as 54 ohm-m, and the depth to the top of third layer of 8m (one half of $AB/_2 = 15$ m). This change is to carry out the forward calculation. The results are shown in Figure 6.22. This provides a good fit to the first half of the sounding curve. Next, a conductor layer is added for the low apparent resistivity near $AB/_2 = 30$m. The resistivity of layer 4 is estimated to be 8000 ohm-m. The forward calculation shows the display in Figure 6.23, where the interactive graphics screen indicate a 4 layer model.

In a final stage, the program is used to perform one full analysis to test the model for adjustments. The results of this run are shown in Table 6.11 and Figure 6.20. The curves displayed during the first part of the interaction show the sensitivity of the sounding curve to each parameter, the resistivity and the thickness of each layer. The fitting error has been reduced by about a factor of 4, from 12 to 3%.

All of the VES data have been interpreted using the Resix computer program. From a hydrological point of view, the interpretations have been correlated with the lithological data from nearby test wells. The agreement between the VES field data, the theoretical curves and the lithological succession of the wells can be considered satisfactory for almost all the test sites. In Tables 6.11, 6.12 and 6.13 the output of the VES interpretations are shown as are the resistivities, thicknesses and the theoretical curves corresponding to these successions (see Appendices 6D and 6E).

6.3.9 Wadi Baysh

6.3.9.1 Soundings of the Upper Part of Wadi Baysh

The first three electrical soundings, TRWB-N1, TRWB-N2 and TRWB-N3 (Figure 6.24), were made near wells BU1, BU2 and BU3 respectively (Table 6.12) where the depth to the fresh water averages 6 m, (Table 6.13). The depth to the water table was 4 m

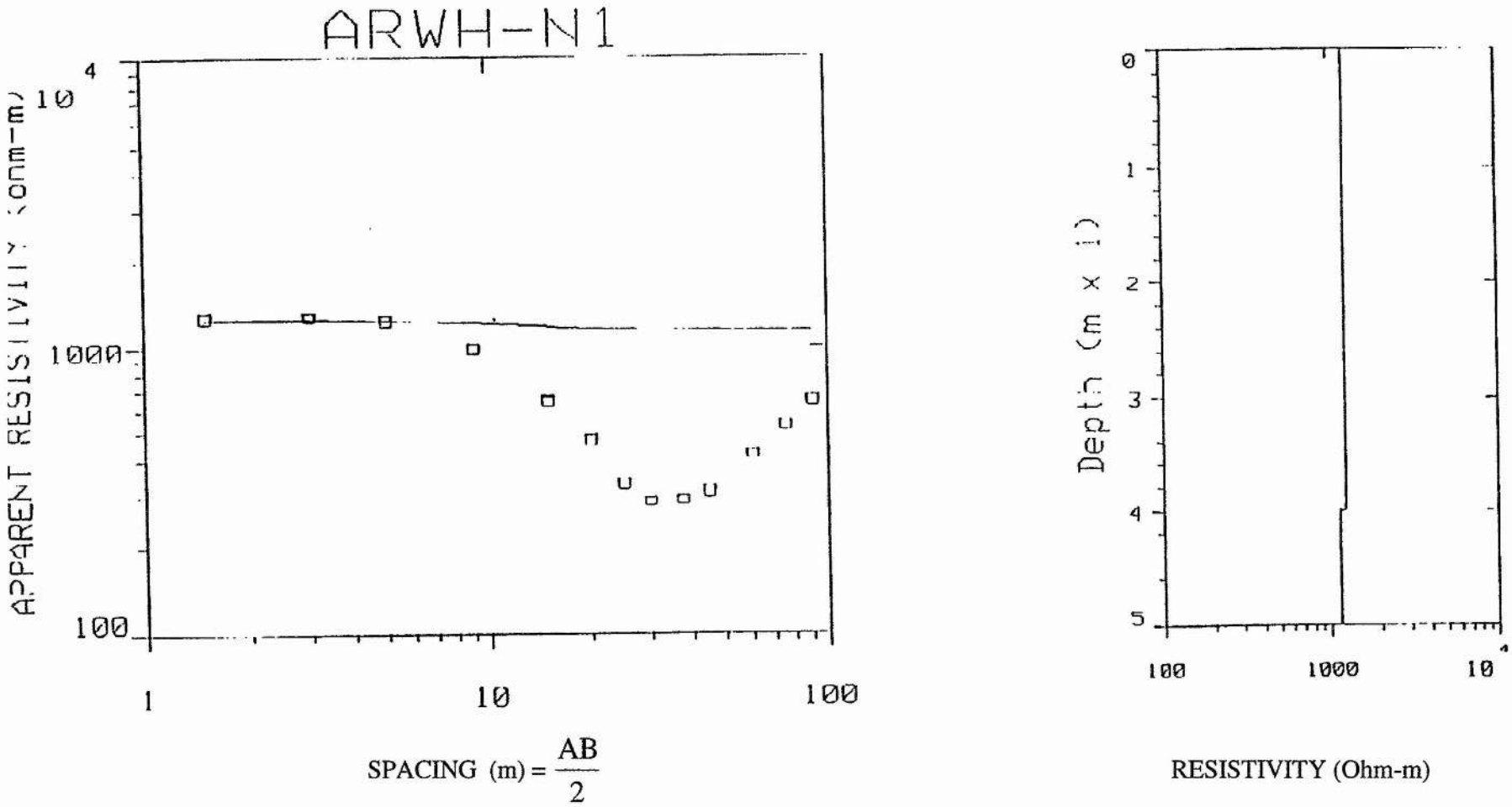

Figure 6.21 VES resistivity curve plots of station ARWH-N1 using resix program to determine the thikness and resistivity of the surface layer.

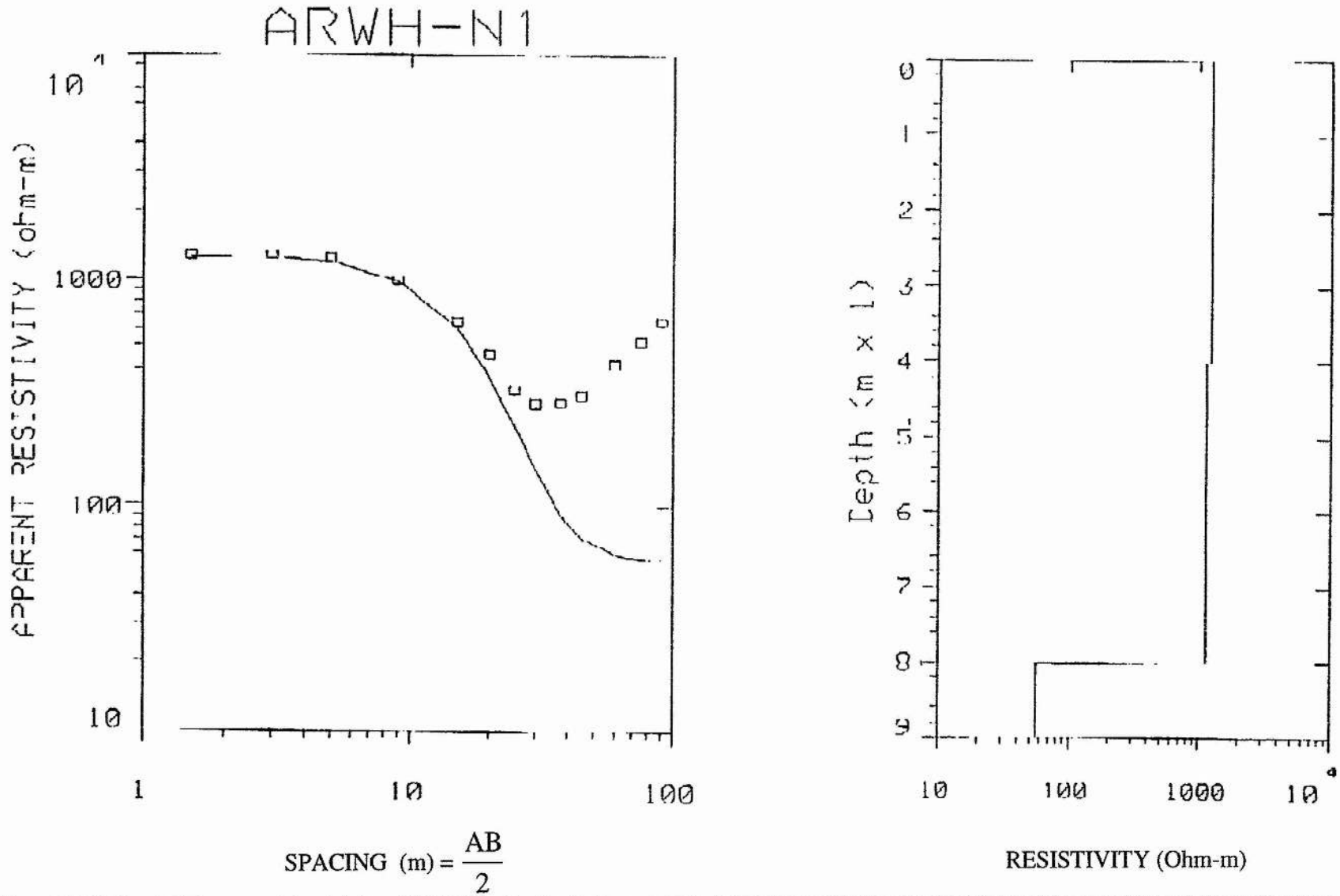

Figure 6.22 VES resistivity curve plots of station ARWH-N1 using the Resix program to determine the thickness and resistivity of the second layer to the surface layer.

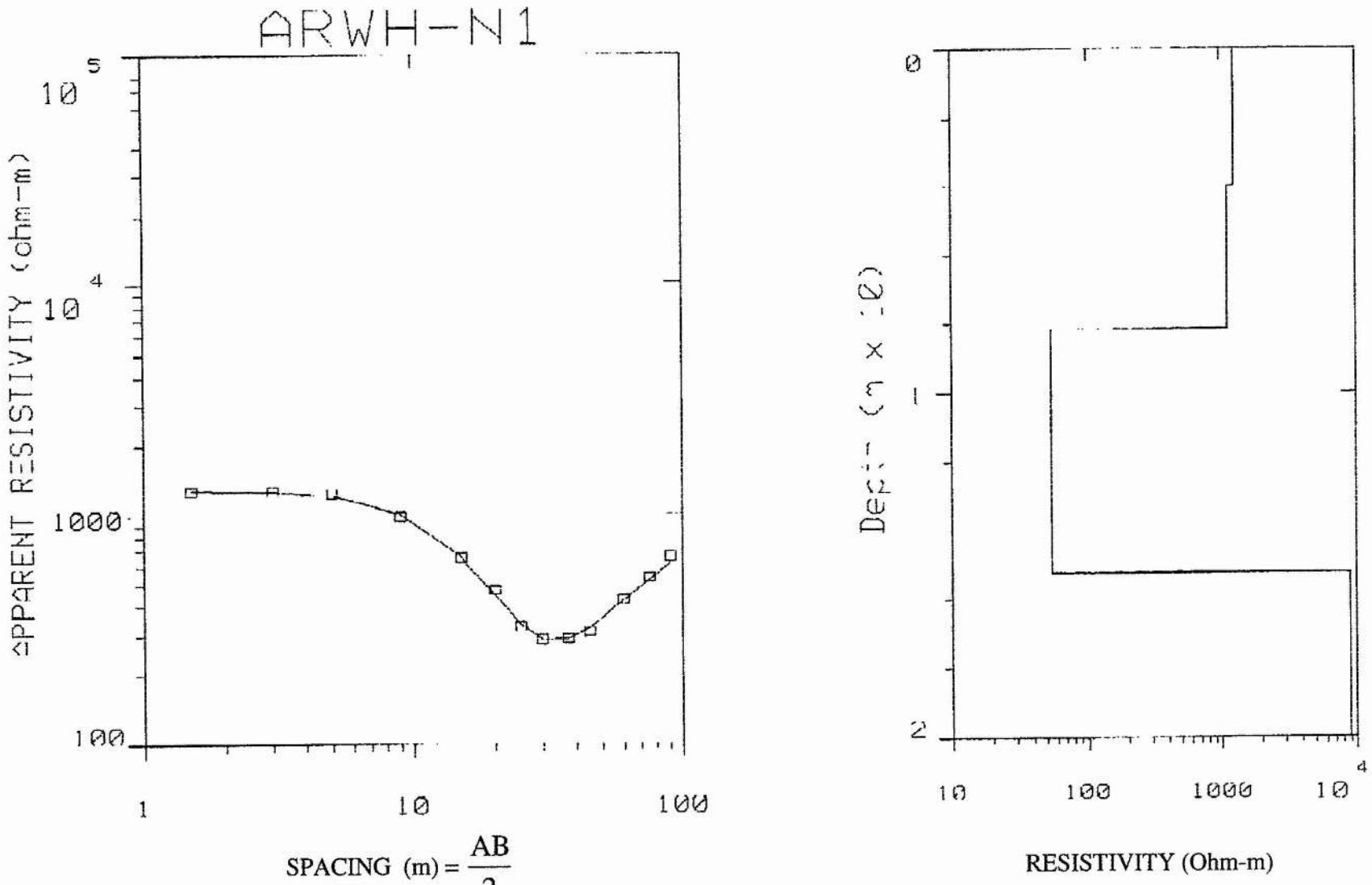

Figure 6.23 VES resistivity curve plots of station ARWH-N1 showing a 4 layer case.

Table 6.12 Resistivity and layer thicknesses of Wadi Baysh and Wadi Habawnah calculated using VES data

Resistivity and layers thickness of wadi Baysh

STATION NO	ρ_1 ohm-m	T_1(m)	ρ_2 ohm-m	T_2(m)	ρ_3 ohm-m	T_3(m)	ρ_4 ohm-m	T_4(m)	ρ_5 ohm-m	Total thickness(m)	Curve Types	
TRWB-N1	586	4	53	4	1584					8	H	($\rho_1>\rho_2<\rho_3$)
TRWB-N2	595	5	75	9	3543					14	H	($\rho_1>\rho_2<\rho_3$)
TRWB-N3	217	2	623	4	58	13	3470			19	KH	($\rho_1<\rho_2>\rho_3<\rho_4$)
TRWB-N4	129	2	108	2	51	14	4700			19	QH	($\rho_1>\rho_2>\rho_3<\rho_4$)
TRWB-N5	130	2	100	4	53	16	5423			23	QH	($\rho_1>\rho_2>\rho_3<\rho_4$)
TRWB-N6	98	1	1549	5	13	14	75			20	KH	($\rho_1<\rho_2>\rho_3<\rho_4$)
TRWB-N7	541	2	190	7	28	15	60			24	QH	($\rho_1>\rho_2>\rho_3<\rho_4$)
TRWB-N8	103	4	245	10	50	13	119			27	KH	($\rho_1<\rho_2>\rho_3<\rho_4$)
TRWB-N9	70	3	154	5	35	13	66	7	115	28	KHA	($\rho_1<\rho_2>\rho_3<\rho_4<\rho_5$)
TRWB-N10	24	5	104	14	71	11	334			30	KH	($\rho_1<\rho_2>\rho_3<\rho_4$)
TRWB-N11	132	4	305	9	45	21	1714			34	KH	($\rho_1<\rho_2>\rho_3<\rho_4$)
TRWB-N12	18	8	82	10	19	17	138			35	KH	($\rho_1<\rho_2>\rho_3<\rho_4$)
TRWB-N13	32	5	144	19	34	10	400			33	KH	($\rho_1<\rho_2>\rho_3<\rho_4$)
TRWB-N14	23	4	39	17	52	14	257			35	AA	($\rho_1<\rho_2<\rho_3<\rho_4$)
TRWB-N15	35	3	74	19	24	10	177			32	KH	($\rho_1<\rho_2>\rho_3<\rho_4$)
TRWB-N16	105	6	11	5	745	10	31	6	11	27	HAA	($\rho_1>\rho_2<\rho_3<\rho_4<\rho_5$)

Resistivity and layers thickness of Wadi Habawnah

STATION NO	ρ_1 ohm-m	T_1(m)	ρ_2 ohm-m	T_2(m)	ρ_3 ohm-m	T_3(m)	ρ_4 ohm-m	T_4(m)	ρ_5 ohm-m	Total thickness(m)	Curve Types	
ARWH-N1	1268	4	1142	4	57	7	6536			16	QH	($\rho_1>\rho_2>\rho_3<\rho_4$)
ARWH-N2	1314	4	385	7	58	6	2950			16	QH	($\rho_1>\rho_2>\rho_3<\rho_4$)
ARWH-N3	2155	2	414	3	1439	8	47	5	772	18	HKH	($\rho_1>\rho_2<\rho_3>\rho_4<\rho_5$)
ARWH-N4	1358	7	705	7	42	16	3457			30	QH	($\rho_1>\rho_2>\rho_3<\rho_4$)
ARWH-N5	1783	7	1325	6	63	12	8	8	1955	33	QQH	($\rho_1>\rho_2>\rho_3>\rho_4<\rho_5$)
ARWH-N6	1508	6	345	7	56	16	6167			29	QH	($\rho_1>\rho_2>\rho_3<\rho_4$)
ARWH-N7	2233	3	2269	7	108	18	5562			28	QH	($\rho_1>\rho_2>\rho_3<\rho_4$)
ARWH-N8	1803	3	721	3	49	23	5710			29	QH	($\rho_1>\rho_2>\rho_3<\rho_4$)
ARWH-N9	1914	3	1562	7	33	13	5824			22	QH	($\rho_1>\rho_2>\rho_3<\rho_4$)
ARWH-N10	1945	2	617	4	1252	7	121	12	3190	25	HKH	($\rho_1>\rho_2<\rho_3>\rho_4<\rho_5$)
ARWH-N11	1094	2	304	11	73	22	2188			35	QH	($\rho_1>\rho_2>\rho_3<\rho_4$)
ARWH-N12	912	3	515	16	33	23	10260			42	QH	(R1>R2>R3<R4)
ARWH-N13	1540	2	513	13	35	19	138			34	QH	($\rho_1>\rho_2>\rho_3<\rho_4$)
ARWH-N14	1085	5	205	12	76	20	3640			37	QH	($\rho_1>\rho_2>\rho_3<\rho_4$)

Table 6.13 VES interpretation data of the total thickness of wadi sediments, water table depth and saturated and unsaturated thicknesses of Wadi Baysh and Wadi Habawnah

COMPUTED PARAMETERS-V.E.S INTERPRETATION OF WADI BAYSH

Well location no.	V.E.S Station no	Location in the wadi	DISTANCE (m) OF WELL to V.E.S	Bed rock resistivity(ohm-m)	Bed rock depth (m)	Water table depth (m)	Saturated zone thickness (m)	Saturated zone resistivity (ohm-m)	Jnsaturated zone thickness (m)
BU1	TRWB-N1	UPPER	3	1584	8	4	2	53	2
BU2	TRWB-N2	UPPER	5	3543	14	5	9	75	3
BU3	TRWB-N3	UPPER	20	3470	19	6	13	58	4
	TRWB-N4	UPPER	___	4700	19	4	14	51	2
	TRWB-N5	UPPER	___	5423	23	6	16	53	4
	TRWB-N6	UPPER	___	75	20	20*	14	75	18
	TRWB-N7	UPPER	___	60	24	24*	14	60	22
Average of the summation				3744	18	6	12	60	4
BM5	TRWB-N8	MIDDLE	10	119	27	14	13	50	12
BM7	TRWB-N9	MIDDLE	10	115	28	21	7	65	19
	TRWB-N10	MIDDLE	___	334	30	19	11	71	17
	TRWB-N11	MIDDLE	___	1714	34	14	20	45	12
BM12	TRWB-N12	MIDDLE	10	138	35	18	17	19	16
Average of the summation				____	30	17	14	50	15
	TRWB-N13	LOWER	___	400	33	23	10	34	21
	TRWB-N14	LOWER	___	257	35	21	14	52	19
BL16	TRWB-N15	LOWER	10	177	32	22	10	24	20
GO	TRWB-N16	LOWER	10	11	27	21	6	31	19
Average of the summation				___	32	22	10	35	20

Continued on next page

Continue table 6.13

COMPUTED PARAMETERS-V.E.S INTERPRETATION OF WADI HABAWNAH

Well location no.	V.E.S Station no	Location in the wadi	DISTANCE (m) OF WELL to V.E.S	Bed rock resistivity(ohm-m)	Bed rock depth (m)	Water table depth (m)	Saturated zone thickness (m)	Saturated zone resistivity (ohm-m)	Jnsaturated zone thickness (m)
HB2	ARWH-N1	UPPER	6	6536	16	8	7	56	6
HB3	ARWH-N2	UPPER	8	2950	16	11	6	58	9
HB6	ARWH-N3	UPPER	10	772	18*	12	5	47	10
Average of the summation				4743	17	10	6	54	8
MT1	ARWH-N4	MIDDLE	10	3457	30	14	15	42	12
H-7-B	ARWH-N5	MIDDLE	5	1955	33	13	12	63	11
MT9	ARWH-N6	MIDDLE	10	6167	29	13	16	56	11
GF2	ARWH-N7	MIDDLE	3	5562	28	10	18	108	8
GF5	ARWH-N8	MIDDLE	3	5710	29	7	22	49	5
NG1	ARWH-N9	MIDDLE	3	5824	22	10	13	33	8
Average of the summation				4794	29	11	16	59	9
MR	ARWH-N10	LOWER	3	3190	25	12	12	121	10
	ARWH-N11	LOWER	___	2188	35	14	21	73	12
HS2	ARWH-N12	LOWER	16	10260	42	19	23	33	17
HS4	ARWH-N13	LOWER	4	138	34*	15	19	35	13
	ARWH-N14	LOWER	___	3640	37	17	20	76	15
Average of the summation				4819	34	15	19	67	13

* It does not represent the total thickness of the wadi deposit because the V.E.S was not deep enought to reach the bedrock.

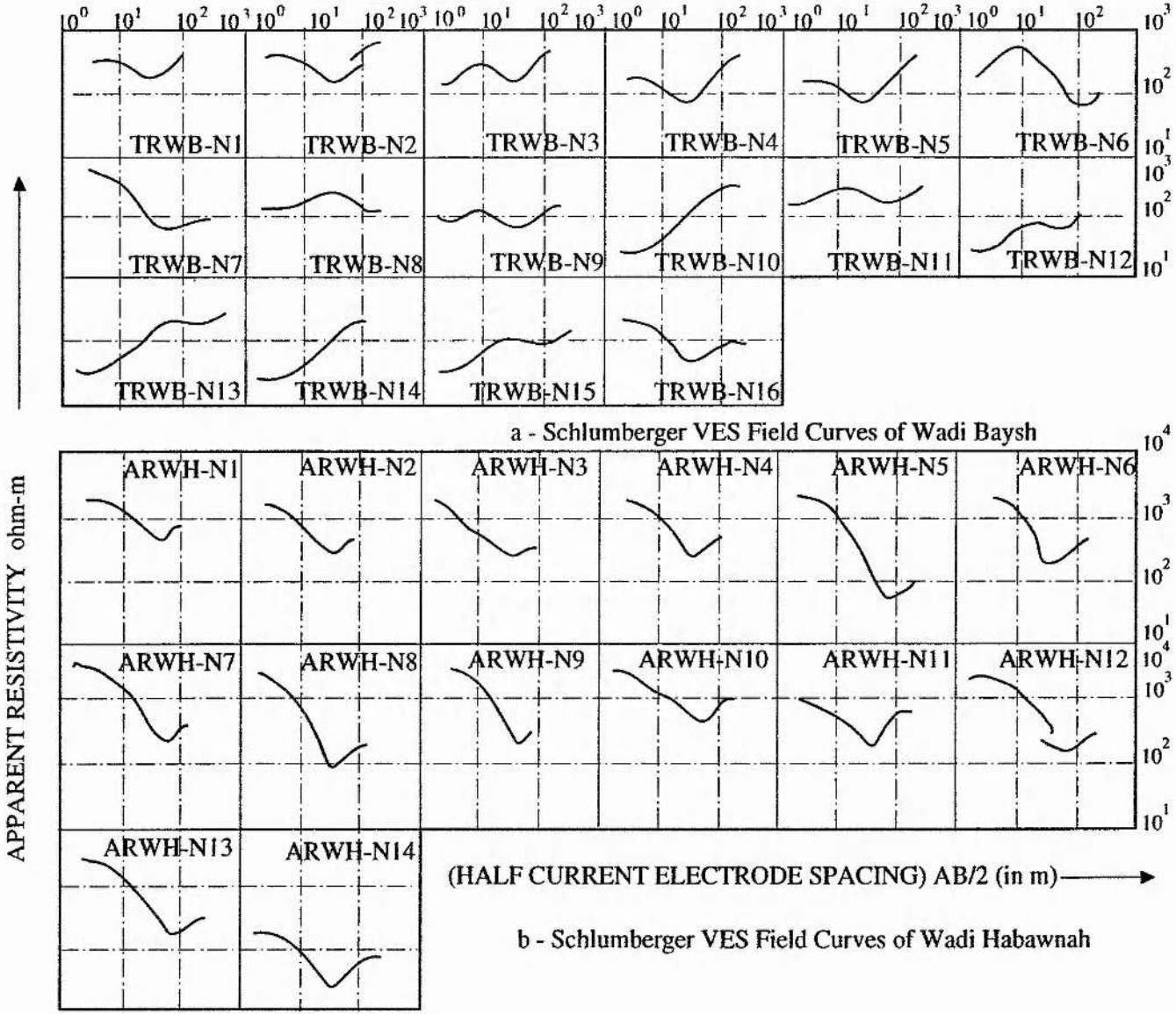

Figure 6.24 Schlumberger VES field curves of Wadi Baysh (a) and Wadi Habawnah (b).

here. Qualitative examination of the TRWB-N1 and TRWB-N2 curves reveals a two layer geoelectric section of the H-type with $\rho_1 > \rho_2 < \rho_3$. The detection of bedrock with a high resistivity of 1587 and 3543 ohm-m at shallow depth, is evidenced by the steeply ascending left limbs of the curves (Figure 6.24 and Appendix 6C).

Examination of the TRWB-N3 curve reveals a three layer geoelectric section of the KH-type with $\rho_1 > \rho_2 < \rho_3 < \rho_4$ and a water depth of 6m. The surface layer shows a low resistivity of 217 ohm-m while the bedrock shows high resistivity (3470 ohm-m) at 19 m, as evidenced by the steep descent of the left branch of the curve, while the right end of the curve branch ascends (Figure 6.24 and Appendix 6C).

Quantitative interpretation of the curve indicates an average depth of 6m to the water table, 18m to the bedrock, with the resistivity of the saturated zone as 60 ohm-m (Table 6.12). Both resistivity surveys and the well depth measurements (Table 6.13) are in good agreement, with an error of less than 10% when comparing the total thickness of the wadi deposits. The water table depth has an error of less than 14% while the saturation thickness has a higher error, between 20% and 33%, for TRWB-N1 and N2, and 10% for TRWB-N3. The rest of the resistivity survey consists of four VES stations namely: TRWB-N4, TRWB-N5, TRWB-N6 and TRWB-N7. There is no well near these VES stations. However their curves reveal a four layer geoelectric section of the QH-type ($\rho_1 > \rho_2 > \rho_3 < \rho_4$), except at TRWB-N6 which shows a KH-type ($\rho_1 < \rho_2 > \rho_3 < \rho_4$).

The results of TRWB-N6 and TRWB-N7 indicate that the water depth is 20m and 24 m below the surface, respectively, but such values are questionable, as field inventory evidence shows water depths of 6 m to 10 m. The resistivity of the third layer of TRWB-N6 is very low (13 ohm-m) with a thickness of 14m. Such a layer of fine grained material (silt to clay) combined with a high salinity aquifer may cause some problems in determining the saturated zone depth. The example, the saturated layer in the previous stations; (resistivities 75 and 60 ohm-m) is covered by a low resistivity thick layer of silt to clay (28 and 13 ohm-m), making the depth of the fresh water at both sites difficult to determine by the VES method.

6.3.9.2 Soundings of the Middle Part of Wadi Baysh

Five vertical electrical soundings were made along the wadi channel towards the south (Figure 6.15). The VES stations TRWB-N8, TRWB-N9 and TRWB-N12 were located close to wells BM5, BM7 and BM12, respectively. The curves from these stations are shown in Figure 6.24. They represent at least a three layer geoelectric section of the KH-type, in which the fresh water level is represented by the upper boundary of the second layer, while the lower boundary could not be determined. The curve interpretation for these stations indicates that the depth to the water table is in the range of 14m to 21m (Table 6.12). This range of values correlates well with the estimated depth of 13m to 19m from well data. A depth of 14m is obtained from TRWB-N8 curve by assuming the resistivity of the third layer as 50 ohm-m. It is necessary to fix this resistivity in order to make the interpreted depth agree precisely with the depth obtained from geological information. This adjusted resistivity value of the third layer is calculated by using the principle of equivalence, with the average resistivity of the aquifer being 50 ohm-m (see Table 6.13). The sounding stations TRWB-N10 and TRWB-N11 were located in an area with no geological information, so that VES survey data are needed to interpret the geology of the aquifer. The aquifer depths at these two resistivity stations are 19m and 14m respectively with resistivities of 71 and 45 ohm-m. The bedrock depth could not be determined in this area using the VES method.

Two further sounding stations TRWB-N13 and TRWB-N14 were situated west of the main channel area both on higher ground. In each case a three layer geoelectric profile was identified, with depths of 24m and 21m, respectively to the aquifer.

6.3.9.3 Sounding of the Lower Part of Wadi Baysh

Two electrical soundings (TRWB-N15 and TRWB-N16) were made approximately 7 km south of Baysh bridge, on the wadi channel and the flood plain to evaluate the aquifer extension in that area. Both of the resistivity stations were correlated geologically with nearby wells, BL16 and G0, respectively. Examination of 75m of borehole log from G0 (Figure 6.13) indicates the presence of eight layers with two aquifer zones bounded by clay and silt. TRWB-N16 was measured near borehole G0, the sounding curve is shown in

Figure 6.23 and Appendix 6C. The presence of four layers is clearly indicated by the HAA-type curves ($\rho_1 > \rho_2 < \rho_3 < \rho_4 < \rho_5$) (Table 6.13 and Figure 6.25).

Preliminary quantitative interpretation of TRWB-N16 curves yields a depth of about 2 m to fresh water (Table 6.13), a depth in a good agreement with 24 m from the borehole at G0 (Tables 6.13 and 6.15).

6.3.10 Wadi Habawnah

Wadi Habawnah was divided into upper, middle and lower parts. Eleven tests of large diameter wells, one borehole and 14 VES curves are available for analysis. The twelve wells were chosen to provide geological control; i.e. HB_2, HB_3, HB_6, MT9, H-7-B, MTI, GF_2, GF_5, MR, NG1, HSI and HS2. All were situated at distances from 5 m to 23 m away from the VES stations (Figure 6.16, Tables 6.12 and 6.14 and Appendix 6C) Figure 6.24 shows the curves of the fourteen soundings. The resistivity curves of eleven of them are characterised as being of QH type with ($\rho 1 > \rho 2 < \rho 3 > \rho 4 < \rho 5$) while ARWH-N3 (in the upper part of the Wadi), ARWH-N5 and ARWH-N10 (in the middle part of the Wadi) are of HKH-type with ($\rho 1 > \rho 2 < \rho 3 > \rho 4 < \rho 5$), QQH-type with ($\rho 1 > \rho 2 > \rho 3 > \rho 4 < \rho 5$) and HKH-type with ($\rho 1 > \rho 2 < \rho 3 > \rho 4 < \rho 5$), respectively (Table 6.12).

6.3.10.1 Soundings of the Upper Part of Wadi Habawnah

In the upper part of Wadi Habawnah there were three VES stations (ARWH-N1, ARWH-N2 and ARWH-N3) and three test wells (HB2, HB3, HB6).

VES TRWH-N1 was located approximately 6 metres east of HB2. The direction of sounding line was EW. The well HB2 indicated the depth to the saturated zone as being 9m and the depth to the bedrock as 16 m (Table 6.13).

The upper two layers in the VES curve interpretations are equal in thickness. The top 4m thick of layer is dry gravel and sand with a resistivity value of 1268 ohm-m. The second is 4m of gravel and sand with silt and considered to extend to the water table. Its resistivity value was interpreted as 1142 ohm-m. This value is somewhat low and probably reflects an unknown fluctuation of the water table.

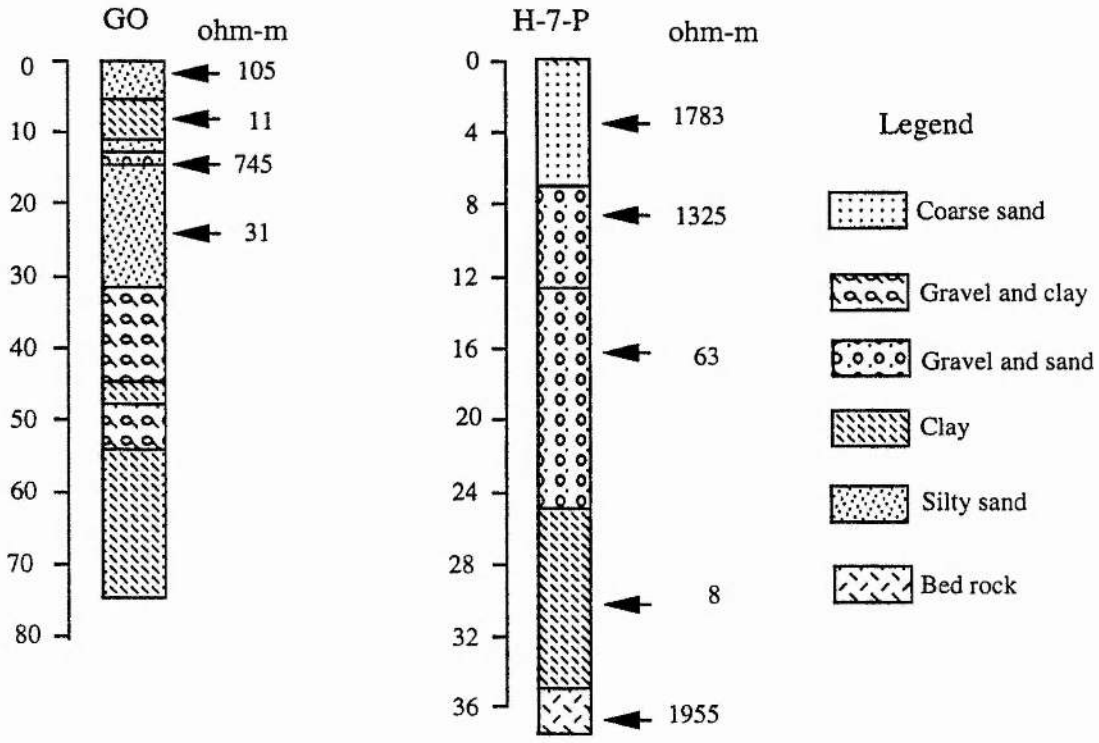

Figure 6.25 Correlation between borehole lithology and VES resistivity data for boreholes GO (Wadi Baysh) and H-7-P (Wadi Habawnah).

Table 6.14 The comparison of VES interpretation of the total thickness of the wadi sediments, water table depth and saturated thickness with field measurements from Wadi Baysh and Wadi Habwanah

Wells measurements of Wadi Baysh				V.E.S interpretation data of Wadi Baysh								
Well location no.	Wadi thickness (m)	Water table depth (m)	Saturated thickness (m)	V.E.S Station no	DISTANCE (m) OF WELL to V.E.S	Wadi thickness (m)	Water table depth (m)	Saturated zone thickness (m)	Saturated zone resistivity (ohm-m)	Error(a) %	Error(b) %	Error(c) %
BU1	6	4	2	TRWB-N1	3	8	4	4	53	14	0	33
BU2	12	6	6	TRWB-N2	5	14	5	9	75	8	9	20
BU3	20	8	12	TRWB-N3	20	19	6	13	58	3	14	4
BM5	24	13	11	TRWB-N8	10	27	14	13	50	6	4	8
BM7	30	17	13	TRWB-N9	10	28	21	7	65	3	11	30
BM12	40	19	21	TRWB-N12	10	35	18	17	18	7	3	11
BL16	60	23	37	TRWB-N15	10	32	22	10	24	30	2	56
GO	75	22	53	TRWB-N16	10	27	21	6	31	47	2	80
Wells measurements of Wadi Habawnah				V.E.S interpretation data of Wadi Habawnah								
Well location no.	Wadi thickness (m)	Water table depth (m)	Saturated thickness (m)	V.E.S Station no	DISTANCE (m) OF WELL to V.E.S	Wadi thickness (m)	Water table depth (m)	Saturated zone thickness (m)	Saturated zone resistivity (ohm-m)	Error(a) %	Error(b) %	Error(c) %
HB2	16	9	7	ARWH-N1	6	16	8	8	56	1	6	4
HB3	17	12	5	ARWH-N2	8	16	11	5	58	-2	4	4
HB6	17	13	4	ARWH-N3	10	18	12	6	47	3	4	20
MT1	32	15	17	ARWH-N4	10	30	14	16	42	3	3	3
H-7-B	33	14	19	ARWH-N5	5	33	13	20	63	0	4	3
MT9	33	14	19	ARWH-N6	10	29	13	16	56	6	4	9
GF2	30	11	19	ARWH-N7	3	28	10	8	108	3	6	9
GF5	24	13	11	ARWH-N8	3	29	6	23	49	9	39	35
NG1	24	12	12	ARWH-N9	3	22	10	12	33	3	9	2
MR	26	14	12	ARWH-N10	3	25	12	13	120	2	8	4
HS2	37	18	19	ARWH-N12	16	42	19	23	73	6	3	10
HS4	38	17	21	ARWH-N13	4	34	15	8	34	5	6	10

Error(a) percentage error of V.E.S interpretation for total thickness compared to field measurment .

Error(b) percentage error of V.E.S interpretation for water table depth compared to field measurment .

Error(c) percentage error of V.E.S interpretation for saturated thickness compared to field measurment .

* It does not represent the total thickness of the wadi deposit because the well was not deep enought to reach the bedrock.

Table 6.15 Saturated and unsaturated thickness of the wells near the geophysical stations

Wadi Habawnah Wells						Wadi Baysh Wells					
Well Location	no.*	Aquifer Thicknes (m	Water table depth (m)	Saturated Thickness (m)	Unsaturated Thickness (m)	Well Location	No*	Aquifer thicknes (m)	Water table depth (m)	Saturated Thickness (m)	Unsaturated Thickness(m)
HB2	Upper	16	9	7	9	BU1	Upper	8	5	3	5
HB3	Upper	17	12	5	12	BU2	Upper	12	6	6	4
HB6	Upper	17	13	4	13	BU3	Upper	20	7	13	7
H-11-P	Upper	20	12	8	12		Average	13	6	7	5
	Average	18	12	6	12						
						BM5	Middle	24	13	11	13
MT1	Middle	32	15	17	15	BM7	Middle	30	17	13	17
H-7-B	Middle	33	14	19	14	BM12	Middle	40	19	16	19
MT9	Middle	33	14	19	14		Average	31	16	13	16
H-3-P	Middle	34	16	18	16						
GF2	Middle	30	11	19	11	BL16	Lower	60	23	37	23
GF5	Middle	24	8	16	13	GO	Lower	75	24	51	24
NG1	Middle	24	12	12	12		Average	77	24	44	21
	Average	30	13	17	14						
MR	Lower	26	14	12	14						
HS2	Lower	37	18	19	18						
HS-4	Lower	38	17	21	17						
H-15-P	Lower	35	16	19	14						
	Average	34	16	18	16						

* These locations show the wadi sections where they are located.

The saturated part of the aquifer is 7m thick with a resistivity of 57 ohm-m (Table 6.12). The bedrock depth is 16m with a resistivity of 6536 ohm-m (Table 6.12). The well lithology HB2 shows two main layers; firstly a 15m layer of gravel, sand and silt, which may be considered as 8m of unsaturated layer and 7m of saturated layer (aquifer). The second layer is the metamorphic bedrock (Tables 6.13 and 6.14). The differences between the two measurements (the resistivity calculation and the well inventory) are less than 10% (Table 6.14).

The VES data for ARWH N2 east of HB3 were derived from a sounding line trending EW, parallel to the main wadi axis. Figure 6.24 shows the VES curve of ARWH-N2. The depth to the water table was interpreted as 11m below the land surface and the bedrock at 16m. The interpretation suggests a simple 3 layer case. The first layer (dry gravels and sands) is 4m thick with resistivity of 1314 ohm-m. The second layer is 7m thick and has a resistivity of 385 ohm-m (Table 6.13). This is a lower resistivity value than that of the top layer and may reflect the influence of the clay within the layer and the moisture of the aquifer below. The saturated zone was best fitted with a resistivity value of 58 ohm-m and thickness of 6m, with the correlation error less than 10% (Table 6.14).

The VES ARWH-N3 is located 10m to the south of test well HB6. The VES curve shows four layers with a total thickness of 18m. The dry zone is characterised by three layers, surface layer, gravel and sand, with a resistivity of 2155 ohm-m, the second layer (silt, sand and gravel) has a resistivity of 414 ohm-m and the third layer (gravel and silty sand) a resistivity of 1439 ohm-m. The saturated zone is reached at a depth of 13m and has a resistivity of 47 ohm-m and a thickness of 5m (Table 6.13). The bedrock resistivity is low (772 ohm-m) suggesting that the bedrock surface is highly fractured or weathered.

Both calculations of the total thickness and the water table depth show errors of less than 10% compared with the well inventory nearby (HB6). However, the thickness of the saturated layer shows errors of 20% (Table 6.13).

6.3.10.2 Soundings of the Middle Part of Wadi Habawnah

The middle part of Wadi Habawnah is considered one of the major areas of agricultural activity along the wadi. It consists of the Al Montasher area to the west, the

lower part of Wadi Thar in the north and extends to Al Nagah in the east (Figure 6.16).

There are six VES stations in this area (ARWH-N4--> ARWH-N9). Quantitative interpretation of the curves shows a good agreement with the well inventory data (MT1, H-7-B, MT9, GF_2, GF_5 and NG1) (Table 6.14) with respect to the thickness of wadi sediment, saturated zone thickness and water table depth, with errors of less than 10% (Table 6.14). The average depth of the saturated zone is 11m. However, bedrock is at an average depth of 29m below the land surface at ARWH-N9 where the elevation is 1192 m above sea level. The average resistivity of the saturated zone is 59 ohm-m while the value for bedrock is 4794 ohm-m (Table 6.13). The lithology of wadi deposits can be classified on the basis of examining VES ARWH-N5, and the adjacent observation well H-7-P (Figures 6.16 and 6.25). Total current electrode separation (AB) of 120m was achieved on an E-W line parallel to the wadi channel at this site. The well inventory indicated the water table depth at 14 m and the bedrock depth at 33m. The surface layer was of 7m of very dry gravel and sand with a resistivity 1783 ohm-m. The second layer was of 6m of sand and gravel with a resistivity of 1325 ohm-m. The saturated zone resisitivity was calculated as 63 ohm-m and was composed of gravel, sand and silt with a thickness of 12 m. The resistivity of the fourth layer suggests the presence of a clay layer with low resistivity of 9 ohm-m and a thickness of 8m. The bed rock resistivity is 1955 ohm-m. It is suggested that the resistivity of the bedrock is low because the bedrock surface is highly fractured or weathered.

6.3.10.3 Soundings of the Lower Part of Wadi Habawnah

The eastern part of Wadi Habawnah is 1 to 2 km wide. It extends from Morykhah in the west, to 10 km east of Al Husaniyah Village into the margin of the Rub al Khali (Figure 6.18). The general topography of the area shows a gentle slope towards the east with an average elevation of 1100m above sea level.

The resistivity survey comprised five resistivity stations (ARWH-N10 --> ARWH-N14) and three test wells (MR, HS2, HS4). The location of these stations is shown in Figure 6.16.

The apparent resistivity curves, of the QH type, are interpreted from VES stations

ARWH-11, ARWH-N12, ARWH-N13 and ARWH-14 (Table 6.12). Resistivity and depth of three layers are calculated. According to the resistivity calculation and the well measurements the lithology of this area can be classified as follows:

1- The unsaturated zone consists of the surface layer (gravel and sand) with resistivity ranging from 912 to 1540 ohm-m. It has an average thickness of 3 m. The second layer (sand and silt) varies in resistivity between 205 and 515 ohm-m, and has a thickness averaging 13 m (Table 6.13).

2- The saturated zone shows two types of lithology. At VES ARWH-N12 and ARWH-N13, the saturated zone consists of sand and silt with a resistivity of 33 and 35 ohm-m and thicknesses of 23 m and 19 m respectively. However, in both VES ARWH-11 and ARWH-14, the saturated zone is of gravel and silty sand with resistivities of 73 and 76 ohm-m and thicknesses of 22 m and 20 m respectively. (Table 6.12 and 6.13).

3- The calculated bedrock depth varies between 25 m and 42 m. It had a resistivity of between 10260 ohm-m and 2188 ohm-m (Table 6.13). At ARWH-13 the bedrock was not reached.

The VES ARWH-N10 plot (Figure 6.24) shows a four layer curve, of the HKH-type. Examination of the nearby test well MR, which is 25m in depth, also shows 4 layers. The surface layer (gravel, sand and silt) is 2m thick with a resistivity of 1945 ohm-m. The second layer is of coarse sand and silt with a thickness of 4m and a resistivity of 617 ohm-m. The third layer is mainly gravel, sand and silt with a thickness of 7m and a resistivity of 1252 ohm-m. These three layers are considered as forming the unsaturated zone. The water depth was measured at 12m below the surface with less than 10% error (Table 6.13). The saturated zone is of gravel and sand, 12m thickness with a resistivity calculated as 121 ohm-m. The top of the bedrock depth is at 24m and it has a resistivity of 3190 ohm-m.

At ARWH-N13, the bedrock depth and the saturated zone thickness could not be determined. The author assumed that the bedrock depth for this station could be reached at the depth of 40 m based on the fact that both upstream (ARWH-N12) and down stream (ARWH-N14) stations show bedrock at depths of between 37 m and 42 m.

In the saturated zone at station ARWH-N13 the calculated resistivities of the upper

(sand and silt), and lower zones were 35 and 131 ohm-m, respectively. It was therefore assumed that the saturated lower zone consisted of gravel and sand such as at station ARWH-N10 where the calculated resistivity of the gravel and sand-rich saturated zone was 121 ohm-m. In conclusion, the succession at station ARWH-N13 can be interpreted as comprising an upper unsaturated zone of gravel and sand (12m), an upper saturated zone of sand and silt (19m) and a lower saturated zone of gravel and sand (9m). Therefore, the bedrock depth is 40m.

6.3.11 Geological Inference

According to the quantitative explanation of the Schlumberger vertical electrical resisistivity sounding exploration, four different sets of geological forms have to be considered in both wadis.

1- A dry surface layer of alluvial deposits with a thickness ranging from 4m to 21m and 5m to 19m, is present in Wadis Baysh and Habawnah, respectively (see Table 6.12). The apparent resistivity of this layer has a higher range of values in Wadi Habawnah than in Wadi Baysh. In Wadi Habawnah the resistivity of the surface layer ranges from 912 to 2233 ohm-m while in Wadi Baysh it ranges from 23 to 745 ohm-m. It is suggested that this difference reflects the presence of fine grained material, such as silt and clay, which characterise the surface layer in Wadi Baysh and the degree of the moisture held in the layer, and contrasts with the sands and gravels at the surface in Wadi Habawnah.

However, the water table depth varied between 7m and 19m and 4m and 24m in Wadi Habawnah and Wadi Baysh respectively (Table 6.13).

The base of the saturated zone in Wadi Habawnah is bounded by hard rock except at station ARWH-N5 below which is a clay layer 8 m in thickness. In Wadi Baysh the saturated zone is underlain by clay except in the upper part of the wadi, where a bedrock of high resistivity is present (see Table 6.12).

2- The water bearing sediments of Wadi Baysh show apparent resistivities varying from less than 30 ohm-m to 120 ohm-m, as shown in the distribution map (Figure 6.26a). Most of the resistivity values of the saturated zone were fell between 30 and 60 ohm-m. In the south east section, resistivities were low (> 30 ohm-m). However, the highest resistivities

are recorded in the middle part of the wadi, ranging between 90 and 120 ohm-m.

In Wadi Habawnah the saturated zone resistivities varied between 25 and 125 ohm-m but most values were between 25 and 50 ohm-m. Generally the lower parts of the wadis are characterised by low resistivity values. However, the highest values were detected in the middle parts of the wadis with values between 100 and 125 ohm-m in which the resistivity decreases towards the west and the east (see Figure 6.26b).

4- The thickness of the saturated zone varies from one place to another:

a) The upper parts of both wadis show thin aquifers with saturated thicknesses ranging from 4m to 12m in Wadi Baysh and from 5m to 7m in Wadi Habawnah.

b) In the middle parts, the average thicknesses increase to 14m and 17m for both wadis. In Wadi Habawnah the thickness increased to 22m in the area of Al Gafader at station ARWH-N8 (Table 6.12).

c) In the lower part of Wadi Baysh the wadi floor deposits increase in thickness rapidly from 30m and 70m to 150 m at well BM7, BL16 and EO, respectively, south of Baysh bridge. In Wadi Habawnah, the deposits increase gradually from about 17m (well HB6) to 40m (well HS3) between Habawnah Village and AlHusaniah (Figure 6.2).

5- In Wadi Habawnah a clay layer occurs under the aquifer in borehole H-7-P and H-15-P (Figure 6.27), similarly in both the middle and the lower parts of Wadi Baysh, a clay layer underlies the saturated aquifer. At some of the survey stations another clay layer lies at the top of the saturated zone, as shown in the resistivity station TRWB-N5 (Figure 6.28a). Elsewhere clays are both below and above the saturated zone (see Figure 6.28b), as at resistivity station TRWB-N16. Such lithological arrangements may give rise to confined or semiconfined aquifers. The clay layers in both wadis show apparent resistivities of less than 12 ohm-m and thicknesses of less than 9m, as revealed from boreholes G0 in Wadi Baysh and H-7-P in Wadi Habawnah (Figure 6.25).

The 5, 16 and 37km longitudinal sections (Figures 6.28a, 6.29b and, 6.30) along the lines CD, A'B and AB, respectively in Wadi Baysh (Figure 6.15) and the 51 km section along the line AB (Figure 6.31) in Wadi Habawnah (Figure 6.16) show the

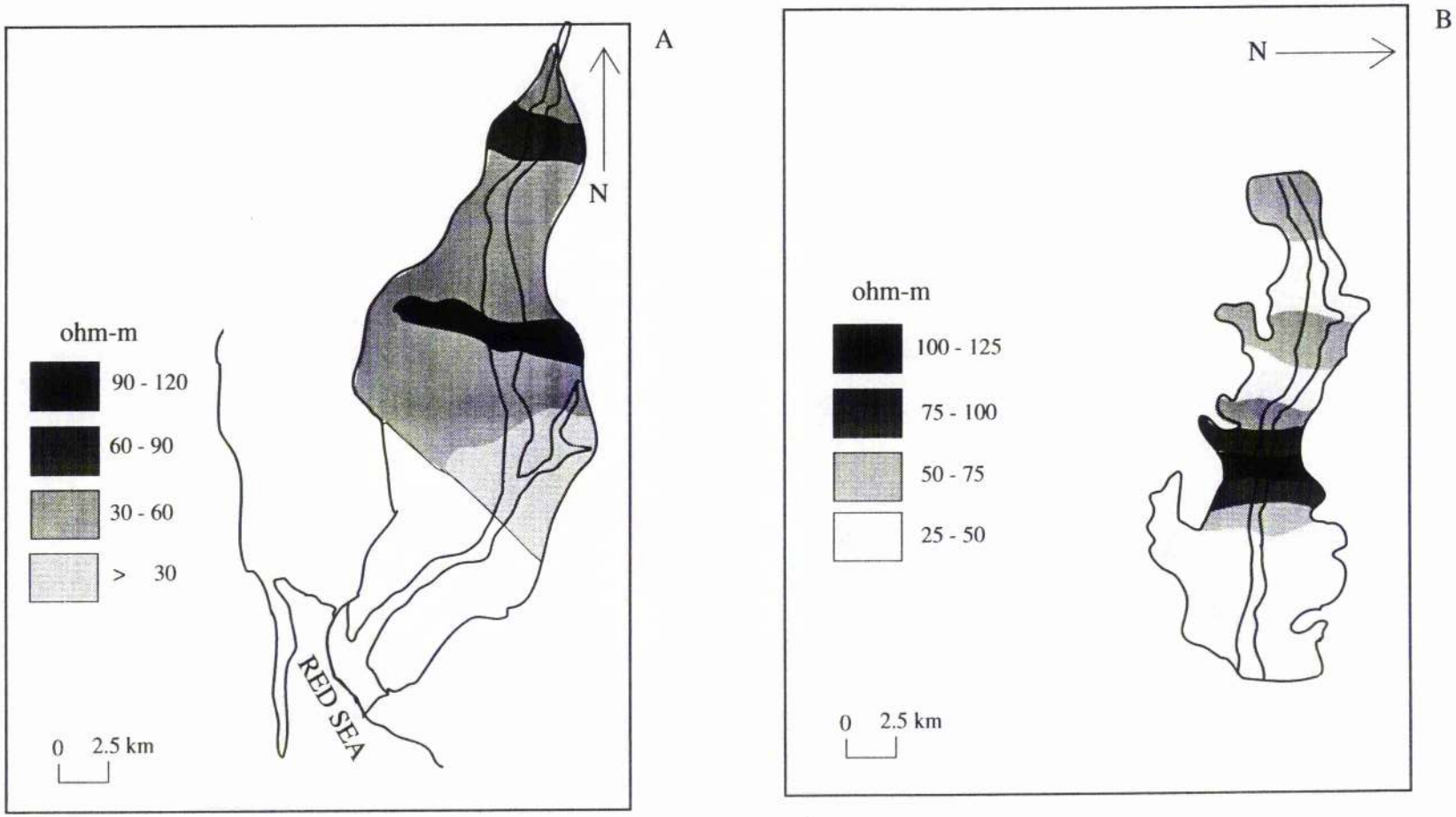

Figure 6.26 The formation resistivity of the saturated zones of Wadi Baysh (A) and Wadi Habawnah (B) aquifers.

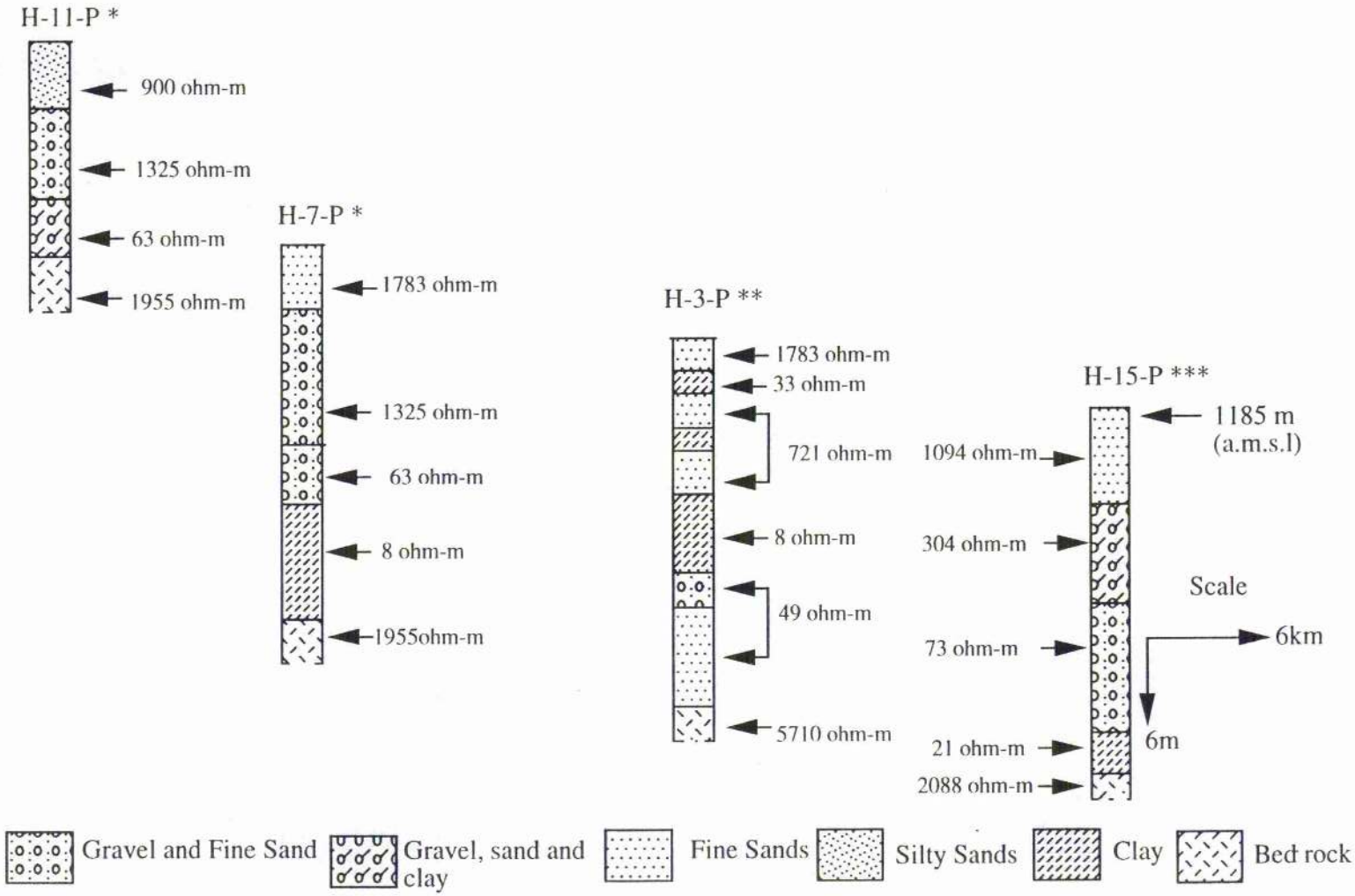

Figure 6.27 The lithology and resistivity values of boreholes H-11-P, H-7-P, H-3-P and H-15-P based on the resistivity stations data nearby ARWH-N5 (*), ARWH-N8(**) and ARWH-N11(***).

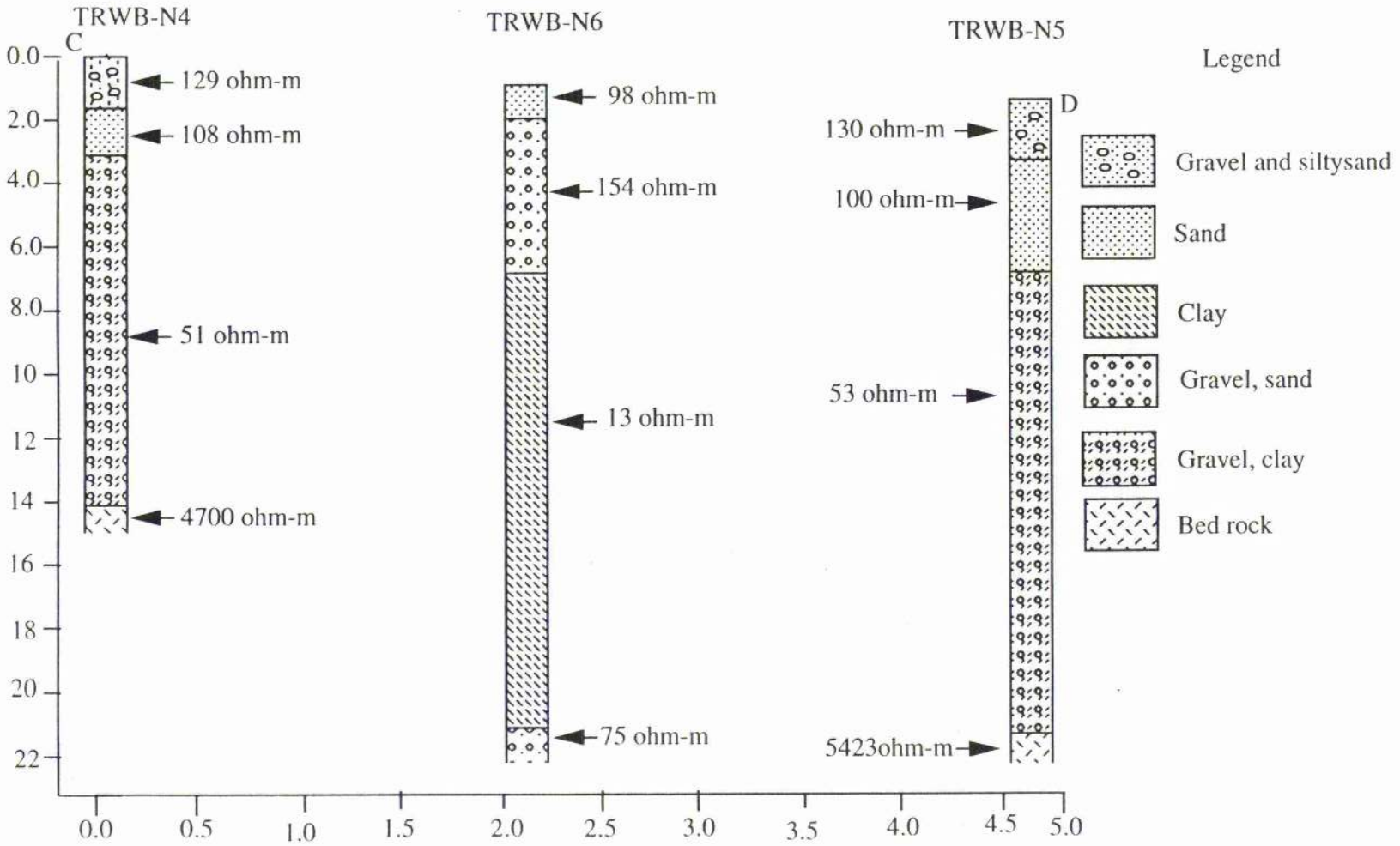

Figure 6.28a Typical resistivity values of the Wadi Baysh sediments along cross section C-D in Figure 6.15

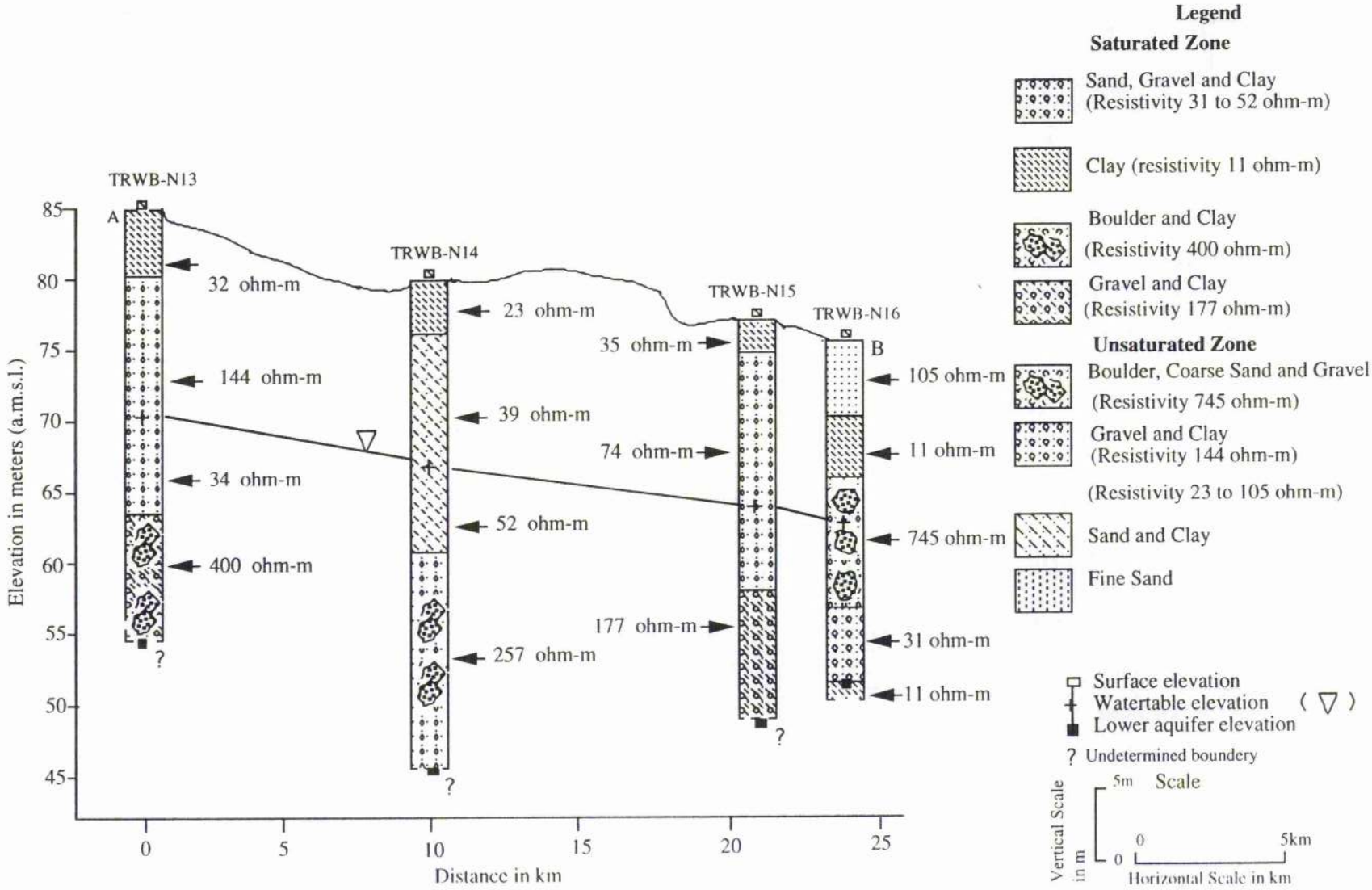

Figure 6.28b A' B Typical resistivity values of the Wadi Baysh sediments along cross section A' B in Figure 6.15.

elevation above the sea level of the surface layer and the water table. The determined bed rock elevation in Wadi Habawnah is also indicated. However, in Wadi Baysh the depth to bedrock could not be estimated in the lower part of the wadi (see Table 6.16).

6.3.12 Errors and Resolution

There is a lack of direct correspondence between the 'standard reference' resistivity models and field measurement shown at some VES stations (TRWB-N1, TREB-N9 and TRWB-N16, Table 6.13. This may be due to the equipment range.

The extreme limit of spread of the current electrodes, and consequently the depth of penetration of current, depends on the power of the current generator and the resistivity characteristics of the sediment type being measured. Both stations had 120m total spread of the current electrodes. This would limit the current penetration to between 30m and 40m below the surface. Accordingly the total thickness of the saturated zone will be affected. For example, VES TRWB-N15 and TRWB-N16 show high percentage differences of 53 % to 35 % in thickness between VES interpretations of 32 and 27m, where the field measurements are 60 and 75m, respectively.

6.3.13 Summary and Discussion

Electrical resistivity soundings employing the Schlumberger configuration were conducted in interval distance of 2 and 6 km approximately. The sounding stations were generally aligned in the E-W direction in Wadi Habawnah and NE to SW parallel to the main channel direction of Wadi Baysh (Figure 6.15 and 6.16). Soundings were located in three main sections; the upper, middle and lower parts of each wadi at control sites near the wells.

The sounding curves mostly represented 4-layer cases of curve types KH and QH in Wadi Baysh while the Wadi Habawnah records were dominated by curves of QH type. Lithological information of dug well and boreholes were vital in refining the interpretation techniques.

White (1988) indicated that improvement in the interpretation of layer depths as obtained by resistivity may best be achieved using control data from boreholes. Figures

Table 6.16 Wadi Baysh and Wadi Habawnah cross section measurements

Wadi Baysh Cross Section Measurement

CROSS SECTION (A -B)

WELL NO	RESISTIVITY STATION NO	HORIZANTAL DISTANCE (km)	ELEVATION in m (a.s.l.) SURFACE	WATER TABLE	BEDROCK
BU1	TRWB-N1	0	130	124	122
BU2	TRWB-N2	2	128	122	116
BU3	TRWB-N3	4	107	100	87
*	TRWB-N6	12	93	85	&
BM5	TRWB-N8	18	70	57	&
BM7	TRWB-N9	21	68	51	&
*	TRWB-N10	24	55	38	&
*	TRWB-N11	26	54	36	&
BM 12	TRWB-N12	30	52	33	&
G0	TRWB-N16	37	45	21	&
CROSS SECTION (C - D)					
*	TRWB-N4	0	100	95	81
*	TRWB-N6	2	93	86	&
*	TRWB-N5	5	96	90	74
CROSS SECTION (E - B)					
*	TRWB-N13	0	87	63	&
*	TRWB-N14	10	60	39	&
BL16	TRWB-N15	22	54	31	&
GO	TRWB-N16	25	45	21	&

Wadi Habawnah Cross Section Measurement

SECTION (F - G)

WELL NO	RESISTIVITY STATION NO	HORIZANTAL DISTANCE (km)	ELEVATION in m (a.s.l.) SURFACE	WATER TABLE	BEDROCK
HB2	ARWH-N1	0	1280	1271	1264
HB3	ARWH-N2	3	1275	1263	1258
HB6	ARWH-N3	6	1265	1252	&
MT1	ARWH-N4	11	1245	1230	1213
MT9	ARWH-N6	16	1225	1212	1191
GF2	ARWH-N7	19	1210	1199	1180
NG1	ARWH-N9	22	1195	1183	1171
MR	ARWH-N10	27	1180	1166	1154
HS2	ARWH-N11	32	1170	1152	1133
H-15-P	**	35	1163	1147	1128
*	ARWH-N12	45	1142	1123	1100
HS4	ARWH-N13	47	1138	1121	&
*	ARWH-N14	51	1125	1108	1088

*Indicates no Existing Well

**Indicates no Resistivity Station

& The bedrock elevation was not determined.

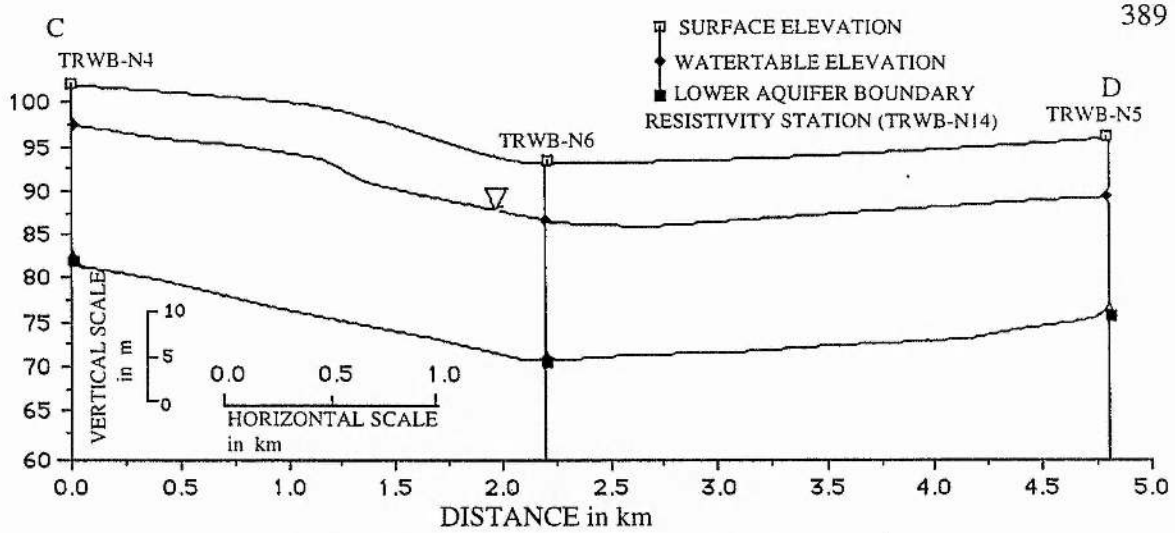

Figure 6.29a CD cross section on Figure 6.15 based on the resistivity interpretation of Wadi Baysh.

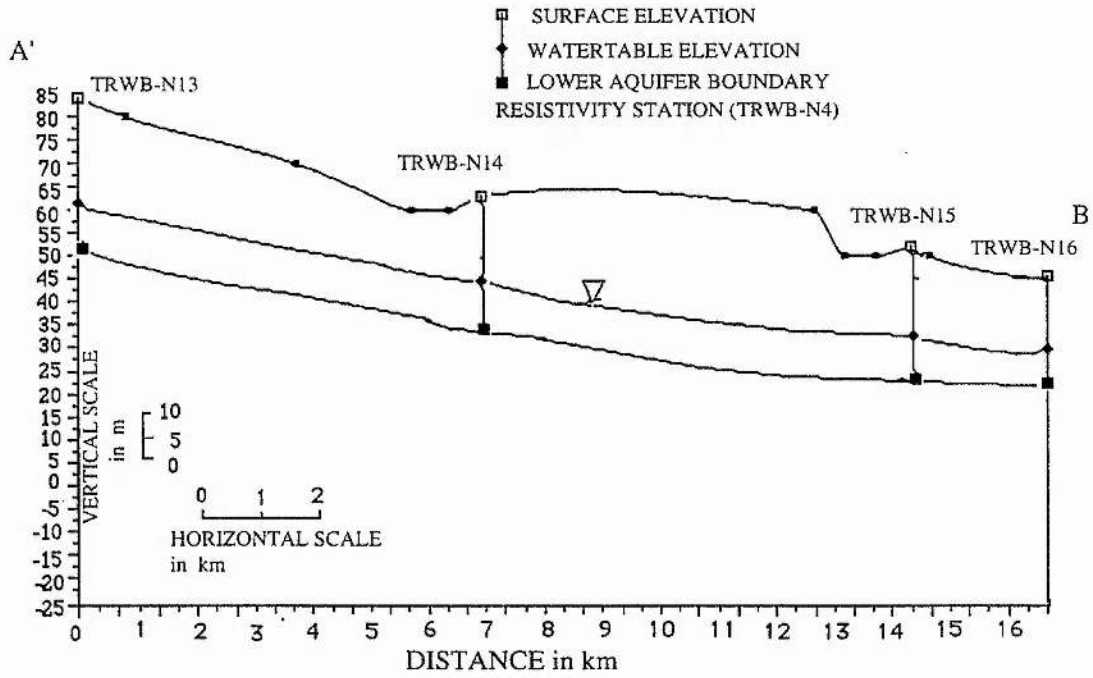

Figure 6.29b A' B cross section on Figure 6.15 based on the resistivity interpretation of Wadi Baysh.

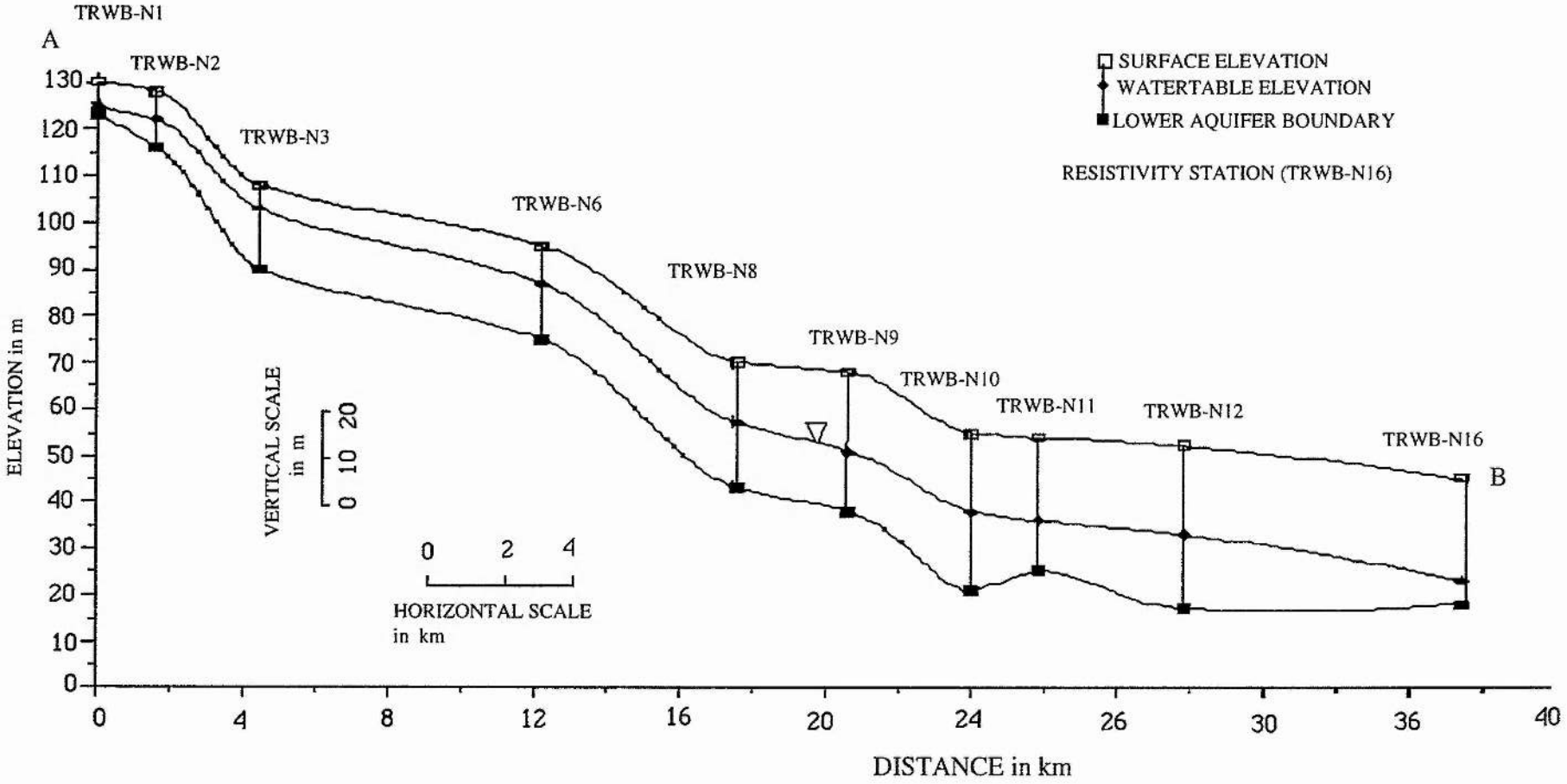

Figure 6.30 Longitudinal section along the line AB in Wadi Baysh (Figure 6.15).

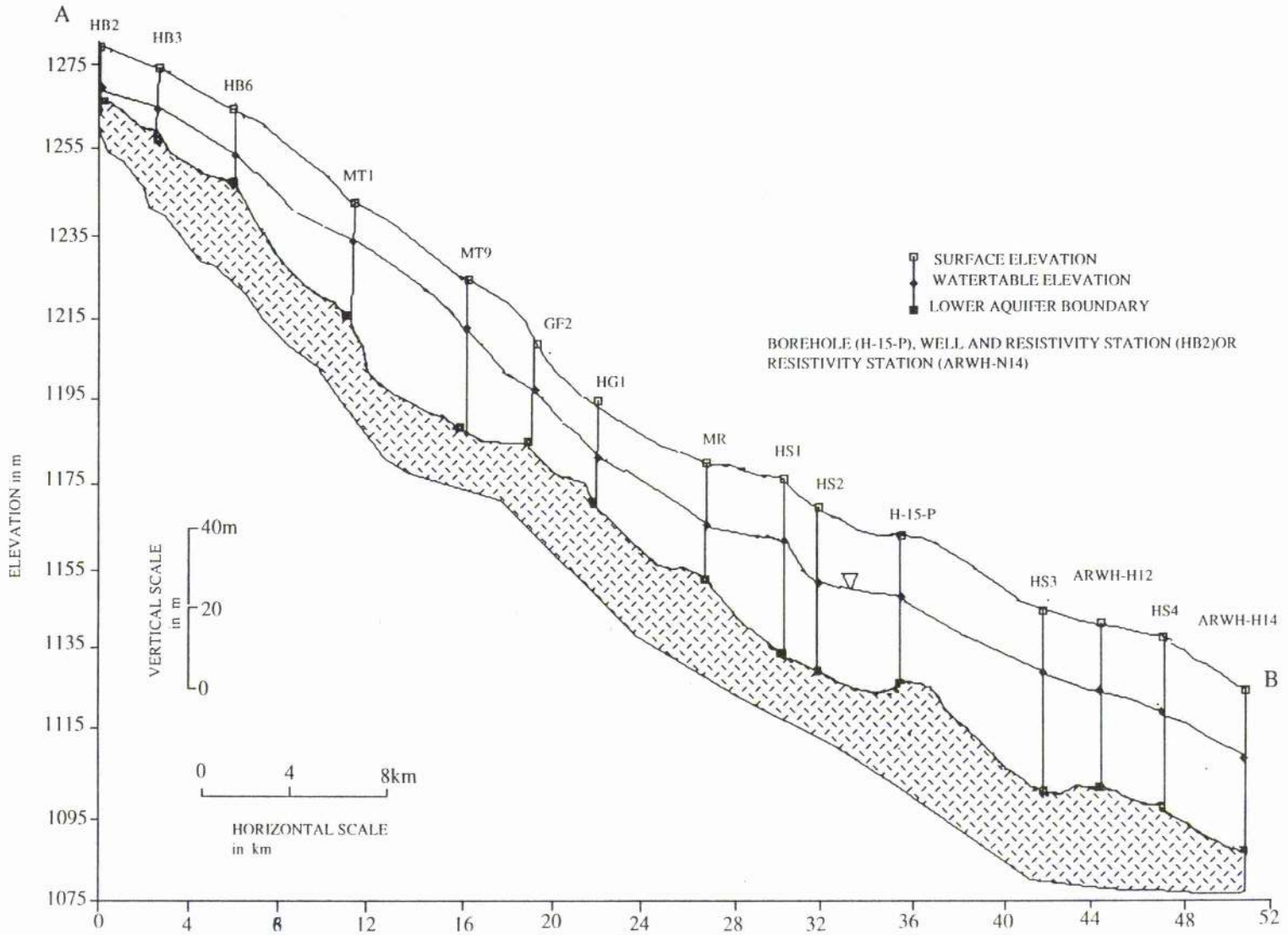

Figure 6.31 Longitudinal section along the line AB in Wadi Habawnah (Figure 6.16).

6.28 and 6.32 show some of the typical sounding wells in the area.

The data were interpreted and adjusted at some locations in relation to the resistivity of the formation on the basis of data on the layer thickness obtained from boreholes and wells nearby.

Bardossy *et al.* (1986) explains that, when the resistivity data are correlated with known lithology type and thickness, the electrical results for a specific layer may be used to show its hydrogeological significance.

Fine sandy clay layers of resistivity equal to 13, 28, and 19 ohm-m) recorded at VES stations of TRWB-N6, N7 and N12, were not found stations TRWB-N8, N9, N10, and N11 (Table 6.11). This indicates a lack of continuity of these layers in the upper-middle part of Wadi Baysh. In Wadi Habawnah, a clay layer which is present at the base of borehole H-7-P, is not recorded in the lower section of borehole H-3-P, but is present again in the middle section of this borehole and also in the lower section of borehole H-15-P (Figure 6.32). This again indicates a lack of continuity of clay deposits.

The upper and middle parts of Wadi Baysh show similar deposits resting on bedrock. This suggests that these separated areas of deposition were subjected to the same sequence of events during at least one stage in their most recent geological history.

Geophysical and lithological data suggest the following:

1- Surface sediments in both wadis show changes in thickness (2 to 20m) of the layers, toward the lower part of the wadi. Fine grained deposits caracterise the lower part of both wadis which may be explained by the down stream decline in energy.

2- The alluvial aquifers in both wadis show variations in thickness. Wadi Baysh and Wadi Habawnah have alluvium thicknesses ranging from 4 to 150m, and 3 to 54m, respectively. The surface deposits down to a depth of 28 m in borehole GO (total depth 150 m) are similar to the deposits in the upper part of Wadi Baysh.

In Wadi Baysh the aquifer resistivity ranges from 19 to 75 ohm-m and the thickness from 4 to 20m. In Wadi Habawnah the resistivity ranges from 33 to 121 ohm-m and the

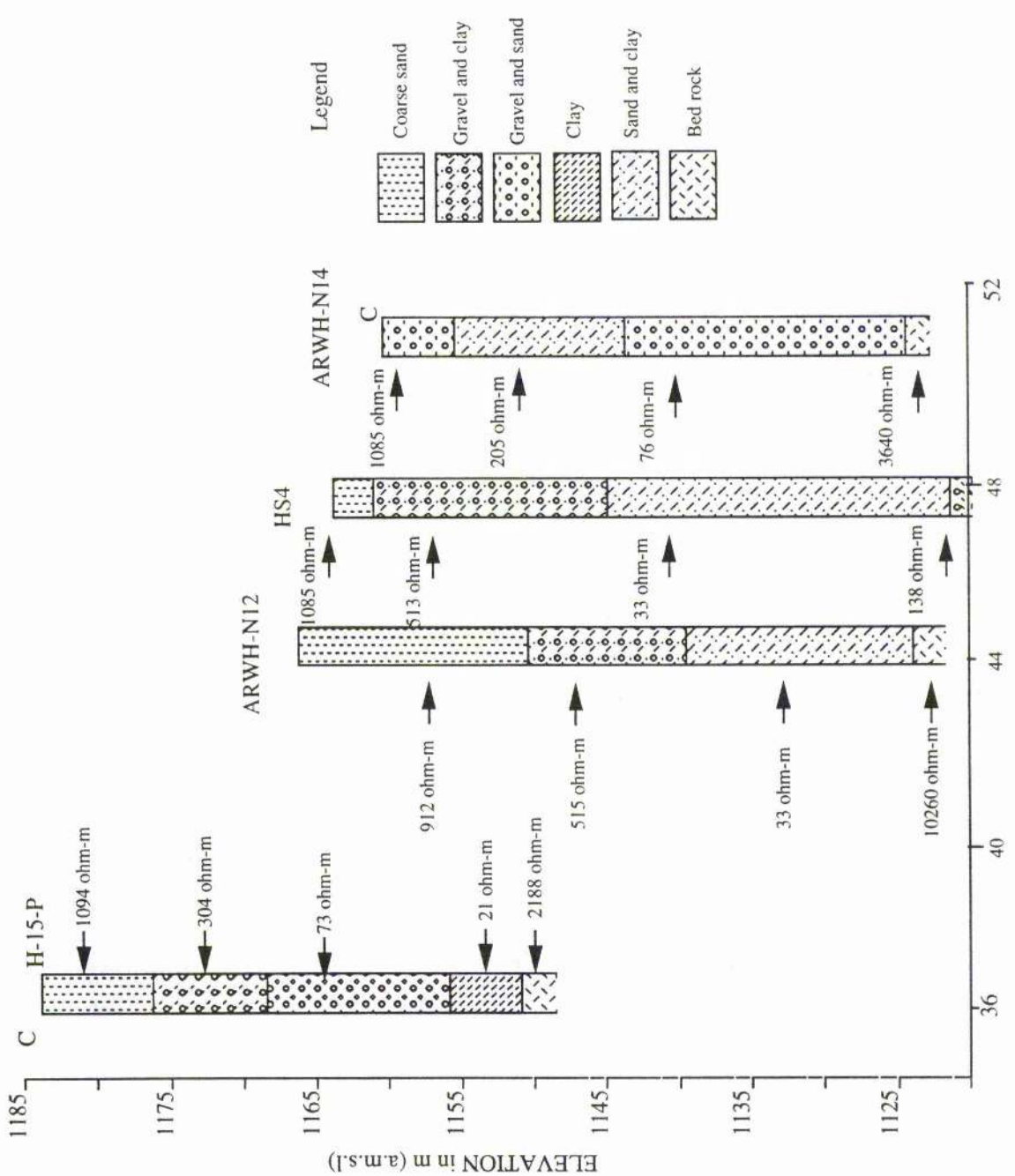

Figure 6.32 Lower part cross section of Wadi Habawnah along the line CD (Figure 6.16).

saturated zone thickness ranges from 7 to 22m. In Wadi Habawnah the five layer curves show higher values of resisitivity which result from a five layer section consisting of, at the top, dry gravel, underlain by dry sand and silt, unsaturated gravel and sand, the saturated zone of the aquifer and the fifth layer is bedrock.

6.4 Conclusion

Surface geophysical techniques have been used successfully in the ground water investigations of both wadis.

The resistivity and seismic refraction surveys confirmed that the thickness of the unconfined aquifer is between 8 and 35 m in Wadi Baysh while in Wadi Habawnah it is between 16 and 42 m. A confined aquifer is developed in the lower part of Wadi Baysh with a depth of 35m.

Resistivity and seismic caracteristics of wadi sediments including the aquifer zone and bedrock are summarised as below:

Wadi Baysh	P-Wave velocity (m s^{-1})	Resistivity (ohm-m)
Surface layer*	169-469	18 - 1549
Aquifer zone*	536-1736	23 - 120
Lower boundary of the aquifer**	***	3470 - 5423

Wadi Habawnah	P-Wave velocity (m s^{-1})	Resistivity (ohm-m)
Surface layer*	322-422	912 - 2269
Aquifer zone*	817 - 1817	25 - 125
Lower boundary of the aquifer**	2615 - 4615	3640 - 10260

* Gravel, sand, silty sand and clay
** Hard rocks (mostly metamorphic and igneous rocks)
*** Unknown

Questions relating to deposits and the depth to bedrock in areas underlain by thedeeper wadi sediments in the lower part of Wadi Baysh remain unanswered. It is important to know about the nature and extent of the unconsolidated sediments that comprise the bulk of the wadi deposits, and whether these materials are an important source of water. The present evidence suggests that wadi sediment has much potential for water supply in the middle and lower parts of both wadis. The alluvial layers are, at best, good

sources of ground water for domestic and farm use. The clay is relatively impermeable, and the fine- grained silty sand deposits will be unlikely sites for the development of productive wells.

CHAPTER SEVEN: THE RELATION BETWEEN THE HYDROGEOLOGICAL AND GEOELECTRICAL PARAMETERS OF THE WADI AQUIFERS

7.1 Introduction

In groundwater studies the longitudinal unit conductance (S_l) and transverse unit resistance (Tr) are powerful tools for aquifer interpretation. Full advantage is taken by combining thickness and electrical resistivity into a single variable, which is used as the basis for evaluation of aquifer properties such as transmissivity.

The physical correlation of the aquifer transmissivity and transverse resistance has been tackled over the past decade. Many contributions have been made to find relationships between the electrical resistivity of the aquifer and its hydrological conductivity, or between transverse resistance and transmissivity, using Vertical Electrical Sounding (VES).

Empirical relationships were obtained using various techniques, some by means of laboratory measurements on rock samples, and others by direct measurements in the field.

The correlation between hydraulic parameters and the corresponding electrical parameters has shown that high apparent formation factors generally correspond to high conductivity (Alger, 1966; Duprat *et al.*, 1970; Henriet, 1976; Kelly, 1977; Worthington, 1977a, b, c; Kosinsky and Kelly, 1981; Urish, 1981 and Ponzini *et al.*, 1984). An inverse relationship between electrical resistivity and hydraulic conductivity has been reported for a glacial outwash aquifer in central Illinois (Heigold *et al.*, 1978). This inverse relationship used data from only three test sites presenting broadly the same hydraulic conductivity but without an adequate knowledge of the porewater resistivity.

Schimschal (1970) indicated an inverse relationship between the above two parameters but for bedded dolomite and limestone with interbedded shale, siltstone and sandstone in New Mexico.

Ponzini *et al.* (1984) described the empirical function that connects the electrical transverse resistance with the hydraulic transmissivity of an aquifer in Toronto valley (Italy), consisting of both unconfined and confined aquifers, mainly of sand and gravel.

The aim of this chapter is to develop surface resistivity techniques for making

quantitative estimates of the water transmitting properties of the wadi floor deposits. A comparison will be made between the present study and that of Ponzini *et al.* (1984) in order to examine the possibility of finding analogous relationships for other aquifer systems.

As a part of the evaluation of the ground water resources in both wadis it provides a good opportunity to study the application of surface resistivity methods for both wadi aquifers, one a largely underdeveloped aquifer (Wadi Baysh) and the second a partially developed aquifer (Wadi Habawnah). Geophysical prospecting by means of Vertical Electrical Sounding (VES) is applied in exploration of the hydrogeology of both wadis in order to define the geometry of the aquifer systems. Aquifer electrical resistivities were determined for 16 and 14 vertical electrical soundings in Wadi Baysh and Wadi Habawnah, respectively (see Figure 6.15 and 6.16). The VES data are compared with well lithology and pumping test data (see Chapter 6).

7.2 Theoretical

Sir Niwas *et al.* (1981) show that, in steady state flow analyses, Darcy's law is analogous to Ohm's law. Darcy's law can be expressed as:

$$V = K\frac{dh}{dL} \tag{7.1}$$

where V is the velocity of the flow, K is the hydraulic conductivity, and $\frac{dh}{dL}$ is the hydraulic gradient. Ohm's Law, governing the flow of electricity through an electrical conductor, may be given as:

$$I = R^{-1}\frac{dE}{dS} \tag{7.2}$$

where I = the electric current (amperes) per unit cross-section of area, R = the resistance (ohms), and $\frac{dE}{dS}$ is the change in the electromotive force (voltage gradient) over unit distance. This analogy makes it possible to simulate the laminar flow of a viscous liquid through a porous medium by the flow of an electric current through a conductor. The voltage, E, is then analogous to the hydraulic head, h; the voltage gradient $\frac{dE}{dS}$ to the hydraulic gradient $\frac{dh}{dL}$, the current, I, to the flow velocity, V. Also the similarity may be noted between the electric current flow lines and the flow lines of a liquid. In addition,

there is similarity between lines of equal voltage and equipotential lines of flow of a liquid (a line in a two dimensional ground water flow field such that the total hydraulic head is the same for all points along the line).

Geoelectric parameters of aquifers were introduced by Maillet (1947) as Dar Zarrouk parameters. For a sequence of n horizontal, homogeneous, and isotropic layers of resistivity ρ_i and thickness h_i, the longitudinal unit conductance, S_i, and transverse unit resistance, T_r, are defined by

$$S_i = \sum_{i=1}^{n} \frac{h_i}{\rho_i} \tag{7.3}$$

and

$$Tr = \sum_{i=1}^{n} h_i \times \rho_i \tag{7.4}$$

Zohdy (1975) indicated that a geoelectric layer is described by two fundamental parameters; its resistivity, ρ_i, and its thickness, h_i, where the subscript, i, indicates the position of the layer in the section. From these two parameters the following variables can be derived as outlined by Zohdy (1975) as:

a - Longitudinal unit conductance, $S_i = \frac{h_i}{\rho_i}$ (7.5)

b - Transverse unit resistance $Tr = h_i \times \rho_i$ (7.6)

These parameters are important when they are used to describe a geoelectric section consisting of several layers. If current flows parallel to the bedding of the column (see Figure 7.1) and layers behave electrically as resistors connected in parallel, the total longitudinal unit conductance, S_i will be:

$$S_i = \sum_{i=1}^{n} \frac{h_i}{\rho_i} = \frac{h_1}{\rho_1} + \frac{h_2}{\rho_2} + \ldots \frac{h_n}{\rho_n} \tag{7.7}$$

If the current flows vertically through the column (see Figures 7.1 and 7.2), then the layers behave as resistors connected. The total transverse resistance, T_r will be:

$$Tr = \sum_{i=1}^{n} h_i \times \rho_i = h_1 \times \rho_1 + h_2 \times \rho_2 \ldots\ldots\ldots + h_n \times \rho_n \tag{7.8}$$

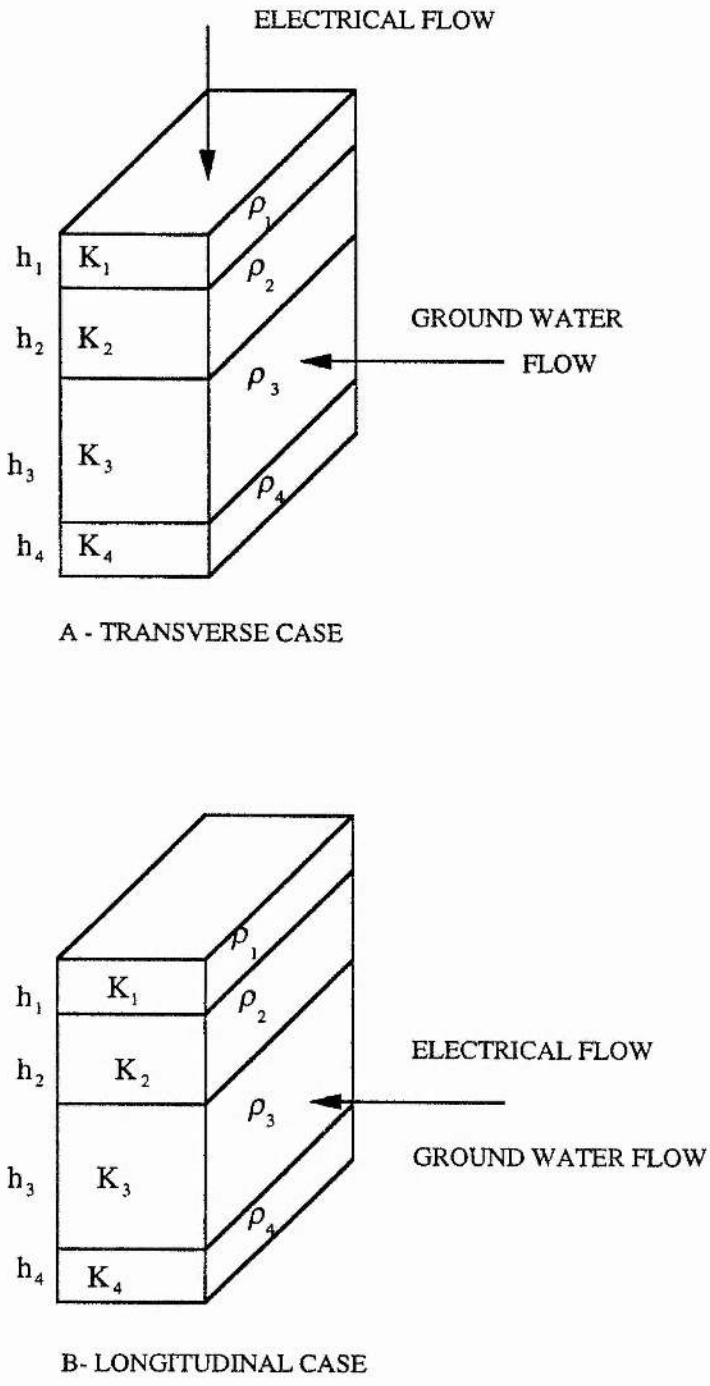

Figure 7.1 Layered models of transverse case (A) and longitudinal case (B), adapted from Kelly and Reiter (1984).

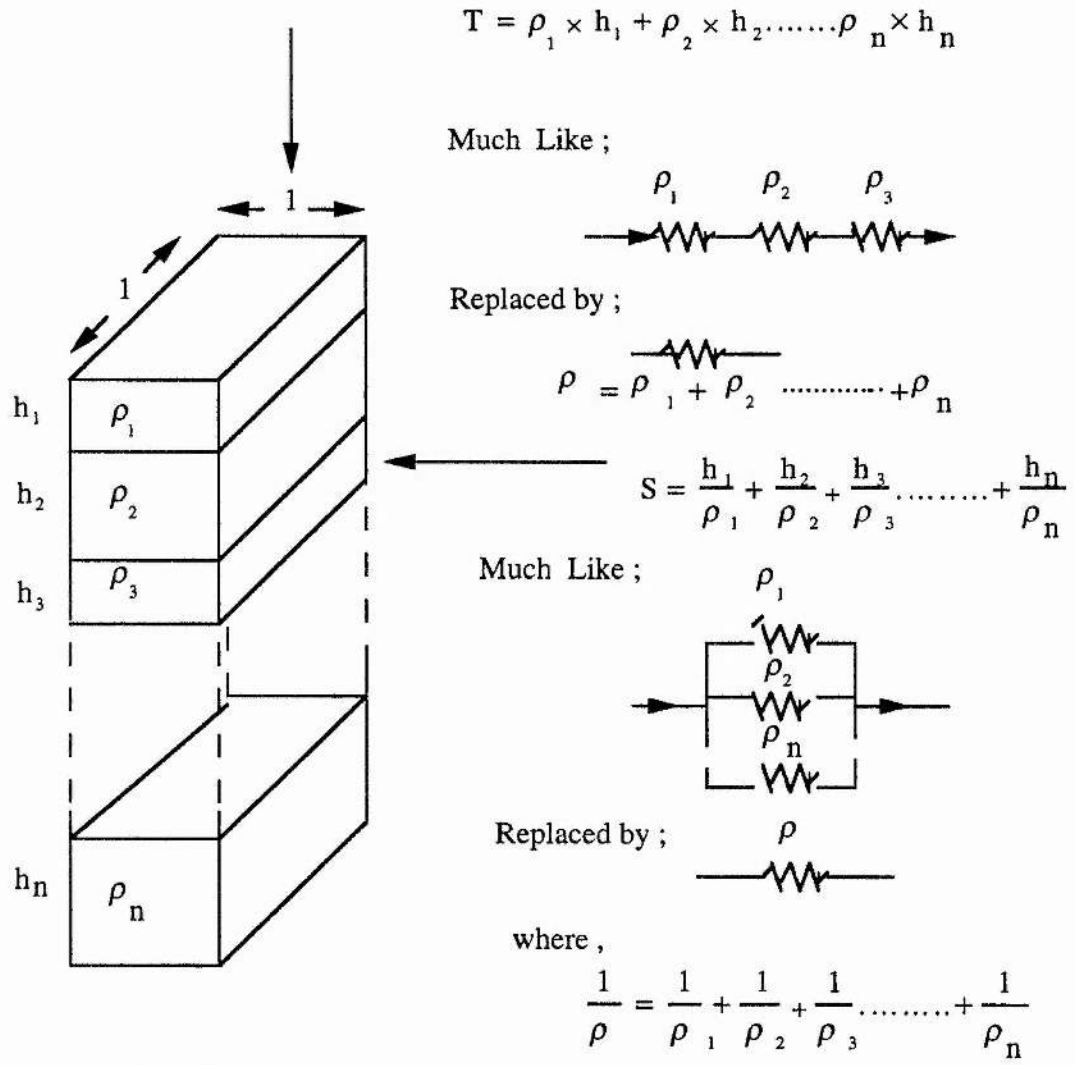

Figure 7.2 Geoelectric parameters (adapted from Zohdi, 1975).

It is analogous to transmissivity used in ground water hydrology, where K_i is the hydrologic conductivity of the ith layer and h_i is the thickness as below:

$$T_i = K_1 \times h_1 + K_2 \times h_2 \ldots\ldots + K_i \times h_i \text{ (Freeze, 1984)} \qquad (7.9)$$

As has been shown, the Dar Zarrouk parameter readily estimates the longitudinal unit conductance, S_i, for the saturated layer by the relationship in equation 7.5.

The saturated layer of the study area is of low resistivity and is sandwiched between higher resistivity layers of the unsaturated zone above and the bedrock below. The longitudinal conductance of the dry layer and of bedrock are very small, and are commonly ignored. Since the pumping test analyses are effectively to determine the transmissivity of the saturated layer, the geoelectric parameter (transverse resistance $Tr = h_i \times \rho_i$) was examined for the same layer.

7.3 Background

7.3.1 Geology and Hydrogeology of the Area

In the present chapter the author refers to the results of the geology, VES data, pumping tests and chemical and physical characteristics of water given in previous chapters, from which the following data are used:

1- Geophysical prospecting consisted of 30 Vertical Electrical Soundings (VES) using the Schlumberger configuration with a maximum $\frac{AB}{2}$ spacing = 130m.

2- Lithological data from well inventory surveys on 80 wells and 17 boreholes.

3- The aquifer hydraulic parameters obtained from 18 pumping tests (large diameter wells).

4- Chemical and physical characteristics of water, with particular reference to the temperature and electrical conductivity from 80 dug wells.

The sediments of both wadis consist of two to four layers (see Table 6.12, Chapter 6). The pumping test data of Chapter 5 are summarised in Table 5.6. The impervious Precambrian crystalline rocks of Wadi Habawnah and the upper part of Wadi Baysh form the internal and lower limits of the sandy gravel aquifer which contains clay with various thicknesses, according to the well inventory. In the middle and lower parts of Wadi Baysh practically impervious clays form the lateral and lower limits of the sandy gravel and silty

sands which form the multi-aquifer systems (see Chapter 8 Section one). The saturated thickness ranged between 11 and 37m in Wadi Baysh while in Wadi Habawnah the range was between 12 and 21m. The unconfined aquifer is the main aquifer in both wadis.

7.3.2 Vertical Electrical Sounding (VES) Results

Sixteen VES were made in Wadi Baysh and 14 in Wadi Habawnah, using maximum Schlumberger array spacings of 75 to 130m, principally to investigate the impervious layers at the bottom of the aquifer system. The surveys were carried out near 18 large diameter wells on which pumping tests had been run.

The VES data were interpreted by the Resix program (see Chapter 6, Section two). The computer-oriented direct or inverse interpretation methods for the VES are capable of resolving the thicknesses and resistivities of various subsurface layers from surface resistivity measurements. These are free from human bias which is always present in the conventional curve matching techniques. From a hydrogeological standpoint the interpretations have been tested utilising the lithology of the nearby wells. The agreement between the theoretical curves, the VES field data and the lithological information of the dug well nearby can be considered satisfactory for almost all the test sites (see Table 6.14).

7.4 Aquifer Parameters Estimation Using VES in Both Wadis

The aquifer parameters may be considered in two main terms: the hydraulic conductivity K (or permeability) and the transmissivity (T).

In single aquifer of thickness h, the transmissivity T may be calculated as follows:

$$T = K \times h \qquad (7.10)$$

Pump testing is an accurate practical method to determine this parameter (Chapter 5). Since there is a limited number of wells in the study area, the author will use the empirical relationships between transmissivity and electrical resistivity techniques. The Resix program was used to compute the Dar Zarrouk parameters (transverse resistance and longitudinal conductance) for all of the interpreted layers (see Table 7.1, Appendices 6A and 6B, Chapter 6 and Section two). Since the saturated thicknesses of the aquifers were determined, the author considered their parameters in both wadis to be correlated with

Table 7.1 Resix computer analysis of VES data and computed geoelectrical parameters of the unconfined aquifers of Wadi Baysh and Wadi Habawnah

Sample No.	Resistivity ohm-m	Thickness meters	Elevation meters	Long. Cond Siemens	Trans. Res. Ohm-m^2
TRWB-N1			130		
	586	4	126	0.0066	2255
	53	4	122	0.0784	220
	1567				
TRWB-N2			128		
	595	5	123	0.0084	2975
	75	9	114	0.1200	675
	3543				
TRWB-N3			107		
	217	2	105	0.0093	434
	623	4	101	0.0064	2491
	58	13	88	0.2230	756
	3470				
TRWB-N4			100		
	129	2	98	0.0146	242
	108	2	96	0.0219	256
	51	14	81	0.2840	740
	4700				
TRWB-N5			96		
	130	2	94	0.0188	317
	100	4	89	0.0409	413
	53	16	73	0.3020	844
	5423				
TRWB-6			93		
	98	1	92	0.0099	95
	1549	5	87	0.0032	778
	13	14	73	1.0400	178
	75				
TRWB-7			86		
	541	2	84	0.0044	1278
	191	7	76	0.0380	1382
	28	14	62	0.5120	408
	60				
TRWB-8			70		
	103	4	66	0.0411	434
	245	10	56	0.0405	2423
	50	13	43	0.2550	647
	119				
TRWB-9			68		
	70	3	65	0.0375	184
	155	5	61	0.0304	729
	35	13	48	0.3700	448
	66	7	41	0.1070	463
	115				
TRWB-10			55		
	24	5	50	0.1870	109
	104	14	37	0.1320	1442
	71	11	26	0.1560	784
	334				

Continued on next page

Table 7.1 continued

Sample No.	Resistivity ohm-m	Thickness meters	Elevation meters	Long. Cond Siemens	Trans. Res. Ohm-m^2
TRWB-11			54		
	132	4	50	0.0304	526
	305	9	41	0.0294	2749
	47	21	20	0.4440	965
	1715				
TRWB-12			52		
	18	8	44	0.4300	138
	82	10	34	0.1210	823
	19	16	18	0.8820	307
	138				
TRWB-13			87		
	32	5	82	0.1460	152
	144	19	64	0.1300	2696
	34	10	54	0.2940	333
	370				
TRWB-14			60		
	23	4	56	0.1760	91
	39	17	39	0.4330	667
	52	14	25	0.2690	728
	257				
TRWB-15			54		
	35	3	51	0.0992	121
	74	19	32	0.2570	1403
	24	10	22	0.4200	237
	177				
TRWB-16			45		
	105	6	39	0.0571	630
	11	5	34	0.4630	54
	745	10	24	0.0134	7447
	31	6	18	0.1950	184
	11				

Wadi Habawnah

Sample No.	Resistivity ohm-m	Thickness meters	Elevation meters	Long. Cond Siemens	Trans. Res. Ohm-m^2
ARWH-N1			1280		
	1268	4	1276	0.0032	5106
	1142	4	1272	0.0036	4628
	57	7	1265	0.1280	416
	6535				
ARWH-N2			1275		
	1314	4	1271	0.0030	5094
	385	7	1264	0.0185	2740
	58	6	1259	0.0941	321
	2950				
ARWH-N3			1265		
	2155	2	1263	0.0010	4738
	414	3	1260	0.0060	1035
	1439	8	1253	0.0052	10810
	47	5	1248	0.1110	249
	772				
ARWH-N4			1245		
	1358	7	1238	0.0051	9388
	705	7	1231	0.0099	4933
	42	16	1216	0.3670	654
	3457				

Continued on next page

Table 7.1 continued

Sample No.	Resistivity ohm-m	Thickness meters	Elevation meters	Long. Cond Siemens	Trans. Res. Ohm-m^2
ARWH-N5			1255		
	1783	7	1248	0.0039	12483
	1325	6	1242	0.0045	7950
	63	12	1230	0.1910	753
	8	8	1222	1.0500	61
	1955				
ARWH-N6			1225		
	1508	6	1219	0.0041	9308
	345	7	1212	0.0191	2273
	56	16	1196	0.2900	926
	6167				
ARWH-N7			1210		
	2233	3	1207	0.0012	5762
	2269	7	1200	0.0032	16201
	108	18	1182	0.1700	1983
	5562				
ARWH-N8			1205		
	1803	3	1202	0.0015	4803
	721	3	1200	0.0039	2024
	49	23	1174	0.4600	1107
	5110				
ARWH-N9			1195		
	1914	3	1192	0.0014	5100
	1562	7	1185	0.0047	11455
	33	13	1172	0.3980	425
	5824				
ARWH-N10			1180		
	1945	2	1178	0.0013	4820
	617	4	1174	0.0063	2381
	1252	7	1167	0.0053	8233
	121	12	1155	0.1010	1486
	3191				
ARWH-N11			1170		
	1095	2	1168	0.0021	2503
	305	10	1157	0.0342	3186
	73	22	1136	0.2960	1595
	2188				
ARWH-N12			1142		
	912	3	1139	0.0038	3119
	515	16	1123	0.0305	8108
	33	23	1100	0.7070	751
	10260				
ARWH-N13			1138		
	1540	2	1136	0.0013	2987
	513	13	1123	0.0253	6664
	34	19	1104	0.5520	657
	138				
ARWH-N14			1125		
	1085	5	1120	0.0044	5206
	205	12	1108	0.0595	2499
	75	20	1088	0.2640	1510
	3640				

aquifer parameters determined from large diameter well pumping tests (see Table 5.6, Chapter 5).

The VES investigation indicated that the main aquifer of both wadis is unconfined. The tests were made at a distance of 3 to 20m from the pumping test wells which gave transmissivities ranging between 75 and 738 m^2/day (see Table 5.6). In Table 7.1 are presented the VES interpretations derived from the Resix program, utilising the successive resistivities and thicknesses as input data (see Chapter 6, section two). From the geological standpoint the interpretations have been tested utilising the borehole lithology of the nearby wells. The agreement between the VES field data and the well lithology nearby show good correlation for almost all of the test sites.

The corresponding geoelectrical parameters of the saturated deposits shows that transverse resistance is between 212 and 1533 ohm-m while the longitudinal conductance is 0.075 to 0.559 siemens. The aquifer resistivity shows a range of 16-120 ohm-m (Table 6.14). Consequently, the true saturated layer resistivity is identified since the thicknesses of these layers are known through the well inventory and borehole lithology (see Chapter 6).

7.5 Corrected Transverse Resistance Versus Transmissivity

Mendolson and Cohen (1982) indicated that, when the layer is isotropic or isotropic equivalent, the average resistivity to current flowing across the bedding (transverse resistivity) may be considered equal to the one flowing parallel to the bedding. The hydraulic transmissivity data of the dug wells, calculated from the large diameter pumping tests, also assume that the hydraulic flow takes place only in the X and Y directions, in other words parallel to the boundaries of the aquifer layer.

Taking into account the effects of porewater resistivity of the saturated layer on the correlation between an electrical parameter and the corresponding hydraulic parameter, Ponzini *et al,* (1984) divided the transverse resistance by porewater resistivity (ρ_w) to obtain a corrected transverse resistance. This is anologous to the apparent formation factor of the saturated layer multiplied by its thickness. In Table 7.2, the data, the measured and calculated parameters that allowed the plotting of the points of Figure 7.3, are given.

In Figure 7.3 the corrected transverse resistance is plotted against the hydraulic

Table 7.2 Field data of the pumping tests and VES data of Wadi Baysh and Wadi Habawnah

Wadi Baysh

WELL No	Location in the wadi	SATURATED THICKNESS H (meters)	WELL DEPTH D (meters)	WATER TEMP. ℃	PORE WATER RESISTIVITY ρ_w ρ_w (Standard 25 °C) ohm-m	ρ_w** at well Temp. ohm-m	TRANSMISSIVITY m^2/DAY T	V.E.S NO.	DISTANCE BETWEEN WELL AND V.E.S (meters)	COMPUTED PARAMETERS-V.E.S INTERPRETATION h meter	ρ (RESISTIVITY) Ohm-m	ρ(TRANSVERSE RESISTANCE(Tr) Ohm-m^2	Normalised Resistivity $Tr/\rho_w = Trn$	LONG-COND ρxh Siemens
BU1	UPPER	2	7	32	21	18	190	TRWB-N1	3	4	53	212	14	0.075
BU2	UPPER	6	12	33	29	24	156	TRWB-N2	5	9	75	675	45	0.120
BU3	UPPER	13	20	32	26	22	87	TRWB-N3	20	13	58	754	50	0.224
BM5	MIDDLE	11	24	32	22	18	75	TRWB-N8	10	13	50	650	43	0.260
BM7	MIDDLE	13	30	31	14	12	147	TRWB-N9	10	7	65	455	30	0.108
BM12	MIDDLE	21	40	32	14	12	150	TRWB-N12	10	17	16	272	18	1.063
BL16	LOWER	37	60	31	6	5	130	TRWB-N15	10	10	24	240	16	0.417

Wadi Habawnah

WELL No	Location in the wadi	SATURATED THICKNESS H (meters)	WELL DEPTH D (meters)	WATER TEMP. ℃	PORE WATER RESISTIVITY PW ρ_w (Standard 25 °C) ohm-m	ρ_w** at well Temp. ohm-m	TRANSMISSIVITY T m^2/DAY	V.E.S STATION NO.	DISTANCE BETWEEN WELL AND V.E.S (meters)	COMPUTED PARAMETERS-V.E.S INTERPRETATION h meter	ρ (RESISTIVITY) Ohm-m	ρ(TRANSVERSE RESISTANCE(Tr) Ohm-m^2	Normalised Resistivity $Tr/\rho_w = Trn$	LONG-COND ρxh Siemens
HB2	UPPER	7	16	27	6	6	207	ARWH-N1	6	7	56	392	65	0.125
HB3	UPPER	4	15	27	5	5	371	ARWH-N2	8	6	58	348	58	0.103
HB6	UPPER	1	17	27	8	7	190	ARWH-N3	10	5	47	235	39	0.106
MT1	MIDDLE	18	31	24	7	7	285	ARWH-N4	10	15	42	630	105	0.357
MT9	MIDDLE	5	33	27	7	7	520	ARWH-N6	10	16	56	896	149	0.286
GF2	MIDDLE	22	30	28	7	7	738	ARWH-N7	3	18	108	1944	324	0.167
GF5	MIDDLE	11	24	27	7	7	281	ARWH-N8	3	22	49	1078	180	0.449
NG1	MIDDLE	12	24	27	7	7	337	ARWH-N9	3	13	33	429	72	0.394
MR	LOWER	13	27	27	8	7	652	ARWH-N10	3	12	120	1440	240	0.100
HS2	LOWER	20	37	30	2	2	734	ARWH-N11	16	21	73	1533	256	0.288
HS4	LOWER	20	38	30	3	3	254	ARWH-N13	4	19	34	646	108	0.559

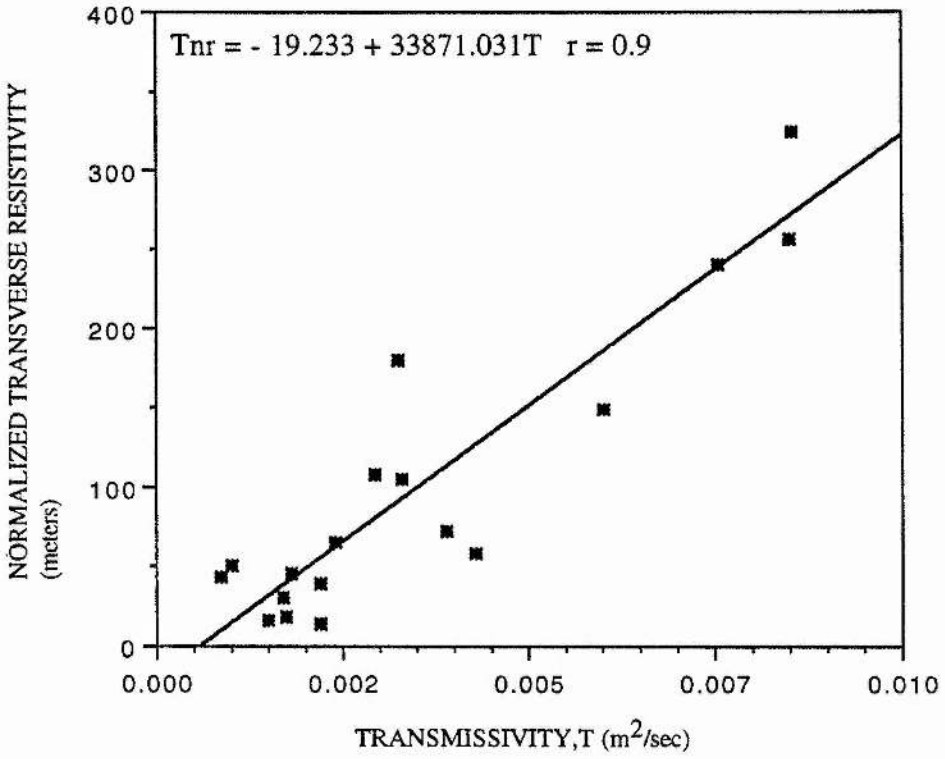

Figure 7.3 Normalized transverse resistivity verses transmissivity for both wadis.

transmissivity obtained by means of VES and pumping tests, respectively, for the alluvial aquifers of Wadi Baysh and Wadi Habawnah. The relationships between normal transverse resistance of the layers multiplied by the thicknesses of the layers are strong for the aquifers of both Wadis. The investigated range of values is sufficiently representative since the linear relationship between the two parameters (T_{rn} and T) shows strong correlation of r = 0.9. This reflects that fact that the equations that govern the flow of water and the flow of electrical current in a porous medium are similar. It indicates that the hydraulic conductivity is high when the flow of the water and of the electrical current move along the same paths. The empirical equation developed for wadi floor sediments is:

$$T_{rn} = -19.233 + 3.3871 \times 10^4 T \qquad (7.11)$$

where T_{rn} is the corrected transverse resistance and T is the transmissivity in m^2/sec

T_{rn} = F (formation factor) x h (the saturated thickness) expressed in metres. This equation is physically reliable in the wadi fill aquifers from which the relationship has been obtained using parameters computed directly in the field.

Applying the empirical relationship elsewhere in the wadis makes it possible to estimate the hydraulic parameters of the aquifer at sites where there are no existing wells. In addition it was possible to determine the aquifer transmissivity at different water levels assuming that the saturated resistivity of fresh water is constant.

In the rainy season, the maximum saturated thickness of the unconfined aquifer reaches to between 1 and 2m below the ground surface in the upper and middle section of both wadis. In the lower sections the saturated layer reaches up to between 2 to 3m below surface in Wadi Habawnah, while in Wadi Baysh it falls to 4 to 5m below ground surface (Farmer's Communication).

Ground water evaporation occurs when the depth to the water table is between 0.5 and 2m (Bower, 1978). The saturated thickness in the upper and the middle sections of both wadis was 2m or less on average below the ground surface. However, in the lower part of the wadis the saturated depth below the ground surface is at least 3m in Wadi Habawnah and 5m in Wadi Baysh and no direct evaporation occurs.

Using the empirical relationships between the transverse resistance and

transmissivity measurements in both wadis, and using the assumed maximum saturated depth, a new approach was used to estimate the hydrological parameters of the unconfined aquifers during the high rain season.

Case - 1 There are VES data but no pumping test data available for nearby sites. Using the above empirical relationship, the transmissivity at the VES site is calculated from the transverse resistivity. Table 7.3 shows the calculated values of the transmissivity for eight locations in Wadi Baysh and three sites in Wadi Habawnah, where no existing pumping wells occur.

Case - 2 Is determining the variations in transmissivity as a result of the water table fluctuation. Table 7.4 shows the maximum transmissivity of the aquifer during the rainy season. The transmissivity can be estimated during the rainy season as the product of the maximum saturated thickness multiplied by the aquifer resistivity, assuming the fresh water resistivity of the aquifer is constant.

Some data show substantial differences between the estimated values of the aquifer transmissivity in the recharge season and the pumping test predictions. However, the values are still within the unconfined aquifer transmissivity range.

As 18 values of the transmissivity values versus VES (T_{rn}) show a range of variation between 6 and 28%, it is concluded that electrical resistivity determined from the VES method can be used to forecast the hydraulic parameters of an aquifer in different seasons with or without existing wells in the area. Such an approach will help to minimise the time of the investigation and the cost of the drilling by giving general information about the aquifer transmissivity in the region and permit identification of the locations for the digging of wells.

7.6 Comparison Between the Ponzini *et al.* (1984) Approach and that of the Present Study

The present method is compared with the Ponzini *et al.* (1984) method since there are similarities between the aquifers of the Baysh-Habawnah study area and those of the Tronto valley. These similarities may be summarised as follows:

Table 7.3 Determination of the aquifer parameters based on the relationship between the hydrogeological and geoelctrical parameters of the aquifer

Wadi Baysh

WELL No	Location in the wadi	SATURATED THICKNESS H (meters)	WELL DEPTH D (meters)	WATER TEMP. ℃	PORE WATER RESISTIVITY ρW: ρ_W (Standard 25 °C) ohm-m	ρ_{W}** at well Temp. ohm-m		TRANSMISSIVITY m^2/DAY T	V.E.S NO.	DISTANCE BETWEEN WELL AND V.E.S (meters)	COMPUTED PARAMETERS-V.E.S INTERPRETATION: h meter	P (RESISTIVITY) Ohm-m	RT(TRANSVERSE RESISTANCE(RT) Ohm-m^2	Normalised Resistivity Tr/ρW = Tm	LONG-COND ρ_{xh} Siemens
BU1	UPPER	2	7	32	21	18		190	TRWB-N1	3	4	53	212	14	0.075
BU2	UPPER	6	12	33	29	24		156	TRWB-N2	5	9	75	675	45	0.120
BU3	UPPER	13	20	32	26	22		87	TRWB-N3	20	13	58	754	50	0.224
&	UPPER				*	21	!	170	TRWB-N4		14	51	714	48	0.275
&	UPPER				*	21	!	193	TRWB-N5		16	53	848	57	0.302
&	UPPER				*	21	!	80	TRWB-N6		14	13	182	12	1.077
&	UPPER				*	21	!	116	TRWB-N7		14	28	392	26	0.500
BM5	MIDDLE	11	24	32	22	18		75	TRWB-N8	10	13	50	650	43	0.260
BM7	MIDDLE	13	30	31	14	12		147	TRWB-N9	10	7	65	455	30	0.108
&	MIDDLE				*	14	!	182	TRWB-N10		11	71	781	52	0.155
&	MIDDLE				*	14	!	206	TRWB-N11		20	46	920	61	0.435
BM12	MIDDLE	21	40	32	14	12		150	TRWB-N12	10	17	16	272	18	1.063
&	LOWER				*	5	!	107	TRWB-N13		10	34	340	23	0.294
&	LOWER				*	5	!	173	TRWB-N14		14	52	728	49	0.269
BL16	LOWER	27	60	31	6	5		130	TRWB-N15	10	10	24	240	16	0.417
QO	LOWER	53	75	31	6	5		119	TRWB-N16	10	6	31	186	12	0.194

Wadi Habawnah

WELL No	Location in the wadi	SATURATED THICKNESS H (meters)	WELL DEPTH D (meters)	WATER TEMP. ℃	PORE WATER RESISTIVITY ρW: ρ_W (Standard 25 °C) ohm-m	ρ_{W}** at well Temp. ohm-m		TRANSMISSIVITY T m^2/DAY	V.E.S STATION NO.	DISTANCE BETWEEN WELL AND V.E.S (meters)	COMPUTED PARAMETERS-V.E.S INTERPRETATION: h meter	P (RESISTIVITY) Ohm-m	RT(TRANSVERSE RESISTANCE(RT) Ohm-m^2	Normalised Resistivity Tr/ρW=Tm	LONG-COND ρ_{xh} Siemens
HB2	UPPER	7	16	27	6	6		207	ARWH-N1	6	7	56	392	65	0.125
HB3	UPPER	4	15	27	5	5		371	ARWH-N2	8	6	58	348	58	0.103
HB6	UPPER	1	17	27	8	7		190	ARWH-N3	10	5	47	235	39	0.106
MT1	MIDDLE	18	31		7	7		285	ARWH-N4	10	15	42	630	105	0.357
H-7-B	MIDDLE	23	35	27	7	7	!	370	ARWH-N5	5	12	63	756	126	0.190
MT9	MIDDLE	5	33	27	7	7		520	ARWH-N6	10	16	56	896	149	0.286
GF2	MIDDLE	22	30	28	7	7		738	ARWH-N7	3	18	108	1944	324	0.167
GF5	MIDDLE	11	24	27	7	7		281	ARWH-N8	3	22	49	1078	180	0.449
NG1	MIDDLE	12	24	27	7	7		337	ARWH-N9	3	13	33	429	72	0.394
MR	LOWER	13	27	27	8	7		652	ARWH-N10	3	12	120	1440	240	0.100
HS2	LOWER	20	37	30	2	2		734	ARWH-N11	16	21	73	1533	256	0.288
&	LOWER				*	3	!	372	ARWH-N12		23	33	759	127	0.697
HS4	LOWER	20	38	30	3	3		254	ARWH-N13	4	19	34	646	108	0.559
&	LOWER				*	3	!	687	ARWH-N14		20	75	1500	250	0.267

& Indicates no existing well but resistivity station

*Predicted based on the average value of the wells

ρ_{W}**=Pat25/1+(0.025*(T-25) (Keller &Frischknecht,1966)

! Calculated based on the following equation Trn(Normalised transverse resistivity) = -19.233 + 3.3871×10^{4}xT the product multiply (24*60*60) to get T= m^2/day

Table 7.4 An new analysis approach of to calculate the hydrological parameters of unconfined aquifers consisting of maximum saturated zone during high rain season using VES data

WADI BAYSH		Saturated Thickens in the Rainy Season					Pumping test prediction		RATIO OF DIFFERENCE BETWEEN
WELL	V.E.S	Location in the Wadi	SATURATED THICKNESS H	RESISTIVITY OF THE SATURATED THICKNESS (P)	CORRECTED TRANSVERSE* RESISTANCE OF THE SATURATED THICKNESS (Tr)	TOTAL AQUIFER TRANSMISSIVITY T (CALCULATED)**	HYDRAULIC CONDUCTIVITY CALCULATED	TOTAL AQUIFER TRANSMISSIVITY T	V.E.S ESTIMATION OF (Tr) AND PUMPING TESTS ESTIMATION OF (T)
No	NO.		(meters)	Ohm-m	Ohm-m^2	m^2/day	m/day	m^2/day	%
BU1	TRWB-N1	UPPER	5	53	18	94	95	475	-67
BU2	TRWB-N2	UPPER	10	75	50	177	26	260	-19
BU3	TRWB-N3	UPPER	18	58	70	227	7	130	27
BM5	TRWB-N8	MIDDLE	22	50	73	236	7	151	22
BM7	TRWB-N9	MIDDLE	28	65	121	359	11	316	6
BM12	TRWB-N12	MIDDLE	38	16	41	152	7	274	-28
BL16	TRWB-N15	LOWER	55	24	88	274	3	190	18

WADI HABAWNAH		Saturated Thickness in the Rainy Season					pumping test prediction		RATIO OF DIFFERENCE BETWEEN
WELL	V.E.S	Location in the Wadi	SATURATED THICKNESS H	RESISTIVITY OF THE SATURATED THICKNESS (P)	CORRECTED TRANSVERSE* RESISTANCE OF THE SATURATED THICKNESS (Tr)	TOTAL AQUIFER TRANSMISSIVITY T (CALCULATED)**	HYDRAULIC CONDUCTIVITY CALCULATED	TOTAL AQUIFER TRANSMISSIVITY T	V.E.S ESTIMATION OF (Ttr) AND PUMPING TESTS ESTIMATION OF (T)
No	NO.		(meters)	Ohm-m	Ohm-m^2	m^2/day	m/day	m^2/day	%
HB2	ARWH-N1	UPPER	14	56	131	382	29	406	-3
HB3	ARWH-N2	UPPER	12.5	58	121	357	74	929	-44
HB6	ARWH-N3	UPPER	15	47	118	349	48	713	-34
MT1	ARWH-N4	MIDDLE	29	42	203	567	17	487	8
MT9	ARWH-N6	MIDDLE	31	56	289	787	27	849	-4
GF2	ARWH-N7	MIDDLE	28	108	504	1335	39	1092	10
GF5	ARWH-N8	MIDDLE	22	49	180	507	18	396	12
NG1	ARWH-N9	MIDDLE	22	33	121	358	28	608	-26
MR	ARWH-N10	LOWER	23	120	460	1222	54	1249	-1
HS2	ARWH-N11	LOWER	33	34	187	526	37	1226	-40
HS4	ARWH-N13	LOWER	34	75	425	1133	12	408	47

* * calculated based on the developed equation in the area where $Trn = -19.233 + 3.3871 \times 10^4 \times T$

* Corrected transverse Resistance of the saturated thickness (Tr) assuming the average well temperature of Wadi Baysh is 15 °C and Wadi Habawnah is 16 °C

1- The aquifers are unconfined in both wadis, consisting mainly of sand and gravel which are similar to the aquifer lithology of the Tronto valley

2- The transverse resistance values for all sites of the saturated layer were normalised by dividing their values by the average value of the pore water resistivity of the aquifer.

3- The transverse resistance of the aquifers of Wadi Habawnah and Wadi Baysh and that found by Ponzini *et al.* in Tronto valley aquifer are the average transverse resistance times the aquifer thickness.

Ponzini *et al.* (1984) developed an empirical function between the transverse electrical resistance of confined and unconfined aquifers (in the March Region, Tronto River, in Italy) and corresponding hydraulic transmissivities. These values of transverse (Tr) resistance were divided by ρ_w to correct for the effect of their porewater resistivities. The empirical relationship for the unconfined aquifer was given by:

$$T_{rn} = a\,T^{0.577} + b \quad , \tag{7.12}$$

where T_{rn} (is corrected transverse resistance) $= \dfrac{Tr}{\rho_w}$, (7.13)

$$a = 3.698 \times 103(s^{0.5777} \times m^{-0.154}) \tag{7.14}$$

and T is the transmissivity in m^2 / sec, and $b = 2.65 \times 10$

For the confined aquifer they derived the equation:

$$T_{rn} = 40.22 \text{ x } T^{0.577} + 17.2 \tag{7.15}$$

These equations are physically reliable only within a transmissivity domain that ranges from 1.4×10^{-4} m^2/sec to 140×10^{-4} m^2/sec. Within this transmissivity range T_{rn} values computed from equation 7.12 differ from the corresponding ones computed from equation 7.15 by less than 10%. The data for the corrected transverse resistance values and the corresponding transmissivities were plotted on a bilogarithmic diagram (see Figures 7.4 and 7.5).

Ponzini *et al.* (1984) indicated that the relationship obtained is curve to linear and direct in the sense that by increasing one parameter the other one also increases. They did not explain in their papers how they evaluated the parameters a and b.

In Figure 7.6 and Table 7.5, two relationships are shown between corrected

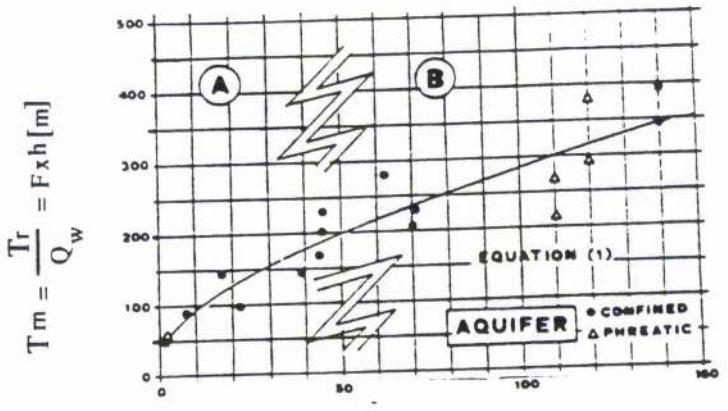

Figure 7.4 Corrected transverse resistance versus transmissivity, plotted on a linear scale (after Ponzini *et al*, 1984).

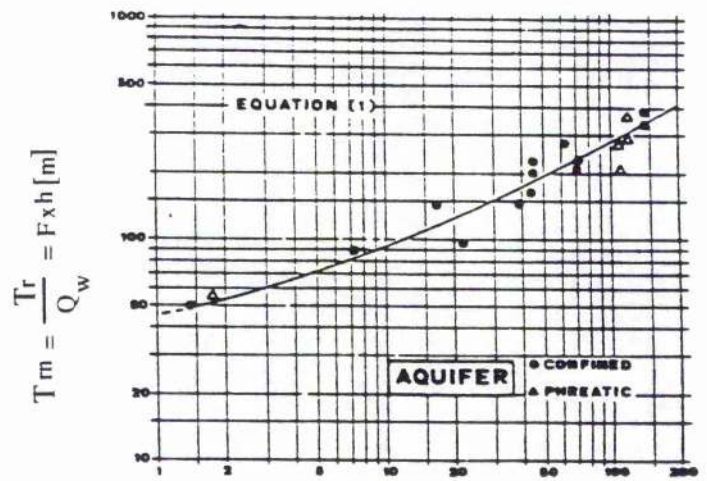

Figure 7.5 Graph to show the corrected transverse resistance versus transmissivity, plotted on log-log scale (after Ponzini *et al*, 1984).

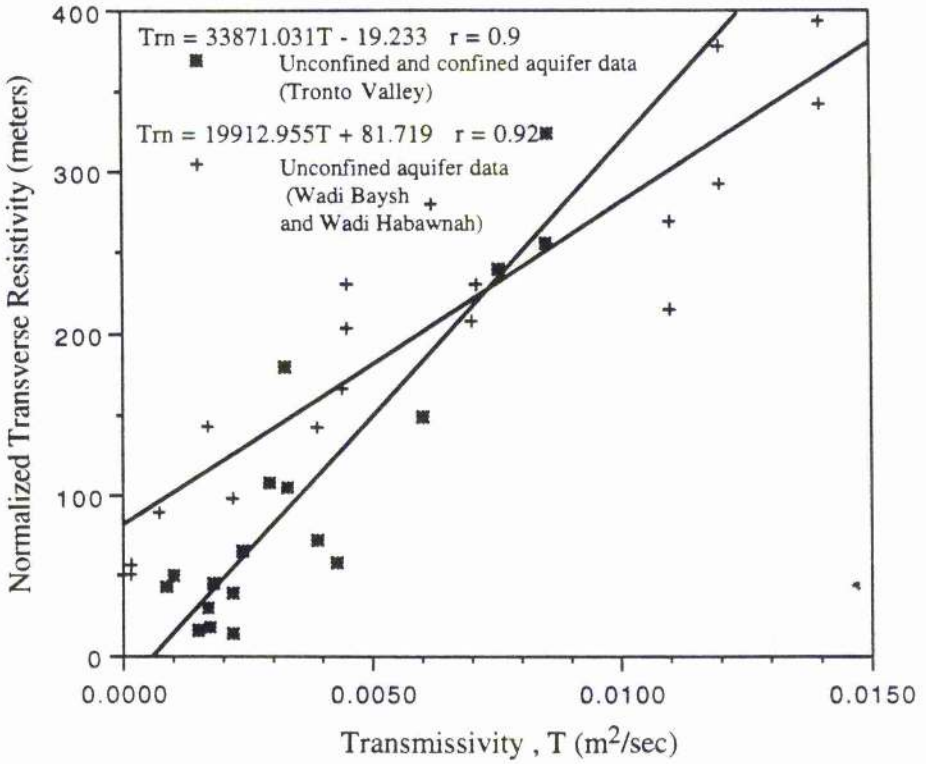

Figure 7.6 Field measurement plots of normalized transverse resistance and transmissivity from both Wadis Baysh and Habawnah and Tronto valley of Italy (After Ponzini et al,1984).

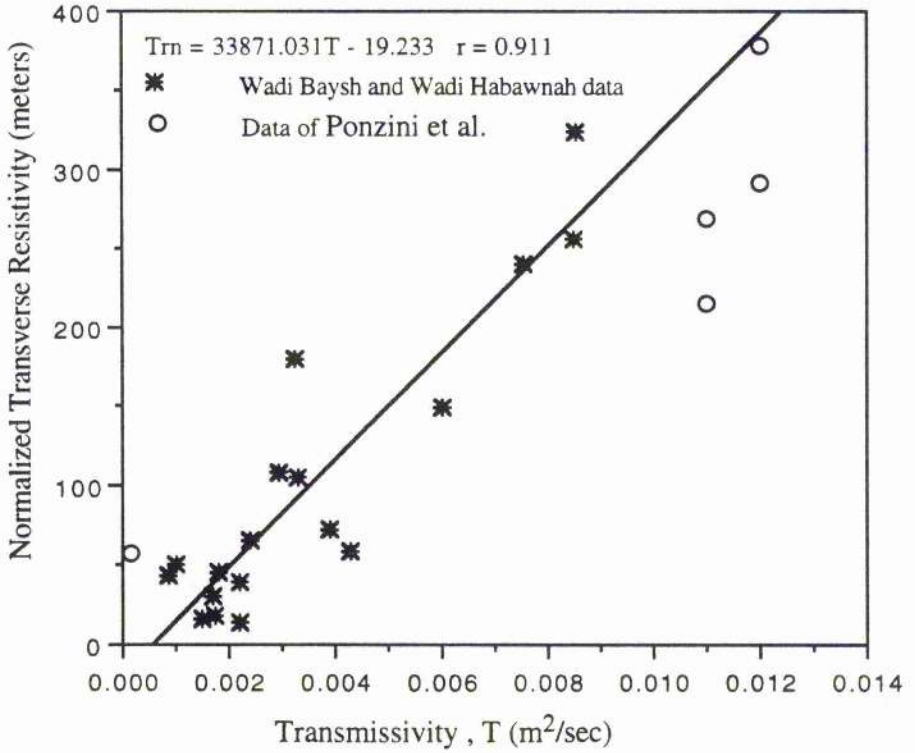

Figure 7.7 Normalized transverse resistivity vers a transmissivity of an unconfined aquifer of Tronto valley and Wadis Baysh and Habawnah.

Table 7.5 The hydraulic transmissivity and transverse electrical resistance of Wadi Baysh and Wadi Habawnah aquifers compared with Tronto valley data (after Ponzini et al. 1984)

Data from Wadi Baysh and Wadi Habawnah.						Ponzini et al Data of Tronto valley (Italy)			
Well no	VES NO	The location in the wadi	Transmissivity T (m^2/day)	Transmissivity T (m^2/sec)	Corrected Transverse Resistance Trn (m)	Well no	Transmissivity T (m^2/Day)	Transmissivity T (m^2/sec)	Corrected Transverse Resistance Trn (m)
BU1	TRWB-N1	UPPER (B)	190	$2.20x10^{-03}$	14	82 C	12	$1.39x10^{-04}$	50
BU2	TRWB-N2	UPPER (B)	156	$1.81x10^{-03}$	45	41 P	14	$1.62x10^{-04}$	57
BU3	TRWB-N3	UPPER (B)	87	$1.01x10^{-03}$	50	85 C	62	$7.18x10^{-04}$	89
BM5	TRWB-N8	MIDDLE (B)	75	$8.68x10^{-03}$	43	54 C	147	$1.70x10^{-03}$	143
BM7	TRWB-N9	MIDDLE (B)	147	$1.70x10^{-03}$	30	80 C	190	$2.20x10^{-03}$	98
BM12	TRWB-N12	MIDDLE (B)	150	$1.74x10^{-03}$	18	129 C	337	$3.90x10^{-03}$	143
BL16	TRWB-N15	LOWER (B)	130	$1.50x10^{-03}$	16	136 C	380	$4.40x10^{-03}$	167
HB2	ARWH-N1	UPPER (H)	207	$2.40x10^{-03}$	65	207 C	389	$4.50x10^{-03}$	204
HB3	ARWH-N2	UPPER (H)	371	$4.29x10^{-03}$	58	207 C	389	$4.50x10^{-03}$	231
HB6	ARWH-N3	UPPER (H)	190	$2.20x10^{-03}$	39	1 C	536	$6.20x10^{-03}$	280
MT1	ARWH-N4	MIDDLE (H)	285	$3.30x10^{-03}$	105	97 C	605	$7.00x10^{-03}$	208
MT9	ARWH-N6	MIDDLE (H)	520	$6.02x10^{-03}$	149	91 C	613	$7.09x10^{-03}$	231
GF2	ARWH-N7	MIDDLE (H)	738	$8.54x10^{-03}$	324	132 P	950	$1.10x10^{-02}$	269
GF5	ARWH-N8	MIDDLE (H)	281	$3.25x10^{-03}$	180	132 P	950	$1.10x10^{-02}$	215
NG1	ARWH-N9	MIDDLE (H)	337	$3.90x10^{-03}$	72	2 P	1037	$1.20x10^{-02}$	292
MR	ARWH-N10	LOWER (H)	652	$7.55x10^{-03}$	240	2 P	1037	$1.20x10^{-02}$	378
HS2	ARWH-N11	LOWER (H)	734	$8.50x10^{-03}$	256	213 C	1210	$1.40x10^{-02}$	343
HS4	ARWH-N13	LOWER (H)	254	$2.94x10^{-03}$	108	213 C	1210	$1.40x10^{-02}$	393

C= Confined aquifer & P= Unconfined aquifer
(B) = Wadi Baysh & (H) Wadi Habawnah

transverse resistance and hydraulic transmissivities obtained by means of VES and pumping tests respectively for floor sediment of Wadis Baysh and Habawnah and the aquifer of the Tronto river.

The plot of all data (Figure 7.6) shows that the data points fall in a broad linear zone which shows that there is an increase in transmissivity with increasing normalised transverse resistivity. The wadi data follow a relatively steeply inclined curve which is close to the origin, whereas the Tronto valley information is more scattered and follows a lower gradient distribution. The plot of Figure 7.6 is less than fully satisfactory because it incorporates data from both confined and unconfined aquifers, and the Tronto valley area is dominated by waters from confined aquifers whereas the wadis are characterised by their unconfined aquifers. Removing data from the confined aquifers (Figure 7.7) reveals a very similar distribution plot with an only slightly decreased breadth of spread in a similar belt showing increase of transmissivity with normalised transverse resistivity. It is suggested that such a plot with similar bounding lines might be of universal application in other aquifers elsewhere.

Thus the saturated layer plays an important role in the sense that the highest hydraulic conductivity corresponds to the highest aquifer thickness while the lowest conductivity corresponds to the lowest aquifer thickness. There is quite an agreement between the wadi floor sediments and the Tronto valley aquifer.

7.7 Summary and Discussion

When attempting to interelate the characteristics of aquifers many facts are involved. In this thesis the study of transverse electrical resistance and hydraulic transmissivity of the aquifers in Saudi Arabia have been compared with those on the Tronto River valley, Italy.

There are similarities between the average resistivity to the current flowing parallel the bedding plane which is equal to that flowing parallel to the bedding in the plane. The hydraulic transmissivity computed from pumping tests also assumes the hydraulic flow is parallel to the aquifer layer. Furthermore, the transverse resistance of the aquifer formation is the more useful parameter to be identified from the interpretation of VES. The computation of the hydraulic conductivity using pumping tests requires extra data.

However, there are other possible sources of errors, such as the effects of grain size distribution, water quality, and permeability.

In both wadis the vertical electrical sounding survey covered most of the area; 18 out of 30 VES were made near the pumping tests as parametric measurements.

The interpretation of the results of VES, together with pumping test results at the same location, were used to establish a relationship between the hydraulic transmissivity and the corrected transverse resistance.

The usefulness of VES for estimating hydraulic parameters depends on the accuracy of the interpretation. From resistivity interpretation, the resistivity and the thickness of the aquifer were determined. The transverse resistance, which is the product of the aquifer resistivity and its thickness, is then calculated for 18 VES sites. To account for the effect of water quality, the transverse resistance is obtained by dividing the resistivity of the water, 5 ohm-m in Wadi Baysh and 6 ohm-m in Wadi Habawnah.

The corrected transverse resistance, T_{rn}, is then plotted on a linear graph versus the corresponding transmissivity value as is obtained from the pumping test. Using regression analysis a best fit line passing through the points is obtained. The relationship obtained in both wadis is a direct linear relation, of the following form:

$$T_{rn} = -19.233 + 3.3871\ 10^4\ T$$

This relationship is similar to the relationship obtained by combining the unconfined data of the Tronto aquifer with that from the study area. To apply the relationship in the sandy gravels of the unconfined aquifers, the corrected transverse resistance values obtained must be substituted in the equation above.

Values of T obtained from the relationship are low with respect to those obtained from the pumping tests. This is due to the fact that the VES and pumping test measurements were made on heterogeneous aquifers, since both of their theories assume isotropic aquifers.

Mazac *et al.* (1985) pointed out that the derived field relationship between the electrical and hydraulic parameters depends on:

1- The accuracy of the geoelectric parameters determined from the field measurements,

usually sounding curves.

2- The accuracy of the hydraulic parameters determined from pumping tests or other less reliable methods.

3- The form of the regression applied to the aquifer.

4- The reliability of the regression equation.

In the study area, the author believes that most factors affect the T values interpreted using the above equation because the aquifer sediments are heterogeneous.

7.8 Conclusion

The VES and large diameter well pumping tests give the opportunity to obtain an empirical function between the aquifer transmissivity and the corresponding corrected transverse resistance. The relationship obtained is generally linear in the sense that, by increasing the T, the Trn will also increase. The transverse resistance of the saturated thickness of the aquifers is the only important parameter for correlation with the hydraulic transmissivity. The computed empirical function is directly utilised for most of the surveyed aquifers and it is also possible to apply it to other aquifers of similar sedimentological properties in the Arabian Shield wadis.

CHAPTER EIGHT: INTERPRETATION OF GEOPHYSICAL LOGS OF WADI AQUIFERS

8.1 Introduction

During the MAWR drilling programme which took place in 1978, a total of 11 core wells were drilled in the lower part of Wadi Baysh and 6 core wells in Wadi Habawnah (Figures 8.1 and 8.2). The core well depth ranged between 44 and 150m in Wadi Baysh, while in Wadi Habawnah wells were between 33 and 39m in depth. Well log records of seven geophysical logs and the grain size analysis data of seventy five core samples were provided by MAWR for the Wadi Baysh drilling wells. However, no such data are available for Wadi Habawnah except general lithological descriptions for the core wells. The following table (Table 8.1) consists of core well depths, their locations and type of data available for analysis for both wadis (see 8.1.1 Section one).

Table 8.1 Location, total depth and altitude of the boreholes in both wadis

Wadi Baysh Well no.	Altitude above sea level (m)	Total depth (m)	Location	
AO *&	37	98.5	17°20'07"N	42°29'77"E
BO*&	65	140	17°34'27"N	42°20'10"E
CO&	50	92	17°13'06"N	42°38'23"E
DO&	80	63	17°13'38"N	42°43'36"E
EO*&	23	150	17°13'27"N	42°34'44"E
FO@	44	44	17°20'12"N	42°29'23"E
GO*&	45	75	17°14'02"N	42°14'00"E
HO*	40	75	17°08'21"N	42°34'07"E
JO*&	22	135	17°15'51"N	42°39'36"E
KO*&	65	102	17°29'04"N	42°27'28"E
IO@	30	143	17°14'05"N	42°36'07"E

Wadi Habawnah Well no.	Altitude above sea level (m)	Total depth (m)	Location	
H-7-P@	1240	33	17°53'00"N	44°10'15"E
H-11-P @	1333	20	17°58'45"N	44°12'10"E
H-3-P @	1204	34	17°52'15"N	44°19'00"E
H-15-P @	1159	35	17°49'00"N	44°32'40"E
H-8-P@	1255	34	17°55'45"N	44°16'23"E
3-N-82@	1209	39	17°49'10"N	44°35'45"E

(*) Well Log data, (&) Sieve analysis data available and (@) general lithology distribution

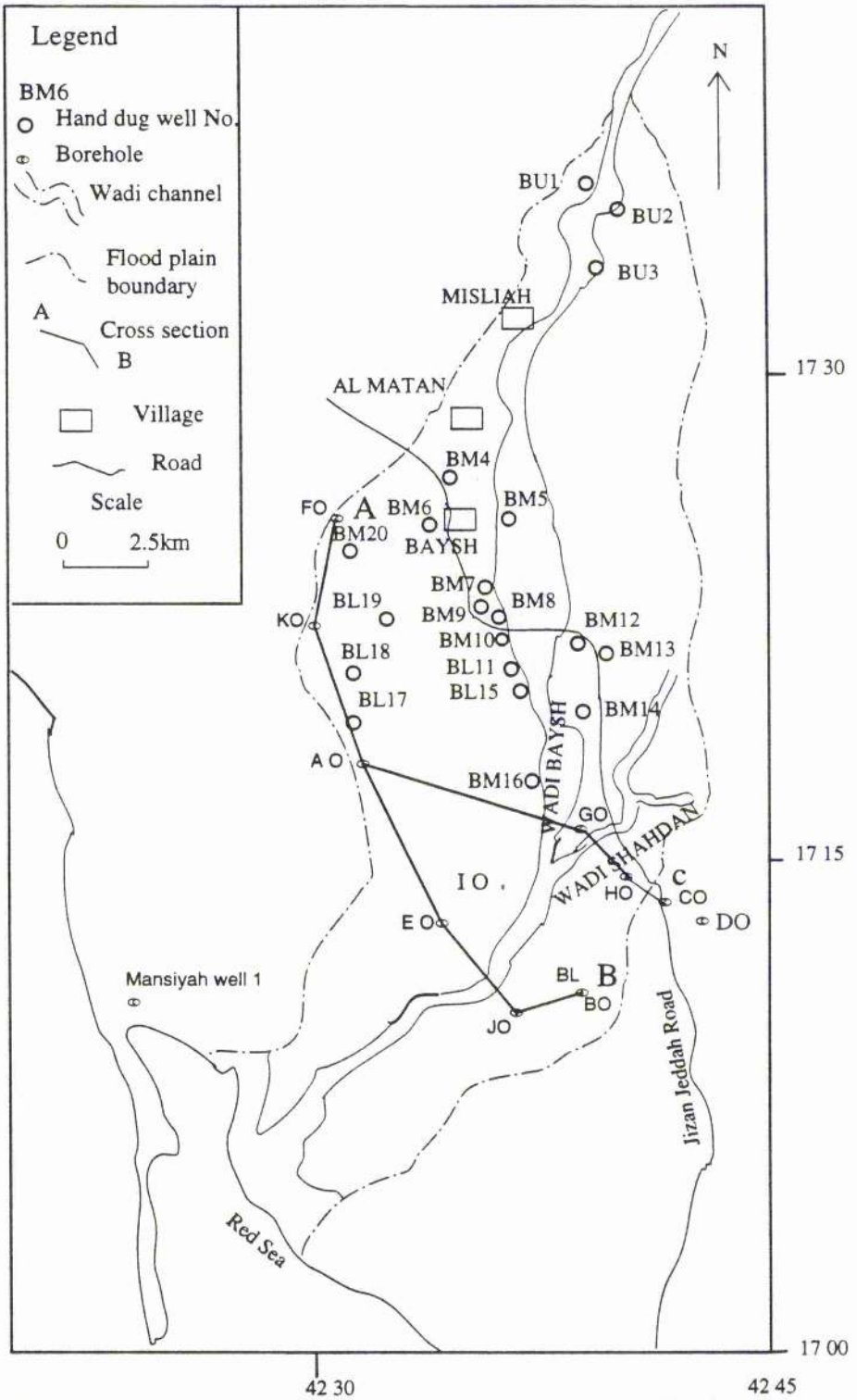

Figure 8.1 Location map of Wadi Baysh hand dug wells , MAWR boreholes and cross section lines (FO,KO,AO,GO,HO,CO and FO,KO,AO,EO,JO).

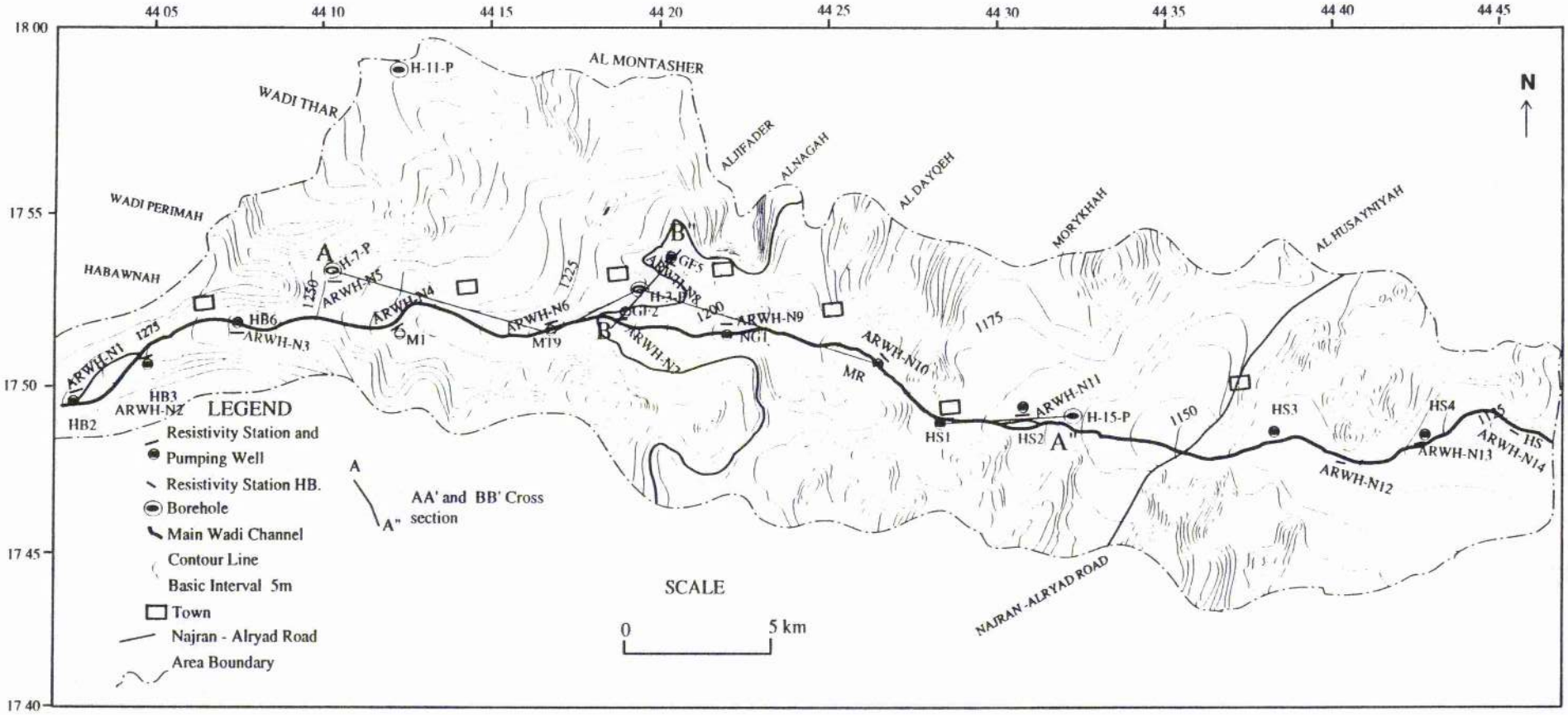

Figure 8.2 Topographic map of Wadi Habawnah showing the locations of resistivity stations, test wells and boreholes .

The borehole lithologies are shown in Tables 8.2 and 8.3. The core wells were equipped with short casing pipes and screwed well caps to provide additional observation points for water level and salinity changes. Unfortunately there are no available records for water salinity or pumping tests except those measurements taken during the drilling project in 1978. The data examined in this chapter are divided into three main sections (One, Two and Three) as follows:

Section One

The lithology of the rocks penetrated by the wells permits identification of the aquifer types on the basis of the lithological characteristics and their location in the stratigraphic sequences of both wadis.

Section Two

The second section deals with grain size analysis of 75 samples collected from different subsurface units in which the permeability and the transmissivity of the aquifers were determined, using the Hazen method, the Masch and Denny method and pumping tests. Computations of ground water flows have been made.

Section Three

In Section three the geophysical logs of Self Potential, Normal Resistivity (long and short) and Natural Gamma Ray emission were used to determine the characteristics of the subsurface lithology in relation to the hydrogeological units of the aquifers. The Archie formula and electrical conductivity data have been used to calculate the formation factors. The graphical relationships between the effective grain size, permeability and formation factor were determined for the wadi floor sediments.

Table 8.2 Borehole lithology data of Wadi Baysh (modified after MAWR records,1978)

Borehole no.	Rock Unit	Thickness m	Total Depth m	Elevation m (a.s.l)
AO	S+Q+S+G+P+S	0-36	97.5	37
	C	36-45.5		
	G+S+G	45.5-59		
	C	59-60.5		
	S+Q	60.5-65		
	C+Q+C	65-79		
	G+S+G	79-97.5		
	Q	97.5-?		
BO	S	0-16	140	65
	C	16-22		
	S+Q+S+Q+S+Q+S+Q	22-64		
	C	64-69		
	S+Q+S+Q	69-108		
	C	108-112		
	G+Q+S	112-115.5		
	C	115.5-117.5		
	S	117.5-120		
	C+Q+C	120-140		
CO	S	0-7	92	50
	C	7 8		
	Q+S+P+S+Q	8.-17		
	C	17-27		
	S+Q+G	27-40		
	C	40-50		
	G	50-54		
	C	54-66		
	G	66-68		
	C+Q	68-92		
DO	S	0-3.5	63	80
	C	3.5-4.5		
	Q+G+S+Q+P+S+Q	4.5-40		
	C	40-41		
	S+Q+S+Q	41-59		
	C	59-63		
EO	S+Q+S+G	0-16.5	150	23
	C	16.5-21		
	S+Q+S	21-34		
	C	34-38		
	S	38-39.5		
	C	39.5-45		
	Q+S+Q+S+G	45-61		
	C	61-63		
	S+Q+S+Q	63-99		
	C	99-111		
	Q+S	111-114		
	C	114-117		
	S	117-119.5		
	C	119.5-124		
	S+Q+S	124-146		
	C	146-150		

Continued on next page

Table 8.2 continued

Borehole no.	Rock Unit	Thickness m	Total Depth m	Elevation m (a.s.l)
FO	S+Q+S+G+Q+P+Q+G+Q	0-26	44	57
	C+P	34-44		
GO	Q+G	0-6.0	75	45
	C	6.0-11.0		
	Q+S+Q	11.0-27		
	C	27-32.5		
	G	32.5-37.5		
	C	37.5-41.5		
	S	41.5-44.5		
	C+P+C+P+C	44.5-75		
HO	S+Q+S+Q+G+Q+G+Q+G	0-52.5	75	40
	C+P+C+P+C	52.5-75		
	S+G	0-12.5	75	40
	C+P+C+H	12.5-75		
KO	S+G	0-10.5	102	65
	C	10.5-11.5		
	G+Q	11.5-37		
	C+P+C+P+C+Q+C+Q	37-102		
IO	S+Q	0-5.0	141	30
	C	5-19.5		
	S	19.5-24		
	C	24-33		
	G+Q+S+G+Q	33-51		
	C	51-62		
	Q+G+Q	62-69		
	C+Q+C+Q+C+Q+C	69-115		
	Q+S+P+	115-132		
	C	132-141		
JO	Q+S	0-4	135	22
	C	4.-5.		
	G+Q+S+Q+S+Q+G+Q+G+Q+	5.-55.5		
	C	55.5-67.5		
	S+G	67.5-71.5		
	C+Q+C	71.5-95		
	P+G	95-97		
	C	97-100		
	G	100-101		
	C	101-113.5		

(Q) Silt,Clay,Sand,

(G)Fine,medium gravel,coarse,medium sand

(P) Basaltic,quarzitic fine gravel,coarse and medium sand

(S)Coarse medium and fine gravel,fine sand

(C) Clay

(H) Hard Rocks (Basalt)

Table 8.3 Borehole data from Wadi Habawnah (MAWR records, 1978)

Borehole no.	Rock Unit	Thikness m	Total Depth m	H-DISTANCE km	ELEVATION m (a.s.l)
H-8-P	coarse sand	16	34	37	1283
	sand ,clay	14			
	gravel,cobbles	4			
	bed rock				
H-11-P	silty sand	6	20	4*	1345
	gravel , cobble:	9			
	gravel .sand	5			
	bed rock				
H-7-P	coarse sand	7	33	35	1264
	gravel cobbles	18			
	clay	8			
	bed rock				
3-N-82	clay, sand	15	39	6**	1245
	gravel,cobbles	19			
	silty sand	5			
	bed rock				
H-3-P	sand	4.5	34	22.5	1220
	clay	1.5			
	sand	3			
	clay	2			
	sand	4			
	clay	7			
	gravel,cobbles	3			
	sand	9			
	bed rock				
H-15-P	sand	8	34	7.25	1185
	clay ,gravel	8			
	gravel ,cobbles	13			
	clay	5			

*Distance from confluence of Wadi Hababah with Wadi Habawnah .
**Distance from confluence of Wadi Sikhi with Wadi Habawnah .

8.2 Section One: Aquifer Type

8.2.1 Wadi Baysh Boreholes and Main Aquifer Types

Alluvial-fan deposits occur in the lower part of Wadi Baysh which occurs on the eastern margin of a basin created by bedrock faulting along the trend of the Red Sea. The upper stratigraphic section of the lower part of Wadi Baysh has been established on the basis of eleven drilled wells. All of the wells penetrate the wadi floor sediment by 44 to 150 m. The underlying hard rock basement was not reached (see Chapter 2). Several alluvial aquifer systems occur bounded with clays.

Two cross sections have been constructed in the area (Figure 8.3). The cross section line (FO-CO), 15 km long, is derived from the data of boreholes FO, KO, AO, GO, HO and CO (see Table 8.2). The section trends N-S between FO, KO and AO parallel to the wadi channel (in the flood plain). The elevation of the tops of these boreholes ranges between 37 and 65m above sea level. The section crosses the main wadi channel at boreholes GO and HO, each of which is 75 m deep. The end of this section is in the flood plain of the left bank of the flow direction at borehole CO, which is 92m deep.

The second cross section is 13 km long (Figures 8.1 and 8.4a) extending from borehole FO to BO, crossing the main wadi channels at boreholes EO and JO whose tops are 22m above sea level. The end of the cross section between JO and BO trends parallel to the wadi channel (in the flood plain). The top of BO is at 65m (See Table 8.1).

The stratigraphic sequence in the lower part of Wadi Baysh is of heterogeneous sediments. It consists of various layers and lenses of sand, silty sand, clays, gravel and boulders. The ground water hydrology in the area can be discussed by grouping the numerous layers into units of hydrologic significance. Accordingly, these layers, listed in Table 8.2 and Figure 6.13, are grouped into two major hydrologic units (Figures 8.3 and 8.4). In order of location from the top to the bottom they are as follows: the upper wadi fill is classified as an unconfined aquifer which locally overlies a confined aquifer (A and B, respectively, in Figures 8.3b and 8.4b).

The unconfined aquifer outcrops at the ground surface while its base rests on an impermeable layer of clay 2-18m thick. The confined aquifer is separated from the ground

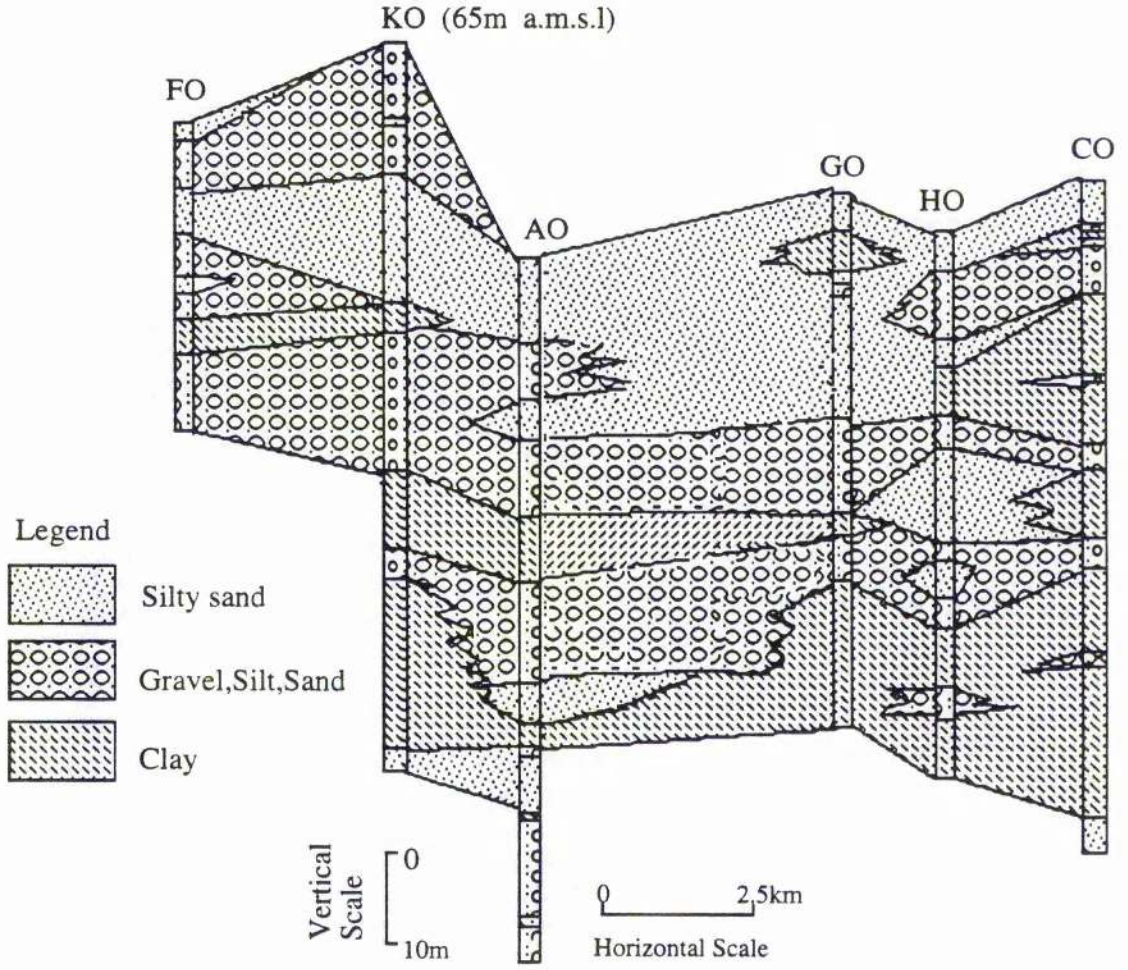

Figure 8.3a Cross section profile trending north west (FO, KO, AO, GO, HO and CO), showing the aquifer lithology in the lower part of Wadi Baysh.

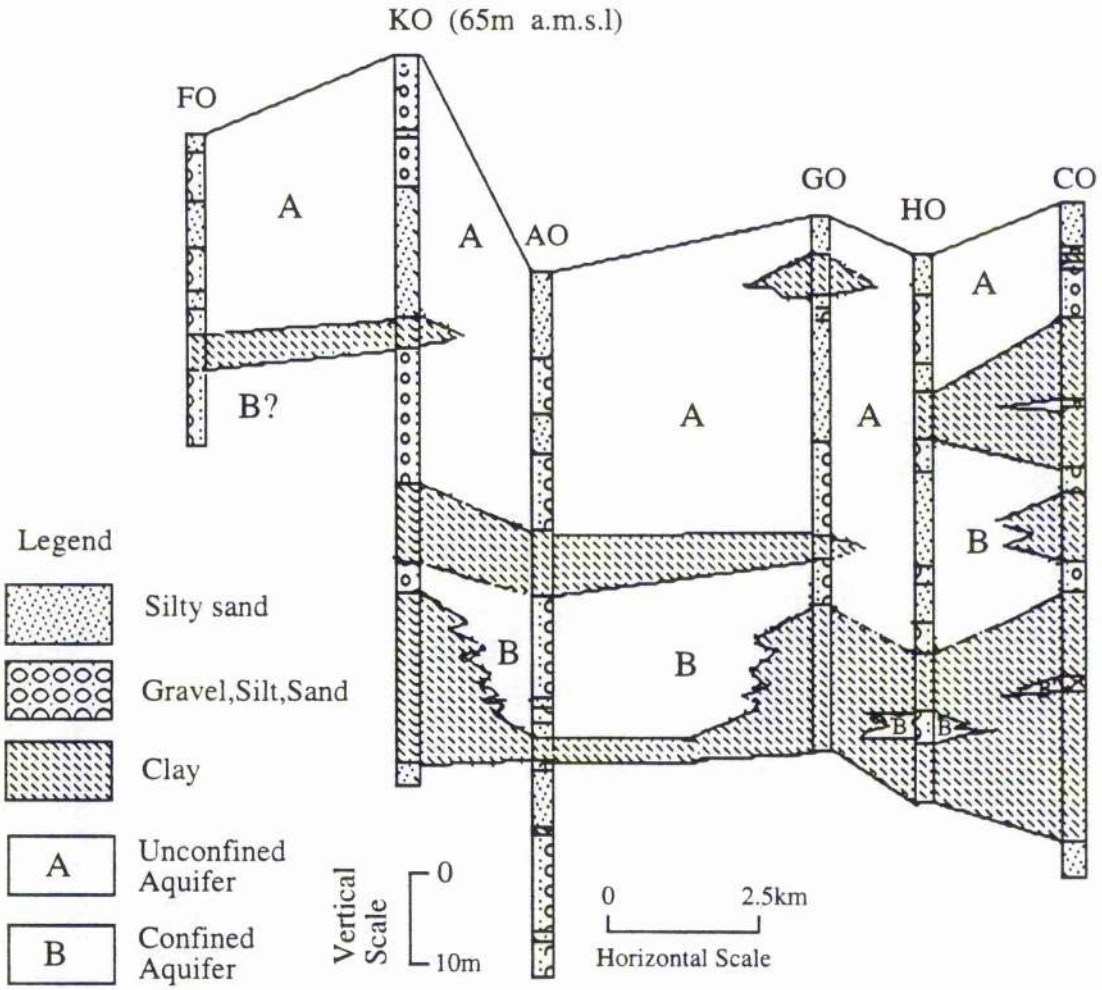

Figure 8.3b Cross section profile trending northwest (FO, KO, AO, GO, HO and CO) showing the aquifer systems of the lower part of Wadi Baysh.

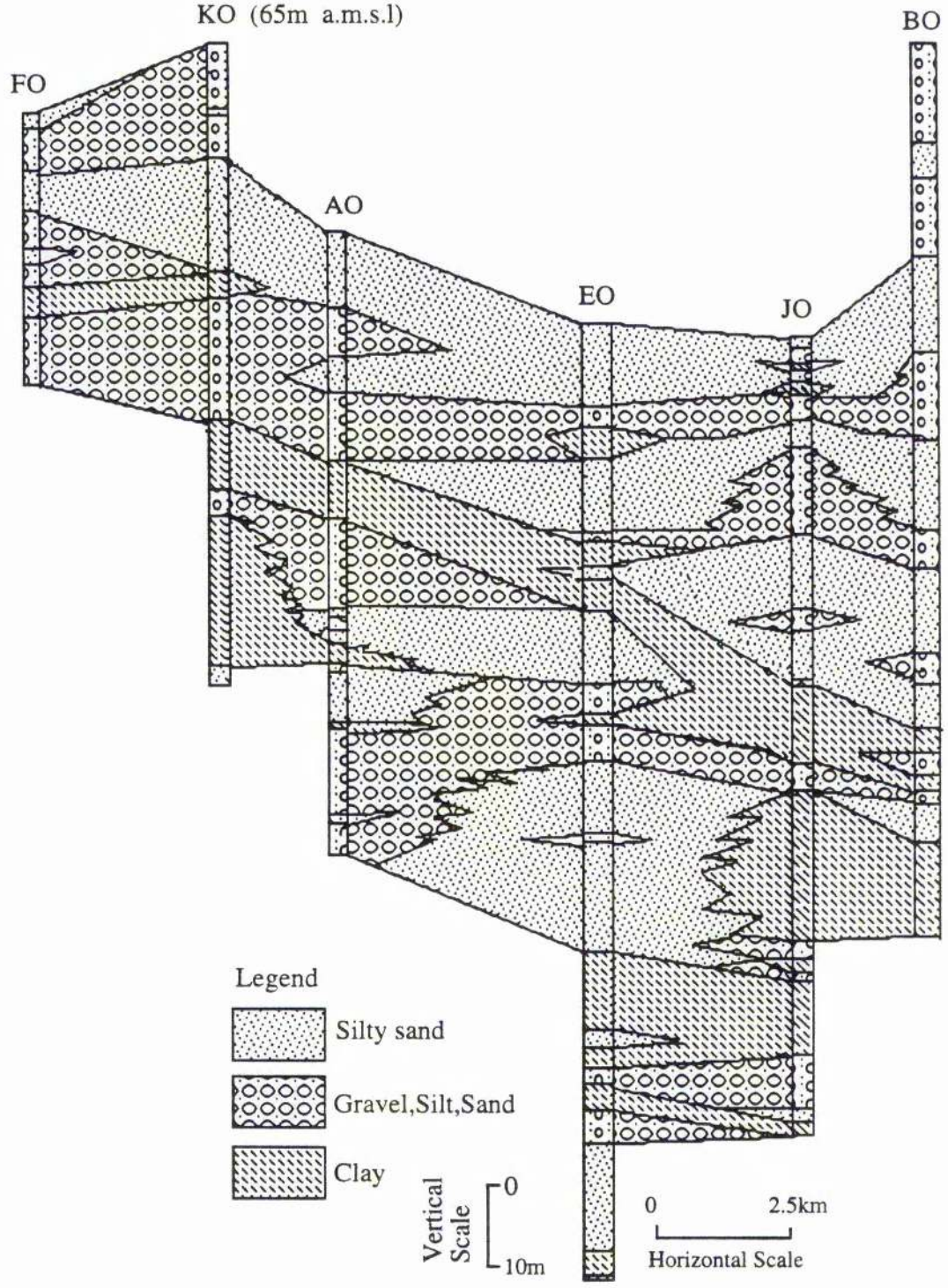

Figure 8.4a Cross section profile trending north south (FO, KO, AO) and west-east AO, EO and JO) and trending again north-south as (JO, BO) in the lower part of Wadi Baysh.

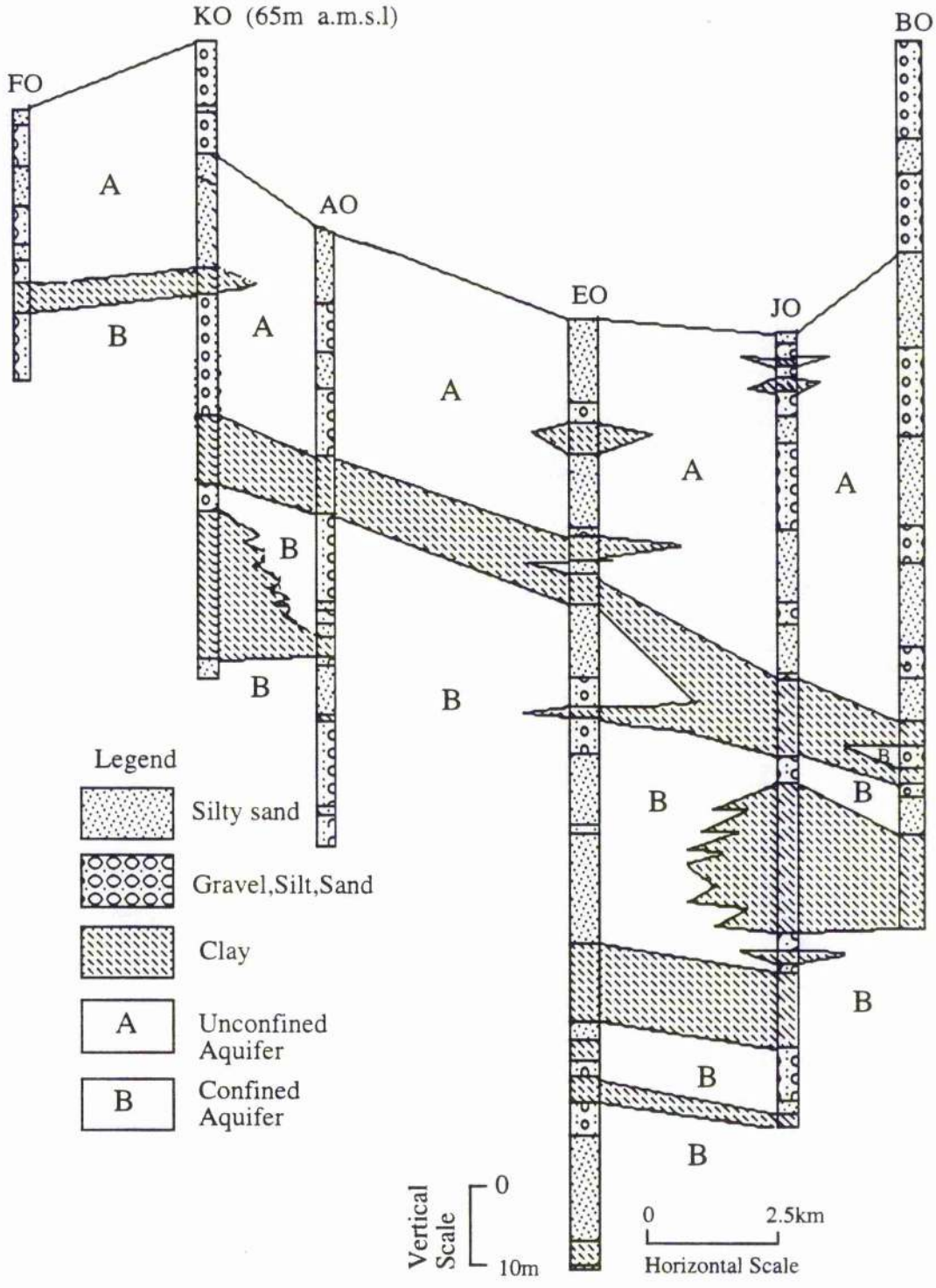

Figure 8.4b Cross section profile trending north south (FO, KO, AO) and west-east (AO, EO, JO) and trending again north-south as (JO, BO) showing the aquifer systems in the lower part of Wadi Baysh.

surface by the unconfined aquifer and the intervening impermeable clay layer (right-hand side of Figures 8.3b and 8.4b).

Layers and lenses of sand and gravel and silty sand occur throughout the aquifers. The gravel is poorly sorted with a maximum grain size of 2 cm.

The greatest thickness of water bearing units in the unconfined aquifer were encountered in borehole BO at 60m. In other boreholes freshwater bearing sequences ranged from 20 to 30m. The confined aquifer is at its greatest thickness of 35m in boreholes AO and EO. It thins above and below a clay horizon in JO and BO.

8.2.2 Wadi Habawnah Boreholes and Main Aquifer Types

The 100m to 2km wide floor of Wadi Habawnah has three types of wadi filling sediments. The six borings, 20 to 39m (Table 8.3 and Figure 6.14) into the wadi floor, make possible the description of the subsurface lithology. The following simplified lithology is shown Figures 8.5 and 8.6. Figure 8.5 is a 36 km section (AA) along the main channel of the wadi parallel to the flow direction. It exhibits a sequence typical of wadi floor deposits. The upper layer in the middle of the wadi channel (borehole H-11-P and H-7-P) consists of silty sand to coarse sand, 3m thick, while in the lower part of the wadi channel (boreholes H-3-P, H-15-P) this layer is thicker with a depth range between 15m and 10m, respectively. In borehole H-3-P there are interbedded lenses of clay with thickness of 1.5 to 2m within sands. An 8m thick layer of clay occurs below the coarse sand in borehole H-3-P with limited extension up and down wadi. The second major layer is of gravel and cobbles which extends along the entire length of the wadi channel. It varies in thicknesses from 13 m to 18 m in boreholes H-11-P and H-7-P, respectively. In the lower part of the wadi, the gravel and cobble layer decreases to 3m in thickness while this thickness again increases in borehole H-15-P consisting of 8m of clay and gravel followed by 13 m of gravel bearing cobbles. The section in Figure 8.6 extends across the wadi. It exhibits a trough shape and is filled with 10-35m of unconsolidated sediment which rests upon the basement complex. The bulk of the wadi floor is underlain by gravels upon which is a layer of sand within which lenses of clay occur in the centre of the wadi. A layer of gravel buries the sands on the northern side of the wadi.

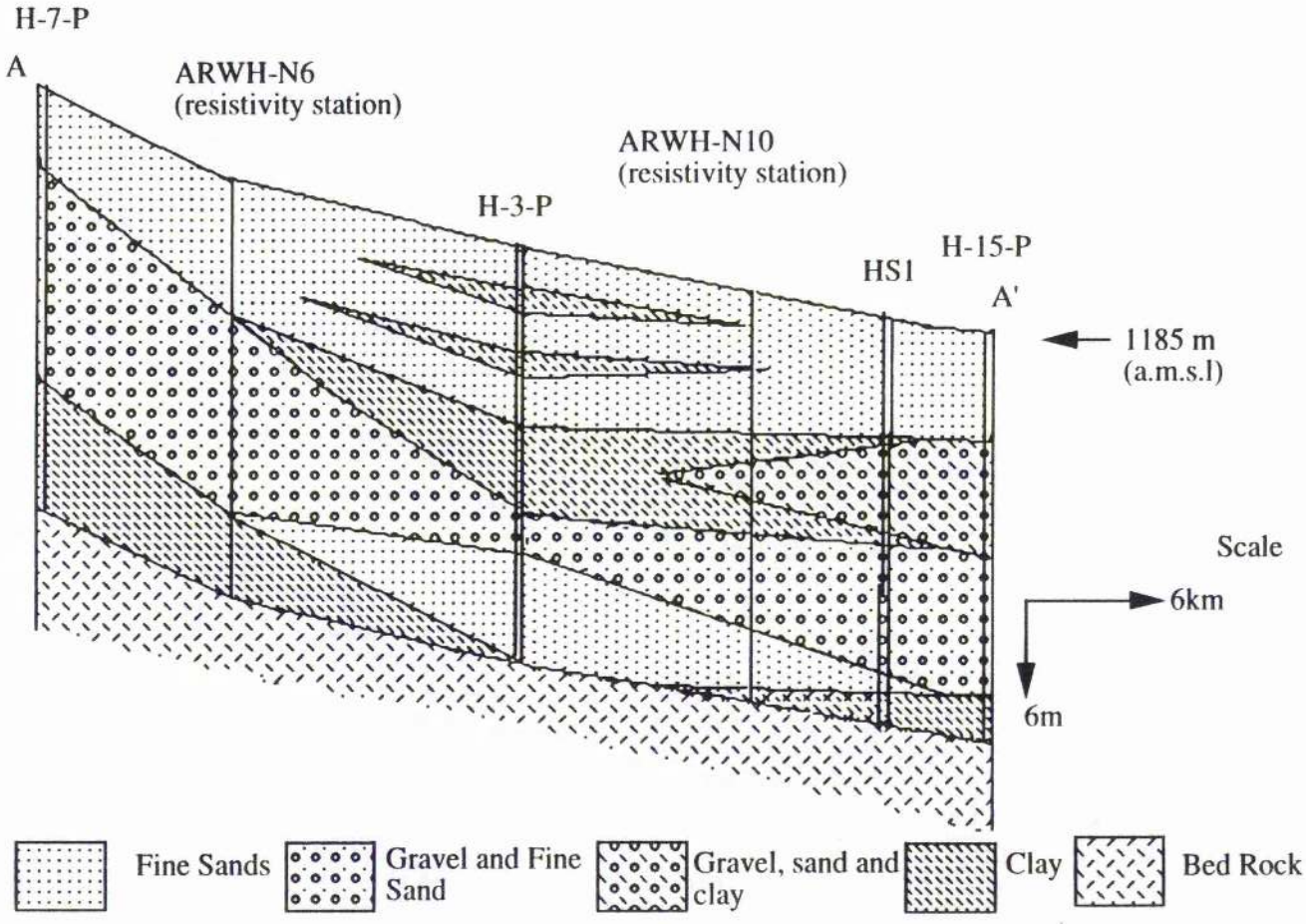

Figure 8.5 Borehole lithology of Wadi Habawnah along the main wadi channel in the flow direction trending west-east.

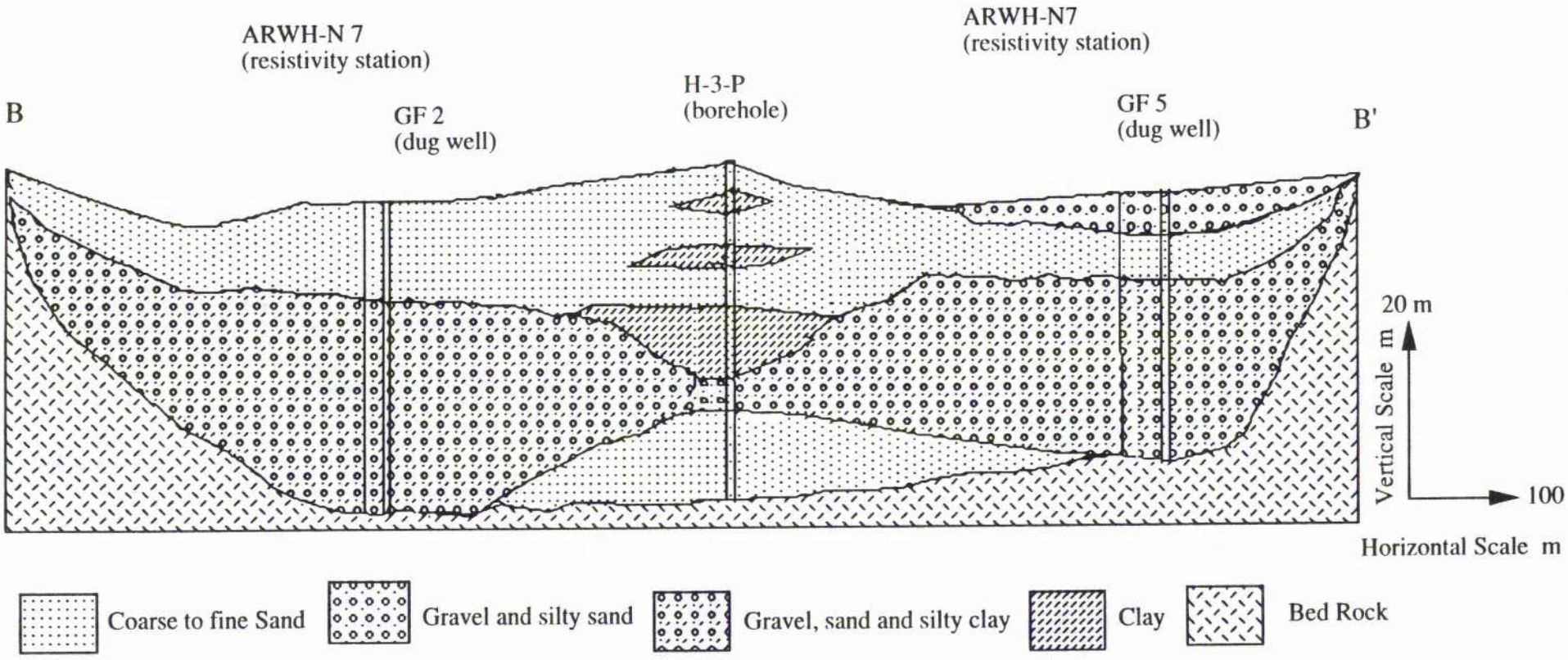

Figure 8.6 Wadi Habawnah cross section (BB') trending north-south, perpendicular to the main wadi flow direction.

Table 8.4 The depth at which the grain size samples have been taken in the various boreholes of Wadi Baysh

Borehole No.	Depth (m)
AO	45.5/46.0
	46.0/47.0
	47.0/48.0
	48.0/49.0
	49.0/50.0
	50.0/51.0
	51.0/52.0
	52.0/53.0

Borehole No.	Depth (m)
BO	54.0/55.0
	55.0/56.0
	56.0/57.0
	57.0/58.0
	58.0/59.0
	59.0/60.0
	60.0/61.0
	61.0/62.0
	62.0/63.0
	76.0/77.0
	77.0/78.0
	78.0/79.0
	79.0/80.0
	80.0/81.0
	81.0/82.0
	97.0/98.0
	98.0/99.0
	99.0/100
	112/113
	113/114

Borehole No.	Depth (m)
CO	37.0/38.0
	38.0/39.0
	39.0/40.0
	50.0/51.0
	51.0/52.0
	52.0/53.0
	53.0/54.0

Borehole No.	Depth (m)
DO	35.0/36.0
	36.0/37.0
	37.0/38.0
	38.0/39.0
	41.0/42.0
	42.0/43.0
	43.0/44.0
	44.0/44.5

Borehole No.	Depth (m)
EO	55.0/56.0
	56.0/57.0
	59.0/60.0
	60.0/61.0
	63.0/64.0
	64.0/65.0
	65.0/66.0
	66.0/67.0
	67.0/68.0
	68.0/69.0

Borehole No.	Depth (m)
JO	42.0/42.5
	42.5/43.5
	43.5/44.5
	44.5/45.0
	45.0/46.5
	64.5/65.5
	65.5/66.5
	120/121
	121/121.5
	121.5/123
	123/124

Borehole No.	Depth (m)
KO	40.5/42.0
	42.0/43.0
	43.0/44.0
	44.0/45.0
	46.0/47.0
	47.0/48.0
	48.0/49.0
	49.0/50.0

8.2.3 Conclusion

According to core wells, which were drilled in the lower part of Wadi Baysh, and 6 core wells in Wadi Habawnah, the well inventory and the geophysical study along the wadi channels of the aquifer systems in Wadi Baysh and Wadi Habwanah were determined as follows:

1-Wadi Baysh

The multi-aquifer system was developed in the lower part the wadi. The upper wadi fill is classified as an unconfined aquifer, which locally overlies a confined aquifer (A and B, respectively, in Figures 8.3b and 8.4b).

The unconfined aquifer outcrops at the ground surface while its base rests on an impermeable layer of clay 2-18m thick. The confined aquifer is separated from the ground surface by the unconfined aquifer and the intervening impermeable clay layer (see Figures 8.3b and 8.4b).

The thickest water bearing units in the unconfined aquifer were encountered in borehole BO at 60m. In the other boreholes, freshwater bearing sequences ranged from 20 to 30m. The confined aquifer is at its thickest (35m) in boreholes AO and EO.

2- Wadi Habawnah

The 100m to 2km wide floor of Wadi Habawnah has three types of wadi filling sediments. The wadi floor sediments exhibit an unconfined to local semi-confined aquifer with thickness varying between <20 to >40 m in the lower part of the wadi. The wadi channel exhibits a trough shape and is filled with unconsolidated sediment which rests upon the basement complex. The bulk of the wadi floor is underlain by gravels, upon which is a layer of sand and within which lenses of clay occur in the centre of the wadi. A layer of gravel buries the sands on the northern side of the wadi. The upper layer in the middle of the wadi channel consists of silty to coarse sand, while in the lower part of the wadi channel this layer is thicker and has a depth ranging between 15m and 10m.

8.3 Section Two: Parameters of the Multi-aquifer System

8.3.1 Introduction

Understanding the hydraulic transmission of groundwater through an aquifer plays a major role in the economic development of groundwater resources. The permeability is one of the most important quantitative measures of such transmission. Masch and Denny (1966) indicated that the permeability is a function of the properties of the medium (particle size, shape, structure, degree of compaction and grain size distribution) since the physical properties of the flowing water (viscosity, and specific weight) are constant.

Grain size analysis has been carried out to determine the aquifer permeability. Analysis of 75 grain size samples provided by MAWR have been used in this study (see Table 8.4). According to the location of the samples below the surface, they are recognised as coming from different parts of the multiaquifer aquifer system.

The geological classification systems of grain size, given in Table 8.5 (after Friedman and Sanders, 1978), is used to provide description of the grain sizes in the area.

Table 8.5 Terms applied to sediments according to grain size (after Friedman and Sanders, 1978)

Limiting particle diameter		Size	Class			
mm	phi					
2048	-11		V.Large		GRAVEL	1m
1024	-10		Large	Boulder		
512	-9		Medium			
256	-8		Small			
128	-7		Large	Cobbles		
64	-6		Small			10^{-1}
32	-5		V. Coarse			
16	-4		Coarse	Pebbles		
8	-3		Medium			10^{-2}
4	-2		Fine			
2	-1		V. Fine			
1	- 0	- (Microns μm)	V. Coarse	Sand		10^{-3}
1/2	+1	500	Coarse			
1/4	+2	250	Medium			
1/8	+3	125	Fine			
1/16	+4	62	V. Fine			10^{-4}
1/32	+5	31	V. Coarse		MUD	
1/64	+6	16	Coarse			
1/128	+7	8	Medium	Silt		10^{-5}
1/256	+8	4	Fine			
1/512	+9	2	V. Fine			
				Clay		

The table shows the standard sizes of sediments with limiting particle diameters and the Ø scale of sediment size, in which phi is equal to $-\log_2$ (the particle diameter in mm). The grain size distribution curves of Appendix 8.B show two kind of grain size ranges, (i) fine to coarse sand and cobbles (somewhat poorly sorted as there is a wide range of grain sizes present) and (ii) well-sorted fine sand.

Grain size analysis by sieving gives raw data in the form of weight percentage of sediments retained on individual screens. In this study the data form the mechanical analyses are plotted as cumulative percentage retained by weight (arithmetical scale on the ordinate) against the grain size in millimetres using a logarithmic scale on the abscissa, with smaller size to the left (see Appendices 8.A and 8.B).

In this method the sample data plot as an S-shaped curve. From the grain size distribution curve, grain size D_{10}, D_{50} and D_{60} were obtained (see Table 8.5). The D refers to the grain size, or apparent diameter, of the aquifer particles where D_{60} = that particle diameter such that 60% of the distribution is finer than this diameter; and D_{10} = that particle diameter such that 10% of the distribution is finer than this diameter. The D_{10} is also called the effective size of the soil. The uniformity coefficient C_u is defined by Preuss and Todd (1966) as follows:

$$C_U = \frac{D_{60}}{D_{10}} \qquad (8.1)$$

The uniformity coefficient C_u gives an idea of grading or particle size distribution in the material, in which the lower values indicate more uniform material or poor grading and higher value, indicate well graded material. Fetter (1988) indicated that a sample with a C_u less than 4 is well-sorted; if the C_u is more than 6 it is poorly sorted. The data of sieve analyses are classified in Table 8.6 as well-sorted (w) or poorly sorted (p). The sediment of the middle aquifer A of well AO is dominated by well-sorted sediment based on the mean C_u value of 4 in a range of C_u between 2 and 7. The core sediment of well BO (see Figures 8.3 and 8.4) is dominated by well to poorly-sorted material in both the upper A and lower aquifers B with values of C_u between 3 and 9 in the upper aquifer (middle section) 4 in the upper aquifer (lower section) and 4 to 5 in the lower aquifer (upper section).

The core sediment of well CO shows very poor sorting with a range of C_u values in

Table 8.6 Grain size Coefficients derived from sieve analysis data showing variations with depth in the lower part of Wadi Baysh

Borehole No.		Middle	Aquifer			Sorting
AO	Depth in m	D10 *	D50 **	D60 ***	CU ****	Range
	45.5/46.0	0.21	1.50	1.85	8.8	p
	46.0/47.0	0.25	1.50	1.90	7.6	p
	47.0/48.0	0.08	0.29	0.40	5.0	m
	48.0/49.0	0.08	0.28	0.40	5.0	m
	49.0/50.0	0.10	0.29	0.32	3.2	w
	50.0/51.0	0.11	0.35	0.62	5.6	m
	51.0/52.0	0.19	0.60	0.81	4.3	m
	52.0/53.0	0.26	1.00	1.50	5.8	m
	54.0/55.0	0.20	0.5	0.90	5	w
	55.0/56.0	0.20	0.6	0.90	5	w
	56.0/57.0	0.18	0.5	0.60	3	w
	57.0/58.0	0.12	0.4	0.50	4	w

Borehole No.		Upper	Aquifer (Middle Section)			Sorting
BO	Depth in m	D10 *	D50 **	D60 ***	CU ****	Range
	54.0/55.0	0.20	5.80	0.80	4.0	w
	55.0/56.0	0.19	0.60	0.80	4.2	m
	56.0/57.0	0.18	0.50	0.60	3.3	w
	57.0/58.0	0.10	0.30	0.40	4.0	w
	58.0/59.0	0.11	0.55	0.90	8.2	p
	59.0/60.0	0.10	0.41	0.55	5.5	m
	60.0/61.0	0.12	0.40	0.70	5.8	m
	61.0/62.0	0.09	0.55	0.80	9.4	p
	62.0/63.0	0.10	0.41	0.50	5.0	m
	76.0/77.0	0.09	0.48	0.60	6.7	p
	77.0/78.0	0.07	0.45	0.60	8.6	p
	78.0/79.0	0.06	0.50	0.60	10.0	p
	79.0/80.0	0.07	0.45	0.58	8.9	p
	80.0/81.0	0.06	0.50	0.75	12.5	p
	81.0/82.0	0.07	0.42	0.60	9.2	p
	MEAN	0.11	0.82	0.65	7.0	p
		Upper	Aquifer (Lower Section)			Sorting
	Depth in m	D10 *	D50 **	D60 ***	CU ****	Range
	97.0/98.0	0.10	0.49	0.65	6.5	p
	98.0/99.0	0.09	0.40	0.60	6.7	p
	99.0/100	0.11	0.33	0.44	4.0	w
	MEAN	0.10	0.41	0.56	5.7	m
		Lower	Aquifer (Upper Section)			Sorting
	Depth in m	D10 *	D50 **	D60 ***	CU ****	Range
	112/113	0.10	0.40	0.70	7.0	p
	113/114	0.20	0.60	0.85	4.3	p
	MEAN	0.15	0.50	0.78	5.6	m

Continued on next page

Table 8.6 continued

Borehole No.		Upper Aquifer				Sorting
CO	Depth in m	D10 *	D50 **	D60 ***	CU ****	Range
	37.0/38.0	0.17	0.40	0.70	4.1	w
	38.0/39.0	0.07	0.70	0.20	3.1	w
	39.0/40.0	0.07	0.65	1.50	23.1	p
	MEAN	0.10	0.58	0.80	10.1	p
		Lower Aquifer				Sorting
	Depth	D10 *	D50 **	D60 ***	CU ****	Range
	meter	0.10	0.70	0.90	9.0	p
	51.0/52.0	0.13	1.80	4.00	30.8	p
	52.0/53.0	0.90	1.10	1.70	1.9	w
	53.0/54.0	0.08	0.80	1.50	18.8	p
	MEAN	0.30	1.10	2.03	15.1	p

Borehole No.		Upper Aquifer				Sorting
DO	Depth in m	D10 *	D50 **	D60 ***	CU ****	Range
	35.0/36.0	0.12	1.00	1.60	13.3	p
	36.0/37.0	0.23	1.10	1.60	7.0	p
	37.0/38.0	0.10	0.30	0.38	3.8	w
	38.0/39.0	0.14	0.35	0.40	2.9	w
		0.15	0.69	1.00	6.7	p

Borehole No.						
EO	Depth	Lower Aquifer				Sorting
DO	meter	D10 *	D50 **	D60 ***	CU ****	Range
	41.0/42.0	0.06	0.37	0.48	8.7	p
	42.0/43.0	0.05	0.30	0.40	8.0	p
	43.0/44.0	0.10	0.40	0.50	5.0	m
	44.0/45.5	0.06	0.40	0.50	8.3	p
	MEAN	0.07	0.37	0.47	7.5	p
Borehole No.		Middle Aquifer (Upper Section)				Sorting
EO	Depth in m	D10 *	D50 **	D60 ***	CU ****	Range
	55.0/56.0	0.18	0.40	0.45	2.5	w
	56.0/57.0	0.15	0.41	0.50	3.3	w
	59.0/60.0	0.20	3.20	4.50	22.5	p
	60.0/61.0	0.35	3.00	4.10	11.7	p
	MEAN	0.22	1.75	2.39	10.0	p
		Middle Aquifer (Middle Section)				Sorting
	Depth in m	D10 *	D50 **	D60 ***	CU ****	Range
	63.0/64.0	0.12	0.35	0.50	4.2	p
	64.0/65.0	0.11	0.30	0.30	2.7	w
	65.0/66.0	0.10	0.30	0.48	4.8	m
	66.0/67.0	0.12	0.32	0.45	3.8	w
	67.0/68.0	0.11	0.80	1.50	13.6	p
	68.0/69.0	0.12	0.34	0.70	5.8	m
	MEAN	0.11	0.40	0.66	5.8	m

Continued on next page

Table 8.6 continued

Borehole No.		Upper	Aquifer			Sorting
JO	Depth in m	D10 *	D50 **	D60 ***	CU ****	Range
	42.0/42.5	0.09	0.65	1.00	11.1	p
	42.5/43.5	0.40	1.50	1.75	4.4	m
	43.5/44.5	0.22	1.20	1.80	8.2	p
	44.5/45.0	0.32	1.75	3.00	9.4	p
	45.0/46.5	0.20	2.00	3.00	15.0	p
		0.25	1.42	2.11	9.6	p
		Middle	Aquifer			Sorting
	Depth in m	D10 *	D50 **	D60 ***	CU ****	Range
	64.5/65.5	0.55	4.00	5.00	9.1	p
	65.5/66.5	0.30	2.00	3.00	10.0	p
	MEAN	0.43	3.00	4.00	9.5	p
		Lower	Aquifer			Sorting
	Depth in m	D10 *	D50 **	D60 ***	CU ****	Range
	120/121	0.07	0.80	1.30	18.6	p
	121/121.5	0.08	1.10	1.60	20.0	p
	121.5/123	0.10	1.70	2.00	20.0	p
	123/124	0.16	1.80	0.28	1.8	w
	MEAN	0.10	1.35	1.30	15.1	p

Borehole No.	Depth	Middle	Aquifer			Sorting
KO	meter	D10 *	D50 **	D60 ***	CU ****	Range
	40.5/42.0	0.13	1.50	2.00	15.4	p
	42.0/43.0	0.20	0.80	1.10	5.5	m
	43.0/44.0	0.19	1.10	1.40	7.4	p
	44.0/45.0	0.15	0.90	1.20	8.0	p
	46.0/47.0	0.20	0.80	1.00	5.0	m
	47.0/48.0	0.18	0.90	1.60	8.9	p
	48.0/49.0	0.13	0.55	1.00	7.7	p
	49.0/50.0	0.16	1.20	1.80	11.3	p
	MEAN	0.17	0.97	1.39	8.6	p

*Grain size that is 10 percent finer by weight
**Grain size that is 50 percent finer by weight
***Grain size that is 60 percent finer by weight
****-Uniformity coefficient D60 /D10
w-well sorted
p - poor sorted

both the upper A and lower aquifers B. The C_u range of the upper aquifer A is between 10 and 30 while in the lower aquifer B it is between 7 and 30. The core sediments of well DO are well-sorted in both the upper and lower sections of the borehole with C_u ranges of 2 to 6 and 3 to 4, respectively. This borehole shows the lithological characteristics near by the southwestern boundary of the catchments area.

The core sediment of well EO, as the mean C_u value of 3 reflects, is generally well-sorted in the middle aquifer B but less well sorted in the upper part of the aquifer B with a Cu range of 1 to 11 and in the lower part of the aquifer B (C_u range 2 to 15). The core sediment of well IO consists of three sections. The upper and the lower sections are poorly sorted with a C_u range of 5 to 10 and 2 to 14 with mean values of 7 and 9 respectively. However, the middle section sediments are well-sorted with C_u values in the range between 3 and 5. The sieve data analyses of well KO core sediment show that the middle aquifer B is poorly sorted with a C_u value range of 5 to 11 and mean of 8.

8.3.2 Hydraulic properties of the Multi-aquifer system

A multi-aquifer system occurs in the lower part of Wadi Baysh. The following definitions of some of the hydraulic properties of aquifers used in this study are adapted from Bear (1979), Kursman *et al.* (1990) and Fetter (1988).

Aquifer

An aquifer is a saturated geological unit that is permeable enough to yield water in a usable quantity to a well. The common aquifers are unconsildated sand and gravels. However, permeable sedimentary rocks (sandstone and limestone) and heavily fractured or weathered rocks (crystalline and volcanic rocks) can also be classified as aquifers. However, ground water occurs in aquifers under two different conditions: unconfined and confined.

An unconfined aquifer is one in which water only partly fills an aquifer. The upper surface of the saturated zone, also called the water table, is free to rise and decline. There are no confining beds between the zone of saturation and the surface. The water in

such aquifers is said to be unconfined (Figure 8.7).

A confined aquifer is an aquifer that is overlain by a confining bed. The confining bed has a significantly lower hydraulic conductivity than the aquifer. A pressure aquifer and an artesian aquifer are a synonyms.

Permeability or Hydraulic Conductivity (K) is the constant of proportionality in Darcy's law (see equation 5.3). It is a measure of the capacity of an aquifer to transmit water (Figure 8.7). Quantitatively the permeability can be defined as the volume of water that will move through a porous medium in unit time under a unit hydraulic gradient through a unit area measured at right angles to direction of flow.

The definition indicates that the permeability is a function of pore water properties as well as the matrix of solid material in the aquifer. The units of permeability are units of length/time commonly used are gpd/ft^2, ft/day, m/day, cm/day. If we rearrange equation 5.3 to solve for K, we obtain

$$K = \frac{Qdl}{Adh} = \frac{(m^3d^{-1})(m)}{(m^2)(m)} = \frac{m}{d} \qquad (8.1)$$

It is clear that equation 8.1 shows that the factors involved in the definition of permeability (hydraulic conductivity) include the volume of water (Q) that will move in a unit time (commonly, a day) under a unit hydraulic gradient (such as meter by meter) through a unit area (such as a square meter). These factors are illustrated in Figure 8.7.

Bouwer (1978), determined different K magnitudes for different kinds of rock in which the unconsolidated materials were considered in this section as follows:

Unconsolidated materials	K(m/d)	
Clay	10^{-8}	-10^{-2}
Fine sand	1	- 5
Medium sand	5	- $2x10^1$
Coarse sand	$2x10^1$	-10^2
Gravel	10^2	-10^3
Sand and gravel mixes	5	-10^2
Clay, sand, gravel mixes (e.g. till)	10^{-3}	-10^{-1}

Transmissivity (T) is the ability (capacity) of an aquifer to transmit water through its thickness. It is the rate of flow of water through a vertical strip of the aquifer one unit wide and extending the full saturated thickness, under hydraulic gradient of 1:1 at the prevailing temperature of the water. Quantitatively the transmissivity is the product of the

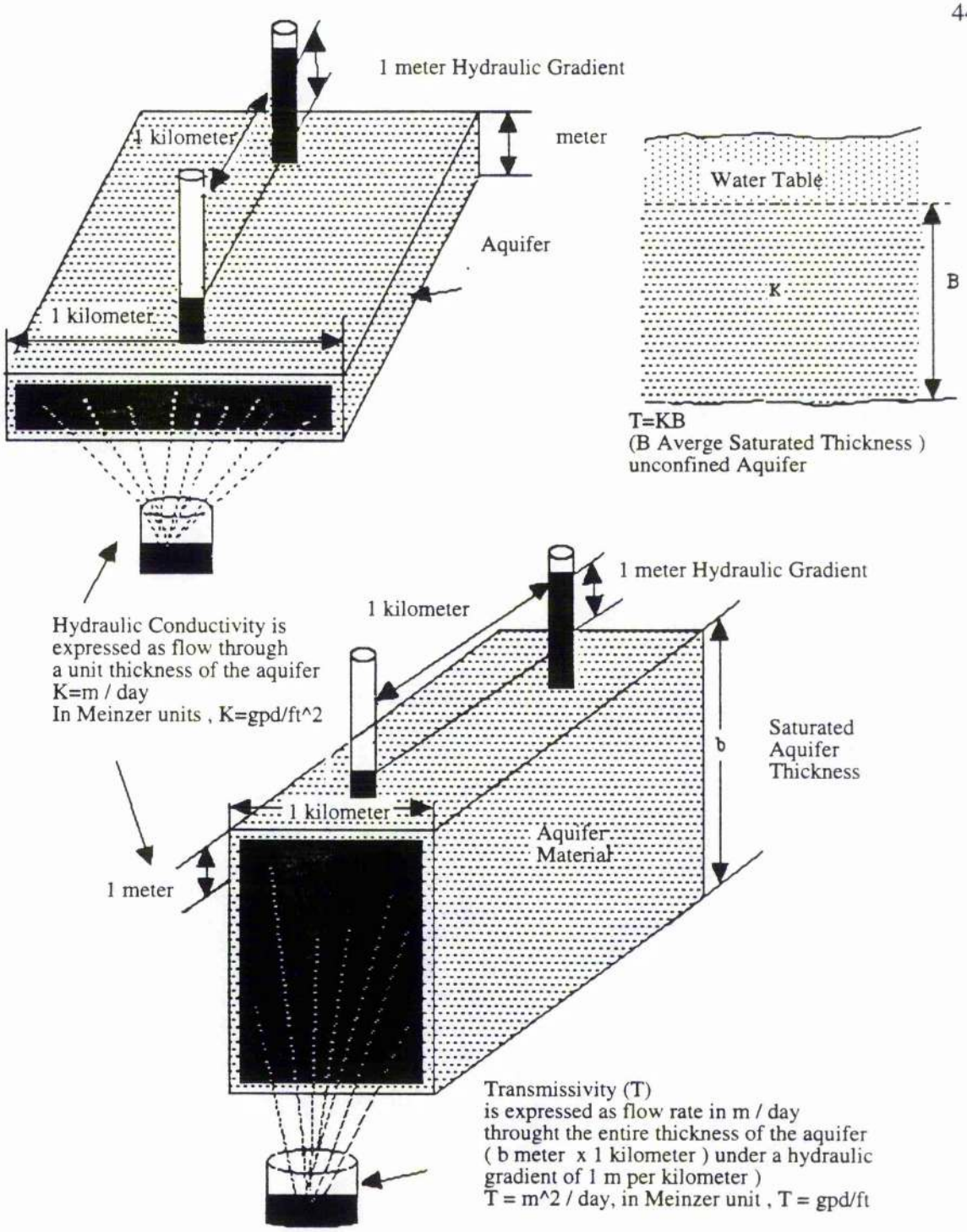

Figure 8.7 Diagram showing the transmissivity and hydraulic conductivity of aquifers.

average hydraulic conductivity K (or permeability) and the thickness of the aquifer b. It is denoted by T (square length / time).

In a single aquifer and a multilayer aquifer the transmissivity, T, may be calculated using the equation (6.9).

The porosity is defined as volume of voids as a % of the bulk volume of material. If the total unit volume (V_T) of an unconsolidated material in which the volume of its solid portion is equal to V_S and the volume of its voids is V_v, then the porosity can be defined as $n = V_v / V_T$. Porosity is usually expressed as a percentage or as a decimal fraction.

As a result of the action of running water, the wadi floor sediments tend to be well-sorted. In addition to grain size sorting, the shape of the grains affects the porosity of the sediments. Sediments of irregular grains will pack less tightly than those composed of sphere-shaped grains. The orientation of particles, if they are not spheres, also influences porosity. The general range of porosity that can be expected for some typical sediments (well sorted sand or gravel to clay) is 25% to 60% (see Fetter, 1988).

8.3.2.1 Permeability or Hydraulic Conductivity (K)

Many investigators have attempted to relate the properties of aquifer material to their transmitting capabilities. In the following, some of these investigators work is described.

The question of what grain size parameters are most effective in determining the relationship with permeability was investigated by Rose and Smith (1957) for Illinois glacial sands. They concluded that the D_{10} size gave the best correlation and that the uniformity coefficient Cu had little or no effect when using the D_{10} size. In contrast, Norris and Fidler (1965) in evaluation of sands from glacial outwash stated that a simple and direct relation appeared to exist between permeability and uniformity coefficient, at least for a specific aquifer.

Equations to predict permeability from the properties of porous media range from the purely theoretical to strictly empirical with varying degrees of applicability to a given situation. Some of the more important equations follow.

One of the earliest empirical equations is that of Hazen (1892):

$$K = C\,(D_{10}) \qquad (8.3)$$

Expressed in cm the D_{10} grain size is the "effective size" and C is a constant which is approximately 100, but is stated to vary in Hazen's observations between 41 and 146 (Taylor, 1948).

Slichter (1899) developed a theoretical equation for uniform spheres of diameter D, from the geometry of the voids.

$$K = \frac{771D^2}{C} \quad cm/sec \tag{8.4}$$

From a regression analysis of tabulated values the constant, C, is found to vary in accordance with the following equation:

$$C = 0.9867\, n^{-3.3} \tag{8.5}$$

where n = porosity.

Terzhagi (1925) derived an equation based on Slichter's equation and extended it to cover sand of non-uniform grain size and variable grain shape.

$$K = \frac{C}{n}\left[\frac{n-0.13}{1-n}\right]^2 D_{10}^2 \quad cm/sec \tag{8.6}$$

where D_{10} = grain size in cm at 10% passing, Y = viscosity of water (e.g. 0.131 c.g.s. at 10°) and C = shape constant.

The parameter Cu varies from 800 for rounded sands to 460 for angular sands.

The equation developed by Fair and Hatch (1933) includes provision for accounting for the proportions of sand sizes contained in the sample. It was developed from dimensional considerations and verified experimentally (Todd, 1959). The equation which gives specific (intrinsic) permeability is:

$$K = \frac{1}{m\left[\frac{(1-n)^2}{n^3}\left(\frac{Q}{100}\sum\frac{P}{D_m}\right)^2\right]} \tag{8.7}$$

where n = porosity, m = packing factor = 5, Q = sand shape factor varying from 6 for spherical grams to 8.7 for angular grains, P = percentage of sand held between adjacent sieves and D_m = geometric mean of rated sizes of adjacent sieves in mm.

Krumbein and Monk (1942; in Masch and Denny, 1966) performed experiments

using sieved and recombined glacial outwash sands.

$$K = a\, D_m^2\, e^{-bs} \tag{8.8}$$

where D_m = geometric mean diameter in mm, s = log standard deviation of size distribution, which is dimensionless, a = constant equal to 760, b = constant equal to 1.31 and e = dimensionless constant equal to 2.718.

Bear (1979) indicated that Kozeny-Carman equation below is obtained from

$$K = C_o \frac{n^3}{(1-n)^2 M_S^2} \tag{8.9}$$

theoretical derivations of Darcy's law to obtain the hydraulic conductivity (K), where M_S is the specific area of the porous matrix (defined per unit volume of solid), C_o is a coefficient for which Carman (1937) suggested the value of 1/5.

Masch and Denny (1966) studied the relation between the permeability and the statistical parameters that describe the grain size distribution of the porous media (unconsolidated sands). A group of curves was defined which incorporated the median, D_{50}, and dispersion to predict the permeability values for aquifer samples.

Equations for permeability provide useful information for specific samples, but these samples may or may not give a representative measure of aquifer permeability. However, the more homogeneous in nature the aquifer material, the more meaningful are the values obtained from samples.

Representative ranges for porosity, specific yield and permeability in naturally occurring sedimentary materials are shown in Table 8.7.

Table 8.7 The porosity, specific yield and permeability of sedimentry material (after Todd, 1970).

Material	Specific Yield (%)	Porosity (%)	Permeability (gpd/ft^2)	Permeability (cm/sec)
Clay	3	45-55	10^{-5}-10^{-3}	10^{-9}-10^{-7}
Silt	5	40-50	10^{-2}-10^{-1}	10^{-6}-10^{-4}
Very fine sand	10	-	1-10^{2}	10^{-4}-10^{-2}
Fine sand	10	30-35	10^{1}-10^{3}	10^{-3}-10^{-1}
Medium sand	25	30-40	10^{2}-10^{3}	10^{-2}-10^{-1}
Coarse sand	25	35-40	10^{2}-10^{4}	10^{-2}-1
Gravel and sand	25	20-35	10^{2}-10^{4}	10^{-2}-1

The above table shows that the specific yield and the permeability increase when the aquifer

material is dominated by coarse grains while the porosity decreases.

As shown previously, there are several methods, which can be used to determine the aquifer permeability. However, due to the available data (grain size distribution of the multiaqifer), Hazen's method and the Mash-Denny method were used here. The determination of the permeability using both methods was based on random field samples of the multiaquifer, which were tested against the permeability determined by pumping test analysis.

The Hazen method is used in this study to determine the aquifer permeability for each aquifer individually. The advantage of applying the Hazen method in the study area is that both of the parameters required to calculate the permeability (the effective grain size, D_{10}, and coefficient C) can be determined from the available data. The Masch and Denny method was adapted to determine the aquifer permeability due to the fact that the average grain size (MD_{50}) and the standard deviation of the aquifer samples (σ) give good relationships with the hydraulic conductivity. Both methods will be discussed further later in this chapter.

The pumping tests

The pumping test is the most reliable method of obtaining the aquifer parameters. The distance drawdown method of the Jacob straightline was used by MAWR to determine the hydraulic properties of the aquifer. This technique may be used if simultaneous observations of the drawdown are made in three or more wells. The pumping tests in these wells provide the average values for the whole depth of the aquifer being exploited. There are no data available on pumping tests for each individual aquifer within the whole section of sediments. The permeability value (m/day) of each well is shown in Table 8.8 and Figure 8.8.

Table 8.8 Aquifer parameters of Wadi Baysh Boreholes (After MAWR, 1978)

Borehole NO	Borehole Depth (m)	Aquifer* Thickness(m)	Transmissivity x10^-3 m^2/sec	Permeability** cm/sec	m/day
AO	97.5	77.5	4	0.0052	4.46
BO	140	120	15	0.0125	10.80
CO	92	72	2.5	0.0035	3.00
DO	63	43	4	0.0093	8.04
EO	150	130	12	0.0092	7.98
JO	141	121	12	0.0099	8.57
KO	102	82	2.8	0.0034	2.95

*Aquifer thickness = Borehole depth - water level depth

** Permeability = Transmissivity / Aquifer thickness (saturated thickness)

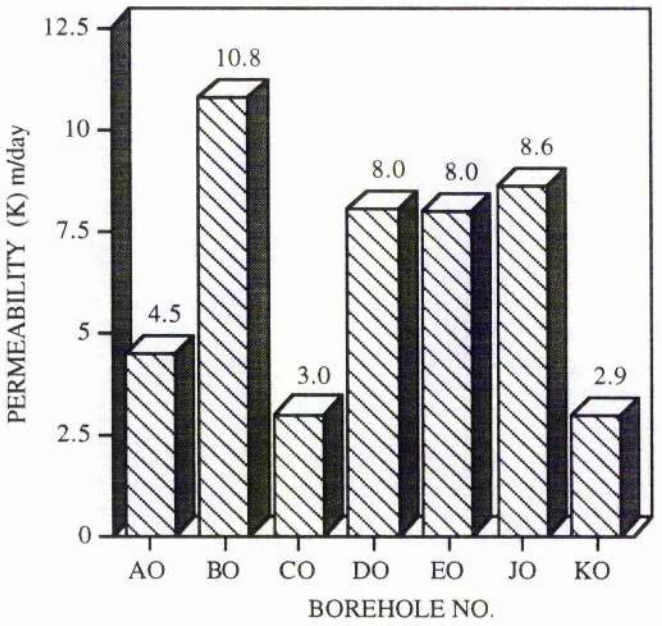

Figure 8.8 Permeability determination (m/day) of Wadi Baysh boreholes using pumping test analysis

Borehole permeabilities vary between 3 and 10.8 m/day. The average permeability values of Wadi Baysh basin were 6.54 m/day with a standard deviation of 3.0 m/day. However those boreholes near to the main wadi channel (BO, EO and IO) show higher permeability than those boreholes nearer the catchment boundary (KO,AO and CO) (see Figure 8.1).

The permeability determinations using the pumping test analyses were compared with the average permeability estimation using the Hazen and Masch & Denny methods.

This study will reveal the effect of average size (MD_{50}) and effective grain size (D_{10}) distribution on the permeability of the multiaquifer fresh water.

8.3.2.1.1 Hazen's Method

The basin sediment of the lower part of Wadi Baysh is characterised by unconsolidated coarse-grained materials which represent the main producers of ground water as a multiaquifer system (see Figures 8.3 and 8.4). The permeability of each aquifer in the study area is estimated from the grain size distribution curves (see Appendix 8B) using the Hazen method. This method is an empirical equation 8.3, described previously, used to approximate the permeability of a sediment on the basis of the effective grain size (D_{10}). The Hazen method is applicable to effective size (D_{10}) of sediment between approximately 0.1 and 3.0mm.

The ground water site investigations have been carried out in the lower part of Wadi Baysh in an area close to the level of the main wadi channel and flood plain. The hydrogeological applicability of the Hazen method has been shown in a study of the permeability of well sediments of this area. There are several aquifers present in the unconsolidated wadi basin sediments, (see Chapter 8. section one). Grain sorting varies from well sorted to poorly sorted. There are eleven ground water observation wells installed in this part of the wadi. The available grain size analyses of well cores are summarised in Appendix 8A for seven observation wells (AO, BO, CO, DO, EO, IO and KO). The permeability of the sediments in each observation well have been calculated by means of the Hazen method, using a coefficient of C based on the degree of the grain size sorting (Tables 8.9 and 8.10).

Table 8.9 Values of coefficient C for different types of sediments (after Fetter, 1988)

Sediment types	Coefficient
very fine sand, poorly sorted	40-80
fine sand, well sorted	40-80
medium sand, well-sorted	80-120
coarse sand, poorly sorted	80-120
coarse sand, well-sorted, clean	120-150

In this study the geometric and arithmetic means of the multiaquifer permeability have been calculated. The geometric mean is determined by taking the natural log of each

Table 8.10 Permeability coeficient calculation using the Hazen method for different depths in the lower part of Wadi Baysh

Borehole No. AO	Depth neter	Middle D10 *	Aquifer D50 **	D60 ***	CU ****	Sorting Range	C (Hazen's coefficient)	Permeability (K) (cm/sec)	Arithmetic mean (K) cm/sec	Geometric mean (K) cm/sec
	45.5/46.0	0.21	1.50	1.85	8.8	p	40	0.018		
	46.0/47.0	0.25	1.50	1.90	7.6	p	40	0.025		
	47.0/48.0	0.08	0.29	0.40	5.0	m	40	0.003		
	48.0/49.0	0.08	0.28	0.40	5.0	m	40	0.003		
	49.0/50.0	0.10	0.29	0.32	3.2	w	80	0.008		
	50.0/51.0	0.11	0.35	0.62	5.6	m	40	0.005		
	51.0/52.0	0.19	0.60	0.81	4.3	m	40	0.014		
	52.0/53.0	0.26	1.00	1.50	5.8	m	40	0.027		
	MEAN	0.16	0.73	0.98	5.7	m	40		0.013	0.0091
Borehole No. BO	Depth neter	Upper D10 *	Aquifer (Middle Section) D50 **	D60 ***	CU ****	Sorting Range	C (Hazen's coefficient)	Permeability (K) (cm/sec)	Arithmetic mean (K) cm/sec	Geometric mean (K) cm/sec
	54.0/55.0	0.20	5.80	0.80	4.0	w	80	0.032		
	55.0/56.0	0.19	0.60	0.80	4.2	m	40	0.014		
	56.0/57.0	0.18	0.50	0.60	3.3	w	80	0.026		
	57.0/58.0	0.10	0.30	0.40	4.0	w	80	0.008		
	58.0/59.0	0.11	0.55	0.90	8.2	p	40	0.005		
	59.0/60.0	0.10	0.41	0.55	5.5	m	40	0.004		
	60.0/61.0	0.12	0.40	0.70	5.8	m	40	0.006		
	61.0/62.0	0.09	0.55	0.80	9.4	p	80	0.006		
	62.0/63.0	0.10	0.41	0.50	5.0	m	40	0.004		
	76.0/77.0	0.09	0.48	0.60	6.7	p	40	0.003		
	77.0/78.0	0.07	0.45	0.60	8.6	p	40	0.002		
	78.0/79.0	0.06	0.50	0.60	10.0	p	40	0.001		
	79.0/80.0	0.07	0.45	0.58	8.9	p	40	0.002		
	80.0/81.0	0.06	0.50	0.75	12.5	p	40	0.001		
	81.0/82.0	0.07	0.42	0.60	9.2	p	40	0.002		
	MEAN	0.11	0.82	0.65	7.0	p	40		0.008	0.0046
	Depth neter	Upper D10 *	Aquifer (Lower Section) D50 **	D60 ***	CU ****	Sorting Range	C (Hazen's coefficient)	Permeability (K) (cm/sec)	Arithmetic mean (K) cm/sec	Geometric mean (K) cm/sec
	97.0/98.0	0.10	0.49	0.65	6.5	p	40	0.004		
	98.0/99.0	0.09	0.40	0.60	6.7	p	40	0.003		
	99.0/100	0.11	0.33	0.44	4.0	w	80	0.010		
	MEAN	0.10	0.41	0.56	5.7	m	40		0.006	0.0047

Continued on next page

Table 8.10 continued

Borehole No.	Depth	Lower	Aquifer (Upper Section)			Sorting	C (Hazen's	Permeability (K)	Arithmetic mean (K)	Geometric mean (K)
BO	neter	D10 *	D50 **	D60 ***	CU ****	Range	coefficient)	(cm/sec)	cm/sec	cm/sec
	112/113	0.10	0.40	0.70	7.0	p	40	0.004		
	113/114	0.20	0.60	0.85	4.3	p	40	0.016		
	MEAN	0.15	0.50	0.78	5.6	m	40		0.010	0.0083
Borehole No.	Depth	Upper	Aquifer			Sorting	C (Hazen's	Permeability (K)	Arithmetic mean (K)	Geometric mean (K)
CO	neter	D10 *	D50 **	D60 ***	CU ****	Range	coefficient)	(cm/sec)	cm/sec	cm/sec
	37.0/38.0	0.17	0.40	0.70	4.1	w	80	0.023		
	38.0/39.0	0.07	0.70	0.20	3.1	w	80	0.003		
	39.0/40.0	0.07	0.65	1.50	23.1	p	40	0.002		
	MEAN	0.10	0.58	0.80	10.1	p	40		0.009	0.0048
	Depth	Lower	Aquifer			Sorting	C (Hazen's	Permeability (K)	Arithmetic mean (K)	Geometric mean (K)
	neter	D10 *	D50 **	D60 ***	CU ****	Range	coefficient)	(cm/sec)	cm/sec	cm/sec
	50.0/51.0	0.10	0.70	0.90	9.0	p	40	0.004		
	51.0/52.0	0.13	1.80	4.00	30.8	p	40	0.007		
	52.0/53.0	0.90	1.10	1.70	1.9	w	80	0.648		
	53.0/54.0	0.08	0.80	1.50	18.8	p	40	0.003		
	MEAN	0.30	1.10	2.03	15.1	p	40		0.165	0.0175
Borehole No.	Depth	Upper	Aquifer			Sorting	C (Hazen's	Permeability (K)	Arithmetic mean (K)	Geometric mean (K)
DO	neter	D10 *	D50 **	D60 ***	CU ****	Range	coefficient)	(cm/sec)	cm/sec	cm/sec
	35.0/36.0	0.12	1.00	1.60	13.3	p	40	0.006		
	36.0/37.0	0.23	1.10	1.60	7.0	p	40	0.021		
	37.0/38.0	0.10	0.30	0.38	3.8	w	80	0.008		
	38.0/39.0	0.14	0.35	0.40	2.9	w	80	0.016		
	MEAN	0.15	0.69	1.00	6.7	p	40		0.013	0.0106
	Depth	Lower	Aquifer			Sorting	C (Hazen's	Permeability (K)	Arithmetic mean (K)	Geometric mean (K)
	neter	D10 *	D50 **	D60 ***	CU ****	Range	coefficient)	(cm/sec)	cm/sec	cm/sec
	41.0/42.0	0.06	0.37	0.48	8.7	p	40	0.001		
	42.0/43.0	0.05	0.30	0.40	8.0	p	40	0.001		
	43.0/44.0	0.10	0.40	0.50	5.0	m	40	0.004		
	44.0/45.5	0.06	0.40	0.50	8.3	p	40	0.001		
	MEAN	0.07	0.37	0.47	7.5	p	40		0.002	0.0017

Continued on next page

Table 8.10 continued

Borehole No.	Depth	Middle	Aquifer (Upper Section)			Sorting	C (Hazen's	Permeability (K)	Arithmetic mean (K)	Geometric mean (K)
EO	neter	D10 *	D50 **	D60 ***	CU ****	Range	coefficient)	(cm/sec)	cm/sec	cm/sec
	55.0/56.0	0.18	0.40	0.45	2.5	w	80	0.026		
	56.0/57.0	0.15	0.41	0.50	3.3	w	80	0.018		
	59.0/60.0	0.20	3.20	4.50	22.5	p	40	0.016		
	60.0/61.0	0.35	3.00	4.10	11.7	p	40	0.049		
	MEAN	0.22	1.75	2.39	10.0	p	40		0.027	0.0234
	Depth	Middle	Aquifer (Middle Section)			Sorting	C (Hazen's	Permeability (K)	Arithmetic mean (K)	Geometric mean (K)
	neter	D10 *	D50 **	D60 ***	CU ****	Range	coefficient)	(cm/sec)	cm/sec	cm/sec
	63.0/64.0	0.12	0.35	0.50	4.2	p	40	0.006		
	64.0/65.0	0.11	0.30	0.30	2.7	w	80	0.010		
	65.0/66.0	0.10	0.30	0.48	4.8	m	40	0.004		
	66.0/67.0	0.12	0.32	0.45	3.8	w	80	0.012		
	67.0/68.0	0.11	0.80	1.50	13.6	p	40	0.005		
	68.0/69.0	0.12	0.34	0.70	5.8	m	40	0.006		
	MEAN	0.11	0.40	0.66	5.8	m	40		0.007	0.0062
Borehole No.	Depth	Upper	Aquifer			Sorting	C (Hazen's	Permeability (K)	Arithmetic mean (K)	Geometric mean (K)
JO	neter	D10 *	D50 **	D60 ***	CU ****	Range	coefficient)	(cm/sec)	cm/sec	cm/sec
	42.0/42.5	0.09	0.65	1.00	11.1	p	40	0.003		
	42.5/43.5	0.40	1.50	1.75	4.4	m	40	0.064		
	43.5/44.5	0.22	1.20	1.80	8.2	p	40	0.019		
	44.5/45.0	0.32	1.75	3.00	9.4	p	40	0.041		
	45.0/46.5	0.20	2.00	3.00	15.0	p	40	0.016		
	MEAN	0.25	1.42	2.11	9.6	p	40		0.029	0.0200
	Depth	Middle	Aquifer			Sorting	C (Hazen's	Permeability (K)	Arithmetic mean (K)	Geometric mean (K)
	neter	D10 *	D50 **	D60 ***	CU ****	Range	coefficient)	(cm/sec)	cm/sec	cm/sec
	64.5/65.5	0.55	4.00	5.00	9.1	p	40	0.121		
	65.5/66.5	0.30	2.00	3.00	10.0	p	40	0.036		
	MEAN	0.43	3.00	4.00	9.5	p	40		0.079	0.0416
	Depth	Lower	Aquifer			Sorting	C (Hazen's	Permeability (K)	Arithmetic mean (K)	Geometric mean (K)
	neter	D10 *	D50 **	D60 ***	CU ****	Range	coefficient)	(cm/sec)	cm/sec	cm/sec
	120/121	0.07	0.80	1.30	18.6	p	40	0.002		
	121/121.5	0.08	1.10	1.60	20.0	p	40	0.003		
	121.5/123	0.10	1.70	2.00	20.0	p	40	0.004		
	123/124	0.16	1.80	0.28	1.8	w	80	0.020		
	MEAN	0.10	1.35	1.30	15.1	p	40		0.007	0.0044

Continued on next page

Table 8.10 continued

Borehole No. KO	Depth meter	Middle D10 *	Aquifer D50 **	D60 ***	CU ****	Sorting Range	C (Hazen's coefficient)	Permeability (K) (cm/sec)	Arithmetic mean (K) cm/sec	Geometric mean (K) cm/sec
	40.5/42.0	0.13	1.50	2.00	15.4	p	40	0.007		
	42.0/43.0	0.20	0.80	1.10	5.5	m	40	0.016		
	43.0/44.0	0.19	1.10	1.40	7.4	p	40	0.014		
	44.0/45.0	0.15	0.90	1.20	8.0	p	40	0.009		
	46.0/47.0	0.20	0.80	1.00	5.0	m	40	0.016		
	47.0/48.0	0.18	0.90	1.60	8.9	p	40	0.013		
	48.0/49.0	0.13	0.55	1.00	7.7	p	40	0.007		
	49.0/50.0	0.16	1.20	1.80	11.3	p	40	0.010		
	MEAN	0.17	0.97	1.39	8.6	p	40		0.012	0.0110

*Grain size that is 10 percent finer by weight
**Grain size that is 50 percent finer by weight
***Grain size that is 60 percent finer by weight
****-Uniformity coefficient D60/D10
w-well sorted
m-well to poor sorted
p - poor sorted

value, finding the mean of the natural values and then calculating the exponential (e^x) of that value to get the geometric mean (see Table 8.10).

All of these results were tested (Tables 8.10 and 8.11) as they were plotted against the D_{10} of the grain size. In Figure 8.9 a strong linear correlation (r = 0.95) between the grain size and the permeability is seen. However, the D_{10} (grain size) shows a higher correlation (r = 0.97) with geometric mean of the permeability (see Table 8.12 and Figure 8.10) while with the arithmetic mean (see Table 8.12), the correlation coefficient is lower (0.582) (see Figure 8.10).

The permeability of wadi floor sediments can therefore be calculated more accurately using the equation below

$$K \text{ (permeability)} = 0.526\ (D_{10})^{2.067} \qquad r = 0.956 \qquad (8.10)$$

where K is cm/sec and the D_{10} is mm.

The average permeability for each borehole has been correlated using the arithmetic and the geometric means versus the permeability from pumping test analysis, due to the fact that the permeability determination using the pumping test represents the average value of the saturated thickness (see Figure 8.11 and Figure 8.12). The boreholes show a similar variation of permeability except the borehole CO in which the arithmetic mean of the permeability has high value of 0.0913 cm/sec. However, the geometric mean of the permeability has a strong correlation with effective grain size (D_{10}) while the arithmetic mean and the pumping test show low correlations of 0.582 and 0.3, respectively.

8.3.2.1.2 Masch and Denny Method

The Masch and Denny method shoes the relationships between permeability and the statistical parameters describing the grain size distributions of unconsolidated sands. It consists of systematic variation of the values of the statistical parameters mainly the median and the inclusive standard deviation (σ_I). The median, i.e., MD_{50}, is used as a measure of the average particle diameter size for the samples constructed where the inclusive standard deviation (STD). σ_I, is used as measure of the dispersion about the median diameter for a given distribution. The expression for σ_I is

Table 8.11 The Determination of the multiaquifer permeability (cm/sec) of Wadi Baysh using Hazen's method

Borehole No.	Depth neter	D10 * mm	Permeability (K) (cm/sec)
AO	45.5/46.0	0.21	0.018
	46.0/47.0	0.25	0.025
	47.0/48.0	0.08	0.003
	48.0/49.0	0.08	0.003
	49.0/50.0	0.10	0.008
	50.0/51.0	0.11	0.005
	51.0/52.0	0.19	0.014
	52.0/53.0	0.26	0.027
BO	54.0/55.0	0.20	0.032
	55.0/56.0	0.19	0.014
	56.0/57.0	0.18	0.026
	57.0/58.0	0.10	0.008
	58.0/59.0	0.11	0.005
	59.0/60.0	0.10	0.004
	60.0/61.0	0.12	0.006
	61.0/62.0	0.09	0.006
	62.0/63.0	0.10	0.004
	76.0/77.0	0.09	0.003
	77.0/78.0	0.07	0.002
	78.0/79.0	0.06	0.001
	79.0/80.0	0.07	0.002
	80.0/81.0	0.06	0.001
	81.0/82.0	0.07	0.002
	97.0/98.0	0.10	0.004
	98.0/99.0	0.09	0.003
	99.0/100	0.11	0.010
BO	112/113	0.10	0.004
	113/114	0.20	0.016
CO	37.0/38.0	0.17	0.023
	38.0/39.0	0.07	0.003
	39.0/40.0	0.07	0.002
	50.0/51.0	0.10	0.004
	51.0/52.0	0.13	0.007
	52.0/53.0	0.90	0.648
	53.0/54.0	0.08	0.003
DO	35.0/36.0	0.12	0.006
	36.0/37.0	0.23	0.021
	37.0/38.0	0.10	0.008
	38.0/39.0	0.14	0.016
	41.0/42.0	0.06	0.001
	42.0/43.0	0.05	0.001
	43.0/44.0	0.10	0.004
	44.0/45.5	0.06	0.001
EO	55.0/56.0	0.18	0.026
	56.0/57.0	0.15	0.018
	59.0/60.0	0.20	0.016
	60.0/61.0	0.35	0.049
	63.0/64.0	0.12	0.006
	64.0/65.0	0.11	0.010
	65.0/66.0	0.10	0.004
	66.0/67.0	0.12	0.012
	67.0/68.0	0.11	0.005
	68.0/69.0	0.12	0.006
JO	42.0/42.5	0.09	0.003
	42.5/43.5	0.40	0.064
	43.5/44.5	0.22	0.019
	44.5/45.0	0.32	0.041
	45.0/46.5	0.20	0.016
	64.5/65.5	0.55	0.121
	65.5/66.5	0.30	0.036
	120/121	0.07	0.002
	121/121.5	0.08	0.003
	121.5/123	0.10	0.004
	123/124	0.16	0.020
KO	40.5/42.0	0.13	0.007
	42.0/43.0	0.20	0.016
	43.0/44.0	0.19	0.014
	44.0/45.0	0.15	0.009
	46.0/47.0	0.20	0.016
	47.0/48.0	0.18	0.013
	48.0/49.0	0.13	0.007
	49.0/5	0.16	0.010

*Grain size that is 10 percent finer by weight

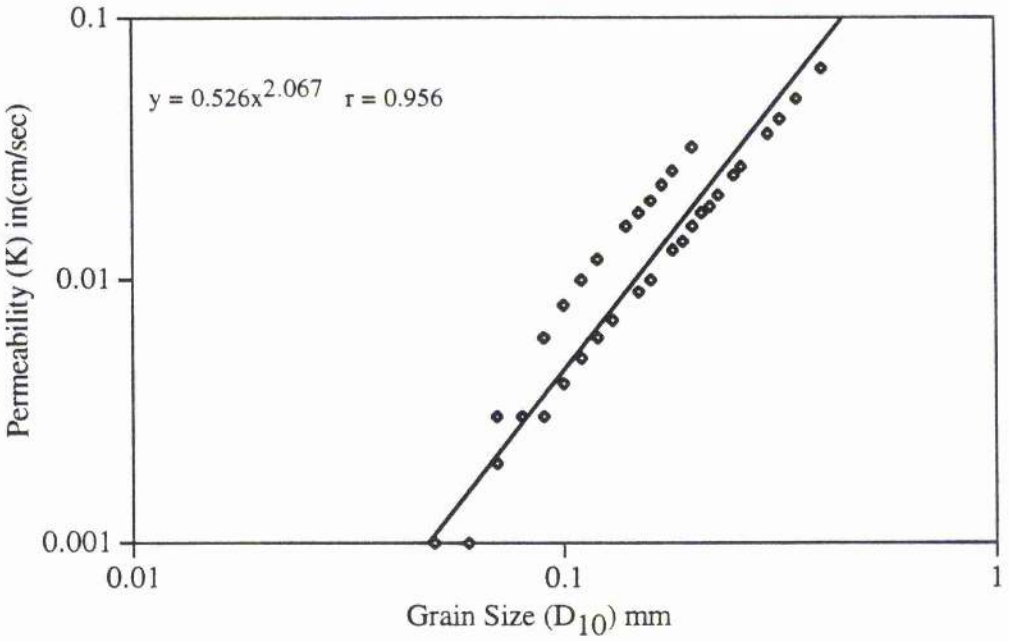

Figure 8.9 Graph relating the grain size (D_{10}) to different values of permeability using Hazen's method.

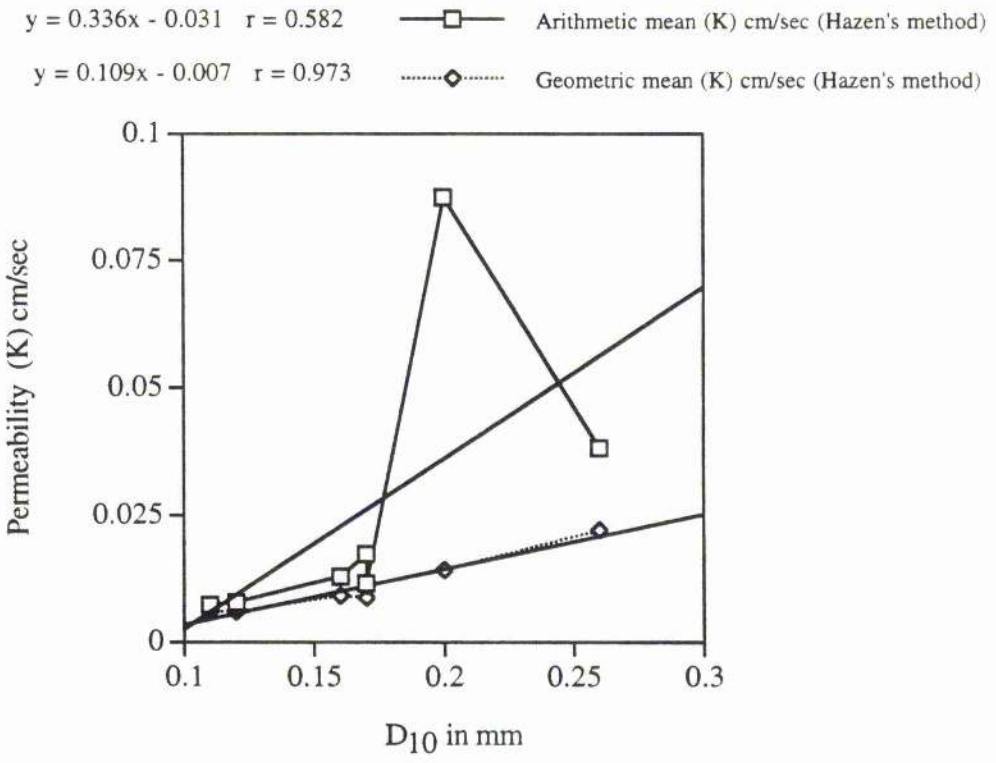

Figure 8.10 The correlation between the effective grain size and the permeabilty using different methods (arithmatic and geometric mean).

Table 8.12 Permeability variation (cm/s) with depth in the Wadi Baysh basin using different methods (Hazen's method, the pumping test and the Masch and Denny method)

		Hazen's Method		**Pumping test**	**Mash and Denny Method***	**Mash and Denny Method****
Borehole NO	Sample	Arithmetic mean (K)	Geometric mean (K)	K	Arithmetic mean (K)	Arithmetic mean (K)
and Depth	Location	cm/sec	cm/sec	**(cm/s)**	cm/sec	cm/sec
AO (45.5/53.0)	Aquifer (A)	**0.0128**	**0.0091**	**0.00593**	**0.00725**	**0.142**
BO (54.0/82.0)	Aquifer (A) (middle section	0.0077	0.0046		0.00406	0.017
BO (97.0/100)	Aquifer (A) (lower section)	0.0056	0.0047		0.00464	0.124***
BO (112/114)	Aquifer (B) (upper section)	0.0100	0.0083		0.00348	0.332
	Mean	**0.0078**	**0.0059**	**0.01364**	**0.00406**	**0.158**
CO (37.0/40.0)	Aquifer (A)	0.0094	0.0048		0.02331***	0.273
CO (50.0/54.0)	Aquifer (B)	0.1653	0.0175		0.02331***	0.095
	Mean	**0.0913**	**0.0141**	**0.00403**	**0.02331*** **	**0.183**
DO (35.0/39.0)	Aquifer (A)	0.0127	0.0106		0.02331***	0.154
DO (41.0/45.5)	Aquifer (B)	0.0019	0.0017		0.02331***	0.125***
	Mean	**0.0073**	**0.0061**	**0.01176**	**0.02331*** **	**0.139**
EO (55.0/69.0)	Aquifer (B) (Middle section	0.0069	0.0062		0.06148	0.014
EO (63.0/69.0)	Aquifer (B) (Lower section)	0.0268***	0.01095***		0.02331	0.125***
	Mean	**0.0172**	**0.0087**	**0.01000**	**0.04240**	**0.0692**
JO (42.0/46.5)	Aquifer (A) aquifer	0.0287	0.0200		0.06148	0.114
JO (64.5/66.5)	Aquifer (B) aquifer	0.0785	0.0416		0.01682	0.071
JO (120/124)	Aquifer (B) aquifer	0.0073	0.0044		0.02331***	**0.010**
	Mean	**0.0382**	**0.0220**	**0.01081**	**0.03387**	0.109
KO (40.5/50.0)	**Aquifer (B) aquifer**	**0.0115**	**0.0110**	**0.00389**	**0.02726**	**0.090**
Basin	**MEAN**	**0.02683**	**0.01095**	**0.00858**	**0.02331**	**0.125**

(K) Hydraulic conductivity cm/sec

* Based on an Inclusive Standard Deviation

** Based on the arithmatic Standerd Deviation

*** Estimated value based on the average of it's group

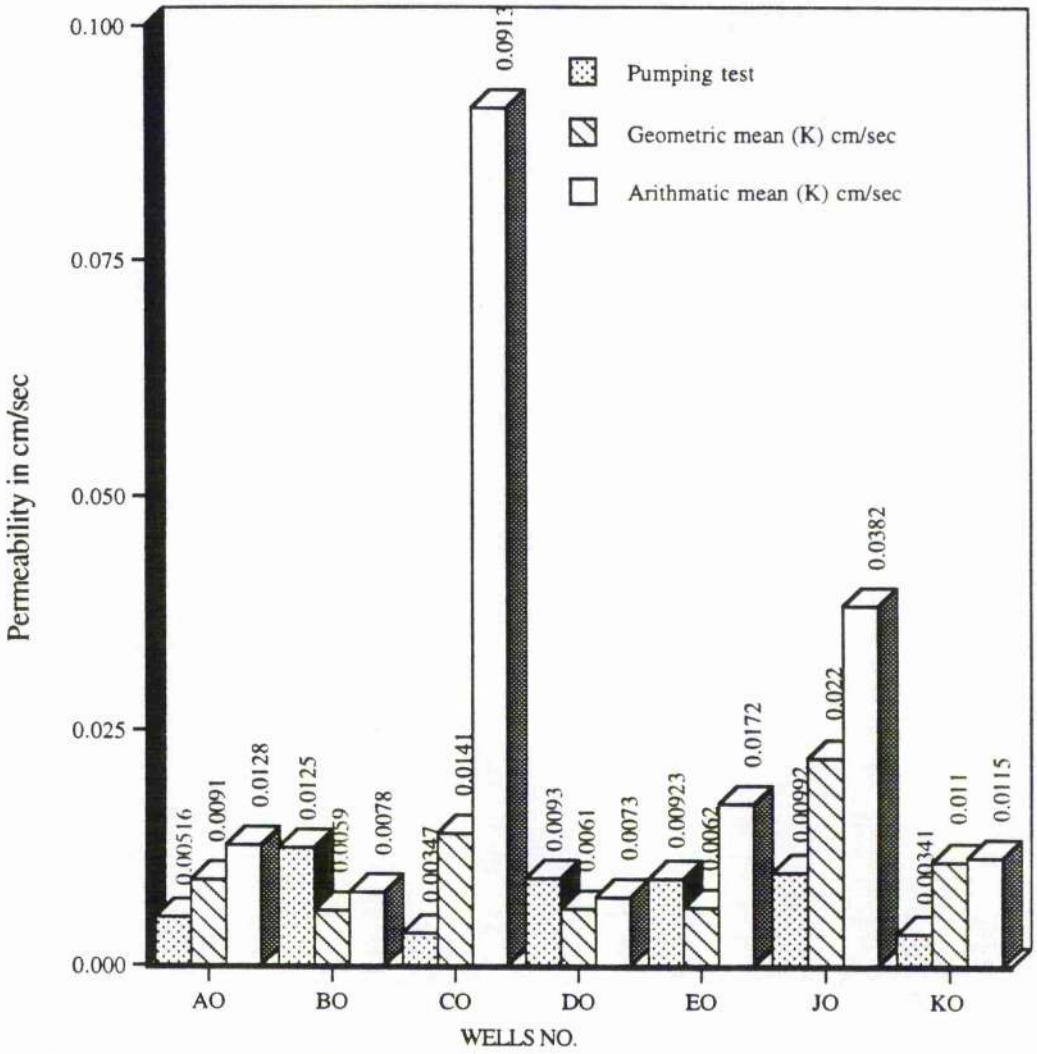

Figure 8.11 Multiaquifer permeability using different methods (the pumping test and Hazen's method-geometric and arithmetic mean).

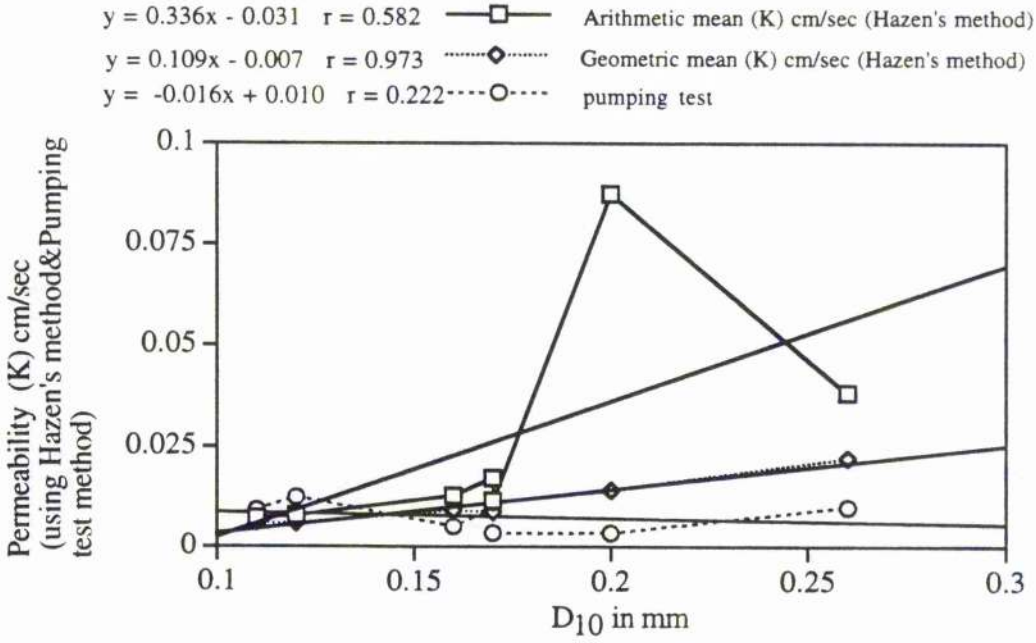

Figure 8.12 The correlation between the effective grain size and the permeabilty using different methods (Hazen's method and the pumping test).

$$\sigma_I = \frac{(\phi 84 - \phi 16)}{4} + \frac{(\phi 95 - \phi 5)}{6.6} \qquad (8.11)$$

The numerical values of (σ_I) range from 0 for a very well sorted distribution to 4 for very poorly sorted ones.

Figure 8.13 shows a family of curves with σ_I values ranging from $0 \leq \sigma_I \geq 1.5$ in increments of 0.25. The dashed portions of various curves for MD_{50} diameter smaller than 3.5 ϕ units represent extrapolations of the existing curves.

Egboka *et al.* (1986) indicated that this method is a most reliable statistical technique for estimating the permeability based on their comparative analysis of transmissivity and hydraulic conductivity values from the Aljali aquifer system of Nigeria.

The Field Samples

To estimate the permeability of the field samples from those predicted by the use of Figure 8.13, it was first necessary to determine the values of the MD_{50} diameter and σ_I parameters for each of the field samples. The MD_{50} diameter values were determined from the size distribution curves for the field samples (see Appendix 8), and the σ_I values were calculated from information obtained from those curves (see Appendix 8.) using equation 8.11 (see Table 8.13). Figure 8.13 was then used to obtain the estimated permeability for each field sample.

Figure 8.13 shows that the permeability values tend to increase with increasing median grain size and to decrease with increasing standard deviation. The grain size and the estimated permeability with their arithmetic mean (based on the inclusive STD) are plotted in Figures 8.14 and 8.15.

The graph relating grain size (MD_{50}) to different values of permeability show low values of correlation (r = 0.067) (see Figure 8.14). However an improved correlation (r = 0.607) exists between the arithmetic mean (MD_{50}) and the permeability for each borehole (AO, BO, CO, DO, EO, IO, KO) (see Table 8.12 and Figure 8.15).

Comparisons between those estimated values and the corresponding permeabilties determined by pumping tests are shown in Figure 8.16.

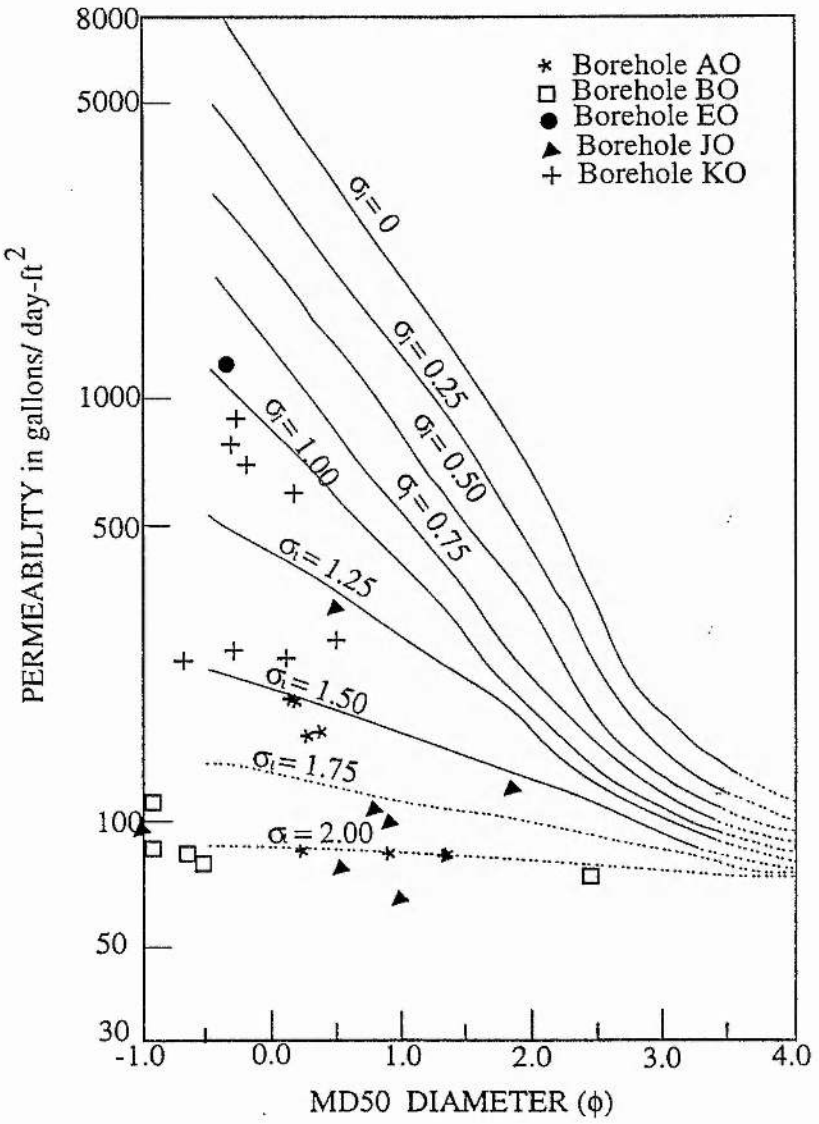

Figure 8.13 Curves used to determine the permeability of the multiaquifer of the Wadi Baysh basin (after Masch and Denny, 1966).

Table 8.13 The determination of the multiaquifer permeability of the Wadi Baysh basin using the Masch and Denny method (1966).

Borehole	Depth	Grain size analysis of multiaquifer											Permeability	
AO	meter	D50 (mm)	D50 (phi)	D95 (mm)	D95 (phi)	D84 (mm)	D84 (phi)	D16 (mm)	D16 (phi)	D5 (mm)	D5 (phi)	σ1	Gallons/day-ft2	m/d
	45.5/46.0	1.50	0.58	15	3.91	8	3.00	0.4	-1.32	0.2	-2.32	2.02	70	3
	46.0/47.0	1.50	0.58	15	3.91	8	3.00	0.4	-1.32	0.2	-2.32	2.02	70	3
	47.0/48.0	0.29	-1.79	4.5	2.17	2	1.00	0.08	-3.64	0.06	-4.06	2.10	75	3
	48.0/49.0	0.28	-1.84	2	1.00	1.2	0.26	0.15	-2.74	0.06	-4.06	1.52	250	10
	49.0/50.0	0.29	-1.79	3	1.58	1	0.00	0.13	-2.94	0.07	-3.84	1.56	230	9
	50.0/51.0	0.35	-1.51	6	2.58	2.1	1.07	0.3	-1.74	0.08	-3.64	1.65	200	8
	51.0/52.0	0.60	-0.74	5	2.32	3	1.58	0.27	-1.89	0.15	-2.74	1.63	210	9
	52.0/53.0	1.00	0.00	8	3.00	6.5	2.70	0.35	-1.51	0.1	-3.32	2.01	85	3
Borehole	Depth	Grain size analysis of multiaquifer											Permeability	
BO	meter	D50 (mm)	D50 (phi)	D95 (mm)	D95 (phi)	D84 (mm)	D84 (phi)	D16 (mm)	D16 (phi)	D5 (mm)	D5 (phi)	σ1	Gallons/day-ft2	m/d
	54.0/55.0	5.80	2.54	9	3.17	7	2.81	0.25	-2.00	0.15	-2.74	2.10		
	55.0/56.0	0.60	-0.74	8	3.00	6.5	2.70	0.25	-2.00	0.15	-2.74	2.04	90	4
	56.0/57.0	0.50	-1.00	7	2.81	6	2.58	0.2	-2.32	0.15	-2.74	2.07	80	3
	57.0/58.0	0.30	-1.74	7	2.81	7	2.81	0.15	-2.74	0.07	-3.84	2.39		
	58.0/59.0	0.55	-0.86	8	3.00	8	3.00	0.13	-2.94	0.1	-3.32	2.44		
	59.0/60.0	0.41	-1.29	7	2.81	7.5	2.91	0.1	-3.32	0.1	-3.32	2.49		
	60.0/61.0	0.40	-1.32	7	2.81	6.5	2.70	0.15	-2.74	0.1	-3.32	2.29		
	61.0/62.0	0.55	-0.86	7.5	2.91	6	2.58	0.1	-3.32	0.07	-3.84	2.50		
	62.0/63.0	0.41	-1.29	8	3.00	6.5	2.70	0.15	-2.74	0.065	-3.94	2.41		
	76.0/77.0	0.48	-1.06	8	3.00	5	2.32	0.12	-3.06	0.06	-4.06	2.41		
	77.0/78.0	0.45	-1.15	7.5	2.91	2	1.00	0.1	-3.32	0.06	-4.06	2.14		
	78.0/79.0	0.50	-1.00	7	2.81	6	2.58	0.1	-3.32	0.08	-3.64	2.45		
	79.0/80.0	0.45	-1.15	7	2.81	2	1.00	0.15	-2.74	0.06	-4.06	1.97		
	80.0/81.0	0.50	-1.00	6	2.58	5	2.32	0.1	-3.32	0.06	-4.06	2.42		
	81.0/82.0	0.42	-1.25	6.5	2.70	6	2.58	0.08	-3.64	0.07	-3.84	2.55		
	Depth	Grain size analysis of multiaquifer											Permeability	
	meter	D50 (mm)	D50 (phi)	D95 (mm)	D95 (phi)	D84 (mm)	D84 (phi)	D16 (mm)	D16 (phi)	D5 (mm)	D5 (phi)	σ1	Gallons/day-ft2	m/d
	97.0/98.0	0.49	-1.03	7	2.81	1.7	0.77	0.09	-3.47	0.08	-3.64	2.04	90	4
	98.0/99.0	0.40	-1.32	1.5	0.58	1	0.00	0.15	-2.74	0.07	-3.84	1.35		
	99.0/100	0.33	-1.60	6.5	2.70	1.5	0.58	0.15	-2.74	0.06	-4.06	1.85		
	MEAN	0.41	-1.30											
	STD	0.08	-3.64											
	Depth	Grain size analysis of multiaquifer											Permeability	
	meter	D50 (mm)	D50 (phi)	D95 (mm)	D95 (phi)	D84 (mm)	D84 (phi)	D16 (mm)	D16 (phi)	D5 (mm)	D5 (phi)	σ1	Gallons/day-ft2	m/d
	112/113	0.40	-1.32	7	2.81	6.5	2.70	0.12	-3.06	0.07	-3.84	2.45		
	113/114	0.60	-0.74	7	2.81	6	2.58	0.25	-2.00	0.1	-3.32	2.07	75	3

Continued on next page

Table 8.13 continued

Borehole	Depth	Grain size analysis of multiaquifer											Permeability	
CO	neter	D50 (mm)	D50 (phi)	D95 (mm)	D95 (phi)	D84 (mm)	D84 (phi)	D16 (mm)	D16 (phi)	D5 (mm)	D5 (phi)	σ1	Gallons/day-ft2	m/d
	37.0/38.0	0.40	-1.32	17	4.09	13	3.70	0.2	-2.32	0.1	-3.32	2.63		
	38.0/39.0	0.70	-0.51	8	3.00	6	2.58	0.1	-3.32	0.07	-3.84	2.51		
	39.0/40.0	0.65	-0.62	17	4.09	7	2.81	0.08	-3.64	0.06	-4.06	2.85		
	Depth	Grain size analysis of multiaquifer											Permeability	
	neter	D50 (mm)	D50 (phi)	D95 (mm)	D95 (phi)	D84 (mm)	D84 (phi)	D16 (mm)	D16 (phi)	D5 (mm)	D5 (phi)	σ1	Gallons/day-ft2	m/d
	50.0/51.0	0.70	-0.51	12	3.58	7	2.81	0.17	-2.56	0.065	-3.94	2.48		
	51.0/52.0	1.80	0.85	9	3.17	8	3.00	0.2	-2.32	0.09	-3.47	2.34		
	52.0/53.0	1.10	0.14	8	3.00	7	2.81	0.19	-2.40	0.06	-4.06	2.37		
	53.0/54.0	0.80	-0.32	8	3.00	6	2.58	0.12	-3.06	0.06	-4.06	2.48		
Borehole	Depth	Grain size analysis of multiaquifer											Permeability	
DO	neter	D50 (mm)	D50 (phi)	D95 (mm)	D95 (phi)	D84 (mm)	D84 (phi)	D16 (mm)	D16 (phi)	D5 (mm)	D5 (phi)	σ1	Gallons/day-ft2	m/d
	35.0/36.0	1.00	0.00	8	3.00	8	3.00	0.2	-2.32	0.07	-3.84	2.37		
	36.0/37.0	1.10	0.14	8	3.00	8	3.00	0.17	-2.56	0.1	-3.32	2.35		
	37.0/38.0	0.30	-1.74	1.5	0.58	1.5	0.58	0.15	-2.74	0.07	-3.84	1.50		
	38.0/39.0	0.35	-1.51	1.5	0.58	1.5	0.58	0.17	-2.56	0.1	-3.32	1.38		
	Depth	Grain size analysis of multiaquifer											Permeability	
	neter	D50 (mm)	D50 (phi)	D95 (mm)	D95 (phi)	D84 (mm)	D84 (phi)	D16 (mm)	D16 (phi)	D5 (mm)	D5 (phi)	σ1	Gallons/day-ft2	m/d
	41.0/42.0	0.37	-1.43	4	2.00	4	2.00	0.06	-4.06	0.06	-4.06	2.43		
	42.0/43.0	0.30	-1.74	4	2.00	4	2.00	0.06	-4.06	0.06	-4.06	2.43		
	43.0/44.0	0.40	-1.32	2	1.00	2	1.00	0.15	-2.74	0.07	-3.84	1.67		
	44.0/45.5	0.40	-1.32	8	3.00	8	3.00	0.07	-3.84	0.06	-4.06	2.78		
EO	Depth	Grain size analysis of multiaquifer											Permeability	
	neter	D50 (mm)	D50 (phi)	D95 (mm)	D95 (phi)	D84 (mm)	D84 (phi)	D16 (mm)	D16 (phi)	D5 (mm)	D5 (phi)	σ1	Gallons/day-ft2	m/d
	55.0/56.0	0.40	-1.32	10	3.32	7	2.81	3.5	1.81	0.1	-3.32	1.26		
	56.0/57.0	0.41	-1.29	7	2.81	1.2	0.26	2	1.00	0.07	-3.84	0.82		
	59.0/60.0	3.20	1.68	2	1.00	1	0.00	2	1.00	0.06	-4.06	0.52		
	60.0/61.0	3.00	1.58	9	3.17	8	3.00	4	2.00	0.1	-3.32	1.23		
	63.0/64.0	0.35	-1.51	9	3.17	8	3.00	6	2.58	0.15	-2.74	1.00		
	64.0/65.0	0.30	-1.74	5	2.32	3	1.58	1.6	0.68	0.1	-3.32	1.08		
	65.0/66.0	0.30	-1.74	1.8	0.85	1.3	0.38	1.2	0.26	0.08	-3.64	0.71		
	66.0/67.0	0.32	-1.64	6	2.58	3	1.58	1.2	0.26	0.07	-3.84	1.30		
	67.0/68.0	0.80	-0.32	2	1.00	2	1.00	1.3	0.38	0.1	-3.32	0.81	1300	53
	68.0/69.0	0.34	-1.56	8	3.00	1	0.00	1.3	0.38	0.06	-4.06	0.97		

Continued on next page

Table 8.13 continued

Borehole JO	Depth meter	Grain size analysis of multiaquifer D50 (mm)	D50 (phi)	D95 (mm)	D95 (phi)	D84 (mm)	D84 (phi)	D16 (mm)	D16 (phi)	D5 (mm)	D5 (phi)	σI	Permeability Gallons/day-ft2	m/d
	42.0/42.5	0.65	-0.62	9	3.17	7.5	2.91	0.075	-3.74	0.065	-3.94	2.74		
	42.5/43.5	1.50	0.58	8	3.00	5.5	2.46	0.25	-2.00	0.1	-3.32	2.07	70	3
	43.5/44.5	1.20	0.26	8	3.00	7	2.81	3	1.58	0.1	-3.32	1.26	450	18
	44.5/45.0	1.75	0.81	9	3.17	8	3.00	0.5	-1.00	0.13	-2.94	1.93	800	33
	45.0/46.5	2.00	1.00	8	3.00	7	2.81	0.4	-1.32	0.065	-3.94	2.08	90	4
	Depth meter	Grain size analysis of multiaquifer D50 (mm)	D50 (phi)	D95 (mm)	D95 (phi)	D84 (mm)	D84 (phi)	D16 (mm)	D16 (phi)	D5 (mm)	D5 (phi)	σI	Permeability Gallons/day-ft2	m/d
	64.5/65.5	4.00	2.00	9	3.17	8	3.00	0.9	-0.15	0.2	-2.32	1.62	200	8
	65.5/66.5	2.00	1.00	9	3.17	7	2.81	0.6	-0.74	0.09	-3.47	1.89	100	4
	Depth meter	Grain size analysis of multiaquifer D50 (mm)	D50 (phi)	D95 (mm)	D95 (phi)	D84 (mm)	D84 (phi)	D16 (mm)	D16 (phi)	D5 (mm)	D5 (phi)	σI	Permeability Gallons/day-ft2	m/d
	120/121	0.80	-0.32	5	2.32	3.5	1.81	0.08	-3.64	0.06	-4.06	2.33		
	121/121.5	1.10	0.14	9	3.17	7	2.81	0.1	-3.32	0.06	-4.06	2.63		
	121.5/123	1.70	0.77	9	3.17	7.5	2.91	0.3	-1.74	0.06	-4.06	2.26		
	123/124	1.80	0.85	9	3.17	7.5	2.91	0.35	-1.51	0.06	-4.06	2.20		
Borehole KO	Depth meter	Grain size analysis of multiaquifer D50 (mm)	D50 (phi)	D95 (mm)	D95 (phi)	D84 (mm)	D84 (phi)	D16 (mm)	D16 (phi)	D5 (mm)	D5 (phi)	σI	Permeability Gallons/day-ft2	m/d
	40.5/42.0	1.50	0.58	9	3.17	7.5	2.91	2	1.00	0.1	-3.32	1.46	300	12
	42.0/43.0	0.80	-0.32	8.5	3.09	6	2.58	4	2.00	0.1	-3.32	1.12	800	33
	43.0/44.0	1.10	0.14	9	3.17	5	2.32	4	2.00	0.08	-3.64	1.11	650	27
	44.0/45.0	0.90	-0.15	7.8	2.96	7	2.81	2	1.00	0.07	-3.84	1.48	400	16
	46.0/47.0	0.80	-0.32	8.3	3.05	4	2.00	3	1.58	0.09	-3.47	1.09	900	37
	47.0/48.0	0.90	-0.15	8	3.00	7	2.81	4	2.00	0.1	-3.32	1.16	700	29
	48.0/49.0	0.55	-0.86	8.5	3.09	7.5	2.91	2	1.00	0.08	-3.64	1.50	380	16
	49.0/50.0	1.20	0.26	9	3.17	8	3.00	2	1.00	0.1	-3.32	1.48	450	18
												MEAN	338	14
												STD	324	13

**Grain size that is 50 percent finer by weight

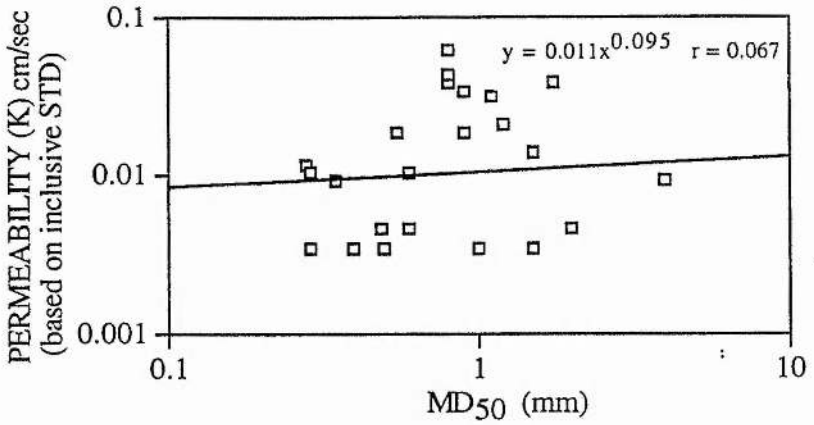

Figure 8.14 Graph relating grain size (D_{50}) to different values of permeability using the Masch and Denny method (inclusive standard deviation).

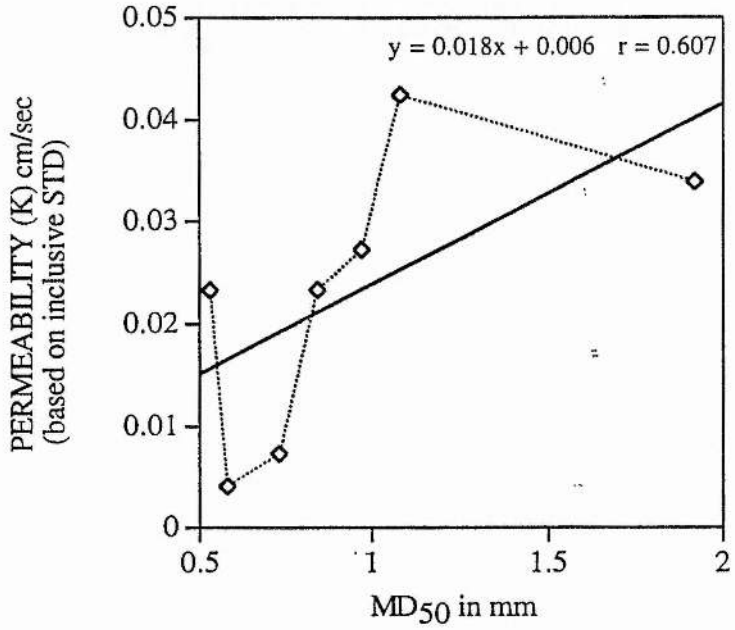

Figure 8.15 The correlation between the arithmetic mean of grain size D_{50} and the permeabilty using the Masch and Denny method (based on an inclusive standard deviation).

8.3.3 Discussion and Interpretation of the Results

The wadi floor sediments have varying permeabilities which depends mainly on their grain size and sorting. The permeabilities using Hazen's method, the Masch & Denny method and pumping tests are given in Tables 8.10, 8.11, 8.12 and 8.14. The author has used the pumping test results as a reference for comparison against the Hazen method and the Masch & Denny method to provide a study of the effects of grain size distribution on the permeability of unconsoildiated aquifer material. Such an investigation, using pumping test data to show the effects of grain size distribution on the permeability of multiaquifer material, has not hitherto been reported. Four stages have been used.

1- Using Hazen's method to estimate a series of permeabilities for the multiaquifer system based on D_{10} size of unconsoildiated material of each aquifer.

2- Using the Masch and Denny method to estimate a series of permeabilities for the multi-aquifer system based on unconsoildiated material, mainly MD_{50} of each aquifer.

3- Using the pumping test method (based mainly on Jacob's method) to determine the average values of the multiaquifer system as an single aquifer.

4- To determine whether the method of Hazen or Masch & Denny could be modified to predict the permeability values of multiaquifer systems of wadi basin based on the grain size distribution parameters.

The permeabilities estimated using the geometric mean of effective grain size (D_{10}) (Hazen's method) show strong correlation with data from pumping tests. However the permeability values are an order of magnitude higher than those values determined from pumping tests. This difference in permeability values can be considered as result of the follows:

1- Since there is a certain degree of cementation and consolidation present in the natural aquifer, the pumping test permeability performed in the multiaquifer system would yield lower permeability values than those obtained from the other methods.

2- The permeability determined using the pumping test was determined considering that the multiaquifer is a single aquifer in which the permeability would be calculated for basin thickness, i.e. Borehole KO has transmissivity = 2.8×10^{-3} m^2/sec divided by the total

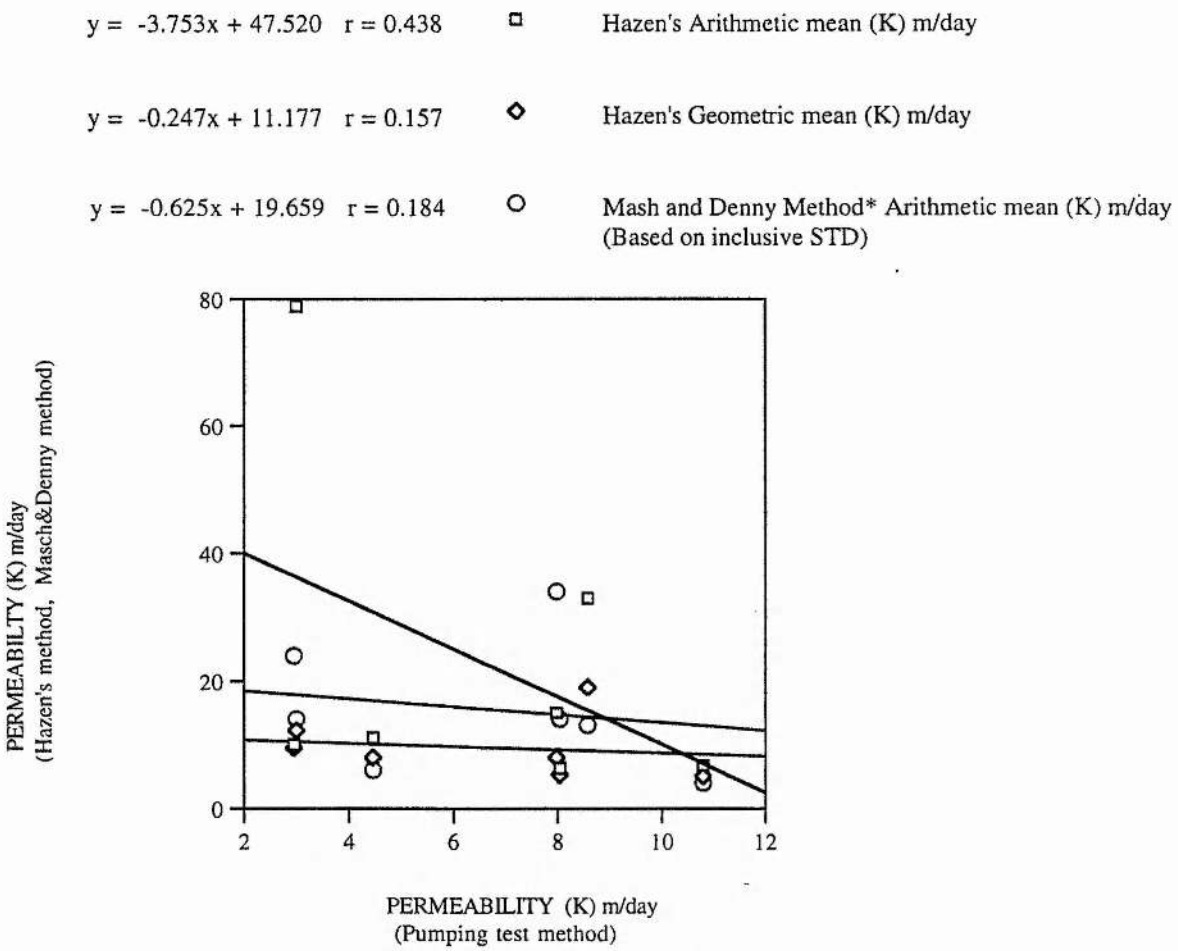

Figure 8.16 Comparison between the permeability of aquifers in Wadi Baysh determined by the pumping test and values estimated using the Hazen and Masch and Denny methods and their modification.

Table 8.14 Permeability variation (m/day) with depth in the Wadi Baysh basin using different methods (Hazen's method, the pumping test and the Masch and Denny method)

		Hazen's Method		**Pumping test**	**Mash and Denny Method***
Borehole NO	Sample	Arithmetic mean (K)	Geometric mean (K)	**K**	Arithmetic mean (K)
and Depth	Location	m/day	m/day	**m/day**	m/day
AO (45.5/53.0)	Aquifer (A)	**11**	**8**	**5**	**6**
BO (54.0/82.0)	Aquifer (A) (middle section	7	4		4
BO (97.0/100)	Aquifer (A) (lower section)	5	4		4
BO (112/114)	Aquifer (B) (upper section)	9	7		3
	Mean	**7**	**5**	**12**	**4**
CO (37.0/40.0)	Aquifer (A)	8	4		14**
CO (50.0/54.0)	Aquifer (B)	143	15		14**
	Mean	**79**	**12**	**3**	**14**
DO (35.0/39.0)	Aquifer (A)	11	9		14**
DO (41.0/45.5)	Aquifer (B)	2	1		14**
	Mean	**6**	**5**	**10**	**14**
EO (55.0/69.0)	Aquifer (B) (Middle section	6	5		53
EO (63.0/69.0)	Aquifer (B) (lower section)	24**	10**		14**
	Mean	**15**	**8**	**9**	**34**
JO (42.0/46.5)	Aquifer (A) aquifer	25	17		15
JO (64.5/66.5)	Aquifer (B) aquifer	68	36		6
JO (120/124)	Aquifer (B) aquifer	6	4		14**
	Mean	**33**	**19**	**9**	**12**
KO (40.5/50.0)	**Aquifer (B) aquifer**	**10**	**9**	**3**	**24**
Basin	**MEAN**	**24**	**10**	**7**	**14**

(K) Hydraulic conductivity cm/sec

* Based on an Inclusive Standard Deviation

** Estimated values based on the average of it's group

thickness of saturated aquifer material (102m) - 20 m (water table depth) = 0.0028 m/sec.

3- The arithmetic mean of the permeability was determined on the limited number of grain size samples which represent some part of the aquifer thickness and not the entire borehole thickness.

4- The Hazen and Masch & Denny methods depend on different grain sizes, D_{10} and D_{50}, which influence the permeability values.

Hazen's method shows that a straight line relationship exists between the logarithm of the permeability and the effective grain size diameter D_{10}. It shows that the permeability, expressed in cm/sec, ranges from 0.08 for very coarse sand to about 0.001 for very fine sand.

The permeability estimation using the family of curves prepared by Masch and Denny shows a poor correlation with grain size (MD_{50}). In Figure 8.15, the maximum values of permeability using the inclusive STD occurred for the range 1.3mm <D_{50}> 0.7mm, and that the permeability decreases for values outside this range. However permeability estimated by pumping tests is higher (Figure 8.17). The average values of the permeability estimated using the arithmetic STD are higher and show a stronger correlation with MD_{50} than those estimated using the inclusive STD. The low estimated values of permeability using the Masch and Denny method (based on the Inclusive SDT) may be due to the predictive curves which were mainly derived from unimodal grain size distributions (Baillieul, 1975), where the inclusive STD (standard deviation) and the median (MD_{50}) for sand samples were controlled in the expermintation. In addition there is a difference between the aquifer pumping test carried out on the site while Masch & Denny method is influenced by the bulk density and packing of the material samples which tends to move the permeability graphs under estimates. Accordingly, the arithmetic STD improves estimation of the permeability over that obtained using an inclusive STD (see Figures 8.14, 8.15, 8.16 and 8.17).

8.3.4 Conclusion

The results of this study confirm that the grain size distribution does have an effect on the permeability of unconsolidated material of a multiaquifer system.

A method of determining permeability values for an effective grain size (D_{10}) (using Hazen's method) and relating the arithmetic and geometric mean permeability to the arithmetic mean size (D_{10}) was achieved. Also the permeabilities were estimated using the Masch and Denny method in which these values are related to geometric mean size, inclusive STD and arithmetic STD of the samples.

Correlations between pumping test permeability values of the multiaquifer material, the effective grain size (D_{10}) and the median grain size diameter (D_{50}) of sample material have been established.

The permeability determination of wadi floor sediments using pumping test analysis has a moderate correlation ($r = 0.438$) with permeability estimation using Hazen method (using arithmetic mean of the permeability). However, the permeability estimation of multiaquifer material using Hazen's method (based on the geometric mean of the permeability) and the Masch & Denny method (based on the Inclusive STD) shows lower correlation values ($r = 0.157$ and 0.184 respectively) compared with the permeability determined by pumping test analysis (see Figure 8.16).

8.4 Section Three: Geophysical Log Analysis

8.4.1 Introduction

Geophysics of the borehole is defined as recording and analysing continuous or point physical property measurements made in test holes or wells. Since geophysical borehole logging was developed for use in oil and gas exploration, there is relatively little published information available on log interpretation for freshwater. Geophysical borehole logging offers a great deal in the way of practical application to hydrology. It includes all techniques of lowering sensing devices into boreholes and recording physical parameters that may be interpreted in terms of the characteristics of the rocks , the fluids contained in the rocks, and construction of the well. According to scientists such as Jones and Buford (1951), Alger (1966) and Keys (1989), geophysical borehole logging can be used to evaluate aquifers, although the parameters of interest in water wells (yield and water quality) are different from those important to oil and gas exploration.

This section discusses the available MAWR data for the geophysical borehole logging in the area. This consists of electric logging (short and normal log and spontaneous potential log) and radioactive logging (a gamma ray log). The main purpose of this section is to provide information using the geophysical log data for ground water investigation rather than how to operate a specific logger. Table 8.16 classifies the principal geophysical logging systems applicable to the ground water in the study area.

Table 8.15 Summary of well logging systems in the lower part of Wadi Baysh.

Chemical Log Physical Type	Open Hole (O) Cased Hole (C) Properties	Lithology	Bed Thickness	Uses Clay &Shale Content	Total Porosity	Effective Porosity
Spontaneous Potential	O	x	x	x		x
Short normal	O	x	x	x		
Long normal	O	x	x	x	x	x
Gamma Ray Log	C	x	x	x		

8.4.2 Data Sources

Spontaneous potential (SP), short normal and long normal resistivity and gamma ray logging, have been run in the cored wells Figure 8.17. From most of the wells there are data records of well logs with the exception of boreholes CO, DO and IO for which the geophysical data are missing. The electrical conductivity measurements were provided during the digging project. The geophysical log charts for every borehole in the area (AO, BO, EO, GO, HO, JO and KO) have been digitised at intervals of 2 metres and replotted. The composite forms the basic documents for a manual interpretation of lithology. The lithological measurements and their descriptions were used to draw the lithological columns. Both the geophysical logs and the lithological columns were compiled together (see Figures 8.18 - 8.24) in order to study their interrelationships with flow in the forms of aquifer parameters determined in the wadi floor sediments.

8.4.3 Geophysical Log Definition

The term geophysical log is adopted from Serra (1984) and in this study relates to a limited number of techniques:

A **log** is defined as a record of one or more curves related to some property in the formation of the well bore.

Borehole Resistivity Logs consist of spontaneous potential logs and normal resistivity logs. A four electrode arrangement is commonly used to measure the resistivity from boreholes similar to the four electrodes used in surface resistivity methods (see Fig. 8.17).

The Spontaneous Potential (SP) log is a measurement of the natural potential difference or self-potential between an electrode in the borehole and a reference electrode at the surface: no artificial currents are applied. SP currents originate principally through the electrochemical effects of salinity differences between the borehole fluid (mud filtrate) and the formation water.

The SP log is used mainly for the evaluation of formation-water resistivity. In defining the values of SP, zero is determined in thick shale or clay intervals where the SP does not change. It is called the shale base line. All values are related to this line.

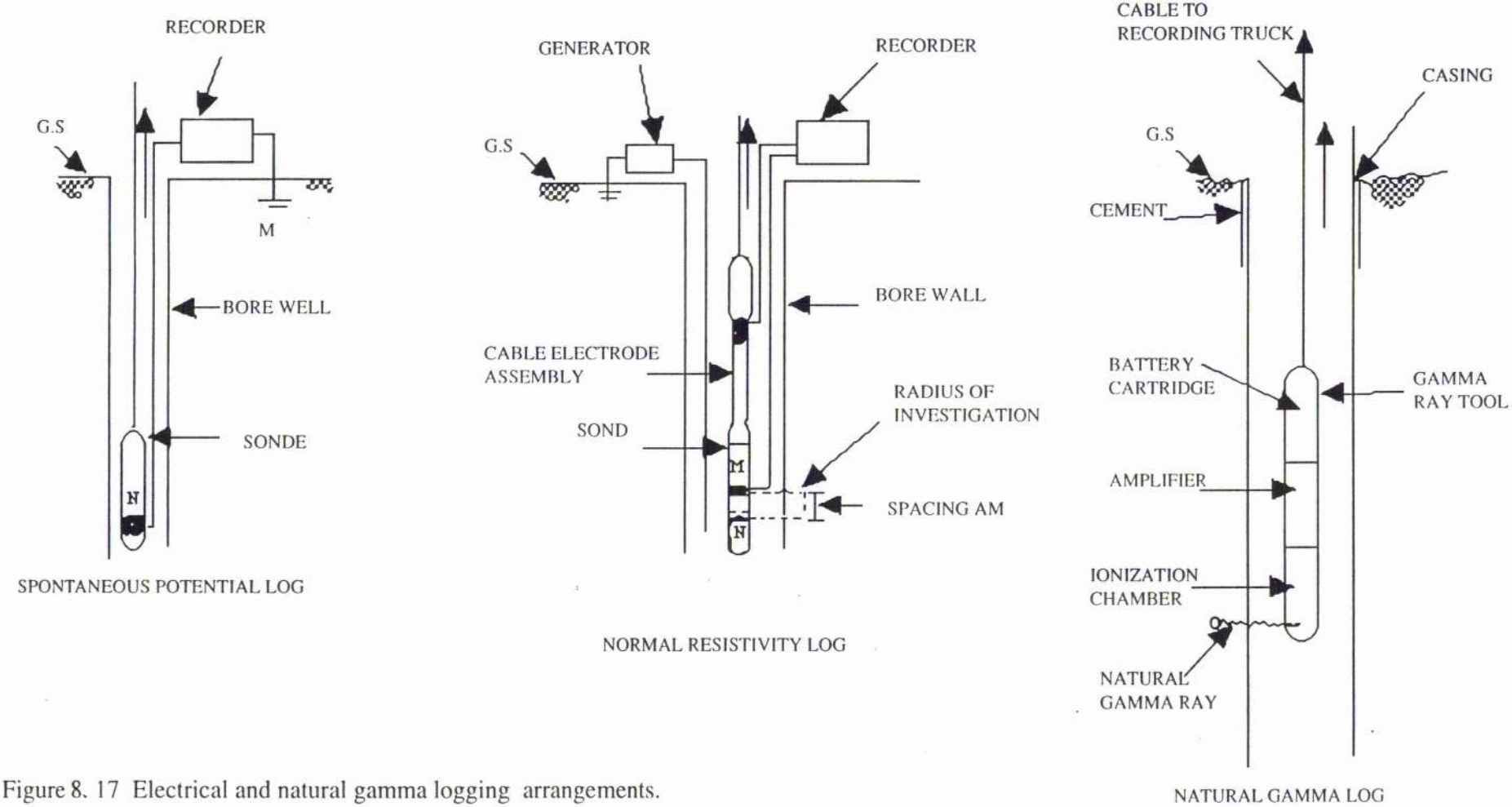

Figure 8. 17 Electrical and natural gamma logging arrangements.

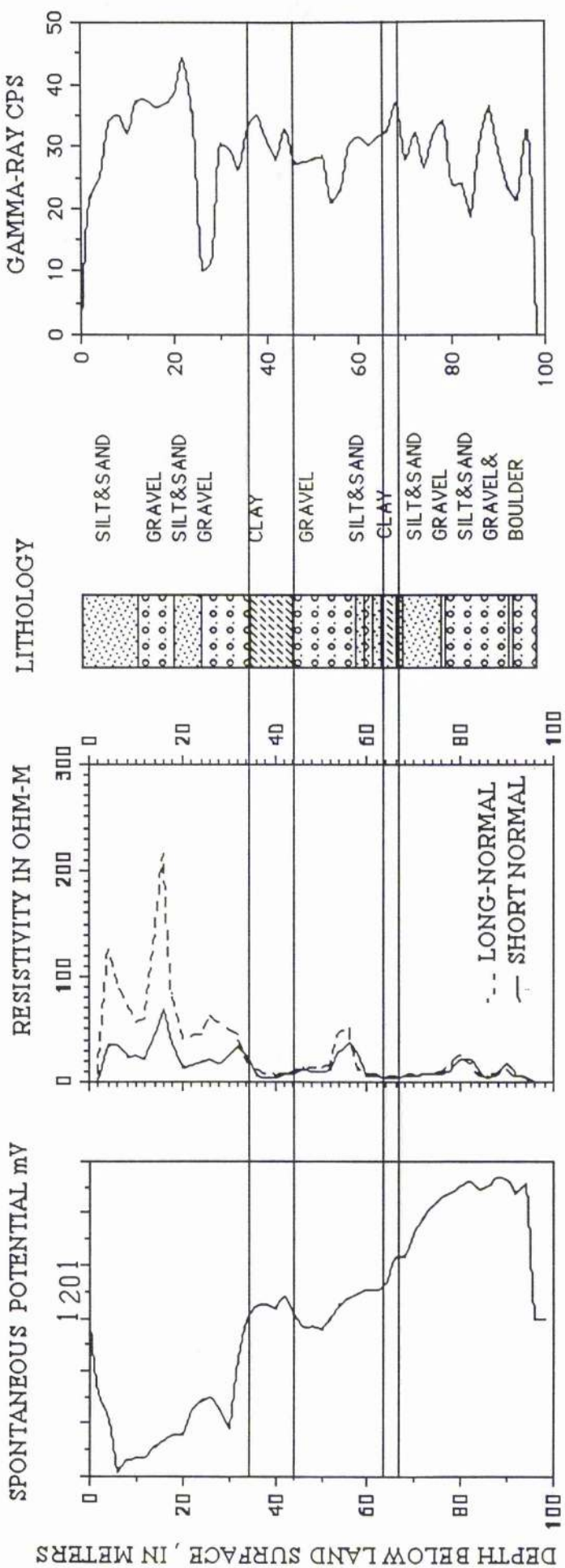

Figure 8.18 A section of lower part of Wadi Baysh deposits illustrated by well logs (borehole AO)

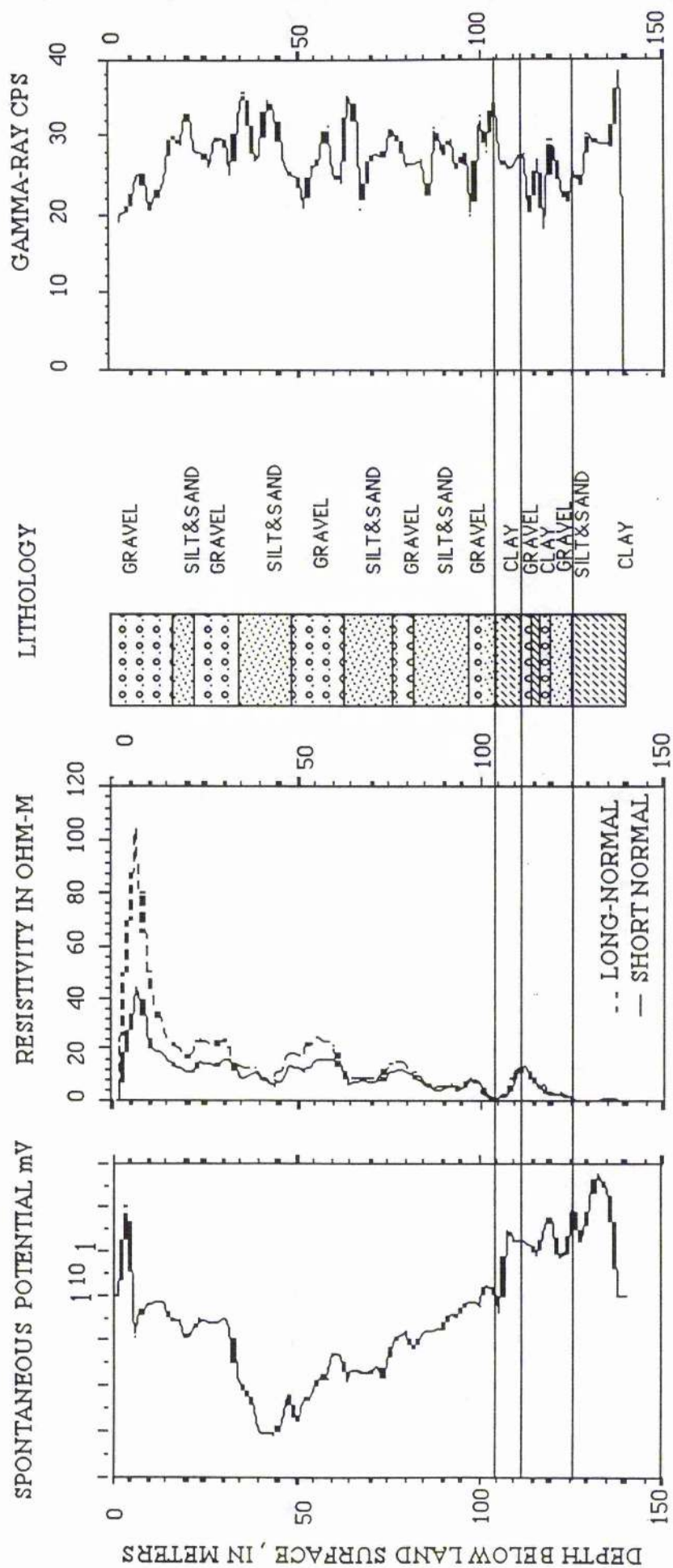

Figure 8.19 A section of lower part of Wadi Baysh deposits illustrated by well logs (borehole BO)

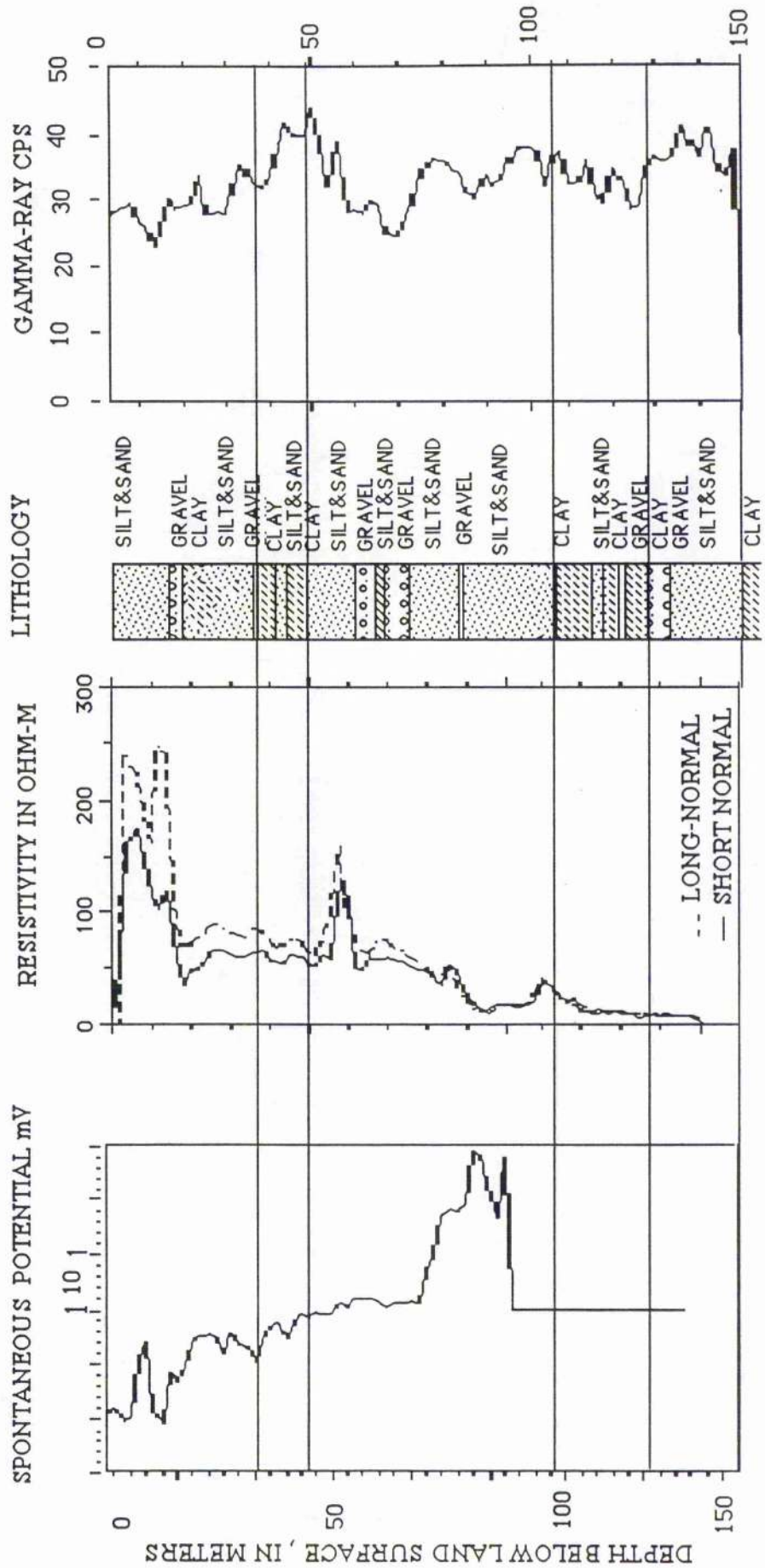

Figure 8.20 A section of lower part of Wadi Baysh deposits illustrated by well logs (borehole EO)

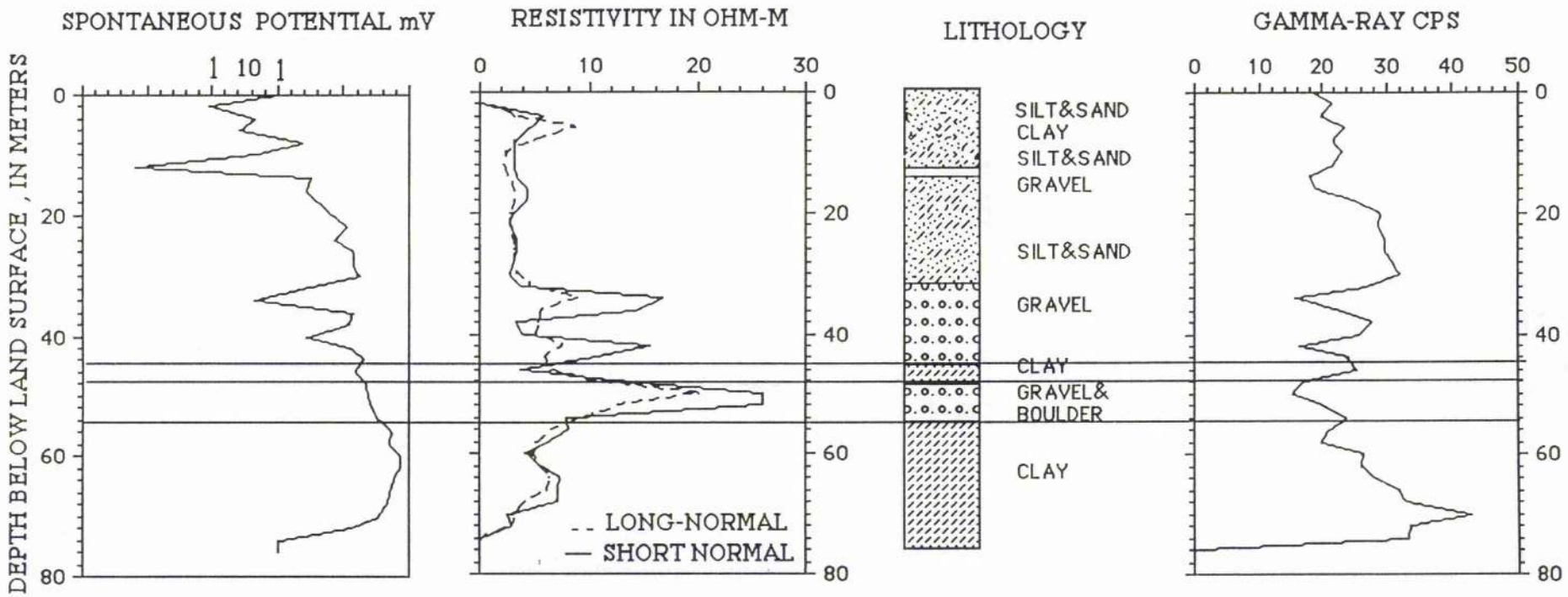

Figure 8.21 A section of lower part of Wadi Baysh deposits illustrated by well logs (borehole GO)

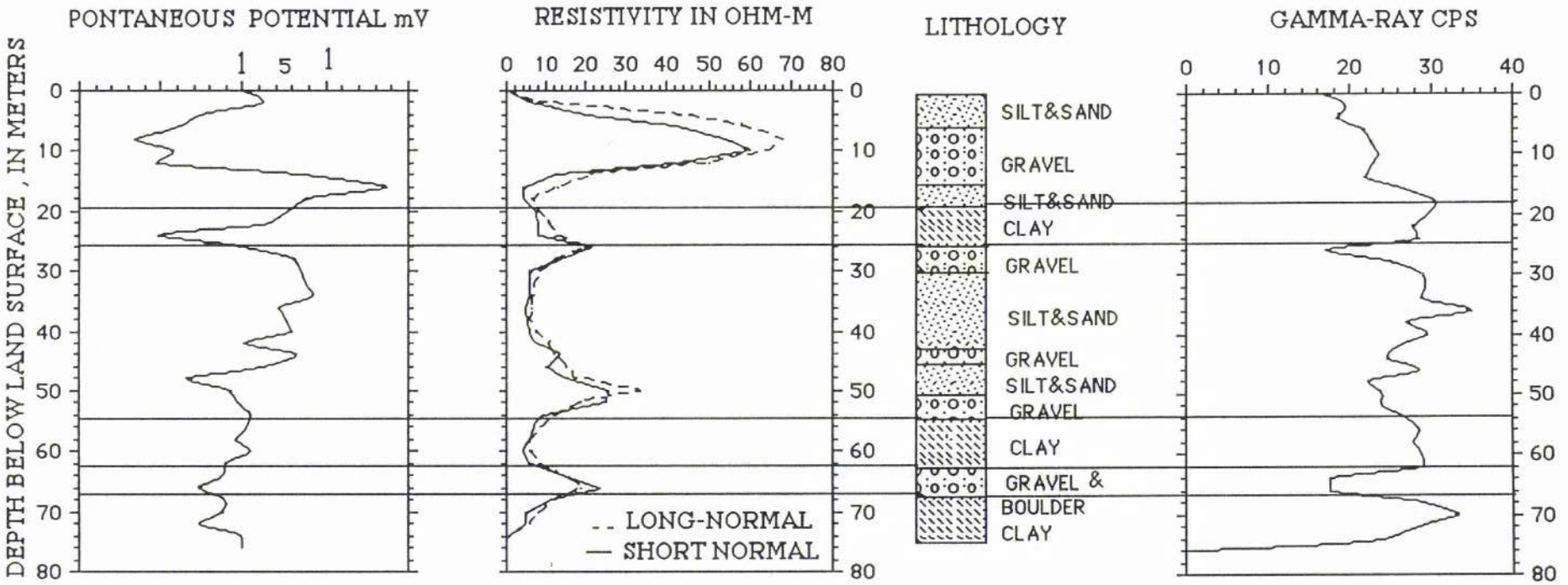

Figure 8.22 A section of lower part of Wadi Baysh deposits illustrated by well logs (borehole HO)

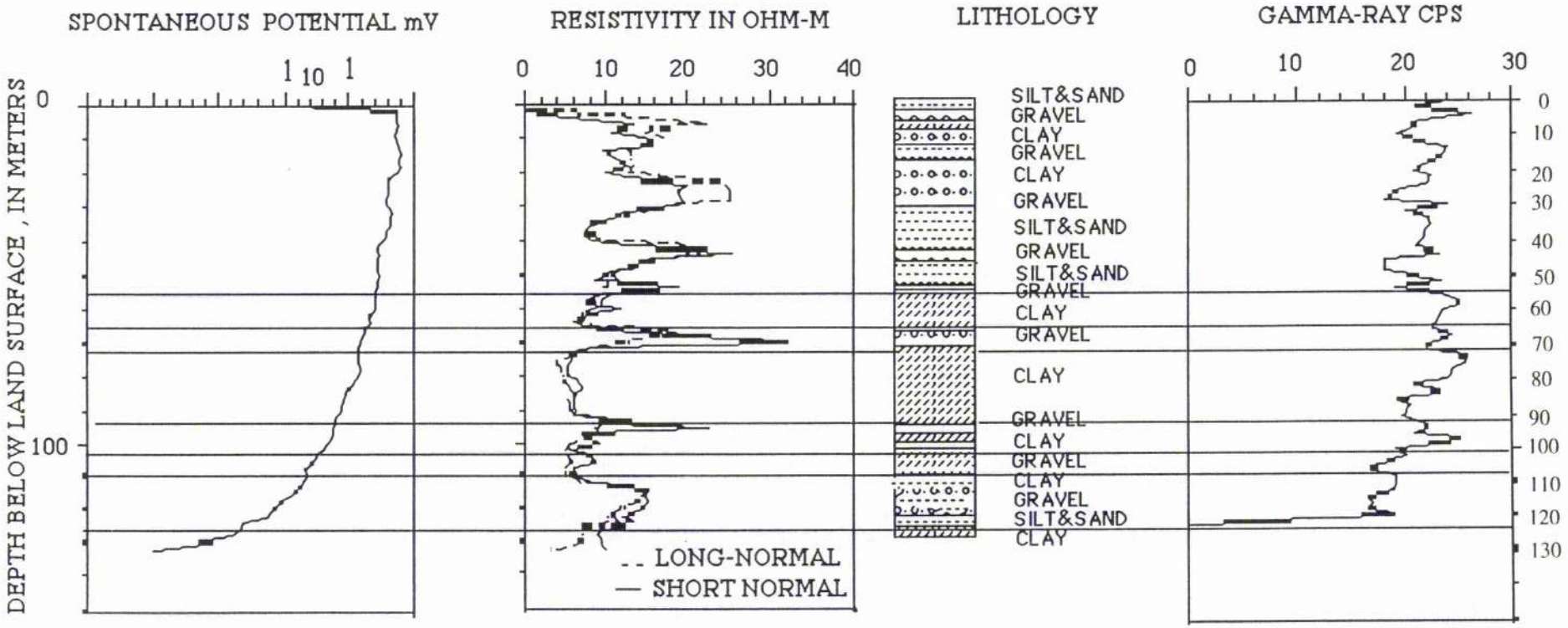

Figure 8.23 A section of lower part of Wadi Baysh deposits illustrated by well logs (borehole JO)

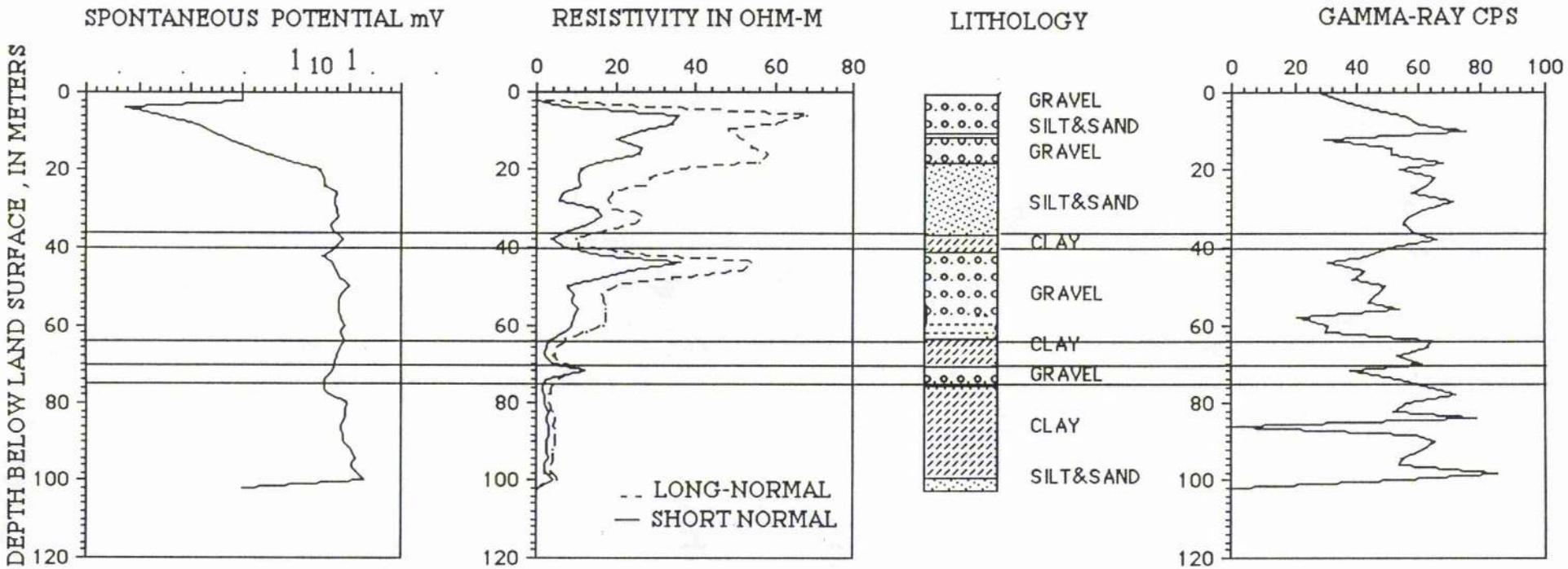

Figure 8.24 A section of lower part of Wadi Baysh deposits illustrated by well logs (borehole KO)

Normal resistivity logs are based on the arrangement of the distance between the electrodes and the voltage. If the distance is small (40 cm), it is called a 'short normal log', and if it is longer (160 cm), it is called a 'long normal log' (see Figure 8.17). The spacing of the current and potential electrodes determines the depth of penetration into the formation for a given borehole diameter. The larger the spacing in relation to the borehole diameter, the deeper the penetration and the lower the bed resolution (Driscoll, 1989).

The permeable zone is indicated by a relatively high porosity on the resistivity logs and relatively low intensity radiation on the natural gamma log.

Nuclear logs are of two general types, those which measure the natural radioactivity of the formation (gamma ray log) and those which detect radiation reflected from or induced in the formation from an artificial source (neutron logs). The radioactive log data used in this study are for gamma rays.

The gamma ray log is a record of formation radioactivity (Figure 8.18). In sediments, the minerals in shales and clays often emit more gamma rays than minerals in gravels and sands. Thus gamma logs can thus be used to differentiate between sand and clay. The gamma log unit is examined as counts per second (CPS). The scale is 0-50 or 1-100.

8.4.4 Geophysical Log Interpretation

By applying all of the above techniques, multiple interpretations of the suite of logs are obtained, and these give more information than the sum of data from the individual logs. For this reason multiple interpretations have been made in order to maximise the information from each well log site. Figures 8.18 - 8.24 are typical of a suite of logs run on each hole and is an example of the synergistic nature of geophysical logs in the study area.

8.4.4.1 SP Logs

All of the boreholes show vertical sequences of relatively low and high permeability beds (clay, silty sand, gravel and sand). The SP curves of boreholes BO, EO, HO, GO and AO, exhibit their maximum deflections opposite permeable water-bearing formations of gravel and sand . Table 8.16 summarises the depths at which the maximum deflection of

SP curves occurs in different boreholes.

Table 8.16 The depth and maximum deflection of SP curves for different boreholes.

Borehole No.	SP Millivolt	Maximum Deflection depth (m)
AO	+10	40
BO	~ +10	120
EO	+25	80
GO	+ 4	50
HO	~ +7	35
KO	+5	80

The MAWR data for borehole JO does not show a baseline in spite of the thick clay layer located at a depth of 70 m. At no point does this curve reflect the variation of the lithology or the water quality. The author assumes that this SP curve (see Figure 8.24) was not recorded properly or that there was an unrecognised equipment malfunction.

In Figure 8.18 correlations using the SP log show that highly permeable layers dominate the lithology in borehole AO. There is no evidence of a clay layer in the SP curves at depth of 40 m. However in most lithological sequences, the clay layer is of small thickness which may make it difficult to detect by the SP methods. Alternatively it may be suggested that, because fine grained sand dominates the lithology, strong SP contrasts found in boreholes penetrating clays, sand and silty sand are absent.

The geometry of SP curves in most of the boreholes (BO, EO, HO, GO, AO) shows a bell shape (see Figures 8.18 - 8.24) indicating the presence of highly permeable layers of wadi floor sediments. However, it does not indicate the actual permeability of these layers. On the basis of the SP deflection value, from the base line of the clays, the water quality shown ranges between +10 and +30 millivolts. The positive value of SP indicates that the water is essentially fresh.

8.4.4.2 Short and Long Normal Resistivity Logs

Short and long normal resistivity logs may be used to qualitatively interpret the lithology in terms of its hydrogeological significance. The log characteristics of the boreholes reflect the same trend for both the short and long curves of resistivity (see Figures 8.18 - 8.24). However, the magnitude of the readings on the long resistivity curve are greater in most cases than those on short resistivity curves. This may be related to the

depth of the measurement in which the long normal resistivity measures deeper into the saturated layer than the short resistivity method.

The resistivity magnitude of both curves is determined for high deflection as in Table 8.17 below.

Table 8.17 The long and short resistivities in ohm-m for the Wadi Baysh boreholes.

		Resistivity ohm-m	
Borehole No	Depth	Short Resistivity	Long Resistivity
AO	18	60	210
	56	30	40
	80	20	20
BO	5	40	105
	25	16	24
	50	16	20
	80	14	16
	115	16	16
EO	5	170	240
	55	140	160
	85	60	60
	100	50	50
FO	8	40	90
	16	45	80
	26	30	35
GO	4	6	9
	34	8	16
	40	6	14
	50	20	26
HO	8	66	68
	25	22	22
	50	24	32
	66	22	22
JO	10	22	16
	30	20	26
	45	26	26
	50	19	19
	65	20	35
	95	10	20
	115	14	14
KO	10	35	65
	50	38	55
	70	15	15

The wadi sediments generally exhibit three ranges of resistivity values:

1- The dry zone of high permeability layers has high resistivity which ranges between 65 and 240 ohm-m, while the low permeability zone shows low resistivity values in the range

of 9 to 16 ohm-m.

2- The saturated zone of the highly permeable layers showed resistivities between 20 and 160 ohm-m.

3- The clay zone, in which the resistivity is very low, had a range of 2 to 14 ohm-m. The long and short resistivity values for Wadi Baysh boreholes are given Table 8.17 .

The resistivity logs show a marked variation in both short and long resistivity caused by changes of the permeability and the saturation conditions. The resistivity techniques permit not only correlation of lithology in the wadi floor sediments, but also enable the high permeability layers to be distinguished from the low permeability layers (clays) which show low values of resistivity (2-14 ohm-m).

8.4.4.3 Natural Gamma Ray Logs

The main uses of natural-gamma logs are for the identification of clay layers for stratigraphic correlation. Such logs have an advantage over electric logs in that they can be used above or below the water table and in open holes as well as cased holes.

The facies identification of wadi floor sediments is easy to achieve using gamma ray logs. Most of the gamma ray curves exhibit a high deflection opposite clay layers, with a range of 30 to 40 CPS (see Figures 8.18 and 8.24), while with gravel and sand layers the intensity falls to 5-25 CPS. In general changes in the grain size of the layer will correlate with changes in gamma ray value, the clay layers producing high gamma ray intensity. Such characteristics, will help to determine the permeable and impermeable layers in the wadi deposits, and so are significant for ground water investigation. The natural-gamma log can be used relatively easily and quickly to estimate the hydrological properties of rocks. Gaur and Singh (1965) established a relationship between natural-gamma intensity and hydraulic conductivity of an oil-bearing sand in India. The relation between natural gamma ray intensity logged in borehole BO and the proportion of clay present is shown in Table 8.18 and Figure 8.19.

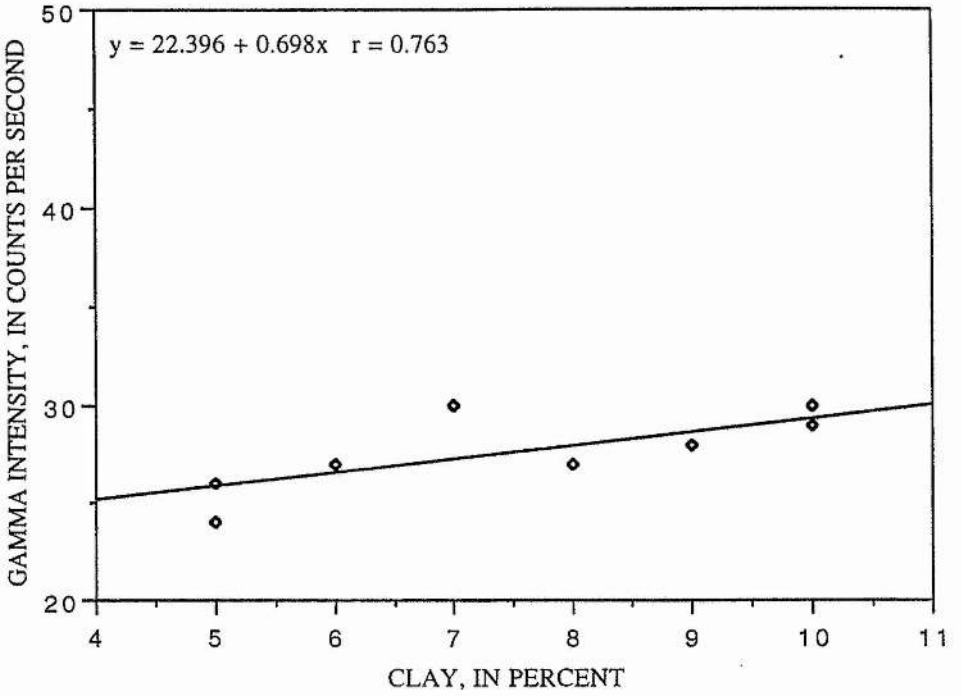

Figure 8.25 Natural gamma intensity and per cent of clay in borehole log BO.

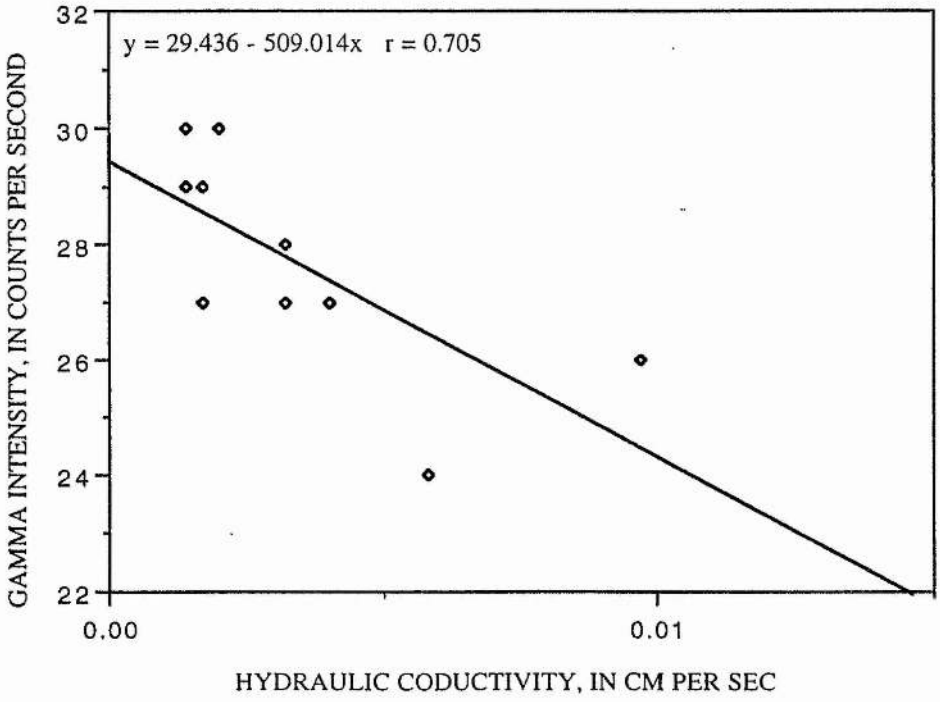

Figure 8.26 Natural gamma intensity and hydraulic conductivity of borehole log BO.

Table 8.18 The relationship between the natural gamma intensity, the percentage of clay and the hydraulic conductivity (K) of the sediments in borehole BO.

Borehole No.	Depth in meters	Clay in percent	Gamma intensity cps	K cm/sec
BO	60/61	5	24	0.0058
	76/77	9	28	0.0032
	77/78	7	30	0.0020
	78/79	10	30	0.0014
	79/80	8	27	0.0017
	80/81	10	29	0.0014
	81/82	10	29	0.0017
	97/98	6	27	0.0040
	98/99	6	27	0.0032
	99/100	5	26	0.0097

Using sieve analyses of sediments from borehole BO (see section two), the clay content plotted against the corresponding values of natural gamma intensity (in counts per second) shows a linear trend with a correlation coefficient of 0.7 (see Figure 8.25).

Hydraulic conductivity is related to effective porosity. The effective porosity is inversely related to clay content. So, the hydraulic conductivity should increase with decreasing clay content. In Figure 8.26 the natural gamma intensity at a specific depth is plotted against hydraulic conductivity derived by the Hazen method. The general negative gradient of the curve confirms that natural-gamma activity decreases with increasing hydraulic conductivity.

8.4.5 Grain Size Versus Permeability Versus Formation Factor

The relationship between grain size, hydraulic conductivity and formation factor is very important in evaluating an aquifer from the log data. In wadi floor sediments, the normal resistivity values (short and long) increase into the saturated coarse layers in which permeability is high. Thus, using the resistivity log to estimate aquifer parameters has dual value in water investigation. Jones and Buford (1951) related grain size to both formation factor and permeability. Alger (1966) used the same data graphically to show that the finer the grain size, the smaller the value of the formation factor, which is contrary to the

findings of oil field characterisation (Keys, 1989).

The contrasting interrelationships between permeability, formation factor and grain size in fresh water aquifers from that of hydrocarbon reservoirs is due to the increase in importance of surface conductance and the decrease in importance of electrolyte conductance (Keys, 1989).

Croft and Dak (1971) tested the Alger method and also demonstrated the relationship between permeability and formation factor using grain size data. However, there is no direct means of interrelating these parameters. Since grain size may be related to both permeability and formation factor, these two parameters have been plotted to provide a graphical method of converting the formation factor to permeability.

In the following section the author will discuss the major parameters used to determine the relationship between the formation factor and the permeability of the wadi floor sediments.

8.4.5.1 Formation Factor (F)

The Formation factor (F) is defined as the formation resisitivity factor, which is a function of the rock texture. It is the ratio of the resistivity of the formation (R_O) to that of the water (R_W) with which it is 100% saturated. It is derived from:

$$F = \frac{R_O}{R_W} \qquad (8.12)$$

Also, the formation factor F can be determined using the Archie formula (see Raghunath, 1982) as follows:

$$F = \frac{a}{Y^m} \qquad (8.13)$$

where Y = porosity, m = cementation factor, which depends upon rock type, and may be closely related to pore geometry rather than cementation (Ridere, 1991). a = a constant

The Humble formula (see Raghunath, 1982) shows the mean values of a and m for an "average" sandstone:

$$F = \frac{0.62}{Y^{2.15}} \qquad [8.14]$$

The value of m is variable within the range 1.8-3. Alger (1966) indicated that " in fresh water sands the usual relationship between F and porosity, $F = \frac{a}{Y^m}$, is not constant.

The value of F is a function of R_w".

According to Sarma and Rao (1962), F decreases as R_w (resistivity of formation water) increases. In addition, they found that computed values of F are appreciably lower than those obtained from the F vs porosity relationships commonly used in petroleum industry log interpretations.

Alger (1966) suggested that surface conductance was the primary factor in variation of F in fresh water sands, concluding that the magnitude of surface conductance is related to the area of surface exposed to the solution. The longer the surface is exposed to the electrolyte, the larger is the total surface conductance. A controlling factor in determining the surface conductance is the interrelationship of grain size to permeability.

8.4.5.2 Water Resistivity (R_W)

In oil wells where the water is the chloride type, the SP is used to calculate R_w using the following formula:

$$SP = K \log (R_m/R_w) \quad (8.15)$$

where SP = log deflection, in millivolts

$$K = 60 \times 0.133\ T \quad (8.16)$$

T = borehole temperature, in degrees Fahrenheit, R_m = resistivity of borehole fluid, in ohm m and R_w = resistivity of formation water, in ohm m

However, Guyod (1966) indicated that the use of the spontaneous potential formula to calculate the water resistivity of fresh formation water is unreliable because the formulation depends on the formation waters having greater resistivity and therefore being more saline than the borehole fluids. In most hydrocarbon exploration the formation waters are saline with NaCl.

Thus, it is not possible to determine or estimate with confidence R_w from the SP curve. Vonhofv (1966) found that calculating the water quality using the SP curve could be achieved "using the empirical relationship between the SP deflection, the electric log and the water quality in glacial aquifers". The conclusions are based on the similarity between the ionic composition of the drilling fluid and formation water, and the resistivity of the drilling fluid being much greater than that of the formation water. Dissolved solids concentrations in the formation water ranged from 1,191 to 3,700 mg/l.

Alger (1966) used the spontaneous potential equation to determine the resistivity of fresh water. He converted all of the anions and cations of the borehole water samples to an equivalent sodium chloride concentration from a salinity-resistivity chart. He assumed that ionic concentration ratios are nearly constant within one ground water region.

Alger extrapolated the relationships between SP, R_w and total dissolved solids (determined from one borehole having an electric log and water analysis) to interpret other boreholes in the region entirely on the basis of their SP deflections. Keys (1989) indicated that the Alger method is not appropriate to calculate the water quality containing less than 10,000 mg/l dissolved solids, unless many other data are available to support the results.

The value of R_w, whether calculated through resistivity measurements or SP, may be used to evaluate water quality. The measurement available is the specific conductance of a water sample at 25°C (77°F), expressed in micromhos per centimetre. It is related to resistivity, expressed in ohm-metres, by the following expression:

$$R_w = \frac{10000}{\text{specific conductance}} \qquad (8.17)$$

The borehole water supply data show the calculation results (Table 8.19) of water resistivity (R_w) derived from specific conductance, as ranging between 2 and 7 ohm-m. This indicates that the formation waters are fresh, confirming the inapplicability of the Guyod (1966) method.

8.4.5.3 Grain Size Versus Formation Factor

The variation of Formation Factor (F) with grain size in the study area is illustrated by the grain size data from sieve analyses, the normal resistivity logs and the water resistivity measurements.

The author has calculated the F values and the porosity of the multiaquifer system (see Table 8.19 and 8.20) on the basis of the ratio of R_O/R_W (see equation 8.12) using data from the normal long and short resistivity logs (see equation 8.12), respectively.

The relationships between Formation Factor, calculated using short and long normal resistivity log data, and D_{10} and D_{50} of grain size were tested as follows:

Table 8.19 Formation Factor measurments based on the short normal resistivity- logs (ohm-m) of Wadi Baysh

Borehole NO	DEPTH Meters	*D10 mm	**D50 mm	TEMP Celsius	EC mmhos	Water resistivity Rw (ohm-m)	Formation resistivity ***Ra (ohm-m)	Formation resistivity ***Ro (ohm-m)	Formation ^ Factor	^^ Porosity %
AO	45.5/46.0	1.50	0.21	37	2175	5	14	18	4	45
	47.0/48.0	0.29	0.08	37	2175	4	9	12	3	49
	49.0/50.0	0.29	0.10	37	2175	4	9	12	3	49
	51.0/52.0	0.35	0.19	37	2175	4	12	16	4	43
	52.0/53.0	1.00	0.26	37	2650	4	30	38	9	28
	Average	**0.69**	**0.17**	**37**	**2270**	**4**	**15**	**19**	**4**	**40**
BO	54.0/55.0	5.80	0.20	38.5	2700	4	14	18	5	39
	56.0/57.0	0.50	0.18	38.5	2700	4	15	20	5	38
	58.0/59.0	0.55	0.11	38.5	2700	4	16	20	5	38
	60.0/61.0	0.40	0.12	38.5	2700	4	16	20	5	38
	62.0/63.0	0.41	0.10	38.5	2700	4	13	17	4	41
	76.0/77.0	0.48	0.09	38.5	2700	4	11	14	3	45
	78.0/79.0	0.50	0.06	38.5	2700	4	12	15	4	41
	80.0/81.0	0.50	0.06	38.5	2700	4	11	14	4	44
	97.0/98.0	0.49	0.10	38.5	2700	4	9	11	3	50
	99.0/100	0.33	0.11	38.5	2700	4	6	8	2	57
	112/113	0.40	0.10	38.5	2700	4	13	17	4	41
	113/114	0.60	0.20	38.5	2700	4	10	13	3	46
	Average	**0.91**	**0.12**	**39**	**2700**	**4**	**12**	**16**	**4**	**43**
EO	55.0/56.0	0.40	0.18	38	5100	2	59	75	38	15
	59.0/60.0	3.20	0.20	38	5100	2	110	139	70	11
	63.0/64.0	0.35	0.12	38	5100	2	50	63	32	16
	65.0/66.0	0.30	0.10	38	5100	2	62	78	39	15
	67.0/68.0	0.80	0.11	38	5100	2	60	76	38	15
	Average	**1.01**	**0.14**	**38**	**, 5100**	**2**	**68**	**86**	**43**	**14**
JO	42.0/42.5	0.65	0.09	38.5	3250	3	13	17	6	36
	43.5/44.5	1.20	0.22	38.5	3250	3	18	23	7	32
	45.0/46.5	2.00	0.20	38.5	3250	3	13	17	5	36
	64.5/65.5	4.00	0.55	38.5	3250	3	11	15	5	39
	65.5/66.5	2.00	0.30	38.5	3250	3	13	17	5	36
	123/124	1.80	0.16	38.5	3250	3	14	18	6	35
	Average	**1.94**	**0.25**	**39**	**3250**	**3**	**14**	**18**	**6**	**36**
KO	40.5/42.0	1.50	0.13	38	5117	2	7	9	4	40
	42.0/43.0	0.80	0.20	38	5117	2	16	21	11	27
	43.0/44.0	1.10	0.19	38	5117	2	36	46	23	19
	47.0/48.0	0.90	0.18	38	5117	2	14	18	9	29
	48/50	0.55	0.16	38	5117	2	8	10	5	37
	Average	**0.97**	**0.17**	**38**	**5117**	**2**	**16**	**21**	**11**	**27**

* Grain size that is 10 percent finer by weight ** Grain size that is 50 percent finer by weight

*** Ro corrected to a standard temperature of 25 Celsius, R0 =Ra*[(Ta+21.5)/(46.5)] ; °C

^ F = Ro/Rw ^^ F=0.62 /(porosity)^2.15

Table 8.20 Formation Factor measurments based on the long normal resistivity-logs (ohm-m) of Wadi Baysh

Borehole NO	DEPTH Meters	*D10 mm	**D50 mm	TEMP Celsius	EC mmhos	Water resistivity Rw (ohm-m)	Formation resistivity ***Ra (ohm-m)	Formation resistivity ***Ro (ohm-m)	Formation ^ Factor	^^ Porosity %
AO	45.5/46.0	0.21	1.50	37	2175	5	11	14	3	49
	47.0/48.0	0.08	0.29	37	2175	4	13	16	4	42
	49.0/50.0	0.10	0.29	37	2175	4	13	17	4	41
	51.0/52.0	0.19	0.35	37	2175	4	18	23	6	36
	52.0/53.0	0.26	1.00	37	2650	4	48	60	15	23
	Average	**0.17**	**0.69**	**37**	**2270**	**4**	**21**	**26**	**6**	**34**
BO	54.0/55.0	0.20	5.80	38.5	2700	4	22	28	8	31
	56.0/57.0	0.18	0.50	38.5	2700	4	25	32	8	30
	58.0/59.0	0.11	0.55	38.5	2700	4	23	30	7	31
	60.0/61.0	0.12	0.40	38.5	2700	4	21	27	7	33
	62.0/63.0	0.10	0.41	38.5	2700	4	13	17	4	41
	76.0/77.0	0.09	0.48	38.5	2700	4	14	18	4	40
	78.0/79.0	0.06	0.50	38.5	2700	4	15	19	5	37
	80.0/81.0	0.06	0.50	38.5	2700	4	14	18	4	40
	97.0/98.0	0.10	0.49	38.5	2700	4	9	11	3	49
	99.0/100	0.11	0.33	38.5	2700	4	4	6	1	69
	112/113	0.10	0.40	38.5	2700	4	13	17	4	41
	113/114	0.20	0.60	38.5	2700	4	10	13	3	46
	Average	**0.12**	**0.91**	**39**	**2700**	**4**	**15**	**20**	**5**	**41**
EO	55.0/56.0	0.18	0.40	38	5100	2	97	123	63	12
	59.0/60.0	0.20	3.20	38	5100	2	100	127	63	12
	63.0/64.0	0.12	0.35	38	5100	2	66	84	42	14
	65.0/66.0	0.10	0.30	38	5100	2	63	80	40	14
	67.0/68.0	0.11	0.80	38	5100	2	72	92	46	13
	Average	**0.14**	**1.01**	**38**	**5100**	**2**	**80**	**101**	**51**	**13**
JO	42.0/42.5	0.09	0.65	38.5	3250	3	14	18	6	36
	43.5/44.5	0.22	1.20	38.5	3250	3	19	25	8	31
	45.0/46.5	0.20	2.00	38.5	3250	3	15	20	6	34
	64.5/65.5	0.55	4.00	38.5	3250	3	11	14	5	39
	65.5/66.5	0.30	2.00	38.5	3250	3	13	16	5	37
	123/124	0.16	1.80	38.5	3250	3	15	19	6	34
	Average	**0.25**	**1.94**	**39**	**3250**	**3**	**14**	**19**	**6**	**35**
KO	40.5/42.0	0.13	1.50	38	5117	2	10	13	7	33
	42.0/43.0	0.20	0.80	38	5117	2	28	36	18	21
	43.0/44.0	0.19	1.10	38	5117	2	54	69	35	15
	47.0/48.0	0.18	0.90	38	5117	2	34	44	22	19
	48/50	0.16	0.55	38	5117	2	20	26	13	24
	Average	**0.17**	**0.97**	**38**	**5117**	**2**	**29**	**37**	**19**	**20**

* Grain size that is 10 percent finer by weight

** Grain size that is 50 percent finer by weight

*** Ro corrected to a standard temperature of 25 Celsius, R0 =Ra*{(Ta+21.5)/(46.5)} ; °C

^ F = Ro/Rw

^^ F=0.62 /(porosity)^2.15

1- F (determined using short normal resistivity data, see Table 8.17) was correlated with D_{10} and D_{50} as two sets of data; full range of F values and the average value of F of each borehole (see Figures 8.27 and 8.28). In Figure 8.27, F shows no correlation with D_{10} and D_{50} ($r = 0.004$ and $r = 0.115$, respectively). The average value of F and D_{10} of each borehole show a better correlation ($r = 0.306$) compared with D_{50}, which shows low correlation ($r = 0.091$, see Figure 8.28).

2- F (determined using long normal resistivity data, see Table 8.18) was correlated with D_{10} and D_{50} as two sets of data; full range of F values and the average value of F for each borehole (see Figures 8.29, 8.30). In Figure 8.29, F shows no correlation with D_{10} ($r = 0.011$) or D_{50} ($r = 0.036$). The average value of F for each borehole shows a better correlation with the average value of D_{10} of each borehole ($r = 0.334$) than with D_{50} which shows virtually no correlation ($r = 0.152$, see Figure 8.30).

Accordingly, the average values of Factor determined from short or long normal resistivity logs of each borehole shows a slight correlation with the average values of both D_{10} and D_{50} ($r= 0.306$ and 0.334 respectively)

An examination of the relationships between the average Formation Factor (using short and long normal resistivity logs of each borehole) and the hydraulic conductivity (K, determined by the Hazen method, the pumping test and the Masch & Denny method) reveals a strong correlation ($r = 0.7$) between only F and K (using Masch & Denny method). No other inter-relationships are statistically significant (Figures 8.31 and 8.32).

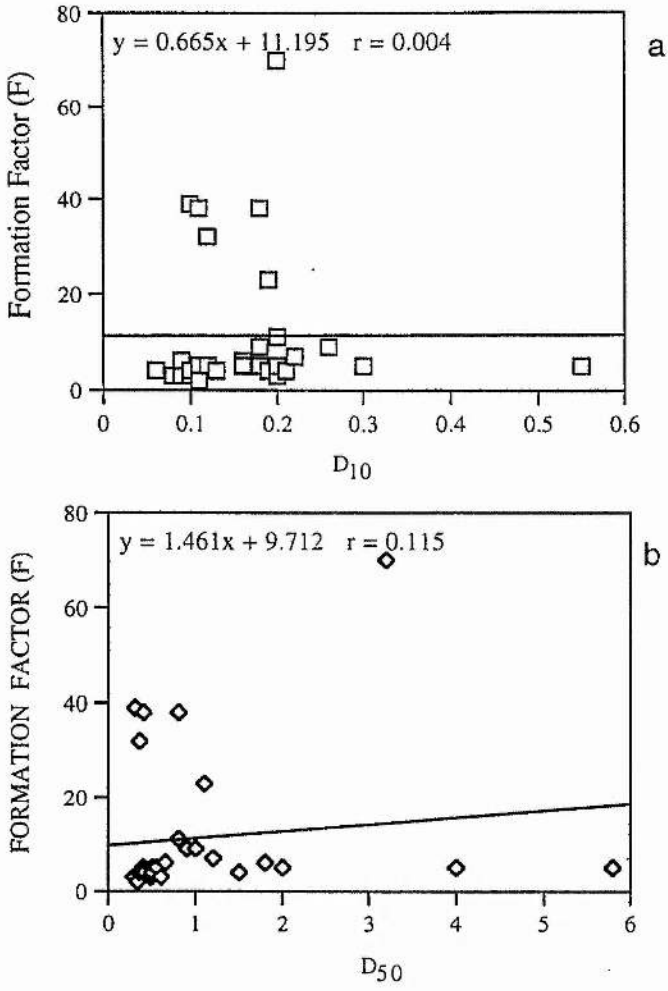

Figures 8.27 The relationship between the grain size D_{10} (a), D_{50} (b) and the Formation Factor determined using the short, normal resistivity logs for Wadi Baysh.

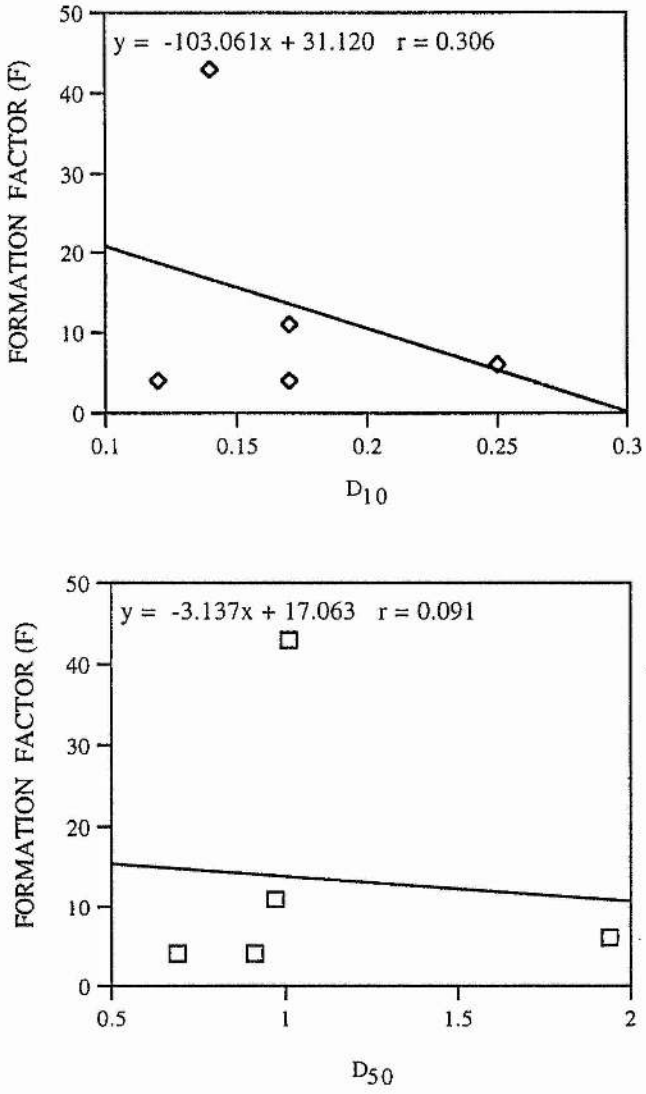

Figures 8.28 The relationship between the average of D_{10} (a) and D_{50} (b) and the average of the Formation Factor (F), determined using the short, normal resistivity logs for Wadi Baysh.

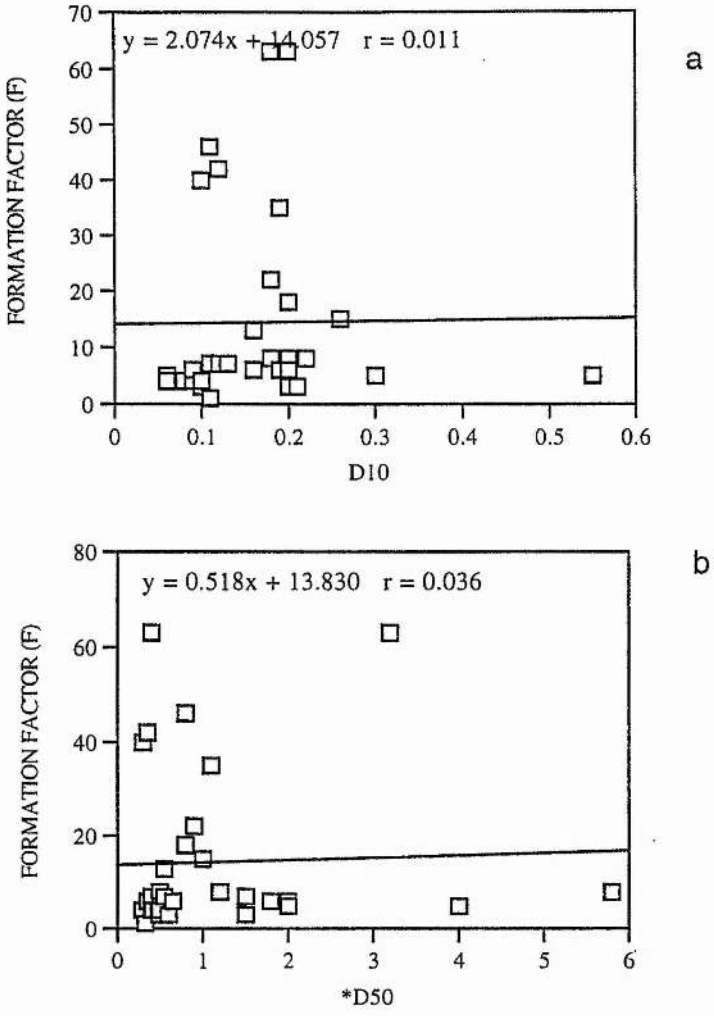

Figures 8.29 The relationship between the grain size D_{10} (a), b (D_{50}) and the Formation Factor determined using the long, normal resistivity logs for Wadi Baysh.

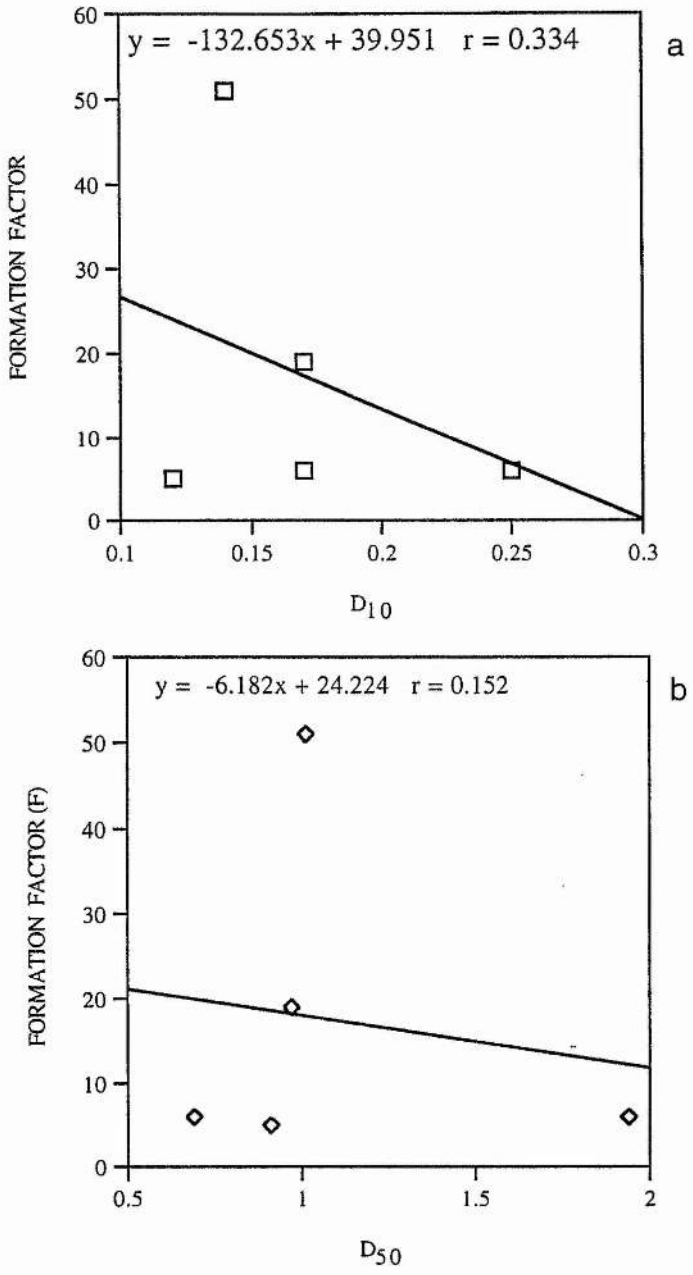

Figures 8.30 The relationship between the average of D_{10} (a) and D_{50} (b) and the average of the Formation Factor (F), determined using the long resistivitynormal logs, for Wadi Baysh.

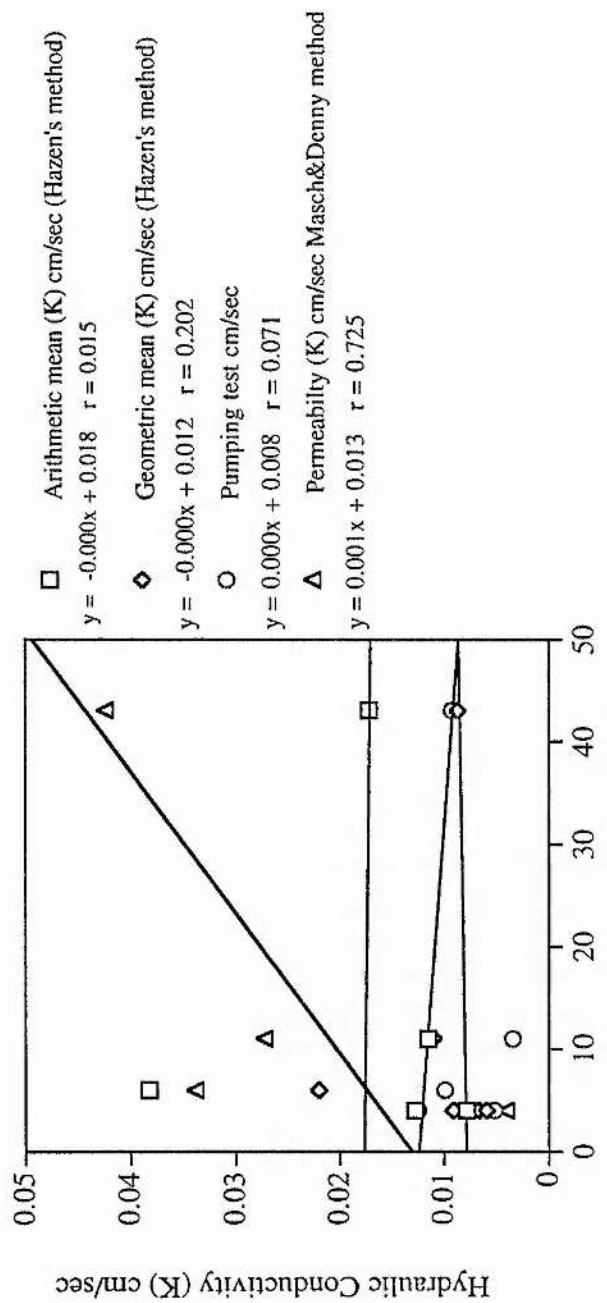

Figure 8.31 The relationship between the Formation Factor (using the short resistivity logs) and the hydraulic conductivity.

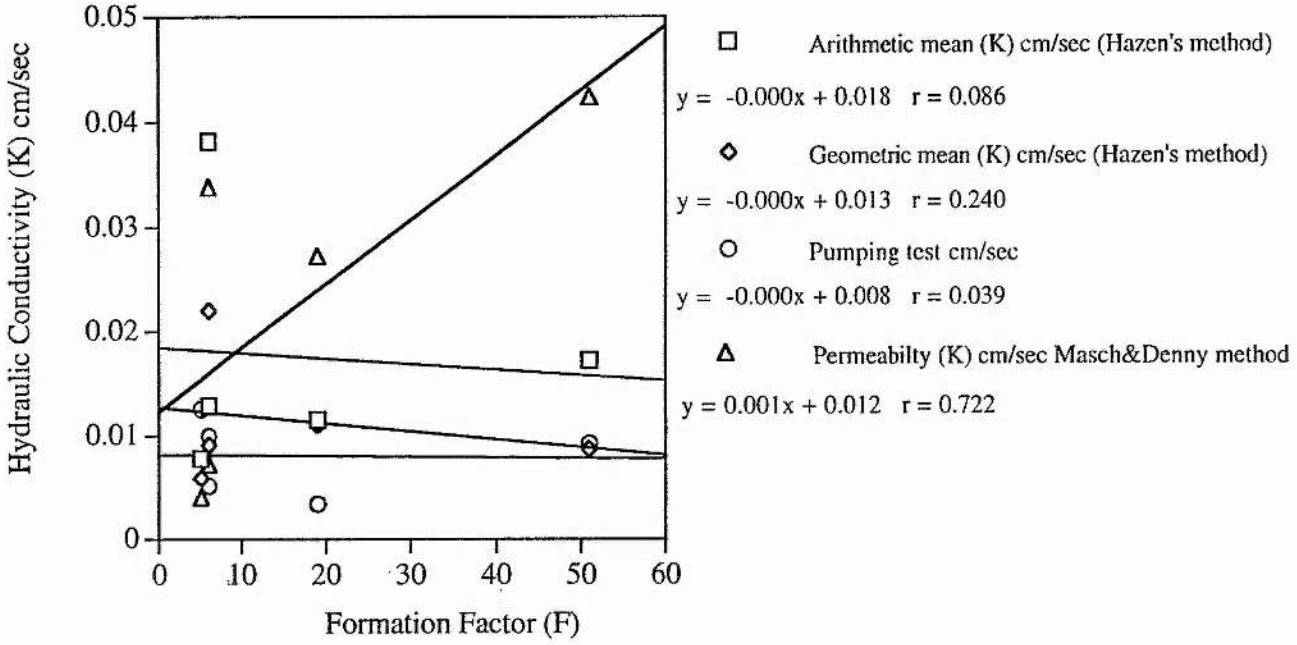

Figure 8.32 The relationship between the Formation Factor (using the long resistivity logs) and the hydraulic conductivity.

8.4.6 Conclusion

The more geophysical logs that show the same geohydrological environments, the greater the benefits which may be gained from logging. The synergistic character of these logs is due to the fact that each type of log measures different parameters. Analysed together each tends to support the conclusions drawn from the others.

Seven spontaneous potential, short resistivity, long resistivity and gamma ray logs illustrated the synergistic nature of the logs. The responses of the resistivity and nuclear logs to saturated wadi sediments are summarised in Figure 8.33 below:

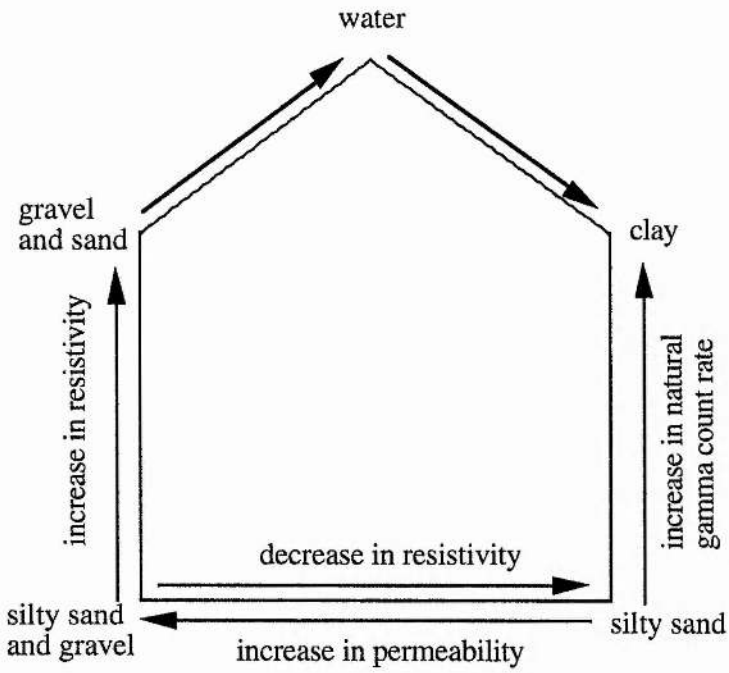

Figure 8.33 Diagram showing the response of the resistivity and the natural gamma logs in the wadi sediments

1- The natural-gamma count rate increases with increasing clay content

2- The resistivity (short and long) decreases with increasing clay content.

3- The resistivity increases with an increase in the permeability while both of them decrease with an increase in the clay content in which the porosity increases

As shown above, the relationships of various logs can help in identifying the hydrogeological characteristics of the wadi sediments. The simplified response of these geophysical parameters for four different logs are listed Table 8.21.

Table 8.21 Well logs parameters of lower parts of Wadi Baysh.

Type of Log	Parameters measured and direction of log deflection	Parameters inferred and direction of log deflection	Index range of wadi floor sediments in the area
Natural gamma ray	Natural gamma radiation increase is to the right	Clay content increase to the right	Clay >30 CPS Silty sand >20<30 CPS Gravel <20 CPS
Resistivity (long and short)	Electrical resistivity increase to right	Formation resistivity increase to the right as permeability increases.	Short resistivity log Clay <10 ohm-m Silty sand >10 ohm-m Gravel >20 ohm-m Long resistivity log Clay <10 ohm-m Silty sand >10<20ohm-m Gravel, sand >20 ohm-m
Spontaneous potential	Natural electrical potential (positive to right)	Clay content	Bell shape > high permeability layer (gravel and sand)

From these logs it is found that the most permeable zone shows the highest resistivity and as indicated by the natural gamma log, the lowest clay content.

The data reported make possible the estimation of permeability and transmissivity from the resistivity curves of the electric logs.

The graphic relationship between the permeability and the Formation Factor in this study shows a greater range of grain size (0.1-6 mm) and Formation Factor (1-50). Alger's (1966) graphs cover a more limited range (e.g. Formation Factor ranged from 1-5 with the grain size from 0.03-3.0 mm). Thus the graph derived above is one of more general application than has been available hitherto.

CHAPTER NINE: FEASIBILITY STUDY OF ARTIFICIAL RECHARGE AND CONJUNCTIVE USE MANAGEMENT OF WATER RESOURCES

9.1 Section One: Feasibility Study of Artificial Recharge

9.1.1 Introduction

Artificial recharge is widely used as a method by which surface water is placed into groundwater storage, where it is not subject to evaporation and is unlikely to be contaminated from surface sources. Where geological conditions are suitable for recharge, the injection of water through wells may be undertaken.

In any area dependent upon pumped water for either domestic or irrigation use, the recharging of the aquifer can be stimulated by artificial methods. They have been used in many areas such as the U.S.A., Europe and Australia. Generally speaking, the countries which rely on the artificial recharge of groundwater are Germany, where about 30% of public water supplies is derived from artificial recharge, and the Netherlands and Sweden, where the corresponding figure is 15% (Ineson, 1970).

In the present study area, characterised by arid and semi arid environments, it is essential to preserve all available surface water, preferably by retaining it in the form of groundwater storage.

The upper part of the catchment of both wadis is characterised by high rainy season flows. Approximately 85% of both wadi catchments comprise rock outcrops and shallow soils, forming valleys which are steep-sided with flat alluvial bases. The rocks are impervious and ensure that a significant portion of the rainfall becomes runoff. About 6 to 14% of rainfall flows as flood water, whereas the rest of the rainfall is lost in evaporation or becomes diverted to terraces in the upper parts of the catchment areas (see Figure 9.1). The flood water which is available to recharge the aquifer occurs during most of the seasons in Wadi Baysh, whereas in Wadi Habawnah it falls during the spring.

In both wadis the economy is dependent on irrigated agriculture using flood waters and pumped groundwater. There are no available data to show the average annual pumping of water in the irrigated area. In Wadi Baysh and Wadi Habawnah there is 1m

Figure 9.1 Agricultural terraces of Asire region dominated with barley, wheat and sorghum plants.

and 2m of the water level pumped per year, respectively. The water record for the lower part of both wadis indicates that the water level ranges between 5 and 23 m below the surface. The water table level has steadily declined in some areas where the flood waters rarely reach, as in observation well KO in Wadi Baysh and H-8-P in Wadi Habawnah (see Figures 8.1 and 8.2). The saturated thicknesses level, which once averaged more than 18 m and 11 m in Wadis Baysh and Habawnah, respectively, has decreased significantly. The greater part of the increased areas of agriculture is served by pumping water from existing aquifers. A survey of areas where water is pumped for irrigation shows a lowering of the water table. The situation is more serious in Wadi Habawnah than in Wadi Baysh, where the aquifers are larger and, consequently, are depleted more slowly. The present rate of decline of the water table could result in limiting the irrigated developments in both wadis.

Generally, aquifers in the arid and semi-arid zone are characterised by the presence of an unsaturated zone. Groundwater flow will take place as a result of infiltration of water beneath the surface. Asano (1985) indicated that infiltration will continue downward but at a decreasing rate until the surface tension forces are equal to the gravitational forces. Once the wetting begins to merge with the underlying saturated zone, the incoming discharge changes direction and flows mainly below the water table and generally parallel to it.

In order to establish successful artificial recharge criteria for the two wadi systems, the author has studied the hydrological characteristics of both wadis. No field experiments for artificial recharge took place during this research. Two parallel approaches have been taken to obtain relevant information. The first was a comprehensive study of the geophysical and pumping tests used to identify suitable areas for artificial recharge; the second was a series of case studies of artificial recharge in other countries, with similar conditions to those in the study area, to serve as a guide for the adoption of artificial recharge methods in the Baysh-Habawnah region.

9.1.2 The Agricultural Systems of Watering

Agriculture in both wadis is characterised by a traditional watering system, which is predominant in Wadi Baysh, whilst there is a more modern system (using pumping) in Wadi Habawnah.

The flood (Sail) irrigation system is the most important system of both traditional and modern farming. However, the flood irrigation system of Wadi Baysh is different from that in Wadi Habawnah.

9.1.2.1 Wadi Baysh Irrigation System

A flood spreading system, based on the traditional water rights code, is applied for irrigation in the middle and lower parts of the wadi, while in the upper parts of the wadi big diameter wells are used for irrigation. According to the local farmers, the existing flood spreading system consists of a series of about 40 temporary earth dikes along the wadi bed (Figure 9.2a). The flood renovates the agricultural land by water diversion systems, which are located along the wadi in the order of the traditional water rights priorities. After the first division gets its requirement of water, the ugoom (1-1.5 meter high) is cut in order to allow the next division downstream to be watered. This procedure is followed until all the agricultural land further downstream in the wadi is irrigated. Within each division, the water distribution is achieved by utilising a network of smaller earth dikes which form small fields.

According to the local farmers, the flood water is absorbed by the soil during a time which varies between one week and three weeks depending on the aridity of the soil and the volume of the flood. The traditional farm planting is performed once the flood water has been absorbed and the plants (mainly sorghum (durah) and barley, with small area of sesame and millet (dukhn)) grow to maturity on moisture stored in the root zone of the soil. The farmers reported that when sufficient water of a single flood is absorbed by the soil, they are able to obtain three harvests of sorghum from the soil (Figure 9.2b).

This traditional system, under existing water priority rights, is insufficient when the flood flow is low. The lower sections of the agricultural land located towards the

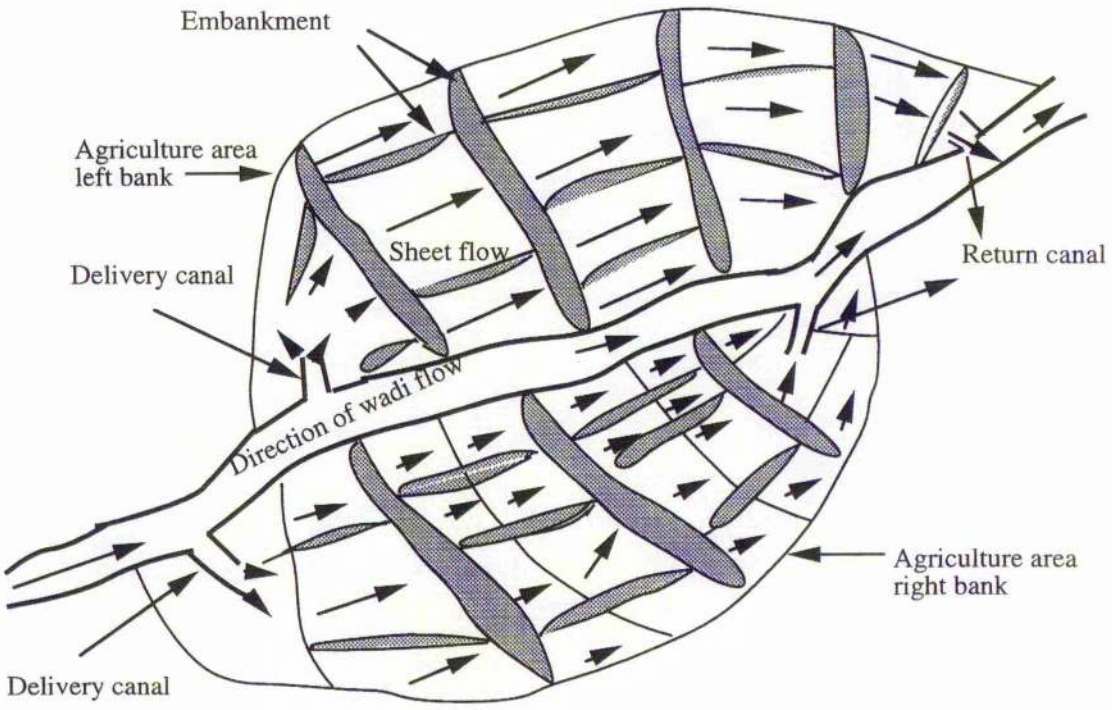

Figure 9.2 a Direct -surface recharge by flooding in Wadi Baysh
(Traditional group system)

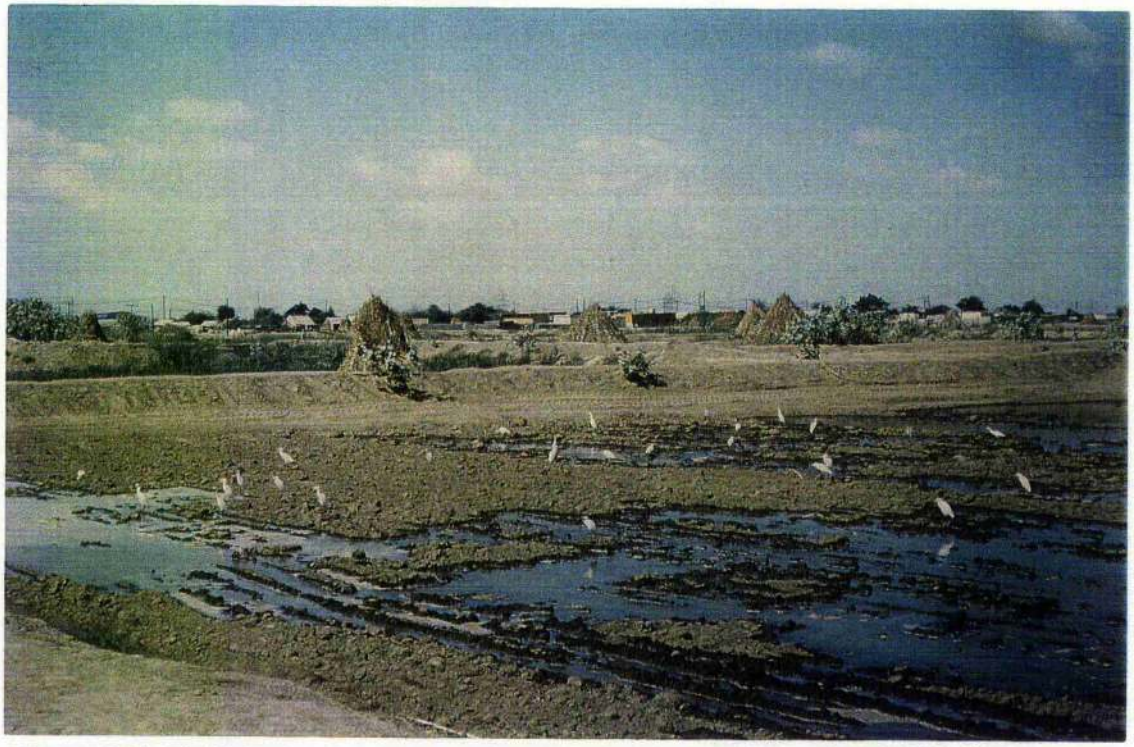

Figure 9.2b Field basin of sorghum showing flood water irrigation in Wadi Baysh. The basin wall has a height of 1 m . In nearby fields is the previous season's harvest.

lower part of the wadi (about 16 km below from Baysh Bridge) usually receive less water than the upper sections. The farmers indicate that every 2 to 6 years they are able to use flood waters to irrigate their farms.

The modern agricultural system of farming in Wadi Baysh is based on the exploitation of groundwater to irrigate the farms using dug wells from which groundwater is pumped to the surface. These farms are located randomly on the flood plain and downstream. The major crops grown under this system are vegetables and melons, in addition to sorghum.

9.1.2.2 Wadi Habawnah Irrigation System

In Wadi Habawnah, the irrigation system takes advantage of the flood (Sail) systems. The agricultural land in Wadi Habawnah is located on both sides of the main wadi channel. Each farm has earth dikes extending towards the main wadi channel, which enables the farms to receive sufficient water during the flood flow. In addition to flood water, each farm has one or more large diameter wells for irrigation (Figure 9.3a). In the lower and middle parts of the wadi, during dry years, the water table may vary between 0.5 and 2 metres above the bed rock, while with sufficient floods the water table reaches 1 to 3 metres below the ground surface (farmers information). Planting is performed when the standing flood is absorbed by the soil. Experiments here have shown that flood irrigation is enough to moisten soil sufficiently to get crops such as barley and wheat to maturity (Figure 9.3b). However, during the dry season, groundwater is used for the irrigation of vegetables and melons.

9.1.2.3 Agricultural Area

The agricultural areas of both wadis have been determined using the topographic maps at a scale of 1:250,000 for Wadi Baysh and 1:50,000 for Wadi Habawnah.

In Wadi Baysh the agricultural area is approximately 27033 ha (see Figure 2.15). The northeastern part of the agricultural area starts about 7.5 km northeast of the village of Misliyh and stretches between Wadi Baysh and Sabya, including the town of Baysh. The agricultural area stops at Al Qawz, a distance of 5 km from the Red Sea, The total

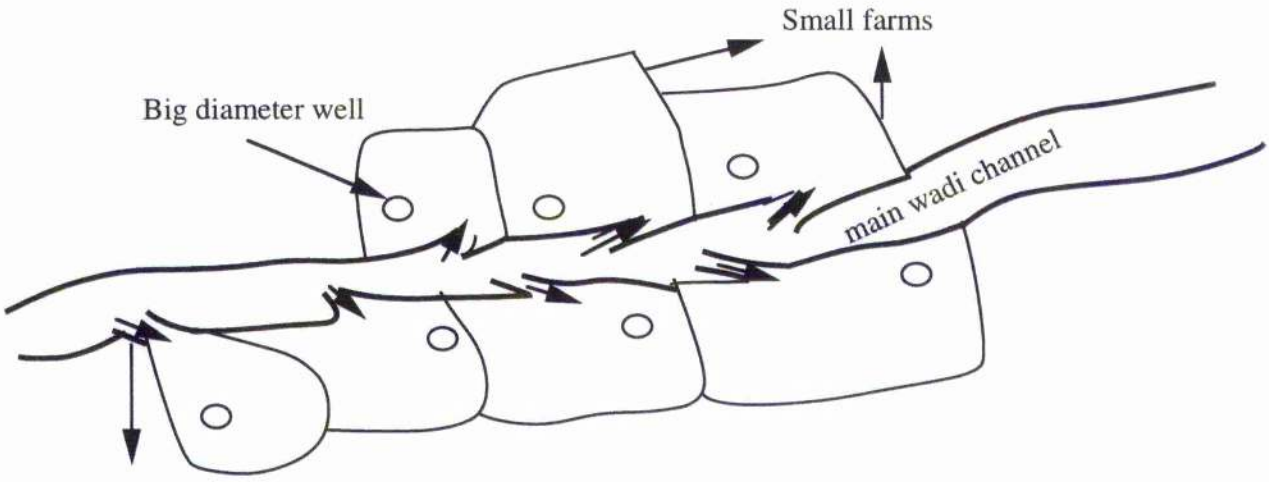

Figure 9.3 a Irrigation system with direct surface recharge by flooding using individual diversion canals (Traditional single system) and big diameter wells in Wadi Habawnah

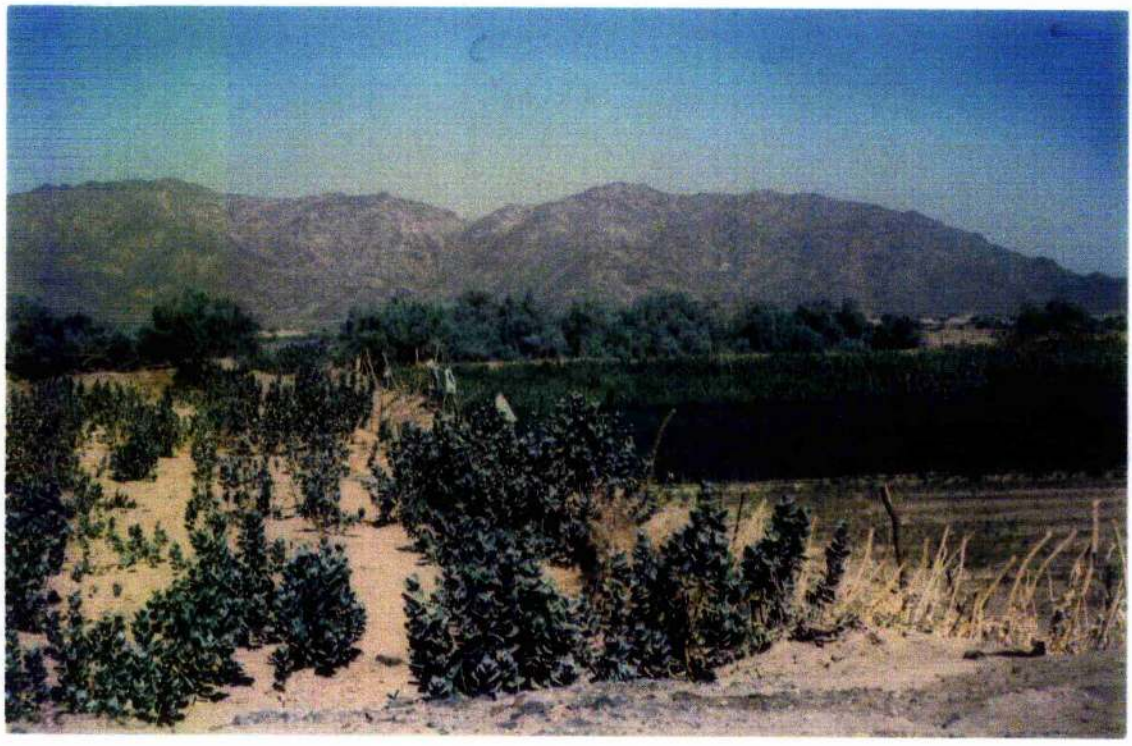

Figure 9.3 b Sorghum and barley fields in Wadi Habawnah, which are irrigated by flood water and groundwater.

length of the agricultural land is 45 km with an average width of 6 km. In Wadi Habawnah the agricultural land is about 11350 ha in area (see Figures 2.16a and 9.4). It starts at Habawnah village and is mostly on both banks of the main channels. Between Wadi Habawnah and Wadi Thar, encompassing the village of Almontasher, about 3400 ha is used for farming. There is no agricultural area in the Abo Khatain mountains (between Aldayqeh village and Morykhah village, see Figure 9.4), but stretching near Al Hausaniah an area of 5300 ha is found.

According to the Agriculture office in Najran, the total area that is suitable for agricultural development in Wadi Habawnah is approximately twenty thousand hectares.

9.1.3 Groundwater Artificial Recharge

Artificial recharge can be defined as a process whereby water is induced artificially to infiltrate the ground from a body of water in quantities, and commonly at rates, in excess of the natural infiltration. Griffis (1976) defines artificial recharge as the movement of water via man-made systems from the surface of the earth to the underground water-bearing strata where it may be stored for future use.

The major advantages using artificial recharge can be summarised as follows:

1 Control of water resources

2 Better use of groundwater reservoirs by recharging close to the points of demand

3 Elimination of evaporation loss

4 Increasing the groundwater supply.

The purpose of this chapter is to examine artificial recharge and identify methods that are most suitable for adoption in the study area. This investigation will consider different design aspects and provide guidelines for studying the feasibility of artificial recharge in specific cases. An extended literature review is a necessary precursor for the study.

The principal methods of artificial recharge currently in use are summarised in Figure 9.5, which is modified from Motts (1983) by the omission of sewage effluent since the recharging by natural water from streams is the main category of artificial recharge required in the study area.

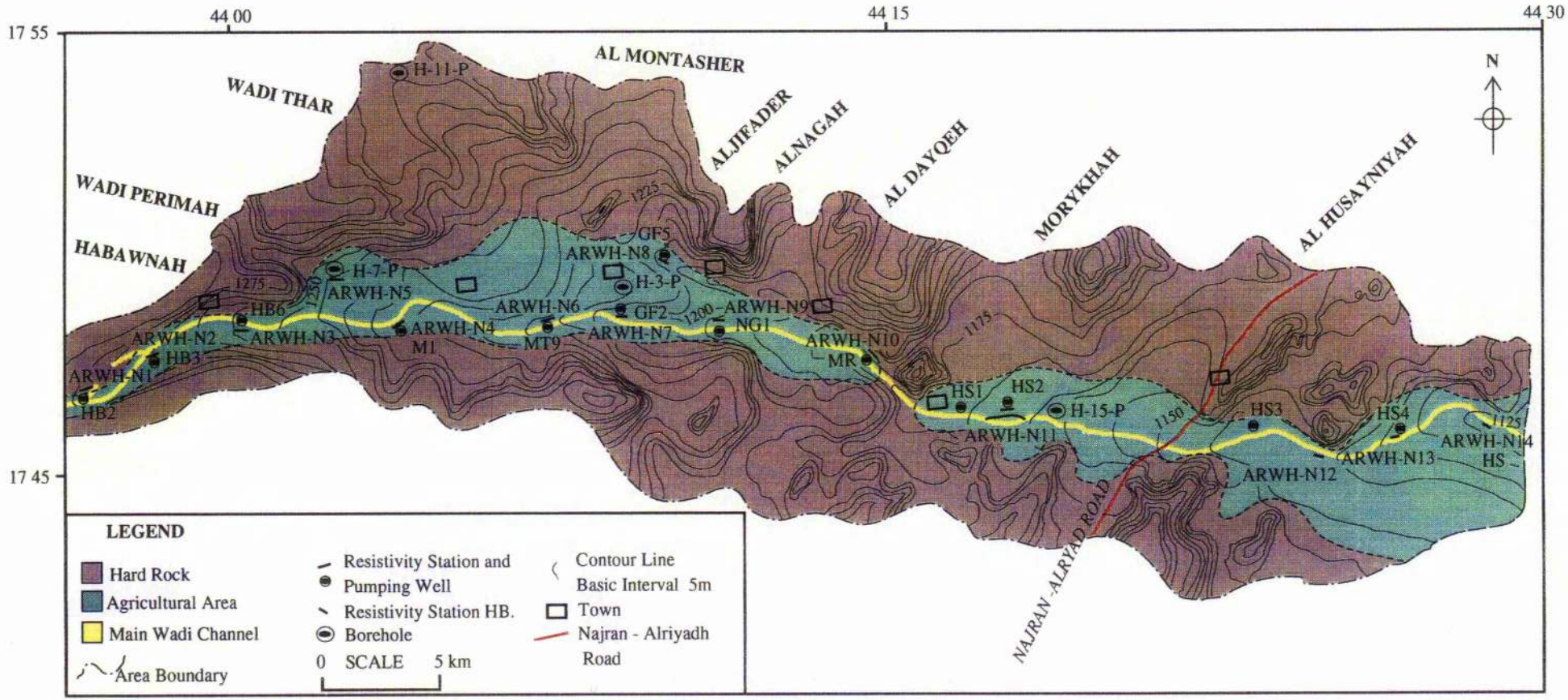

Figure 9.4 Agricultural Map of Wadi Habawnah.

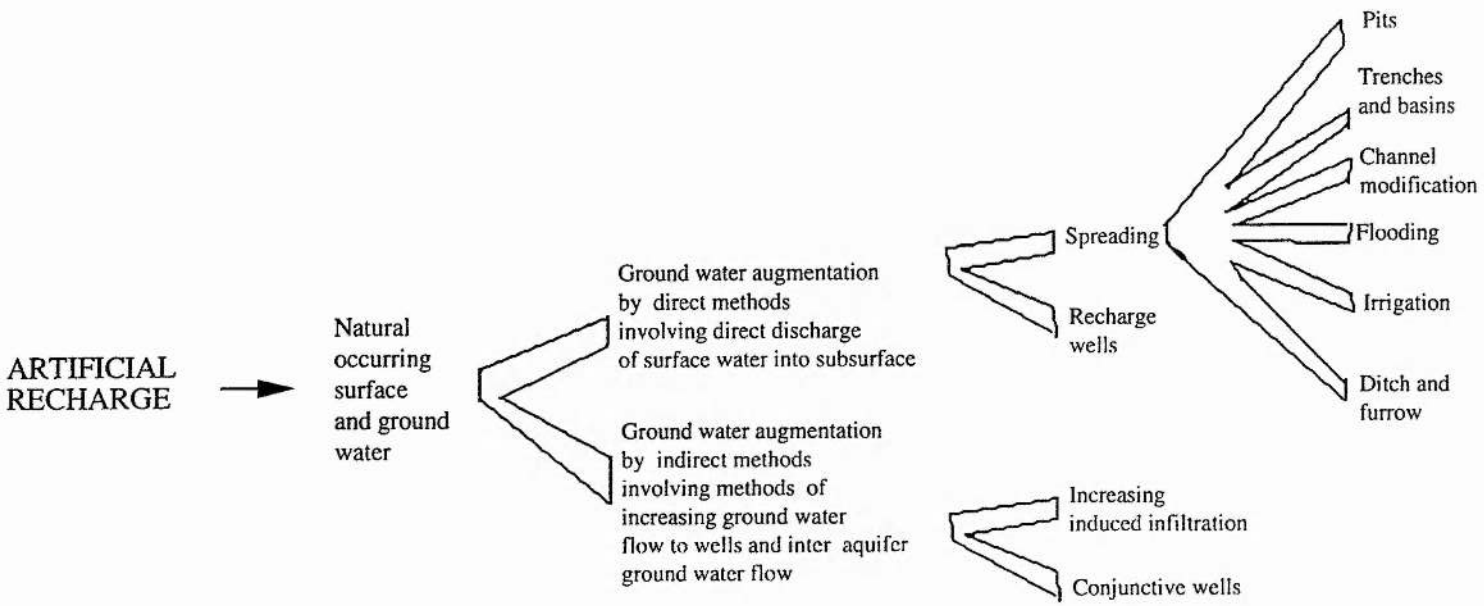

Figure 9.5 Flow Chart Showing Principal Methods of Artificial Recharge (modified from Motts, 1983)

The artificial recharge of naturally occurring surface water may be further subdivided into groundwater augmentation by indirect methods involving the inducement of surface and ground water towards pumping wells and by direct methods involving the discharge of surface water into the subsurface via spreading or recharge wells.

Both direct and indirect methods of artificial recharge will be addressed. The direct methods consist of spreading basins, recharge pits, shafts, ditches and recharge wells. Indirect methods are induced infiltration (enhanced stream bed infiltration) and conjunctive wells.

9.1.3.1 Methods of Artificial Recharge

The most common method of artificial recharge is to spread water over a large surface area. This spreading, which allows the water to sink into underlying aquifers, is the basis of traditional recharge in Wadi Baysh. Two primary methods of water spreading commonly in use are off-channel spreading and on-channel spreading.

9.1.3.1.1 Off-Channel Spreading

Off-channel spreading consists of transferring water from a channel to areas characterised by high infiltration rates. It is achieved most commonly by building dikes or levees. The size and shape of the infiltration basins depend primarily on land availability, slope and soil conditions (Todd, 1980). In the study area storm runoff would need to be diverted for recharge. Desilting basins may be required before water is released to the next infiltration basins. Figure 9.6 shows a typical case in which water is diverted into abandoned gravel pits located near the wadi channel. The basins fill and the excess water is passed along a spillway canal back to the wadi channel.

Todd (1980) indicated that ditch and furrow methods are less frequently used in off-channel artificial recharge. These ditches and furrows are mainly shallow and flat bottomed excavations in the ground, into which water is diverted. Three layouts may be used (see Figure 9.7):

1 Contour. The ditch follows the ground contour

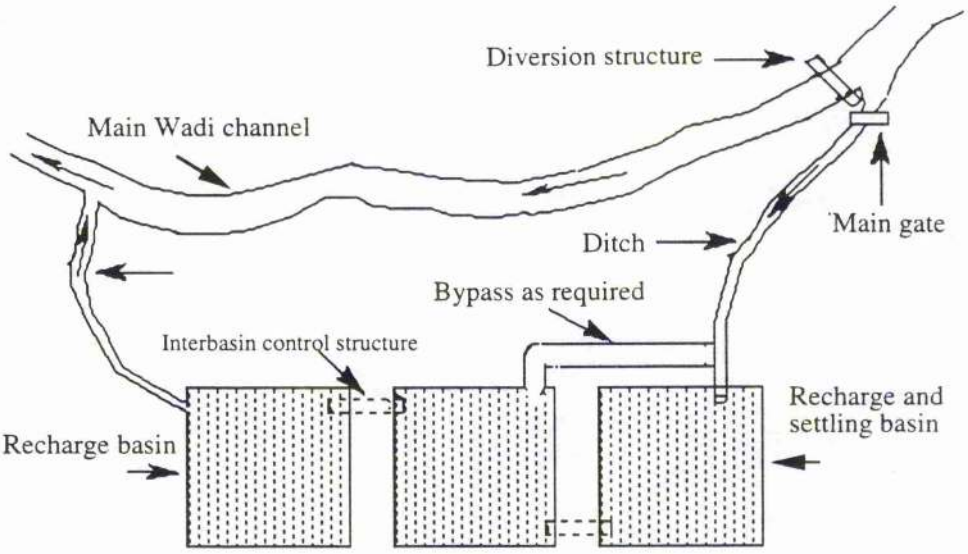

Figure 9.6 Simple plan of basin type recharge flood plain

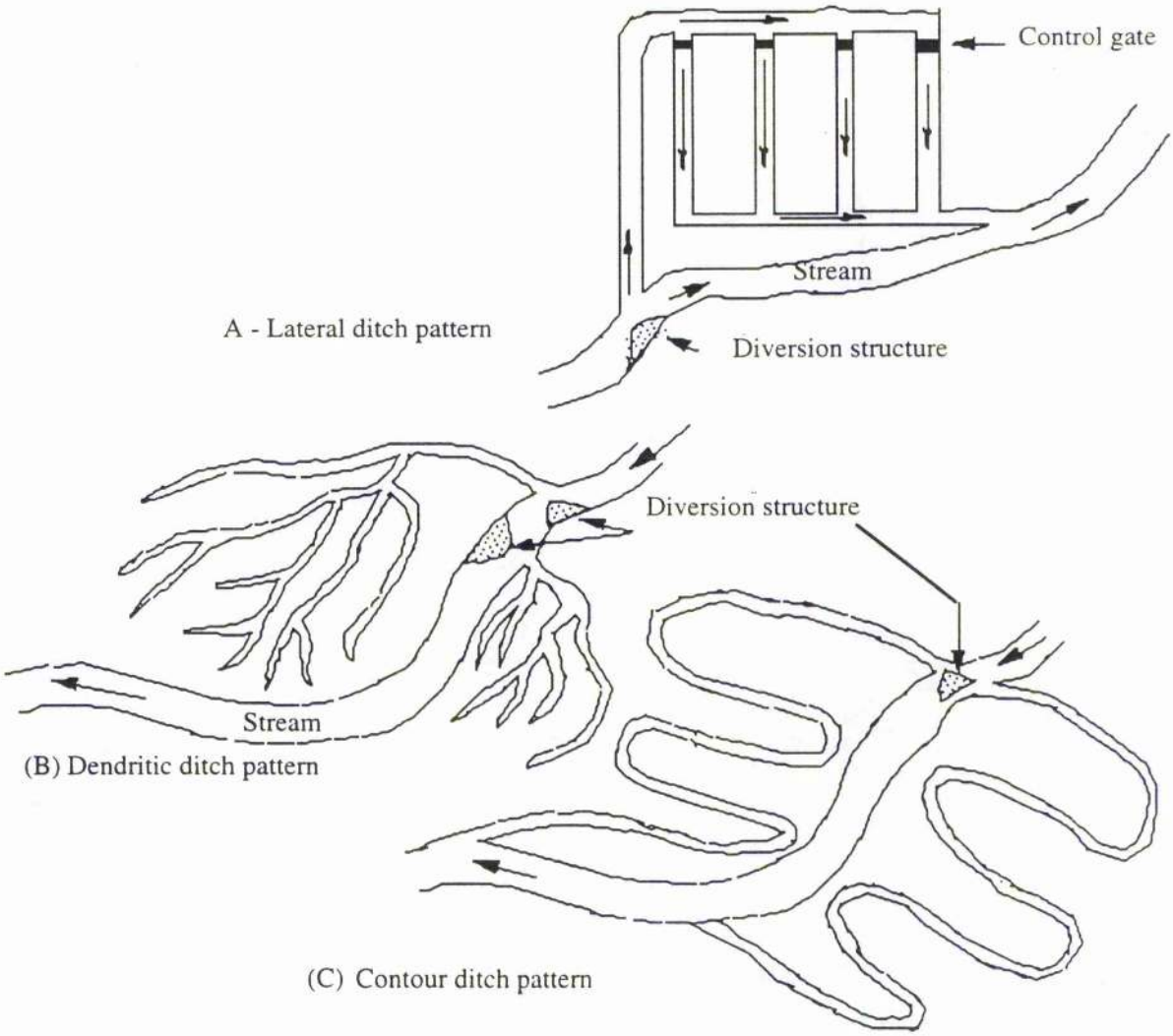

Figure 9.7 Typical ditch and furrow systems. (a) Lateral. (b) Dendritic.(c) contour.

2 Tree-shaped (Dendritic ditch pattern). The main ditch successively branches into smaller ditches

3 Lateral. A series of small ditches extend laterally from a main ditch

9.1.3.1.1.1 Selection of Spreading Areas

Suitable places to spread water are bordering streams and below a mountain channel (Figure 9.8a and b). These elevated areas generally consist of coarse material and are too rough for agricultural purposes. However such areas are useful for water spreading. The agricultural area in neither wadi is suitable for spreading methods since clay and silty clay (both impervious materials), which exists between the ground surface and the aquifer, prevents the free downward movement of the percolating water (Figure 9.9). Surface slopes ranging from 3 to 60m per km are found to be suitable for spreading areas (Husiman, 1983). In the study area the slopes are about 3m per km.

The artificial introduction of water is preferably made outside the flood channels on gravel deposits, also, commonly, on low benches bordering the streams, or on the elevated land near the mountains. Such terrain is typically underlain by very absorbent sediments.

Locating diversion structures on wadi channels requires careful design. The flood channels convey flow over the wadi deposits, which are rarely confined within permanent banks. Each successive storm brings down varying quantities of silt, sand, gravel and boulders. If diversion works are improperly designed or located on these streams, the debris carried by the flood flow will accumulate above the works and divert the stream out of its channel. Thus, in all cases, adequate provision should be made to permit large floods to pass without damage to the diversion works, or to enter the channels intended to convey water uncontrolled to the spreading recharge systems.

9.1.3.1.1.2 Spreading basins

Spreading basins provide a common method of artificial recharge in which the surface spreading of water is used to recharge the basins. Pettyjohn (1981) indicated that

a

b

Figure 9.8 Suitable spreading areas for groundwater recharge. a) Area below the mountain channel consisting of boulders and gravel, which makes it too rough for agricultural use but is ideal for groundwater recharge (Wadi Habawnah). b) Similar site in the Wadi Baysh area.

Figure 9.9 Agricultural area consisting of a thick layer (3m) of clay and silt near Mislyah village, Wadi Baysh

the basins used for the spreading methods of recharge are commonly built by modest excavation in the existing terrain, or by placing low head dams across natural water ways.

Dvorcek and Peterson (1971) explained that the optimum artificial recharge by spreading methods can be achieved when highly permeable soils are maintained above the aquifer. Under such conditions, Hausaniah and Olsthoorm (1983) showed that the recharge in basins and ditches depends on three factors: (1) the infiltration rate; (2) the percolation rate and (3) the capacity for horizontal water movement. The infiltration rate is defined as the rate at which the water is picked up by the soil. At the beginning of the spreading operation, where the aquifer is assumed to be homogeneous up to the ground surface, the infiltration rate is equal to the percolation rate.

The operation of a spreading system is comparable to an irrigation system except that, instead of attempting to hold the moisture within the root zone of the irrigated crop, rapid percolation into the aquifer is encouraged.

Oaksford (1985) indicates that artificial recharge requires a large area, permeable surface material, a simple construction to run the system and little or no water pre-treatment.

The combined availability of relatively large land areas, permeable surface materials, hydraulic connections and downward gradient will lead to significant quantities of recharge from the land surface to the aquifer. Figure 9.10 shows a scheme of water diverted from an intermittent stream to a settling basin and then to an infiltration basin. Adopting such a method would provide storage of the water for irrigation needs and purification by filtering of fine materials in the settling basin.

9.1.3.1.2 On-Channel Spreading

In on-channel spreading, the main wadi channel is used for water spreading, with improvements made to increase the infiltration capacity. This can be achieved by scraping, levelling, widening, ditching and building sand dikes in the wadi bed. These wadi channel modifications both increase the rate of infiltration and reduce the water velocity allowing more time for infiltration (see Figure 9.11).

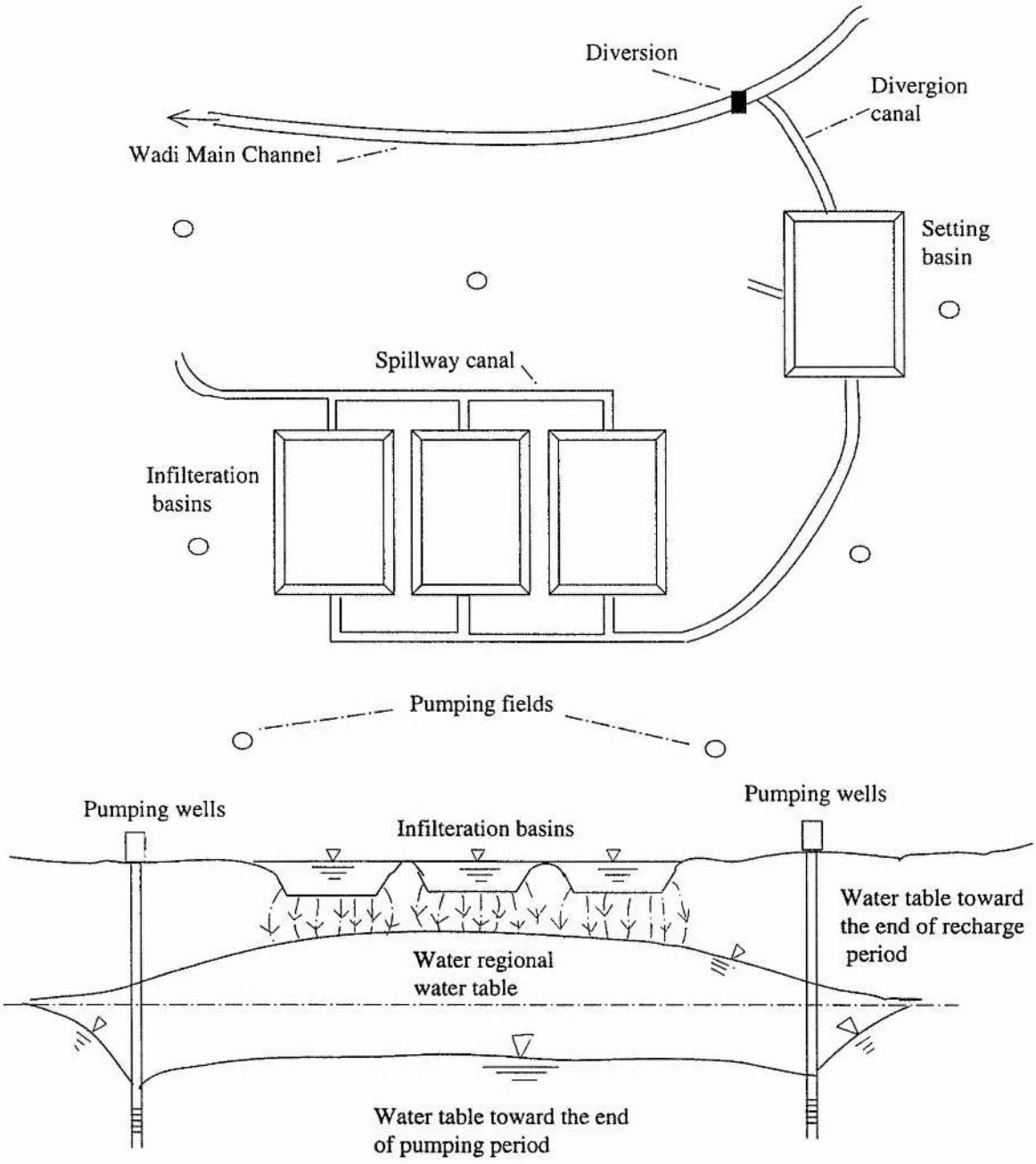

Figure 9.10 Schematic plan for suggested artificial recharge by means of an infiltration basin (modified from Bear, 1979). The wells are located at some distance from the infiltration basin to allow for a minimum retention time in the ground before pumping.

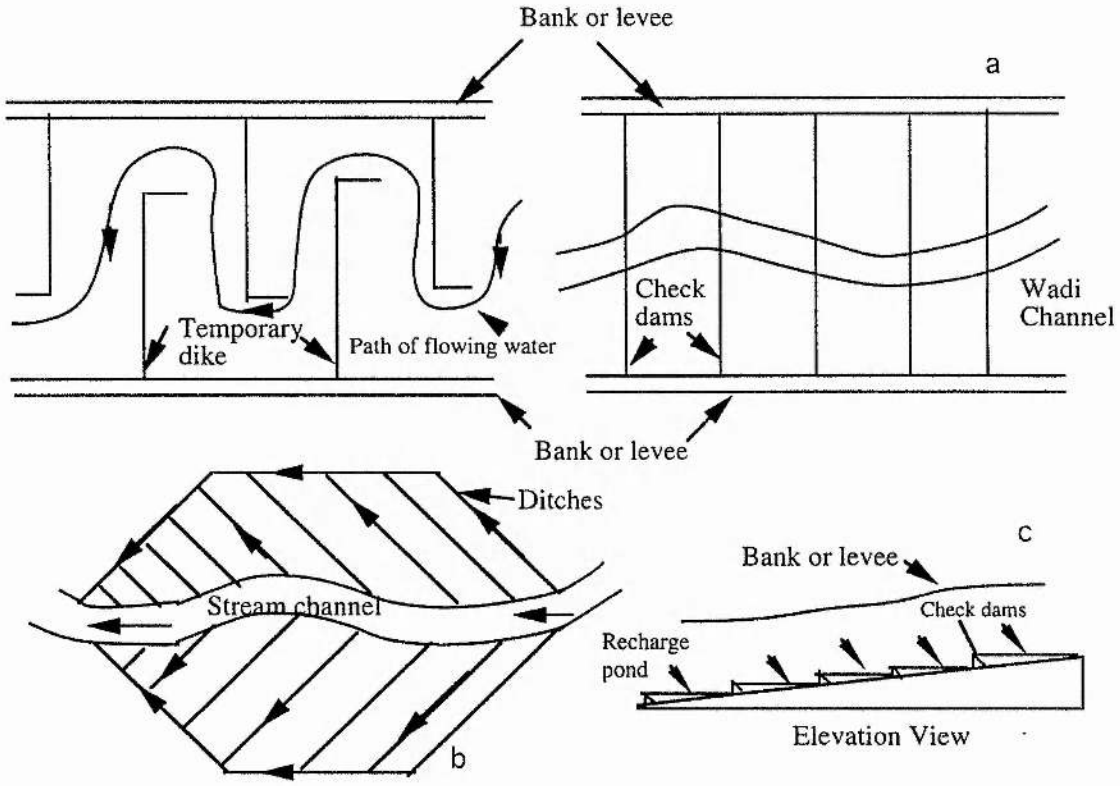

Figure 9.11 Wadi channel modification for artificial recharge using (a) diversions, (b) ditches, (c) check dams (modified from Todd, 1964).

Recharge basins for groundwater can be demonstrated by the Leaky-Acres project in Fresno, California. This project consists of 47.4 ha of surface area (Nightingale *et al.*, 1973). It is divided into 10 basins to replenish the groundwater, which is overdrawn by pumping for municipal water supply. The water source for the project is the King River, which is diverted to the basins through an irrigation canal. The average infiltration rate is 0.12 m/day. Bouwer (1978) indicated that 32.8 m/year is the long term infiltration while the total annual recharge volume is 15.6×10^6 m^3 for the entire project.

9.1.3.1.3 Artificial Recharge by Well Injection

Artificial recharge using well injection (Figure 9.12) is required when the aquifer is situated at some depth below the ground surface and overlain by a semi-pervious layer with large resistance against vertical water movement (see Figure 9.9). in this case surface spreading recharge is not appropriate. However, injection wells can be used in unconfined aquifers where small areas are available for surface spreading.

The most important factor to be considered in using injection wells is the danger of pore clogging, primarily caused by an entrance rate into the aquifer which is one to two orders of magnitude higher than that with spreading ditches (Huisman *et al.* 1983). Such problems (clogging) could be avoiding by storing the flood water in the upstream dam for enough time to permit the suspended material to settle.

The main causes for clogging in injection wells are the presence of air bubbles in the recharge water.

Air bubbles may be entrained during injection due to the free fall of the water when the injection pipe ends some distance above the water level in the well casing. The air may then come out of solution when the water pressure drops below atmospheric. The entrapment of air can easily be prevented by carrying the supply pipe some distance below the water level in the well (Huisman *et al.* 1983). Suspended sediment may be washed into the pores of the aquifer, blocking passageways through which the water

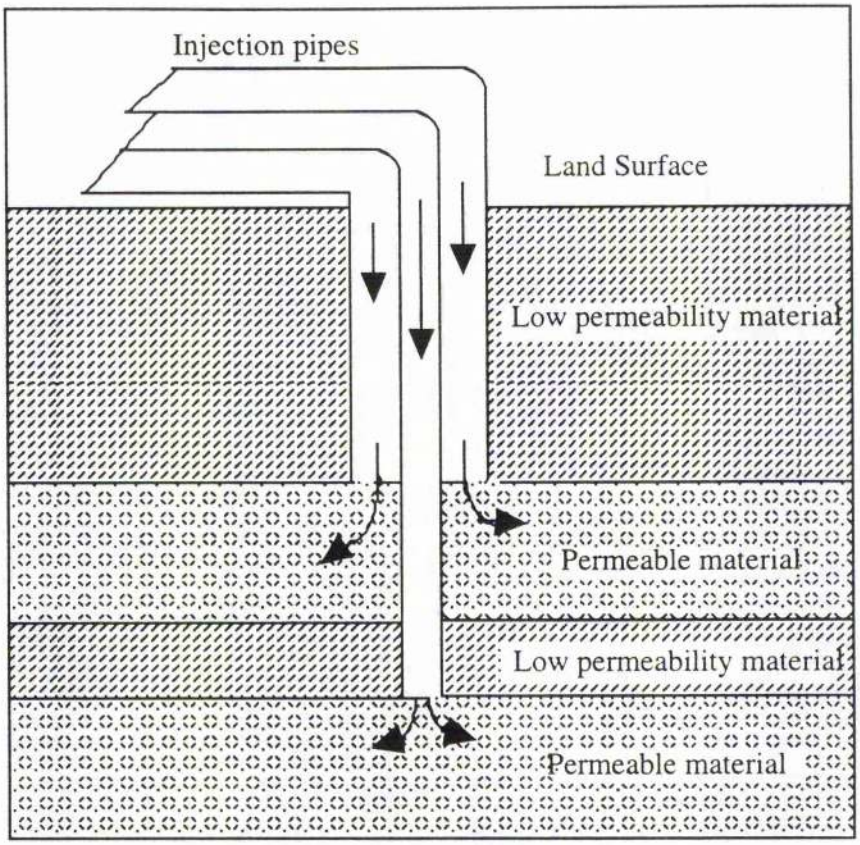

Figure 9.12a Schematic diagram showing multiaqufer recharge well (modified from Pettyjohn, 1981).

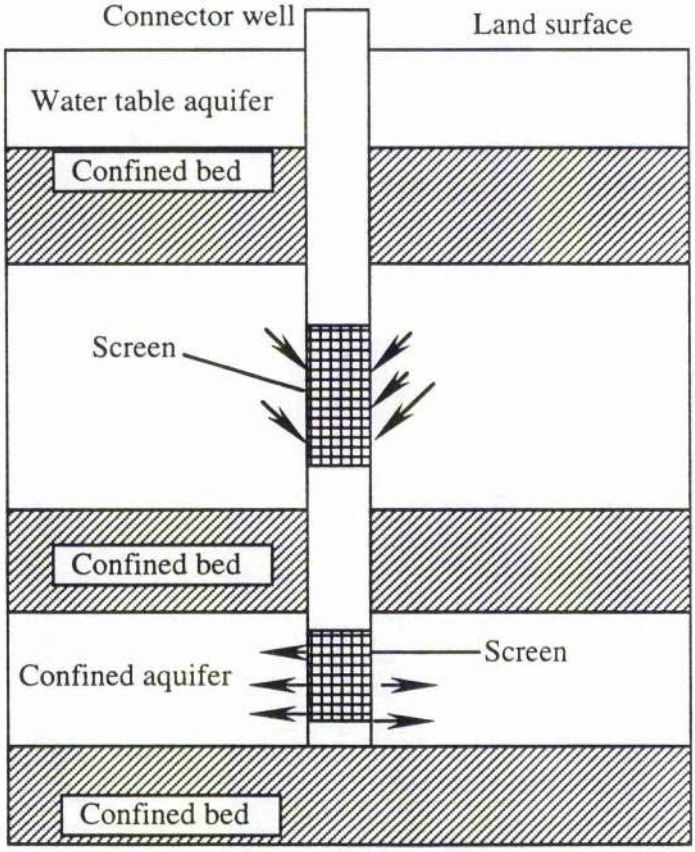

Figure 9.12b Connector well use in aquifer recharge where water flows from aquifer of greater potentiometric head to aquifer of lesser potentiometeric head (modified from Watkins, 1977).

needs to travel. Neither of these factors has significant effect on coarse, permeable aquifers (Oaksford, 1985).

The case study of El Paso, Texas shows a typical example for the well injection method. El Paso, Texas, is located in an arid area with a water supply problem. Water is not abundant in the region, with the annual rainfall averaging about 200mm (Knorr, 1985). Recharging of the Hueco Bolson aquifer is accomplished through injection wells. This injection project gives 10mgd (38,000 m^3/day) of recharge for the potable water supply.

The sedimentary deposit throughout the injection interval is fluvial and contains gravel, silt and clay lenses. The horizontal permeability of the recharge level averages about 8133 l/day/m^2 with a porosity averaging about 20%. The coefficient of transmissibility is about 1242 m^3/day/m and the specific yield is about 10%. The average well injection rate is planned to rise to 700gpm (Daniel *et al.* 1985).

9.1.4 Factors Affecting Infiltration

The common factors that affect infiltration are the hydraulic conductivity of the surface layer, the presence of soil gases in the non-saturated zone and the changes in the soil structure during infiltration (Todd, 1980).

During spreading operations the water contains suspended solids which may clog the soil with silt or mud near the surface. Water containing less than 1000 mg/l of suspended solids is generally acceptable for spreading (United Nations, 1975).

Bear (1979) explained that the surface spreading methods are recommended when the maintenance of high infiltration rates is economically feasible. Depending on the soil type, the infiltration shows various rates.

Gravel:	3-15 m/day
Gravel and sand:	3 m/day
Fine sand and sandstone:	2 m/day
Sand and silt:	0.5 m/day

These infiltration rates represent initial values because, as infiltration continues through an artificial recharge basin, the base gradually becomes clogged (Figure 9.13).

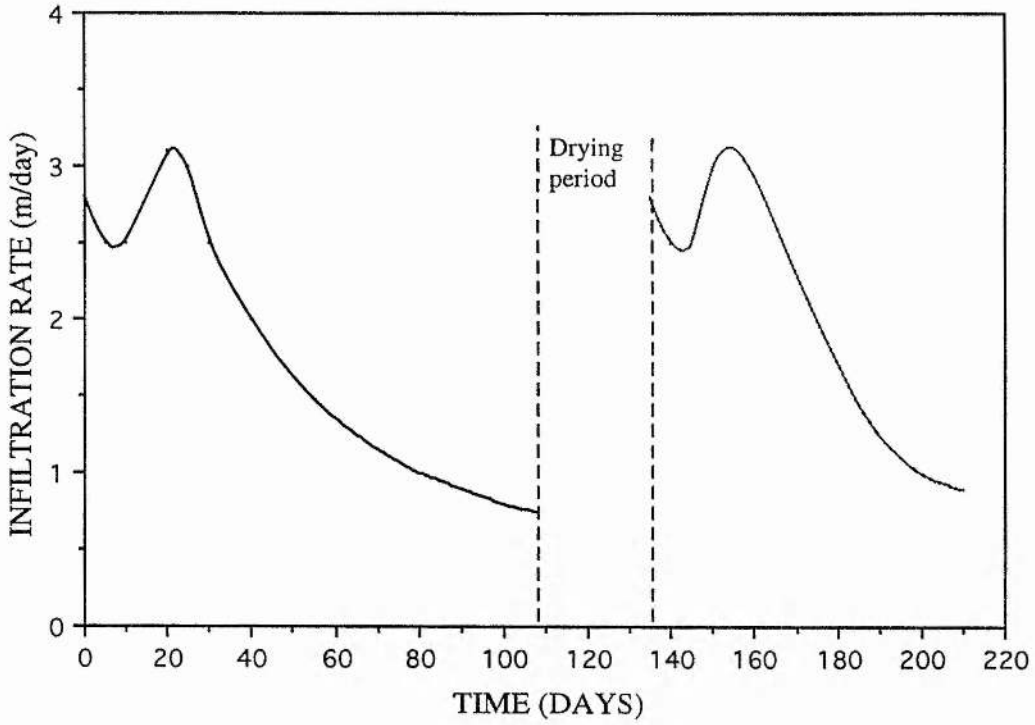

Figure 9.13 Infiltration rate variation with time, after Bear, 1979. The drying period shows that the reduction in infiltration occurs because of the dispersion and swelling of soil particles after wetting. The drying period zone after the reduction in infiltration rate (exponential form curves) is due to the clogging of the soil pores at the bottom of the basin, which is due to the retention of the suspended soilds (from flash floods). By drying the basin and scrubbing the surface layer, the infiltration rate can be increased almost to its initial value and the basin is then put back to use (Bear 1979).

9.1.4.1 Effect of Particle Size and Distribution

The texture of the surface soil is a starting point for the classification of soil permeability in a groundwater basin. High permeability is very important in site selection. The physical and chemical conditions that control the water transmitting character (permeability of hydraulic conductivity) throughout the period of recharge determine the long term recharge efficiency of a site (Husman, 1983).

The transmission of recharge water through the soil surface is affected by the particle size distribution and the continuity of the pores in the soil, as in aquifers. Generally, high intake rates are associated with soils that consist of coarse grain sizes (sands/gravels; Pettyjohn, 1981).

9.1.4.2 Chemical Composition

The impact of dissolved inorganic chemical constituents on the maintenance and magnitude of recharge rates is dependent upon the chemical quality of the water to be spread. The cations that predominate in natural waters and soils are calcium, magnesium, sodium and potassium. The dispersion of a soil when recharged with a natural water is dependent on a weighted ratio of the cation contents called the Sodium Absorption Ratio or SAR (U.S. Salinity Laboratory Staff, 1954). Potassium is normally not present in large amounts so when most soils come to chemical equilibrium with a water that has an SAR approaching 15, dispersion will begin to affect the structure of the soil and decrease the intake rates.

However, both wadis show SAR values of less than 15, i.e. the soil will not be affected using the groundwater for irrigation (see Chapter 4).

The bicarbonate and carbonate anions can affect the chemical equilibrium by the precipitation of $CaCO_3$ and $MgCO_3$ in the soil, thus increasing the relative amount of Na^+. This is important under irrigation or in recharge where frequent intermittent drying concentrates the solutions in the soil surface. Normally, where flood spreading is carried out over extended periods Ca^{2+} and CO_3^{2-} concentrations will be in equilibrium with the water being spread (U.S. Salinity Laboratory Staff, 1954).

9.1.4.3 Effect of Clogging

Continued downward water flow through any soil provides internal transport of suspended matter as well as any dissolved matter. Particle movement can result only in a progressive decrease in the size continuity and number of larger water-transmitting pores in a soil profile. The most significant source of fine particles is the suspended load of the recharge flood waters.

Surface maintenance of the spreading basins breaks down the aggregates and keeps the pore spaces open in the recharge area.

9.1.4.4 Flow of Water and Air in Soils

In general, water movement in the vadose zone ignores the effects of air in the pores. It is assumed that air in the vadose zone is displaced without viscous resistance so that it can escape. However, Bianchi and Haskell (1968) noted that, in the field, the infiltration rate is reduced significantly when the air flow is impeded by the presence of lateral obstructions, or impervious layers in unconfined aquifers.

In the case of unsaturated flow, Oaksford (1985) indicated that hydraulic conductivity in a fine-grained medium does not decrease as rapidly with increasing soil tension as it does in a coarse medium. Although a coarse medium may be more conductive under saturated conditions than a fined-grained medium, a fine-grained medium may transmit more water under certain unsaturated conditions. The conductive, coarse medium, if located in a profile of fine-grained material, will, under certain unsaturated conditions, actually impede flow until enough water has accumulated to fill its relatively large pores through which most flow takes place.

9.1.4.5 Turbidity

Turbidity is a measurement of the amount of suspended material in the water. Based on experience in California (Nightingale and Bianchi, 1977), it is suggested that the upper limit of turbidity at which no recharge should be carried out is 75 NTU (nephelometric turbidity units). Using this criterion, it was established that recharge could commence about 21 days after receipt of water in a reservoir after a flood event.

9.1.5 Recharge Conditions in Both Wadis

The geological and hydrological studies of both wadis have been presented in previous chapters of the thesis. These introduced the examination of the rainfall-runoff season, the groundwater flow system and the structure of wadi deposits.

9.1.5.1 A Rainfall Runoff Season

Wadi Baysh is characterised by rainfall during all four seasons while in Wadi Habawnah, although there are flows in the winter and the spring, there is no runoff during the rest of the year. The rainfall runoff volumes differ greatly in the two wadis. Both have high rainfall runoffs in the spring. In April, the Wadi Baysh record shows 195mcm of rainfall and 13mcm of runoff while in Wadi Habawnah there is 149mcm of rainfall and 11.7mcm of runoff. During the summer and autumn there is no rain in Wadi Habawnah, while in Wadi Baysh, August has the highest rainfall and runoff volume of the summer season (139mcm and 8.9mcm, respectively). The autumn is characterised by low rainfall and runoff volumes of 70mcm and 4.8mcm, respectively.

Recharge from local rainfall is the sole replenishment of the natural fresh water resource. The evaporation rate per year exceeds the rainfall in the lower part of Wadi Baysh (3330 mm/y evaporation and 150 mm/y rainfall while Wadi Habawnah shows 3400 mm evaporation and 40 mm rainfall; see Chapter 3). Most recharge results from the infiltration of runoff that collects in the main wadi channel, averaging of 75 and 10 mcm for Wadi Baysh and Wadi Habawnah respectively from rainfall events of more than 350 mm/y in Wadi Baysh and 150 mm/y in Wadi Habawnah.

The characteristics of both wadis are summarised in Table 3.17. Both wadi basins show a good average hydraulic conductivity of 1.6 m/h, (Chapter 4). In Wadi Baysh, the infiltration area (the area of the main wadi channel) is approximately 45 km^2 while in Wadi Habawnah it is smaller (27 km^2).

The upper parts of both wadis are characterised by the low dissolved solids concentration (<600mg/l in Wadi Baysh and <1400mg/l in Wadi Habawnah). The lower parts of both wadis show higher concentrations, 600mg/l to 3800mg/l in Wadi Baysh and 1400mg/l to <3500mg/l in Wadi Habawnah (see Figure 4.36). The total dissolved solids

concentrations are generally lower in the aquifer of the upper parts of both wadis and increase with distance downstream.

9.1.5.2 Groundwater Flow System

Depth to the water table varies throughout both wadis, but is greater in the lower parts. Depth to the water in the recharge area is typically 3 to 5m and increases basinward to 8 to 23m. This increase in water depth towards the lower parts of the wadis is influenced by well pumping rates and the irregularity of floodwater delivery (see Chapters 3 and 5). The hydraulic gradient of the water table resembles that of the land surface, but is somewhat gentler. Groundwater moves perpendicular to the mountain front and toward the lower part of the wadi, where it either discharges or blends with the existing underflow. Groundwater velocities are of the order of few metres to a few tens of metres per year. Velocities are generally greater near the mountain fronts, where gradients are steeper and permeabilities are higher than those in the interior of the basins (see Chapters 5 and 8). Groundwater generally occurs in the unconfined aquifers, but semiconfined to confined aquifers exist where there are extensive, fine-grained facies of fill deposits of the lower parts of both wadis (see Chapter 8). Aquifers, some of which discharge more than 576 m^3/day as unconfined types and 1000 m^3/day as confined from, are found extensively in the eastern part of Wadi Habawnah and the southwestern part of Wadi Baysh.

Groundwater is recharged to the alluvial aquifer as (1) infiltration of precipitation and runoff along mountain fronts (mountain front recharge); (2) infiltration along the wadi channels that generally traverse the central axis of basins (basin-centre recharge) and (3) underflow from the wadi tributaries from higher altitude. Of the above three modes of recharge, mountain front recharge and the infiltration along the wadi channel account for most of the groundwater in storage. Mountain front recharge occurs within an indeterminate zone that begins in the hardrock-alluvium contact and extends into the lower part of the wadi. A large part of the recharge occurs in the coarse grained wadi deposits that drain the mountains.

The infiltration along the wadi channel recharges the wadi aquifers and for this the lower parts of both wadis depend on flood water infiltration directly into the alluvium.

Underflow of groundwater from the wadi tributaries at higher altitudes contributes to the recharge of several sections of the main channel in both wadis. Underflow from Wadi Thar in the northern part and from Wadi Sayhan in the western part contribute to the recharge of Wadi Habawnah. Likewise Wadi Qura and Wadi Shahdan contribute to recharge of the Wadi Baysh groundwater.

Groundwater discharge from both wadis occurs through (1) discharge to the wadi by way of springs (Fatyhah village and 2km north east of Mislyah village); (2) evapotranspiration from the area where the water table is shallow and (3) groundwater pumping.

Groundwater discharged from underflows moves down Wadi Qura and Wadi Baysh (Fatyhah village) and exits through a narrow alluvium filled gap between the mountains. In Wadi Habawnah, the pumping is now the dominant discharge mechanism. Over a period of 20 years pumping has lowered stable water levels by 12 to 20m near Al Hausaniah (Wadi Habawnah) and Well No GO (Wadi Baysh), respectively (see Table 6.18). The groundwater hydrology of the aquifers in both wadis is summarised in Figure 9.14.

9.1.5.3 Structure of Wadi Deposits

In the upper reaches, wadi channels are well defined. However, in the lower reaches, as the valley bottom widens and channel slope is reduced, wide alluvial channels develop and the courses of the active channels may change significantly from one flood event to another.

The wadi channels have been filled with sediments deposited by flooding streams. A significant decrease in slope occurs between the upper and lower parts of the wadi floor. The depositional environment changes from that of a rapidly moving stream to that of slow flow in the lower part of the wadi basins course. Sediment is deposited in the relatively flat, lower valley floor. In the latter the deposits change texture with depth, fine

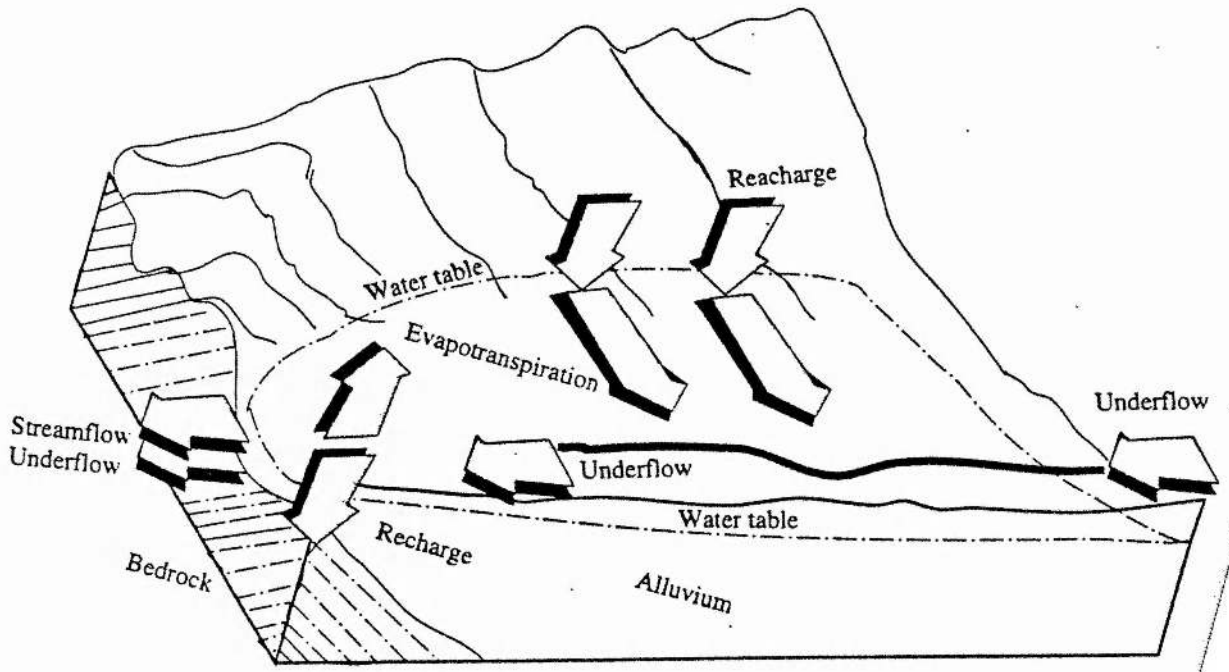

Figure 9.14 Diagram to show the recharge, movement, and discharge of groundwater.

impermeable layers occurring at several positions and serving to confine the groundwater system (Figures 8.3a, 8.4a and 8.5)

The lower parts of both wadis are characterised by eolian deposits, which are graded granular deposits of rock and soil material transported and deposited by windblown dunes which are significant near the Red Sea coast in Wadi Baysh and towards the Empty Quarter Desert in Wadi Habawnah. The sands may serve very effectively for recharging aquifers in both wadis, but the sand dunes are located at the end of the hydrological channel system and rarely receive surface waters.

9.1.5.4 Infiltration Field Tests

Since surface water becomes groundwater either naturally or through infiltration at artificial recharge basins or injection wells, identification of permeable soil profiles and site selection is extremely important.

The double-ring system introduced by Johnson (1963) has been used in both wadis for the measurements of relative vertical infiltration rates (Figures 9.15 and 9.16). The double-ring is an artificial method which introduces the construction of small experimental ponds on the dry bed of a wadi channel. A steel cylindrical tube 30 cm in diameter is inserted in the soil with another of 60 cm diameter inserted concentrically around it. The large diameter tube is used to act as a buffer to reduce undesirable lateral flow and to force the flow vertically downward. During the measurements, both tubes are flooded continuously with water. The amount of water required to maintain a constant head within the inner ring and the time required to achieve this condition are measured. Several readings of the volume of infiltration water and the corresponding times are made until a nearly steady state is reached. Such tests were carried out at several sites along the main channels in the upper, middle and lower parts of both wadis to establish the range of infiltration characteristics of the surface soils. In all, a total of 12 infiltration tests were performed, 6 in each wadi (Figures 9.17 and 9.18). The infiltration site numbers were designated first with the letter F followed by the initial letter of the wadi and the section of the wadi, and then each site is numbered insequence from upstream to downstream

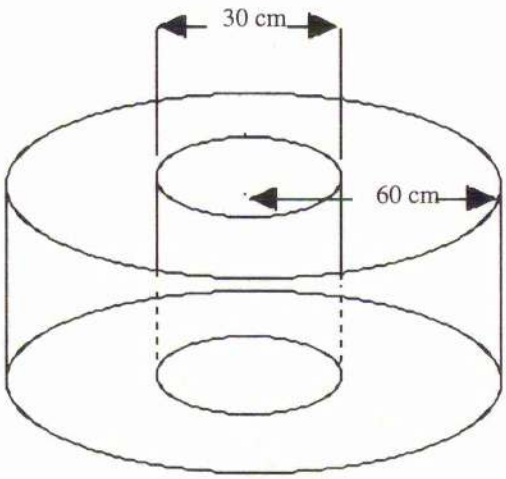

Figure 9.15 Sketch for double - ring system (30 and 60 cm diameter) as used in both wadis for comparison and measuring of relative vertical infiltration rates

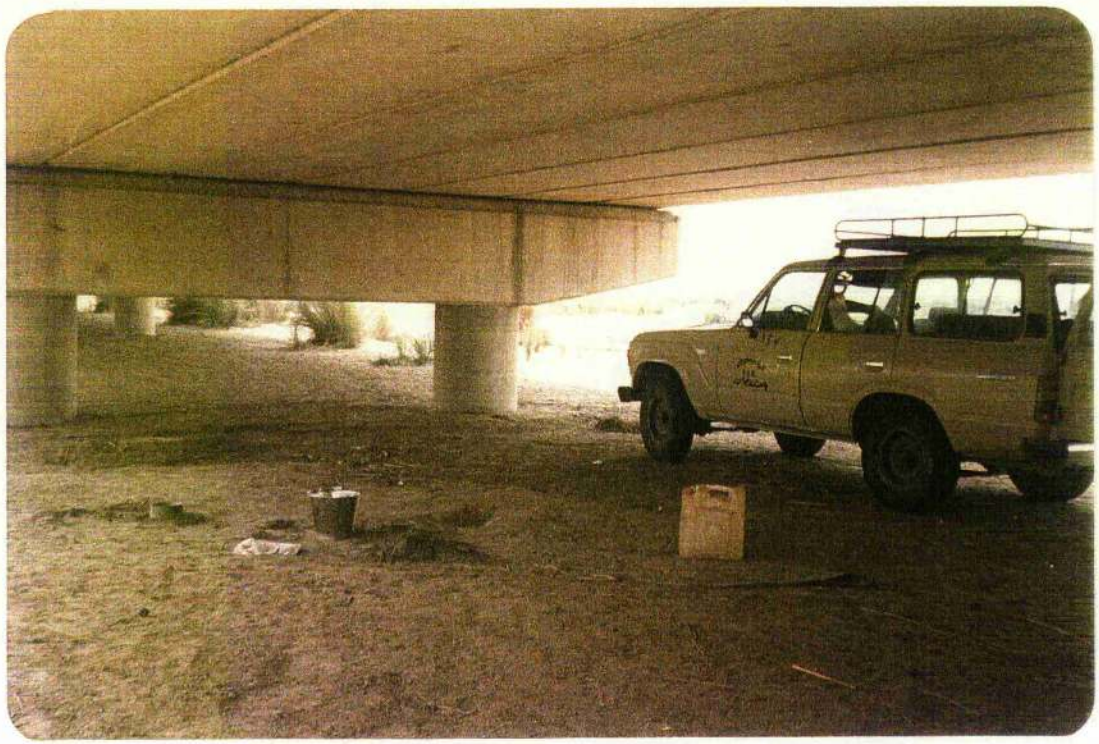

Figure 9.16 Infiltration field test station FBM4 under Wadi Baysh Bridge showing the double ring instrumentation.

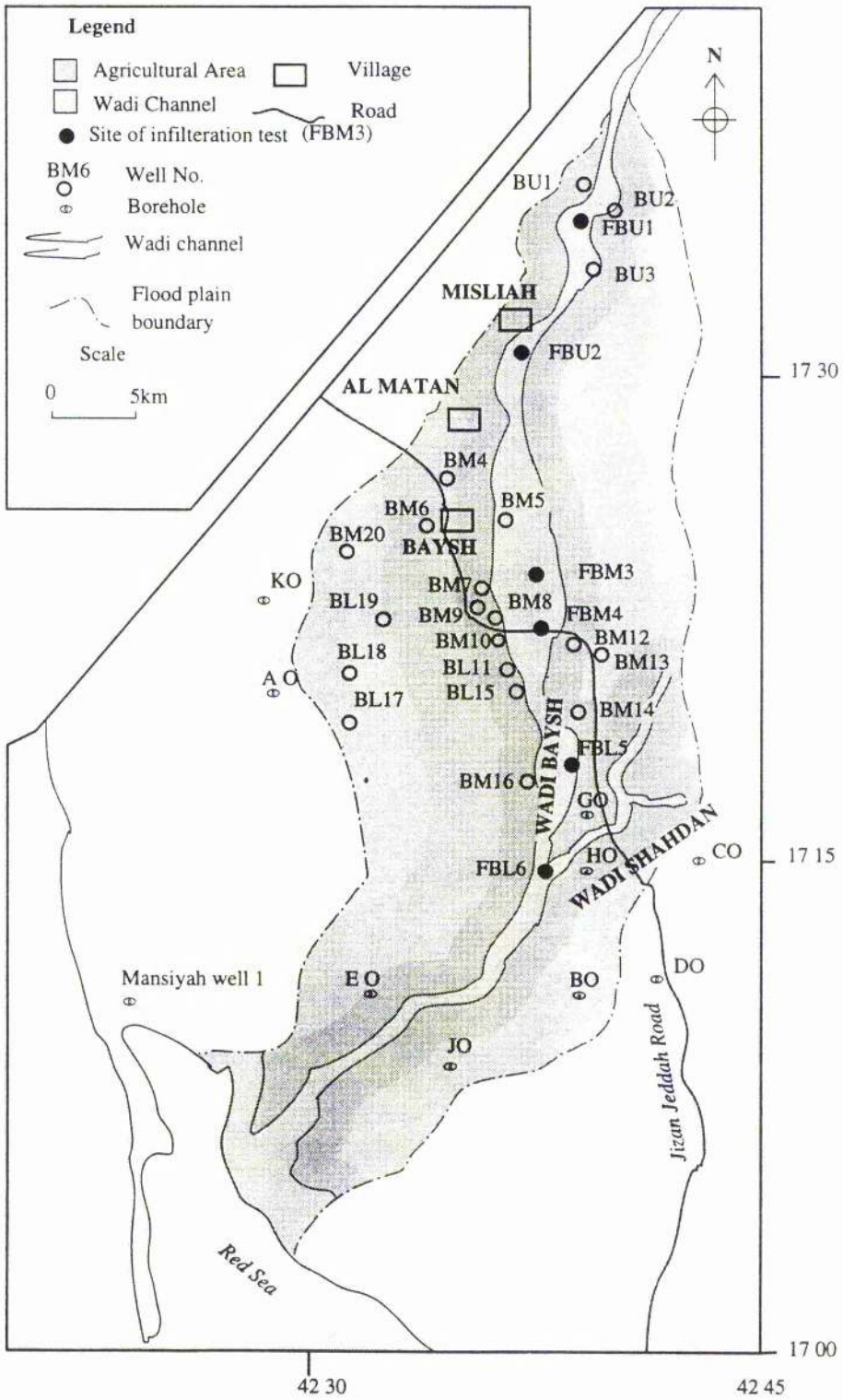

Figure 9.17 Location map of Wadi Baysh wells and infiltration tests.

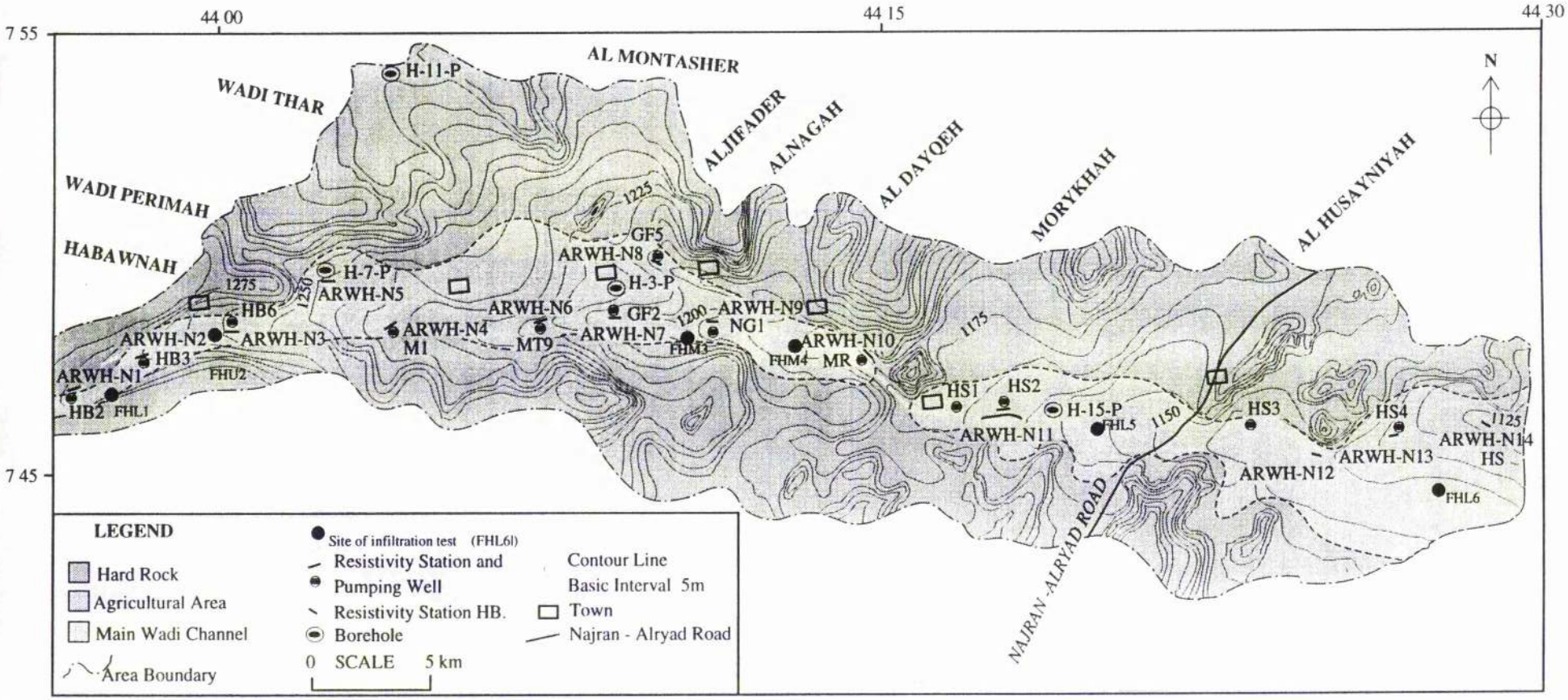

Figure 9.18 Location map of Infiltration tests in Wadi Habawnah.

as following: Wadi Baysh (FBU1, FBM5, FBL8) and Wadi Habawnah (FHU1, FHM5, FHL8).

9.1.5.4.1 Infiltration Data Interpretation

The point infiltration rates measured are expressed in cm/h in Figures 9.19 and 9.20 for Wadi Baysh and Habawnah, respectively. The rates at each site decrease with time after the maximum initial infiltration values. The infiltration curves vary greatly for each wadi. In Wadi Baysh, the infiltration ranged between 0.053 and 0.3 cm/min while the infiltration rate of Wadi Habawnah ranged between 0.021 and 0.23 cm/min with an average of 0.132 cm/min. However, the average value can be used for each wadi for artificial recharge evaluation.

9.1.6 Isopotential Contour Line

The Isopotential contour line maps are drawn on the basis of sixty points of water level measurements in Wadi Habawnah and twenty points in Wadi Baysh in addition to the resistivity measurements (chapter 6) and throughout these data points the contours were constructed assuming a linear hydraulic gradient between them (Figures 9.21). The direction of the underground flow is roughly parallel to the wadi beds; i.e. a general direction from NE to SW for Wadi Baysh (from the foothills toward the Red Sea) and from W to E for Wadi Habawnah (from the highlands toward the Al Rub Al Khali desert). The contour maps of both wadis show that the slope of the water table is influenced by the wadis. The piezometric gradient of Wadi Habawnah varies from 17m per km in the upper part to 6m per km in the lower part of the wadi while in Wadi Baysh it varies from 20m per km in the upper part to 2m per km in the lower part of the wadi. Both wadis show a steep gradient in the upper part of the wadi. The depth to the water table in the upper part of both wadis shows a variation of 4 to 6 metres below the surface while in the lower parts the depth reaches 15 to 23 metres.

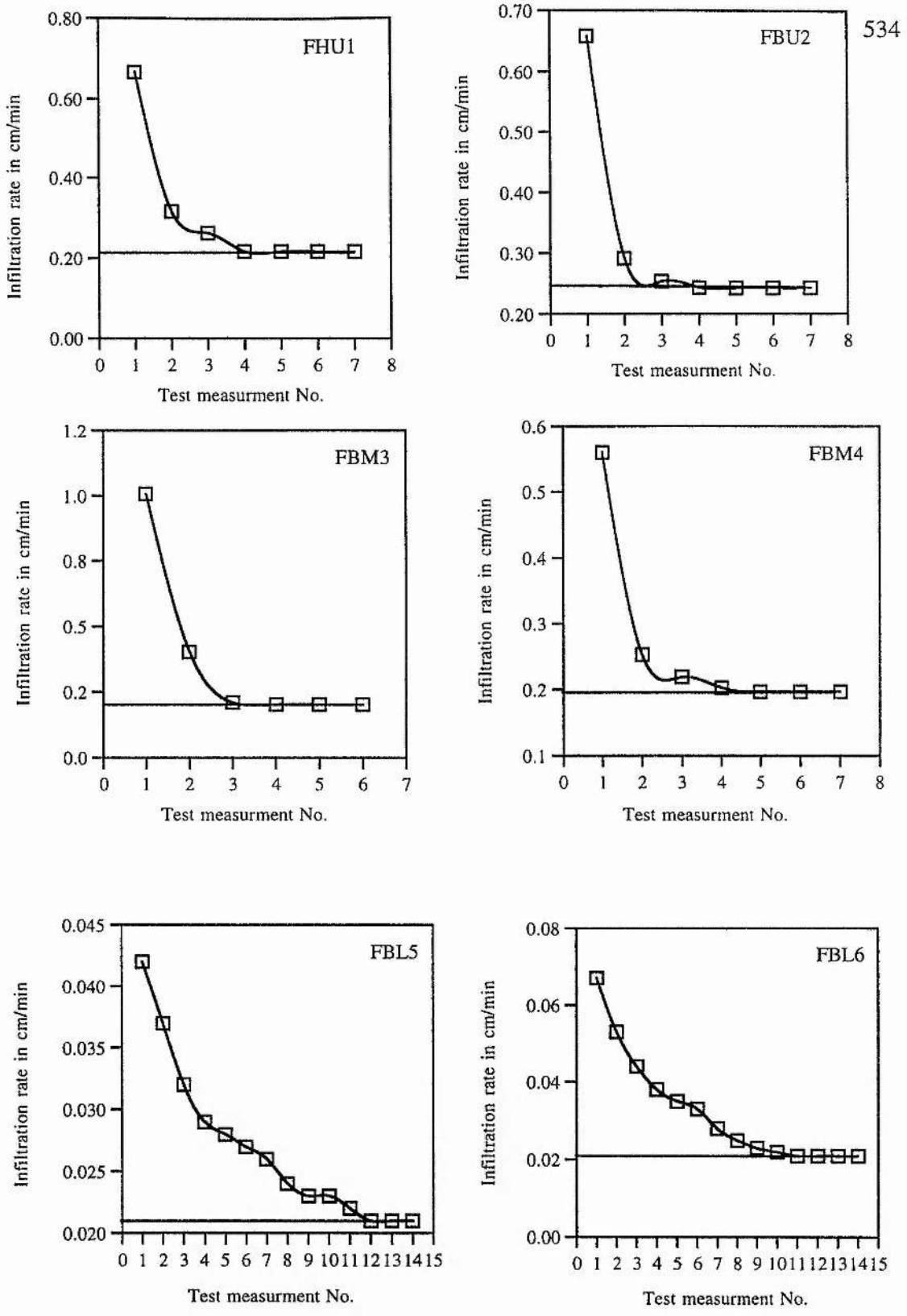

Figure 9.19 Measuremient of infiltration curves along Wadi Baysh main channels (Figure 9.17)

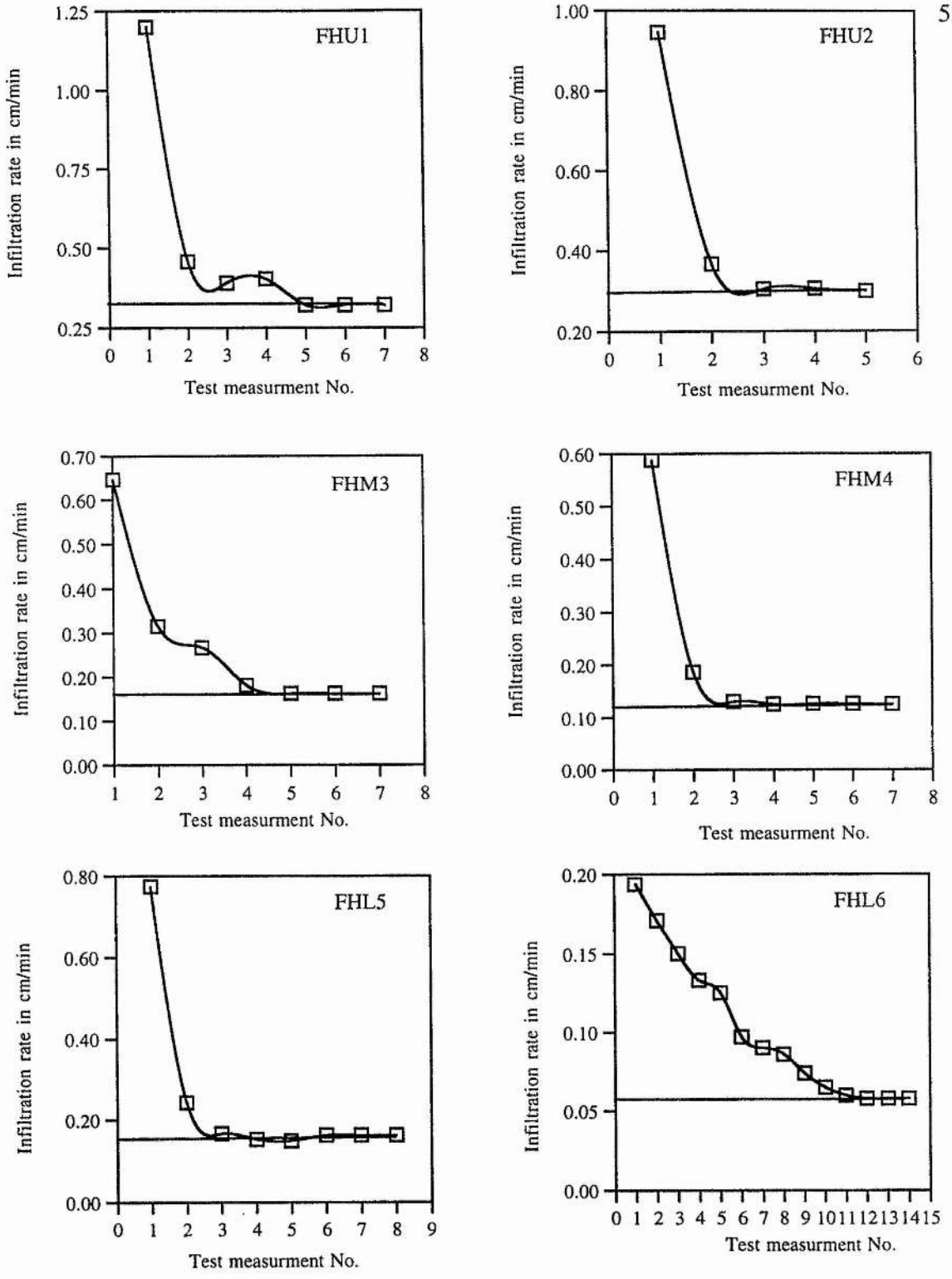

Figure 9.20 Measurement of infiltration curves along Wadi Habawnah main channels (Figure 9.18)

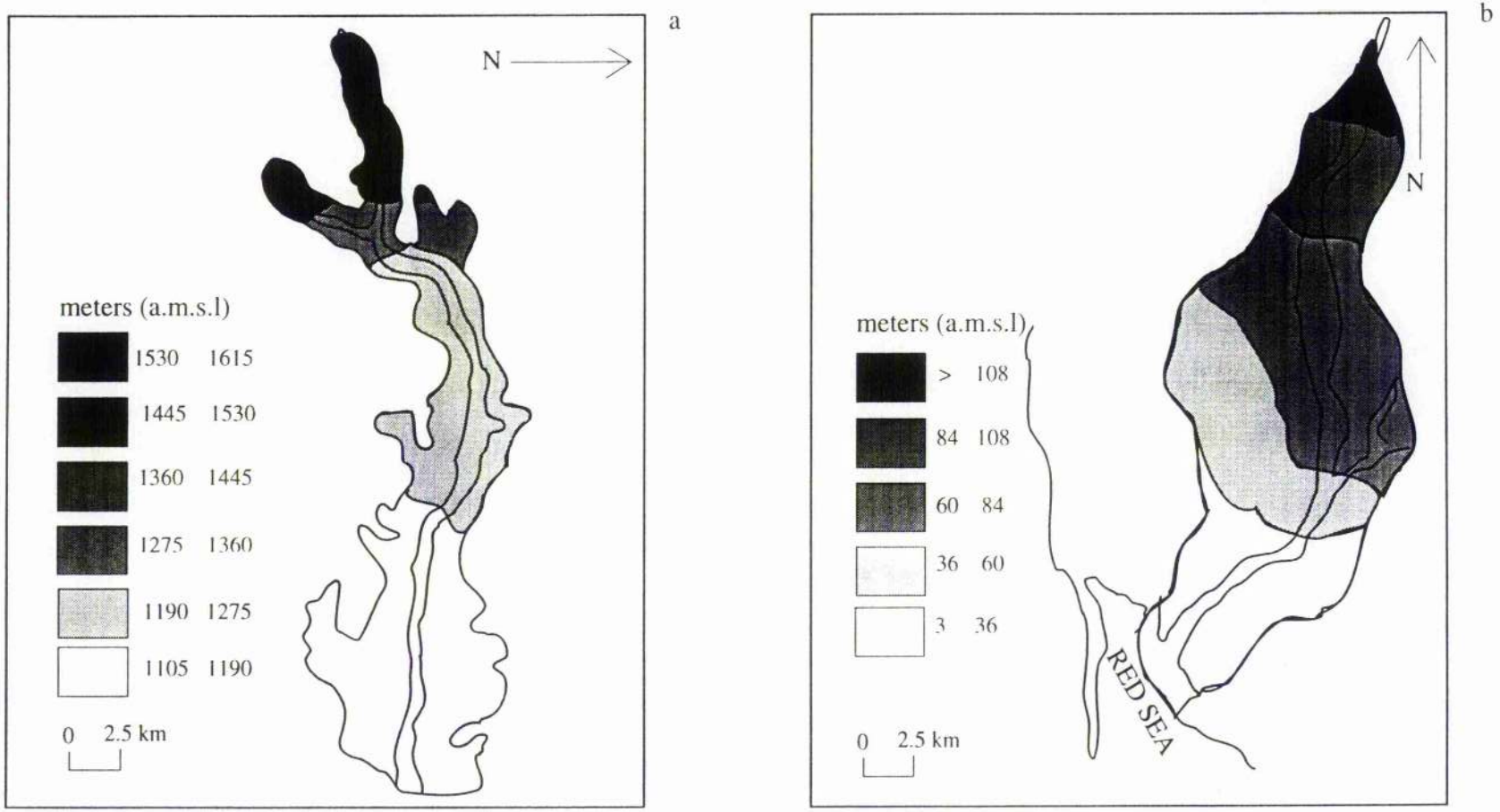

Figure 9.21 Isopotential contour map of Wadi Habawnah (a) and Wadi Baysh (b) groundwater

There is no record of water level measurements to show a seasonal pattern of fluctuation. However, the farmer interviews indicate that the water level reaches 2 to 3m below the surface during the flood season.

Figure 9.22 shows distribution maps of the floor sediments of Wadi Baysh and Wadi Habawnah. In Wadi Baysh, the sediment thickness varies between less than 16m in the upper part to 48m in the central sectors 112m in the lower wadi.

The Wadi Habawnah sediments have a range of thicknesses between 4 and 19m in the upper part while in the middle the sediment thickness range is between 19 and 34m (Figure 9.22). In the lower wadi, the sediments reach a thickness of more than 34m. However, the well inventory shows a thickness of 50 near the Hausaniah bridge.

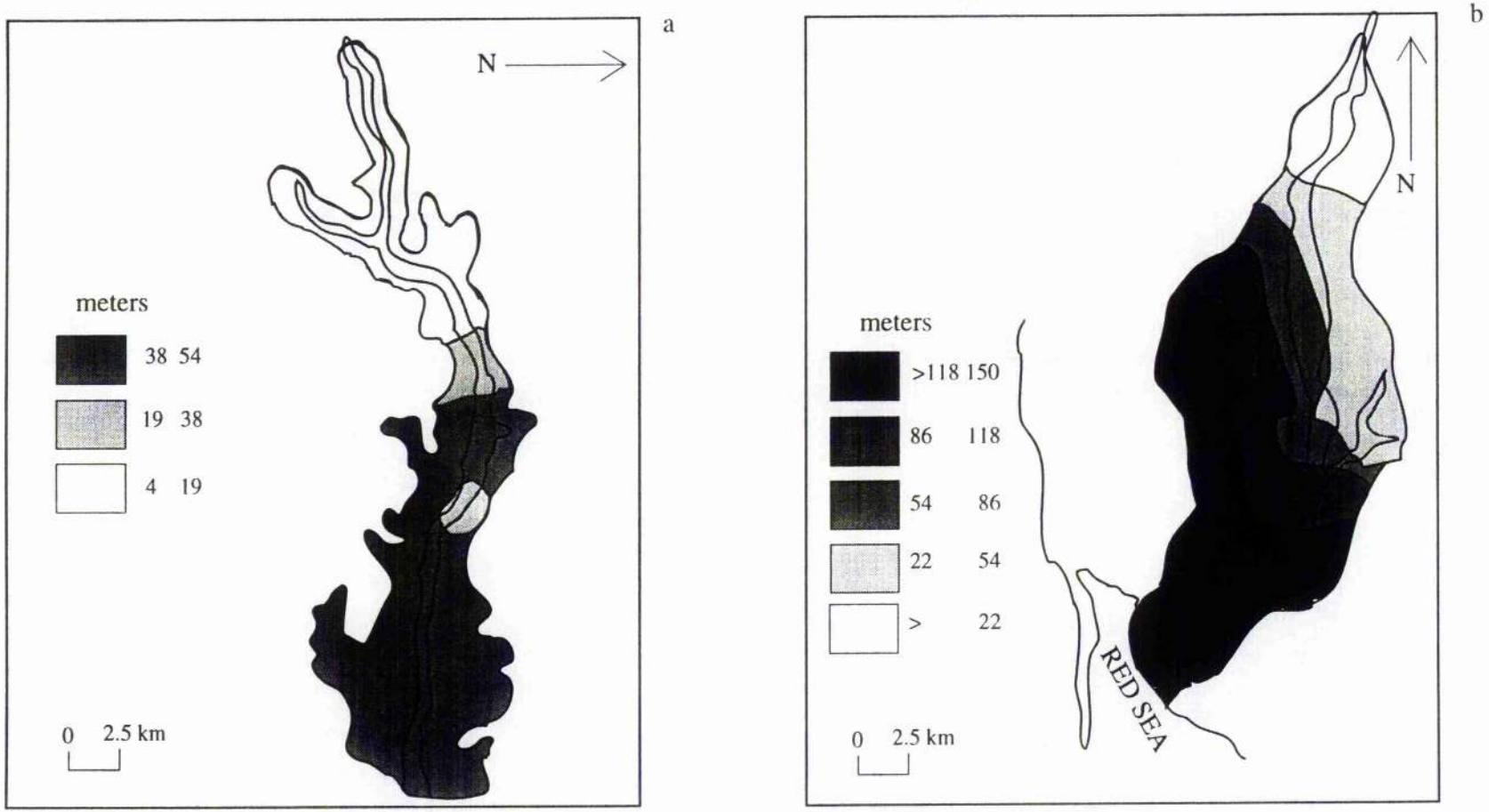

Figure 9.22 Map showing thickness variation of Wadi Habawnah (a) and Wadi Baysh (A) aquifers

9.2 Section Two: Conjunctive Use Management of Water Resources

9.2.1 Introduction

Groundwater has an important role in agricultural systems in arid and semi-arid wadis where the water availability fluctuates. As more and more users are competing for limited quantities of water, water management is being recognised as a need that must be addressed.

Integrating the groundwater and the flood water during the wet season in conjunctive use will help to provide efficient management. Conjunctive use is the co-ordinated and planned operation of both surface and ground water supplies to meet water requirements while also conserving water (Todd, 1980). Dracup (1970) states that the greatest potential for conjunctive use management lies in alleviating the problems associated with hydrological uncertainty: utilising the underground storage capacity of an aquifer for containing artificially recharged surface water during wet periods to provide adequate water supplies during dry periods.

The water resources have long been neglected in both wadis. The increasing demand has now largely changed the traditional concept to include the conjunctive operation of dams and aquifers as resources.

The water resources (the groundwater and flood water of both wadis) can be planned to increase the efficient use of water by determining the most desirable guidelines for water utilisation. Accordingly, proper use of recharge of flood waters and the extraction of groundwater will conserve the supplies and provide for the maximisation of the economic returns from the use of water for irrigation.

With a system consisting of a dam and an aquifer a hydrological study (see Chapter 3), could provide detail to enable:

1- The determination of the dam capacity

2- The determination of the area that can be served by the system.

3- The range of the draft from the reservoir and the water volume that could be pumped from the aquifer.

The flood waters and groundwater studied in previous chapters have been analysed to determine the amount of surface storage that can be provided and to establish a pattern for allocating the available water to surface and subsurface storage. In this section, the water budget model of the surface reservoir and the aquifer will be discussed for both wadis.

The valid of resources depends on the correct identification of the hydrological cycle components which are important to water balance computations for surface waters and aquifers.

Most practising hydrogeologists consider the policy that, in any year, abstraction should not exceed replenishment. In other words, if the demand exceeds the amount of replenishment by either natural or artificial means, the groundwater level would be lowered. The perennial yield concept of management practice is based on the theoretical annual quantity which replenishes the aquifer.

Four states of groundwater resources development were recognised by Jones (1972) in groundwater balance computations (Table 9.1).

Table 9.1 Development and management of water resources

State of development		State of resource	Management state
1st	Youth	$I_n > O_a + O_n$	Unappreciated but desirable
2st	Maturity	$I_n = O_a + O_n$	Necessary
3st	Old age	$I_n < O_a + O_n$	Essential
4st	Rejuvenation	$I_n + I_a = O_a + O_n$	Essential

where I_n = natural input, I_a = Artificial input, O_n = natural output and O_a = Artificial output.

These management policies determine the importance of the degree of management practice. The above criteria were considered in this study to assess the status of groundwater development in the two wadis and to recognise the form of the management practice that may be required for to maintain the use of the present groundwater and flood water in the area.

In any area, the hydrological cycle components control both the natural and artificial flow of groundwater in the basin. The water balance depends mainly on the recharge and discharge storage calculation, which can be expressed as follows:

Recharge = Discharge + Change in permanent groundwater storage.

The very important components of the recharge area in both wadis can be assumed as follows:

Groundwater replenishment

1 Infiltration

2 Underground Flow

Groundwater Discharge

1 Evaporation

2 Subsurface outflow to the wadi channel

3 Artificial withdrawal by Pumping

9.2.2 Groundwater Replenishment

9.2.2.1 Infiltration

Channel transmission loss is seen as flow reduction, which takes place when the flood flows occur in normally dry stream beds. Lane (1983) indicated that the transmission loss reduces the volume of runoff progressively at points downstream along the channel. The wadi floors are filled with porous alluvial deposits into which water infiltrates readily. Both wadis are characterised by permeable material with an average of 1.6 m/hr of hydraulic conductivity based on the pumping test analyses (see Chapter 5), which suggests that conditions for surface recharge are favourable. In Wadi Habawnah, the groundwater recharge as channel transmission losses from the monthly records have been determined (see Table 3.21). The average annual recharge is approximately equal to 3mcm. However, in Wadi Baysh, the average annual recharge about 31% of the average annual flood volume (see Chapter 3), which is equal to 21mcm.

9.2.2.2 Underground Flow

The amount of groundwater that enters the lower part of Wadi Baysh and Wadi Habawnah as under flow through the unconsolidated wadi fill near the Baysh Bridge and Al Montacher, respectively, have been estimated as part of the water budget for both wadis. The amount of under flow could not be measured directly, but an estimate has been made using a version of Darcy's Law, Q = KIA, where Q is the amount of water flowing through a selected cross section of the saturated material K, the average hydraulic conductivity of the material is the amount of water in m/day that flows through a cross-sectional area of $1m^2$ under a hydraulic gradient of 1.0 at the prevailing water temperature. I is the hydraulic gradient and A is the area of the saturated cross-section in m^2.

9.2..2.2.1 Wadi Baysh Recharge

The location of the section for which under flow was computed is about 5 km to the west of Wadi Baysh Bridge. The method used in obtaining information needed to determine the under flow area is discussed below.

There are two or three main aquifers as shown in the cross-section FO, KO, AO, GO, HO, CO, and the cross-section FO, KO, AO, EO, JO, BO (see Figures 8.3b and 8.4b, respectively). All the aquifers consist of unconsolidated wadi floor deposits of silty sand, sandy gravel and gravel underlying and bounding the north-western and south-eastern sides of clays in which the hydraulic conductivity is assumed to be very low.

The lithology and extent of the unconsolidated materials that compose the aquifer have been determined from the examination of well lithology data, the study of the grain size analyses, from the well inventory in the area, from geophysical methods including geophysical well logs, a seismic refraction survey and an electrical resistivity survey. Neither the electrical resistivity nor the seismic refraction surveys predicted the presence of thick sections of saturated unconsolidated fill within the upper 30 to 40 m near the Baysh Bridge. The greatest thickness of sand and gravel revealed along the electrical sounding profile was 40 m and lies between well AO and borehole GO. The borehole

lithology is shown in cross-section A-C (Figure 8.1). The materials that compose the unconfined and confined aquifers are represented by cross-section A-A' in Chapter 8 section one.

Water is unconfined in the upper part of the saturated zone, while in the lower part of boreholes CO, GO and EO it is confined by thin discontinuous beds of clay. The confining beds themselves are broken by unconfined aquifers (see borehole JO, EO and GO, section A), and there may be appreciable movement of water between the two types of aquifers.

The quantity of under flow through the saturated unconsolidated wadi fill of Wadi Baysh has been computed at sections A A' and B-B'. Each cross-section was divided into sub-sections on the basis of the presence of the clay layer (see Figures 8.3 and 8.4 in which the unconfined and confined aquifers are identified as A and B, respectively).

The lithological sequences of the central part of the section permit the unconfined and confined aquifers to be recognised independently. However, in both the eastern and western sides of the section the aquifer types are not so readily defined because they are marked by the intersection of the water table and an impermeable layer (clay), which extends beneath BO and JO in the east and between HO and CO in the west. The minimum width of the central section is estimated to be about 12 km (AO-GO-HO, Figure 8.1).

The thickness of the saturated unconfined aquifer in the central part of the section is about 18m at well AO. If 18m is used as an average thickness for the entire 12 km section, the saturated cross-sectional area would be 270,000 m^2 for the minimum width of 12 km. A further figure of 45000 m^2 is added for the remainder of the section giving an estimated 310,000 m^2 for the maximum width of 15 km.

The average hydraulic gradient of the under flow across the section was determined from the nearby well measurements and is about 0.0002 (Chapter 5). The hydraulic conductivity (K) was estimated using pumping test analyses from wells BO, KO, CO and AO. The average hydraulic conductivity was 7 m/day (see Table 8.14).

$$Q = (7 \text{ m/day}) \times (0.002) \times (270{,}000 m^2) = 3780 \ m^3/day$$

Applied to the section of maximum width (B-B^1), the equation yields:

$$Q = (7 \text{ m/day}) \times (0.002) \times (310{,}000 \text{ m}^2) = 4340 \text{ m}^3\text{/day}$$

The quantity of under flow through the clay layer is negligible. The total under flow from Wadi Baysh toward the lower area is, therefore, between 1.38 x 10^6 m^3 a year. and, 1.58 x 10^6 m^3 a year, and it probably averages about 1.48 x 10^6 m^3 a year. In the quantitative assessment of this particular component of groundwater replenishment, the water contour map (Figure 9.21a) plays an important role. This isopotential contour line on the contour map indicates the slope of the water table of the wadis. The hydraulic gradient (i = dh/dI) and the length of equipotential line effectively represents the actual length of the subsurface flow (L). The third parameter is the transmissivity (T) obtained from the analysis of the pumping test data (see Table 5.6). These three parameters are used in the most convenient form of Darcy's Law (Q = T x i x L) to make the assessment. The subsurface flow (Q) = (T_{ave} = 133m^2/day) x (i = 0.0022) x (L = 13000m) =

$$3803 \text{ m}^3\text{/day} = 1.4\text{x}10^6 \text{ m}^3\text{/year}$$

9.2.2.2.2 Wadi Habawnah Recharge

The location of the section for which under flow was computed is about 8 km to the east of Habawnah village and about 0.5 km to the east of Al Montasher village (see Figure 8.2). The quantity of under flow through Wadi Habawnah has been computed at sections A-A^1 of the saturated unconsolidated wadi fill. The aquifer is bounded from both sides by the impermeable layer (hardrock), which extends beneath the section.

The section in Figure 8.6 extends across the wadi. It exhibits a trough shape and is filled with 0 to 35m of unconsolidated sediment, which rests upon the basement complex. The bulk of the wadi floor is underlain by gravels upon which is a layer of sand which has lenses of clay occurring in the centre of the wadi. A layer of gravel buries the sands on the northern side of the wadi.

The average hydraulic gradient of the under flow across the section was estimated at about 0.006. The average hydraulic conductivity (K) was determined using the

pumping test analysis (see Chapter 5), which is equal to the average hydraulic conductivity used (34 m/day; see Table 5.6).

$$Q = (34\ m/day) \times (0.006) \times (11m \times 1000) = 2244\ m^3/day$$

$$= 8x10^5\ m^3/year$$

The subsurface flow (Q) using the isopotential contour line (Figure 9.20b) =

$$(T_{ave} = 415m^2/day) \times (i = 0.006) \times (L = 1000m) = 2490\ m^3/day$$

$$2495\ m^3/day = 9x10^5\ m^3/year$$

Both methods show agreement for estimating the wadi subsurface flows.

9.2.3 Groundwater Discharge

9.2.3.1 Evaporation

The study area is in an arid to semi-arid zone, characterised by hot weather and irregular rainfall. In Wadi Baysh, the average annual rainfall is 500mm for the upper part of the catchment, falling to 165mm on the lower part of the catchment area (station SA-106) and the potential evaporation is 3352mm/y (see Table 3.16). In Wadi Habawnah, the potential evaporation in the lower part of the catchment is 4070mm/y, where is the annual mean of the rainfall is 62mm at station N-223. The upper part of the catchment shows lower evaporation and evapotranspiration, but receives higher rainfall. At Sarat Abidah and Abha, the annual values of potential evaporation range between 1100 and 2678mm/yr and between 177 and 839mm/yr, respectively. The annual rainfall at Sarat Abidah and Abha is 155mm and 175mm, respectively.

The foothills of Wadi Baysh (Malaki station) are characterised by higher values of PE and PT than the station in the lower part of the wadi (SA-106; see Table 3.16), close to the Red Sea. The PE and PT average daily rates for the lower part of Wadi Baysh were determined as 9 and 6mm, while Wadi Habawnah has average daily rates of PE and PT of 11 and 5mm, respectively. However, because of the short duration of most runoff events in both Wadi basins, the author has assumed that the effect of the evaporation on the channel transmission losses is small and insignificant.

9.2.3.2 Subsurface Outflow to the Wadi Channel

Near Baysh Bridge in Wadi Baysh there are surface water flows with an average of 2000 m^3/day flowing towards the south west (field estimation). The author assumed that as a result of the quartzite dyke crossing that part of the wadi channel, about one kilometre to the north of Baysh Bridge (near the outlet of Wadi Quara), such a dike may force the groundwater flow to the surface. However, in Wadi Habawnah, this was not found to be the case during the field study nor was there information indicating that there is subsurface out flow.

Considering the subsurface outflow in the upper part of Wadi Baysh, the total aquifer discharge per year would be equal to 730000 m^3/year.

9.2.3.3 Artificial Withdrawal by Pumping

There are no data available to determine the total pumping flow in both wadis. However, interviews with farmers indicated that the water table level of the Wadi Baysh aquifer fluctuates by about 1m per year while in Wadi Habawnah if varies between 1 and 3m per year.

Assuming there is no regional recharge taking place in both wadis, the annual pumping volume can be estimated as follows:

Annual pumping volume = The water table depth per year x the agricultural area x the specific yield (for further information see section 9.2.7).

It is assumed that the saturated thicknesses decrease by an average of 1m and 2m per year in Wadi Baysh and Wadi Habawnah, respectively and the agricultural areas are 27033 and 11355 ha respectively are known.

An approximation of the total volume of water that was pumped per year from Wadi Baysh and Habawnah would be equal to the product of the specific yield (0.08 and 0.04 respectively) times the agricultural area of each wadi times the average decline of water table level per year.

Accordingly, the annual volumes of pumped water in Wadi Baysh and Wadi Habawnah are about $21x10^6$ m^3 and $9x10^6$ m^3, respectively

9.2.4 Recharge Budget Model of the Aquifer of Both Wadis

The water budget analysis of both main wadi aquifers can be written as:

$$R_V + I_{in} - I_{out} = \pm \Delta S \quad (9.1)$$

where R_V = Recharge from the reservoir, I_{in} = Subsurface inflow, I_{out} = Subsurface outflow (pumping well) and ΔS = Change in the aquifer storage.

9.2.4.1 Surface Reservoir

Water may be drawn from the floods impounded above construction dams by gravity flow. This which is diverted from the drainage channel directly to the point of use, or stored in the aquifer by natural or artificial means and pumped to the surface when needed. Cluff (1985) suggested that, in arid and semi-arid lands, water harvesting systems should be implemented by using compartment reservoirs. Compartment reservoirs keep the water concentrated into a volume with as small a surface area as possible. Evaporation control on the compartment reservoir can be improved by placing an evaporation control barrier such as floating thin polyethylene plastic sheets or concrete slabs made with lightweight aggregate on the surface (Cluff, 1967, 1987).

Topographic conditions may be the governing factor in the adoption of conjunctive use design. There are a few feasible surface reservoir sites in the upper part of both wadis basin. The assumed dams of Wadi Baysh and Wadi Habawnah can be located at the outlet stations SA-124 and N-404, respectively, due to the fact that both outlet stations are below a major part of the catchment area of both wadis. The maximum capacity of the reservoir should be designed to accommodate the 100 year flood (see Table 3.37). Accordingly, the suggested volume of the assumed reservoir would be equal to 70mcm and 42mcm for Wadi Baysh and Wadi Habawnah, respectively.

9.2.4.2 Reservoir Water Budget Model

The reservoir water budget model is based on the concept that no water infiltrates into the ground during flood control. The hydrological components of this model can be expressed as:

$$R = Q_i + P - E - Q_o - Q_s \pm \Delta S \quad (9.2)$$

where $R, Q_i, P, E, Q_o, Q_s, \pm\Delta S$ represent recharge, surface inflow, precipitation, evaporation from the reservoir controlled outflow, over-spilling and change in surface storage. However, flood records for both wadis show a seasonality influence. In Wadi Habawnah, the flood occurs in the spring while in Wadi Baysh it occurs during each season, with each flood lasting for a minimum of one week and a maximum of a month (farmer interview).

The flood flow data are for the period 1970-1985 (15 years) for Wadi Baysh and Wadi Habawnah (see Chapter 3).

Equation 9.2 can be reduced to equation 9.3 due to the following:

1- The precipitation in the lower parts is very low

2- The surface water is not continually flowing and depends totally on the flood water

3- The spillway losses occur only in very rare cases.

$$R = -E + \Delta S \text{ or } R_V = -E\,A_{ave} + \Delta V \text{ (expressed in unit of volume)} \quad (9.3)$$

where R_v is flood volume, A_{ave} is the average water surface area of the reservoir and ΔV is the decrease in the volume of stored water. Equation 9.3 was applied assuming that the flood water was stored for one month before it was released downstream for artificial recharge purposes. Data given in Table 9.2 provide details of the average monthly flood water volume (R_v) in both wadis over a 15 year period (assuming that each month is 30 days). These values are accumulated during a month, which is considered to be the monthly amount of water stored in the assumed reservoir with the corresponding recharge efficiency. The recharge efficiency for each month was calculated as the ratio between the flood volume stored in the reservoir and the net volume before the water release (product of flood volume minus the evaporation during that month). The annual

Table 9.2 Monthly storage data of assumed surface reservoir and artificial recharge flow for both wadis.

WADI HABAWNAH (Average flood volumes (1970-1985))

Month	Stored volume (mcm)	Water surface area (km^2)	PT volume mcm	Recharge volume mcm	Recharge efficiency (%)
DEC	0	0.48	0.2016	0.00	0.0
JAN	0.23	0.48	0.2016	0.03	12.3
FEB	0	0.48	0.2016	0.00	0.0
MAR	0.434	0.48	0.2016	0.23	53.5
APR	11.74	0.48	0.2016	11.54	98.3
MAY	1.69	0.48	0.2016	1.49	88.1
JUN	0.05	0.48	0.2016	0.00	0.0
JUL	0.02	0.48	0.2016	0.00	0.0
AUG	0	0.48	0.2016	0.00	0.0
SEP	0	0.48	0.2016	0.00	0.0
OCT	0	0.48	0.2016	0.00	0.0
NOV	0	0.48	0.2016	0.00	0.0
ANNUAL	**1 4**			**1 3**	**9 3**
T50	19	0.48	0.2016	18.80	98.9
T100	24	0.48	0.2016	23.80	99.2

WADI BAYSH (Average flood volumes(1970-1985))

Month	Stored volume (mcm)	Water surface area (km^2)	PT volume m^3	Recharge volume mcm	Recharge efficiency (%)
DEC	2.25	1.4	0.588	1.7	73.9
JAN	3.19	1.4	0.588	2.6	81.6
FEB	4.86	1.4	0.588	4.3	87.9
MAR	7.09	1.4	0.588	6.5	91.7
APR	13.04	1.4	0.588	12.5	95.5
MAY	10.16	1.4	0.588	9.6	94.2
JUN	5.77	1.4	0.588	5.2	89.8
JUL	8.79	1.4	0.588	8.2	93.3
AUG	8.9	1.4	0.588	8.3	93.4
SEP	4.8	1.4	0.588	4.2	87.8
OCT	3.06	1.4	0.588	2.5	80.8
NOV	2.57	1.4	0.588	2.0	77.1
ANNUAL	**7 4**			**6 7**	**9 0**
T50	56	1.4	0.588	55.4	99.0
T100	70	1.4	0.588	69.4	99.2

T50 = 50 year flood
T100 = 100 year flood

Table 9.3 Annual storage calculation in mcm of flood, irrigation water supplay and artificial recharge flow for both wadis.

WADI BAYSH					WADI HABAWNAH			
Year	Annual flood water (mcm)	Flood water (cumulative volume) (mcm)	Annual water demand (mcm)	Water demand (cumulative volume) (mcm)	Annual flood water (mcm)	Flood water (cumulative volume) (mcm)	Annual water demand (mcm)	Water demand (cumulative volume) (mcm)
1970	22	22	65	65	2.3	2	8	8
1971	86	108	65	130	15.8	18	8	16
1972	134	242	65	195	25.9	44	8	24
1973	46	288	65	260	2	46	8	32
1974	87	375	65	325	11.2	57	8	40
1975	77	452	65	390	10.2	67	8	48
1976	45	497	65	455	4.9	72	8	56
1977	37	534	65	520	2.7	75	8	64
1978	35	569	65	585	1.9	77	8	72
1979	40	609	65	650	4.3	81	8	80
1980	38	647	65	715	4	85	8	88
1981	96	743	65	780	17	102	8	96
1982	121	864	65	845	12.4	115	8	104
1983	151	1015	65	910	19.4	134	8	112
1984	66	1081	65	975	6.9	141	8	120
1985	111	1192	65	1040	11.3	152	8	128
2020*	197				55			
2070**	226				65			

WADI BAYSH					WADI HABAWNAH			
Year	Annual flood water (mcm)	Flood water (cumulative volume) (mcm)	Annual water demand (mcm)	Water demand (cumulative volume) (mcm)	Annual flood water (mcm)	Flood water (cumulative volume) (mcm)	Annual water demand (mcm)	Water demand (cumulative volume) (mcm)
1970	22	22	70	70	2.3	2	9	9
1971	86	108	70	140	15.8	18	9	18
1972	134	242	70	210	25.9	44	9	27
1973	46	288	70	280	2	46	9	36
1974	87	375	70	350	11.2	57	9	45
1975	77	452	70	420	10.2	67	9	54
1976	45	497	70	490	4.9	72	9	63
1977	37	534	70	560	2.7	75	9	72
1978	35	569	70	630	1.9	77	9	81
1979	40	609	70	700	4.3	81	9	90
1980	38	647	70	770	4	85	9	99
1981	96	743	70	840	17	102	9	108
1982	121	864	70	910	12.4	115	9	117
1983	151	1015	70	980	19.4	134	9	126
1984	66	1081	70	1050	6.9	141	9	135
1985	111	1192	70	1120	11.3	152	9	144

Continued on next page

Table 9.3 contiued

	WADI BAYSH				WADI HABAWNAH			
Year	Annual flood water (mcm)	Flood water (cumulative volume) (mcm)	Annual water demand (mcm)	Water demand (cumulative volume) (mcm)	Annual flood water (mcm)	Flood water (cumulative volume) (mcm)	Annual water demand (mcm)	Water demand (cumulative volume) (mcm)
1970	22	22	75	75	2.3	2	10	10
1971	86	108	75	150	15.8	18	10	20
1972	134	242	75	225	25.9	44	10	30
1973	46	288	75	300	2	46	10	40
1974	87	375	75	375	11.2	57	10	50
1975	77	452	75	450	10.2	67	10	60
1976	45	497	75	525	4.9	72	10	70
1977	37	534	75	600	2.7	75	10	80
1978	35	569	75	675	1.9	77	10	90
1979	40	609	75	750	4.3	81	10	100
1980	38	647	75	825	4	85	10	110
1981	96	743	75	900	17	102	10	120
1982	121	864	75	975	12.4	115	10	130
1983	151	1015	75	1050	19.4	134	10	140
1984	66	1081	75	1125	6.9	141	10	150
1985	111	1192	75	1200	11.3	152	10	160

*50 year flood
**100 year flood

average recharge volume (flood water) is 75 and 10mcm and the recharge efficiency during the year is 93% and 90%, respectively, for Wadi Habawnah and Wadi Baysh.

The problem is to determine the reservoir capacity required to satisfy different policies by assuming different constant demands of 65, 70 and 75 mcm for Wadi Baysh and 8, 9 and 10 mcm for Wadi Habawnah per year. All of these demands have been assumed to be adjusted to take into account evaporation, precipitation losses, etc.

The mass curve is drawn in Figures 9.23, 9.24 and 9.25. The figures show the plotting of the cumulative supply and demand curves as indicated in Table 9.3. Both wadis show different wet and dry periods. The maximum deficits and excesses of assumed storage under different demands are summarised in Table 9.4 as follows:

Table 9.4 Wadi Baysh and Wadi Habawnah maximum deficit and excess water over a 10 year period.

Wadi Baysh Demand	Volume of max deficit (mcm)	Period (year)	Volume of max excess (mcm)	Period (year)
75	178	10	17	1
70	123	4	72	3
65	68	4	152	3
Wadi Habawnah				
10	24.8	9	14	4
9	13.8	4	17	7
8	2.8	1	24.2	5

However, the maximum deficits to be met from storage are 178 mcm and 24.8 mcm from Wadi Baysh and Wadi Habawnah, respectively.

Both wadi flood records were analysed, which involved keeping track of the excess and deficit throughout the 15 years. Calculations were facilitated by a tabular approach (see Tables 9.5 and 9.6). The first three columns of Tables 9.5 and 9.6 show the year, the supply and the different assumed demands. Volume is in mcm per year. The comparison between the annual flood water as a supply and the different assumed demands on an annual basis provides details of the deficit which must be met from storage or the excesses which demand more volume. These are shown in columns 4 and 5 of Tables 9.5 and 9.6 Column 6 keeps a running record of the volume in the assumed reservoir and is based on the assumption that the reservoir contains the 1970 flood water. This running total is particularly valuable for showing the amount of water still left in the

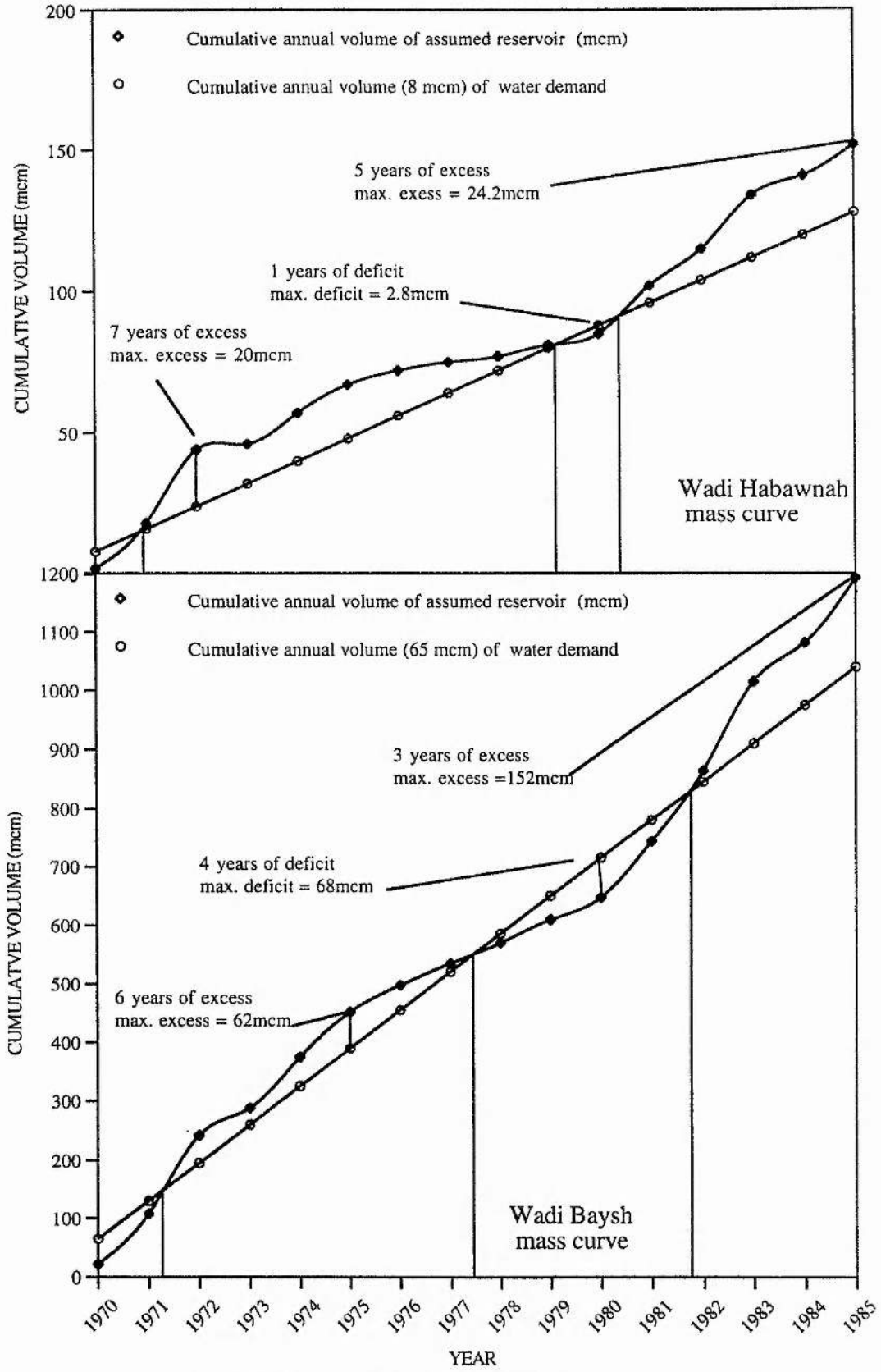

Figure 9.23 Mass curves of assumed reservoir showing the cumulative volume of annual inflow assuming 8mcm and 65mcm of water demand for Wadi Habawnah (upper) and Wadi Baysh (lower), respectively.

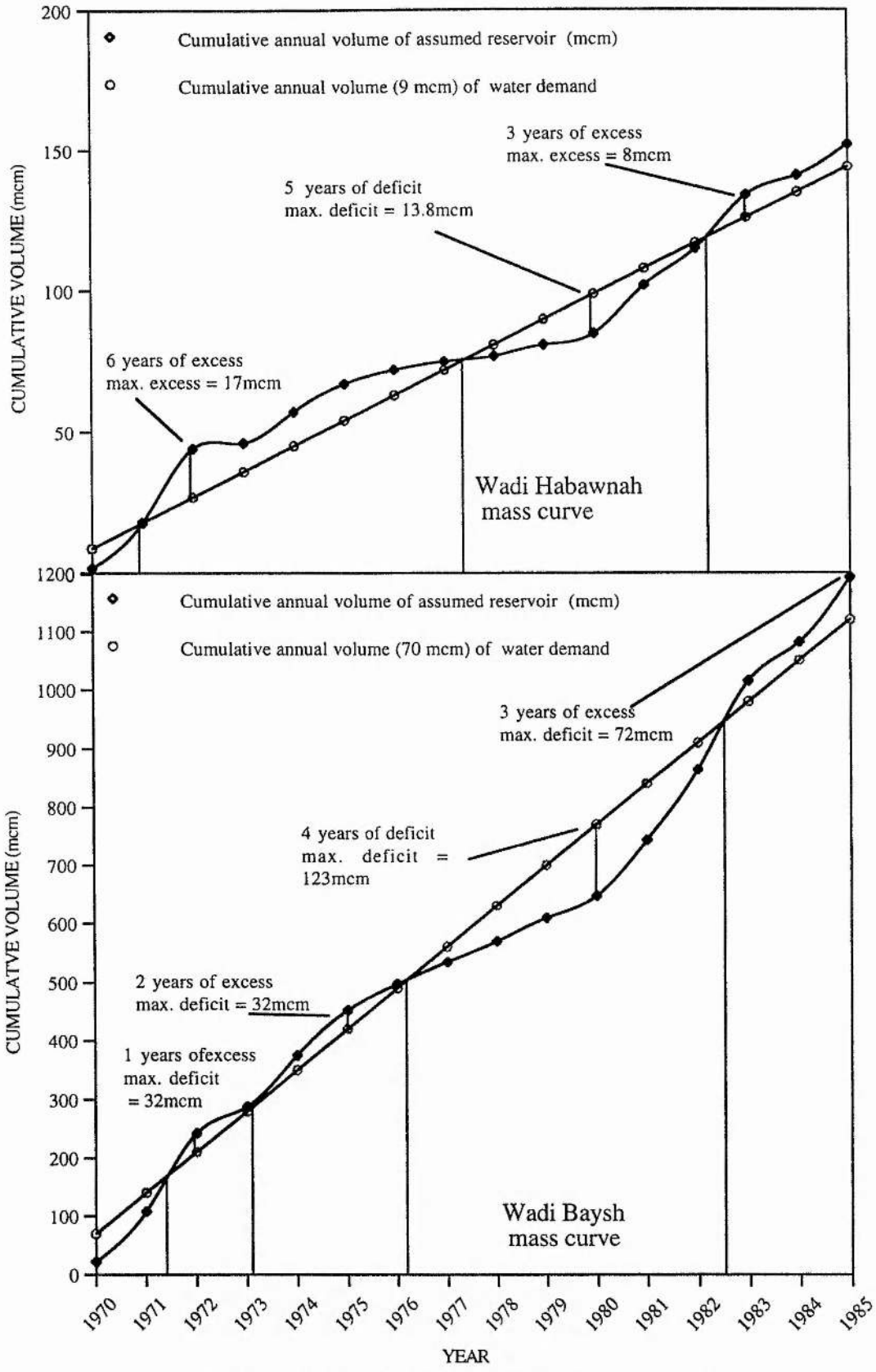

Figure 9. 24 Mass curves of assumed reservoir showing the cumulative volume of annual inflow assuming 9mcm and 70mcm of water demand for Wadi Habawnah (upper) and Wadi Baysh (lower), respectively.

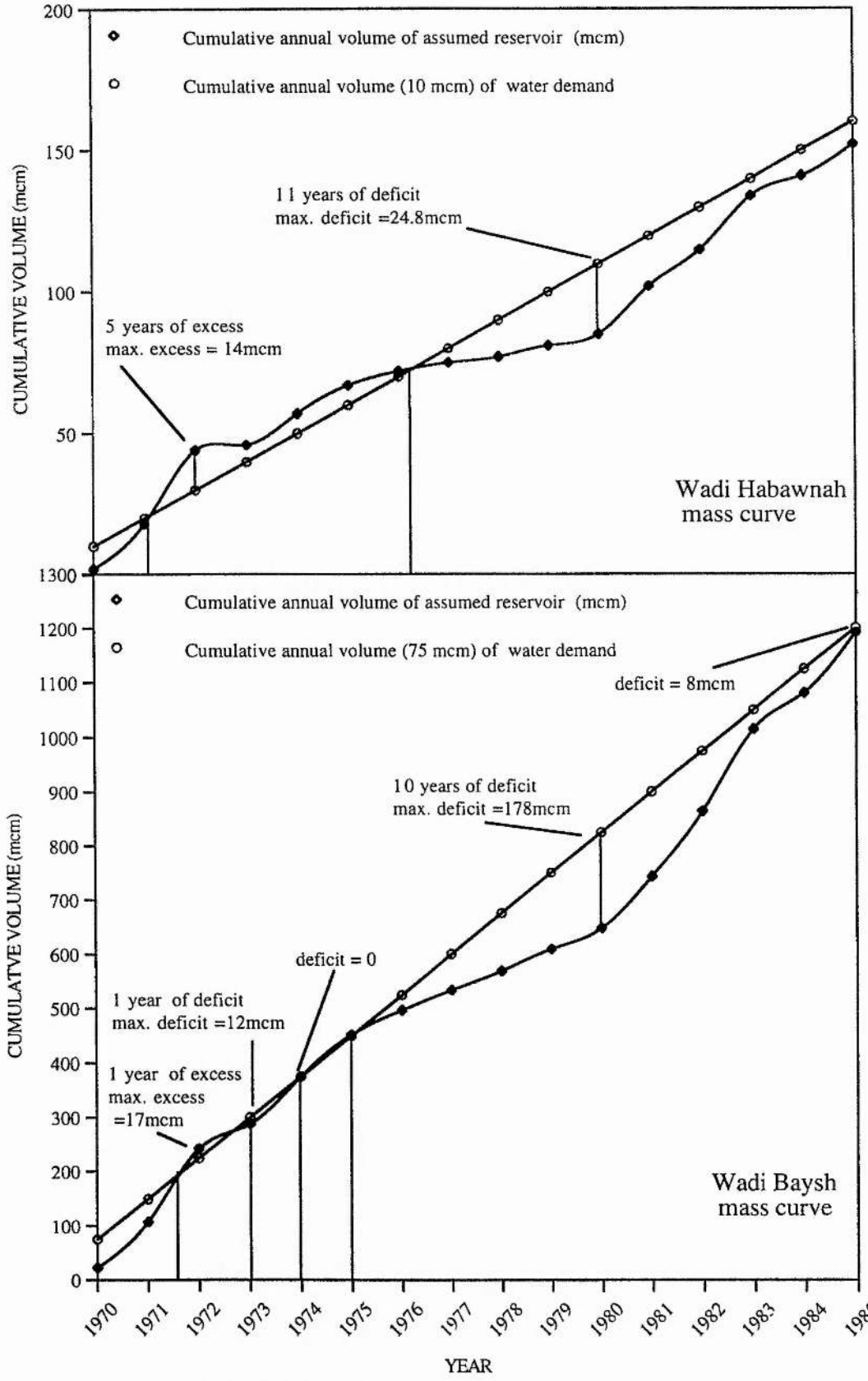

Figure 9.25 Mass curves of assumed reservoir showing the cumulative volume of annual inflow and assuming 10mcm and 75mcm of water demand for Wadi Habawnah (upper) and Wadi Baysh (lower), respectively.

Table 9.5 Annual storage calculation in mcm of flood, assuming different annual volume of water supplay for irrigation and artificial recharge flow for Wadi Habawnah

WADI HABAWNAH

YEAR	SUPPLY	DEMAND	DEFICIT	EXCESS	VOLUME
	mcm	mcm	mcm	mcm	mcm
1970	2.3	8	5.7		-5.7
1971	15.8	8		7.8	2.1
1972	25.9	8		17.9	20
1973	2	8	6		14
1974	11.2	8		3.2	17.2
1975	10.2	8		2.2	19.4
1976	4.9	8	3.1		16.3
1977	2.7	8	5.3		11
1978	1.9	8	6.1		4.9
1979	4.3	8	3.7		1.2
1980	4	8	4		-2.8
1981	17	8		9	6.2
1982	12.4	8		4.4	10.6
1983	19.4	8		11.4	22
1984	6.9	8	1.1		20.9
1985	11.3	8		3.3	**24.2**
Water Balance			**35**	**59.2**	**24.2**
2020*	55	8		47	47
2070**	65	8		57	57

YEAR	SUPPLY	DEMAND	DEFICIT	EXCESS	VOLUME
	mcm	mcm	mcm	mcm	mcm
1970	2.3	9	6.7		-6.7
1971	15.8	9		6.8	0.1
1972	25.9	9		16.9	17
1973	2	9	7		10
1974	11.2	9		2.2	12.2
1975	10.2	9		1.2	13.4
1976	4.9	9	4.1		9.3
1977	2.7	9	6.3		3
1978	1.9	9	7.1		-4.1
1979	4.3	9	4.7		-8.8
1980	4	9	5		-13.8
1981	17	9		8	-5.8
1982	12.4	9		3.4	-2.4
1983	19.4	9		10.4	8
1984	6.9	9	2.1		5.9
1985	11.3	9		2.3	**8.2**
Water Balance			**43**	**51.2**	**8.2**
2020*	55	9		46	45
2070**	65	9		56	55

Continued on next page

Table 9.5 continued

YEAR	SUPPLY	DEMAND	DEFICIT	EXCESS	VOLUME
	mcm	mcm	mcm	mcm	mcm
1970	2.3	10	7.7		-7.7
1971	15.8	10		5.8	-1.9
1972	25.9	10		15.9	14
1973	2	10	8		6
1974	11.2	10		1.2	7.2
1975	10.2	10		0.2	7.4
1976	4.9	10	5.1		2.3
1977	2.7	10	7.3		-5
1978	1.9	10	8.1		-13.1
1979	4.3	10	5.7		-18.8
1980	4	10	6		-24.8
1981	17	10		7	-17
1982	12.4	10		2.4	-15.4
1983	19.4	10		9.4	-6
1984	6.9	10	3.1		-9.1
1985	11.3	10		1.3	**-7.8**
Water Balance			**51**	**43.2**	**-7.8**
2020*	55	10		45	45
2070**	65	10		55	55

* 50 year flood

* *100 year flood

Table 9.6 Annual storage calculation in mcm of flood, assuming different annual volume of water supplay for irrigation and artificial recharge flow for Wadi Baysh

WADI BAYSH

YEAR	SUPPLY	DEMAND	DEFICIT	EXCESS	VOLUME
	mcm	mcm	mcm	mcm	mcm
1970	22	65	43		-43
1971	86	65		21	-22
1972	134	65		69	47
1973	46	65	19		28
1974	87	65		22	50
1975	77	65		12	62
1976	45	65	20		42
1977	37	65	28		14
1978	35	65	30		-16
1979	40	65	25		-41
1980	38	65	27		-68
1981	96	65		31	-37
1982	121	65		56	19
1983	151	65		86	105
1984	66	65		1	106
1985	111	65		46	**152**
Water Balance			**192**	**344**	**152**
2020*	197	65		132	132
2070**	226	65		161	293

YEAR	SUPPLY	DEMAND	DEFICIT	EXCESS	VOLUME
	mcm	mcm	mcm	mcm	mcm
1970	22	70	48		-48
1971	86	70		16	-32
1972	134	70		64	32
1973	46	70	24		8
1974	87	70		17	25
1975	77	70		7	32
1976	45	70	25		7
1977	37	70	33		-26
1978	35	70	35		-61
1979	40	70	30		-91
1980	38	70	32		-123
1981	96	70		26	-97
1982	121	70		51	-46
1983	151	70		81	35
1984	66	70	4		31
1985	111	70		41	**72**
Water Balance			**231**	**303**	**72**
2020*	197	70		127	122
2070**	226	70		156	273

Continued on next page

Table 9.6 continued

YEAR	SUPPLY	DEMAND	DEFICIT	EXCESS	VOLUME
	mcm	mcm	mcm	mcm	mcm
1970	22	75	53		-53
1971	86	75		11	-42
1972	134	75		59	17
1973	46	75	29		-12
1974	87	75		12	0
1975	77	75		2	2
1976	45	75	30		-28
1977	37	75	38		-66
1978	35	75	40		-106
1979	40	75	35		-141
1980	38	75	37		-178
1981	96	75		21	-157
1982	121	75		46	-111
1983	151	75		76	-35
1984	66	75	9		-44
1985	111	75		36	**-8**
Water Balance			**271**	**263**	**-8**
2020*	197	75		122	122
2070**	226	75		151	273

reservoir. A comparison of the available supply and the different suggested demands in both wadis over a 15 year period is summarised in Table 9.7 as follows:

Table 9.7 A summary of the reservoir budget using 15 years of flood records for both wadis

Wadi Habawnah

Demand mcm	No. of years of excess	No. of years of deficit	Total net (mcm)
8	8	8	24.2 excess
9	8	8	8.2 excess
10	8	8	-7.8 deficit
Wadi Baysh			
65	9	7	152 excess
70	8	8	72 excess
75	8	8	-8 deficit

Considering the average values of the 15 year record as a good overall average for the annual water demand in both wadis, the accumulative deficit in 45 years time would be equivalent to 24mcm in each wadi using 10 and 75 mcm as demand policy for Wadi Habawnah and Wadi Baysh respectively. The 50 year flood volume (55mcm and 197mcm for Wadi Habawnah and Wadi Baysh, respectively) would cover such a deficit in the long run with the basin storage excesses being 31mcm and 98mcm for Wadi Habawnah and Wadi Baysh, respectively.

9.2.5 Water Demand and Irrigable Area

The traditional type of irrigation in both wadis is almost entirely dependent upon the flood waters. If an irrigation system is to be built which supplies regulated flows according to the demand of the plants, it is necessary to acquire knowledge on the exact time distribution of the water demands of the various crops during the year. However, the water demands for various crops during the year are different. Furthermore, it depends on the soil type, climate conditions, salt content of soil, etc.

To provide a more reliable source of irrigation water in order to meet the demand of the crops, there should be conjunctive of groundwater and surface water should be used.

9.2.5.1 Water Demand for Sorghum and Barley

In this study, only sorghum and barley will be considered, because they are the dominant plants in both wadi agricultural areas (about 96% of the crops, Agricultural Office, personal communication).

The water demand for these crops is 300 m^3 per month per hectare (Scottish crop Research institute, 1995).

Since there were previously three suggestions for water supply policy, the author examined these for the different crop seasons in both wadis assuming that all the agricultural area was planted (see Table 9.8).

Table 9.8 Irrigated area per season for various yearly water budgets in both wadis.

Wadi Baysh Surface Storage	Monthly Water Demand	One Season	Two Seasons	Three Seasons	Four Seasons
m^3	m^3/ha	no. ha	no. ha	no. ha	no. ha
75000000	300	83333	41667	27778	20833
65000000	300	72222	36111	24074	18056
60000000	300	66667	33333	22222	16667

Wadi Habawnah Surface Storage	Monthly Water Demand	One Season	Two Seasons	Three Seasons	Four Seasons
m^3	m^3/ha	no. ha	no. ha	no. ha	no. ha
10000000	300	11111	5556	3704	2778
9000000	300	10000	5000	3333	2500
8000000	300	8889	4444	2963	2222

The characteristics of the demand rules indicate that the irrigation area of Wadi Baysh will reach the maximum of sustainable crops in one to two seasons. However, the irrigation area can be supplied with water for crops in three seasons if the 75mcm/year is applied. The four season crop policy can not be implemented because the water budget will irrigate only 16667 ha to 20833 ha, whereas the existing area is 27033 ha.

In Wadi Habawnah, one season of crops can be applied per year using 10 mcm of water since the total irrigation area is 11350 ha. However, all of the water supply policy will fail to meet the demand for two, three and four seasons crops due to the limited water supply.

9.2.6 Conjunctive Use Management

9.2.6.1 Introduction

Conjunctive use management can lead to a successful long-running project if skillful management is applied at an early stage. The water balances of both wadis have been estimated to a reasonable degree of accuracy. The youthful state of development management practice is unappreciated but desirable where the water input component exceeds the total natural and artificial water output (see Table 9.1).

Effective conjunctive use management would be necessary in the mature state, where the water input is equal to the sum of the natural and artificial water output. However, during the old age and rejuvenation states, conjunctive use management practice becomes essential for development in order to protect the water resource from further damage. Since the flood waters and groundwaters are used in such a development, the accurate assessment of both permanent and temporary storage and perennial yield is critical. Such careful management would help to avoid the minimisation of the aquifer because ignoring such practice would produce many undesirable effects.

9.2.6.2 Development State of Water Resources

According to previous flood and ground water budget estimations, the state of resources can be demonstrated. The natural inflow in Wadi Baysh is found to be equal to the combined natural and artificial outflow. In Wadi Habawnah, the water budget demonstrates that the natural inflow is lower than the combined natural and artificial outflow.

The development of conjunctive use has been assessed in the light of the Jones'criteria (1972),. The water balance of the Wadi Baysh (assuming that the water demand was 75mcm/yr) demonstrates that the resource is in the **mature state**. However, the water budget of Wadi Habawnah (assuming a demand of 10mcm/yr) suggests that the resource has passed into the **old age state** of development. However, the author argues that such a stage of development might not have been reached since there has been no severe drop in the level of the water table.

9.2.6.3 Perennial Yield

The perennial yield is the optimum groundwater yield, in the broad sense, rather than the safe yield, because the optimum yield does not depend on the recharge alone as does the safe yield.

The groundwater perennial yield defines the rate at which water can be withdrawn without producing adverse effects such as the progressive depletion of water resources, land subsidence, degradation of groundwater quality, excessive pumping costs and interference with prior water rights (Todd, 1980). Hence, the maximum quantity of water extracted from the aquifer depends on the perennial yield

The present groundwater regimes in both wadis show two different perennial yield cases. In Wadi Baysh, the irrigation depends mainly on flood water, which puts the perennial yield in a 'safe' state. In Wadi Habawnah, the artificial discharge is equivalent to the perennial yield. With regard to the water balance of Wadi Habawnah, the amount of perennial yield is about $5x10^6$mcm/yr ($4x10^6$-$9x10^6$ mcm/yr). The total recharge volume compared to the artificial withdrawal is about 44% of the estimated minimising yield.

9.2.7 Groundwater in Storage

The amount of groundwater in storage is the groundwater volume. It can be determined by multiplying the average saturated thickness of the aquifer by the area over which the aquifer is already extended and further multiplied by the specific yield (the ratio of the volume of water a rock or soil will yield by gravity drainage to the rock or soil). In a confined aquifer, the specific yield is equivalent to the storativity (storage coefficient) as follows:

Groundwater in storage (GS) = M x A x S

where M = the saturated thickness, A = Area of groundwater basin and S = specific yield. The nature of the present aquifer in both wadis can be assumed as unconfined to leaky confined in Wadi Baysh and the saturated thickness is approximately 18m. However, in Wadi Habawnah, the saturated thickness is approximately 11m.

The storage coefficient values of the Wadi Baysh basin (MWRA, 1978) ranges from $1x10^{-2}$ to $1.95x10^{-1}$ with an average value of 0.08. In Wadi Habawnah the storage coefficient ranges from 1.5×10^{-2} to 9.39×10^{-2} (see Table 5.6) with an average value of 0.045. Therefore, the volume of groundwater in storage for the present basin area in each wadi is:

1- Wadi Baysh.

$$GS = (A = 27033x10^4 m^2) \times (M = 18m) \times (S = 0.08) = 389 \text{ mcm}$$

where

A is the agricultural area of Wadi Baysh = 27033 ha

2- Wadi Habawnah

$$GS = (A = 11350x10^4 m^2) \times (M = 11m) \times (S = 0.04) = 49 \text{ mcm}$$

where

A is the agricultural area of Wadi Habawnah = 11350 ha

9.2.8 Summary and Conclusion

Both wadis show that excellent conditions prevail for the spreading of flood waters for replenishment of the underground supply, but the introduction of any permanent, extensive spreading system in the stream bed of the lower part of the wadi would be difficult without first acquiring the privately owned lands and the construction of some form of permanent bank protection.

The aquifers in both wadis show conditions that are favourable for recharge. These are:

1- A good value and range of aquifer permeability in both wadis.

2- The underlying aquifers are unconfined in most of Wadi Habawnah and in the upper part of Wadi Baysh, which is characterised by a sufficiently low water table to allow additional storage.

3- The lower parts of both wadis contain semi-confined to confined aquifers. The ability to recharge them by direct or indirect methods would improve prospects for agricultural development in both wadis.

4- Most of the upper and middle parts of both wadis are favourable for groundwater storage because of the unconfined nature of the aquifers coupled with high infiltration rates.

5- The lower parts of both wadis show unconsolidated alluvial multi-aquifers containing coarse sediments which represent favourable conditions for artificial recharge using well injection.

6- The unconfined aquifer shows high to moderate transmissivity, which would allow the lateral movement of recharge water without building up the groundwater mound that rises into the basins.

7- The agricultural land is characterised with a surface layer of thick clay (3.6 m) where the hydraulic conductivity is low. This will restrict the infiltration to unacceptably low rates. Such an area could be treated with a suitable artificial recharge method of injection.

Reservoir operation has been simulated for the 50 and 100 year periods and for three demand alternatives (65, 70 and 75mcm/year of water budget in Wadi Baysh and 8,

9, and 10 mcm of water budget in Wadi Habawnah). The mass curve analysis revealed the relation between the irrigable area and the conjunctive use policy for each alternative as shown.:

Table 9.9 Percentage exiting agricultural land which could be irrigated in relation to matured crop harvest according to different values of water demands

Wadi Baysh Annual water demand mcm	Irrigable area (ha) for one seasons	Irrigable area (ha) for two seasons	Irrigable area (ha) for three seasons	Irrigable area (ha) for four seasons
75	308%	**154%**	**103%**	77%
65	267%	**134%**	**89%**	67%
60	247%	**123%**	**82%**	62%

Wadi Habawnah Annual water demand mcm	Irrigable area (ha) for one seasons	Irrigable area (ha) for two seasons	Irrigable area (ha) for three seasons	Irrigable area (ha) for four seasons
10	**98%**	49%	33%	24%
9	**88%**	44%	29%	22%
8	**78%**	39%	26%	20%

As can be seen from table 9.9, the increase in percentile rrigable area is due to the decrease of the number of crop seasons. It seems that conjuctive use would be optimal if a demand of 75mcm/year was adopted with three crop seasons in the year. This would allow a 3% increase in the irrigable area without affecting the safe yield. In Wadi Habawnah, the benefits obtained from irrigation are limited to one crop season in the year in which 98% of the irrigable area can be used. This occurs only if the 10mcm demand conjuctive use policy is adopted for irrigation.

The author believes that the results from this simulation will give a more reliable indication of the actual benefit for irrigation systems in which the risk of failure is very low.

As a conjunctive use feasibility study of the area, the interest has been in how the groundwater can best gain from the flood water and vice versa (Figures 9.26 and 27). As a result, the combined flood and ground water system could be developed through conjunctive use management for improve agricultural productivity in the area. The groundwater resources development can be achieved by determining the maximum withdrawal rate possible without causing undesirable effects.

A plan to ensure a steady state relationship between the surface and subsurface storage would help to manage the perennial yield and minimise the mining yield. Accordingly, the results show that building a reservoir in both wadis is economically justifiable. In spite of that, neither dam will extend the irrigable area significantly, but both will help to distribute the flood water more efficiently, using artificial methods such as artificial groundwater recharge. In addition such a plan will help to reduce evaporation effects and increase the subsurface water storage for irrigation needs besides protecting the agricultural lands from flash floods.

Considering the existing traditional irrigation system in both wadis, the wadi channel remains the main source of recharge water in which 31% of the wadi seepage reaches the saturated zone.

To improve the flood spreading system in both wadis, the author suggests building long narrow channels with a width and depth of 2 and 3m, respectively (see Figure 9.28). Such a plan will help to distribute the flood water to recharge the aquifer and to enhance the groundwater quality.

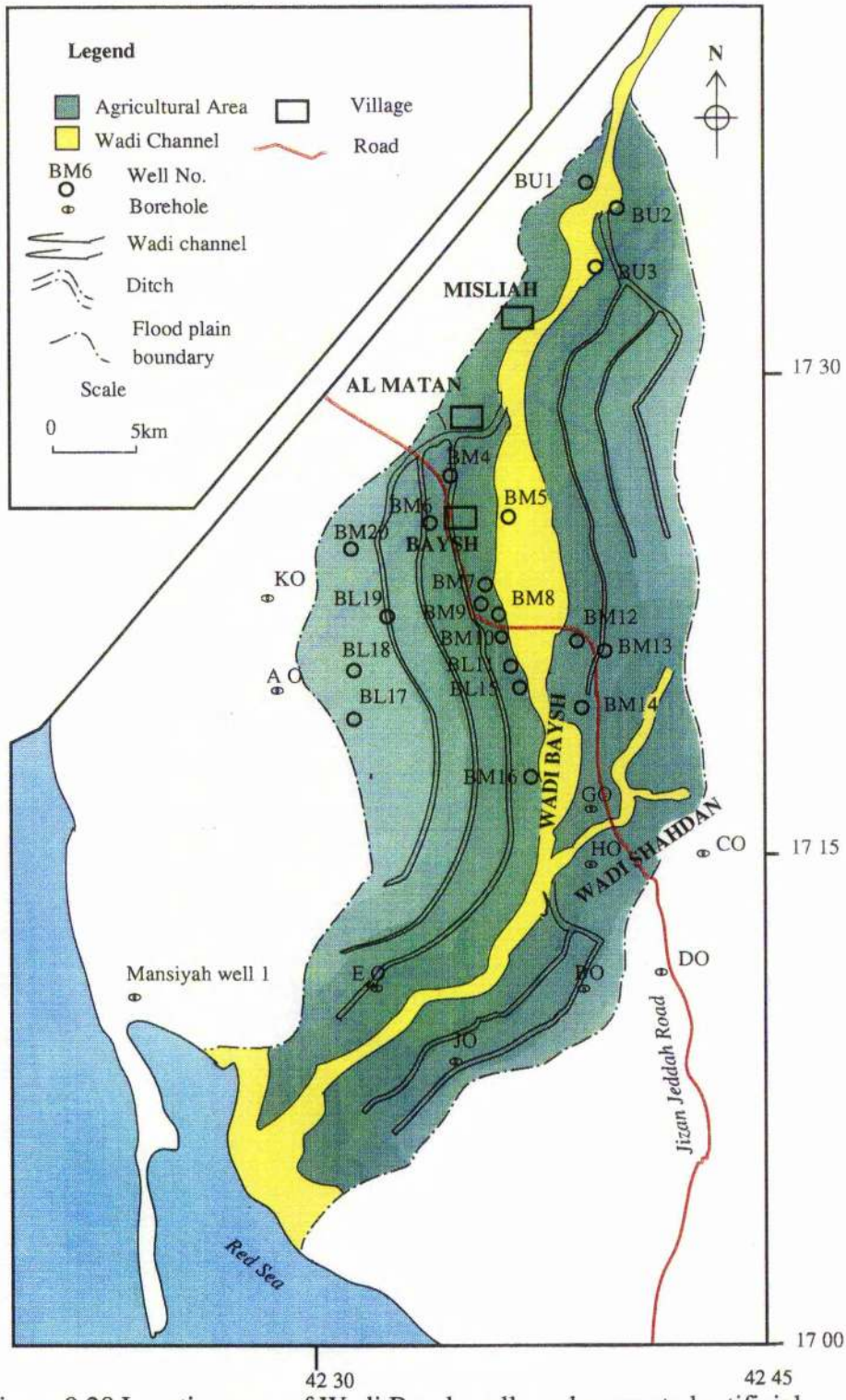

Figure 9.28 Location map of Wadi Baysh wells and suggested artificial recharge ditch system.

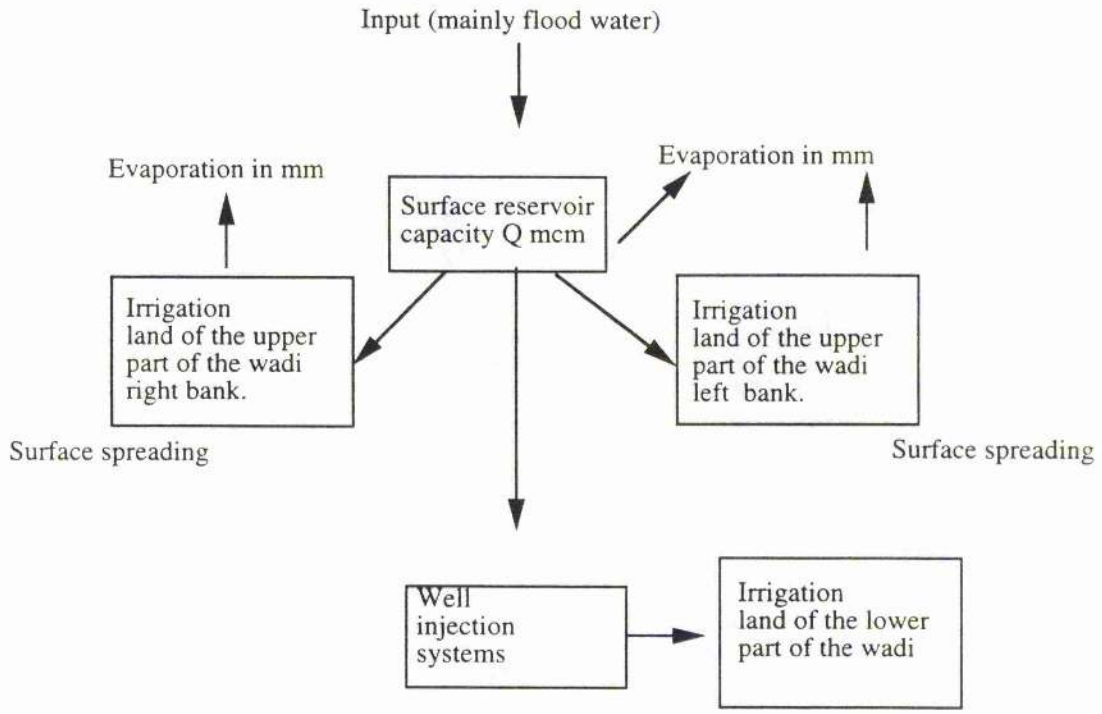

Figure 9.26 Schematic representation of the suggested system of conjunctive use in both wadis .

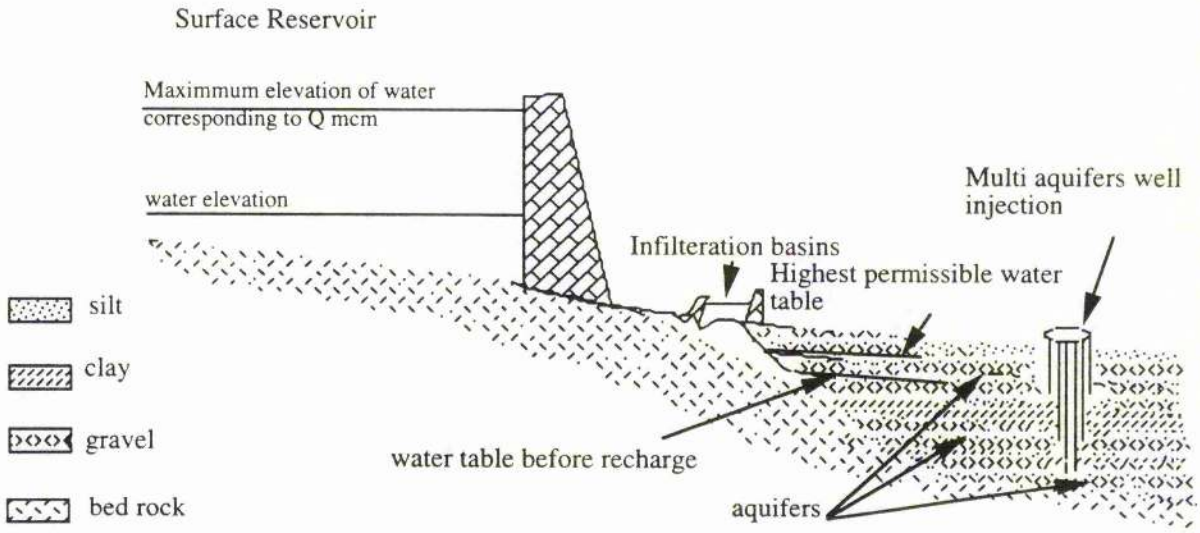

Figure 9.27 Diagrammatic vertical cross section through the suggested system of artificial recharge in both wadiss

CHAPTER TEN: SUMMARY, CONCLUSIONS AND RECOMMENDATIONS

10.1 Summary and Conclusions

The southern part of the Asir region (Najran region and Tehamah Asir) of Saudi Arabia includes some of the best agricultural land in the country, produces quite a significant quantity of crops and thereby is one of the major suppliers of food to the Asir and Najran regions. Rainfall is variable causing floods in any season in Wadi Baysh, and during the spring in Wadi Habawnah. The latter is an area that experiences monsoonal climatic conditions and suffers serious shortages of flood recharge during the summer period, due to prolonged dry conditions.

The study has been carried out in Wadi Baysh and Wadi Habawnah, both of which contain ephemeral streams that originate in Asir Mountains. Wadi Baysh, which drains an area of 4987 km^2, is partly bounded by the Red Sea and on the southeast by the Yemen Arab Republic. It rises to 700m in the foothills and above 3000m at the head of the wadi.

Wadi Habawnah is in the extreme southeast of Asir province and leads towards the Rub Al Khali desert. The wadi, which drains 4640 km^2, rises at over 3000m and falls eastwards to about 1200m above sea level.

The upper hard-rock areas comprise about 85% of the watershed of both wadis. These areas are rugged and mountainous, developed on igneous and metamorphic rocks. The lower areas have little relief and are primarily underlain by alluvium.

In winter, most rain falls in the mountains because this area is affected by the north-westerly air flow. In spring, the rainfall falls mainly in the high land while the low areas in the eastern part of Wadi Habawnah and in the Tehamah plain receive little rain as they are subjected to south-easterly monsoon air flow.

During the summer the Wadi Baysh foothills receive precipitation while the eastern slopes receive no rain because the southwest monsoon rain falls only on the western slopes of the mountains. The N-S orientation of the Asir Mountains creates a barrier, the eastern slopes being in a rain shadow.

At higher elevations Wadi Baysh receives an annual rainfall of up to 662mm, with a mean of 400mm while Wadi Habawnah receives an average annual rainfall of 150mm in the upper part of the catchment area. There is a direct correlation between the mean annual rainfall and the elevation in both wadis. The hydrological potential evaluations of the Wadi Baysh and Wadi Habawnah runoff records have been performed on the basis of 16 years and 3 years of observation respectively. The flood volume of Wadi Baysh shows a mean of 75 mcm while for Wadi Habawnah it is 10 mcm per year.

Estimated magnitudes of floods with 2, 10, 50 and 100 year return periods. are 66, 128, 157 and 185 mcm in Wadi Baysh and 8, 20, 26 and 33 mcm in Wadi Habawnah.

Groundwater samples collected from 62 and 20 hand dug wells in Wadi Habawnah and Wadi Baysh respectively have been analysed for concentrations of the major ions (Ca^{2+}, Mg^{2+}, Na^{+}, K^{+}, CO_3^{2-}, HCO_3^{-}, SO_4^{2-} and Cl^{-}) and some trace elements (Fe^{2+}, Mn^{2+}, Ni^{2+}, Pb^{2+} and Al^{3+}).

Calcium, sodium, magnesium, sulphate and chloride are present in high concentrations in the water in the lower part of both wadis. This indicates a high natural abundance of these ions and may point to their high solubility .

Waters from wells vary considerably in their composition. There are positive correlations of Na^{+},Ca^{2+},Mg^{2+},Cl^{-} and SO_4^{2-} with total dissolved solids (TDS). K^{+}, HCO_3^{-} and CO_3^{2-}, show poor correlations with TDS. This suggests that aquifer waters mix in various proportions with recharge water.

The correlation coefficient of Cl^{-} against Na^{+} in the aquifer of Wadi Baysh has a higher value (0.9) than that of Wadi Habawnah (0.79). In Wadi Baysh simple dissolution or mixing between waters is the main process in the aquifer. However, in Wadi Habawnah the analyses show that the Cl^{-} concentration exceeds the Na^{+} concentration, possibly due to reverse ion exchange, where $CaCl_2$ type water is abundant. (Ca^{2+}+Mg^{2+}) and ($HCO_3^{-} + SO_4^{2-}$) are strongly correlated in both wadis suggesting that simple dissolution and mixing are the main processes in the aquifers.

In Wadi Habawnah the cation composition is dominated by calcium (40-60%) with

subsidiary magnesium (20-30%), while sulphate (40-60%) is the dominant anion with subsidiary chloride (30-50%). In terms of hydrochemical facies, the groundwater of Wadi Habawnah is principally a calcium-sulphate type. Sodium-chloride and magnesium-sulphate water types are also present but less common.

In Wadi Baysh the water type is characteristically of the calcium-sodium-chloride facies with some examples of magnesium-sulphate or calcium bicarbonate water types. Chloride, the stable fraction, normally represents 20-30% of the groundwater anions. In Wadi Baysh simple dissolution is dominant for 30% of the samples, of the Ca (HCO_3) and NaCl water type. However, some 30% are Ca^{2+} and SO_4^{2-} dominant, suggesting a mixed water or a water exhibiting simple dissolution.

Only 6% of the Wadi Baysh groundwater samples are of $CaSO_4$ and Na Cl water types. This contrasts with 79% of the Wadi Habawnah samples being of Ca SO_4 type about half of which are from the upper part of the wadi. With the exception of a few scattered sites in each wadi most of the groundwater samples are sub-saturated.

Principal Component Analysis shows that the Wadi Habawnah groundwater has a high loading of total dissolved solids, sodium, calcium, chloride and sulphate. These high values of groundwater constituents are most likely the result of evaporation.

Bicarbonate has significantly loaded components 2, 3 and 4 reflecting dissolution of minerals by groundwater. The low variance associated with this component probably reflects buffering of the HCO_3^- content by CO_2 exchange between groundwater and the atmosphere. Also there is loading of saturation indices of aragonite. It may indicate precipitation of aragonite and possibly calcite within the basin fill.

Water type classification, based on the average ionic content with low standard deviation that dominates the groundwater in each zone of each wadi (upper, middle and lower zone), has been applied. Accordingly, in Wadi Baysh and Wadi Habawnah three main water types can be identified:

The upper part of Wadi Baysh (Misliyah area) is characterised by Water Type (I) as calcium sulphate rich. Water Type (II) is of calcium sulphate and sodium chloride waters which represent the groundwater in the middle zone (Baysh area). Water Type (III) is

calcium sulphate and sodium chloride waters. It occurs in the lower part, in semi confined to confined aquifers (basin area).

Wadi Habawnah: Water Type (I) is calcium sulphate dominates the recharge area (Al Khanig, Alharashf, Al Majma and Habawnah village area). Water Type (II) is calcium sulphate water with chloride becoming increasingly dominant in the middle part (Almuntasher, Alnagah, Al Daugah and Morayekhah areas). The unconfined to semi confined aquifer in the Wadi Habawnah outlet is characterised by Type (III), calcium sulphate and sodium chloride waters.

The dominant chemical processes occurring in the groundwaters of both wadis continue throughout the aquifer in the flow direction. Simple mixing between waters with different degrees of salinity, from recharge area to discharge area, is likely to be the main chemical process dominating the study areas. The recharge area and the evaporation processes play important roles in defining the groundwater types of both wadis.

The groundwater is used mainly for domestic and agricultural water supply. In the upper and middle parts of both wadis the groundwaters are more suitable for drinking and irrigation than in the lower parts of the wadis. In both wadis the drinking water quality is within the recommended limits in the upper and middle sections. The trace elements Fe^{2+} and Mn^{2+} exceed the EEC solute limits slightly with concentrations of 0.725-0.964 and 0.154-0.186 mg/l, respectively. The groundwater hardness is 234 to 1694 mg/l in Wadi Baysh and 313 to 2045 mg/l in Wadi Habawnah.

The groundwaters in the lower parts of Wadi Baysh and Wadi Habawnah are moderately saline.

The sodium hazard is low to medium in both wadis. Plants with moderate salt tolerance can be grown in most instances without special practices for salinity control. In Wadi Habawnah, the SAR ranges between 2 and 6 while in Wadi Baysh it shows a range between less than 1 to 7, which suggests that most of the water falls within the category of medium to high salinity hazard in both wadis.

Thus most of the waters are not suitable for most crops. Nevertheless, selective cropping patterns (such as barley, sorghum, wheat palm tree) would be appropriate in areas

having high salinity hazard, such as the lower parts of both wadis.

Since the safe margin of Residual Carbonate (RC) is 204 meq/l, the present sets of data indicate that the water of both wadis is suitable for agricultural use. In the lower part of both areas, most of the wells show high salinities but with ionic compositions maintaining a suitable balance for agricultural purposes.

For the present sets of data from the lower parts of both wadis, the evaluation of the groundwater conditions may need to be based on the salinity conditions rather than the SAR and RC. This is because the lower parts of both wadis are characterised by high evaporation and low rainfall (120 mm-80 mm). Using groundwater with high salinity for irrigation would damage the agricultural water supply. A subsurface drainage system to reduce the evaporation effect and the planting of suitable crops (wheat, sorghum and corn) for such high salinity groundwaters in this part of the study area is recommended.

The main problems in the determination of aquifer parameters are to find the most suitable analytical methods. Although a range of different methods is available, each is valid only under a set of limited assumptions concerning aquifer homogeneity, isotropy, and uniformity in thickness, which are seldom, if ever, satisfied.

The Papadopulos-Cooper (1967) method was most suitable method to evaluate the properties of the unconfined aquifer using the pumping tests for large diameter wells.

The transmissivity value for the unconfined aquifers in Wadi Baysh is 134 m^2/day while the average of the transmissivity of Wadi Habawnah aquifers is 515 m^2/day. These transmissivity values are moderate to high on the basis of the Ghearghe (1979) criteria .

Both wadis show high values of transmissivity in the main course of the wadi system, where highly permeable wadi floor sediments are present, but lower values outside the main channel where sediments of low permeability are present.

The storativity (S) values obtained using the Papadopulos and Cooper method, although theoretically exact, are questionable from the practical viewpoint.

The volumetric method was not helpful in determining a realistic value for the storativity. All the values calculated were very low. This method needs a long record of draw down to avoid the effects of well storage on the draw down compared to the aquifer

drain. Such long period testing was not possible at the sites investigated.

The modified Ferris method, using approximation techniques, gives reliable results for determining the storativity of the unconfined aquifers (storage coefficient) using the large diameter well tests. Step draw down testing shows that the efficiency of wells examined in both wadis is high. The values obtained confirm that large diameter wells are suitable for water supply in the wadis of the Arabian shield. It is calculated that the pumping rate in the upper and middle part of Wadi Baysh and in the lower part of Wadi Habawnah should be within the range of 400 and 215 m^3/day to satisfy a high percentage of well efficiency.

The Quaternary deposits of both wadis and the uppermost area can be traced continuously from local wells, boreholes and also by seismic refraction surveys. Lithologies recorded in wells indicate that this material is predominantly composed of interbeded gravel, silt and medium to coarse sand. The Quaternary deposits range from 6 to 150 m in thickness in Wadi Baysh and from 4 to 50 m in Wadi Habawnah.

The unconsolidated surface sediment (alluvium) in both wadis, is characterised by low seismic velocities (200 to 600 m s^{-1}). This suggests a high total porosity and potential water storage capacity and may be a useful guide to unconsolidated aquifers. The uppermost layer, 80% of the total area of both wadis, has a low seismic velocity.

The seismic refraction study shows that in both wadis the aquifers consist of three main zones; unsaturated zone, saturated zone, and bedrock. The unsaturated zone thickness varied between 3 and 29 m in thickness with P-wave velocities ranging between 200 and 600 m s^{-1}. The saturated thicknesses varied between 3 and 30 meters in Wadi Habawnah and in the upper -middle parts of Wadi Baysh while in the lower part it was not determined. The lower aquifer boundaries in Wadi Habawnah and in the upper and middle parts of Wadi Baysh were defined as a contact with igneous and metamorphic rocks with P-wave velocity ranging between 2675 and 4615 m s^{-1}.

Electrical resistivity soundings employing the Schlumberger configuration were conducted in the upper, middle and lower parts of each wadi at control sites near wells. The sounding curves mostly represented 4-layer cases of curve types KH and QH in Wadi

Baysh while the Wadi Habawnah records were dominated by curves of type QH. Lithological information from dug wells and boreholes was vital in refining the interpretation techniques.

The surface sediments increase in thickness (2 to 20m) down both wadis. Fine grained deposits characterise the lower sections of both wadis. The alluvial aquifers in both wadis vary in thickness. Wadi Baysh and Wadi Habawnah have alluvium thicknesses ranging from 4 to 150m, and 3 to 54m, respectively. The surface deposits down to a depth of 28 m in borehole GO (total depth 150 m) are similar to those in the upper part of Wadi Baysh.

In Wadi Baysh the aquifer resistivity ranges from 19 to 75 ohm-m and the thickness from 4 to 20m . In Wadi Habawnah the resistivity ranges from 33 to 121 ohm-m and the saturated zone thickness ranges from 7 to 22 m. In Wadi Habawnah the five layer curves show higher values of resistivity which result from a five layer section consisting of, at the top, dry gravel, underlain by dry sand and silt, unsaturated gravel and sand, the saturated zone of the aquifer and the fifth layer is bedrock.

The resistivity and seismic refraction surveys confirmed that the thickness of the unconfined aquifer is between 4 and 35 m in Wadi Baysh while in Wadi Habawnah it is between 7 and 42 m. A confined aquifer is developed in the lower part of Wadi Baysh with a thickness of 35m. The P-wave velocities of the aquifers ranges between 536 and 1817 m s^{-1} in both wadis. Questions relating to the deposits and the depth to bedrock in areas underlain by the deeper wadi sediments in the lower part of Wadi Baysh remain unanswered. In both wadis the aquifers show resistivities ranging between 23 and 125 ohm-m . The bedrock (igneous and metamorphic) resistivity in the upper and middle parts of Wadi Baysh and along Wadi Habawnah show values range between 3400 and 10260 ohm-m. However, it is important to know about the nature and extent of the unconsolidated sediments that comprise the bulk of the wadi deposits, and whether these materials are an important source of water. The present evidence suggests that wadi sediment have much potential for water supply in the middle and lower parts of both wadis. The alluvial layers are, at best, good sources of ground water for domestic and farm use.

The clay is relatively impermeable, and the fine- grained silty sand deposits will be unlikely sites for the development of productive wells.

In both wadis the VES surveys covered most of the area; 18 out of 30 VES, were made near the pumping tests as parametric measurements. The interpretation of the results of VES, together with pumping test results at the same location, were used to establish a relationship between the hydraulic transmissivity and the corrected transverse resistance.

There are similarities between the average resistivity and the current flowing parallel the bedding plane. The hydraulic transmissivity computed from pumping tests also assumes the hydraulic flow is parallel to the aquifer layer. Furthermore, the transverse resistance of the aquifer formation is the more useful parameter to be identified from the interpretation of VES.

From resistivity interpretation, the resistivity and the thickness of the aquifer were determined. The transverse resistance, which is the product of the aquifer resistivity and its thickness, was then calculated for 18 VES sites. To account for the effect of water quality, the transverse resistance was obtained by dividing the resistivity of the field measurement by the resistivity of the water, 5 ohm-m in Wadi Baysh and 6 ohm-m in Wadi Habawnah.

The corrected transverse resistance, Trn, is then plotted on a graph versus the corresponding transmissivity value as obtained from pumping tests. Using regression analysis a best fit line passing through the points is obtained. The relationship obtained in both wadis is direct and linear :

$$Trn = -19.233 + 3.3871 \times 10^4 T$$

To apply the relationship in the sandy gravels of the unconfined aquifers, the corrected transverse resistance values are substituted in the equation. Values of T obtained from the relationship are low with respect to those obtained from pumping tests. This is due to the fact that the VES and pumping test measurements were made on heterogeneous aquifers, whereas both of their theories assume isotropic aquifers.

In the study area, the author believes that many factors affect the T values interpreted using the above equation because the aquifer sediments are heterogeneous.

The VES and large diameter well pumping tests give the opportunity to obtain an

empirical function between the aquifer transmissivity and the corresponding corrected transverse resistance. The relationship obtained is generally linear in the sense that, by increasing the T, the Trn will also increase. The transverse resistance of the saturated thickness of the aquifers is the only important parameter for correlation with the hydraulic transmissivity. The computed empirical function is directly utilised for most of the surveyed aquifers and it is also possible to apply it to other aquifers of similar sedimentological properties in the Arabian Shield wadis.

Interpretation of geophysical logs of wadi aquifers

1-Wadi Baysh

A multi-aquifer system is present beneath the lower part the wadi. The upper wadi fill is classified as an unconfined aquifer, which locally overlies two confined aquifers.

The unconfined aquifer outcrops at the ground surface while its base rests on an impermeable layer of clay 2-18m thick. The confined aquifer is separated from the ground surface by the unconfined aquifer and the intervening impermeable clay layer.

The thickest water bearing units in the unconfined aquifer were encountered in borehole BO at 60m. In the other boreholes, freshwater bearing sequences ranged from 20 to 30m in thickness. The confined aquifer is at its thickest (35m) in boreholes AO and EO.

2- Wadi Habawnah

The 100m to 2km wide floor of Wadi Habawnah has three types of wadi filling sediments. The unconfined to locally semi-confined aquifer with thickness varying between <20 to >40m occurs in the lower part of the wadi. The wadi channel exhibits a trough shape and is filled with unconsolidated sediment, which rests upon the basement complex. The bulk of the wadi floor is underlain by gravels, upon which is a layer of sand within which lenses of clay occur in the centre of the wadi. A layer of gravel buries the sands on the northern side of the wadi. The upper layer in the middle of the wadi channel consists of silty to coarse sand, while in the lower part of the wadi channel this layer is thicker and has a depth ranging between 15m and 10m.

Grain size distribution affects the permeability of unconsolidated material in a multiaquifer system. The Hazen method of determining permeability values for an effective

grain size (D_{10}) and relating the arithmetic and geometric mean permeability to the arithmetic mean size (D_{10}) was applied to wadi floor sediments. Permeabilities were estimated using the Masch and Denny method which relates them to inclusive STD of the samples.

The more geophysical logs that show the same geohydrological environments, the greater the benefits which may be gained from logging. The synergistic character of these logs is due to the fact that each type of log measures different parameters. Analysed together each tends to support the conclusions drawn from the others.

Seven spontaneous potential, short resistivity, long resistivity and gamma ray logs illustrated the synergistic nature of the logs. The responses of the resistivity and nuclear logs to saturated wadi sediments are summarised below:

1- The natural-gamma count rate increases with increasing clay content.

2- The resistivity (short and long) decreases with increasing clay content.

3- The resistivity increases with an increase in the permeability while both parameters decrease with an increase in the clay content.

These relationships between the geophysical logs can help in identifying the hydrogeological characteristics of the wadi sediments. The simplified response of these four different logs can be summarised as follows :

1- The main aquifers in both wadis show index range <30 CPS and <200 ohm-m for the natural gamma logs and long & short resistivity logs respectively.

2- Natural gamma ray of the clay layer is >30 CPS while the resistivity logs (short and long) give < 10 ohm-m.

Thus the most permeable zone shows the highest resistivity and, as indicated by the natural gamma log, has the lowest clay content.

In both wadis excellent conditions prevail for the spreading of flood waters for replenishment of the underground supply. However the introduction of any permanent, extensive spreading system in the stream bed of the lower part of the wadi would be difficult without first acquiring the privately owned lands and the construction of some form of permanent bank protection.

The aquifers in both wadis show conditions that are favourable for recharge. These are:

1 A good horizontal value and range of aquifer permeability in both wadis.

2 The underlying aquifers are unconfined in most of Wadi Habawnah and the upper part of Wadi Baysh, which has a sufficiently low water table to allow additional storage.

3- Most of the upper and middle parts of both wadis are favourable for groundwater storage because of the unconfined nature of the aquifers coupled with high infiltration rates.

4- The lower parts of both wadis contain semi-confined to confined aquifers. The ability to recharge these by direct or indirect methods would be helpful for the agricultural development in both wadis.

5- The lower parts of both wadis show multi-aquifers containing coarse sediments which present favourable conditions for artificial recharge using well injection.

6- The unconfined aquifer shows high to moderate transmissivity, which would allow the lateral movement of recharge water without building up the groundwater mound that rises to be surface.

7- The agricultural land is characterised with a thick surface layer of clay (3.6 m) in which the hydraulic conductivity is low. This will restrict the infiltration to unacceptably low rates. Such an area would need to be treated with a suitable artificial recharge method of injection.

Reservoir operation has been simulated for the 50 and 100 year periods and for three demand alternatives (65, 70 and 75 mcm/year of water budget in Wadi Baysh and 8, 9, and 10 mcm of water budget in Wadi Habawnah). The mass curve analysis revealed the relationship between the irrigable area and the conjuctive use policy for each alternative as shown:

Wadi Baysh Annual water demand mcm	Irrigable area (ha) for one season	Irrigable area (ha) for two seasons	Irrigable area (ha) for three seasons	Irrigable area (ha) for four seasons
75	308%	**154%**	**103%**	77%
65	267%	**134%**	**89%**	67%
60	247%	**123%**	**82%**	62%

Wadi Habawnah Annual water demand mcm	Irrigable area (ha) for one season	Irrigable area (ha) for two seasons	Irrigable area (ha) for three seasons	Irrigable area (ha) for four seasons
10	**98%**	49%	33%	24%
9	**88%**	44%	29%	22%
8	**78%**	39%	26%	20%

As can be seen from the table, the increase in irrigable area is due to the decrease of the number of crop seasons. It seems that conjuctive use will be optimal if a demand of 75 mcm/year was adopted with three crop seasons in the year. This would allow a 3% increase in the irrigable area without affecting the safe yield. In Wadi Habawnah, the benefits obtained from irrigation are limited to one crop season in the year in which 98% of the irrigable area can be used. This occurs only if the 10 mcm demand conjuctive use policy is adopted for irrigation.

The author believes that the results from this simulation will give a more reliable indication of the actual benefit for irrigation systems in which the risk of failure is very low.

As a conjunctive use feasibility study of the area, the interest has been in how the groundwater can best gain from the flood water and vice versa. As a result, the flood and ground water system might be developed using conjunctive use management for good agricultural productivity in the area. The groundwater resources development can be achieved by determining the maximum withdrawal rate possible without causing undesirable effects.

A plan to ensure a steady state relationship between the surface and subsurface storage would help to manage the perennial yield and minimise the mining yield. Accordingly, the results show that building a reservoir in both wadis is economically justifiable. In spite of that, neither dam will extend the irrigable area significantly, but both will help to distribute the flood water more efficiently, using artificial methods such as artificial groundwater recharge. Also, such a plan will help to reduce evaporation effects and increase the subsurface water storage for irrigation needs besides protecting the agricultural lands from flash floods.

Considering the existing traditional irrigation system in both wadis, the wadi channel remains the main source of recharge water in which 31% of the wadi seepage

reaches the saturated zone.

To improve the flood spreading system in both wadis, the author suggests building long narrow channels with a width and depth of 2 and 3m, respectively (see Figures 9.25). Such a plan will help to distribute the flood water to recharge the aquifer and to enhance the groundwater quality.

10.2 Recommendations

The following suggestions for future research are recommended due to the problems that were noted during the collection and analysis of the data on which this thesis is based.

1- For ease of planning research on the water resources of Saudi Arabia it is of great importance that the Hydrogeology and Hydrology Departments of the Ministry of Agricultural and Water Resources should establish a section to co-ordinate data collection and distribution in order to improve access to the data and to encourage more research.

2- In order to improve data collection it is important that the Hydrogeology and Hydrology Departments of THE Ministry of Agricultural and Water Resources should install automatic water level recorders in existing observation wells to determine the groundwater storage. Long term measurements would enhance the accuracy of estimating the water balance in the area.

3- No core material from boreholes in either wadi were available due to the lack of storage systems to keep them in sequence. Any future drilling programme should be accompanied not only by logs of the cores but ideally by curated storage of the materials.

4- The computation of the groundwater budget in both wadis would be more reliable if the irrigation return flow as well as the artificial withdrawal of groundwater were determined. To reach such a goal it is recommended that in future a time record should

be kept of pumping wells in hours, per day, season and annually.

5- Both wadis show limited water resources in which every drop of water is valuable. Accordingly, the farmers should be educated to know the water quantity that they need for irrigation. Also they should be encouraged to use subsurface irrigation to minimise the evaporation effects around the crops.

6- It is highly recommended that future investigations should include field experiments in both wadis in order to determine the recharge rates using the existing flood spreading systems.

7- Studying the quantities of silt carried in flood waters and their influence on groundwater recharge rates would help determine processes of aquifer recharge and this in future would indicate the nature and numbers of disilting basin to be used in the recharge procedure.

8-Trapping of 70 mcm and 10 mcm of runoff each year in Wadi Baysh and Wadi Habawnah by retaining dams in both wadis could extend the time available for infiltration and increase the recharge to the aquifer to compensate for increased pumping elsewhere.

9- Initial capital investment is needed to ensure that the programme for the conjuctive use of water resources based on both surface reservoirs and pumping wells could be established.

Bibliography

Abdul-kar, H.M., 1988. Development of agriculture in Tihamah: Regional growth and development in the Jizan region, Saudi Arabia. (PhD. Thesis: University of Arizona).

Al-Hageri, F.Y., 1977. Groundwater studies of Wadi Qudaid. Institute of applied geology, King Abdulaziz University, Jeddah, Saudi Arabia. Research series no. **2**. 132-178

Al-Jerash, M.A., 1982, Rainfall runoff relationship in south west Saudi Arabia, *Journal of the Faculty of Arts and Humanities,* King Abdulaziz University, Volume **2**, 175-199.

Al-Jarash, M.A., 1989. The climatic water balance in Saudi Arabia 1970-1986. Scientific Publishing Centre, King Abdulaziz University, Jeddah, Saudi Arabia. 441pp

Al-Otaiby, A.A., 1981. The Quaternary evolution of Wadi Bishah (Saudi Arabia): A morpho-climatic interpretation. (M.A. Thesis: Michigan State University).

Al-Qurashi, M.D.A., 1981. Synoptic climatology of the rainfall in the Southwest region of Saudi Arabia (M.Sc. Thesis: Western Michigan University, United States of America).

Alehaideb, I., 1985. Precipitation distribution in the Southwest of Saudi Arabia (PhD. Thesis: Arizona State University).

Alger, R.P., 1966. Interpretation of electric logs in fresh water wells in unconsolidated formations. In *Society of Professional Well Log Analysts Annual Logging Symposium* **7**, Tulsa, Okla. Transactions: Houston, Society of Professional Well Log Analysts, CC1-25.

Anderson, R.E., 1979. Geology of the Wadi 'Atf (sheet 17/43 A) and Mayza scale 1: 100,000. *Saudi Arabian Directorate General of Mineral Resources Bulletin* **25**, 33 pp.

Asano, T., 1985. Overview. In: Artificial recharge of groundwater (Edited by T. Asano). 3-20. Butterworth, Boston.

Back, W., and B.B. Hanshaw, 1965, Chemical geohydrology. Adv. Hydrosci., 1, pp. 49-109.

Baillieul, T.A., 1975. A reconnaissance survey of the cover sands in the Republic of Botswana. *Journal of Sedimentary Petrology* , **45**, 494-503.

Ball, J.W., Jenne, E.A., and Nordstrom, D.K., 1980, WATEQ2- a computerised chemical model for trace and major element speciation and mineral equilibrium of natural waters. In chemical modelling in aqueous systems (ed. E.A. Jenne), ACS Symposium 93,pp. 815-835.

Bardossy, A., Bogardi, I. and Kelly, W.E., 1986. Geostatistical analysis of geoelectric estimates for specific capacity. *Journal of Hydrology.* **84**, 81-95.

Barker, R.D. and Worthington, P.F., 1973. Some hydrogeophysical properties of the Bunter Sandstone of Northwest England. *Geoexploration* **11**, 151-170.

Barry, R., 1992. Mountain weather and climate: Routledge: London. 226-283

Bear, J., 1979. Hydraulics of groundwater: New York, McGraw-Hill. 19-89

Bianchi, W.C. and E.,Jr., Huskell,1968. Field observations compared to the Dupint Forcheimen theory for mound heights under a recharge basin. *Water Resources Research* **4**(5) 1049-1057.

Bianchi, W.C., Nightingale, H.I. and McCormick, R.L., 1978. Fresno, California, subsurface drain collector - deep well recharge system. *Journal.American Works Association.* **70**(8), 427-435.

Bierschenk, W.H., 1963. Determining well efficiency by multiple step-drawdown tests. *International Association of Scientific Hydrology. Publication.* **64,** 493-507.

Bouwer, H., 1978, Ground water hydrology: McGraw-Hill, New York, 480 p

Bose, R.N., Chatterjee, D. and Sen, A.K., 1973. Electrical resistivity surveys for ground water in the Aurangabad sub-division, Gaya District, Bihar, India. *Geoexploration* **11**, 171-181.

Brown, G.F., 1960. Geomorphology of Western and Central Saudi Arabia. *21st. International. Geology. Conference. Copenhagen, Report* **21**, 150-159.

Brown, G.F., 1970. Eastern margin of the Red Sea and the coastal structures in Saudi Arabia: *Philosophical Transactions of the Royal Society of London*, Ser. A. **267**, 75-87.

Brown, G.F. and Jackson, R.O., 1959. Geologic map of the Asir quadrangle, Kingdom of Saudi Arabia: United States. Geological Survey Miscellaneous Geologic Investigation Map **I-217 A**, scale 1:500,000; reprint, Saudi Arabian Directorate General of Mineral Resources, Geologic Map **GM-217 A**.

Brown D.L., 1971. Techniques for quality of water interpretations from calibrated geophysical logs. *Groundwater.* **9**, 25-38.

Brown, L.H. and Coheme, J., 1972. A study of the agroclimatology of the highlands of eastern Africa. Technical note no. **175**, 41-65 World Meteorological Organisation, Geneva.

Carman, P.C., 1937. Fluid flow through a granular bed. *Transactions of the Institution of Chemical Engineers (London)***15,** 150-156.

Chapman, R.W., 1978. Geology. In: Quaternary period in Saudi Arabia, 1 (Edited by S. S. Al-Sayari and J. G. Zotl), 4-18. Springer-Verlag Wien.

Chebotarev, I.I., 1955. Metamorphism of natural waters in the crust of weathering. Geochemica et Cosmochimica. *Acta.* **8**, 22-48, 137-170, 198-212.

Cherry, J.A., Shaikh, A.U., Tallman, D.E. and Nicholson, R.V., 1979. Arsenic species as an indicator of redox conditions in groundwater. *Journal of Hydrology.* **43**, 577-580.

Chow, V.T., 1964. Handbook of applied hydrology: McGraw-Hill. Inc., section **24.** New York.

Clark, A., 1989. Lakes of the Rub al Khali. Aramco World **3**, 28-33.

Cluff, C.B., 1967. Rafts: a new way to control evaporation. *Crops and Soils Magazine, November.23-30*

Cluff, C.B., 1985. Development and evaluation of water harvesting systems. *Report* **OURR-A-001-AR12(6)**, Arizona Water Resources Research Center, University of Arizona, Tucson, Arizona.5.1-5.22

Cluff, C.B., 1987. Water harvesting systems in arid lands. *Kuwait Symposium on Management and Technology of Water Resources in Arid Zones*, Kuwait. 13pp.

Colman, R.G., Fleck, R.J., Hedge, C.E. and Ghent, E.D., 1977. The volcanic rocks of southwest Saudi Arabia and opening of the Red Sea. Red Sea Research 1970-1975: *Saudi Arabian Directorate General of Mineral Resources Bulletin* **22**, D1-D30.

Colman, R.G., Hadley, D.G., Fleck, R.J., Hedge, C.E. and Donato, M.M., 1979. The Miocene Tihamah Asir ophiolite and its bearing on the opening of the Red Sea. Evolution and mineralization of the Arabian-Nubian Shield: King Abdulaziz University, Institute of Applied Geology, *I.A.G. Bulletin* 3, **1**, 173-186.

Cordery, I., Pilgrim D.H. and Doran, D. G., 1983. Some hydrological characteristics of arid western New South Wales. Hydrology and water resources Symposium, Institution of Engineers of Australia. National Conference Publication. no. **83/13**, 287-292.

Covington, A.K., Robinson, R.A. and Bates, R.C., 1966. The ionisation constant of deuterium oxide from 5° to 50°. *Journal of Physical Chemistry* **16**, No 2, 3820-3824.

Critchfield, H., 1974. General climatology: Englewood Cliffs, N.J. Prentice-Hall, 235-241.

Croft, M.G., 1971. A method of calculating permeability from electric logs. *United States.Geological Survey Professional Paper* **750B**, B265-B269.

Dansby, D.A., 1992. Graphical Well Analysis Package Version 2.0. Oceanside, CA.

Davis, J.C., 1986, Statistics and data analysis in geology, second edition, Wiley, New York. 502-515

De Marsily, G., 1986. Quantitative hydrogeology: Academic Press, London, Ch-8.

Development-Hydrogeological Section, 1978. Investigation and detailed studies for the agricultural development of South Thama, Vol. **A3**, Part 3 Geology and Hydrogeology. Ministry of Water Resources and Agriculture, Riyadh, Saudi Arabia.

Division of Hydrology, 1967. Hydrological Informations No. **12**. Ministry of Water Resources and Agriculture, Riyadh, Saudi Arabia.

Division of Hydrology, 1971. Hydrological Informations No. **50**. Ministry of Water Resources and Agriculture, Riyadh, Saudi Arabia.

Division of Hydrology, 1973. Hydrological Year Book, Area I, IV and VI. Ministry of Water Resources and Agriculture, Riyadh, Saudi Arabia.

Division of Hydrology, 1974. Hydrological Publication No. **72**. Ministry of Water Resources and Agriculture, Riyadh, Saudi Arabia.

Division of Hydrology, 1981. Rainfall report for the period 1971-1975. Vol. **1** No. 98. Ministry of Water Resources and Agriculture, Riyadh, Saudi Arabia.

Division of Hydrology, 1981. Rainfall report for the period 1976-1980. Vol. **1** No. 98. Ministry of Water Resources and Agriculture, Riyadh, Saudi Arabia.

Division of Hydrology, 1981. Rainfall report for the period 1980. Vol. **1** No. 96. Ministry of Water Resources and Agriculture, Riyadh, Saudi Arabia.

Division of Hydrology, 1988. Climate Atlas of Saudi Arabia. Ministry of Water Resources and Agriculture, Saudi Arabia.

Division of Hydrology, 1988. Habawnah basin report. Report, Vol. **B1**. Ministry of Water Resources and Agriculture, Riyadh, Saudi Arabia.

Division of Hydrology, 1988. Habawnah basin sediment report. Report, Vol. **B8**. Ministry of Water Resources and Agriculture, Riyadh, Saudi Arabia.

Division of Hydrology, 1988. Habawnah basin surface water data. Final Report. Vol. **B1, B2** and **B4**. Ministry of Water Resources and Agriculture, Riyadh, Saudi Arabia.

Dobrin, M.B. and Savit, C.H., 1988. Introduction to geophysical prospecting, 4th edition: New York, McGraw-Hill, Ch-11.

Domenico, P. A., 1972, Concepts and Models in Groundwater Hydrology. McGraw-Hill, New York.

Drever, J.I., 1982. The geochemistry of natural waters: London, Prentice-Hall,Ch-9.

Drever, J.I. and Smith, C.L., 1978. Cyclic wetting and drying of the soil zone as an influence on the chemistry of ground water in arid terrains. *American Journal of Science*. **278**, 1448-1454.

Drew, W.M., 1972. Evaporation control: a comparative study of six evaporation restriction media. AQUA, State Rivers and Supply Commission of Victoria. 15-37pp

Driscoll, F.G., 1989. Groundwater and Wells, 2nd edition: St Paul, Minnesota, Johnson Division, Ch-6, Ch-8 and Ch-16.

Duprat, A., Simler, L. and Ungemach, P., 1970. Contribution de la prospection éléctrique à la récherche des caracteristiqes hydrodinamiques d'un milieu aquifère.*Terres Eaux*. **23, 63.**

Durfor, C.N., and Becker, E., 1964. Public water supplies of the 100 largest cities in the United States, 1962, *United States. Geological Survey Water-Supply Paper 1812*. 64 pp.

Durov, S.A., 1948. Natural waters and graphic representation of their composition: *Nauk SSSR Doklady*. **59**, 87-90.

Dvoracek, M.J. and Peterson, S.H., 1971. Artificial recharge in Water Resources Management. *American Society of Civil Engineering Journal of Irrigation and Drainage Division*. **97**, no. IR2, 210-232.

Eaton, G.P. and Watkins, J.S., 1970. The use of seismic refraction and gravity methods in hydrogeological investigations. *Geology Survey Canada, Economic Geology . Report* No. **26**, 544-568.

Eden. R.N. and Hazel, C.P., 1973. Computer and graphical analysis variable discharge pumping test of wells. *Institution of Engineers of Australia. Civil Engineering Transactions.* **5-10.**

Edgell, H.S., 1990. Evolution of the Rub al Khali desert. *Journal of King Abdulaziz University Earth Science.*, vol. **3**, Special Issue: 1st Saudi Symposium on Earth Science, Jeddah, 109-126.

Edmunds, W.M., 1977. Groundwater geochemistry controls and processes. Proceedings Conference on Groundwater Quality Measurement, Prediction and Protection. 115-47. Water Research Centre, Medmenham, England.

Egboka, C.E. and Umk, K.O., 1986. Comparative analysis of transmissivity and hydraulic conductivity values from the Aljali aquifer system of Nigeria. *Journal of Hydrol.*ogy **83**, 185-196.

El-Khatib, A.B., 1980, Seven Green Spikes (2nd edition): Darx Al-Asfahani, Jeddah, Ch-4,Ch-9 and Ch-14.

Eriksson, E., 1985. Principal and applications of hydrochemistry: Chapman and Hall, London, 187 pp. *Examples from Tanzania. In: Agroclimatology of the highlands of eastern Africa*

Fair, G.M., and Hatch, L.P., 1933. Fundamental factors governing the streamline flow of water through sand. *Journal American Works Association.* **25**, 1551-1565.

Fairer, G.M., 1982, Reconnaissance geology of the Wadi Baysh quadrangle, sheet **17/42B**, scale 1:100,000. Kingdom of Saudi Arabia: Saudi Arabian Deputy Ministry for Mineral Resources Open-File Report US Geological Survey- **OF-02-85**, 23 pp.

Fairer, G.M., 1985. Geologic map of the Wadi Baysh quadrangle, sheet 17 F, scale 1 :250,000. Kingdom of Saudi Arabia: Saudi Arabian Deputy Ministry for Mineral Resources Technical Record Map **GM-77A**, with text, 23 pp.

Ferris, J.G., Knowles, B.O., Brown, R.H. and Stallman, R.W., 1962. Theory of aquifer tests. *United States. Geological Survey Water Supply* Paper, **1536-E**.174 pp.

Fetter, C.W., 1988. Applied hydrogeology: Ohio, Merrill Publishing Company, 2nd edition.438-442.

Freeze, R.A. and Cherry, J.A., 1979. Groundwater: Prentice Hall, Inc., Englewood Cliffs, NJ. Ch-7.

Friedman, G.M. and Sanders, J.E., 1978. Principles of Sedimentology: John Wiley and Sons, New York.Ch-3

Gaur, R.S. and Singh, I., 1965. Relation between permeability and gamma-ray intensity for the Oligocene sand of an Indian field, India (Republic): *Oil and Natural Gas Communication. Bull.* **2**, 74-77.

Gettings, M.E. and Stoeser, D.B., 1981. A tabulation of radiometric age determination for the Kingdom of Saudi Arabia: *United States. Geological Survey Saudi Arabian Mission* Miscellaneous Document **20**, 52 pp.

Ghearghe, A., 1978. Processing and synthesis of hydrological data. Abacus press, Tunbridge Wells, Keut.Ch-3.

Gillmann, M., 1968. Primary results of a geological and geophysical reconnaissance of the Jizan coastal plain in Saudi Arabia: AIME Regional Tech. Symposium, Rebt., 2nd edition, Dahran, 189-208.

Gorham, E., 1961. Factors influencing supply of major ions to inland waters with special reference to the atmosphere. *Bulletin Geol, Geological Society of America* **72**, 795-840.

Greenwood, W.R., 1985. Geologic map of Bir Idamah quadrangle, sheet 18 G, scale 1:250,000. Kingdom of Saudi Arabia: Saudi Arabian Deputy Ministry for Mineral Resources Technical Record Map **GM-79 A, C**, with text, 30 pp.

Greenwood, W.R., Stoeser, D.B., Flesck, R.J. and Stacy, J.S., 1982. Late Proterozoic island arc complexes and tectonic belts in the southern part of Arabian Shield, Kingdom of Saudi Arabia: Deputy Ministry for Mineral Resources Open-File *Report* **USGS-OF-02-8**, 46 pp.

Griffis, G.L., 1976. Artificial recharge in the Grand Prarie, Arkansas. *Bull.* **810** August Agricultural Experiment Station, University of Arkansas, Fayettville, Arkansas.

Guyod, H., 1966. Interpretation of electric and gamma ray logs in water wells. *Log Analyst* **6**, no. 5, 29-44.

Hantush, M.S., 1964. Hydraulics of wells. In: Advances in hydroscience, (Edited by V. T. Chow). Vol. **1**, 281-432. Academic Press, New York

Hastenrath, A., Hafez, A. and Kaczmarczyk, E.B., 1979. A contribution to the dynamic climatology of Arabia. Archiv fur Meterologic Geophysiks und Bioklimatologic. Serie B.**27,** 103-120.

Hawkins, L.V. and Maggs, D., 1961. Nomograms for determining maximum errors and limiting conditions in seismic refraction survey with a blind zone problem *Geophysical. Prospecting*. **9**, 526-32.

Heigold, P.C., Gilkerson, R.H., Reed, P.C. and Cartwright, K., 1978. Mapping Aquifer Transmissivity by surface electrical methods. *EOS .American Geophysical Union Transactions* **59**, no.4, April.

Heiland, C.A., 1963. Geophysical Exploration. Hafner Publishing Co., New York. Ch-9 and Ch-11

Hellwig, D.H.R, 1974. Evaporation of water from sand, 5: The effect of evaporation on the concentration of salts dissolved in water stored in sand. *Journal of Hydrology*. **21**, 101-110.

Hem, J.D., 1989. Study and interpretation of the chemical characteristics of natural water: *UNITED STATES. Geological Survey Water Supply* Paper **1473**. 263 pp.

Henderson, P., 1986. Inorganic geochemistry. Pergamon Press, London. Ch-10.

Henriet, J.P., 1976. Direct applications of the Dar Zarrouk parameters in ground water surveys. *Geophysiscs Prospecting.* **24**, 344-353.

Hotzl, H. and Zotl, J.G., 1984. Climatic changes during the Quaternary period. Quaternary period in Saudi Arabia. (Edited by J. G. Zotl): Springer-Verlag, Wien and New York 360pp.

Huisman, L. and Olsthoorn, T.N., 1983. Artificial groundwater recharge: Pitman Advanced Publishing Program, Boston, Massachusetts.Ch-1 and Ch-2.

Ineson, J., 1970. Hydrogeological and groundwater aspects of artificial recharge. Proceedings of a conference held at the University of Reading. v. **1**, 1-23.

Interpex Limited, 1990. Resix computer programme. DC resistivity data interpretation software, Golden, CO, USA .

Italconsult, 1965. Land and water surveys on Wadi Jizan, U.N. Special Fund Project. FAO, Rome.

Italconsult, 1973. Climate in area VI south. Hydrological special paper No. **2**, Ministry of Water Resources and Agriculture, Saudi Arabia.

Jacob, C.E., 1944. Notes on determining permeability by pumping tests under watertable conditions. *United States. Geology Survey, Open File Report.* 26pp

Jacob, C.E., 1947. Drawdown test to determine effective radius of artesian well. *Transactions, American Society of Civil Engineering* **112**, Paper 2321, 1047-1064.

Johnson, P., Scheibner, E. and Smith, A., 1987. Basement fragments, accreted tectonostratigraphic terranes, and overlap sequences: Elements in the tectonic evolution of the Arabian Shield. Geodynamics Series. *Transactions, American Geophysical Union.* **17**, 323-343.

Johnston, R.J., 1980. Multivariate statistical analysis in geography. Longman Inc., New York.150-165.

Jones, G.P., 1972. Management of underground water resources. *Quarterly Journal of Engineering Geology.* **4**, 317-328.

Jones, O.R., Goss, D.W. and Schneider, A.D., 1974. Surface plugging during basin recharge of turbid water. *Transactions American Society of Agricultural Eng*ineers **17**, no. 6, 1011-1019.

Jones, P.H. and Buford, T.B., 1951. Electric logging applied to groundwater exploration.*Geophysics*. **16**(1), 115-139.

Keller, G.V. and Frischknecht, F.C., 1966. Electrical methods in Geophysical Prospecting. Pergamon Press, Oxford Ch-4 and Ch-5

Kelly, W.E., 1977. Geoelectric sounding for estimating aquifer hydraulic conductivity. *Ground Water* . **15**, No. 6, 420-424.

Kelly, W.E. and Frolich, R.K., 1985. Relationships between aquifer electrical and hydraulic properties. *Ground Water*. **23**, No. 2, 182-189.

Kennedy, V.C. and Brown, T.E., 1966. Experiments with a sodium-ion electrode as a means of studying cation-exchange rates: National Conference on Clay and Clay Minerals, 13th, Madison 1964, *Proceedings*, 351-352.

Keys, W.S., 1968. Well logging in ground-water hydrology. *Ground Water*. **6**, No. 1, 10-19.

Keys, W.S., 1989. Borehole geophysics applied to ground-water investigations. National

Water Well Association, Dublin, Ohio.Ch-1, Ch-4 and Ch-10.

Keys, W.S and MacCary, L.M., 1971. Application of borehole geophysics to water-resources invistigation. Water resources investigations of the United States Geological Survey (Chapter E1 - Book 2).

Kister, L.R. and Hardt, W.F., 1966. Salinity of the ground water in western Pinal County, Arizona *United States. Geological Survey Water Supply* Paper **1819-E**, 21pp.

Knorr, D.B. and Cliett, T., 1985. Proposed groundwater recharge at El Paso, Texas. In: Artificial recharge of groundwater (Edited by T. Asano). 425-480. Butterworth, Boston.

Ku, H.F.H. and Simmons, D.L., 1983. Recharge basins for storm water management on Long Island, New York. Proceedings of the NWWA Eastern Regional Conference on Ground Water Management, Orlando, Florida. 17-43.

Kursman, G.P. and Ridder, N.A., 1990. Analysis and evaluation of pumping test data, 2nd edition: International institute for land reclamation and improvement. Wageningen, The Netherlands. Ch-1.

Lennox, D.H., 1966. Analysis of step-drawdown test. *Journal. Hydraulics Division. Proceeding of American Society of Civil Engineers.* 92(HY6), 25-48.

Lichtlen, W.F., Stannard, D.I. and Kouma, E., 1980. Investigation of artificial recharge of aquifers in Nebraska, water resources investigations. 80-93. September. United States. Geological Survey, Lincoln, Nebraska.

Lloyd, J.W. and Heathcote, J.A., 1985. Natural inorganic hydrochemistry in relation to groundwater. Clarendon Press, Oxford. 296 pp.

Maclaren International Limited, 1978. Water and agricultural development studies. Arabian Shield. Hydrogeological investigations, Annex. 3 Report to the Ministry of Agriculture and Water, Saudi Arabia.

Maillet, R., 1947. The fundamental equations of electrical prospecting.*Geophys.* **XII**, No. 4, 529-556. MAP technical notes 7, 54 pp.

Masch, D.F. and Denny, K.J., 1966. Grain size distribution and its effect on the permeabilty of unconsolidated sands.*Water Resources Research* **2**, No.4, 665-677.

Minister of Agriculture and Water, 1978. Hydrogeological information in Arabian Shield and Tehamat Asir, Minister of Agriculture and Water, Riyadh, Saudi Arabia

Mazac, O., Cislerova, M. and Vogel, T., 1988. Application of geophysical methods in describing spatial variability of saturated hydraulic conductivity in the zone of aeration. *Journal of Hydrology* **103**, 117-126.

Mazac, O., Kelly, W.E. and Landa, I.A., 1985. Hydrogeophysical model for relationships between electrical and hydraulic properties of aquifers. *Journal of Hydrol.*ogy **79**, 1-19.

Mazor, E., 1991. Applied chemical and isotopic groundwater hydrology: Open University Press, Ch-5 and Ch-6.

McClure, H.A., 1978. Ar Rub Al Kali. In: Quaternary period in Saudi Arabia. (Edited by J. G. Zotl): Springer-Verlag, Wien and New York, 252-263.

McKee, E.D., 1963. Origin of the Nubian and similar sandstone: *Geologische. Geological Rundschau.* Bd. **52,** 551-587.

Mendolson, K.S. and Cohen, M.H., 1982. The effect of grain anisotropy on the electrical properties of sedimentary rocks.*Geophysics* 47(2), 257-263.

Ministry of Agriculture and Water, 1984. Water atlas of Saudi Arabia, Riyadh, 112 pp.

Mooney, H.M.and E. Orellana, 1966, Master table and curves for vertical electrical sounding over layered structures. Interciencia, Madrid. 34pp.

Mooney, H.M., 1977. Handbook of engineering geophysics: Bison Instruments Inc. United States of America.
130pp

Moore, J.McM., 1983. Tectonic fabric and structural control of mineralization in the southern Arabian Shield: a compilation based on satellite imagery interpretation. Saudi Arabian Deputy Ministry for Mineral Resources. *Open-File Report* **USGS-OF-03-105**, 34 pp.

Motts, W.S., 1983. Feasability of increasing water supplies and preventing environmental damage by artificial recharge in Massachusetts. Publication no. **132** Jan. Water Resources Research. Center, University of Massachusetts, Amherst, Massachusetts. Compiled by O'Hare, M.P., D.M., Fairchild, P.A. Hajali and L.W. Canter, 1986. Artificial recharge of groundwater. Lewis Publisher, Michigan. Ch-2.

Muller, E., 1977. Agriculture development of South Tihamah. Unpublished reports for Saudi Arabian Ministry of Agriculture and Water by German Consultants Frankfurt a.m.

Nieuwold, S., 1974. The influence of aspect and elevation on daily rainfall: Some examples from Tanzania. In Agroclimatology of the highland of eastern Africa, No. 389, 16-23. Geneva: World Meteorological Organisation.

Nightingale, H.I. and Bianchi, W.C., 1973. Ground water recharge for urban use: Leaky-Acres project. *Ground Water* **11**(6): 36-43.

Norris, S.E. and Fidler, R.E., 1965. Relation of permeability to partical size in glacial-outwash aquifer at Piketon, Ohio. *United States. Geological Survey Professional Paper* **525D**, D203-D206.

Oaksford, E.T., 1985. Artificial recharge methods, hydraulics and monitoring. In: Artificial recharge of groundwater (Edited by T. Asano). Butterworth, Boston 69-128.

Pacl, J., 1973. Orographic influences on distribution of precipitation; physiographical factors and hydrological approaches. In: Distribution of precipitation in mountainous area, Vol. **1**, No. 326, 67-72. Geneva: World Meteorological Organisation.

Pallister, J.S., 1982. Reconnaissance geology of the Jabal al Ilman quadrangle, sheet 18/44 A, scale 1:100,000. Kingdom of Saudi Arabia: Saudi Arabian Deputy Ministry for Mineral Resources *Open-File Report* **USGS-OF-02-90**, text, 61 pp.

Palmer, D., 1981. An introduction to the generalised reciprocal method of seismic refraction interpretation. *Geophysics* **46**, No. 11, 1508-1518.

Papadopulos, I.S. and Cooper, H.H., 1967. Drawdown in a well of large diameter. *Water Resources Research* **3**, 241-244.

Parker, T.W.H., 1982 Assessment of the mineral potential of the Kutam-Al Halahia district, south east Asir: Saudi Arabian Deputy Ministry for Mineral Resources Open-File Report RF-OF-02-22, scale 1:100,000; text, 98pp

Pettyjohn, W.A., 1981. Introduction to artificial ground water recharge. **EPA-600/2-81-236**, Oct. (Edited by R. S. Kerr). Environmental Research Laboratory, United States. Environmental Protection Agency, Ada, Oklahoma.

Philby, H.St.J.B., 1952. Arabian highlands. Duckworth, London.Ch-9

Piper, A.M., 1944. A graphic procedure in geochemical interpretation of water analyses. *Transaction, Amercan Geophysics Union*. **25** 914-923.

Plummer, L.N., Jones, B.F. and Truesdell, A.H., 1984. WATEQF- A fortran IV version of WATEQ: a computer program for calculating chemical equilibrium of natural waters. *United States. Geological Survey Water-Resources Investigation* . **76-13**.

Ponzini, G., Ostroman, A. and Molinari, M., 1984. Empirical relationship between electrical traverse resistance and hydraulic transmissivity. *Geoexploration*. **22**, 1-15.

Powers, R.W., Ramirez, L.F., Redmond, C.D. and Elberg, E.L.,Jr, 1966. Geology of the Arabian Peninsula-sedimentary geology of SaudiArabia:*United States. Geological Survey Professional Paper* **560D**, D147.

Preuss, F.A. and Todd, D.K., 1966. Specific yield of unconsolidated alluvium, Water Resources Center Contribution No. **76**.12-18 University of California, Berkeley, California.

Qari, M.T., 1990. Geological analysis of parts of the southern Arabian Shield based on Landsat TM imagery (PhD. Thesis: University College, London).

Rankama, K., and T.G., Sahama, 1950, Geochemistry: Chicago, University of Chicago Press, 912 p.

Raghunath, H.M., 1982. Ground water. Wiley Eastern Ltd, New Delhi.pages.Ch-8

Riofinex Geological Mission, 1978, An investigation of the geology and exploration potential of the wadi Wassat-Kutam District, south east Asir, Saudi Arabia: Riofinex Geological Mission (Saudi Arabia) Report RF-1978-3, 129 pp.

Rider, M.H., 1991. The geological interpretation of well logs. Caithness, Whittles Publishing.175pp

Robertson, F.N., 1991. Geochemistry of ground water in alluvial basins of Arizona and adjacent parts of Nevada, New Mexico, and California. United States. Geological survey professional paper 1406-C. 90pp.

Robinove, C.J., Langford, R.H. and Brookhart, J.W., 1958. Saline-water resources of North Dakota: *United States. Geological Survey Water Supply Paper* **1428**, 132 pp.

Rorabaugh, M.J., 1953. Graphical and theoretical analysis of step-drawdown test of artesian well. *Proceedings, American Society of Civil Engineering* **79**, separate no. 362, 23pp

Rose, H.G. and Smith, H.F., 1957. A method for determining permeability and specific capacity from effective grain size. *Illinois State Water Survey Circular*, no. **59**.3pp

Rubin, Y., Mavko, G. and Harris, J., 1992. Mapping permeability in heterogeneous aqufers using hydrologic and seismic data, *Water Resources Research* **28**, no.7, 1809-1816.

Sable, E.G., 1982. Reconnaissance geology of the Najran quadrangle, sheet 17/44 C, scale 1:100,000. Kingdom of Saudi Arabia: Saudi Arabian Deputy Ministry for Mineral Resources *Open-File Report* **USGS-OF-03-7**, text, 25 pp.

Sable, E.G., 1985. Geologic map of the Wadi Najran quadrangle, sheet 17 G, scale 1: 250,000. Kingdom of Saudi Arabia: Saudi Arabian Deputy Ministry for Mineral Resources Technical Record Map **GM-78A**, with text, 17pp.

Sarma, V.V.J. and Rao, V.B., 1962. Variation of electrical resistivity of river sands, calcite, and quartz powders with water content. *Geophysics* **27**, 470-479.

Sawyer, J., 1956. The physical and dynamical problems of orographic rain. *Weather* . **11**(12), 375-381.

Schimschal, U., 1981. The relationship of geophysical measurements to hydraulic conductivity at the Brantley Damsite, New Mexico. *Geoexploration* . **19**. 115-125

Scottish Crop Research Institute, 1995. Personal communication, Dundee.

Seidell, A., 1952. Solubilities, I, 3th edition. *American Chemistery. Socity /* Van Nostrand, Princeton, New Jersey.

Sen, Z., 1983. Large diameter well evaluations and applications for the Arabian Shield, in Symposium on water resources in Saudi Arabia, management, treatment and utilisation, v. 1 college of Engineering, King Saudi University, Riyadah, A257-A270.

Serra, O., 1984. Fundamentals of well-log interpretation: Elsevier Science Publishers B. V., Amsterdam Ch-1 and Ch-3.

Sillen, L.G. and Martell, A.E., 1967. Stability constants-supplement no. 1: Ljunggren, P., 1955. Geochemistry and radioactivity of some Mn and Fe bog ores. *Geologiska Foreningen Stockholm, Forhandlingar* . **77**, 33-44.

Sir Niwas and Singhal, D.C., 1981. Estimation of aquifer transmissivity from Dar-Zarrouk parameters in porous medium. *Journal. Hydrology.* **50**, 393-399.

Sir William Halcrow and Partners, 1972. Irrigation development in the Wadi Jizan. Ministry of Water Resources and Agriculture, Saudi Arabia. 39pp

Sjogren, B., 1984. Shallow refraction seismics. Chapman and Hall, London. Ch-2 and Ch-3

Skinner, A.C., 1988. Practical experience of borehole performance evaluation. *Journal. Institute of Water Environment and Management.* **2**, 332-340.

Slichter, C.S., 1899. Theoretical investigation of the motion of ground waters. *United States. Geological Survey, 19th Ann. Report.* **2**, 322 pp.

Sorman, A.U., Abdulrazzak, M.J., 1987, Regional flood discharge analysis south west region of the Kingdom of Saudi Arabia, V.P. Singh (ed.), Regional flood analysis. 11-25 D. Reidel Publishing Company.

Sogreah, 1967. Agriculture: provisional reconnaissance report, area vi, Saudi Arabia. Report prepared for the Ministry of Agriculture and Water, in connection with the water and Agricultural Development studies of Area vi, Ar Riyadh, DECEMBER. Sorman, A.U. and Abdulrazzak, M.J., 1993. Infiltration-recharge through wadi beds in arid regions. *Hydrological Sciences Journal* **38**, no 3, 173-187.

Sowayan, A.M. and Allayla, R., 1989. Origin of saline ground water in Wadi Ar-Rumah, Saudi Arabia. *Ground Water.* **27**(4), 481-490.

Stoeser, D. and Camp, V., 1985. Pan-African microplate accretion of the Arabian Shield. *Bulletin, American Society of Geology.* **96**, 817-826.

Suess, M.J., 1982. Examination of water for pollution control. v.**2**. Pergamon Press, Oxford. 555pp

Szikszay, M., Teissedre, J.M., Barner, U. and Matsui, E., 1981. Geochemical and isotopic characteristics of spring and groundwater in the state of Sao Paulo, Brazil. *Journal of Hydrology.* **54**, 23-32.

Taha, M., Harb, S., Nagib, M. and Tantawy, A., 1981. The climate of the Near East. In: Climates of southern and western Asia. **9**, 183-229. Elsevier, New York.

Taylor, D., 1948. Fundamentals of soil mechanics. John Wiley and Sons, Inc., New York.Ch-4.

Terzhagi, C., 1925. Principle of soil mechanics. *Engineering News Record.* **95**, 742-746.

Theis, C.V., 1935. The relation between the lowering of the piezometric surface and the rate and duration of discharge of a well using ground-water storage. *Trans. Am. Geophysic. Union* . **16**, 519-524.

Todd, D.K., 1959. Groundwater Hydrology. Wiley, New York. 336pp.

Todd, D.K., 1970. The water encyclopedia. Water information center, Port Washington, New York 559 pp.

Todd, D.K., 1980. Groundwater Hydrology, 2nd edition. Wiley and Sons, New York. 535 pp.

Truesdell, A.H. and Jones, B.F., 1974. WATEQ, a computer program for calculating chemical equilibria of natural waters. *United States.Geological Survey Journal of Research.* **2**, 233-248.

United States Environmental Protection Agency, 1975. National interim primary drinking water regulations, Part 141. Federal Register **40**(248), DECEMBER. 59566-59588

United States. Salinity Laboratory Staff, 1954. Diagnosis and improvement of saline and alkali soils. *United States. Dept. of Agriculture Handbook.* **60**, 160 pp.

UNESCO, 1979. Map of the world distribution of arid regions: explanatory note. 9 -13

Ungemach, P., Mostaghimi, F. et Duprat, A., 1969. Essais de détermination du coefficient d'émmagasinement en nappe libre application à la nappe alluvial du rhin. *Bulletin. International association of Scientific Hydrology.XIV.* **36,** 169-189.

United Nations, 1975. Groundwater storage and artificial recharge. National resources/water Series no. 2 **ST/ESA/13**. Dept. Econ. Social Aff. 270 pp.

Urish, D.W., 1981. Electrical resistivity-hydraulic conductivity relationships in glacial outwash deposits. *Water Resources Research* **17**, No. 5, 1401-1408.

Urish, D.W., 1983. The practical application of surface electrical resistivity to detection of ground-water pollution. *Ground Water.* **21**, No. 2, 144-152.

Viessman, W.Jr, Knapp, J.W., Lewis, G. and Harbaugh., T.E., 1977. Introduction to hydrology, 2nd edition. 157-229: IEP, New York.

Vonhofv, J.A., 1966. Water quality determination from spontaneous-potential electric log curves. *Journal of Hydrology.* **4**, no.4, 341-347.

Walton, W.C., Hills, D.L. and Grundeen, G.M., 1967. Recharge from induced streambed infiltration under varying groundwater levels and stream-stage conditions. *Bull.* **6**, June. Water Research Center, University of Minnesota, Minneapolis, Minnesota. 42pp

White, C.C., Houston, J.F.T. and Barker, R.D., 1988. The Victoria Province drought relief, I. Geophysical sitting of boreholes. *Ground Water.* **26**, no. 3, 309-316.

WHO, 1971. International Standards for Drinking Water.3ed.(WHO), Geneva.131pp

Wilcox, L.V., 1955. Classification and use of irrigation waters. *United States.Dept. of Agriculture Circ.* **969**.75pp

Wilson, E.M., 1990. Engineering Hydrology. 4th edition: MacMillan Education Ltd, London.Ch-9

Wilson, I.G., 1973. Ergs. *Sedimentary Geology.* **10**, 77-106.

Worthington, P.F., 1977a. Influence of matrix conduction upon hydrogeophysical relationships in arenaceous aquifers. *Water Resources Research* **13**(1).87-92pp

Worthington, P.F., 1977b. Reply to Kelly's Comments on: Influence of matrix conduction upon hydrogeophysical relationships in arenaceous aquifers. *Water Resources Research* **13**(6).1024pp

Worthington, P.F., 1977c. Geophysical investigations of groundwater resources in the Kalahari Basin. *Geophysics* **42**(4).838-849

Zohdy, A.R., 1975. Automatic interpretation of Schlumberger sounding curves using modified Dar Zarrouk functions. *United States. Geol. Surv. Bull.* **1313-E**.39pp

Zohdy, A.R., Eaton, G.P. and Mabey, D.R., 1980. Application of surface geophysics to ground-water investigations. Techniques of Water-Resources Investigations of the United States Geological Survey, Book **2**. 116pp

Zohdy, A.A.R., 1969b. Anew method for differential resistivity sounding. *Geophysics*, **34**. 924-943.

Appendix 5A Data from large diameter well tests from Wadi Baysh.

WADI BAYSH (BU1)

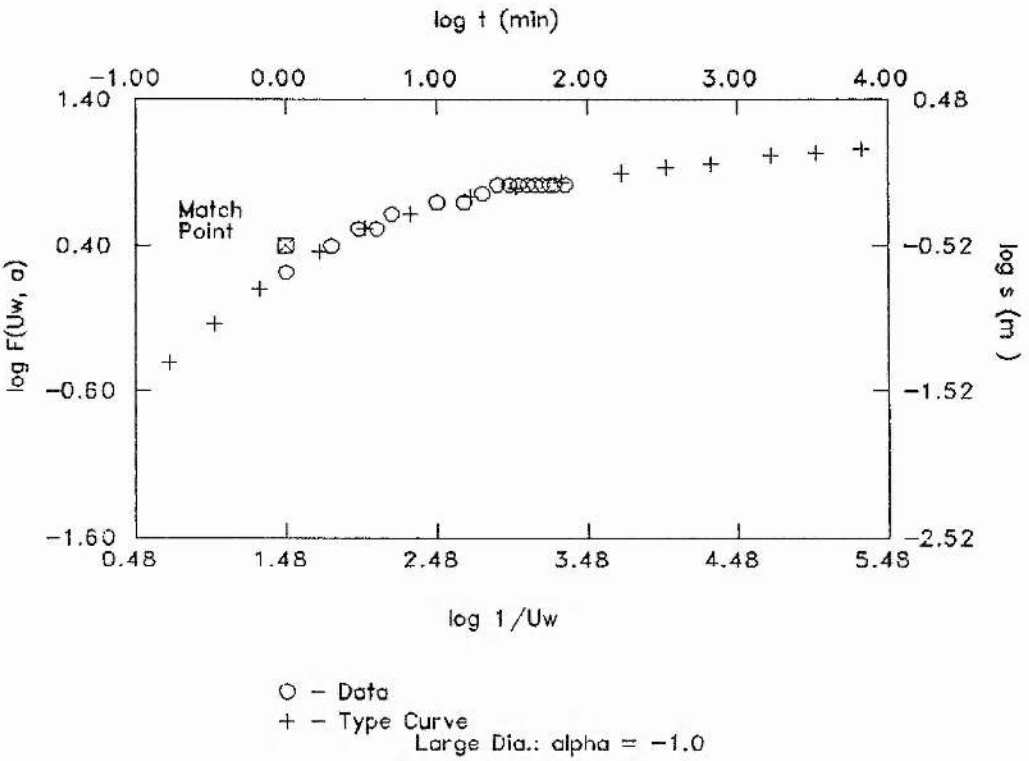

MATCH POINT		SOLUTION	
t	= 1.000E+0000	Transmissivity (T)	= 2.186E−0003 sq m/sec
s	= 3.048E−0001	Hydraulic Conductivity (K)	= 1.093E−0003 m/sec
1/Uw	= 3.020E+0001	Storativity (S)	= 1.000E−0001
F(Uw, a)	= 2.512E+0000		

WELL INFORMATION	
WELL IDENTIFICATION	: BU1
DATE OF AQUIFER TEST	: 1/7/89
AQUIFER THICKNESS (b)	: 2.000E+0000 m
DISCHARGE RATE (Q)	: 2.880E+0002 cu m/day
EFFECTIVE RADIUS	: 1.200E+0000 m
WELL RADIUS AT MEASURED WATER LEVELS (rc)	: 1.200E+0000 m

WADI BAYSH (BU2)

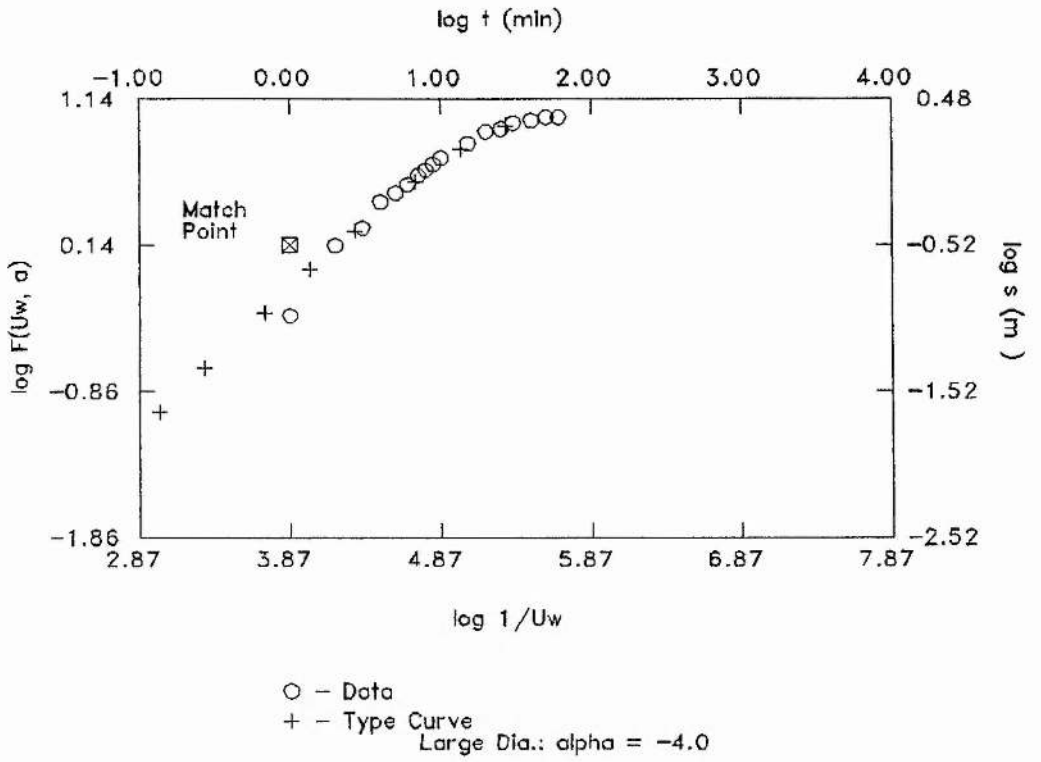

MATCH POINT			SOLUTION		
t	=	1.000E+0000	Transmissivity (T)	=	1.802E-0003 sq m/sec
s	=	3.048E-0001	Hydraulic Conductivity (K)	=	3.003E-0004 m/sec
1/Uw	=	7.413E+0003	Storativity (S)	=	1.000E-0004
F(Uw, a)	=	1.380E+0000			

WELL INFORMATION	
WELL IDENTIFICATION	: BU2
DATE OF AQUIFER TEST	: 2/7/89
AQUIFER THICKNESS (b)	: 6.000E+0000 m
DISCHARGE RATE (Q)	: 4.320E+0002 cu m/day
EFFECTIVE RADIUS	: 1.700E+0000 m
WELL RADIUS AT MEASURED WATER LEVELS (rc)	: 1.700E+0000 m

WADI BAYSH (BU3)

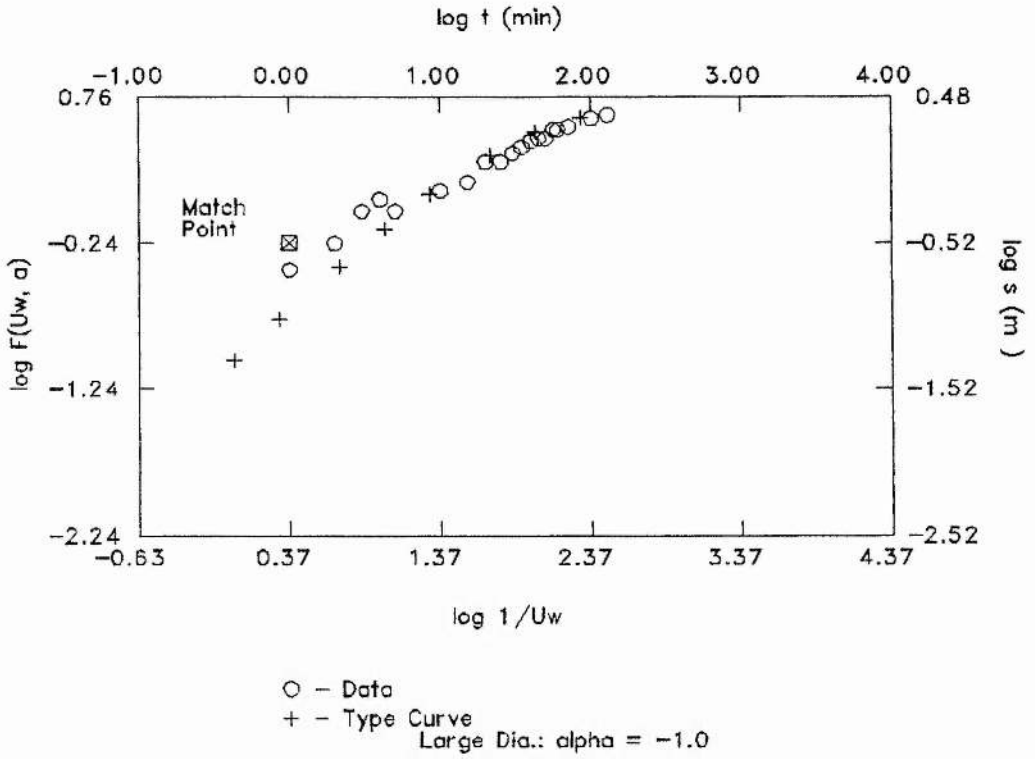

MATCH POINT		SOLUTION	
t	= 1.000E+0000	Transmissivity (T)	= 1.002E-0003 sq m/sec
s	= 3.048E-0001	Hydraulic Conductivity (K)	= 8.347E-0005 m/sec
1/Uw	= 2.344E+0000	Storativity (S)	= 1.000E-0001
F(Uw, a)	= 5.754E-0001		

WELL INFORMATION	
WELL IDENTIFICATION	: BU3
DATE OF AQUIFER TEST	: 3/7/89
AQUIFER THICKNESS (b)	: 1.200E+0001 m
DISCHARGE RATE (Q)	: 5.760E+0002 cu m/day
EFFECTIVE RADIUS	: 2.500E+0000 m
WELL RADIUS AT MEASURED WATER LEVELS (rc)	: 2.500E+0000 m

WADI BAYSH (BM5)

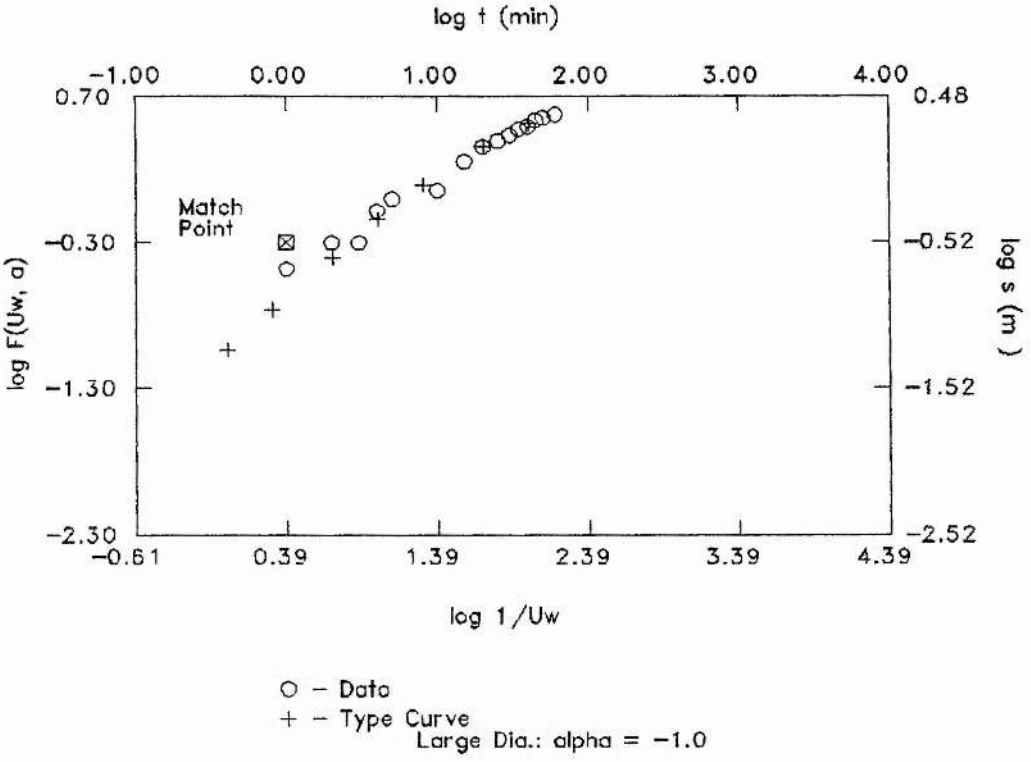

MATCH POINT			SOLUTION		
t	=	1.000E+0000	Transmissivity (T)	=	8.724E-0004 sq m/sec
s	=	3.048E-0001	Hydraulic Conductivity (K)	=	7.930E-0005 m/sec
1/Uw	=	2.455E+0000	Storativity (S)	=	1.000E-0001
F(Uw, a)	=	5.012E-0001			

WELL INFORMATION	
WELL IDENTIFICATION	: BM5
DATE OF AQUIFER TEST	: 4/7/89
AQUIFER THICKNESS (b)	: 1.100E+0001 m
DISCHARGE RATE (Q)	: 5.760E+0002 cu m/day
EFFECTIVE RADIUS	: 1.500E+0000 m
WELL RADIUS AT MEASURED WATER LEVELS (rc)	: 1.500E+0000 m

WADI BAYSH (BM7)

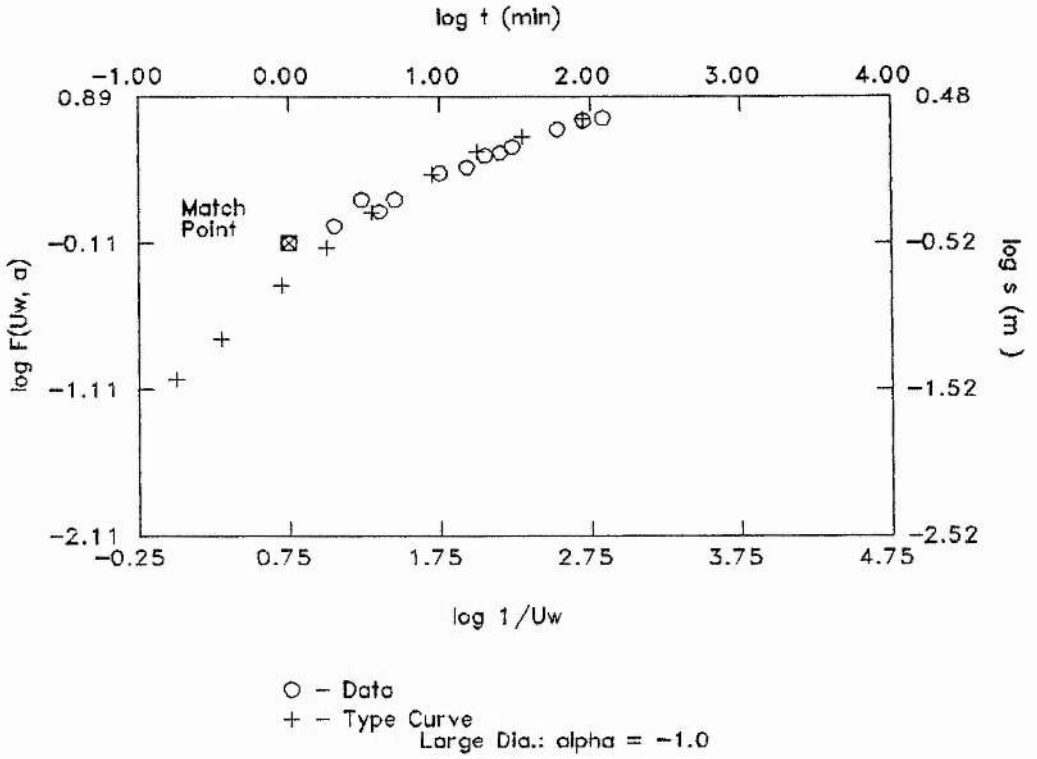

MATCH POINT		SOLUTION	
t	= 1.000E+0000	Transmissivity (T)	= 1.689E-0003 sq m/sec
s	= 3.048E-0001	Hydraulic Conductivity (K)	= 1.299E-0004 m/sec
1/Uw	= 5.623E+0000	Storativity (S)	= 1.000E-0001
F(Uw, a)	= 7.762E-0001		

WELL INFORMATION	
WELL IDENTIFICATION	: BM7
DATE OF AQUIFER TEST	: 5/7/89
AQUIFER THICKNESS (b)	: 1.300E+0001 m
DISCHARGE RATE (Q)	: 7.200E+0002 cu m/day
EFFECTIVE RADIUS	: 1.600E+0000 m
WELL RADIUS AT MEASURED WATER LEVELS (rc)	: 1.600E+0000 m

WADI BAYSH (BM12)

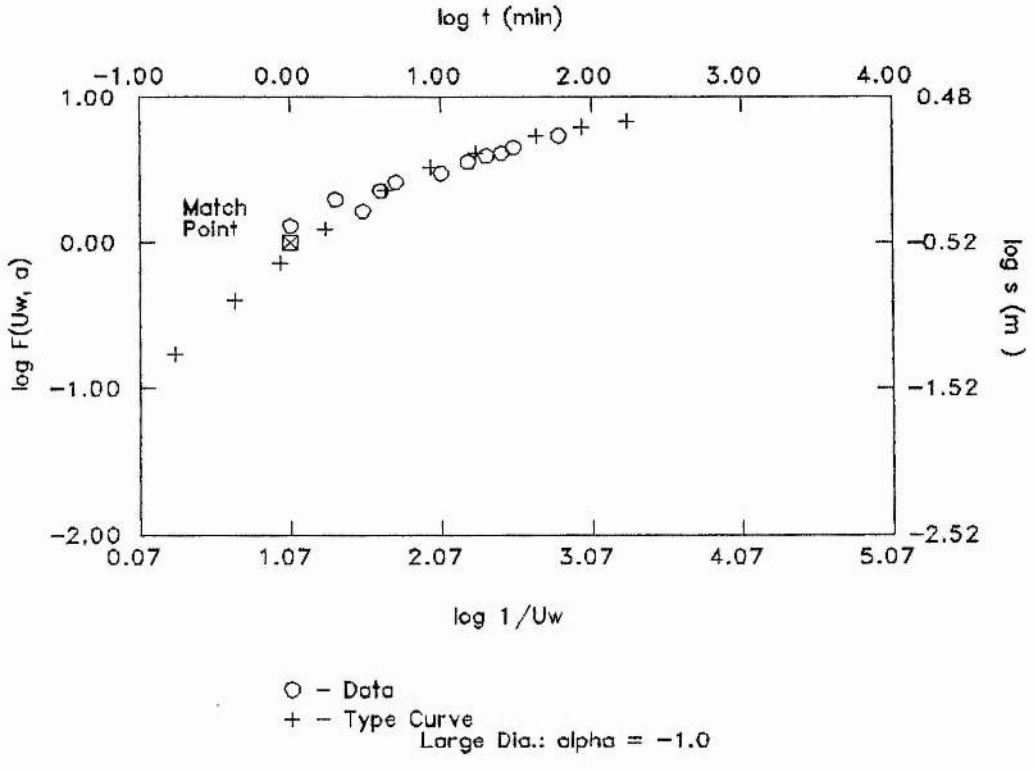

MATCH POINT			SOLUTION		
t	=	1.000E+0000	Transmissivity (T)	=	1.741E-0003 sq m/sec
s	=	3.048E-0001	Hydraulic Conductivity (K)	=	8.288E-0005 m/sec
1/Uw	=	1.175E+0001	Storativity (S)	=	1.000E-0001
F(Uw, a)	=	1.000E+0000			

WELL INFORMATION	
WELL IDENTIFICATION	: BM12
DATE OF AQUIFER TEST	: 6/7/89
AQUIFER THICKNESS (b)	: 2.100E+0001 m
DISCHARGE RATE (Q)	: 5.760E+0002 cu m/day
EFFECTIVE RADIUS	: 1.200E+0000 m
WELL RADIUS AT MEASURED WATER LEVELS (rc)	: 1.200E+0000 m

WADI BAYSH (BL16)

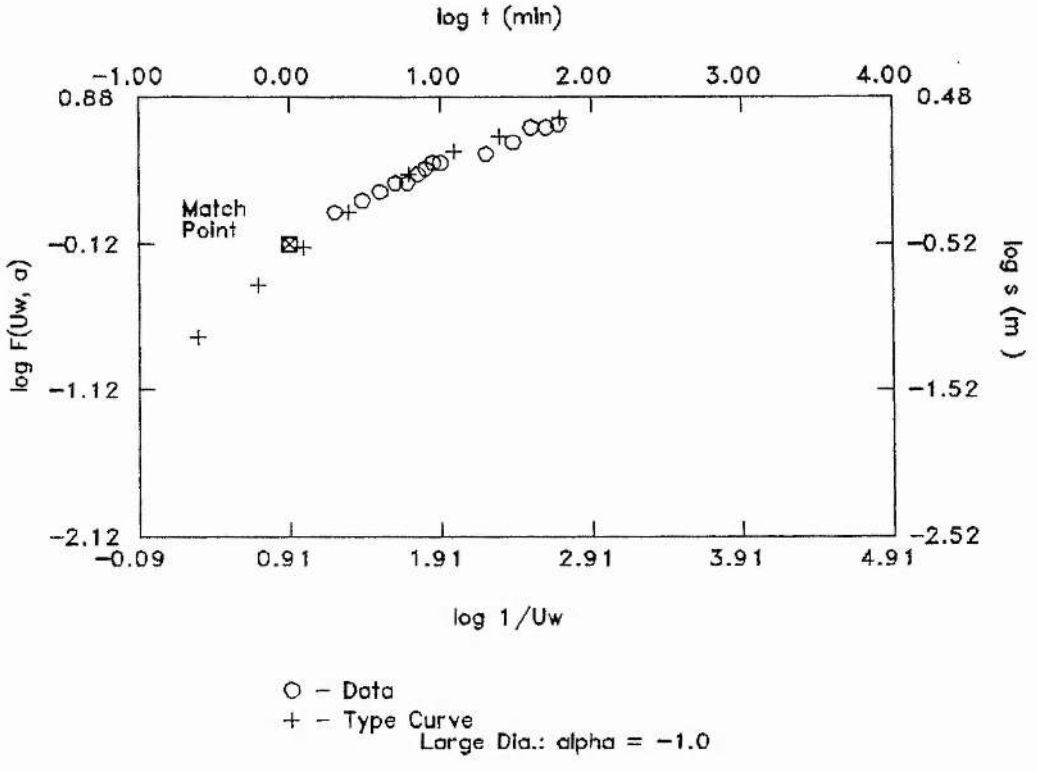

MATCH POINT		SOLUTION	
t	= 1.000E+0000	Transmissivity (T)	= 1.485E-0003 sq m/sec
s	= 3.048E-0001	Hydraulic Conductivity (K)	= 4.015E-0005 m/sec
1/Uw	= 8.128E+0000	Storativity (S)	= 1.000E-0001
F(Uw, a)	= 7.586E-0001		

WELL INFORMATION	
WELL IDENTIFICATION	: BL16
DATE OF AQUIFER TEST	: 7/7/89
AQUIFER THICKNESS (b)	: 3.700E+0001 m
DISCHARGE RATE (Q)	: 6.480E+0002 cu m/day
EFFECTIVE RADIUS	: 1.500E+0000 m
WELL RADIUS AT MEASURED WATER LEVELS (rc)	: 1.500E+0000 m

Appendix 5B Data from large diameter well tests from Wadi Habawnah.

WADI HABAWNAH (HB2)

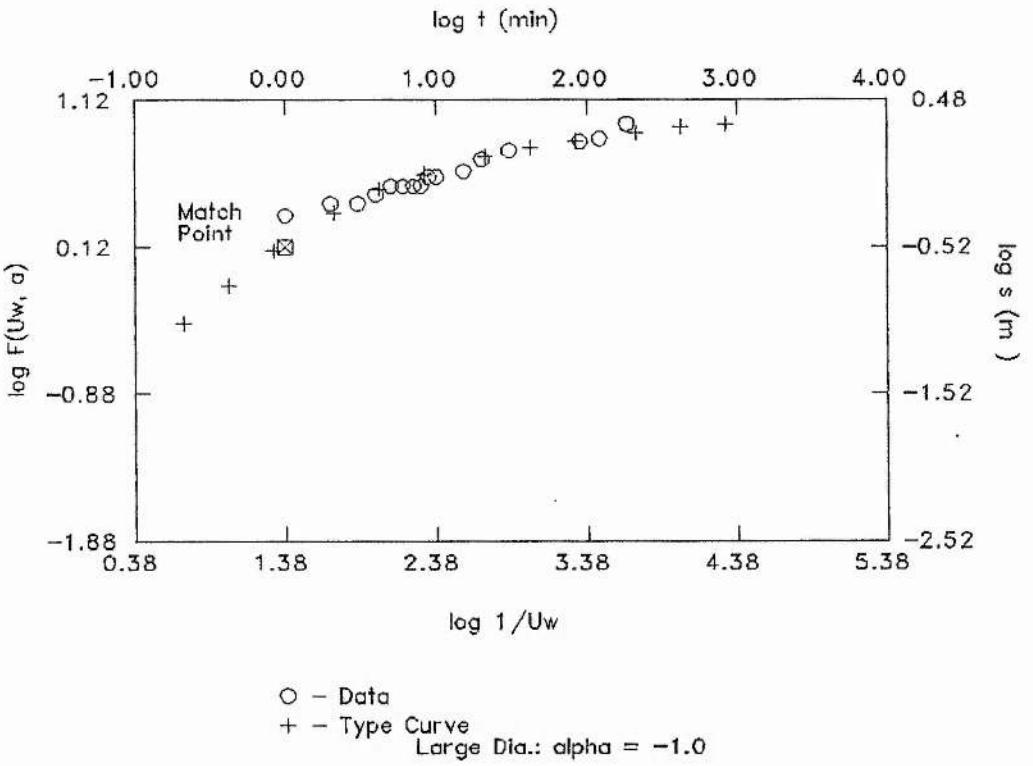

MATCH POINT		SOLUTION	
t	= 1.000E+0000	Transmissivity (T)	= 2.406E-0003 sq m/sec
s	= 3.048E-0001	Hydraulic Conductivity (K)	= 1.266E-0004 m/sec
1/Uw	= 2.399E+0001	Storativity (S)	= 1.000E-0001
F(Uw, a)	= 1.318E+0000		

WELL INFORMATION	
WELL IDENTIFICATION	: HS2
DATE OF AQUIFER TEST	: 18/6/89
AQUIFER THICKNESS (b)	: 1.900E+0001 m
DISCHARGE RATE (Q)	: 6.040E+0002 cu m/day
EFFECTIVE RADIUS	: 1.500E+0000 m
WELL RADIUS AT MEASURED WATER LEVELS (rc)	: 1.500E+0000 m

WADI HABAWNAH (BH3)

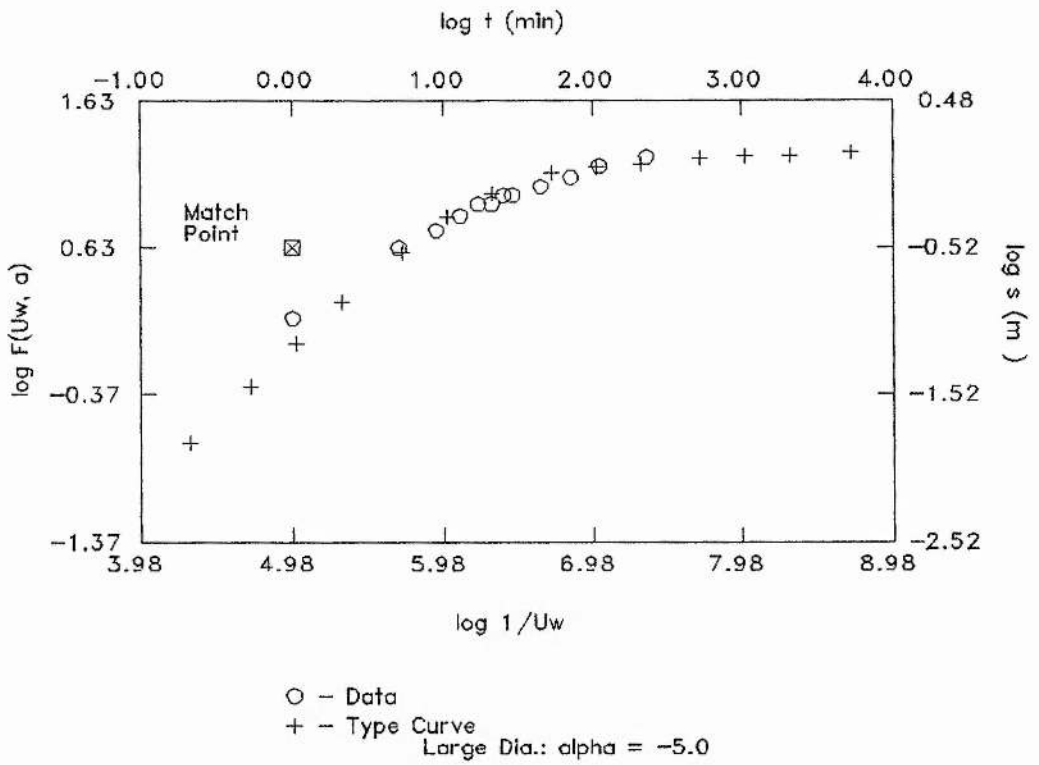

MATCH POINT		SOLUTION	
t	= 1.000E+0000	Transmissivity (T)	= 4.267E-0003 sq m/sec
s	= 3.048E-0001	Hydraulic Conductivity (K)	= 8.533E-0004 m/sec
1/Uw	= 9.550E+0004	Storativity (S)	= 1.000E-0005
F(Uw, a)	= 4.266E+0000		

WELL INFORMATION	
WELL IDENTIFICATION	: HB3
DATE OF AQUIFER TEST	: 10/6/89
AQUIFER THICKNESS (b)	: 5.000E+0000 m
DISCHARGE RATE (Q)	: 3.310E+0002 cu m/day
EFFECTIVE RADIUS	: 1.400E+0000 m
WELL RADIUS AT MEASURED WATER LEVELS (rc)	: 1.400E+0000 m

WADI HABAWNAH (HB6.DTA)

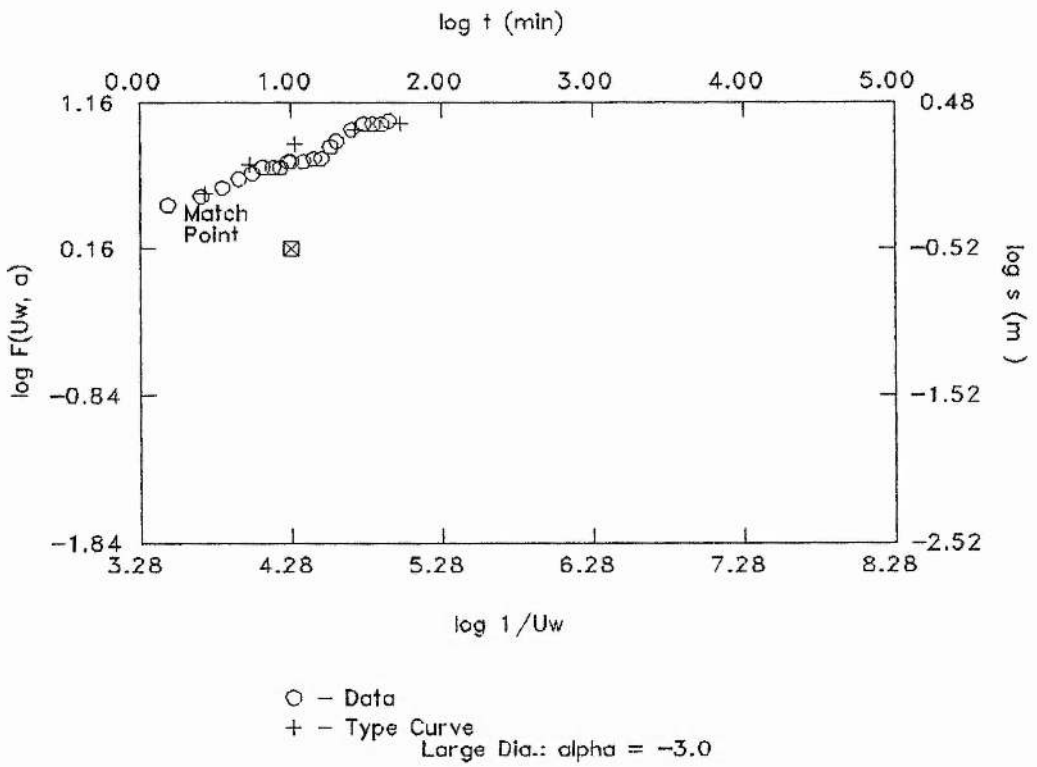

MATCH POINT			SOLUTION		
t	=	1.000E+0001	Transmissivity (T)	=	2.201E-0003 sq m/sec
s	=	3.048E-0001	Hydraulic Conductivity (K)	=	5.504E-0004 m/sec
1/Uw	=	1.905E+0004	Storativity (S)	=	1.000E-0003
F(Uw, a)	=	1.445E+0000			

WELL INFORMATION	
WELL IDENTIFICATION	: HB6
DATE OF AQUIFER TEST	: 11/6/89
AQUIFER THICKNESS (b)	: 4.000E+0000 m
DISCHARGE RATE (Q)	: 5.040E+0002 cu m/day
EFFECTIVE RADIUS	: 1.500E+0000 m
WELL RADIUS AT MEASURED WATER LEVELS (rc)	: 1.500E+0000 m

WADI HABAWNAH (MT1)

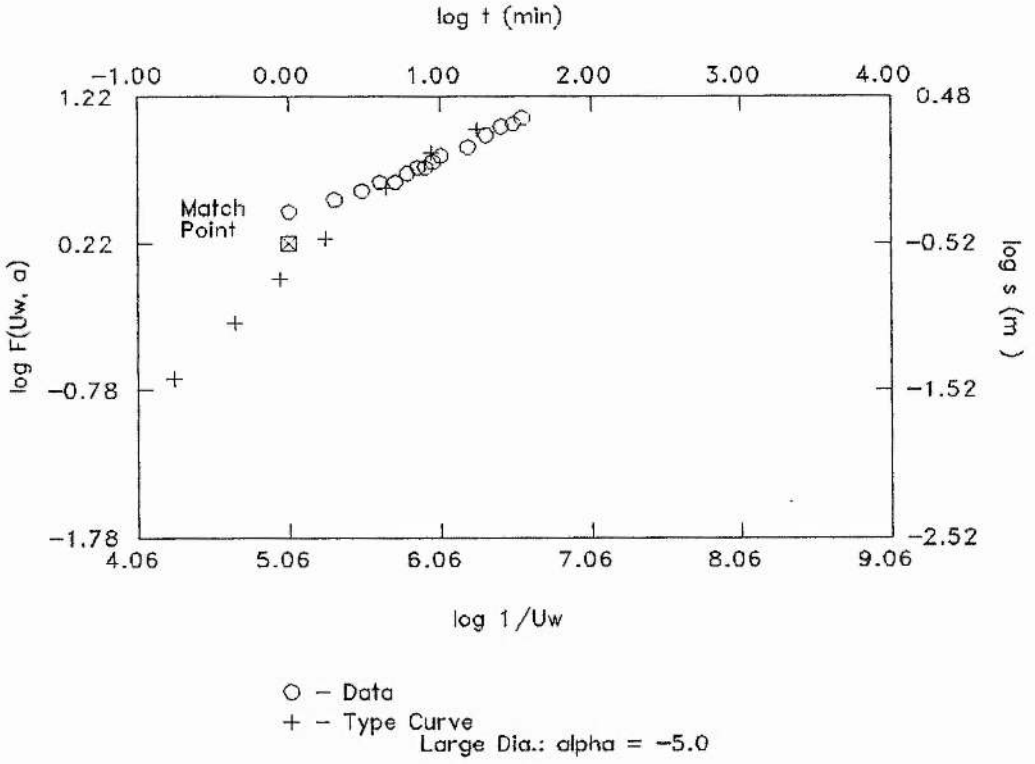

MATCH POINT			SOLUTION		
t	=	1.000E+0000	Transmissivity (T)	=	3.250E-0003 sq m/sec
s	=	3.048E-0001	Hydraulic Conductivity (K)	=	1.912E-0004 m/sec
1/Uw	=	1.148E+0005	Storativity (S)	=	1.000E-0005
F(Uw, a)	=	1.660E+0000			

WELL INFORMATION	
WELL IDENTIFICATION	: MT1
DATE OF AQUIFER TEST	: 12/6/89
AQUIFER THICKNESS (b)	: 1.700E+0001 m
DISCHARGE RATE (Q)	: 6.480E+0002 cu m/day
EFFECTIVE RADIUS	: 1.500E+0000 m
WELL RADIUS AT MEASURED WATER LEVELS (rc)	: 1.500E+0000 m

WADI HABAWNAH (MT9)

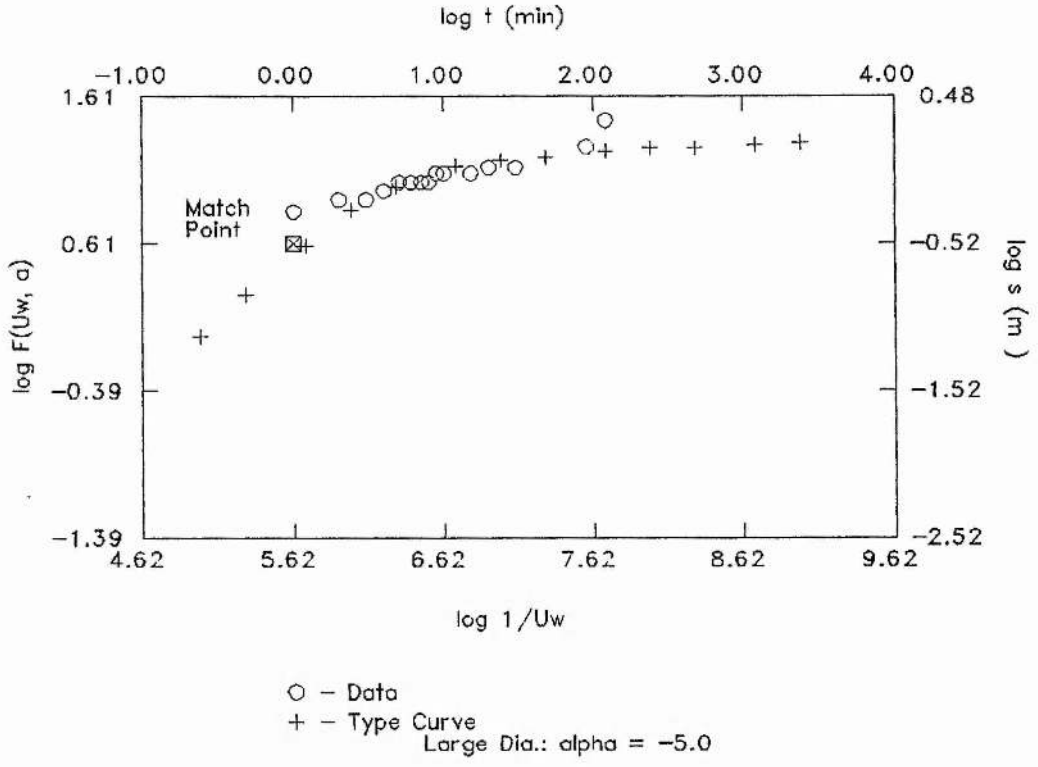

MATCH POINT			SOLUTION		
t	=	1.000E+0000	Transmissivity (T)	=	6.020E−0003 sq m/sec
s	=	3.048E−0001	Hydraulic Conductivity (K)	=	3.168E−0004 m/sec
1/Uw	=	4.169E+0005	Storativity (S)	=	1.000E−0005
F(Uw, a)	=	4.074E+0000			

WELL INFORMATION	
WELL IDENTIFICATION	: MT9
DATE OF AQUIFER TEST	: 13/6/89
AQUIFER THICKNESS (b)	: 1.900E+0001 m
DISCHARGE RATE (Q)	: 4.890E+0002 cu m/day
EFFECTIVE RADIUS	: 1.500E+0000 m
WELL RADIUS AT MEASURED WATER LEVELS (rc)	: 1.500E+0000 m

WADI HABAWNAH (GF2)

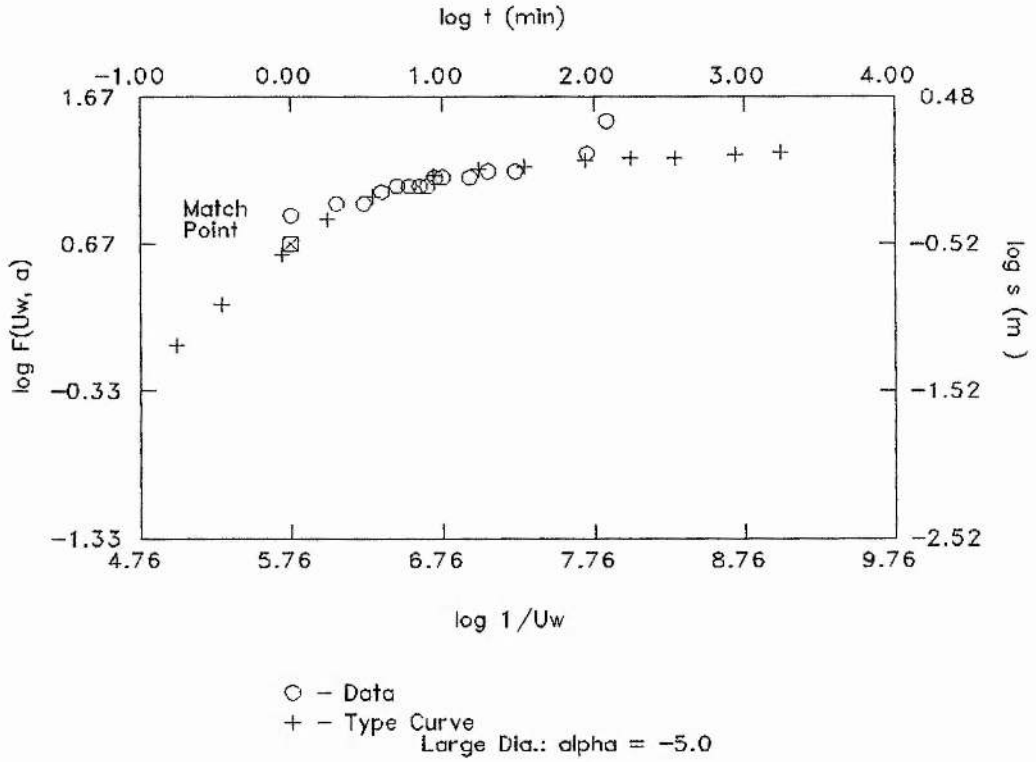

MATCH POINT		SOLUTION	
t	= 1.000E+0000	Transmissivity (T)	= 8.537E−0003 sq m/sec
s	= 3.048E−0001	Hydraulic Conductivity (K)	= 4.493E−0004 m/sec
1/Uw	= 5.755E+0005	Storativity (S)	= 1.000E−0005
F(Uw, a)	= 4.677E+0000		

WELL INFORMATION	
WELL IDENTIFICATION	: GF2
DATE OF AQUIFER TEST	: 14/6/89
AQUIFER THICKNESS (b)	: 1.900E+0001 m
DISCHARGE RATE (Q)	: 6.040E+0002 cu m/day
EFFECTIVE RADIUS	: 1.500E+0000 m
WELL RADIUS AT MEASURED WATER LEVELS (rc)	: 1.500E+0000 m

WADI HABAWNAH (GF5)

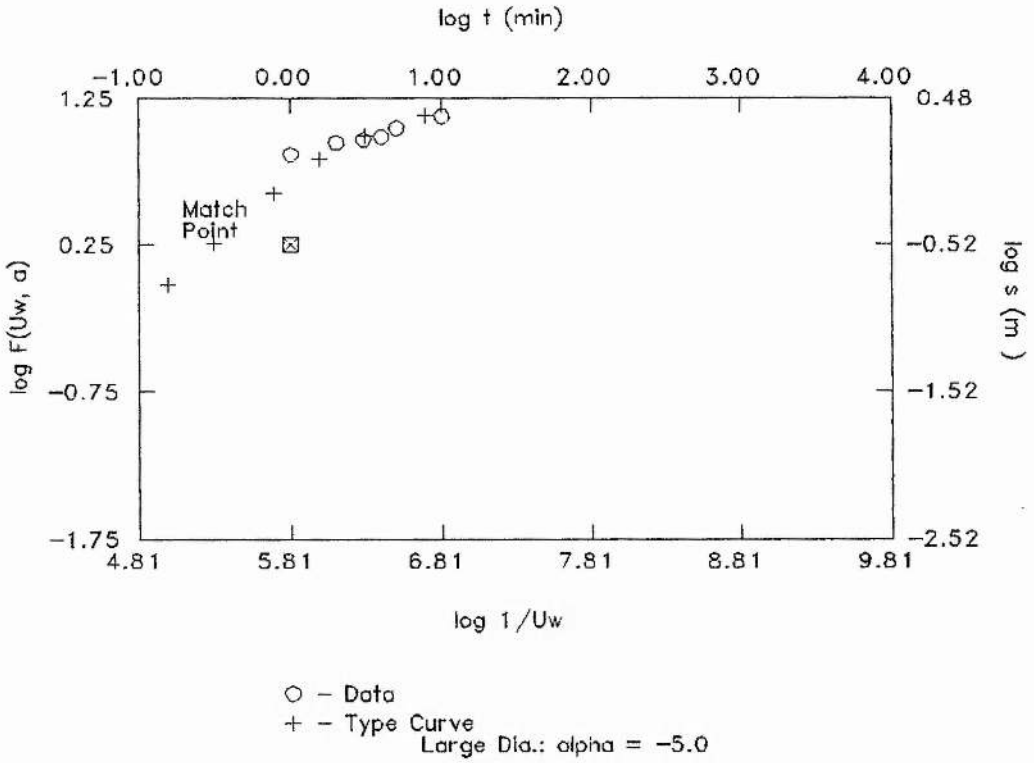

MATCH POINT			SOLUTION		
t	=	1.000E+0000	Transmissivity (T)	=	3.246E-0003 sq m/sec
s	=	3.048E-0001	Hydraulic Conductivity (K)	=	2.029E-0004 m/sec
1/Uw	=	6.457E+0005	Storativity (S)	=	1.000E-0005
F(Uw, a)	=	1.778E+0000			

WELL INFORMATION	
WELL IDENTIFICATION	: GF5
DATE OF AQUIFER TEST	: 15/6/89
AQUIFER THICKNESS (b)	: 1.600E+0001 m
DISCHARGE RATE (Q)	: 6.040E+0002 cu m/day
EFFECTIVE RADIUS	: 1.500E+0000 m
WELL RADIUS AT MEASURED WATER LEVELS (rc)	: 1.500E+0000 m

WADI HABAWNAH (NG1)

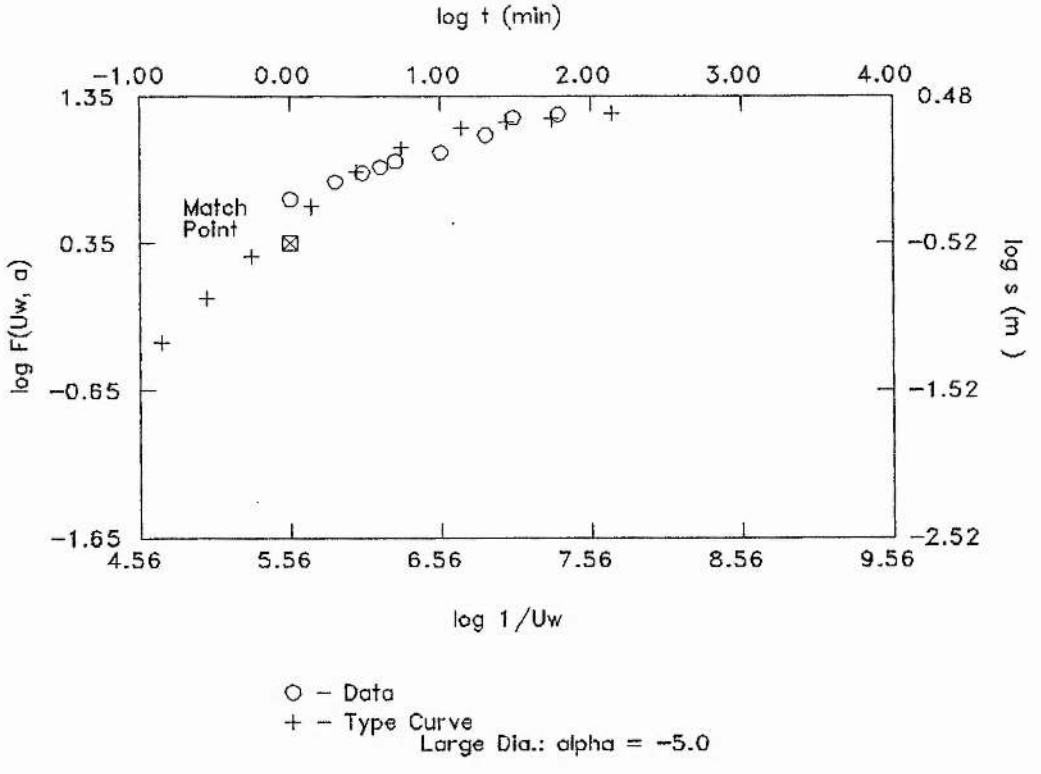

MATCH POINT			SOLUTION		
t	=	1.000E+0000	Transmissivity (T)	=	3.897E-0003 sq m/sec
s	=	3.048E-0001	Hydraulic Conductivity (K)	=	3.247E-0004 m/sec
1/Uw	=	3.631E+0005	Storativity (S)	=	1.000E-0005
F(Uw, a)	=	2.239E+0000			

WELL INFORMATION

WELL IDENTIFICATION	: NG1
DATE OF AQUIFER TEST	: 17/6/89
AQUIFER THICKNESS (b)	: 1.200E+0001 m
DISCHARGE RATE (Q)	: 5.760E+0002 cu m/day
EFFECTIVE RADIUS	: 1.500E+0000 m
WELL RADIUS AT MEASURED WATER LEVELS (rc)	: 1.500E+0000 m

WADI HABAWNAH (MR)

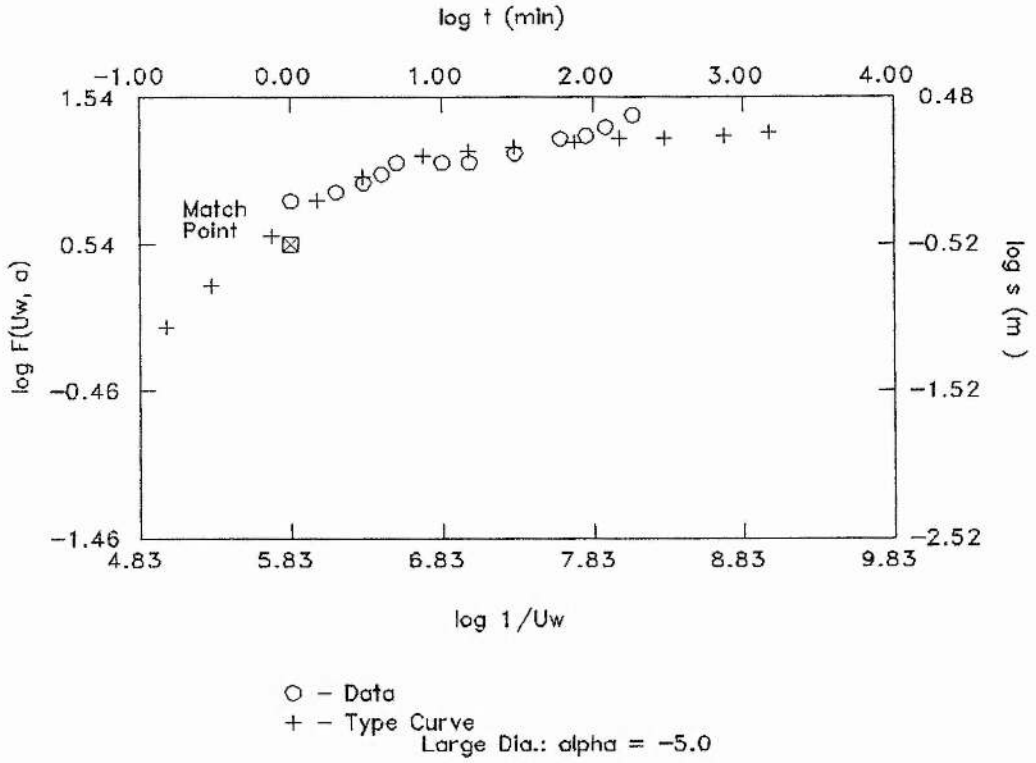

MATCH POINT		SOLUTION	
t	= 1.000E+0000	Transmissivity (T)	= 7.544E-0003 sq m/sec
s	= 3.048E-0001	Hydraulic Conductivity (K)	= 6.287E-0004 m/sec
1/Uw	= 6.761E+0005	Storativity (S)	= 1.000E-0005
F(Uw, a)	= 3.467E+0000		

WELL INFORMATION	
WELL IDENTIFICATION	: MR
DATE OF AQUIFER TEST	: 16/6/89
AQUIFER THICKNESS (b)	: 1.200E+0001 m
DISCHARGE RATE (Q)	: 7.200E+0002 cu m/day
EFFECTIVE RADIUS	: 1.500E+0000 m
WELL RADIUS AT MEASURED WATER LEVELS (rc)	: 1.500E+0000 m

WADI HABAWNAH (HS2)

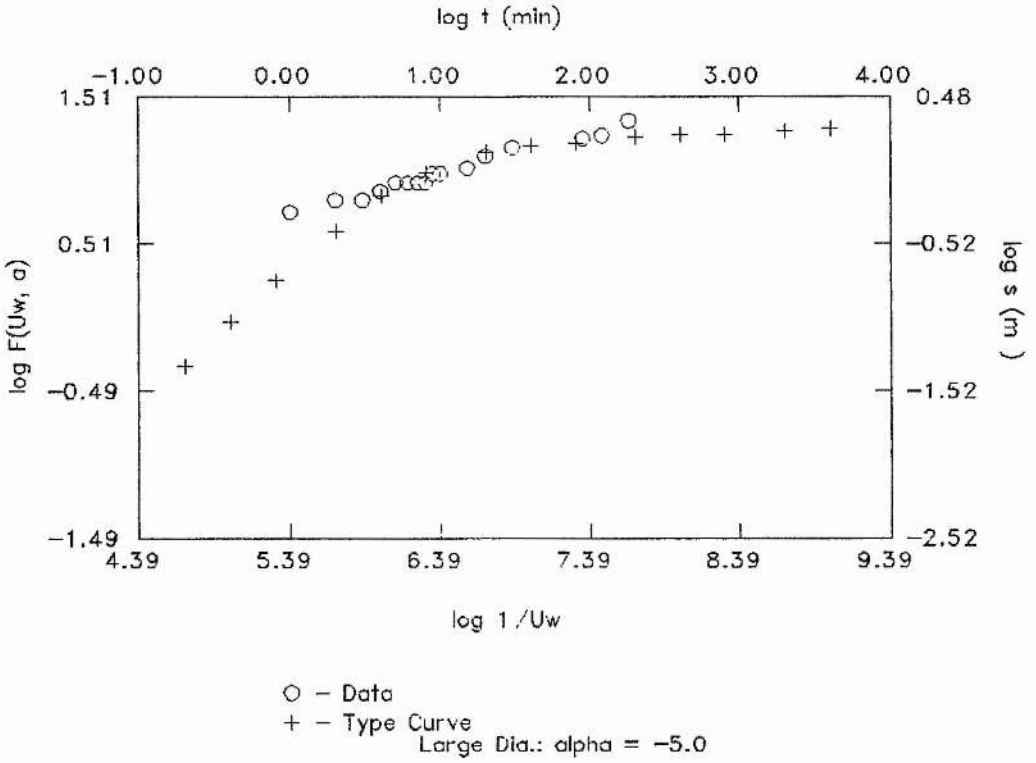

WELL INFORMATION	
WELL IDENTIFICATION	: HS2
DATE OF AQUIFER TEST	: 18/6/89
AQUIFER THICKNESS (b)	: 1.900E+0001 m
DISCHARGE RATE (Q)	: 6.040E+0002 cu m/day
EFFECTIVE RADIUS	: 1.500E+0000 m
WELL RADIUS AT MEASURED WATER LEVELS (rc)	: 1.500E+0000 m

WADI HABWANAH (HS4)

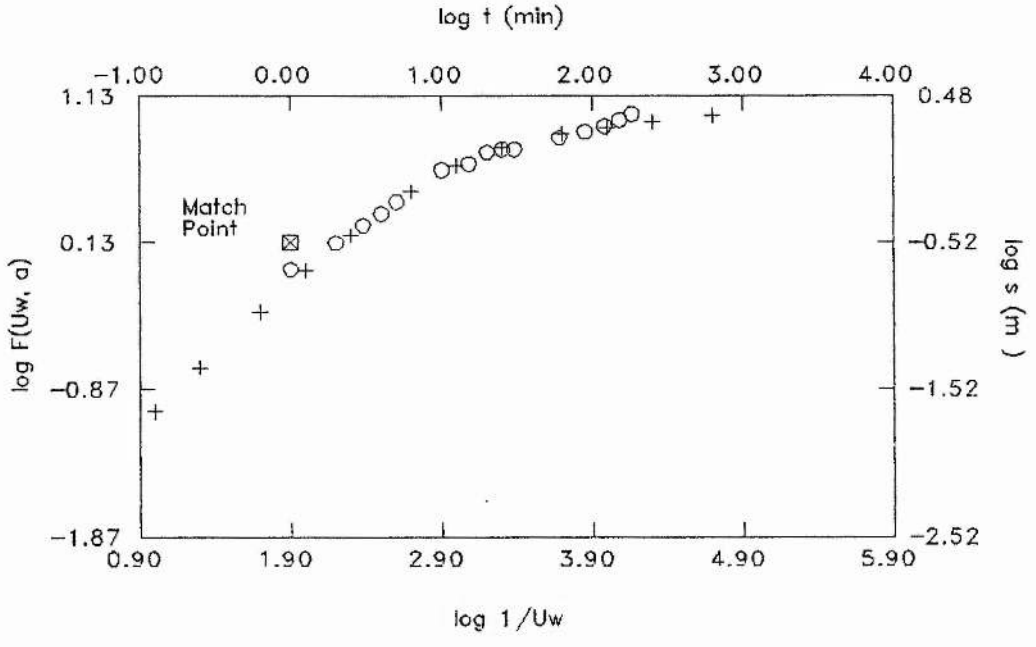

MATCH POINT			SOLUTION		
t	=	1.000E+0000	Transmissivity (T)	=	2.935E-0003 sq m/sec
s	=	3.048E-0001	Hydraulic Conductivity (K)	=	1.398E-0004 m/sec
1/Uw	=	7.943E+0001	Storativity (S)	=	1.000E-0002
F(Uw, a)	=	1.349E+0000			

WELL INFORMATION	
WELL IDENTIFICATION	: HS4
DATE OF AQUIFER TEST	: 19/6/89
AQUIFER THICKNESS (b)	: 2.100E+0001 m
DISCHARGE RATE (Q)	: 7.200E+0002 cu m/day
EFFECTIVE RADIUS	: 1.500E+0000 m
WELL RADIUS AT MEASURED WATER LEVELS (rc)	: 1.500E+0000 m

Appendix 6A
Time-distance curves of Wadi Baysh and Wadi Habawnah which are intended to illustrate the seismic refraction data in both wadis.

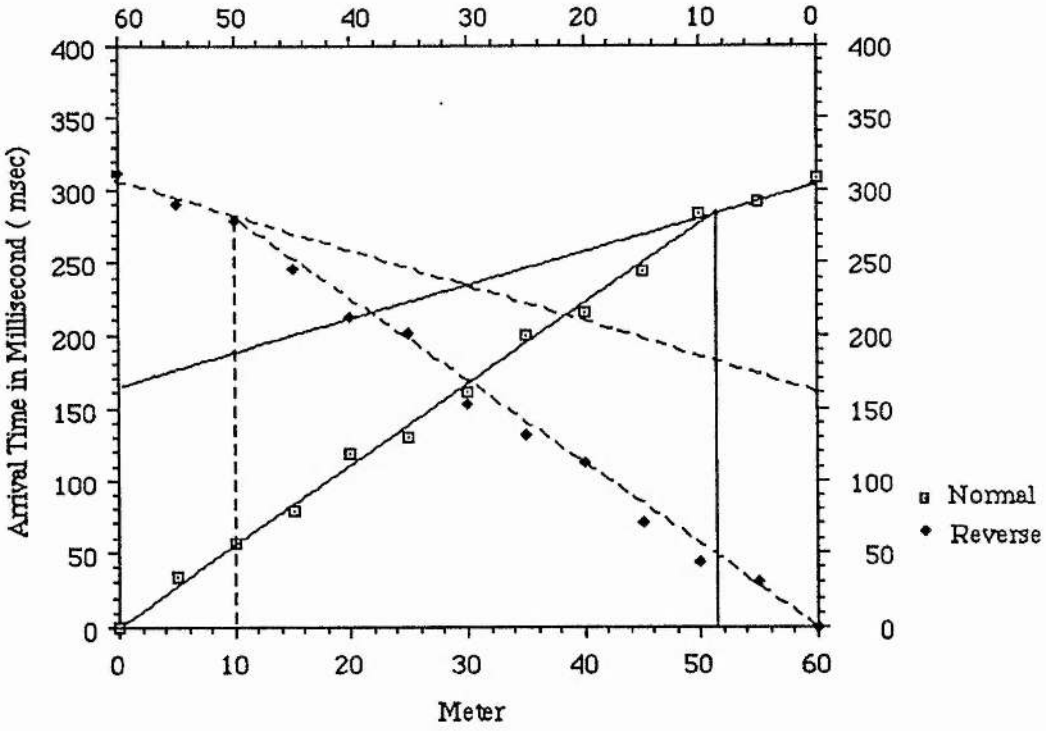

Geophone Distance From Shotpoint A&B in Meter (Station no .B S1)

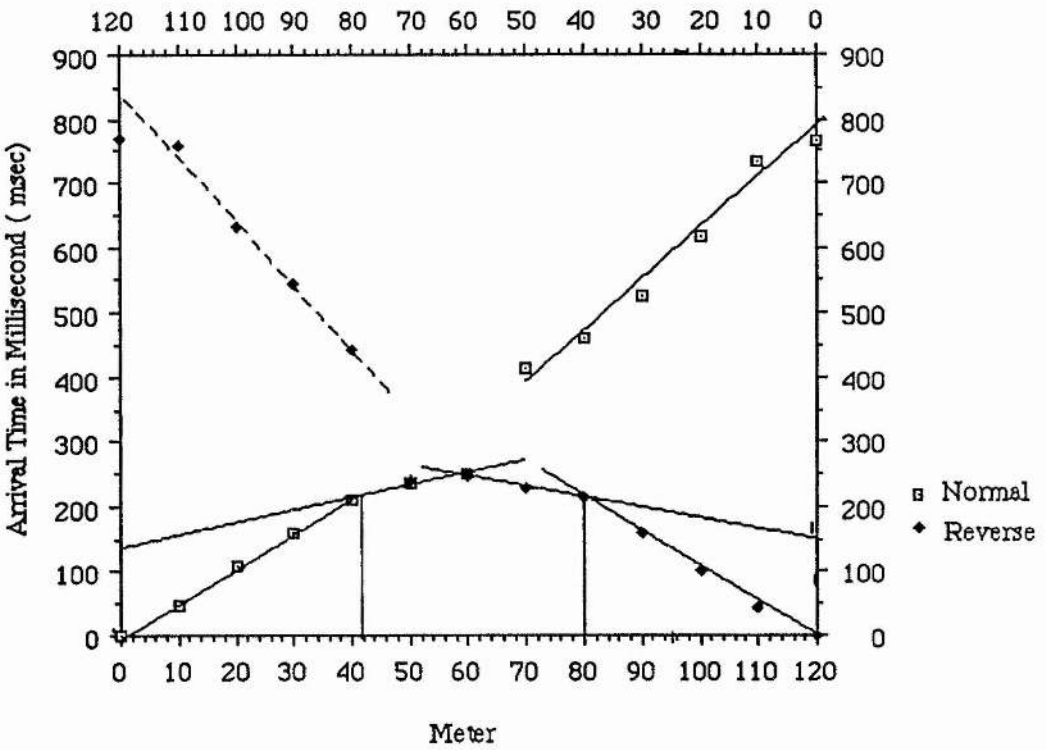

Geophone Distance From Shotpoint A&B in Meter (Station no . B S2)

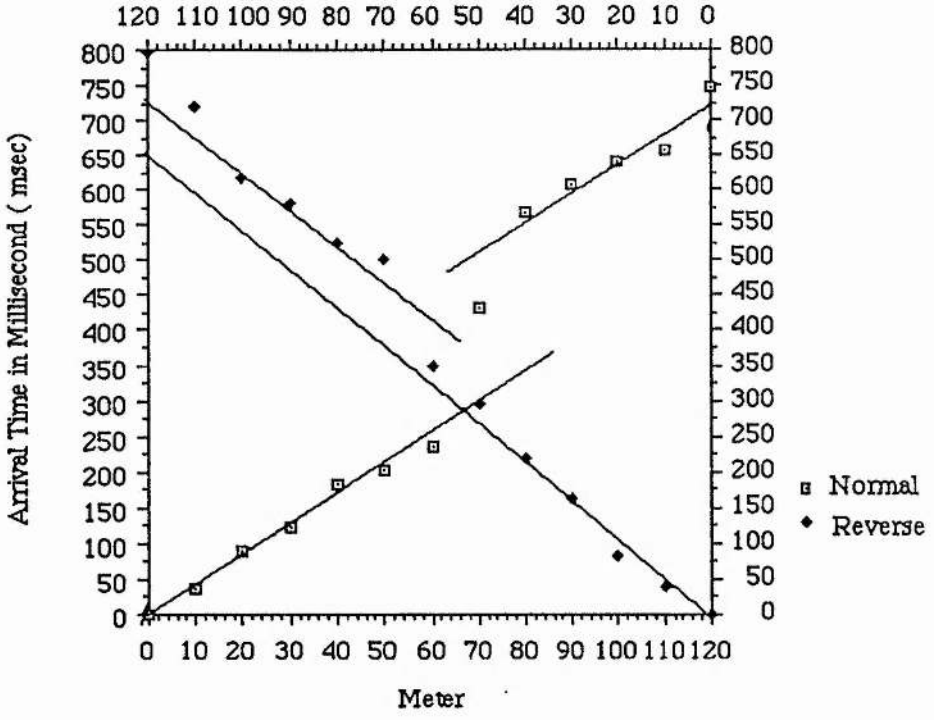

Geophone Distance From Shotpoint A&B in Meter (Station no . BS3)

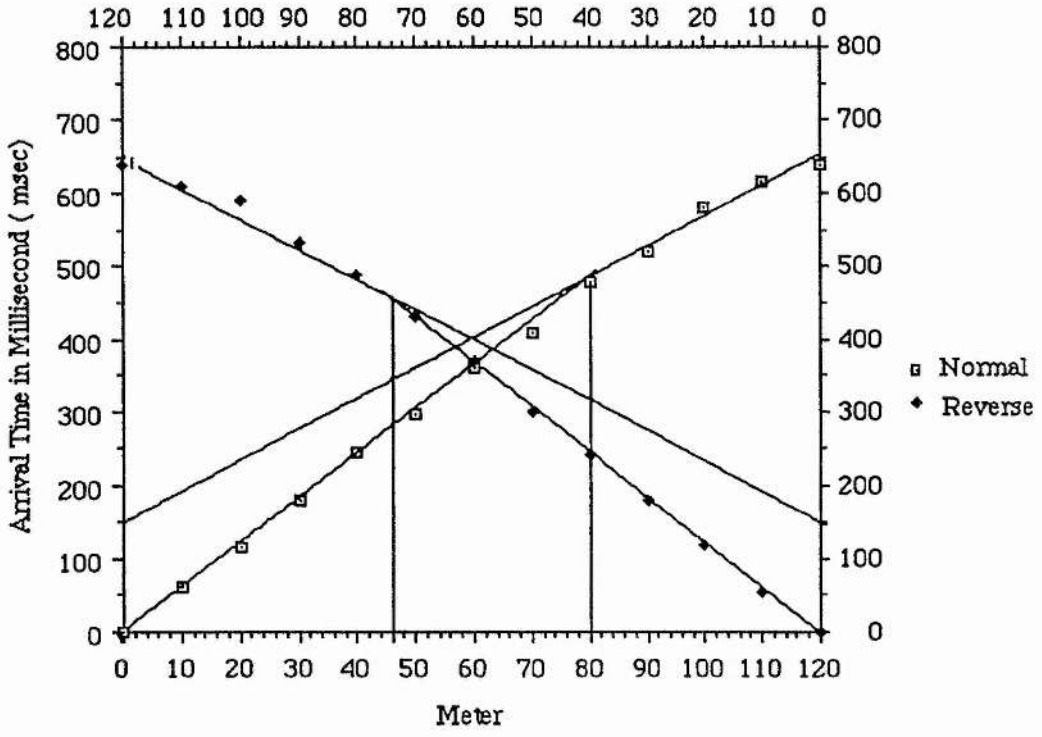

Geophone Distance From Shotpoint A&B in Meter (Station no . BS4)

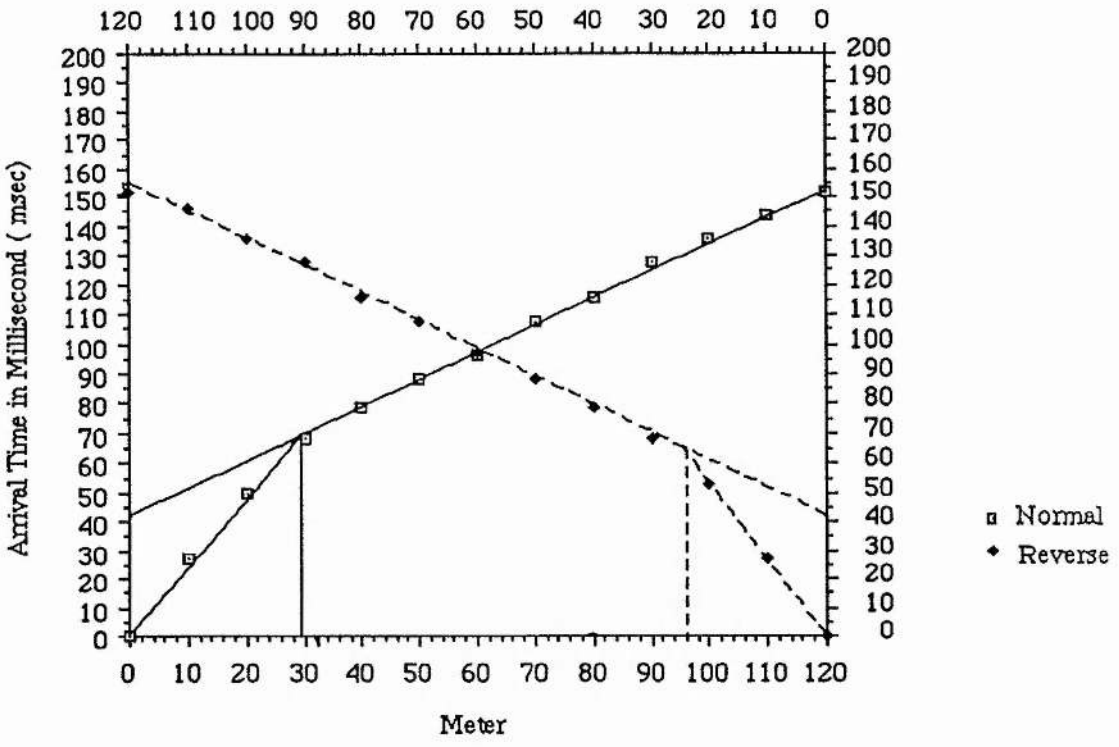

Geophone Distance From Shotpoint A&B in Meter (Station no . B S5)

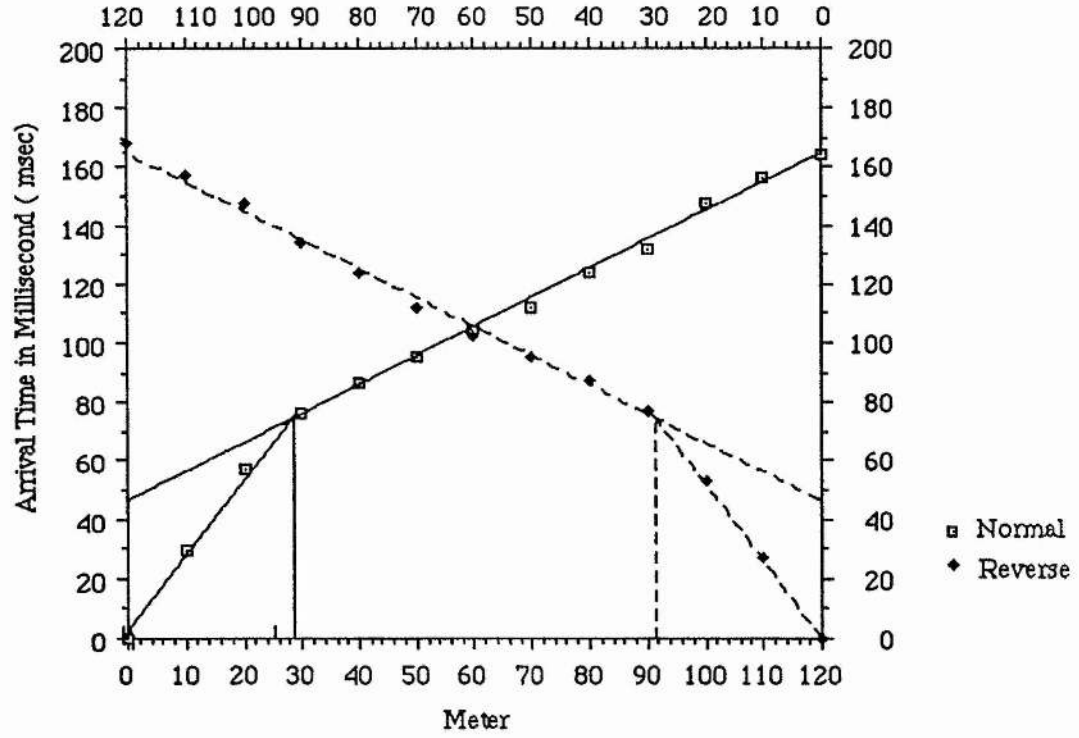

Geophone Distance From Shotpoint A&B in Meter (Station no . B S6)

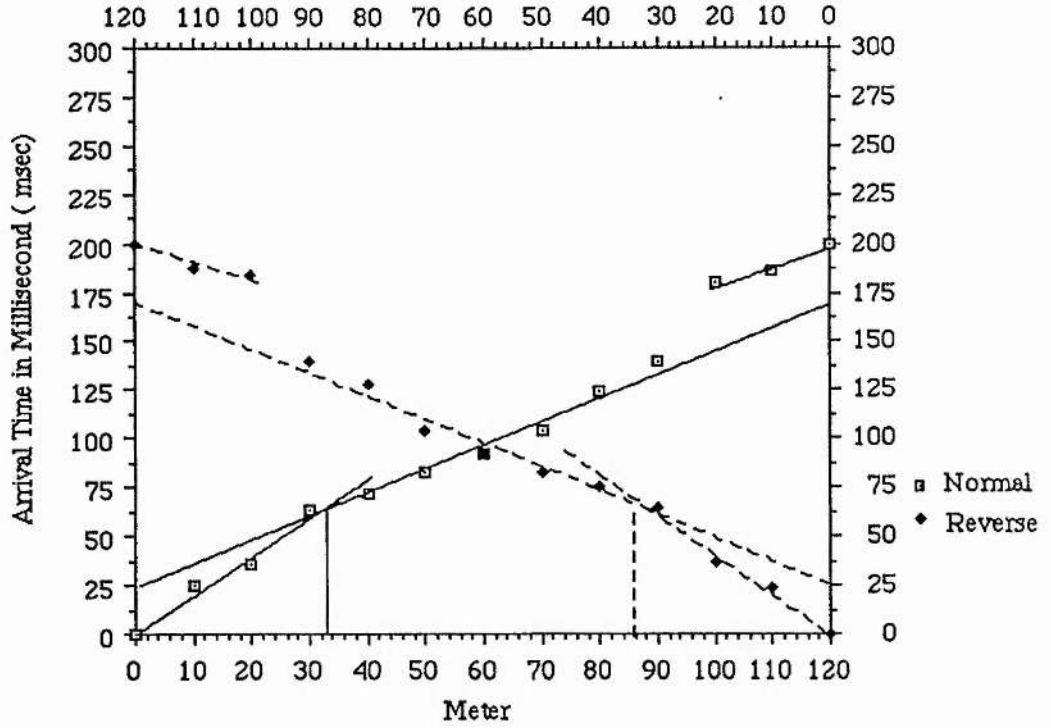

Geophone Distance From Shotpoint A&B in Meter (Station no . B S7)

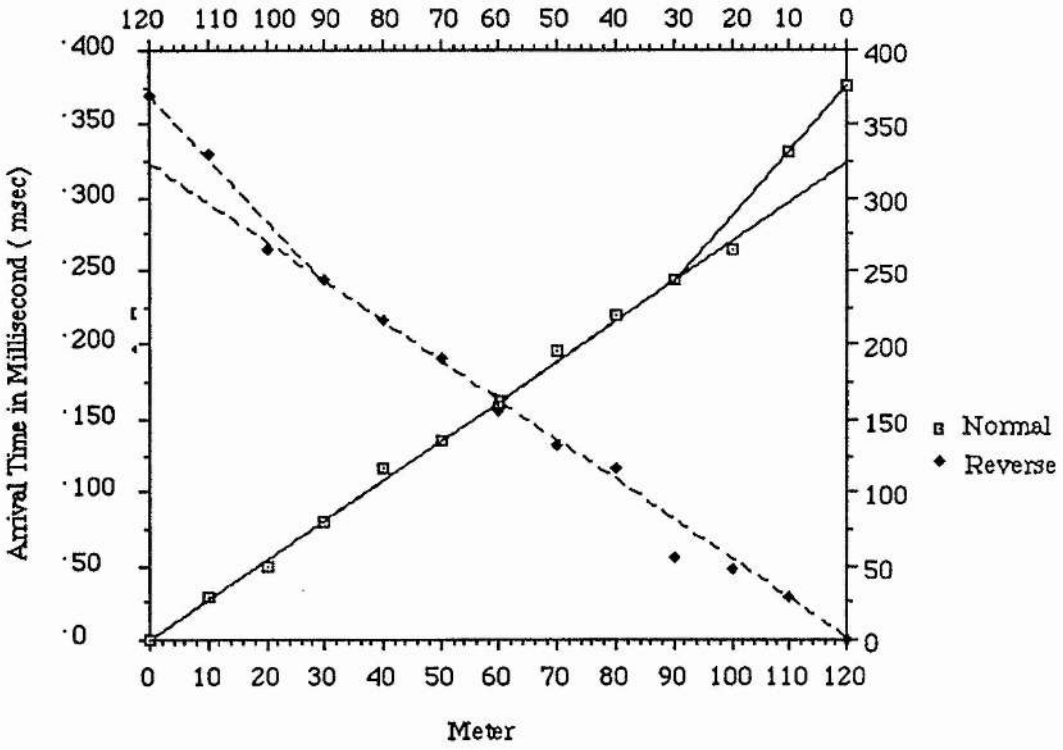

Geophone Distance From Shotpoint A&B in Meter (Station no . B S8)

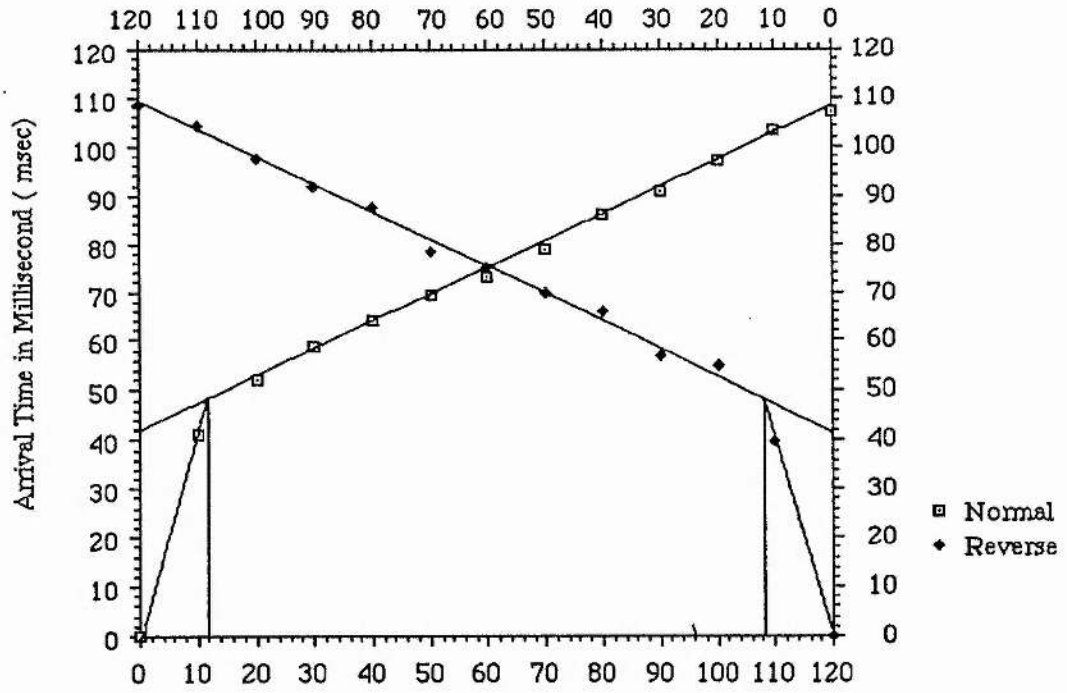
Arrival Time in Millisecond (msec)
Normal
Reverse
Geophone Distance From Shotpoint A&B in Meter (Station no BS9)

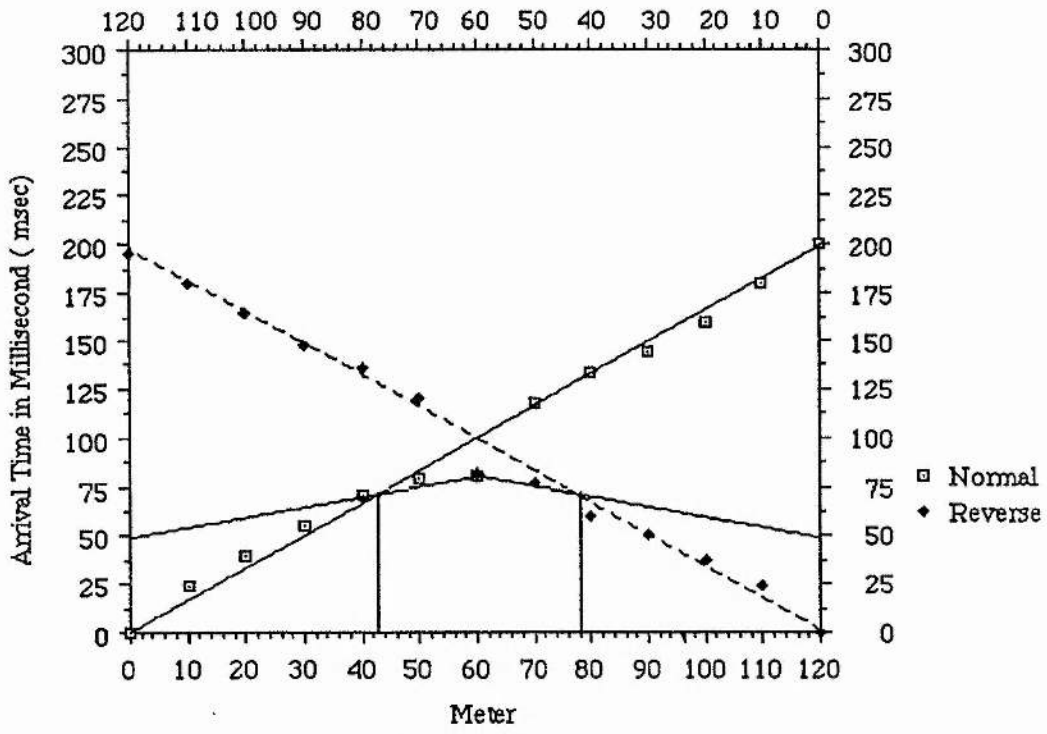
Arrival Time in Millisecond (msec)
Normal
Reverse
Meter
Geophone Distance From Shotpoint A&B in Meter (Station no BS10)

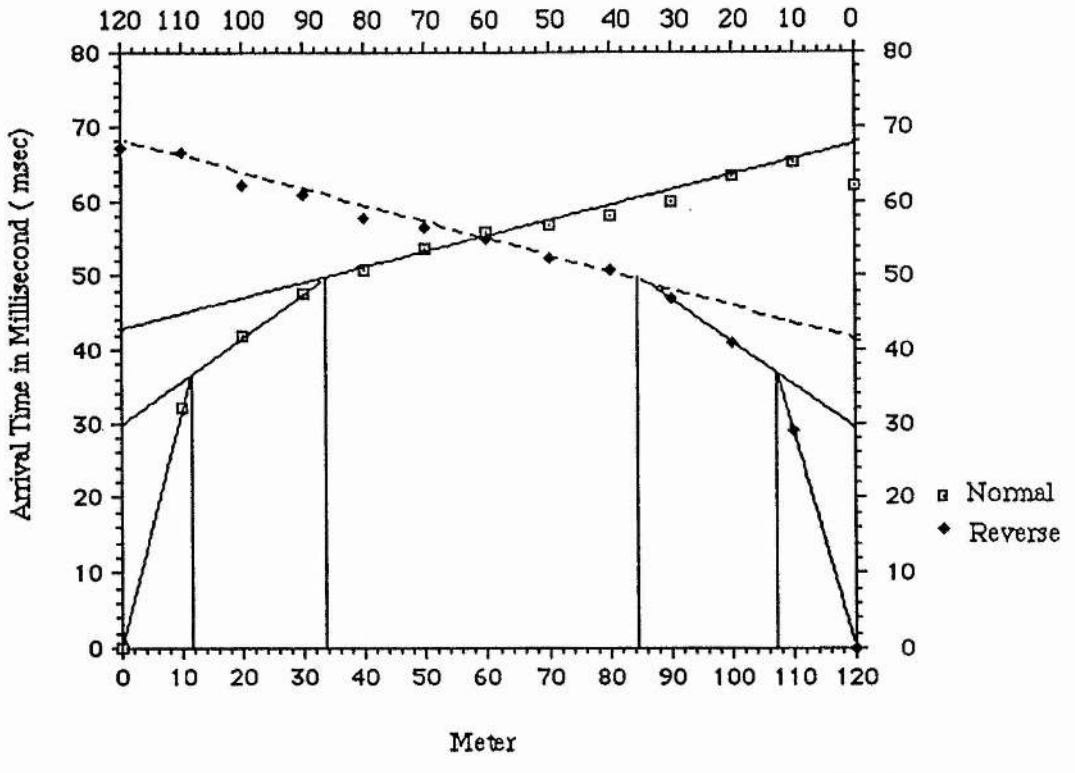

Geophone Distance From Shotpoint A&B in Meter (Station no HS1)

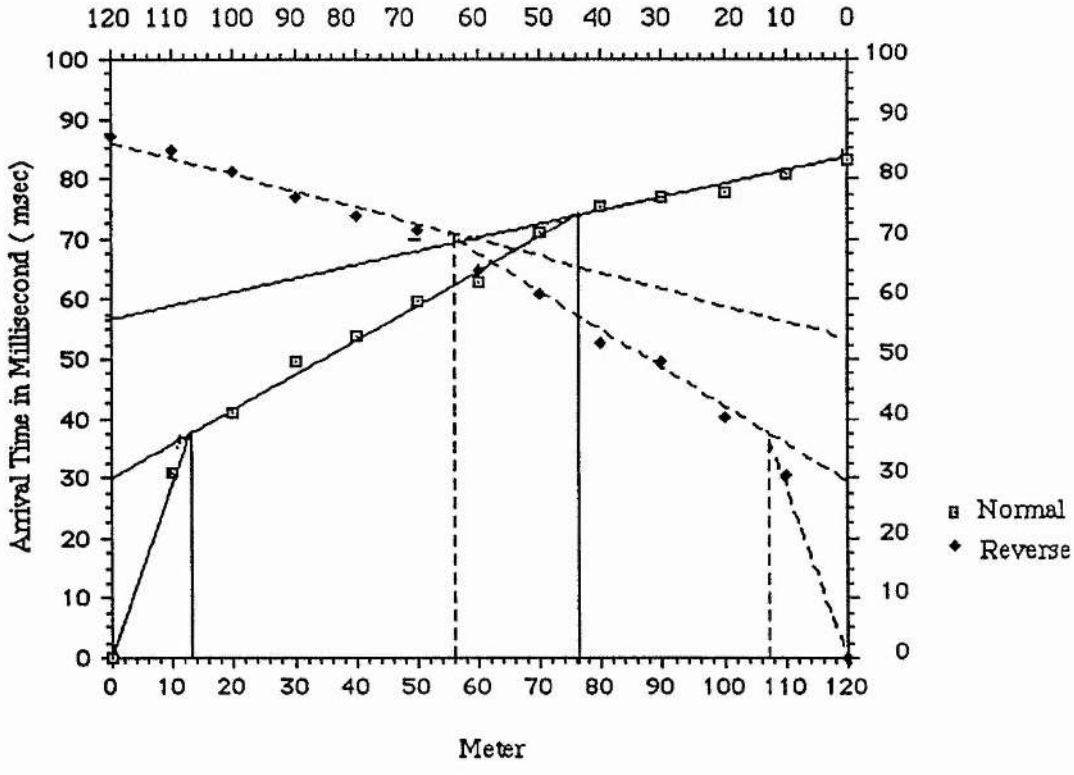

Geophone Distance From Shotpoint A&B in Meter (Station no HS2)

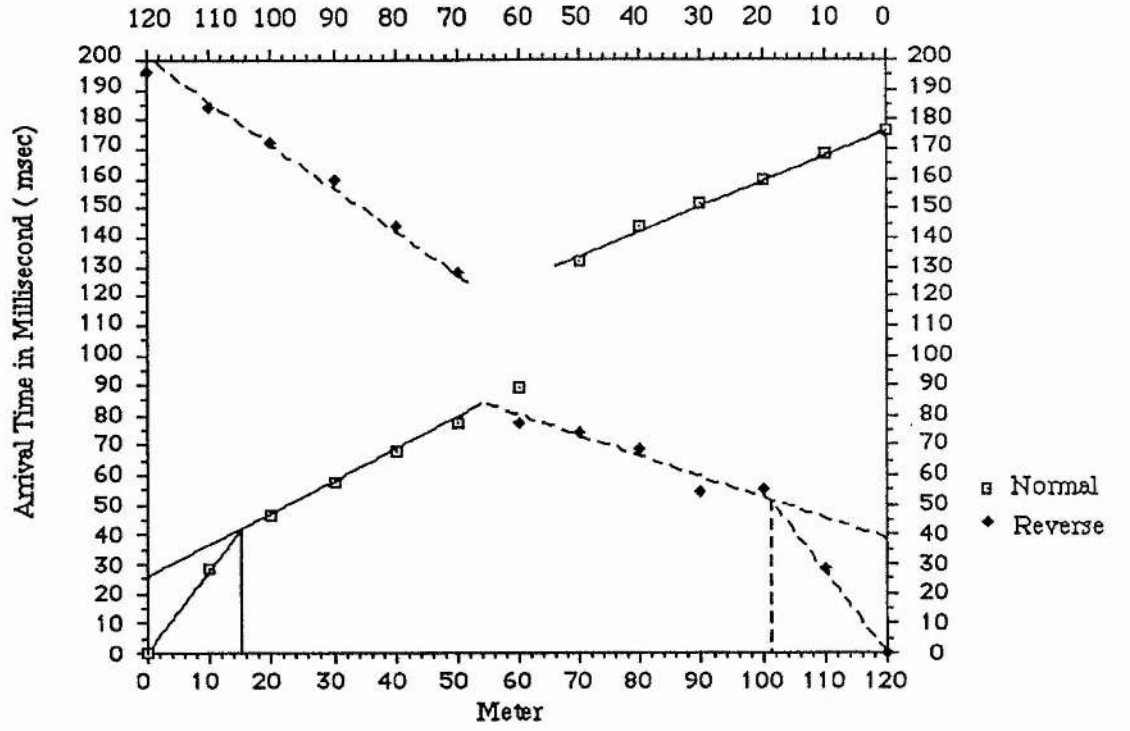

Geophone Distance From Shotpoint A&B in Meter (Station no . HS3)

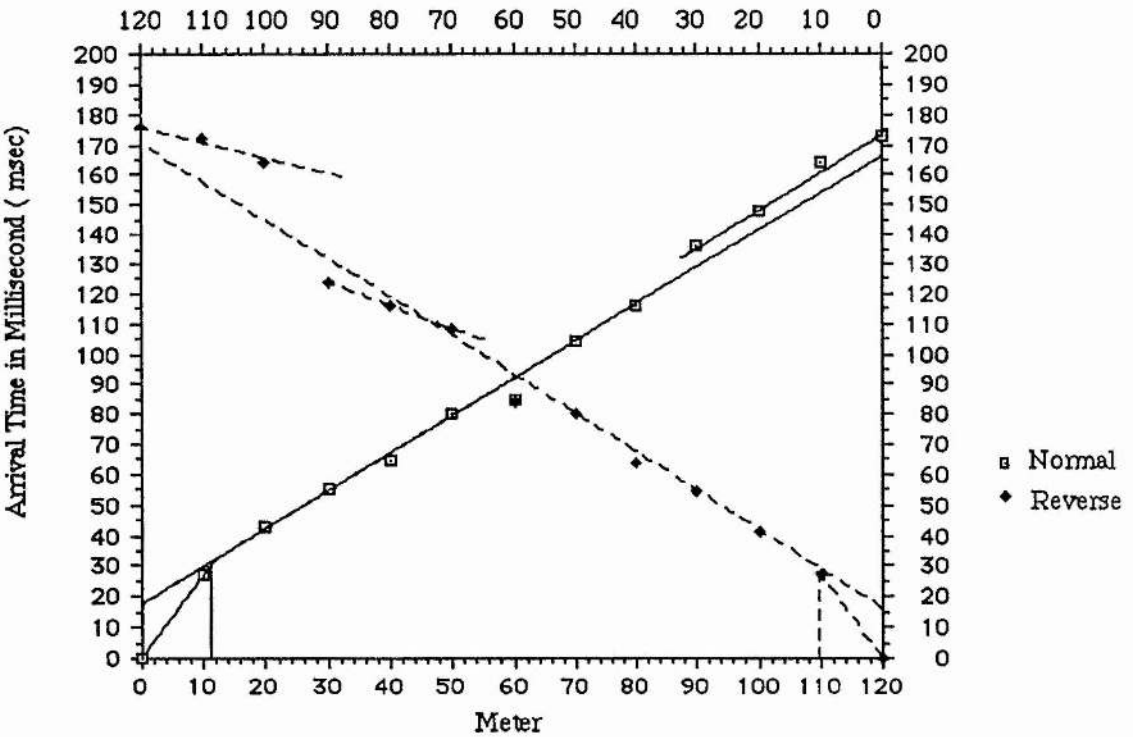

Geophone Distance From Shotpoint A&B in Meter (Station no HS4)

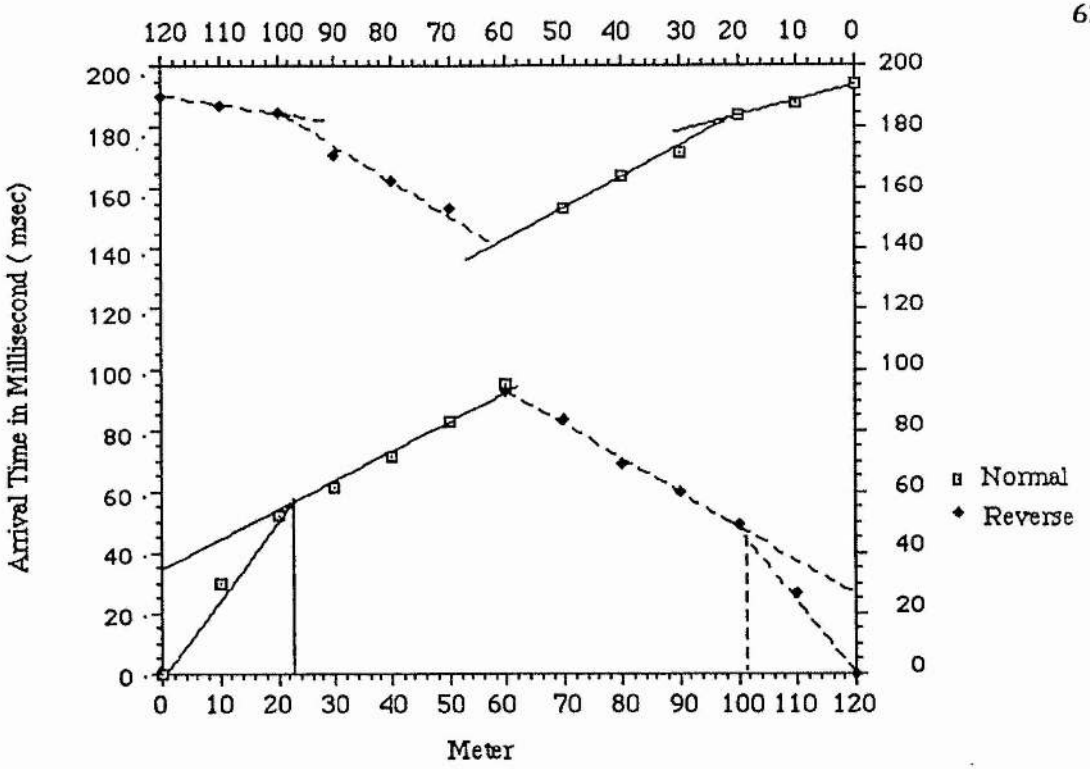

Geophone Distance From Shotpoint A&B in Meter (Station no . HS5)

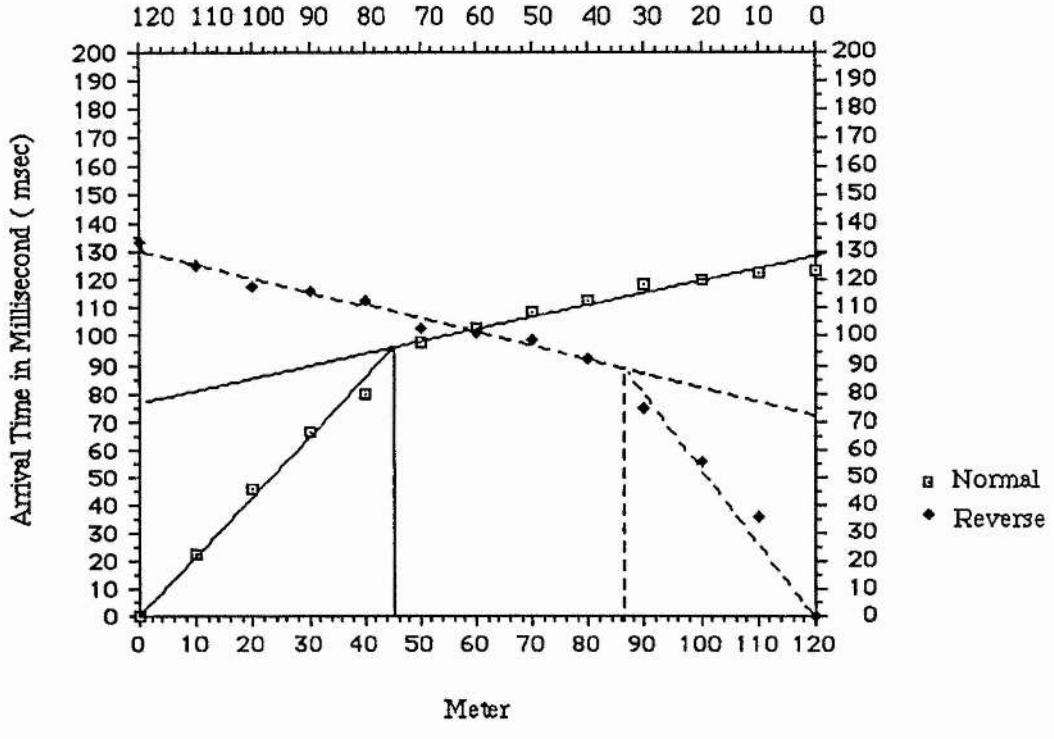

Geophone Distance From Shotpoint A&B in Meter (Station no . HS6)

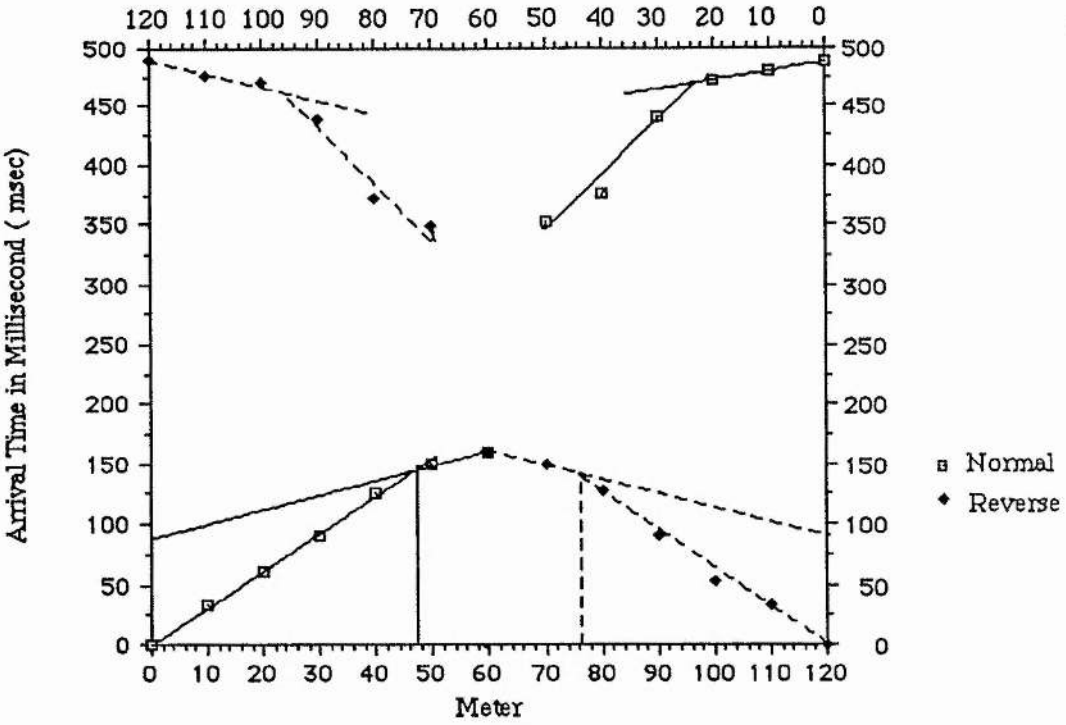

Geophone Distance From Shotpoint A&B in Meter (Station no HS7)

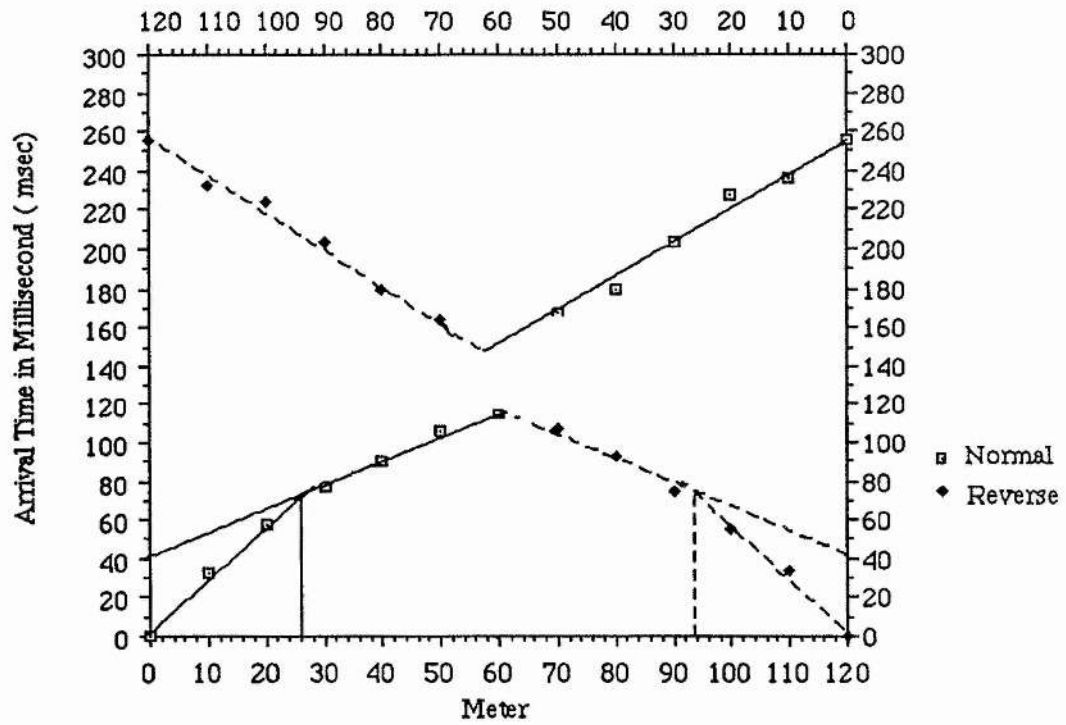

Geophone Distance From Shotpoint A&B in Meter (Station no HS8)

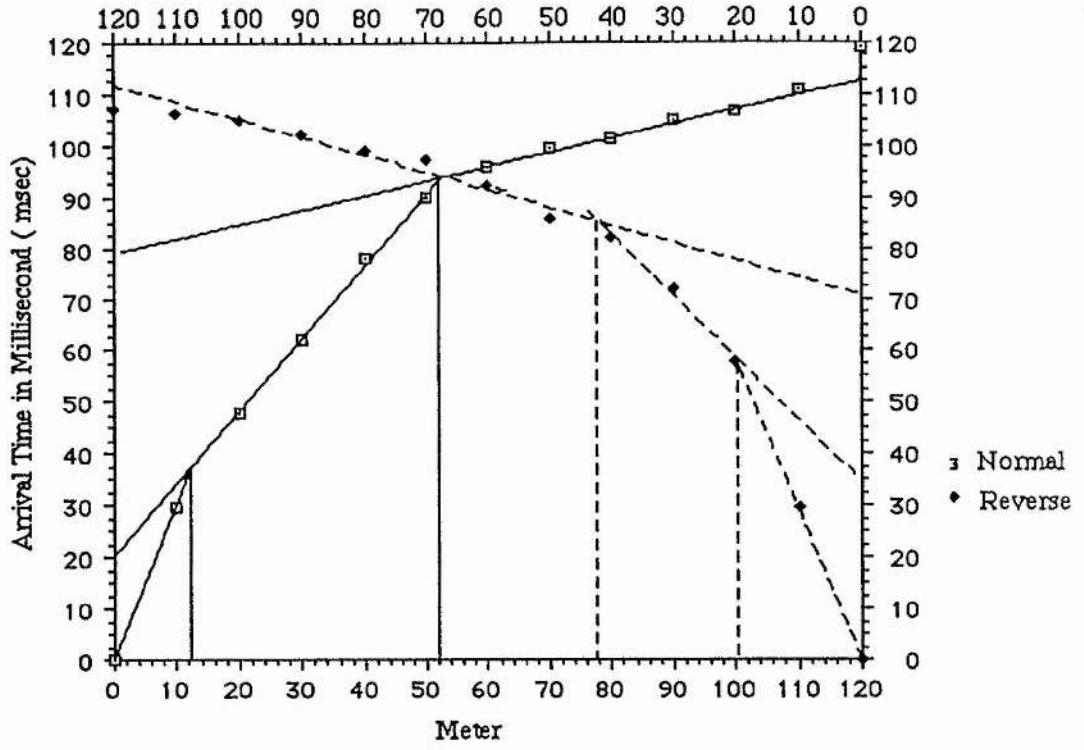

Geophone Distance From Shotpoint A&B in Meter (Station no HS9)

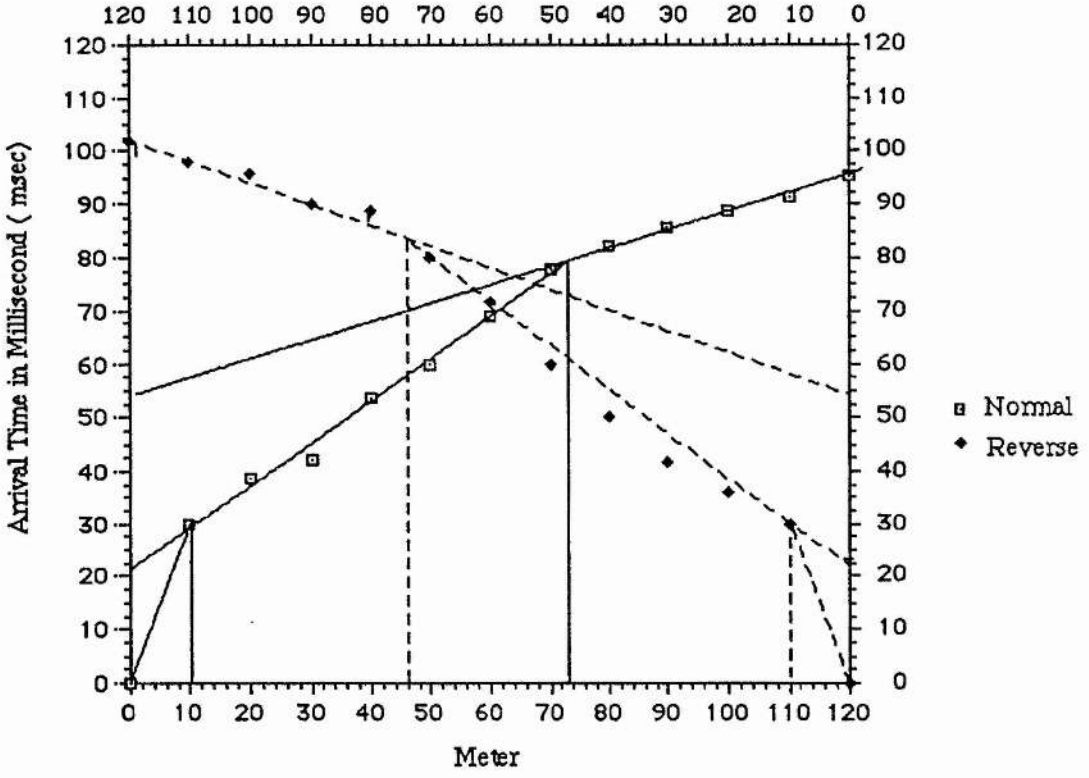

Geophone Distance From Shotpoint A&B in Meter (Station no . HS10)

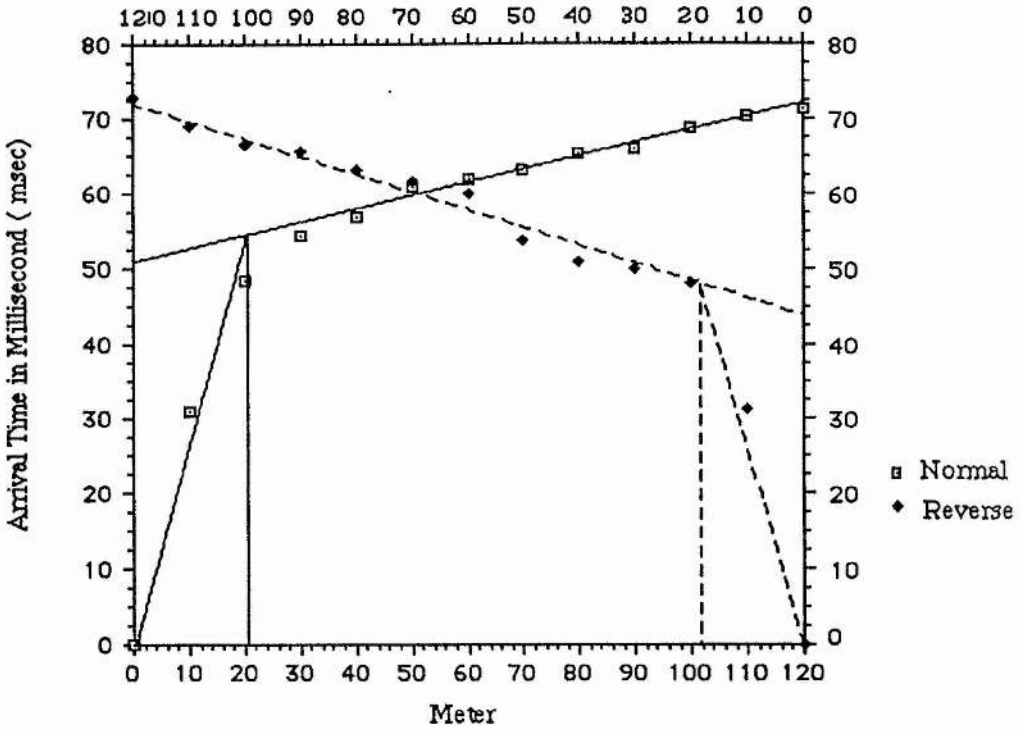

Geophone Distance From Shotpoint A&B in Meter (Station no . HS11)

Appendix 6B Mooney's computer program list.

```
      DIMENSION W(10),V(10),VA(10),VB(10),ALPH(10),BETA(10), Q(10),
     1  A(10),B(10),TAI(10),TBI(10),HA(10),HB(10),DA(10),DB(10),P(10),
     2  TITLE(8)
C SET M = 1 IF INTERCEPT TIMES ARE IN MILLISECONDS, M = 0 IF IN SECONDS.
C N = NUMBER OF LAYERS, INCLUDING HALF-SPACE. ALSO, N = NUMBER OF TRAVEL-
C     TIME SEGMENTS.
C X = PROFILE LENGTH FROM A TO B, IN METERS, KILOMETERS, OR FEET.
C VA(I) = APPARENT VELOCITIES FROM A END, I = 1,N.
C VB(I) = APPARENT VELOCITIES FROM B END  I = 1,N.
C TAI(I) = INTERCEPT TIMES FROM A END, I = 2,N.
C TBI(I) = INTERCEPT TIMES FROM B END, I = 2,N.
C INPUT DATA ARE CHECKED TO ASSURE THAT THEY SATISFY RECIPROCITY AT LEAST
C     WITHIN 10 PERCENT.
C IF B-END INTERCEPT TIMES, TBI, ARE NOT SUPPLIED AS INPUT, THE PROGRAM WILL
C     COMPUTE THEM FROM RECIPROCITY.  INSERT A BLANK CARD WHERE THEY ARE
C     CALLED FOR AS INPUT DATA.
 400  PRINT 401
 401  FORMAT (1H1)
C  N=NUMBER OF LAYERS OR TRAVEL TIME SEGMENTS, X=END-TO-END SPREAD LENGTH.
      READ 405,M,N,X,(TITLE(I),I=1,6)
 405  FORMAT (2I2,F8.0,6A8)
      IF (N) 640,640,407
 407  READ 410,(VA(I),I=1,N)
 410  FORMAT (9F8.0)
      READ 410, (VB(I),I = 1,N)
      READ 410, (TAI(I),I=2,N)
      READ 410, (TBI(I),I=2,N)
      TAI(1) = 0.
      TBI(1) = 0.
      PRINT 411,(TITLE(I),I=1,6),X
 411  FORMAT (2X,6A8,15HSPREAD LENGTH =  ,F8.0,//)
      PRINT 412
 412  FORMAT ('  INPUT DATA' //10X,'LAYER',10X,'APPARENT', 10X,
     1  'APPARENT',10X,'INTERCEPT', 9X,'INTERCEPT'/ 23X,'VELOCITIES, A',
     2  5X,'VELOCITIES, B',7X,'TIMES, A',10X,'TIMES, B'//)
      IF (M) 414,417,414
 414  PRINT 415, (I,VA(I),VB(I),TAI(I),TBI(I),I=1,N)
 415  FORMAT (I12,F22.2,F18.2,F17.1,F18.1)
      DO 416 I = 2,N
      TAI(I) = TAI(I)/1000.
 416  TBI(I) = TBI(I)/1000.
      GO TO 419
 417  PRINT 418, (I,VA(I),VB(I),TAI(I),TBI(I),I=1,N)
 418  FORMAT (I12,F22.2,F18.2,F17.4,F18.4)
 419  CONTINUE
 421  DO 430 I = 2,N
      TBB = TAI(I) + X*(1./VA(I) - 1./VB(I))
      IF (TBI(I)) 422,422,423
 422  TBI(I) = TBB
      GO TO 430
 423  TAEND = TAI(I) + X/VA(I)
      TBEND = TBI(I) + X/VB(I)
      ERROR = ABS (TAEND/TBEND - 1.)
      IF (ERROR - 0.10) 430,424,424
 424  PRINT 425,I
 425  FORMAT (5X,    74HAPPARENT VELOCITY AND TIME INTERCEPT DATA ARE IN
     1CONSISTENT AT LAYER NUMBER   ,I2,/,7X,56HEND-TO-END TRAVEL TIMES D
     2IFFER BY MORE THAN 10 PERCENT.       ,//)
 430  CONTINUE
      V(1) = (VA(1) + VB(1))*.5
      DO 570 M = 2,N
      K = 1
      ALPH(1) = ASIN (V(1)/VB(M))
      BETA(1) = ASIN (V(1)/VA(M))
      IF (M-2) 500,500,510
 500  A(1) = (ALPH(1) + BETA(1))*.5
```

```
      W(2) = (ALPH(1) - BETA(1))*.5
      V(2) = V(1)/SIN (A(1))
      GO TO 550
  510 A(1) = ALPH(1) - W(2)
      B(1) = BETA(1) + W(2)
  520 K = K+1
      VV = V(K)/V(K-1)
      P(K) = ASIN (VV*SIN (A(K-1)))
      Q(K) = ASIN (VV*SIN (B(K-1)))
      IF (K+1-M) 530,540,540
  530 A(K) = P(K) - W(K+1) + W(K)
      B(K) = Q(K) + W(K+1) - W(K)
      ALPH(K) = A(K) + W(K+1)
      BETA(K) = B(K) - W(K+1)
      GO TO 520
  540 A(K) = (P(K) + Q(K))*.5
      B(K) = A(K)
      W(K+1) = W(K) + (P(K) - (K))*.5
      ALPH(K) = A(K) + W(K+1)
      BETA(K) = B(K) - W(K+1)
      V(K+1) = V(K)/SIN (A(K))
  550 KK = K-1
      HHA = 0.
      HHB = 0.
      IF (KK) 561,561,551
  551 DO 561 I = I,KK
      HH = COS (ALPH(I)) + COS (BETA(I))
      HH = HH/V(I)
      HHA = HHA + HH*HA(I)
  560 HHB = HHB + HH*HB(I)
  561 CONTINUE
      R = V(K)/(COS (ALPH(K)) + COS (BETA(K)))
      HA(K) = R*(TAI(K+1) - HHA)
      HB(K) = R*(TBI(K+1) - HHB)
      DA(1) = HA(1)
      DB(1) = HB(1)
      IF (K-1) 570,570,569
  569 DA(K) = DA(K-1) + HA(K)
      DB(K) = DB(K-1) + HB(K)
  570 CONTINUE
      DO 580 J = 2,N
  580 W(J) = W(J)*57.2958              +0.001
      PRINT 620
  620 FORMAT (/// 2X,18HCOMPUTED STRUCTURE  // 9X,5HLAYER, 6X,8HVELOCITY
     1 ,  6X,11HTHICKNESS A, 4X,11HTHICKNESS B, 8X,3HDIP,10X,7HDEPTH A,
     2    8X,7HDEPTH B //)
      I = 1
      PRINT 625, I, V(I), HA(I), HB(I),DA(I), DB(I)
  625  FORMAT (I12,3F15.2,15X,2F15.2)
      IF (N-2) 632,632,627
  627 NN = N - 1
      PRINT 630,(I, V(I), HA(I), HB(I), W (I),DA(I),DB(I),I=2,NN)
  630 FORMAT (I12,6F15.2)
  632 PRINT 635,N,V(N),W(N)
  635 FORMAT (I12,F15.2,30X,F15.2)
      PRINT 638
  638 FORMAT (/////
     1  5X,'OUTPUT DATA ARE PRINTED TO TWO DECIMAL PLACES,'/
     1  5X,'BUT NO IMPLICATION IS INTENDED THAT THE SEISMIC'/
     1  5X,'RESULTS HAVE THIS DEGREE OF RELIABILITY.')
      GO TO 400
  640 CONTINUE
      END
```

Appendix 6C Resistivity data of Wadi Baysh and Wadi Habawnah.

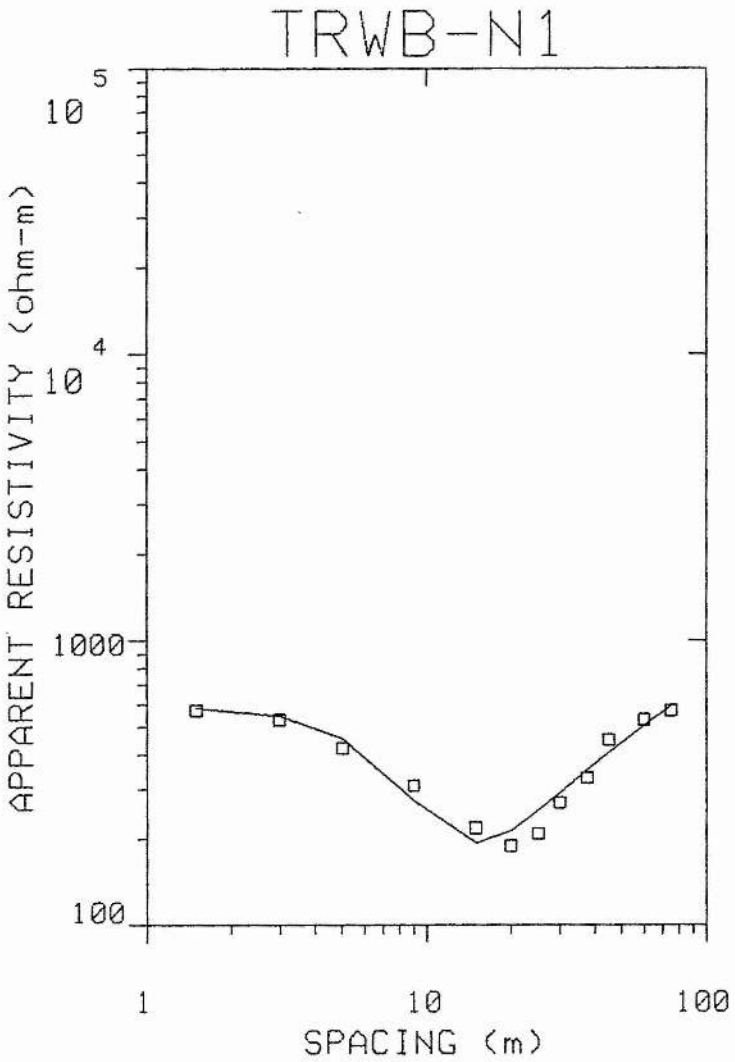
TRWB-N1
APPARENT RESISTIVITY (ohm-m)
10^5
10^4
1000
100
1
10
100
SPACING (m)

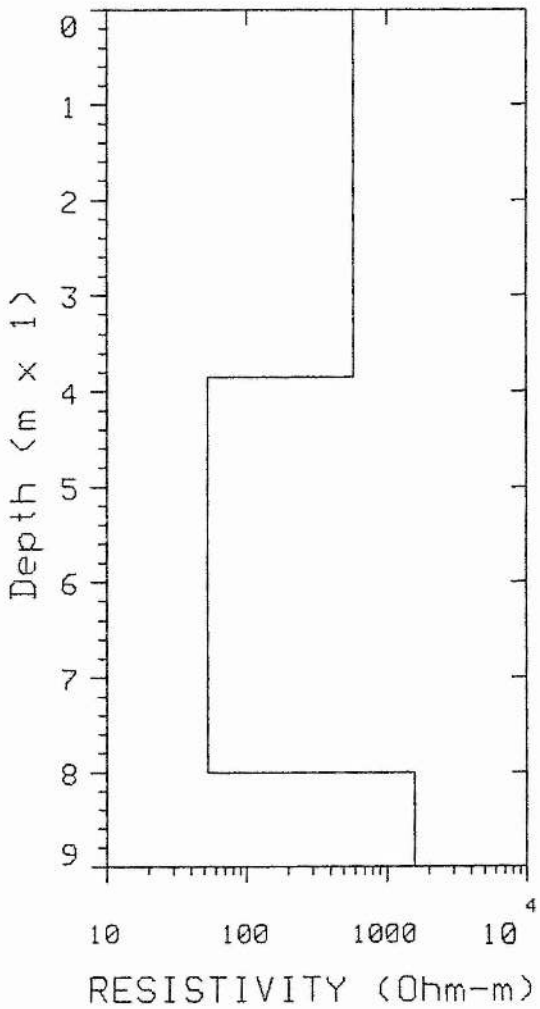
Depth (m x 1)
0
1
2
3
4
5
6
7
8
9
10
100
1000
10^4
RESISTIVITY (Ohm-m)

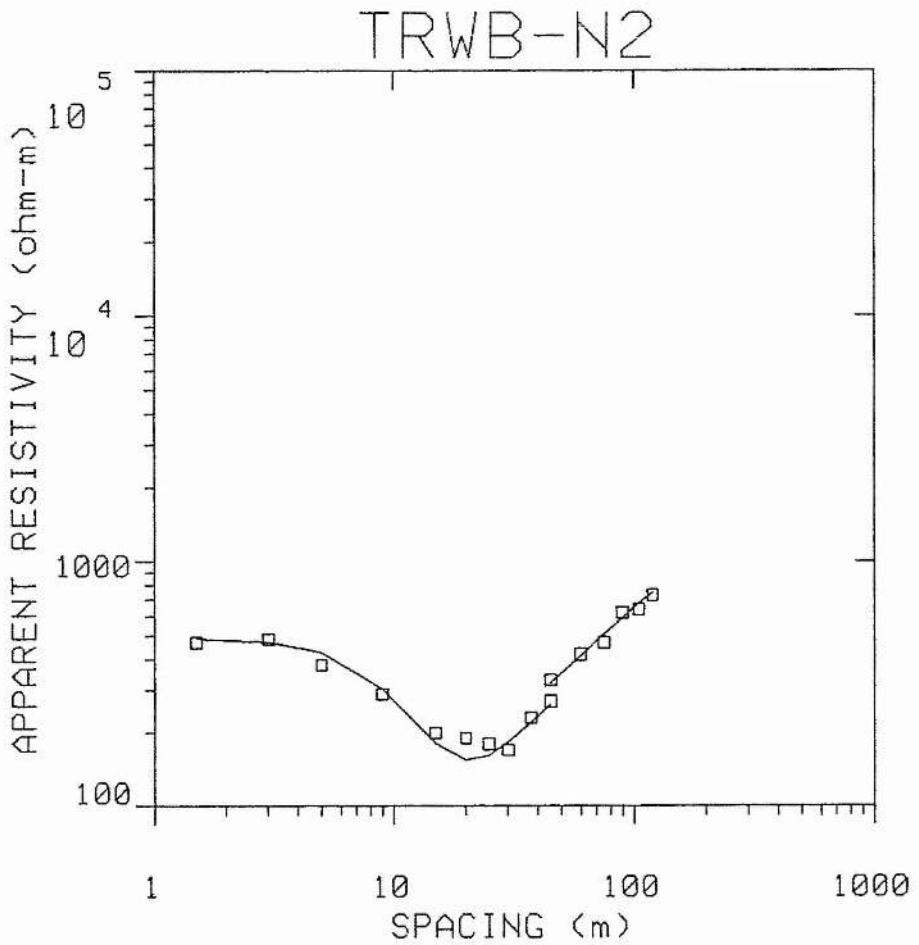
TRWB-N2
APPARENT RESISTIVITY (ohm-m)
10^5
10^4
1000
100
1
10
100
1000
SPACING (m)

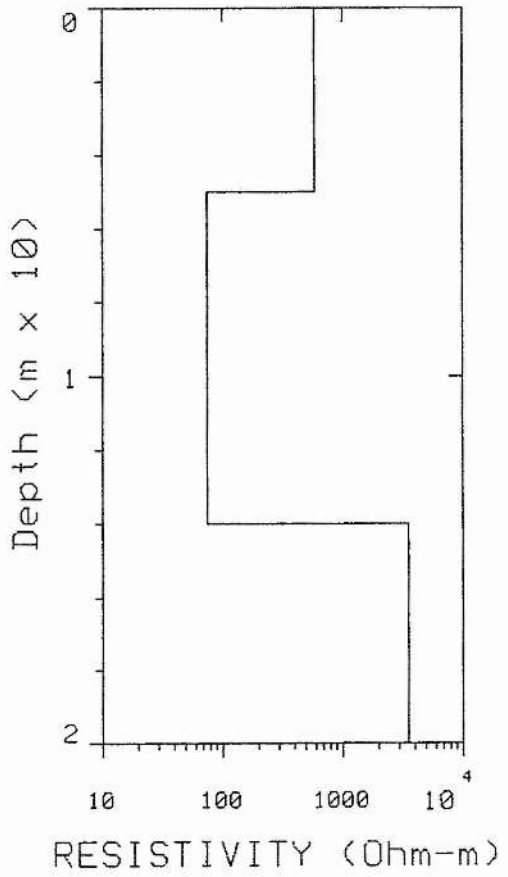
Depth (m x 10)
0
1
2
10
100
1000
10^4
RESISTIVITY (Ohm-m)

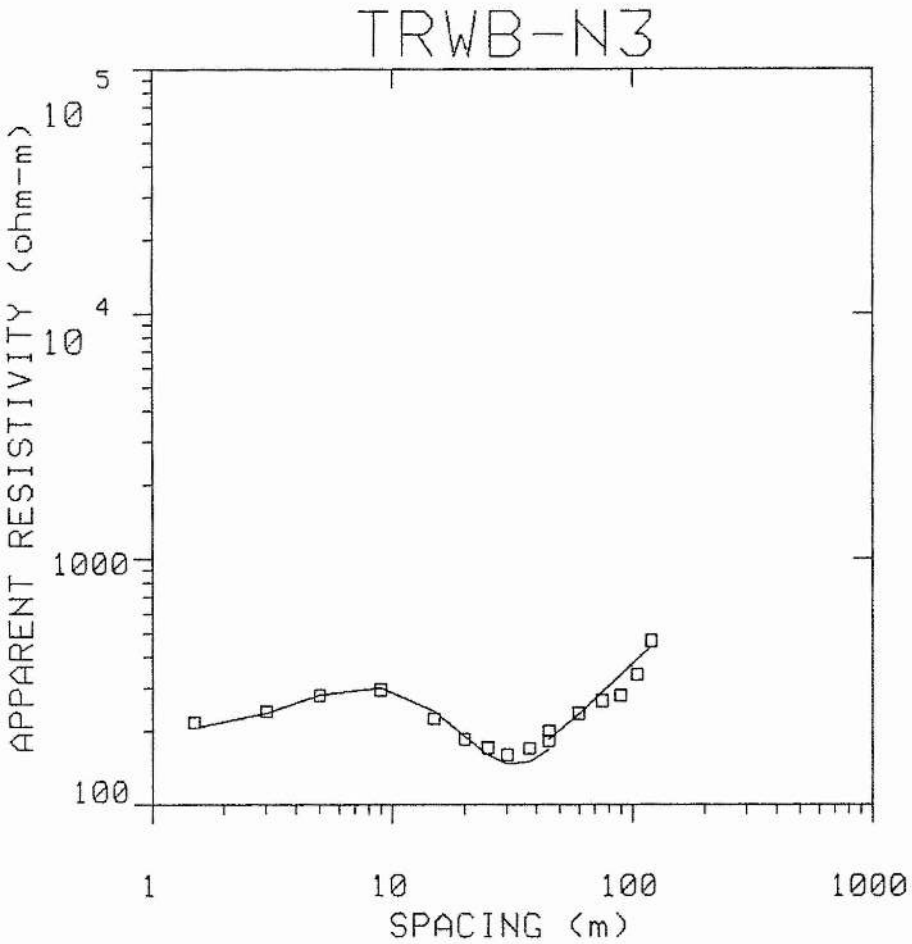
TRWB-N3
APPARENT RESISTIVITY (ohm-m)
10^5
10^4
1000
100
1
10
100
1000
SPACING (m)

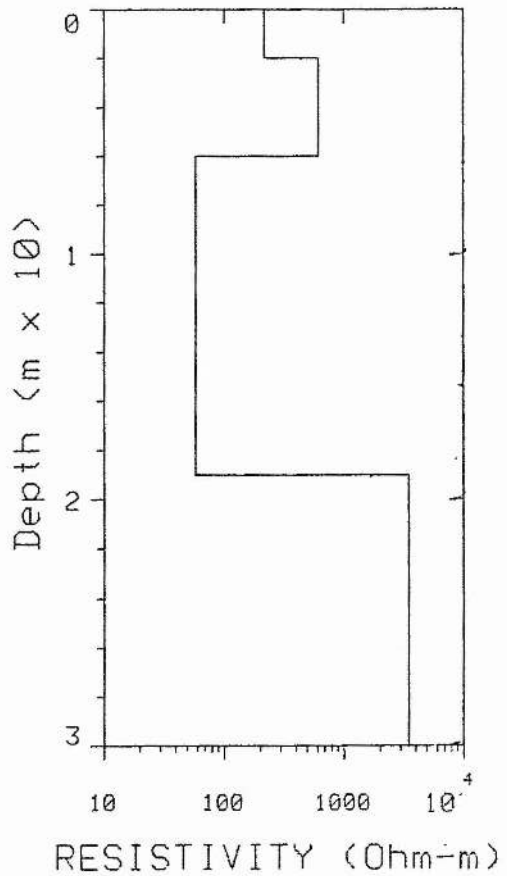
Depth (m x 10)
0
1
2
3
10
100
1000
10^4
RESISTIVITY (Ohm-m)

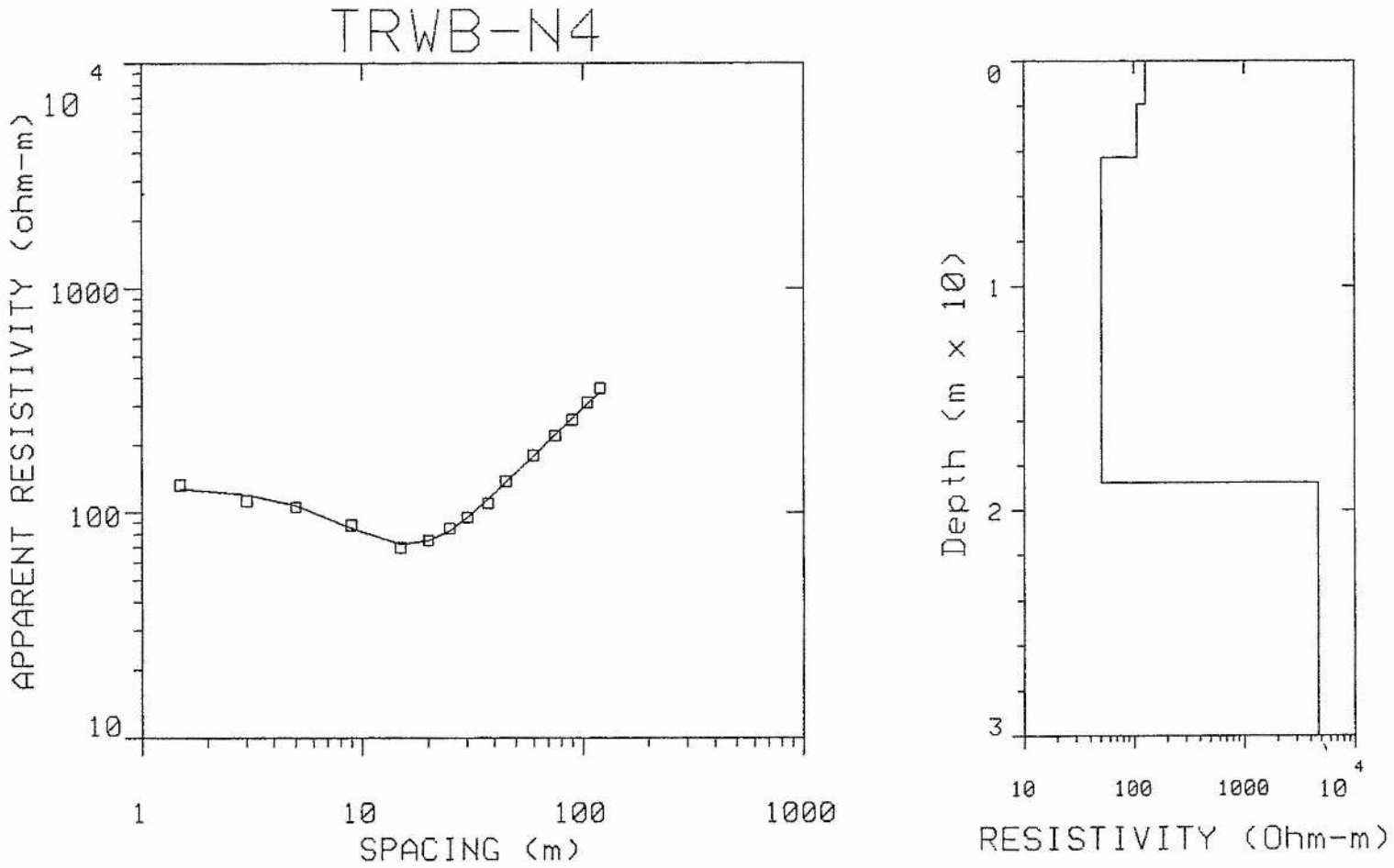
TRWB-N4
APPARENT RESISTIVITY (ohm-m)
10
4
1000
100
10
1
10
100
1000
SPACING (m)
Depth (m x 10)
0
1
2
3
10
100
1000
10
4
RESISTIVITY (Ohm-m)

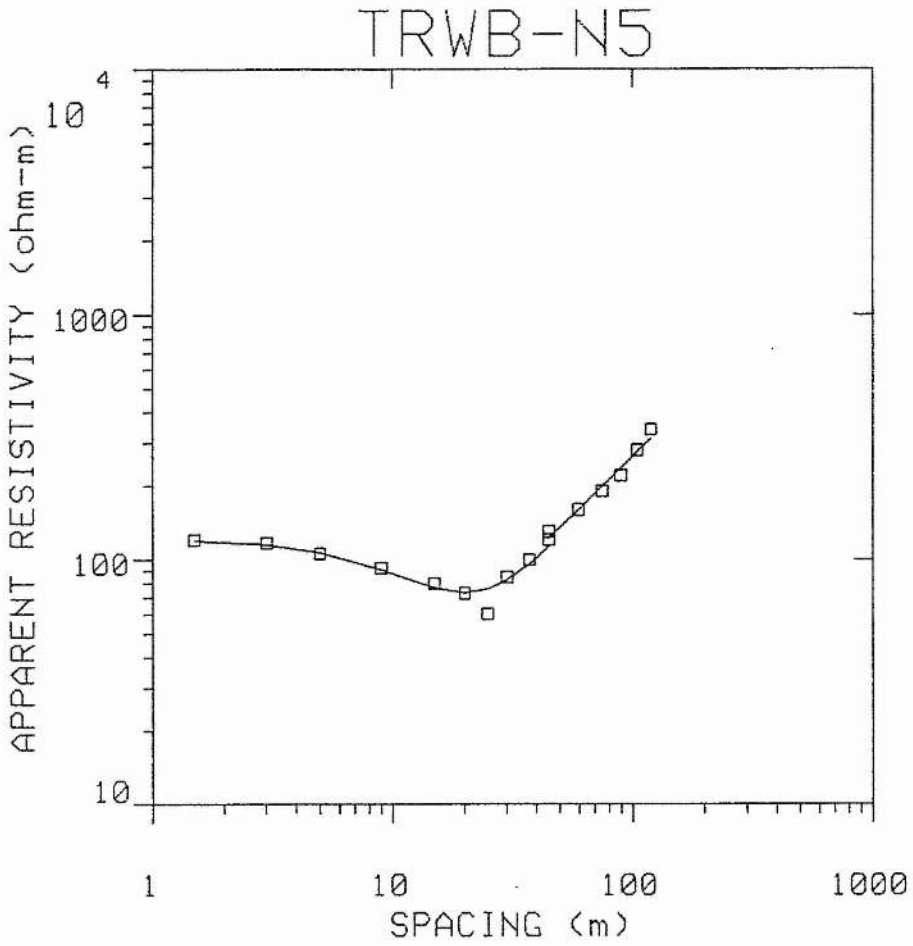
TRWB-N5
APPARENT RESISTIVITY (ohm-m)
10^4
1000
100
10
1
10
100
1000
SPACING (m)

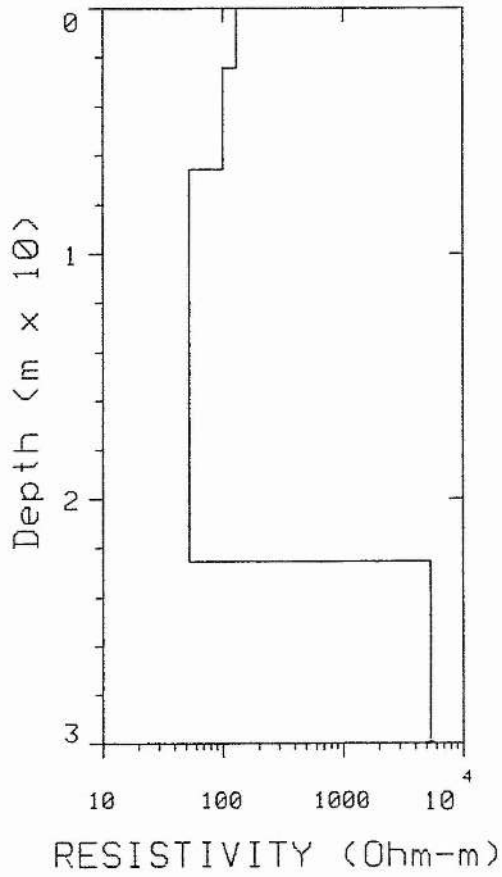
Depth (m x 10)
0
1
2
3
10
100
1000
10^4
RESISTIVITY (Ohm-m)

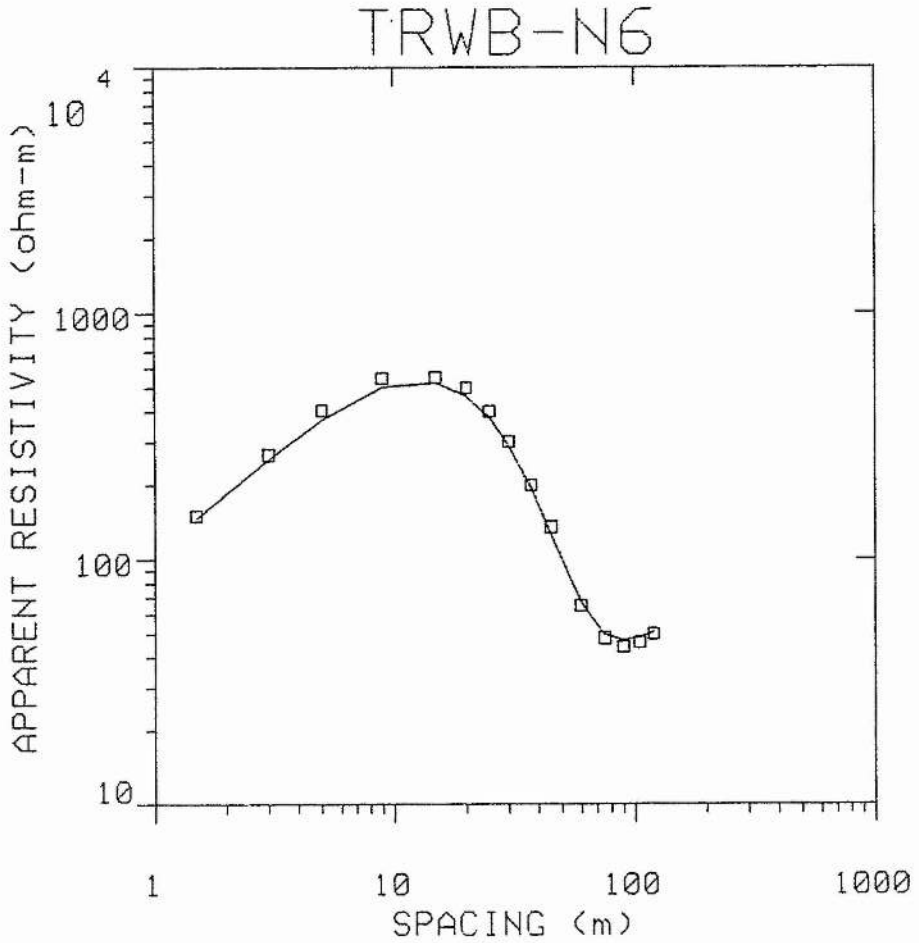
TRWB-N6
APPARENT RESISTIVITY (ohm-m)
10 4
1000
100
10
1
10
100
1000
SPACING (m)

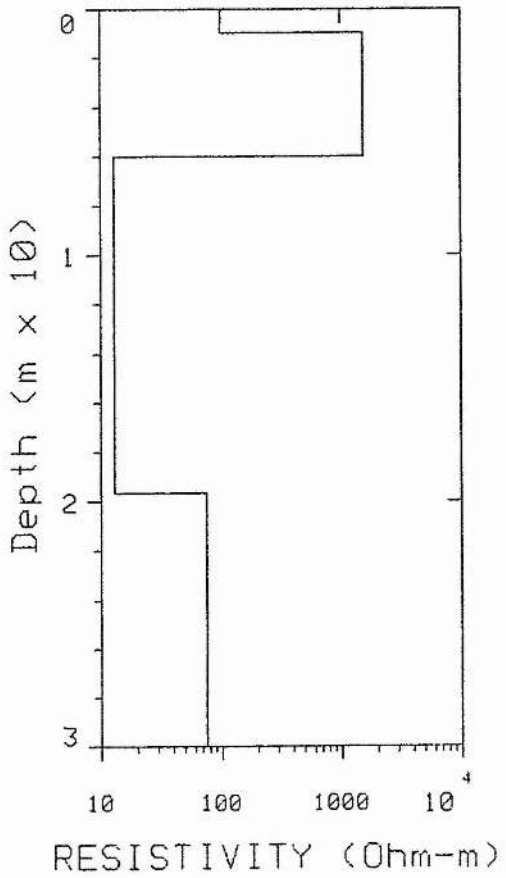
Depth (m x 10)
0
1
2
3
10
100
1000
10 4
RESISTIVITY (Ohm-m)

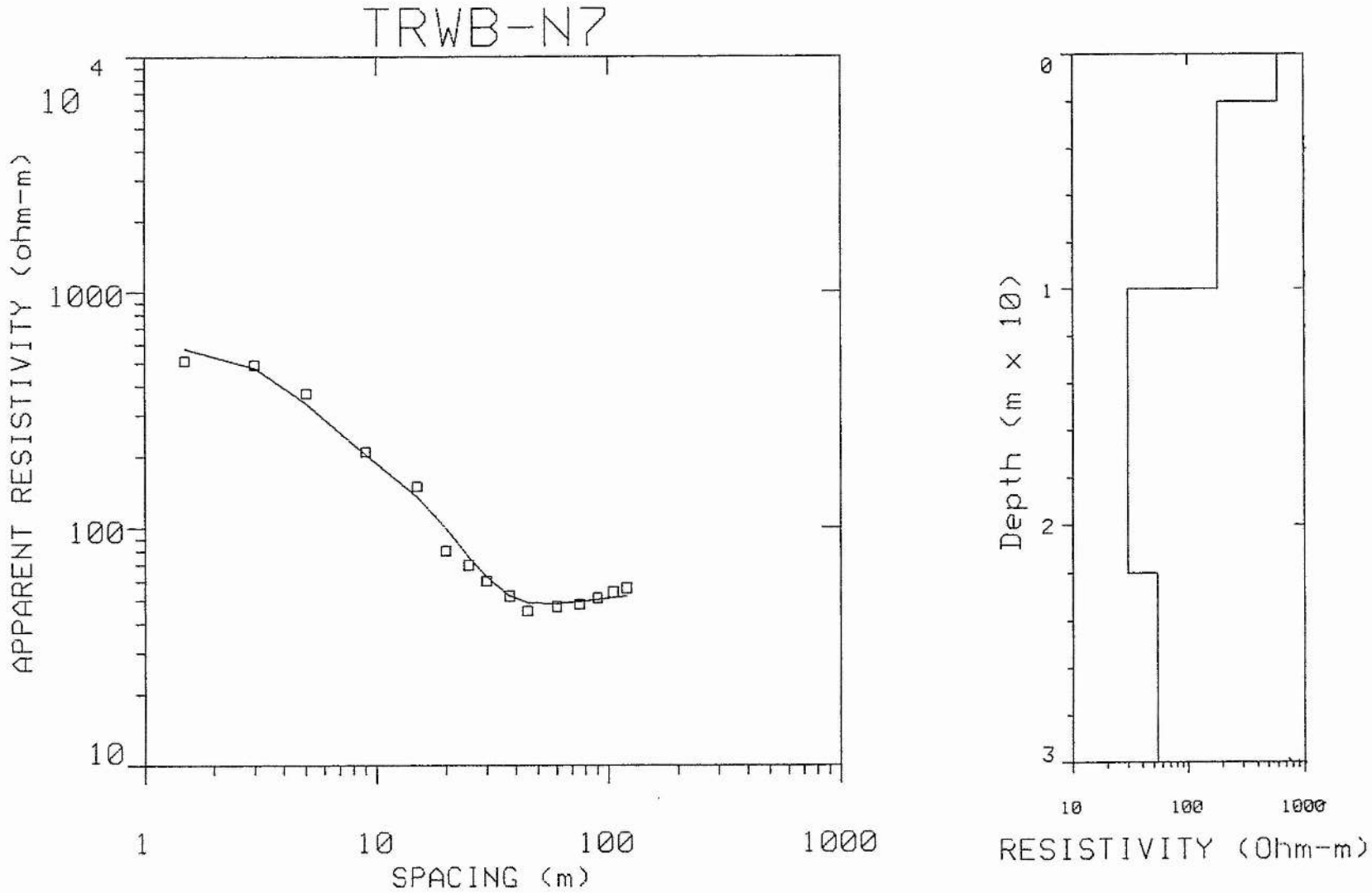
TRWB-N7
APPARENT RESISTIVITY (ohm-m)
10^4
1000
100
10
1
10
100
1000
SPACING (m)
Depth (m x 10)
0
1
2
3
10
100
1000
RESISTIVITY (Ohm-m)

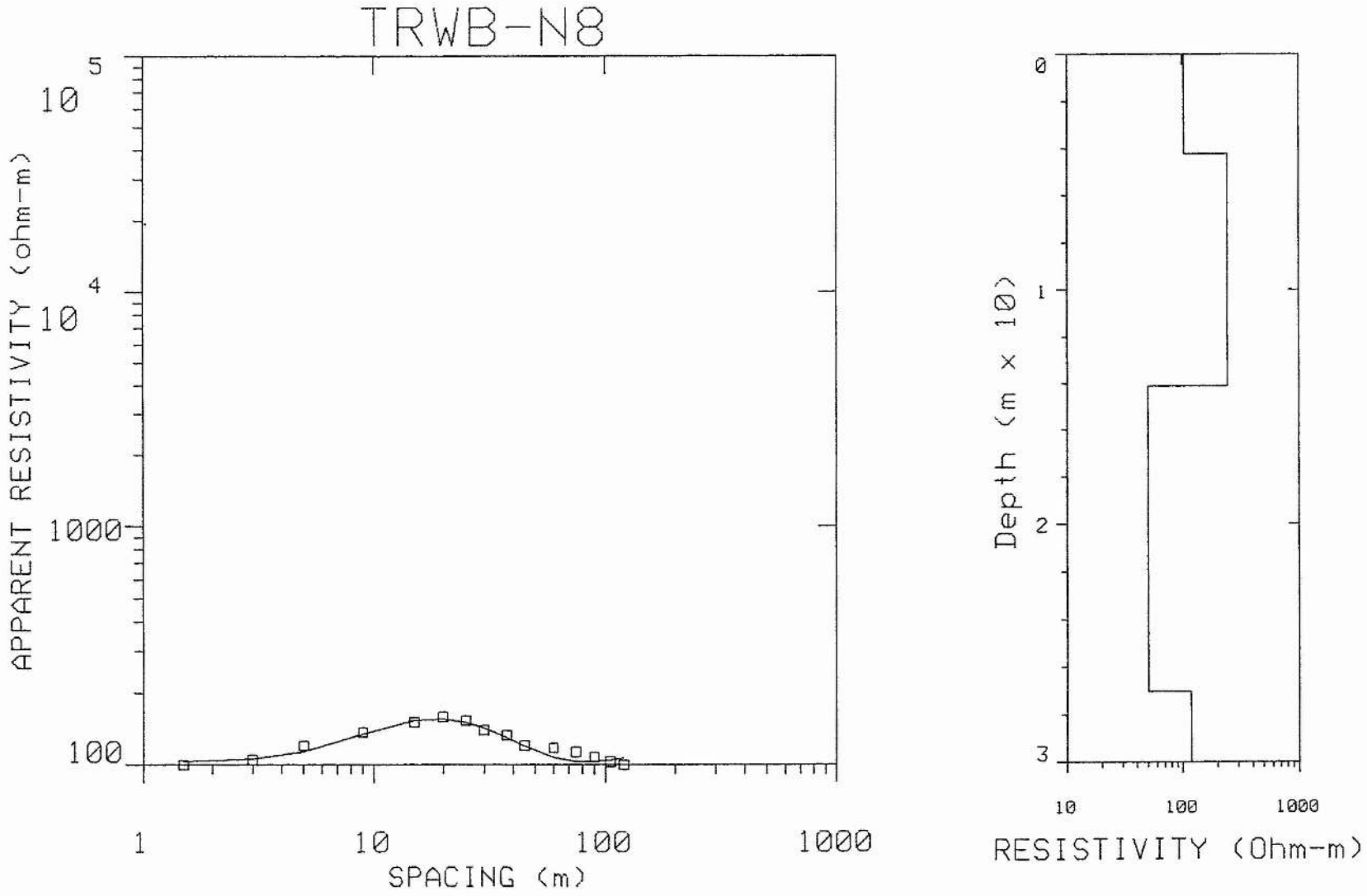
TRWB-N8
APPARENT RESISTIVITY (ohm-m)
10^5
10^4
1000
100
1
10
100
1000
SPACING (m)
Depth (m x 10)
0
1
2
3
10
100
1000
RESISTIVITY (Ohm-m)

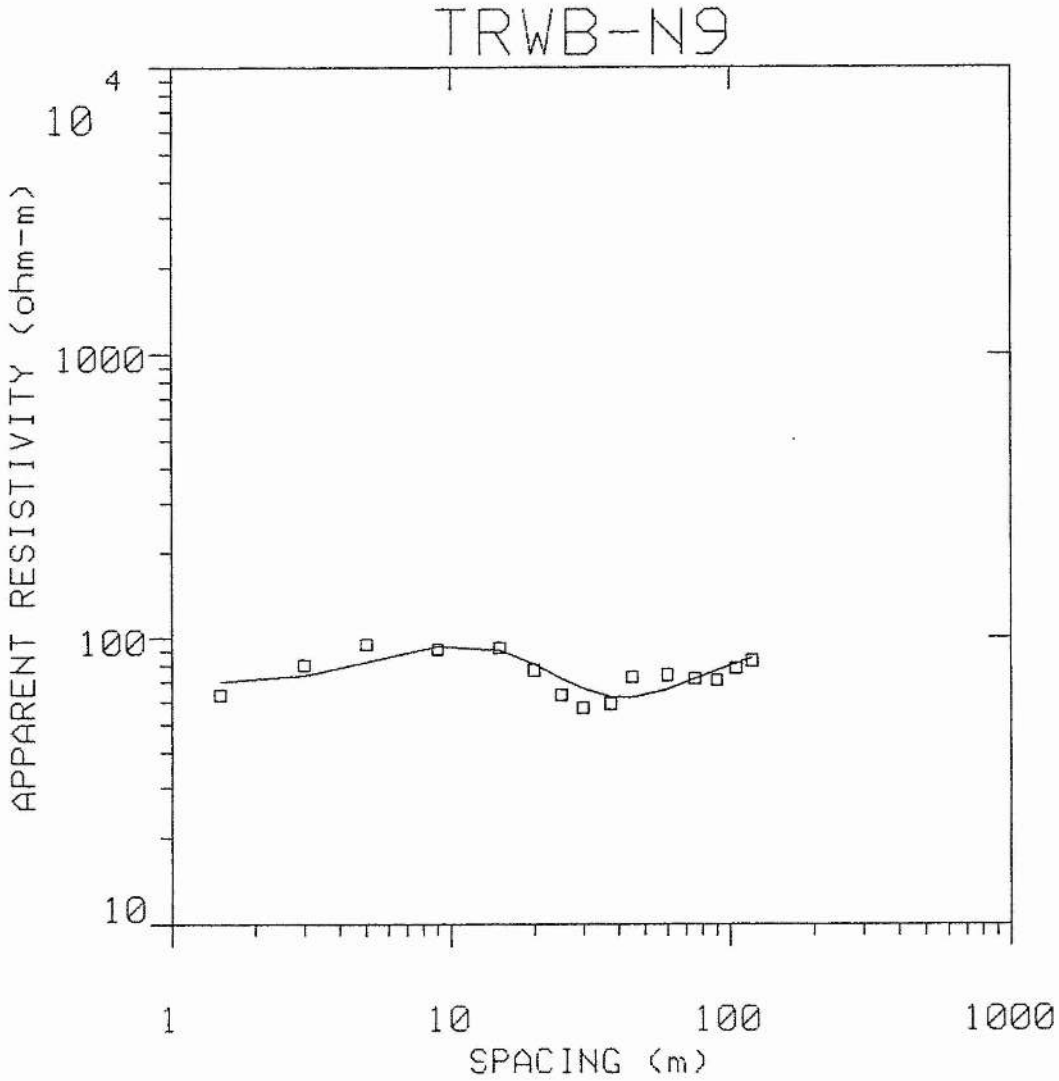
TRWB-N9
APPARENT RESISTIVITY (ohm-m)
10 4
1000
100
10
1
10
100
1000
SPACING (m)

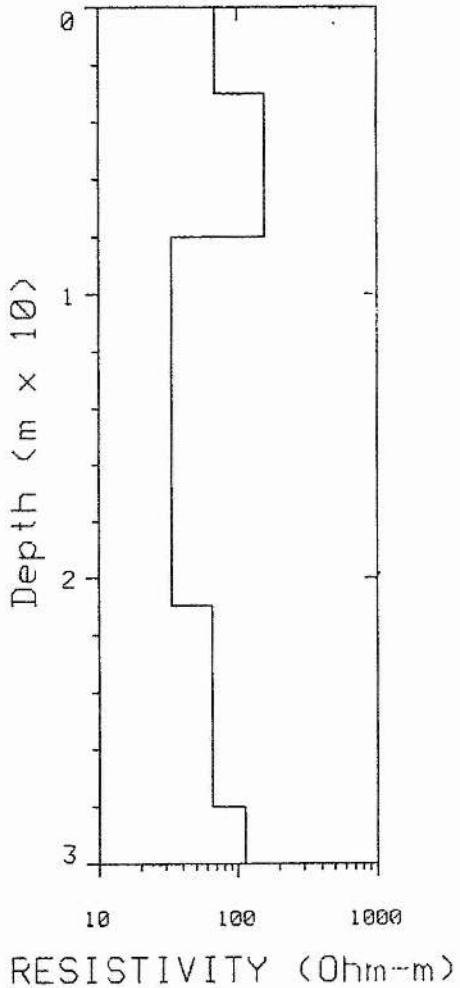
Depth (m x 10)
0
1
2
3
10
100
1000
RESISTIVITY (Ohm-m)

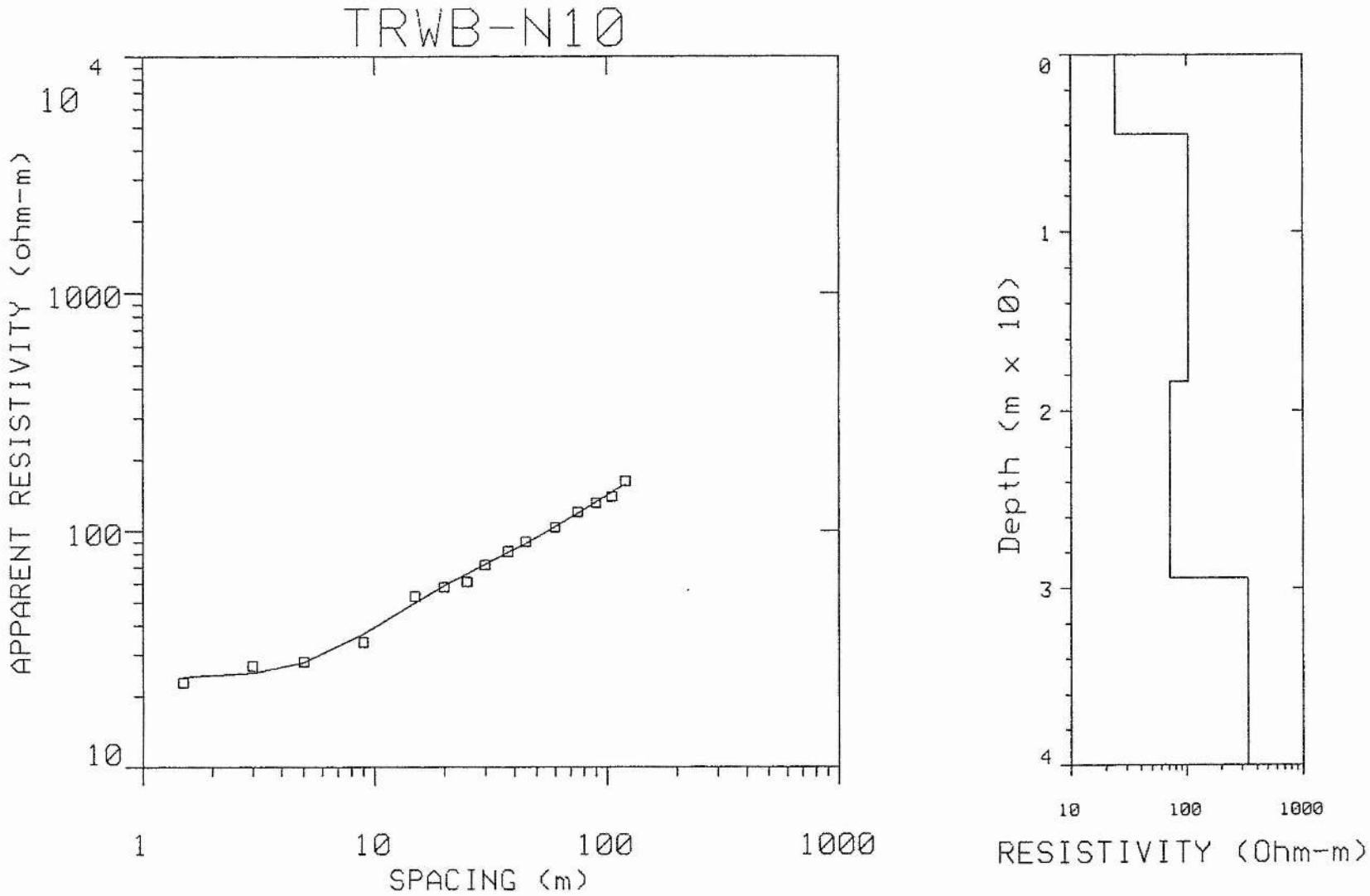
TRWB-N10
APPARENT RESISTIVITY (ohm-m)
10^4
1000
100
10
1
10
100
1000
SPACING (m)
Depth (m x 10)
0
1
2
3
4
10
100
1000
RESISTIVITY (Ohm-m)

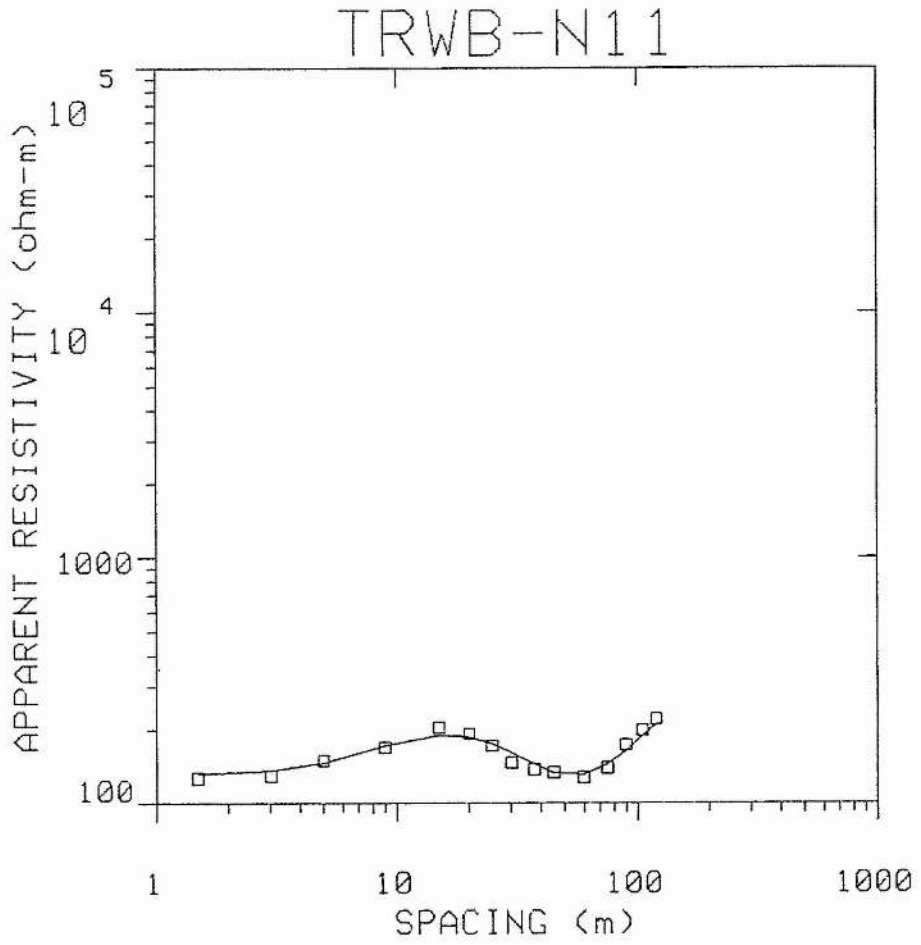
TRWB-N11
APPARENT RESISTIVITY (ohm-m)
10^5
10^4
1000
100
1
10
100
1000
SPACING (m)

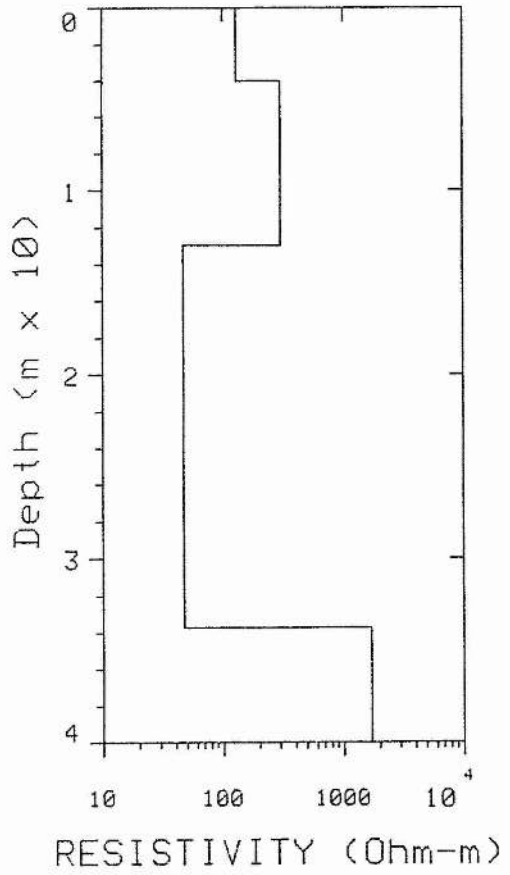
Depth (m x 10)
0
1
2
3
4
10
100
1000
10^4
RESISTIVITY (Ohm-m)

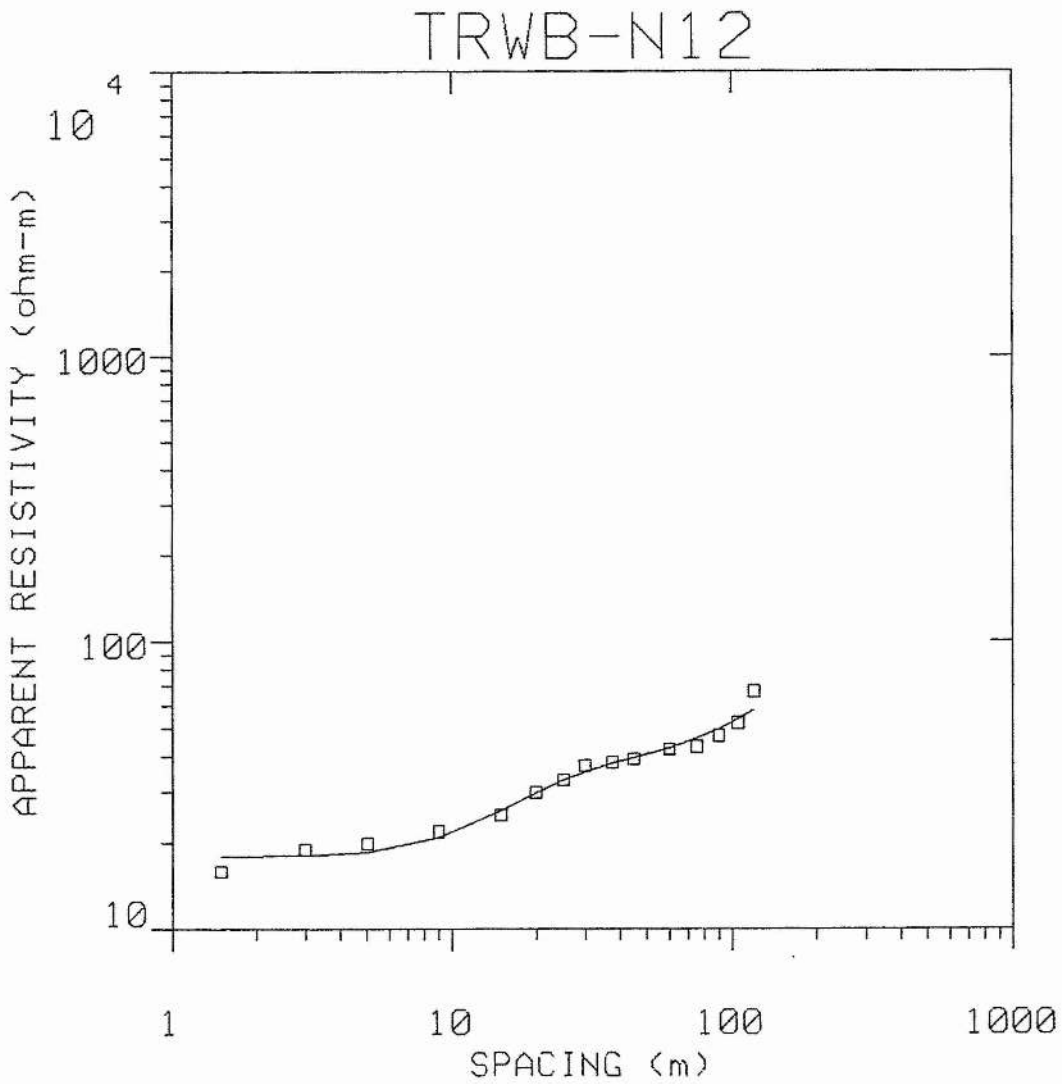
TRWB-N12
APPARENT RESISTIVITY (ohm-m)
10 4
1000
100
10
1
10
100
1000
SPACING (m)

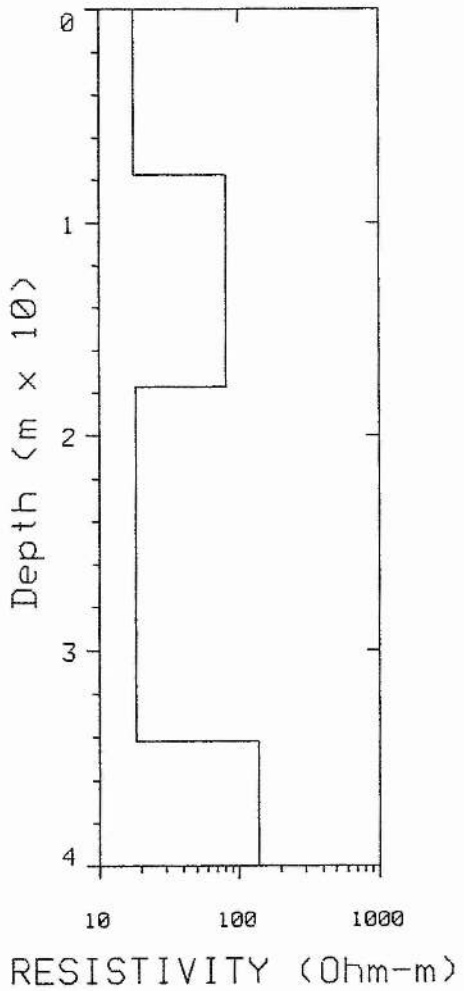
Depth (m x 10)
0
1
2
3
4
10
100
1000
RESISTIVITY (Ohm-m)

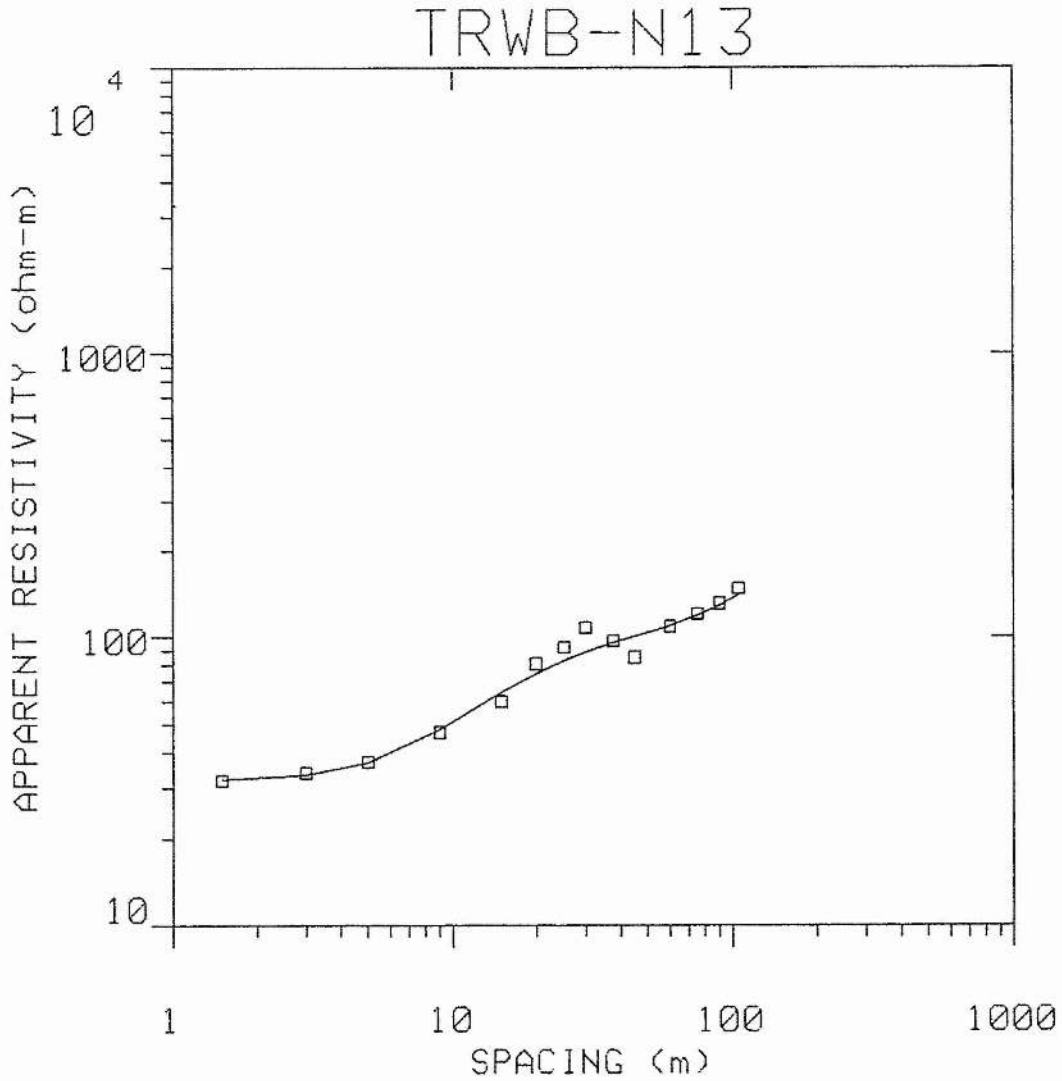
TRWB-N13
APPARENT RESISTIVITY (ohm-m)
10^4
1000
100
10
1
10
100
1000
SPACING (m)

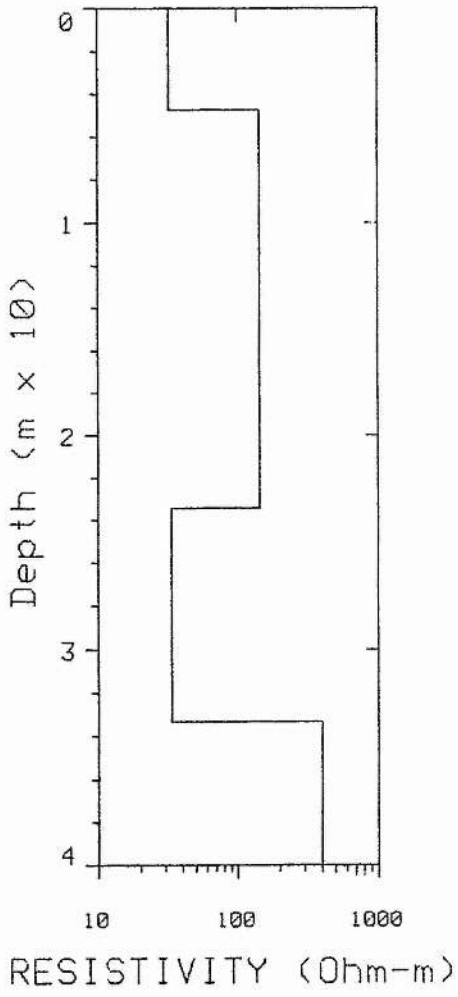
Depth (m x 10)
0
1
2
3
4
10
100
1000
RESISTIVITY (Ohm-m)

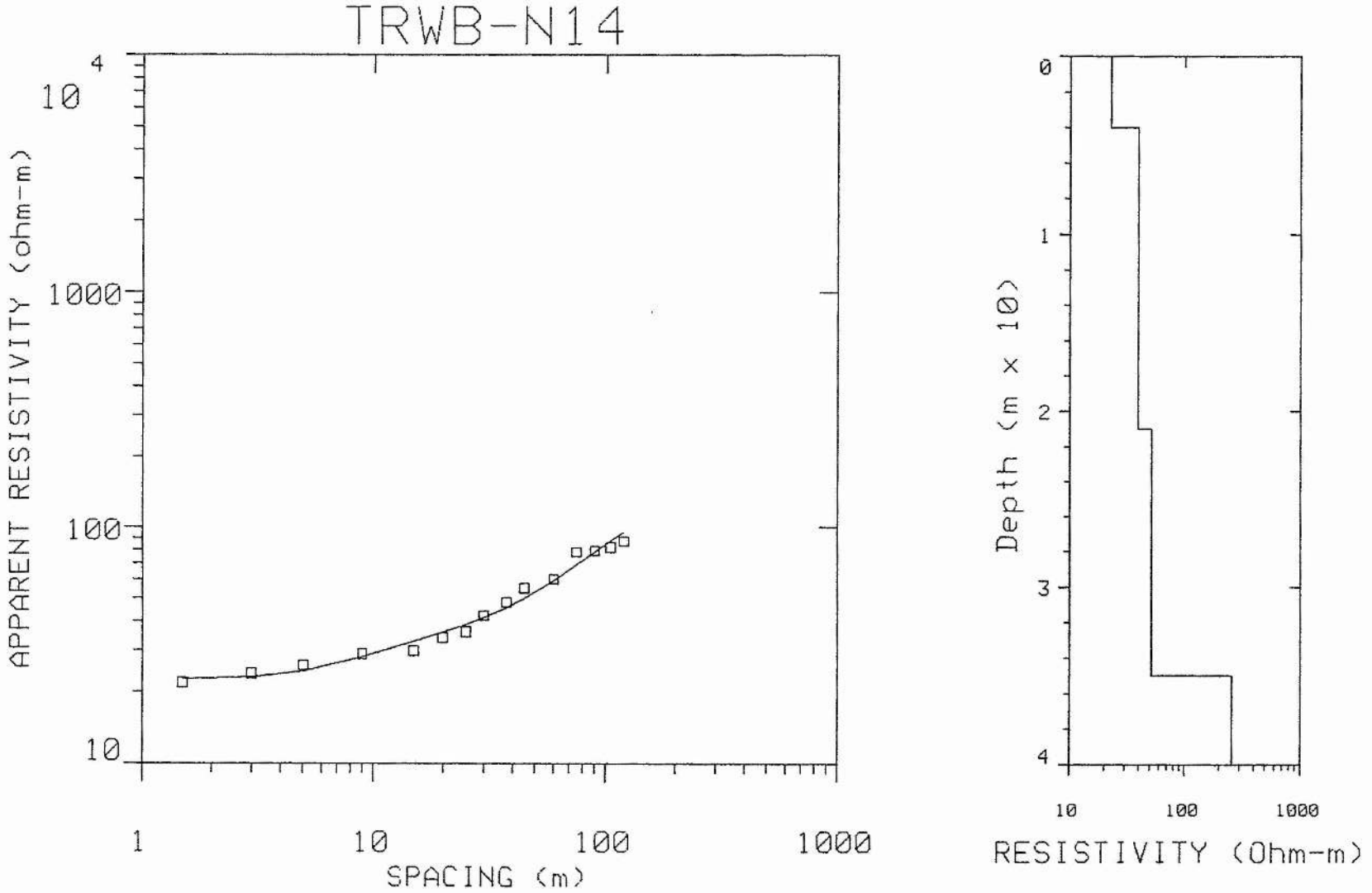
TRWB-N14
APPARENT RESISTIVITY (ohm-m)
10^4
1000
100
10
1
10
100
1000
SPACING (m)
Depth (m x 10)
0
1
2
3
4
10
100
1000
RESISTIVITY (Ohm-m)

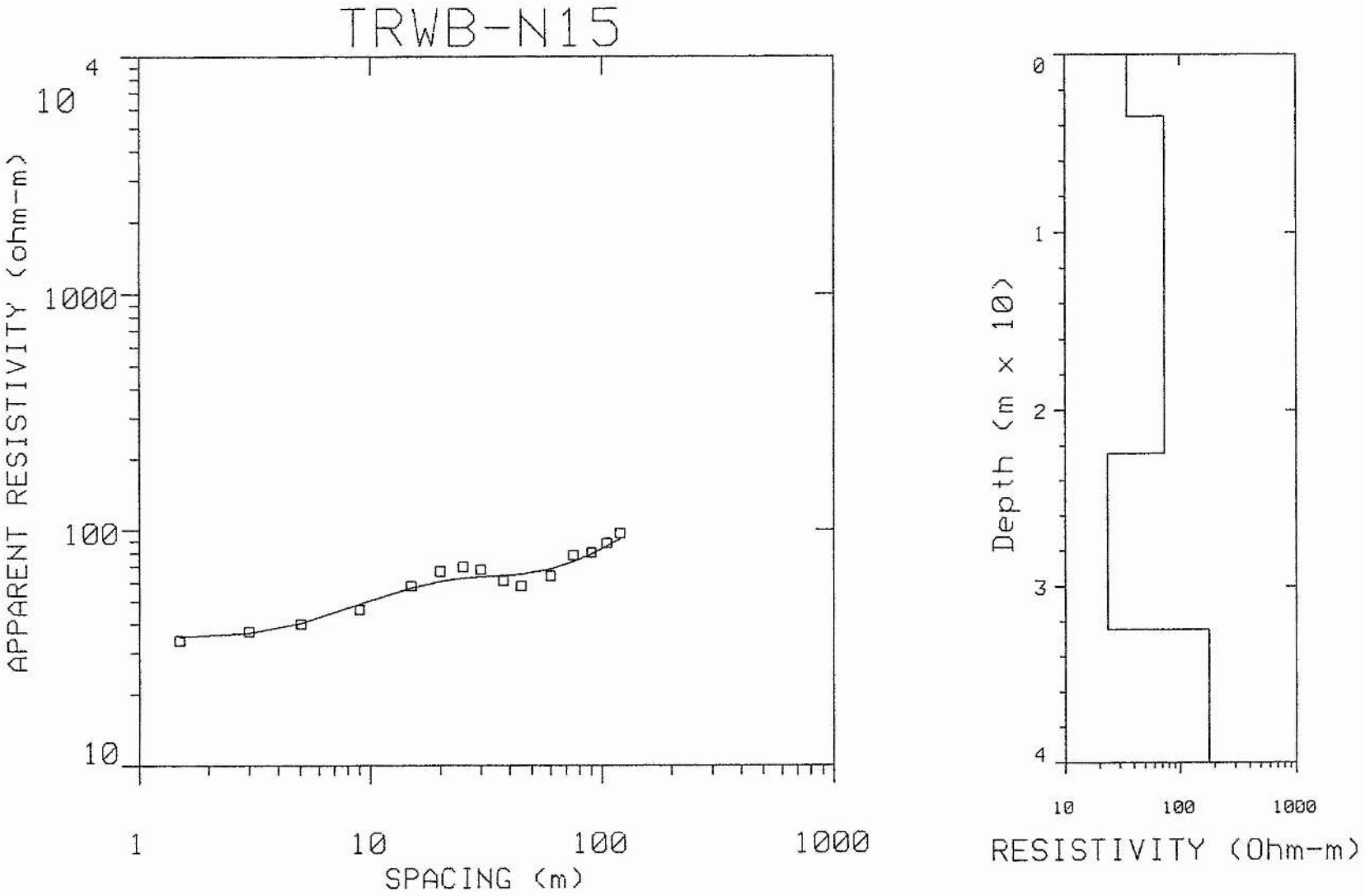
TRWB-N15
APPARENT RESISTIVITY (ohm-m)
10 4
1000
100
10
1
10
100
1000
SPACING (m)
Depth (m x 10)
0
1
2
3
4
10
100
1000
RESISTIVITY (Ohm-m)

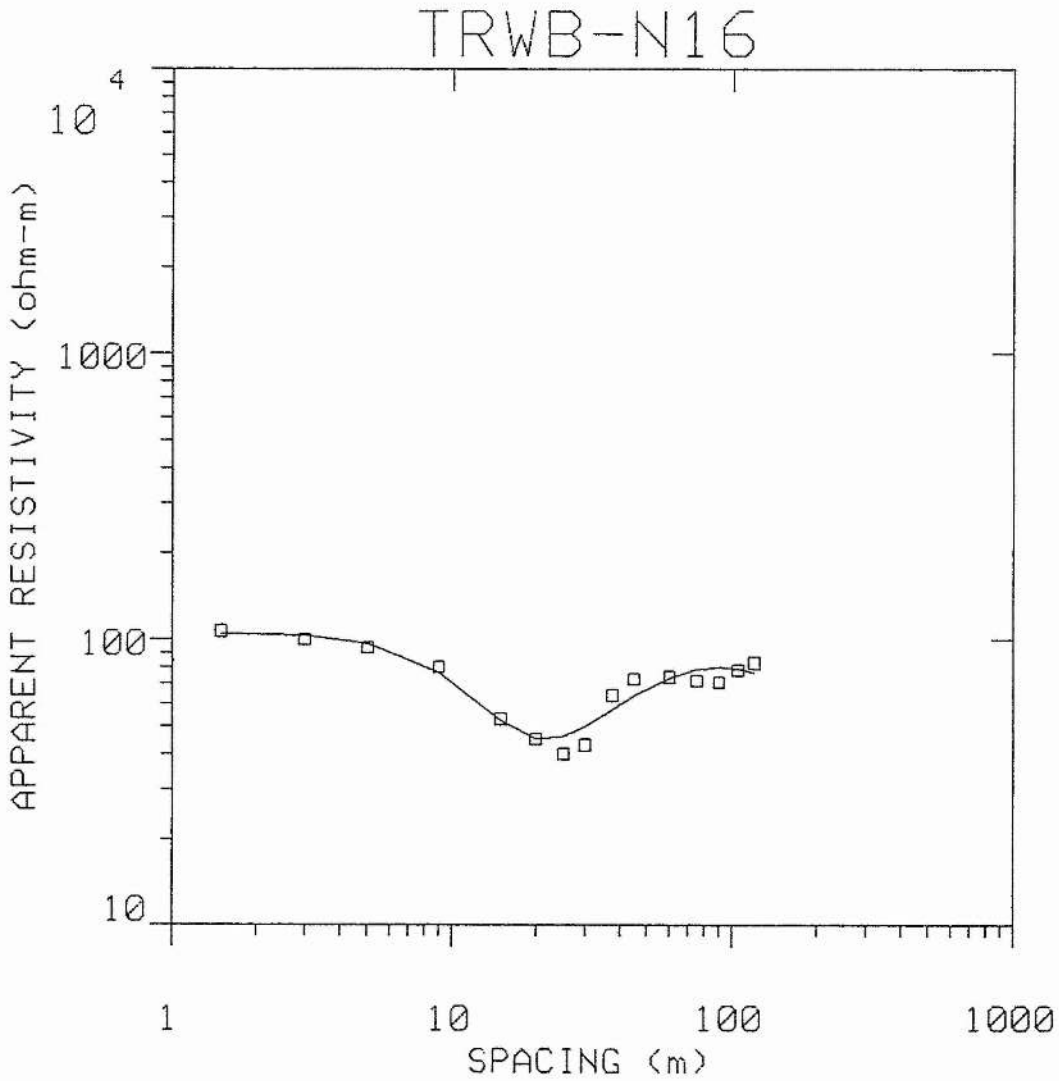
TRWB-N16
APPARENT RESISTIVITY (ohm-m)
10^4
1000
100
10
1
10
100
1000
SPACING (m)

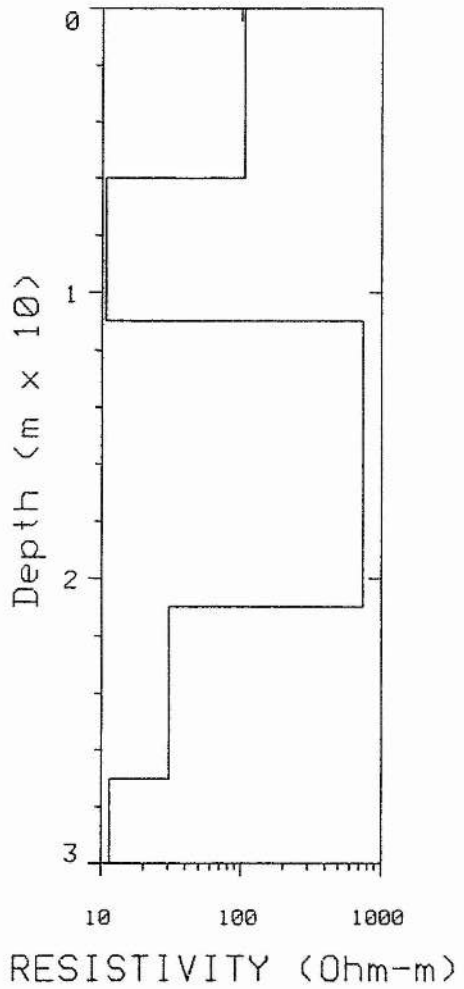
Depth (m x 10)
0
1
2
3
10
100
1000
RESISTIVITY (Ohm-m)

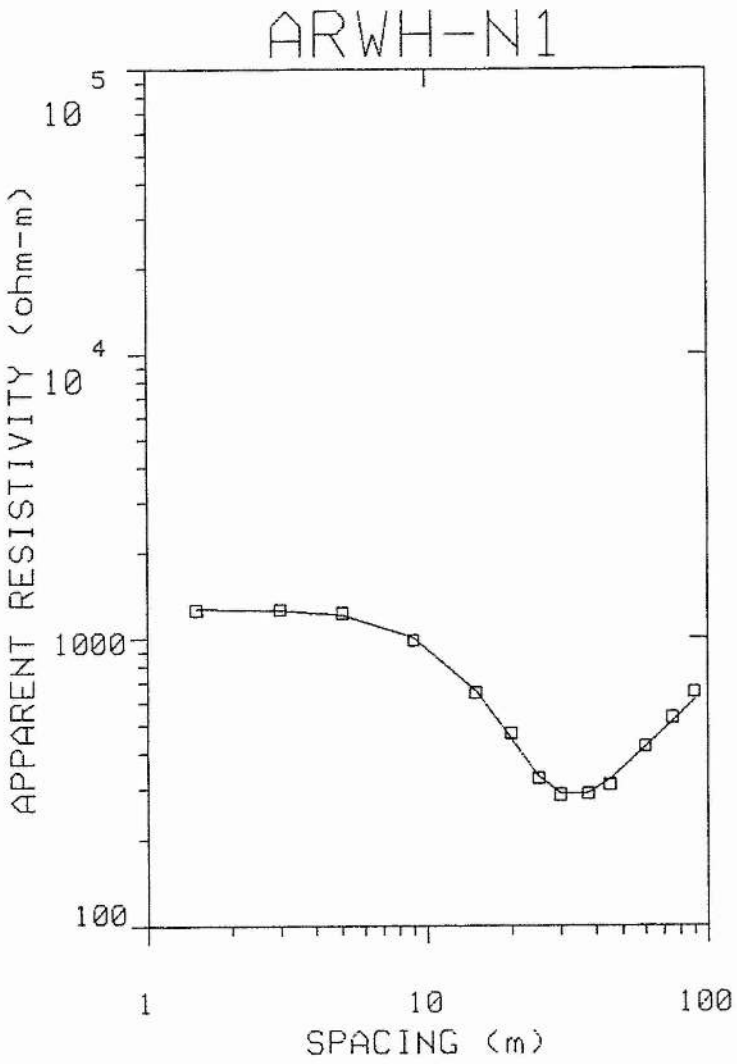
ARWH-N1
APPARENT RESISTIVITY (ohm-m)
10^5
10^4
1000
100
1
10
100
SPACING (m)

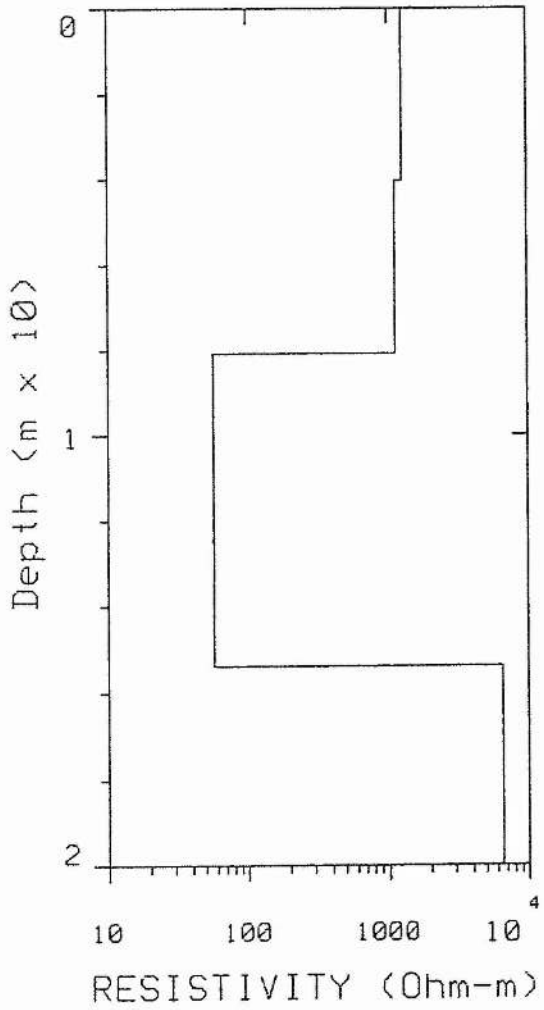
Depth (m x 10)
0
1
2
10
100
1000
10^4
RESISTIVITY (Ohm-m)

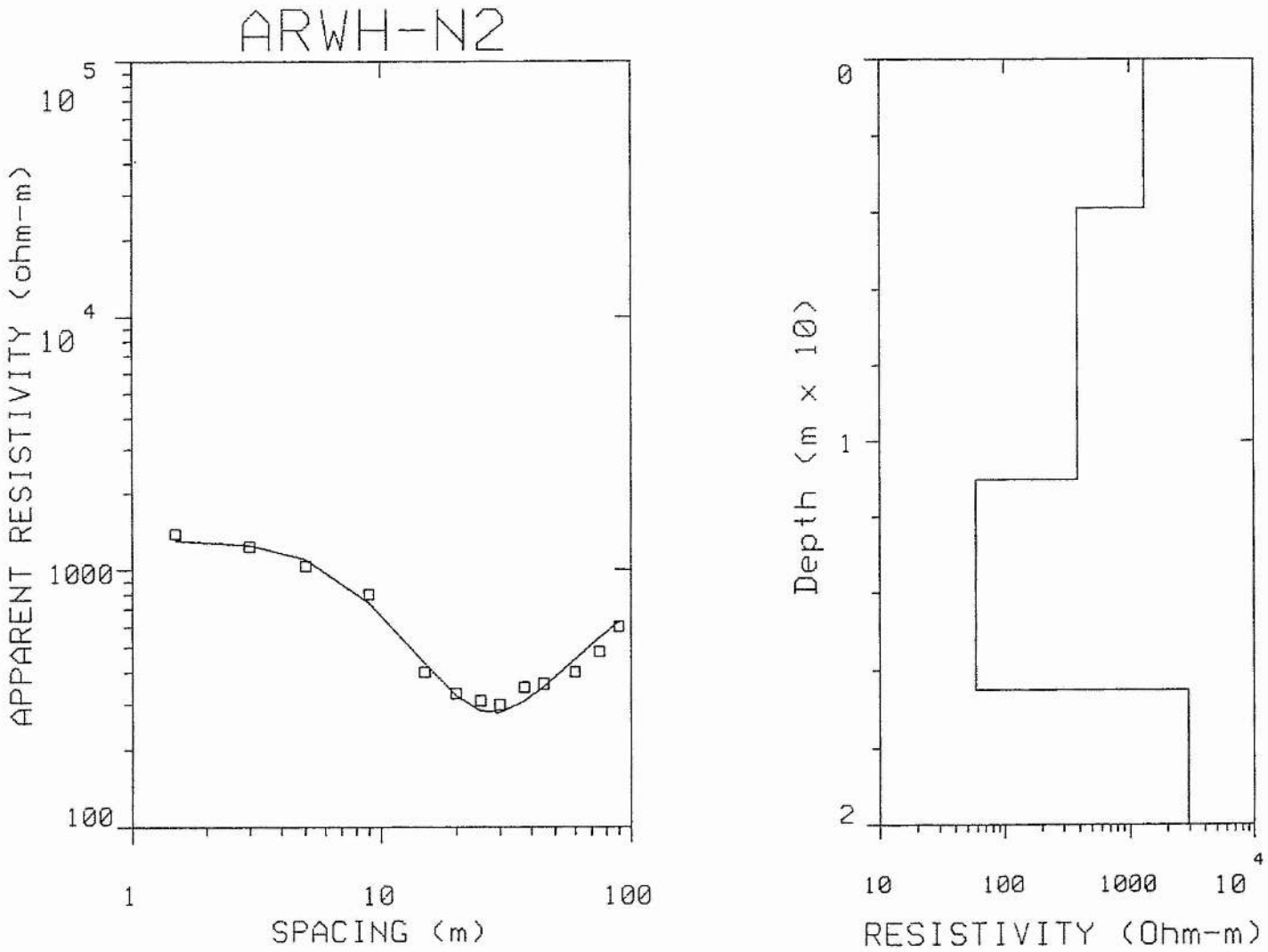
ARWH-N2
APPARENT RESISTIVITY (ohm-m)
10^5
10^4
1000
100
1
10
100
SPACING (m)
Depth (m x 10)
0
1
2
10
100
1000
10^4
RESISTIVITY (Ohm-m)

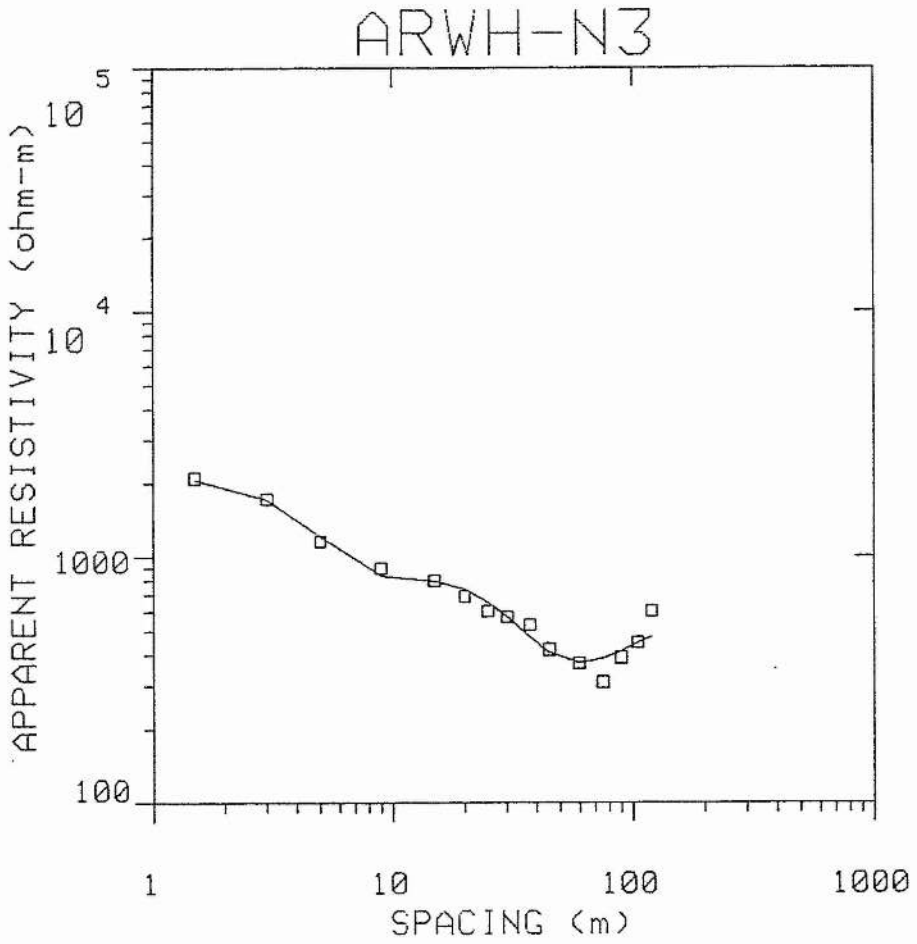
ARWH-N3
APPARENT RESISTIVITY (ohm-m)
10 5
10 4
1000
100
1
10
100
1000
SPACING (m)

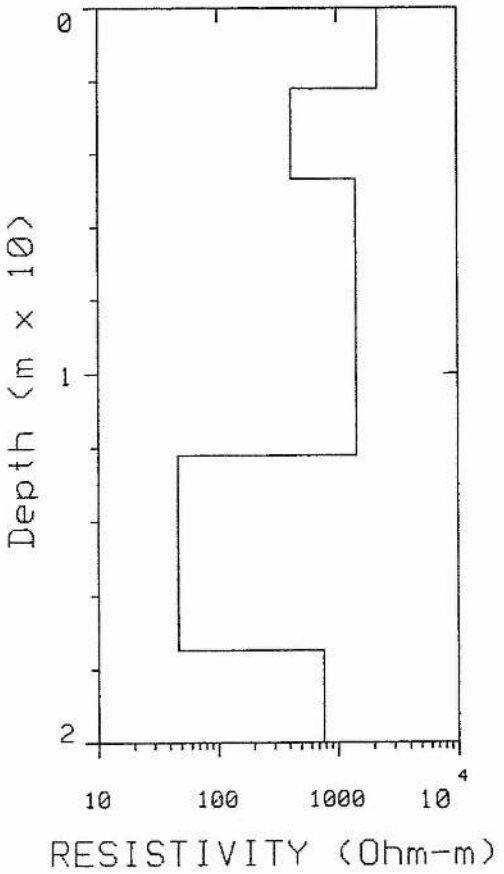
Depth (m x 10)
0
1
2
10
100
1000
10 4
RESISTIVITY (Ohm-m)

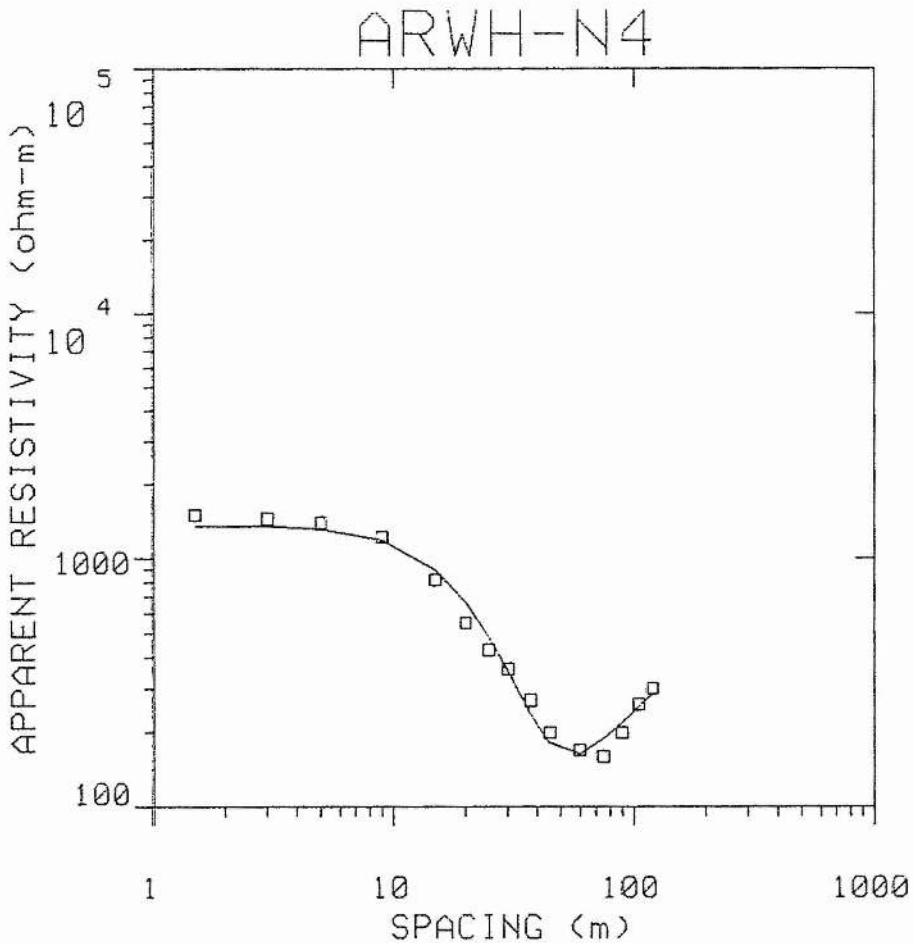
ARWH-N4
APPARENT RESISTIVITY (ohm-m)
10 5
10 4
1000
100
1
10
100
1000
SPACING (m)

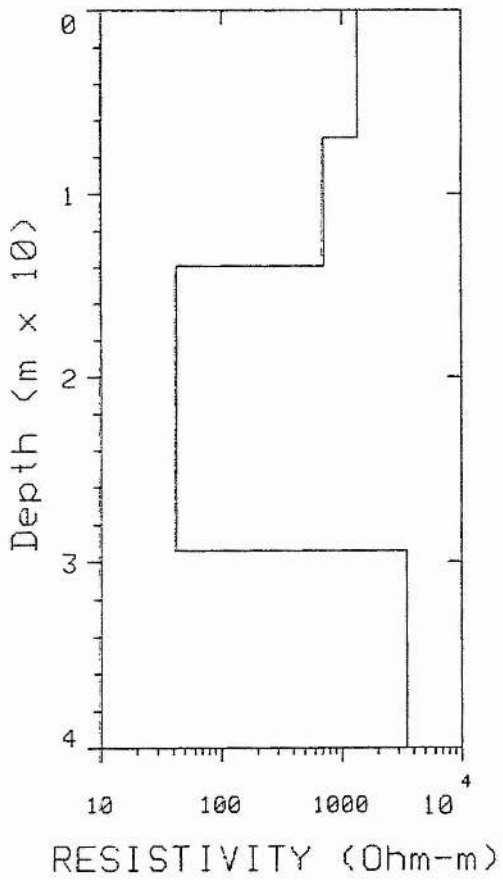
Depth (m x 10)
0
1
2
3
4
10
100
1000
10 4
RESISTIVITY (Ohm-m)

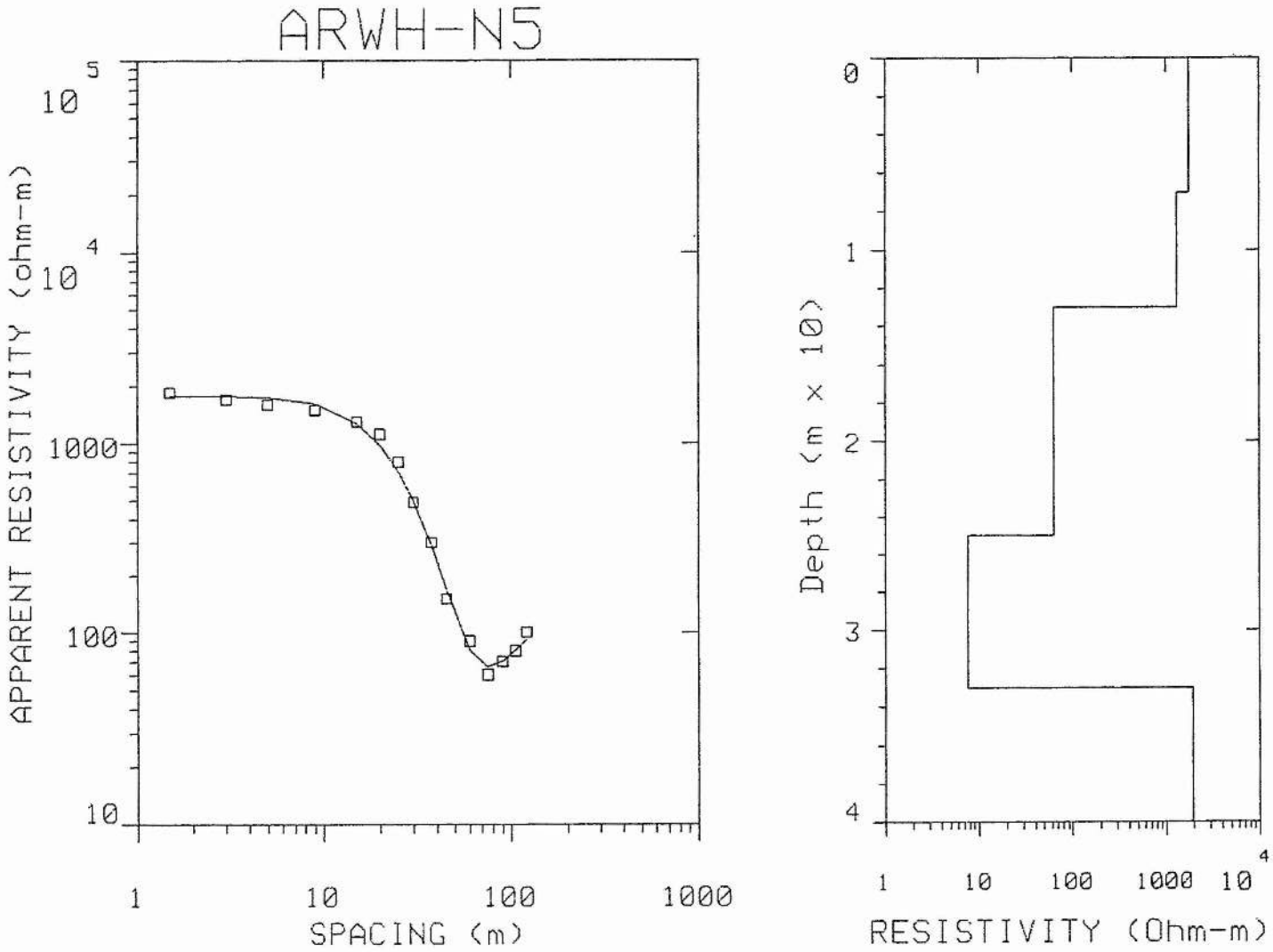
ARWH-N5
APPARENT RESISTIVITY (ohm-m)
10^5
10^4
1000
100
10
1
10
100
1000
SPACING (m)
Depth (m x 10)
0
1
2
3
4
1
10
100
1000
10^4
RESISTIVITY (Ohm-m)

Appendix 8 Grain size distribution curves for sediments from borehole lithology AO, BO, CO, DO, GO, IO, JO and KO in the lower part of Wadi Baysh

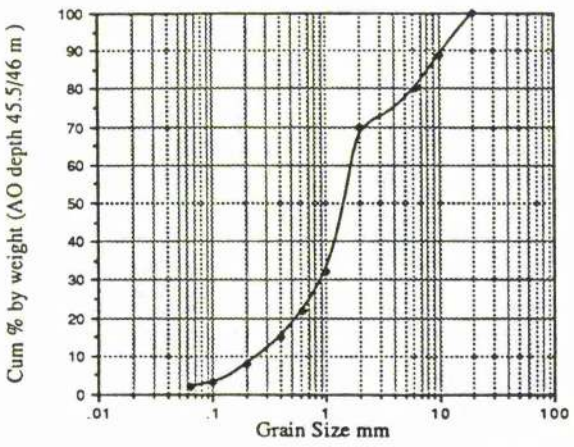
Cum % by weight (AO depth 45.5/46 m)
Grain Size mm

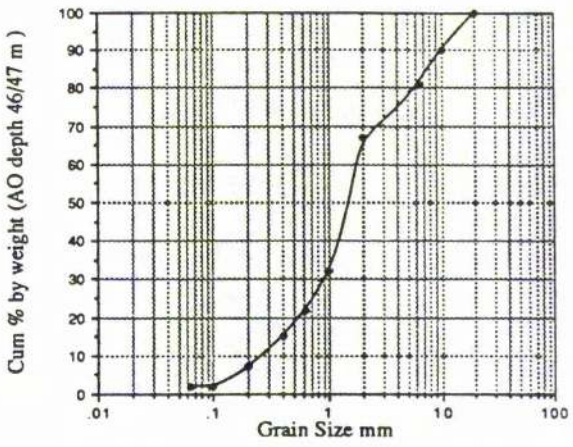
Cum % by weight (AO depth 46/47 m)
Grain Size mm

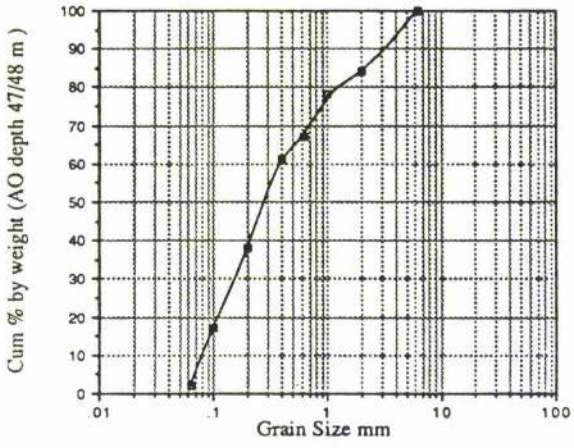
Cum % by weight (AO depth 47/48 m)
Grain Size mm

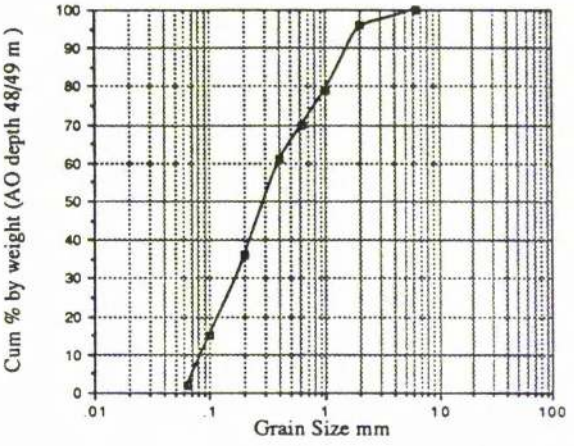
Cum % by weight (AO depth 48/49 m)
Grain Size mm

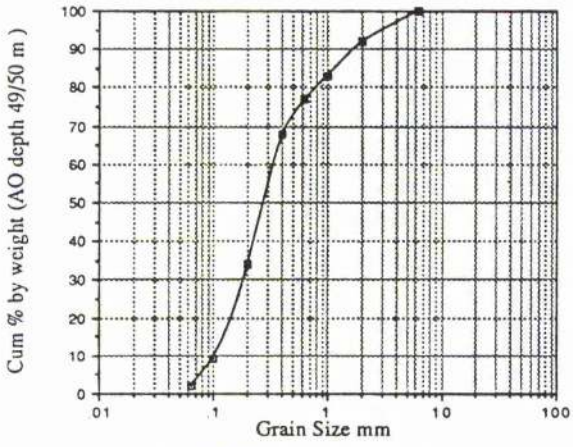
Cum % by weight (AO depth 49/50 m)
Grain Size mm

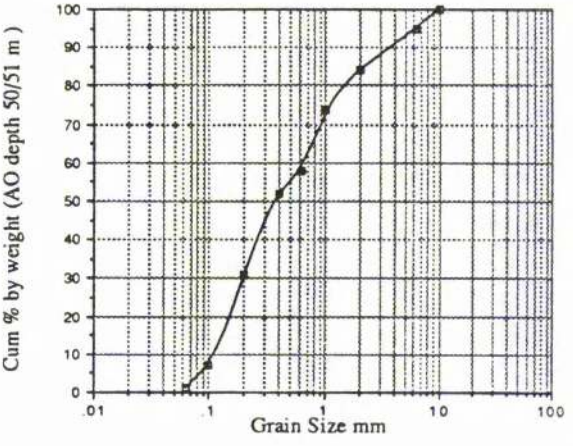
Cum % by weight (AO depth 50/51 m)
Grain Size mm

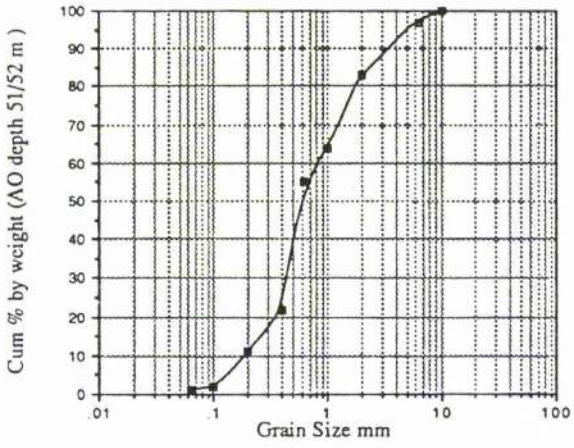
Cum % by weight (AO depth 51/52 m)
Grain Size mm

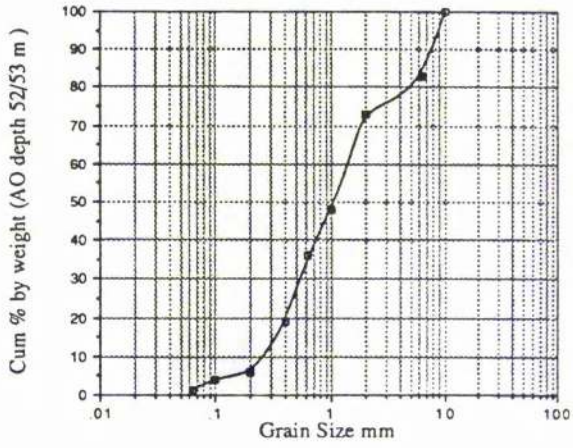
Cum % by weight (AO depth 52/53 m)
Grain Size mm

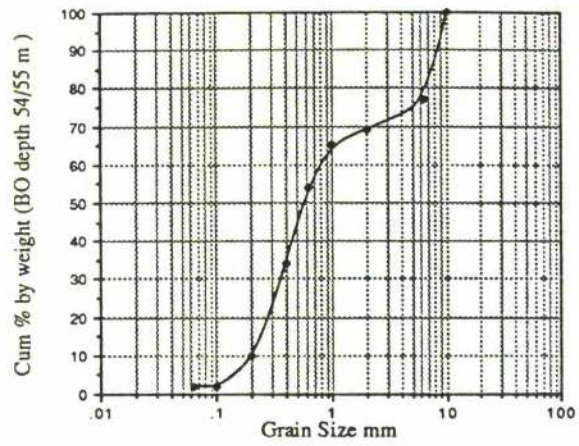
Cum % by weight (BO depth 54/55 m)
Grain Size mm

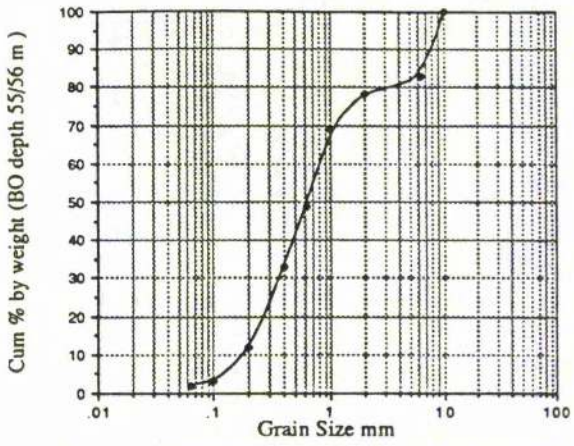
Cum % by weight (BO depth 55/56 m)
Grain Size mm

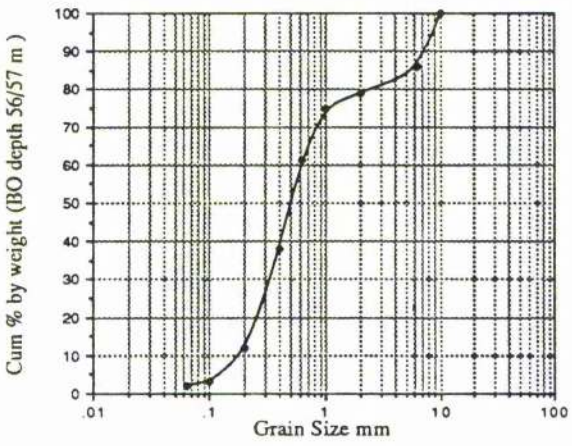
Cum % by weight (BO depth 56/57 m)
Grain Size mm

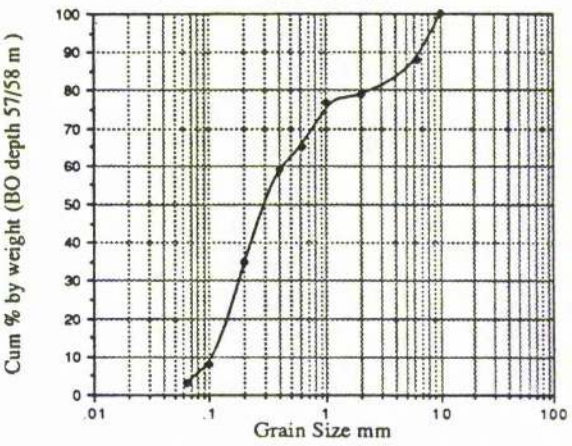
Cum % by weight (BO depth 57/58 m)
Grain Size mm

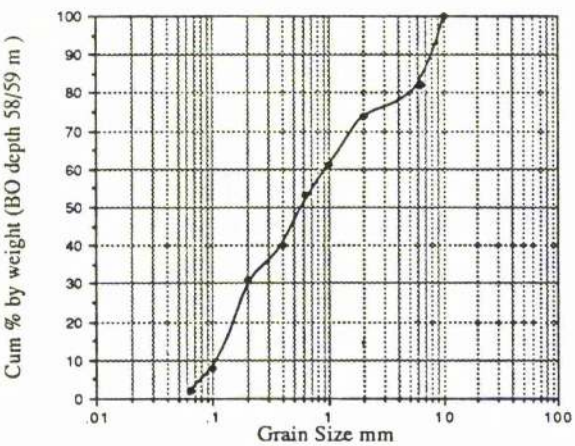
Cum % by weight (BO depth 58/59 m)
Grain Size mm

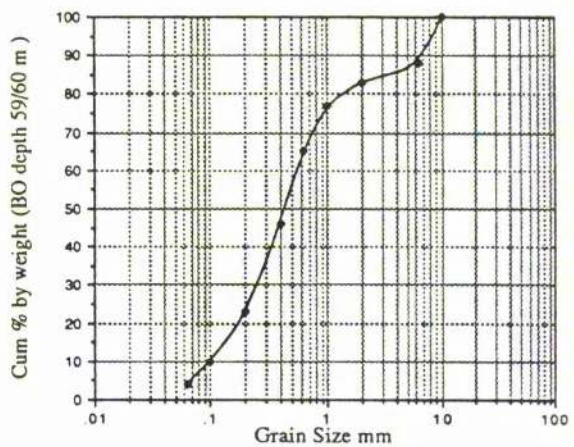
Cum % by weight (BO depth 59/60 m)
Grain Size mm

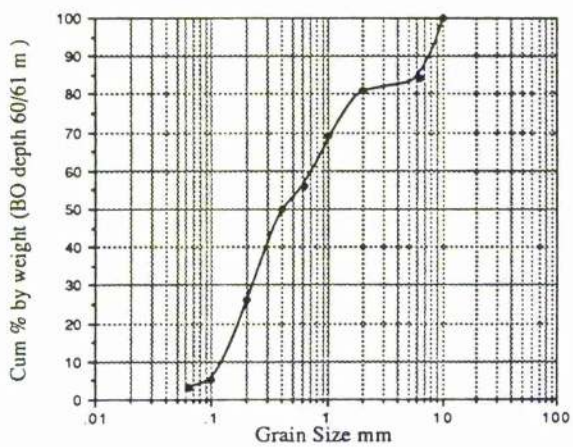
Cum % by weight (BO depth 60/61 m)
Grain Size mm

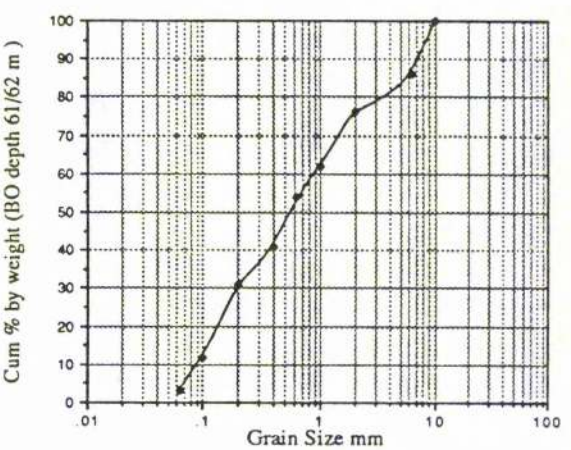
Cum % by weight (BO depth 61/62 m)
Grain Size mm

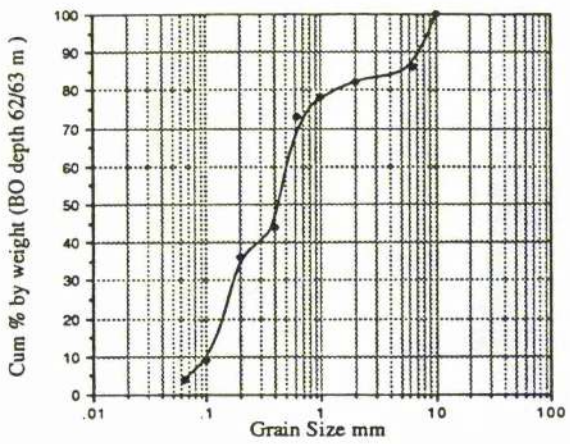
Cum % by weight (BO depth 62/63 m)
Grain Size mm

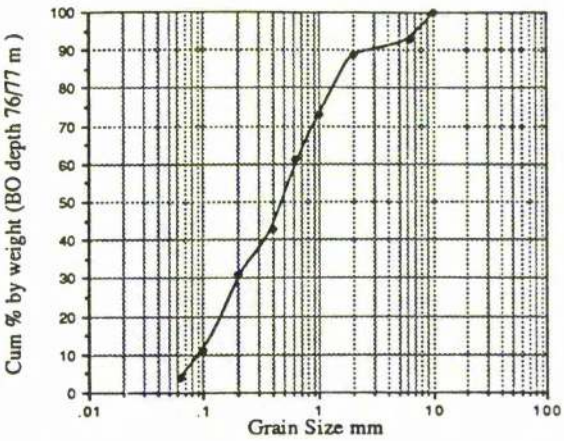
Cum % by weight (BO depth 76/77 m)
Grain Size mm

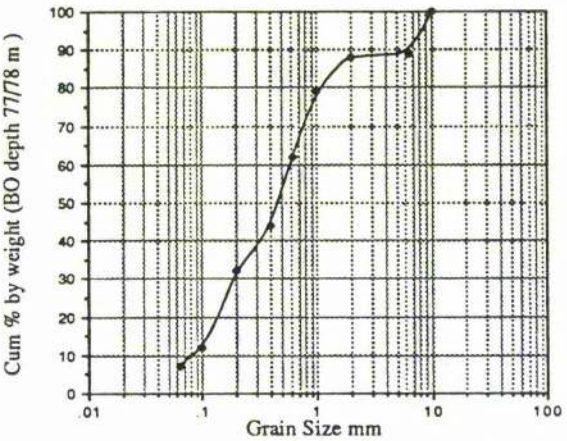
Cum % by weight (BO depth 77/78 m)
Grain Size mm

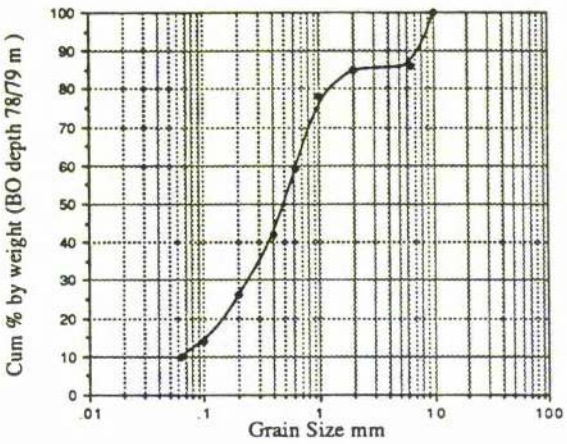
Cum % by weight (BO depth 78/79 m)
Grain Size mm

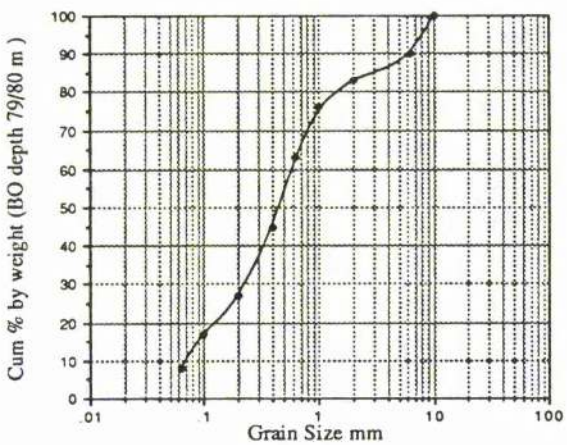
Cum % by weight (BO depth 79/80 m)
Grain Size mm

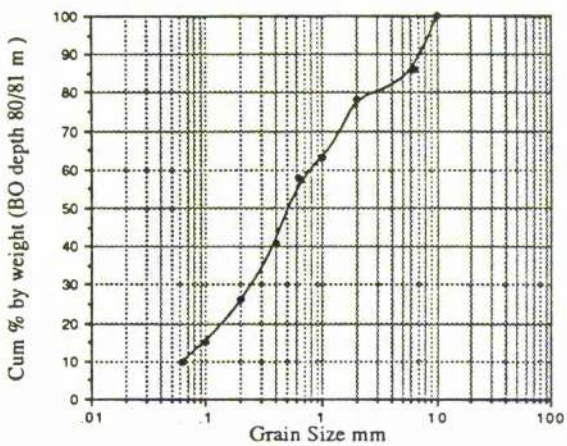
Cum % by weight (BO depth 80/81 m)
Grain Size mm

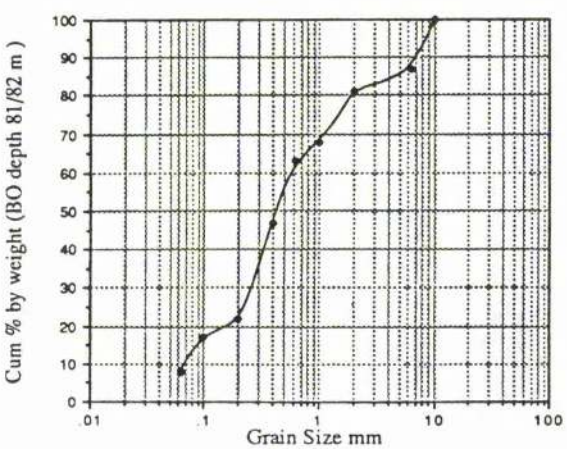
Cum % by weight (BO depth 81/82 m)
Grain Size mm

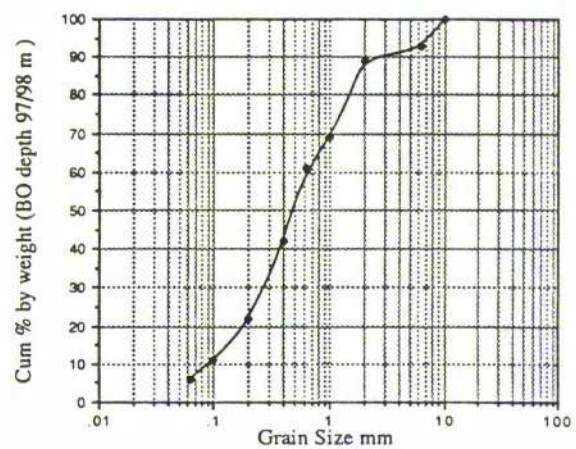
Cum % by weight (BO depth 97/98 m)
Grain Size mm

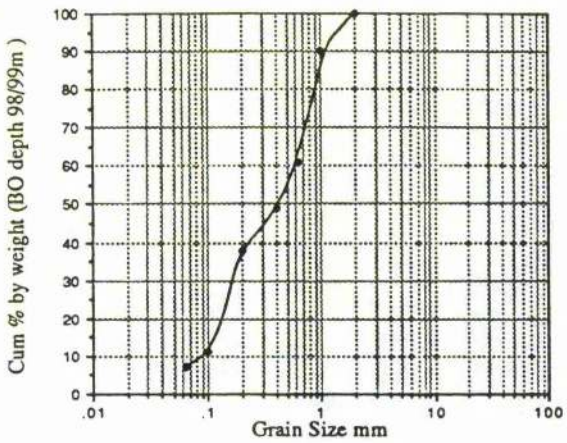
Cum % by weight (BO depth 98/99m)
Grain Size mm
100
90
80
70
60
50
40
30
20
10
0
.01
.1
1
10
100

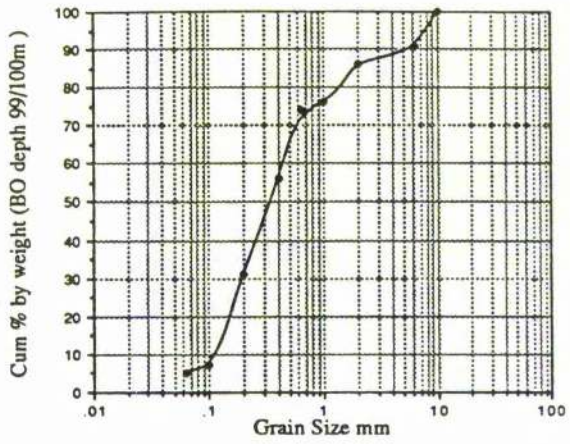
Cum % by weight (BO depth 99/100m)
Grain Size mm
100
90
80
70
60
50
40
30
20
10
0
.01
.1
1
10
100

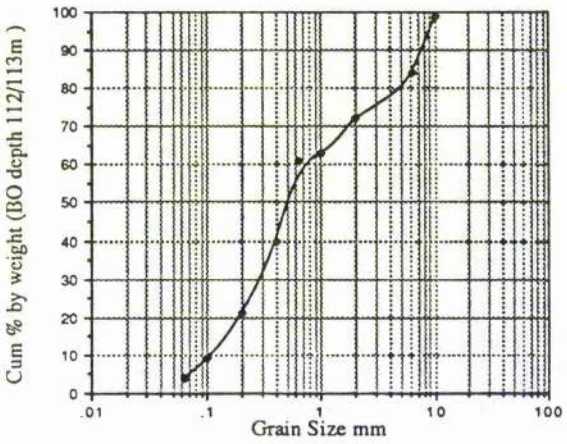
Cum % by weight (BO depth 112/113m)
Grain Size mm
100
90
80
70
60
50
40
30
20
10
0
.01
.1
1
10
100

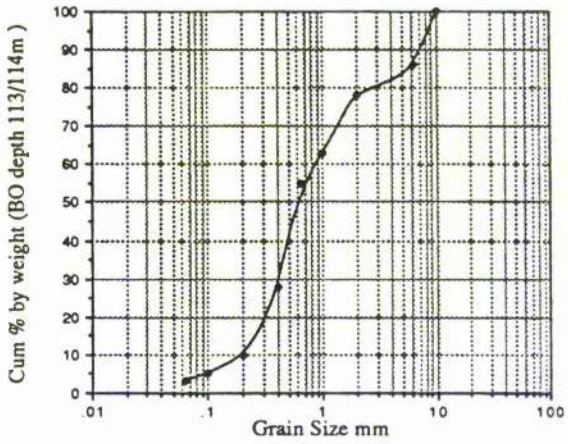
Cum % by weight (BO depth 113/114m)
Grain Size mm
100
90
80
70
60
50
40
30
20
10
0
.01
.1
1
10
100

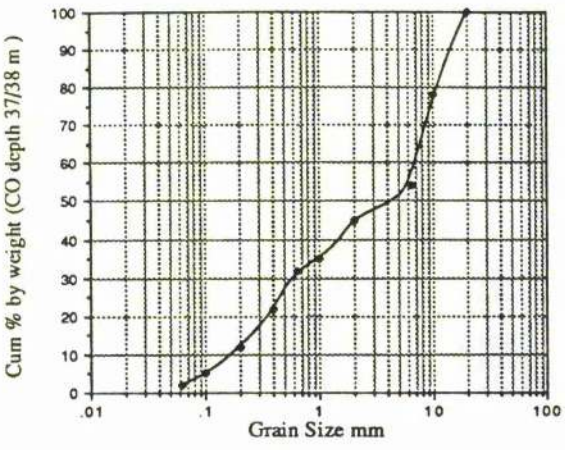
Cum % by weight (CO depth 37/38 m)
Grain Size mm

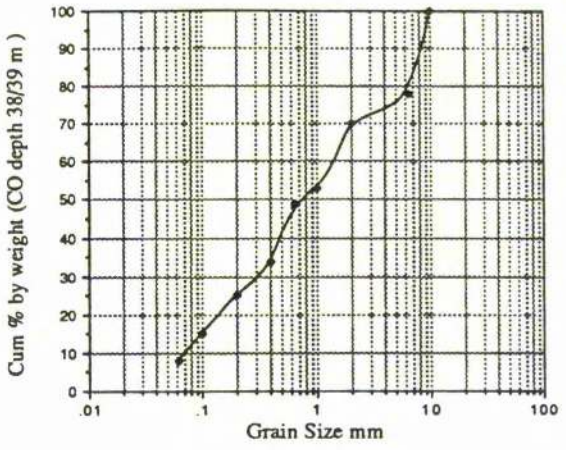
Cum % by weight (CO depth 38/39 m)
Grain Size mm

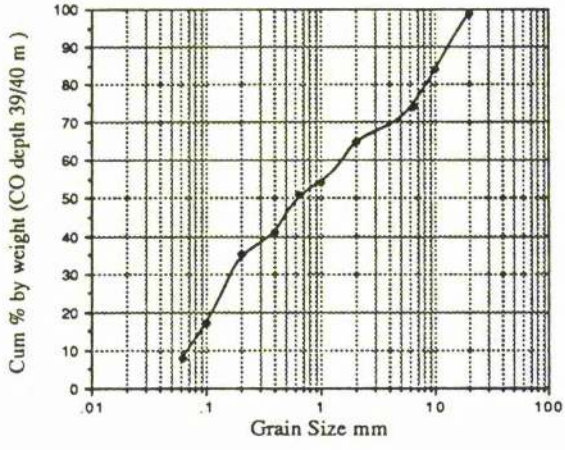
Cum % by weight (CO depth 39/40 m)
Grain Size mm

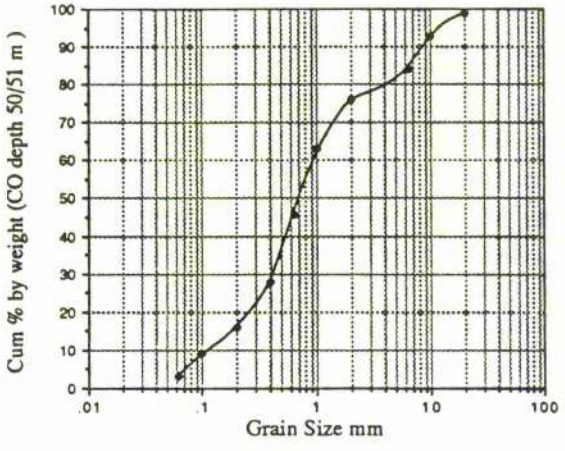
Cum % by weight (CO depth 50/51 m)
Grain Size mm

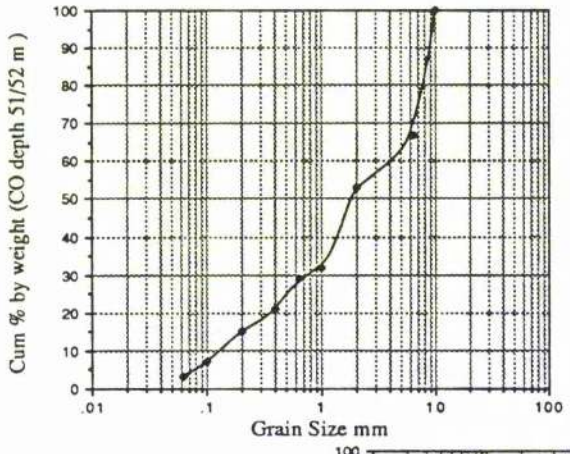
Cum % by weight (CO depth 51/52 m)
Grain Size mm

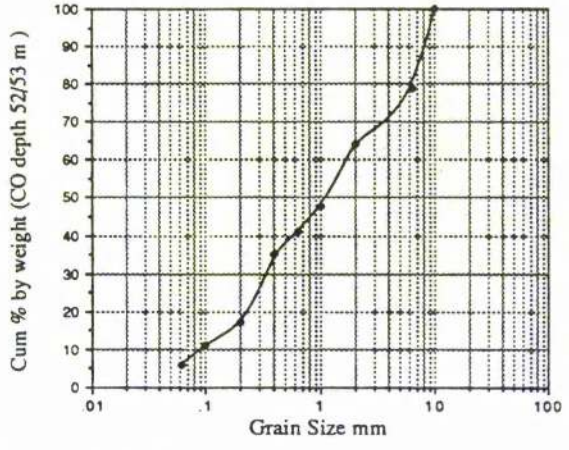
Cum % by weight (CO depth 52/53 m)
Grain Size mm

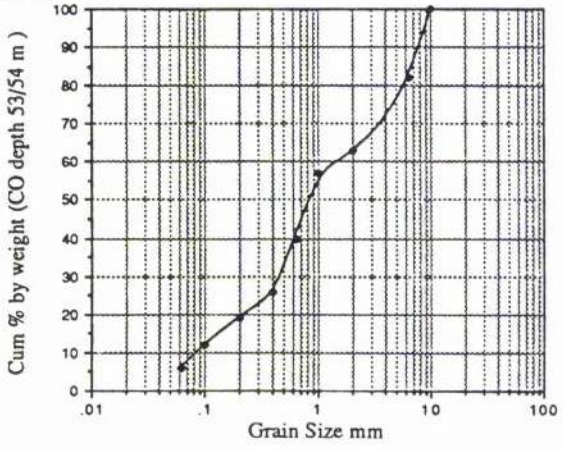
Cum % by weight (CO depth 53/54 m)
Grain Size mm

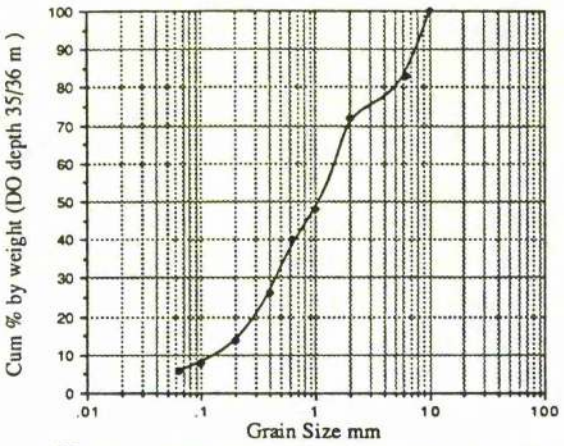
Cum % by weight (DO depth 35/36 m)
Grain Size mm

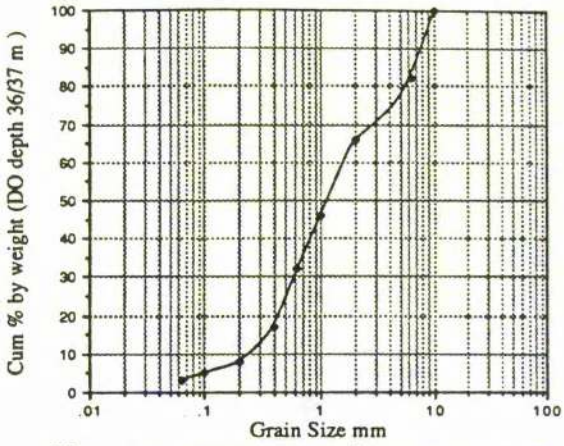
Cum % by weight (DO depth 36/37 m)
Grain Size mm

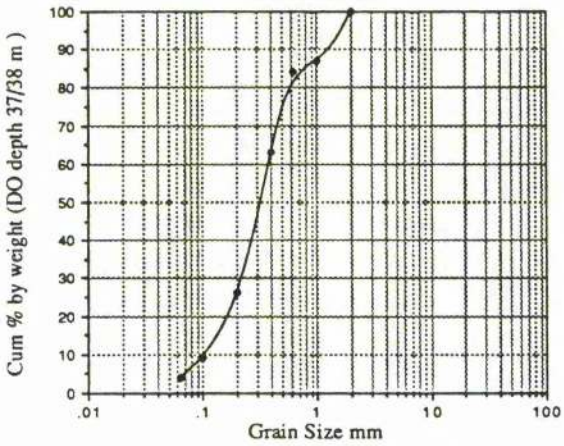
Cum % by weight (DO depth 37/38 m)
Grain Size mm

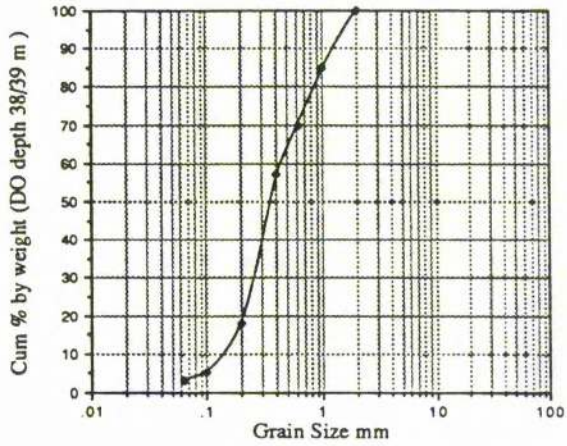
Cum % by weight (DO depth 38/39 m)
Grain Size mm

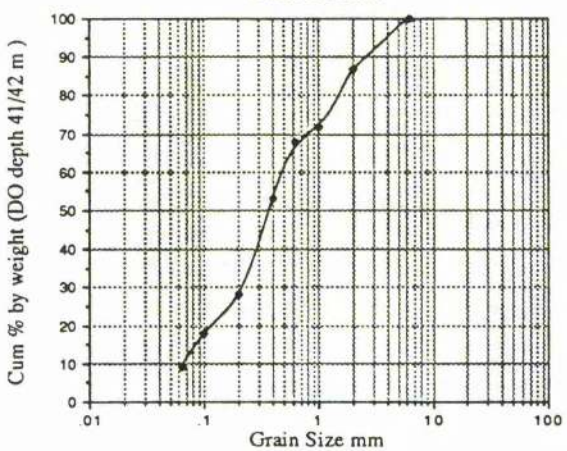
Cum % by weight (DO depth 41/42 m)
Grain Size mm

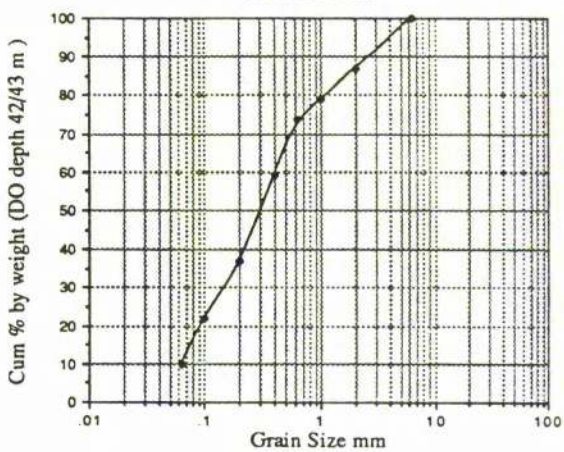
Cum % by weight (DO depth 42/43 m)
Grain Size mm

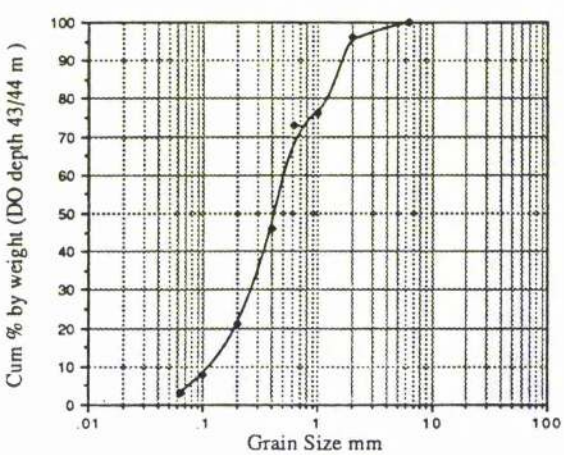
Cum % by weight (DO depth 43/44 m)
Grain Size mm

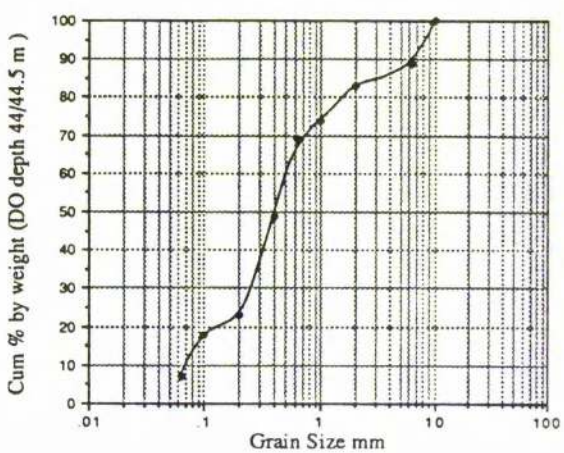
Cum % by weight (DO depth 44/44.5 m)
Grain Size mm

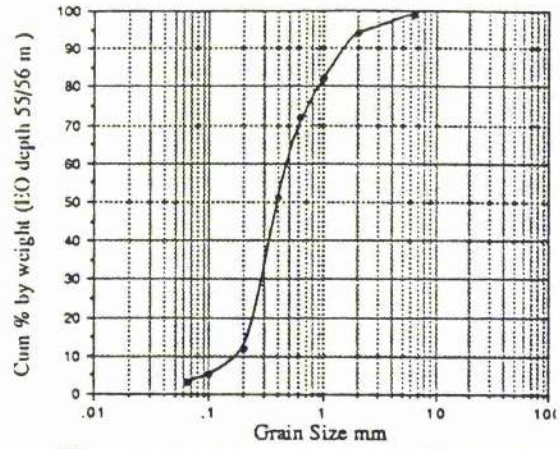
Cum % by weight (I:O depth 55/56 m)
Grain Size mm

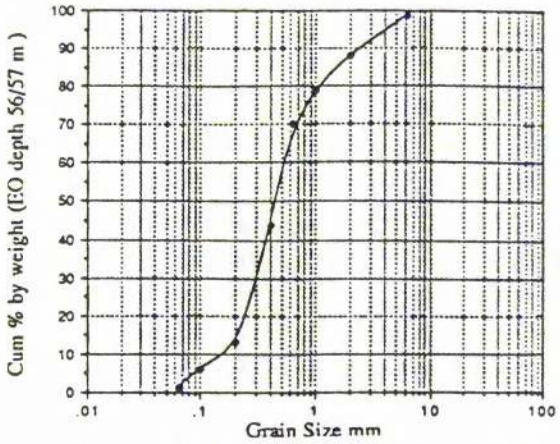
Cum % by weight (I:O depth 56/57 m)
Grain Size mm

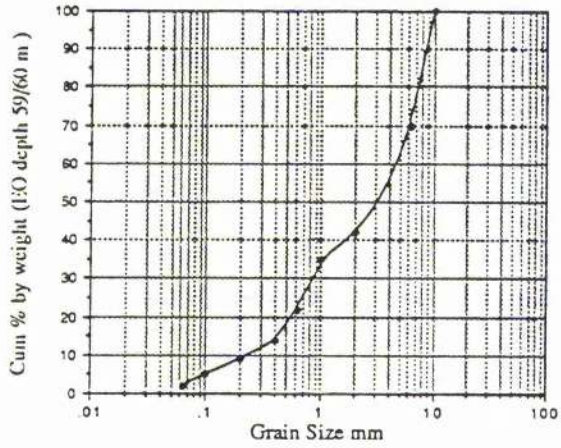
Cum % by weight (I:O depth 59/60 m)
Grain Size mm

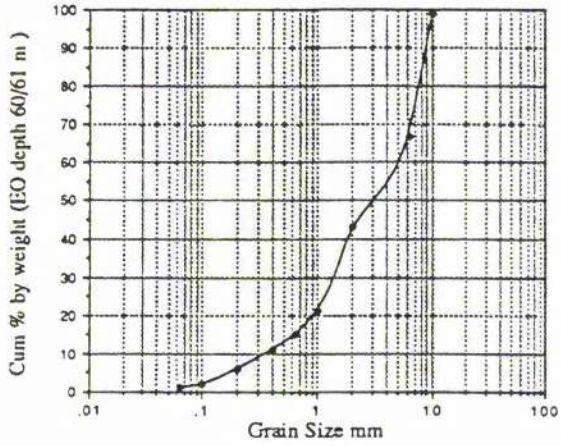
Cum % by weight (I:O depth 60/61 m)
Grain Size mm

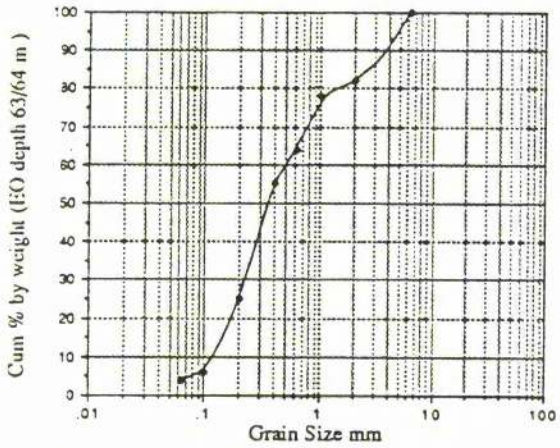
Cum % by weight (I:O depth 63/64 m)
Grain Size mm

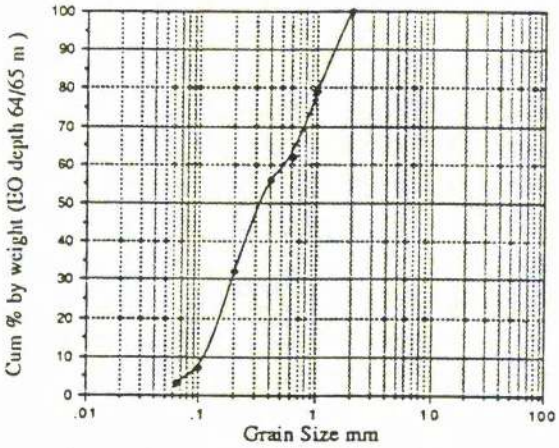
Cum % by weight (I:O depth 64/65 m)
Grain Size mm

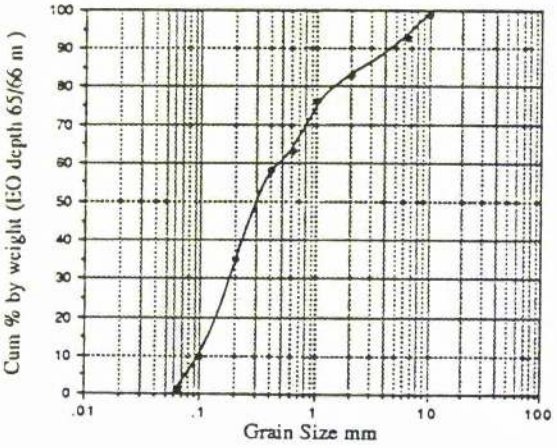
Cum % by weight (I:O depth 65/66 m)
Grain Size mm

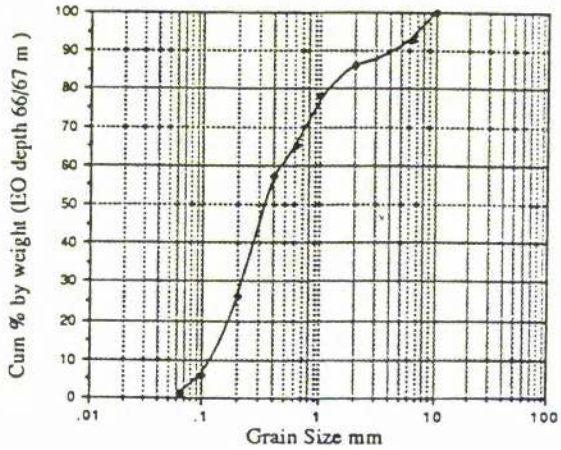
Cum % by weight (I:O depth 66/67 m)
Grain Size mm

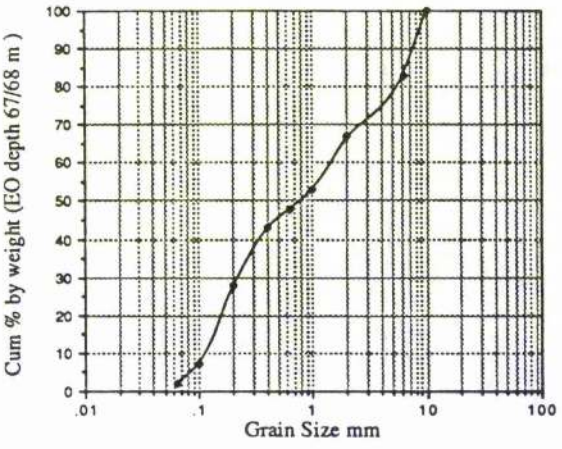
Cum % by weight (EO depth 67/68 m)
100
90
80
70
60
50
40
30
20
10
0
.01
.1
1
10
100
Grain Size mm

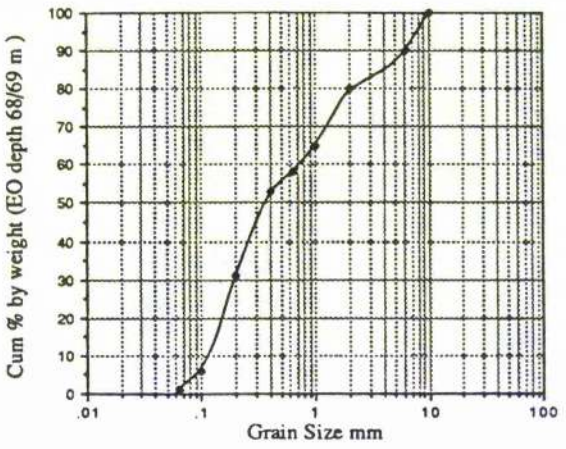
Cum % by weight (EO depth 68/69 m)
100
90
80
70
60
50
40
30
20
10
0
.01
.1
1
10
100
Grain Size mm

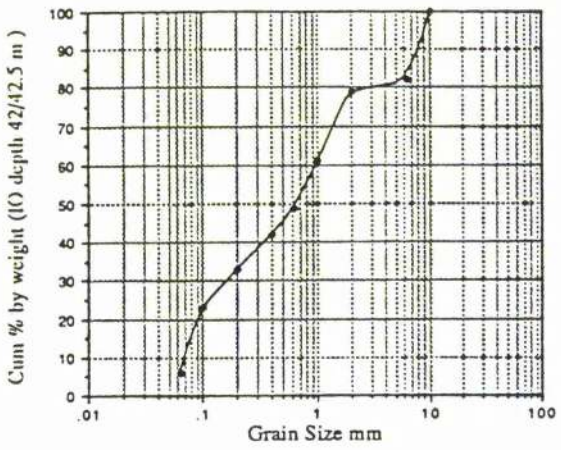
Cum % by weight (IO depth 42/42.5 m)
Grain Size mm

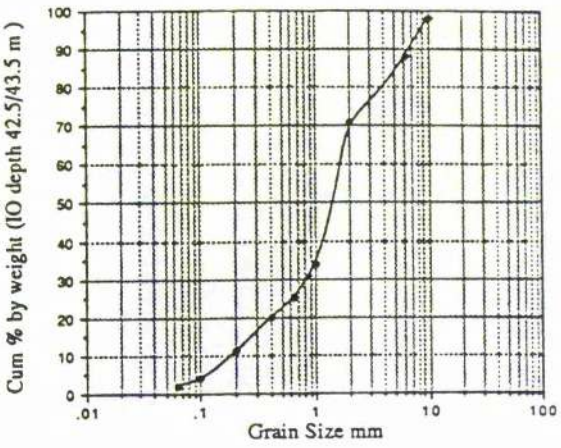
Cum % by weight (IO depth 42.5/43.5 m)
Grain Size mm

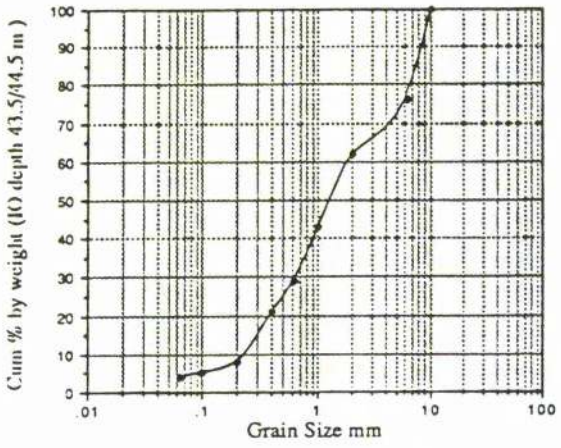
Cum % by weight (IO depth 43.5/44.5 m)
Grain Size mm

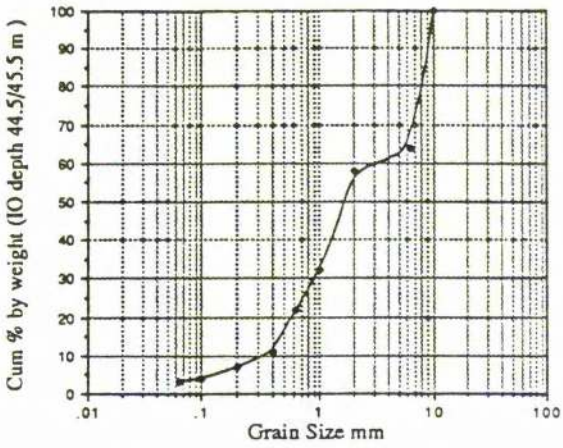
Cum % by weight (IO depth 44.5/45.5 m)
Grain Size mm

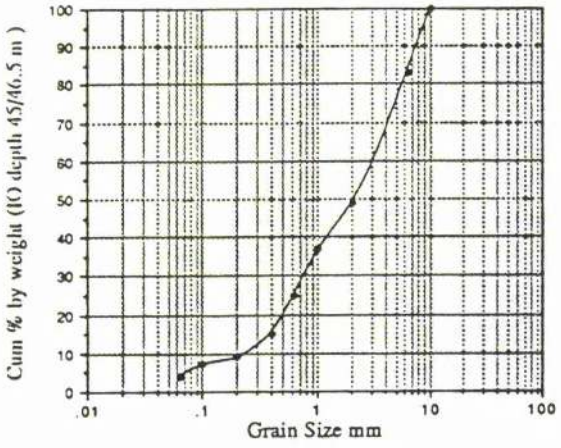
Cum % by weight (IO depth 45/46.5 m)
Grain Size mm

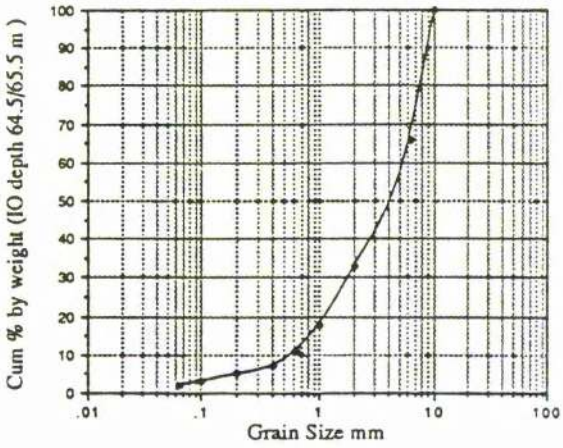
Cum % by weight (IO depth 64.5/65.5 m)
Grain Size mm

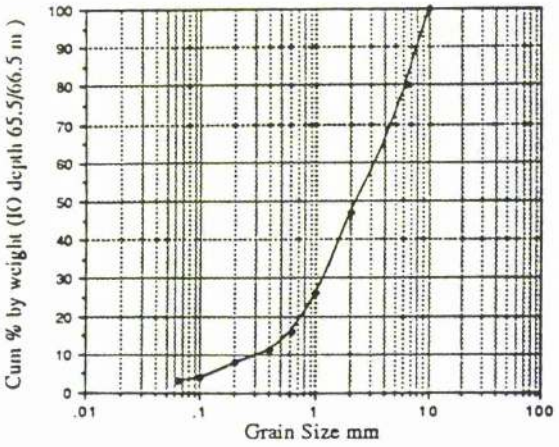
Cum % by weight (IO depth 65.5/66.5 m)
Grain Size mm

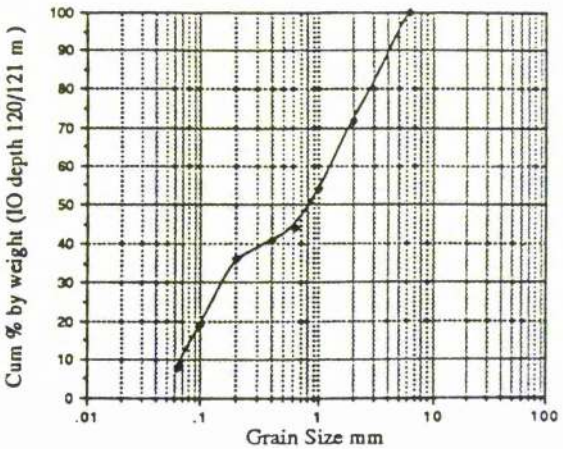
Cum % by weight (IO depth 120/121 m)
Grain Size mm

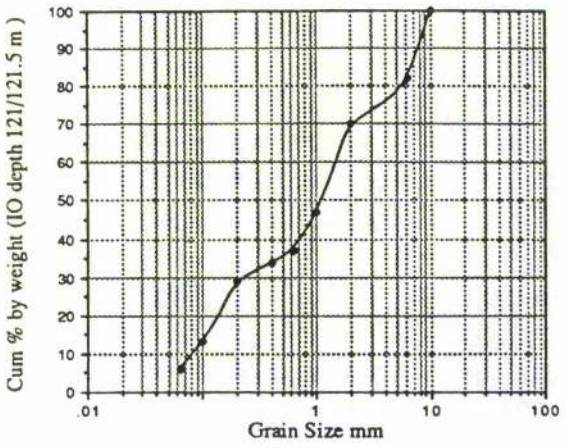
Cum % by weight (IO depth 121/121.5 m)
Grain Size mm
0
10
20
30
40
50
60
70
80
90
100
.01
1
10
100

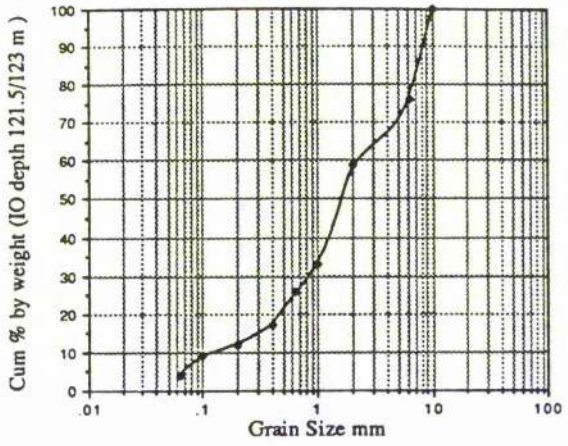
Cum % by weight (IO depth 121.5/123 m)
Grain Size mm
0
10
20
30
40
50
60
70
80
90
100
.01
.1
1
10
100

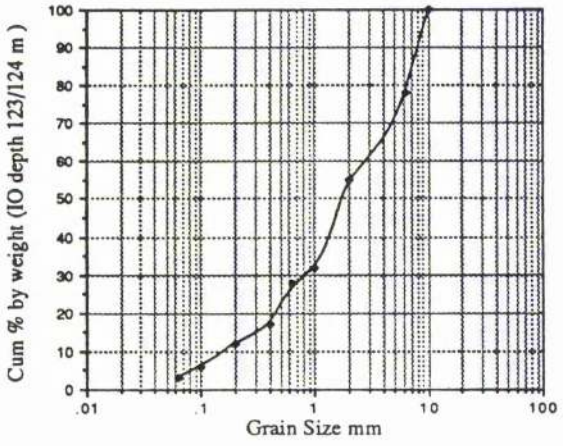
Cum % by weight (IO depth 123/124 m)
Grain Size mm
0
10
20
30
40
50
60
70
80
90
100
.01
.1
1
10
100

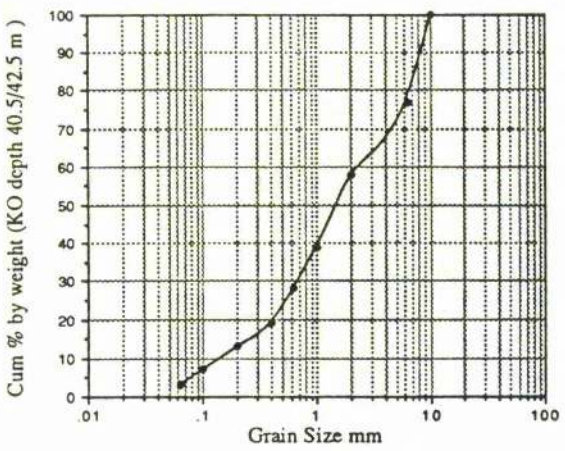
Cum % by weight (KO depth 40.5/42.5 m)
Grain Size mm

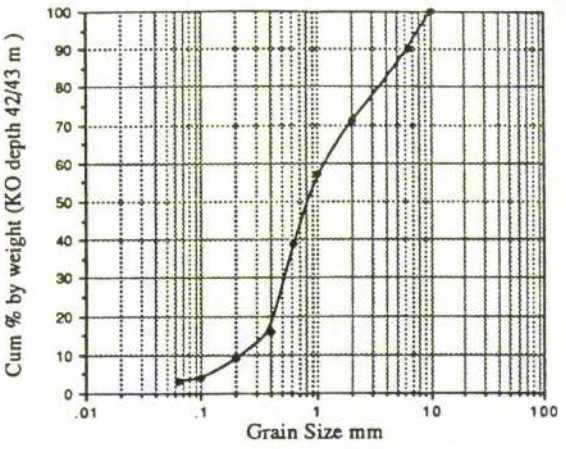
Cum % by weight (KO depth 42/43 m)
Grain Size mm

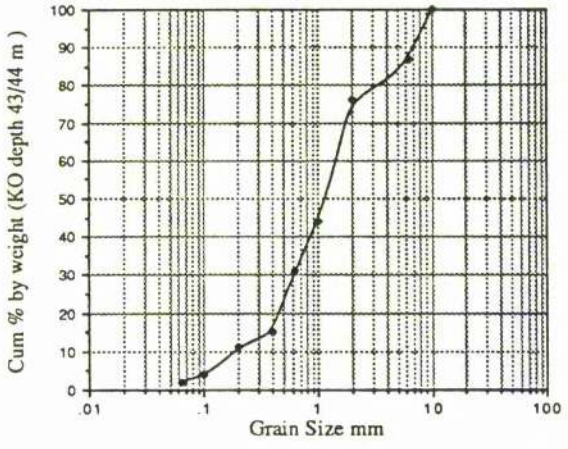
Cum % by weight (KO depth 43/44 m)
Grain Size mm

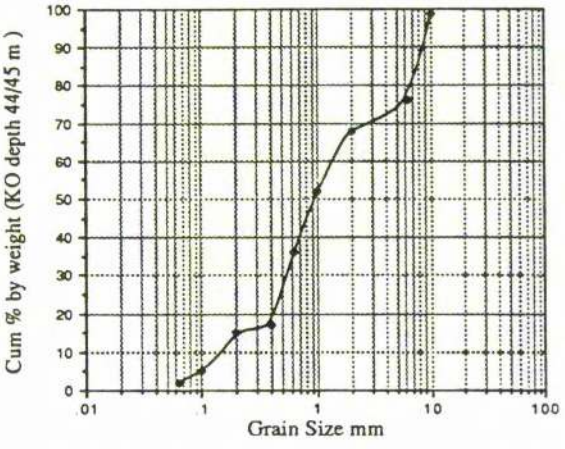
Cum % by weight (KO depth 44/45 m)
Grain Size mm

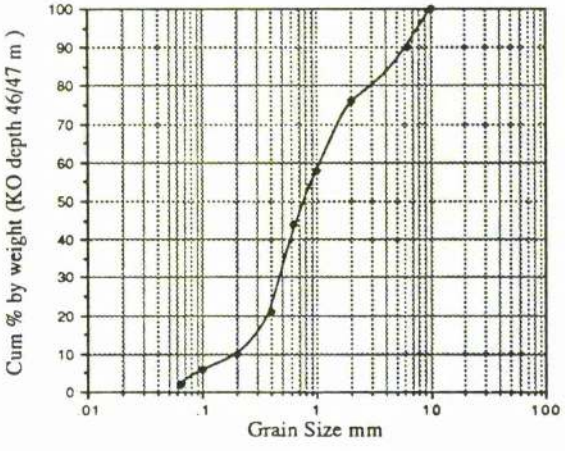
Cum % by weight (KO depth 46/47 m)
Grain Size mm

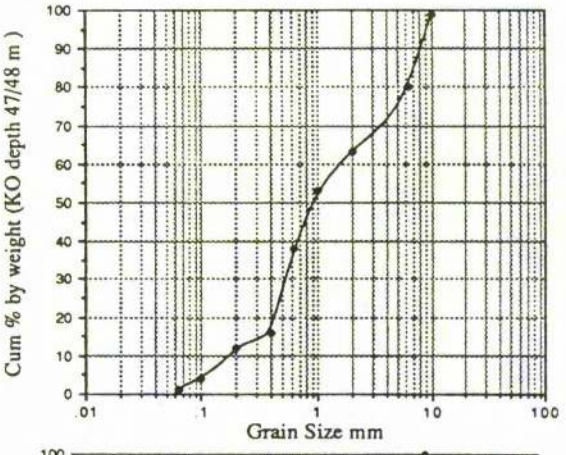
Cum % by weight (KO depth 47/48 m)
Grain Size mm

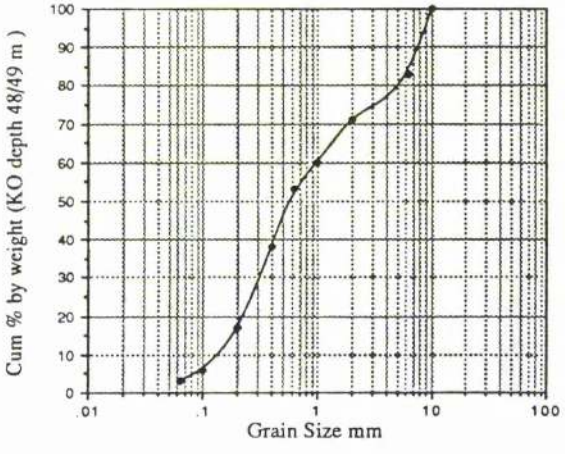
Cum % by weight (KO depth 48/49 m)
Grain Size mm

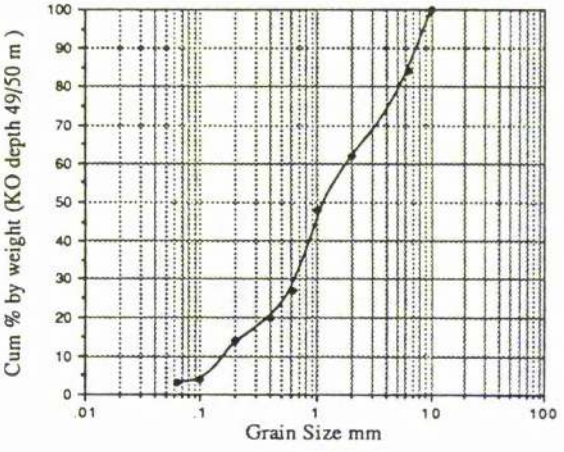
Cum % by weight (KO depth 49/50 m)
Grain Size mm